British Journal of Pharmacology

October 1992

Volume 107 Number 2 pages 271–634

Br. J. Pharmacol. (1992), **107**, 273–275

SPECIAL REPORT

Non-specific activity of (±)-CP-96,345 in models of pain and inflammation

[1]Atsushi Nagahisa, Rinko Asai, Yoshihito Kanai, Akio Murase, Megumi Tsuchiya-Nakagaki, Toshiyuki Nakagaki, Tiee-Cherng Shieh & Kana Taniguchi

Department of Medicinal Biology, Central Research Division, Pfizer Inc., 5-2 Taketoyo, Aichi 470-23, Japan

The non-peptide NK_1 receptor antagonist, CP-96,345, and its **2R,3R** enantiomer CP-96,344, which is not an NK_1 receptor antagonist ($IC_{50} > 10\,\mu M$), were evaluated for antinociceptive and anti-inflammatory activities in several classical models of pain and inflammation in the rat. Both CP-96,345 and CP-96,344 reduced carrageenin-induced paw oedema and hyperalgesia, and attenuated the second phase of formalin-induced paw licking with equal potency. These results indicate that NK_1 antagonism is not responsible for the activity of (±)-CP-96,345 in the above animal models.

Keywords: CP-96,345; non-peptide NK_1 receptor antagonist; pain; inflammation

Introduction The discovery of non-peptide NK_1 receptor antagonist, CP-96,345 [(2S,3S)-*cis*-2-(diphenylmethyl)-N-[(2-methoxyphenyl)methyl)-1-azabicyclo[2.2.2]octan-3-amine] (Snider *et al.*, 1991) has been a major breakthrough in our ability to investigate the role of substance P (SP) and NK_1 receptor responses in a variety of *in vitro* and *in vivo* biological systems.

Recently, several investigators studied CP-96,345 in well-established models of pain and inflammation and implicated NK_1 receptor responses in mustard oil- (Lembeck *et al.*, 1992) and capsaicin-induced (Nagahisa *et al.*, 1992) neurogenic plasma extravasation in carrageenin-induced foot oedema and hyperalgesia (Birch *et al.*, 1992), and in formalin- (Birch *et al.*, 1992), acetic acid- (Nagahisa *et al.*, 1992) and hot plate- (Lecci *et al.*, 1991) induced nociceptive responses. However, a number of these studies were carried out using racemic (±)-CP-96,345 (Birch *et al.*, 1992; Lecci *et al.*, 1991).

In other pharmacological studies, CP-96,345 has been shown to lower blood pressure in intact anaesthetized dogs (Constantine *et al.*, 1992). Since CP-96,344, the **2R,3R** enantiomer of CP-96,345, which is not a SP antagonist, was equally potent, the hypotensive activity CP-96,345 seems to be unrelated to SP antagonism.

In order to ascertain that the previous observations made with racemic (±)-CP-96,345 are indeed due to NK_1 antagonism, we evaluated CP-96,345 and CP-96,344 in several models of pain and inflammation.

Methods *Binding studies* Binding experiments were conducted on brain and spinal cord membrane preparations from rat, essentially according to previously described procedures (Snider *et al.*, 1991). Briefly, tissue preprations (0.1–0.2 mg membrane protein per assay tube) were incubated with test compounds and radiolabelled SP (0.36 nM [^{125}I]-SP and 1 nM [^{3}H]-SP for brain and spinal cord, respectively) at 25°C for 1 h. Non-specific binding was determined in the presence of 1 μM SP.

Carrageenin-induced foot oedema and hyperalgesia in rat Male Sprague-Dawley rats (90–125 g) were used for all experiments. Rat foot inflammation was induced by subplantar injection of 0.1 ml of a 1% solution of carrageenin in saline. To determine the extent of oedema, volumes of the injected foot were measured at various time points with a water-displacement plethysmometer (model TK-101, Unicom). Hyperalgesia was assessed by measuring nociceptive pressure thresholds with an analgesymeter (Ugo Basile). CP-96,345 and CP-96,344 (dihydrochloride salts) were dissolved in 0.1% methyl cellulose-water or saline and given orally 60 min before or subcutaneously 30 min before the carrageenin injection, respectively. Results were compared against vehicle control.

Formalin-induced paw licking in rat Formalin-induced paw licking was induced by intraplantar injection with 50 μl of 5% formalin in saline (Dubuisson & Dennis, 1977). CP-96,345 and CP-96,344 were dissolved in methyl cellulose-saline and given s.c. 30 min before formalin injection. Animals were placed in 2 l clear beakers (1 per beaker) and duration of licking behaviour was determined for 15–25 min (for second phase).

Materials Dihydrochloride salts of CP-96,345 [(2S,3S)-*cis*-2-(diphenylmethyl)-N-[(2-methoxyphenyl)methyl)]-1-azabicyclo [2.2.2]octan-3-amine] and CP-96,344 [(2R,3R)-*cis*-2-(diphenylmethyl)-N-[(2-methoxyphenyl)methyl)]-1-azabicyclo[2.2.2] octan-3-amine] were synthesized in the Central Research Division, Pfizer Inc., as previously described (Lowe *et al.*, 1992). Carrageenin was purchased from Zushikagaku Laboratory Inc., Japan. Substance P was purchased from Peptide Institute, Japan, and [^{3}H]-SP and [^{125}I]-SP were from New England Nuclear. Male Sprague-Dawley rats were purchased from Oriental Yeast Company, Japan.

Results *Binding studies* CP-96,345 potently inhibited SP binding in membrane preparations from brain and spinal cord of rat with IC_{50} values (95% confidence limits) of 45 (8–81) and 160 (86–220) nM, respectively. The binding of CP-96,345 was stereospecific in that the **2R,3R** enantiomer, CP-96,344, was inactive up to 10 μM. The results are consistent with an earlier finding in which bovine caudate tissue was used (Snider *et al.*, 1991).

Carrageenin-induced foot oedema in rat Intraplantar injection of carrageenin caused a rapid increase in the paw volume, reaching a maximum 3 h after injection. Both CP-96,345 and CP-96,344, inhibited foot oedema in a dose-dependent manner, with statistically significant effects observed at 30 and 45 mg kg^{-1}, s.c. (62 and 93 μmol kg^{-1}) (Figure 1a). Essentially equivalent effects were observed when CP-96,345 and CP-96,344 were administered orally.

Carrageenin-induced hyperalgesia in rat Intraplantar injection of carrageenin caused a reduction in the nociceptive

[1] Author for correspondence.

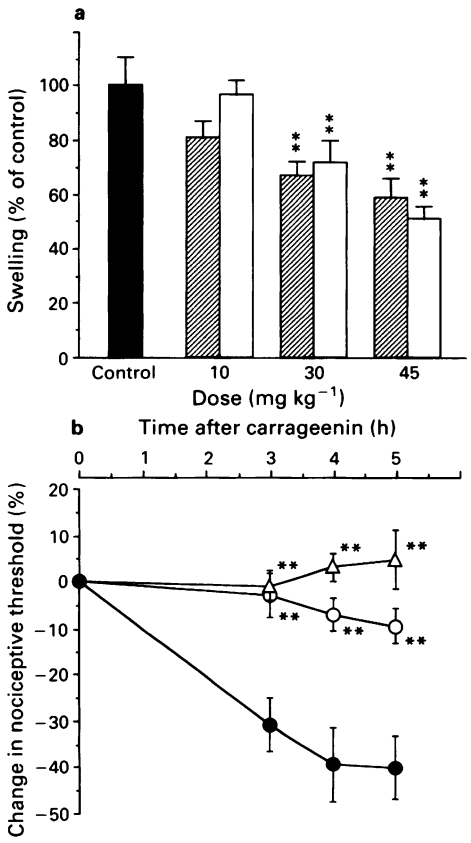

Figure 1 (a) Effects of CP-96,345 (hatched columns) and CP-96,344 (open columns) on carrageenin-induced foot oedema in rat. Solid column indicates vehicle-treated animals. The foot volumes were measured at 3 h after intraplantar injection of 1% carrageenin. Test compounds were given subcutaneously 30 min before carrageenin. Each column represents mean data from 5 animals; vertical lines show s.e.means. (b) Effects of CP-96,345 and CP-96,344 on carrageenin-induced hyperalgesia in rats. Symbols indicate animals treated with 45 mg kg^{-1} s.c. of CP-96,345 (○) and CP-96,344 (△) or vehicle control (●). Each point represents mean data from 8 animals; vertical lines show s.e.means. $^{**}P<0.01$ significantly different from vehicle control by 1-way ANOVA, Dunnett's test.

pressure threshold 3, 4 and 5 h after injection. CP-96,345 and CP-96,344 completely blocked the hyperalgesic response at 45 mg kg^{-1}, s.c. (Figure 1b).

Formalin-induced paw licking in rat Intraplantar injection of formalin caused a characteristic biphasic licking response. The duration of the second phase of the response was 217 ± 14 s (mean ± s.c.). CP-96,345 and CP-96,344 inhibited the second phase of the response in a dose-dependent fashion with equal potency. Statistically significant effects were observed at 30 and 45 mg kg^{-1} s.c. (Figure 2).

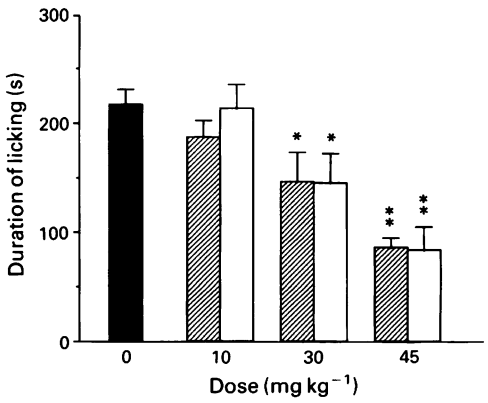

Figure 2 Effects of CP-96,345 (hatched columns) and CP-96,344 (open columns) on the second phase of the formalin-induced paw licking response in rats. Solid column indicates vehicle-treated animals. Each column represents mean data from 5–6 animals; vertical lines show s.e.means. $^{*}P<0.05$ and $^{**}P<0.01$ significantly different from vehicle control by 1-way ANOVA, Dunnett's test.

Discussion The racemic mixture of CP-96,345 has been reported to show antinociceptive and anti-oedema activity in the carrageenin-induced hyperalgesia and foot oedema models in the rat, as well as to inhibit the formalin-induced licking response in the rat (Birch *et al.*, 1992). Based on these results, it was suggested that SP is a mediator of the effects observed in these two well-characterized models of inflammation and pain. In our studies, CP-96,344, the **2R,3R** enantiomer of CP-96,345, which is inactive as an NK_1 antagonist ($IC_{50}>10\ \mu M$) in rat brain and spinal cord, reduced carrageenin-induced paw oedema and hyperalgesia, and attenuated the second phase of the formalin-induced paw licking response, with potency equal to CP-96,345. These results do not suggest a mediator role of SP in the above models.

In contrast, we have previously shown that CP-96,345 stereoselectivity inhibited mustard oil-induced rat foot oedema in rats and acetic acid-induced writhing in mice (Lembeck *et al.*, 1992; Nagahisa *et al.*, 1992). Thus, NK_1 receptor responses appear to play a role in these animal models of pain and inflammation.

Recently, both CP-96,345 and CP-96,344 have been shown to interact with Ca^{2+} channel binding sites (Schmidt *et al.*, 1992). In our hands, verapamil (30 mg kg^{-1} p.o.) inhibited carrageenin-induced rat foot oedema and hyperalgesia as well as the formalin-induced response (data not shown) suggesting that the Ca^{2+} antagonist activity might account for the non-specific pharmacological effects of CP-96,345 and CP-96,344.

We conclude that studies in which the racemic mixture of CP-96,345 are used may lead to erroneous conclusions.

The authors wish to thank Dr J.A. Lowe III, Dr R.M. Snider and Dr H.-J. Hess for helpful discussion.

References

BIRCH, P.J., HARRISON, S.M., HAYES, A.G., ROGERS, H. & TYERS, M.B. (1992). The non-peptide NK_1 receptor antagonist, (±)-CP-96,345, produces antinociceptive and anti-oedema effects in the rat. *Br. J. Pharmacol.*, **105**, 508–510.

CONSTANTINE, J.W., LEBEL, W.S. & WOODY, H.A. (1991). Inhibition of tachykinin-induced hypotension in dogs by CP-96,345, a selective blocker of NK-1 receptor. *Naunyn-Schmeidebergs Arch Pharmacol.*, **344**, 471–477.

DUBUISSON, D. & DENNIS, S.G. (1977). The formalin test: a quantitative study of the analgesic effects of morphine, meperidine, and brain stem stimulation in rats and cats. *Pain*, **4**, 161–174.

LECCI, A., GIULIANI, S., PATACCHINI, R., VITI, G. & MAGGI, C.A. (1991). Role of NK_1 tachykinin receptors in thermonociception: effect of (±)-CP-96,345, a non-peptide substance P antagonist, on the hot plate test in mice. *Neurosci. Lett.*, **129**, 299–302.

LEMBECK, F., DONNERER, J., TSUCHIYA, M. & NAGAHISA, A. (1992). The non-peptide tachykinin antagonist, CP-96,345, is a potent inhibitor of neurogenic inflammation. *Br. J. Pharmacol.*, **105**, 527–530.

LOWE, J.A., DROZDA, S.E., SNIDER, R.M., LONGO, K.P., ZORN, S.H., MORRONE, J., JACKSON, E.R., MCLEAN, S., BRYCE, D.K., BORDNER, J., NAGAHISA, A., KANAI, Y., SUGA, O. & TSUCHIYA, M. (1992). The discovery of (2S,3S)-cis-2-(diphenylmethyl)-N-(2-methoxyphenyl)methyl)-1-azabicyclo[2.2.2]octan-3-amine as a novel, nonpeptide substance P antagonist. *J. Med. Chem.*, **35**, 2591–2600.

NAGAHISA, A., KANAI, Y., SUGA, O., TANIGUCHI, K., TSUCHIYA, M., LOWE, J.A. & HESS, H.-J. (1992). Antiinflammatory and analgesic activity of a non-peptide substance P receptor antagonist. *Eur. J. Pharmacol.*, **217**, 191–195.

SCHMIDT, A.W., MCLEAN, S. & HEYM, J. (1992). The substance P receptor antagonist CP-96,345 interacts with Ca^{2+} channels. *Eur. J. Pharmacol.*, **215**, 351–352.

SNIDER, R.M., CONSTANTINE, J.W., LOWE, J.A., LONGO, K.P., LEBEL, W.S., WOODY, H.A., DROZDA, S.E., DESAI, M.C, VINICK, F.J., SPENCER, R.W. & HESS, H.-J. (1991). A potent nonpeptide antagonist of the substance P (NK_1) receptor. *Science*, **251**, 435–437.

(Received June 2, 1992
Accepted June 29, 1992)

Br. J. Pharmacol. (1992), **107**, 276–281

Characterization of histamine receptor sub-types regulating prostacyclin release from human endothelial cells

Helen A. Bull, P.F. Courtney, M.H.A. Rustin & [1]Pauline M. Dowd

Department of Dermatology and Academic Unit, The Department of Surgery, University College and Middlesex School of Medicine, London

1 The histamine receptor sub-types that are involved in the initiation and maintenance of prostacyclin (PGI_2) release from human endothelial cells have been investigated.

2 Endothelial cells cultured from umbilical vein (HUVEC) were incubated with either histamine, the selective H_1-receptor agonists, 2-methyl histamine (2-MeHA) or thiazolylethylamine (ThEA), the H_1-agonist/H_3-antagonist, β-histine (β-His), the selective H_2-agonist, dimaprit, the H_2-agonist/H_3-antagonist, impromidine, the selective H_3-agonist, (**R**)α-methylhistamine ((**R**)α-MeHA) and the H_3-antagonist, thioperamide.

3 The H_1-agonists and the H_3-agonist (**R**)α-MeHA induced a concentration (100 nM–1 mM) and time-dependent release of PGI_2 as determined by radioimmunoassay for 6-keto-$PGF_{1\alpha}$, but were less potent than histamine itself. The rank order of potency was the same following 30 min and 24 h incubation, i.e. histamine > ThEA > 2-MeHA >> β-His > (**R**)α-MeHA.

4 Histamine and 2-MeHA (1 μM–1 mM), ThHEA (10 μM–1 mM) and (**R**)α-MeHA (1 mM), but not β-His, induced a significantly greater increase in PGI_2 release after 24 h incubation than after 30 min incubation ($P < 0.05$).

5 Neither the selective H_2-agonist, dimaprit, nor the H_2-agonist/H_3-antagonist, impromidine alone induced release of PGI_2.

6 The H_1-antagonist, mepyramine (10 μM), abolished release of PGI_2 induced by histamine, the H_1-agonists and (**R**)α-MeHA but the H_2-antagonist cimetidine (10 μM) and the H_2/H_3-antagonist, burimamide (10 μM) did not significantly modulate PGI_2 release.

7 Although the H_3-agonist (**R**)α-MeHA induced release of PGI_2, it failed to modulate PGI_2 release in the presence of histamine.

8 Low concentrations of the H_3-antagonist, thioperamide (100 nM) did not modulate histamine release of PGI_2 at all but after 24 h incubation, thioperamide (10^{-4} M) partially reduced PGI_2 release in the presence of histamine.

9 These results indicate that PGI_2 from HUVEC is initiated and maintained via histamine H_1-receptor occupancy. There appears to be no involvement of either H_2- or H_3-receptors in this particular endothelial cell histaminergic response.

Keywords: Histamine receptors; endothelial cells; prostacyclin

Introduction

Histamine released from basophils, mast cells and nerve fibres, is a potent mediator of both local and systemic inflammatory and allergic reactions (Beaven, 1976). Although it has been shown to mediate plasma extravasation, leukocyte margination and increased vasodilatation, its mode of action on vascular endothelium is poorly understood.

Stimulation of cultured endothelial cells with histamine induces release of prostaglandins (Baenziger *et al.*, 1980). In human umbilical vein endothelial cells (HUVEC), histamine induces rapid release of prostacyclin (PGI_2)(Alhenc-Gelas *et al.*, 1982). This release is inhibited by the classic histamine H_1-antagonist, mepyramine and by the dihydropyridine calcium channel antagonist, nifedipine (Bull & Dowd, 1990). Endothelial cells are reported to show tachyphylaxis to repeated stimulation with histamine, the return of PGI_2 synthesizing capacity being dependent on the clearance and metabolism of histamine by serum-derived diamine oxidases (Haddock *et al.*, 1987). In contrast to histamine, release of PGI_2 from HUVEC incubated with the cytokine interleukin-1 (IL-1) is characterized by a delayed onset of 4–6 h but thereafter is continuous up to 48 h so long as the agonist is present (Rustin *et al.*, 1989). In the light of these results we examined the response of HUVEC to prolonged exposure to histamine and the results of our initial experiments demonstrated that, in the absence of serum, histamine induced release of PGI_2 was biphasic. The initial rapid release of PGI_2 was followed by a lag phase of 2 h, after which time release of PGI_2 began again and continued up to 24 h (Bull *et al.*, 1989). The mechanisms underlying this biphasic response are at present unclear. The initial response to histamine appears to be facilitated by histamine H_1-receptor occupancy as the H_1-receptor antagonsit, mepyramine, blocks PGI_2 release. However, studies on human cerebral arteries have demonstrated that vasodilatation is mediated by both H_1- and H_2-receptors (Ottosson *et al.*, 1988) and following brachial artery infusions in man, increased forearm blood was initiated by histamine H_1 receptor occupancy and maintained by H_1- and H_2-receptor occupancy (Chipman & Glover, 1976).

Recently, a third class of histamine receptor has been described on cerebral cortex (Arrang *et al.*, 1983) and peripheral nerve terminals (Ishikawa & Sperelakis, 1987) which mediates histamine regulation of its own synthesis and release. The existence of this histamine H_3-receptor sub-type on cells that respond to exogenous histamine has not been

[1] Author for correspondence at: Department of Dermatology, The Middlesex Hospital, Mortimer Street, London W1N 8AA.

investigated.

The involvement of receptor sub-classes in pharmacological responses is determined by the use of specific receptor agonists and antagonists. The development of a histamine H_3-receptor agonist and antagonist (Arrang *et al.*, 1987) in addition to the already available H_1- and H_2-receptor agonists and antagonists, have made it possible to determine the role of histamine receptor sub-types in human endothelial cell responses to histamine.

We have therefore sought to characterize the receptor subtypes that initiate and maintain histamine release of PGI_2 from human endothelial cells.

A preliminary account of this work was presented at the annual meeting of The British Society for Investigative Dermatology, Newcastle upon Tyne, September 17–18, 1990.

Methods

Endothelial cell culture

Human endothelial cells were harvested from umbilical cord veins and cultured as previously described (Bull *et al.*, 1988). Umbilical cords were collected immediately following delivery and placed in Hanks balanced salt solution (HBSS). Only untraumatized sections were used. The vein was cannulated and flushed with sterile HBSS until the effluent ran clear of red blood cells. At this stage, collagenase (type 1 CLS *Clostridium histolyticum*) (0.1% w/v final concentration) was prepared in HBSS. The vein was filled with collagenase solution, both ends sealed and the cord was incubated for 20 min at 37°C. At the end of the incubation period, the contents of the vein were flushed out with culture medium 199 (M199) containing 100 u ml^{-1} penicillin, 100 $\mu g\ ml^{-1}$ streptomycin, 50 $\mu g\ ml^{-1}$ amphotericin B and 2 mM glutamine. The cells were centrifuged at 200 *g* for 5 min, resuspended in complete culture medium consisting of M199 supplemented with 20% pooled human serum and plated out in 25 cm^2 culture flasks. The endothelial cell nature of the cultured cells was confirmed by positive staining for von Willebrand Factor protein (Wagner *et al.*, 1982). In these experiments, 1st passage cultures grown in 24 well culture dishes were used and each individual experiment was performed using endothelial cells cultured from a separate umbilical cord.

Agonist-induced release of prostacyclin from endothelial cells

Confluent monolayers of endothelial cells grown in 24 well culture plates were washed once with M199 alone. Each well of endothelial cells was then overlayed with 500 µl of M199 containing the different histamine receptor agonists at concentrations of 100 nM to 1 mM. The cells were incubated at 37°C in 5% CO_2/95% humidified air for up to 24 h and then the supernatants were removed from individual wells and frozen at − 20°C for subsequent radioimmunoassay (RIA) of 6-keto-prostaglandin $F_{1\alpha}$ (6-keto-$PGF_{1\alpha}$). At the end of each experiment, the endothelial cells were trypsinized (0.25% w/v trypsin in calcium and magnesium free HBSS) and counted manually in an improved Neubauer Chamber (Weber, UK). Concentrations of 6-keto-$PGF_{1\alpha}$ were expressed as ng per 10^4 cells.

The effect of specific antagonists on prostacyclin release from endothelial cells

The concentrations of antagonists used in these experiments did not stimulate PGI_2 release following 24 h incubation with cells alone.

Prostacyclin assay

PGI_2 levels were measured with a radioimmunoassay (RIA) for 6-keto-$PGF_{1\alpha}$ (the stable hydrolysis product of PGI_2) as previously described (Bull *et al.*, 1988). Briefly, each assay tube contained 50 µl of endothelial cell supernatant, 3,000 c.p.m. [^{3}H]-6-keto-$PGF_{1\alpha}$ in 50 µl assay buffer (0.07 M NaCl, 0.07 M PO_4, pH 7.4) and 50 µl of antiserum. The standard curve covered the range 3.9 pg to 1 ng of 6-keto-$PGF_{1\alpha}$. The assay tubes were incubated overnight at 4°C and the bound tritiated 6-keto-$PGF_{1\alpha}$ was separated from unbound by dextran charcoal precipitation; 200 µl of supernatant was counted in 2 ml of Ecoscint scintillation fluid (National Diagnostics). The 6-keto-$PGF_{1\alpha}$ antiserum exhibited cross-reactivity of less than 1% with other major prostaglandins of the 1 and 2 series and the limit of sensitivity of the assay was 5 pg. The inter-assay and intra-assay coefficients of variation for the 6-keto-$PGF_{1\alpha}$ radioimmunoassay were 7.56 ($n = 10$) and 3.88 ($4 = 10$) respectively.

The cell supernatants were assayed without prior extraction and measurements were made at two dilutions.

Analysis of data

The results have been corrected for basal release of PGI_2 from unstimulated HUVEC following both 30 min and 24 h incubation. They are expressed as mean ± s.e.mean % 6-keto-$PGF_{1\alpha}$ released relative to release induced by 100 µM histamine, which was included in all experiments as a positive control. The data were analysed by Student's *t* test for paired data; agonist-induced release of PGI_2 after 30 min incubation was compared to basal release after 30 min and agonist-induced release of PGI_2 after 24 h incubation was compared to agonist-induced release of PGI_2 after 30 min. The effects of the different antagonists on agonist-induced PGI_2 release were compared to agonist-induced release of PGI_2 alone after 30 min and 24 h incubation. $P < 0.05$ was considered to be statistically significant.

Materials

Culture medium and antibodies were obtained from Gibco, Paisley, UK. Histamine was obtained from Sigma Chemical Co., Poole, UK and collagenase from Cambridge Biochemicals, UK.

The histamine receptor agonists 2-methylhistamine (2MeHA), beta-histine (β,His), thiazolethylamine (ThEA), impromidine and dimaprit and the receptor antagonists mepyramine, burimamide and cimetidine were a generous gift from Dr Parsons, Smith Kline and French, Welwyn, UK. The H_3-receptor agonist, (R)α-methylhistamine ((R)α-MeHA) and the H_3-receptor antagonist, thioperimide were generous gifts from Prof. Schwartz and Dr Arrang, Centre Paul Borca de l'INSERM, Paris, France.

The 6-keto-$PGF_{1\alpha}$ antiserum was a gift from Dr M. Greaves, Royal Hallamshire Hospital, Sheffield, UK and the 6-keto-$PGF_{1\alpha}$ standard was obtained from Cayman Chemicals, U.S.A. and the tritiated compound from Amersham p.l.c., UK.

Results

PGI_2 was released in a concentration (100 nM–1 mM) and time-dependent manner from HUVEC incubated with either histamine, the selective H_1 receptor agonists ThEA and 2-MeHA or the H_1-receptor agonist/H_3-receptor antagonist, β-His, although the receptor agonists were less potent than histamine itself (Figure 1). The rank order of potency was histamine > ThEA > 2-MeHA >> β-His and was the same after both 30 min or 24 h incubation (Table 1). In HUVEC incubated for 30 min with histamine (1 µM–1 mM), 2-MeHA

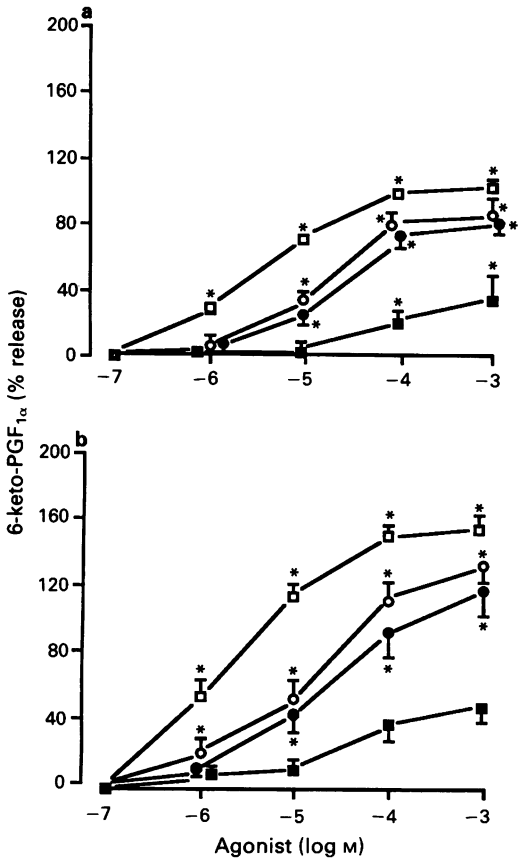

Figure 1 Histamine H_1-receptor agonists induced the release of prostacyclin (PGI_2) from human umbilical vein endothelial cells (HUVEC) incubated with either histamine (□) or the H_1-receptor agonists, thiazolylethylamine (○), 2-methylhistamine (●) and β-histine (■) (100 nM–1 mM) for (a) 30 min or (b) 24 h. Results are expressed as the mean of 8–16 experiments and the vertical bars represent s.e.mean.
*$P < 0.05$ indicates a significant increase in agonist-induced PGI_2 release compared to basal release in (a) and compared to release after 30 min in (b).

Table 1 Concentrations of histamine agonists eliciting half maximal release of prostacyclin (PGI_2) from human umbilical vein endothelial cells (HUVEC) following 30 min or 24 h incubation

	30 min	*24 h*
Histamine	$3.62 \pm 0.47 \times 10^{-6}$ M	$3.24 \pm 0.63 \times 10^{-6}$ M
ThEA	$1.16 \pm 0.21 \times 10^{-5}$ M	$7.62 \pm 1.53 \times 10^{-6}$ M
2-MeHA	$2.21 \pm 0.56 \times 10^{-5}$ M	$1.05 \pm 0.54 \times 10^{-5}$ M
β-His	$6.80 \pm 3.20 \times 10^{-5}$ M	$4.57 \pm 1.65 \times 10^{-5}$ M
(R)α-MeHA	$1.15 \pm 0.33 \times 10^{-4}$ M	$6.61 \pm 2.08 \times 10^{-5}$ M

ThEA, thiazolylethylamine; 2-MeHA, 2-methylhistamine; β-His, β-histine; (R)α-MeHA, Rα-methylhistamine.

(10 μM–1 μM), ThEA (1 μM–1 mM) and β-His (1 mM), PGI_2 release was significantly increased over basal release. In cells incubated with either histamine, 2-MeHA (1 μM–1 mM) or ThEA (10 μM–1 mM), there was a significantly greater increase in PGI_2 release after 24 h incubation compared with release after 30 min. However, β-His did not significantly increase PGI_2 release between 30 min and 24 h incubation.

The selective H_2-agonist, dimaprit and the H_2-agonist/H_3-antagonist, impromidine (1 μM–1 mM) failed to induce release of PGI_2 following either 30 min or 24 h incubation ($n = 3$, data not shown).

Having identified those agonists that induced release of PGI_2 from HUVEC following 30 min incubation and a significant increase in release between 30 min and 24 h, we then undertook experiments to establish whether they were acting solely through the H_1-receptor.

The dose-dependent release of PGI_2 from HUVEC incubated with increasing concentrations of 2-MeHA was abolished by the H_1-receptor antagonist, mepyramine (10 μM) (Figure 2). Neither the H_2-receptor antagonist, cimetidine (10 μM) nor the H_2-/H_3-receptor antagonist, burimamide (10 μM) significantly modulated PGI_2 release following either 30 min or 24 h incubation.

Mepyramine (10 μM) also abolished the concentration-dependent release of PGI_2 from HUVEC incubated with ThEA (Figure 3). However, neither cimetidine (10 μM) nor burimamide (10 μM) modulated PGI_2 release from HUVEC following either 30 min or 24 h incubation.

Release of PGI_2 induced by β-His was abolished by co-incubation with mepyramine (10 μM) but neither cimetidine (10 μM) nor burimamide (10 μM) significantly modulated PGI_2 release, as shown in Figure 4.

The H_3-receptor agonsit (R)α-MeHA induced a concentration dependent release of PGI_2 from HUVEC following 30 min and 24 h incubation (Figure 5). There was a significantly greater increase in PGI_2 release over 24 h compared to 30 min in HUVEC incubated with 1 mM (R)α-

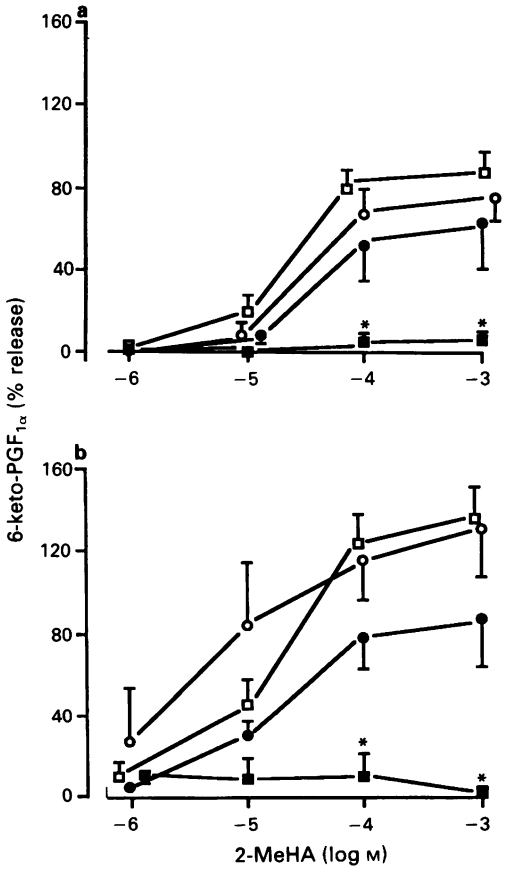

Figure 2 The effect of histamine receptor antagonists on prostacyclin (PGI_2) release induced by 2-methylhistamine (2-MeHA). HUVEC were incubated with 2-MeHA (1 μM–1 mM) alone (□) or in the presence of mepyramine (■), cimetidine (●) or burimamide (○) (each 10 μM) for either (a) 30 min or (b) 24 h. Results are expressed as the mean of 4 experiments and the vertical bars represent s.e.mean.
*$P < 0.05$ denotes significant inhibition of PGI_2 release at each timepoint.

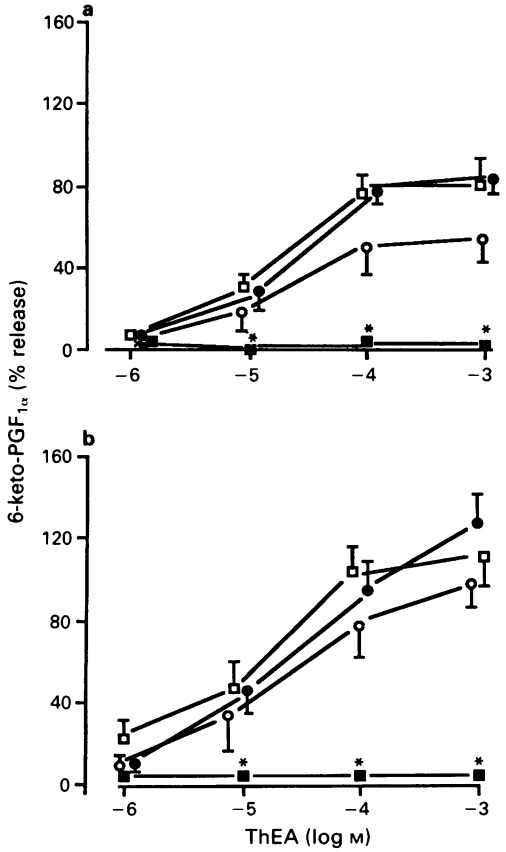

Figure 3 The effect of histamine receptor antagonists on prostacyclin (PGI_2) release induced by thiazolylethylamine (ThEA). HUVEC were incubated with ThEA (1 μM–1 mM) alone (□) or in the presence of mepyramine (■), cimetidine (●) or burimamide (○) (each 10 μM) for either (a) 30 min or (b) 24 h. Results are expressed as the mean of 4 experiments and the vertical bars represent s.e.mean.
*$P < 0.05$ denotes significant inhibition of PGI_2 release at each timepoint.

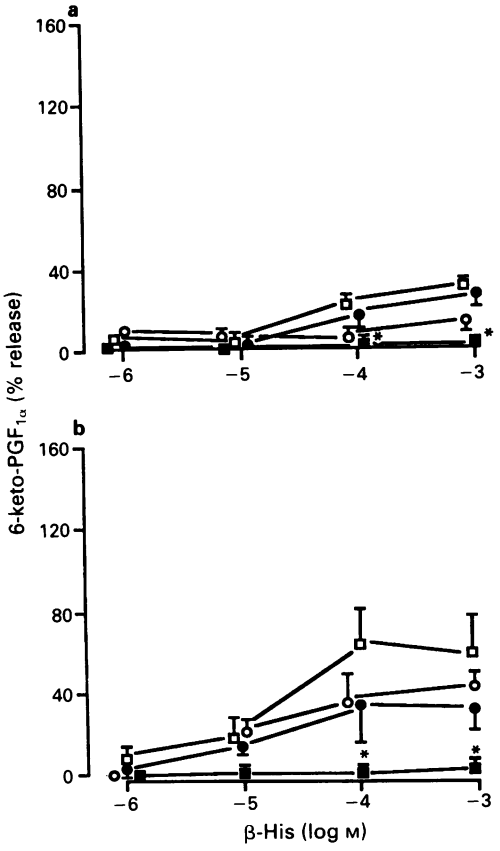

Figure 4 The effect of histamine receptor antagonists on prostacyclin (PGI_2) release induced by β-histine (β-His). HUVEC were incubated with β-His (1 μM–1 mM) alone (□) or in the presence of mepyramine (■), cimetidine (●) or burimamide (○) (each 10 μM) for either (a) 30 min or (b) 24 h. Results are expressed as the mean of 4 experiments and the vertical bars represent s.e.mean.
*$P < 0.05$ denotes significant inhibition of PGI_2 release at each timepoint.

MeHA but not with lower concentrations. In HUVEC co-incubated with (R)α-MeHA (1 μM or 1 mM) and histamine (100 nM–1 mM) for either 30 min or 24 h, no further significant change in PGI_2 release was observed. PGI_2 release induced by (R)α-MeHA (10 μM– 1 mM) was abolished by the H_1-antagonist, mepyramine (1 μM–10 μM) following both 30 min and 24 h incubation (Figure 6).

The H_3 receptor antagonist, thioperamide (100 nM–1 mM) failed to induce PGI_2 release (Figure 7). Thioperamide (100 nM) did not modulate histamine-induced release of PGI_2 after either 30 min or 24 h incubation but thioperamide (100 μM) partially blocked the increase in PGI_2 release following 24 h incubation whilst having no effect on PGI_2 release after 30 min incubation.

Discussion

Exposure of HUVEC to histamine induces the release of the potent vasodilator, PGI_2, in a time- and concentration-dependent manner. The present studies have demonstrated that the response of HUVEC to histamine following both 30 min and 24 h incubation is mimicked by the selective H_1-agonists ThEA and 2-MeHA and that the response of HUVEC to these agonists is blocked by the H_1-antagonist, mepyramine. The lack of effect of the selective H_2-agonist, dimaprit and the H_2-/H_3-antagonist, impromidine on PGI_2 release from HUVEC demonstrates that PGI_2 release is not initiated via the H_2-receptor sub-type in these cells. Both 2-MeHA and ThEA have weak H_2-receptor activity (Ganellin, 1982) and occupancy of H_2-receptors may potentiate the response initiated via the H_1-receptor as indicated in other vascular beds (Ottosson *et al.*, 1988). However, neither of the H_2-receptor antagonists, burimamide or cimetidine, significantly altered the dose-response curves of PGI_2 release from HUVEC incubated with either 2-MeHA or ThEA indicating that H_2-receptor occupancy does not modulate the response initiated via the H_1-receptor in these cells.

The third H_1-agonist used in these studies, β-His, was found to be a poor agonist for PGI_2 release and did not induce a significantly greater increase in PGI_2 release after 24 h compared to release after 30 min. The reason for this is unclear. However, β-His is only a weak H_1-agonist and there is evidence to indicate that it is also an H_3-antagonist in brain. The selective H_3-agonist, (R)α-MeHA induced a concentration-dependent release of PGI_2 from HUVEC that was significantly greater after 24 h than after 30 min incubation in cells incubated with 1 mM (R)α-MeHA. In HUVEC incubated with (R)α-MeHA and histamine, the dose-response curve for PGI_2 release was not significantly different from that for PGI_2 release from HUVEC incubated with histamine alone. The lack of any synergistic or additive effect of 1 mM (R)α-MeHA on histamine-induced PGI_2 release from HUVEC indicates that (R)α-MeHA may have some action on H_1-receptors in these cells. This was confirmed by the observation that mepyramine blocked (R)α-MeHA-induced release of PGI_2.

In contrast to (R)-α-MeHA, the H_3-receptor antagonist, thioperamide, failed to induce release of PGI_2 from HUVEC.

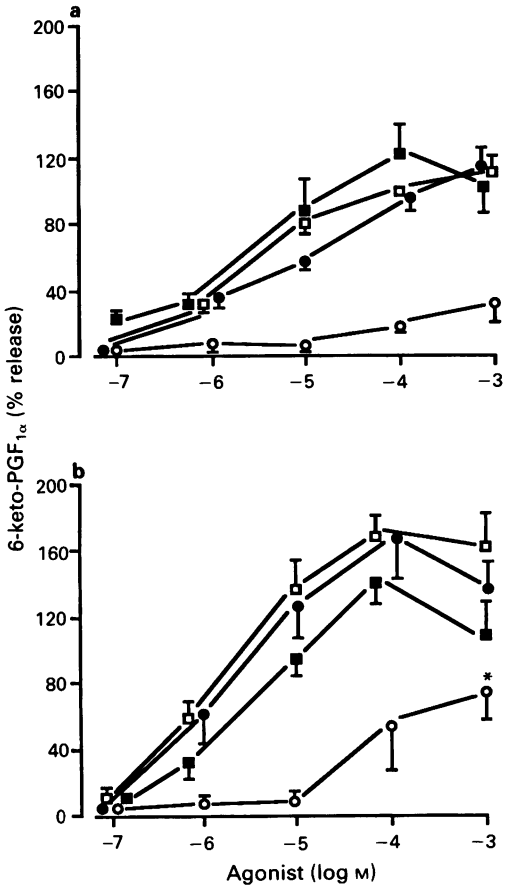

Figure 5 (R)α-methylhistamine ((R)α-MeHA) modulation of histamine-induced prostacyclin (PGI_2) release. HUVEC were incubated with (R)α-MeHA (1 μM–1 mM) alone (○), histamine (1 μM–1 mM) alone (□) or histamine (1 μM–1 mM) in the presence of (R)α-MeHA (1 μM) (●) or (R)α-MeHA (1 mM) (■) for (a) 30 min or (b) 24 h. Results are expressed as the mean of 4 experiments and the vertical bars represent s.e.mean.
*$P < 0.05$ indicates a significant increase in agonist-induced PGI_2 release compared to basal release in (a) and compared to release after 30 min in (b).

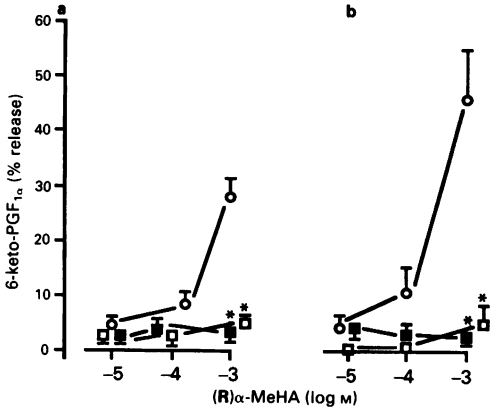

Figure 6 Mepyyramine modulation of (R)α-methylhistamine ((R)α-MeHA)-induced prostacyclin (PGI_2) release. HUVEC were incubated with (R)α-MeHA (10 μM–1 mM) alone (○) or in the presence of mepyramine 1 μM (□) or 10 μM (■) for either (a) 30 min or (b) 24 h. Results are expressed as the mean of 3 experiments and the vertical bars represent s.e.mean.
*$P < 0.05$ denotes significant inhibition of PGI_2 release at each timepoint.

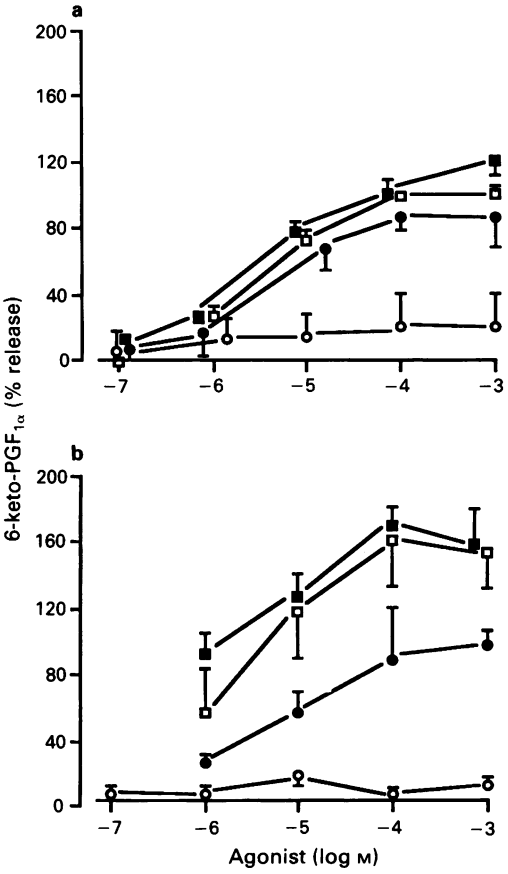

Figure 7 Thioperamide modulation of histamine induced prostacyclin (PGI_2) release. HUVEC were incubated with thioperamide (100 nM–1 mM) alone (○), histamine (1 μM–1 mM) alone (□) or histamine (1 μM–1 mM) in the presence of thioperamide (100 nM) (■) or thioperamide (100 μM)) (●) for either (a) 30 min or (b) 24 h. Results are expressed as the mean of 4 experiments and the vertical bars represent s.e.mean.

Furthermore, at concentrations that Arrang *et al.* (1987) found to be efficacious in their experiments (100 nM), thioperamide did not modulate histamine-induced release of PGI_2. At the higher concentration (100 μM), thioperamide had no effect on histamine-induced PGI_2 release after 30 min but did partially reduce the increase over 24 h. The mechanism of this effect is unclear; concentrations of thioperamide greater than 100 μM have been demonstrated to compete with [^{3}H]-mepyramine binding to H_1-receptors in membranes of guinea-pig cerebellum (Arrang *et al.*, 1987) and similar binding may occur in HUVEC.

In conclusion therefore, the results of these experiments demonstrate that PGI_2 release from HUVEC is initiated and maintained via histamine H_1-receptor occupancy. There appears to be no involvement of either H_2- or H_3-receptors in this response. Whether this is because HUVEC do not possess either of these histamine receptor sub-types or solely because they are not involved in release of PGI_2 is not known. Only with the successful cloning of all of the different histamine receptor sub-types will definitive proof of cell and tissue distribution of these receptors become available.

H.A.B. is supported by a grant from The Sir Jules Thorn Charitable Trust. P.F.C. was supported by a grant from The National Eczema Society, U.K. We would like to thank Prof. Schwartz and Dr Arrang, Centre Paul Broca de l'INSERM, Paris, France for providing the H_3-receptor agonist (R)α-methylhistamine ((R)α-MeHA) and the H_3-receptor, antagonist, thioperamide and Dr Parsons, Smith Kline and French, Welwyn, UK for providing the histamine receptor agonists, 2-methylhistamine (2MeHA), beta-histine (β-His). thiazolylethylamine (ThEA), impromidine and dimaprit and the receptor antagonists, mepyramine, burimamide and cimetidine.

References

ALHENC-GELAS, F., TSAI, S.J., CALLAHAN, K.S., CAMPBELL, W.B. & JOHNSON, A.R. (1982). Stimulation of prostaglandin formation by vasoactive mediators in cultured human endothelial cells. *Prostaglandins*, **24**, 723–740.

ARRANG, J.-M., GARBARG, M., LANCELOT, J.-C., LECOMTE, J.-M., POLLARD, H., ROBBA M., SCHUNACK, W. & SCHWARTZ, J.-C. (1987). Highly potent and selective ligands for histamine H_3-receptors. *Nature*, **327**, 117–123.

ARRANGE, J.-M., GARBARG, M. & SCHWARTZ, J.-C. (1983). Auto-inhibition of brain histamine release mediated by a novel class (H_3) of histamine receptor. *Nature*, **302**, 832–837.

BAENZIGER, N.L., FORCE, L.E. & BECHNER, P.R. (1980). Histamine stimulates prostacyclin synthesis in cultured human umbilical vein endothelial cells. *Biochem. Biophys. Res. Commun.*, **92**, 1435–1440.

BEAVEN, M.A. (1976). Histamine. *N. Engl. J. Med.*, **294**, 30–36, 320–325.

BULL, H.A. & DOWD, P.M. (1990). Interleukin-1 potentiates histamine-induced release of prostacyclin from human endothelial cells. *Br. J. Pharmacol.*, **101**, 703–709.

BULL, H.A., PITTILO, R.M., WOOLF, N. & MACHIN, S.J. (1988). The effect of nicotine on human endothelial cell release of prostaglandins and morphology. *Br. J. Exp. Pathol.*, **69**, 413–422.

BULL, H.A., RUSTIN, M.H.A. & DOWD, P.M. (1989). Release of prostacyclin from cultured human endothelial cells following prolonged exposure to histamine. *Br. J. Dermatol.*, **120**, 757–766.

CHIPMAN, P. & GLOVER, W.E. (1976). Histamine H_2 receptors in the human peripheral circulation. *Br. J. Pharmacol.*, **56**, 494–496.

GANELLIN, C.R. (1982). Chemistry and structure activity relationships of drugs acting at histamine receptors. In *Pharmacology of Histamine Receptors*. ed. Ganellin, C.R. & Parsons, M.E. pp. 10–102. Bristol: John Wright & Songs Ltd.

HADDOCK, R.C., MACK, P., FOGERTY, F.J. & BAENZIGER, N.L. (1987). Role of receptors in metabolic interaction of histamine with vascular endothelial cells and skin fibroblasts. *J. Biol. Chem.*, **262**, 10220–10228.

ISHIKAWA, S. & SPERELAKIS, N. (1987). A novel class (H_3) of histamine receptors on perivascular nerve terminals. *Nature*, **327**, 158–160.

OTTOSSON, A., JANSEN, I. & EDVINSSON, L. (1988). Characterisation of histamine receptors in isolated human cerebral arteries. *Br. J. Pharmacol.*, **94**, 901–907.

RUSTIN, M.H.A., BULL, H.A. & DOWD, P.M. (1989). The effect of human recombinant interleukin 1α on release of prostacyclin from human endothelial cells. *Br. J. Dermatol.*, **120**, 153–160.

WAGNER, D.D., OLMSTED, J.B. & MARDER, V.J. (1982). Immunolocalization of von Willebrand protein in Weibel-Palade bodies of human endothelial cells. *J. Cell. Biol.*, **95**, 355–360.

(Received June 19, 1991
Revised March 15, 1992
Accepted May 22, 1992)

Br. J. Pharmacol. (1992), **107**, 282–287

Participation of protein kinase C in endothelin-1-induced contraction in rat aorta: studies with a new tool, calphostin C

[1] Hiroyuki Shimamoto, [2] Yoriko Shimamoto, Chiu-Yin Kwan & Edwin E. Daniel

Smooth Muscle Research Program, Division of Physiology and Pharmacology, Department of Biomedical Sciences, Faculty of Health Sciences, McMaster University, 1200 Main Street West, Hamilton, Ontario, Canada L8N 3Z5

1 Calphostin C at 10^{-6} M was shown to be selective and highly effective in inhibiting contractile responses of rat aortae to 12-*o*-tetradecanoylphorbol-13-acetate, while it had no effect on contractile responses to elevated KCl.

2 In the rat aorta, endothelin-1 (ET-1) developed a sustained tonic contraction dose-dependently in both normal Ca^{2+}-containing Krebs and Ca^{2+}-free Krebs containing 1 mM EGTA. Calphostin C (10^{-6} M), a selective protein kinase C inhibitor, antagonized the maximal tensions for cumulative addition of 10^{-8} M ET-1 by 13.2% in Ca^{2+}-containing medium and 25.8% in Ca^{2+}-free Krebs containing 1 mM EGTA.

3 In both Ca^{2+}-containing medium and Ca^{2+}-free Krebs containing 1 mM EGTA, precontraction with 10^{-8} M ET-1 had no effects on the contractile response to subsequently added 10^{-6} M 12-*o*-tetradecanoylphorbol-13-acetate (TPA), an activator of protein kinase C.

4 In Ca^{2+}-free Krebs containing 1 mM EGTA, precontraction with 10^{-6} M TPA potentiated the contractile response to subsequently added 10^{-8} M ET-1, whereas this potentiation was abolished by pretreatment with 10^{-6} M calphostin C. The mechanism of the TPA-induced potentiating effect remains to be determined.

5 These results suggest that the participation of protein kinase C in the 10^{-8} M ET-1-induced contraction may be 13.2% and 25.8% in the presence and absence of extracellular Ca^{2+}, respectively, and that mechanisms other than protein kinase C may be predominantly responsible for ET-1-induced tonic contraction.

Keywords: Endothelin-1; protein kinase C; phorbol ester; 12-*o*-tetradecanoylphorbol-13-acetate; calphostin C; rat aorta; smooth muscle (vascular)

Introduction

Endothelin-1 (ET-1) which is a 21 amino acid peptide isolated from the culture medium of porcine aortic endothelial cells (Yanagisawa *et al.*, 1988), induces a potent and prolonged vasoconstrictor response in isolated vascular tissue. Although there is a variability in the dependence of the constrictive effect of ET-1 on the extracellular Ca^{2+} concentration, influx of extracellular Ca^{2+} is necessary for the full expression of the contractile responses to ET-1. ET-1-induced Ca^{2+} mobilization consists of two components, one dependent on Ca^{2+} influx and the other dependent on the utilization of intracellular Ca^{2+} (Chabrier *et al.*, 1989; Ohlstein *et al.*, 1989; Bolger *et al.*, 1990; Deng & Schiffrin, 1991). ET-1 induces a slowly-developing and sustained contraction in normal Ca^{2+}-containing Krebs. On the other hand, under experimental conditions where Ca^{2+} is depleted such as pretreatment with caffeine and histamine/or noradrenaline in Ca^{2+}-free buffer containing EGTA in the rat aorta (Itoh *et al.*, 1991) or porcine coronary artery (Kodama *et al.*, 1989), the contractile response to ET-1 is markedly reduced, but still present.

It has been proposed that activation of protein kinase C may be involved in the sustained component of the ET-1-induced contraction (Chabrier *et al.*, 1989; Ohlstein *et al.*, 1989). However, there have been contradictory reports on the participation of protein kinase C in the vasoconstrictor effects of ET-1 in Ca^{2+}-free buffer (Kodama *et al.*, 1989; Itoh *et al.*, 1991), which is, at least in part, due to lack of specific protein kinase C inhibitors (Rüegg & Burgess, 1989). Recently, it has been shown that calphostin C which is produced by *Cladosporium cladosporioides* (Kobayashi *et al.*, 1989a) inhibits protein kinase C activity more effectively and more selectively than other protein kinase C inhibitors do, suggesting that calphostin C is a potent as well as a more selective inhibitor of protein kinase C (Kobayashi *et al.*, 1989b).

In this study, in order to assess the participation of protein kinase C in the ET-1-induced contraction, we have examined the effect of calphostin C on the ET-1-induced contraction and the interactions between contractile responses to ET-1 and 12-*o*-tetradecanoylphorbol-13-acetate (TPA), a typical protein kinase C activator.

Methods

Isolated tissues

Male Wistar rats (250–300 g, body weight) were killed by cervical dislocation. Descending aortae were isolated rapidly and placed in normal Krebs solution containing (mM) NaCl 115.5, KCl 4.6, $CaCl_2$ 2.5, $MgSO_4$ 1.2, NaH_2PO_4 1.2, $NaHCO_3$ 21.9 and glucose 11.0 (pH 7.4–7.5). Fat and connective tissues were removed and 3 mm rings were mounted in 9 ml- or 3 ml-organ baths connected to a force transducer (Grass FT03C) and a pen recorder (Gould 2800). The vascular endothelium was removed by gently rubbing the intimal surface of the aorta with a wooden stick. The removal of endothelium was confirmed in some tissues by assessing whether 10^{-6} M acetylcholine could relax the aorta when

[1] Visiting scientist from the First Department of Internal Medicine, Hiroshima University School of Medicine, Hiroshima, Japan and author for correspondence at the above (Canadian) address.
[2] Visiting scientist from Nakamura Hospital, Hiroshima, Japan.

precontracted with 10^{-7} M phenylephrine. Tissue baths were warmed to 37°C, and bubbled with 95%O_2/5%CO_2. The rings were equilibrated for 20 min before stretching the vascular tissues to approximately 2 g. Then, aortic rings were allowed to equilibrate for 120 min before starting the experiments. Tension was recorded isometrically.

Subsequently, stimulation of the aortic rings with 60 mM KCl was repeated every 30 min until a reproducible contraction was obtained. All subsequent contractile responses in each vessel were expressed as a percentage of the last contractile response to 60 mM KCl in the rat aorta. For Ca^{2+}-free Krebs, Ca^{2+} was omitted from the Krebs solution and 1 mM EGTA was added.

Contractility studies

After a period of equilibration with KCl stimulation, concentration-response curves for ET-1 in normal Ca^{2+}-containing Krebs and Ca^{2+}-free Krebs containing 1 mM EGTA were obtained by cumulative addition to the organ bath in 0.5 log dose increments. In these curves, the maximal contraction was attained by 10^{-8} M ET-1.

The effect of calphostin C, a selective protein kinase C inhibitor, on ET-1-induced concentration-response curves was assessed in normal Ca^{2+}-containing Krebs and Ca^{2+}-free Krebs containing 1 mM EGTA. Tissues were incubated for 1 h in calphostin C-containing medium. In our preliminary study using the rat aorta, contractile responses to 10^{-6} M TPA or 60 mM KCl were obtained in the absence and presence of 3×10^{-7} M, 10^{-6} M and 3×10^{-6} M calphostin C. Calphostin C (3×10^{-7} M) inhibited the maximal tension of 10^{-6} M TPA-induced contraction by 53.3 ± 10.9% ($P<0.01$). Contractile responses to 10^{-6} M TPA were completely inhibited by 10^{-6} M calphostin C ($P<0.01$), whereas 10^{-6} M calphostin C had no effect on 60 mM KCl-induced contraction. Calphostin C (3×10^{-6} M) abolished 10^{-6} M TPA-induced contraction ($P<0.01$), but it also reduced contractile responses to 60 mM KCl ($P<0.05$) (Figure 1). Because protein kianse C apparently does not participate in KCl-induced contraction (Takuwa *et al.*, 1988; Haller *et al.*, 1990), 10^{-6} M calphostin C appeared to be the appropriate concentration. In this study, therefore, we used 10^{-6} M calphostin C as a selective protein kinase C inhibitor. In either normal Krebs or Ca^{2+}-free Krebs containing 1 mM EGTA, cumulative concentration-response curves for ET-1 were obtained in the absence and presence of 10^{-6} M calphostin C.

The relationship between ET-1- and TPA-induced contractions was investigated in normal Ca^{2+}-containing Krebs and Ca^{2+}-free Krebs containing 1 mM EGTA. In normal Krebs, after ET-1-induced contractions had developed, they slowly reversed to a level less than 20% of the contraction to 60 mM KCl. Then 10^{-6} M TPA was applied to these ET-1-desensitized tissues. In the Ca^{2+}-free medium, aortic rings were challenged with 10^{-8} M ET-1 at the zenith of 10^{-6} M TPA-pretreated contractions. Furthermore, when the 10^{-8} M ET-1-induced contraction was maximal, 10^{-6} M TPA was added to the tissue bath. In the presence of 10^{-6} M calphostin C, the same experimental procedures were repeated in both Ca^{2+}-containing medium and Ca^{2+}-free Krebs containing 1 mM EGTA. The agonist-induced increase in tension of aortic strips precontracted with 10^{-8} M ET-1 or 10^{-6} M TPA was compared with the tension development elicited by this agonist in the absence of precontraction.

Statistical analysis

All values are presented as mean ± s.d. Data were analyzed by nonparametric Wilcoxon U test. A value of $P<0.05$ was considered statistically significant.

Drugs

Drugs used in this study were endothelin-1 (Bachem Inc, Torrance, CA, U.S.A.), TPA (Sigma Chemical Company, St. Louis, MO, U.S.A.), calphostin C (Kamiya Biomedical Co. CA, U.S.A.), EGTA (ethylene glycol-*bis*(β-aminoethyl ether)-*N,N,N,N*-tetracetic acid, Sigma), and dimethylsulphoxide (DMSO, Sigma). TPA and calphostin C were dissolved in DMSO. The maximal concentration of DMSO was ⩽0.1% and had no effect on the contractility of the rat aorta. Calphostin C was used immediately after being dissolved.

Results

Effects of calphostin C on endothelin-1-induced contractions

In normal Ca^{2+}-containing Krebs, ET-1 produced a sustained tonic contraction in the rat aorta in a concentration-dependent manner (Figure 2). ET-1 also elicited a smaller (Table 1), but sustained tonic contraction dose-dependently in Ca^{2+}-free Krebs containing 1 mM EGTA (Figure 3). There was no significant difference in the maximal tension between response to cumulative addition of 10^{-8} M ET-1 and that to

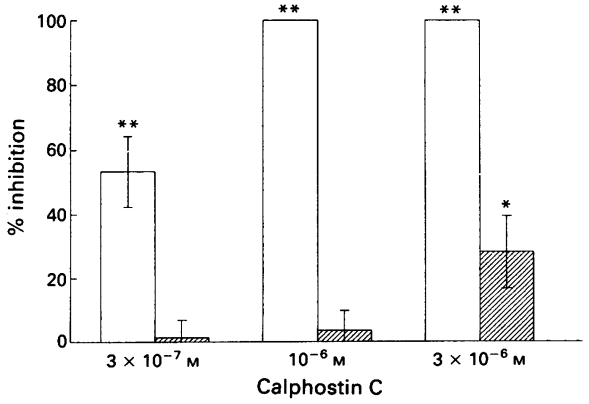

Figure 1 Inhibitory effects (% inhibition: percentage inhibition of maximal tension) of calphostin C on 12-*o*-tetradecanoylphorbol-13-acetate (TPA)-induced contraction (open column) and KCl-induced contraction (hatched column). Rat aortic rings were incubated for 1 h in 3×10^{-7} M, 10^{-6} M, or 3×10^{-6} M calphostin C-containing medium. Contractile responses to 10^{-6} M TPA or 60 mM KCl were obtained in the absence and presence of calphostin C. Each column shows the mean percentage decrease in the maximal tension of 6 experiments; vertical bars show s.d.
*$P<0.05$; **$P<0.01$; statistical significance of percentage differences in the absence and presence of calphostin C.

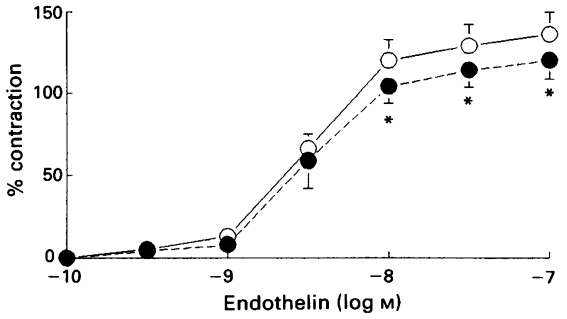

Figure 2 Effects of calphostin C on endothelin-1-induced contractions in normal Ca^{2+}-containing Krebs. Concentration-response curves for endothelin-1 were obtained in the absence (○, $n = 8$) and presence of 10^{-6} M calphostin C (●, $n = 8$). Contractions are expressed as percentage of 60 mM KCl-induced contraction.
*$P<0.05$; statistical significance of difference in the absence and presence of 10^{-6} M calphostin C.

Table 1 Comparison of the maximal tension between cumulative addition of 10^{-8} M endothelin-1 (ET-1) and a single dose of endothelin-1 (10^{-8} M) in the presence and absence of calphostin C

	Maximal tension (%)	
	Ca^{2+}-containing normal Krebs	*Ca^{2+}-free Krebs + 1 mM EGTA*
Cumulative addition of 10^{-8} M ET-1		
Control	120.4 ± 12.7 ($n = 8$)	25.2 ± 6.0($n = 8$)
	‡ $P < 0.05$	‡ $P < 0.05$
Calphostin C 10^{-6} M	104.5 ± 10.5 ($n = 8$)	18.7 ± 5.0($n = 8$)
A single dose of 10^{-8} M ET-1		
Control	129.1 ± 11.0 ($n = 8$)	24.0 ± 5.2 ($n = 8$)
	‡ $P < 0.01$	‡ $P < 0.05$
Calphostin C 10^{-6} M	108.1 ± 11.4 ($n = 8$)	16.9 ± 4.8 ($n = 7$)

Data are means ± s.d. Contractions are expressed as percentage of 60 mM KCl-induced contraction in Ca^{2+}-containing normal Krebs. Aortic rings were incubated with calphostin C (10^{-6} M) for 1 h before addition of endothelin-1. Endothelin-1-induced contractions were obtained in the absence (control) and presence of calphostin C (10^{-6} M).

a single dose of 10^{-8} M ET-1 (Table 1). Calphostin C (10^{-6} M), acting as a selective protein kinase C inhibitor, inhibited ET-1-induced contraction with a significant decrease in the maximal tension in both Ca^{2+}-containing medium and Ca^{2+}-free Krebs containing 1 mM EGTA (both $P < 0.05$, see Figures 2 and 3). Average percentage inhibitions of the maximal tensions for cumulative addition of 10^{-8} M ET-1 by 10^{-6} M calphostin C were 13.2% in normal Ca^{2+}-containing medium and 25.8% in Ca^{2+}-free Krebs containing 1 mM EGTA. In other words, the contribution of protein kinase C in ET-1-induced contraction appeared to be 13.2% and 25.8% in Ca^{2+}-containing medium and Ca^{2+}-free Krebs containing 1 mM EGTA, respectively. These data are summarized in Table 1.

Relationship between endothelin-1- and TPA-induced contractions in normal Ca^{2+}-containing Krebs solution

In Ca^{2+}-containing medium, 10^{-8} M ET-1 elicited a slowly-developing, sustained contraction which developed maximal tensions of 129.1 ± 11.0% compared to 60 mM KCl (100%) ($n = 8$). These contractions subsided gradually. Washing several times with normal Krebs containing 10^{-8} M ET-1 during spontaneous relaxation in tissues precontracted with 10^{-8} M ET-1 had no effect on rate of decay of the aortic tension. After the tension decreased to a level less than 20% of the 60 mM KCl-induced contraction (average 6.4 h later after the first exposure to 10^{-8} M ET-1), exposure to 10^{-6} M TPA elicited a sustained contraction with the maximal tension of 135.6 ± 21.0% ($n = 8$) (Figure 4). In untreated tissues, 10^{-6} M TPA elicited a slowly-developing and much more sustained contraction compared to that induced by 10^{-8} M ET-1 in normal Krebs (Figure 5). The maximal response to 10^{-6} M TPA in the absence of precontraction with 10^{-8} M ET-1 was 125.9 ± 10.1% ($n = 8$), which was not significantly different from the maximal tension elicited by 10^{-6} M TPA with 10^{-8} M ET-1-induced precontraction (see Table 2).

Calphostin C (10^{-6} M) completely abolished 10^{-6} M TPA-induced contraction in the presence and absence of precontraction with 10^{-8} M ET-1 (Figure 4,5). Calphostin C (10^{-6} M) decreased the maximal tension of 10^{-8} M ET-1 significantly (108.1 ± 11.4%, $n = 8$, $P < 0.01$, Table 2). In tissues pretreated with 10^{-6} M calphostin C, the 10^{-6} M TPA-induced contraction was abolished, and the contractile response to subsequent addition of 10^{-8} M ET-1 was not different from 10^{-8} M ET-1-induced contraction initiated in the presence of 10^{-6} M calphostin C without the preceding addition of 10^{-6} M TPA (Figure 5, Table 3).

Relationship between endothelin-1- and TPA-induced contractions in Ca^{2+}-free Krebs containing 1 mM EGTA (Figure 6)

In Ca^{2+}-free Krebs containing 1 mM EGTA, 10^{-8} M ET-1 induced a small, but sustained contraction with the maximal tension of 24.0 ± 5.2% of KCl (60 mM)-induced contractions ($n = 8$) (Table 4). These tonic contractions faded slowly.

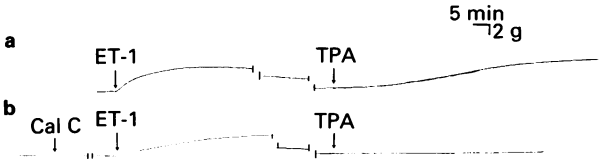

Figure 4 Typical tracings of effects of 10^{-6} M calphostin C (Cal C) on contractile responses to endothelin-1 (10^{-8} M ET-1) and subsequently added 12-*o*-tetradecanoylphorbol-13-acetate (10^{-6} M TPA) in normal Ca^{2+}-containing Krebs. After 10^{-8} M ET-1-induced contraction spontaneously decreased to a level less than 20% of the 60 mM KCl-induced contraction, 10^{-6} M TPA was added in the absence (a) and presence of 10^{-6} M calphostin C (b).

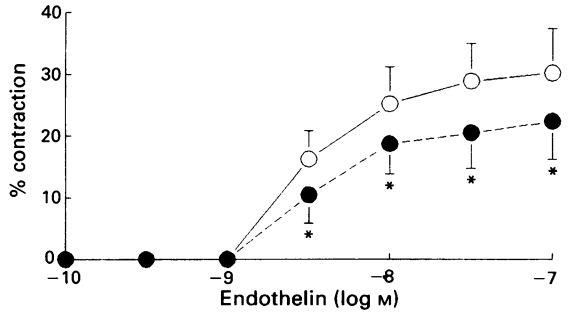

Figure 3 Effects of calphostin C on endothelin-1-induced contractions in Ca^{2+}-free Krebs containing 1 mM EGTA. Concentration-response curves for endothelin-1 were obtained in the absence (○, $n = 8$) and presence of 10^{-6} M calphostin C (●, $n = 8$). Contractions are expressed as percentage of 60 mM KCl-induced contraction in normal Ca^{2+}-containing Krebs.
*$P < 0.05$; statistical significance of difference in the absence and presence of 10^{-6} M calphostin C.

Table 2 Effects of endothelin-1 (ET-1 10^{-8} M) and subsequently added 12-*o*-tetradecanoylphorbol-13-acetate (TPA 10^{-6} M) on rat aortic rings pretreated with calphostin C in Ca^{2+}-containing normal Krebs solution

		Maximal tension (%)	
Treatments	*Number*	*ET-1 (10^{-8} M)*	*TPA (10^{-6} M)*
Control	8	129.1 ± 11.0	135.6 ± 21.0
Control	8	‡ $P < 0.01$	125.9 ± 10.1
Calphostin C 10^{-6} M	8	108.1 ± 11.4	0.0 ± 0.0
Calphostin C 10^{-6} M	6		0.0 ± 0.0

Data are means ± s.d. Contractions represent increments in tension produced by each agonist, and are expressed as percentage of 60 mM KCl-induced contraction. After ET-1-induced contraction spontaneously reduced to a level less than 20% of the 60 mM KCl contraction, TPA (10^{-6} M) was added. Some tissues were incubated with calphostin C (10^{-6} M) for 1 h before addition of ET-1 (10^{-8} M).

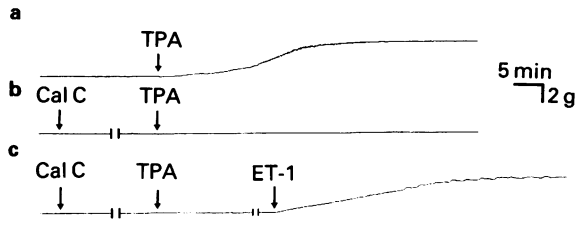

Figure 5 Typical chart records showing the effect of 10^{-6} M calphostin C (Cal C) on contractile responses to 12-*o*-tetradecanoylphorbol-13-acetate (10^{-6} M TPA) and subsequently added 10^{-8} M endothelin-1 (ET-1) in normal Ca^{2+}-containing Krebs. TPA (10^{-6} M) elicited a sustained contraction (a). With 10^{-6} M calphostin C, the 10^{-6} M TPA-induced contraction was abolished (b), whereas subsequently added 10^{-8} M ET-1 elicited a sustained contraction (c).

Table 3 Effects of 12-*o*-tetradecanoylphorbol-13-acetate (TPA 10^{-6} M) and subsequently added endothelin-1 (ET-1 10^{-8} M) on rat aortic rings pretreated with calphostin C in Ca^{2+}-containing normal Krebs solution

Treatments	*Number*	*Maximal tension (%)* *TPA (10^{-6} M)*	*ET-1 (10^{-8} M)*
Calphostin C 10^{-6} M	6	0.0 ± 0.0	116.9 ± 18.5
Calphostin C 10^{-6} M	6		113.7 ± 13.5

Data are means ± s.d. Contractions represent increments in tension produced by each agonist, and are expressed as percentage of 60 mM KCl. Tissues were incubated with calphostin C (10^{-6} M) for 1 h before addition of TPA (10^{-6} M). Calphostin C inhibited the TPA (10^{-6} M)-induced contraction completely, after which, ET-1 (10^{-8} M) was added.

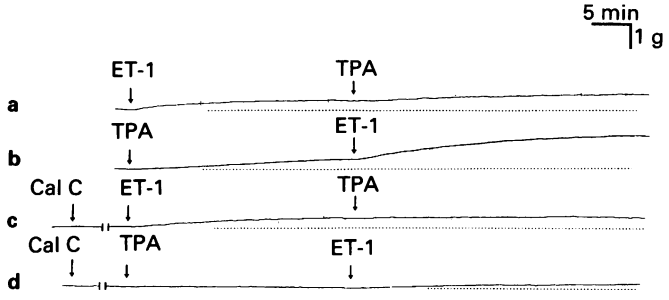

Figure 6 Typical tracings of effects of 10^{-6} M calphostin C (Cal C) on agonist-induced contractions in Ca^{2+}-free Krebs containing 1 mM EGTA. (a) Effects of addition of 12-*o*-tetradecanoylphorbol-13-acetate (10^{-6} M TPA) on aortic rings precontracted with endothelin-1 (10^{-8} M ET-1). (b) Effects of addition of 10^{-8} M ET-1 on tissues precontracted with 10^{-6} M TPA. ET-1 (10^{-8} M)-induced contraction was potentiated by the precontraction with 10^{-6} M TPA. (c) Calphostin C (10^{-6} M Cal C) abolished 10^{-6} M TPA-induced contraction in tissues precontracted with 10^{-6} M ET-1. (d) Calphostin C (10^{-6} M) abolished the potentiating effect of 10^{-6} M TPA on contractile response to subsequently added 10^{-8} M ET-1.

Readministration of 10^{-8} M ET-1 during spontaneous relaxation in tissues precontracted with 10^{-8} M ET-1 failed to elicit a second contraction in either normal Ca^{2+}-containing Krebs or Ca^{2+}-free Krebs containing 1 mM EGTA. In Ca^{2+}-free Krebs containing 1 mM EGTA, 10^{-6} M TPA initiated a small and sustained contraction, which was abolished completely by 10^{-6} M calphostin C (Table 5). Precontraction induced by 10^{-8} M ET-1 did not change the 10^{-6} M TPA-induced contraction (Table 4). In contrast, pretreatment with 10^{-6} M TPA significantly potentiated the following 10^{-8} M ET-1-induced contraction ($P<0.01$) (Table 5).

Table 4 Effects of endothelin-1 (ET-1 10^{-8} M) and subsequently added 12-*o*-tetradecanoylphorbol-13-acetate (TPA 10^{-6} M) on rat aortic rings pretreated with calphostin C in Ca^{2+}-free Krebs solution containing 1 mM EGTA

Treatments	*Number*	*Maximal tension (%)* *ET-1 (10^{-8} M)*	*TPA (10^{-6} M)*
Control	8	24.0 ± 5.2	31.1 ± 17.1
Control	6	‡$P<0.05$	26.7 ± 14.2
Calphostin C 10^{-6} M	7	16.9 ± 4.8	0.0 ± 0.0
Calphostin C 10^{-6} M	8		0.0 ± 0.0

Data are means ± s.d. Contractions represent increments in tension by each agonist, and are expressed as percentage of 60 mM KCl in Ca^{2+}-containing normal Krebs solution. After ET-1 (10^{-8} M)-induced contraction reached maximum tension, TPA (10^{-6} M) was added in the absence (control) and presence of calphostin C (10^{-6} M).

Calphostin C (10^{-6} M) reduced 10^{-8} M ET-1-induced contractions in Ca^{2+}-free medium ($P<0.05$) (Table 4). In the presence of 10^{-6} M calphostin C, there was no significant difference in the maximal tension of 10^{-8} M ET-1-induced contraction with and without the preceding treatment with 10^{-6} M TPA; that is, the potentiating effect of 10^{-6} M TPA on the subsequent 10^{-8} M ET-1-induced contraction was abolished by 10^{-6} M calphostin C (Table 5).

Discussion

In this study, the role of protein kinase C in the mechanism responsible for the vasoconstrictor effects of ET-1 in the rat aorta was determined. The antagonistic effects of 10^{-6} M calphostin C, a protein kinase C inhibitor shown to be effective and selective at this concentration, on ET-1-induced concentration-response curves demonstrated that the participation of protein kinase C in the 10^{-8} M ET-1-induced contraction was small, 13.2% in normal Ca^{2+}-containing Krebs and 25.8% in Ca^{2+}-free Krebs. These results are supported by additional data on interactions between the contractile responses to ET-1 and TPA, an established protein kinase C activator. TPA-induced contraction was not affected by precontraction with ET-1 in either Ca^{2+}-containing medium or Ca^{2+}-free Krebs containing 1 mM EGTA. Thus, mechanisms other than protein kinase C may be predominantly responsible for the ET-1-induced tonic sustained contraction. The experimental evidence and the rationale for this conclusion are discussed below.

Proposed role of protein kinase C in endothelin-1-induced contraction as studied with protein kinase C inhibitors

ET-1 induced a tonic and sustained contraction in normal Ca^{2+}-containing Krebs. Incubation with Ca^{2+}-free Krebs containing 1 mM EGTA decreased ET-1-mediated tension markedly, showing that the ET-1-induced contractions were largely Ca^{2+}-dependent. However, in Ca^{2+}-free Krebs containing 1 mM EGTA there was a significant residual contraction which was not affected by 10^{-6} M nifedipine (data not shown). The vasoconstrictor effects of ET-1 in Ca^{2+}-free Krebs containing 1 mM EGTA may be mediated either through Ca^{2+} mobilization from intracellular sources which are not easily accessible to external EGTA or through Ca^{2+}-independent mechanisms. The most likely mechanism for contraction independent of Ca^{2+} is activation of protein kinase C. In most vascular smooth muscles, phorbol esters which activate protein kinase C produce, like ET-1, a slow-

Table 5 Effects of 12-*o*-tetradecanoylphorbol-13-acetate (TPA 10^{-6} M) and subsequently added endothelin-1 (ET-1 10^{-8} M) in Ca^{2+}-free Krebs solution containing 1 mM EGTA

Treatments	*Number*	*Maximal tension (%)* *TPA (10^{-6} M)*	*ET-1 (10^{-8} M)*	
Control	8	27.1 ± 13.5	50.7 ± 9.5	] $P<0.01$
Control	6		25.4 ± 6.7	
Calphostin C 10^{-6} M	8	0.0 ± 0.0	17.6 ± 4.2	
Calphostin C 10^{-6} M	6		18.7 ± 5.5	

Data are means ± s.d. Contractions represent increments in tension by each agonist, and are expressed as a percentage of 60 mM KCl. After TPA (10^{-6} M)-induced contraction reached a plateau, ET-1 (10^{-8} M) was added. Precontraction with TPA (10^{-6} M) potentiated contractile response to ET-1 (10^{-8} M), whereas this potentiation was prevented by preincubation with calphostin C (10^{-6} M).

developing and sustained contraction (Abdel-Latif, 1986; Rasmussen *et al.*, 1987), which may support a role for protein kinase C in regulating tonic contraction in vascular smooth muscle (Rasmussen *et al.*, 1987). A role for protein kinase C in contractile response to ET-1 is also suggested by data showing that in cultured vascular smooth muscle (Resink *et al.*, 1988; Ohlstein *et al.*, 1989), ET-1 generates diacylglycerol, which can subsequently activate protein kinase C (Nishizuka, 1986). On the basis of experiments with staurosporine or 1-(5-isoquinolinesulphonyl)-2-methylpiperazine (H-7), putative protein kinase C inhibitors, some reports proposed an important role of activation of protein kinase C in the contractile response to ET-1 in rabbit aorta (Ohlstein *et al.*, 1989; Sugiura *et al.*, 1989). Although both staurosporine (Omura *et al.*, 1977) and H-7 (Hidaka *et al.*, 1984) have been widely employed as protein kinase C inhibitors, both these agents inhibit the ATP binding site of protein kinase C, a region with a high degree of sequence homology in most kinases (Hidaka *et al.*, 1984; Tamaoki *et al.*, 1986; Nakadate *et al.*, 1988; Kobayashi *et al.*, 1989b). Therefore, these two agents may include non-specific effects on various smooth muscle contractions (Rüegg & Burgess, 1989). Also our preliminary results using rat aortae demonstrated that H-7 and staurosporine inhibited KCl-induced contraction with a potency equivalent to or higher than TPA-induced contraction (data not shown). Because of a lack of specificity, the interpretation of the effects induced by staurosporine and H-7 needs re-evaluation. In contrast, calphostin C is reported to interact specifically with the regulatory domain of protein kinase C, a region lacking homology with other known kinases (Kobayashi *et al.*, 1989b). In this study, 10^{-6} M calphostin C inhibited 10^{-6} M TPA-induced contractions completely, whereas 60 mM KCl-induced contractions were unaffected. Therefore, calphostin C is a potent as well as selective inhibitor of protein kinase C. Our results using 10^{-6} M calphostin C suggest that protein kinase C is responsible for only a small portion of the contractile response to ET-1, 13.2% and 25.8% in normal Ca^{2+}-containing normal Krebs and Ca^{2+}-free Krebs containing 1 mM EGTA, respectively.

Possible mechanisms other than protein kinase C which are responsible for endothelin-1-induced contraction in Ca^{2+}-free Krebs containing 1 mM EGTA

An intracellular Ca^{2+} mobilization by ET-1 has been observed in cultured vascular smooth muscle cells (Miasiro *et al.*, 1988) and such an effect usually involves the polyphosphoinositide cycle, resulting in a release of inositol 1,4,5-triphosphate which causes Ca^{2+} release from the intracellular Ca^{2+} store (Abdel-Latif, 1986). Although the basal polyphosphoinositide turnover was reduced in Ca^{2+}-free medium containing EGTA, ET-1 produced similar percentage increases over basal levels to those observed in the presence of extracellular Ca^{2+} (Ohlstein *et al.*, 1989). Also fluorescent studies have shown that ET-1 produces a rise in concentration of intracellular Ca^{2+} even in the absence of extracellular Ca^{2+} (Marsden *et al.*, 1989).

EGTA at 1 mM removes superficial membrane-bound Ca^{2+} and also some of the intracellular Ca^{2+} pool (Guan *et al.*, 1988). Nevertheless, contractions produced by ET-1 in Ca^{2+}-free Krebs containing 1 mM EGTA are probably mediated, to some extent, by release of Ca^{2+} from sequestered intracellular stores which are not readily accessible to EGTA. The observations with the fluorescent Ca^{2+} indicators have shown that during smooth muscle contractile response to ET-1, elevation of intracellular free Ca^{2+} levels was transient, returning to near resting levels while force was maintained tonically at high levels (Hirata *et al.*, 1988; Komuro *et al.*, 1988; Miasiro *et al.*, 1988; Marsden *et al.*, 1989; Murakawa *et al.*, 1990). These findings suggest that Ca^{2+} mobilization from intracellular Ca^{2+} pool may not entirely account for this sustained contraction. Therefore, mechanisms of ET-1-induced contraction other than protein kinase C and intracellular Ca^{2+} require further evaluation.

Interaction between endothelin-1-induced contraction and TPA-induced contraction

In this study, the contractions induced by cumulative application of TPA and ET-1 were assessed in normal Ca^{2+}-containing Krebs and Ca^{2+}-free Krebs containing 1 mM EGTA, in order to clarify the relationships between the mechanisms of action of these two agents. If contractile responses to TPA and ET-1 are mediated through different mechanisms, the contractions induced by cumulative applications of two agents may be additive. In contrast, if TPA- and ET-1-contractions are induced by common mechanisms, the first agent-induced precontraction may reduce the second agent-induced contraction.

In the present study, in tissues pretreated and desensitized with ET-1 in normal Ca^{2+}-containing Krebs, TPA-induced contraction was not different from one without pretreatment of ET-1. However, because TPA-induced contraction was not relaxed to a level less than 50% of the control 60 mM KCl contraction after 6–8 h exposure to TPA, we could not investigate the effect of ET-1 in TPA-desensitized tissues. On the other hand, TPA-induced contraction was not affected by precontraction with ET-1 in Ca^{2+}-free Krebs containing 1 mM EGTA. Similar observations have been reported by Itoh *et al.* (1991). These data suggest different mechanisms of TPA- and ET-1-induced contractions, which is consistent with the conclusion that protein kinase C activation is responsible for only 25% of 10^{-8} M ET-1-induced contraction in Ca^{2+}-free medium.

On the other hand, precontraction with TPA potentiated ET-1-induced contraction in Ca^{2+}-free Krebs containing 1 mM EGTA. This potentiation of ET-1 was abolished in the presence of calphostin C. As mentioned above, since the contractile response to ET-1 in Ca^{2+}-free Krebs containing 1 mM EGTA may be, to some degree, due to utilization of Ca^{2+} from the intracellular store, pretreatment with TPA

might enhance the mobilization of intracellular Ca^{2+} or increase the sensitivity of the contractile apparatus to Ca^{2+}. Jiang & Morgan (1987) have demonstrated using aequorin in the rat and ferret aortae, that phorbol esters-induced contractions were not associated with an increase in intracellular Ca^{2+} concentration in Ca^{2+}-free medium containing EGTA, suggesting that phorbol esters potentiate a vasocontraction without altering the concentration of intracellular Ca^{2+}. Several other studies proposed that activation of protein kinase C by vasoactive substances or phorbol esters increases the sensitivity of myofilaments to Ca^{2+} (Adelstein & Sellers, 1987; Drenth *et al.*, 1989; Mori *et al.*, 1990; Nishimura *et al.*, 1990), which may explain the potentiating effects of phorbol ester on ET-1-induced contraction in this study.

This work was supported by a term-grant, a Visiting Scientist Award from the Heart and Stroke Foundation of Canada (H.S.), and a Career Investigator Award from the Heart and Stroke Foundation of Ontario (C.Y.K.).

References

ABDEL-LATIF, A.A. (1986). Calcium-mobilizing receptors, polyphosphoinositides, and the generation of second messengers. *Pharmacol. Rev.*, **38**, 227–272.

ADELSTEIN, R.S. & SELLERS, J.R. (1987). Effects of calcium on vascular smooth muscle contraction. *Am. J. Cardiol.*, **59**, 4B–10B.

BOLGER, G.T., LIARD, F. & JARAMILLO, J. (1990). Tissue selectivity and calcium dependence of contractile responses to endothelin. *J. Cardiovasc. Pharmacol.*, **15**, 946–958.

CHABRIER, P.E., AUGUET, M., ROUBERT, P., LONCHAMPT, M.O., GILLARD, V., GUILLON, J.-M., DELAFLOTTE, S. & BRAQUET, P. (1989). Vascular mechanism of action of endothelin-1: Effect of Ca^{2+} antagonists. *J. Cardiovasc. Pharmacol.*, **13** (Suppl. 5), s32–s35.

DENG, L.Y. & SCHIFFRIN, E.L. (1991). Calcium dependence of effects of endothelin on rat mesenteric microvessels. *J. Physiol. Pharmacol.*, **69**, 798–804.

DRENTH, J.P.H., NISHIMURA, J., NOUAILHETAS, V.L.A. & VAN BREEMEN, C. (1989). Receptor-mediated C-kinase activation contributes to alpha-adrenergic tone in rat mesenteric resistance artery. *J. Hypertension*, **7** (Suppl. 4), s41–s45.

GUAN, Y.Y., KWAN, C.Y. & DANIEL, E.E. (1988). The effects of EGTA on vascular smooth muscle contractility in calcium-free medium. *Can. J. Physiol. Pharmacol.*, **66**, 1053–1056.

HALLER, H., SMALLWOOD, J.I. & RASMUSSEN, H. (1990). Protein kinase C translocation in intact vascular smooth muscle strips. *Biochem. J.*, **270**, 375–381.

HIDAKA, H., INAGAKI, M., KAWAMOTO, S. & SASAKI, Y. (1984). Isoquinolinesulfonamides, novel and potent inhibitors of cyclic nucleotide dependent protein kinase and protein kinase C. *Biochemistry*, **23**, 5036–5041.

HIRATA, Y., YOSHIMI, H., TAKATA, S., WATANABE, T.X., KUMAGAI, S., NAKAJIMA, K. & SAKAKIBARA, S. (1988). Cellular mechanism of action by a novel vasoconstrictor endothelin in cultured rat vascular smooth muscle cells. *Biochem. Biophys. Res. Commun.*, **154**, 868–875.

ITOH, H., HIGUCHI, H., HIRAOKA, N., ITO, M., KONISHI, T., NAKANO, T. & LEDERIS, K. (1991). Contraction of rat thoracic aorta strips by endothelin-1 in the absence of extracellular Ca^{2+}. *Br. J. Pharmacol.*, **104**, 847–852.

JIANG, M.J. & MORGAN, K.G. (1987). Intracellular calcium levels in phorbol ester-induced contractions of vascular muscle. *Am. J. Physiol.*, **253**, (Heart Circ. Physiol. 22), H1365–H1371.

KOBAYASHI, E., ANDO, K., NAKANO, H., IIDA, T., OHNO, H., MORIMOTO, M. & TAMAOKI, T. (1989a). Calphostins (UCN-1028), novel and specific inhibitors of protein kinase C–I. fermentation, isolation, physico-chemical properties and biological activities. *J. Antibiotics*, **42**, 1470–1474.

KOBAYASHI, E., NAKANO, H., MORIMOTO, M. & TAMAOKI, T. (1989b). Calphostin C (UCN-1028C), a novel microbial compound, is a highly potent and specific inhibitor of protein kinase C. *Biochem. Biophys. Res. Commun.*, **159**, 548–553.

KODAMA, M., KANAIDE, H., ABE, S., HIRANO, K., KAI, H. & NAKAMURA, M. (1989). Endothelin-induced Ca-independent contraction of the porcine coronary artery. *Biochem. Biophys. Res. Commun.*, **160**, 1302–1308.

KOMURO, I., KURIHARA, H., SUGIYAMA, T., TAKAKU, F. & YAZAKI, Y. (1988). Endothelin stimulates c-fos and c-myc expression and proliferation of vascular smooth muscle cells. *F.E.B.S. Lett.*, **238**, 249–252.

MARSDEN, P.A., DANTHULURI, N.R., BRENNER, B.M., BALLERMANN, B.J. & BROCK, T.A. (1989). Endothelin action on vascular smooth muscle involves inositol triphosphate and calcium mobilization. *Biochem. Biophys. Res. Commun.*, **158**, 86–93.

MIASIRO, N., YAMAMOTO, H., KANAIDE, H. & NAKAMURA, M. (1988). Does endothelin mobilize calcium from intracellular store sites in rat aortic vascular smooth muscle cells in primary culture? *Biochem. Biophys. Res. Commun.*, **156**, 312–317.

MORI, T., YANAGISAWA, T. & TAIRA, N. (1990). Phorbol 12,13-dibutyrate increases vascular tone but has a dual action on intracellular calcium levels in porcine coronary arteries. *Naunyn-Schmiedebergs Arch. Pharmacol.*, **341**, 251–255.

MURAKAWA, K., KOHNO, M., YOKOKAWA, K., YASUNARI, K., HORIO, T., KURIHARA, N. & TAKEDA, T. (1990). Endothelin-induced renal vasoconcentration and increase in cytosolic calcium in renal vascular smooth muscle cells. *Clin. Exp. Hyper-Theory. Practice*, **A12**, 1037–1048.

NAKADATE, T., JENG, A.Y. & BLUMBERG, P.M. (1988). Comparison of protein kinase C functional assays to clarify mechanisms of inhibitor action. *Biochem. Pharmacol.*, **37**, 1541–1545.

NISHIMURA, J., KHALIL, R.A., DRENTH, J.P. & VAN BREEMEN, C. (1990). Evidence for increased myofilament Ca^{2+} sensitivity in norepinephrine-activated vascular smooth muscle. *Am. J. Physiol.*, **259** (Heart Circ. Physiol. 28), H2–H8.

NISHIZUKA, Y. (1986). Studies and perspectives of protein kinase C. *Science*, **233**, 305–312.

OHLSTEIN, E.H., HOROHONICH, S. & HAY, D.W.P. (1989). Cellular mechanisms of endothelin in rabbit aorta. *J. Pharmacol. Exp. Ther.*, **250**, 548–555.

OMURA, S., IWAI, Y., HIRANO, A., NAKAGAWA, A., AWAYA, J., TSUCHIYA, H., TAKAHASHI, Y. & MASUMA, R. (1977). A new alkaloid AM-2282 of streptomyces origin, taxonamy, fermentation, isolation and preliminary characterization. *J. Antibiot.*, **30**, 275–281.

RASMUSSEN, H., TAKUWA, Y. & PARK, S. (1987). Protein kinase C in the regulation of smooth muscle contraction. *FASEB J.*, **1**, 177–185.

RESINK, T.J., SCOTT-BURDEN, T. & BÜHLER, F.R. (1988). Endothelin stimulates phospholipase C in cultured vascular smooth muscle cells. *Biochem. Biophys. Res. Commun.*, **157**, 1360–1368.

RÜEGG, U.T. & BURGESS, G.M. (1989). Staurosporine, K-252 and UCN-01: potent but nonspecific inhibitors of protein kinases. *Trends. Pharmacol. Sci.*, **10**, 218–220.

SUGIURA, M., INAGAMI, T., HARE, G.M.T. & JOHNS, J.A. (1989). Endothelin action: inhibition by a protein kinase C inhibitor and involvement of phosphoinositols. *Biochem. Biophys. Res. Commun.*, **158**, 170–176.

TAKUWA, Y., KELLEY, G., TAKUWA, N. & RASMUSSEN, H. (1988). Protein phosphorylation changes in bovine carotid artery smooth muscle during contraction and relaxation. *Mol. Cell Endocrinol.*, **60**, 71–86.

TAMAOKI, T., NOMOTO, H., TAKAHASHI, I., KATO, Y., MORIMOTO, M. & TOMITA, F. (1986). Staurosporine, a potent inhibitor of phospholipid/Ca^{++} dependent protein kinase. *Biochem. Biophys. Res. Commun.*, **135**, 397–402.

YANAGISAWA, M., KURIHARA, H., KIMURA, S., TOMOBE, Y., KOBAYASHI, M., MITSUI, Y., YAZAKI, Y., GOTO, K. & MASAKI, T. (1988). A novel potent vasoconstrictor peptide produced by vascular endothelial cells. *Nature*, **332**, 411–415.

(Received March 1, 1992
Revised May 18, 1992
Accepted May 22, 1992)

Br. J. Pharmacol. (1992), **107**, 288–295

Inhibition by adrenergic neurone blocking agents of the relaxation induced by BRL 38227 in vascular, intestinal and uterine smooth muscle

[1] J.L. Berry, R.C. Small, S.J. Hughes, R.D. Smith, A.J. Miller, M. Hollingsworth, G. Edwards & A.H. Weston

Smooth Muscle Research Group, Department of Physiological Sciences, University of Manchester, Oxford Road, Manchester, M13 9PT

1 The adrenergic neurone blocking agents, guanethidine and bretylium, have been tested for inhibitory activity against the actions of some relaxant drugs (BRL 38227, noradrenaline, sodium nitroprusside, theophylline) in vascular, intestinal and uterine smooth muscle.

2 In guinea-pig isolated taenia caeci pre-contracted with KCl (25 mM), BRL 38227 (0.1–10 μM) and noradrenaline (10 nM–100 μM) each caused concentration-dependent relaxation. Guanethidine and bretylium (50 μM) each antagonized the relaxation to BRL 38227 but not that to noradrenaline. At high concentration (500 μM), the adrenergic neurone blocking agents antagonized the action of BRL 38227 and, to some extent, that of noradrenaline.

3 In rat isolated aorta pre-contracted with noradrenaline (300 nM), BRL 38227 (0.0125–3.2 μM) and sodium nitroprusside (0.3–100 nM) each produced concentration-dependent smooth muscle relaxation. Guanethidine and bretylium (5–500 μM) each antagonized the action of BRL 38227 without antagonizing that of sodium nitroprusside.

4 Rats were pretreated with 17-β oestradiol benzoate. Tension waves were then induced from segments of isolated, oestrogen-dominated uterus by transmural electrical stimulation or by oxytocin (0.2 nM). These tension waves were inhibited by BRL 38227 (0.025–3.2 μM) or theophylline (0.05–0.8 mM) in a concentration-dependent manner. Guanethidine (50 μM) antagonized the action of BRL 38227 in both the electrically- and oxytocin-driven tissues. In the electrically-driven tissues, guanethidine (50 μM) did not antagonize the inhibition to theophylline.

5 In KCl (25 mM)-treated guinea-pig taenia caeci, guanethidine (50 μM) inhibited the efflux of $^{86}Rb^+$ evoked by BRL 38227 (10 μM) but not that evoked by noradrenaline (10 μM). In contrast, apamin (100 nM) reduced the efflux of $^{86}Rb^+$ which was promoted by noradrenaline, but did not affect efflux induced by BRL 38227.

6 It is concluded that the adrenergic neurone blocking agents, guanethidine and bretylium (each at 50 μM), selectively inhibit the relaxant action of BRL 38227 in vascular, intestinal and uterine smooth muscle. If this inhibition reflects direct blockade of the K^+-channel (K_{KCO}) which is opened by BRL 38227, then the adrenergic neurone blocking agents act as inhibitors selective for K_{KCO} as opposed to the small, apamin-sensitive (SK_{Ca}) and large (BK_{Ca}) conductance, Ca^{2+}-dependent K^+-channels.

Keywords: Guinea-pig taenia caeci; rat aorta; rat uterus; guanethidine; bretylium; BRL 38227; noradrenaline; $^{86}Rb^+$ efflux; K^+-channels; smooth muscle

Introduction

Kirpekar *et al.* (1978) studied the ability of the adrenergic neurone blocking agent, guanethidine, to suppress the neural release of noradrenaline from the spleen of the cat perfused *in situ*. These workers demonstrated that the K^+-channel blockers, tetraethylammonium (TEA) and 4-aminopyridine (4-AP), could inhibit this effect of guanethidine. Stutzin *et al.* (1983) subsequently showed that apamin, an inhibitor of small, Ca^{2+}-dependent K^+-channels (SK_{Ca}), could antagonize the guanethidine-induced inhibition of contractile responses to the electrical stimulation of noradrenergic nerves in the guinea-pig isolated vas deferens. These workers proposed that guanethidine opened Ca^{2+}-dependent K^+-channels in the plasmalemma of the neurone terminal and that the resultant hyperpolarization inhibited neurotransmitter release. The reversal by TEA or 4-AP of guanethidine-induced adrenergic neurone blockade in rat anococcygeus (Smith & Weston, 1991) is consistent with a K^+-channel opening effect of guanethidine, although other mechanisms such as displacement of guanethidine by TEA or 4-AP (Drukarch *et al.*, 1989) cannot be excluded.

In contrast to these investigations, other studies with adrenergic neurone blocking agents suggest that these drugs may function as K^+-channel inhibitors. For example, when bretylium was applied either extracellularly or intracellularly to chick cardiac myocytes it reduced the outward K^+-current induced by a depolarizing voltage step (Bkaily *et al.*, 1988). Support for the view that guanethidine and bretylium may act as K^+-channel inhibitors is derived from studies of guinea-pig and bovine trachealis muscle. In guinea-pig trachealis, guanethidine and bretylium attenuated the relaxant actions of potassium channel openers (KCOs) such as BRL 38227, RP 52891, SDZ PCO 400 and pinacidil without inhibiting the relaxant effects of theophylline or isoprenaline (Berry *et al.*, 1992; Small *et al.*, 1992). Furthermore, guanethidine, bretylium and debrisoquine each attenuated BRL 38227-induced $^{86}Rb^+$ efflux from bovine trachealis (Berry *et al.*, 1992). In contrast to the effects of the adrenergic neurone blocking agents, charybdotoxin (an inhibitor of the large conductance, Ca^{2+}-dependent K^+-channel (BK_{Ca})) antagonized the relaxant actions of isoprenaline and theophylline in guinea-pig trachealis without antagonizing the actions of KCOs such as cromakalim, pinacidil, RP 49356 and SDZ PCO 400 (Jones *et al.*, 1990; Murray *et al.*,

[1] Author for correspondence.

1991; Small *et al.*, 1992). The fact that the adrenergic neurone blocking agents antagonized the relaxant actions of KCOs in guinea-pig trachea, without antagonizing those of isoprenaline or theophylline, therefore suggests that the adrenergic neurone blocking agents may selectively inhibit the K^+-channel opened by KCOs (K_{KCO}) as opposed to BK_{Ca} (Berry *et al.*, 1992; Small *et al.*, 1992).

The experiments of the present study were performed to determine whether adrenergic neurone blocking agents could selectively antagonize the action of KCOs in smooth muscle other than that of the airways. In addition, more insight was sought as to the inhibitory selectivity of the neurone blocking agents for the various types of K^+-channel known to exist in the plasmalemma of smooth muscle cells.

Methods

Experiments with guinea-pig taenia caeci

Guinea-pigs (400–550 g) of either sex were killed by stunning and bleeding. Segments of taenia caeci, approximately 10 mm in length, were excised from the animals and set up for the isometric recording of tension changes under an initial, imposed tension of 1 g. Following a 20 min equilibration period, KCl (25 mM) was added to the bath fluid and the contractile response allowed 20 min to develop. The tissues were then washed 3 times at 10 min intervals and allowed to equilibrate for 20 min before again adding KCl (25 mM) to the bath fluid. The contractile response to KCl was allowed to develop for 30 min (by which time it had reached a plateau) before constructing a cumulative log concentration-effect curve either to BRL 38227 (0.1–100 μM) or to noradrenaline (10 nM–100 μM). Concentration increments (0.5 $\log_{10}$ unit) of the relaxant drug were then made at 8 min (BRL 38227) or 2 min (noradrenaline) intervals.

Following construction of the log concentration-effect curve for the relaxant drug, test tissues were equilibrated (40 min, including exchange of bath fluid at 10 and 20 min) with a modifying agent (guanethidine or bretylium, each 50 or 500 μM). The test tissues were then subjected to a third challenge with KCl (25 mM); 30 min after the KCl addition, the log concentration-effect curve for the relaxant drug was reconstructed in the presence of the modifying agent. Time-matched control tissues were treated similarly, but were not exposed to the modifying agent. All relaxant responses were measured as a proportion (%) of the mechanical tone extant when commencing construction of the log concentration-effect curve, the position of zero tone being determined at the end of the experiment by washing with normal Krebs solution.

Experiments with rat isolated aorta

Male Sprague-Dawley rats (250–350 g) were killed by stunning and bleeding. The thoracic aorta was excised from the animals and the mid section of each aorta was cut into two segments approximately 0.5 cm in length. Each segment of aorta was opened by cutting along its longitudinal axis and the endothelium removed by rubbing with a cotton bud moistened with Krebs solution. Threads were attached to the longitudinally-cut edges of each tissue segment with fine hooks. The tissues were then set up for the isometric recording of tension changes under an initial, imposed tension of 1 g.

Following a 45 min equilibration period, noradrenaline (300 nM) was added to the bath fluid and the resultant contraction recorded for 10 min. The tissue was then washed with drug-free Krebs solution. Two further applications of noradrenaline were made. When the contractile response to the third noradrenaline challenge had reached equilibrium, a cumulative concentration-effect curve either for BRL 38227 (0.0125–3.2 μM) or for sodium nitroprusside (0.3–100 nM) was constructed. Two fold (BRL 38227) or three fold (sodium nitroprusside) concentration increments were made at 5 min intervals. When the maximal effect of the relaxant drug had been recorded, the tissues were washed with drug-free Krebs solution. Test tissues were then equilibrated (30 min) with Krebs solution containing guanethidine (5 μM) or bretylium (5 μM). Noradrenaline (300 nM) was then again applied to the test tissues and the log concentration-effect curve for the relaxant agent in the presence of the adrenergic neurone blocking agent was determined. Similar concentration-effect curves for the relaxant agents were subsequently constructed in the presence of greater (50 or 500 μM) concentrations of the adrenergic neurone blocking agent. Time-matched control tissues were treated similarly to test tissues but were not exposed to guanethidine or bretylium.

Experiments with rat isolated uterus

Female Sprague-Dawley rats (250–350 g) were treated with 17-β oestradiol benzoate (100 μg kg^{-1}, s.c.); 18–24 h later, the animals were killed by stunning and exsanguination. The oestrogen-dominated uteri were excised and each uterine horn was cut into two segments of approximately equal length. Tissue segments from one uterine horn were set up for transmural electrical stimulation essentially as described by Hollingsworth (1975). The two tissue segments from the other uterine horn were not arranged for transmural stimulation but all tissues were set up for the isometric recording of tension changes of the longitudinal muscle layer (Granger *et al.*, 1985) in Krebs solution containing propranolol (1 μM). The initial, imposed tension was 1 g.

In order to induce uterine tension waves, tissues arranged for transmural stimulation were stimulated at 32 Hz with 40 V pulses of 1 ms duration. These pulses were delivered in trains of 4 s duration at a train frequency of 1 min^{-1}. For tissues not subjected to transmural stimulation, uterine tension waves were induced by the addition of oxytocin (0.2 nM) to the bath fluid. A 15 min period was allowed for the development of tension waves of near-constant amplitude and frequency. A cumulative concentration-effect curve for BRL 38227 (0.025–3.2 μM) or theophylline (0.05–0.8 mM) was constructed by their addition in two fold concentration increments at 10 min intervals. All tissues were subsequently washed with relaxant-free Krebs solution and tension wave activity was allowed to recover. The induction of uterine tension waves was then discontinued by switching off the stimulator or by washing the tissues with oxytocin-free Krebs solution as appropriate; 40 min later, guanethidine (50 μM) was added to the bath fluid of test tissues and vehicle added to that of control tissues. Following 15 min tissue incubation with either guanethidine or vehicle, uterine tension waves were again induced by transmural stimulation or the addition of oxytocin (0.2 nM) to the Krebs solution as appropriate; 15 min later, the cumulative log concentration-effect curve for the relaxant was reconstructed in the presence of the guanethidine (test tissues) or vehicle (time-matched control tissues).

The integral of uterine mechanical activity was measured on line with a Research Machines 380Z microcomputer as previously described (Foster & Hollingsworth, 1985; Granger *et al.*, 1985). The response to a given concentration of relaxant drug was calculated by expressing the integral of mechanical activity recorded in the final 5 min of tissue exposure as a proportion (%) of the integral of activity recorded in the 5 min before drug administration. $-\log EC_{50}$ values for relaxant agents were calculated by linear regression of the probit of response versus $\log_{10}$ molar concentration.

Studies of $^{86}Rb^+$ efflux from guinea-pig taenia caeci

The efflux of $^{86}Rb^+$ from guinea-pig taenia caeci was studied by the method described by Weir & Weston (1986). In brief, strips of taenia caeci (length approximately 1.25 cm) were

impaled on hypodermic needles and loaded with $^{86}Rb^+$ by incubation for 90 min in Krebs solution maintained at 37°C and gassed with a mixture of 95% O_2 and 5% CO_2. This loading solution contained 185 kBq ml^{-1} $^{86}Rb^+$ and the Rb^+ concentration was less than 50 μM. Following loading with the radiotracer, each tissue strip was transferred to the first of a series of efflux tubes each containing 3 ml of K^+-rich (25 mM) Krebs solution gassed with a mixture of 95% O_2 and 5% CO_2 and maintained at 37°C. Each tissue strip was transferred to the next tube in the series at 2 min intervals. At the end of the efflux period the contents of each of the efflux tubes was assayed for radioactivity in a gamma counter. Each tissue strip was blotted and similarly assayed for radioactivity.

In the case of test tissues, BRL 38227 (10 μM) or noradrenaline (10 μM) was present in the efflux medium for the periods 28–44 min or 28–34 min respectively, from the start of the efflux. In the case of time-matched control tissues, the efflux medium contained the appropriate vehicle for BRL 38227 or noradrenaline over the same time periods. In experiments where the effects of modifying agents (apamin, 100 nM or guanethidine, 50 μM) alone, or in combination with BRL 38227 (10 μM) or noradrenaline (10 μM) were examined, the modifying agent (or appropriate vehicle) was added to the efflux medium for the whole of the efflux period.

The efflux data were expressed in terms of the rate coefficient (fractional loss of $^{86}Rb^+$ from the tissue standardized for a 1 min period, expressed as a percentage).

Drugs and solutions/statistical analysis of results

Drug concentrations are expressed in terms of the molar concentration of the active species. The following substances were used: apamin (Sigma), bretylium tosylate (Wellcome Foundation), BRL 38227 ((−)-6-cyano-3,4-dihydro-2,2-dimethyl-trans-4-(2-oxo-1-pyrrolidyl)-2H-benzo[b]pyran-3-ol, SmithKline Beecham Pharmaceuticals), guanethidine sulphate (Ciba), (-)-noradrenaline bitartrate (Sigma), 17-β oestradiol benzoate (Sigma), oxytocin acetate (Sigma), propranolol hydrochloride (ICI), sodium nitroprusside (Sigma), theophylline (Sigma).

Stock solutions of noradrenaline were prepared in 0.1 M HCl. Dilutions from these stocks were prepared with twice-distilled water containing 0.57 mM ascorbic acid as an antioxidant. Stock solutions of BRL 38227 were prepared in 70% ethanol. 17-β Oestradiol benzoate was prepared in arachis oil. Stock solutions of other drugs were prepared in twice-distilled water.

The Krebs solution had the following composition (mM): NaCl 118, KCl 4.8, $CaCl_2$ 2.5, $MgSO_4$ 1.2, KH_2PO_4 1.2, $NaHCO_3$ 25 and glucose 11.1. This solution (pH 7.4) was maintained at 37°C and was gassed with a mixture of 95% O_2 and 5% CO_2.

The significance of differences between means was assessed by use of a two-tailed, unpaired t test. The null hypothesis was rejected when $P<0.05$.

Results

Experiments with guinea-pig taenia caeci

When KCl (25 mM) was added to the Krebs solution bathing strips of guinea-pig taenia caeci, the tissues generated tension. The contractile response to KCl took approximately 25 min to reach equilibrium and thereafter was well-sustained. The subsequent administration of BRL 38227 (0.1–10 μM) caused concentration-dependent relaxation. The slope of the log concentration-effect curve for BRL 38227 was very steep (Figure 1) and the EC_{50} for BRL 38227 was approximately 1 μM (Table 1). Concentrations of BRL 38227 which generated <50% or >95% of the maximal response generally produced well-sustained relaxation whereas rhythmic tension waves were often superimposed on relaxations which ranged from 60–90% of the maximal response.

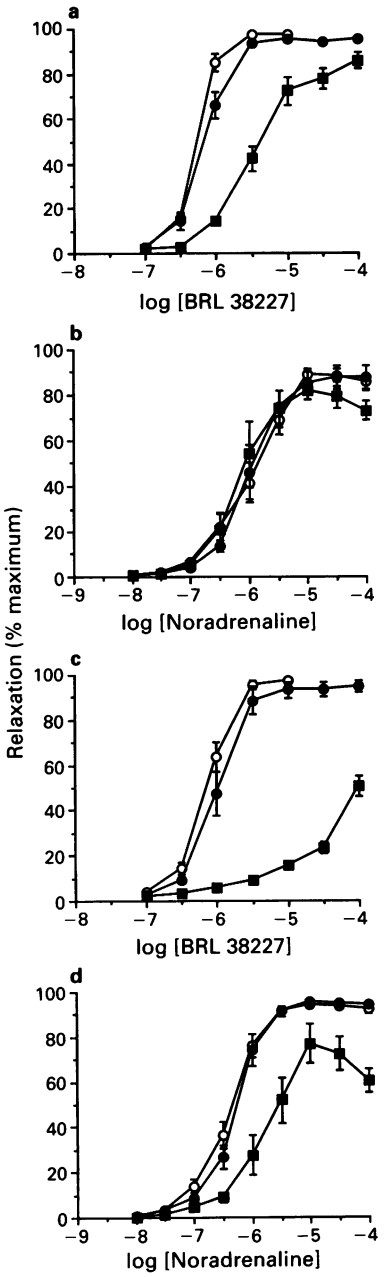

Figure 1 The effects of guanethidine (50 and 500 μM) on the relaxant actions of BRL 38227 and noradrenaline in the guinea-pig taenia caeci pre-contracted with KCl (25 mM). Abscissae: $\log_{10}$ molar concentration of BRL 38227 (a and c) or noradrenaline (b and d). Ordinates: relaxation as a % of the tone induced by KCl (25 mM). In each panel (○) indicates the pooled (control and test tissues) initial log concentration-effect curve for the relaxant agent; (●) indicates the subsequent curve obtained in vehicle-treated, time-matched control tissues and (■) indicates the subsequent curve obtained in test tissues equilibrated with guanethidine 50 μM (a and b) or 500 μM (c and d). Data indicate the means (± s.e.mean, vertical bars) of values from at least 6 tissues.

Noradrenaline (10 nM–100 μM) also caused concentration-dependent suppression of the contraction evoked by KCl (Figure 1). The EC_{50} for noradrenaline was approximately 1 μM (Table 1). The relaxation produced by each concentration of noradrenaline developed very rapidly. Marked fade of the relaxation often occurred before the next concentration increment, although this fade became less marked for

Table 1 The effects of adrenergic neurone blocking agents on the potency of some relaxant drugs

Tissue/agonist	*Time-matched controls*	*Guanethidine* (50 μM)	*Time-matched controls*	*Guanethidine* (500 μM)
Guinea-pig taenia caeci				
BRL 38227	6.16 ± 0.06	5.36 ± 0.07*	6.00 ± 0.08	†
Noradrenaline	6.00 ± 0.10	6.09 ± 0.14	6.26 ± 0.07	5.66 ± 0.10*
Rat aorta				
BRL 38227	7.02 ± 0.07	6.26 ± 0.04*	6.96 ± 0.07	6.13 ± 0.05*
Sodium nitroprusside	8.20 ± 0.04	8.15 ± 0.10	8.20 ± 0.04	8.48 ± 0.11*
Electrically-driven rat uterus				
BRL 38227	6.96 ± 0.09	4.79 ± 0.35*	‡	‡
Theophylline	3.91 ± 0.10	3.46 ± 0.24	‡	‡
Oxytocin-driven rat uterus				
BRL 38227	6.84 ± 0.01	5.14 ± 0.26*	‡	‡

Tissue/agonist	*Time-matched controls*	*Bretylium* (50 μM)	*Time-matched controls*	*Bretylium* (500 μM)
Guinea-pig taenia caeci				
BRL 38227	6.16 ± 0.07	5.77 ± 0.04*	6.05 ± 0.06	†
Noradrenaline	6.16 ± 0.11	6.18 ± 0.08	6.15 ± 0.11	5.69 ± 0.14*
Rat aorta				
BRL 38227	6.72 ± 0.01	6.23 ± 0.09*	6.70 ± 0.07	†
Sodium nitroprusside	8.33 ± 0.12	8.03 ± 0.09	8.31 ± 0.07	8.39 ± 0.14

Data indicate mean (± s.e.mean) values of $-\log EC_{50}$ derived from a minimum of 6 tissues.
*indicates a significant ($P<0.05$) difference from the corresponding value in the time-matched control tissues;
†indicates a non-calculable value and ‡indicates an experiment not performed.

noradrenaline concentrations producing >90% of the maximal response. For both noradrenaline and BRL 38227, the maximal relaxant response was equivalent to 90–100% of the tone prior to administration of the relaxant agent.

The addition of guanethidine (50 μM) to the Krebs solution bathing test tissues modified neither the contraction evoked by KCl, nor the relaxant action of noradrenaline. However, guanethidine (50 μM) antagonized the relaxation to BRL 38227, producing a rightward (approximately 6 fold) shift of the log concentration-relaxation curve, together with a reduction in the slope (Figure 1a,b; Table 1). Guanethidine (500 μM) again failed to modify the contractile response of the taenia caeci to KCl, but profoundly antagonized the action of BRL 38227, shifting the log concentration-effect curve more than 30 fold to the right. Guanethidine (500 μM) also caused some antagonism of the relaxation to noradrenaline, shifting the log concentration-effect curve approximately 4 fold to the right and reducing the maximal response (Figure 1c,d; Table 1).

Bretylium (50 μM) did not modify contraction of the taenia caeci to KCl, nor did it antagonize the relaxation to noradrenaline. In contrast, bretylium (50 μM) shifted the log concentration-effect curve for BRL 38227 approximately 3 fold to the right, and slightly reduced the maximal response (Figure 2a,b; Table 1). The contractile response of the taenia caeci to KCl was not modified by bretylium (500 μM). However, this higher concentration of bretylium profoundly reduced the slope of the log concentration-effect curve to BRL 38227. Bretylium (500 μM) also antagonized the relaxation to noradrenaline, shifting the log concentration-effect curve approximately 3 fold to the right (Figure 2c,d; Table 1).

Experiments with rat isolated aorta

Noradrenaline (300 nM)-induced contraction of rat aorta was suppressed by BRL 38227 (0.0125–3.2 μM) and by sodium nitroprusside (0.3–100 nM), in both cases in a concentration-dependent manner. The EC_{50} value for BRL 38227 was close to 0.1 μM and that for sodium nitroprusside was close to 6 nM (Table 1). For each agent E_{max} was very close to full suppression of the noradrenaline-induced contraction. Guanethidine (5, 50 or 500 μM) did not significantly affect the noradrenaline-induced contraction, but caused a concentration-dependent rightward shift in the log concentration-effect curve of BRL 38227. Guanethidine (50 or 500 μM) did not, however, antagonize the relaxant action of sodium nitroprusside. Indeed, the highest concentration of guanethidine shifted the log concentration-effect curve for sodium nitroprusside approximately 2 fold to the left (Figure 3; Table 1).

Bretylium (5 or 50 μM) did not significantly modify the noradrenaline-induced contraction of the aorta, but caused a concentration-dependent rightward shift of the log concentration-effect curve of BRL 38227. At a concentration of 500 μM, however, bretylium significantly reduced (by 30.9 ± 1.0%; $n = 4$) the noradrenaline-induced contraction and markedly depressed the log concentration-effect curve for BRL 38227. In contrast, bretylium (50 and 500 μM) caused no significant change in the position of the log concentration-effect curve for sodium nitroprusside (Figure 4 and Table 1).

Experiments with rat isolated uterus

Cumulative administration of BRL 38227 (0.025–3.2 μM) or theophylline (0.05–0.8 mM), produced a concentration-dependent reduction in both the amplitude and the frequency of oxytocin (0.2 nM)-induced tension waves. These agents also reduced the amplitude of the tension waves which were generated by transmural electrical stimulation (Figure 5).

In approximately 30% of tissues, the addition of guanethidine (50 μM) to the Krebs solution bathing the test tissues prevented the generation of oxytocin- or electrically-induced tension waves. In test preparations which had been challenged with theophylline, the addition of guanethidine frequently inhibited oxytocin-induced tension wave activity and these tissues could therefore not be used to assess the interactions between guanethidine and the relaxant drugs. In the presence of guanethidine (50 μM) the log concentration-inhibition curve for BRL 38227 against electrically-induced

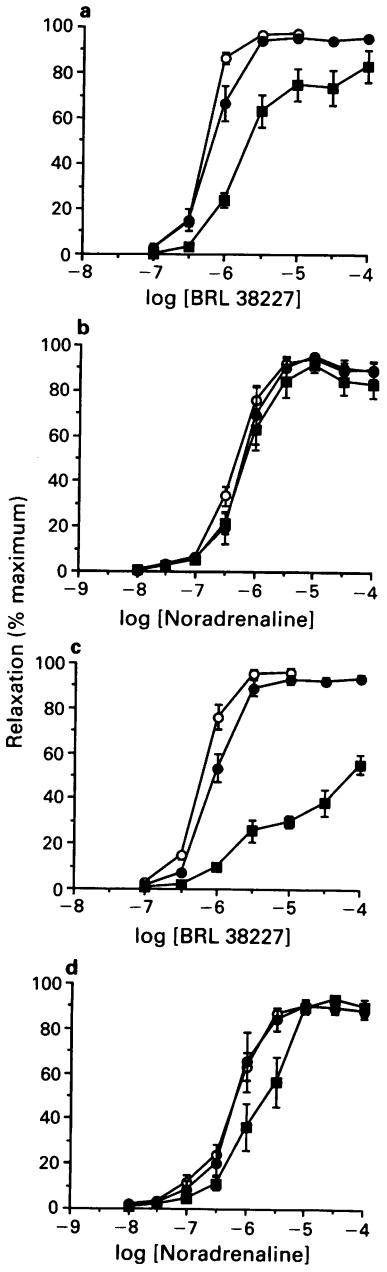

Figure 2 The effects of bretylium (50 and 500 μM) on the relaxant actions of BRL 38227 and noradrenaline in the guinea-pig taenia caeci pre-contracted with KCl (25 mM). Abscissae: $\log_{10}$ molar concentration of BRL 38227 (a and c) or noradrenaline (b and d). Ordinates: relaxation as a % of the tone induced by KCl (25 mM). In each panel (○) indicates the pooled (control and test tissues) initial log concentration-effect curve for the relaxant agent; (●) indicates the subsequent curve obtained in vehicle-treated, time-matched control tissues and (■) indicates the subsequent curve obtained in test tissues equilibrated with bretylium 50 μM (a and b) or 500 μM (c and d). Data indicate the means (± s.e.mean, vertical bars) of values from at least 6 tissues.

tension waves was shifted rightward approximately 150 fold (Table 1). However, a similar shift was not observed in the time-matched control tissues (Figure 5). The log concentration-effect curve for theophylline was moved very slightly to the right in the presence of guanethidine (50 μM), while the equivalent curve in the time-matched control tissues shifted marginally to the left. However, the position of the log concentration-effect curve for theophylline observed in the presence of guanethidine did not significantly differ from that observed in the time-matched control tissues (Table 1).

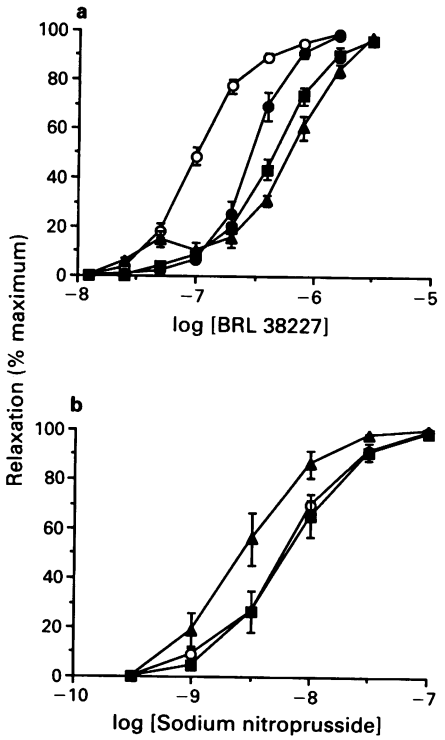

Figure 3 The effects of guanethidine (5, 50 and 500 μM) on the relaxant actions of BRL 38227 (a) and sodium nitroprusside (b) in rat aorta precontracted with noradrenaline (300 nM). Abscissae: $\log_{10}$ molar concentration of BRL 38227 (a) or sodium nitroprusside (b). Ordinates: relaxation as a % of the tone induced by noradrenaline (300 nM). In each panel, (○) indicates the pooled (all curves except the initial curve) log concentration-effect curves of the relaxant agent as observed in time-matched control tissues; (●), (■) and (▲) indicate the log concentration-effect curves of the relaxant agent obtained in test tissues equilibrated with guanethidine 5, 50 and 500 μM respectively. Data indicate the means (± s.e.mean, vertical bars) of values from at least 6 tissues.

In tissues driven by oxytocin (0.2 nM), guanethidine (50 μM) caused a 50 fold rightward shift of the log concentration-effect curve for BRL 38227 (Table 1). A similar rightward shift was not observed in the time-matched control tissues. In the oxytocin-driven tissues, the high proportion of theophylline- and guanethidine-treated tissues which failed to generate tension waves in response to oxytocin prevented a rigorous study of the interaction between guanethidine and theophylline.

Studies of $^{86}Rb^+$ efflux from guinea-pig taenia caeci

In both test and control tissues, the $^{86}Rb^+$ efflux rate coefficient had declined to a relatively stable (approximately 1.5% min^{-1}) value within 22 min of the start of the efflux period. In control tissues, the $^{86}Rb^+$ efflux rate coefficient changed very little throughout the remainder of the efflux period. The addition of BRL 38227 (10 μM) or noradrenaline (10 μM) to the efflux medium increased the $^{86}Rb^+$ efflux rate coefficient compared with the vehicle-treated control tissues. The effect was evident throughout the period of drug exposure (Figure 6).

Apamin (100 nM) and guanethidine (50 μM) did not themselves modify the efflux rate coefficient for $^{86}Rb^+$ (data not shown). However, apamin (100 nM) significantly reduced the increase in $^{86}Rb^+$ efflux evoked by noradrenaline (10 μM) without modifying the increase in efflux evoked by BRL 38227 (10 μM). In contrast, guanethidine (50 μM) significantly reduced the increase in $^{86}Rb^+$ efflux evoked by BRL 38227

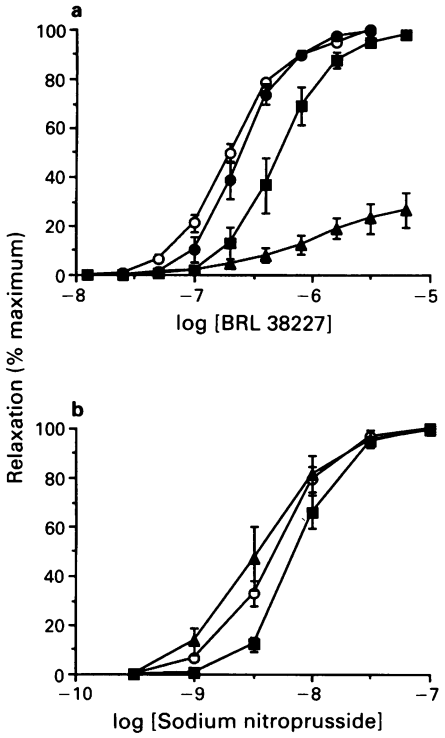

Figure 4 The effects of bretylium (5, 50 and 500 μM) on the relaxant actions of BRL 38227 (a) and sodium nitroprusside (b) in rat aorta precontracted with noradrenaline (300 nM). Abscissae: $\log_{10}$ molar concentration of BRL 38227 (a) or sodium nitroprusside (b). Ordinates: relaxation as a % of the tone induced by noradrenaline (300 nM). In each panel, (○) indicates the pooled (all curves except the initial curve) log concentration-effect curves of the relaxant agent as observed in time-matched control tissues; (●), (■) and (▲) indicate the log concentration-effect curves of the relaxant agent obtained in test tissues equilibrated with bretylium 5, 50 and 500 μM respectively. Data indicate the means (± s.e.mean, vertical bars) of values from at least 6 tissues.

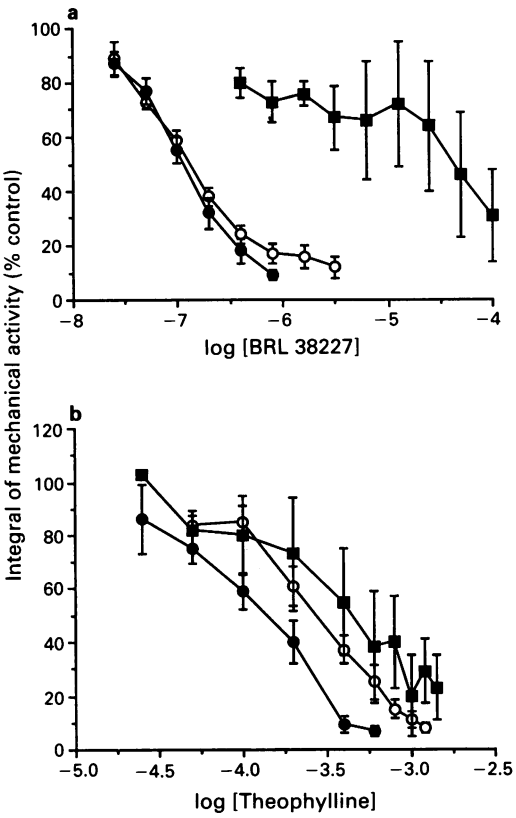

Figure 5 The influence of guanethidine (50 μM) on the inhibitory actions of BRL 38227 and theophylline in the transmurally-stimulated rat isolated uterus. Abscissae: $\log_{10}$ molar concentration of BRL 38227 (a) or theophylline (b). Ordinates: integrated mechanical activity as a % of that recorded prior to administration of BRL 38227 or theophylline. In each panel, (○) indicates the pooled (control and test tissues) initial log concentration-effect curve for the relaxant agent; (●) indicates the subsequent curve obtained in time-matched control tissues and (■) indicates the subsequent curve obtained in test tissues equilibrated with guanethidine (50 μM). Data indicate the means (± s.e.mean, vertical bars) of values from at least 6 tissues. Propranolol (1 μM) was present throughout these experiments.

(10 μM) but had no effect on the increase in efflux evoked by noradrenaline (10 μM) (Figure 6).

Discussion

The tissue specificity of adrenergic neurone blocking agents as antagonists of KCOs

The adrenergic neurone blocking agents, guanethidine and bretylium, inhibit the tracheal relaxant actions of BRL 38227, pinacidil, RP 52891 and SDZ PCO 400 in concentrations that do not antagonize the relaxation to isoprenaline or theophylline (Berry *et al.*, 1992; Small *et al.*, 1992). In the present study, guanethidine and bretylium (each 50 μM) were each shown to inhibit the relaxant action of BRL 38227 in the guinea-pig taenia caeci, without modifying that of noradrenaline (Figures 1 and 2). Similarly, these agents inhibited the relaxant action of BRL 38227 in rat isolated aorta without inhibiting the relaxant action of sodium nitroprusside (Figures 3 and 4) and in the transmurally stimulated rat uterine horn, guanethidine (50 μM) inhibited the action of BRL 38227 without affecting that of theophylline (Figure 5). These findings suggest that the antagonism of KCOs by adrenergic neurone blocking agents is selective and occurs in a variety of different smooth muscle preparations. An unexpected finding of the present study was that, in noradrenaline-treated rat aorta, guanethidine (500 μM) caused a minor (2 fold) leftward shift in the log concentration-effect curve for sodium nitroprusside (Table 1). Hu *et al.* (1992) have reported that incubation of rat aorta with noradrenaline can potentiate sodium nitroprusside by enhancing activation of the guanylate cyclase-cyclic GMP system. Such a mechanism is unlikely to account for the leftward shift of the log concentration-effect curve for sodium nitroprusside observed in the presence of guanethidine (500 μM), for a similar shift was not observed in the presence of the lower (50 μM) concentration of guanethidine tested. Furthermore, guanethidine (500 μM) failed to modify the contraction of the aorta induced by noradrenaline (300 nM). Accordingly, a reduction in the amount of pre-existing mechanical tone cannot account for the minor potentiation of sodium nitroprusside observed in the presence of guanethidine (500 μM) and the mechanism underlying the potentiation therefore remains unclear.

Mechanisms by which adrenergic neurone blocking agents inhibit the smooth muscle relaxant actions of KCOs

In guinea-pig trachealis, guanethidine and bretylium reduced the relaxations produced by the KCOs BRL 38227, RP 52891, SDZ PCO 400 and pinacidil (Berry *et al.*, 1992; Small *et al.*, 1992). In guinea-pig taenia caeci and rat aorta, guanethidine and bretylium each inhibited the relaxant action of BRL 38227 and, furthermore, guanethidine inhibited the

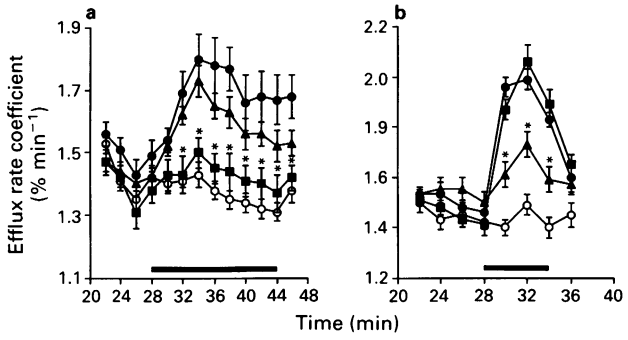

Figure 6 The effects of apamin (100 nM) and guanethidine (50 μM) on the actions of 10 μM BRL 38227 (a) and 10 μM noradrenaline (b) in promoting the efflux of $^{86}Rb^+$ from strips of guinea-pig taenia caeci preloaded with the radiotracer. In each panel the abscissa scale indicates the time (min) measured from the start of the efflux period. The ordinate scale indicates the efflux rate coefficient (% per min). (a) Shows the effects of vehicle alone (○); BRL 38227 (10 μM) alone (●); BRL 38227 (10 μM) in combination with apamin (100 nM) (▲); and BRL 38227 (10 μM) in combination with guanethidine (50 μM) (■). (b) Shows the effects of vehicle alone (○); noradrenaline (10 μM) alone (●); noradrenaline (10 μM) in combination with apamin (100 nM) (▲) and noradrenaline (10 μM) in combination with guanethidine (50 μM) (■). Data points indicate the means of values from at least 10 tissue strips. Vertical bars indicate s.e. mean. Where used, apamin or guanethidine were present throughout. The horizontal bar indicates the period for which BRL 38227 (a) or noradrenaline (b) or their vehicles were present.
*indicates a significant ($P<0.05$ difference) from the corresponding data point in the efflux curve for BRL 38227 alone (a) or for noradrenaline alone (b).

action of BRL 38227 in the transmurally-stimulated rat uterus (present study). Adrenergic neurone blocking agents, including guanethidine, bretylium and debrisoquine also reduced BRL 38227-induced $^{86}Rb^+$ efflux from bovine trachealis (Berry *et al.*, 1992) and guanethidine had a similar effect in guinea-pig taenia caeci (present study). In addition, bretylium is known to inhibit the outward K^+-current induced by the application of depolarizing voltage steps to chick cardiac myocytes (Bkaily *et al.*, 1988).

The ability of the adrenergic neurone blocking agents to antagonize both the smooth muscle relaxation and $^{86}Rb^+$ efflux which are stimulated by the KCOs (Berry *et al.*, 1992; Small *et al.*, 1992; present study) could indicate that these agents act directly as blockers of K_{KCO}. However, much speculation still surrounds the site and mechanism of action of the KCOs. Early studies (Standen *et al.*, 1989) indicated that an intermediate conductance (135pS), ATP-sensitive K^+-channel was involved. However, more recent data strongly suggest that a small conductance (10–20 pS) K^+-channel, the ATP- and Ca^{2+}-sensitivity of which remains to be determined, is the target activated by these agents (Kajioka *et al.*, 1991; Nakao & Bolton, 1991; Noack *et al.*, 1992a,b). Furthermore, the on-cell patch clamp studies of Kajioka *et al.* (1991), together with the results of binding experiments (Bray & Quast, 1992), are consistent with the view that the KCOs may act at a site which is discrete from the actual membrane K^+-channel, where they may initiate a series of biochemical changes which culminate in the channel opening. At present, therefore, it remains possible that the adrenergic neurone blocking agents could antagonize the action of the KCOs either at their primary binding site or by interfering with the biochemical changes by which they promote K^+-channel opening.

Are adrenergic neurone blocking agents selective K^+-channel inhibitors?

Charybdotoxin is a relatively selective inhibitor of the large conductance, Ca^{2+}-dependent K^+-channel (BK_{Ca}) (Cook & Quast, 1990). In guinea-pig isolated trachealis, charybdotoxin inhibited the relaxant action of isoprenaline, salbutamol, salmeterol and theophylline without inhibiting the relaxant action of KCOs such as cromakalim, pinacidil and RP 49356 (Jones *et al.*, 1990; Murray *et al.*, 1991; Cook & Small, 1992). This suggests that the relaxation of tracheal smooth muscle to agonists at β-adrenoceptors and to theophylline is mediated, at least in part, by the opening of BK_{Ca} channels. The fact that neither guanethidine (50 μM) nor bretylium (50 μM) antagonized isoprenaline or theophylline in relaxing guinea-pig isolated trachealis (Boyle *et al.*, 1987; Berry *et al.*, 1992; Small *et al.*, 1992) therefore suggests that these agents do not inhibit the activity of BK_{Ca} channels.

Apamin is a highly selective inhibitor of the small, Ca^{2+}-dependent K^+-channel (SK_{Ca}) (Cook & Quast, 1990). In guinea-pig taenia caeci, apamin inhibited the relaxant action of noradrenaline and the ability of noradrenaline to promote the efflux of $^{86}Rb^+$ from tissue preloaded with the radiotracer (Allen *et al.*, 1985; Weir & Weston, 1986; present study). In contrast, apamin failed to inhibit the ability of cromakalim to relax the taenia caeci (Weir & Weston, 1986) or the ability of cromakalim or its active enantiomer, BRL 38227, to promote $^{86}Rb^+$ efflux from the tissue (Weir & Weston, 1986; present study). These findings suggest that the relaxant action of noradrenaline in the taenia caeci, but not that of cromakalim, is mediated by the opening of SK_{Ca} channels in the plasmalemma. The present observations, that neither guanethidine (50 μM) nor bretylium (50 μM) inhibited the relaxant action of noradrenaline in the taenia caeci, and that guanethidine (50 μM) failed to modify the ability of noradrenaline to promote $^{86}Rb^+$ efflux from the tissue, indicate that, at this concentration, the adrenergic neurone blocking agents do not inhibit the apamin-sensitive SK_{Ca} channel.

If the ability of the adrenergic neurone blocking agents to inhibit the relaxant actions of KCOs in the trachea (Berry *et al.*, 1992; Small *et al.*, 1992) and in the aorta, taenia caeci and uterus (present study) indeed reflects their ability to inhibit the opening of K_{KCO}, then this can be achieved at concentrations (up to 50 μM) which do not also inhibit the opening of BK_{Ca} and SK_{Ca} channels. The adrenergic neurone blocking agents may therefore exhibit selectivity as inhibitors of K_{KCO} as opposed to other types of K^+-channel. It should be noted, however, that in the present study, a higher concentration (500 μM) of guanethidine or bretylium did profoundly antagonize BRL 38227 and, to a lesser extent, noradrenaline on the taenia caeci (Figures 1 and 2). This could suggest that, at high concentrations, the adrenergic neurone blocking agents can also inhibit SK_{Ca}.

J.L.B. was supported by Sandoz Pharma Ltd, G.E. by Pfizer Central Research, S.J.H. by the Medical Research Council, R.C.S. by Sandoz Pharma and the National Asthma Campaign, R.D.S. by Roche Products Ltd.

References

ALLEN, S.L., BEECH, D.J., FOSTER, R.W., MORGAN, G.P. & SMALL, R.C. (1985). Electrophysiological and other aspects of the relaxant action of isoprenaline in guinea-pig isolated trachealis. *Br. J. Pharmacol.*, **86**, 843–854.

BERRY, J.L., SMALL, R.C. & FOSTER, R.W. (1992). Tracheal relaxation induced by potassium channel opening drugs: its antagonism by adrenergic neurone blocking agents. *Br. J. Pharmacol.*, (in press).

BKAILY, G., PAYET, M.D., BENABDERRAZIK, M., SAUVE, R., RENAUD, J.F., BACANER, M. & SPERELAKIS, N. (1988). Intracellular bretylium blocks Na^+ and K^+ currents in heart cells. *Eur. J. Pharmacol.*, **151**, 389–397.

BOYLE, J.P., DAVIES, J.M., FOSTER, R.W., MORGAN, G.P. & SMALL, R.C. (1987). Inhibitory responses to nicotine and transmural stimulation in hyoscine-treated guinea-pig isolated trachealis; an electrical and mechanical study. *Br. J. Pharmacol.*, **90**, 733–744.

BRAY, K.M. & QUAST, U. (1992). A specific binding site for K^+-channel openers in rat aorta. *J. Biol. Chem.*, (in press).

COOK, N.S. & QUAST, U. (1990). Potassium Channel Pharmacology. In *Potassium Channels: Structure, Classification, Function and Therapeutic Potential.* ed. Cook, N.S., pp. 181–231. Chichester: Ellis Horwood Ltd.

COOK, S.J. & SMALL, R.C. (1992). Role of K^+-channel opening in salmeterol-induced relaxation of trachealis muscle. *Br. J. Pharmacol.*, **106**, 12P.

DRUKARCH, B., KITS, K.S., LEYSEN, J.E., SCHEPENS, E. & STOOF, J.C. (1989). Restricted usefulness of tetraethylammonium and 4-aminopyridine for the characterization of receptor-operated K^+-channels. *Br. J. Pharmacol.*, **98**, 113–118.

FOSTER, R.W. & HOLLINGSWORTH, M. (1985). Microcomputer integration of tension development, a versatile aid to concentration: response data collection and analysis. *Br. J. Pharmacol.*, **85**, 389P.

GRANGER, S.E., HOLLINGSWORTH, M. & WESTON, A.H. (1985). A comparison of several calcium antagonists on uterine, vascular and cardiac muscles from the rat. *Br. J. Pharmacol.*, **85**, 225–262.

HOLLINGSWORTH, M. (1975). Mechanical responses of rat isolated uterine horns to transmural stimulation. *Br. J. Pharmacol.*, **55**, 41–46.

HU, Z.W., HONDA, K., MURAD, F. & HOFFMAN, B.B. (1992). Prolonged exposure to catecholamines enhances sensitivity of smooth muscle relaxation induced by sodium nitroprusside and atriopeptin. *J. Pharmacol. Exp. Ther.*, **260**, 756–761.

JONES, T.R., CHARETTE, L., GARCIA, M.L. & KACZOROWSKI, G.J. (1990). Selective inhibition of relaxation of guinea-pig trachea by charybdotoxin, a potent Ca^{2+}-activated K^+-channel inhibitor. *J. Pharmacol. Exp. Ther.*, **255**, 697–706.

KAJIOKA, S., KITAMURA, K. & KURIYAMA, H. (1991). Guanosine diphosphate activates an adenosine 5'-triphosphate-sensitive K^+-channel in the rat portal vein. *J. Physiol.*, **444**, 397–418.

KIRPEKAR, M., KIRPEKAR, S.M. & PRAT, J.C. (1978). Reversal of guanethidine blockade of sympathetic nerve terminals by tetraethylammonium and 4-aminopyridine. *Br. J. Pharmacol.*, **62**, 75–78.

MURRAY, M.A., BERRY, J.L., COOK, S.J., FOSTER, R.W., GREEN, K.A. & SMALL, R.C. (1991). Guinea-pig isolated trachealis: the effects of charybdotoxin on mechanical activity, membrane potential changes and the activity of plasmalemmal K^+-channels. *Br. J. Pharmacol.*, **103**, 1814–1818.

NAKAO, K. & BOLTON, T.B. (1991). Cromakalim-induced potassium current in single dispersed smooth muscle cells of rabbit artery and vein. *Br. J. Pharmacol.*, **102**, 155P.

NOACK, Th., DEITMER, P., EDWARDS, G. & WESTON, A.H. (1992a). Characterisation of potassium currents modulated by BRL 38227 in rat portal vein. *Br. J. Pharmacol.*, **106**, 717–726.

NOACK, Th., EDWARDS, G., DEITMER, P., GREENGRASS, P., MORITA, T., ANDERSSON, P.-O., CRIDDLE, D., WYLLIE, M. & WESTON, A.H. (1992b). The involvement of potassium channels in the action of ciclazindol in rat portal vein. *Br. J. Pharmacol.*, **106**, 17–24.

SMALL, R.C., BERRY, J.L., FOSTER, R.W., BLARER, S. & QUAST, U. (1992). Analysis of the relaxant action of SDZ PCO 400 in airway smooth muscle from the ox and guinea-pig. *Eur. J. Pharmacol.*, (in press).

SMITH, R.D. & WESTON, A.H. (1991). Studies on the interaction between guanethidine and potassium channel blockers in rat anococcygeus. *Br. J. Pharmacol.*, **102**, 161P.

STANDEN, N.B., QUAYLE, J.M., DAVIES, N.W., BRAYDEN, J.E., HUANG, Y. & NELSON, M.T. (1989). Hyperpolarizing vasodilators activate ATP-sensitive K^+-channels in arterial smooth muscle. *Science*, **245**, 177–180.

STUTZIN, A., PARAVIC, F., ORMENO, G. & ORREGO, F. (1983). Guanethidine effects on the guinea-pig vas deferens are antagonized by the blockers of calcium-activated potassium conductance, apamin, methylene blue and quinine. *Mol. Pharmacol.*, **23**, 409–416.

WEIR, S.W. & WESTON, A.H. (1986). Effect of apamin on responses to BRL 34915, nicorandil and other relaxants in the guinea-pig taenia caeci. *Br. J. Pharmacol.*, **88**, 113–120.

(Received April 28, 1992
Revised May 18, 1992
Accepted May 22, 1992)

Br. J. Pharmacol. (1992), **107**, 296–302

The actions of two sensory neuropeptides, substance P and calcitonin gene-related peptide, on the canine hepatic arterial and portal vascular beds

P.G. Withrington

Department of Pharmacology, Faculty of Basic Medical Sciences, Queen Mary and Westfield College, Mile End Road, London E1 4NS

1 The two peptides, calcitonin gene-related peptide (CGRP) and substance P (SP) were administered individually as bolus injections into the separately perfused hepatic arterial and portal vascular beds of the anaesthetized dog to assess their actions and relative molar potencies at these sites.

2 CGRP caused an immediate dose-related increase in hepatic arterial flow when injected close-arterially, reflecting a fall in resistance. This vasodilator effect was slightly increased by the prior administration of the selective β_2-adrenoceptor antagonist, ICI 118,551.

3 On a molar basis, CGRP was more potent as an hepatic arterial vasodilator than the non-selective β-adrenoceptor agonist, isoprenaline (Iso).

4 Intra-portal injection of CGRP also evoked hepatic arterial vasodilatation unaccompanied by other cardiovascular changes.

5 CGRP in doses up to 10 nmol had no effect on portal vascular resistance when administered intra-portally.

6 SP evoked a rapid, dose-related increase in hepatic arterial flow when injected intra-arterially. The molar ED_{50} for this hepatic vasodilatation was 40.2 fmol, significantly less than the ED_{50} for either CGRP or Iso. SP was the most potent hepatic arterial vasodilator yet examined. The vasodilator effect of SP was slightly potentiated by prior β_2-adrenoceptor blockade.

7 SP caused hepatic arterial vasodilatation when administered by intra-portal injection; its absolute and relative potency was much reduced.

8 SP when injected intra-portally caused a graded increase in hepatic portal inflow resistance. The molar potency for this portal vasoconstriction was significantly greater than that for noradrenaline (NA); however, the maximum increase in portal resistance was significantly less to SP than to NA.

9 In view of the location of the peptides CGRP and SP within the afferent innervation of the liver, it is proposed that they play an important function in controlling the hepatic microvasculature in response to sensory stimuli, particularly those arising from changes in portal blood composition secondary to change in metabolic activity within the gastrointestinal tract (GIT).

10 Since the peptides are released from the GIT into the hepatic portal inflow, they may modify hepatic arterial blood flow, the extent of which is related to events within the GIT.

Keywords: Substance P; calcitonin gene related peptide; liver circulation; hepatic sensory innervation; portal system; hepatic artery; hepatic vasodilatation; portal vasoconstriction

Introduction

Substantial current interest in the microcirculation centres around the physiological significance and potential therapeutic value of a group of peptides, histochemically located in many vascular beds, with potent and varying actions on vascular and extravascular smooth muscle.

Calcitonin gene-related peptide (CGRP) is a 37 amino acid peptide, produced as a consequence of alternative processing of the calcitonin gene. It causes marked vasodilatation of peripheal vascular beds such as the mesenteric circuit (Marshall *et al.*, 1986) and spleen (Withrington, 1989). In the rat, CGRP has been identified, histochemically, within nerves in the tunica adventitia and media of the intra-hepatic distribution of both the hepatic artery and portal vein; staining reactions which are substantially reduced by bilateral vagotomy (Sasaki *et al.*, 1986). Substance P (SP) is a potent hypotensive agent with a widespread distribution throughout the body. It has been identified in nerves within the tunica adventitia of both the hepatic artery and portal vein of the rat (Sasaki *et al.*, 1984) and of man (Carlei *et al.*, 1988). The cell bodies of the SP-containing nerves in the portal vein and hepatic artery have been localized in the rat, by the technique of retrograde tracing, to spinal sensory ganglia T_8–T_{13} (Barja & Mathison, 1984). Simultaneous staining for both SP and CGRP has demonstrated their co-location within the innervation of the liver vasculature of the guinea-pig (Goehler *et al.*, 1988). Abrogation of these staining reactions to SP and CGRP occurs in the rat liver when capsaicin, the sensory neurotoxin, had been previously administered at the neonatal stage (Burt *et al.*, 1987). These observations indicate that the two peptides are associated with the hepatic sensory innervation and could modulate hepatic haemodynamics subsequent to their release from afferent nerve endings within the liver.

SP and CGRP are widely distributed throughout the gastrointestinal tract (Pernow, 1983; Uddman *et al.*, 1986) from where they may be released into the venous drainage to enter the liver in the portal vein. Therefore, the two peptides could modify hepatic arterial inflow, although present only in the portal supply, by using the 'transhepatic' routes (Richardson & Withrington, 1978b).

Since both SP and CGRP could influence hepatic haemodynamics either by release within the liver or entry in the portal vein, then a detailed analysis of the actions of the two peptides on hepatic arterial and portal vasculature is appropriate. The activity of CGRP on the liver vasculature has not

been reported previously although some of the present data has been presented in both a preliminary (Withrington, 1987b) and review (Withington & Richardson, 1990) form. Melchiorri *et al.*, (1977) described many of the hepatic vascular responses to SP and other tachykinins in the dog; the present experiments communicated in a preliminary form (Withrington, 1987a) confirm many of their observations and extend them.

Methods

The experiments were performed on 13 dogs (mean weight 25.4 ± 1.2 kg; range 15.0–32.0 kg) anaesthetized with an intravenous mixture of chloralose and urethane (50 and 500 mg kg^{-1} respectively) after induction with methohexitone sodium (6 mg kg^{-1}). The trachea was cannulated although respiration was always spontaneous. The right femoral vein was cannulated to administer additional anaesthetic when appropriate. The right femoral artery was cannulated to provide hourly blood samples for analysis of arterial P_{CO_2}, P_{O_2} and pH; $NaHCO_3$ was administered i.v. (1.0 mmol min^{-1}) if considered necessary to maintain normal arterial pH. The left carotid artery was cannulated and connected to a strain gauge transducer (Statham P23Gb) to provide continuous registration of systemic blood pressure; heart rate was derived electronically from this signal. Body temperature was maintained within normal limits, as indicated by a buccal thermometer, with either table heaters or overhead lamps. The animals were heparinised (500 iu kg^{-1}) once perfusion had started and half this dose administered hourly.

The surgery and perfusion circuits required for separate hepatic arterial and portal perfusion have been described in detail recently (Corder & Withrington, 1988; Withrington *et al.*, 1990) and in all major details the same procedures were adopted here. Essentially the hepatic artery was cannulated and perfused with arterial blood derived from the cannulated left femoral artery. Incorporated into the arterial perfusion circuit was an electromagnetic flow probe (Cardiovascular Instruments) to measure phasic and mean flows (HABF), a strain gauge transducer (Statham P23Gb) to measure mean perfusion pressure (HAPP) and a T piece to permit the intra-arterial administration of vasoactive substances. The signals were continuously recorded on a chart recorder (Devices M19) and also processed by an IBM PC-XT computer programmed to calculate hepatic arterial vascular resistance (HAVR). In some of these hepatic arterial perfusion experiments the spleen was removed and a catheter inserted into the splenic vein and advanced down into the portal vein; vasoactive substances could then be injected intra-portally. Once the arterial perfusion had been successfully established then the preparation remained stable for between 4 to 6 h. In most experiments, therefore, between 8 and 12 complete dose-response curves to various vasoactive agonists could be obtained. In the present experiments at least one, and usually two dose-response curves to either SP and CGRP were constructed in each experiment. These numbers are indicated in the text. Between dose-response curves to the peptides a partial dose-response curve to the test agonist, in this case isoprenaline was repeated to ascertain that no change in the arterial responses to that agonist had occurred either as the result of prior administration of either of the peptides or as the consequence of deterioration in the preparation.

The technique for perfusion of the portal inflow requires retrograde cannulation of the splenic vein followed by ligation of the portal vein immediately beyond the entrance of the superior mesenteric vein. The diverted mesenteric drainage can then be pumped from a reservoir, under controlled conditions of pressure and flow, into the cannulated hepatic end of the portal vein. An electromagnetic flow probe, strain gauge pressure transducer and a 'T' piece are incorporated into the perfusion circuit. A long polythene cannula was inserted into a femoral vein and advanced along the interior vena cava (IVC) to a point opposite the hepatic veins to provide a continous recording of IVC pressure (IVCP). From these recordings of mean hepatic portal flow (HPVF), mean hepatic portal perfusion pressure (HPVP) and IVCP, hepatic portal inflow vascular resistance (HPVR = HPVP-IVCP/HPVF)) was calculated. Vasoactive substances could be injected directly into the portal stream through the 'T' piece.

The flow probes were calibrated with whole blood at the end of each experiment and the liver weighed so that all flows could be expressed in terms of 100 g weight.

Drugs used and vehicles

Vasoactive substances (isoprenaline, CGRP, SP, noradrenaline) were washed in with saline (0.9% w/v NaCl solution) to give a constant injectate of 2.0 ml. Human α-CGRP (Bachem) and SP (Sigma) were made up in sterile saline which contained human serum albumin (10 mg ml^{-1}; Elstree) and polypep (2.5 mg ml^{-1}; low viscosity; Sigma). These additions to the vehicle reduced non-specific binding of CGRP and SP onto plastic surfaces. Close arterial or intraportal injections of the vehicle plus additions did not alter either hepatic arterial or portal vascular resistances. (±)-Isoprenaline hydrochloride (Pharmax Ltd.) and (−)-noradrenaline acid tartrate (Winthrop) were diluted immediately before use with normal saline and containers maintained in ice. In three of the hepatic arterial perfusions the selective β_2-adrenoceptor antagonist, ICI 118,551 (erythro-DL-1-(-7-methylindan-4-yloxy)-3-isopropylamino-butan-2-ol; mol wt 277) was administered by intra-arterial injection, after the initial control responses to adrenaline, substance P and calcitonin gene-related peptide had been obtained.

Statistics

Results are presented as mean ± standard errors of the mean (s.e.mean). Tests for significance refer to either Student's *t* or paired *t* tests. Individual molar ED_{50} values were calculated for each individual dose-response curve as a percentage of the maximum response for that curve; arithmetic mean molar ED_{50} values were then calculated.

Results

Control values

In the 8 hepatic arterial perfusion experiments the mean liver weight was 580 ± 35 g representing 2.30 ± 0.06% of the body weight. The initial mean hepatic arterial blood flow, perfusion pressure and inflow vascular resistance were 210 ± 14.1 ml min^{-1}, 161 ± 5.4 mmHg and 0.79 ± 0.05 mmHg ml^{-1} min, respectively. In the five hepatic portal perfusion experiments the mean liver weight was 547 ± 25 g. The mean initial hepatic portal venous flow was 218 ± 37 ml min^{-1} whilst the mean hepatic portal venous pressure was 9.36 ± 0.44 mmHg. Since the mean IVC pressure was 1.22 ± 0.38 mmHg then the mean hepatic portal perfusion pressure was 8.14 ± 0.09 mmHg and the calculated hepatic portal inflow resistance 0.043 ± 0.008 mmHg ml^{-1} min. Once portal perfusion had started, the mean initial systemic blood pressure was 130 ± 8.8 mmHg. These hepatic arterial and portal control values are similar to those reported previously from this laboratory (Corder *et al.*, 1988; Withrington *et al.*, 1990).

Hepatic arterial vascular responses to intra-arterial injections

Isoprenaline The hepatic arterial vascular response to intra-arterial bolus doses of the non-selective β-adrenoceptor agonist isoprenaline (Iso) was a short lasting, dose-

dependent, increase in arterial flow (Figure 1), representing a fall in inflow resistance and hepatic arterial vasodilatation. In each of the hepatic arterial perfusions, a complete dose-response curve to Iso was constructed (Figure 2). The mean threshold dose for the vasodilator effect was either 0.05 or 0.10 nmol whilst the maximum response was achieved at between 20 and 50 nmol. The mean maximum increase in hepatic arterial blood flow to Iso was 61.6 ± 11% of control; the mean reduction in inflow resistance was 38.9 ± 4.2% of control. The mean molar ED_{50} for Iso i.e. the mean molar dose to reduce the hepatic arterial inflow resistance to 50% of the maximum response to Iso in each experiment, was 0.97 ± 0.32 nmol. All these values are within the range previously reported for responses to Iso in similar preparations (Withrington *et al.*, 1990).

Calcitonin gene-related peptide In 5 hepatic arterial perfusions intra-arterial bolus injections of CGRP were made over the dose range 0.1–200 pmol to construct 8 complete dose-response curves from threshold to maximum. At each dose above threshold (usually 0.5 or 1.0 pmol) the peptide caused an increase in arterial flow of slightly longer duration than to iso (Figure 1) and graded with dose (Figures 1 and 2). A vasoconstrictor response to CGRP was never observed. The maximum increase in flow to CGRP was 36.1 ± 5.1% control and the mean maximum fall in resistance was 28.1 ± 2.8% of the control. Both these values are significantly less than the maximum changes in flow and resistance to Iso ($P < 0.05$ for both). The mean molar ED_{50} for CGRP was 10.7 ± 2.44 pmol; a value significantly less ($P < 0.01$) than that for Iso.

Substance P In 6 of the arterial preparations SP was administered by close arterial bolus injections over the dose-range 1.0 fmol to 10 pmol to construct 9 complete dose-response curves (Figure 2). The vascular response consisted of a dose related increase in blood flow of short duration and characteristically of rapid onset (Figure 1). An hepatic arterial vasoconstrictor response to SP was never observed. In most preparations the threshold dose was between 1.0 and 5.0 fmol; much lower than any vasodilator peptide yet examined in this preparation. The maximum arterial vasodilator response was achieved at between 1.0 and 5.0 fmol SP. The mean molar ED_{50} for SP was 40.2 ± 10.4 fmol; a value significantly less than either CGRP ($P < 0.01$) or Iso ($P < 0.001$). The mean maximum increase in hepatic arterial blood flow to SP was 77.0 ± 10.0% ($n = 9$) of the pre-injection control flow and the mean maximum reduction in hepatic arterial inflow vascular resistance was 46.9 ± 3.1% expressed as a percentage reduction of the control pre-injection resistance. These maximum changes in flow and resistance are significantly different from the maximum values for CGRP ($P < 0.01$; $P < 0.001$ respectively) but not to those for Iso ($P > 0.1$ for both). The paper speed in these

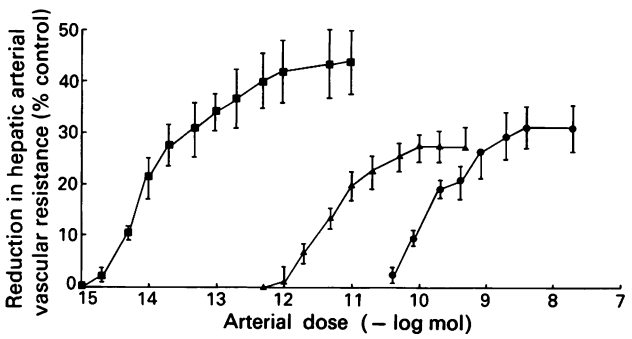

Figure 2 Mean results obtained in 8 liver perfusions illustrating the relationship between the percentage reduction in hepatic arterial vascular resistance from control (vasodilatation) in response to the close arterial molar dose of substance P (■, $n = 5–9$), calcitonin gene-related peptide (▲, $n = 5–8$) and the non selective β-adrenoceptor agonist, isoprenaline (●, $n = 8$). Individual symbols represent the means and the vertical lines the standard errors of those means.

experiments did not permit a discriminating resolution of the latent interval between bolus administration and the start of the local vascular response; statistical analysis of the time course of onset of the arterial vasodilatation to SP compared with either Iso or CGRP was not possible.

Hepatic arterial responses after β_2-adrenoceptor blockade

In 3 preparations dose-response curves to Iso, CGRP and SP were constructed before, and after, the i.v. administration of the β_2-adrenoceptor antagonist, ICI 118,551 (3.6 μmol kg^{-1}) which caused a significant increase in mean perfusion pressure from a mean control of 148 ± 1.1 mmHg to 157 ± 0.7 mmHg ($P < 0.01$), a reduction in control mean hepatic arterial mean blood flow from 224 ± 2.6 ml min^{-1} to 172 ± 3.9 ml min^{-1} ($P < 0.001$) and therefore a significant increase in basal hepatic arterial vascular resistance from 0.67 ± 0.01 mmHg ml^{-1} min to 0.93 ± 0.02 mmHg ml^{-1} min ($P < 0.001$). In each experiment the hepatic arterial vasodilator responses to Iso were antagonized as indicated by the shift of the dose-response curve to the right (Figure 3) and by a 6–10 times increase in the molar ED_{50}. In contrast, the responses to both CGRP and SP were not antagonized but, apparently, potentiated since the dose-response curves to these peptides were shifted to the left whilst the molar ED_{50} for each was reduced by a factor 6–10 and 25–30 times, respectively. The changes in the molar ED_{50} to Iso, SP and CGRP after β_2-adrenoceptor blockade were significant ($P < 0.01$, 0.05 and 0.01 respectively; paired t test; $n = 3$). The shift to the left for the peptide-induced vasodilator responses reflects the consequence of an increased basal vascular tone from which any vasodilatator responses were evoked.

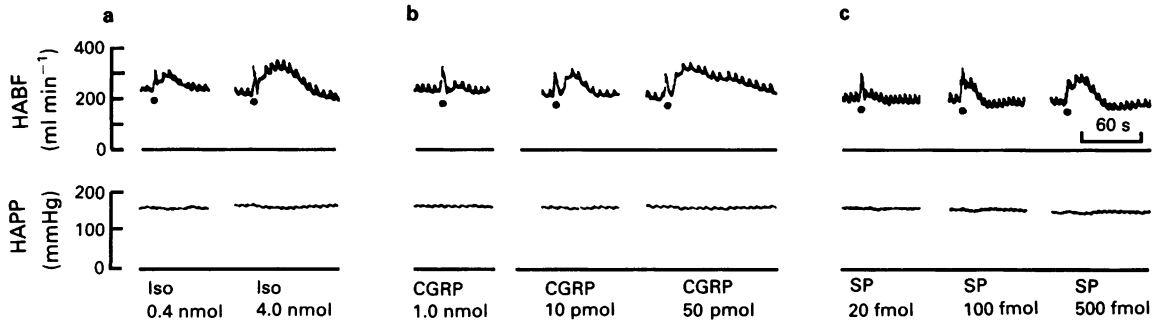

Figure 1 Experimental records illustrating the changes in hepatic arterial blood flow (HABF) and hepatic arterial perfusion pressure (HAPP) in response to the intra-arterial bolus injections of (a) the non-selective β-adrenoceptor agonist, isoprenaline (Iso, 0.4 and 40 nmol), (b) calcitonin gene-related peptide (CGRP, 1.0, 10 and 50 pmol) and (c) substance P (SP, 20, 100, 500 fmol). Liver weight 502 g.

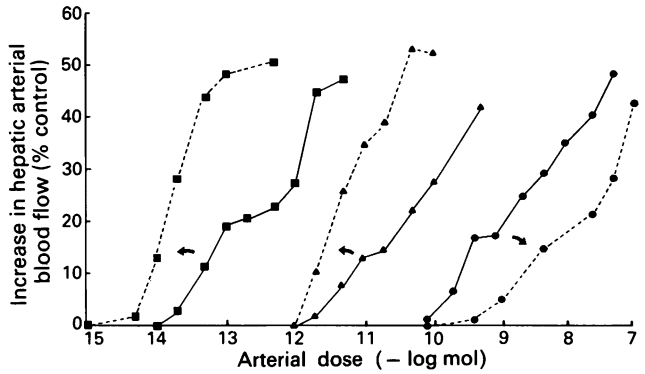

Figure 3 Results obtained in one experiment (liver weight 602 g) illustrating the relationship between the percentage increase in hepatic arterial blood flow (vasodilatation) in response to the close arterial injection of substance P (■), calcitonin gene-related peptide (▲) and isoprenaline (●) before (continuous lines ——) and after (broken lines – – –) the i.v. administration of the selective β_2-adrenoceptor antagonist, ICI 118,551 (3.6 μmol kg^{-1}). The mean (± s.e.) control perfusion pressure and flow was 161 ± 1.7 mmHg and 200 ± 1.90 ml min^{-1} before, and 158 ± 0.33 mmHg and 154 ± 4.41 ml min^{-1} after, ICI 118,551.

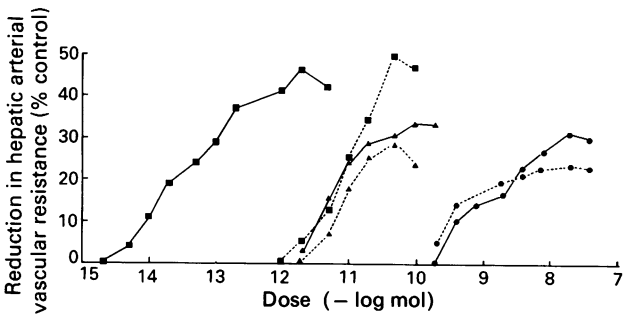

Figure 4 The results obtained in a single experiment (liver weight 642 g) illustrating the relationships between the percentage reduction in hepatic arterial vascular resistance (vasodilatation) and the intra-arterial (continuous line, ——) and intra-portal (interrupted line – – –) molar dose of substance P (■), calcitonin gene-related peptide (▲) and isoprenaline (●). The mean (± s.e.) control values for pressure perfusion and flow were 130 (± 2.41) mmHg and 165 (± 7.3) ml min^{-1}, respectively (n = 45).

Hepatic arterial vascular responses to intra-portal bolus injections

Isoprenaline In the present experiments, Iso was administered as a bolus injection in graded doses into the portal vein, via the splenic vein, as described in the Methods. The effect was to induce vasodilatation of the hepatic arterial vasculature (Figure 4) without significant changes in systemic parameters. A ratio (portal bolus dose required to produce the same arterial response as that evoked by the intra-arterial molar ED_{50} dose/arterial molar ED_{50} dose) was calculated. For Iso, in the present experiments the arterial ED_{50} was 0.97 nmol and the portal dose to produce the same hepatic arterial vasodilator response was 4.7 nmol giving a mean portal/arterial dose ratio of 4.87.

Calcitonin gene-related peptide CGRP was also administered intra-portally over the dose range 1.0–500 pmol and caused hepatic arterial vasodilatation at doses above 10 pmol in (Figure 4) the absence of any systemic changes. In these experiments, the mean arterial molar ED_{50} for CGRP was 4.7 pmol whilst the mean portal dose to evoke the same arterial vasodilatation was 55 pmol giving a portal/arterial dose ratio of 11.7

Substance P SP was administered as an intra-portal bolus over the dose-range 0.1 fmol to 10 pmol. The hepatic arterial vascular response to intra-portal SP, once the threshold dose had been achieved, was always vasodilatation. The threshold portal dose of SP to cause hepatic arterial vasodilatation was usually 1.0 pmol. The mean arterial molar ED_{50} dose for SP was 42 fmol; however, it was clear in all these experiments that there was a substantial shift in the position of the hepatic arterial dose response curve to intra-portal SP (Figure 4) since a much larger dose of SP was required to be administered intra-portally to obtain the equivalent hepatic arterial vasodilatation to any dose of SP administered intra-arterially. The mean intra-portal dose of SP to induce the same arterial dilatation as the arterial ED_{50} was 13.3 pmol giving a portal/arterial dose ratio of 317.

Hepatic portal vascular responses to intra-portal injections

Noradrenaline Intra-portal bolus injections of nordrenaline (NA) were made in all 5 portal perfusion experiments over the dose range 0.5–600 nmol to provide a test agonist for molar comparisons. Graded increases in portal perfusion pressure were obtained (Figure 5) which reflect increases in portal inflow resistance; vascular responses previously shown (Richardson & Withrington, 1978a) to be mediated by α-adrenoceptors since they are antagonized by phentolamine. In the present series, the threshold intra-portal dose of NA was 6.0 nmol; the molar ED_{50} could not be calculated since high intra-portal doses of NA caused marked systemic cardiovascular changes which altered the conditions of the perfusion.

Calcitonin gene-related peptide Intra-portal bolus injections of CGRP were made in 3 experiments over the dose range 0.1–10 nmol. There was no clear change in portal inflow pressure in either direction (Figure 5) indicating, at constant volume, no equivocal change in portal inflow resistance. The larger intra-portal doses of CGRP were accompanied by systemic effects such as hypotension and tachycardia, indicating the biological activity of the injectate, its entrance into the systemic circuit and survival, at high dose levels, after passage through the liver and cardiopulmonary circuit.

Substance P Intra-portal bolus injections of SP were made in 4 portal perfusion experiments over the dose-range 1.0 pmol–10 nmol. In contrast to the effects of CGRP, there were graded increases in heptic portal inflow pressure (Figure 5), indicating, at constant portal inflow volume, an increase in portal inflow resistance. At the higher intra-portal bolus doses of SP, there were marked systemic effects indicating entry of the peptide into the systemic circulation causing peripheral vasodilatation and hypotension. A comparison of the molar dose-response curves of SP and NA (Figure 6) reveals that, in terms of increasing the hepatic portal inflow resistance SP is more potent than NA since the mean threshold

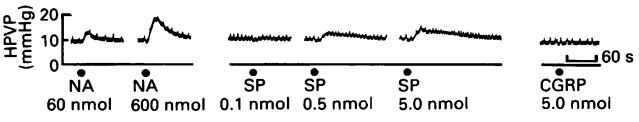

Figure 5 Experimental records illustrating the changes in hepatic portal venous pressure (HPVP) in response to the intra-portal bolus injections of noradrenaline (NA, 60 and 600 nmol), substance P (SP, 0.1, 0.5 and 5.0 nmol) and calcitonin gene-related peptide (CGRP, 5.0 nmol). The portal circuit was perfused at constant flow (200 ml min^{-1}) throughout with blood derived from the mesenteric circuit. Liver weight 577 g.

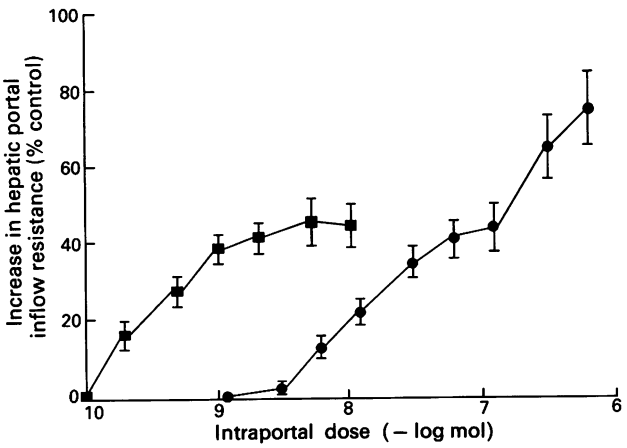

Figure 6 Mean results obtained in 5 portal perfusions illustrating the relationship between the percentage increase in portal vascular resistance compared with control (portal vasoconstriction) and the intra-portal molar dose of substance P (■) and noradrenaline (●). Individual symbols represent the means and the vertical lines the standard errors of either 4 or 5 observations.

dose to SP (either 0.1 or 0.2 pmol) and NA (1.0 or 0.6 nmol) were very different and the intra-portal dose of SP required to elevate the portal inflow resistance by 30% of the control was significantly less ($P < 0.01$) for SP (mean 0.87 ± 0.11 nmol) than the mean value for NA (22.7 ± 3.7 nmol). However, it was apparent that the mean maximum increase in portal inflow resistance for SP ($52.4 \pm 7.1\%$) was significantly less ($P < 0.05$) than that achieved with the highest doses of NA (mean $82.7 \pm 9.8\%$ increase in HPVR) used in these experiments, even though these doses did not, for reasons outlined above, evoke the maximum change possible in response to NA administration.

Discussion

The present study clearly demonstrates the high molar potency and intrinsic vasodilator efficacy of the two sensory neuropeptides, SP and CGRP, in inducing hepatic arterial vasodilatation. Using the molar ED_{50} (the molar dose to reduce hepatic arterial vascular resistance to 50% of the maximum effect) as a basis for comparison then SP and CGRP were over 24,000 and 90 times, respectively, more potent than the non-selective β-adrenoceptor agonist, isoprenaline. These values reveal SP to be the most potent hepatic arterial vasodilator yet examined. The mechanism of these vasodilator responses does not involve activation of β_2-adrenoceptors since the responses were not inhibited by selective blockade with ICI 118,551. Recent evidence (Brizzolara & Burnstock, 1991) suggests that the origin of the vasodilator response is different for the two peptides since in isolated rings of the rabbit hepatic artery the relaxant properties of SP were annulled by removal of the endothelium whilst the responses to CGRP were unaffected.

In contrast, SP and CGRP were very different in their potencies and vascular actions on the hepatic portal resistance sites. CGRP, in intra-portal bolus doses up to 10 nmol, produced no change in portal inflow resistance in either direction. This has been observed with many peptides that are active vasodilator agents on the hepatic arterial circuit (Withrington & Richardson, 1986). Although SP was inactive on portal resistance over the fmol and pmol range of intra-portal injections, when the dose of SP was increased into the nmol range then graded increases in portal inflow resistance were obtained. These doses of SP were considerably higher than those administered into the portal vein by Melchiorri *et al.* (1977) who failed to observe any changes in portal inflow resistance to SP. The portal vasoconstriction observed to SP was, in the present experiments, dose-related but the intrinsic efficacy for SP was lower than that for NA. The precise anatomical site of intra-hepatic portal resistance cannot be established with the present experiment, but isolated preparations of the portal vein have been shown to contract to SP (Mastrangelo *et al.*, 1983) which would indicate that the intrahepatic pre-sinusoidal terminations of the portal vein may be sensitive to this agonist property of SP.

Both CGRP and SP cause hepatic arterial vasodilatation when injected into the portal vein without any accompanying cardiovascular changes indicative of systemic entry of the peptide. These results confirm previous observations (Richardson & Withrington, 1978b; Lautt *et al.*, 1984) describing 'transhepatic' routes whereby vasoactives substances present in one of the hepatic inflow circuits may nevertheless modify the inflow resistance of the other circuit. The marked rightward shift in the location of the dose-response curve (Figure 4) relating the hepatic arterial vasodilator response to SP as the result of intra-portal administration may be related to the ability of SP to increase portal inflow resistance. An increase in inflow resistance as a result of presinusoidal portal constriction would lead to substantial changes in hepatic microcirculation and redistribution of peptide and reduced access to arterial resistance sites. However, the reduced arterial response to intra-portal SP may also reflect a rapid destruction of SP following intra-portal administration (Melchiorri *et al.*, 1977) since over 80% of portal infused SP is eliminated by the liver (Lembeck *et al.*, 1978).

Although the precise mechanisms and route by which vasoactive substances present in the portal inflow have access to the arterial resistance sites have not been established, the functional implications are substantial since it implies that, in the present context, portal levels of SP and CGRP may determine hepatic arterial inflow.

The principal source of systemic plasma SP appears to be the gut (Gamse *et al.*, 1978) but due to the rapid hepatic destruction the portal plasma levels of SP are 4–5 times that circulating in the peripheral systemic plasma. The elevated systemic plasma levels of CGRP and SP reported in liver disease (Bendtsen *et al.*, 1991; Hortnagl *et al.*, 1984) demonstrate the normal function of the liver in clearing the peptides from the circulation and, more relevant in the present context, the vasodilator activity of these levels of the peptides since they were associated with significant reductions in peripheral vascular resistance. Normally, such levels of CGRP and SP, originating from the GIT, would enter the liver in the portal inflow where they could initiate substantial alterations in the hepatic microcirculation including increased arterial inflow into the sinusoids. In addition, portal levels of both peptides may be increased by activity within the gut related to the digestive process. In vascular perfused, isolated small intestine preparations of guinea-pig (Baron *et al.*, 1983; Donnerer *et al.*, 1984), dog (Manaka *et al.*, 1989) and man (Grider, 1989) significant release of SP into the venous effluent may accompany either experimental stretch of the preparation or electrical field stimulation at high frequencies (40 Hz). There is, to date, little evidence of the release of CGRP from the GI tract in response to physiological stimuli although mesenteric periarterial nerve stimulation (Fujimori *et al.*, 1989) does evoke substantial overflow of CGRP into the venous effluent following activation at frequencies within the physiological range.

In addition to their distribution along the GI tract both SP and CGRP-like immunoreactivity has been demonstrated within the liver itself. The peptides are usually co-located within nerves fibres associated with vascular structures. The staining characteristics of these fibres are abrogated after treatment of the animals with the sensory neurotoxin, capsaicin, indicating an intimate relationship between SP, CGRP and the sensory innervation of the hepatic vasculature. These reported observations on the intrahepatic location of SP and

CGRP and the present study showing the high molar potency of the peptides as hepatic arterial vasodilators prompts a re-examination of the role of the afferent innervation in the control of hepatic haemodynamics.

In the rat isolated liver, increases in portal perfusate osmolarity were accompanied by an increase in hepatic vagal afferent discharge (Adachi *et al.*, 1976); experimental elevations of portal osmolarity has been established to lead to hepatic arterial vasodilatation in both the cat (Lautt *et al.*, 1977) and dog (Richardson & Withrington, 1979). Whilst some of the arterial vasodilatation may be due to direct smooth muscle relaxation due to hyperosmolarity a component may be due to the intrahepatic release of sensory neuropeptides concomitant with afferent terminal activation.

In the guinea-pig, elevated portal pressure leads to an increase in afferent activity in filaments of the hepatic splanchnic nerve (Niijima, 1977), a procedure which is known to cause reduction in hepatic arterial inflow resistance (Richardson & Withrington, 1978b). Lautt *et al.* (1985) have proposed that this reciprocity between the two inflow circuits of the liver may depend upon the intrahepatic synthesis and release of adenosine; another contributory factor may be the release of sensory neuropeptides, SP and CGRP both of which are substantially more potent as hepatic arterial vasodilators than adenosine.

In addition, sensory mechanisms exist within the portal inflow system sensitive to changes in portal glucose concentration (Nijiima, 1982), portal sodium levels (Andrews & Orbach, 1974) and portal blood temperature (Adachi & Nijiima, 1982) as detected by increased afferent activity in either hepatic vagal or splanchnic nerve filaments. Clearly there now exists a mechanism by which hepatic microcirculatory events and the distribution of portal blood may be modified by afferent activity sensing changes in the portal inflow composition. An essential component leading to an appropriate re-distribution of portal blood is the release of highly potent vasodilator neuropeptides from the afferent innervation with access to arterial smooth muscle resistance sites.

It has been established experimentally that there are significant increases in total liver blood flow during digestion and that a component of this is arterial vasodilatation. The release of the potent vasodilator peptides SP and CGRP from both the gut and the sensory innervation to the liver itself may play a contributory role in this hyperaemia and in this way relate the hepatic arterial supply to events within the gastrointestinal tract.

References

ADACHI, A. & NIIJIMA, A. (1982). Thermosensitive afferent fibres in hepatic branch of the vagus nerve in guinea-pig. *J. Auton. Nerv. System.*, **5**, 101–109.

ADACHI, A., NIIJIMA, A. & JACOBS, H.L. (1976). An hepatic osmoreceptor mechanism in the rat: electrophysiological and behavioral studies. *Am. J. Physiol.*, **231**, 1043–1049.

ANDREWES, W.H.H. & ORBACH, J. (1974). Sodium receptors activating some nerves of perfused rabbit livers. *Am. J. Physiol.*, **227**, 1273–1275.

BARJA, F. & MATHISON, R. (1984). Sensory innervation of the rat portal vein and hepatic artery. *J. Auton. Nerv. System.*, **10**, 117–125.

BARON, S.A., JAFFE, B.M. & GINTZLER, A.R. (1983). Release of substance P from the enteric nervous system: direct quantitation and characterization. *J. Pharmacol. Exp. Ther.*, **227**, 365–368.

BENDTSEN, F., SCHIFTER, S. & HENRIKSEN, J.H. (1991). Increased circulating calcitonin gene-related peptide (CGRP) in cirrhosis. *J. Hepatol.*, **12**, 118–123.

BRIZZOLARA, A.L. & BURNSTOCK, G. (1991). Endothelium-dependent and endothelium-independent vasodilatation of the hepatic artery of the rabbit. *Br. J. Pharmacol.*, **103**, 1206–1212.

BURT, A.D., GILLON, M., WISSE, E., POLAK, J.M. & MACSWEEN, R.N.M. (1987). Distribution of calcitonin gene related peptide (CGRP) and substance P containing nerves in the liver: an immuno-histochemical study. *Gut*, **28**, A1330.

CARLEI, F., LYGIDAKIS, M.J., SPERANZA, V., BRUMMELKAMP, W.H., MCGURRIN, J.F., PIETROLETTI, R., LEZOCHE, E. & BOSTWICK, D.G. (1988). Neuro-endocrine innervation of the hepatic vessels in the rat and in man. *J. Surg. Res.*, **45**, 417–426.

CORDER, R. & WITHRINGTON, P.G. (1988). The actions of neuropeptide Y and peptide YY on the hepatic arterial and portal vascular beds of the anaesthetised dog. *Br. J. Pharmacol.*, **94**, 1149–1156.

DONNERER, J., BARTHO, L., HOLZER, P. & LEMBECK, F. (1984). Intestinal peristalsis associated with release of immunoreactive substance P. *Neuroscience*, **11**, 913–918.

FUJIMORI, A., SAITO, A., WATANABE, T., UCHIYAMA, Y., KAWASAKI, H. & GOTO, K. (1989). Neurogenic vasodilatation and release of calcitonin gene related peptide (CGRP) from perivascular nerves in the rat mesenteric artery. *Biochem. Biophys. Res. Commun.*, **165**, 1391–1398.

GAMSE, R., MROZ, E., LEEMAN, S. & LEMBECK, F. (1978). The intestine as the principal source of immunoreactive substance P in plasma of the cat. *Naunyn-Schmiedebergs Arch. Pharmacol.*, **305**, 17–21.

GOEHLER, L.E., STERNINI, C. & BRACHA, N.C. (1988). Calcitonin gene releated peptide immuno-reactivity in the biliary pathway and liver of the guinea-pig: distribution and co-localisation with substance P. *Cell Tissue Res.*, **253**, 145–150.

GRIDER, J.R. (1989). Identification of neurotransmitters regulating intestinal peristatic reflex in humans. *Gastroenterology*, **97**, 1414–1419.

HORTNAGL, H., LENZ, K., SINGER, E.A., KLEINBERGER, G. & LOCHS, H. (1984), Substance P is markedly increased in plasma of patients with hepatic coma. *Lancet*, **i**, 480–483.

LAUTT, W.W., LEGARE, D.J. & D'ALMEIDA, M. (1985). Adenosine as putative regulator of hepatic arterial flow (the buffer response). *Am. J. Physiol.*, **248**, H331–H338.

LAUTT, W.W., LEGARE, D.J. & DANIELS, T.R. (1984). The comparative effect of administration of substances via the hepatic artery or portal vein on hepatic arterial resistance, liver blood volume and hepatic extraction in cats. *Hepatol.*, **4**, 497–502.

LAUTT, W.W., MACLACHLAN, T.L. & BROWN, L.C. (1977). The effect of hypertonic infusions on hepatic blood flows and liver volume in the cat. *Can. J. Physiol. Pharmacol.*, **55**, 1339–1344.

LEMBECK, F., HOLZER, P., SCHWEDITSCH, M. & GAMSE, R. (1978). Elimination of substance P from the circulation of the rat and its inhibition by bacitracin. *Naunyn-Schmiedebergs Arch. Pharmacol.*, **305**, 9–16.

MANAKA, H., MANAKA, Y., KOSTOLANSKA, F., FOX, J.E.T. & DANIEL, E.E. (1989). Release of VIP and substance P from isolated perfused canine ileum. *Am. J. Physiol.*, **257**, G182–190.

MARSHALL, I., AL-KALWIM, S.J., HOLMAN, J.J. & CRAIG, R.K. (1986). Human and rat α-CGRP but not calcitonin cause mesenteric vasodilatation in rats. *Eur. J. Pharmacol.*, **123**, 217–222.

MASTRANGELO, D., MATHISON, R. & HUGGEL, H. (1983). Post-junctional localisation of substance P receptors in rat portal vein. *Pharmacology*, **27**, 305–318.

MELCHIORRI, P., TONELLI, F. & NEGRI, L. (1977). Comparative circulatory effects of substance P, eledoisin and physalemin in the dog. In *Substance P.*, ed. von Euler, U.S. & Pernow, B. pp. 311–319. New York: Raven Press.

NIIJIMA, A. (1977). Afferent discharges from venous pressoreceptors in the liver. *Am. J. Physiol.*, **232**, C76–81.

NIIJIMA, A. (1982). Glucose-sensitive afferent nerve fibres in the hepatic branch of the vagus nerve in the guinea pig. *J. Physiol.*, **332**, 315–323.

PERNOW, B. (1983). Substance P. *Pharmacol. Rev.*, **35**, 75–141.

RICHARDON., P.D.I. & WITHRINGTON, P.G. (1978a). Alpha and beta adrenoceptors in the hepatic portal venous bed of the dog. *Br. J. Pharmacol.*, **62**, 376P.

RICHARDSON, P.D.I. & WITHRINGTON, P.G. (1978b). Pressure-flow relationships and the effects of noradrenaline and isoprenaline on the simultaneously perfused hepatic arterial and portal venous vascular beds in the dog. *J. Physiol.*, **282**, 451–470.

RICHARDSON, P.D.I. & WITHRINGTON, P.G. (1979). Effects of intraportal infusions of hypertonic solutions on hepatic haemodynamics in the dog. *J. Physiol.*, **301**, 82–83P.

SASAKI, Y., HAYASHI, N., KASAHARA, A., MATSUDA, H., FUSAMOTO, H., SATO, H., HILLYARD, C.J., GIRGIS, S., MACINTYRE, I., WEMSON, P., SHIOSAKA, S., TOHYAMA, M., SHIOTANI, Y. & KAMADA, T. (1986). Calcitonin gene related peptide in the hepatic and splanchnic systems of the rat. *Hepatol.*, **6**, 676–681.

SASAKI, Y., KAMADA, T., HAYASHI, N., SATO, N., KASAHARA, A., FUSAMOTO, H., SHIOSAKA, S., TOHYAMA, M. & SHIOTANI, Y. (1984). Immunohistochemical distribution of glucagon, substance P and vasoactive intestinal polypeptide in hepatic vasculature of the rat. *Hepatol.*, **4**, 1184–1189.

UDDMAN, R., EDVINSSON, L., EKBLAD, E., HAKANSON, R. & SUNDLER, F. (1986). Calcitonin gene-related peptide (CGRP): perivascular distribution and vasodilator effects. *Reg. Peptides.*, **15**, 1–23.

WITHRINGTON, P.G. (1987a). Substance P: the most potent hepatic arterial vasodilator yet examined? *J. Hepatol.*, **4**, 16.

WITHRINGTON, P.G. (1987b). The vasodilator potency of calcitonin gene related peptide on the hepatic arterial vasculature of the dog. *Br. J. Pharmacol.*, **90**, 198P.

WITHRINGTON, P.G. (1989). The relaxant properties of human calcitonin gene-related peptide on vascular and extravascular (capsular) smooth muscle of the isolated blood-perfused spleen of the anaesthetised dog. *Br. J. Pharmacol.*, **96**, 823–828.

WITHRINGTON, P.G., DHUME, V.G., CROXTON, R. & GERBES, A.L. (1990). The actions of human atrial natriuretic factor on hepatic arterial and portal vascular beds of the anaesthetised dog. *Br. J. Pharmacol.*, **99**, 810–814.

WITHRINGTON, P.G. & RICHARDSON, P.D.I. (1986). Hepatic haemodynamics and microcirculation. In *Regulation of hepatic metabolism.* ed. Thurman, R.G., Kauffman, F.C. & Jungermann, K. pp. 27–53. New York and London: Plenum Press.

WITHRINGTON, P.G. & RICHARDSON, P.D.I. (1990). Liver Blood Flow. In *Hepatology; a textbook of liver disease.* ed. Zakim, D. & Boyer, T.D. pp. 30–48. Philadelphia: W.B. Saunders Company.

(Received December 2, 1991
Revised May 12, 1992
Accepted May 22, 1992)

Br. J. Pharmacol. (1992), **107**, 303–310

Differential cardiovascular and neuroendocrine effects of epinine and dopamine in conscious pigs before and after adrenoceptor blockade

L.J. van Woerkens, *F. Boomsma, *A.J. Man in 't Veld, †M.M. Bevers & [1] P.D. Verdouw

Laboratory for Experimental Cardiology, Thoraxcentre, Erasmus University Rotterdam; *Department of Internal Medicine I, Academic Hospital Rotterdam 'Dijkzigt' Rotterdam; and †Clinic for Veterinary Obstetrics, University of Utrecht, The Netherlands

1 The effects of epinine or dopamine (both $1-10\,\mu g\,kg^{-1}\,min^{-1}$) on systemic haemodynamics and plasma concentrations of catecholamines and prolactin were studied in conscious pigs before and after combined non-selective α- and β-adrenoceptor blockade.

2 The plasma concentrations of the two compounds did not differ from each other over the entire dose-range.

3 Epinine increased aortic blood flow (AoBF, 24 ± 6%), which was due to an increase in heart rate (HR) for doses less than $10\,\mu g\,kg^{-1}\,min^{-1}$. At $10\,\mu g\,kg^{-1}\,min^{-1}$, HR decreased slightly (10 ± 3%, as compared to the value obtained at $5\,\mu g\,kg^{-1}\,min^{-1}$) and stroke volume increased up to 15% ($P<0.05$). Mean arterial pressure (MAP, 99 ± 3 mmHg at baseline) decreased dose-dependently (14 ± 2%, $P<0.05$) up to the infusion rate of $5\,\mu g\,kg^{-1}\,min^{-1}$, but increased by 4.0 ± 1.8 mmHg during infusion of $10\,\mu g\,kg^{-1}\,min^{-1}$. Systemic vascular resistance (SVR) decreased up to 23 ± 3% for doses less than $10\,\mu g\,kg^{-1}\,min^{-1}$, but did not change further during infusion of the highest dose. LV$dP/dt_{max}$ increased during the two highest infusion rates up to 22 ± 6% ($P<0.05$). After the infusion was stopped there was an abrupt increase in HR (18 ± 4%, $P<0.05$) and a further decrease in SVR before all parameters returned to baseline.

4 Dopamine caused increases in AoBF (27 ± 3%) similar to epinine, the only difference being that HR continued to increase (32 ± 5%) and MAP (13 ± 3%) and SVR continued to decrease (31 ± 3%) over the entire dose-range. The increase in LV$dP/dt_{max}$ at the highest dose (48 ± 4%, $P<0.05$) was more pronounced than with epinine.

5 Adrenoceptor blockade inhibited all epinine-induced changes, but did not affect the dopamine-induced changes in AoBF, SVR and MAP, but attenuated the increases in HR and LV$dP/dt_{max}$.

6 Noradrenaline (NA) and adrenaline (Ad) concentrations did not change during infusion of epinine or dopamine, but NA increased by 50% within 2.5 min after stopping the infusion of epinine. After adrenoceptor blockade NA and Ad concentrations did not change during infusion of dopamine, which contrasted with a decrease of 55 ± 5% ($P<0.05$) in NA during infusion of epinine.

7 Prolactin concentrations decreased gradually from 480 ± 40 pg ml^{-1} to 270 ± 50 pg ml^{-1} ($P<0.05$) during infusion of epinine, but did not change significantly during dopamine infusion.

8 The differential effects of epinine and dopamine on MAP, SVR, plasma NA (before and after adrenoceptor blockade) and prolactin, leads us to conclude that in conscious pigs, epinine is a more potent α, β_2 and D_2-receptor agonist, but a weaker D_1-receptor agonist than dopamine.

Keywords: Epinine; dopamine; adrenoceptor blockade; prolactin; systemic haemodynamics; plasma concentration of catecholamines; conscious pigs

Introduction

Intravenous administration of dopamine has proved to be useful in some patients with congestive heart failure, but poor absorption after oral administration seriously limits its use in the chronic treatment of this disorder (Goldberg, 1974). Therefore, there has been a long-lasting search for dopamine-like drugs that are active after oral administration. This has led to the development of ibopamine, the di-*iso*-butyrylester of epinine (N-methyldopamine), for the chronic treatment of congestive heart failure (Casagrande *et al.*, 1985). Ibopamine is a prodrug, which itself is devoid of pharmacological activity. It is rapidly hydrolyzed by plasma esterases to the active moiety epinine (Randolph *et al.*, 1983; Pocchiari *et al.*, 1986; Rajfer *et al.*, 1986). Epinine, like dopamine, is a polar compound which is not able to cross the blood brain barrier. The drug has a rather short half life and is metabolized rapidly to N-methyldopamine 3-*O* sulphate and N-methyldopamine 4-*O* sulphate, which are devoid of any pharmacological activity (Ferrini *et al.*, 1987). The cardiovascular actions of epinine have been studied and compared to those of dopamine, but the investigations have been performed exclusively in anaesthetized animals (Itoh *et al.*, 1985; Nichols & Ruffolo, 1987; Nichols *et al.*, 1987; Shebuski *et al.*, 1987; Kopia *et al.*, 1988). Epinine stimulates non-selectively α- and β-adrenoceptor and dopamine (D) receptors. Stimulation of D_2-receptors inhibits ganglionic and noradrenergic neurotransmission, preferentially at high levels of sympathetic activity (Lokhandwala & Barratt, 1982). Because during anaesthesia there may be high sympathetic activity, we studied the cardiovascular actions of epinine and dopamine in conscious pigs, thereby avoiding the possible interference of anaesthesia.

To elucidate its mechanisms of action, we studied the cardiovascular effects of infusions of epinine and those of

[1] Author for correspondence at: Laboratory for Experimental Cardiology, Thoraxcentre, Erasmus University Rotterdam, P.O. Box 1738, 3000 DR Rotterdam, The Netherlands.

dopamine before and after non-selective blockade of the α- and β-adrenoceptors, in order to delineate the contribution of D_1-receptor, β_2- and α-adrenoceptor stimulation to the overall vasodilator response to these drugs. We also determined arterial plasma concentrations of catecholamines, since dopamine and epinine may inhibit noradrenergic neurotransmission and noradrenaline release by presynaptic α_2- and D_2-receptor stimulation. Furthermore, plasma prolactin was measured as a specific D_2-receptor-mediated response, since stimulation of D_2-receptors in the pituitary gland inhibits release of prolactin (Moore & Bloom, 1978).

Methods

The experimental procedures were approved by the Committee on Animal Experimentation of the Erasmus University Rotterdam, and complied with the guidelines for the care and use of laboratory animals as outlined by the council of the American Physiology Society.

Surgical procedures

After an overnight fast, cross-bred Landrace x Yorkshire pigs of either sex (19–21 kg at the time of surgery, HVC, Hedel, The Netherlands), pretreated with 600 mg of a mixture of procaine penicillin-G and benzathine penicillin-G intramuscularly (Duplocillin, Gist-Brocades NV, Delft, The Netherlands), were sedated with an intramuscular injection of 30 mg kg^{-1} ketamine HCl (Aeskoket, Aesculaap BV, Boxtel, The Netherlands). Subsequently the animals were intubated and mechanically ventilated with a mixture of oxygen and nitrous oxide (1:2) to which 1–4% (v/v) enflurane (Ethrane, Abbott BV, Amsterdam, The Netherlands) was added. Under sterile conditions, a jugular vein and a common carotid artery were cannulated for infusion of drugs or solvent and measurement of arterial blood pressure, respectively. The chest was opened via the third left intercostal space and an electromagnetic flow probe (Skalar, Delft, The Netherlands) was positioned around the ascending aorta for the measurement of aortic blood flow. The heart was exposed via the fifth intercostal space and a pressure transducer (Konigsberg Instruments Inc., Pasadena, C.A., U.S.A.) was implanted into the left ventricle of the heart through its apex for recording of left ventricular pressure. The left atrium was cannulated for recording of left atrial pressure which, together with the arterial blood pressure, was used for calibration of the Konigsberg transducer signals. The wires were then tunnelled to the back, the chest was closed and the animals were allowed to recover.

Post-surgical period

The animals received daily intravenous doses of 500 mg amoxicillin (Clamoxil, Beecham Farma BV, Amstelveen, The Netherlands) and, during the first week only, 500 mg kanamycin 10% (Alfasan, Woerden, The Netherlands) to prevent infection. Catheters were flushed daily with an isotonic saline solution containing 500 iu ml^{-1} heparin (Thromboliquine, Organon Teknika BV, Boxtel, The Netherlands). During the first weeks of the post-operative recovery period the animals were daily adapted to the laboratory facilities (8 to 10 sessions), while haemodynamic parameters were monitored. The experimental protocols were executed when systemic haemodynamics remained stable for at least one hour, usually 2–3 weeks after instrumentation.

Experimental protocol

On the day of the experiment, 4 doses of either epinine or dopamine were infused at incremental rates of 1, 2.5, 5 and 10 μg kg^{-1} min^{-1} for 10 min each. At the end of each infusion step and at 2.5, 5, 10 and 15 min of the post-infusion period, systemic haemodynamic parameters were recorded and 4 ml of arterial blood was withdrawn for determination of plasma concentrations of catecholamines and prolactin. Experiments were performed before and after combined blockade of α-adrenoceptors with phentolamine (1 mg kg^{-1}, Bom *et al.*, 1988) and of β-adrenoceptors with propranolol (0.5 mg kg^{-1} + 0.5 mg kg^{-1} h^{-1}, Duncker *et al.*, 1987). Phentolamine was administered 25 min and propranolol 15 min before the start of the infusion of epinine or dopamine. The infusion of propranolol was continued throughout the infusion of epinine and dopamine. The stability of the cardiovascular condition of each animal was evaluated by infusion of the solvent at identical volumes (0.2, 0.5, 1.0 and 2.0 ml min^{-1} for 10 min) as used during the infusion of the drugs. Infusions of the drugs or solvent were in random order and experiments in the same animals were separated by at least 24 h. All measurements were performed while the animals were quietly resting in a constraining jacket.

Plasma catecholamine and prolactin determinations

Catecholamines (noradrenaline, adrenaline and dopamine) and epinine were measured simultaneously by high performance liquid chromatography with gradient elution and with fluorimetric detection (Van der Hoorn *et al.*, 1989; Boomsma *et al.*, 1991). We encountered a methodological problem with determinations of dopamine, but not with those of the other catecholamines, in pig plasma. Despite the routine addition of the anti-oxidant glutathione in a final concentration of 1.2 mg ml^{-1} in tubes of 10 ml, dopamine appeared to disappear rapidly from pig plasma, contrary to our experiences with human plasma. When, however, blood was containing ten times more glutathione, dopamine was found to be stable in pig plasma. Concentrations of epinine and dopamine in plasma prepared from blood collected in tubes containing these high amounts of glutathione, yielded similar concentrations of epinine and dopamine over the entire infusion range (1–10 μg kg^{-1} min^{-1}, $n = 5$). The mechanism of the rapid disappearance of dopamine in pig plasma is currently under investigation in our laboratory. Arterial plasma porcine prolactin concentrations were estimated by a specific, homologous double-antibody radioimmunoassay (Bevers *et al.*, 1978). The intra- and interassay coefficients of variation were 1.8% and 15.1%, respectively. The sensitivity of the assay was 0.2 μg l^{-1}.

Drugs

Epinine was a gift from Dr C. Casagrande (Zambon Research, Milan, Italy) and prepared daily in physiological saline (0.9% NaCl) and infused in concentrations of 5 μg ml^{-1}. Epinine appeared to be contaminated with dopamine by 0.66%. Dopamine (dopamine HCl, ICN Pharmaceuticals Holland BV, Zoetermeer, The Netherlands), propranolol (ICI Farma, Rotterdam, The Netherlands) and phentolamine (Regitine, Ciba-Geigy BV, Arnhem, The Netherlands) were obtained from the Pharmacy of the University Hospital Rotterdam 'Dijkzigt'.

Data presentation and analysis

Stroke volume was approximated by the ratio of ascending aortic blood flow and heart rate, because cardiac output (which equals the sum of ascending aortic blood flow and coronary blood flow) could not be calculated as coronary blood flow (4–6% of cardiac output) was not determined. Because central venous blood pressure was not measured, systemic vascular resistance was approximated by the ratio of mean aortic blood pressure and ascending aortic blood flow.

All data are presented as the mean ± s.e.mean. The significance of the effects of the drugs has been evaluated by comparing the changes from baseline induced by the drugs to

the changes from baseline during infusion of the solvent, by analysis of variance. Significance was accepted for $P<0.05$. A Bonferroni correction was used because of comparison for multiple measurements.

Results

Stability of animal preparation

Infusion of the solvent did not affect any of the cardiovascular parameters or arterial plasma catecholamine levels (Table 1).

Cardiovascular changes during infusion of epinine before and after adrenoceptor blockade

Infusion of epinine increased ascending aortic blood flow (AoBF) dose-dependently up to 22% (Figure 1). At the lower dose-range, the increase was exclusively due to an increase in heart rate (HR, 17 ± 6%, $P<0.05$), but during infusion of 10 μg kg^{-1} min^{-1}, HR decreased from 132 ± 8 beats min^{-1} (at 5 μg kg^{-1} min^{-1}) to 125 ± 5 beats min^{-1} ($P<0.05$) and stroke volume increased from 23.7 ± 1.7 ml to 27.6 ± 2.5 ml ($P<0.05$). Mean arterial blood pressure (MAP) decreased dose-dependently during infusions up to 5 μg kg^{-1} min^{-1}, but increased by 4.0 ± 1.8 mmHg ($P<0.05$) during infusion of

Table 1 Effect of solvent on cardiovascular parameters and plasma catecholamines in 10 conscious pigs

	Baseline	*Solvent* (ml min^{-1} for 10 min) *0.2*	*0.5*	*1*	*2*
Systemic haemodynamics					
CO (l min^{-1})	2.61 ± 0.15	2.60 ± 0.15	2.60 ± 0.14	2.58 ± 0.14	2.61 ± 0.13
MAP (mmHg)	98 ± 3	99 ± 4	98 ± 3	98 ± 3	98 ± 3
HR (beats min^{-1})	111 ± 4	111 ± 5	111 ± 4	109 ± 4	111 ± 4
LV$dP/dt_{max}$ (mmHg s^{-1})	3140 ± 120	3100 ± 120	3060 ± 120	3080 ± 130	3150 ± 150
LVEDP (mmHg)	8.7 ± 0.4	8.8 ± 0.4	8.8 ± 0.4	8.8 ± 0.4	8.9 ± 0.5
SVR (mmHg min l^{-1})	37.4 ± 2.2	37.7 ± 2.3	37.8 ± 2.3	38.0 ± 2.2	37.9 ± 2.2
SV (ml)	24.0 ± 1.7	23.7 ± 1.5	23.9 ± 1.5	24.2 ± 1.6	23.9 ± 1.5
Arterial plasma catecholamines					
Dopamine (pg ml^{-1})	19 ± 5	16 ± 4	15 ± 3	15 ± 3	29 ± 6
Noradrenaline (pg ml^{-1})	211 ± 31	186 ± 21	191 ± 20	182 ± 17	268 ± 69
Adrenaline (pg ml^{-1})	130 ± 41	123 ± 24	147 ± 24	115 ± 25	131 ± 29

Data are mean ± s.e.mean. CO = cardiac output; MAP = mean arterial blood pressure; HR = heart rate; LV$dP/dt_{max}$ = maximal rate of rise in left ventricular pressure; LVEDP = left ventricular end-diastolic pressure; SVR = systemic vascular resistance; SV = stroke volume.

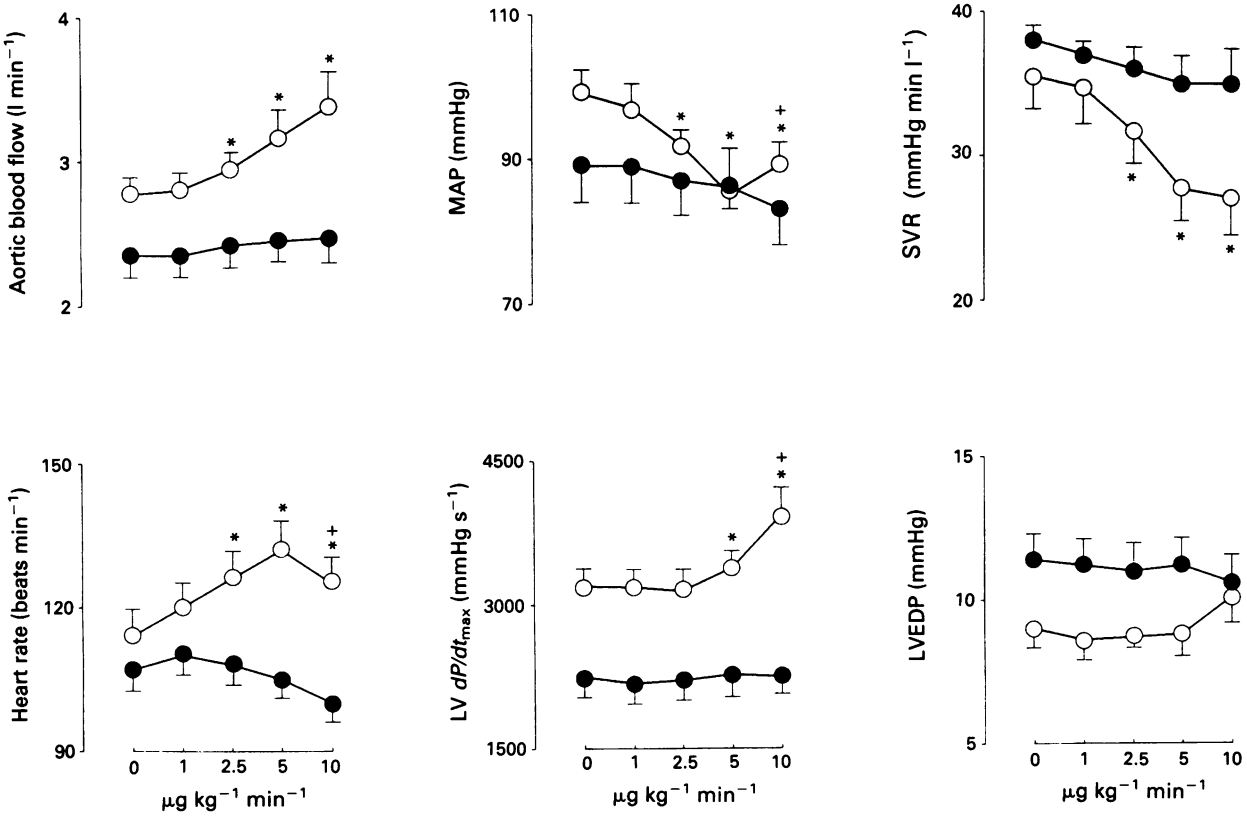

Figure 1 Cardiovascular effects of consecutive 10 min infusions of epinine in conscious pigs. Infusions were performed before (open symbols, $n = 10$) and after combined non-selective α- and β-adrenoceptor blockade (closed symbols, $n = 5$). Data are presented as mean and the bars show s.e.mean. *$P<0.05$ versus pre-drug value (0 μg kg^{-1} min^{-1}). $^{+}P<0.05$ versus value obtained after 5 μg kg^{-1} min^{-1}.

the highest dose. Calculation of the arterial pulse pressure (difference between systolic and diastolic arterial blood pressure) revealed no change for doses less than 5 μg kg^{-1} min^{-1} (46 ± 4 mmHg), but an increase to 51 ± 3 mmHg ($P<0.05$) during infusion of 10 μg kg^{-1} min^{-1}, as systolic arterial blood pressure increased by 4.1 ± 2.2 mmHg, compared to the value observed at 5 μg kg^{-1} min^{-1}, while diastolic arterial blood pressure did not change. In view of the changes in AoBF and MAP it can be calculated that systemic vascular resistance (SVR) decreased by 27 ± 3% ($P<0.05$) in the dose-range of 1–5 μg kg^{-1} min^{-1}, but it did not change further during infusion of the highest dose. LV$dP/dt_{max}$ increased only slightly (6 ± 2%, $P<0.05$) during infusion of 5 μg kg^{-1} min^{-1}, but rose markedly (22 ± 6%, $P<0.05$) during infusion of the highest dose. Left ventricular end-diastolic pressure was not influenced at any dose.

After non-selective α- and β-adrenoceptor blockade, infusion of epinine no longer affected any of the cardiovascular parameters (Figure 1).

The cardiovascular effects exerted by dopamine were similar to those of epinine in the dose range of 1–5 μg kg^{-1} min^{-1}, but during infusion of 10 μg kg^{-1} min^{-1} there were some differences: HR continued to increase and SVR continued to decrease (Figure 2). Finally, at the highest dose the dopamine-induced increase in LV$dP/dt_{max}$ (1440 ± 110 mmHg s^{-1}) was considerably larger than after epinine (680 ± 210 mmHg s^{-1}, $P<0.05$).

Blockade of the α- and β-adrenoceptors neither affected the dopamine-induced increase in AoBF nor the dopamine-induced decreases in MAP and SVR (Figure 2). HR still increased, but this was significant only at the highest dose. LV$dP/dt_{max}$ also increased, but the effect (690 ± 160 mmHg s^{-1}) was attenuated as compared to the increment without blockade (1440 ± 110 mmHg s^{-1}, $P<0.05$).

Cardiovascular effects of epinine and dopamine during the post-infusion period

Immediately after the epinine infusions had been stopped, HR increased by 49 ± 5 beats min^{-1} (40 ± 5%) and LV$dP/dt_{max}$ increased by 680 ± 170 mmHg s^{-1} (18 ± 5%) (Table 2) over the values observed at the end of the infusion of the highest dose. This 'withdrawal-tachycardia' was most likely a reflex mechanism, since it coincided with a fall in SVR. AoBF and HR remained elevated, but all other parameters returned to baseline values in the susequent recovery period. Adrenoceptor blockade not only prevented the epinine-induced changes during the infusion period, but also the 'withdrawal-tachycardia' was no longer seen.

After the dopamine infusions had been stopped, all parameters returned gradually towards baseline values (Table 2). HR was still elevated after 15 min. A similar pattern of changes was observed when the dopamine infusions were performed after adrenoceptor blockade (Table 2).

Arterial plasma concentrations of catecholamines during infusion of epinine before and after adrenoceptor blockade

Plasma concentrations of epinine increased in a dose-dependent manner up to 62,020 ± 3,980 pg ml^{-1} during infusion of epinine (Figure 3). During the subsequent washout period, there was a very rapid decline in plasma levels to 3,690 ± 410 pg ml^{-1} after 2.5 min and 430 ± 90 pg ml^{-1} after 15 min. A similar dose-response curve was found when the epinine infusions were repeated after adrenoceptor blockade (Figure 3).

Plasma dopamine concentrations increased dose-dependently from 42 ± 24 pg ml^{-1} at baseline to 620 ± 226 pg ml^{-1}

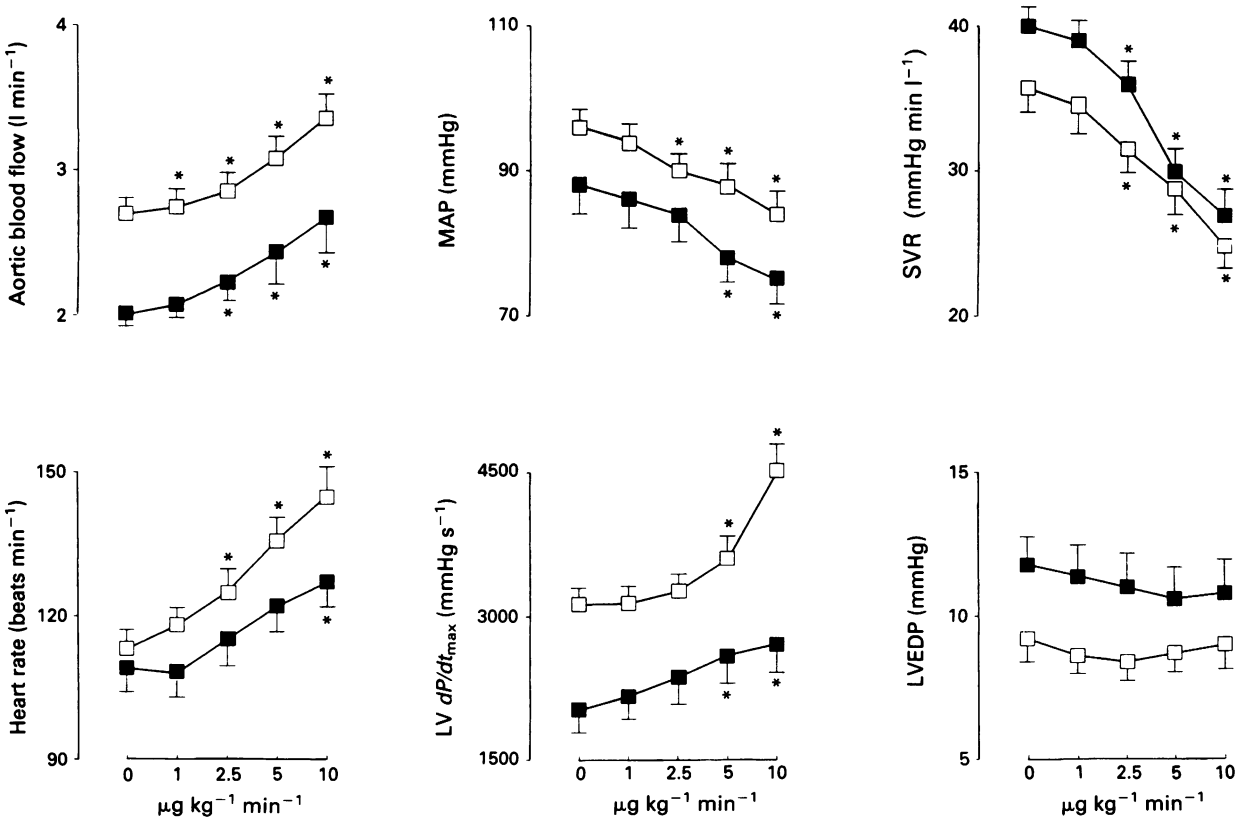

Figure 2 Cardiovascular effects of consecutive 10 min infusions of dopamine in conscious pigs. Infusions were performed before (open symbols, $n = 10$) and after combined non-selective α- and β-adrenoceptor blockade (closed symbols, $n = 5$). Data are presented as mean and the bars show s.e.mean. *$P<0.05$ versus pre-drug value (0 μg kg^{-1} min^{-1}).

Table 2 Cardiovascular effects of epinine and dopamine during the post-infusion period

		n	*After*	*Post-infusion period (min)*			
		Baseline	(10 μg kg^{-1} min^{-1})	*2.5*	*5*	*10*	*15*
CO	E	2.77 ± 0.11	3.38 ± 0.25*	3.56 ± 0.23*	3.29 ± 0.24*	3.07 ± 0.08*	2.84 ± 0.09*
(l min^{-1})	D	2.69 ± 0.11	3.36 ± 0.17*	3.02 ± 0.17*†	2.70 ± 0.07*†	2.64 ± 0.11†	2.57 ± 0.11†
	αβE	2.35 ± 0.16	2.47 ± 0.17	2.40 ± 0.15	2.38 ± 0.14	2.33 ± 0.15	2.28 ± 0.12
	αβD	2.00 ± 0.12	2.67 ± 0.26*	2.33 ± 0.14*†	2.30 ± 0.14†	2.15 ± 0.14†	2.12 ± 0.15†
MAP	E	99 ± 3	89 ± 4*	85 ± 3*	92 ± 4	97 ± 4†	100 ± 4†
(mmHg)	D	96 ± 2	84 ± 3*	95 ± 5†	99 ± 4†	101 ± 4†	89 ± 7
	αβE	89 ± 8	83 ± 6*	84 ± 6	88 ± 6	89 ± 7	89 ± 7
	αβD	88 ± 6	75 ± 4*	88 ± 5†	91 ± 3†	96 ± 5*†	95 ± 5*†
HR	E	114 ± 7	125 ± 5*	174 ± 6*†	158 ± 6*†	144 ± 7*†	137 ± 8*†
(beats min^{-1})	D	113 ± 5	145 ± 8*	136 ± 9*†	130 ± 9*†	126 ± 9*†	123 ± 9*†
	αβE	107 ± 5	100 ± 4*	107 ± 3	104 ± 3	102 ± 6	100 ± 6
	αβD	109 ± 6	127 ± 7*	106 ± 2	111 ± 7†	106 ± 6†	103 ± 6†
LV$dP/dt_{max}$	E	3190 ± 210	3930 ± 300*	4620 ± 350*†	4280 ± 320*	3810 ± 320*	3670 ± 350
(mmHg)	D	3120 ± 200	4560 ± 250*	4220 ± 190*	3970 ± 350*†	3820 ± 450*†	3480 ± 360†
	αβE	2250 ± 210	2250 ± 170	2250 ± 160	2230 ± 150	2290 ± 200	2250 ± 180
	αβD	2020 ± 250	2710 ± 330*	2370 ± 310	2490 ± 310	2450 ± 300†	2390 ± 290†
LVEDP	E	9.0 ± 0.7	10.1 ± 1.0	9.1 ± 0.9†	8.4 ± 0.9†	9.0 ± 1.0	9.1 ± 1.0
(mmHg)	D	9.2 ± 0.8	9.0 ± 0.9	8.8 ± 1.1	8.3 ± 1.1	8.3 ± 0.9	9.0 ± 1.0
	αβE	11.4 ± 0.9	10.6 ± 1.1	11.0 ± 1.4	10.2 ± 1.2	10.2 ± 1.2	10.0 ± 1.2
	αβD	11.8 ± 1.0	10.8 ± 1.2	10.8 ± 1.3	11.6 ± 1.2	11.4 ± 1.2	11.2 ± 1.1
SVR	E	35.5 ± 2.3	27.1 ± 2.6*	24.3 ± 2.3*	28.0 ± 2.6*	30.5 ± 2.0*†	33.8 ± 2.0†
(mmHg l^{-1} min)	D	35.7 ± 1.8	24.9 ± 1.5*	29.9 ± 1.8*†	35.0 ± 0.8†	36.2 ± 1.4†	37.0 ± 1.5†
	αβE	37.7 ± 0.7	34.5 ± 2.7	36.5 ± 2.6†	38.4 ± 3.0†	40.1 ± 2.8†	40.7 ± 2.4†
	αβD	41.3 ± 0.6	27.0 ± 2.4*	36.3 ± 2.2†	38.6 ± 2.1†	42.9 ± 2.3†	43.1 ± 2.7†
SV	E	24.2 ± 1.8	27.6 ± 2.5*	21.4 ± 1.9†	21.5 ± 1.8†	22.1 ± 1.3†	21.9 ± 1.4†
(ml)	D	24.1 ± 1.7	23.4 ± 1.4	23.1 ± 2.0	22.8 ± 2.1	23.1 ± 2.3	22.6 ± 2.4
	αβE	22.4 ± 1.1	25.9 ± 2.7	22.6 ± 0.6	23.4 ± 1.9	24.4 ± 2.8	24.1 ± 1.9
	αβD	19.1 ± 0.7	22.0 ± 0.4	22.2 ± 1.3	22.4 ± 1.6	21.2 ± 0.5	21.8 ± 1.0
Noradrenaline	E	261 ± 64	235 ± 22	345 ± 35†	290 ± 24	247 ± 22	308 ± 82
(pg ml^{-1})	D	326 ± 142	417 ± 46	278 ± 33†	301 ± 45†	253 ± 38†	251 ± 49†
	αβE	1170 ± 250	570 ± 120*	650 ± 120*	570 ± 110*	520 ± 90*	550 ± 120*
	αβD	1260 ± 230	1230 ± 240	840 ± 240†	860 ± 120*†	800 ± 170*	710 ± 180*†
Adrenaline	E	109 ± 19	103 ± 8	118 ± 19	124 ± 13	139 ± 23	159 ± 38
(pg ml^{-1})	D	92 ± 12	80 ± 15	117 ± 21	98 ± 29	103 ± 28	121 ± 17†
	αβE	262 ± 81	457 ± 195	497 ± 172	441 ± 152	520 ± 277	641 ± 366
	αβD	279 ± 59	218 ± 52*	186 ± 64*	220 ± 52	194 ± 63	224 ± 85

Data are mean ± s.e.mean. E = epinine; D = dopamine; αβE = epinine after adrenoceptor blockade; αβD = dopamine after adrenoceptor blockade; CO = cardiac output; MAP = mean arterial blood pressure; HR = heart rate; SV = stroke volume; LV$dP/dt_{max}$ = maximum rate of rise of left ventricular end-diastolic pressure; LVEDP = left ventricular end-diastolic pressure; SVR = systemic vascular resistance; SV = stroke volume.
*$P<0.05$ versus baseline; †$P<0.05$ versus 10 μg kg^{-1} min^{-1}.

during infusion of epinine, and fell rapidly after the infusions had been stopped (data not shown). These changes in dopamine can be fully accounted for by the contamination of 10 μg kg^{-1} min^{-1} of epinine with 0.66% of dopamine. A similar pattern of changes in dopamine was seen when the epinine infusions were repeated after adrenoceptor blockade.

Plasma noradrenaline concentrations (NA) did not change during infusion of epinine (Figure 4), but increased from 235 ± 22 pg ml^{-1} (at the end of the infusion of 10 μg kg^{-1} min^{-1}) to 345 ± 35 pg ml^{-1} ($P<0.05$) (Table 2) during the first 2.5 min of the post-infusion period and returned to baseline in the following minutes. NA increased sharply from 160 ± 30 pg ml^{-1} to 1040 ± 170 pg ml^{-1} ($P<0.05$) after α-adrenoceptor blockade, and rose further to 1360 ± 230 pg ml^{-1} after additional β-adrenoceptor blockade (Figure 4). During the additional infusion of epinine there was a decrease in NA to 570 ± 120 pg ml^{-1} ($P<0.05$ versus baseline), which continued into the post-infusion period

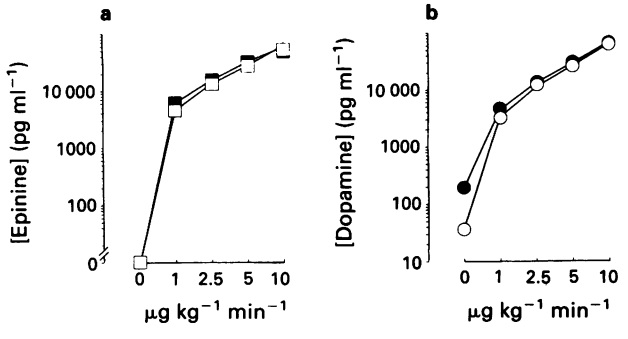

Figure 3 Arterial plasma levels of epinine and dopamine during intravenous infusion of (a) epinine and (b) dopamine in conscious pigs, respectively. Infusions were performed before (open symbols) and after (closed symbols) adrenoceptor blockade.

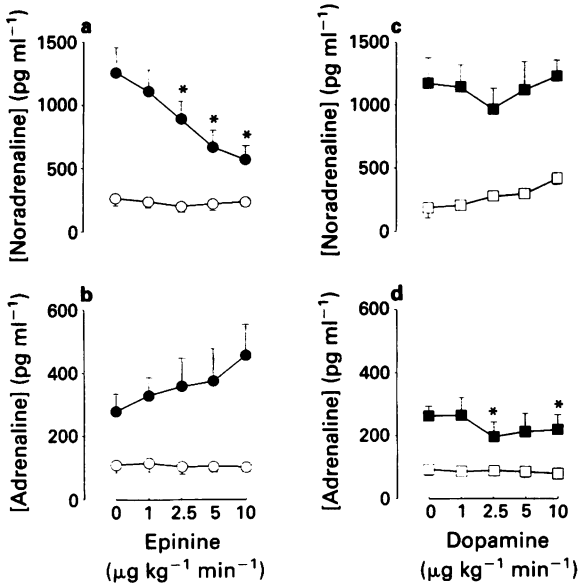

Figure 4 Arterial plasma catecholamine concentrations during intravenous infusion of epinine and of dopamine, respectively. Infusions were performed before (open symbols, $n = 10$) and after (closed symbols, $n = 5$) combined non-selective α- and β-adrenoceptor blockade. Data are presented as mean and the bars show s.e.mean. $^*P < 0.05$ versus pre-drug value (0 μg kg^{-1} min^{-1}).

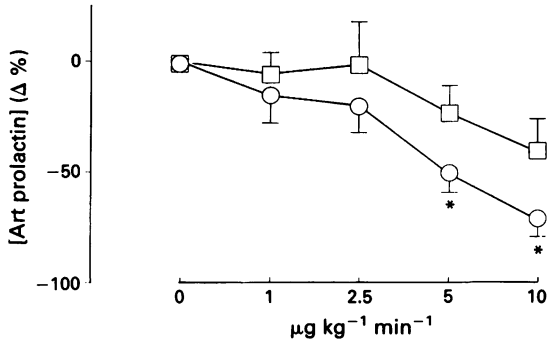

Figure 5 Changes in arterial plasma concentrations of prolactin (Art prolactin) during infusion of epinine (○) and of dopamine (□). Data are presented as mean and the bars show s.e.mean. $^*P < 0.05$ versus pre-drug value (0 μg kg^{-1} min^{-1}).

(Figure 4, Table 2). The increase, previously seen in the early post-infusion period before adrenoceptor-blockade (from 235 ± 22 pg ml^{-1} to 345 ± 35 pg ml^{-1}) was, however, not significant (570 ± 120 to 650 ± 120 pg ml^{-1}). Plasma concentrations of adrenaline (Ad) did not change during infusion of epinine, either before or after adrenoceptor blockade (Table 2, Figure 4).

Arterial plasma concentrations of catecholamines during infusion of dopamine before and after adrenoceptor blockade

Plasma dopamine concentrations increased up to 62,400 ± 4,210 pg ml^{-1} during infusion of dopamine (Figure 3). This dose-response curve was not affected by adrenoceptor blockade. During the post-infusion period the dopamine concentration rapidly declined to 2,110 ± 290 and 1,230 ± 120 pg ml^{-1} after 2.5 and 5 min, but it was still elevated after 15 min (data not shown). During the dopamine infusions, before adrenoceptor blockade, NA and Ad were similar to the concentrations seen during the epinine infusions. However, in contrast to epinine, dopamine did not decrease NA after adrenoceptor blockade (Figure 4). Also, in contrast to what was observed after stopping epinine, NA did not rise during the early washout period (Table 2).

Arterial plasma concentrations of prolactin during infusion of epinine and dopamine

Arterial concentrations of prolactin decreased gradually ($P < 0.05$) during the infusion of epinine, but they did not change significantly during dopamine (Figure 5).

Discussion

The cardiovascular effects of epinine and dopamine have been compared in several studies (Itoh *et al.*, 1985; Nichols & Ruffolo, 1987; Nichols *et al.*, 1987; Shebuski *et al.*, 1987; Kopia *et al.*, 1988). These studies, however, have all been performed in animals under anaesthesia and this condition may have influenced the results. For instance, Itoh *et al.* (1985) reported that heart rate decreased after epinine, while Kopia *et al.* (1988) noticed an increase in heart rate, in anaesthetized dogs for a dose-range similar to that used in our study. In the present investigation the animals were conscious, thus avoiding any possible interference of anaesthetic agents with the haemodynamic effects of the drugs under study. The animals had been carefully adapted to the laboratory conditions, as reflected by the stability of the cardiovascular condition and arterial plasma catecholamine concentrations during infusion of the solvent. Moreover, the plasma concentrations of noradrenaline and adrenaline in our instrumented animals were very similar to those reported by Barrand *et al.* (1981) for conscious, non-instrumented pigs of the same age and weight. This strongly suggests that the stability of the haemodynamic status and the catecholamine concentrations indeed reflects the fact that the animals were not disturbed.

In the range of 1–5 μg kg^{-1} min^{-1}, epinine and dopamine caused similar changes in LV$dP/dt_{max}$, heart rate, left ventricular end-diastolic pressure and arterial blood pressure. The relation between the increase in heart rate and the decrease in arterial blood pressure during the infusion of epinine suggests that a baroreflex-mediated withdrawal of vagal tone could be involved in the change in heart rate.

Changes in LV$dP/dt_{max}$ are frequently interpreted as changes in inotropy, but the dependency of LV$dP/dt_{max}$ on heart rate, pre- and afterload may limit the value of LV$dP/dt_{max}$ as an index of myocardial contractility. The similarity in changes in both LV$dP/dt_{max}$ as well as in heart rate, pre- and afterload during infusion of epinine and dopamine, however, suggests that epinine and dopamine had equal effects on myocardial contractility. This positive inotropic effect was probably also the reason that stroke volume increased at this dose as systemic vascular resistance and left ventricular end-diastolic pressure were not affected and mean arterial blood pressure even slightly increased.

Combined non-selective α- and β-adrenoceptor blockade prevented all haemodynamic effects of epinine, which strongly suggests that stimulation of α- and β-adrenoceptors underlies the mechanism of action of epinine. However, this conclusion is premature as both arterial prolactin and noradrenaline concentrations, the latter only after α- and β-adrenoceptor blockade, progressively decreased during infusion of epinine. Both effects can be explained by stimulation of D_2-receptors. Prolactin release from the pituitary gland is directly inhibited through stimulation of D_2-receptors (Moore & Bloom, 1978). Noradrenergic neurotransmission is inhibited by D_2-receptors located either on ganglionic cells (minor effect) or located prejunctionally on postganglionic sympathetic nerve fibres, thus diminishing

noradrenaline release and spill-over into plasma. The latter process becomes mainly activated at higher levels of sympathetic nerve traffic, as is the case during non-selective α-adrenoceptor blockade (Lokhandwala & Barratt, 1982). Such a phenomenon was recently confirmed in healthy volunteers where ibopamine, the prodrug of epinine, blunted the rise in plasma noradrenaline during physical exercise, whereas it had no effect on the normal basal values of plasma noradrenaline (Girbes *et al.*, 1992). The unchanged systemic vascular resistance, during epinine infusion after non-selective adrenoceptor blockade, indicates that the 'direct' vasodilator capacity of epinine via D_1-receptor activation is limited. However, under the experimental conditions of the current protocol an 'indirect' D_2-receptor mediated contribution to the overall vasodilator effect of epinine is difficult to demonstrate for two reasons: Firstly, when sympathetic tone is not elevated, as in our animals, such a mechanism probably contributes little to the vasodilator effect of epinine. Secondly, a D_2-receptor-mediated reduced α-adrenoceptor vasoconstrictor tone, as witnessed by a fall in plasma noradrenaline after infusion of epinine during adrenoceptor blockade, would not have produced vasodilatation, since α-adrenoceptors were blocked. Therefore, our data do not exclude the possibility that epinine exerts an 'indirect' vasodilator action through D_2-receptors when sympathetic tone is elevated, as is the case in severe forms of congestive heart failure. To delineate the contribution of such a D_2-receptor mediated vasodilatation, studies with selective D_2-adrenoceptor antagonists are required.

That epinine indeed has a D_2-agonist action, which is even more potent than that of dopamine, can be concluded from the decrease in prolactin concentrations. Thus since the decrease in systemic vascular resistance by dopamine was not affected by combined α- and β-adrenoceptor blockade, and dopamine is apparently a weaker D_2-agonist than epinine in the dose-range tested, it must follow that dopamine is a more potent D_1-agonist than epinine. When we compare the magnitude of the changes in $LVdP/dt_{max}$ and heart rate during infusion of epinine and dopamine to those observed with a number of dihydropyridine calcium antagonists, that do not possess positive inotropic properties (Duncker *et al.*, 1988), the β_1-agonist activity of epinine and dopamine appears to be rather weak from a quantitative point of view. These data support earlier observations in *in vitro* experiments and in the intact anaesthetized animals that epinine and dopamine share similar but relatively weak β-adrenoceptor agonist activity as compared to isoprenaline and that the effects of epinine are more selectively mediated through β_2-adrenoceptors, whereas dopamine is non-selective or relatively β_1-selective depending on the animal species or tissue that was used (Ferrini & Miragoli, 1986; Nichols & Ruffolo, 1987; English *et al.*, 1988; Deighton *et al.*, 1990; Bravo *et al.*, 1991). Furthermore, we have shown previously that D_1-receptors do not play a major role in the heart, under physiological conditions (Van Woerkens *et al.*, 1991). The lack of a pronounced positive inotropic action of epinine was recently confirmed by infusion of epinine in patients with moderate heart failure due to ischaemic heart disease (Rousseau *et al.*, 1992).

At $10\,\mu g\,kg^{-1}\,min^{-1}$ the α-adrenoceptor agonistic activity of epinine appears to exceed that of dopamine, because during infusion of that dose arterial blood pressure and systemic vascular resistance started to increase and heart rate to decrease. Additional evidence here is the abrupt increase in heart rate and plasma noradrenaline and the fall in arterial blood pressure, and systemic vascular resistance, immediately after the infusion of epinine had been stopped. This vasodilatation was, most likely, due to an abrupt disappearance of α-adrenoceptor agonistic activity at lower plasma concentrations of epinine. Furthermore, these changes were all prevented by previous adrenoceptor blockade. With dopamine a sudden increase in heart rate and noradrenaline and a decrease in arterial blood pressure and vascular resistance were not seen, which is evidence that a sudden loss of α-adrenoceptor agonistic activity after stopping the infusion of dopamine did not occur. Furthermore, plasma noradrenaline did not increase after stopping dopamine. Finally, considering the facts that (1) the observed vasodilatation with epinine was due to β_2-adrenoceptor activation (α- and β-adrenoceptor blockade inhibited the epinine-induced vasodilatation), (2) that α- and β-adrenoceptor blockade did not affect the vasodilator response to dopamine, and (3) that dopamine is the weaker α-adrenoceptor agonist, it also follows that epinine is a more potent β_2-adrenoceptor agonist than dopamine.

These data lead us to suggest that in the conscious pigs and in the dose-range tested ($1-10\,\mu g\,kg^{-1}\,min^{-1}$), epinine is a weaker D_1-agonist, but a more potent D_2, β_2- and α-agonist than dopamine, while the β_1-agonistic potency of both compounds is rather weak, if present at all. Further studies are required to investigate whether epinine has any affinity for D_3, D_4 or D_5, the recently described dopamine receptor subtypes (Sibley & Monsma, 1992) and to delineate the role of the different receptors in the haemodynamic profile of epinine or its prodrug, ibopamine, in healthy man and in patients with congestive heart failure (Man in 't Veld, 1991).

References

BARRAND, M.A., DAUNCEY, M.J. & INGRAM, D.L. (1981). Changes in plasma noradrenaline and adrenaline associated with central and peripheral thermal stimuli in the pig. *J. Physiol.*, **316**, 139–152.

BEVERS, M.M., WILLEMSE, A.H. & KRUIP, TH.A.M. (1978). Plasma prolactin levels in the sow during lactation and the postweaning period as measured by radioimmunoassay. *Biol. Reprod.*, **19**, 628–634.

BOM, A.H., DUNCKER, D.J., SAXENA, P.R. & VERDOUW, P.D. (1988). 5-Hydroxytryptamine-induced tachycardia in the pig: possible involvement of a new type of 5-hydroxytryptamine receptor. *Br. J. Pharmacol.*, **93**, 663–671.

BOOMSMA, F., ALBERTS, G., HOORN, F.A.J., MAN IN 'T VELD, A.J. & SCHALEKAMP, M.A.D.H. (1992). Simultaneous determination of free catecholamines and epinine and estimation of total epinine and dopamine in plasma and urine by HPLC with fluorimetric detection. *J. Chromatogr.*, **574**, 109–117.

BRAVO, G., GHYSEL-BURTON, J., JAUMIN, P. & GODFRAIND, T. (1991). A comparison of the inotropic effects of dopamine and epinine in human isolated cardiac preparations. *J. Pharmacol. Exp. Ther.*, **257**, 439–443.

CASAGRANDE, C., GHIRARDI, P. & MARCHETTI, G. (1985). Ibopamine. In *New Drugs Annual: Cardiovascular Drugs*. Vol. 3 ed. Scriabine, A. pp. 173–196. New York: Raven Press.

DEIGHTON, N.M., MOTOMURA, S., SÖHLMANN, W., ZERKOWSKI, H.R. & BRODDE, O.E. (1990). β-adrenoceptor-mediated inotropic effects of dopamine and epinine in human isolated right atrium. *Br. J. Pharmacol.*, **99**, (Suppl. 1), 116P.

DUNCKER, D.J., SAXENA, P.R. & VERDOUW, P.D. (1987). Systemic hemodynamic and beta-adrenoceptor antagonistic effects of bisoprolol in conscious pigs: a comparison with propranolol. *Arch. Int. Pharmacodyn. Ther.*, **290**, 54–63.

DUNCKER, D.J., SAXENA, P.R. & VERDOUW, P.D. (1988). Systemic hemodynamics of dihydropyridine derivatives in conscious pigs with or without propranolol. *Eur. J. Pharmacol.*, **156**, 401–409.

ENGLISH, T.A.H., GRISTWOOD, R.W., OWEN, P.A.A., SAMPFORD, K.A. & WALLWORK, J. (1988). Effects of dopamine on human ventricle in vitro: comparison with effects of isoprenaline, epinine and ibopamine. *Br. J. Pharmacol.*, **87**, 203P.

FERRINI, R. & MIRAGOLI, G. (1986). Activity of ibopamine on some isolated organs. *Arzneim. Forsch.*, **36**, 312–317.

FERRINI, R., MERLO, L. & MIRAGOLI, G. (1987). Pharmacological characterization of epinine 3-O-sulphate and 4-O-sulphate. *Arch. Int. Pharmacodyn.*, **289**, 37–45.

GIRBES, A.R.J., VAN VELDHUIZEN, D.J., GREVINT, R.M., SMIT, A.J. & REITSMA, W.D. (1992). Effects of ibopamine on exercise-induced increase in norepinephrine in normal men. *J. Cardiovasc. Pharmacol.*, **19**, 371–375.

GOLDBERG, L.I. (1974). Dopamine – clinical uses of an endogenous catecholamine. *N. Engl. J. Med.*, **291**, 707–710.

ITOH, H., HOHLI, J., RAJFER, S. & GOLDBERG, L. (1985). Comparison of the cardiovascular actions of dopamine and epinine in the dog. *J. Pharmacol. Exp. Ther.*, **233**, 87–93.

KOPIA, G., OHLSTEIN, E. & RUFFOLO, R. (1988). Systemic and coronary hemodynamic actions of the novel inotropic agent, ibopamine, and the de-esterified metabolic and active form, epinine: Relationship to left ventricular performance in the dog. *J. Pharmacol. Exp. Ther.*, **246**, 434–440.

LOKHANDWALA, M.F. & BARRETT, R.J. (1982). Cardiovascular dopamine receptors: physiological, pharmacological and therapeutic implications. *J. Auton. Pharmacol.*, **3**, 189–215.

MAN IN 'T VELD, A.J. (1991). Ibopamine in the treatment of heart failure. *Am. J. Med.*, **90** (sub5B), 50S–54S.

MOORE, R.Y. & BLOOM, F.E. (1978). Central catecholamine neuron systems: anatomy and physiology of the dopamine systems. *Annu. Rev. Neurosci.*, **1**, 129–169.

NICHOLS, A. & RUFFOLO, R. (1987). Evaluation of the alpha and beta adrenoceptor-mediated activities of the novel, orally active inotropic agent, ibopamine, in the cardiovascular system of the pithed rat: comparison with epinine and dopamine. *J. Pharmacol. Exp. Ther.*, **242**, 455–463.

NICHOLS, A., SMITH, J., SHEBUSKI,R. & RUFFOLO, R. (1987). Comparison of the effects of the novel inotropic agent, ibopamine, with epinine, dopamine and fenoldopam on renal vascular dopamine receptors in the anaesthetized dog. *J. Pharmacol. Exp. Ther.*, **242**, 573–578.

POCCHIARI, F., PATACCINI, R., CASTELNOVO, P., LONGO, A., PARO, M. & CASAGRANDE, C. (1986). Ibopamine, an orally active dopamine-like drug: Metabolism and pharmocokinetics in dogs. *Arzneim. Forsch.*, **36**, 341–344.

RANDOLPH, W.C., SWAGZDIS, J.E., JOSEPH, G.L. & GIFFORD, R. (1983). Circulating levels of epinine and epinine conjugates in rat, dog and man following oral administration of ibopamine. *Pharmacologist*, **25**, 117.

RAJFER, S.L., ROSSEN, J.D., DOUGLAS, F.L., GOLDBERG, L.I. & KARRISON, T. (1986). Effects of long-term therapy with oral ibopamine on resting hemodynamics and exercise capacity in patients with heart failure: Relationship to the generation of N-methyldopamine and to plasma norepinephrine levels. *Circulation*, **73**, 740–749.

ROUSSEAU, M.F., RAIGOSO, J., VAN EYLL, C., VAN MECHELEN, H., MUSSO, N.R., LOTTI, G. & POULEUR, H. (1992). Effects of intravenous epinine administration on left ventricular systolic performance, coronary hemodynamics and circulating catecholamines in patients with heart failure. *J. Cardiovasc. Pharmacol.*, **19**, 155–162.

SHEBUSKI, R., FUJITA, T., SMITH, J. & RUFFOLO, R. (1987). Comparison of the alpha adrenoceptor activity of dopamine, ibopamine and epinine in the pulmonary circulation of the dog. *J. Pharmacol. Exp. Ther.*, **241**, 6–12.

SIBLEY, D.R. & MONSMA, F.J. (1992). Molecular biology of dopamine receptors. *Trends Pharmacol. Sci.*, **13**, 61–69.

VAN DER HOORN, F.A.J., BOOMSMA, F. MAN IN 'T VELD, A.J. & SCHALEKAMP, M.A.D.H. (1989). Determination of catecholamines in human plasma by high-performance liquid chromatography: comparison between a new method with fluorescence determination and an established method with electrochemical determination. *J. Chromatogr.*, **487**, 17–28.

VAN WOERKENS, L.J., DUNCKER, D.J., DEN BOER, M.O., MCFALLS, E.O., SASSEN, L.M.A., SAXENA, P.R. & VERDOUW, P.D. (1991). Evidence against a role for dopamine D_1 receptors in the porcine myocardium. *Br. J. Pharmacol.*, **104**, 246–250.

(Received March 12, 1992
Revised May 1, 1992
Accepted May 26, 1992)

Br. J. Pharmacol. (1992), **107**, 311–316

Effects of lignocaine and quinidine on the persistent sodium current in rat ventricular myocytes

Yue-Kun Ju, David A. Saint & [1] Peter W. Gage

John Curtin School of Medical Research, Australian National University, Canberra, Australia

1 The effects of the Class 1 antiarrhythmic agents lignocaine and quinidine on action potentials, and on sodium currents and potassium currents activated by depolarization, were examined in rat isolated ventricular myocytes by the whole cell, tight seal recording technique.

2 Tetrodotoxin and lignocaine shortened, whereas quinidine prolonged, the duration of the plateau phase of action potentials.

3 At low concentrations, lignocaine and quinidine blocked a persistent sodium current that was resistant to inactivation but they had only a small effect on the transient sodium current. At higher concentrations, they also blocked the transient sodium current.

4 Quinidine, but not tetrodotoxin or lignocaine, depressed potassium currents activated by depolarization and this could account for the prolongation of the plateau phase caused by quinidine.

5 It is suggested that block of the persistent sodium current may be responsible, at least in part, for the antiarrhythmic action of lignocaine and quinidine.

Keywords: Sodium current; Class 1 antiarrhythmic drugs; cardiac muscle; lignocaine; quinidine

Introduction

Lignocaine and quinidine are widely used in the management of ventricular arrhythmias. Both decrease the maximum rate of rise of ventricular action potentials and have been classified as Class 1 antiarrhythmic agents (Vaughan Williams, 1981) which share the common property of acting primarily on sodium channels. It is generally considered that these drugs suppress arrhythmias by blocking the sodium channels that cause rapid depolarization during an action potential and then quickly inactivate. Arrhythmias would be less likely in the presence of such agents because of an increase in threshold or a decrease in conduction velocity of action potentials.

We have recently described a small, very slowly inactivating, tetrodotoxin (TTX)-sensitive sodium current in rat myocytes (Saint *et al.*, 1992). There is considerable indirect evidence for such a current e.g. the decrease in duration of action potentials in dog Purkinje fibres caused by TTX (Coraboeuf *et al.*, 1979). As this current becomes activated close to the resting membrane potential (Saint *et al.*, 1992), it would contribute to the pacemaker current. Drugs that depress the persistent sodium current should act as antiarrhythmic agents by increasing the interval between action potentials and slowing the heart rate. Indeed, TTX has been shown to have an antiarrhythmic action *in vivo* (Abraham *et al.*, 1989).

We show here that both lignocaine and quinidine block the persistent sodium current at clinically relevant concentrations (Rosen *et al.*, 1975; Hoffman *et al.*, 1975) that have relatively little effect on the transient sodium current. These observations raise the possibility that the antiarrhythmic effects of these drugs are due, at least in part, to depression of the persistent sodium current.

Methods

Isolation of ventricular myocytes

Single ventricular myocytes were obtained by enzymatic dissociation of adult rat hearts using a Langendorff method (Farmer *et al.*, 1983). Briefly, adult Wistar rats were killed by cervical dislocation 20 to 30 min after an intraperitoneal injection of 2000 units of heparin. The heart was quickly excised and rinsed in calcium-free Tyrode solution cooled to 0°C and bubbled with oxygen. It was then perfused via the aorta with calcium-free Tyrode solution at 37°C for 5 min to remove blood from the chambers. The Tyrode solution contained (mM): NaCl 133, KCl 4.0, NaH_2PO_4 1.2, $MgCl_2$ 1.2, TES (N-tris(hydroxymethyl)-methyl-2 aminoethanesulphonic acid) 10, glucose 11, pH adjusted to 7.4 ± 0.5 with NaOH. The perfusing solution was then changed to one containing 25 μM calcium, collagenase (1 mg ml^{-1}; Worthington CLS II), protease (0.1 mg ml^{-1}; Sigma type XIV) and foetal calf serum (1 μl ml^{-1}). Success in the procedure was indicated by the heart becoming pale, enlarged and flaccid after 30–40 min perfusion with this enzyme solution. The ventricles were then removed, chopped into small pieces in fresh Tyrode solution containing 25 μM calcium, and gently triturated to dissociate the cells. Cell suspensions were centrifuged, the sedimented myocytes washed with 200 μM Ca^{2+}-Tyrode solution, then resuspended in 1 mM Ca^{2+}-Tyrode solution before being plated onto glass coverslips and maintained at room temperature.

Electrophysiological recording and data analysis

Currents were recorded from myocytes by the tight seal, whole cell technique (Hamill *et al.*, 1981). In order to obtain reproducible results, currents were usually recorded 10 to 15 min after achieving the whole-cell configuration. Analogue compensation available on the amplifier (Axopatch 1D) was used to minimize capacitative transients and leakage currents. Removal of residual leakage and capacitative currents was achieved by digital scaling and subtraction of the current generated by a 20 mV hyperpolarizing pulse preceding each test pulse.

Solutions and drugs

For simultaneous recording of sodium and potassium currents, the pipette solution contained (mM): KF 120, K-EGTA 10, $MgCl_2$ 1, $CaCl_2$ 2, ATP 10, TES 10, pH adjusted to 7.4 ± 0.05 with KOH. For recording sodium currents in

[1] Author for correspondence at: JCSMR, GPO Box 334 Canberra, ACT 2601, Australia

isolation, the pipette solution contained (mM): CsF 50, NaF 70, K-EGTA 20, $CaCl_2$ 2, TES 10, ATP 10, pH adjusted to 7.4 ± 0.05 with KOH. Electrodes typically had resistances of 1.5 to 2.0 MΩ when filled with pipette solution. Experiments were performed at room temperature (22 to 25°C) in a bath solution normally containing (mM): NaCl 130, KCl 5.4, $MgCl_2$ 1, $CaCl_2$ 2, CsCl 5, $CoCl_2$ 5, TES 10, NaOH 5, glucose 10, pH adjusted to 7.4 ± 0.05 with NaOH.

Quinidine sulphate dihydrate (Aldrich-chemie D-7924 Steinheim) and lignocaine (Sigma Chemical, St. Louis, MO, U.S.A.) were dissolved in test solutions.

Results

The effects of tetrodotoxin, lignocaine and quinidine on action potentials in rat isolated ventricular myocytes are shown for comparison in Figure 1. At the concentrations used, tetrodotoxin and lignocaine had little effect on the amplitude of action potentials but affected their plateau phase. It can be seen in Figure 1 that tetrodotoxin (0.1 μM) and lignocaine (25 μM) shortened the duration of the plateau phase. Quinidine (10 μM) had a more complicated effect, as shown in Figure 1c: the amplitude of the action potential was slightly reduced and repolarization after the peak was initially more rapid but the plateau phase was prolonged. The opposite effects of lignocaine and quinidine on the duration of the plateau phase of action potentials agree with previous observations (e.g. Colatsky, 1982).

The plateau phase of cardiac action potentials is due to a balance of inward and outward currents at the plateau potential. A drug which disturbs the balance of these currents should affect the plateau. For example, TTX would be expectred to affect the plateau because it has been shown at this concentration (0.1 μM) to block a persistent, inward sodium current that would be present at the plateau potential (Saint *et al.*, 1992). The effect of 50 μM TTX on the persistent sodium current can be seen in Figure 2. The currents were generated in an isolated myocyte by a voltage step to − 40 mV from a prepulse potential of − 150 mV (holding potential − 100 mV). In the standard extracellular solution, the rapidly decaying transient inward current (truncated in Figure 2, peak amplitude − 25.3 nA) was followed by a slowly inactivating persistent current which had an amplitude of about − 100 pA after 150 ms. Application of 50 μM TTX blocked the persistent current completely while causing an incomplete block of the transient current (residual peak amplitude − 2.8 nA). The effects of TTX were readily reversible, as shown by the trace labelled 'wash'. That this persistent current blocked by TTX is carried by sodium ions was confirmed by replacing the extracellular sodium ions with choline. This substitution depressed both transient and persistent sodium currents (Figure 2).

The reduced duration of the plateau phase of the action potential caused by lignocaine (Figure 1b) would be explained if lignocaine also blocked the persistent sodium

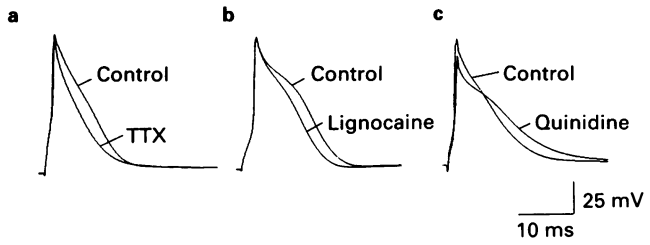

Figure 1 Effects of 0.1 μM tetrodotoxin (TTX) (a), 25 μM lignocaine (b) and 10 μM quinidine (c) on action potentials in isolated ventricular myocytes of the rat.

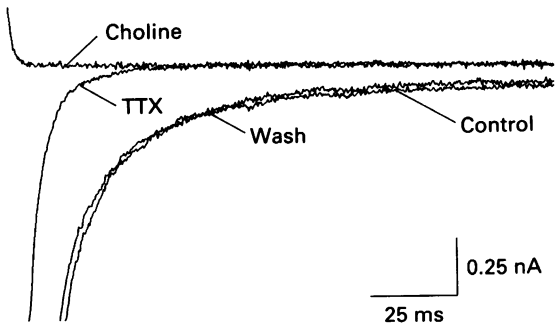

Figure 2 Block of the persistent inward current by tetrodotoxin (TTX, 50 μM) and by substitution of choline for sodium in the bath solution. The four current traces were elicited in a rat isolated myocyte by voltage steps to − 40 mV from a pre-pulse potential of − 150 mV in the normal bath solution (Control), in bath solution containing 50 μM TTX (TTX), after washing out the TTX with normal bath solution (Wash) and in bath solution containing choline instead of sodium (Choline).

current. This possibility was therefore tested. The effect of lignocaine on the persistent sodium current is illustrated in Figure 3a. At a concentration of 200 μM, lignocaine clearly blocked the persistent sodium current while not completely blocking the transient sodium current (the peak amplitude of the transient current was reduced from 30.1 to 2.7 nA). The degree of block of the persistent sodium current by the lignocaine was checked with 50 μM TTX which completely blocks the persistent sodium current (Figure 2). Addition of TTX (50 μM) caused no further reduction in the amplitude of the persistent sodium current (Figure 3a) indicating that the lignocaine had completely blocked this current. It can be seen

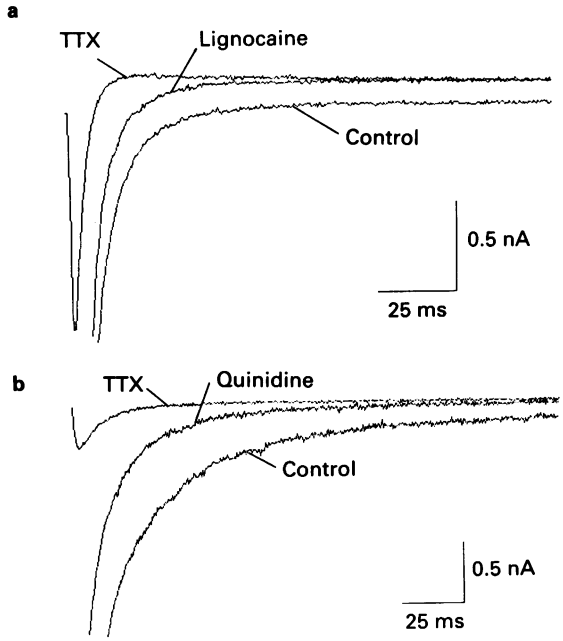

Figure 3 Block of the persistent sodium current by lignocaine and quinidine. All current traces were elicited by voltage steps to − 40 mV from a prepulse potential of − 150 mV. (a) The traces shown were recorded in control solution (Control), then in a solution containing 200 μM lignocaine, then in a solution containing 200 μM lignocaine plus 50 μM tetrodotoxin (TTX). (b) The traces were recorded in control solution (Control), in a solution containing 40 μM quinidine, and in a solution containing 40 μM quinidine plus 50 μM TTX.

in Figure 3a, however, that the addition of TTX caused a further reduction in the amplitude of the transient sodium current.

Quinidine had a similar effect on the persistent sodium current (Figure 3b). At a concentration of 40 μM, quinidine caused significant depression of the persistent sodium current whereas the transient current was much less affected (the peak amplitude of the transient current was reduced from − 68 to − 11 nA). Again, most of the persistent sodium current must have been blocked by the quinidine because there was little further depression of the persistent current when 50 μM TTX was added to the solution (Figure 3b).

In experiments such as those illustrated in Figure 3, it appeared that lignocaine and quinidine were blocking the persistent sodium current more effectively than the transient sodium current. The selective effect of these drugs on the persistent sodium current was even clearer when lower concentrations were used. The selective effect of a lower concentration of lignocaine is illustrated in Figure 4. Currents generated by voltage steps to − 50 mV from a pre-potential of − 150 mV are shown at both low (a) and high (b) gains so that the transient and persistent currents can be clearly seen. Traces obtained before introduction of the drug are marked C. Lignocaine, at a concentration of 12.5 μM, caused only slight depression of the transient current (from − 47.5 to − 39 nA) but there was significant depression of the persistent current. With a higher concentration of lignocaine (100 μM), there was much more depression of the transient current which now had a peak amplitude of 16 nA but there was little further depression of the persistent current, indicating that it had been completely blocked by the lower concentration of lignocaine. This was confirmed in several experiments by demonstrating that 50 μM TTX caused no further depression of the persistent sodium current. A comparison of the effects of low (12.5 to 25 μM) and high (100 to 200 μM) concentrations of lignocaine on the transient and persistent sodium currents can be seen in Table 1. There was no significant difference ($P > 0.05$, Student's t test) in the depression of the persistent sodium current with low and high concentrations of lignocaine whereas the transient sodium current was significantly smaller in solutions containing the higher concentrations of lignocaine.

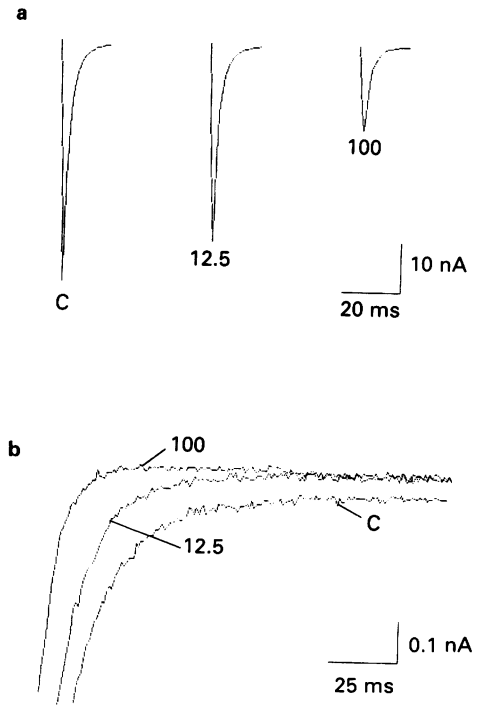

Figure 4 Differential sensitivity of the transient and persistent sodium current to lignocaine. The currents, evoked by voltage steps to − 50 mV from a prepulse potential of − 150 mV, are shown at low gain in (a) and at higher gain in (b) to reveal the persistent current. The records, all from the same cell, were obtained in control solution (labelled C), a solution containing 12.5 μM lignocaine (labelled 12.5) and a solution containing 100 μM lignocaine (labelled 100).

Quinidine at low concentrations, also selectively and reversibly blocked the persistent sodium current, as illustrated in Figure 5. Sodium currents were first recorded in control solution (C). After addition of 5 μM quinidine to the bath, the peak transient current was reduced by only 12% (from − 86.5 to − 77.5 nA, Figure 5a), but the persistent current was substantially reduced in amplitude (Figure 5b). These effects of quinidine could be reversed by washing the drug out of the bath, as illustrated by the traces marked W in Figure 5.

Effects of 5–10 μM and 40–120 μM quinidine on transient and persistent sodium currents are summarised in Table 2. There was no significant difference ($P > 0.05$, Student's t test) in the amount of persistent sodium current blocked by the low and high concentrations of quinidine. In contrast, the transient sodium current was more effectively blocked by the higher concentrations of quinidine. It is clear from these results that the persistent sodium current is more sensitive to block by quinidine than is the transient sodium current: 5 or 10 μM quinidine caused an essentially complete block of the persistent current but, on average, only a 26% block of the transient sodium current.

As both lignocaine and quinidine block the persistent sodium current, why does quinidine not shorten the plateau phase of action potentials? A possible explanation is that quinidine depresses the outward current that balances the inward current and eventually causes repolarization. The effects of tetrodotoxin, lignocaine and quinidine on outward currents were therefore investigated. In these experiments, inward sodium current was blocked by substituting choline for sodium in the extracellular solution. The currents shown in Figure 6 were generated by voltage steps to + 40 mV from a holding potential of − 140 mV. They consisted of a transient peak which subsided to a plateau. TTX (50 μM, a) and lignocaine (100 μM, b) caused a slight depression of the outward current which may have been due to block of a small outward sodium current at + 40 mV in the extracellular solution containing choline instead of sodium. In contrast, quinidine (20 μM, c) caused a large depression of both the transient and sustained components of the outward current as has been reported previously (Hiraoka *et al.*, 1986; Imaizumi & Giles, 1987; Balser *et al.*, 1991). In the presence of quinidine, the transient outward current was decreased in amplitude and decayed more rapidly. There was also a large decrease in the amplitude of the sustained outward current. Such effects could well explain the prolongation caused by quinidine in the plateau phase of the action potential (Figure 1c).

Discussion

We have shown that tetrodotoxin, lignocaine and quinidine block a persistent sodium current in rat ventricular myocytes. Lignocaine and quinidine do this at concentrations that are within their therapeutic ranges (Rosen *et al.*, 1975; Hoffman *et al.*, 1975). At the same concentrations, they had much less effect on the transient sodium current. A wide range of concentrations was not tested because accurate determination of smaller depressions of the persistent sodium current would be very difficult. Moreover, our primary interest was in the mechanism of the action of these drugs in the therapeutic range. The results clearly show that the persistent sodium current was much more sensitive than the transient sodium

Table 1 Depression of transient and persistent sodium currents by low and high concentrations of lignocaine

Low concentration of lignocaine (12.5 to 25 μM)

Cell	*Lignocaine* (μM)	ΔI_p (pA)	I_{tc} (nA)	$\Delta I_p/I_{tc}$ (%)	I_{td} (nA)	$(I_{tc}-I_{td})/I_{tc}$ (%)	*Vt* (mV)
1	25	− 118	− 49.0	0.24	− 44.0	10.2	− 50
2	25	− 149	− 44.0	0.34	− 38.5	12.5	− 40
3	25	− 122	− 41.5	0.29	− 33.5	19.3	− 50
4	25	− 90	− 48.5	0.19	− 33.5	30.9	− 40
5	12.5	− 89	− 34.5	0.26	− 23.5	31.9	− 40
6	12.5	− 95	− 33.0	0.29	− 23.5	28.8	− 40
7	12.5	− 170	− 69.5	0.24	− 53.0	23.7	− 50
8	12.5	− 103	− 47.5	0.22	− 39.5	16.8	− 50
9	25	− 103	− 35.0	0.29	− 30.0	14.3	− 40
	mean	− 115	− 44.7	0.26	− 35.4	20.9	
	1 s.e.mean	9.29	3.73	0.02	3.18	2.74	

High concentration of lignocaine (100 to 200 μM)

Cell	*Lignocaine* (μM)	ΔI_p (pA)	I_{tc} (nA)	$\Delta I_p/I_{tc}$ (%)	I_{td} (nA)	$(I_{tc}-I_{td})/I_{tc}$ (%)	*Vt* (mV)
1	200	− 115	− 28.0	0.41	− 13.5	51.8	− 40
2	200	− 158	− 48.5	0.33	− 17.0	64.9	− 40
3	100	− 114	− 36.5	0.31	− 13.0	64.4	− 40
4	200	− 264	− 78.5	0.34	− 4.50	94.3	− 50
5	100	− 103	− 47.5	0.22	− 16.5	65.3	− 40
6	100	− 79	− 42.5	0.19	− 22.5	47.1	− 50
7	100	− 103	− 45.0	0.23	− 28.5	36.7	− 50
8	100	− 116	− 50.0	0.23	− 19.5	61.0	− 40
9	100	− 215	− 21.5	1.00	− 13.0	39.5	− 40
10	200	− 142	− 30.0	0.47	− 2.65	91.2	− 40
11	100	− 110	− 41.5	0.27	− 21.0	49.4	− 40
	mean	− 138	− 42.7	0.36	− 15.6	60.5	
	1 s.e.mean	16.6	4.54	0.07	2.28	5.66	

The symbols denote: ΔI_p, the change in amplitude of the persistent sodium current (measured at the end of a 150 ms test pulse to V_T); I_{tc}, the peak amplitude of the transient current in control solution; I_{td}, the peak amplitude of the transient current in the presence of the drug. The holding potential was − 100 mV.

Table 2 Depression of transient and persistent sodium currents by low and high concentrations of quinidine

Low concentration of quinidine (5 to 10 μM)

Cell	*Quinidine* (μM)	ΔI_p (pA)	I_{tc} (nA)	$\Delta I_p/I_{tc}$ (%)	I_{td} (nA)	$(I_{tc}-I_{td})/I_{tc}$ (%)	*Vt* (mV)
1	5	− 102	− 86.5	0.12	− 77.5	10.4	− 50
2	10	− 86	− 32.0	0.27	− 26.0	18.8	− 60
3	10	− 83	− 20.0	0.42	− 17.0	15.0	− 40
4	5	− 125	− 66.7	0.19	− 35.6	46.6	− 40
5	5	− 161	− 76.5	0.21	− 61.1	20.1	− 40
6	5	− 148	− 36.5	0.41	− 22.8	37.5	− 40
7	5	− 156	− 37.9	0.41	− 31.2	17.7	− 40
8	5	− 155	− 55.1	0.28	− 30.0	45.6	− 40
	mean	− 127	− 51.4	0.29	− 37.6	26.5	
	1 s.e.mean	11.5	8.32	0.04	7.35	5.11	

High concentration of quinidine (40 to 120 μM)

Cell	*Quinidine* (μM)	ΔI_p (pA)	I_{tc} (nA)	$\Delta I_p/I_{tc}$ (%)	I_{td} (nA)	$(I_{tc}-I_{td})/I_{tc}$ (%)	*Vt* (mV)
1	40	− 95	− 31.0	0.31	− 10.5	66.1	− 40
2	40	− 83	− 32.5	0.26	− 9.00	72.3	− 40
3	40	− 176	− 68.0	0.26	− 11.0	83.8	− 50
4	80	− 122	− 66.7	0.18	− 5.77	91.3	− 40
5	120	− 175	− 76.5	0.23	− 1.54	98.0	− 40
6	80	− 194	− 36.5	0.53	− 8.40	77.0	− 40
7	80	− 150	− 41.0	0.37	− 4.20	89.8	− 40
	mean	− 142	− 50.3	0.30	− 7.20	82.6	
	1 s.e.mean	16.3	7.29	0.04	1.32	4.30	

The meanings of the symbols are as for Table 1

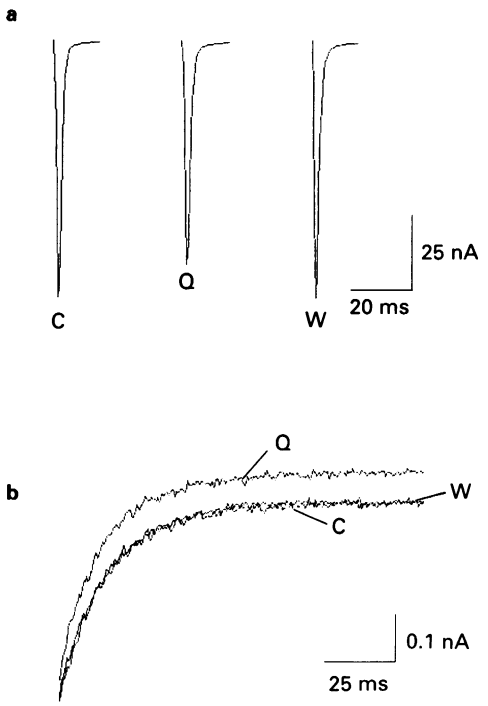

Figure 5 Differential sensitivity of the transient and persistent sodium current to quinidine. The currents, evoked by voltage steps to − 50 mV from a prepulse potential of − 150 mV, are shown at low gain in (a) and at higher gain in (b) to reveal the persistent current. The records, all from the same cell, were obtained in control solution (labelled C), in a solution containing 5 μM quinidine (labelled Q), and back in control solution after washing out the quinidine (labelled W).

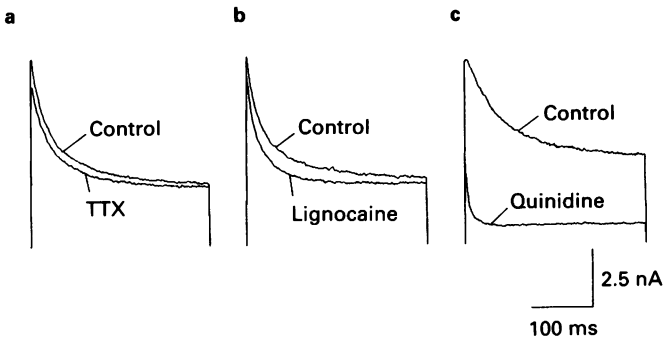

Figure 6 Effects of tetrodotoxin (TTX, 50 μM), lignocaine (100 μM) and quinidine (20 μM) on potassium currents. Choline was substitued for extracellular sodium and the currents shown were elicited by a voltage step to + 40 mV from a potential of − 140 mV. (a) and (b) contain records from the same cell; (c) from another.

current to both lignocaine and quinidine.

As the persistent sodium current is partially activated at − 70 mV and is 50% activated at about − 50 mV (Saint *et al.*, 1992), it would contribute an inward current that would increase in amplitude with progressive depolarization during a pacemaker potential. Block of such a current would tend to slow the rate of depolarization during the pacemaker potential and hence reduce the rate of firing of action potentials. Furthermore, cardiac muscle fibres would be less excitable when the persistent sodium current is blocked. It seems very likely, therefore, that the antiarrhythmic effects of lignocaine and quinidine are due, at least in part, to their effect on the persistent sodium current.

Although both lignocaine and quinidine blocked the persistent sodium current, they had different effects on the plateau phase of action potentials (Figure 1). This can be attributed to the depression of voltage-activated potassium currents caused by quinidine, an effect that has been well described previously (Hiraoka *et al.*, 1986; Imaizumi & Giles, 1987; Balser *et al.*, 1991).

It would be interesting to know why the persistent sodium current is more sensitive to these drugs than the transient sodium current. One possible explanation is that the drugs block open channels. If sodium channels were open for a longer time during the persistent sodium current, the probability of block by a 'blocking' drug would be increased Alternatively, binding of these drugs to sodium channels may be both time- and potential-dependent, being greater at later times and more depolarized potentials, whether or not channels are open.

Indeed, depression of sodium currents by lignocaine in cardiac muscle shows both of these forms of use-dependence (Clarkson *et al.*, 1988; Makielski *et al.*, 1991; Starmer *et al.*, 1991). Because of the different voltage-dependence of activation and inactivation of the transient and persistent sodium currents, it has been suggested that the two currents are generated by two different kinds of channel (Saint *et al.*, 1992). The difference may be very subtle, perhaps due to the presence or absence of a labile 'subunit'. Different modes of activity of sodium channels have been described (Nilius, 1988) and the probability of different modes appears to be influenced by intracellular modulators (Zhou *et al.*, 1991). However, the evidence presented here does not allow evaluation of these hypotheses. Whatever the basis of the persistent sodium current, the channels responsible for the persistent current are clearly more susceptible to block by TTX, lignocaine and quinidine than channels responsible for the transient sodium current. Discovery of the reason for this may lead to the introduction of new treatments for arrhythmias that depend on modifying the levels of endogenous modulators of the persistent sodium current.

This work was supported by a grant from the National Heart Foundation of Australia. We are grateful to Mrs B. McLachlan and M. Robertson for their assistance.

References

ABRAHAM, S., BEATCH, G.N., MACLEOD, B.A. & WALKER, M.J.A. (1989). Antiarrhythmic properties of tetrodotoxin against occlusion-induced arrhythmias in the rat: a novel approach to the study of the antiarrhythmic effects of ventricular sodium channel blockade. *J. Pharmacol. Exp. Ther.*, **251**, 1166–1171.

BALSER, J.R., BENNETT, P.B., HONDEGHEM, L.M. & RODEN, D.M. (1991). Suppression of time-dependent outward current in guinea pig ventricular myocytes. *Circ. Res.*, **69**, 519–529.

CLARKSON, C.W., FOLLMER, C.H., TEN EICK, R.E., HONDEGHEM, L.M. & YEH, J.Z. (1988). Evidence for two components of sodium channel block by lidocaine in isolated cardiac myocytes. *Circ. Res.*, **63**, 869–878.

COLATSKY, T.J. (1982). Mechanisms of action of lidocaine and quinidine on action potential duration in rabbit cardiac Purkinje fibers. *Circ. Res.*, **50**, 17–27.

CORABOEUF, E., DEROUBAIX, E. & COULOMBE, A. (1979). Effect of tetrodotoxin on action potentials of the conducting system in the dog heart. *Am. J. Physiol.*, **236**, H561–H567.

FARMER, B.B., MANCINA, M., WILLIAMS, E.S. & WATANABE, A.M. (1983). Isolation of calcium tolerant myocytes from adult rat hearts: review of the literature and description of a method. *Life Sci.*, **33**, 1–18.

HAMILL, O.P., MARTY, A., NEHER, E., SAKMANN, B.& SIGWORTH, F.J. (1981). Improved patch-clamp techniques for high resolution current recording from cells and cell-free membrane patches. *Pfügers Arch.*, **391,** 85–100.

HIRAOKA, M., SAWADA, K. & KAWANO, S. (1986). Effects of quinidine on plateau currents of guinea-pig ventricular myocytes. *J. Mol. Cell. Cardiol.*, **18,** 1097–1106.

HOFFMAN, B.F., ROSEN, M.R. & WIT, A.L. (1975). Electrophysiology and pharmacology of cardiac arrhythmias. VII. Cardiac effects of quinidine and procaine amide. *Am. Heart J.*, **89,** 804–808.

IMAIZUMI, Y. & GILES, W.R. (1987). Quinidine-induced inhibition of transient outward current in cardiac muscle. *Am. J. Physiol.*, **253,** H704–H708.

MAKIELSKI, J.C., ALPERT, L.A. & HANCK, D.A. (1991). Two components of use-dependent block of sodium current by lidocaine in voltage clamped cardiac Purkinje cells. *J. Mol. Cell. Cardiol.*, **23,** 95–102.

NILIUS, B. (1988). Modal gating behavior of cardiac sodium channels in cell-free membrane patches. *Biophys. J.*, **53,** 857–862.

ROSEN, M.R., HOFFMAN, B.F. & WIT, A.L. (1975). Electrophysiology and pharmacology of cardiac arrhythmias. V. Cardiac antiarrhythmic effects of lidocaine. *Am. Heart J.*, **89,** 526–536.

SAINT, D.A., JU, Y.K. & GAGE, P.W. (1992). A persistent sodium current in rat ventricular myocytes. *J. Physiol.*, **453,** 219–231.

STARMER, C.F., NESTERENKO, V.V., UNDROVINAS, A.I., GRANT, A.O. & ROSENSHTRAUKH, L.V. (1991). Lidocaine blockade of continuously and transiently accessible sites in cardiac sodium channels. *J. Mol. Cell. Cardiol.*, **23,** 73–83.

VAUGHAN-WILLIAMS, E.M. (1981). Classification of antidysrhythmic drugs. In *Pharmacology of anti-arrhythmic agents*, ed. SZEKERS, L., pp. 125–150. Oxford: Pergamon.

ZHOU, J., POTTS, J.F., TRIMMER, J.S., AGNEW, W.S. & SIGWORTH, F.J. (1991). Multiple gating modes and the effect of modulating factors on the μI sodium channel. *Neuron*, **7,** 775–785.

(Received March 24, 1992
Revised May 22, 1992
Accepted May 26, 1992)

Br. J. Pharmacol. (1992), **107**, 317–321

A perfusion system for the long term study of macrophage activation

Jamil Assreuy & [1] Salvador Moncada

Wellcome Research Laboratories, Langley Court, Beckenham, Kent BR3 3BS

1 A closed system was developed for perfusing J774 macrophages in columns. The cells were perfused for up to 100 h, at which time they were still viable.

2 Stimulation with increasing concentrations (0.01–10 $\mu g\ ml^{-1}$) of bacterial lipopolysaccharide (LPS) caused the cells to produce increasing amounts of nitrite in the perfusion medium. This production was time-dependent, reaching a plateau by 48–50 h.

3 The nitrite accumulation caused by 0.1 $\mu g\ ml^{-1}$ of LPS was augmented by priming the cells for 2 h with increasing amounts of interferon-γ. The nitrite accumulation also reached a plateau under these conditions.

4 N-iminoethyl-L-ornithine (L-NIO, 30 μM) completely inhibited the accumulation of nitrite whereas dexamethasone (0.3 μM) caused 60–70% inhibition.

5 Perfusion of the cells without L-arginine prevented the nitrite accumulation. Replacement of this amino acid after 20 or 50 h of perfusion led to a rapid generation of nitrite, the levels of which continued to increase for the duration of the experiment.

6 Thus, the perfusion system can be used to study the kinetics of the activation of the NO synthase and most likely other parameters in J774 cells and probably other cells in culture. An observation already of interest is that the 'disappearance' of the NO synthase after its activation can be prevented or reduced by removal of L-arginine from the medium.

Keywords: Nitric oxide; macrophage; interferon-γ; L-arginine; J774 cells; perfusion

Introduction

It is now well established that a variety of cells can generate nitric oxide (NO) from the amino acid L-arginine through the activity of NO synthase. This enzyme exists in two forms, one constitutive and the other inducible by stimuli such as bacterial lipopolysaccharide (LPS) and/or several cytokines (for a review, see Moncada *et al.*, 1991).

The induction of the macrophage NO synthase causes these cells to become cytostatic or cytotoxic to tumour cells (Hibbs *et al.*, 1988), bacteria (Granger *et al.*, 1990) and protozoa (Liew *et al.*, 1990). Furthermore, it has been demonstrated that NO produced by activated macrophages can cause metabolic abnormalities in the macrophage itself (Drapier & Hibbs, 1988). The induction of NO synthase in macrophages is inhibited by cycloheximide (Marletta *et al.*, 1988), showing that the process is dependent on *de novo* protein synthesis. Glucocorticoids also inhibit the induction of the NO synthase (Di Rosa *et al.*, 1990), although the mechanism by which they achieve this is not yet known. The potent inhibitory effect of glucocorticoids on NO synthase induction may explain some of their anti-inflammatory effects (Moncada *et al.*, 1991). In contrast, some L-arginine analogues, including N^G-monomethyl-L-arginine (L-NMMA) and N-iminoethyl-L-ornithine (L-NIO) inhibit the enzyme directly (McCall *et al.*, 1991).

Most of the studies so far on the activation of macrophages *in vitro* have been carried out on plates, coverslips, etc. In general, these systems are sampled at the end of the experiment so that the dynamic aspects of the cell response are not studied. Because of this, we thought that it would be of interest to develop a perfusion system to study these cells. We have perfused macrophages attached to microcarrier beads in a closed column system in sterile conditions over prolonged periods. This method, which is similar to that previously used in our laboratory to study endothelial cells (Gryglewski *et al.*, 1986), allows the activation of macrophages to be studied in a dynamic way. Such a system may easily be optimized for other cell types in order to study the kinetics of NO synthase induction and other related parameters.

[1] Author for correspondence.

Methods

Cell culture and attachment to the beads

The murine macrophage cell line J774 (ATCC TIB 67) was grown in suspension culture in Techne stirrer bottles, spun at 25 r.p.m. and incubated at 37°C in RPMI 1640 medium containing 25 mM N-2-hydroxyethylpiperazine-N′-2-ethanesulphonic acid (HEPES) and supplemented with 10% foetal calf serum (FCS), 2 mM glutamine, 100 u ml^{-1} penicillin and 100 $\mu g\ ml^{-1}$ streptomycin. The cells were subcultured by removing 95% of the cell suspension and replacing it with fresh growth medium. The medium used for the cell attachment to the beads and for the column perfusion was Dulbecco's modified Eagle's medium (DMEM) containing 30 mM HEPES, supplemented with 10% FCS, 2 mM glutamine, 200 u ml^{-1} penicillin, 200 $\mu g\ ml^{-1}$ streptomycin and 50 $\mu g\ ml^{-1}$ gentamycin. In addition, the medium was supplemented with glucose (final concentration 20 mM; Granger *et al.*, 1990). On the day of the experiment, the cells ($2–4 \times 10^8$) were collected by centrifugation, resuspended in DMEM and added to 1.5 g of hydrated Cytodex 3 beads in a spinner bottle. The beads had been washed and left in medium the day before the experiment. The volume was made up to 100 ml with medium and the bottle was incubated for 2–3 h at 37°C with occasional stirring. The beads were then allowed to settle down, the supernatant was removed by aspiration and the beads were washed three times with medium to remove the non-adherent cells. Cell count was carried out by nuclei enumeration in a haemocytometer (Sanford *et al.*, 1951).

Column set-up and washing

The system resembles that described by Gryglewski *et al.* (1986), except that the present one operates in a closed circuit. Each perfusion system consisted of a jacketed K16/20 chromatographic column (Pharmacia) with the ends closed with flow adaptors. Medium was pumped through the column at 2 ml min^{-1} via a heated glass coil which also served as a bubble trap. The column effluent went to a glass reservoir bottle from where it was again pumped through the column. The cap of the reservoir bottle was pierced, in addition to the inlet (for column effluent) and outlet (to pump), by one piece of polythene tubing with a three-way valve at the tip for sample collection. To relieve the small vacuum created by repeated sample collection, the cap was pierced by an injection needle, fitted with a disposable filter unit (0.2 μm). Therefore, the incoming air was sterilized on line. All glass parts were siliconized. Inside a laminar flow cabinet, the system was opened and 3–3.5 ml packed beads containing $1-3 \times 10^7$ cells ml^{-1} packed beads were added to the column and 100 ml of medium was added to the reservoir bottle. The column was closed and the whole system was transferred to the bench. Perfusion was then started and the temperature was maintained at 37°C by means of a water circulator. Under these conditions the system can be run indefinitely without bacterial contamination. At the end of the experiment, each system was dismantled, washed with plenty of water, reassembled and then sequentially washed by pumping, without recirculation, with: 100 ml of household detergent (5% v/v); 250 ml of water; 150 ml of polymyxin B sulphate (10 μg ml^{-1}); 250 ml of NaOH 0.2 N; 500 ml of sterile water and 100 ml 70% (v/v) ethanol. This washing protocol was important to reduce contamination with LPS to a minimum. After drying, the complete system was wrapped in plastic bags and sterilized by gamma radiation. The glass reservoir bottle was sterilized by autoclaving.

Cell activation

When the cells were activated by LPS alone, it was added directly to the reservoir bottle at the concentrations indicated. Priming with interferon-γ (IFN-γ) was carried out in a small volume of medium (usually 5 ml for each 3 ml of packed beads) for 2 h at 37°C. The beads were then added to the column as described. The effects of N-iminoethyl-L-ornithine (L-NIO), dexamethasone and polymyxin B were studied by adding these agents at the beginning of the perfusion directly to the reservoir bottle at the concentrations indicated. DMEM without arginine was used for the arginine deprivation/replacement experiments. The FCS used to make this medium was not dialysed and under these conditions initial L-arginine levels were 13.4 ± 0.5 μM ($n = 3$). At the times indicated, L-arginine was dissolved in DMEM without the amino acid, the solution was sterilized by filtration (0.2 μm) and injected into the system to yield the normal level of L-arginine. Although DMEM contains 400 μM L-arginine, after the addition of antibiotics, glucose, HEPES and serum the final concentration was 351 ± 10.2 μM ($n = 9$).

Biochemical assays

All measurements were carried out in the perfusion medium. Nitrite (NO_2^-) was measured by chemiluminescence assay as described (Palmer *et al.*, 1987). Total nitrate (NO_3^-) was measured by converting NO_3^- to NO_2^-, using the NO_3^- reductase method (Schmidt *et al.*, 1989).

Materials

The following materials were obtained from the sources indicated: phenol-extracted LPS from *Salmonella typhosa* 0901 (Difco); recombinant mouse IFN-γ (Genzyme); dexamethasone sodium phosphate (Merck, Sharp and Dohme); L-NIO (Wellcome); cell culture media (Gibco); FCS (Flow) and Cytodex 3 (Pharmacia).

Results

Dose-response curves to lipopolysaccharide

Activation with LPS induced a dose-dependent increase in NO_2^- levels in the perfusion effluent medium (Figure 1). This effect was noticeable even at doses as low as 0.01 μg ml^{-1}, while 10 μg ml^{-1} induced an increase of about 6 fold, when compared to control columns. The time course of the increase in NO_2^- was similar at all doses of LPS used. Six hours after the beginning of the perfusion, the NO_2^- levels were low, although higher than in medium alone (0.46 ± 0.07, $n = 6$ compared to 1.14 ± 0.67 nmol ml^{-1}, $n = 3$ for LPS 0.1 μg ml^{-1}). A steep increase occurred between 6 and 30 h and after 50 h the NO_2^- levels tended to plateau. The proportion of NO_2^-/NO_3^- was 1:1 and was not altered in any experiment. At the end of the perfusion time, the L-arginine level had decreased from 351 ± 10.2 μM ($n = 6$) to 237 ± 14.6 μM ($n = 3$ for LPS 0.1 μg ml^{-1}), representing a consumption of about 40% of the initial level. This L-arginine consumption was similar for all LPS concentrations used. By this time the cell viability was high, as the levels of lactate dehydrogenase found in the medium represented 20–45% of total enzyme content in J774 cells (data not shown). Unlike NO_2^- production, there was no clear dose-effect relationship between LPS and/or IFN-γ concentrations and cell viability.

Dose-response curves to interferon-γ

The concentration of 0.1 μg ml^{-1} of LPS was chosen as the closest to the ED_{50}. When this concentration of LPS was added to the J774 cells after a priming of 2 h with different doses of IFN-γ (see Methods section), an enhanced production of NO_2^- was observed. This amplification of the LPS response by IFN-γ was dose-dependent with an ED_{50} of about 75 u of the cytokine (Figure 2). In the absence of added LPS, the cytokine induced a small increase in NO_2^- levels (Figure 2) that was virtually abolished by 25 μg ml^{-1} of

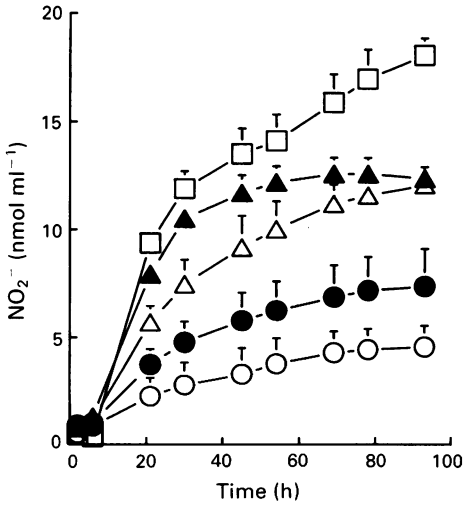

Figure 1 Time-course of NO_2^- production in perfused J774 cells activated by bacterial lipopolysaccharide (LPS). Control(○); 0.01 (●); 0.1 (△); 1.0 (▲) and 10 (□) μg ml^{-1}. The endotoxin was added to the medium at the beginning of the perfusion and, at the indicated time intervals, samples of the medium were withdrawn for the measurements. Each point represents mean (± s.e.mean, vertical bars) of 4–5 columns.

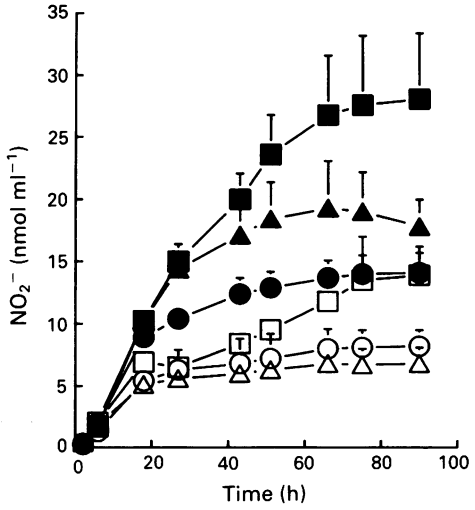

Figure 2 Time-course of NO_2^- production in perfused J774 cells primed with interferon-γ (IFN-γ). The open symbols show activation by IFN-γ alone (○, 25; △, 75; □, 150 u); the closed symbols are the same concentrations of IFN-γ plus bacterial lipopolysaccharide 0.1 μg ml^{-1} (●, 25;▲, 75; ■ 150 u). Each point represents mean (± s.e.mean, vertical bars) of 3 columns.

polymyxin B in the medium (from 6.8 ± 1.3 to 1.1 ± 0.27 nmol ml^{-1}, $n = 3$, data not shown).

Effects of N-iminoethyl-L-ornithine and dexamethasone

We next studied the effects of dexamethasone and of L-NIO on the perfused J774 macrophages. The concentrations employed were approximately 10 fold higher than the IC_{50} (50 nM for dexamethasone, Di Rosa *et al.*, 1990; 3 μM for L-NIO, McCall *et al.*, 1991). When either of these two compounds was added to the system at the beginning of the perfusion and the cells were stimulated with IFN-γ (75 u) plus LPS (0.1 μg ml^{-1}), a significant decrease in NO_2^- levels was found. However, L-NIO proved to be more potent in this regard, inhibiting completely the NO synthase activity whereas the corticosteroid caused only 60–70% inhibition (Figure 3).

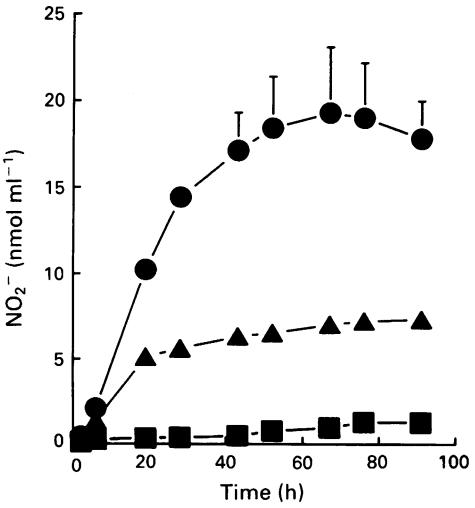

Figure 3 Inhibition by dexamethasone and N-iminoethyl-L-ornithine (L-NIO) of the production of NO_2^- by perfused J774 cells activated by interferon-γ (IFN-γ) and bacterial lipopolysaccharide (LPS). (●) Activation by IFN-γ (75 u) and LPS (0.1 μg ml^{-1}); (▲) inhibition by dexamethasone 0.3 μM; (■) inhibition by L-NIO 30 μM. Each point represents mean (± s.e.mean, vertical bars) of 3 columns.

Perfusion in L-arginine-free medium and the effects of replacement of L-arginine

When L-arginine was omitted from the medium, the cells produced virtually no NO_2^- after activation with IFN-γ and LPS (Figure 4). When, after 20 of 50 h of perfusion, L-arginine was replaced to the levels of normal DMEM, a rise in NO_2^- accumulation was observed. However, this rise had a time-course different from that observed when L-arginine was present throughout the perfusion, so that NO_2^- accumulation increased almost linearly with time, the levels of NO_2^- attained were higher and no plateau was seen up to the end of perfusion (Figure 4). For instance, the cells in normal medium produced NO_2^- at a rate of 0.63 nmol ml^{-1} h^{-1} in the first 24 h of perfusion whereas this rate was doubled (1.25 nmol ml^{-1} h^{-1}) in the same period when the amino acid was replaced after 20 h of perfusion. More importantly, the total NO_2^- concentration was 400% greater in the latter than in the former situation.

Discussion

Perfusion of columns of microcarriers containing endothelial cells has provided valuable information about the biology of the L-arginine: NO pathway (Palmer *et al.*, 1987; 1988; Palmer & Moncada, 1989). This system has also been applied to the study of this pathway in smooth muscle cells (Bernhardt *et al.*, 1991). We now describe the characteristics of the perfusion system when a macrophage cell line was used.

J774 cells, like mouse macrophages (Stuehr & Marletta, 1987), show a dose-dependent production of NO_2^- in response to LPS. The time-course of NO_2^- production in the closed system we used was essentially the same as for J774 cells activated in bottles or in plates by a mixture of LPS and IFN-γ (Di Rosa *et al.*, 1990). The effect of LPS on the induction of NO synthase was enhanced by IFN-γ. Since the time-courses of cell activation by LPS alone or by the endotoxin and IFN-γ are very similar, this suggests that the

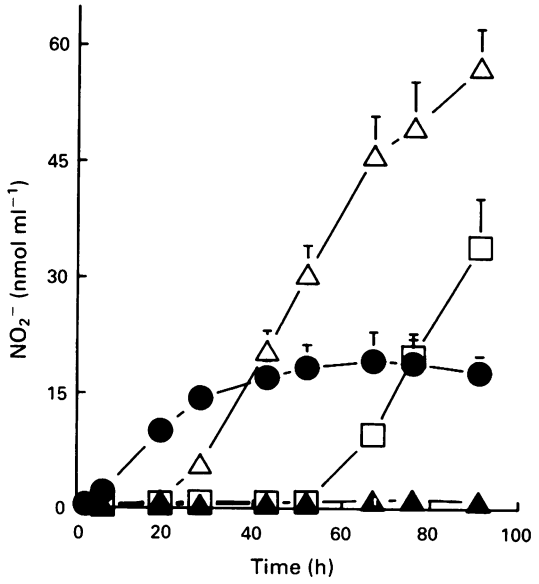

Figure 4 Time-course of NO_2^- production in normal DMEM and in DMEM without L-arginine in perfused J774 cells activated with interferon-γ (IFN-γ) and bacterial lipopolysaccharide (LPS). Control in medium with L-arginine (●) and in medium without L-arginine (▲). Effect of adding L-arginine at 20 h (△) and at 50 h (□) of perfusion. The cells were primed with 75 u of IFN-γ in normal DMEM and washed three times with DMEM without L-arginine before the column was set up. LPS was present at 0.1 μg ml^{-1}. Each point represents mean (± s.e.mean, vertical bars) of 3 columns.

cytokine produces only a quantitative change in the activation of the macrophages. Furthermore the effect of IFN-γ seems to occur rapidly for incubation of the cells with IFN-γ for as little as 2 h was enough to enhance the effect of LPS.

The small production of NO_2^- caused by IFN-γ alone in the absence of added LPS was largely prevented by polymyxin B, an antibiotic known to inactivate LPS (Weinberg *et al.*, 1978). This indicates that even with careful washing, some LPS remains in the system. Although we did not find a direct inducing effect of IFN-γ, this could be attributable to the low concentrations and the short time of contact with the cytokine. Murine macrophages cultured on plates have been shown to produce NO_2^- when kept in contact with high concentrations (500 u ml^{-1}) of IFN-γ in the presence of polymyxin B (Stuehr & Marletta, 1987).

The process of induction of the NO synthase in J774 macrophages is inhibited dose-dependently by glucocorticoids (Di Rosa *et al.*, 1990). The mechanism of this effect is not clear yet but involves binding of the steroid to specific receptors. Furthermore, this effect occurs *in vivo* and the inhibition can be achieved at plasma concentrations found following therapeutic administration (Di Rosa *et al.*, 1990). Therefore, inhibition of the induction of NO synthase by glucocorticoids is likely to explain, at least in part, some of their anti-inflammatory and immunosuppressive actions. L-arginine analogues have been employed as a means of unravelling and confirming the involvement of NO in a variety of processes (Moncada *et al.*, 1991). These analogues inhibit J774 macrophage and rat polymorphonuclear leukocyte NO synthase activity either reversibly (L-NMMA) or irreversibly (L-NIO) (McCall *et al.*, 1991). In our system, the level of inhibition of J774 cell NO synthase was very similar to that reported for these cells when cultured on plates (Di Rosa *et al.*, 1990).

L-Arginine is the biological substrate for the generation of NO (Hibbs *et al.*, 1988; Palmer *et al.*, 1988). In activated macrophages, about one third of consumed L-arginine gives rise to L-citrulline and NO_2^-/NO_3^- (products of NO synthase) at the expense of the arginase pathway (Granger *et al.*, 1990). This also seems to be the case in our experiments, since the total L-arginine consumption was approximately 140 μM and the $NO_2^- + NO_3^-$ production was 40–50 μM; the rest was presumably used by arginase.

In the absence of exogenous L-arginine J774 cells did not generate NO_2^- following the induction of the enzyme. However, replacement of the amino acid at 20 or 50 h after induction led to a rapid and continuous increase in the NO_2^- levels. Thus, these cells, in spite of having high levels of L-arginine (Hecker *et al.*, 1990), have little or no ability to use it for the generation of NO and are therefore totally dependent on the supply of exogenous amino acid for this purpose. This confirms previous results in macrophages on plates (Drapier & Hibbs, 1988; Takema *et al.*, 1991). In addition, this suggests that these cells may be different from endothelial cells which seem able to generate L-arginine from L-citrulline and use it for NO generation (Palmer *et al.*, 1988; Hecker *et al.*, 1990). The higher NO_2^- accumulation after L-arginine replacement at 20 h of perfusion was indicative of an increase in the uptake of the amino acid induced by the activation process. Indeed, L-arginine uptake in J774 cells has been shown to be doubled by activation with LPS plus IFN-γ (Bogle, Baydoun, Pearson, Moncada & Mann, unpublished observations).

If the plateau in NO_2^- accumulation which occurs in J774 cells after about 48 h of perfusion and also in mouse peritoneal macrophages after 50–60 h of activation (Stuehr & Marletta, 1987; Takema *et al.*, 1991) reflects deactivation of NO synthase, one would expect little or no NO_2^- accumulation when L-arginine was replaced at this stage of perfusion. The finding that NO_2^- production occurred at a very high rate when L-arginine was replaced after 50 h of perfusion indicates that NO synthase was still active. Therefore, it is possible that NO produced by the cells is somehow involved in the deactivation of NO synthase.

We thank Neale Foxwell for his skilful technical assistance during the setup of the column system. We also thank Gill Henderson and Annie Higgs for their help in preparing the manuscript. J.A. is on leave from Department of Pharmacology, ICB/CCS, Brazil and is supported by a fellowship of Conselho Nacional de Desenvolvimento Cientifico e Tecnologico (CNPq), Brazil.

References

BERNHARDT, J., TSCHUDI, M.R., DOHI, Y., GUT, I., URWYLER, B., BUHLER, F.R. & LUSCHER, T.F. (1991). Release of nitric oxide from human vascular smooth muscle cells. *Biochem. Biophys. Res. Commun.*, **180,** 907–912.

DI ROSA, M., RADOMSKI, M., CARNUCCIO, R. & MONCADA, S. (1990). Glucocorticoids inhibit the induction of nitric oxide synthase in macrophages. *Biochem. Biophys. Res. Commun.*, **172,** 1246–1252.

DRAPIER, J.-C. & HIBBS, J.B. Jr. (1988). Differentiation of murine macrophages to express nonspecific cytotoxicity for tumor cells in L-arginine-dependent inhibition of mitochondrial iron-sulphur enzymes in the macrophage effector cells. . *Immunol.*, **140,** 2829–2838.

GRANGER, D.L., HIBBS, J.B. Jr., PERFECT, J.R. & DURACK, D.T. (1990). Metabolic fate of L-arginine in relation to microbiostatic capability of murine macrophages. *J. Clin. Invest.*, **85,** 264–273.

GRYGLEWSKI, R.J., MONCADA, S. & PALMER, R.M.J. (1986). Bioassay of prostacyclin and endothelium-derived relaxing factor (EDRF) from porcine aortic endothelial cells. *Br. J. Pharmacol.*, **87,** 685–694.

HECKER, M., SESSA, W.C., HARRIS, H.J., ANGGARD, E.E. & VANE, J.R. (1990). The metabolism of L-arginine and its significance for the biosynthesis of endothelium-derived relaxing factor: cultured endothelial cells recycle L-citrulline to L-arginine. *Proc. Natl. Acad. Sci. U.S.A.*, **87,** 8612–8616.

HIBBS, J.B. Jr., TAINTOR, R.R., VAVRIN, Z. & RACHLIN, E.M. (1988). Nitric oxide: a cytotoxic activated macrophage effector molecule. *Biochem. Biophys. Res. Commun.*, **157,** 87–94.

LIEW, F.Y., MILLOT, S., PARKINSON, C., PALMER, R.M.J. & MONCADA, S. (1990). Macrophage killing of Leishmania parasite in vivo is mediated by nitric oxide from L-arginine. *J. Immunol.*, **144,** 4794–4797.

MARLETTA, M.A., YOON, P.S., IYENGAR, R., LEAF, C.D. & WISHNOK, J.S. (1988). Macrophage oxidation of L-arginine to nitrite and nitrate: nitric oxide is an intermediate. *Biochemistry*, **27,** 8706–8711.

MCCALL, T.B., FEELISCH, M., PALMER, R.M.J. & MONCADA, S. (1991). Identification of N-iminoethyl-L-ornithine as an irreversible inhibitor of nitric oxide synthase in phagocytic cells. *Br. J. Pharmacol.*, **102,** 234–238.

MONCADA, S., PALMER, R.M.J. & HIGGS, E.A. (1991). Nitric oxide: physiology, pathophysiology and pharmacology. *Pharmacol. Rev.*, **43,** 109–142.

PALMER, R.M.J., ASHTON, D.S. & MONCADA, S. (1988). Vascular endothelial cells synthesize nitric oxide from L-arginine. *Nature*, **333,** 664–666.

PALMER, R.M.J., FERRIGE, A.G. & MONCADA, S. (1987). Nitric oxide release accounts for the biological activity of endothelium-derived relaxing factor. *Nature*, **327,** 524–526.

PALMER, R.M.J. & MONCADA, S. (1989). A novel citrulline-forming enzyme implicated in the formation of nitric oxide by vascular endothelial cells. *Biochem. Biophys. Res. Commun.*, **158,** 348–352.

SANFORD, K.K., EARLE, W.R. & EVANS, V.J. (1951). The measurement of proliferation in tissue cultures by enumeration of cell nuclei. *J. Natl. Cancer Inst.*, **11,** 773–795.

SCHMIDT, H.H.H., WILKE, P., EVERS, B. & BOHME, E. (1989). Enzymatic formation of nitrogen oxides from L-arginine in bovine brain cytosol. *Biochem. Biophys. Res. Commun.*, **165,** 284–291.

STUEHR, D.J. & MARLETTA, M.A. (1987). Induction of nitrite/nitrate synthesis in murine macrophages by BCG infection, lymphokines or interferon-γ. *J. Immunol.*, **139,** 518–525.

TAKEMA, M., INABA, K., UNO, K., KAKIHARA, K.-I., TAWARA, K. & MURAMATSU, S. (1991). Effect of L-arginine on the retention of macrophage tumoricidal activity. *J. Immunol.*, **146,** 1928–1933.

WEINBERG, J.B., CHAPMAN, H.A. & HIBBS, J.B., Jr. (1978). Characterization of the effects of endotoxin on macrophage tumor cell killing. *J. Immunol.*, **121,** 72–80.

(Received April 6, 1992)
Revised May 12, 1992
Accepted May 26, 1992)

Br. J. Pharmacol. (1992), **107**, 322–328

Rabbit isolated renal artery contractions by some tryptamine derivatives, including 2-methyl-5-HT, are mediated by a 5-HT_1-like receptor

Sreekanth Tadipatri, *Wasyl Feniuk & [1] Pramod R. Saxena

Department of Pharmacology, Faculty of Medicine and Health Sciences, Erasmus University Rotterdam, Post box 1738, 3000 DR Rotterdam, The Netherlands and *Glaxo Group Research, Ware, Herts, U.K.

1 Despite the fact that 5-hydroxytryptamine (5-HT)-induced contractions of the rabbit isolated renal artery are mediated by a receptor belonging to the heterogeneous 5-HT_1-like category, we observed that the so-called selective 5-HT_3 receptor agonist, 2-methyl-5-HT, caused a concentration-dependent contraction of this vessel. This study was therefore undertaken to analyze the effects of 2-methyl-5-HT in the renal artery segments, either quiescent or precontracted with U46619 (10^{-7} M). α-Methyl-5-HT and 5-methoxytryptamine, which have high affinities for 5-HT_2 and 5-HT_4 receptors, respectively, were used for comparison.

2 In the precontracted vessel segments, the maximum contractile responses obtained with 2-methyl-5-HT, α-methyl-5-HT, 5-methoxytryptamine and 5-HT were similar to those in the quiescent segments. However the pD_2 values were higher in the precontracted segments, making them about 4–100 fold more sensitive.

3 Neither MDL 72222 (10^{-6} M) nor tropisetron (3×10^{-6} M) suppressed renal artery contractions elicited by 5-HT, 2-methyl-5-HT, α-methyl-5-HT or 5-methoxytryptamine, thus ruling out the involvement of 5-HT_3 as well as 5-HT_4 receptors.

4 On the other hand, both methiothepin (10^{-8} and 10^{-7} M) and ketanserin (10^{-7} and 10^{-6} M) caused a rightward shift of agonist concentration-effect curves. The two antagonists had similar pA_2 values against the different agonists tested on either quiescent or precontracted vessels, but ketanserin (apparent pA_2: 6.6 to 7.0) was between 20–100 fold less potent than methiothepin (apparent pA_2: 8.4 to 8.8).

5 The results of this functional study permit us to conclude that the contractile effects of 2-methyl-5-HT as well as α-methyl-5-HT and 5-methoxytryptamine on the rabbit isolated renal artery are mediated by a 5-HT_1-like receptor. Since, in addition, the reported ligand binding affinity of 2-methyl-5-HT at 5-HT_3 receptors is similar to both the ligand binding affinity and the functional pD_2 at 5-HT_1 sites, this compound cannot be regarded as a selective 5-HT_3 receptor agonist. Similarly, α-methyl-5-HT and 5-methoxytryptamine have only a limited selectivity for 5-HT_2 and 5-HT_4 receptors, respectively.

Keywords: 5-HT receptors; 5-hydroxytryptamine; 2-methyl-5-hydroxytryptamine; α-methyl-5-hydroxytryptamine; rabbit renal artery

Introduction

The receptors for 5-hydroxytryptamine (5-HT) can be classified on the basis of selective agonists and antagonists into four main types, namely 5-HT_1-like, 5-HT_2, 5-HT_3 and 5-HT_4 receptors (see Bradley *et al.*, 1986; Saxena & Villalón, 1990). The compounds which are considered relatively selective agonists at these receptors are: 5-carboxamidotryptamine (5-HT_1-like), sumatriptan (a particular 5-HT_1-like subtype), α-methyl-5-HT (5-HT_2), 1-(2,5-dimethoxy-4-iodophenyl)-2-aminopropane hydrochloride (DOI; 5-$HT_{1C/2}$), 2-methyl-5-HT (5-HT_3), 5-methoxytryptamine (5-HT_1-like and 5-HT_4) and renzapride (5-HT_4). Similarly, methiothepin (5-HT_1-like and 5-HT_2), ketanserin (5-HT_2), MDL 72222 (5-HT_3) and tropisetron (5-HT_3 and, in high concentrations, 5-HT_4) are regarded as selective antagonists.

The contractile effect of 5-HT in the rabbit isolated renal artery is mimicked by 5-carboxamidotryptamine, sumatriptan, α-methyl-5-HT and 5-methoxytryptamine, but not DOI, and antagonized by methiothepin (potently) and ketanserin (moderately), but not MDL 72222. Therefore, the pharmacological properties of the 5-HT receptor in the rabbit isolated renal artery most closely resemble those described for the heterogeneous 5-HT_1-like category (Tadipatri *et al.*, 1991). Yet, we recently noticed that 2-methyl-5-HT, a compound considered as a selective 5-HT_3 receptor agonist, elicited concentration-dependent contractions of this artery. Though it is reported that 2-methyl-5-HT has affinity for 5-HT_1 binding sites (Hoyer, 1989; Ismaiel *et al.*, 1990, Van Wijngaarden *et al.*, 1990) and can even sometimes elicit functional responses in tissues containing a 5-HT_1 receptor subtype (Schoeffter & Hoyer, 1990; Hamel & Bouchard, 1991; Sumner, 1991; Bax *et al.*, 1992), none of the investigations conclusively demonstrated this putative lack of selectivity by using appropriate antagonists. It is for this reason that we have now performed a thorough analysis of the mechanism of action of 2-methyl-5-HT in the rabbit renal artery. For comparison, we included in this analysis α-methyl-5-HT and 5-methoxytryptamine, both of which contracted the artery in our previous investigation (Tadipatri *et al.*, 1991), but had not been challenged with any antagonist. Lastly, as the responses to 5-HT and 5-carboxamidotryptamine were potentiated in vessel segments precontracted with U44169 (Tadipatri *et al.*, 1991), we tried to establish if this was also true for 2-methyl-5-HT, α-methyl-5-HT and 5-methoxytryptamine. Some of the results of this investigation have been reported to the British Pharmacological Society (Tadipatri & Saxena, 1992).

[1] Author for correspondence.

Methods

Tissue preparation

New Zealand white rabbits (ENKI, Helmond, The Netherlands), weighing 2.0–2.8 kg, were killed by injections of pentobarbitone sodium (Nembutal; 60 mg kg^{-1}) into a marginal ear vein. The right and left renal arteries were cleaned of fat and connective tissue *in situ*, and placed in Krebs solution (composition in mM: NaCl 118, KCl 4.7, $CaCl_2$ 2.5, $MgSO_4$ 1.2, $NaHCO_3$ 25, KH_2PO_4 1.2 and glucose 8.3, pH 7.4). Ring segments (3–5 mm length) were prepared carefully under a microscope and suspended between two stainless steel wire hooks (0.2 mm diameter) inserted into the lumen to record changes in isometric tension. Subsequently, the vessel segments were placed in organ bath chambers filled with 8 ml Krebs solution maintained at 37°C and bubbled constantly with a 95% O_2 and 5% CO_2 gas mixture. No attempt was made to remove the endothelium. At the end of the experiment, the relaxation to 10^{-7} M methacholine was measured. Though only those preparations which showed a vasodilator response were included in the study, it should be recalled that, unlike methacholine, 5-HT does not elicit vasodilatation (Tadipatri *et al.*, 1991).

Contractile tension was measured with a Harvard isometric transducer and the preparations were maintained at an initial resting tension of 2 g. During the equilibration period, the Krebs solution was exchanged at 15 min intervals and the vascular segments were re-stretched to the resting tension. This procedure was repeated three times. After equilibration, the contractile response to 30 mM KCl was ascertained and the preparations washed. Since the sensitivity to 5-carboxamidotryptamine and 5-HT was substantially increased in vascular segments precontracted with a submaximal concentration (10^{-7} M) of U46619 (Tadipatri *et al.*, 1991), the experiments were conducted in both quiescent and precontracted vessels. In about 50% of the vessel segments U46619 did not elicit contraction though KCl produced its normal response.

Determination of agonist potency

5-HT was added to the fluid bathing the renal artery preparations by use of cumulative concentration schedule, allowing sufficient time for the effects of each concentration to become fully established before adding the next concentration, until a maximum response (E_{max}) was obtained or relaxation started to occur. After frequent washing tissues were left for at least 30 min before re-challenging with either 5-HT or another agonist. On each preparation, one or two concentration-effect curves to 5-HT were obtained; previous experiments had shown that at least three consecutive concentration-effect curves to 5-HT were reproducible (Tadipatri *et al.*, 1991). One preparation was used as a control in which the concentration-effect curve to 5-HT was repeated, while concentration-effect curves to various other agonists (2-methyl-5-HT, α-methyl-5-HT and 5-methoxytryptamine) were constructed on other preparations from the same animal.

Determination of antagonist potency

Concentration-effect curves to 5-HT were established in the rabbit renal artery as described above. One preparation was used as a control and a single concentration of an antagonist was added to the other organ baths. An antagonist equilibration time of 30 min was allowed before agonist concentration-effect curves were re-determined.

Analysis of the data

The concentration-effect curves for the agonists were analyzed by means of a computerized curve fitting technique described by De Lean *et al.* (1978). The parameters thus obtained (i.e. pD_2 and E_{max}) were averaged for the respective agonists. In the case of antagonists, the shifts in the agonist-induced concentration-effect curves were calculated from the pD_2 values in each individual preparation before and after addition of an antagonist. The slope and apparent pA_2 values were calculated from equations described by Kenakin (1987). All data are presented as means ± s.e.mean. Student's *t* test was used to evaluate the significance of the differences in the slope, pD_2 and E_{max} values.

Compounds

Apart from pentobarbitone (Nembutal: Sanofi, Paris, France), the compounds used in this study were kindly supplied by or purchased from the companies mentioned: 5-hydroxytryptamine creatinine sulphate (Sigma Chemical Co., St. Louis, U.S.A.), tropisetron (ICS 205-930; gift: Sandoz, Basel, Switzerland), ketanserin tartrate (gift: Janssen Pharmaceutica, Beerse, Belgium), 1αH,3α,5αH-tropan-3yl-3,5-dichlorobenzoate (MDL 72222; gift: Merrell Dow Research Institute, Strasbourg, France), methacholine bromide (Janssen Chimica, Beerse, Belgium), methiothepin malelate (gift: Hoffman La Roche, Mijdrecht, The Netherlands), 5-methoxytryptamine hydrochloride (Research Biochemicals Inc., Natick, U.S.A.), 2-methyl-5-hydroxytryptamine (gift: Glaxo, Ware, U.K.), α-methyl-5-hydroxytryptamine maleate (gift: Glaxo, Ware, U.K.), and 9,11-dideoxy-11α,9,α-epoxymethano-prostaglandin $F_{2\alpha}$ (U46619; The Upjohn Chemical Company, Kalamazoo, U.S.A.).

Results

Agonist studies in the absence or presence of U46619

The concentration-effect curves obtained with 5-HT, 2-methyl-5-HT, α-methyl-5-HT and 5-methoxytryptamine on the rabbit isolated renal artery, either quiescent or precontracted with U46619 (10^{-7} M), are shown in Figure 1. In both cases, all four agonists elicited renal artery contractions; the maximum responses obtained with 2-methyl-5-HT, α-methyl-5-HT and 5-methoxytryptamine were comparable to those with the first administration of 5-HT (Figure 1; Table 1). The rank order of potency in the quiescent vessels was α-methyl-5-HT = 2-methyl-5-HT > 5-HT > 5-methoxytryptamine. Compared to the quiescent vessels, the precontracted vessels were more sensitive to these agonists, but the increase in the sensitivity was most marked with 5-HT (100 fold), followed in the decreasing order by α-methyl-5-HT (30 fold), 5-methoxytryptamine (10 fold) and 2-methyl-5-HT (4 fold). Consequently, the rank order of potency in the vessels precontracted with U44169 was α-methyl-5-HT = 5-HT> 2-methyl-5-HT> 5-methoxytryptamine (Table 1).

Analysis of agonist-induced contractions

The renal artery contractions elicited by the agonists 5-HT (Figure 2), 2-methyl-5-HT (Figure 3), α-methyl-5-HT (Figure 4) and 5-methoxytryptamine (Figure 5) were analyzed both in the absence (quiescent vessels) and presence of U46619 (precontracted vessels), using the antagonists MDL 72222 (10^{-6} M), tropisetron (3×10^{-6} M), ketanserin (10^{-7} and 10^{-6} M) and methiothepin (10^{-8} and 10^{-7} M). It should be noticed that neither MDL 72222 nor tropisetron antagonized the contractile responses to these agonists, including 2-methyl-5-HT which is considered selective for the 5-HT_3 receptor. On the other hand, both methiothepin and, to a lesser extent, ketanserin caused a rightward shift of the concentration-effect curves. In some cases, particularly with the higher concentration (10^{-7} M) of methiothepin, there was some depression of the maximum responses.

In Table 2 are shown the slopes and apparent pA_2 values

of ketanserin and methiothepin against the agonists 5-HT, 2-methyl-5-HT, α-methyl-5-HT and 5-methoxytryptamine, both in the quiescent and precontracted vessels. The slopes did not differ from unity. Though the apparent pA_2 values of ketanserin (6.6 to 7.0) and methiothepin (8.4 to 8.8) against the different agonists were similar, irrespective of the initial tension of the vessel, ketanserin was between 20–100 fold less potent than methiothepin.

Discussion

The rabbit isolated renal artery is a tissue where the contractile effect of 5-HT is mediated by a 5-HT_1-like receptor (Tadipatri *et al.*, 1991). The main aim of the present study in the rabbit isolated renal artery was to analyze the effects of the selective 5-HT_3 receptor agonist, 2-methyl-5-HT, as well as α-methyl-5-HT and 5-methoxytryptamine, which are considered relatively selective for 5-HT_2 and 5-HT_4 receptors, respectively (Bradley *et al.*, 1986; Saxena & Villalón, 1990). Indeed, as 2-methyl-5-HT, α-methyl-5-HT and 5-methoxytryptamine are commonly used for receptor characterization, it is important to keep validating the selectivity of such compounds which are employed in the characterization of receptors.

Effect of agonists in quiescent and precontracted vascular segments

Sahin-Erdemli *et al.* (1991) have reported that, unless the basal tone is slightly increased with prostaglandin $F_{2\alpha}$ virtually no contractions are noticed in the guinea-pig iliac

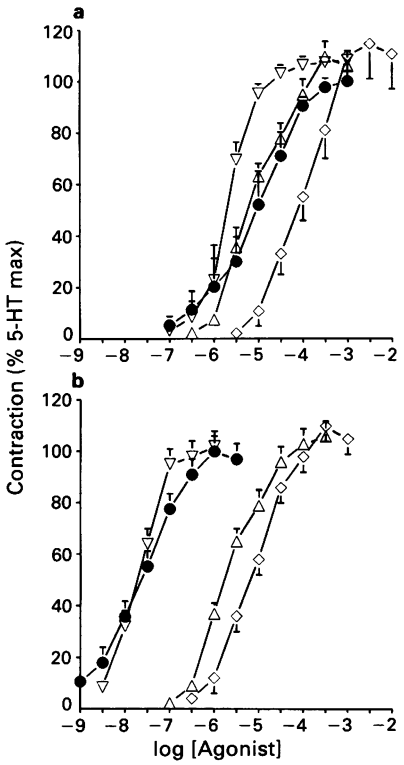

Figure 1 Rabbit isolated renal artery: concentration-response curves to 5-hydroxytryptamine (5-HT, ●), 2-methyl-5-HT (△), α-methyl-5-HT (▽) and 5-methoxytryptamine (◇) in quiescent vessels (a) and in vessels precontracted with U46619 (10^{-9} M) (b). Points represent mean (with s.e.mean shown by vertical bars) of the increase in force expressed as a percentage of the initial maximal responses to 5-HT. $n = 4-6$, except in the case of 5-HT in precontracted vessels where $n = 18$.

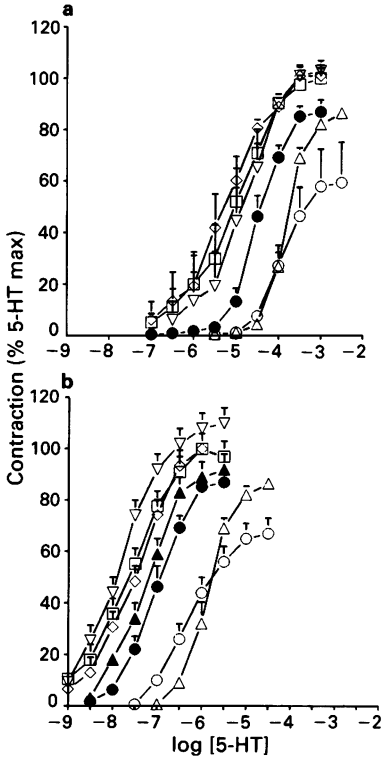

Figure 2 Rabbit isolated renal artery: concentration-response curves to 5-hydroxytryptamine (5-HT) in quiescent vessels (a) and in vessels precontracted with U46619 (10^{-9} M) (b); control (□) and in the presence of tropisetron (3×10^{-6} M, ◇), MDL 72222 (10^{-6} M, ▽), methiothepin (10^{-8} M, ● or 10^{-7} M, ○) or ketanserin (10^{-7} M, ▲ or 10^{-6} M, △). Points represent mean (with s.e.mean shown by vertical bars) of the increase in force expressed as a percentage of the initial maximal responses to 5-HT. $n = 4-6$.

Table 1 The pD_2 and E_{max} values of 5-HT receptor agonists calculated from concentration-effect curves obtained on the rabbit isolated renal artery, either quiescent or precontracted with U46619 (10^{-7} M)

	Quiescent vessels		*Precontracted vessels*	
Agonist	E_{max}	pD_2	E_{max}	pD_2
5-HT 1st curve	100	5.1 ± 0.1	100	7.1 ± 0.2
5-HT 2nd curve	109 ± 3	5.2 ± 0.2	not tested	not tested
2-Methyl-5-HT	103 ± 7	5.6 ± 0.3	107 ± 21	6.2 ± 0.3
α-Methyl-5-HT	109 ± 4	5.7 ± 0.2	120 ± 7	7.2 ± 0.3
5-Methoxytryptamine	117 ± 14	4.3 ± 0.2	119 ± 6	5.3 ± 0.2

The pD_2 value and maximal response (E_{max}) were calculated by a computerized analysis of the individual curves according to De Lean *et al.* (1978). Values are mean ± s.e.mean. ($n = 4-6$). The maximal response is expressed as percentage of the initial E_{max} obtained for 5-HT.

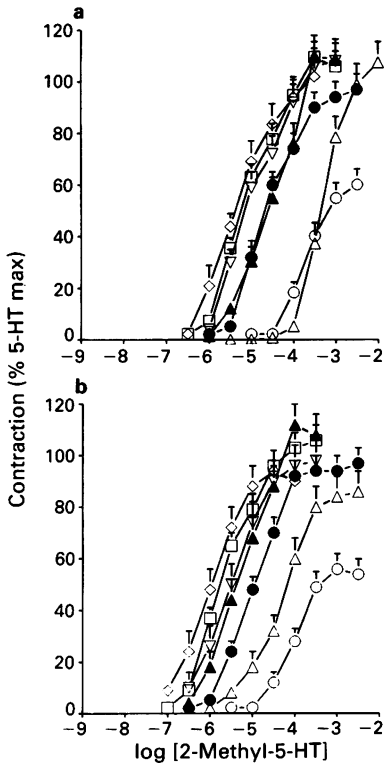

Figure 3 Rabbit isolated renal artery: concentration-response curves to 2-methyl-5-HT in quiescent vessels (a) and in vessels precontracted with U46619 (10^{-9} M) (b); control (□) and in the presence of tropisetron (3×10^{-6} M, ◇), MDL 72222 (10^{-6} M, ▽), methiothepin (10^{-8} M, ● or 10^{-7} M, ○) or ketanserin (10^{-7} M, ▲ or 10^{-6} M, △). Points represent mean (with s.e.mean shown by vertical bars) of the increase in force expressed as a percentage of the initial maximal responses to 5-HT. $n = 4-6$.

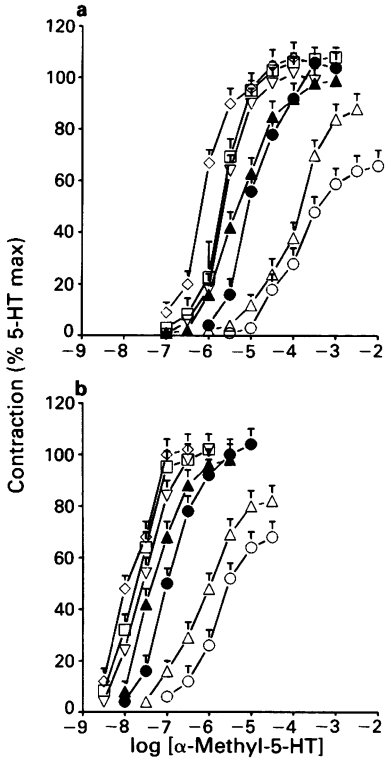

Figure 4 Rabbit isolated renal artery: concentration-response curves to α-methyl-5-HT in quiescent vessels (a) and in vessels precontracted with U46619 (10^{-9} M) (b); control (□) and in the presence of tropisetron (3×10^{-6} M, ◇), MDL 72222 (10^{-6} M, ▽), methiothepin (10^{-8} M, ● or 10^{-7} M, ○) or ketanserin (10^{-7} M, ▲ or 10^{-6} M, △). Points represent mean (with s.e.mean shown by vertical bars) of the increase in force expressed as a percentage of the initial maximal responses to 5-HT. $n = 4-6$.

artery following stimulation of 5-HT_1-like receptors by 5-HT, 5-carboxamidotryptamine or sumatriptan. Though both 5-HT and 5-carboxamidotryptamine do contract the rabbit renal artery by themselves, such contractions are also clearly potentiated, approximately 100 and 1500 fold, respectively, in vessels in which the basal tone is augmented with the thromboxane receptor agonist, U46619 (Tadipatri *et al.*, 1991). The present study shows that such an interaction also existed between U46619 and the other tryptamine derivatives (2-methyl-5-HT, 5-methoxytryptamine and α-methyl-5-HT), but the extent of potentiation was much less (4, 10 and 30 fold, respectively). We do not know the reason for this variability, but it may indicate subtle differences in the receptors involved. It was further noticed that in about 50% of the vessel segments tested, U46619 was inactive as an agonist, though other agonists including KCl were active. Such a variation in the agonist action has also been reported for a prostaglandin D_2 analogue, where its action varied from full agonism to no agonism in different pieces of the same kind of tissue (Leff *et al.*, 1990).

Nature of 5-HT receptors mediating contractions to the tryptamine derivatives

MDL 72222 (Fozard, 1984) and tropisetron (Richardson *et al.*, 1985) are potent antagonists at 5-HT_3 receptors, and high concentrations (10^{-6} M) of tropisetron can also block 5-HT_4 receptors (Dumuis *et al.*, 1988a,b). Since in the present experiments neither MDL 72222 (10^{-6} M) nor tropisetron (3×10^{-6} M) suppressed the responses to 5-HT, 2-methyl-5-HT, α-methyl-5-HT or 5-methoxytryptamine, the involvement of both 5-HT_3 and 5-HT_4 receptors can be ruled out. This is despite the fact that 2-methyl-5-HT and 5-methoxytryptamine have high affinities at the 5-HT_3 (Richardson *et al.*,1985) and 5-HT_4 (Dumuis *et al.*, 1988a,b) receptors, respectively.

Ketanserin is a prototype 5-HT_2 receptor antagonist and its antagonism against the responses to 5-HT, 2-methyl-5-HT, α-methyl-5-HT and 5-methoxytryptamine may suggest the involvement of 5-HT_2 receptors. Some findings, however, indicate that this is probably not so: (i) the pA_2 value of ketanserin for the 5-HT_2 receptor is above 8 (Van Nueten *et al.*, 1981; Feniuk *et al.*, 1985; Mylecharane, 1991), while in the present investigation its apparent pA_2 values were between 6.8–7.3, (ii) the selective 5-HT_2 receptor agonist, DOI (see Saxena & Villalón, 1990) was ineffective in contracting the rabbit renal artery (Tadipatri *et al.*, 1991), and (iii) methiothepin, which has a high affinity for both 5-HT_1-like receptors and 5-HT_2 receptors (Bradley *et al.*, 1986; Saxena & Villalón, 1990), potently antagonized the rabbit renal artery contractions induced by the tryptamine derivatives used here (apparent pA_2: 8.4–8.8). It is, therefore, more likely that these agonists act via a 5-HT_1-like receptor and ketanserin is a weak antagonist at this receptor. This conclusion is strengthened by the fact that even sumatriptan-induced contractions of the rabbit renal artery are antagonized by ketanserin with a similar potency (Tadipatri *et al.*, 1991). Furthermore, ketanserin has also been reported to possess affinity for the 5-HT_1-like receptor mediating contractile responses in the rabbit saphenous vein (Martin *et al.*, 1990; Van Heuven *et al.*, 1990).

Selectivity of the tryptamine derivatives at the 5-HT receptors

The tryptamine derivatives α-methyl-5-HT, 2-methyl-5-HT and 5-methoxytryptamine have high activity at 5-HT_2, 5-HT_3

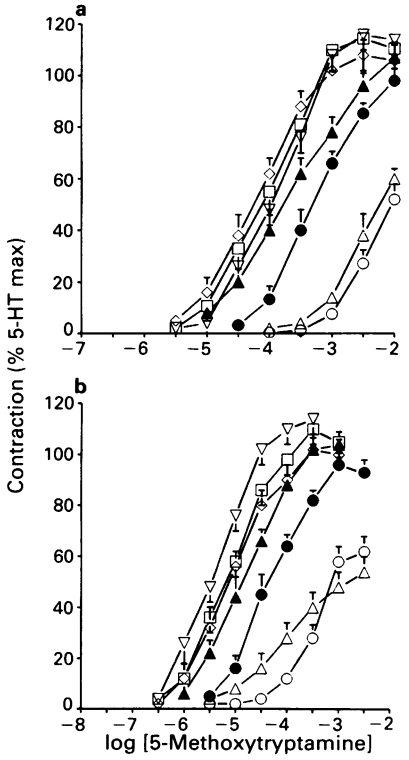

Figure 5 Rabbit isolated renal artery: concentration-response curves to 5-methoxytryptamine in quiescent vessels (a) and in vessels precontracted with U46619 (10^{-9} M) (b); control (□) and in the presence of tropisetron (3×10^{-6} M, ◇), MDL 72222 (10^{-6} M, ▽), methiothepin (10^{-8} M, ● or 10^{-7} M, ○) or ketanserin (10^{-7} M, ▲ or 10^{-6} M, △). Points represent mean (with s.e.mean shown by vertical bars) of the increase in force expressed as a percentage of the initial maximal responses to 5-HT. $n = 4-6$.

and 5-HT_4 receptors, respectively, and the first two compounds are often even considered selective for the 5-HT_2 and 5-HT_3 receptors, respectively (see Bradley *et al.*, 1986; Saxena & Villalón, 1990). Yet, the present analysis of the functional responses using appropriate antagonists for the first time clearly demonstrates that 2-methyl-5-HT contracts the rabbit isolated renal artery via a 5-HT_1-like receptor.The same is also true for α-methyl-5-HT and methoxytryptamine. Therefore, the selectivity of these tryptamine derivatives at the 5-HT receptors seems rather limited. Indeed, this conclusion is supported by ligand binding data, reported in several publications (Engel *et al.*, 1986; Hoyer, 1989; Fozard, 1990; Ismaiel *et al.*, 1990; Van Wijngaarden *et al.*, 1990) and summarized in Table 3, which show appreciable affinities for 2-methyl-5-HT (pK_i: 5.6–6.4), α-methyl-5-HT (pK_i: 6.8–7.2) and 5-methoxytryptamine (pK_i: 5.9–8.4) at the 5-HT_{1A}, 5-HT_{1C} or 5-HT_{1D} binding sites. Apart from the ligand binding data, functional responses have also been observed with these compounds in several tissues where a particular 5-HT_1 receptor subtype seems to be predominant (see Table 3). In particular, it may be noted that in the case of 2-methyl-5-HT neither the pK_i values at the 5-HT_1 binding sites nor the pD_2 value found in the rabbit renal artery (present results) are much different from the pK_i (5.9–7.1) (Kilpatrick *et al.*, 1987; Hoyer & Neijt, 1988; Van Wijngaarden *et al.*, 1990) or pD_2 (5.7) (Richardson & Buchheit, 1988) values at the 5-HT_3 receptor. Similarly, for α-methyl-5-HT the pK_i values at the 5-HT_1 binding sites (6.8–7.4) are comparable to the pK_i values reported at the 5-HT_2 binding site (6.1–6.9) (Engel *et al.*, 1986; Hoyer, 1989; Ismaiel *et al.*, 1990) or the pD_2 values determined by us in the rabbit isolated renal artery. Also, for 5-methoxytryptamine the pK_i values at the 5-HT_1 binding sites (5.9–8.4) (Hoyer, 1989; Ismaiel *et al.*, 1990) are comparable to the pD_2 values reported at the 5-HT_4 receptors (7.0 and 7.6) (Dumuis *et al.*, 1988b; Craig & Clarke, 1990) as well as to those in the rabbit isolated renal artery (present results).

Admittedly, the pD_2 values of α-methyl-5-HT (5.6), 2-methyl-5-HT (5.7) and 5-methoxytryptamine (4.3) on the quiescent rabbit renal artery are low, but precontraction of the vessel with U46619 increased the sensitivity by 10–30 fold. This suggests that, potentially, these compound can have a high activity via some 5-HT_1-like receptors. Indeed, as shown in Table 3, all three tryptamine derivatives showed a particularly high affinity (pD_2 values: 7.2, 8.8 and 8.4, respectively) for the 5-HT_1 receptor mediating endothelium-dependent relaxations in the porcine vena cava (Sumner, 1991). Though the two other tryptamines were not investigated, the pD_2 value of α-methyl-5-HT in eliciting endothelium-dependent relaxations of the rabbit jugular vein was 8.4 (Martin *et al.*, 1990). These tryptamine derivatives had intermediate activity (pD_2: 5.2–6.8) in eliciting the dog saphenous vein contraction (Feniuk *et al.*, 1985) and certain other responses (e.g. human pial artery contraction, endothelium-dependent porcine coronary artery relaxation) that are probably mediated by 5-HT_{1D} receptors (Hamel & Bouchard, 1991; Molderings *et al.*, 1989; Schoeffter & Hoyer, 1990) (Table 3). It is, however, interesting to note that 2-methyl-5-HT was found inactive at the 5-HT_1 receptor mediating either tracheal smooth muscle contraction or tracheal blood vessel dilatation in the sheep (Webber *et al.*, 1990). Similarly, α-methyl-5-HT was inactive at the smooth muscle 5-HT_1-like receptor mediating relaxations in the rabbit jugular vein (Sumner, 1991).

In conclusion, our results show that the contractile effect of 2-methyl-5-HT as well as α-methyl-5-HT and 5-

Table 2 The slope and apparent pA_2 values of ketanserin and methiothepin against the contractile responses to 5-HT, 2-methyl-5-HT, α-methyl-5-HT and 5-methoxytryptamine on the rabbit isolated renal artery, either quiescent (QV) or precontracted with U46619 (10^{-7} M; PCV).

		Ketanserin		*Methiothepin*	
		Slope	*pA_2*	*Slope*	*pA_2*
5-HT	QV	NA	6.6 ± 0.1†	NA	8.6 ± 0.4†
	PCV	0.7 ± 0.2	7.0 ± 0.2	0.8 ± 0.3	8.5 ± 0.1
2-Methyl-5-HT	QV	0.8 ± 0.2	6.8 ± 0.1	1.2 ± 0.1	8.4 ± 0.2
	PCV	0.7 ± 0.2	6.8 ± 0.1	1.4 ± 0.2	8.7 ± 0.3
α-Methyl-5-HT	QV	1.3 ± 0.1	7.0 ± 0.3	0.7 ± 0.2	8.8 ± 0.1
	PCV	0.8 ± 0.1	7.3 ± 0.2	1.2 ± 0.3	8.6 ± 0.4
5-Methoxytryptamine	QV	1.1 ± 0.3	6.9 ± 0.2	1.5 ± 0.4	8.7 ± 0.2
	PCV	1.2 ± 0.2	7.2 ± 0.1	1.4 ± 0.3	8.8 ± 0.4

Values are mean ± s.e.mean. ($n = 4-6$). †pK_B values (data from Tadipatri *et al.*, 1991); NA, not applicable as only one dose of the antagonist had been used in these experiments

Table 3 Some reported radioligand binding (pK_i) or functional (pD_2*) affinities of α-methyl-5-HT, 5-methoxytryptamine and 2-methyl-5-HT on 5-HT receptors

	5-HT$_{1A}$	*5-HT$_{1C}$*	*5-HT$_{1D}$*	*5-HT$_{1?}$***	*5-HT$_2$*	*5-HT$_3$*	*5-HT$_4$*
2-Methyl-5-HT							
pK_i	5.6[a], 5.9[b], 5.8[c]	5.9[a], 6.2[b], 6.3[c]	6.4[a], 5.9[b], 5.8[c]		5.0[a], <5[b], <5[c]	5.8[c], 5.9[d] 5.9[d], 7.1[e]	–
pD_2	–	–	5.2[f]	7.2[g]	–	5.7[h]	<5[i], <5[j]
α-Methyl-5-HT							
pK_i	7.1[a], 7.4[b] 7.1[k]	7.2[a], 6.8[b], 7.2[k]	6.8[b]		6.9[a], 6.1[b], 6.9[k]	6.8[k]	–
pD_2	–	–	6.6[f], 5.4[l] 5.7[n]	8.8[g], 5.7[m] 8.1[n]	6.1[m], 6.6[n]	–	6.8[j]
5-Methoxytryptamine							
pK_i	8.0[a], 5.9[b]	7.6[a], 6.2[b]	8.4[b], 6.0[b]		5.5[a], <5[b]	4.5[d]	–
pD_2	–	–	6.8[l], 5.9[o]	8.4[g]	–	<4[h]	7.0[i], 7.6[j]

*The pD_2 shown are on the basis of the predominant receptor present in the tissue studied; **5-HT$_{1?}$ means that the receptor subtype does not positively correlate with any of the 5-HT$_1$ binding site.
[a] Hoyer (1989); [b] Ismaiel *et al.* (1990); [c] van Wijngaarden *et al.* (1990); [d] Hoyer & Neijt (1988); [e] Kilpatrick *et al.* (1987); [f] Hamel & Bouchard (1991); [g] Sumner (1991); [h] Richardson & Buchheit (1988); [i] Dumuis *et al.* (1988b); [j] Craig & Clarke (1990); [k] Engel *et al.* (1986); [l] Schoeffter & Hoyer (1990); [m] Feniuk *et al.* (1985); [n] Martin *et al.* (1990); [o] Molderings *et al.* (1989).

methoxytryptamine, which is more marked in the precontracted rabbit isolated renal artery segments, can be mediated by a 5-HT$_1$-like receptor. Since, in addition, the ligand binding affinity of 2-methyl-5-HT at 5-HT$_3$ receptors is similar to both the ligand binding affinity and the functional pD_2 at 5-HT$_1$ sites, this compound cannot be regarded as a selective 5-HT$_3$ receptor agonist. Similarly, α-methyl-5-HT and 5-methoxytryptamine have only a limited selectivity for 5-HT$_2$ and 5-HT$_4$ receptors, respectively. Thus, it cannot be overemphasized that, without the proper use of complementary antagonists, the nature of 5-HT receptors involved in a particular response may be incorrectly interpreted. Though we cannot categorically state that such was the case in the putative charcterization of 5-HT$_3$ receptors in the human temporal artery (see Edvinsson & Jansen, 1989; Lance, 1991), in view of the present results, at the very least, it needs confirmation.

This investigation was partly supported by a grant from Glaxo Group Research, Ware, U.K.

References

BAX, W.A., VAN HEUVEN-NOLSEN, D., BOS, E., SIMOONS, M.L. & SAXENA, P.R. (1992). 5-HT$_2$ receptors and a receptor resembling the 5-HT$_{1D}$ receptor subtype mediate contractions in human saphenous vein. *Br. J. Pharmacol.*, **105**, 99P.

BRADLEY, P.B., ENGEL, G., FENIUK, W., FOZARD, J.R., HUMPHREY, P.P.A., MIDDLEMISS, D.N., MYLECHARANE, E.J., RICHARDSON, B.P. & SAXENA, P.R. (1986). Proposals for the classification and nomenclature of functional receptors for 5-hydroxytryptamine. *Neuropharmacology*, **25**, 563–576.

CRAIG, D.A. & CLARKE, D.E. (1990). Pharmacological characterization of a neuronal receptor for 5-hydroxytryptamine in guinea-pig ileum with properties similar to the 5-hydroxytryptamine$_4$ receptors. *J. Pharmacol. Exp. Ther.*, **352**, 1378–1386.

DE LEAN, A., MUNSON, P.J. & RODBARD, R. (1978). Simultaneous analysis of families of sigmoidal curves: application to bioassay, radioligand assay and physiological dose-response curves. *Am. J. Physiol.*, **235**, 97–102.

DUMUIS, A., BOUHELAL, R., SEBBEN, M. & BOCKAERT, J. (1988a). A 5-HT receptor in the central nervous system, positively coupled with adenyl cyclase, is antagonized by ICS 205-930. *Eur. J. Pharmacol.*, **146**, 187–188.

DUMUIS, A., BOUHELAL, R., SEBBEN, M., CORY, R. & BOCKAERT, J. (1988b). A non-classical 5-hydroxytryptamine receptor positively coupled with adenyl cyclase in the central nervous system. *Mol. Pharmacol.*, **34**, 880–887.

EDVINSSON, L. & JANSEN, I. (1989). Characterization of 5-HT receptors mediating contractions of human cerebral, meningeal and temporal arteries: target for GR 43175 in acute treatment of migraine? *Cephalalgia*, **9** (Suppl. 10), 39–40.

ENGEL, G., GÖTHERT, M., HOYER, D., SCHLICKER, E. & HILDEBRAND, K. (1986). Identity of inhibitory presynaptic 5-hydroxytryptamine (5-HT) autoreceptors in the rat brain cortex with 5-HT$_{1B}$ binding sites. *Naunyn-Schmiedebergs Arch. Pharmacol.*, **332**, 1–7.

FENIUK, W., HUMPHREY, P.P.A. & WATTS, A.D. (1985). A comparison of 5-hydroxytryptamine receptors mediating contraction in rabbit aorta and dog saphenous vein: evidence for different 5-HT receptor types obtained by use of selective agonists and antagonists. *Br. J. Pharmacol.*, **86**, 697–704.

FOZARD, J.R. (1984). MDL 72222, a potent and highly selective antagonist at neuronal 5-hydroxytryptamine receptors. *Naunyn-Schmiedebergs Arch. Pharmacol.*, **326**, 36–44.

FOZARD, J.R. (1990). Agonists and antagonists of 5-HT$_3$ receptors. In *Cardiovascular Pharmacology of 5-Hydroxytryptamine*. ed. Saxena, P.R., Wallis, D.I., Wouters, W. & Bevan, P. pp. 101–115. Dordrecht: Kluwer Academic Publishers.

HAMEL, E. & BOUCHARD, D. (1991). Contractile 5-HT$_1$ receptors in human isolated pial arterioles: correlation with 5-HT$_{1D}$ binding sites. *Br. J. Pharmacol.*, **102**, 227–233.

HOYER, D. (1989). 5-hydroxytryptamine receptors and effector coupling mechanisms in peripheral tissues. In *The Peripheral Actions of 5-Hydroxytryptamine*. ed. Fozard, J.R. pp. 72–99. Oxford: Oxford University Press.

HOYER, D. & NEIJT, H.C. (1988). Identification of serotonin 5-HT$_3$ recognition sites in membranes of N1E-115 neuroblastoma cells by radioligand binding. *Mol. Pharmacol.*, **33**, 303–309.

ISMAIEL, A.M., TITELER, M., MILLER, K.J., SMITHS, T.S. & GLENNON, R.A. (1990). 5-HT$_1$ and 5-HT$_2$ binding profiles of the serotonergic agents α-methyl-serotonin and 2-methyl-serotonin. *J. Med. Chem.*, **33**, 755–758.

KENAKIN, T.P. (1987). *Pharmacologic Analysis of Drug-receptor Interaction*. p. 213. New York: Raven Press.

KILPATRICK, G.J., JONES, B.J. & TYERS, M.B. (1987). Identification and distribution of 5-HT$_3$ receptors in rat brain using radioligand binding. *Nature*, **330**, 746–748.

LANCE, J.W. (1991). 5-Hydroxytryptamine and its role in migraine. *Eur. Neurol.*, **31**, 279–281.

LEFF, P., DOUGALL, I.G., HARPER, D.H. & DAINTY, I.A. (1990). Errors in agonist affinity estimation: do they and should they occur in isolated tissue experiments? *Trends Pharmacol. Sci.*, **11**, 64–67.

MARTIN, G.R., LEFF, P. & MACLENNAN, S.J. (1990). Tryptamine fingerprints in the classification of 5-hydroxytryptamine receptors. In *Cardiovascular Pharmacology of 5-Hydroxytryptamine*. ed. Saxena, P.R., Wallis, D.I., Wouters, W. & Bevan, P. pp. 157–162. Dordrecht: Kluwer Academic Publishers.

MOLDERINGS, G.J., ENGEL, G., ROTH, E. & GOTHERT, M. (1989). Characterization of an endothelial 5-hydroxytryptamine (5-HT) receptor mediating relaxation of the porcine coronary artery. *Naunyn-Schmiedebergs Arch. Pharmacol.*, **340**, 300–308.

MYLECHARANE, E.J. (1991). 5-HT_2 receptor antagonists and migraine therapy. *J. Neurol.*, **288** (Suppl. 1), S45–S52.

RICHARDSON, B.P. & BUCHHEIT, K.H. (1988). The pharmacology, distribution and function of 5-HT_3 receptors. In *Neuronal Serotonin*. ed. Osborne, N.N. & Hamon, M. pp. 465–507. Chichester: John Wiley and Sons, Ltd.

RICHARDSON, B.P., ENGEL, G., DONATSCH, P. & STADLER, P.A. (1985). Identification of serotonin M-receptor subtypes and their specific blockade by a new class of drugs. *Nature*, **316**, 126–131.

SAHIN-ERDEMLI, I., HOYER, D., STOLL, A., SEILER, M.P. & SCHOEFFTER, P. (1991). 5-HT_1-like receptors mediate 5-hydroxytryptamine-induced contraction guinea-pig isolated iliac artery. *Br. J. Pharmacol.*, **102**, 386–390.

SAXENA, P.R. & VILLALÓN, C.M. (1990). Cardiovascular effects of serotonin agonists and antagonists. *J. Cardiovasc. Pharmacol.*, **15** (Suppl. 7), S17–S34.

SCHOEFFTER, P. & HOYER, D. (1990). 5-Hydroxytryptamine (5-HT)-induced endothelium-dependent relaxation of pig coronary arteries is mediated by 5-HT receptors similar to the 5-HT1D receptor subtype. *J. Pharmacol. Exp. Ther.*, **252**, 387–395.

SUMNER, M.J. (1991). Characterization of the 5-HT receptor mediating endothelium-dependent relaxation in porcine vena cava. *Br. J. Pharmacol.*, **102**, 938–942.

TADIPATRI, S., VAN HEUVEN-NOLSEN, D., FENIUK, W. & SAXENA, P.R. (1991). Analysis of the 5-HT receptors mediating contraction in the rabbit isolated renal artery. *Br. J. Pharmacol.*, **104**, 887–894.

TADIPATRI, S. & SAXENA, P.R. (1992). Is 2-methyl-5-hydroxytryptamine a selective 5-HT_3 receptor agonist? *Br. J. Pharmacol.*, **105**, 34P.

VAN HEUVEN-NOLSEN, D., TYSSE KLASEN, T.H., LUO, Q.F. & SAXENA, P.R. (1990). 5-HT1-like receptors mediate contractions of the rabbit saphenous vein. *Eur. J. Pharmacol.*, **191**, 375–382.

VAN NUETEN, J.M., JANSSEN, P.A.J., VAN BEEK, J., XHONNEUX, R., VERBEURERN, T.J. & VANHOUTTE, P.M. (1981). Vascular effects of ketanserin (R 41 468), a novel antagonist of 5-HT_2 serotonergic receptors. *J. Pharmacol. Exp. Ther.*, **218**, 217–230.

VAN WIJNGAARDEN, I., TULP, M.Th.M. & SOUDIJN, W. (1990). The concept of selectivity in 5-HT receptor research. *Eur. J. Pharmacol.*, **188**, 301–312.

WEBBER, S.E., SALONEN, R.O. & WIDDICOMBE, J.G. (1990). Receptors mediating the effects of 5-hydroxytryptamine on the tracheal vasculature and smooth muscle of sheep. *Br. J. Pharmacol.*, **99**, 21–26.

(Received May 1, 1992
Accepted May 26, 1992)

Br. J. Pharmacol. (1992), **107**, 329-333

Capsazepine reversal of the antinociceptive action of capsaicin *in vivo*

[1]M.N. Perkins & E.A. Campbell

Sandoz Institute for Medical Research, Gower Place, London WC1E 6BN

1 This study was designed to investigate the antinociceptive activity of capsaicin in acute and persistent nocifensor behavioural models and to determine whether this was mediated via a specific receptor interaction, by use of the antagonist, capsazepine.

2 Capsaicin administered systemically in low doses produced antinociception in the knee joint hyperalgesia, rat paw pressure, rat and mouse tail flick and mouse hot plate nocifensor models with similar efficacy in all tests.

3 The novel competitive capsaicin antagonist, capsazepine, prevented the capsaicin-induced antinociception when administered systemically in the range 50–100 μmol kg^{-1}.

4 Capsazepine administered by itself had no antinociceptive actions.

5 These data describe a joint hyperalgesic model in the rat which does not rely on extreme nocifensor behavioural endpoints and it is suggested this is a useful model for investigating mechanisms in persistent pain.

6 This is the first demonstration of antagonism by capsazepine of the behavioural antinociceptive properties of capsaicin and provides further evidence that capsaicin acts to reduce nociceptive thresholds via a specific receptor.

Keywords: Capsaicin; capsazepine; antinociception

Introduction

Capsaicin (8-methyl-N-vanillyl-6-noneamide) is the major pungent extract from hot peppers of the capsicum family. It has the unique property of selectively activating polymodal nociceptors following local or systemic administration.

It has been well established that large systemic doses of capsaicin in the neonatal animal are neurotoxic to small umymelinated C-fibres (Jancso *et al.*, 1977) and these high dose treatments lead to a very long lasting or even permanent increase in nociceptive thresholds (Hayes *et al.*, 1981a; Gamse *et al.*, 1982; Buck & Burks, 1986).

Following administration of small acute doses of capsaicin, however, there is a period of insensitivity to further noxious stimuli (Hayes *et al.*, 1991b) which is distinct from the toxic effects. The selectivity of capsaicin for peripheral polymodal nociceptors has made it of particular interest to those studying pain mechanism. The pharmacological and physiological basis for this selectivity has, however, remained unclear.

Recently, the development of the first competitive antagonist for capsaicin (capsazepine, 2-[2-(4-chlorphenyl) ethylamino-thiocarbonyl]-7,8-dihydroxy-2,3,4,5-tetrahydro-1H-2-benzazepine) has been reported (Bevan *et al.*, 1991; Dray *et al.*, 1991). Capsazepine antagonized the excitatory actions of capsaicin *in vitro* in a variety of preparations in a competitive manner (Bevan *et al.*, 1991). It also antagonized the excitatory actions of capsaicin *in vivo* and in man (Dray *et al.*, 1991; Dickenson *et al.*, 1991; Dickenson & Dray, 1991).

We now show that capsazepine can prevent the antinociceptive actions of capsaicin in a number of acute and persistent nocifensor models.

Methods

In all nocifensor tests CD-1 mice (20–25 g) or Sprague Dawley rats were used. Drugs were supplied by Sigma or, in the case of capsaicin and capsazepine, were synthesized here. Statistical analysis was by unpaired *t*-test or Mann-Whitney U test as appropriate.

Tail flick

Female mice (20–25 g) or female rats (100–120 g) had all drugs administered s.c. 60 min before testing. Latency to tail withdrawal from a focused noxious heat beam (55°C) was measured. Capsazepine was co-administered with capsaicin or administered by itself.

Hot plate

The latency (s) to foot lick in female mice on a hot plate at 55°C was determined 60 min after s.c. administration of drugs. Capsazepine was co-administered with capsaicin.

Paw pressure

Female rats (100–120 g) were injected intraplantar unilaterally with 100 μl of 1% carrageenin (lambda). Paw pressure threshold (g) was determined by a modified Randal & Sellitoe (1957) test, the modification being that the paw withdrawal threshold was measured immediately before injection of carrageenin and 3 h subsequently. Vehicle-treated animals were run with every experiment and comparisons made with the vehicle-treated animals. The end point was the withdrawal of the paw. Drugs or vehicle were administered 60 min before testing at the 3 h time point and capsazepine was co-administered with capsaicin or on its own. In all cases testing was done blind.

Uric acid/Freund's adjuvant-induced hyperalgesia

Female Wistar rats (100–120 g) were anaesthetized and injected with 100 μl of either sodium urate crystals or Freund's complete adjuvant into one knee; 18–24 h (urate injections) or 64–70 h (Freund's) later the animal was placed with each hind paw on a separate pressure transducer and a

[1] Author for correspondence.

downward force was exerted evenly until an online readout of the load borne by both legs indicated that the uninjected leg was bearing 10 g. At this point the animal was removed from the transducers and the load borne by the injected leg measured. The animals would be less tolerant of pressure on the injected leg which would be manifested in a lower load being tolerated by that leg (i.e. less than 100 g). This reduced load was the measure of hyperalgesia.

For the determination of the time course the hyperalgesia was expressed as absolute loading. The drug responses at 18–24 h or 64–70 h, depending on the model were, however, expressed as a percentage of the maximum possible response, when both legs would be bearing the same load, using the formula:

$$\frac{\text{test reading from injected leg} - \text{average of initial three readings}}{100 - \text{average of initial three readings}} \times 100$$

As there were three readings taken before drug administration in all cases each animal acted as its own control, with the addition of separate animals receiving vehicle only, to establish the lack of vehicle effects.

Results

Hot plate

Capsaicin (20 μmol kg^{-1}, s.c.) significantly increased the latency to foot lick on the hot plate in mice from 7.5 s to 8.9 s (see Figure 1). This dose of capsaicin has previously been found to be a sub-maximal antinociceptive dose in rats and mice (Campbell *et al.*, 1998). Capsazepine given concomitantly at 50 μmol kg^{-1}, s.c. prevented the antinociceptive action of capsaicin. Increasing the capsazepine dose to 200 μmol kg^{-1}, s.c. did not have any further effect nor did it show any antinociceptive activity by itself.

Tail flick

Capsaicin (20 μmol kg^{-1}, s.c.) increased tail flick latency in both mice (11.1 ± 1.7 to 23.4 ± 2.3 s) and in rats (7.9 ± 1.9 s to 23.8 ± 3.0 s). Figure 2 shows partial reversal of this effect by capsazepine at 20 μmol kg^{-1}, s.c. (16.8 ± 2.2 s) with full reversal at 100 μmol kg^{-1}, s.c. in mice (10.9 ± 2.2 s) and rats (11.5 ± 3.6 s). Capsazepine by itself at 100 μmol kg^{-1}, s.c., in mice, had no effect (9.9 ± 2.2 s).

Paw pressure

Three hours after intraplantar injection of carrageenin the paw pressure threshold had fallen by 43% from 93 ± 5.4 g to 54 ± 4.3 g (see Figure 3). Capsaicin (20 μmol kg^{-1}, s.c.) administered 60 min before the 3 h reading reversed this hyperalgesia raising the threshold to 107 ± 17 g. Capsazepine (10 μmol kg^{-1}, s.c.) administered with capsaicin prevented this antinociceptive effect (see Figure 3). Capsazepine by itself (100 μmol kg^{-1}, s.c.) had no effect.

Uric acid/Freund's adjuvant-induced hyperalgesia

The maximum tolerated weight borne by the leg receiving uric acid or adjuvant fell sharply within 5 h after the injection and continued to fall until by 18 h after injection the injected leg would sustain approximately 40% of the original

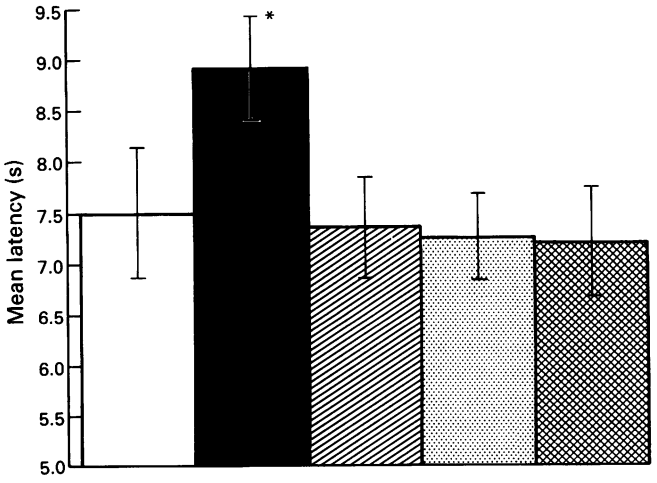

Figure 1 Latencies (mean with s.e.mean shown by vertical bars) to foot licking in hot plate test in mice (all $n = 10$) following capsaicin (20 μmol kg^{-1}, s.c. in all groups) or capsaicin with capsazepine. Open column: naive animals receiving vehicle s.c. only: solid column: capsaicin 20 μmol kg^{-1}, s.c.; hatched column: capsaicin with capsazepine 50 μmol kg^{-1}, s.c.; dotted column: capsaicin with capsazepine 100 μmol kg^{-1}, s.c.; cross-hatched: capsaicin with capsazepine 200 μmol kg^{-1}, s.c.
*$P < 0.05$, Student's t test.

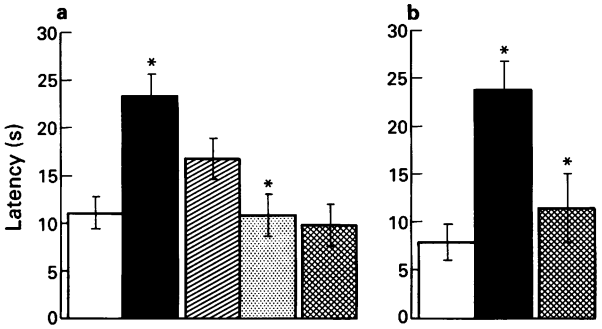

Figure 2 Latencies (mean with s.e.mean shown by vertical bars, $n = 10$) to tail flick withdrawal in mice and rats following capsaicin (20 μmol kg^{-1}, s.c. in all groups) or capsaicin with capsazepine. (a) Open column: vehicle; solid column: capsaicin 20 μmol kg^{-1}, s.c.; hatched column: capsaicin with capsazepine at 20 μmol kg^{-1}, s.c.; dotted column: capsaicin with capsazepine at 100 μmol kg^{-1}, s.c.; cross-hatched column: capsazepine alone at 100 μmol kg^{-1}, s.c. (b) Open column: vehicle; solid column: capsaicin 20 μmol kg^{-1}, s.c.; cross-hatched column: capsaicin with capsazepine at 100 μmol kg^{-1}, s.c.
*$P < 0.05$ Mann-Whitney U-test.

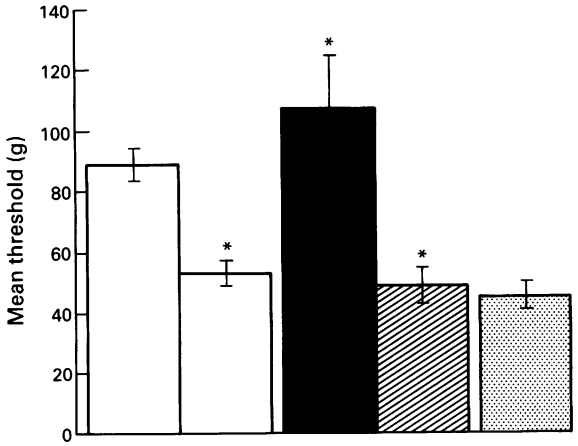

Figure 3 Paw pressure thresholds (mean with s.e.mean shown by vertical bars, $n = 10$) in rats following capsaicin (20 μmol kg^{-1}, s.c.) or capsaicin with capsazepine. The two open columns are, respectively, the thresholds immediately after vehicle injection but just prior to a unilateral intraplantar injection of carrageenan and 3 h subsequent to the carrageenan. Solid column: capsaicin s.c.; hatched column: capsaicin with capsazepine 100 μmol kg^{-1}, s.c.; dotted column: capsazepine 100 μmol kg^{-1}, s.c.

force. Figure 4 shows the magnitude and time course of the hyperalgesia following uric acid and Freund's adjuvant injection. As can be seen the magnitude of the response was the same following uric acid or Freund's adjuvant injection, the only difference being the recovery period. In all animals the hyperalgesic response was stable for the preceding 1.5 h prior to injection of drugs (Figures 5–7). Vehicle injections had no effect on the response (Figure 7) for the entire duration of the experiment and the responses in animals that received no drug or vehicle treatment were indistinguishable from vehicle-treated (data not shown).

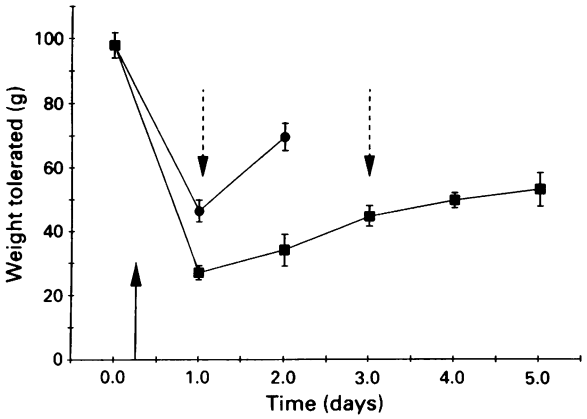

Figure 4 Time course of weight tolerated by hind leg of rats following intra-articular injection of Freund's adjuvant or uric acid to induce hyperalgesia (see Methods). All values are mean with s.e.mean shown by vertical bars ($n = 8$); (●) thresholds following uric acid injections; (■) thresholds after Freund's adjuvant injection. The arrow marks the time of injection (just after the initial threshold reading).

Conventional analgesics/anti-inflammatory agents were effective in both models. Morphine 2–16 mg kg^{-1}, s.c. was effective in reversing the hyperalgesia in both the uric acid and Freund's model (see Figure 5) and this was naloxone reversible (2.5–5 mg kg^{-1}, s.c.). Subcutaneous non-steroidal anti-inflammatory drugs (NSAIDs) were also effective at reversing the hyperalgesia, indomethacin (5–10 mg kg^{-1}), ibuprofen (1–50 mg kg^{-1}), paracetamol (100–500 mg kg^{-1}) and aspirin (100–200 mg kg^{-1}) produced a maximum effect of up to 80% of maximum possible response (see Figure 6).

Capsaicin (20 μmol kg^{-1}, s.c.) administered either 18 h in the case of uric acid-induced hyperalgesia or 3 days after Freund's injection showed a similar reversal of the hyperalgesia (see Figure 7) with a peak response of 50–60% of maximum possible response. The maximum response to capsaicin was 3–4 h after administration and the total duration of its antinociceptive activity 5–6 h giving a mean response of 30–40% over this period. Capsazepine (100 μmol kg^{-1}, s.c.) effectively prevented this antinociceptive action of capsaicin (see Figure 7).

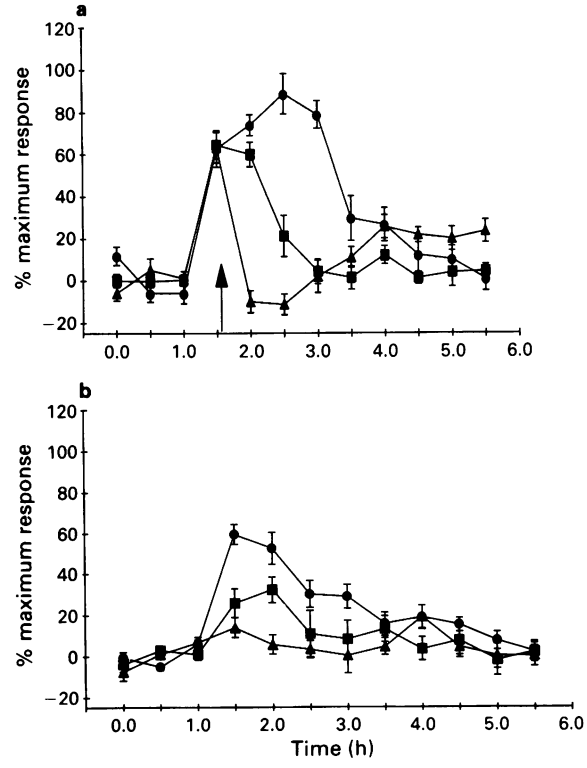

Figure 5 Time course of load tolerated by hind limb 24 h following intra-articular injection of uric acid (a) or on the third day after Freund's adjuvant (b) in rats. Morphine was injected immediately after the 1 h reading in all cases and all values are mean with s.e.mean shown by vertical bars ($n = 8–10$). Anti-hyperalgesic action of morphine at 2 mg kg^{-1}, s.c. (■) and 8 mg kg^{-1}, s.c. (●) given 18 h after uric acid injection; (▲) reversal of the morphine (8 mg kg^{-1}, s.c.) response by naloxone (5 mg kg^{-1}, s.c.) administered just after the 1.5 h reading (arrow marks time). (b) Anti-hyperalgesic action of morphine at 4 mg kg^{-1}, s.c. (■) and 8 mg kg^{-1}, s.c. (●) given 3 days after Freund's adjuvant injection; (▲) antagonism of morphine (8 mg kg^{-1}, s.c.) by co-administration of naloxone (2.5 mg kg^{-1}, s.c.).

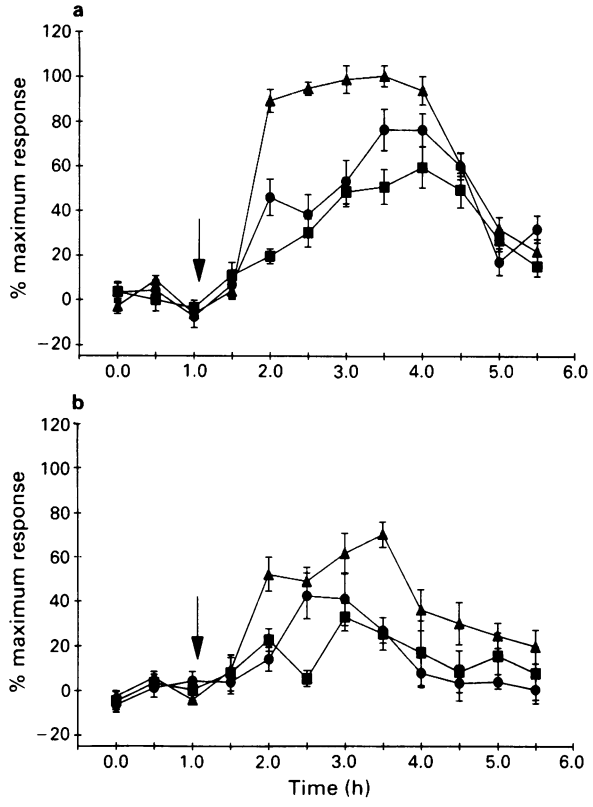

Figure 6 Time course of load tolerated by hind limb 24 h following intra-articular injection of uric acid (a) or on the third day after Freund's adjuvant (b) in rats. Paracetamol was injected immediately after the 1 h reading in all cases, marked by an arrow, and all values are mean with s.e.mean shown by vertical bars ($n = 8–10$). (a) Anti-hyperalgesic action of paracetamol at 50 mg kg^{-1}, s.c. (■); 100 mg kg^{-1}, s.c. (●) and 500 mg kg^{-1}, s.c. (▲) given 24 h after uric acid injection. (b) Anti-hyperalgesic action of paracetamol at 50 mg kg^{-1}, s.c. (■), 100 mg kg^{-1}, s.c. (●) and 500 mg kg^{-1}, s.c. (▲) given 3 days after Freund's adjuvant injection.

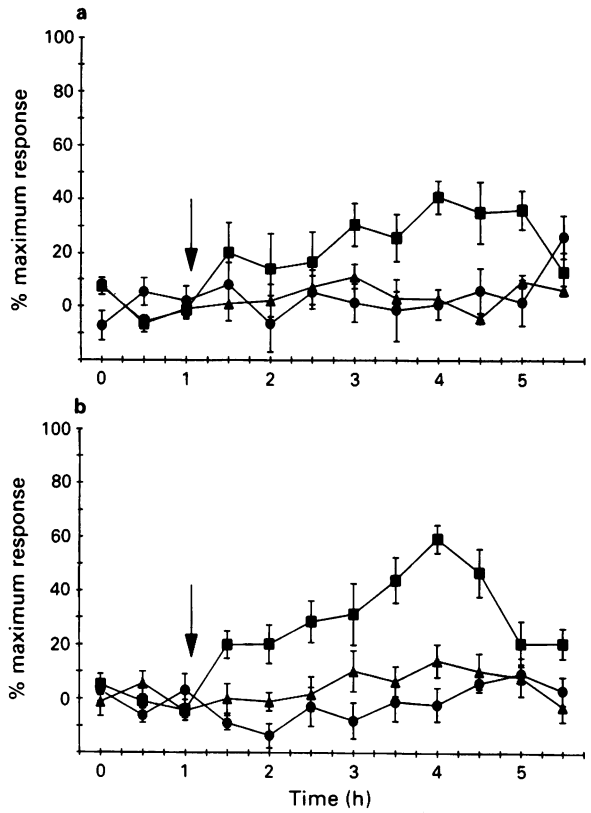

Figure 7 Time course of load tolerated (mean with s.e.mean shown by vertical bars, $n = 10$) by hind limb 24 h following intra-articular injection of uric acid (a) or on the third day after Freund's adjuvant (b) in rats In both (a) and (b) (■) shows the effect of capsaicin (20 μmol kg^{-1}, s.c.) injected immediately after the 1 h reading, marked by an arrow; (●) shows the response to capsaicin (20 μmol kg^{-1}, s.c.) which is abolished by concomitant injection of capsazepine (100 μmol kg^{-1}); (▲) response to the vehicle.

Irritancy of capsaicin

Although no quantification was undertaken, it was consistently noted that whenever capsazepine was injected concomittantly with capsaicin at 100 μmol kg^{-1}, s.c. or greater there were no behavioural signs indicating irritancy. When capsaicin was injected by itself the animals would typically turn to the injection site and lick and/or scratch at the area around the injection for 5–10 s.

Discussion

These data confirm the antinociceptive activity of capsaicin in various behavioural models *in vivo* using a dose (20 μmol kg^{-1}, s.c.) which is in agreement with previous studies relating to the acute analgesic actions of capsaicin (Dickenson & Dray, 1991; Hayes *et al.*, 1981a, b).

In addition, these data are further evidence that capsazepine is an effective antagonist of capsaicin *in vivo*. They also demonstrate that the antinociceptive actions of capsaicin as manifested in behavioural models are mediated through a specific capsaicin receptor that is likely to be the same as that described previously using *in vitro* preparations (Wood *et al.*, 1988; Bevan *et al.*, 1991; Dray *et al.*, 1991; Dickenson & Dray, 1991).

In addition, this is the first paper describing the use of the modified uric acid- and Freund's adjuvant-induced knee joint hyperalgesic model. Both the uric acid and Freund's-induced hyperalgesia respond well to morphine and NSAIDs, the latter effect being consistent with previous studies showing that both these agents have pronounced pro-inflammatory actions such effects being causal to the subsequent development of hyperalgesia (Lam & Ferrell, 1991; Dubner, 1992). These models both show a stable degree of hyperalgesia over the time course of the experiment which is demonstrated by both the responses obtained prior to drug administration as well as the lack of effect of vehicle injections.

The tendency for greater efficacy of both morphine and paracetamol seen in the uric acid model could either reflect the shorter time scale involved with uric acid and, by implication, a less severe response or that other factors become important in maintaining the hyperalgesia in the more persistent Freund's model. One could speculate that these could be either a neuropathic element or possibly involvement of the sympathetic innervation as has ben described in other models (Levine *et al.*, 1985; McMahon, 1991).

Further characterization of the Freund's model needs to be done but we consider that this model has an advantage over previous ones in that the end point in terms of behaviour is not an overt nocifensor response, such as vocalisation or gross withdrawal. Instead of this more extreme response, the animal spares the use of the leg with the inflamed joint and as such could be regarded as of greater relevance to man.

The analgesia seen with capsaicin in this study is consistent with previous reports describing the analgesic properties of capsaicin. It is important to note that these antinociceptive actions of capsaicin are distinct from the longer lasting sensory deficits seen with higher doses (Hayes *et al.*, 1981a; Gamse *et al.*, 1982). The results in the more persistent Freund's-induced hyperalgesia also suggest that capsaicin analogues would be useful clinically as analgesics in chronic pain conditions.

Capsazepine has been shown to antagonize the actions of capsaicin *in vitro* (Bevan *et al.*, 1991) in several neuronal preparations. Antagonism of capsaicin-evoked depolarization of dorsal root ganglion cells in culture and other indices of depolarization using ion flux give IC_{50} values of 0.5–1 μM. Schild analysis in such preparations provides evidence for this antagonism being of a reversible and competitive nature. In more integrated preparations such as the neonatal spinal cord tail preparation *in vitro*, hemisphected mouse spinal cord or rat saphenous nerve/skin preparation capsazepine antagonizes capsaicin-evoked neuronal excitation with similar IC_{50} values (Dray *et al.*, 1991; Dickenson & Dray, 1991).

Capsazepine has also been shown to be an effective antagonist of capsaicin-evoked activity *in vivo*. Dorsal horn neurones in the anaesthetized rat respond to systemic capsaicin with an increase in firing rate and this is reversed by capsazepine given systemically at 100 μmol kg^{-1}, s.c. (Dickensen *et al.*, 1991; Dickenson & Dray, 1991).

In the present study the antinociceptive actions of capsaicin were antagonized by capsazepine with doses in the range 50–100 μmol kg^{-1}, s.c. It is impossible to say whether this antagonism is at peripheral or central capsaicin receptors but it is interesting that in a previous study, capsazepine given intrathecally was able to reverse systemic capsaicin-evoked activity in the dorsal horn, implying a central site of action, at least in part, for the excitatory actions of capsaicin (Dickenson *et al.*, 1991; Dray, 1992).

The lack of any antinociceptive activity of capsazepine by itself suggests that it is very unlikely that capsaicin antagonists *per se* will be of use as analgesic agents. It also implies that any possible endogenous 'capsaicin-like' ligand is unlikely to be involved in evoking nocifensor behaviour. The role and, indeed existence, of such a ligand is unknown.

References

BEVAN, S., HOTHI, S., HUGHES, G.A., JAMES, I.F., RANG, H.P., SHAH, K., WALPOLE, C.S.J. & YEATS, J.C. (1991). Development of a competitive antagonist for the sensory neurone excitant capsaicin. *Br. J. Pharmacol.*, **102,** 77P.

BUCK, S.H. & BURKS, T.F. (1986). The neuropharmacology of capsaicin: review of some recent observation. *Pharmacol. Rev.*, **38,** 179–226.

CAMPBELL, E.A., DRAY, A. & PERKINS, M.N. Comparison of capsaicin and olvanil as antinociceptive agents *in vivo* and *in vitro*. *Br. J. Pharmacol.*, **98,** 907P.

DICKENSON, A.H. & DRAY, A. (1991). Selective antagonism of capsaicin by capsazepine: evidence for a spinal site in capsaicin-induced anti-nociception. *Br. J. Pharmacol.*, **104,** 1045–1049.

DICKENSON, A.H., DRAY, A., HUGHES, G.A. & WALPOLE, C.S.J. (1991). The selective capsaicin antagonist capsazepine inhibits capsaicin-induced anti-nociception: electrophysiological studies in rodents. *Br. J. Pharmacol.*, **102,** 79P.

DRAY, A. (1992). Neuropharmacological mechanisms of capsaicin and related substances. *Biochem. Pharmacol.*, (in press).

DRAY, A., CAMPBELL, E.A., HUGHES, G.A., PATEL, I.A., PERKINS, M.N., RANG, H.P., RUEFF, A., SENO, N., URBAN, L. & WALPOLE, C.S.J. (1991). Antagonism of capsaicin-induced activation of C-fibres by a selective capsaicin antagonist, capsazepine. *Br. J. Pharmacol.*, **102,** 78P.

DUBNER, R. (1992). Hyperalgesia and expanded receptive fields. *Pain*, **48,** 3–4.

GAMSE, R., PETSHE, U., LEMBECK, F. & JANCSO, F. (1982). Capsaicin applied to peripheral nerve inhibits axoplasmic transport of substance P and somatostatin. *Brain Res.*, **239,** 447–462.

HAYES, A.G., SCADDING, J.W., SKINGLE, M. & TYERS, M.B. (1981a). Effects of neonatal capsaicin on nociceptive thresholds in the mouse and rat. *J. Pharm. Pharmacol.*, **33,** 183–185.

HAYES, A.G., SKINGLE, M. & TYERS, M.B. (1981b). Effects of single doses of capsaicin on nociceptive thresholds in the rodent. *Neuropharmacology*, **20,** 505–511.

JANCSO, G., KIRALY, E. & JANCSO-GABOR, A. (1977). Pharmacologically induced selective degeneration of chemosensitive primary sensory neurons. *Nature*, **270,** 741–742.

LAM, F.Y. & FERRELL, W.R. (1991). Neurogenic component of different models of acute inflammation in the rat knee. *Ann. Rheum. Dis.*, **50,** 747–751.

LEVINE, J.D., MOSKOWITZ, M.A. & BASBAUM, A.I. (1985). The contribution of neurogenic inflammation in experimental arthritis. *J. Immunol.*, **135,** 843s–847s.

MCMAHON, S.B. (1991). Mechanisms of sympathetic pain. *Br. Med. Bull.*, **47,** 584–600.

RANDALL, L.O. & SELITTO, J.J. (1957). A method for the measurement of analgesic activity on inflamed tissue. *Arch. Int. Pharmacodyn.*, **4,** 409–419.

WOOD, J.N., WINTER, J., JAMES, I.F., RANG, H.P., YEATS, J. & BEVAN, S. (1988). Capsaicin-induced ion fluxes in dorsal root ganglion cells in culture. *J. Neurosci.*, **8,** 3208–3220.

(Received April 21, 1992
Revised May 25, 1992
Accepted May 28, 1992)

Br. J. Pharmacol. (1992), **107**, 334–340

Investigations into neuropeptide Y-mediated presynaptic inhibition in cultured hippocampal neurones of the rat

[1]David Bleakman, †Neil L. Harrison, *William F. Colmers & Richard J. Miller

Department of Pharmacological and Physiological Sciences, and †Department of Anesthesia and Critical Care, The University of Chicago, 947 E. 58th Street, Chicago, IL 60637, U.S.A. and *Department of Pharmacology, University of Alberta, Edmonton, Canada

1 We have examined the effects of neuropeptide Y (NPY) on synaptic transmission and $[Ca^{2+}]_i$ signals in rat hippocampal neurones grown in culture. $[Ca^{2+}]_i$ in individual neurones displayed frequent spontaneous fluctuations often resulting in an elevated plateau $[Ca^{2+}]_i$. These fluctuations were reduced by tetrodotoxin (1 μM) or combinations of the excitatory amino acid antagonists 6-cyano-7-dinitroquinoxaline (CNQX) (10 μM) and aminophosphonovalerate (APV) (50 μM), indicating that they were the result of glutamatergic transmission occurring between hippocampal neurones.

2 $[Ca^{2+}]_i$ fluctuations were also prevented by Ni^{2+} (200 μM), by the $GABA_B$ receptor agonist, baclofen (10 μM) and by NPY (100 nM) or Y_2 receptor-selective NPY agonists. Following treatment of cells with pertussis toxin, NPY produced only a brief decrease in $[Ca^{2+}]_i$ fluctuations which rapidly recovered.

3 Perfusion of hippocampal neurones with 50 mM K^+ produced a large rapid increase in $[Ca^{2+}]_i$. This increase was slightly reduced by NPY or by a combination of CNQX and APV. The effects of CNQX/APV occluded those of NPY. NPY had no effect on Ba^{2+} currents measured in hippocampal neurones under whole cell voltage-clamp even in the presence of intracellular GTP-γ-S. On the other hand, Ba^{2+} currents were reduced by both Cd^{2+} (200 μM) and baclofen (10 μM).

4 Current clamp recordings from hippocampal neurones demonstrated the occurrence of spontaneous e.p.s.ps and action potential firing which were accompanied by increases in $[Ca^{2+}]_i$. This spontaneous activity and the accompanying $[Ca^{2+}]_i$ signals were prevented by application of NPY (100 nM). When hippocampal neurones were induced to fire trains of action potentials in the absence of synaptic transmission, these were accompanied by an increase in cell soma $[Ca^{2+}]_i$. NPY (100 nM) had no effect on these cell soma $[Ca^{2+}]_i$ signals. NPY (100 nM) also had no effect on inward currents generated in hippocampal neurones by micropipette application of glutamate (50 μM).

5 Thus, NPY is able to abolish excitatory neurotransmission in hippocampal cultures through a pertussis toxin-sensitive mechanism. However, no effect of NPY on Ca^{2+} influx into the cell soma of these hippocampal neurones could be discerned. These results are consistent with a localized presynaptic inhibitory effect of NPY on glutamate release in hippocampal neurones in culture.

Keywords: Glutamate; calcium channels; presynaptic inhibition; G-proteins; calcium signals; neuropeptide Y receptors

Introduction

Neuropeptide Y (NPY) is a 36 amino acid neuropeptide which is abundantly distributed in both the central and peripheral nervous systems (Chronwall *et al.*, 1985). The peptide is thought to act as a neurotransmitter at both peripheral neuroeffector junctions and in the brain. NPY-containing fibres and receptors are widely distributed within the central nervous system (Chronwall *et al.*, 1985; Lynch *et al.*, 1989). For example, the CA1 region of the hippocampus is innervated by NPY-immunoreactive axons and terminals which make numerous synaptic contacts with the dendrites of hippocampal neurones (Haas *et al.*, 1987). Previous measurements in brain slices have demonstrated that NPY effectively suppresses transmission at the Schaffer collateral/CA1 synapse (Colmers *et al.*, 1985; 1987; 1988; 1991; Haas *et al.*, 1987). In rat hippocampal slices, NPY acts at a presynaptic site in area CA1, very possibly at the presynaptic terminal itself, as NPY did not affect the antidromic excitability of the presynaptic axons and did not affect the Ca^{2+}-dependent action potential in the presynaptic CA3 pyramidal cells (Colmers *et al.*, 1988). Although the mechanism of its action is unknown, there is no evidence that activation of potassium channels at the presynaptic terminal is involved (Colmers *et al.*, 1988; Klapstein & Colmers, 1992).

NPY is one of a group of agents which has been shown to reduce neurotransmitter release from a variety of peripheral neurones. This is accompanied by a reduction of the neuronal Ca^{2+} current and Ca^{2+} influx into the cell soma (Walker *et al.*, 1988; Schofield & Ikeda, 1988; Thayer & Miller, 1990; Hirning *et al.*, 1990; Bleakman *et al.*, 1991). These effects are mediated by the Y_2 subtype of NPY receptors, as are the effects of NPY in the hippocampal slice (Bleakman *et al.*, 1991; Colmers *et al.*, 1991). Binding studies support the presence of Y_2 receptors for NPY in the hippocampus (Sheikh *et al.*, 1989; Li & Hexum, 1991). The peripheral effects of NPY are mediated by pertussis toxin-sensitive G-proteins (Schofield & Ikeda, 1988; Ewald *et al.*, 1988; Walker *et al.*, 1988; Hirning *et al.*, 1990; Wiley *et al.*, 1990), although in the hippocampal slice preparation the effects of NPY were reported to be resistant to pertussis toxin (PTX) (Colmers & Pittman, 1989). In order to investigate further the mechanism of action of NPY, we have made measurements of its effects on spontaneous synaptic transmission between hippocampal neurones in culture and combined these with measurements of its effects on Ca^{2+} influx into these cells.

Methods

Instrumentation

The methods used for this study have been described previously in detail (Thayer *et al.*, 1988). Briefly, for excitation of the fluorescent calcium probe fura-2, the collimated beam

[1] Author for correspondence at: Department of Pharmacological and Physiological Sciences, University of Chicago, 947 East 58th Street, Chicago, IL 60637, U.S.A.

of light from a 200W Hg arc lamp was passed through a dual spectrophotometer (Phoenix Instruments, Philadelphia, PA, U.S.A.) which alternated wavelengths from 340 to 380 nm by means of a spinning chopper (60 Hz). The light source was placed outside a darkened Faraday cage which enclosed the vibration isolation table supporting a microscope. A fused silica lens was positioned to focus light upon a liquid light guide (3 mm × 1 mm, Oriel, Stratford, CT, U.S.A.) and a similar lens, placed at the terminating end of the guide, was positioned to direct light through the epifluorescent illuminator of the microscope. The light guide eliminated problems associated with vibration from the chopper and electrical noise from the arc lamp. The light was reflected off a dichroic mirro (Nikon, DM 400) and focused through a 70 × oil immersion objective (E. Leitz Inc., Rockleigh, NJ, U.S.A., numerical aperture 1.15). The emission fluorescence was selected for wavelengths with a 480 nm barrier filter and recordings were spatially defined with an adjustable rectangular diaphragm. The fluorescence emission was analyzed with a photomultiplier tube (bialkali) and discriminator (APED II; Thorn EMI Gencom Inc., Plainview, NY, U.S.A.). The discriminator output was converted to pulses which were then integrated by passing the signal through an 8 pole Bessel filter at 500 Hz. The gain on this detection system could be adjusted from 1 to 100 fold by increasing the pulse length. The conversion of light intensity to voltage by this process was confirmed to be linear over the range of the light levels used in these experiments. The signal from the filter was fed into one channel of an analog to digital convertor computer system (PDP-11/73, Indec Systems, Sunnyvale, CA, U.S.A.). The signals from two photodiodes, each placed in a small portion of the light beam directed toward the monochromators, were connected to two additional channels of the analog to digital convertor.

Sorting the fluorescence output into signals corresponding to excitation at these two wavelengths was performed entirely by software written in BASIC-23 (Cheshire Data, Indec Systems). The photomultiplier output was sorted into signals from 340 and 380 nm excitation by use of the photodiode outputs at timing signals and the output observed on-line throughout the experiment.

Cover slips (25 mm diameter), plated with cells, were mounted in the perfusion chamber which was positioned on the opening of the microscope stage. The solution change in the cell superfusion system approximated a step occuring over 10 s. The tubing between the large media reservoirs and the inlet to the chambers delayed the onset of the solution change by an additional 10 s. Figures have been corrected for the perfusion delay.

Calibration and analysis

Records were corrected for experimentally determined background values and the ratio of 340/380 nm fluorescence calculated off-line. Ratios were converted to free $[Ca^{2+}]_i$ by the equation, $[Ca^{2+}]_i = K(R - R_{min})/(R_{max} - R)$ in which R is the 340/380 nm fluorescent ratio (Grynkiewicz *et al.*, 1985). The maximum ratio (R_{max}), the minimum ratio (R_{min}) and the constant K (the product of the dissociation product for fura-2 and the ratio of the free and bound forms of the dye at 380 nm) were determined from a fit to a standard curve using the above equation with a non-linear least squares analysis programme (Fabatio & Fabatio, 1979). The standard curve was determined for the fura-2 salt in calibration buffer (in mM: 4-(2-hydroxyethyl)-1-piperazineethanesulphonic acid (HEPES) 20, KCl 120, NaCl 5, $MgCl_2$ 1, pH 7.1) containing 10 mM ethylene glyco *bis* (β-aminoethyl)-N,N,N',N'-tetra-acetic acid (EGTA), $Ks = 3696 \times 10^6\ M^{-1}$ with calculated amounts of Ca^{2+} added to give free calcium concentrations ranging between approximately 0 and 2000 mM. Identical calibration curves were obtained if CsCl was used to replace KCl. Experiments performed over long periods of time (> 30 s) were digitally filtered with an algorithm which added 1/2 the value of each data point to 1/4 of the value of each neighbouring point. The data were cycled through this routine 5 times. The $[Ca^{2+}]_i$ traces in patch-clamp experiments were digitally filtered by a single cycle through an 11 point moving average algorithm.

Cell culture

Hippocampal regions were dissected from the brains of E16-19 rat embryos. Neurones were dissociated with combinations of papain and mechanical trituration (Heuttner & Baughmann, 1986), and plated onto confluent cortical astrocytes on poly-D-lysine coated glass cover slips; cultures were treated with fluorodeoxy uridine (10 μM) after 24 h and were then maintained for up to six weeks in Minimal Eagle's Medium supplemented with 2 mM L-glutamine and 5% horse serum (HyClone).

Whole-cell patch clamp

The tight seal whole-cell configuration of the patch-clamp technique (Hamill *et al.*, 1981) was used to record transmembrane I_{Ca} or I_{Ba} alone from single cells and for measuring I_{Ca} while simultaneously measuring $[Ca^{2+}]_i$ transients. Cells were mounted in a perfusion chamber and thoroughly rinsed with buffer. Due to the extensive arborizations of the hippocampal neurones it was difficult to obtain good spatial control of the membrane voltage. Detailed kinetic analysis of the current was therefore not attempted. Indications of poor voltage control were manifest as the all or none activation of the currents in the low membrane potential range (−20 to −30 mV), a slow time-dependent activation in the voltage range −20 to +10 mV and slow deactivation of the currents following repolarization to −80 mV. If any of these characteristics were displayed, experiments were discarded. Acceptable recordings using these criteria represented approximately 20% of the cells from which recordings were made. Background fluorescence was recorded after formation of a giga-seal but before breaking into the cell, thus accounting for fluorescence contributed by the fura-2 in the pipette. Since the pipette approached the cell from above, the objective was focussed below the pipette near the middle of the cell to minimize the pipette fluorescence. Fluorescence recordings were made from the cell soma alone. Full diffusion of the fura-2 into the cell occurs over a period of 1–3 min. For the 'perforated patch technique', amphotericin-B (150 μg ml^{-1}) was present in the pipette and access was obtained within 2 min as indicated by an increase in the amplitude of the capacitance transient. If the whole cell configuration and internal perfusion occurred, the cell deteriorated within 2 min. Currents recorded by a List EPC-7 amplifier were filtered by an 8-pole low-pass Bessel filter with a cut-off frequency of 200 Hz and stored on computer. Linear leak corrections were performed by averaging sixteen, 10 mV hyperpolarizing pulses from the holding potential. The d.c. component of the averaged leak current was then modelled so as to increase the signal to noise ratio. Digital summation of this leak template after appropriate scaling with the current obtained during depolarizing test pulses provided the leak correction. Series resistance compensation of approximately 40–80% was possible with the uncompensated portion of the series resistance ranging between 1.8 and 3 MOhm. Peak I_{Ca} and I_{Ba} values rarely exceeded 1.5 nA or 2.5 nA respectively, giving approximate maximum voltage errors of 4.5 mV and 7.5 mV. Cells were discarded when the steady leakage current at the holding potential was greater than 5% of the peak inward current. All experiments were performed at room temperature. Under current clamp conditions action potentials were evoked by brief current pulses (0.5–2 nA; 4–8 ms). Recordings were accepted for analysis if the resting potential exceeded −50 mV, the input resistance

exceeded 200 MOhms and the basal $[Ca^{2+}]_i$ was below 200 nM. All experiments were performed at room temperature (22–25°C).

Fura-2 fluorescence experiments

Experiments in which fura-2 fluorescence alone was measured were performed on coverslips of cells loaded for 30 min at 37°C with 5 μM fura-2 acetoxy methyl ester. Cells were then washed twice with buffer and allowed to incubate for a further 30 min at 37°C. These loading conditions generally resulted in moderate fluorescence similar to that observed for cells dialyzed under whole cell patch clamp with 100 μM fura-2 pentapotassium salt in the patch pipette.

Drugs and chemicals

Extracellular solutions For experiments performed under current-clamp conditions, the solutions were composed of (in mM): NaCl 138, $CaCl_2$ 2, $MgCl_2$ 1, KCl 5, HEPES 10, glucose 10 adjusted to pH 7.4 with NaOH. Voltage clamp experiments were performed with cells perfused with solutions containing (in mM): tetraethylammonium chloride (TEACl) 143, $CaCl_2$ 2, $MgCl_2$ 1, HEPES 10, glucose 10, pH adjusted to 7.4 with TEA hydroxide. $BaCl_2$ 2 mM was substituted for $CaCl_2$ for experiments in which the I_{Ba} was measured. For experiments in which glutamate was applied by micropressure from a pipette (approximately 0.5–1 MOhm tip resistance) using a Picospritzer (6 p.s.i., 30 ms) the extracellular solutions contained no added Mg^{2+}, 3 μM glycine and 0.5 μM tetrodotoxin (TTX). For the micropressure application the pipette was placed approximately 50 μm from the cell.

Pipette solutions Solutions for voltage-clamp experiments containing (in mM): CsCl 135, $MgCl_2$ 1, HEPES 10, diTris phosphocreatinine 14, MgATP 3.6, 50 U ml^{-1} creatinine phosphokinase, adjusted to pH 7.1 with CsOH. For the measurement of I_{Ba}, I_{Ca} or experiments during which micropressure application of glutamate was performed, 10 mM 1,2-bis(2-aminophenoxy)ethane-N',N',N',N''-tetra acetic acid (BAPTA) was also present in the patch pipette. For combined I_{Ca} and $[Ca^{2+}]_i$ transients, 100 μM fura-2 pentapotassium salt was present in the patch pipette. The patch pipettes for current clamp contained (in mM): fura-2 pentapotassium salt 0.1, K gluconate 145, $MgCl_2$ K_2ATP 5, HEPES 5, pH 7.2, osmolality, 310 mosmol kg^{-1}. Amphotericin-B (150 μg ml^{-1}) was included in the patch pipette for the perforated patch experiments.

All reagents were of the highest commercial grade. Fura-2 pentapotassium salt was obtained from Molecular Probes Inc., Eugene, OR. Neuropeptide Y from Richeleau Biochemicals, Quebec and 6-cyano-7-dinitroquinoxaline (CNQX) from Research Biochemicals Inc. All other agents were obtained from Sigma Chemical Company.

Results

Hippocampal neurones form excitatory synapses with one another in culture (Forsythe & Westbrook, 1988; Abele *et al.*, 1990). Under conditions which optimize N-methyl-D-aspartate (NMDA) receptor stimulation, i.e. perfusion in the presence of glycine (10 nM) and in the absence of added Mg^{2+}, hippocampal neurones show frequent large fluctuations in their $[Ca^{2+}]_i$ (Abele *et al.*, 1990). These fluctuations result from spontaneous glutamatergic transmission between the cells. Spontaneous fluctuations in $[Ca^{2+}]_i$, which sometimes fused into a persistent plateau, were also observed in the present experiments. As indicated in Figure 1, fluctuations in $[Ca^{2+}]_i$ were prevented by a combination of CNQX (10 μM) and aminophosphonovalerate (APV) (50 μM), by TTX (1 μM), by Ni^{2+} (200 μM) and reduced by the $GABA_B$ agonist, baclofen (10 μM).

NPY and its homologue PYY (100 nM) were also effective in reducing $[Ca^{2+}]_i$ fluctuations in these hippocampal cultures (Figures 1e and 2a). Peptides which act at the Y_2 receptor for NPY, such as NPY 13-36 (100 nM), were also inhibitory (Figure 2a). We examined these effects further by treating cultures overnight with pertussis toxin (PTX, 150 ng ml^{-1},

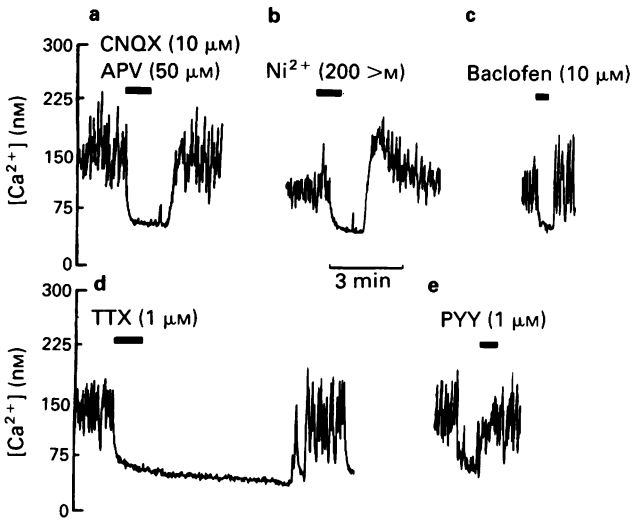

Figure 1 Typical examples of spontaneous fluctuations in $[Ca^{2+}]_i$ observed in single hippocampal neurones in culture. Shown are the effects of perfusion with solutions containing (a) CNQX (10 μM) and APV (50 μM); (b) Ni^{2+} (200 μM); (c) baclofen (10 μM), (d) TTX (1 μM) and (e) PYY (100 nM). For abbreviations, see text.

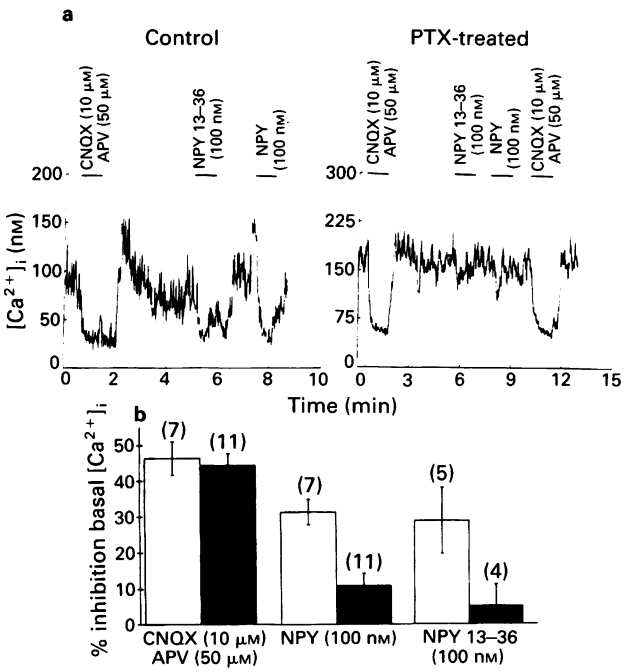

Figure 2 (a) Records of spontaneous $[Ca^{2+}]_i$ fluctuations in hippocampal neurones and the effects of neuropeptide Y (NPY, 100 nM) and NPY 13-36 (100 nM) under control conditions and following pretreatment with pertussis toxin (PTX, 150 ng ml^{-1}, 17–20 h). Also shown is the effect of a combination of CNQX (10 μM) and APV (50 μM). (b) Histogram summarizing the effects of PTX treatment (150 ng ml^{-1}, 17–20 h) on the NPY (100 nM), NPY 13-36 (100 nM) and CNQX/APV-dependent reduction in the mean $[Ca^{2+}]_i$. The reduction in $[Ca^{2+}]_i$ was calculated from an average of thirty, 1 s values prior to and following application of the agents shown. The numbers in parentheses are the number of cells on which the agents were tested. Open columns: controls; solid columns: PTX-treated (*n*). For abbreviations, see text.

17–20 h). Following such treatment, NPY (100 nM) became largely ineffective in reducing fluctuations in $[Ca^{2+}]_i$. In PTX-treated cultures, addition of NPY (100 nM) usually produced a transient reduction in the prevailing $[Ca^{2+}]_i$ which quickly reversed. This contrasted with the control situation where addition of NPY (100 nM) reduced $[Ca^{2+}]_i$ to a greater extent and this persisted throughout the period of application (Figure 2a). Quantitation of these differences indicated that PTX-treatment greatly reduced the inhibitory effects of NPY (100 nM) and NPY 13-36 (100 nM) but not those produced by the combination of CNQX (10 μM) and APV (50 μM) (Figure 2b).

We next examined the ability of NPY (100 nM) to inhibit neuronal voltage-sensitive Ca^{2+} currents in hippocampal neurones. Perfusion of hippocampal neurones with a solution containing 50 mM KCl (iso-osmotically substituted for NaCl) produced large and rapid increases in $[Ca^{2+}]_i$ (Figure 3). Treatment of cells with NPY (100 mM) reduced this increase by 13.6 ± 3.8% ($n = 8$). A combination of CNQX (10 μM)/APV (50 μM), reduced the response by a similar amount (17.3 ± 4.5%, $n = 7$). In the presence of CNQX (10 μM) and APV (50 μM) no additional effect of NPY (100 nM) was discernable ($\Delta = 5.0 \pm 2.9\%$, $n = 7$). We interpret this result as follows. The response to 50 mM K^+ is mostly due to direct depolarization of the cell under observation. A small component of the effect is due to glutamate release from adjoining cells which make synaptic contact with the observed cell. When this minor component is blocked by CNQX/APV, NPY (100 nM) has no further effect.

It has been shown elsewhere that agonists acting at $GABA_B$ or A_1 adenosine receptors and which effectively

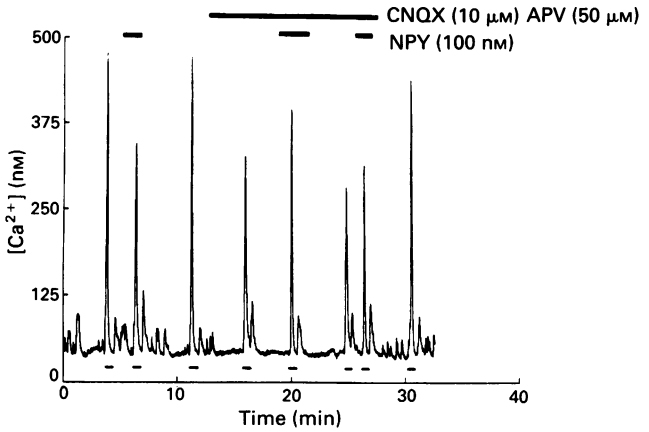

Figure 3 A typical experiment illustrating increases in a single hippocampal neurone $[Ca^{2+}]_i$ resulting from 30 s perfusions with solutions containing 50 mM KCl and showing the inhibitory effects of neuropeptide Y (NPY, 100 nM), CNQX (10 μM) plus APV (50 μM), and CNQX (10 μM) plus APV (50 μM) plus NPY (100 nM). For abbreviations, see text.

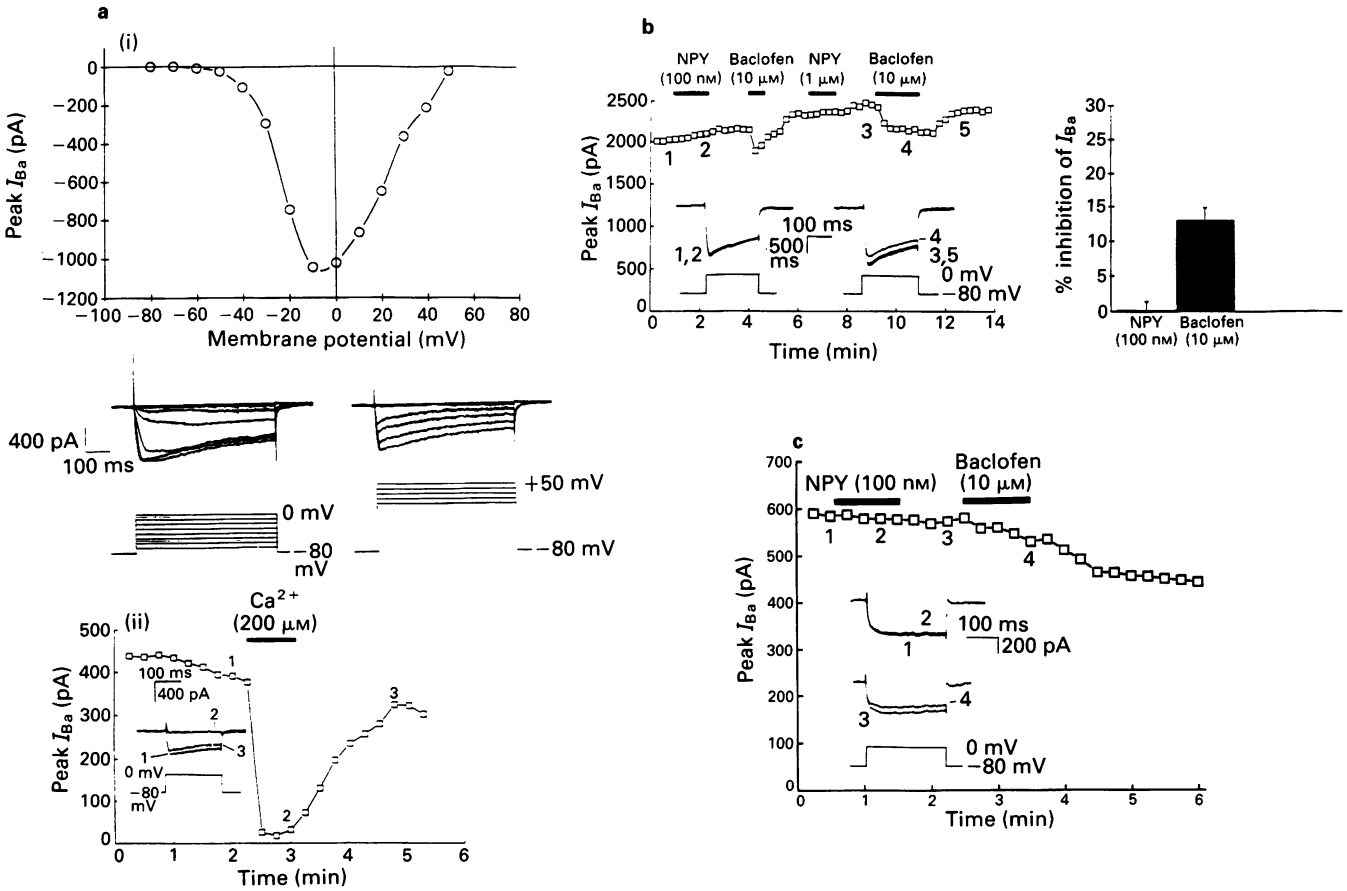

Figure 4 (a) (i) Ba^{2+} current (I_{Ba}) recorded in single hippocampal neuronal cell bodies under voltage-clamp conditions and associated current/voltage relationship in a single hippocampal neurone. $V_h = -80$ mV. (ii) Time course illustrating the inhibitory effect of Cd^{2+} (200 μM) on the I_{Ba}. Insets show the individual current records as denoted in the time course. (b) Time course of the effect of neuropeptide Y (NPY, 100 nM and 1 μM) and baclofen on the I_{Ba} recorded in a hippocampal neurone cell soma. The insets show individual current traces. The histogram summarizes the effects of NPY (100 nM) and baclofen (10 μM) on the recorded I_{Ba}. The inhibition produced was calculated by plotting the peak I_{Ba} as a function of time for at least three data points prior to the addition of the drug. The time course was then plotted as a linear function and the decline in the I_{Ba} extrapolated to the point at which the effects of the drug were stable. The expected magnitude of the I_{Ba} was then calculated and used to obtain the inhibition produced ($n = 5$). (c) Time course showing the effect of NPY (100 nM) and baclofen (10 μM) on the I_{Ba} recorded with GTP-γ-S (150 μM) in the patch pipette. Baclofen produced a 12.9 ± 2.1% inhibition of the I_{Ba} measured 2 min following drug application. NPY produced a 1.9 ± 1.5% inhibition 2 min following application to the same cells ($n = 4$).

block excitatory transmission in the hippocampal slice and in culture, also inhibit the Ca^{2+} current (I_{Ca}) recorded in the cell body of hippocampal neurones (Scholz *et al.*, 1990; Scholz & Miller, 1991a,b). Figure 4a illustrates the I_{Ba} recorded in the cell soma of one of these neurones, as well as its inhibition by Cd^{2+}. Figure 4b shows that the $GABA_B$ agonist, baclofen (10 μM) reduced I_{Ba} in these neurones, whereas NPY (100 nM and 1 μM) was without effect. Inhibition of I_{Ba} was also examined with the non-hydrolyzable analogue of GTP, GTP-γ-S, in the patch pipette (Figure 4c). GTP-γ-S enhances the inhibitory effects of neurotransmitters on neuronal Ca^{2+} currents and renders them irreversible (Dolphin & Scott, 1987). Thus we argued that GTP-γ-S might reveal any small effects of NPY on the I_{Ba} which might not be readily apparent. In the present study inclusion of GTP-γ-S in the patch pipette (150 μM) produced a reduction in the activation rate of the I_{Ba} similar to that reported in other studies (Bean, 1989). However NPY (100 nM) was still without effect whereas baclofen (10 μM) now irreversibly reduced the I_{Ba} in the same cells.

We now tested the possibility that the membrane of an effect of NPY on the I_{Ba} was the result of dialysis of some essential intracellular component necessary for coupling of the NPY receptor to the somatic Ca^{2+} channels. With the pore-forming antibiotic amphotericin-B (150 μg ml^{-1}) in the pipette, electrical access to the cell occurs but dialysis of large intracellular components is prevented (Rae *et al.*, 1991). Under these conditions NPY still had no effect on the I_{Ba} recorded in the cell soma, while in the same neurone, baclofen (10 μM) reduced the I_{Ba} (inhibition for NPY = 0.1 ± 0.7%, baclofen = 18.5 ± 2.4% $n = 3$, mean ± s.d.).

In order to test the possibility that NPY directly blocks postsynaptic glutamate receptors, we also examined the effect of NPY on inward currents recorded in hippocampal neurones generated by 30 ms applications of glutamate (50 μM). Figure 5 shows such an experiment in which the inward current observed was unaffected by NPY (100 nM). In the same neurone it was possible to reduce the glutamate-activated currents using APV (50 μM) and CNQX (10 μM) (not shown).

Current clamp recordings were used to analyze further the effects of NPY. As can be seen in Figure 6a, recordings from cultured hippocampal neurones revealed the presence of excitatory postsynaptic potentials (e.p.s.ps) that sometimes triggered action potentials. In the presence of NPY (100 nM), the spontaneous activity and the resulting increase in $[Ca^{2+}]_i$ was abolished (Figure 6a and b). NPY had no effect on the resting membrane potential of the cells. The observed activity and associated increases in $[Ca^{2+}]_i$ were also prevented by a combination of CNQX (10 μM) and APV (50 μM) (not shown). In addition, spontaneous e.p.s.ps and the accompanying elevated $[Ca^{2+}]_i$ observed in the absence of evoked trains of action potentials could also be prevented by NPY (12 of 15 cells examined). Furthermore, e.p.s.ps could also be abolished by baclofen (10 μM), Ni^{2+} (200 μM), and NPY 13-36 (100 nM) (not illustrated). It should be noted that in 3 cells examined (1 of 15 cells under current clamp conditions and 2 of 32 cells under fura-2 AM recording conditions), NPY produced an increase in the spontaneous activity accompanied by a depolarization or rise in the basal $[Ca^{2+}]_i$ (not shown). Interestingly, this effect was not mimicked by NPY 13-36 which may suggest that it is not due to activation of Y_2 receptors for NPY. Since this effect occurred so infrequently we did not examine it in detail.

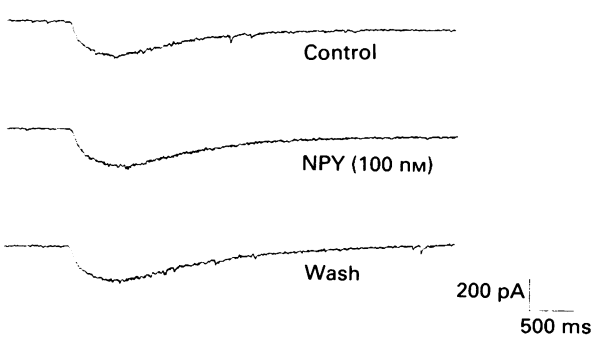

Figure 5 Inward currents associated with pressure ejection application of glutamate (50 μM) for brief periods (ejected under positive pressure of 6 p.s.i., picospritzer, 30 ms) at a holding potentials of −60 mV. Individual examples showing averaged currents (of 5 sweeps of data, 20 s apart) for application of glutamate (50 μM, 30 ms) in the absence of neuropeptide Y (NPY, 100 nM), in the presence of NPY (100 nM) and following washout of the peptide. The data shown are representative of 4 separate experiments.

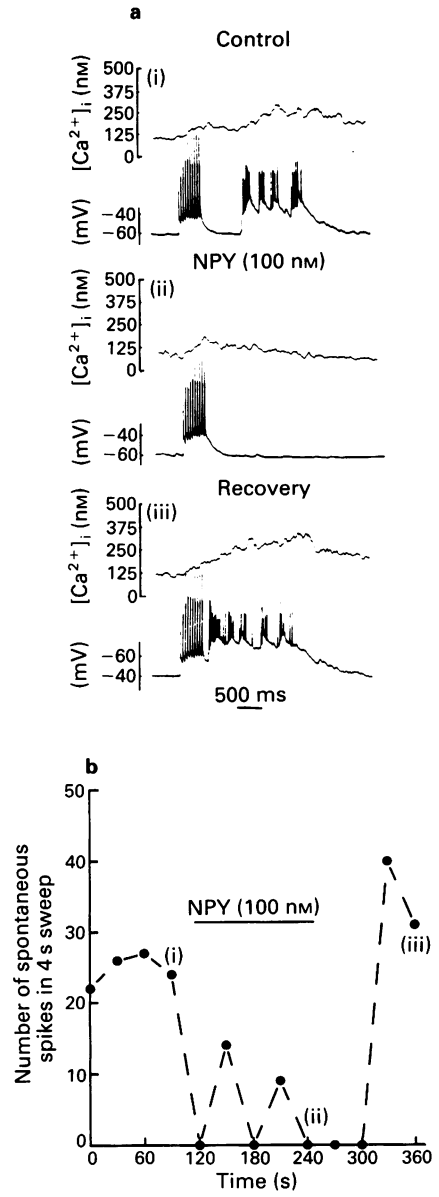

Figure 6 (a) Current clamp records and simultaneous $[Ca^{2+}]_i$ measurements in cells under whole cell patch clamp with 100 μM fura-2 in the patch pipette. Action potentials were evoked by brief current injection (4–8 ms, 100–700 pA). Records show sweeps in the absence (i), presence (ii) and 2 min following washout (iii) of neuropeptide Y (NPY, 100 nM). (b) Plot illustrating the effect of NPY (100 nM) on synaptic activity for the data shown in (a). The total number of action potentials observed in a 4 s sweep of collected data has been plotted for each successive sweep. Sweeps of data were collected every 30 s and NPY (100 nM) included in the perfusion solution as denoted by the horitzontal bar.

Increases in $[Ca^{2+}]_i$ could also be produced when cells were induced to fire trains of action potentials following brief injections of depolarizing current as shown in Figure 6a. NPY (100 nM) had no effect on the magnitude of the action potential-induced increases in $[Ca^{2+}]_i$ in the cell soma. In some experiments, CNQX (10 μM) and APV (50 μM) were included in the perfusing solutions to prevent spontaneous activity; again, NPY (100 nM) had no effect on the magnitude of the action potential-induced increases in $[Ca^{2+}]_i$ in the cell soma. Under these conditions the mean change in the peak increase in $[Ca^{2+}]_i$ in the presence of NPY (100 nM) was $3.5 \pm 6.0\%$ ($n = 6$).

Discussion

The presence observations confirm previous reports showing that NPY can effectively inhibit excitatory glutamate-mediated synaptic transmission in the hippocampus (Colmers *et al.*, 1985; 1987; 1988; 1991; Haas *et al.*, 1987; Abele *et al.*, 1990). Although the precise mechanism by which NPY produces these effects remains unclear, the data suggest several possible explanations, and eliminate others.

NPY is extensively distributed in the peripheral nervous system (Lundberg *et al.*, 1982; Sundler *et al.*, 1983) and is an effective inhibitor of neurotransmitter release at a number of peripheral neuroeffector junctions (Sundler *et al.*, 1983; Wahlestedt *et al.*, 1985; Stretton & Barnes, 1988; Grundemar *et al.*, 1988; Walker *et al.*, 1988; Wiley *et al.*, 1990). NPY has been shown to inhibit the I_{Ca} in the cell bodies of rat DRG neurones (Walker *et al.*, 1988), enteric neurones (Hirning *et al.*, 1990) and sympathetic neurones (Schofield & Ikeda, 1988). These are all tissues in which the peptide also blocks neurotransmitter release (Lundberg *et al.*, 1982; Friel *et al.*, 1986; Walker *et al.*, 1988; Wiley *et al.*, 1990). Furthermore in these peripheral neurones, NPY appears to inhibit selectively the N-type Ca^{2+} channel (Hirning *et al.*, 1990; Wiley *et al.*, 1990; Plummer *et al.*, 1991), which has been associated with providing Ca^{2+} influx associated with neurotransmitter release (Miller, 1990). The coupling of the NPY receptor and the Ca^{2+} channels appears to be mediated by a PTX-sensitive G-protein. In DRG cells, NPY has no effect on other membrane properties, suggesting a single site of action of the Y_2 NPY receptor (Bleakman *et al.*, 1991).

An important question is whether inhibition of the neuronal I_{Ca} underlies the presynaptic inhibitory effects of NPY in the central nervous system as well. A number of neurotransmitters that are capable of inhibiting Ca^{2+} currents in central neurones such as $GABA_B$ agonists, A_1 adenosine agonists and NPY (reviewed in Miller, 1990; see also Chemevskaya *et al.*, 1981; Toselli *et al.*, 1989; Fisher & Johnston, 1990; Pennington & Kelly, 1990; Scholz *et al.*, 1990; Scholz & Miller, 1991a,b) can also inhibit synaptic transmission in cultured hippocampal neurones (Abele *et al.*, 1990; Scholz *et al.*, 1990; Scholz & Miller, 1991a,b). We have shown elsewhere that the inhibitory effects of A_1 adenosine and $GABA_B$ agonists are mediated by pertussis toxin-sensitive G-proteins and are associated with inhibition of Ca^{2+} influx monitored in the soma of these cells (Scholz *et al.*, 1990; Scholz & Miller, 1991a,b). Nevertheless, the latter two receptors can also increase I_K in central neurones (Greene & Haas, 1985). Although NPY also inhibits excitatory synaptic transmission in rat hippocampal slices and cultures, it differs from $GABA_B$ or A_1 adenosine agonists in that it has no effect on postsynaptic ion channels including the Ca^{2+} channels either in the slice (Colmers *et al.*, 1987; 1988) or in culture. In addition no effect of NPY on the I_{Ba} was seen when washout of intracellular components was prevented by the use of the perforated patch technique. All of this contrasts with the effects of NPY on peripheral neurones where it produces large inhibitory effects on the I_{Ca} using precisely the same paradigms (Hirning *et al.*, 1990; Thayer & Miller, 1990; Bleakman *et al.*, 1991; Plummer *et al.*, 1991). It is particularly interesting to note that NPY did not reduce Ca^{2+} influx into the neuronal soma in response to a train of action potentials. In these experiments, no effect on resting membrane potential was observed, indicating that there also appears to be no effect of NPY on resting K^+ conductance in the cell body. Nevertheless a selective activation of a K^+ conductance in the nerve terminal cannot be ruled out entirely. Finally, the possibility that the inhibitory action of NPY was due to an effect on the postsynaptic response to endogenously released glutamate was also examined. We show that glutamate applications to the cell soma, in the absence of synaptic transmission, were unaffected by NPY.

The simplest hypothesis for the mechanism of NPY action is that it inhibits Ca^{2+} influx, but that its receptors and their physiological effects are selectively localized to presynaptic terminals. There is both physiological and anatomical evidence consistent with this hypothesis. In the hippocampal slice, applications of low concentrations of 4-aminopyridine (4-AP) blocked the presynaptic inhibition mediated by NPY. However, lowering the extracellular concentration of Ca^{2+} completely restored the ability of NPY to inhibit transmitter release (Colmers *et al.*, 1988; Klapstein & Colmers, 1992), which is consistent with a mechanism involving regulation of Ca^{2+} influx. Also consistent with this hypothesis is evidence from autoradiographic studies that indicate the presence of NPY receptors in strata oriens and radiatum, where the terminals of the excitatory input to the pyramidal neurones are found. However, few receptors are found in the cell body layer (Martel *et al.*, 1986; 1990). An alternative hypothesis is that NPY blocks glutamate release by a mechanism which does not require it to block Ca^{2+} influx. For example, there is evidence for such a mechanism mediating at least part of the inhibition of transmitter release produced by adenosine at some mammalian neuromuscular junctions (Silinsky, 1986). However one would predict that if NPY interfered with glutamate release at a step subsequent to Ca^{2+} entry, then this inhibition should not be sensitive to manipulations of presynaptic Ca^{2+} presumably caused by 4-AP as observed (Colmers *et al.*, 1988; Colmers *et al.*, 1991). Thus, we conclude that NPY appears to abolish excitatory neurotransmission in cultured hippocampal neurones by preventing glutamate release from presynaptic nerve terminals and that the NPY receptors in the hippocampus are located at or near these terminals.

D.B. was supported by a Fulbright Fellowship. R.J.M. was supported by grants DA-02121, MH-40165 and IP30-DK-42086, a Digestive Diseases Research Center Core Grant. W.F.C. was supported by the M.R.C. (Canada) and is an Alberta Heritage Foundation for Medical Research Scholar. We would like to thank P.S. Chard for assistance in some of these experiments, M. Jones for his assistance in the experiments shown in Figure 5 and L. Hornberger for the cell culture.

References

ABELE, A.E. & MILLER, R.J. (1990). Potassium channel activators abolish excitotoxicity in cultured hippocampal pyramidal neurons. *Neurosci. Lett.*, **115**, 195–200.

ABELE, A.E., SCHOLZ, K.P., SCHOLZ, W.K. & MILLER, R.J. (1990). Excitotoxicity induced by enhanced excitatory neurotransmission in cultured hippocampal pyramidal neurons. *Neuron*, **4**, 413–419.

BEAN, B.P. (1989). Neurotransmitter inhibition of neuronal calcium current by changes in channel voltage dependence. *Nature*, **340**, 153–156.

BLEAKMAN, D., COLMERS, W.F., FOURNIER, A. & MILLER, R.J. (1991). Neuropeptide Y inhibits Ca^{2+} influx into cultured rat dorsal root ganglion neurons via a Y_2 receptor. *Br. J. Pharmacol.*, **103**, 1781–1789.

CHEMEVSKAYA, N.I., OBUKHOV, A.G. & KRISHTAL, O.A. (1991). NMDA receptor agonists selectivity block N-type calcium channels in hippocampal neurons. *Nature*, **349**, 418–420.

CHRONWALL, B.M., DIMAGGIO, D.A., MASSARI, V.J., PICKEL, V.M., RUGGIERO, D.A. & O'DONOHUE, T.L. (1985). The anatomy of neuropeptide Y containing neurons in the rat brain. *Neurosci.*, **15**, 1159–1181.

COLMERS, W.F., KLAPSTEIN, G.J., FOURNIER, ST. PIERRE, S. & TREHERNE, K.A. (1991). Presynaptic inhibition by neuropeptide Y in rat hippocampal slice *in vitro* is mediated by a Y_2-receptor. *Br. J. Pharmacol.*, **102**, 41–44.

COLMERS, W.F. & PITTMAN, Q.J. (1989). Presynaptic inhibition by neuropeptide Y and baclofen in hippocampus: Insensitivity to pertussis toxin treatment. *Brain Res.*, **498**, 99–104.

COLMERS, W.F., LUKOWIAK, K.D. & PITTMAN, Q.J. (1985). Neuropeptide Y reduces orthodromically evoked population spikes in rat hippocampal CA1 by a possibly presynaptic mechanism. *Brain Res.*, **346**, 404–408.

COLMERS, W.F., LUKOWIAK, K.D. & PITTMAN, Q.J. (1987). Presynaptic action of neuropeptide Y in area CA1 of the rat hippocampal slice. *J. Physiol.*, **383**, 285–299.

COLMERS, W.F., LUKOWIAK, K.D. & PITTMAN, Q.J. (1988). Neuropeptide Y action in the rat hippocampal slice: site and mechanism of presynaptic action. *J. Neurosci.*, **8**, 3827–3837.

DOLPHIN, A.C. & SCOTT, R.H. (1987). Calcium channel currents and their inhibition by (−) baclofen in rat sensory neurones: modulation by guanine nucleotides. *J. Physiol.*, **386**, 1–17.

EWALD, D.A., STERNWEIS, P.C. & MILLER, R.J. (1988). G_O induced coupling of neuropeptide Y receptors to calcium channels in sensory neurones. *Proc. Natl. Acad. Sci. U.S.A.*, **85**, 3633–3637.

FABATIO, A. & FABATIO, F. (1979). Calculator programs for computing the composition of solutions containing multiple metal and ligands used for experiments in skinned muscle cells. *J. Physiol. (Paris)*, **75**, 463–505.

FISHER, R. & JOHNSTON, D. (1990). Differential modulation of single voltage gated calcium channels by cholinergic and adrenergic agonists in adult rat hippocampal neurons. *J. Neurophysiol.*, **64**, 1291–1302.

FORSYTHE, I.D. & WESTBROOK, G.L. (1988). Slow excitatory postsynaptic currents mediated by N-Methyl-D-aspartate receptors in cultured mouse central neurons. *J. Physiol.*, **396**, 515–534.

FRIEL, D.D., WALKER, M.W. & MILLER, R.J. (1986). Neuropeptide Y: a powerful modulator of epithelial ion transport. *Br. J. Pharmacol.*, **88**, 425–443.

GREENE, R.W. & HAAS, H.L. (1985). Adenosine actions on CA1 pyramidal neurones in rat hippocampal slices. *J. Physiol.*, **366**, 119–127.

GRUNDEMAR, L., WIDMARK, E., WALDECK, B. & HAKANSON, R. (1988). NPY: presynaptic inhibition by vagally induced contractions in the guinea-pig trachea. *Regul. Pept.*, **23**, 309–313.

GRYNKIEWICZ, G., POENIE, M. & TSIEN, R.Y. (1985). A new generation of calcium indicators with greatly improved fluorescence properties. *J. Biol. Chem.*, **260**, 3440–3450.

HAAS, H.L., HERMANN, A., GREENE, R.W. & CHAN-PALAY, V. (1987). Action and location of neuropeptide tyrosine (Y) in hippocampal neurons of the rat slice preparation. *J. Comp. Neurol.*, **257**, 208–215.

HAMILL, A., MARTY, E., NEHER, E., SAKMANN, B. & SIGWORTH, F. (1981). An improved patch clamp technique for high resolution current recordings from cells and cell free membrane patches. *Pflügers Arch.*, **391**, 85–100.

HEUTTNER, J.E. & BAUGHMANN, R.W. (1986). Primary cultures of identified neurons from the visual cortex of post natal rats. *J. Neurosci.*, **6**, 3044–3060.

HIRNING, L.D., FOX, A.P. & MILLER, R.J. (1990). Inhibition of calcium currents in cultured rat myenteric neurons by neuropeptide Y: evidence for direct receptor/channel coupling. *Brain Res.*, **532**, 120–130.

KLAPSTEIN, G.J. & COLMERS, W.F. (1992). 4-Aminopyridine and low Ca^{2+} differentiate presynaptic inhibition mediated by neuropeptide Y, baclofen and 2-chloroadenosine in rat hippocampal CA1 *in vitro*. *Br. J. Pharmacol.*, **105**, 470–474.

LI, W. & HEXUM, T.D. (1991). Characterization of neuropeptide Y (NPY) receptors in human hippocampus. *Brain Res.*, **553**, 167–170.

LUNDBERG, J.M., TERENIUS, L., HOKFELT, T., MARTLING, C.R., TATEMOTO, K., MUTT, V., POLAK, J., BLOOM, S.R. & GOLDSTEIN, M. (1982). Neuropeptide Y (NPY)-like immunoreactivity in peripheral noradrenergic neurons and effects of NPY on sympathetic function. *Acta Physiol. Scand.*, **116**, 477–480.

LYNCH, D.R., WALKER, M., MILLER, R.J. & SNYDER, S.H. (1989). Neuropeptide Y receptor binding sites in rat brain: ^{125}I-peptide YY and ^{125}I-neuropeptide Y imply receptor heterogeneity. *J. Neurosci.*, **9**, 2607–2619.

MARTEL, J.C., FOURNIER, A., ST-PIERRE, S. & QUIRON, R. (1990). Quantitative autoradiographic distribution of [^{125}I]Bolton-Hunter neuropeptide Y receptor binding sites in rat brain. Comparison with [^{125}I]peptide YY receptor sites. *Neuroscience*, **36**, 255–283.

MARTEL, J.C., ST. PIERRE, S. & QUIRION, R. (1986). Neuropeptide Y receptors in rat brain: autoradiographic localization. *Peptides*, **7**, 55–60.

MILLER, R.J. (1990). Receptor mediated regulation of calcium channels and neurotransmitter release. *FASEB J.*, **4**, 3291–3299.

PENNINGTON, N.J. & KELLY, J.S. (1990). Serotonin receptor activation reduces calcium current in an acutely dissociated adult central neurone. *Neuron*, **2**, 1453–1463.

PLUMMER, M.R., RITTENHOUSE, A., KANEVSKY, M. & HESS, P. (1991). Neurotransmitter modulation of calcium channels in rat sympathetic neurons. *J. Neurosci.*, **11**, 2339–2349.

RAE, J., COOPER, K., GATES, P. & WATSKY, M. (1991). Low access resistance perforated patch recordings using amphotericin B. *J. Neurosci. Methods*, **37**, 15–26.

SHEIKH, S.P., HAKANSON, R. & SCHWARTZ, T.W. (1989). Y1 and Y2 receptors for neuropeptide Y. *FEBS Lett.*, **245**, 209–214.

SCHOFIELD, C.G. & IKEDA, S.K. (1988). Neuropeptide Y blocks a calcium current in C cells of bullfrog sympathetic ganglion. *Eur. J. Pharmacol.*, **151**, 131–134.

SCHOLZ, K.P. & MILLER, R.J. (1991a). Analysis of adenosine actions of Ca^{2+} currents and synaptic transmission in cultured rat hippocampal pyramidal neurones. *J. Physiol.*, **435**, 373–393.

SCHOLZ, K.P. & MILLER, R.J. (1991b). GABA-B receptor mediated inhibition of Ca^{2+} currents and synaptic transmission in cultured rat hippocampal neurones. *J. Physiol.*, **444**, 669–686.

SCHOLZ, K.P., SCHOLZ, W.K. & MILLER, R.J. (1990). Analysis of presynaptic inhibitions of calcium currents induced by baclofen in pyramidal and nonpyramidal neurons cultured from rat hippocampus. *Soc. Neurosci.*, **16**, 793 (abs).

SILINSKY, E.M. (1986). Inhibition of transmitter release by adenosine: are Ca^{2+} currents depressed or are the intracellular effects of Ca^{2+} impaired. *Trends Pharmacol. Sci.*, **7**, 180–185.

STRETTON, C.D. & BARNES, P.J. (1988). Modulation of cholinergic transmission in guinea-pig trachea by neuropeptide Y. *Br. J. Pharmacol.*, **93**, 672–678.

SUNDLER, F., MOGHIMZADEH, E., HAKANSON, R., EKLUND, M. & EMSON, P. (1983). Nerve fibers in the gut and pancreas of the rat displaying neuropeptide Y immunoreactivity. Intrinsic and extrinsic origin. *Cell Tiss. Res.*, **230**, 487–493.

THAYER, S.A., STUREK, M. & MILLER, R.J. (1988). Measurement of neuronal Ca^{2+} transients using simultaneous microfluorimetry and electrophysiology. *Pflügers Arch.*, **412**, 216–223.

THAYER, S.A. & MILLER, R.J. (1990). Regulation of intracellular free calcium concentration in single rat dorsal root ganglion neurones *in vitro*. *J. Physiol.*, **425**, 85–115.

TOSELLI, M., LANG, J., COSTA, T. & LUX, H.D. (1989). Direct modulation of voltage dependent calcium channels by muscarinic activation of a pertussis toxin sensitive G-protein in hippocampal neurons. *Pflügers Arch.*, **415**, 255–261.

WAHLESTEDT, C., YANAIHARA, N. & HAKANSON, R. (1985). Evidence for different pre and postsynaptic junctional receptors for neuropeptide Y and related properties. *Regul. Pept.*, **13**, 317–328.

WALKER, M.W., EWALD, D.A., PERNEY, T.M. & MILLER, R.J. (1988). Neuropeptide Y modulates neurotransmitter release and Ca^{2+} currents in rat sensory neurons. *J. Neurosci.*, **8**, 2438–2446.

WILEY, J.W., GROSS, R.A., LU, Y. & MACDONALD, R.L. (1990). Neuropeptide Y reduces calcium current and inhibits acetylcholine release in nodose neurones via a pertussis toxin sensitive mechanism. *J. Neurophysiol.*, **63**, 1499–1507.

(Received February 18, 1992
Revised May 11, 1992
Accepted May 28, 1992)

Br. J. Pharmacol. (1992), **107**, 341–346

Effect of adenosine and adenosine analogues on cyclic AMP accumulation in cultured mesangial cells and isolated glomeruli of the rat

Ana Olivera & [1]*Jose M. Lopez–Novoa

Fundaciòn Jimenez Diaz–Consejo Superior de Investigaciones Cientificas, Madrid and *Departamento de Fisiologia y Farmacologia, Universidad de Salamanca, Salamanca, Spain

1 Changes in intracellular levels of adenosine 3':5'-cyclic monophosphate (cyclic AMP) were studied in rat isolated glomeruli and cultured glomerular mesangial cells exposed to adenosine and to the preferential A_1 receptor agonist N^6-**R**-1-methyl-2-phenylethyl adenosine (**R**-PIA), or the potent A_2 adenosine receptor agonist 5-(N-ethylcarboxamide)adenosine (NECA).

2 Whereas NECA and adenosine triggered a dose-dependent increase in cyclic AMP values with EC_{50} values of approximately 10^{-6} M and 3×10^{-5} M respectively, **R**-PIA lowered cyclic AMP levels at concentrations of 10^{-6} M or less and increased them at higher concentrations.

3 The time-course of the increase induced by 10^{-6} M NECA was slower than that induced by 10^{-4} M adenosine. Adenosine produced a maximal stimulation within the first minute, whereas the effect of NECA in both glomeruli and mesangial cells was noticeable only from the second minute of incubation.

4 The effects of the agonists **R**-PIA and NECA on the cyclic AMP system were blocked respectively by the A_1 adenosine receptor antagonist, 8-cyclopentyl-1, 3-dipropylxanthihe (DPCPX) at 10^{-6} M and the A_2 antagonist N-(2-dimethylaminoethyl)-N-methyl-4-(2, 3, 6, 7-tetrahydro-2,b-dioxo-1, 3-dipropyl-1H-purin-8-yl) benzene sulphonamide (PD115,199) at 10^{-6} M. Theophylline, a known antagonist of adenosine receptors, inhibited the action of adenosine on cyclic AMP in mesangial cells. Dipyridamole, an inhibitor of the uptake of adenosine by the cells, enhanced the response to adenosine.

5 These results suggest the existence of A_1 and A_2 adenosine receptors with opposite actions on intracellular levels of cyclic AMP in both glomeruli and mesangial cells. Adenosine seems to increase cyclic AMP through the activation of a surface adenosine receptor with pharmacological properties distinct from those exhibited by the A_2 adenosine receptor.

Keywords: Adenosine; adenosine receptors; cyclic AMP; glomeruli; mesangial cells; NECA; RPIA; kidney; xanthines

Introduction

Adenosine modulates important kidney functions, mainly local blood flow (Spielman *et al.*, 1980), renin secretion (Murray & Churchill, 1985) and glomerular filtration rate (GFR) (Osswald *et al.*, 1978). The two main types of adenosine receptor related to the adenylate cyclase system, A_1 and A_2, have been localized or characterized in several kidney structures that are involved in the regulation of these functions, i.e. the renal microvasculature (Freissmuth *et al.*, 1987), juxtaglomerular cells (Churchill & Churchill, 1985) and glomeruli (Abboud & Dousa, 1983).

Glomeruli possess A_1 and A_2 receptors (Freissmuth *et al.*, 1987) and respond to adenosine with an increase in the accumulation of adenosine 3':5'-cyclic monophosphate (cyclic AMP) (Abboud & Dousa, 1983), although the distribution of these receptors on the different types of glomerular cells and the ability of each population to respond to adenosine remain unexplored. Intraglomerular mesangial cells seem to be important in the control of GFR by virtue of their contractile properties (Kon & Ichikawa, 1985) and we have previously shown that adenosine causes these cells and isolated glomeruli to contract (Lopez–Novoa *et al.*, 1987; Olivera *et al.*, 1989). This suggests a role for mesangial cells in the reduction of the GFR induced by adenosine.

In the present study we have set out to identify functional A_1 and A_2 receptors in glomerular mesangial cells and isolated glomeruli by studying the effects of the relatively selective adenosine agonists N^6-**R**-1methyl-2-phenylethyl-adenosine (**R**-PIA) (A_1) and 5-(N-ethylcarboxamide)adenosine (NECA) (A_2) on the intracellular content of cyclic AMP. We also investigated the effect of adenosine on the intracellular accumulation of cyclic AMP in mesangial cells.

[1] Author for correspondence at: Jose M. Lopez–Novoa, Dept. of Physiology and Pharmacology, Faculty of Medicine, Avda. Campo Charro s/n, 37007 Salamanca, Spain.

Methods

Glomerular isolation and mesangial cell culture

Glomeruli were isolated from Wistar rats weighing 200 to 250 g by successive mechanical sieving (105 and 75 μm) as previously described (Rodriguez–Puyol *et al.*, 1986). The final preparation consisted of glomeruli without Bowman's capsule and without afferent or efferent arterioles. Tubular contamination was less than 5%.

For mesangial cell culture, glomeruli isolated from Wistar rats weighing 150 to 200 g by successive mechanical sieving (150 and 50μm), were treated with collagenase (300 u ml^{-1}), plated in 35 mm plastic tissue culture dishes (Costar) and maintained in the conditions previously described (Olivera *et al.*, 1989; Rodriguez–Puyol *et al.*, 1989). The culture medium consisted of RPMI 1640 supplemented with 10% foetal calf serum, L-glutamine (1 mM), penicillin (0.66 μg ml^{-1}), streptomycin sulphate (60 μg ml^{-1}), and buffered with HEPES, pH 7.2. The culture medium was changed every two days. Studies were performed on day 21 or 22, at which time epithelial cells were no longer detected in the culture dishes. The identity of the cells was confirmed by morphological and functional criteria previously described (Olivera *et al.*, 1989; Rodriguez–Puyol *et al.*, 1989).

Intracellular and intraglomerular cyclic AMP determination

Cells were incubated for 5 min in Tris-glucose buffer (Composition mM:Tris 20, NaCl 130, KCl 10, sodium acetate 10 and glucose 5, pH 7.4) with 2.5 mM $CaCl_2$. The buffer was then aspirated and replaced by the same buffer containing adenosine or the adenosine analogues. At the times indicated, the medium was aspirated, and the cells washed twice with ice-cold buffer. Intracellular cyclic AMP was extracted twice with 1.0 ml absolute ethanol. Cells were scraped from the dishes and protein measured by the method of Lowry *et al.* (1951). In the experiments in which forskolin was used to stimulate adenylate cyclase, the preincubation and incubation buffers also contained 5 μM forskolin. When adenosine antagonists or dipyridamole were used, they were also present in the preincubation and incubation buffers.

Isolated glomeruli were resuspended in ice-cold Tris-glucose buffer containing 2.5 mM $CaCl_2$. Five aliquots of 50 μl were taken from this pool for protein determination, and samples of 500 μl were added to polystyrene tubes and kept in ice. The glomerular suspension was placed in a shaking water bath at 37°C for 20 min. After this preincubation period, 500 μl of the same buffer containing the substances to be tested was added to the suspension. The incubation was terminated at different times (1, 2, 5 and 30 min) by adding 2 ml of ice-cold buffer and centrifuging for 30 s in a microfuge at 1000 *g*. Supernatants were aspirated and replaced by 1 ml of absolute ethanol. The ethanolic extraction of intraglomerular cyclic AMP was performed twice.

Ethanolic extracts from each sample were pooled and evaporated in a stream of nitrogen. Dried samples were resuspended and cyclic AMP was assayed with a commercial kit. The recovery of cyclic AMP during the extraction procedure, determined as percentage of recovery of [^{3}H]-cyclic AMP added to the sample (2000–3000 c.p.m.), was greater than 89% in all cases. The inter- and intra-assay coefficients of variation were 11.9% and 8.4% respectively. Cross-reactivities with the adenosine and adenosine agonists and antagonists used were: adenosine, 10^{-4} M: 0.00151%; **R**-PIA, 10^{-6} M: 0.0066%; NECA 10^{-6} M: 0.0061%; 8-cyclopentyl-1, 3-dipropylxanthine (DPCPX) 10^{-6} M: 0.0036%; N2(2-dimethylaminoethyl) - N - methyl - 4 - (2,3,6,7 - tetrahydro-2,6-dioxo-1, 3-dipropyl-1H-purin-8-yl)benzenesulphonamide PD115,199 10^{-6} M: 0.0073% (n = 5–7).

Materials

Adenosine, **R**-PIA (N^6-**R**-1-methyl-2-phenylethyl adenosine), NECA (5-(N-ethylcarboxamide)adenosine), theophylline (1,3-dimethylxanthine), forskolin (7-acetoxy-8,13-epoxy-1φ,6β, 9-trihydroxylabd-14-ene-11-one), collagenase type 1A from *Clostridium histolyticum*, and L-glutamine were purchased from Sigma (St Louis, MO, U.S.A.). DPCPX (8-cyclopentyl-1,3-dipropylxanthine) and PD115,199 (N-(2-dimethylaminoethyl) -N-methyl-4-(2, 3, 6, 7-tetrahydro-2,6-dioxo-1,3-dipropyl-1H-purin -8-yl) benzenesulphonamide) were kind gifts from Warner–Lambert, Parke Davis, Ann Arbor, Michigan, U.S.A. Adenosine deaminase was purchased from Boehringer Mannheim GmbH, Germany. Dipyridamole (Persantin) and isoprenaline (Aleudrin) were from Boehringer Ingelheim, Barcelona, Spain. Penicillin was obtained from Laboratorios Level SA, Barcelona, Spain, Streptomycin sulphate was obtained from Antibioticos SA, Madrid, Spain and amphotericin B from Squibb Industria Farmaceutica S.A., Barcelona, Spain. RPMI 1640, Hanks balanced salt solution and foetal calf serum were obtained from Flow Laboratories, Woodcock Hill, UK. The [^{125}I]-cyclic AMP (single range) assay system was purchased from Amersham.

Statistics

Values are given as mean ± s.e. mean. Statistical differences between means were assessed either by the Kruskal–Wallis test or by one way/two way analysis of variance, followed by Scheffé's test. $P<0.05$ was considered to be statistically significant.

Results

Effects of adenosine and adenosine analogues on cyclic AMP accumulation

Adenosine induced a concentration-dependent increase in the intracellular cyclic AMP content in mesangial cells with an EC_{50} of approximately 3×10^{-5} M, that was statistically significant from unstimulated values in the supramicromolar range (Figure 1). The potent A_2 adenosine analogue, NECA, also induced a concentration-dependent increase in cyclic AMP, with an EC_{50} of approximately 10^{-6} M. The relatively selective A_1 agonist **R**-PIA, had a dual effect, i.e. it decreased cyclic AMP content at concentrations lower than 10^{-6} M, but caused an increase at concentrations above 10^{-6} M.

To test for possible endogenous adenosine synthesis in mesangial cells that might explain the relatively high doses needed to obtain a response, the cells were preincubated for 10 min in the presence of adenosine deaminase (2 u ml^{-1}) to inactivate endogenous adenosine before washing and incubating with adenosine for 5 min. The pretreatment with adenosine deaminase did not significantly modify basal cyclic AMP levels (basal: 11.4 ± 0.8, n = 18; adenosine deaminase: 14.7 ± 3.6 pmol mg^{-1} protein; n = 7) or the effect of adenosine 10^{-4} M (adenosine: 25.3 ± 5.4, n = 12; adenosine + adenosine deaminase: 28.0 ± 7.1 pmol mg^{-1} protein; n = 7).

In subsequent experiments adenosine was used at 10^{-4} M, a concentration giving a maximal response and the concentration used in previous studies (Olivera *et al.*, 1989). Adenosine analogues were used at 10^{-6} M, at which concentration **R**-PIA caused contraction of mesangial cells (unpublished results).

Time course changes in cyclic AMP levels

The time-courses of changes in cyclic AMP content induced by the agonists and adenosine in isolated glomeruli and

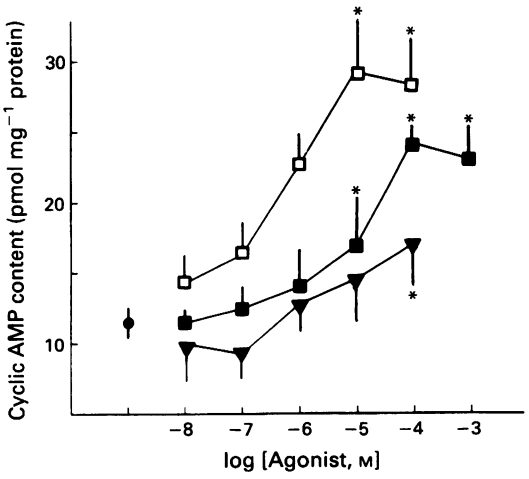

Figure 1 Concentration-response curves for adenosine (■), NECA (□) and **R**-PIA (▼) on intracellular cyclic AMP accumulation in mesangial cells after 5 min incubation. Values are mean with s.e.mean (vertical lines) of 7–12 experiments.
Asterisks represent significant differences ($P<0.05$ or higher, Scheffé test), compared with basal (●).

untreated mesangial cells, and in cells prestimulated with forskolin 5 μM, are shown in Figures 2, 3 and 4, respectively. In mesangial cells, adenosine induced an increase in cyclic AMP within the first minute of stimulation that was maintained for at least 5 min, before falling to basal levels by 10 min (Figure 3). However, levels of cyclic AMP increased again after 15 min incubation with adenosine and remained elevated up to 30 min (Control: 9.8 ± 1.2, $n = 9$; adenosine: 16.2 ± 4.5 pmol mg^{-1} protein, $n = 13$). In glomeruli, a slight and statistically insignificant enhancement of intraglomerular cyclic AMP remained after 30 min of incubation (9.5 ± 0.1, $n = 7$ *versus* 6.4 ± 0.9 pmol mg^{-1} protein in control conditions, $n = 10$). The rapid response to adenosine (within 1 min) occurred both in isolated glomeruli (Figure 2) and in forskolin – prestimulated and untreated mesangial cells (Figures 3 and 4), but the increase in cyclic AMP induced by NECA in these preparations was considerably slower (Figures 2, 3 and 4). In contrast to the effect of adenosine or NECA, the A_1 agonist **R**-PIA either had no significant effect or reduced the intracellular cyclic AMP content in isolated glomeruli and mesangial cells. When the agonists **R**-PIA and NECA were added together, each at 0.5 or 1 × 10^{-6} M, both to isolated glomeruli and cultured mesangial cells, the response was similar to that induced by adenosine (data not shown).

Effect of adenosine A_1 and A_2 receptor blockade

Neither **R**-PIA nor NECA is completely subtype specific. To establish that their observed actions were mediated by A_1 and A_2 receptors respectively, the effects of adding the potent A_1 antagonist 8-cyclopentyl-1,3-dipropylxanthine (DPCPX) and the A_2 antagonist PD115,199 both at 10^{-6} M, were examined. The increase in cyclic AMP induced by NECA was blocked by the relatively selective A_2 antagonist, but not by the A_1 antagonist, whereas the A_1 antagonist blocked the inhibitory effect of **R**-PIA in forskolin-pretreated cells (Figure 5). The antagonists alone had no effect on cyclic AMP content.

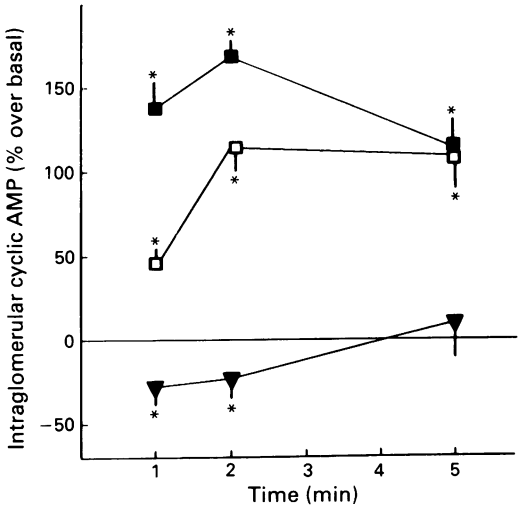

Figure 2 Time-course of changes in intraglomerular cyclic AMP in isolated glomeruli induced by 10^{-6} M adenosine (■), 10^{-6} M **R**-PIA (▼) and 10^{-6} M NECA (□). Data are expressed as a percentage over basal cyclic AMP at each time. Values are mean with s.e.mean (vertical lines) of 8–15 experiments.
Asterisks represent significant differences ($P < 0.05$ or higher, Scheffé test), compared with control values.

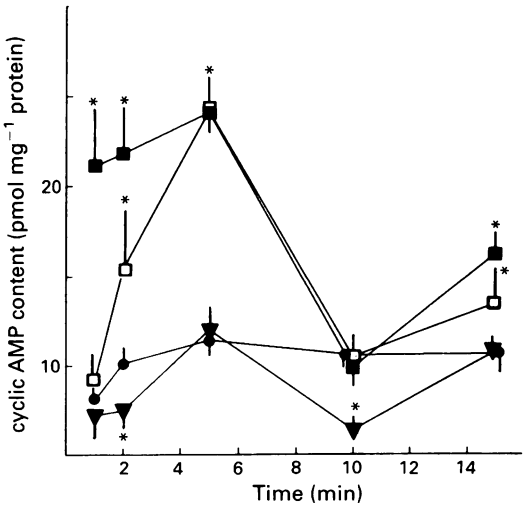

Figure 3 Time-course of changes in intracellular cyclic AMP content induced by 10^{-4} M adenosine (■), 10^{-6} M **R**-PIA (▼) or 10^{-6} M NECA (□) in glomerular mesangial cells. Values are mean with s.e.mean (vertical lines) of 9–18 experiments.
Asterisks represent significant differences ($P < 0.05$ or higher, Scheffé test), compared with control values (●).

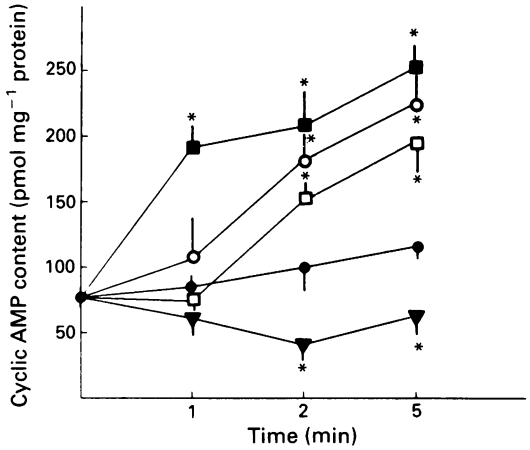

Figure 4 Time-course of changes in intracellular cyclic AMP content induced by adenosine analogues in forskolin-treated mesangial cells. Treatments are 10^{-4} M adenosine (■), 10^{-6} M **R**-PIA (▼), 10^{-6} M NECA (□) or 10^{-6} M NECA + DPCPX (○). Values are mean with s.e.mean (vertical lines) of 6–18 experiments.
Asterisks represent significant differences ($P < 0.05$ or higher, Scheffé test), compared with control values (●).

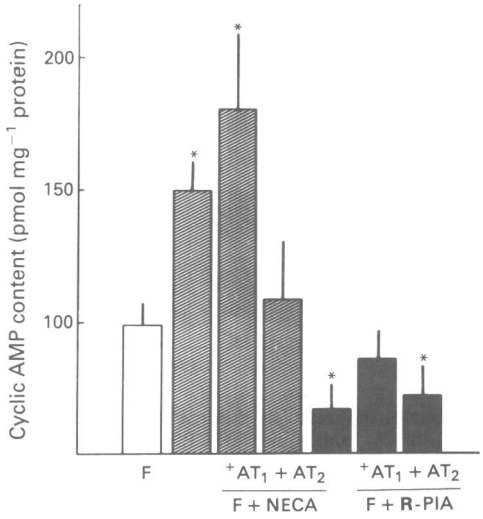

Figure 5 Effects of the relatively selective antagonists PD115,199 (AT_2, 10^{-6} M and DPCPX (AT_1, 10^{-6} M) on the changes in cyclic AMP induced by 10^{-6} M **R**-PIA or 10^{-6} M NECA in mesangial cells. Cells were preincubated in the presence of forskolin (F, 5 μM) for 5 min and incubated with the agonists for 2 min. Values are mean with s.e.mean (vertical lines) of 4–8 experiments.
Asterisks represent significant differences ($P < 0.05$ or higher, Scheffé test), compared with control values.

To determine the type of adenosine receptor involved in the response to adenosine, the effects of the same antagonists were tested. Neither of the antagonists modified the stimulation of cyclic AMP production by adenosine in either forskolin pretreated or untreated mesangial cells (Figure 6) or in isolated glomeruli (results not shown). Only when both antagonists were used together, each at 5×10^{-7} M, was an inhibition of the effect of adenosine observed. A similar result was obtained when both antagonists were used together at a concentration of 5×10^{-6} M each. The inhibition was partial in cells pretreated with forskolin and almost maximal (not significantly different from the inhibition induced by theophylline) in non-pretreated cells (Figure 6).

Effects of theophylline and dipyridamole

To demonstrate further that the effect of adenosine is mediated by a specific membrane receptor and not by an intracellular receptor or by the action of products of adenosine metabolism, we studied the action of theophylline and dipyridamole on the stimulation of cyclic AMP accumulation by adenosine. Theophylline, a methylxanthine used as an adenosine receptor antagonist, inhibited the increase in cyclic AMP induced by adenosine (Figure 7). This effect was specific for adenosine receptors since theophylline at the same concentration (10^{-4} M) failed to inhibit the increase in cyclic AMP induced by isoprenaline (10^{-4} M) (control: 11.4 ± 0.8, $n = 18$; isoprenaline: 32.0 ± 6.6, $n = 7$; $P<0.01$; isoprenaline + theophylline: 35.6 ± 3.8 pmol mg^{-1} protein, $n = 7$; $P<0.01$ *versus* control). On the other hand, dipyridamole, a drug that inhibits the transport of adenosine into the cells, potentiated the increase in cyclic AMP induced by adenosine in mesangial cells (adenosine alone: 122 ± 19% $n = 12$; dipyridamole + adenosine: 159 ± 15%, $n = 13$, $P<0.05$, by the Kruskal–Wallis test). Theophylline at 10^{-4} M did not significantly modify intracellular cyclic AMP (Figure 7) but dipyridamole used alone augmented cyclic AMP content over basal values (control: 11.4 ± 0.8, $n = 18$; dipyridamole: 25.2 ± 1.3 pmol mg^{-1} protein, $n = 6$, $P<0.01$).

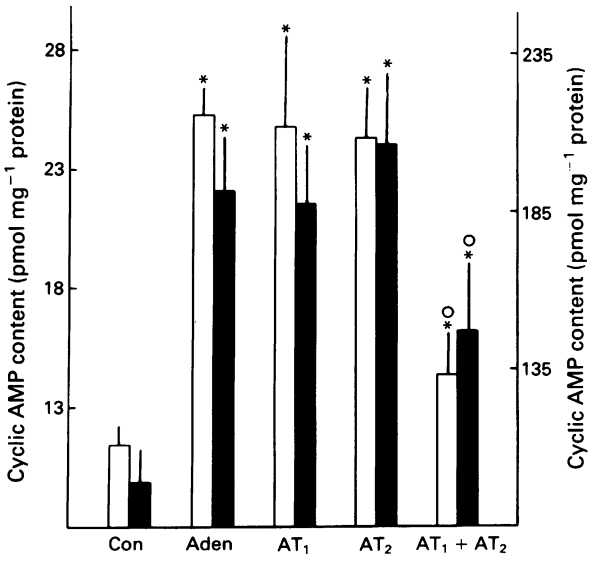

Figure 6 Effects of the relatively selective A_2 antagonist PD115,199 (AT_2, 10^{-6} M) or A_1 antagonist DPCP × (AT_1, 10^{-6} M) or both (AT_1 + AT_2, 10^{-6} M) on the increase in cyclic AMP induced by 10^{-4} M adenosine (Aden) in mesangial cells in the presence (hatched columns, right ordinate scale) or absence (open columns, left ordinate scale) of forskolin. Forskolin-treated cells were preincubated in the presence of forskolin (5 μM) for 5 min and incubated with adenosine for 2 min. Values are mean with s.e.mean (vertical lines) of 5–8 experiments.
Asterisks represent significant differences ($P<0.05$ or higher, Scheffé test), compared with control values (Con). Circles represent significant differences ($P<0.05$ or higher, Scheffé test) compared with adenosine.

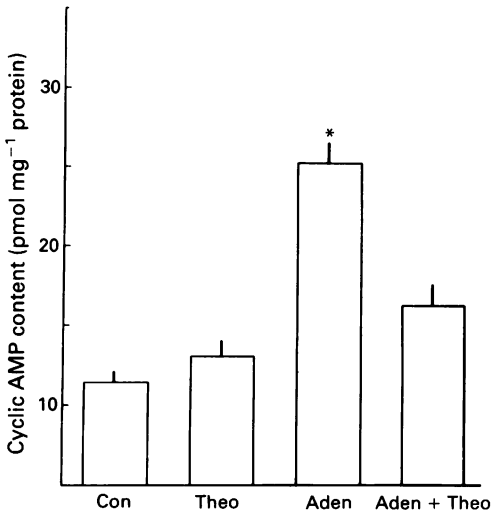

Figure 7 Effect of the adenosine receptor antagonist theophylline (Theo, 10^{-4} M) on the stimulatory response to 10^{-4} M adenosine (Aden) on intracellular cyclic AMP accumulation in mesangial cells. Values are mean with s.e.mean (vertical lines) of 7–18 experiments.
Asterisks represent significant differences ($P<0.01$, Kruskall–Wallis test) *versus* control values (Con).

Discussion

While there have been some previous *in vivo* and *in vitro* studies of the effects of adenosine and adenosine analogues on glomeruli and glomerular function (Osswald *et al.*, 1978; Abboud & Dousa, 1983; Hall *et al.*, 1985; Freissmuth *et al.*, 1978; Lopez-Novoa *et al.*, 1987) no studies have been reported on the effects of these compounds on different types of glomerular cell. Thus the primary purpose of this work was to study in glomerular mesangial cells the effect of adenosine and its analogues on intracellular cyclic AMP, one of the most important messengers mediating the effects of adenosine (Londos *et al.*, 1980; Shimizu, 1983) and involved in regulating cellular responses (Ross & Gilman, 1980).

The results presented here suggest the existence of both A_1 and A_2 adenosine receptors on mesangial cells and in that respect complement information already reported for whole glomeruli. One of the widely accepted criteria for the demonstration of distinct adenosine receptor subtypes has been the differential effects obtained with relatively selective adenosine agonists (Londos *et al.*, 1980; Daly, 1982; Burns *et al.*, 1987a). We used **R**-PIA as a relatively selective A_1 agonist (Daly, 1982) and NECA as a potent A_2 adenosine agonist, although it also binds to the A_1 receptor (Bruns *et al.*, 1987a; Daly, 1982). Adenosine and NECA raised cyclic AMP levels in mesangial cells and isolated glomeruli, whereas **R**-PIA at doses up to 10^{-6} M decreased cyclic AMP content in both mesangial cells and glomeruli. The rank-order of potency for the increase in cyclic AMP (NECA > adenosine > **R**-PIA) is the one expected for an A_2-mediated response, whereas the inhibitory effect of **R**-PIA suggests the existence of classical A_1 or R_i (Londos *et al.*, 1980) adenosine receptors in glomeruli and mesangial cells. The dose-response effect of **R**-PIA was biphasic because of its ability to bind to A_2 receptors at high concentrations. The A_1 receptor, which has been shown to be of high affinity (Londos *et al.*, 1980; Bruns *et al.*, 1987a), was activated at low doses of **R**-PIA, and the A_2 receptor, which is supposed to be of low affinity, was activated at high doses of **R**-PIA. When the basal activity of the adenylate cyclase was enhanced by

forskolin, the inhibitory effect of **R**-PIA was more evident. Forskolin pretreatment was used in some of the experiments because the slight changes that may be induced by different compounds are more easily observed when cyclase activity is enhanced.

Further evidence of the involvement of A_1 and A_2 adenosine receptor subtypes in the inhibitory (**R**-PIA) and stimulatory (NECA) responses, comes from the fact that the highly selective A_1 adenosine antagonist DPCPX (PD116,948, Haleen *et al.*, 1987), inhibited the effect of **R**-PIA on cyclic AMP, but not that of NECA, in forskolin-pretreated mesangial cells. However, the potent A_2 antagonist PD115,119 (Bruns *et al.*, 1987b) blocked the stimulatory effect of NECA, but not the inhibitory effect of **R**-PIA.

Adenosine, like the agonist NECA, increased cyclic AMP accumulation in isolated glomeruli and mesangial cells. The increase in cyclic AMP levels induced by adenosine in mesangial cells was insufficient to reach statistical significance at micromolar concentrations. The relatively high doses necessary to obtain a response with adenosine cannot be explained in terms of endogenous synthesis of adenosine by the cultures since treatment with adenosine deaminase affected neither basal values of cyclic AMP nor the stimulatory action of adenosine on intracellular cyclic AMP content. Both adenosine-stimulated and basal cyclic AMP levels in the glomeruli were very similar to those reported by Abboud & Dousa (1983). Although the contribution of epithelial and endothelial glomerular cells to the adenosine-induced rise in intraglomerular cyclic AMP has not been studied, mesangial cells seem to be the main source of cyclic AMP in the glomerulus (Mene *et al.*, 1989).

In theory, adenosine could cause an increase in cyclic AMP levels either through a stimulatory coupling to adenylate cyclase or an inhibitory action on cyclic AMP breakdown (Shenolikar, 1988). Several studies have provided evidence that adenosine acts via coupling of its receptor to adenylate cyclase rather than by an action on cyclic AMP phosphodiesterase (Londos *et al.*, 1980; Shimizu, 1983; Arend *et al.*, 1987; Burnatowska-Hledin & Spielman, 1991). In isolated glomeruli, adenosine appeared to act by stimulating adenylate cyclase (Abboud & Dousa, 1983). From our results in mesangial cells we cannot discount the possibility of an action of adenosine on the phosphodiesterase. However, the effect of dipyridamole, a compound that inhibits adenosine transport into the cells, seems to support the interpretation of an action of adenosine via a surface receptor coupled to adenylate cyclase. Dipyridamole has been shown to inhibit cyclic AMP phosphodiesterase in some cells (Abboud & Dousa, 1983; Schoeffter *et al.*, 1987), and increases basal levels of cyclic AMP in glomeruli (Abboud & Dousa, 1983) and in our mesangial cell cultures. The enhancement by dipyridamole of the stimulatory action of adenosine could be the result of the inhibition of cyclic AMP phosphodiesterase by this compound. Nevertheless, the existence of an inhibitory intracellular P site for high doses of adenosine (Londos *et al.*, 1980; Garcia-Sainz & Torner, 1985) in mesangial cells cannot be ruled out, and dipyridamole, by blocking adenosine transport, may prevent access of adenosine to this site.

The present results demonstrate the involvement of a specific surface receptor for adenosine. First, theophylline, a known inhibitor of the interaction of adenosine with its surface receptors (Schwabe *et al.*, 1985), inhibits the stimulatory effect of adenosine on glomerular (Abboud & Dousa, 1983) and mesangial cell content of cyclic AMP. Secondly, the addition of dipyridamole to inhibit adenosine uptake into the cell, potentiates the increase induced by adenosine in intraglomerular (Abboud & Dousa, 1983) or intracellular cyclic AMP. These results argue strongly against an action of adenosine as a precursor for intracellular ATP synthesis, the substrate for cyclic AMP formation, and also against the possible mediation of products of intracellular adenosine deamination elicited by adenosine.

The receptor involved in the response to adenosine in these glomerular cells seems to exhibit properties different from those described for A_1 and A_2 receptors. First, the relatively selective antagonists PD115,199 and DPCPX when used separately, failed to inhibit the response to adenosine either in glomeruli or mesangial cells whether or not they were preincubated with forskolin, and only when the antagonists were added together, did they block the adenosine response. Secondly, the stimulatory effect of adenosine was observed 1 min earlier than the effect of NECA. The stimulation of cyclic AMP described in other cells for adenosine or adenosine analogues is not usually observed before 2 min of incubation and it is usually maximal from 5 to 30 min (Van Calker *et al.*, 1979; Jonzon *et al.*, 1985; Arend *et al.*, 1987; Gatti *et al.*, 1988). In mesangial cells and isolated glomeruli, NECA showed the typical stimulation time-course, but the effect of adenosine was consistently faster. These results suggest that the action of adenosine on cyclic AMP is characteristic of neither A_1 nor A_2 adenosine receptor subtypes. Adenosine surface receptors with unusual pharmacological and physiological properties have already been described in several cell types (Chin & DeLorenzo, 1986; Arend *et al.*, 1988; Belloni *et al.*, 1989; Ali *et al.*, 1990), and these receptors have sometimes been called A_3 receptors (Ribeiro & Sebastiao, 1986). An alternative explanation could be the existence in mesangial cells of two types of A_2 receptor, A_{2a} and A_{2b}. The A_{2b}, the low affinity A_2 adenosine receptor, has been described only in brain and fibroblasts, and cannot bind the A_2 antagonist PD115,199 (Bruns *et al.*, 1987b). In addition, it is possible that the occupation of both A_1 and A_2 receptors by high doses of adenosine produces a synergistic interaction similar to that described for α- and β-adrenoceptors in parathyroid cells (McKinney *et al.*, 1989). This latter hypothesis is supported by the fact that when the agonists **R**-PIA and NECA were used together at 0.5 or 1×10^{-6} M each, both in isolated glomeruli and cultured mesangial cells, the response was neither like that to **R**-PIA nor like that to NECA, but was similar to that induced by adenosine.

In summary, our findings demonstrate that both A_1 and A_2 adenosine receptors are present in glomeruli and in cultured glomerular mesangial cells. The results with the selective antagonists and the different time-courses of cyclic AMP accumulation produced by adenosine and its agonist analogues suggest that the effect of adenosine may not be mediated solely by activation of an A_2-like adenosine receptor.

This work has been partially supported by grants from the National Institute of Health of Spain (FIS 1873/88), and Dirección General de Investigación Cientifica Y Técnica (Grant PM88-0013-C02), A.O. is a fellow of the Plan de Formación de Personal Investigador, Spanish Ministerio de Educación y Ciencia. We specially thank Warner Lambert Research Laboratories, Michigan, U.S.A., and Dr F. Anton, Medical Director, Parke-Davis Spain, Barcelona, for the gift of the adenosine antagonists. We also acknowledge the help of Prof. Otto Uttenthal in reviewing the manuscript.

References

ABBOUD, H.E., & DOUSA, T.P. (1983). Action of adenosine on cyclic 3',5'nucleotides in glomeruli. *Am. J. Physiol.*, **244**, F633-F638.

ALI, H., CUNHA-MELO, J.R., SAUL, W.F., & BEAVEN, M.A. (1990). Activation of phospholipase C via adenosine receptors provides synergistic signals for secretion in antigen-stimulated RBL-2H3 cells. Evidence for a novel adenosine receptor. *J. Clin. Invest.*, **265**, 715-753.

AREND, L.J., SONNENBURG, W.K., SMITH, W.L. & SPIELMAN, W.S. (1987). A_1 and A_2 adenosine receptors in rabbit cortical collecting tubule cells, modulation of hormone-stimulated cAMP. *J. Clin. Invest.*, **79**, 710-714.

AREND, L.J., BURNATOWSKA-HLEDIN, M.A. & SPIELMAN, W.S. (1988). Adenosine receptor-mediated calcium mobilization in cortical collecting tubule cells. *Am. J. Physiol.*, **255**, C581-C588.

BURNATOWSKA-HLEDIN, M.A. & SPIELMAN, W.S. (1991). Effects of adenosine on cAMP production and cytosolic Ca^{2+} in cultured rabbit medullary thick limb cells. *Am. J. Physiol.*, **260**, C143-C150.

BELLONI, F.L., BELARDINELLI, L., HALPERIN, C. & HINTZE, T.H. (1989). An unusual receptor mediates adenosine-induced SA nodal bradycardia in dogs. *Am. J. Physiol.*, **256**, H1553-H1564.

BRUNS, R.F., LU, G.H. & PUGSLEY, T.A. (1987a). Adenosine receptor subtypes: binding studies. In *Topics and Perspectives in Adenosine Research*. ed. Gerlach, E. & Becker, B.F. pp.59-73. Berlin: Springer-Verlag.

BRUNS, R.F., FERGUS, J.H., BADGER, E.W., BRISTOL, J.A., SANTAY, L.A. & HAYS, S.J. (1987b). PD 115,199: an antagonist ligand for adenosine A_2 receptors. *Naunyn-Schmiedebergs Arch. Pharmacol.*, **335**, 64-69.

CHIN, J.H. & DELORENZO, R.J. (1986). A new class of adenosine receptors in brain. Characterization by 2-Chloro[^{3}H]-adenosine binding. *Biochem. Pharmacol.*, **35**, 847-856.

CHURCHILL, P.C. & CHURCHILL, M.C. (1985). A_1 and A_2 adenosine receptor activation inhibits and stimulates renin secretion of rat renal cortical slices. *J. Pharmacol. Exp. Ther.*, **232**, 589-594.

DALY, J.W. (1982). Adenosine receptors: targets for future drugs. *J. Med. Chem.*, **25**, 197-207.

FREISSMUTH, M., HAUSLEITHNER, V., TUISL, E., NANOFF, C. & SCHUTZ, W. (1987). Glomeruli and microvessels of the rabbit kidney contain both A_1 and A_2 adenosine receptors. *Naunyn-Schmiedebergs Arch. Pharmacol.*, **335**, 438-441.

GARCIA-SAINZ, J.A. & TORNER, M.L. (1985). Rat fat cells have three types of adenosine receptors (Ra, Ri and P). Differential effects of pertussis toxin. *Biochem. J.*, **232**, 439-443.

GATTI, G., MADEDDU, L., PANDIELLA, A., POZZAN, T. & MALDONESI, J. (1988). Second-messenger generation in PC12 cells. Interactions between cyclic AMP and Ca^{2+} signals. *Biochem. J.*, **255**, 753-760.

HALEEN, S.J., STEFFEN, R.P. & HAMILTON, H.W. (1987). PD 116,948, a highly selective A_1 adenosine receptor antagonist. *Life Sci.*, **40**, 555-561.

HALL, J.E., GRANGER, J.P. & HESTER, R.L. (1985). Interactions between adenosine and angiotensin II in controlling glomerular filtration. *Am. J. Physiol.*, **248**, F340-F346.

JONZON, B., NILSSON, J. & FREDHOLM, B.B. (1985). Adenosine receptor-mediated changes in cyclic AMP production and DNA synthesis in cultured arterial smooth muscle cells. *J. Cell Physiol.*, **124**, 441-456.

KON, V. & ICHIKAWA, I. (1985). Hormonal regulation of glomerular filtration. *Annu. Rev. Med.*, **36**, 515-531.

LONDOS, C., COOPER, D.M. & WOLFF, J. (1980). Subclasses of external adenosine receptors. *Proc. Natl. Acad. Sci. U.S.A.*, **77**, 2251-2254.

LOPEZ-NOVOA, J.M., ARRIBA, G., BARRIO, V. & RODRIGUEZ-PUYOL, D. (1987). Adenosine induces a calcium-dependent glomerular contraction. *Eur. J. Pharmacol.*, **134**, 365-367.

LOWRY, O.H., ROSEBROUGH, N.J., FARR, A.L. & RANDALL, R. (1951). Protein measurement with the Folin phenol reagent. *J. Biol. Chem.*, **193**, 265-275.

MCKINNEY, J.S., DESOLE, M.S. & RUBIN, R.P. (1989). Convergence of cAMP and phosphoinositide pathways during rat parotid secretion. *Am. J. Physiol.*, **257**, C651-C657.

MENE, P., SIMONSON, M.S. & DUNN, M.J. (1989). Physiology of the mesangial cell. *Physiol. Rev.*, **69**, 1347-1424.

MURRAY, R.D. & CHURCHILL, P.C. (1985). Concentration dependency of the renal vascular and renin secretory response to adenosine receptor agonists. *J. Pharmacol. Exp. Ther.*, **232**, 189-193.

OLIVERA, A., LAMAS, S., RODRIGUEZ-PUYOL, D. & LOPEZ-NOVOA, J.M. (1989). Adenosine induces mesangial cell contraction by an A_1-type receptor. *Kidney Int.*, **35**, 1300-1305.

OSSWALD, H., SPIELMAN, W.S. & KNOX, F.G. (1978). Mechanisms of adenosine-mediated decreases in glomerular filtration rate in dogs. *Circ. Res.*, **43**, 465-469.

RIBEIRO, J.A. & SEBASTIAO, A.M. (1986). Adenosine receptors and calcium: basis for proposing a third (A_3) class adenosine receptor. *Prog. Neurobiol.*, **26**, 179-209.

RODRIGUEZ-PUYOL, D., ARRIBA, G., BLANCHART, A., SANTOS, J.C., CARAMELO, C., FERNANDEZ-CRUZ, A., HERNANDO, L. & LOPEZ-NOVOA, J.M. (1986). Lack of a direct regulatory effect of ANF on prostaglandins and renin release by isolated rat glomeruli. *Biochem. Biophys. Res. Commun.*, **138**, 496-501.

RODRIGUEZ-PUYOL, D., LAMAS, S., OLIVERA, A., LOPEZ-FARRE, A., ORTEGA, G., HERNANDO, L. & LOPEZ-NOVOA, J.M. (1989). Actions of Cyclosporine A on cultured rat mesangial cells. *Kidney Int.*, **35**, 632-637.

ROSS, E.M. & GILMAN, A. (1980). Biochemical properties of hormone-sensitive adenylate cyclase. *Annu. Rev. Biochem.*, **49**, 533-564.

SCHOEFFTER, P., LUGNIER, C., DEMESY-WAELDELE, F. & STOCLET, J.C. (1987). Role of cyclic AMP- and cyclic GMP-phosphodiesterases in the control of cyclic nucleotide levels and smooth muscle tone in rat isolated aorta. A study with selective inhibitors. *Biochem. Pharmacol.*, **36**, 3965-3972.

SCHWABE, U., UKENA, D. & LOHSE, M.J. (1985). Xanthine derivates as antagonists at A_1 and A_2 adenosine receptors. *Naunyn-Schmiedebergs Arch. Pharmacol.*, **330**, 212-221.

SHENOLIKAR, S. (1988). Protein phosphorylation: hormones, drugs, and bioregulation. *FASEB J.*, **2**, 2753-2764.

SHIMIZU, H. (1983). Adenosine receptors associated with the adenylate cyclase system. In *Physiology and Pharmacology of Adenosine Derivates*. ed. Daly, J.W., Kuroda, Y., Phillis, J.W., Shimizu, H. & Ui, M. pp.31-40. New York: Raven Press.

SPIELMAN, W.S., BRITTON, S.L. & FIKSEN-OLSEN, M.J. (1980). Effect of adenosine on the distribution of renal blood flow in dogs. *Circ. Res.*, **46**, 449-456.

VAN CALKER, D., MÜLLER, M. & HAMPRECHT, B. (1979). Adenosine regulates via two different types of receptors, the accumulation of cyclic AMP in cultured brain cells. *J. Neurochem.*, **33**, 999-1005.

(Received August 8, 1991
Revised May 18, 1992
Accepted May 29, 1992)

Br. J. Pharmacol. (1992), **107**, 347–351

Inhibition of sympathetic hypertensive responses in the guinea-pig by prejunctional histamine H_3-receptors

[1]J.A. Hey, M. del Prado, R.W. Egan, W. Kreutner & R.W. Chapman

Schering-Plough Research Institute, Bloomfield, NJ 07003, U.S.A.

1 The effect of (**R**)-α-methylhistamine, a selective H_3-histamine receptor agonist, was examined on the neurogenic hypertension and tachycardia that is induced by stimulation of areas in the medulla oblongata of guinea-pigs. Electrical medullary stimulation (32 Hz, 3–5 s trains, 0.5–1.0 ms square pulse, 25–400 μA) produced intensity-dependent increases in blood pressure and a more variable tachycardia.

2 (**R**)-α-methylhistamine inhibited the hypertension and tachycardia due to submaximal CNS stimulation. The inhibition of hypertension by (**R**)-α-methylhistamine was dose-dependent (10–300 μg kg^{-1}, i.v.) and was not seen at high intensities of stimulation.

3 (**R**)-α-methylhistamine (300 μg kg^{-1}, i.v.) did not attenuate the pressor response to adrenaline (1 and 3 μg kg^{-1}, i.v.), indicating that the effect of (**R**)-α-methylhistamine was not mediated by a postjunctional action on smooth muscle.

4 The inhibition of CNS-induced hypertension by (**R**)-α-methylhistamine (300 μg kg^{-1}, i.v.) was blocked by the H_3 antagonists, thioperamide (ID_{50} = 0.39 mg kg^{-1}, i.v.), impromidine (ID_{50} = 0.22 mg kg^{-1}, i.v.) and burimamide (ID_{50} = 6 mg kg^{-1}, i.v.). The rank order potency of these antagonists is consistent with activity at the H_{3B} receptor subtype. Chlorpheniramine (30 μg kg^{-1}, i.v.) and cimetidine (3 mg kg^{-1}, i.v.) did not antagonize the inhibition of CNS-hypertension by (**R**)-α-methylhistamine.

5 These results suggest that (**R**)-α-methylhistamine inhibits sympathetic hypertensive responses in guinea-pigs by activation of prejunctional H_3-receptors, possibly located on postganglionic nerve terminals. Furthermore, on the basis of the rank order potency to different H_3-antagonists, it appears that the H_{3B}-receptor subtype is involved with H_3-receptor responses on vascular sympathetic nerves.

Keywords: Histamine H_3-receptors; (**R**)-α-methylhistamine; presynaptic inhibition; neurogenic hypertension; sympathetic neurotransmission; thioperamide; impromidine; burimamide

Introduction

Histamine exerts an inhibitory effect on neurotransmitter release by a prejunctional mechanism in CNS and peripheral autonomic neural systems (Arrang *et al.*, 1983; 1988; Schlicker *et al.*, 1988; 1990). This action is mediated by activation of prejunctional histamine H_3-receptors, a mechanism that is pharmacologically distinct from the classical postjunctional H_1- and H_2-mediated responses to histamine (Timmerman, 1990). Furthermore, recent studies of radioligand binding have revealed two classes of H_3-binding sites designated H_{3A} and H_{3B}, with different sensitivities to the H_3-antagonists, thioperamide and burimamide (West *et al.*, 1990). Therefore, the possibility exists for a tissue selective distribution of H_3-receptor subtypes.

There has been some controversy about the role of H_3-receptors on nerve fibres innervating blood vessels. The early work by Ishikawa & Sperelakis (1987) showed that histamine can depress sympathetic neurotransmission in the mesenteric artery by interacting with prejunctional H_3-receptors that are located on the perivascular nerve terminals. Activation of prejunctional H_3-receptors also inhibited electrically-induced release of [^{3}H]-noradrenaline from human saphenous vein (Molderings *et al.*, 1991). Although Schneider *et al.* (1991) found no evidence for H_3-receptor-mediated inhibition of [^{3}H]-noradrenaline release in the rat vena cava *in vitro*, this same group reported H_3-receptor mediated inhibition of the neurogenic vasopressor response in rats *in vivo* (Malinowska & Schlicker, 1991).

The present studies were undertaken to investigate H_3-receptor modulation of sympathetic vascular responses caused by stimulation of the dorsal medulla oblongata in the anaesthetized guinea-pig. This species has been used previously to identify an inhibitory role for H_3-receptors on neurogenic responses in the ileum (Trzeciakowski, 1987; Menkveld & Timmerman, 1990), duodenum (Coruzzi *et al.*, 1991) and airways (Ichinose *et al.*, 1989; 1990). In addition, the potencies of thioperamide, burimamide and impromidine were examined in order to identify the H_3-receptor subtype responsible for the modulation of sympathetically-evoked vascular responses.

Methods

Animal preparation

Male Hartley guinea-pigs (450–600 g, Charles River, Bloomington, MA, U.S.A.) were anaesthetized with α-chloralose (125 mg kg^{-1}, i.p.) and surgically prepared by catheterization of the trachea, jugular vein and carotid artery. Animals were mechanically ventilated (volume = 4 ml, frequency = 45 breaths min^{-1}) and paralyzed with gallamine (2 mg kg^{-1}, i.v.). The arterial catheter was connected to a pressure transducer for blood pressure (BP) and heart rate (HR) measurements. Pulmonary insufflation pressure (PIP) was measured from a side port in the tracheal cannula and changes in PIP were used to measure bronchoconstriction (Hey *et al.*, 1990a). All physiological parameters were recorded on a MI^2, M-3000 signal processing centre (Modular Instruments, Malvern, PA, U.S.A.).

Electrical stimulation of the medulla

Animals were positioned in a Kopf stereotaxic apparatus (David Kopf Inst., Tujunga, CA, U.S.A.) and an incision was made to expose the dorsal aspect of the skull. A section of the bone overlying the cerebellum was removed. A portion of cerebellar tissue that covers the floor of the fourth ventri-

[1] Author for correspondence.

cle was removed to expose obex (the most caudal structure on the floor of the fourth ventricle). Concentric bilateral electrodes were inserted into the dorsal medulla. Regions of the dorsal medulla that elicited the largest hypertensive responses with the least changes in airway tone were selected. The stereotaxic coordinates that yielded these effects were: A 1.0–2.0 mm, L 1.5 mm and V 2.0 mm in relation to obex. This area, which was empirically identified through mapping, is more anterior and ventral than the dorsal bronchoconstrictor area previously identified in the guinea-pig (Hey *et al.*, 1990a). To minimize tissue dimpling, the electrodes were placed 1.0 mm ventral to the target site and then gently retracted to the appropriate stereotaxic coordinates.

The medulla was electrically stimulated with a Grass (S88) dual stimulator connected to the electrodes by means of stimulus isolation units with constant current output (Grass Instruments, Quincy, MA, U.S.A.). The stimulation parameters used to evoke cardiovascular responses were: 32 Hz, 3–5 s trains, 0.5–1.0 ms square pulse and varying intensities from 25–400 μA. The train rate was approximately 180 s. Upon completion of each experiment, a supramaximal stimulus (400 μA) was used to confirm that the intensity range used in the study was submaximal for each animal.

Pharmacological studies

To characterize the hypertensive response to medullary stimulation each animal received, in a step-wise fashion, an increasing stimulation intensity (25–400 μA) and peak changes in BP and HR were recorded for each stimulus train. All animals had been pretreated with ipratropium bromide (10 μg kg^{-1}, i.v.), to block CNS-induced cholinergic bronchospasm and the effects of medullary stimulation on vagal innervation to the heart (Hey *et al.*, 1990a).

The cardiovascular responses to CNS stimulation were evaluated before and after (**R**)-α-methylhistamine (10–300 μg kg^{-1}, i.v.). (**R**)-α-methylhistamine was administered 5 min before medullary stimulation and peak responses were recorded to each stimulus intensity (25–400 μA). The effect of (**R**)-α-methylhistamine (300 μg kg^{-1}) on the hypertensive response due to exogenous adrenaline (1 and 3 μg kg^{-1}, i.v.) was studied to determine whether (**R**)-α-methylhistamine was acting by a postjunctional action on smooth muscle.

To establish the type of histamine receptor involved in the response to (**R**)-α-methylhistamine, animals were treated with chlorpheniramine (30 μg kg^{-1}, i.v.), cimetidine (3 mg kg^{-1}, i.v.), or thioperamide (3 mg kg^{-1}, i.v.) 10 min before (**R**)-α-methylhistamine (300 μg kg^{-1}). In a separate set of experiments, impromidine (0.1–1.0 mg kg^{-1}), burimamide (3–30 mg kg^{-1}) and thioperamide (0.1–3.0 mg kg^{-1}) were evaluated against a single dose of (**R**)-α-methylhistamine (300 μg kg^{-1}) to determine the relative potency of H_3-antagonist activity. From these results, the ID_{50} (the dose causing a 50% blockade of the effect of (**R**)-α-methylhistamine) was calculated for each H_3-antagonist.

Drugs used

Gallamine triethiodide, α-chloralose, chlorpheniramine maleate, cimetidine, ipratropium bromide and (−)-adrenaline bitartrate were purchased from Sigma Chemical Co. (St. Louis, MO. U.S.A.). (**R**)-α-methylhistamine hydrochloride, burimamide and thioperamide were synthesized at Schering-Plough Research (Bloomfield, NJ, U.S.A.). Impromidine was a gift from Smith-Kline-Beecham (King of Prussia, PA, U.S.A.). Thioperamide was dissolved in DMSO. All other drugs were dissolved in 0.9% v/v saline. Doses were calculated as their free base.

Statistics

The statistical evaluation of the results was performed by one-way analysis of variance (ANOVA) and Student's *t* test for paired and unpaired comparisons; $P<0.05$ was considered statistically significant.

Results

Baseline BP and HR in ipratropium-treated guinea-pigs were 54 ± 5 mmHg and 302 ± 7 beats min^{-1}, respectively. Bilateral electrical stimulation of regions within the medulla oblongata evoked intensity-dependent increases in both BP and HR (Figure 1). The responses to CNS stimulation were near maximal at 100 μA, as higher intensities did not yield larger increases in BP or HR. Repeated stimulation intensity response curves could be generated in the same animal without dimunition or augmentation of the hypertensive or tachycardia responses (data not shown). Treatment with (**R**)-α-methylhistamine (300 μg kg^{-1}, i.v.) caused decreases in baseline BP (12 ± 2 mmHg) and HR (34 ± 2 beats min^{-1}) ($n = 4$). (**R**)-α-methylhistamine (300 μg kg^{-1}, i.v.) attenuated the CNS-induced hypertensive and tachycardia responses between 25–100 μA as indicated by a shift in the stimulus intensity-response curves (Figure 1). At higher stimulus intensities such as 400 μA, (**R**)-α-methylhistamine did not inhibit these cardiovascular responses (Figure 1). In these studies, the changes in BP were consistent and reproducible, while the changes in HR were more variable, so we focused on changes in BP as a measure of H_3-modulation of the neurogenic responses.

The dose-dependent inhibition of CNS-induced hypertension by (**R**)-α-methylhistamine (10–300 μg kg^{-1}, i.v.) was studied at 75 μA (Figure 2), which was submaximal but produced consistent changes in BP. To avoid the develop-

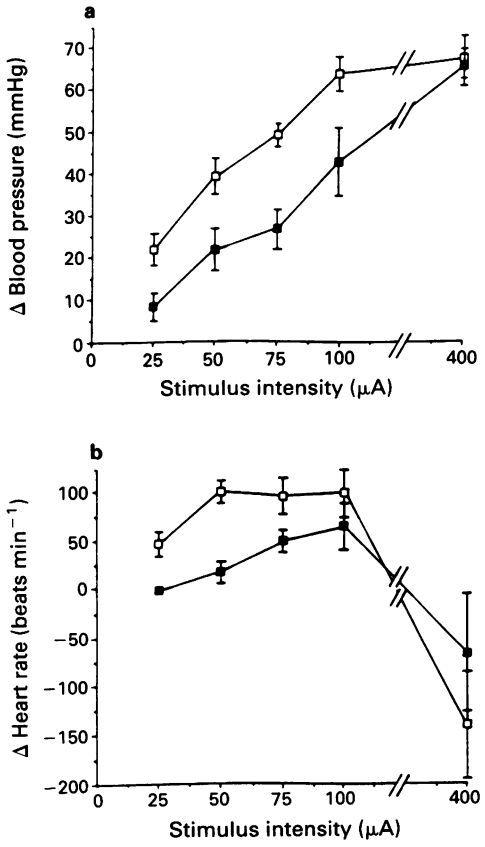

Figure 1 (a) Hypertensive and (b) tachycardia responses to CNS stimulation in the absence and presence of (**R**)-α-methylhistamine. Responses in (**R**)-α-methylhistamine (300 μg kg^{-1}, i.v.)-treated animals (●) were significantly ($P<0.05$) less than in control animals (○) that received only the CNS stimulation. Values represent the mean (± s.e.mean shown by vertical bars) ($n = 4$) increase in blood pressure and heart rate due to CNS stimulation.

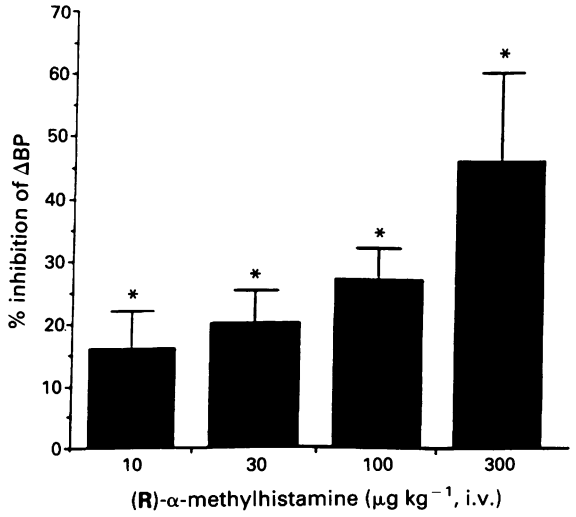

Figure 2 Dose-dependent inhibitory effects of (R)-α-methylhistamine on CNS-induced hypertension. The graph shows responses (ΔBP) at a stimulus intensity of 75 μA. Values are the mean (± s.e.mean shown by vertical bars) ($n = 4-7$).

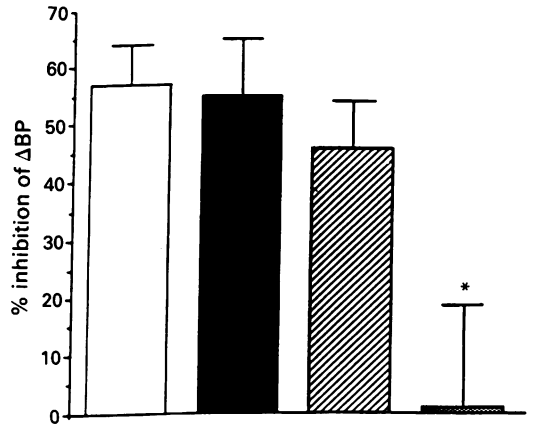

Figure 3 Effects of histamine H_1-, H_2- and H_3-antagonists on the inhibition of CNS-induced hypertension by (R)-α-methylhistamine. The graph illustrates the effect on blood pressure (ΔBP) of (R)-α-methylhistamine (300 μg kg^{-1}, i.v.) given alone (open column), or in the presence of chlorpheniramine (30 μg kg^{-1}; solid column), cimetidine (3 mg kg^{-1}; hatched column), or thioperamide (3 mg kg^{-1}; stippled column). The stimulus-intensity was 75 μA. *$P < 0.05$ compared to (R)-α-methylhistamine alone. Values represent the mean (± s.e.mean shown by vertical bars) ($n = 4$).

ment of tachyphylaxis, each animal received a single dose of (R)-α-methylhistamine. Under these conditions, 300 μg kg^{-1} of (R)-α-methylhistamine produced a maximal inhibition of 48 ± 10%. Higher doses of (R)-α-methylhistamine could not be tested, because they cause histamine H_1-receptor-mediated responses (Hey *et al.*, 1992). The ED_{50} (dose producing 50% of maximal inhibition) for (R)-α-methylhistamine was 100 μg kg^{-1}, i.v. To determine whether the action of (R)-α-methylhistamine was prejunctional or postjunctional, we studied its effect on the hypertensive response to intravenous adrenaline. There was no difference in the magnitude of the hypertensive responses to (−)-adrenaline (1 and 3 μg kg^{-1}) between saline-treated (ΔBP = 21 ± 2 and 71 ± 4 mmHg) and (R)-α-methylhistamine-treated (300 μg kg^{-1}; ΔBP = 22 ± 5 and 73 ± 4, respectively) animals ($n = 3-6$), indicating a prejunctional site of action for (R)-α-methylhistamine.

The selective H_3-antagonist, thioperamide (3 mg kg^{-1}, i.v.), blocked the inhibitory effect of (R)-α-methylhistamine on CNS-induced hypertension (Figure 3). In contrast, chlorpheniramine (30 μg kg^{-1}) and cimetidine (3 mg kg^{-1}), at doses that block H_1- and H_2-receptor mediated responses, did not block the action of (R)-α-methylhistamine.

To determine a rank order potency of the H_3-antagonists, thioperamide, impromidine and burimamide, were given before a single dose of (R)-α-methylhistamine (300 μg kg^{-1}, i.v.) (Figure 4). Impromidine (ID_{50} = 0.22 mg kg^{-1}, i.v.) and thioperamide (ID_{50} = 0.39 mg kg^{-1}, i.v.) were essentially equipotent in blocking the inhibitory effects of (R)-α-methylhistamine. Burimamide (ID_{50} = 6 mg kg^{-1}, i.v.) was 15 fold weaker than impromidine or thioperamide.

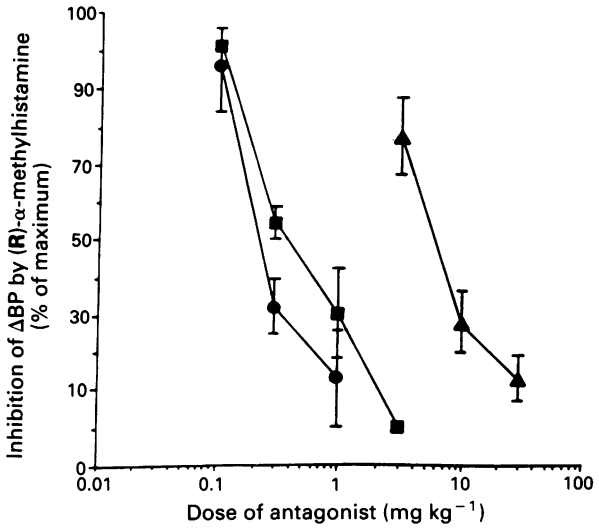

Figure 4 Potencies of H_3-antagonists on (R)-α-methylhistamine inhibition of CNS-induced hypertension. The graph shows the response to (R)-α-methylhistamine (300 μg kg^{-1}, i.v.) in the presence of increasing doses of impromidine (●), thioperamide (■) and burimamide (▲). The values represent the mean (± s.e.mean shown by vertical bars) ($n = 4-5$) percentage maximum inhibition of CNS-induced hypertension. Maximum inhibition produced by 300 μg kg^{-1} of (R)-α-methylhistamine was 47 ± 12%.

Discussion

The present study demonstrates that activation of prejunctional H_3-receptors, with the selective H_3-agonist, (R)-α-methylhistamine, produces an inhibition of centrally-evoked hypertension and tachycardia in guinea-pigs. The inhibition by (R)-α-methylhistamine of CNS-induced hypertension is dose-related and dependent upon the stimulus intensity. Furthermore, the effect of (R)-α-methylhistamine is blocked by pretreatment with H_3-antagonists. These results are consistent with the findings of Ishikawa & Sperelakis (1987) who showed that activation of prejunctional perivascular H_3-receptors inhibits sympathetic neurotransmission. Other investigators have recently shown that (R)-α-methylhistamine inhibits the release of noradrenaline from postganglionic sympathetic nerves in pigs and in guinea-pigs (Schlicker *et al.*, 1990; Luo *et al.*, 1991; Malinowska & Schlicker, 1991). Our studies build upon the growing body of work that establishes that the H_3-receptor is an important prejunctional inhibitory modulator both in the CNS (Schwartz *et al.*, 1986; 1991; Arrang *et al.*, 1983; 1988) and in the periphery (Ichinose *et al.*, 1990).

The sympathetically driven hypertensive responses that are elicited by activation of structures within the dorsal medulla have been well characterized in cats (Alexander, 1949; Chai & Wang, 1968), rabbits (Goodchild & Dampney, 1985) and, more recently, in guinea-pigs (Hey *et al.*, 1990b). These hypertensive events are mediated by activation of bulbospinal

sympathetic pathways as they are blocked with α-adrenoceptor antagonists, ganglionic blockers such as hexamethonium and spinal cord transection with lignocaine (Hey *et al.*, 1990b). Our results in guinea-pigs indicate that (**R**)-α-methylhistamine inhibits the hypertension produced by electrical stimulation of the dorsal medulla (Hey *et al.*, 1992) and that the effects of (**R**)-α-methylhistamine are not blocked by H_1- or H_2-receptor antagonists. On the other hand, thioperamide, which is a selective H_3-antagonist (Arrang *et al.*, 1987) blocks the effect of (**R**)-α-methylhistamine, implicating the H_3-receptor. Additional dose-response studies with the H_3-antagonists, thioperamide, impromidine and burimamide reveal an antagonist potency profile that is consistent with an H_{3B}-receptor subtype (West *et al.*, 1990) mediating responses on vascular sympathetic neurotransmission. It should be noted, however, that these *in vivo* findings may also reflect a possible uneven tissue distribution and/or metabolism of these antagonists. Nevertheless, these conclusions are consistent with those of West *et al.* (1990) that the guinea-pig mesenteric artery contains the H_{3B} receptor.

In a recent study in rats, Malinowska & Schlicker (1991) found that (**R**)-α-methylhistamine inhibited the pressor response to sympathetic nerve stimulation. The results from our study confirm and extend these findings. We demonstrate an inhibitory effect of (**R**)-α-methylhistamine on sympathetically-driven hypertension in guinea-pigs. This species is highly responsive to (**R**)-α-methylhistamine (Trzeciakowski, 1987; Ichinose *et al.*, 1989; 1990; Menkveld & Timmerman, 1990; Coruzzi *et al.*, 1991) including inhibitory effects on sympathetic neurotransmission in perivascular nerves (Ishikawa & Sperelakis, 1987). However, the H_3-mediated effects on blood pressure responses *in vivo* have not been previously shown in the guinea-pig. Furthermore, although an inhibitory effect of (**R**)-α-methylhistamine on electrically-stimulated contractile responses in the guinea-pig isolated myocardium has been reported (Luo *et al.*, 1991), this is the first report describing an inhibitory effect of (**R**)-α-methylhistamine on neurally stimulated tachycardia *in vivo*. Finally, Malinowska & Schlicker (1991) used only thioperamide to characterize the H_3-effects of (**R**)-α-methylhistamine. In our study, we have used thioperamide, impromidine and burimamide to characterize this more fully as an H_{3B}-receptor-mediated response.

(**R**)-α-methylhistamine appears to inhibit the CNS-induced hypertension by a prejunctional mechanism on sympathetic nerves. The fact that the inhibitory effect of (**R**)-α-methylhistamine is dependent on the stimulus intensity and is less at supramaximal intensities is consistent with a prejunctional site of action (Starke, 1987; van der Vliet *et al.*, 1990). This had been demonstrated by other peripherally acting prejunctional inhibitory modulators such as α_2-adrenoceptor agonists and $GABA_B$ receptor agonist (Armstrong & Boura, 1973; Doxey *et al.*, 1977; Kohlenbach & Schlicker, 1990). Further evidence that (**R**)-α-methylhistamine acts prejunctionally comes from the studies of Ishikawa & Sperelakis (1987), who demonstrated an inhibition by H_3-receptor activation of postganglionic sympathetic perivascular nerve terminals in guinea-pigs. Histamine H_3-receptor activation also depresses ganglionic neurotransmission (Tamura *et al.*, 1988), so we cannot rule out a possible ganglionic component. On the other hand, there is no evidence to support the notion that (**R**)-α-methylhistamine inhibits sympathetic outflow to vascular nerves at the level of the CNS (McLeod *et al.*, 1991) and it is unlikely that (**R**)-α-methylhistamine acts postjunctionally on smooth muscle because it did not inhibit pressor responses to i.v. adrenaline. The finding that (**R**)-α-methylhistamine lowered basal blood pressure and heart rate without causing the reflex tachycardia also suggests an effect on vascular sympathetic nerves rather than dilatation of vascular smooth muscle. Furthermore, the fact that our studies were performed in the presence of ipratropium bromide to block peripheral muscarinic receptors also rules out the possibility that bradycardia and hypotensive effects of (**R**)-α-methylhistamine were the result of activation of vagal output from the CNS (McLeod *et al.*, 1991).

In summary, our findings indicate that (**R**)-α-methylhistamine inhibits sympathetic hypertensive responses in guinea-pigs by activation of prejunctional H_3-receptors, possibly located on postganglionic nerve terminals. Furthermore, our results suggest that the H_{3B}-receptor subtype is involved with H_3-receptor responses on vascular sympathetic nerves. It is speculated that activation of the prejunctional H_3-receptor in allergic reactions may contribute to local vascular engorgement by inhibiting sympathetic vasoconstrictor tone to the affected vascular bed.

The authors gratefully acknowledge the typing skills of Ms Carol Battle.

References

ALEXANDER, R.S. (1949). Tonic and reflex functions of medullary cardiovascular centers. *Am. J. Physiol.*, **149**, 205–217.

ARMSTRONG, J.M. & BOURA, A.L.A. (1973). Effects of clonidine and guanethidine on peripheral sympathetic nerve function in the pithed rat. *Br. J. Pharmacol.*, **47**, 850–852.

ARRANG, J.-M., DEVAUX, B., CHODKIEWICZ, J.P. & SCHWARTZ, J.-C. (1988). H_3-Receptors control histamine release in human brain. *J. Neurochem.*, **51**, 105–108.

ARRANG, J.-M., GARBARG, M., LANCELOT, J.C., LECOMTE, J.M., POLLARD, H., ROBBA, M., SCHUNACK, W. & SCHWARTZ, J.C. (1987). Highly potent and selective ligands for histamine H_3-receptors. *Nature*, **327**, 117–123.

ARRANG, J.-M., GARBARG, M. & SCHWARTZ, J.-C. (1983). Auto-inhibition of brain histamine release mediated by a novel class (H_3) of histamine receptor. *Nature*, **302**, 832–837.

CHAI, C.Y. & WANG, S.C. (1968). Integration of sympathetic cardiovascular centers. *Am. J. Physiol.*, **149**, 205–217.

CORUZZI, G., POLI, E. & BERTACCINI, G. (1991). Histamine receptors in isolated guinea pig duodenal muscle: H_3-receptors inhibit cholinergic transmission. *J. Pharmacol. Exp. Ther.*, **258**, 325–331.

DOXEY, J.C. (1977). Effect of clonidine on cardiac acceleration in pithed rats. *J. Pharm. Pharmacol.*, **29**, 173–174.

GOODCHILD, A.K. & DAMPNEY, R.A.L. (1985). A vasopressor cell group in the rostral dorsomedial medulla of the rabbit. *Brain Res.*, **360**, 24–32.

HEY, J.A., DEL PRADO, M. & CHAPMAN, R.W. (1990a). Activation of a novel medullary pathway elicits a vagal, cholinergic bronchoconstriction in guinea pigs. *Pulmon. Pharmacol.*, **3**, 53–54.

HEY, J.A., DEL PRADO, M. & CHAPMAN, R.W. (1990b). Sympathetic modulation of CNS-induced bronchospasm in guinea pigs. *Am. Rev. Respir. Dis.*, **141**, A844.

HEY, J.A., DEL PRADO, M., EGAN, R.W., KREUTNER, W. & CHAPMAN, R.W. (1992). (**R**)-α-methylhistamine augments neural, cholinergic bronchospasm in guinea pigs by histamine H_1-receptor activation. *Eur. J. Pharmacol.*, **211**, 421–426.

ICHINOSE, M., STRETTON, C.D., SCHWARTZ, J.-C. & BARNES, P.J. (1989). Histamine H_3-receptors inhibit cholinergic neurotransmission in guinea-pig airways. *Br. J. Pharmacol.*, **97**, 13–15.

ICHINOSE, M., BELVISI, M.G. & BARNES, P.J. (1990). Histamine H_3-receptors inhibit neurogenic microvascuar leakage in airways. *J. Appl. Physiol.*, **68**, 21–25.

ISHIKAWA, S. & SPERELAKIS, N. (1987). A novel class (H_3) of histamine receptors on perivascular nerve terminals. *Nature*, **327**, 152–160.

KOHLENBACH, A. & SCHLICKER, E. (1990). GABA-B receptor-mediated inhibition of the neurogenic vasopressor response in the pithed rat. *Br. J. Pharmacol.*, **100**, 365–369.

LUO, X.-L., TAN, Y.-H. & SHENG, B.-H. (1991). Histamine H_3 receptors inhibit sympathetic neurotransmission in guinea-pig myocardium. *Eur. J. Pharmacol.*, **204**, 311–314.

MALINOWSKA, B. & SCHLICKER, E. (1991). H_3 receptor-mediated inhibition of neurogenic vasopressor response in pithed rats. *Eur. J. Pharmacol.*, **205**, 307–310.

MCLEOD, R., GERTNER, S. & HEY, J.A. (1991). Central H_3 modulation of vagal tone and blood pressure in the conscious guinea pig. *Eur. J. Pharmacol.*, **209**, 141–142.

MENKVELD, G.J. & TIMMERMAN, H. (1990). Inhibition of electrically evoked contractions of guinea pig ileum preparation mediated by the histamine H_3 receptor. *Eur. J. Pharmacol.*, **186,** 343–347.

MOLDERINGS, G.J., WEISSENBORN, G., SCHLICKER, E. & GÖTHERT, M. (1991). Pharmacological characterization of the inhibitory presynaptic histamine receptors on the sympathetic nerves of the human saphenous vein. *Naunyn-Schmiedebergs Arch. Pharmacol.*, **344** (Suppl), R73.

SCHLICKER, E., BETZ, R. & GÖTHERT, M. (1988). Histamine H_3 receptor-mediated inhibition of serotonin release in the rat brain cortex. *Naunyn-Schmiedebergs Arch. Pharmacol.*, **337,** 588–590.

SCHLICKER, E., BETZ, R. & GOTHERT, M. (1990). Histamine H_3 receptor-mediated inhibition of noradrenaline release in pig retina discs. *Naunyn-Schmiedebergs Arch. Pharmacol.*, **324,** 497–501.

SCHNEIDER, D., SCHLICKER, E., MALINOWSKA, B. & MOLDERINGS, G. (1991). Noradrenaline release in the rat vena cava is inhibited by γ-aminobutyric acid via $GABA_B$ receptors but not affected by histamine. *Br. J. Pharmacol.*, **104,** 478–482.

SCHWARTZ, J.C., ARRANG, J.M., GARBARG, M. & KORNER, M. (1986). Properties and roles of the three subclasses of histamine receptors in brain. *J. Exp. Biol.*, **124,** 203–224.

SCHWARTZ, J.C., ARRANG, J.M., GARBARG, M., POLLARD, H. & RUAT, M. (1991). Histaminergic transmission in the mammalian brain. *Physiol. Rev.*, **71,** 1–51.

STARKE, K. (1987). Presynaptic α-autoreceptors. *Rev. Physiol. Biochem. Pharmacol.*, **107,** 73–146.

TAMURA, K., PALMER, J.M. & WOOD, J.D. (1988). Presynaptic inhibition produced by histamine at nicotinic synapses in enteric ganglia. *Neurosci.*, **25,** 171–179.

TIMMERMAN, H. (1990). Histamine H_3 ligands just pharmacological tools or potential therapeutic agents? *J. Med. Chem.*, **33,** 4–11.

TRZECIAKOWSKI, J.P. (1987). Inhibition of guinea pig ileum contractions mediated by a class of histamine receptors resembling the H_3 subtypes. *J. Pharmacol. Exp. Ther.*, **243,** 874–880.

VAN DER VLIET, A., BAST, A. & TIMMERMAN, H. (1990). Autoinhibition of histamine release by H_3 receptors in rat brain cortex depends on stimulation frequency. *Agents Actions*, **30,** 206–209.

WEST, R.E., JR, ZWEIG, A., SHIH, N.-Y., SIEGEL, M.I., EGAN, R.W. & CLARK, M. (1990). Identification of two H_3-histamine receptor subtypes. *Mol. Pharmacol.*, **38,** 610–613.

(Received March 26, 1992
Revised May 28, 1992
Accepted May 29, 1992)

Br. J. Pharmacol. (1992), **107**, 352–355

Inhibition of noradrenaline release in the rat vena cava via prostanoid receptors of the EP_3-subtype

Gerhard Molderings, [1]Barbara Malinowska & [2]Eberhard Schlicker

Institut für Pharmakologie und Toxikologie, Rheinische Friedrich-Wilhelms-Universität Bonn, Reuterstraße 2 b, D-5300 Bonn 1, Germany

1 In segments of the rat vena cava preincubated with [^{3}H]-noradrenaline and superfused with physiological salt solution (containing desipramine and corticosterone), we studied the effects of prostaglandins of the D, E and F series, of a prostacyclin analogue and a thromboxane-mimetic and of subtype-selective prostaglandin E-receptor (EP-receptor) ligands on the electrically (0.66 Hz)-evoked tritium overflow.

2 The electrically-evoked tritium overflow was inhibited by prostaglandin E_2 (maximum inhibition by about 80%; pIC_{40} 7.49). The effect of prostaglandin E_2 was not affected by rauwolscine, which, by itself, increased the evoked overflow; the α_2-adrenoceptor antagonist was added to the superfusion medium in all subsequent experiments. Indomethacin failed to affect either the evoked tritium overflow or its inhibition by prostaglandin E_2.

3 The inhibitory effect of prostaglandin E_2 on the electrically-evoked tritium overflow was not altered by the EP_1-receptor antagonist, AH 6809 (6-isopropoxy-9-oxoxanthene-2-carboxylic acid) at a concentration at least 30 fold higher than its pA_2 value at EP_1-receptors. The following compounds mimicked the effect of prostaglandin E_2 showing the following rank order of potencies: misoprostol (EP_2-/EP_3-receptor agonist) $\simeq$ sulprostone (EP_1-/EP_3-receptor agonist) $\simeq$ prostaglandin E_1 = prostaglandin E_2 >> iloprost (EP_1-/IP-receptor agonist) = prostaglandin $F_{2\alpha}$. The evoked overflow was not affected by high concentrations of prostaglandin D_2 or the thromboxane-mimetic U46619 (9,11-dideoxy-11α, 9α-epoxymethano-prostaglandin $F_{2\alpha}$).

4 The present results suggest that the postganglionic sympathetic nerve fibres innervating the rat vena cava are endowed with presynaptic EP_3-receptors. They are not tonically activated by endogenously formed products of cyclo-oxygenase and do not interact with the presynaptic α_2-adrenoceptors.

Keywords: Rat vena cava; postganglionic sympathetic neurones; noradrenaline release; presynaptic EP_3-receptors; presynaptic α_2-receptors; receptor interactions; prostaglandin E_2; sulprostone; misoprostol; indomethacin

Introduction

Prostaglandin E_2 (PGE_2) inhibits noradrenaline release from the vascular postganglionic sympathetic nerve endings (for review, see Hedqvist, 1977; Starke, 1977; Güllner, 1983; Malik & Sehic, 1990). No information is so far available with respect to the prostaglandin E-receptor subtype involved in this effect in vascular tissues (EP_1, EP_2 or EP_3; for review of prostaglandin E (PGE)-receptor subtypes, see Coleman *et al.*, 1990). We, therefore, decided to address this question using the rat vena cava. Furthermore, the effects of prostaglandins of the D and F series and of an analogue of prostacyclin and a thromboxane A_2-mimetic on noradrenaline release were studied. Finally, the inhibitory effect of PGE_2 on noradrenaline release was also examined in vascular segments in which formation of endogenous prostaglandins was inhibited by indomethacin or in which the presynaptic α_2-adrenoceptors on the postganglionic sympathetic nerve fibres (Göthert & Kollecker, 1986) were blocked by rauwolscine.

A preliminary account of the present results was given to the 33rd Spring Meeting of the Deutsche Gesellschaft für Pharmakologie und Toxikologie (Malinowska & Schlicker, 1992).

Methods

Cranial segments of the inferior vena cava from male Wistar rats were ligated at both ends and incubated for 30 min with physiological salt solution (37°C; for composition, see below) containing [^{3}H]-noradrenaline 0.1 μmol l^{-1} (specific activity 43.7 Ci $mmol^{-1}$). The veins were mounted vertically in an organ bath, between two parallel platinum electrodes (1.5 cm long), and under a tension of 0.5 g. The adventitial surface was superfused with [^{3}H]-noradrenaline-free physiological salt solution of 37°C at 2 ml min^{-1}. The composition of the solution was (mmol l^{-1}): NaCl 118, NaH_2PO_4 1.2, $NaHCO_3$ 25.0, KCl 4.7, $CaCl_2$ 1.6, $MgSO_4$ 1.2, glucose 11.0, ascorbic acid 0.3, Na_2EDTA 0.03 (aerated with 95% O_2 and 5% CO_2). The solution contained desipramine 0.6 μmol l^{-1} and corticosterone 40 μmol l^{-1} (for inhibition of neuronal and extraneuronal noradrenaline uptake, respectively) throughout the superfusion. Five periods (duration 6 min each) of electrical stimulation (rectangular pulses of 100 mA and 0.3 ms; 0.66 Hz) were applied to each vein after 93 (S_1), 117 (S_2), 141 (S_3), 165 (S_4) and 189 (S_5) min of superfusion. The superfusate was collected in 3 or 6 min fractions. The radioactivity in the superfusate samples and veins was determined by liquid scintillation counting.

Calculations and statistics

Tritium efflux was calculated as the percentage of tritium present in the vein at the start of the respective collection period. Basal ^{3}H efflux was expressed as the percentage of tritium efflux during the collection period immediately before S_2 (t_2), S_3 (t_3), S_4 (t_4) and S_5 (t_5). Stimulation-evoked ^{3}H overflow was calculated by subtraction of the basal efflux (assumed to decrease linearly from the collection period before to that 12–15 min after the start of stimulation) from the total efflux during stimulation and the subsequent 6 min

[1] Permanent address: Zakład Farmakodynamiki, Akademia Medyczna, Mickiewicza 2C, 15-122 Białystok 8, Poland.
[2] Author for correspondence.

and was expressed as a percentage of tissue tritium at the start of stimulation. In order to quantify the effects of prostanoids (added to the medium in three increasing concentrations 9 min before and during S_3, S_4 and S_5) on basal and evoked overflow, the ratios t_3/t_2, t_4/t_2 or t_5/t_2 and S_3/S_2, S_4/S_2 or S_5/S_2 obtained in the presence of the drug under study were compared to the corresponding ratios obtained in its absence. For quantification of the effects of rauwolscine, indomethacin and AH 6809 (added to the medium from 27 min before S_2 onward), the percentage of ^3H efflux during t_2 or the tritium overflow evoked by S_2 in veins exposed to the drug under study was compared to the respective parameter in untreated veins.

Results are given as means ± s.e.mean. Student's t test for unpaired data was used for comparison of mean values. If two or more experimental series were compared to the same control series, the t test was subjected to Bonferroni's procedure.

Drugs

The following drugs were used: (−)-[ring-2,5,6-^{3}H]-noradrenaline (NEN, Dreieich, Germany); AH 6809 (6-isopropoxy-9-oxoxanthene-2-carboxylic acid; Glaxo, Ware, England); corticosterone, prostaglandin D_2, E_1, E_2, $F_{2\alpha}$ (Sigma, Munich, Germany); desipramine hydrochloride (CIBA-Geigy, Wehr, Germany); iloprost, sulprostone (Schering, Berlin, Germany); indomethacin (MSD Sharp & Dohme, Munich, Germany); misoprostol (Searle, Skokie, IL, U.S.A.); rauwolscine hydrochloride (Roth, Karlsruhe, Germany); U46619 (9,11-dideoxy-11α,9α-epoxymethano-prostaglandin $F_{2\alpha}$; Biosigma, Munich, Germany). Stock solutions were prepared with water (AH 6809, desipramine, rauwolscine), saline (iloprost; ampoules provided by the manufacturer), 1,2-propanediol (corticosterone), ethanol (indomethacin, misoprostol, PGD_2, PGE_1, PGE_2, $PGF_{2\alpha}$, sulprostone) or dimethylsulphoxide (U46619) and diluted with physiological salt solution to the concentration required. The solvents did not affect basal and evoked tritium overflow.

Results

Basal tritium efflux

The percentage of tritium efflux during t_2 and the ratios t_3/t_2, t_4/t_2 and t_5/t_2 (t_n/t_2) were used for quantification of basal ^3H efflux (for further details, see Methods). The percentage of tritium efflux during t_2 was not affected by rauwolscine 1 μmol l^{-1}, indomethacin 3 μmol l^{-1} or AH 6809 10 μmol l^{-1} (Table 1). The ratios t_3/t_2, t_4/t_2 and t_5/t_2 were 0.96 ± 0.03, 0.88 ± 0.02 and 0.85 ± 0.03, respectively, in 7–9 control experiments (i.e. prostanoids absent) performed on vascular segments exposed to rauwolscine. These ratios were not changed by omission of rauwolscine or by addition of indomethacin or AH 6809 (results not shown). The ratio t_n/t_2 was not affected by most of the prostanoids or slightly decreased (by up to 27%; results not shown). Since preliminary experiments had shown that sulprostone 1 μmol l^{-1} markedly increased basal efflux, only lower concentrations of this prostanoid (1–100 nmol l^{-1}) were examined in subsequent experiments.

Electrically-evoked tritium overflow

Tritium overflow evoked by S_2 and the ratios S_3/S_2, S_4/S_2 and S_5/S_2 (S_n/S_2) were used for quantification of evoked overflow (for further details, see Methods). Tritium overflow evoked by S_2 was increased by rauwolscine 1 μmol l^{-1} (by 277%), but not further affected by indomethacin 3 μmol l^{-1} or AH 6809 10 μmol l^{-1} (Table 1). The ratios S_3/S_2, S_4/S_2 and S_5/S_2 were 1.03 ± 0.04, 1.01 ± 0.06 and 0.93 ± 0.07 in the control series mentioned above. These ratios were not affected by omission of rauwolscine or addition of indomethacin or AH 6809 (results not shown). In the following paragraphs, the S_n/S_2 ratios obtained in the presence of prostanoids are given, expressed as percentages of the respective control values.

The electrically evoked ^3H overflow was inhibited by PGE_2 10–1000 nmol l^{-1} in a concentration-dependent manner; essentially the same concentration-response curve was obtained for the prostanoid both in the absence and presence of rauwolscine 1 μmol l^{-1} (Figure 1a). All further experiments were therefore performed in the presence of rauwolscine. Indomethacin 3 μmol l^{-1}, added to the superfusion medium to inhibit the production of endogenous prostaglandins, had no significant effect on the concentration-response curve to PGE_2 (Figure 1b).

In another series of experiments, the effects of prostaglandins D_2 and $F_{2\alpha}$ and of iloprost and U46619 were studied (Figure 2, open symbols). $PGF_{2\alpha}$ and iloprost inhibited the electrically-evoked tritium overflow only at concentrations > 100 nmol l^{-1}. PGD_2 and U46619 failed to affect the evoked overflow even at concentrations of up to 1 μmol l^{-1}.

Next, experiments were carried out to investigate the involvement of prostaglandin EP-receptor subtypes in the effect of PGE_2. The concentration-response curve for PGE_2 was not affected by a high concentration (10 μmol l^{-1}) of the EP_1-receptor antagonist AH 6809 (Figure 1c). Amongst a range of prostaglandin E analogues tested, PGE_1, the EP_2-/EP_3-receptor agonist, misoprostol and the EP_1/EP_3-receptor agonist, sulprostone were found to be as potent as PGE_2 (Figure 2, closed symbols).

Table 1 Effect of rauwolscine, indomethacin and AH 6809 on the basal and electrically (0.66 Hz)-evoked tritium overflow from superfused rat vena cava segments preincubated with [^{3}H]-noradrenaline

Drug(s) (μmol l^{-1})	n	*Basal ^3H efflux* (t_2)[a] (expressed as % of tissue tritium × min^{-1})	*Evoked ^3H overflow* (S_2) (expressd as % of tissue tritium[b])
–	13	0.25 ± 0.02	0.92 ± 0.07
Rauwolscine 1	50	0.23 ± 0.01	3.47 ± 0.16*
Rauwolscine 1 + indomethacin 3	16	0.21 ± 0.01	2.77 ± 0.21
Rauwolscine 1 + AH 6809 10	13	0.17 ± 0.01	2.95 ± 0.33

The veins were superfused with isotope-free physiological salt solution containing desipramine 0.6 μmol l^{-1} plus corticosterone 40 μmol l^{-1}. Rauwolscine, indomethacin and/or AH 6809 were added to the medium from 27 min before S_2 onward. Five 6 min periods of transmural electrical stimulation (S_1–S_5) were administered to each vein. Means ± s.e.mean of n experiments.
*$P < 0.001$, compared to the rauwolscine-free value.
[a]t_2 represents the 3 min period of superfusate sampling immediately before S_2.
[b]Evoked overflow in excess of basal efflux.

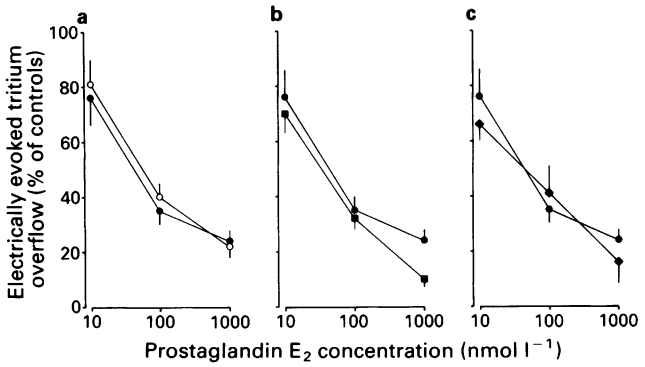

Figure 1 The effect of prostaglandin E_2 on the electrically-evoked ^3H overflow from rat vena cava segments preincubated with [^3H]-noradrenaline. Mean inhibitory concentration-effect curves to prostaglandin E_2 in the absence (open symbols) and presence (closed symbols) of rauwolscine 1 μmol l^{-1} (●); rauwolscine + indomethacin 3 μmol l^{-1} (■); or rauwolscine + AH 6809 10 μmol l^{-1} (◆). All points are means from 4–9 experiments with s.e.mean shown by vertical lines. All values below 75% were significantly different ($P \leq 0.05$) from the corresponding controls (prostaglandin E_2 absent).

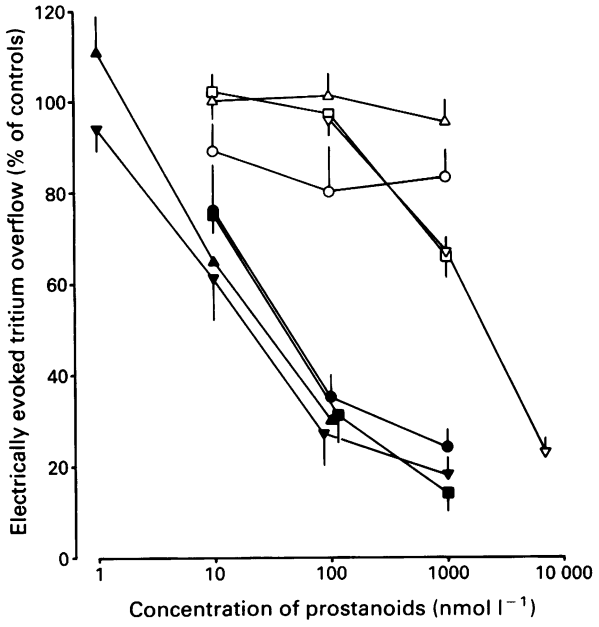

Figure 2 The effect of prostanoids on the electrically-evoked ^3H overflow from rat vena cava segments preincubated with [^3H]-noradrenaline. Mean inhibitory concentration-effect curves to prostaglandin E_2 (●); prostaglandin E_1 (■); misoprostol (▼); sulprostone (▲); prostaglandin D_2 (○); prostaglandin $F_{2\alpha}$ (□); iloprost (▽) and U46619 (△). Each point is the mean from 5–9 separate experiments with s.e.mean shown by vertical lines (not shown are the s.e.mean values for sulprostone 10 nmol l^{-1}, 100 nmol l^{-1} and prostaglandin $F_{2\alpha}$ 100 nmol l^{-1}, which were 15, 8 and 4% of controls, respectively). All values below 75% were significantly different ($P \leq 0.05$) from the corresponding controls.

Since the maximum inhibitory effect of PGE_2 and related compounds was about 80%, pIC_{40} values were determined to quantify the potencies of the 8 drugs (Table 2). The following rank order of potencies was obtained: misoprostol $\simeq$ sulprostone $\simeq$ PGE_1 = PGE_2 >> $PGF_{2\alpha}$ = iloprost >> PGD_2 or U46619.

Table 2 Potencies of prostanoids for their inhibitory effect on the electrically-evoked ^3H overflow from superfused rat vena cava segments preincubated with [^3H]-noradrenaline

Prostanoid	*pIC_{40}*
Misoprostol	7.97
Sulprostone	7.85
Prostaglandin E_1	7.66
Prostaglandin E_2	7.61[a]
Iloprost	5.87
Prostaglandin $F_{2\alpha}$	~5.8[b]
Prostaglandin D_2	<6.0
U46619	<6.0

pIC_{40} values were determined from the concentration-response curves shown in Figure 2.
[a]The pIC_{40} value for prostaglandin E_2 was 7.49 in the absence of rauwolscine (Figure 1a), 7.74 in the presence of rauwolscine plus indomethacin (Figure 1b) and 7.76 in the presence of rauwolscine plus AH 6809 (Figure 1c).
[b]Approximate value, obtained by extrapolation.

Discussion

In the present study, superfused segments of the rat vena cava preincubated with [^3H]-noradrenaline were used for the analysis of prostanoid-induced effects. The electrically-evoked tritium overflow in this tissue was shown to be Ca^{2+}-dependent and tetrodotoxin-sensitive and may be assumed to represent quasi-physiological noradrenaline release from the postganglionic sympathetic nerve fibres (Göthert & Kollecker, 1986). A variety of presynaptic receptors have been shown to occur in this tissue, including inhibitory α_2-adrenoceptors (Göthert & Kollecker, 1986), 5-HT_{1B}- (Molderings *et al.*, 1987) and $GABA_B$-receptors (Schneider *et al.*, 1991) or facilitatory β_2-adrenoceptors and angiotensin II-receptors (Göthert & Kollecker, 1986).

As expected, noradrenaline release in the rat vena cava was inhibited by PGE_2 and PGE_1. Iloprost, which is a stable analogue of prostacyclin (the principal product of arachidonic acid released in response to adrenergic nerve stimulation in blood vessels; for review, see Malik & Sehic, 1990), was markedly less potent than PGE_2 in inhibiting noradrenaline release. $PGF_{2\alpha}$ (which has been shown previously to inhibit or facilitate noradrenaline release from blood vessels; for review, see Starke, 1977; Malik & Sehic, 1990) was also markedly less potent than PGE_2 in inhibiting noradrenaline release in the rat vena cava. PGD_2 (which increased noradrenaline release in dog mesenteric arteries; Nakajima & Toda, 1984) and U46619 were ineffective in the present model, even at high concentrations. The data therefore implicate a role for EP-receptors in prostanoid-induced inhibition of electrically-evoked noradrenaline release.

Next, the question was addressed as to which subtype of EP-receptor (according to the classification of Coleman *et al.*, 1990) is involved in the inhibitory effect of PGE_2 and PGE_1 on noradrenaline release in the rat vena cava. The effect of PGE_2 was mimicked by the EP_1-/EP_3-receptor agonist, sulprostone and the EP_2-/EP_3-receptor agonist, misoprostol, which were both at least as potent in this respect as PGE_2. Iloprost, which is equipotent with PGE_2 at EP_1-receptors and markedly less potent than PGE_2 at EP_2- and EP_3-receptors (Sheldrick *et al.*, 1988), was 55 fold less potent than PGE_2 in the present model. Moreover, the EP_1-receptor antagonist, AH 6809, at a concentration which was at least 30 fold higher than its pA_2 value at EP_1-receptors (Coleman *et al.*, 1985), failed to affect the concentration-response curve of PGE_2. Taken together, these data suggest that the effect of PGE_1 and PGE_2 is mediated via EP_3-receptors. The same holds true for the presynaptic receptor for PGE_2 on postganglionic sympathetic nerve fibres innervating non-vascular

tissues, namely the rat trachea (Racké *et al.*, 1991), the guinea-pig vas deferens (Coleman *et al.*, 1987) and atrium (Beckman & Knirk, 1991; Mantelli *et al.*, 1991), and the human iris-ciliary body (Ohia & Jumblatt, 1991).

Our data obtained with $PGF_{2\alpha}$, PGD_2 and U46619 can be easily reconciled with the view that the sympathetic nerve endings are endowed with presynaptic EP_3-receptors and that additional presynaptic receptors for prostanoids, e.g. FP-receptors, are lacking. Thus, the potencies of these drugs in inhibiting noradrenaline release in the present model are in good agreement with their potencies in contracting the chick ileum (an EP_3-receptor containing preparation; Coleman *et al.*, 1990). The equipotent concentrations ($PGE_2 = 1$) were 116, >1500 and >400, respectively, in the chick ileum and ~ 65, $\gg 41$ and $\gg 41$, respectively, in the present model.

To answer the question as to whether noradrenaline release, under the experimental conditions of the present study, is also inhibited by endogenously formed arachidonic acid metabolites, experiments with indomethacin were carried out. If the EP_3-receptors were tonically activated by endogenous prostanoids, one would expect that noradrenaline release would be increased by indomethacin (due to interruption of an inhibitory effect produced by endogenous prostanoids); moreover, one would expect that the inhibitory effect of exogenously added PGE_2 on noradrenaline release would be enhanced since the exogenously added prostaglandin has to compete for the EP_3-receptor only with a small amount of endogenously formed prostanoids. The lack of effect of indomethacin on noradrenaline release, and its modulation by PGE_2 argue against a tonic activation of the EP_3-receptors by endogenous prostanoids. These findings are at variance with results reported for several other vascular preparations (for review, see Hedqvist, 1977; Starke, 1977; Malik & Sehic, 1990).

Finally, the question was addressed as to whether an interaction occurs between the EP_3-heteroreceptors and the α_2-autoreceptors. Interactions between presynaptic EP- and α_2-receptors have been shown to occur on peripheral (Hedqvist, 1974; Ohia & Jumblatt, 1990) and central noradrenergic neurones (Allgaier *et al.*, 1989). In the latter studies, blockade of the α_2-adrenoceptors, activated by endogenously released noradrenaline, enhanced the inhibitory effect of PGE_2 on noradrenaline release. In the model of the rat vena cava, such an interaction does not appear to exist since the effect of PGE_2 was virtually identical in the absence and presence of the α_2-adrenoceptor antagonist, rauwolscine (which was added to the superfusion medium in subsequent experiments in order to increase noradrenaline release). On the other hand, an interaction betwen the presynaptic 5-HT_{1B}- and α_2-receptors has been previously shown for the rat vena cava (Molderings & Göthert, 1990).

In conclusion, the present results suggest that the sympathetic nerve fibres supplying the rat vena cava are endowed with inibitory EP_3-receptors. The latter are not tonically activated by endogenously formed prostanoids. An interaction between the EP_3- and α_2-receptors does not appear to occur.

This study was supported by the Deutsche Forschungsgemeinschaft (Bonn, Germany). B.M. is recipient of a fellowship provided by the Alexander von Humboldt-Stiftung (Bonn, Germany). We wish to thank Mrs R. Hell and Mrs K. Thur for their skilled technical assistance, Mrs R. Korneli and Mrs S. Rudat for typing the manuscript and the pharmaceutical companies CIBA-Geigy, Glaxo, MSD Sharpe & Dohme, Schering and Searle for gifts of drugs.

References

ALLGAIER, C., JÄGER, T. & HERTTING, G. (1989). Endogenous noradrenaline impairs the prostaglandin-induced inhibition of noradrenaline release. *Naunyn-Schmiedebergs Arch. Pharmacol.*, **340**, 472–474.

BECKMAN, R. & KNIRK, U. (1991). Presynaptic effects of prostaglandins on adrenergic neurotransmission in guinea pig atria in vitro. *Naunyn-Schmiedebergs Arch. Pharmacol.*, **344**, (Suppl), R 83.

COLEMAN, R.A., HUMPHREY, P.P.A. & KENNEDY, I. (1985). Prostanoid receptors in smooth muscle: further evidence for a proposed classification. In *Trends in Autonomic Pharmacology*, Vol 3. ed. Kalsner, S. pp. 35–49. London: Taylor and Francis.

COLEMAN, R.A., KENNEDY, I., SHELDRICK, R.L.G. & TOLOWINSKA, I.Y. (1987). Further evidence for the existence of three subtypes of PGE_2-sensitive (EP-)-receptors. *Br. J. Pharmacol.*, **91**, 407P.

COLEMAN, R.A., KENNEDY, I., HUMPHREY, P.P.A., BUNCE, K. & LUMLEY, P. (1990). Prostanoids and their receptors. In *Comprehensive Medicinal Chemistry. The Rational Design, Mechanistic Study and Therapeutic Application of Chemical Compounds*, Vol. 3. ed. Emmett, J.C. pp. 643–714. Oxford: Pergamon.

GÖTHERT, M. & KOLLECKER, P. (1986). Subendothelial β_2-adrenoceptors in the rat vena cava: facilitation of noradrenaline release via local stimulation of angiotensin II synthesis. *Naunyn-Schmiedebergs Arch. Pharmacol.*, **334**, 156–165.

GÜLLNER, H.G., (1983). The interactions of prostaglandins with the sympathetic nervous system – a review. *J. Autonom. Nerv. Syst.*, **8**, 1–12.

HEDQVIST, P. (1974). Prostaglandin action on noradrenaline release and mechanical responses in the stimulated guinea-pig vas deferens. *Acta Physiol. Scand.*, **90**, 86–93.

HEDQVIST, P. (1977). Basic mechanisms of prostaglandin action on autonomic neurotransmission. *Annu. Rev. Pharmacol. Toxicol.*, **17**, 259–279.

MALIK, K.U. & SEHIC, E. (1990). Prostaglandins and the release of the adrenergic transmitter. *Ann. N.Y. Acad. Sci.*, **604**, 222–236.

MALINOWSKA, B. & SCHLICKER, E. (1992). EP_3 receptor-mediated inhibition of noradrenaline release from the postganglionic sympathetic nerve fibres of the rat vena cava. *Naunyn-Schmiedebergs Arch. Pharmacol.*, **345** (Suppl), R 107.

MANTELLI, L., AMERINI, S., RUBINO, A. & LEDDA, F. (1991). Prejunctional prostanoid receptors on cardiac adrenergic terminals belong to the EP_3 subtype. *Br. J. Pharmacol.*, **102**, 573–576.

MOLDERINGS, G.J., FINK, K., SCHLICKER, E. & GÖTHERT, M. (1987). Inhibition of noradrenaline release in the rat vena cava via presynaptic 5-HT_{1B} receptors. *Naunyn-Schmiedebergs Arch. Pharmacol.*, **336**, 245–250.

MOLDERINGS, G.J. & GÖTHERT, M. (1990). Mutual interaction between presynaptic α_2-adrenoceptors and 5-HT_{1B} receptors on the sympathetic nerve terminals of the rat inferior vena cava. *Naunyn-Schmiedebergs Arch. Pharmacol.*, **341**, 391–397.

NAKAJIMA, M. & TODA, N. (1984). Neuroeffector actions of prostaglandin D_2 on isolated dog mesenteric arteries. *Prostaglandins*, **27**, 407–419.

OHIA, S.E. & JUMBLATT, J.E. (1990). Prejunctional inhibitory effects of prostanoids on sympathetic neurotransmission in the rabbit iris-ciliary body. *J. Pharmacol. Exp. Ther.*, **255**, 11–16.

OHIA, S.E. & JUMBLATT, J.E. (1991). Prejunctional prostaglandin receptors in the human iris-ciliary body. *Current Eye Res.*, **10**, 967–975.

RACKE, K., BÄHRING, J. & WESSLER, I. (1991). Release of endogenous noradrenaline from rat isolated trachea is inhibited via prostglandin receptors of the EP_3 subtype. *Naunyn-Schmiedebergs Arch. Pharmacol.*, **344** (Suppl. 2), R 128.

SCHNEIDER, D., SCHLICKER, E., MALINOWSKA, B. & MOLDERINGS, G. (1991). Noradrenaline release in the rat vena cava is inhibited by γ-aminobutyric acid via $GABA_B$ receptors but not affected by histamine. *Br. J. Pharmacol.*, **104**, 478–482.

SHELDRICK, R.L.G., COLEMAN, R.A. & LUMLEY, P. (1988). Iloprost – a potent EP_1- and IP-receptor agonist. *Br. J. Pharmacol.*, **94**, 334P.

STARKE, K. (1977). Regulation of noradrenaline release by presynaptic receptor systems. *Rev. Physiol. Biochem. Pharmacol.*, **77**, 1–124.

(Received March 11, 1992
Revised May 26, 1992
Accepted May 29, 1992)

Br. J. Pharmacol. (1992), **107**, 356–360

Effects of the bradykinin antagonist, HOE 140, in experimental acute pancreatitis

T. Griesbacher & [1]F. Lembeck

Department of Experimental and Clinical Pharmacology, University of Graz, Universitätsplatz 4, A-8010 Graz, Austria

1 The novel bradykinin antagonist, HOE 140, completely blocked the fall in rabbit blood pressure caused, not only by i.v. bradykinin, but also by i.v. kallikrein. This shows that both the effects of exogenously administered bradykinin and those of endogenously released kinins are antagonized by HOE 140.

2 Acute pacreatitis was induced in rats by i.v. infusion of the cholecystokinin analogue, caerulein. This treatment resulted in massive oedema of the pancreas, increased activities of amylase and lipase in serum and a characteristic, biphasic fall in blood pressure.

3 HOE 140 prevented the caerulein-induced pancreatic oedema and the second phase of hypotension whereas NPC 349, a widely used, but short-acting, bradykinin antagonist did not show a significant inhibition. HOE 140, in contrast to its inhibitory effects on caerulein-induced pancreatic oedema and hypotension, significantly augmented the increases in amylase and lipase activities in serum.

4 It is concluded that in this model of acute pancreatitis, the release of kinins induces pancreatic oedema and hypotension. Prevention by HOE 140 of the kinin-induced oedema allows the pancreatic enzymes to leave the tissue without hindrance and thus will diminish subsequent pathological events. It is suggested that the results obtained with the highly potent and long-acting bradykinin antagonist, HOE 140, provide a pharmacological basis for a clinical trial in acute pancreatitis.

Keywords: Bradykinin antagonists; HOE 140; pancreatitis (experimental); caerulein; hypotension; plasma protein extravasation; serum amylase; serum lipase

Introduction

Acute pancreatitis, which is associated with a considerable mortality rate, is characterized by a massive oedema of the gland and the adjacent retroperitoneal tissue, interstitial activation of proteolytic enzymes, increases of serum amylase and lipase activities, hypovolaemia, hypoalbuminaemia, pulmonary oedema and severe pain. To induce experimental pancreatitis in animals, a number of procedures are used. These include ligation of the pancreatic duct, injection of bile salts into the pancreatic duct, infusion of oleic acid, or infusion of the cholecystokinin (CCK) analogue, caerulein (Adler *et al.*, 1986). The latter procedure produces hyperstimulation of the exocrine secretion of pancreatic enzymes and leads to morphological changes similar to those seen in acute pancreatitis in man (Willemer *et al.*, 1990). Some of the clinical symptoms of acute pancreatitis have been attributed to the activation of the kallikrein-kinin system (Ruud *et al.*, 1985). Therefore, in the present work, the effects of a novel, potent and long-acting bradykinin (BK) antagonist, HOE 140 (Lembeck *et al.*, 1991; Hock *et al.*, 1991; Wirth *et al.*, 1991; Griesbacher & Lembeck, 1991), were investigated in caerulein-induced experimental pancreatitis in the rat.

Methods

Rabbit blood pressure

Rabbits of either sex (3.5–5.0 kg) were anaesthetized with pentobarbitone sodium (35 mg kg^{-1}, i.v.). Blood pressure was monitored in a carotid artery with a Statham pressure transducer. The stability of the blood pressure and the corneal reflex were used as indices of the depth of the anaesthesia. Bradykinin (BK; 1 or 3 nmol kg^{-1}) or kallikrein (1 or 3 u kg^{-1}) were injected into a jugular vein at intervals of 10 min. HOE 140 (3 nmol kg^{-1}) was then given i.v.. The injections of BK or kallikrein were repeated 5–15 min later.

Caerulein-induced pancreatitis in rats

Surgical procedure Female Sprague–Dawley rats (260 ± 30 g) were anaesthetized by simultaneous i.p. injection of pentobarbitone sodium (40 mg kg^{-1}) and phenobarbitone sodium (160 mg kg^{-1}). Captopril (50 μmol kg^{-1}, i.p.), an inhibitor of kininase II, was injected, at the same time, to augment the actions of any kinins released. Kininase II is present in many tissues (Lembeck *et al.*, 1990). Blood pressure in a carotid artery was monitored throughout the experiment with a Statham pressure transducer. A jugular vein was cannulated to allow the infusion of either caerulein (4 nmol kg^{-1} h^{-1}) or of saline (0.034 ml min^{-1}) for a period of 120 min. The BK antagonists, HOE 140 (100 nmol kg^{-1}) or NPC 349 (1 μmol kg^{-1}), or a corresponding volume (0.5 ml kg^{-1}) of a 154 mM sodium chloride solution (saline) were injected s.c. 30 min before, or 10–45 min after, the start of the caerulein infusion. At the end of the experiment the animals were killed by decapitation and blood was collected for the determination of serum amylase and lipase activity.

Quantification of pancreatic oedema To quantify the pancreatic oedema, 5 mg kg^{-1} of Evans blue, which binds quantitatively to serum albumin (Rawson, 1943), was injected i.v. immediately before the start of the i.v. infusion of caerulein or saline. At the end of the infusion, the rats were exsanguinated and perfused with 30 ml saline via the aorta. The portion of the pancreas adjacent to the duodenum was excised and weighed. It was then dried in a vacuum centrifuge, reweighed and the difference between wet and dry weight was used as a measure for the water content of the tissue. The dried tissues were then

[1] Author for correspondence.

immersed for 24 h at 50°C in formamide in order to extract the Evans blue (Gamse *et al.*, 1980). The amount of dye in the supernatant was determined photometrically at 620 nm (Saria & Lundberg, 1983).

Determination of serum enzyme activities Serum amylase activity was measured with a kinetic colour test using 2-chloro-4-nitrophenyl-D-maltoheptoside (Amylase test kit Roche, Germany). Serum lipase activity was measured by the reduction of the turbidity due to cleavage of triolein to monoglyceride and oleic acid (Monotest Lipase, Boehringer Mannheim, Germany). The limit of detection for amylase was 11 u l^{-1} and for lipase 16 u l^{-1}.

Substances used

HOE 140 (D-Arg-[Hyp^3, Thi^5, D-Tic^7, Oic^8]-bradykinin, a gift from Hoechst AG, Germany), NPC 349 (D-Arg-[Hyp^3, Thi^{5,8}, D-Phe^7]-bradykinin, NovaBiochem, Switzerland), caerulein (Sigma, U.S.A.) and bradykinin (Bachem, Switzerland) were dissolved in saline at a concentration of 1 mM. Porcine pancreatic kallikrein (Sigma, U.S.A.) was dissolved in 50% (v/v) ethanol and dilutions made with saline. Pentobarbitone sodium (Nembutal) was purchased from Sanofi Santé (France). Phenobarbitone sodium (Apoka, Austria) was dissolved in saline at a concentration of 80 mg ml^{-1}. Captopril was obtained from Squibb-von Heyden GmbH (Austria). Evans blue was purchased from Sigma (U.S.A.).

Statistical analysis

The hypotensive effects of BK and kallikrein in the rabbit before and after HOE 140 were compared by the Quade test (Conover, 1980). Comparisons between the different treatment groups in the rat were made by nonparametric multiple comparisons (Zar, 1984).

Results

Inhibition by HOE 140 of endogenously released kinins in the rabbit

The basal blood pressure of anaesthetized rabbits was about 110 mmHg. Intravenous injections of BK (1 or 3 nmol kg^{-1}) caused dose-dependent brief (about 1 min) falls in blood pressure. Comparable hypotensive effects could be elicited by i.v. injections of kallikrein (1 or 3 u kg^{-1}). HOE 140 (3 nmol kg^{-1}, i.v.) completely blocked the actions of these doses of BK and kallikrein; higher doses of BK (10 nmol kg^{-1}) and kallikrein (10 u kg^{-1}) induced only a minute fall in blood pressure when HOE 140 had been given previously (Figure 1). The inhibitory effect of HOE 140 was long-lasting: 120 min after the injection of HOE 140 the actions of BK or kallikrein were still reduced (not shown in the figure).

Caerulein-induced pancreatitis in rats

Blood pressure The basal blood pressure was 90–110 mmHg in all experimental groups. In control rats, which had received saline as s.c. injection and as i.v. infusion, the blood pressure fell by about 10–15 mmHg during the 2 h period of the i.v. infusion of saline. Pretreatment with HOE 140 (100 nmol kg^{-1}, s.c.) had no effect on the basal blood pressure or on the blood pressure during the i.v. infusion of saline. The i.v. infusion of caerulein caused a biphasic fall in blood pressure (Figure 2). The first hypotensive phase (about −20 mmHg) occurred during the first 15 min of the caerulein infusion. A further drop in blood pressure set in after 25–30 min, reaching minimal values of 70 ± 10 mmHg at 45–55 min. During the remaining time of the caerulein infusion, the blood pressure recovered slowly. In animals pretreated s.c. with HOE 140, the caerulein infusion still induced the initial fall in blood pressure during the first 25 min. However, the second phase of the caerulein-induced hypotension was abolished by HOE 140.

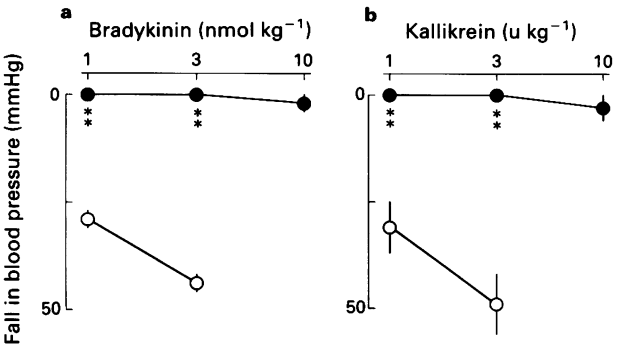

Figure 1 Fall in mean arterial pressure in anaesthetized rabbits elicited by i.v. injections of bradykinin (a) or of kallikrein (b). Open symbols are values obtained before, closed symbols are values obtained 5–15 min after, an i.v. injection of HOE 140 (3 nmol kg^{-1}). Mean values with s.e.mean (vertical lines); $n = 3$.
Significance of difference from control values: $^{**}P<0.01$.

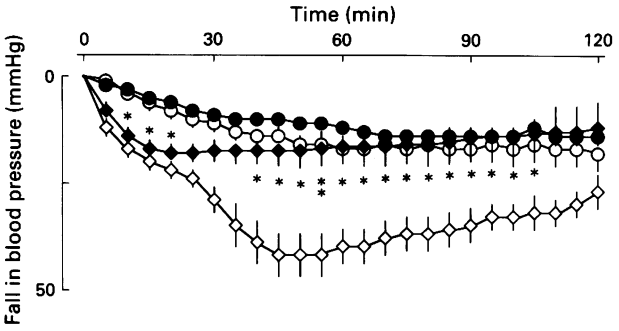

Figure 2 Fall in mean arterial pressure in anaesthetized rats during an i.v. infusion of caerulein (diamonds) or of saline (circles). Closed symbols are the values obtained from animals pretreated with HOE 140 (100 nmol kg^{-1}, s.c.); values obtained in control animals are given as open symbols. Mean values with s.e.mean (vertical lines); $n = 10$ in each of the 4 groups.
Asterisks denote significant differences ($^{*}P<0.05$; $^{**}P<0.01$) between groups above and below the asterisks.

Pancreatic oedema The infusion of caerulein led to a massive swelling of the pancreas which extended into the retroperitoneal area adjacent to the pancreas. A jelly-like oedema clearly separated the individual lobules and the pancreas had an almost transparent appearance. The water content of the tissue increased about three fold. The massive extravasation of Evans blue showed that a large amount of plasma proteins had accumulated in the interstitial space. In animals injected s.c. with HOE 140 (100 nmol kg^{-1}) 30 min before the caerulein infusion, caerulein did not induce any changes in the macroscopic appearance of the pancreas and the effects on the water content of the tissue and on plasma protein extravasation were completely abolished. HOE 140, when it was injected up to 25 min after the start of the caerulein infusion, also significantly inhibited the caerulein-induced pancreatic oedema (Figure 3). In contrast, NPC 349 (1 μmol kg^{-1}) was completely inactive when injected 30 min before caerulein. When NPC 349 was injected 10 min after the start of the caerulein infusion, the pancreatic oedema seemed to be smaller, but the effect was not statistically significant (Figure 3).

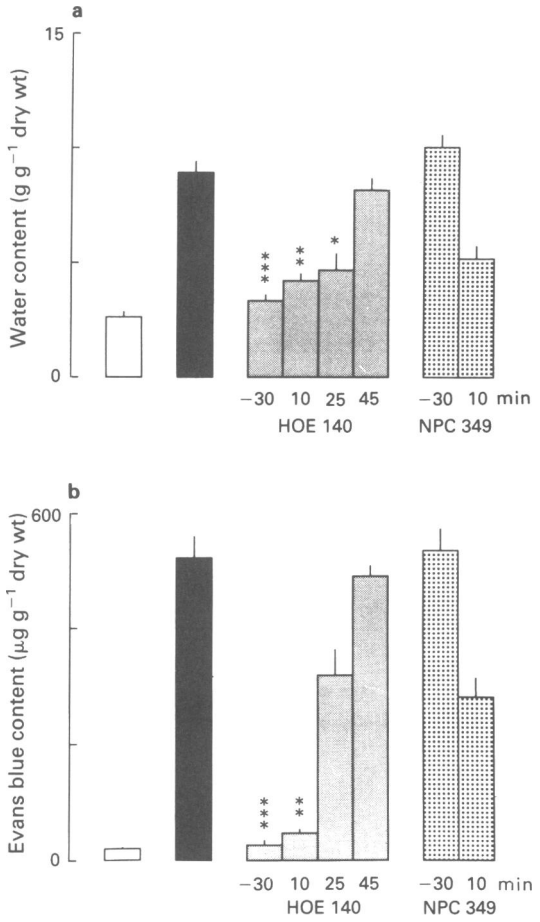

Figure 3 Oedema of the pancreas of rats quantified as water content (a) and as Evans blue content (b). Open columns show basal values obtained in animals receiving an i.v. infusion of saline, and solid columns show the effect of caerulein (8 nmol kg^{-1} infused i.v. within 120 min). Six further groups of rats were injected with bradykinin antagonists HOE 140 (100 nmol kg^{-1}, shaded columns) or NPC 349 (1 μmol kg^{-1}, stippled columns) either 30 min before, or 10, 25 or 45 min after the start of the caerulein infusion.
Significance of difference from the effect of caerulein alone (solid column): $^{*}P<0.05$,.$^{**}P<0.01$; $^{***}P<0.001$. Column heights represent mean values, vertical lines show s.e.mean; $n = 6-13$.

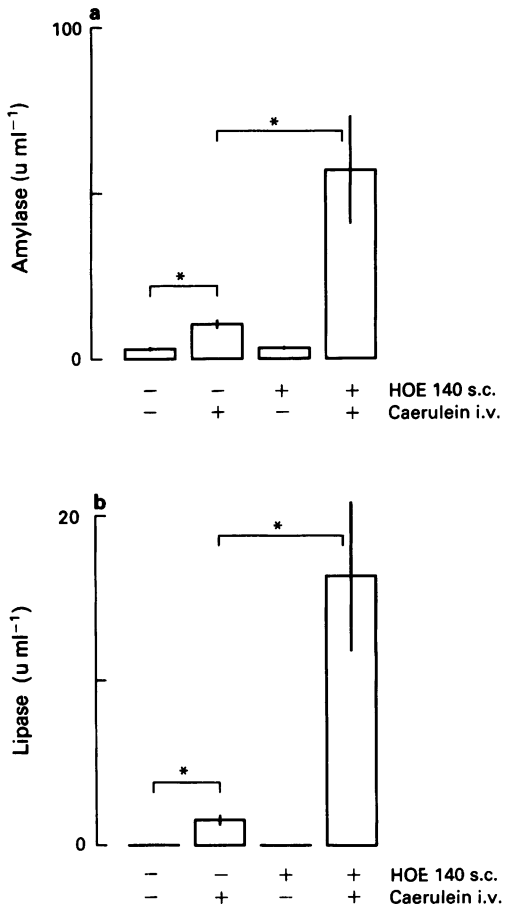

Figure 4 Serum activities of amylase (a) and lipase (b) in rats. Infusion of caerulein (8 nmol kg^{-1} within 120 min); pretreatment with HOE 140 (100 nmol kg^{-1}, s.c.) 30 min before the caerulein infusion. Control animals received corresponding volumes of saline instead of caerulein or HOE 140. Mean values with s.e.mean (vertical lines); $n = 10$ in each of the 4 groups.
Significance of difference between the groups indicated by brackets: $^{*}P<0.05$.

Enzyme activities in serum After pretreatment with HOE 140 alone, the serum activity of amylase was the same as in control animals. In rats pretreated s.c. with saline, the i.v. infusion of caerulein increased the serum activity of amylase significantly and this caerulein-induced elevation in serum amylase activity was augmented approximately 6 fold in rats pretreated with HOE 140 (Figure 4).

The activity of lipase in serum was below the limit of detection in the two groups of rats which received an i.v. infusion of saline. Caerulein induced a rise in serum lipase activity which was about 10 times larger in rats pretreated with HOE 140 (Figure 4).

Discussion

HOE 140 is a selective antagonist of exogenously administered BK across a wide spectrum of *in vitro* and *in vivo* tests and has a much higher potency and a longer duration of action than all other BK antagonists previously available (Lembeck *et al.*, 1991; Hock *et al.*, 1991; Wirth *et al.*, 1991; Griesbacher & Lembeck, 1991). In experiments on the kallikrein-induced fall in the blood pressure of rabbits we have now demonstrated that the actions of endogenously released kinins are also antagonized by HOE 140. Kallikrein, an enzyme discovered in urine and pancreatic extracts (see Werle, 1970), splits BK or lysyl-BK from a precursor, kininogen. The kinins thus formed are responsible for the resulting fall in blood pressure. Rabbits were used for initial experiments comparing the effects of BK and kallikrein because in the rat, a different kinin, Ile-Ser-BK, is released from kininogen by other enzymes such as trypsin. Ile-Ser-BK has all of the characteristic actions of kinins such as fall in blood pressure or increase in vascular permeability (Greenbaum, 1989). HOE 140 also blocks the fall in blood pressure and the plasma protein extravasation evoked by i.v. injected BK in the rat (Lembeck *et al.*, 1991).

Activation of CCK receptors seems to be involved in several forms of experimental pancreatitis because CCK antagonists have been found to have alleviating effects in such models (see Woodruff & Hughes, 1991). Hyperstimulation of the exocrine function of the pancreas by the CCK analogue, caerulein, results in increases in the serum activities of amylase and lipase (Silverman *et al.*, 1989) as well as in morphological changes similar to those observed in human acute pancreatitis (Willemer *et al.*, 1990).

Acute pancreatitis is characterized by pancreatic and retroperitoneal oedema and severe hypotension. In experimental models, the hypotension was associated with a major redistribution of body fluids. A great proportion of the measured loss in blood volume could be explained by the fluid found in

the peritoneal cavity (ascites) and the gain in volume of the pancreas itself (Ryan *et al.*, 1964). Since the transfusion of blood (Nugent & Atendido, 1966) or ascitic fluid (Ellison *et al.*, 1981) from animals with pancreatitis to healthy animals caused hypotension in the recipients, the involvement of vasoactive substances, such as kinins or histamine, has been postulated.

If kinins are released into the tissue they could also be responsible for the intense pain which is a major symptom of acute pancreatitis in man. BK is probably the most potent endogenous algesic substance and acts on capsaicin-sensitive afferent nerves (Juan & Lembeck, 1974). This type of nerve fibre is present in the pancreas (Sharkey *et al.*, 1984) and has also been studied in several experimental models for visceral pain (Ness & Gebhart, 1990).

Kinins in biological fluids have usually been measured by bioassay on the rat uterus or on the guinea-pig ileum. Similarly, kininogen was quantified as BK-like activity generated by trypsin. Using these methods, it has been found that, in experimental acute pancreatitis, the plasma levels of BK increase (Satake *et al.*, 1973) whereas those of kininogen decrease (Ryan *et al.*, 1964).

In order to prove that kinins are responsible for some of the clinical signs in acute pancreatitis, specific antagonists have to be employed. The failure of one of the earlier BK antagonists to protect against the hypotension in experimental pancreatitis (Berg *et al.*, 1989) had cast some doubt on the pathogenic role of kinins in this disease. However, the BK antagonist used in this earlier study belongs to a group of BK antagonists the effects of which are only very short-lasting *in vivo* (Griesbacher & Lembeck, 1987; Griesbacher *et al.*, 1989).

When the long-acting BK antagonist, HOE 140, became available, the proposed role of kinins in acute pancreatitis could be investigated in detail. Thus, the model of caerulein-induced pancreatitis in rats was chosen. The animals developed an acute interstitial oedema of the pancreas with hypotension and increased serum activities of amylase and lipase. This is comparable to the form of pancreatitis most frequently found in clinical situations in man (Büchler, 1991). No necroses were induced by the experimental procedure.

HOE 140 prevented the formation of the pancreatic oedema and the second phase of the hypotension in rats given an i.v. infusion of caerulein. These effects may, thus, be attributed to the release of endogenous kinins. The extravasation of plasma proteins was observed only in the pancreas but not in other organs. This effect was abolished by HOE 140 and shows that liberation of kinins, under the experimental conditions used, only occurs within the pancreas. HOE 140 did not inhibit the oedema formation when it was administered at a time (45 min) when, in the absence of HOE 140, the caerulein-induced hypotension had fully developed (compare Figure 2 and Figure 3). Therefore, it is strongly indicated that the hypotension observed in acute pancreatitis is not due to a kinin-induced vasodilatation but rather to a massive loss of plasma into the pancreatic oedema. A widely used, short-acting BK antagonist, NPC 349, was almost inactive even when used at a dose that was 10 times higher than that of HOE 140.

The effect of HOE 140 on the caerulein-induced increases in serum amylase and lipase activities were surprising. Instead of reducing the increase in enzyme activities there was an augmentation of up to ten fold. An explanation of this result could be that, while the oedema is present, a large proportion of both enzymes is trapped in the pancreas but when the oedema is prevented by the BK antagonist, the enzymes can leave the gland without hindrance. Accumulation of these enzymes in the oedematous pancreas will, no doubt, eventually lead to further tissue damage.

The severity of acute pancreatitis in man does not correlate with the serum levels of amylase and lipase, but rather with the pancreatic oedema and acites, the extent of pancreatic and extrapancreatic necrosis, and subsequent bacterial contamination which finally determine the risk of mortality (Büchler, 1991). The mortality rate is also highly correlated with the degree of hypoalbuminaemia (Imrie *et al.*, 1976). Pancreatic oedema is an essential factor in the development of pancreatic necroses (Klöppel *et al.*, 1986) and of hypoalbuminaemia. A therapeutic procedure counteracting the oedema formation is, therefore, of paramount therapeutic value. Since the present investigation shows that HOE 140 potently blocks the hypotension and the formation of the pancreatic oedema, the results provide a pharmacological basis for a clinical trial of HOE 140 in acute pancreatitis.

References

ADLER, G., KERN, H.F. & SCHEELE, G.A. (1986). Experimental models and concepts in acute pancreatitis. In *The Exocrine Pancreas*. ed. Go, V.L.W., Brooks, F.P., DiMagno, E.P., Gardner, J.D., Lebenthal, E., & Scheele, G.A. pp. 407–421. New York: Raven Press.

BERG, T., SCHLICHTING, E., ISHIDA, H. & CARRETERO, O.A. (1989). Kinin antagonist does not protect against the hypotensive response to endotoxin, anaphylaxis or acute pancreatitis. *J. Pharmacol. Exp. Ther.*, **251**, 731–734.

BÜCHLER, M. (1991). Objectification of the severity of acute pancreatitis. *Hepato-Gastroenterol.*, **38**, 101–108.

CONOVER, W.J. (1980). *Practical Nonparametric Statistics*. 2nd ed. pp.295–299. New York: Wiley.

ELLISON, E.C., PAPPAS, T.N., JOHNSON, J.A., FABRI, P.J. & CAREY, L.C. (1981). Demonstration and characterization of the hemoconcentrating effect of ascitic fluid that accumulates during hemorrhagic pancreatitis. *J. Surg. Res.*, **30**, 241–248.

GAMSE, R., HOLZER, P. & LEMBECK, F. (1980). Decrease of substance P in primary afferent neurones and impairment of neurogenic plasma extravasation by capsaicin. *Br. J. Pharmacol.*, **68**, 207–213.

GREENBAUM, L.M. (1989). Discovery and role of T-kininogen. In *The Kallikrein-Kinin System in Health and Disease*. ed. Fritz, H., Schmidt, I. & Dietze, G. pp.301–309. Braunschweig: Limbach.

GRIESBACHER, T. & LEMBECK, F. (1987). Actions of bradykinin antagonists on bradykinin-induced plasma extravasation, venoconstriction, prostaglandin E_2 release, nociceptor stimulation and contraction of the iris sphincter muscle in the rabbit. *Br. J. Pharmacol.*, **92**, 333–340.

GRIESBACHER, T. & LEMBECK, F. (1991). Bradykinin antagonists with high potency and long duration of action *in vivo*. *Naunyn-Schmiedebergs Arch. Pharmacol.*, **343**, R103.

GRIESBACHER, T., LEMBECK, F. & SARIA, A. (1989). Effects of the bradykinin antagonist B4310 on smooth muscles and blood pressure in the rat, and its enzymatic degradation. *Br. J. Pharmacol.*, **96**, 531–538.

HOCK, F.J., WIRTH, K., ALBUS, U., LINZ, W., GERHARDS, H.J., WIEMER, G., HENKE, S., BREIPOHL, G., KÖNIG, W., KNOLLE, J. & SCHÖLKENS, B.A. (1991). Hoe 140 a new potent and long acting bradykinin-antagonist: *in vitro* studies. *Br. J. Pharmacol.*, **102**, 769–773.

IMRIE, C.W., ALLAM, B.F. & FERGUSON, J.C. (1976). Hypocalcaemia of acute pancreatitis: the effect of hypoalbuminaemia. *Curr. Med. Res. Opin.*, **4**, 101–116.

JUAN, H. & LEMBECK, F. (1974). Actions of peptides and other algesic agents on paravascular pain receptors of the isolated perfused rabbit ear. *Naunyn-Schmiedebergs Arch. Pharmacol.*, **283**, 151–164.

KLÖPPEL, G., DREYER, T., WILLEMER, S., KERN, H.F. & ADLER, G. (1986). Human acute pancreatitis: its pathogenesis in the light of immunocytochemical and ultrastructural findings in acinar cells. *Virchows Arch.*, **A409**, 791–803.

LEMBECK, F., GRIESBACHER, T. & ECKHARDT, M. (1990). Demonstration of extrapulmonary activity of angiotensin converting enzyme in intact tissue preparations. *Br. J. Pharmacol.*, **100**, 49–54.

LEMBECK, F., GRIESBACHER, T., ECKHARDT, M., HENKE, S., BREIPOHL, G., & KNOLLE, J. (1991). New, long-acting, potent bradykinin antagonists. *Br. J. Pharmacol.*, **102**, 297–304.

NESS, T.J. & GEBHART, G.F. (1990). Visceral pain: a review of experimental studies. *Pain*, **41**, 167–234.

NUGENT, F.W. & ATENDIDO, W. (1966). Hemorrhagic pancreatitis. *Postgrad. Med.*, **40**, 87–94.

RAWSON, R.A. (1943). The binding of T-1824 and structurally related diazo dyes by plasma proteins. *Am. J. Physiol.*, **138**, 708–717.

RUUD, T.E., AASEN, A.O., KIERULF, P., STADAAS, J. & AUNE, S. (1985). Studies on the plasma kallikrein-kinin system in peritoneal exudate and plasma during experimental acute pancreatitis in pigs. *Scand. J. Gastroenterol.*, **20**, 877–882.

RYAN, J.W., MOFFAT, J.G. & THOMPSON, A.G. (1964). Role of bradykinin in the development of acute pancreatitis. *Nature*, **204**, 1212–1213.

SARIA, A. & LUNDBERG, J.M. (1983). Evans blue fluorescence: quantitative and morphological evaluation of vascular permeability in animal tissues. *J. Neurosci. Meth.*, **8**, 41–49.

SATAKE, K., ROZMANITH, J.S., APPERT, H. & HOWARD, J.M. (1973). Hemodynamic change and bradykinin levels in plasma and lymph during experimental actute pancreatitis in dogs. *Ann. Surg.*, **178**, 659–662.

SHARKEY, K.A., WILLIAMS, R.G. & DOCKRAY, G.J. (1984). Sensory substance P innervation of the stomach and pancreas; demonstration of capsaicin-sensitive sensory neurons in the rat by combined immunohistochemistry and retrograde tracing. *Gastroenterology*, **87**, 914–921.

SILVERMAN, M., ILRADI, C., BANK, S., KRANZ, V. & LENDVAI, S. (1989). Effects of the cholecystokinin receptor antagonist L-364,718 on experimental pancreatitis in mice. *Gastroenterology*, **96**, 186–192.

WERLE, E. (1970). Discovery of the most important kallikreins and kallikrein inhibitors. In *Bradykinin, Kallidin, and Kallikrein, Handbook of Experimental Pharmacology*, Vol. 25. ed. Erdös, E.G. pp. 1–6. Berlin, Heidelberg, New York: Springer.

WILLEMER, S., BIALEK, R., KÖHLER, H. & ADLER, G. (1990). Caerulein-induced acute pancreatitis in rats: changes in glycoprotein-compostion of subcellular membrane systems in acinar cells. *Histochemistry*, **95**, 87–96.

WIRTH, K., HOCK, F.J., ALBUS, U., LINZ, W., ALPERMANN, H.G., ANAGNOSTOPOULOS, H., HENKE, S., BREIPOHL, G., KÖNIG, W., KNOLLE, J. & SCHÖLKENS, B.A. (1991). Hoe 140 a new potent and long acting bradykinin-antagonist: *in vivo* studies. *Br. J. Pharmacol.*, **102**, 774–777.

WOODRUFF, G.N. & HUGHES, J. (1991). Cholecystokinin antagonists. *Annu. Rev. Pharmacol. Toxicol.*, **31**, 469–501.

ZAR, J.H. (1984). *Biostatistical Analysis*. 2nd ed. pp. 199–201. Englewood Cliffs, N.J.: Prentice–Hall.

(Received January 30, 1992
Accepted May 29, 1992)

Br. J. Pharmacol. (1992), **107**, 361–366

Nitric oxide synthase responsible for L-arginine-induced relaxation of rat aortic rings *in vitro* may be an inducible type

[1]Hideki Moritoki, Shougo Takeuchi, Tetsuhiro Hisayama & Wataru Kondoh

Department of Chemical Pharmacology, Faculty of Pharmaceutical Sciences, University of Tokushima, Shomachi, Tokushima 770, Japan

1 Characteristics of L-arginine-induced non-endothelial nitric oxide (NO) formation in rat isolated thoracic aorta were investigated.

2 Relaxation to L-arginine in arterial rings devoid of endothelium developed about 2 h after the first challenge with L-arginine and reached a maximum after a further 4 h of incubation.

3 After the arteries had relaxed in response to L-arginine, guanosine 3':5'-cyclic monophosphate (cyclic GMP) production was stimulated. In fresh arteries that had not yet relaxed in response to L-arginine, L-arginine failed to elevate cyclic GMP levels.

4 Glucocorticoids, actinomycin D and polymyxin B prevented the development of L-arginine-induced relaxation and L-arginine-stimulated increase in cyclic GMP formation.

5 Once L-arginine-induced relaxation developed, these agents no longer suppressed the relaxation and increase in cyclic GMP formation to L-arginine.

6 From these results, it is suggested that in the isolated thoracic aorta of the rat, endotoxin in the medium triggers induction of a non-endothelial NO synthase during prolonged incubation, which accelerates production of NO from added L-arginine to cause relaxation of the arteries via cyclic GMP. Glucocorticoids and protein synthesis inhibitors may prevent induction of NO synthase. It is suggested that the NO synthase mediating the production of muscle-derived NO from L-arginine is an inducible type.

Keywords: L-Arginine; relaxation; muscle-derived nitric oxide; glucocorticoid; protein synthesis inhibitors; polymyxin B; NO synthase induction

Introduction

Endothelium-derived relaxing factor (EDRF) is now thought to be either nitric oxide (NO) or a related NO-containing compound (Ignarro *et al.*, 1987; Palmer *et al.*, 1987) synthesized from the terminal guanidino nitrogen atom of L-arginine in the vascular endothelial cells (Palmer *et al.*, 1988; Schmidt *et al.*, 1988). We have previously shown that in the rat thoracic aorta, L-arginine induced relaxation and an increase in guanosine 3':5'-cyclic monophosphate (cyclic GMP) production, irrespective of whether the endothelium was present or absent (Moritoki *et al.*, 1990; 1991; Ueda *et al.*, 1990). The L-arginine-induced relaxation and cyclic GMP production were inhibited by N^G-nitro L-arginine (Moore *et al.*, 1990), N^G-monomethyl L-arginine (Hibbs *et al.*, 1987; Palmer *et al.*, 1988), N^G-nitro L-arginine methyl ester (Mülsch & Busse, 1990; Rees *et al.*, 1990b), haemoglobin (Martin *et al.*, 1985) and methylene blue (Gruetter *et al.*, 1981; Martin *et al.*, 1985). Therefore we have concluded that L-arginine-induced relaxation may be mediated by NO derived from vascular smooth muscles, but not the endothelium, and proposed that the NO thus formed be termed muscle-derived NO (MDNO). In addition, L-arginine-induced relaxation was detectable 2 h after the start of the experiments and increased progressively to reach a maximum in 6 h, suggesting the induction of NO synthesizing mechanisms.

In the present studies, we examined further the characteristics of L-arginine-induced, non-endothelial NO formation, with special reference to the type of NO synthase.

[1] Author for correspondence.

Methods

Organ bath experiments

Male Wistar rats of 8–9 weeks old (297 ± 15 g, $n = 15$) were used. The thoracic aortae were rapidly removed, freed of adhering fat and connective tissues, and cut into ring segments of 3 mm length with parallel razors. Each segment was set up in a 10 ml organ bath essentially by the method described by Bevan *et al.* (1975). Briefly, two stainless steel wires were inserted into the lumen of the aortic ring. One wire was connected to a transducer and the other U-shaped wire was anchored to a plastic holder. The holder was mounted on tissue bath filled with 10 ml Krebs solution gassed with 5% CO_2 in O_2. The solution had the following composition (mM): NaCl 115.3, KCl 4.9, $CaCl_2$ 2.5, $MgSO_4$ 1.2, KH_2PO_4 1.2, $NaHCO_3$ 25.0, disodium edetate (EDTA) 0.03, ascorbic acid 0.11 and glucose 11.1. To maintain constant responsiveness of the preparations in the prolonged studies, the experiments were carried out at 34°C. The arteries were equilibrated for 2 h before the start of the experiments at an optimal resting tension of 1.0 g for producing the largest response to phenylephrine; during this time phenylephrine was applied every 30 min to check tension development. Then L-arginine was applied cumulatively every 1 h to the arteries precontracted with phenylephrine.

To study relaxation, the arteries were precontracted with the EC_{80} concentration of phenylephrine (0.1 μM), and then L-arginine was added cumulatively in a volume of 7~20 μl. Responses were recorded isometrically.

For the removal of the endothelium, the lumen of the arteries were rubbed with cotton thread before setting up in an organ bath, and endothelial removal was confirmed by the loss of sensitivity to acetylcholine at the start and end of the experiments.

When examining the effects of protein synthesis inhibitors such as dexamethasone, the arterial segments were immersed in the medium containing these inhibitors immediately after isolation and throughout the experiments.

Assay of cyclic GMP

After confirming that the L-arginine-induced relaxation reached a constant level by application of 10 μM L-arginine at 60 min intervals, the preparations were incubated with the EC_{80} concentration of phenylephrine for 5 min. Then the preparations were transferred to the medium containing 10 μM L-arginine. After 1 min of incubation, the preparations were quickly frozen in liquid nitrogen, and the level of cyclic GMP was determined by radioimmunoassay with commercially available kits as previously described (Moritoki *et al.*, 1991).

Statistical analysis

The statistical significance of differences was analyzed by Student's unpaired *t* test, and *P* values of less than 0.05 were considered as significant. Values are expressed as means ± s.e.mean.

Materials

The materials used were L-arginine hydrochloride, dexamethasone acetate, prednisolone acetate, hydrocortisone acetate, polymyxin B sulphate, puromycin, actinomycin D, cycloheximide, phenylephrine hydrochloride, acetylcholine chloride, ATP and sodium nitroprusside (Sigma Chemical Co. Ltd., St Louis, Mo, U.S.A.), and kits for radioimmunoassay of cyclic GMP (Yamasa Shouyu Co. Ltd., Chohshi, Japan).

Results

L-arginine-induced, endothelium-independent relaxation

After equilibration of the endothelium-free rat thoracic aorta in Krebs solution for 2 h, L-arginine was applied repetitively every 1 h. The first application of L-arginine at concentrations of up to 300 μM did not induce relaxation. However, on the second application, relaxation to L-arginine did develop and thereafter increased time-dependently to reach a steady level on the 6th application (Figure 1).

Effects of glucocorticoids and other protein synthesis inhibitors on the L-arginine-induced relaxation

The arteries were immersed in the medium containing glucocorticoids or protein synthesis inhibitors immediately after they had been excised, and the compounds were present throughout the experiments. As shown in Figure 1, dexamethasone at a concentration of 1 μM prevented both development and time-dependent increase in L-arginine-induced relaxation; even 10 h after the start of the experiments, L-arginine did not relax the arteries (data not shown).

As shown in Figures 2 and 3, the glucocorticoids, hydrocortisone (1 μM) and prednisolone (3 μM), and the protein synthesis inhibitors, cycloheximide (10 μM), puromycin (1 μM) and actinomycin D (0.1 μM) had essentially similar inhibitory effects.

On the other hand, neither endothelium-dependent relaxations induced by acetylcholine and ATP, nor endothelium-independent relaxation induced by nitroprusside were affected by these compounds (data not shown). The EC_{50} values of acetylcholine in normal and dexamethazone (1 μM)-treated arteries were 60.0 ± 14.6 nM and 52.4 ± 6.0 nM (n = 5), respectively, and those of nitroprusside in normal

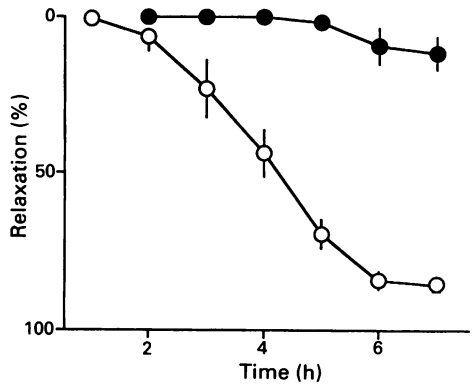

Figure 1 Prevention by dexamethasone of the time-dependent development of L-arginine-induced relaxation of endothelium-free rat thoracic aorta. The experiments were started after equilibration of the arteries for 2 h. The arteries were first contracted with 0.1 μM phenylephrine to produce tone, and then 10 μM L-arginine was applied every 60 min. Dexamethasone, when used, was added to the medium immediately after excision of the artery and also during the experiments. Relaxations are expressed as percentages of the contraction induced by the EC_{80} concentration of phenylephrine (0.1 μM). Abscissa scale indicates the time after the first challenge with L-arginine. (○) Control; (●) with 1 μM dexamethasone. Values are means for preparations from 5 rats; vertical lines show s.e.mean.

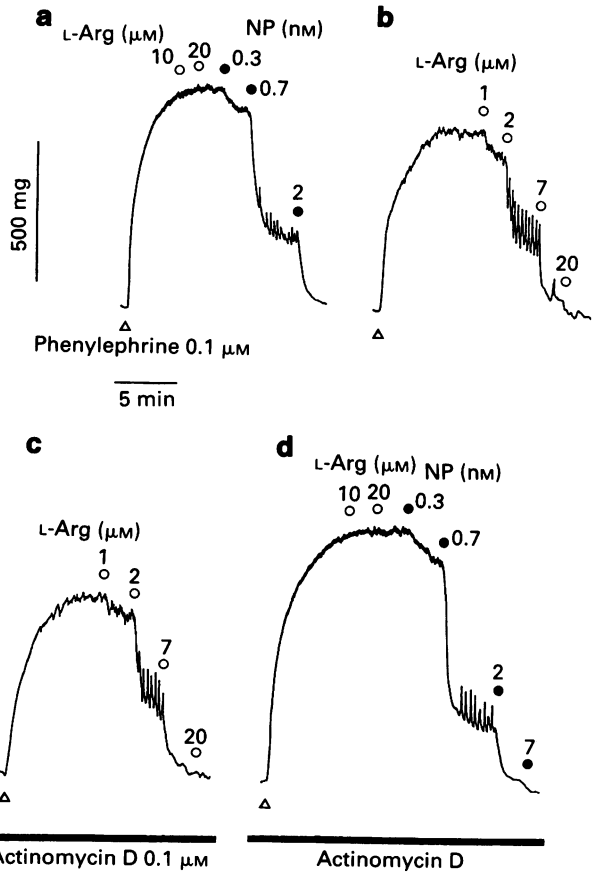

Figure 2 Typical tracings showing the effect of actinomycin D on the phenylephrine-induced contraction and L-arginine-induced relaxation. (a) At the start of the experiments, the aorta was contracted with 0.1 μM phenylephrine, and L-arginine (L-Arg) was applied; (b) 6 h after the start of the experiments, the response to L-arginine was determined. (c) After confirming that the aorta had relaxed fully in response to L-arginine, actinomycin D was applied for 4 h, then the effect of L-arginine was examined. (d) The arteries were treated with 0.1 μM actinomycin D immediately after the excision and throughout the experiments. Six hours after the start of the experiments, the aorta was contracted with 0.1 μM phenylephrine, and then the effects of L-arginine and nitroprusside (NP) were examined.

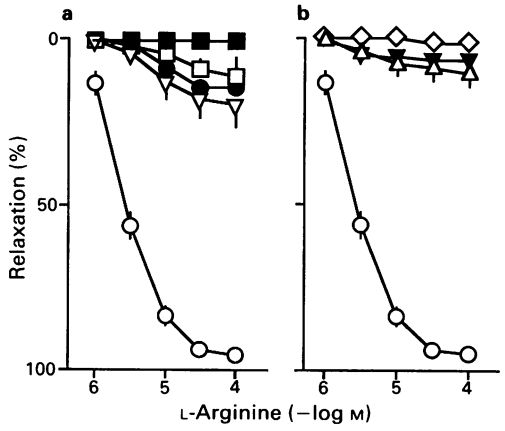

Figure 3 Preventive effects of glucocorticoids, polymyxin B, cycloheximide, actinomycin D and puromycin on the L-arginine-induced relaxation of endothelium-free rat thoracic aorta. Six hours after the start of the experiments, responses of the arteries to L-arginine were examined. L-Arginine was added cumulatively. Experimental conditions are as for Figures 1 and 2. (a) (○) Control; (▽) 1 μM dexamethasone; (□) 1 μM hydrocortisone; (●) 3 μM prednisolone; (■) 100 μM polymyxin B. (b) (◇) 0.1 μM Actinomycin D; (△) 10 μM cycloheximide; (▼) 1 μM puromycin. Values are means for preparations from 5 rats; vertical lines show s.e.mean.

and dexamethazone (1 μM)-treated arteries were 0.58 ± 0.08 nM and 0.62 ± 0.19 nM (n = 5), respectively.

Polymyxin B (100 μM) had an inhibitory effect essentially similar to actinomycin D on the development of L-arginine-induced relaxation (Figure 3).

Effect of dexamethasone on the phenylephrine-induced contraction

Six hours after the start of the experiments when the arteries had gained constant responsiveness to L-arginine, contraction induced by phenylephrine was slightly attenuated (Figures 2 and 4a). The time course of the change in tension development induced by 0.1 μM phenylephrine is shown in Figure 4b. Treatment with 1 μM dexamethasone throughout the experiments, besides suppressing the L-arginine-induced relaxation, prevented the time-dependent reduction of the contraction.

Essentially similar effects were observed with 0.1 μM actinomycin D and 1 μM cycloheximide, but these agents rather augmented, to some extent, the phenylephrine-induced contraction (Figure 4b).

Effects of dexamethasone and actinomycin D on cyclic GMP formation

L-Arginine stimulated cyclic GMP production in preparations that had relaxed in response to L-arginine (Figure 5). L-Arginine at a concentration of 10 μM increased cyclic GMP formation from the control level of 0.60 ± 0.14 pmol mg^{-1} protein to 4.87 ± 0.48 pmol mg^{-1} protein in 1 min (n = 6). However, in arteries that had failed to relax in response to L-arginine after treatment with 1 μM dexamethasone or 0.1 μM actinomycin D, L-arginine did not stimulate cyclic GMP formation.

On the other hand, endothelium-dependent cyclic GMP formation stimulated by ATP used as a reference was not affected by these inhibitors (data not shown).

Effects of dexamethasone and actinomycin D on the arteries sensitized to L-arginine

After confirming that the arteries had relaxed in response to L-arginine, glucocorticoids or actinomycin D were applied to the preparations for more than 4 h; then the effect of L-

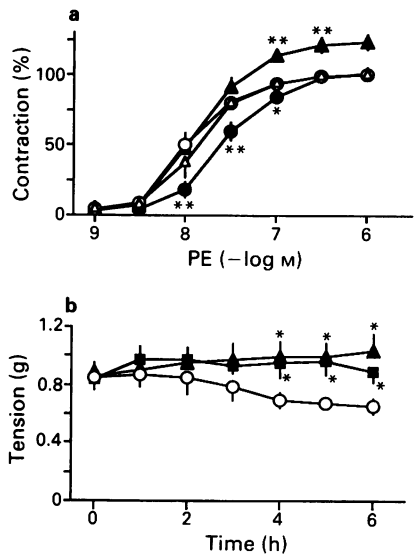

Figure 4 Time course of change in phenylephrine-induced contractions of rat thoracic aorta in the absence and presence of dexamethasone and actinomycin D. (a) Phenylephrine was cumulatively applied and the preparation was rinsed with fresh Krebs solution every 15 min. Actinomycin D, when used, was applied to another aorta immediately after excision, and present throughout the experiments. Phenylephrine-induced contractions were monitored every 60 min and the responses to phenylephrine at the first and 6th application were plotted. The responses of the arteries were determined at the start of the experiments in the absence (○) and presence (△) of actinomycin D. The responses of the arteries were determined 6 h after the start of the experiments in the absence (●) and presence (▲) of actinomycin D. (b) Contractions induced by 0.1 μM phenylephrine were plotted every 60 min, and expressed as g tension. Abscissa scale indicates time after the first challenge with L-arginine: (○) control; (■) with 1 μM dexamethasone; (▲) with 0.1 μM actinomycin D. Values are means for preparations from 5 rats; vertical lines show s.e.mean.
$^{*}P<0.05$; $^{**}P<0.01$ compared with respective control.

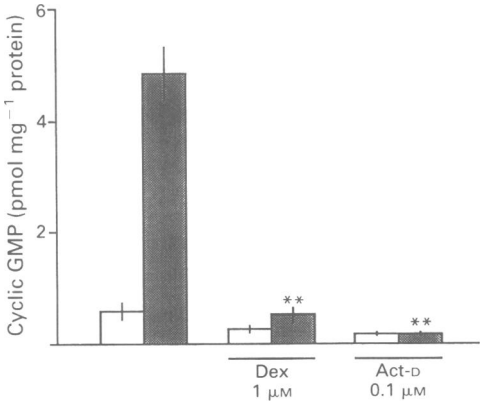

Figure 5 Preventive effects of dexamethasone and actinomycin D on the L-arginine-stimulated increase in cyclic GMP formation. The levels of cyclic GMP were measured after confirming that relaxation induced by 10 μM L-arginine had reached a steady level (6 h after the start of the experiments). The preparations were incubated with the EC_{80} concentration of phenylephrine (0.1 μM) for 5 min and then with 10 μM L-arginine. Amounts of cyclic GMP were determined in 1 min. Dexamethasone and actinomycin D, when used, were added immediately after isolation of the arteries and also throughout the experiments. Open columns, basal level of cyclic GMP; closed columns, cyclic GMP level in the presence of 10 μM L-arginine; underlined columns, cyclic GMP formation in the preparation treated with 1 μM dexamethasone (Dex) or 0.1 μM actinomycin D (Act-D). Columns represent means of values (n = 6) from 5 rats; vertical lines indicate s.e.mean.
$^{**}P<0.01$ compared with control value.

arginine was re-tested. In contrast to the preventative effects produced by prophylactic application of glucocorticoids and actinomycin D, treatment with these inhibitors after the preparation had gained responsiveness to L-arginine, no longer suppressed L-arginine-induced relaxation and L-arginine-stimulated increase in cyclic GMP formation (Figure 6 and see Figure 2).

Discussion

It has been known for many years that EDRF (NO) is produced in the endothelium in response to various agonists and causes the relaxation of vascular smooth muscle (Furchgott & Zawadzki, 1980). NO has also been demonstrated to play a regulatory role in various systems such as the central nervous system (Garthwaite *et al.*, 1988; Bredt & Snyder, 1989; Knowles *et al.*, 1989), non-adrenergic, non-cholinergic system (Gillespie *et al.*, 1989; Gibson *et al.*, 1990), and platelets (Radomski *et al.*, 1990). We have found that L-arginine induced endothelium-independent relaxation and an increase in cyclic GMP levels in rat thoracic aorta. Because L-arginine-induced responses were inhibited by the inhibitors of NO ~ cyclic GMP pathway, such as N^G-monomethyl L-arginine methyl ester, N^G-nitro L-arginine, haemoglobin and methylene blue, we have concluded that vascular smooth muscle also has the ability to produce NO and that L-arginine-induced responses were mediated by the muscle-derived NO (Moritoki *et al.*, 1990; 1991).

In the present studies, L-arginine-induced relaxation and L-arginine-stimulated increase in cyclic GMP formation in the aortic smooth muscle were found to be prevented by prophylactic treatment with protein synthesis inhibitors such as glucocorticoids, cycloheximide, actinomycin D and puromycin. Although these agents augmented slightly the phenylephrine-induced contraction, it seems unlikely that this enhanced tone counteracts the arginine-induced relaxation, and that these agents generally impair responsiveness of the aorta to contractile and relaxing agents, because relaxations induced by ATP, acetylcholine and nitroprusside were not affected by the protein synthesis inhibitors. In this respect, it has been reported that glucocorticoids prevented induction of NO synthesis in macrophages (Rosa *et al.*, 1990), vasculature (Knowles *et al.*, 1990; Rees *et al.*, 1990a; Smith *et al.*, 1991), cultured endothelial cells (Radomski, *et al.*, 1990) and renal mesangial cells (Pfeilschifter, 1991), and prevented time-dependent loss of phenylephrine-induced tone (Rees *et al.*, 1990a; Julou-Schaffer *et al.*, 1991). In addition, the protein synthesis inhibitor, cycloheximide (Busse & Mülsh, 1990; Rees *et al.*, 1990a; Fleming *et al.*, 1991; Jorens *et al.*, 1991; Mollace *et al.*, 1991), the inhibitor of RNA synthesis, actinomycin D (Lloyd *et al.*, 1987; Frasier-Scott *et al.*, 1988; Warner & Libby, 1989) and puromycin (Green *et al.*, 1990) blocked induction of NO synthase in macrophages and vascular smooth muscle cells.

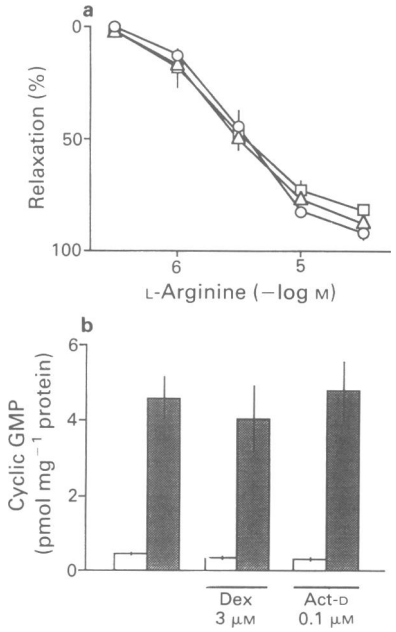

Figure 6 Failure of dexamethasone or actinomycin D to prevent inductions of L-arginine-evoked relaxation and L-arginine-stimulated formation of cyclic GMP in the endothelium-free arteries that had already been sensitized to L-arginine. Experimental conditions are as for Figures 1 and 3, except that dexamethasone was applied after confirming that the arteries had relaxed in response to L-arginine. (a) Shows L-arginine-induced relaxation: (○) control; (△) with 1 μM dexamethasone; (□) 0.1 μM actinomycin D. (b) Shows cyclic GMP formation: Open column, basal level of cyclic GMP; closed columns, cyclic GMP level induced by 10 μM L-arginine; underlined columns: L-arginine-induced cyclic GMP formation in the preparations treated with 3 μM dexamethasone (Dex) or 0.1 μM actinomycin D (Act-D). Columns represent means of values (n = 6) from 5 rats; vertical lines indicate s.e.mean.

Two types of enzymes responsible for biosynthesis of NO have been documented. One is a constitutive type which is localized in the endothelium, and the other is an inducible type found in macrophages (Marletta *et al.*, 1988; Stuehr *et al.*, 1989; Hiki *et al.*, 1990). The present findings are reminiscent of previous observations that a NO synthase is induced in the vascular smooth muscle cells in culture (Busse & Mülsch, 1990; Knowles *et al.*, 1990; Mollace *et al.*, 1991), that vascular smooth muscle cells produced NO in response to endotoxin (Fleming *et al.*, 1990; 1991) or interleukin-1β (French *et al.*, 1991) via the L-arginine ~ NO pathway, and that induction of the enzyme is inhibited by glucocorticoids (Knowles *et al.*, 1990; Rees *et al.*, 1990a) or cycloheximide (Busse & Mülsch, 1990; Mollace *et al.*, 1991; Fleming *et al.*, 1991; French *et al.*, 1991).

In addition, the fact that more than a few hours of incubation of the preparation with Krebs solution was necessary for L-arginine to induce relaxation and an increase in formation of cyclic GMP further supports the idea that the NO synthase mediating L-arginine-induced relaxation is an inducible type similar to that localized in macrophages (Stuehr & Marletta, 1987; Stuehr *et al.*, 1989: Jorens *et al.*, 1991).

On the basis of these observations it appears that L-arginine-induced responses are probably mediated by an inducible NO synthase localized in the vascular smooth muscle.

Moreover, the protein synthesis inhibitors were effective only when applied before the arteries were sensitized to L-arginine. Once L-arginine-induced relaxation had developed, these inhibitors could no longer prevent the relaxation. These results imply that once the enzyme is induced, the inhibitors are without effect, and further provide presumptive evidence for the idea that L-arginine-induced responses are mediated by inducible NO synthase in the vascular smooth muscle.

Polymyxin B, that binds to lipopolysaccharide and neutralizes its activity (Weinberg *et al.*, 1978; Danner *et al.*, 1989), has been reported to prevent spontaneous reduction of phenylephrine-induced tone possibly due to induction by lipopolysaccharide of an NO synthase (Rees *et al.*, 1990a). Similarly, in the present experiments, polymyxin B also prevented development of L-arginine-induced relaxation, suggesting the possible induction of an NO synthase by lipopolysaccharide contamination of the Krebs solution which has been noted (Rees *et al.*, 1990a).

It has been reported that phenylephrine-induced tone was time-dependently decreased due to induction of NO synthase, and thus NO (Rees *et al.*, 1990a). It is speculated that during prolonged incubation with phenylephrine, endotoxin is liberated into the bathing solution to accelerate induction of NO synthase. In our studies, however, the extent of the

reduction of phenylephrine-induced contraction was less than that previously reported. In our experimental conditions, however, replacement of the bathing solution every 15 min may minimize accumulation of endotoxin, which in turn reduces induction of NO synthase, thus resulting in less fade of phenylephrine-induced contraction. It is suggested, however, that even when phenylephrine-induced contraction was less affected, a small amount of induced NO synthase could produce sufficient amounts of NO when excess L-arginine was supplemented.

Recently, vascular endothelial cells in culture, besides having a constitutive NO synthase, has been shown to express an inducible NO synthase after activation with interferon-γ and lipopolysaccharide (Radomski *et al.*, 1990; Salvemini *et al.*, 1990), because the generation of NO in the endothelium was inhibited by cycloheximide and glucocorticoids (Radomski *et al.*, 1990). Possible induction of an NO synthase mediating L-arginine-induced vasorelaxation observed in the present experiments, does not represent the induction of the enzyme in the endothelium, because the L-arginine-induced relaxation and increase in cyclic GMP production were observable after removal of the endothelium. Nevertheless, in the endothelium-intact preparations, possible contribution of inducible NO synthase in the endothelium to the L-arginine-induced responses cannot be ruled out.

In summary, vascular smooth muscle can produce NO when excess L-arginine is present. The NO synthase responsible for L-arginine-induced relaxation and cyclic GMP formation is concluded to be of an inducible type. Further studies are needed to clarify the inducer(s) for the NO synthase mediating formation of muscle-derived nitric oxide (MDNO).

This work was in part supported by a Grant-in-Aid for Scientific Research C from the Ministry of Education, Science and Culture of Japan (63571045 and 03671054), The Fujisawa Foundation, and The Suzuken Memorial Foundation.

References

BEVAN, J.A., DUCKLES, S.P. & LEE, T.J-F. (1975). Histamine potentiation of nerve- and drug-induced responses of a rabbit cerebral artery. *Circ. Res.*, **36**, 647–653.

BREDT, D.S. & SNYDER, S.H. (1989). Nitric oxide mediates glutamate-linked enhancement of cGMP levels in the cerebellum. *Proc. Natl. Acad. Sci., U.S.A.*, **86**, 9030–9033.

BUSSE, R. & MÜLSCH, A. (1990). Induction of nitric oxide synthase by cytokines in vascular smooth muscle cells. *FEBS Lett.*, **275**, 87–90.

DANNER, R.L., JOINER, K.A., RUBIN, M., PATTERSON, W.H., JOHNSON, N., AYERS, K.M. & PARRILLO, J.E. (1989). Purification, toxicity, and antiendotoxin activity of polymyxin B nonapeptide. *Antimicrob. Agents Chemother.*, **33**, 1428–1434.

DI ROSA, M., RADOMSKI, M., CARNUCCIO, R. & MONCADA, S. (1990). Glucocorticoids inhibit the induction of nitric oxide synthase in macrophages. *Biochem. Biophys. Res. Commun.*, **172**, 1246–1252.

FLEMING, I., GRAY, G.A., JULOU-SCHAEFFER, G., PARRATT, J.R. & STOCLET, J-C. (1990). Incubation with endotoxin activates the L-arginine pathway in vascular tissue. *Biochem. Biophys. Res. Commun.*, **171**, 562–568.

FLEMING, I., GRAY, G.A., SCHOTT, C. & STOCLET, J-C. (1991). Inducible but not constitutive production of nitric oxide by vascular smooth muscle cells. *Eur. J. Pharmacol.*, **200**, 375–376.

FRASIER-SCOTT, K., HATZAKIS, H., SEONG, D., JONES, C.M. & WU, K.K. (1988). Influence of natural and recombinant interleukin-2 on endothelial cell arachidonate metabolism. Induction of de novo synthesis of prostaglandin H synthase. *J. Clin. Invest.*, **82**, 1877–1883.

FRENCH, J.F., LAMBERT, L.E. & SAGE, R.C. (1991). Nitric oxide synthase inhibitors inhibits interleukin-1β-induced depression of vascular smooth muscle. *J. Pharmacol. Exp. Ther.*, **259**, 260–264.

FURCHGOTT, R.F. & ZAWADZKI, V. (1980). The obligatory role of endothelial cells in the relaxation of arterial smooth muscle by acetylcholine. *Nature*, **288**, 373–376.

GARTHWAITE, J., CHARLES, S.L. & CHESS-WILLIAMS, R. (1988). Endothelium-derived relaxing factor release on activation of NMDA receptors suggests role as intracellular messenger in the brain. *Nature*, **336**, 385–388.

GIBSON, A., MIRZAZADEH, G., HOBBS, A.J. & MOORE, P.K. (1990). L-N^G-monomethyl arginine and L-N^G-nitroarginine inhibit non-adrenergic, non-cholinergic relaxation of the mouse anococcygeus muscle. *Br. J. Pharmacol.*, **99**, 602–606.

GILLESPIE, J.S., LIU, X. & MARTIN, W. (1989). The effects of L-arginine and N^G-monomethyl L-arginine on the response of the rat anococcygeus muscle to NANC nerve stimulation. *Br. J. Pharmacol.*, **98**, 1080–1082.

GREEN, E., TODD, B. & HEATH, D. (1990). Mechanism of glucocorticoid regulation of alkaline phosphatase gene expression in osteoblast-like cells. *Eur. J. Biochem.*, **188**, 147–153.

GRUETTER, C.A., KADOWITZ, P.J. & IGNARRO, L.J. (1981). Methylene blue inhibits coronary arterial relaxation and guanylate cyclase activation by nitroglycerin, sodium nitrite, and amyl nitrite. *Can. J. Physiol. Pharmacol.*, **59**, 150–156.

HIBBS Jr., J.B., TAINTOR, R.R. & VAVRIN, Z. (1987). Macrophages cytotoxicity: Role of L-arginine deiminase and imino nitrogen oxidation to nitrite. *Science*, **235**, 473–476.

HIKI, K., YUI, Y., HATTORI, R., EIZAWA, H., KOSUGA, K. & KAWAI, C. (1991). Three regulation mechanisms of nitric oxide synthase. *Eur. J. Pharmacol.*, **206**, 163–164.

IGNARRO, L.J., BUGA, G.M., WOOD, K.S., BYRNS, R.E. & CHAUDHURI, G. (1987). Endothelium-derived relaxing factor produced and released from artery and vein is nitric oxide. *Proc. Natl. Acad. Sci. U.S.A.*, **84**, 9265–9269.

JORENS, P.G., VAN OVERVELD, F.J., BULT, H., VERMEIRE, P.A. & HERMAN, A.G. (1991). L-Arginine-dependent production of nitrogen oxides by rat pulmonary macrophages. *Eur. J. Pharmacol.*, **200**, 205–209.

JULOU-SCHAEFFER, G., GRAY, G.A., FLEMING, I., SCHOTT, C., PARRATT, J.R. & STOCLET, J-C. (1990). Loss of vascular responsiveness induced by endotoxin involves L-arginine pathway. *Am. J. Physiol.*, **259**, H1038–1043.

KNOWLES, R.G., PALACIOS, M., PALMER, R.M.J. & MONCADA, S. (1989). Formation of nitric oxide from L-arginine in the central nervous system: A transduction mechanism for stimulation of the soluble guanylate cyclase. *Proc. Natl. Acad. Sci. U.S.A.*, **86**, 5159–5162.

KNOWLES, R.G., SALTER, M., BROOKS, S.L. & MONCADA, S. (1990). Anti-inflammatory glucocorticoids inhibit the induction by endotoxin of nitric oxide synthase in the lung, liver, and aorta of the rat. *Biochem. Biophys. Res. Commun.*, **172**, 1042–1048.

LLOYD, C.J., CARY, D.A. & MENDELSOHN, F.A. (1987). Angiotensin converting enzyme induction by cyclic AMP and analogues in cultured endothelial cells. *Mol. Cell. Endocrinol.*, **52**, 219–225.

MARLETTA, M.A., YOON, P.S., IYENGER, R., LEAF, C.D. & WISHNOK, J.S. (1988). Macrophage oxidation of L-arginine to nitrite and nitrate: nitric oxide is an intermediate. *Biochemistry*, **27**, 8706–8711.

MARTIN, W., VILLIANI, G.M., JOTHIANANDAN, D. & FURCHGOTT, R.F. (1985). Selective blockade of endothelium-dependent and glyceryl trinitrate-induced relaxation by hemoglobin and by methylene blue in the rabbit aorta. *J. Pharmacol. Exp. Ther.*, **232**, 708–716.

MOLLACE, V.M., SALVEMINI, D., ANGGARD, E. & VANE, J. (1991). Nitric oxide from vascular smooth muscle cells: regulation of platelet reactivity and smooth muscle cell guanylate cyclase. *Br. J. Pharmacol.*, **104**, 633–638.

MOORE, P.K., AL-SWAYEH, O.A., CHONG, N.W.S., EVANS, R.A. & GIBSON, A. (1990). L-N^G-nitro arginine (L-NOARG), a novel L-arginine-reversible inhibitor of endothelium-dependent vasodilatation *in vitro*. *Br. J. Pharmacol.*, **99**, 408–412.

MORITOKI, H., HISAYAMA, T. & UEDA, H. (1990). L-Arginine induces vasodilation by a mechanism involving nitric oxide formation. *Blood Vessels*, **27**, 48.

MORITOKI, H., UEDA, H., YAMAMOTO, H., HISAYAMA, T. & TAKEUCHI, S. (1991). L-Arginine induces relaxation of rat aorta possibly through non-endothelial nitric oxide formation. *Br. J. Pharmacol.*, **102**, 841–846.

MÜLSCH, A. & BUSSE, R. (1990). N^G-Nitro-L-arginine (N^5-[imino-(nitroamino)methyl]-L-ornithine) impairs endothelium-dependent dilations by inhibiting cytosolic nitric oxide synthesis from L-arginine. *Naunyn–Schmiedebergs Arch. Pharmacol.*, **341,** 143–147.

PALMER, R.M.J., ASHTON, D.S. & MONCADA, S. (1988). Vascular endothelial cells synthesize nitric oxide from L-arginine. *Nature*, **333,** 664–666.

PALMER, R.M.J., FERRIGE, A.G. & MONCADA, S. (1987). Nitric oxide release accounts for the biological activity of endothelium-derived relaxing factor. *Nature*, **327,** 524–526.

PFEILSCHIFTER, J. (1991). Anti-inflammatory steroids inhibit cytokine induction of nitric oxide synthase in rat renal mesangial cells. *Eur. J. Pharmacol.*, **195,** 179–180.

RADOMSKI, M.W., PALMER, R.M.J. & MONCADA, S. (1990). Glucocorticoids inhibit the expression of an inducible, but not the constitutive, nitric oxide synthase in vascular endothelial cells. *Proc. Natl. Acad. Sci. U.S.A.*, **87,** 10043–10047.

REES, D.D., CELLEK, S., PALMER, R.M.J. & MONCADA, S. (1990a). Dexamethasone prevents the induction by endotoxin of a nitric oxide synthase and the associated effects on vascular tone: an insight into endotoxin shock. *Biochem. Biophys. Res. Commun.*, **173,** 541–547.

REES, D.D., SCHULZ, R., HODSON, H.F., PALMER, R.M.J. & MONCADA, S. (1990b). Identification of some novel inhibitors of the vascular nitric oxide synthase *in vivo* and *in vitro*. In *Nitric Oxide from L-Arginine: a Bioregulatory System.* ed. Moncada, S. & Higgs, E.A. pp.485–487. Amsterdam: Elsevier.

SALVEMINI, D., KORBUT, R., ÄNGGÄRD, E. & VANE, J. (1990). Immediate release of a nitric oxide-like factor from bovine aortic endothelial cells by Escherichia coli lipopolysaccharide. *Proc. Natl. Acad. Sci. U.S.A.*, **87,** 2593–2597.

SCHMIDT, H.H.H.W., KLEIN, M.M., NIROOMAND, F. & BÖHME, E. (1988). Is arginine a physiological precursor of endothelium-derived nitric oxide? *Eur. J. Pharmacol.*, **148,** 293–295.

SMITH, R.E.A., PALMER, R.M.J. & MONCADA. S. (1991). Coronary vasodilatation induced by endotoxin in the rabbit isolated perfused heart is nitric oxide-dependent and inhibited by dexamethasone. *Br. J. Pharmacol.*, **104,** 5–6.

STUEHR, D.G., GROSS, S.S., SAKUMA, I., LEVI, R. & NATHAN, C.F. (1989). Activated murine macrophages secrete a metabolite of arginine with the bioactivity of endothelium-derived relaxing factor and the chemical reactivity of nitric oxide. *J. Exp. Med.*, **169,** 1011–1020.

STUEHR, D.G. & MARLETTA, M.A. (1987). Induction of nitrite/nitrate synthesis in murine macrophages by BCG infection, lymphokines, or interferon-γ. *J. Immunol.*, **139,** 518–525.

UEDA, H., YAMAMOTO, T., HISAYAMA, T. & MORITOKI, H. (1990). Possible mechanism of arginine-induced vasodilation. *Jpn. J. Pharmacol.*, **52,** 378p.

WARNER, S.J.C. & LIBBY, P. (1989). Human vascular smooth muscle cells, target for and source of tumor necrosis factor. *J. Immunol.*, **142,** 100–109.

WEINBERG, J.B., CHAPMAN, Jr., H.A. & HIBBS, Jr. J.B. (1978). Characterization of the effects of endotoxin on macrophage tumor cell killing. *J. Immunol.*, **121,** 72–80.

(Received January 31, 1992
Revised May 11, 1992
Accepted May 29, 1992)

Br. J. Pharmacol. (1992), **107**, 367–374

Activation of P_1- and P_{2Y}-purinoceptors by ADP-ribose in the guinea-pig taenia coli, but not of P_{2X}-purinoceptors in the vas deferens

[1]Charles H.V. Hoyle & Gareth A. Edwards

Department of Anatomy & Developmental Biology, University College London, Gower Street, London WC1E 6BT

1 The activity of adenosine 5'-diphosphoribose (ADP-ribose), a ribosylated purine nucleotide, was investigated on the carbachol-contracted taenia coli, a tissue possessing P_1- (A_2) and P_{2Y}-purinoceptors and on the guinea-pig vas deferens which possesses P_{2X}-purinoceptors.

2 In the vas deferens, where ATP (1 μM–1 mM) produced concentration-dependent contractions, ADP-ribose was without effect at concentrations up to 1 mM.

3 In the taenia coli, ADP-ribose (0.1 μM–1 mM) produced concentration-dependent relaxations with a potency similar to that of adenosine, but less than that of ATP. The pD_2 values for ADP-ribose, adenosine and ATP were 4.5 ± 0.07 (27), 4.4 ± 0.10 (9) and 5.5 ± 0.14 (21), respectively. The time-course of the relaxations elicited by ADP-ribose was found to be significantly longer than that for ATP and significantly shorter than that for adenosine.

4 The P_1-purinoceptor antagonist, 8-phenyltheophylline (5 μM), produced parallel rightward shifts in the concentration-response curves of the relaxations of the taenia coli elicited by ADP-ribose and adenosine but not ATP.

5 Dipyridamole (0.3 μM), a purine nucleoside uptake inhibitor, potentiated the responses to adenosine and ADP-ribose in the taenia coli. These potentiations were sensitive to 8-phenyltheophylline (5 μM).

6 Reactive blue 2, a P_{2Y}-purinoceptor antagonist, antagonized the inhibitory responses of ADP-ribose and ATP in the taenia coli, without significantly altering the inhibitory responses of either adenosine or noradrenaline.

7 In the presence of the potassium channel blocker, apamin (0.3 μM), the inhibitory responses of ADP-ribose were severely attenuated, and the inhibitory responses of ATP in the taenia coli were converted to transient contractions. Further addition of 8-PT blocked the residual responses of ADP-ribose.

8 The P_2-purinoceptor antagonist, suramin (500 μM), antagonized responses to ATP and ADP-ribose, but not adenosine. Further addition of 8-PT antagonized the residual responses to ADP-ribose, but not to ATP.

9 It is concluded that ADP-ribose has a mixed pharmacological profile, evoking both P_1 (A_2)-purinoceptor-mediated responses and P_{2Y}-purinoceptor-mediated responses, while being inert at P_{2X}-purinoceptors. It is suggested that ADP-ribose may provide a useful starting point for the generation of structural analogues which have specific activity at the P_{2Y}-purinoceptor.

Keywords: ADP-ribose; apamin; ATP; guinea-pig intestine; purinoceptors; reactive blue 2; smooth muscle; suramin; guinea-pig vas deferens

Introduction

Purine nucleosides and nucleotides have long been known to have potent extracellular actions on a variety of tissues. As early as 1929, Drury & Szent-György published findings of cardiac and vascular actions of adenine compounds. Since then, purine derivatives have also been shown to have potent pharmacological activity in many peripheral organs and the central nervous system. ATP has been proposed as the principle neurotransmitter from some non-adrenergic, non-cholinergic nerves and to be a co-transmitter with noradrenaline, acetylcholine and other substances (see Burnstock, 1972; 1976; 1990; Hoyle & Burnstock, 1991a).

Based on criteria of differences in relative agonist potencies, selective antagonism and differences in transduction mechanisms, Burnstock (1978) proposed that two types of purinoceptors could be distinguished: P_1- and P_2-purinoceptors. Both these classes of purinoceptors have subsequently been found not to be homogeneous groups and have been further subdivided (see Hoyle & Burnstock, 1991b). The P_1-purinoceptors, which have a relative agonist potency order of adenosine ≥ adenosine monophosphate (AMP) > adenosine diphosphate (ADP) ≥ adenosine 5'-triphosphate (ATP), have been divided into A_1 and A_2 subtypes (see Burnstock & Buckley, 1985), and a third subclass of P_1-purinoceptors, A_3 (Ribeiro & Sebastião, 1986; Sebestião & Ribeiro, 1988) has more recently been proposed.

P_2-purinoceptors, which have an agonist potency order of ATP ≥ ADP > AMP ≥ adenosine, were subdivided by Burnstock & Kennedy (1985), into P_{2X}- and P_{2Y}-purinoceptors, based largely on the rank order of agonist potency of structural analogues of ATP and also on the activity of antagonists at the P_{2X}-purinoceptor. The P_2-purinoceptor has been further subclassified (Gordon, 1986), with P_{2T}-purinoceptors, activated by ADP, suggested as being present only on thrombocytes and megakaryocytes, and P_{2Z}-receptors, activated by ATP^{4-}, mediating permeabilisation of mast cells and other blood cells.

It has been suggested that adenine dinucleotides, including

[1] Author for correspondence.

nicotinamide-adenine dinucleotide (NAD) and nicotinamide-adenine dinucleotide phosphate (NADP), might act on a receptor class distinct from P_1- and P_2-purinoceptors (Hoyle, 1990). Adenosine 5'-diphosphoribose (ADP-ribose) is chemically related to NAD and NADP, and NAD can be regarded as ADP-ribose covalently attached to the vitamin nicotinamide by a high energy β-N-glycosidic bond. ADP-ribose itself is an ADP moiety with a second ribose sugar attached to the β-phosphate via an esteric linkage. An increasing number of studies have provided evidence suggesting that mono/poly (ADP-ribose) may regulate the activities of a number of enzymes, either by covalent attachment to, or by physical association with, these enzymes (Hussain *et al.*, 1989). ADP-ribosylation of specific proteins is thought to occur in almost all forms of life and almost all compartments of the cell, and has been implicated in the control of a number of biological events (Hayaishi & Ueda, 1977; Ueda & Hayaishi, 1985). Although its intracellular roles have been widely researched, the pharmacological profile of ADP-ribose on extracellular receptors has not to our knowledge been evaluated.

Since ADP-ribose is an adenine nucleotide it was thought that it would be more likely to act upon P_2- than P_1-purinoceptors and therefore the tissues chosen for investigation were the guinea-pig vas deferens, which has P_{2X}-purinoceptors on the smooth muscle, and the taenia coli which possesses P_{2Y}-purinoceptors (Burnstock & Kennedy, 1985). The taenia coli also possesses P_1-purinoceptors of the A_2 subtype (Burnstock *et al.*, 1984).

Methods

Guinea-pig taenia coli

Male guinea-pigs, weighing between 300 and 600 g, were killed by a blow to the head and exsanguination. The ventral and medial taenia coli were dissected free. Segments, approximately 2 cm long, were suspended in 5 or 10 ml organ-baths containing modified Krebs solution of the following composition (mM): NaCl 133, KCl 4.7, NaH_2PO_4 1.4, $NaHCO_3$ 16.3, $MgSO_4$ 0.6, $CaCl_2$ 2.5 and glucose 7.7 (Bülbring, 1953). The organ-baths were constantly gassed with 95% O_2/5% CO_2 and the organ-baths and reservoirs of Krebs solution were maintained at 36–37°C.

The strips of taenia coli were initially loaded with a tension of 1 g and were then allowed to equilibrate for approximately 45 min, with the bathing solution being changed every 15 min. Contractions were recorded by either a Dynamometer UF1 or Grass FTOC3 force-displacement transducer, and displayed on a Grass 79D polygraph.

Carbachol (100 nM) was used to induce a sustained submaximal (approximately 80%) contraction upon which the relaxant effects of the test drugs were demonstrable. When the maximal relaxation due to the applied drug had been observed, the organ-bath was washed several times with fresh Krebs solution. After 7–10 min, carbachol was re-added and the next concentration of the drug tested. The drugs were usually tested in multiples of 1 and 3 decades of concentration units; intermediate concentrations were tested in those cases where there was a steep concentration-response relationship. This was carried out in a range of concentrations from below the threshold for observable response to maximal response or a maximal organ-bath concentration of 1 mM (or 0.5 mM in the case of adenosine).

When dipyridamole, 8-phenyltheophylline (8-PT) or reactive blue 2 (RB2) were used, the agent was added to the stock of Krebs solution and the preparations were allowed to equilibrate for 30 min. Apamin was added directly to the organ-bath and allowed to equilibrate for minimum of 20 min.

Responses to ADP-ribose, ATP and noradrenaline were tested first in the absence of RB2 and then compared with responses on the same preparations in the presence of RB2. Since RB2 tends to have a general desensitizing action on all drugs responses beyond a period of about 2 h (Burnstock & Warland, 1987), only one non-cumulative concentration-response curve was performed on each preparation once RB2 had been added to the organ-bath.

Because of the limited availability of suramin, and the relatively high concentrations that are needed, full concentration-response relationships were not determined in its presence. Instead, concentrations of agonists that produced approximately a 50% relaxation under control conditions were tested following incubation of the preparation in suramin for 30 min, and again in the additional presence of 8-PT. Also, because full concentration-relaxation relationships for ADP-ribose could not be obtained in the presence of apamin, in one series of experiments concentrations of ADP-ribose that produced approximately 50% relaxations in the control situation were tested in the presence of apamin, and again in the additional presence of 8-PT.

Guinea-pig vas deferens

Male guinea-pigs, weighing between 300 and 600 g were killed by a blow to the head and exsanguination, their abdomens were opened and the vasa deferentia removed. Segments, 2 cm long, were suspended in 5 or 10 ml organ-baths containing modified Krebs solution (as described above). The organ-baths were constantly gassed with 95% O_2/5% CO_2 and were maintained at 36–37°C.

The preparations were allowed to equilibrate for at least 30 min under a resting tension of approximately 1 g, with the bathing solution being changed every 15 min. Contractile responses were recorded as described above. Concentration-response curves were obtained following the non-cumulative addition of ATP in a range from below the threshold of observable response to 1 mM. The concentrations tested were in multiples of 1 and 3 decades of concentration units. For ADP-ribose a range of concentrations between 1 μM and 1 mM were tested in a non-cumulative manner. After the maximal response to the applied drug had been observed, the organ bath was washed several times with fresh Krebs solution and 7–10 min were allowed before the next application of a drug.

A series of experiments was carried out in order to assess possible effects of ADP-ribose on the response to ATP. Having established a concentration-response relationship of ATP on a preparation, ADP-ribose (1 μM–1 mM) was added to the organ-bath and after an interval ranging from 2 to 22 min ATP was again tested.

Drugs used

Adenosine 5'-diphosphoribose, adenosine 5'-triphosphate (sodium salt), adenosine hemisulphate, noradrenaline ((±)-L-arterenol bitartrate), apamin, 8-phenyltheophylline and reactive blue 2 (Cibracron blue 3GA) were all obtained from Sigma. Dipyridamole (Persantin) was supplied by Boehringer Ingelheim. 8-Phenyltheophylline was dissolved in 80% v/v methanol/20% molar NaOH to produce a stock solution of 10 mM; noradrenaline was dissolved in 0.1 mM ascorbic acid to produce a stock solution of 10 mM and adenosine was dissolved in Krebs solution to give a stock of 10 mM; subsequent dilutions of all three drugs were in distilled water. In order to obtain an organ-bath concentration of 0.5 mM, 500 μl of the adenosine stock was added to the 10 ml organ-bath, while other additions were of 30 μl or 100 μl. All other drugs were made up in distilled water to produce stock solutions so that additions to the 10 ml organ-bath were 30 μl or 100 μl, and those to the 5 ml organ-baths were 15 μl or 50 μl.

Analysis of results

In the experiments on the taenia coli, responses were calculated as the percentage reduction of the carbachol-induced contraction. The mean response of the preparations from each animal was calculated at each concentration of the test-drug used. These mean responses for each animal were then subjected to a probit transformation (Bliss, 1935; Finney, 1971) which converts the sigmoidal log-concentration curve to a straight line. Linear regression of the probit values against log concentration was then carried out in order to interpolate the log-concentrations yielding 1, 5, 10, 20, 35, 50, 65, 80, 90, 95 and 99% responses (Hoyle & Greenberg, 1988). The means and standard errors of the log concentrations for each of these percentage points were calculated and used to plot the summed concentration-response curve. This method averages the concentration-response curve horizontally and therefore avoids a bias towards a lower slope (see Waud, 1975). Since the range of response from 1–99% is used, this method is also more informative than taking the mean of linear regression over the 20–80% portion of the concentration-response curve.

In the experiments where dipyridamole, 8-PT or RB2 were used, the means and the standard errors of the pD_2 values (negative logarithm of EC_{50}) were calculated from the concentration-response relationships and were then used in Student's paired t tests. The slopes of the concentration-response curves in the presence of an agent were also compared with the control curves by paired t tests.

In the experiments with apamin, maximal relaxation of the carbachol-contraction in response to ADP-ribose was not attained at the concentrations tested. Analysis by the method outlined above was therefore inappropriate; the results were analysed by Students paired t test of the mean relaxant responses produced by ADP-ribose at concentrations of 10 μM, 30 μM and 100 μM.

Measurements of the time to reach maximum response were made for responses to ATP, adenosine and ADP-ribose at approximately their EC_{50} concentrations in the control experiments. Such measurements were also made in the presence of dipyridamole (0.3 μM), which is an inhibitor of nucleoside uptake (Kolassa *et al.*, 1970).

In experiments on the vas deferens the responses to the drugs were expressed relative to the response elicited by the administration of ATP (1 mM). The means and standard errors of the average response of the preparations from each animal for each concentration applied were calculated

In the text, values are presented as mean ± s.e.mean with the number of replicates given in parentheses. When mulitiple comparisons were made, analysis of variance followed by Tukey's procedure was used. For all tests a probability level of 0.05 or less was considered significant.

Table 1 Carbachol-contracted guinea-pig taenia coli: pD_2 values of the inhibitory responses of ADP-ribose, ATP, noradrenaline (NA) and adenosine, and the effects of 8-phenyltheophylline (8-PT), dipyridamole (Dip), and reactive blue 2 (RB2)

Agents	$pD_2 \pm$ s.e. (n)
ADP-ribose	4.50 ± 0.07 (27)
ADP-ribose + 5 μM 8-PT	4.12 ± 0.07 (7)*
ADP-ribose + 0.3 μM Dip	5.54 ± 0.24 (4)*
ADP-ribose + 0.3 μM + 5 μM 8-PT	4.31 ± 0.10 (4)*
ADP-ribose + 30 μM RB2	3.96 ± 0.17 (7)*
ATP	5.50 ± 0.14 (21)
ATP + 5 μM 8-PT	5.39 ± 0.15 (7)
ATP + 30 μM RB2	4.59 ± 0.16 (9)*
Adenosine	4.40 ± 0.10 (9)*
Adenosine + 5 μM 8-PT	3.69 ± 0.08 (5)
Adenosine + 0.3 μM Dip	5.84 ± 0.22 (4)*
Adenosine + 0.3 μM Dip + 5 μM 8-PT	4.67 ± 0.16 (4)*
NA	6.50 ± 0.34 (7)
NA + 30 μM RB2	6.20 ± 0.12 (7)

*$P<0.05$, paired t test against control

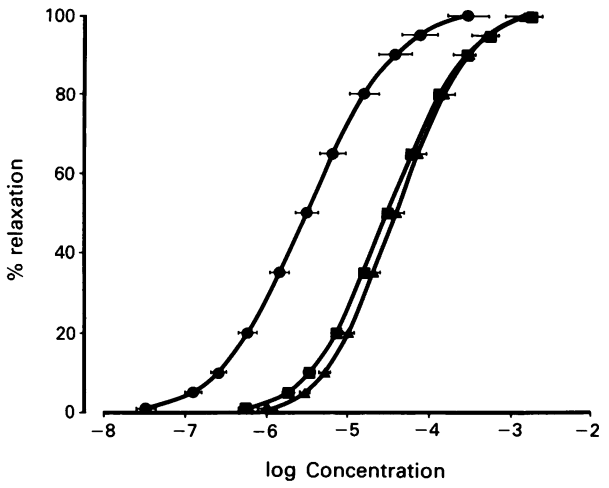

Figure 1 Concentration-response curves for ATP (●, $n = 21$), ADP-ribose (■, $n = 27$) and adenosine (▲, $n = 9$) in causing relaxation of carbachol-contracted guinea-pig taenia coli. The points represent the mean and the horizontal lines the s.e.mean.

Results

Guinea-pig taenia coli

The results of the experiments carried out on the taenia coli are summarised in Tables 1 and 2.

ADP-ribose, in a concentration range of 0.1 μM to 1 mM, produced concentration-dependent relaxations of the carbachol-contracted taenia coli with a pD_2 value of 4.50 ± 0.07 (27). ATP (0.03 μM–1 mM) produced concentration-dependent relaxations with a pD_2 value of 5.50 ± 0.14 (21). Adenosine (0.3 μM–500 μM) produced concentration-dependent relaxations with a pD_2 value of 4.40 ± 0.10 (9). The concentration-response curves for ADP-ribose, ATP and adenosine are illustrated in Figure 1.

The time taken for the peak response to half-maximal concentrations of ATP, adenosine and ADP-ribose to develop were all significantly different from one another, with mean times (s) to reach maximum response being 9 ± 1 (21) for ATP, 14 ± 1 (27) for ADP-ribose, and 21 ± 3 (9) for adenosine.

Effects of 8-phenyltheophylline

The effects of 8-PT (5 μM) on the concentration-response relationships for adenosine, ADP-ribose and ATP are shown in Figure 2.

8-PT (5 μM) produced significant rightward shifts in the concentration-response curves of both adenosine and ADP-ribose, with the pD_2 value of adenosine being reduced from 4.34 ± 0.15 to 3.69 ± 0.08 (5) ($P<0.01$) and the pD_2 value of ADP-ribose being reduced from 4.47 ± 0.05 to 4.12 ± 0.07 (7) ($P<0.01$). The shift in the pD_2 value for adenosine was significantly greater than that for ADP-ribose ($P<0.01$). No significant change was found in the slope of the concentration-response curves for either drug in the presence of 8-PT.

For ATP no significant changes were found in either the

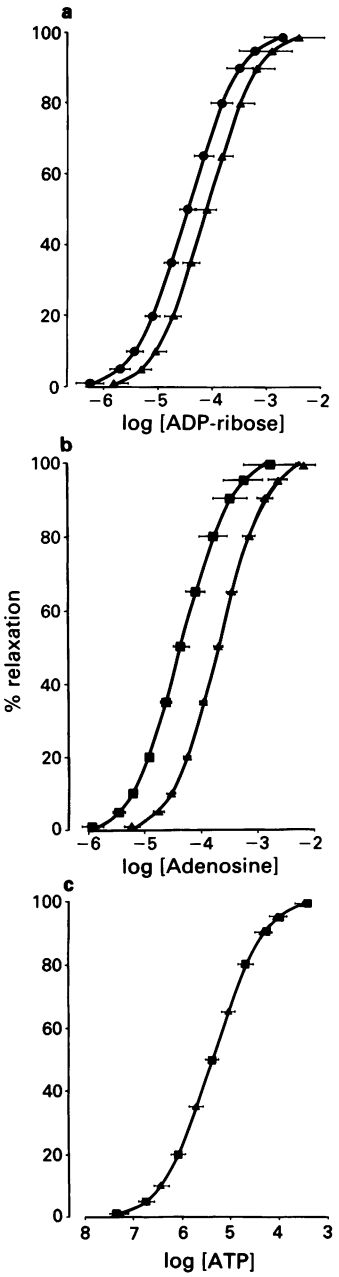

Figure 2 Effect of 8-phenyltheothylline (8-PT, 5 μM) on the inhibitory responses of carbachol-contracted guinea-pig taenia coli to ADP-ribose, adenosine and ATP. Concentration-response curves are shown for (a) ADP-ribose prior to administration of 8-PT (●) and in the presence of 8-PT (▲) ($n = 7$); (b) adenosine prior to administration of 8-PT (■) and in the presence of 5 μM 8-PT (▲) ($n = 5$); and (c) ATP prior to administration of 8-PT (■) and in the presence of 8-PT (▲) ($n = 7$). The points represent the mean and the horizontal lines the s.e.mean.

pD_2 values, which altered from 5.39 ± 0.15 to 5.39 ± 0.17 (7), or the slope of the concentration-response curve, in the presence of 8-PT.

Effects of dipyridamole

In the presence of dipyridamole (0.3 μM) no observable changes in the levels of spontaneous activity or the sensitivity of the taenia preparations to carbachol were noted. The effects of dipyridamole (0.3 μM), and 8-PT (5 μM) in the presence of dipyridamole (0.3 μM), on the concentration-response relationships for ADP-ribose and adenosine are shown in Figure 3. Relaxant responses evoked by ATP were

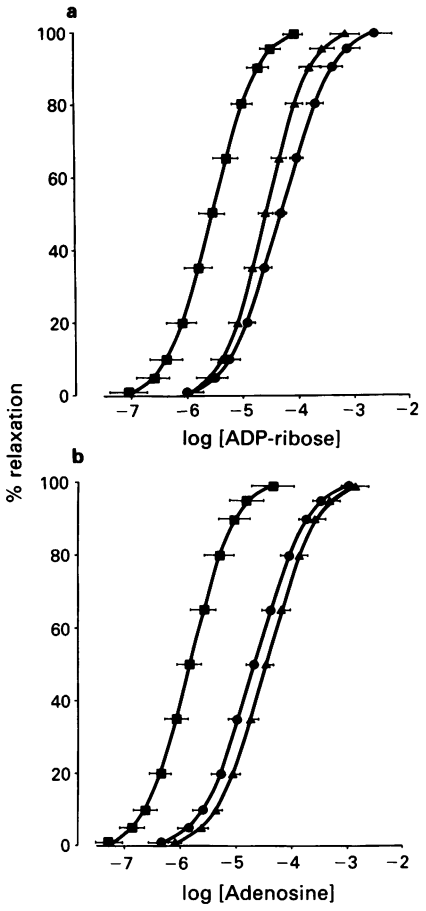

Figure 3 Effects of dipyridamole (0.3 μM) and 8-phenyltheophylline (8-PT, 5 μM) in the presence of dipyridamole on the inhibitory responses of carbachol-contracted guinea-pig taenia coli to ADP-ribose and adenosine. Concentration-response curves are shown for (a) ADP-ribose in the absence of dipyridamole and 8-PT (▲), in the presence of dipyridamole (■), and in the presence of dipyridamole plus 8-PT (●); and (b) adenosine in the absence of dipyridamole and 8-PT (▲), in the presence of dipyridamole (■), and in the presence of dipyridamole plus 8-PT (●). The points represent the mean and the horizontal lines the s.e.mean.

unaffected by dipyridamole (0.3 μM). In the absence and presence of dipyridamole the pD_2 values for ATP were 5.44 ± 0.10 (4) and 5.44 ± 0.15 respectively. There was no significant difference between the slopes of the concentration-response relationships.

The concentration-response curves of both adenosine and ADP-ribose were significantly shifted to the left in the presence of dipyridamole (0.3 μM). The pD_2 value of adenosine increased from 4.48 ± 0.15 to 5.84 ± 0.22 (4) ($P < 0.001$), while that of ADP-ribose shifted from 4.59 ± 0.13 to 5.54 ± 0.24 (4) ($P < 0.02$). The shift in the pD_2 value for adenosine was significantly greater than that for ADP-ribose ($P < 0.01$). No significant changes were found in the slopes of the concentration-response curves for either drug in the presence of dipyridamole (0.3 μM).

In the presence of dipyridamole (0.3 μM), 8-PT (5 μM) produced rightward shifts in the concentration-response curves of adenosine and ADP-ribose. The pD_2 values of adenosine was significantly reduced from 5.84 ± 0.22 to 4.67 ± 0.16 (4) ($P < 0.01$) and the pD_2 value of ADP-ribose was reduced from 5.54 ± 0.24 to 4.31 ± 0.10 (4) ($P < 0.01$). The shift in the pD_2 value for adenosine in the presence of dipyridamole, produced by 8-PT, was not significantly different from that for ADP-ribose. No significant changes were found in the slopes of the concentration-response curves for either agonist.

Analysis of the responses to EC_{50} concentrations of adenosine showed a significant lengthening of the time to reach maximal response in the presence of dipyridamole (0.3 μM). Prior to the addition of dipyridamole the time taken to reach maximal response for adenosine was 23 ± 6 s (4), while in the presence of dipyridamole, adenosine (EC_{50} value) brought about a response taking a mean of 57 ± 10 s (4) ($P<0.05$). A significant change was also found in the time to reach maximal response to ADP-ribose (EC_{50} value), taking a mean of 13 ± 2 s to reach maximal response in the control experiments, and 24 ± 6 s (4) ($P<0.05$) to reach a maximal response in the presence of dipyridamole.

Effects of apamin

In the presence of apamin (0.3 μM) a considerable increase in the frequency and magnitude of spontaneous activity of the taenia preparations was seen, although the magnitude of the contractions elicited by carbachol (0.1 μM) was not significantly affected. At low concentrations of ATP (1–30 μM) the normal inhibitory responses were greatly reduced or abolished. At higher concentrations of ATP (100 μM–1 mM), the normal inhibitory responses were converted to transient contractions.

The inhibitory responses induced by ADP-ribose at 10 μM, 30 μM and 100 μM were significantly reduced in the presence of apamin (0.3 μM), but contractile responses were not unmasked. The mean percentage relaxation induced by ADP-ribose at 10 μM was significantly reduced from 22.8 ± 5.1% to 4.7 ± 2.0% (9) ($P<0.01$), while relaxations to ADP-ribose at 30 μM were reduced from 44.4 ± 9.2% to 13.1 ± 3.0% (9) ($P<0.01$) and relaxations to ADP-ribose at 100 μM were reduced from 70.9 ± 8.0% to 19.7 ± 5.0% (9) ($P<0.001$). In a further series of experiments, when the concentration of ADP-ribose was adjusted to produce a near 50% relaxation (log [ADP-ribose] = 4.5 ± 0.20 (4), which produced a relaxation of 50.4 ± 2.47%), apamin (0.3 μM) reduced this response to 15.7 ± 4.3%, and further incubation with 8-PT (5 μM) caused the relaxant response to be reduced to 1.0 ± 4.0%. The effects of both apamin and 8-PT were significant ($P<0.01$ and $P<0.05$, respectively).

Effects of reactive blue 2

In the presence of RB2 (30 μM) no effect was seen on the carbachol-induced contractions of the strips of taenia coli. The effects of RB2 (30 μM) on the concentration-response relationships for ADP-ribose, ATP and noradrenaline are illustrated in Figure 4.

At a concentration of 30 μM, RB2 produced a significant rightward shift in the ADP-ribose concentration-response curve, reducing the pD_2 value from 4.41 ± 0.19 to 3.96 ± 0.17 (7) ($P<0.02$). The slope of the ADP-ribose concentration-response curve was not significantly altered.

The concentration-response curve of ATP was also subjected to a rightward parallel shift in the presence of RB2 (30 μM), with the pD_2 value being reduced from 5.52 ± 0.25 to 4.59 ± 0.16 (9) ($P<0.01$) in the presence of RB2 (30 μM). No significant differences were found in the slopes of these concentration-response curves.

No significant change was seen in the slope or the pD_2 values of the concentration-response curves for either adenosine or noradrenaline in the presence of RB2 (30 μM). For adenosine the pD_2 values in the absence and presence of RB2 were 4.56 ± 0.05 (6) and 4.60 ± 0.07, respectively. For noradrenaline, in the absence of RB2 the pD_2 was 6.49 ± 0.12 (7), compared with a value of 6.20 ± 0.12 in presence of RB2.

Effects of suramin

The effects of suramin (500 μM) on responses to adenosine, ATP and ADP-ribose are summarised in Table 2. Suramin had no significant effect on the relaxant responses to adenosine, but significantly reduced the responses evoked by ATP and ADP-ribose. Further addition of 8-PT (5 μM) antagonized the responses to adenosine, did not significantly affect the residual responses to ATP, but significantly inhibited the residual responses to ADP-ribose (Table 2).

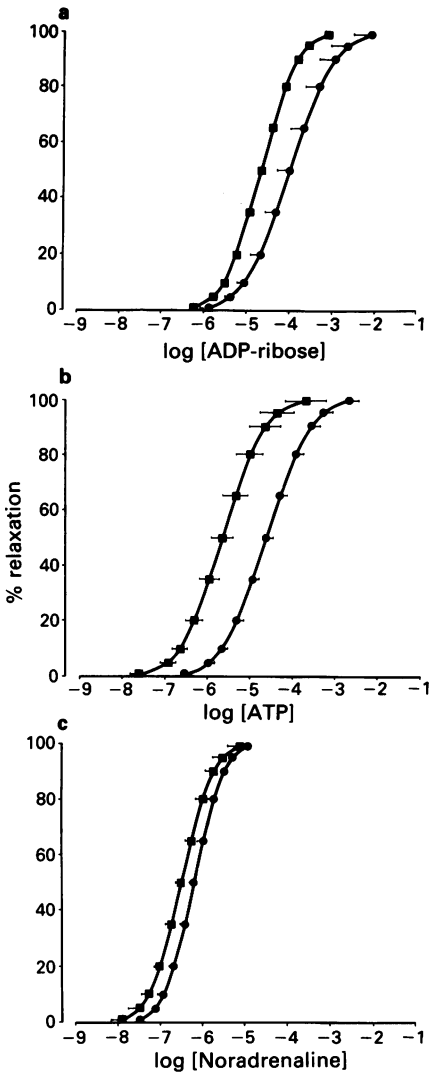

Figure 4 Effect of reactive blue 2 (RB2, 30 μM) on the inhibitory responses of carbachol-contracted guinea-pig taenia coli to ADP-ribose. Concentration-response curves are shown for (a) ADP-ribose in the absence of RB2 (■) and in the presence of RB2 (●) ($n = 7$); (b) ATP in the absence of RB2 (■), and in the presence of RB2 (●) ($n = 9$); and (c) noradrenaline in the absence of RB2 (■), and in the presence of RB2 (●) ($n = 7$). The points represent the mean and the horizontal lines the s.e.mean.

Guinea-pig vas deferens

ATP, tested in a range of concentrations of 1 μM to 1 mM, produced concentration-dependent transient contractions in the guinea-pig vas deferens. The mean increase in tension elicited by ATP at 1 mM was 1.50 ± 0.49 g (7). ADP-ribose in a range of concentrations from 1 μM to 1 mM failed to produce any observable change in the tension of the vas deferens preparations.

There were no changes in the response of the vas deferens preparations to ATP when ADP-ribose, at various concentrations from 1 μM to 1 mM, was allowed to incubate in the organ-baths for various times from 2–22 min prior to administration of ATP.

Table 2 Effects of suramin (500 μM), alone and in combination with 8-phenyltheophylline (8-PT, 5 μM) on the relaxant responses to adenosine, ATP and ADP-ribose in the carbachol-contracted guinea-pig taenia coli

		Relaxation (%)		
Agonist	*−log(conc)*	*Control*	*+Suramin*	*+Suramin and 8-PT*
Adenosine	4.4 ± 0.13	55.3 ± 5.78	56.2 ± 12.01	6.8 ± 1.39[a]
ATP	5.6 ± 0.24	55.9 ± 7.10	15.5 ± 9.24[b]	8.6 ± 3.35
ADP-ribose	4.4 ± 0.06	58.2 ± 7.57	35.7 ± 8.25[b]	1.7 ± 1.73[a]

Data are given as mean ± s.e.mean, from at least four animals. The concentration of the agonists (first column) that produced approximately a 50% relaxation of the carbachol-contracted taenia coli were subsequently tested in the presence of suramin (500 μM), and in the presence of suramin plus 8-PT (5 μM). Statistical significances were (paired Student's *t* tests): [a]$P<0.05$ versus suramin; [b]$P<0.05$ versus control.

Discussion

The results from the experiments on the taenia coli show that ADP-ribose is pharmacologically active in this tissue, producing concentration-dependent relaxations with a potency similar to that of adenosine. The antagonism of the inhibitory responses to ADP-ribose by 8-PT (5 μM) indicates that these responses, at least in part, are mediated through P_1-purinoceptors.

The potentiation of the action of adenosine on the guinea-pig taenia coli by dipyridamole (0.3 μM) and the antagonism by 8-PT, found in this study is consistent with previous studies (Satchell *et al.*, 1972; Satchell & Burnstock, 1975; Burnstock *et al.*, 1984). The potentiation of the inhibitory actions of ADP-ribose by dipyridamole indicates that ADP-ribose might have been degraded to adenosine which contributed to the overall response. The potentiation of ADP-ribose by dipyridamole and the sensitivity to 8-PT strongly indicate that adenosine, from some source or other, was involved in the overall response.

The extracellular catabolism of adenine nucleotides is thought to occur by sequential stepwise degradation such that ATP is catabolized to ADP then to AMP, and then to adenosine with at least three enzymes being involved (Gordon, 1986; Fleetwood *et al.*, 1989; Culic *et al.*, 1990). The final common ectoenzyme in the conversion of adenine 5'-nucleotides to adenosine is 5'-nucleotidase, which is thought to be exclusively localized on the extracellular face of the plasma membrane (De Pierre & Karnovsky, 1974). All of the naturally occurring ribo- and deoxyribo-nucleotide 5'-monophosphates are substrates of 5'-nucleotidase, while nucleotide 5'-diphosphates and -triphosphates are not substrates of the enzyme, but do inhibit it (Burger & Lowenstein, 1970).

If the degradation of ADP-ribose to adenosine occurs as a result of the actions of the same ectoenzymes that are thought to act on ATP to produce adenosine, resulting in the ability of dipyridamole to potentiate ADP-ribose, it is strange that in the absence of dipyridamole the actions of ADP-ribose were antagonized by 8-PT while those of ATP were not, and that dipyridamole did not potentiate ATP.

Alternatively, indirect activation of P_1-purinoceptors by ADP-ribose could be brought about by the evoked release of purine compounds from the muscle itself. Nucleotides and dinucleotides have been shown to be able to induce release of labelled adenosine from rodent vas deferens (Stone, 1981), and it is possible that a similar mechanism could occur in the taenia coli. Further experiments are needed to determine whether or not ADP-ribose evokes release of adenosine from the guinea-pig taenia coli.

The findings of increased spontaneous activity, the reduction of inhibitory responses to ATP and the appearance of contractile responses to ATP in the presence of apamin (0.3 μM) are consistent with the findings of other studies (Banks *et al.*, 1979; Maas & Den Hertog, 1979; Maas *et al.*, 1980; Brown & Burnstock, 1981; Fedan *et al.*, 1984). That the inhibitory responses to ADP-ribose were strongly attenuated by apamin indicates that for at least part of its action ADP-ribose shares characteristics associated with activation of P_2-purinoceptors rather than P_1-purinoceptors. Although apamin antagonizes P_2-purinoceptor-mediated activity, it is not specific for this receptor type since its mechanism involves the blocking of calcium-dependent potassium channels. Thus, an action of ADP-ribose on P_2-purinoceptors cannot be definitely concluded from the results with apamin alone. However, it is known that apamin does not antagonize the activity of adenosine on the guinea-pig taenia coli (Brown & Burnstock, 1981); thus it can be said that the activity of ADP-ribose cannot be solely limited to activation of adenosine receptors.

Further evidence for the involvement of P_2-purinoceptors in the action of ADP-ribose on the taenia coli comes from the experiments carried out with RB2 and suramin. The antagonism of the inhibitory responses to ATP but not to adenosine or noradrenaline in the presence of RB2 is consistent with the findings of Burnstock *et al.* (1986), and with the view that in this tissue, at this concentration RB2 is a selective antagonist at P_{2Y}-purinoceptors. Thus, the antagonism of the inhibitory responses to ADP-ribose and ATP by RB2, but not to adenosine, indicates that the inhibitory responses to ADP-ribose were mediated, at least in part, by P_{2Y}-purinoceptors. Suramin is selective antagonist of P_2-purinoceptors (Dunn & Blakeley, 1988; Hoyle *et al.*, 1990), but it does not discriminate between the P_{2X} and P_{2Y} subtypes (Hoyle *et al.*, 1990). Nevertheless, the antagonism by suramin of responses to ATP and ADP-ribose, but not adenosine, further supports the case that ADP-ribose is acting on P_2-purinoceptors in the taenia coli.

It is also interesting to note that both apamin and suramin, at the concentrations tested, blocked the responses to ATP to a greater extent than they did ADP-ribose, and that the residual responses to ADP-ribose (but not ATP) were inhibited by 8-PT. The fact that a combination of apamin and 8-PT, or suramin and 8-PT, was needed almost to abolish the responses to ADP-ribose, rather than any one of these antagonists alone, is further evidence that both P_1- and P_2-purinoceptors are involved in the responses to ADP-ribose.

The contractile responses of the guinea-pig vas deferens to ATP have been noted in several studies, and the P_2-purinoceptors mediating such contractions were defined as P_{2X}-purinoceptors (Burnstock & Kennedy, 1985). The results of the present study, showing that ADP-ribose over a concentration range of 1 μM to 1 mM had no effect on the tension of the preparations of the vas deferens, are in agreement with the results of Fedan *et al.* (1986), who found ADP-ribose to be without activity in this tissue, even at a concentration of 10 mM. ADP-ribose was found to be similarly inert in producing any changes in the response of the vas deferens to ATP. These results imply that ADP-ribose is neither an agonist nor an antagonist of P_{2X}-purinoceptors.

The mixed pharmacology of ADP-ribose can be said to be remarkable considering its structural similarity to ATP, from

which it varies only by the replacement of the terminal phosphate by a ribose moiety. This replacement of a phosphate by a ribose group somehow conferred an additional P_1-purinoceptor activity on ADP-ribose that is lacked by ATP, while also removing its ability to act as an agonist of P_{2X}-purinoceptors.

The compound adenosine 5'-(2-fluorodiphosphate) (ADPβF) has been shown to be a specific agonist for P_{2Y}-purinoceptors (Hourani *et al.*, 1988). Although the relaxation of the guinea-pig taenia coli evoked by ADPβF is unaffected by 8-PT (Hourani *et al.*, 1988), it has been suggested that ADPβF can act on P_1-purinoceptors mediating relaxation of the rabbit jugular vein (Wood *et al.*, 1989). Nevertheless it is interesting to note that substitution on the β-phosphate of ADP by either F^- or a ribose moiety can confer P_{2Y} specificity over P_{2X}. Furthermore, if this ribose moiety is also linked to a nicotinamide group, forming NAD, all P_2-purinoceptor activity is lost (Burnstock & Hoyle, 1985).

In conclusion, it can be said that ADP-ribose has a mixed pharmacological profile. The inhibitory responses to ADP-ribose in the guinea-pig taenia coli appear to involve adenosine acting on a P_1-purinoceptor, probably via an indirect mechanism involving either partial degradation of ADP-ribose to adenosine or the induction of release of adenosine from the muscle itself. It would seem appropriate that future experiments might investigate whether adenosine is formed or released during the course of ADP-ribose action. ADP-ribose also appears to act on P_{2Y}-purinoceptors in the taenia coli while having no observable action on the P_{2X}-purinoceptors of the guinea-pig vas deferens. This selectivity between the two P_2-purinoceptor subtypes indicates that ADP-ribose could be a useful parent compound in the development of a specific P_{2Y}-purinoceptor agonist if a modification could be made which eliminates its P_1-purinoceptor activity. Also, the activity of ADP-ribose might indicate that in addition to its ubiquitous distribution as an intracellular regulatory compound, during evolution it may also have developed a role as a messenger involved in cell to cell communication.

The authors thank Gillian Knight for technical assistance. G.A.E. is grateful for financial support from the Clothworkers Association and the Mason Foundation.

References

BANKS, B.E.C., BROWN, C., BURGESS, G.M., BURNSTOCK, G., CLARET, M., COCKS, T.M. & JENKINSON, D.H. (1979). Apamin blocks certain neurotransmitter-induced increases in potassium permeability. *Nature*, **282**, 415–417.

BLISS, C.I. (1935). The calculation of dosage-mortality curve. *Ann. Appl. Biol.*, **22**, 134–167.

BROWN, C. & BURNSTOCK, G. (1981). Evidence in support of P_1/P_2-purinoceptor hypothesis in guinea-pig taenia coli. *Br. J. Pharmacol.*, **73**, 617–624.

BÜLBRING, E. (1953). Measurements of oxygen consumption in smooth muscle. *J. Physiol.*, **122**, 111–134.

BURGER, R.M. & LOWENSTEIN, J.M. (1970). Preparation and properties of 5'-nucleotidase from smooth muscle of small-intestine. *J. Biol. Chem.*, **245**, 6274–6280.

BURNSTOCK, G. (1972). Purinergic nerves. *Pharmacol. Rev.*, **24**, 509–581.

BURNSTOCK, G. (1976). Do some nerves release more than one transmitter? *Neuroscience*, **1**, 239–248.

BURNSTOCK, G. (1978). A basis for distinguishing two types of purinergic receptors. In *Cell Membrane Receptors for Drugs and Hormones*. ed. Straub, R. & Bolis, L. pp. 107–118, New York: Raven Press.

BURNSTOCK, G. (1990). Co-transmission. *Arch. Int. Pharmacodyn. Ther.*, **304**, 7–33.

BURNSTOCK, G. & BUCKLEY, N.J. (1985). The classification of receptors for adenosine and adenine nucleotides. In *Methods Used in Adenosine Research*. (Methods in Pharmacology Series). ed. Paton, D.M. pp. 193–212. New York: Raven Press.

BURNSTOCK, G. & HOYLE, C.H.V. (1985). Actions of adenine dinucleotides in the guinea-pig taenia coli: NAD acts indirectly on P_1-purinoceptors; NADP acts like a P_2-purinoceptor agonist. *Br. J. Pharmacol.*, **84**, 825–831.

BURNSTOCK, G. & KENNEDY, C. (1985). Is there a basis for distinguishing two types of P_2-purinoceptor? *Gen. Pharmacol.*, **16**, 433–440.

BURNSTOCK, G., HILLS, J.M. & HOYLE, C.H.V. (1984). Evidence that the P_1-purinoceptor in the guinea-pig taenia coli is an A_2-subtype. *Br. J. Pharmacol.*, **81**, 533–541.

BURNSTOCK, G., HOPWOOD, A.M., HOYLE, C.H.V., REILLY, W.M., SAVILLE, V.L., STANLEY, M.D.A. & WARLAND, J.J.I. (1986). Reactive blue 2 selectivity antagonizes the relaxant responses to ATP and its analogues which are mediated by the P_{2Y}-purinoceptor. *Br. J. Pharmacol.*, **89**, 857P.

BURNSTOCK, G. & WARLAND, J.J.I. (1987). P_2-purinoceptors of two subtypes in rabbit mesenteric artery: RB2 selectively inhibits responses mediated via the P_{2Y}- but not the P_{2X}-purinoceptor. *Br. J. Pharmacol.*, **90**, 383–391.

CULIC, O., SABOLIC, I. & ZANIC-GRUBISIC, T. (1990). The stepwise hydrolysis of adenine nucleotides by ectoenzymes of rat renal brush-border membranes. *Biochem. Biophys. Acta.*, **1030**, 143–151.

DE PIERRE, B.W. & KARNOVSKY, M.L. (1974). Ectoenzymes of the guinea-pig polymorphonuclear leukocyte. *J. Biol. Chem.*, **249**, 7121–7129.

DRURY, A.N. & SZENT-GYÖRGYI, A. (1929). The physiological activity of adenine compounds with special reference to their action upon mammalian heart. *J. Physiol.*, **68**, 213–237.

DUNN, P.M. & BLAKELEY, A.G. (1988). Suramin: a reversible P_2-purinoceptor antagonist in the mouse vas deferens. *Br. J. Pharmacol.*, **93**, 243–245.

FEDAN, J.S., HOGABOOM, G.K. & O'DONNELL, J.P. (1984). Comparison of the effects of apamin, a Ca^{2+}-dependent K^+ channel blocker, and ANAPP3, a P_2-purinergic receptor antagonist in the guinea-pig vas deferens. *Eur. J. Pharmacol.*, **104**, 327–334.

FEDAN, J.S., HOGABOOM, G.K. & O'DONNELL, J.P. (1986). Further comparison of the contractions of the smooth muscle of the guinea-pig isolated vas deferens induced by ATP and related analogs. *Eur. J. Pharmacol.*, **129**, 279–291.

FINNEY, D.J. (1971). *Probit Analysis*. 3rd edition. Cambridge: Cambridge University Press.

FLEETWOOD, G., COADE, S.B., GORDON, J.L. & PEARSON, I.D. (1989). Kinetics of adenine nucleotide catabolism in coronary circulation of rats. *Am. J. Physiol.*, **256**, H1565–1572.

GORDON, J.L. (1986). Extracellular ATP: effects, source and fate. *Biochemistry*, **233**, 309–319.

HAYAISHI, O. & UEDA, K. (1977). Poly (ADP-ribose) and ADP-ribosylation of proteins. *Annu. Rev. Biochem.*, **46**, 95–116.

HOURANI, S.M.D., WELFORD, L.A., LOIZOU, G.D. & GUSACK, N.J. (1988). Adenosine 5'-(2-fluorodiphosphate) is a selective agonist at P_2-purinoceptors mediating relaxation of smooth muscle. *Eur. J. Pharmacol.*, **147**, 133–136.

HOYLE, C.H.V. (1990). Pharmacological activity of adenine dinucleotides in periphery: possible receptor classes and transmitter function. *Gen. Pharmacol.*, **21**, 827–831.

HOYLE, C.H.V. & BURNSTOCK, G. (1991a). ATP receptors and their physiological roles. In *Adenosine in the Nervous System*. ed. Stone, T.W. pp. 43–76, London: Academic Press.

HOYLE, C.H.V. & BURNSTOCK, G. (1991b). Purinergic receptors. In *Receptor Data for Biological Experiments: A Guide to Drug Selectivity*. ed. Doods, H.N. & van Meel, J.C.A. pp. 54–61. New York: Ellis Horwood.

HOYLE, C.H.V. & GREENBERG, M.B. (1988). Actions of adenyl compounds in invertebrates from several phyla: evidence for internal purinoceptors. *Comp. Biochem. Physiol.*, **90C**, 113–122.

HOYLE, C.H.V., KNIGHT, G.E. & BURNSTOCK, G. (1990). Suramin antagonizes responses to P_2-purinoceptor agonists and purinergic nerve stimulation in the guinea-pig urinary bladder and taenia coli. *Br. J. Pharmacol.*, **99**, 617–621.

HUSSAIN, M.Z., GHANI, Q.P. & HUNT, T.K. (1989). Inhibition of propylhydroxylase by poly (ADPR) and phosphoribosyl-AMP. *J. Biol. Chem.*, **264**, 7850–7855.

KOLASSA, N., PFLEGEG, K. & RUMMER, W. (1970). Specificity of adenosine uptake into the heart and inhibition of dipyridamole. *Eur. J. Pharmacol.*, **9**, 265–268.

MAAS, A.J.J. & DEN HERTOG, A. (1979). The effect of apamin on the smooth muscle cells of the guinea-pig taenia coli. *Eur. J. Pharmacol.*, **58**, 151–156.

MAAS, A.J.J., DEN HERTOG, A., RAS, R. & VAN DEN AKKER, J. (1980). The action of apamin on the guinea-pig taenia coli. *Eur. J. Pharmacol.*, **67**, 265–274.

RIBEIRO, J.A. & SEBASTIAO, A.M. (1986). Adenosine receptors and calcium: A basis for proposing a third (A_3) adenosine receptor. *Prog. Neurobiol.*, **26**, 179–209.

SATCHELL, D.J. & BURNSTOCK, G. (1975). Comparison of inhibitory effects on guinea-pig taenia coli of adenosine nucleotides and adenosine in presence and absence of dipyridamole. *Eur. J. Pharmacol.*, **32**, 324–328.

SATCHELL, D.J., LYNCH, A., ROURKE, P.M. & BURNSTOCK, G. (1972). Potentiation of the effects of exogenously applied ATP and purinergic nerve stimulation on the guinea-pig taenia coli by dipyridamole and hexobendine. *Eur. J. Pharmacol.*, **19**, 343–350.

SEBASTIAO, A.M. & RIBEIRO, J.A. (1988). On the adenosine receptor and adenosine inactivation of the rat diaphragm neuromuscular junction. *Br. J. Pharmacol.*, **94**, 109–120.

STONE, T.W. (1981). Action of adenine dinucleotides on vas deferens, guinea-pig taenia coli and bladder. *Eur. J. Pharmacol.*, **75**, 93–102.

UEDA, K. & HAYAISHI, O. (1985). ADP-ribosylation. *Annu. Rev. Biochem.*, **54**, 73–100.

WAUD, D.R. (1975). Analysis of dose-response curves. In *Methods in Pharmacology*, Vol. 3, Smooth Muscle. ed. Daniel, E.E. & Paton, D.M. pp. 471–506. New York: Raven Press.

WOOD, B.E., SQUIRE, A., O'CONNOR, S.E. & LEFF, P. (1989). ADP-β-F is not a selective P_{2Y}-receptor agonist in rabbit jugular vein. *Br. J. Pharmacol.*, **98**, 794P.

(Received April 23, 1992
Accepted June 1, 1992)

Br. J. Pharmacol. (1992), **107**, 375–381

Antagonism of synaptic potentials in ventral horn neurones by 6-cyano-7-nitroquinoxaline-2,3-dione: a study in the rat spinal cord *in vitro*

[1] A.E. King, J.A. Lopez-Garcia & [2] M. Cumberbatch

Department of Physiology, University of Leeds, Leeds LS2 9NQ

1 The rat spinal cord *in vitro* has been used to assess the effect of 6-cyano-7-nitroquinoxaline-2,3-dione (CNQX) on the dorsal root evoked extracellular ventral root reflex (DR-VRR) and the intracellular excitatory postsynaptic potential (e.p.s.p.) in ventral horn neurones and motoneurones.

2 CNQX (1–5 μM) produces a selective and dose-dependent reduction in the amplitude of the monosynaptic component of the DR-VRR recorded from lumbar spinal segments.

3 With low intensity dorsal root stimulation CNQX selectively attenuates the amplitude of the short latency intracellular e.p.s.p. (70% reduction, $P<0.005$) and its rise-time (75%, $P<0.01$) without affecting the half-time to decay.

4 When high intensity stimulation is used CNQX significantly attenuates the amplitude of the e.p.s.p. (56%, $P<0.005$), rise-time (76%, $P<0.01$) and abolishes the short latency spike. In addition longer latency synaptic components are attenuated and the half-time to decay significantly reduced (47%, $P<0.005$).

5 The results with CNQX are compared to D-aminophosphonovalerate and discussed in relation to the recruitment of low versus high threshold afferents. The data supports an involvement of non-NMDA receptors in transmission through both mono- and polysynaptic pathways in the ventral horn.

Keywords: Spinal cord; quinoxalinediones; motoneurones; excitatory amino acids; excitatory synaptic potentials

Introduction

The quinoxalinedione derivatives 6-cyano-7-nitroquinoxaline-2,3-dione (CNQX) and 6,7-dinitroquinoxaline-2,3-dione (DNQX) act as amino acid antagonists with a selectivity targeted towards receptors of the non-N-methyl-D-aspartate (NMDA) variety (Honoré *et al.*, 1988). Affinity ratios in binding studies for the quinoxalinediones indicate a strong preference for α-amino-3-hydroxy-5-methyl-4-isoxazole propionate (AMPA) and kainate receptors over NMDA receptors (Honoré *et al.*, 1988). Iontophoretic experiments in hippocampus (Andreasen *et al.*, 1989), spinal cord (Honoré *et al.*, 1988) and other areas of the central nervous system (Davies & Collingridge, 1990) confirm that these antagonists more effectively attenuate excitations produced by exogenous AMPA, quisqualate (Quis) or kainate over NMDA. The quinoxalinediones are therefore useful pharmacological tools for the elucidation of the role of non-NMDA receptors in the vertebrate central nervous system

In the amphibian spinal cord the quinoxalinediones selectively reduce the early monosynaptic component in the dorsal root evoked extracellular ventral root reflex (DR-VRR) whilst the longer latency components are relatively unaffected (Fletcher *et al.*, 1988). In rat Long *et al.* (1990) reported that CNQX was a potent antagonist of the short latency monosynaptic component of the ventral root reflex recorded from sacro-coccygeal segments of the spinal cord. These authors did not describe the effects of CNQX on longer latency components of the reflex. Taken overall the available extracellular data support a role for CNQX-sensitive receptors such as kainate and AMPA receptors in transmission from low threshold afferents onto motoneurones. The resistance of the early monosynaptic component of the ventral root reflex recorded in rat to antagonism by selective NMDA antagonists such as D-aminophosphonovalerate (D-AP5) strengthens this argument (Long *et al.*, 1988). In contrast longer latency components within the ventral root reflex generated by high threshold afferents are strongly attenuated by selective NMDA antagonists (Evans *et al.*, 1982; Evans, 1989) arguing for a role for NMDA receptors in transmission through polysynaptic pathways activated by high threshold afferents. However, the effect of the quinoxalinediones on these longer latency components of the mammalian ventral root reflex is unknown.

Intracellular data on the effects of the quinoxalinedione derivatives on synaptic potentials is accumulating. In the hippocampus, for example, CNQX has revealed an NMDA-mediated component of transmission through the Schaffer collateral-commissural pathway (Davies & Collingridge, 1989). In the spinal cord, intracellular data are available only for the dorsal horn; Yoshimura & Jessel (1990) reported that synaptic responses generated by A- delta and C fibres in substantia gelatinosa neurones are antagonized by CNQX. CNQX also antagonizes a fast excitatory postsynaptic potential produced in deep dorsal horn neurones by low frequency dorsal root stimulation (Gerber & Randic, 1989). To date there are no intracellular data available on the effects of quinoxalinedione antagonists on neurones of the mammalian ventral horn including motoneurones.

In the present study the main aim has been to assess the effects of CNQX on intracellularly recorded dorsal root-evoked synaptic potentials elicited in rat lumbar ventral horn neurones *in vitro*. The selective NMDA antagonist D-AP5 which is known to antagonize preferentially polysynaptic potentials in the mammalian ventral horn (Evans, 1989) has been used for comparison purposes. The two antagonists, CNQX and D-AP5, have also been used in combination with each other. In order to confirm earlier data on the effect of CNQX on the synchronized monosynaptic component of the ventral horn reflex and to determine an effect, if any,

[1] Author for correspondence.
[2] Present address: Department of Physiology, The Medical School, University Walk, Bristol BS8 1TD.

on longer latency synaptic components, the DR-VRR was recorded. Some of the preliminary results have appeared in abstract form (King & Lopez-Garcia, 1991).

Methods

The spinal cords of young male or female rats 10–12 days after birth and weighing less than 30 g were used for all experiments. For a complete description of the dissection see King *et al.* (1990). Briefly, under urethane anaesthesia (dose: 2 g kg^{-1}, i.p.) a dorsal laminectomy was performed to reveal the lumbar spinal cord with attached dorsal and ventral roots (L3–6). The cord was rapidly excised and placed in ice cooled artificial CSF for hemisection. The hemisected cord was submerged in a bath, cut surface uppermost, and superfused continuously with oxygenated (95% O_2-5% CO_2) Krebs solution (mM: NaCl 128, KCl 1.9, KH_2PO_4 1.2, $MgSO_4$ 1.3, $CaCl_2$ 2.4, $NaHCO_3$ 26, glucose 10, pH 7.4, 28–30°C) at a rate of 5 ml min^{-1}.

Drugs (NMDA and Quis, D-AP5 and CNQX from Cambridge Research Biochemicals; D-serine from Sigma) were dissolved in this solution and perfused through separate gravity feed inlets in a fixed volume (10–25 ml). Concentrations of 1–5 μM CNQX were chosen for the experiments on the effects of CNQX on synaptic responses for several reasons. Firstly with these concentrations the antagonism could be reversed over a time scale (45–60 min) realistic for maintaining a stable intracellular recording. A feature of the antagonism produced by CNQX is its slow and sometimes incomplete reversibility especially at higher concentrations (Andreasen *et al.*, 1989). Secondly CNQX at a concentration as low as 10 μM is known to have an effect on the strychnine-insensitive glycine receptor which modulates responses to NMDA (Birch *et al.*, 1988).

For intracellular recordings, 3 M potassium acetate-filled microelectrodes with a 60–100 MΩ d.c. resistance were routinely used and signals were amplified through an Axoclamp 2A system. Records were stored on Racal FM tape for subsequent off-line computer analysis. For the averaged samples illustrated, the data were digitized at a minimum rate of 3kHz. All data are expressed as mean ± s.e.mean and for statistical comparisons, Student's *t* test was used. Motoneurones were identified on the basis of the appearance of a short latency spike following low intensity (< 50 μA, 50 μs) antidromic stimulation of the segmental ventral root. Cells which did not respond to antidromic stimulation were classed as ventral horn neurones. The pattern of antagonism produced by CNQX and D-AP5 was equivalent so the data from both groups have been combined. For synaptic activation of neurones, two stimulation conditions, 'low' and 'high', were employed; low intensity was considered as less than 80 μA,60 μs while high intensity was from 100 μA,100 μs up to 500 μA,500 μs. These values are based on those of Thompson *et al.* (1990) who showed, in the same preparation, that the low intensity would activate exclusively A beta, Group I and Group II fibres whilst the high intensity would activate in addition A delta, C and Group III/IV afferent fibres.

For extracellular recording of the segmental DR-VRR the lumbar dorsal and ventral roots were pulled into tight fitting glass suction electrodes constructed from capillary glass and filled with Krebs solution. Constant current stimuli (up to 1.0 mA, 500 μs) were applied via suction electrodes on L3–L6 dorsal roots.

Results

The intracellular data base is comprised of recordings from 27 ventral horn neurones and 12 motoneurones. The mean resting membrane potential for the 39 neurones was −73.6 ± 1.2 mV and the mean input resistance was 16.2 ± 8 MΩ. The extracellular data were obtained from simultaneous ventral root recordings during the intracellular experiments and from an additional 10 preparations from which only ventral root recordings were performed.

Antagonism of the extracellular DR-VRR

Supramaximal stimulation of dorsal roots produces a short latency (5.7 ± 0.2 ms, $n = 25$), highly synchronized population spike followed by longer latency (> 10 ms) asynchronous synaptic activity. This is recorded extracellularly from the ventral root as the DR-VRR. The effects of the antagonists CNQX (1–5 μM) and D-AP5 (10–50 μM) on the DR-VRR were tested. CNQX (1–5 μM) produced a potent and dose-dependent preferential antagonism of the highly synchronized monosynaptic component of the DR-VRR. This effect is illustrated in Figure 1 which shows an example of a DR-VRR recorded in control versus antagonist containing Krebs solution. Note the strong attenuation of the amplitude of the short latency component in the presence of 5 μM CNQX (Figure 1c) compared to 50 μM D-AP5 (Figure 1b). Superfusion of D-AP5 (50 μM) in contrast had very little effect on the short latency monosynaptic component although a modest decrease of 11% was produced in the example shown in Figure 1b; the mean reduction of this component in the presence of D-AP5 (10–50 μM) was 13 ± 4%.

CNQX up to 1 μM had little effect on the amplitude of the longer latency component of the DR-VRR (see graph of Figure 1). However the highest concentration of 5 μM CNQX produced variable reductions in the amplitude (mean value 32%; range 0–75%). D-AP5 (10–50 μM) more consistently antagonizes this component (Figure 1b) with a 27 ± 6% reduction in amplitude ($n = 15$).

Antagonism of exogenous agonists

The effect of CNQX on bath-applied Quis and NMDA was assessed intracellularly. Superfusion of 30 μM Quis produced a rapidly developing membrane depolarization of 10–20 mV (Figure 2a) which elicited high frequency cell firing and was followed by a return to baseline. A similar profile of excitation was produced by 50 μM NMDA although these responses typically decayed more slowly back to the resting membrane potential. CNQX over a range of 1–5 μM consistently produced a reversible attenuation of the depolarization induced by 30 μM Quis (Figure 2a). The dose-dependency of the reduction in the amplitude of the Quis induced depolarization in the presence of CNQX is illustrated in the graph of Figure 2. CNQX up to 5 μM had no significant effect on NMDA-induced depolarizations (Figure 2b and graph).

Antagonism of intracellularly recorded synaptic potentials

At low stimulus intensities (< 80 μA,60 μs) a short latency (5.6 ± 0.72 ms, $n = 16$) presumed monosynaptic e.p.s.p. was generated. This was followed by a longer latency (28.1 ± 4.1 ms, $n = 17$) subthreshold polysynaptic e.p.s.p. which took several hundred milliseconds (mean 611.9 ± 112.9 ms, $n = 17$) to decay completely. The half time to decay (defined as the time taken for the e.p.s.p. amplitude to decay to half its maximum value) was 104.3 ± 4.1 ms. An example from a single motoneurone is shown in Figure 3a where the stimulus strength was set just below monosynaptic spike threshold at 30 μA,50 μs. At high stimulus intensities (100 μA,100 μs to 500 μA,500 μs) a short latency (5.4 ± 0.45 ms, $n = 14$) monosynaptic spike was followed by longer latency (89.9 ± 29.4 ms, $n = 16$) polysynaptic potentials which took several seconds (mean 4.9 ± 1.3 s, $n = 11$) to decay. The mean half-time to decay for these polysynaptic responses was 322.6 ± 33.6 ms, $n = 16$. Examples of the synaptic excitation produced by high intensity stimulation are shown in Figure 4.

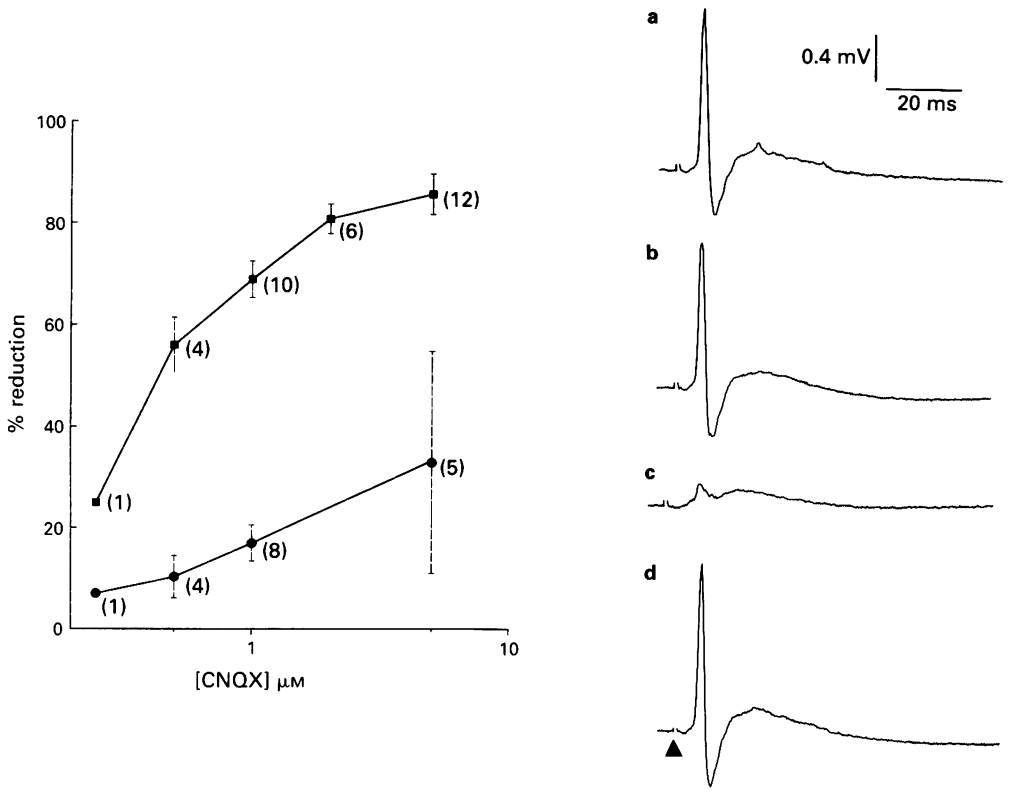

Figure 1 Antagonism of the extracellular dorsal root evoked ventral root reflex (DR-VRR) by 6-cyano-7-nitroquinoxaline-2,3-dione (CNQX) and D-aminophosphonovalerate (D-AP5). The DR-VRR (average of 5 samples) recorded in (a) control Krebs solution (b) D-AP5 (50 μM) (c) CNQX (5 μM) and (d) 30 min following return to control Krebs solution. Stimulus artifact indicated in this and other figures by (▲). Graph shows the concentration-dependent reduction in the mean amplitude of the short latency (■) and long latency (●) components of the extracellular DR-VRR by CNQX (0.25–5 μM). Values are mean with s.e.mean (vertical bars), number of trials per data point indicated in parentheses.

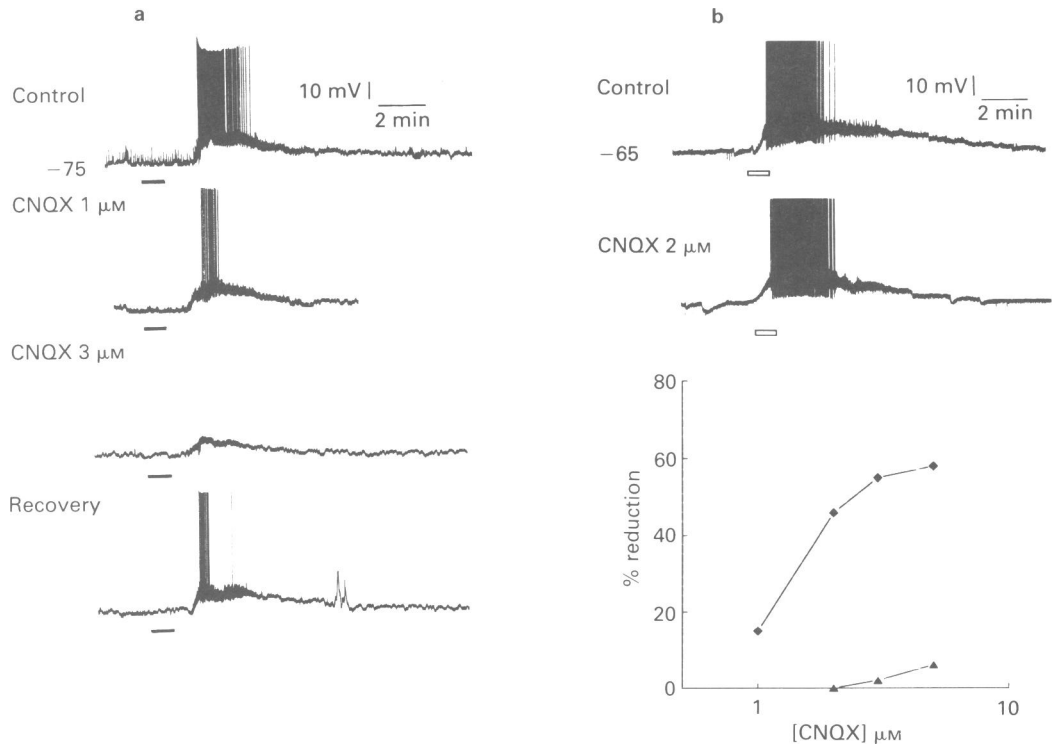

Figure 2 Antagonism of exogenous quisqualate (Quis, 30 μM) and N-methyl-D-aspartate (NMDA, 50 μM) by 6-cyano-7-nitroquinoxaline-2,3-dione (CNQX). (a) Dose-dependent reduction in Quis depolarization produced by 1 and 3 μM CNQX and partial recovery following 45 min in normal Krebs solution. (b) In another neurone 2 μM CNQX fails to antagonize the NMDA depolarization. Duration of agonist superfusion is indicated by the solid (Quis) and open (NMDA) horizontal bars. Graph shows selective antagonism by 1–5 μM CNQX against Quis (◆) vs NMDA (▲) depolarizations; data points obtained from single preparations except for 3 μM ($n = 2$) and 5 μM CNQX ($n = 3$).

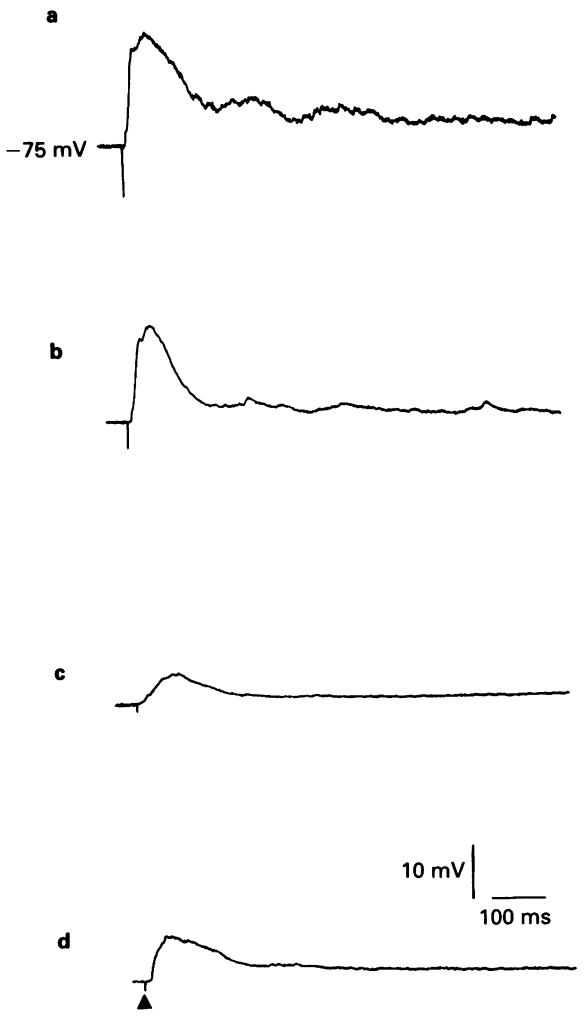

Figure 3 Effects of CNQX and D-AP5 on an e.p.s.p. produced in a motoneurone by low intensity (30 μs,50 μA) dorsal root stimulation. (a) Control Krebs solution; (b) 50 μM D-AP5; (c) 5 μM CNQX; (d) partial recovery following 45 min wash in control Krebs solution. All e.p.s.p. records in this and subsequent figures are the average of 5 sweeps. For abbreviations, see legends to Figures 1 and 2.

The effects of 1–5 μM CNQX and 50 μM D-AP5 were tested against intracellular e.p.s.ps in these two conditions; low versus high intensity stimulation of dorsal roots. When testing the antagonists, three parameters were measured; e.p.s.p. peak amplitude (mV), rise-time (mV ms^{-1}) and half-time to decay (ms). The results are summarized in Table 1.

Under conditions of low intensity dorsal root stimulation CNQX (1–5 μM) and D-AP5 (10–50 μM) had contrasting effects on the e.p.s.p. as illustrated in Figure 3. CNQX strongly attenuated the amplitude of the short latency e.p.s.p. and significantly reduced its rise-time (Figure 3 and Table 1). The mean e.p.s.p. amplitude was reduced from a control value of 12.7 ± 1.7 mV to 3.8 ± 1.0 mV ($n = 16$, $P<0.005$ level) representing a 70% reduction. The rise-time of the e.p.s.p. reduced by 75% from 6.3 ± 1.9 to 3.9 ± 1.2 ms ($P<0.01$). CNQX had a small and statistically insignificant effect on the half-time to decay of the e.p.s.p. (Table 1). In contrast the main action of D-AP5 was to reduce the half-time to decay from a control value of 112.5 ± 17.9 ms to 65.0 ± 7.8 ms ($n = 10$, $P<0.01$) without substantially reducing the amplitude or rise-time of the short latency e.p.s.p. (Figure 3b, Table 1).

At high stimulus intensities CNQX (1–5 μM) reduced the amplitude and rise-time of the short latency e.p.s.p. (Figure 4a and Table 1), the effect of which is to abolish spike initiation (Figure 4a). In the presence of CNQX the short latency e.p.s.p. mean amplitude was reduced from a control value of 16.0 ± 2.2 mV to 6.9 ± 1.8 ($n = 12$, $P<0.005$, Table 1) representing a 56% reduction while the mean rise-time was reduced by 76% ($P<0.01$). However, in addition CNQX antagonized longer latency components of the postsynaptic potential as illustrated in the motoneurone of Figure 4a. In this example the e.p.s.p. half-time to decay decreased from a control value of 580 ms to 281 ms in CNQX. The data in Table 1 indicate a statistically significant 47% reduction ($P<0.005$) in the mean half-time to decay for the synaptic responses in control Krebs solution (mean value of 298 ± 48.8 ms, $n = 12$) versus CNQX (mean value of 156 ± 23.4 ms). D-AP5 reduced the e.p.s.p. mean half-time to decay (Figure 4b and Table 1) indicating the expected potent effect of this antagonist against longer latency polysynaptic potentials. Table 1 shows a modest but significant 28% reduction in the mean amplitude of the short latency e.p.s.p. from a control value of 17.3 ± 1.8 mV to 12.4 ± 2.1 mV ($n = 10$, $P<0.005$) although the mean e.p.s.p. rise-time and spike initiation were unaffected by D-AP5 (Figure 4b).

The extent of antagonism produced by 1–5 μM CNQX and 50 μM D-AP5 against the short versus long latency com-

Table 1 Effects of the antagonists 6-cyano-7-nitroquinoxaline-2,3-dione (CNQX, 1–5 μM), D-aminophosphonovalerate (D-AP5, 50 μM) on dorsal root evoked e.p.s.ps produced by 'low' (<80 μA,60 μs) and 'high' (100 μA,100 μs to 500 μA,500 μs) intensity stimulation

	Control	*CNQX*	*Control*	*D-AP5*	*Control*	*CNQX + D-AP5*
Low Intensity						
Rise-time (mV ms^{-1})	6.3 ± 1.9	1.6 ± 0.5 (**, 75%)	3.9 ± 1.2	3.8 ± 1.3 (2%)	5.6 ± 1.6	1.1 ± 0.3 (**, 80%)
e.p.s.p. amplitude (mV)	12.7 ± 1.7	3.8 ± 1.0 (***, 70%)	11.9 ± 2.3	10.1 ± 2.8 (15%)	13.1 ± 2.6	2.4 ± 0.9 (***, 81%)
Half-time to decay (ms)	96.4 ± 14.1	72.1 ± 11.3 (25%)	112.5 ± 17.9	65.0 ± 7.8 (**, 42%)	82.5 ± 16.7	22.5 ± 10.3 (***, 72%)
High intensity						
Rise-time (mV ms^{-1})	7.6 ± 2.4	1.8 ± 0.6 (**, 76%)	4.4 ± 1.2	4.1 ± 1.4 (7%)	11.9 ± 3.9	2.0 ± 0.5 (**, 82%)
e.p.s.p. amplitude (mV)	16.0 ± 2.2	6.9 ± 1.8 (***, 56%)	17.3 ± 1.8	12.4 ± 2.1 (***, 28%)	23.7 ± 3.3	6.4 ± 1.6 (***, 72%)
Half-time to decay (ms)	298 ± 48.8	156 ± 23.4 (***, 47%)	272.1 ± 37	170.3 ± 27.6 (***, 55%)	320 ± 69.0	60.1 ± 9.9 (**, 81%)

Results are shown as mean ± s.e.mean values.
Statistical significance levels : $^{**}P<0.01$; $^{***}P<0.005$ and % reductions are shown in parentheses.

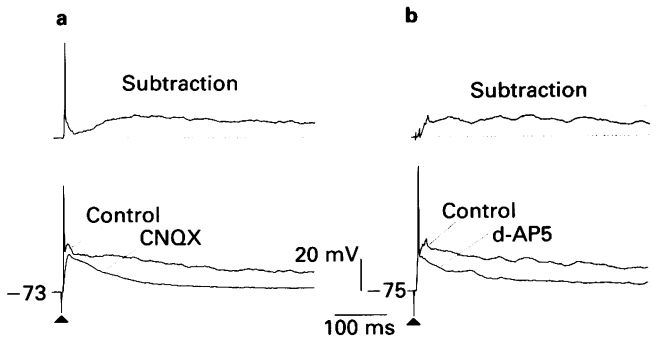

Figure 4 Antagonism by (a) CNQX (5 μM) and (b) D-AP5 (50 μM) of short latency vs long latency e.p.s.ps produced in two motoneurones by high intensity dorsal root stimulation. Note the characteristic reduction in the short latency e.p.s.p. amplitude and rise-time with CNQX. Lower panels; averaged e.p.s.p. elicited in control Krebs solution and reduction of the e.p.s.p. in presence of the antagonist. Upper panels; mathematical subtraction of the two records (control vs antagonist). Resulting profile is that part of the e.p.s.p. removed by either CNQX or D-AP5 (see text for details). Stimulus intensities used were (a) 100 μs,400 μA and (b) 100 μs,200 μA. See legends to Figures 1 and 2 for abbreviations.

ponents of the postsynaptic potential produced by high intensity dorsal root stimulation can be visualized by performing a digital subtraction protocol (Forsythe & Westbrook, 1988). An example is illustrated in Figure 4 (upper panels); the subtracted record represents the synaptic components eliminated by the antagonist. CNQX antagonized the short latency e.p.s.p. with abolition of the monosynaptic spike and additionally attenuated the longer latency subthreshold e.p.s.ps. In contrast, the predominant effect of D-AP5 was an attenuation of the longer latency subthreshold e.p.s.p. (Figure 4b) with no effect on the short latency spike.

CNQX is known to antagonize NMDA responses via an action at the strychnine-insensitive glycine receptor (Birch *et al.*, 1988). This action of CNQX is offset by D-serine and in separate experiments the antagonism produced by 5 μM CNQX against motoneurone e.p.s.ps recorded in the presence of 0.1–1 mM D-serine was tested. Under these conditions, CNQX still reduced both the short latency e.p.s.p. spike and the long latency subthreshold e.p.s.ps produced by high intensity dorsal root stimulation. In the example of Figure 5 the amplitude of the short latency e.p.s.p. was reduced from 25 mV to 17 mV and the initial spike abolished by CNQX. The e.p.s.p. half-time to decay decreased from 90 ms to 30 ms. The mean % reduction of the e.p.s.p. amplitude and half-time to decay produced by CNQX in the presence of D-serine was 30% and 52% ($n = 4$) respectively.

The antagonism produced by superfusion of a combination of 5 μM CNQX and 50 μM D-AP5 was assessed against e.p.s.ps produced by low and high intensity dorsal root stimulation. The degree of antagonism produced by the two antagonists applied together exceeded that produced by one antagonist alone (see Table 1). Following low intensity stimulation the postsynaptic e.p.s.p. was virtually abolished in the presence of a combination of CNQX and D-AP5 (Figure 6a), the mean amplitude was reduced from a control value of 13.1 ± 2.6 mV to 2.4 ± 0.9 mV ($n = 10$). This represents a reduction of 81% compared to an average reduction of 70% by CNQX or 15% by D-AP5 alone (Table 1). In 4 ventral horn neurones the e.p.s.p. was completely abolished by CNQX and D-AP5. With high intensity stimulation although the e.p.s.p. amplitude was strongly attenuated, a more distinct synaptic potential with an amplitude of 5–10 mV (mean 6.4 ± 1.6 mV) remained in the presence of the two antagonists (Figure 6b). A 72% reduction in the mean e.p.s.p. amplitude was measured (Table 1).

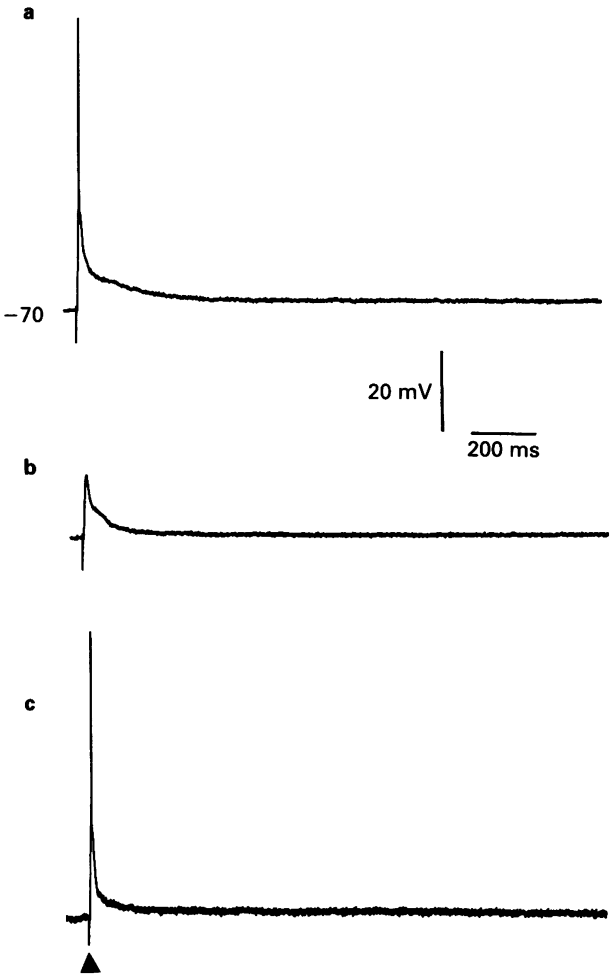

Figure 5 The effect of 6-cyano-7-nitroquinoxaline-2,3-dione (CNQX) in the presence of D-serine. Records are of the e.p.s.p. (stimulus intensity 150 μs,150 μA) recorded from a motoneurone in normal Krebs solution containing (a) 1 mM D-serine and (b) 1 mM D-serine plus 50 μM CNQX. Partial recovery after removal of CNQX is shown in (c).

Discussion

In the lumbar segments of the rat spinal cord, as in sacrococcygeal segments (Long *et al.*, 1990), CNQX has a preferential antagonistic effect against the short latency monosynaptic component of the extracellularly recorded DR-VRR. Intracellularly in ventral horn neurones this is seen as a reduction in the amplitude and rise-time of the early e.p.s.p. below that required for spike initiation. The selectivity of CNQX against the short latency synaptic component is demonstrated clearly under conditions of low stimulus intensity where the amplitude of the subthreshold e.p.s.p. is significantly attenuated. The low stimulus intensities used in this study have been shown previously to activate predominantly low threshold, large diameter afferents, namely Group I and II afferents (Thompson *et al.*, 1990; King *et al.*, 1990) which make monosynaptic connections onto motoneurones. This intracellular data strengthens the view that the postsynaptic action of these afferents is mediated mainly by non-NMDA receptors (Evans, 1989) such as the AMPA receptor for which CNQX has a high affinity (Honoré *et al.*, 1988). Previously kynurenate, which similarly but less potently discriminates in favour of non-NMDA receptors, has been shown to be a potent inhibitor of the Ia e.p.s.p. (Jahr & Yoshioka, 1986).

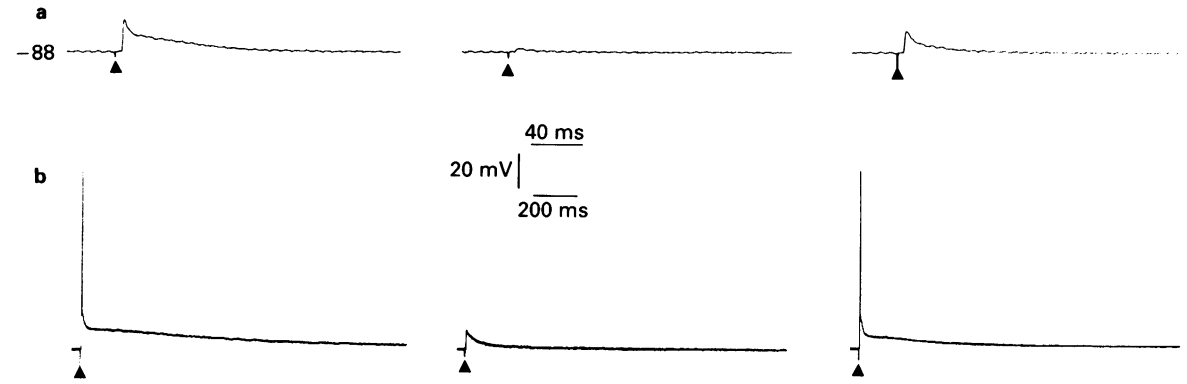

Figure 6 Antagonism produced by co-application of CNQX (5 μM) and D-AP5 (50 μM). Motoneurone e.p.s.p. elicited by (a) low intensity (50 μA,50 μs) and (b) high intensity (200 μA,200 μs) dorsal root stimulation. Left panels (upper and lower): e.p.s.ps recorded in control Krebs medium; middle panels: in presence of a combination of CNQX (5 μM) and D-AP5 (50 μM); (c) recovery. Note presence of residual e.p.s.p. especially in (b). For abbreviations see legends to Figures 1 and 2.

At high stimulus intensities CNQX has a dual effect on the dorsal root evoked e.p.s.p., namely a reduction in the amplitude of the short latency e.p.s.p. with abolition of the spike and a reduction in the half-time to decay of the e.p.s.p. Under these conditions it is likely that both low and high threshold afferents are active in generating the long duration polysynaptic e.p.s.p. in ventral horn neurones. High threshold afferents such as A delta and C arising from muscle, joint and skin mechanoreceptors terminate largely in superficial dorsal horn and activate motoneurones via polysynaptic relays which generate the withdrawal reflex (Eccles & Lundberg, 1959). Intracellular studies *in vitro* show that natural and electrical stimulation of such afferents produce in rat lumbar motoneurones slowly decaying polysynaptic e.p.s.ps similar to the CNQX-sensitive synaptic responses described in this study (King *et al.*, 1990; Thompson *et al.*, 1990). It must be inferred from this then that such afferents mediate at least part of their postsynaptic effects onto ventral horn neurones including motoneurones via CNQX-sensitive receptors such as kainate or quisqualate/AMPA receptors. However the present data cannot discriminate between an effect of CNQX on the final synapse onto motoneurones or earlier synapses within the pathway. Previous studies using the NMDA antagonist D-AP5 have emphasized its selectivity against the long latency components of both the extracellularly recorded DR-VRR (Evans, 1989) and the polysynaptic e.p.s.p. (Fletcher *et al.*, 1988). Such data has been collectively interpreted as indicating a major role for NMDA receptors within multisynaptic spinal pathways. The present study indicates that the contribution of non-NMDA receptor types to synaptic transmission within these pathways may have been considerably underestimated. A role for non-NMDA receptors in polysynaptic spinal pathways has been implicated by studies with non-selective antagonists such as kynurenate which attenuate all components of the DR-VRR (Long *et al.*, 1988). Additionally, in rat substantia gelatinosa, A delta and C afferent-evoked monosynaptic e.p.s.ps are antagonized by CNQX and kynurenate (Yoshimura & Jessel, 1990).

Under appropriate conditions NMDA-mediated synaptic transmission in the central nervous system can be facilitated by glycine (Johnson & Ascher, 1987). This effect is mediated by an action of glycine at a strychnine-insensitive binding site which is allosterically linked to the NMDA receptor and is susceptible to antagonism by CNQX (Birch *et al.*, 1988). Several factors in this study argue against antagonism of NMDA-mediated responses by an action at this site by CNQX as an explanation for the observed reduction of longer latency polysynaptic e.p.s.ps in ventral horn cells. The concentration of CNQX used in this study was 1–5 μM which is below the limit of 10 μM at which the effect on NMDA becomes significant (Birch *et al.*, 1988; Hablitz & Sutor, 1990; Davies & Collingridge, 1990). Furthermore this concentration-range of CNQX antagonizes depolarizations to exogenous Quis with little effect on NMDA. More significantly, superfusion of D-serine which reduces the effects of CNQX on this glycine binding site (Birch *et al.*, 1988) does not influence the profile of antagonism produced by CNQX in ventral horn neurones. In the rat spinal cord, glycine fails to augment the depolarization to NMDA (Birch *et al.*, 1988) indicating that it may be present at saturating concentrations endogenously. Supporting this is the fact that in the ventral horn, unlike some other areas e.g. cortex (Thomson, 1990), CNQX discriminates effectively between NMDA and Quis even in the absence of glycine or D-serine.

The profile of antagonism produced both intracellularly and extracellularly for D-AP5 is similar to that described previously, namely a selective attenuation of longer latency synaptic components (Evans *et al.*, 1982; Fletcher *et al.*, 1988; Long *et al.*, 1988). However, when high intensity dorsal root stimulation is employed, a modest reduction of the amplitude of the short latency e.p.s.p. is measured. The reason for this is unclear since others have reported no consistent effect of D-AP5 on this component (Flatman *et al.*, 1987; Long *et al.*, 1988). Such a result may be explained by postulating a minor NMDA receptor-mediated contribution to the synaptic activation of motoneurones by low threshold Group I and II afferents. A role for NMDA receptors in monosynaptic transmission has been demonstrated in vertebrate spinal cord (Corradetti *et al.*, 1985; Dale & Roberts, 1985) and in cultured hippocampal and spinal neurones (Forsythe & Westbrook, 1988). In a population of dorsal horn neurones, D-AP5 reduced the peak amplitude of A delta-evoked monosynaptic e.p.s.ps by around 20% (Yoshimura & Jessel, 1990).

Co-application of CNQX and D-AP5 fails to abolish completely ventral horn synaptic potentials particularly under conditions of high intensity dorsal root stimulation. Similar findings have been reported for substantia gelatinosa neurones (Yoshimura & Jessel, 1990), vertebrate motoneurones (Alford & Grillner, 1990) and hippocampal neurones (Davies & Collingridge, 1989). These data can be interpreted in two ways; an involvement of receptors to putative transmitters other than amino acids or a high concentration of endogenous transmitter in the synaptic cleft overcoming competitive blockade. Further pharmacological studies will be required to differentiate between these two possibilities.

The use of a diverse range of amino acid receptor antagonists in the spinal cord has led to a generalized scheme whereby it is proposed that non-NMDA receptors mediate short latency, monosynaptic transmission whereas NMDA

receptors mediate predominantly longer latency polysynaptic transmission (Evans, 1989). The results of this study with CNQX do not contradict this but also suggest that it may be simplistic and that a significant component of polysynaptic transmission, at least onto ventral horn neurones, is relayed via non-NMDA receptors such as AMPA/quisqualate or kainate type. Similarly, on the basis of evidence presented here and other studies (Corradetti *et al.*, 1985; Dale & Roberts, 1985; Forsythe & Westbrook, 1988), a case can be made for involvement of NMDA receptors in short latency mono- or di-synaptic responses. Ultimately, independent classes of muscle or cutaneous afferents and the involvement of the different types of amino acid receptors in transmission onto second order dorsal or ventral horn neurones must be analysed separately rather than collectively since it is likely that differences exist. For example in the ventral but not dorsal horn, nociceptive sensory responses appear to be in part mediated by NMDA receptors (Headley *et al.*, 1987). One desirable way to achieve this would be to test selective amino acid antagonists against naturally evoked sensory responses (Headley *et al.*, 1987; Honore *et al.*, 1988; Salt & Eaton, 1989).

This research was supported by the Wellcome Trust and the University of Leeds Research Fund.

References

ALFORD, S. & GRILLNER, S. (1990). CNQX and DNQX block non-NMDA synaptic transmission but not NMDA-evoked locomotion in lamprey spinal cord. *Brain Res.*, **506**, 297–302.

ANDREASEN, M., LAMBERT, J.D.C. & SKOVGAARD JENSEN, M. (1989). Effects of new non-N-methyl-D-aspartate antagonists on synaptic transmission in the *in vitro* rat hippocampus. *J. Physiol.*, **414**, 317–336.

BIRCH, P.J., GROSSMAN, C.J. & HAYES, A.G. (1988). 6,7-dinitroquinoxaline-2,3-dion and 6-nitro,7-cyano-quinoxaline-2,3-dion antagonise responses to NMDA in the rat spinal cord via an action at the strychnine-insensitive glycine receptor. *Eur. J. Pharmacol.*, **156**, 177–180.

CORRADETTI, R., KING, A.E., NISTRI, A., ROVIRA, C. & SIVILOTTI, L. (1985). Pharmacological characterization of D-aminophosphonovaleric acid antagonism of amino acid and synaptically evoked excitations on frog motoneurones *in vitro*: an intracellular study. *Br. J. Pharmacol.*, **86**, 19–25.

DALE, N. & ROBERTS, A. (1985). Dual component amino-acid-mediated synaptic potentials: excitatory drive for swimming in *Xenopus* embryos. *J. Physiol.*, **363**, 35–59.

DAVIES, S.N. & COLLINGRIDGE, G.L. (1989). Role of excitatory amino acid receptors in synaptic transmission in area CA1 of rat hippocampus. *Proc. R. Soc.*, B, **236**, 373–384.

DAVIES, S.N. & COLLINGRIDGE, G.L. (1990). Quinoxalinediones as excitatory amino acid antagonists in the vertebrate central nervous system. *Int. Rev. Neurobiol.*, **32**, 281–303.

ECCLES, R.M. & LUNDBERG, A. (1959). Synaptic actions in motoneurones by afferents which may evoke the flexion reflex. *Arch. Ital. Biol.*, **97**, 199–221.

EVANS, R.H. (1989). The pharmacology of segmental transmission in the spinal cord. *Prog. Neurobiol.*, **33**, 255–279.

EVANS, R.H., FRANCIS, A.A., JONES, A.W., SMITH, D.A.S. & WATKINS, J.C. (1982). The effects of a series of ω-phosphonic α-carboxylic amino acids on electrically evoked and excitant amino acid-induced responses in isolated spinal cord preparations. *Br. J. Pharmacol.*, **75**, 65–75.

FLATMAN, J.A., DURAND, J., ENGBERG, I. & LAMBERT, J.D.C. (1987). Blocking the monosynaptic EPSP in spinal cord motoneurones with inhibitors of amino acid excitation. In *Excitatory Amino Acid Transmission*. ed. Hicks, T.P., Lodge, D. & McLennan, H., pp. 285–292. New York: Alan R. Liss Inc.

FLETCHER, E.J., MARTIN, D., ARAM, J.A., LODGE, D. & HONORÉ, T. (1988). Quinoxalinediones selectively block quisqualate and kainate receptors and synaptic events in rat neocortex and hippocampus and frog spinal cord *in vitro*. *Br. J. Pharmacol.*, **95**, 585–597.

FORSYTHE, I. & WESTBROOK, G. (1988). Slow excitatory postsynaptic currents mediated by N-methyl-D-aspartate receptors on cultured mouse central neurones. *J. Physiol.*, **396**, 515–534.

GERBER, G. & RANDIC, M. (1989). Participation of excitatory amino acid receptors in the slow excitatory synaptic transmission in the rat spinal dorsal horn *in vitro*. *Neurosci. Lett.*, **106**, 220–228.

HABLITZ, J.J. & SUTOR, B. (1990). Excitatory postsynaptic potentials in rat neocortical neurones in vitro. III. Effects of a quinoxalinedione non-NMDA receptor antagonist. *J. Neurophysiol.*, **64**, 1282–1290.

HEADLEY, P.M., PARSONS, C.G. & WEST, D.C. (1987). The role of N-methyl-aspartate receptors in mediating responses of rat and cat spinal neurones to defined sensory stimuli. *J. Physiol.*, **385**, 169–188.

HONORÉ, T., DAVIES, S.N., DREJER, J., FLETCHER, E., JACOBSEN, P., LODGE, D. & NIELSEN, F.E. (1988). Quinoxalinediones: potent competitive non-NMDA glutamate receptor antagonists. *Science*, **241**, 701–703.

JAHR, C.E. & YOSHIOKA, K. (1986). Ia afferent excitation of motoneurones in the in vitro new-born rat spinal cord is selectively antagonized by kynurenate. *J. Physiol.*, **370**, 515–530.

JOHNSON, J.W. & ASCHER, P. (1987). Glycine potentiates the NMDA response in cultured mouse brain neurones. *Nature*, **325**, 529–531.

KING, A.E. & LOPEZ-GARCIA, J.A. (1991). Extracellular and intracellular comparison of the effects of 6-cyano-7-nitroquinoxaline-2,3-dione (CNQX) and D-amino-5-phosphonovalerate (d-APV) on synaptic responses of rat ventral horn neurones *in vitro*. *Eur. J. Neurosci.*, Suppl. 4, S3186.

KING, A.E., THOMPSON, S.W.N. & WOOLF, C.J. (1990). Characterization of the cutaneous input to the ventral horn *in vitro* using the isolated spinal cord-hindlimb preparation. *J. Neurosci. Meth.*, **35**, 39–46.

LONG, S.K., EVANS, R.H., CULL, L., KRIJZER, F. & BEVAN, P. (1988). An *in vitro* mature spinal cord preparation from the rat. *Neuropharmacol.*, **27**, 541–546.

LONG, S.K., SMITH, D.A.S., SIAREY, R.J. & EVANS, R.H. (1990). Effects of 6-cyano-7-nitroquinoxaline-2,3-dione (CNQX) on dorsal root-, NMDA-, kainate- and quisqualate-mediated depolarization of rat motoneurones *in vitro*. *Br. J. Pharmacol.*, **100**, 850–854.

SALT, T.E. & EATON, S.A. (1989). Function of non-NMDA and NMDA receptors in synaptic response to natural somatosensory stimulation in the ventrobasal thalamus. *Exp. Brain Res.*, **77**, 646–652.

THOMPSON, S.W.N., KING, A.E. & WOOLF, C.J. (1990). Activity-dependent changes in rat ventral horn neurones *in vitro*; summation of prolonged afferent evoked postsynaptic depolarizations produce a D-2-amino-5-phosphonovalerate acid sensitive wind-up. *Eur. J. Neurosci.*, **2**, 638–649.

THOMSON, A.M. (1990). Augmentation by glycine and blockade by 6-cyano-7-nitroquinoxaline-2,3-dione (CNQX) of responses to excitatory amino acids in slices of rat neocortex. *Neuroscience*, **39**, 69–79.

YOSHIMURA, M. & JESSEL, T. (1990). Amino acid-mediated EPSPs at primary afferent synapses with substantia gelatinosa neurones in the rat spinal cord. *J. Physiol.*, **430**, 315–335.

Received March 24, 1992
Revised May 20, 1992
Accepted June 1, 1992)

Br. J. Pharmacol. (1992), **107**, 382–386

Calmodulin antagonists inhibit endothelium-dependent hyperpolarization in the canine coronary artery

Tetsuhiko Nagao, Stephane Illiano & [1]Paul M. Vanhoutte

Center for Experimental Therapeutics, Baylor College of Medicine, One-Baylor Plaza, Houston, Texas 77030, U.S.A.

1 The effects of the calmodulin antagonists, calmidazolium and fendiline were investigated on endothelium-dependent hyperpolarization in the canine coronary artery. The membrane potential of vascular smooth muscle cells was measured with the microelectrode technique.

2 Smooth muscle cells of the canine coronary artery had a resting membrane potential of −50 mV. Bradykinin and the Ca^{2+}-ionophore, A23187, induced concentration- and endothelium-dependent hyperpolarization. The hyperpolarization induced by a supramaximal concentration of bradykinin (10^{-6} M) reached approximately 20 mV.

3 Calmidazolium (10^{-5} M) and fendiline (10^{-4} M) inhibited hyperpolarization induced by bradykinin and A23187. By contrast, calmidazolium did not affect the hyperpolarization induced by lemakalim, an opener of ATP-sensitive K^+-channels.

4 These observations suggest that calmodulin is involved in the generation of endothelium-dependent membrane hyperpolarization of vascular smooth muscle.

Keywords: A23187; bradykinin; calcium; calmidazolium; endothelium-derived hyperpolarizing factor (EDHF); fendiline; lemakalim

Introduction

Calcium ions (Ca^{2+}) are important messenger in various intracellular physiological processes. Calmodulin, a calcium-binding protein, plays a crucial role in some Ca^{2+}-dependent responses; i.e., the metabolism of nucleotides, the release of neurotransmitters or hormones, and the contractions of muscle cells (Cheung, 1980). For example, in vascular smooth muscle cells, intracellular Ca^{2+} derived either from the extracellular space or intracellular stores, binds to calmodulin, activates myosin light chain kinase, phosphorylates myosin light chain, and leads to the actin-myosin interaction to cause muscle contraction (Kamm & Stull, 1985).

The endothelium modulates the tone of underlying vascular smooth muscle cells by releasing non-prostanoid endothelium-derived relaxing factors (EDRFs; Furchgott & Zawadzki, 1980). Previous work suggests that there are more than one EDRF (Hoeffner *et al.*, 1989; Boulanger *et al.*, 1989). Among them, nitric oxide (Furchgott, 1988; Ignarro *et al.*, 1987; Palmer *et al.*, 1987) or a related compound (Myers *et al.*, 1990) is regarded as a major EDRF. Another, yet unidentified factor causing membrane hyperpolarization, has been named endothelium-derived hyperpolarizing factor (EDHF: Bény & Brunet, 1988; Chen *et al.*, 1988; Feletou & Vanhoutte, 1988; Taylor & Weston, 1988). EDHF inactivates voltage-dependent Ca^{2+}-channels by hyperpolarizing the membrane of the vascular smooth muscle and leads to its relaxation (Taylor & Weston, 1988). The hyperpolarization is inhibited by glibenclamide, a blocker of ATP-sensitive K^+-channels, in middle cerebral arteries of the rabbit (Standen *et al.*, 1989; Brayden, 1990) suggesting the involvement of this class of K^+-channels in the generation of endothelium-dependent hyperpolarizations. However, conflicting results are reported in other vascular beds (Fujii *et al.*, 1990; Chen *et al.*, 1991; Van de Voorde *et al.*, 1992). Although subtypes of K^+-channels may not be identical between those activated by EDHF and those by an opener of ATP-sensitive channels, they share a common mechanism of action in that they both hyperpolarize the membrane of smooth muscle cells by opening K^+-channels. Thus, it seems appropriate to compare responses to EDHF and that to an opener of ATP-sensitive K^+-channels, such as lemakalim.

The release of EDRF is dependent on Ca^{2+} (Singer & Peach, 1982) and the synthesis of nitric oxide requires calmodulin in the cerebellum of the rat (Bredt & Snyder, 1990), and porcine and bovine aortic endothelial cells (Busse & Mülsch, 1990; Förstermann *et al.*, 1991). However, it is unknown whether or not endothelium-dependent hyperpolarizations require calmodulin for their generation. The present experiments were designed to examine, in the canine coronary artery, the effects of calmodulin antagonists on endothelium-dependent hyperpolarizations, and for comparison, on hyperpolarizations induced by lemakalim.

Methods

Mongrel dogs of either sex (12–28 kg) were anaesthetized with an intravenous injection of pentobarbitone (30 mg kg^{-1}, Abbott Laboratories, North Chicago, IL, U.S.A.). The hearts were excised and put immediately in ice cold modified Krebs-Ringer bicarbonate solution [millimolar concentration: NaCl 118.3, KCl 4.7, $CaCl_2$ 2.5, $MgSO_4$ 1.2, KH_2PO_4 1.2, $NaHCO_3$ 25.0, edetate calcium disodium (CaEDTA) 0.026, and glucose 11.1 (control solution), aerated with 95% O_2 and 5% CO_2]. Diagonal branches of the left anterior descending artery were isolated, cut into 5 mm segments, split along the longitudinal axis, and pinned down on the bottom of an organ chamber (1.5 ml capacity) with the endothelial side facing upward. The tissues were superfused with warm control solution (3 ml min^{-1}). After 90 min of incubation, a glass microelectrode (tip resistance 40–80 megaohms), filled with 3 M KCl and held by means of a micromanipulator (Narishige, Tokyo, Japan), was inserted into a smooth muscle cell (Nagao & Vanhoutte, 1991; 1992). Although impalements were possible both from the intimal or adventitial side of the vessel, changes in membrane potential were larger and more sensitive to agonists with the former procedure (data not shown). Thus, the electrical signal was recorded from the intimal side and was amplified by means of a recording amplifier (World Precision Instruments, New Haven, CT, U.S.A.). The membrane potential was monitored continuously on an oscilloscope (Textronix 5223,

[1] Author for correspondence.

Beaverton, OR, U.S.A.) and recorded on a paper recorder (Gould TA550, Cleveland, OH, U.S.A.). The following criteria were used to assess the validity of a successful impalement: (a) a sudden negative shift in voltage followed by (b) a stable negative voltage for more than 1 min and (c) an instantaneous return to the previous voltage level on dislodgement of the microelectrode. In some preparations, the endothelial cells were removed by gentle rubbing of the intimal surface with a scalpel blade. Amplitudes of hyperpolarizations induced by bradykinin or A23187 were determined by continuous recordings of membrane potential from a single cell, since these hyperpolarizations were transient in nature. Calmidazolium (10^{-5} M) and fendiline (10^{-4} M) were given more than 60 min before the administration of the agonists. The effects of calmidazolium on lemakalim-induced hyperpolarizations were examined by means of repeated impalements of the cells, since these hyperpolarizations were sustained for more than 30 min. The experiments with the calmodulin antagonists were performed in the presence of dimethylsulphoxide (0.1 volume %), either as a solvent of the antagonists or as vehicle. All experiments were performed in the presence of indomethacin (10^{-5} M) to inhibit the formation of endogenous vasoactive prostanoids.

Drugs

The drugs used were A23187, bradykinin (Sigma, St Louis, MO, U.S.A.), calmidazolium (Boehringer Mannheim, GmbH, Germany), fendiline, indomethacin (Sigma) and lemakalim (Beecham, U.K.). A23187 (10^{-3} M), calmidazolium (10^{-2} M) and fendiline (10^{-1} M) were dissolved in dimethyl sulphoxide (DMSO). Lemakalim (1.7×10^{-4} M) was prepared in ethanol. Stock solutions of indomethacin were prepared in equal molar concentration of Na_2CO_3 to adjust the pH to around 7.4. The final bath concentrations were 0.1, 0.3, 0.6 volume % for DMSO, ethanol and Na_2CO_3, respectively. All other drugs were dissolved in distilled water.

Statistical analysis

The results were expressed as means ± s.e.mean; n represents the number of animals examined. The statistical significance of observed differences was tested with Student's unpaired t test (two-tailed) or analysis of variance followed by Scheffé's F test. P values less than 0.05 were considered to be statistically significant.

Results

Smooth muscle cells of canine coronary arteries had a resting membrane potential of -49 ± 0.6 mV (Table 1). Calmidazolium (10^{-5} M) depolarized the membrane by 1 mV and fendiline (10^{-4} M) by 3 mV (Table 1). The maximal hyperpolarization induced by bradykinin (10^{-6} M, a supramaximal concentration) approximated 20 mV.

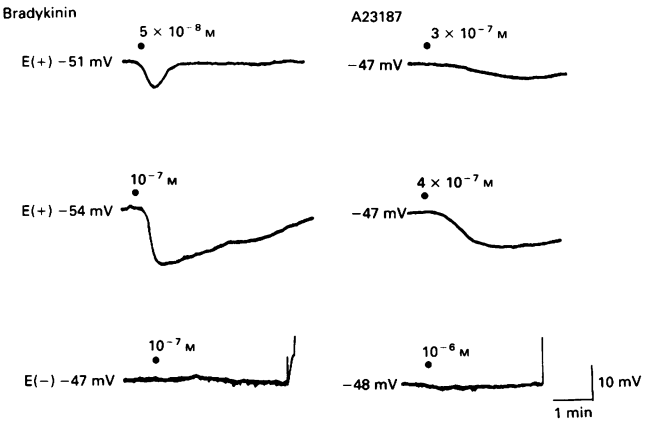

Figure 1 Effect of bradykinin and A23187 on the membrane potential of the canine coronary artery. The recordings in the presence of endothelium were obtained from the same animal, and those in the absence of endothelium were recorded from a different dog. The sudden discontinuations of the recordings (by upward deflection) in the bottom panel show dislodgements of a microelectrode. E(+): with endothelium, E(−): without endothelium.

Bradykinin induced concentration-dependent hyperpolarizations (Figure 1). The hyperpolarization was not observed in tissues without endothelium ($n = 3$, Figure 1). At 5×10^{-8} M, bradykinin evoked submaximal hyperpolarizations (averaging 10 mV). Calmidazolium (10^{-5} M) abolished the endothelium-dependent hyperpolarization induced by bradykinin (5×10^{-8} M), and as a consequence, the membrane potential during the administration of bradykinin was significantly less negative in the presence of calmidazolium (Figure 2). Fendiline (10^{-4} M), also inhibited the hyperpolarization induced by the same concentration of the kinin (Figure 3).

The calcium ionophore A23187 induced concentration-dependent membrane hyperpolarization (Figure 1), which was observed in tissues with, but not in those without endothelium ($n = 3$, Figure 1). Calmidazolium (10^{-5} M) abolished the hyperpolarization induced by A23187 (2 to 4×10^{-7} M; the concentration of A23187 was determined in each animal to achieve approximately 10 mV of hyperpolarization), and the membrane potential during the administration of A23187 was significantly less negative in the presence of calmidazolium (Figure 4).

Lemakalim (5×10^{-7} M, a submaximal concentration) hyperpolarized the membrane by 16 mV in control experiments. Calmidazolium (10^{-5} M) did not affect the hyperpolarization induced by the K^+-channel opener significantly, and the membrane potential in the presence of lemakalim was comparable, regardless of the presence or absence of calmidazolium (Figure 5).

Table 1 Membrane potential in canine coronary vascular smooth muscle

	Membrane potential (mV)	*Number of impalements*	*Number of animals*
Control: with endothelium	-49 ± 0.6	14	7
Without endothelium	-50 ± 0.8	14	5
Vehicle (DMSO, 0.1%)	-48 ± 0.6	26	10
Calmidazolium (10^{-5} M)	-47 ± 0.4*	18	9
Fendiline (10^{-4} M)	-45 ± 0.6*	5	3

Values are mean ± s.e.mean.
*Statistically significant difference ($P < 0.05$) between the tissue treated with the vehicle (DMSO: dimethyl sulphoxide) and with the inhibitors of calmodulin.

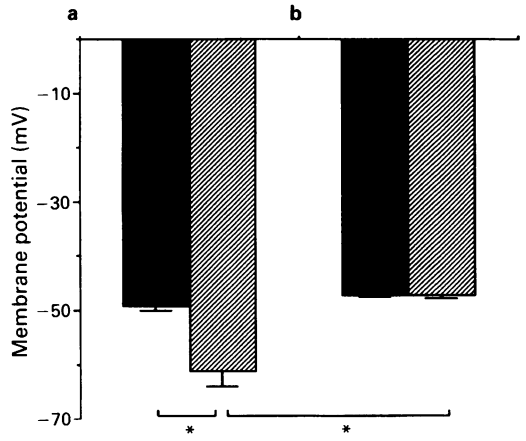

Figure 2 Amplitudes of membrane hyperpolarizations induced by bradykinin (5×10^{-8} M) in the absence (a) or presence (b) of calmidazolium (10^{-5} M), in the canine coronary artery. The solid and hatched columns represent membrane potential before and after the administration of bradykinin, respectively. The effects of bradykinin were determined by continuous recordings of membrane potential from a single cell. Data are shown as mean with s.e.mean indicated by vertical bars ($n = 4$). *Significant difference: $P < 0.05$, analysis of variance.

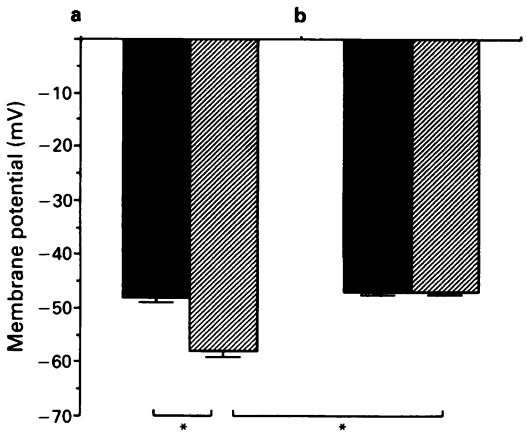

Figure 4 Amplitudes of membrane hyperpolarizations induced by A23187 ($2-4 \times 10^{-7}$ M) in the absence (a) or presence (b) of calmidazolium (10^{-5} M), in the canine coronary artery. The solid and hatched columns represent membrane potential before and after the administration of A23187, respectively. The effects of A23187 were determined by continuous recordings of membrane potential from a single cell. Data are shown as mean with s.e.mean indicated by vertical bars ($n = 4$). *Significant difference: $P < 0.05$, analysis of variance.

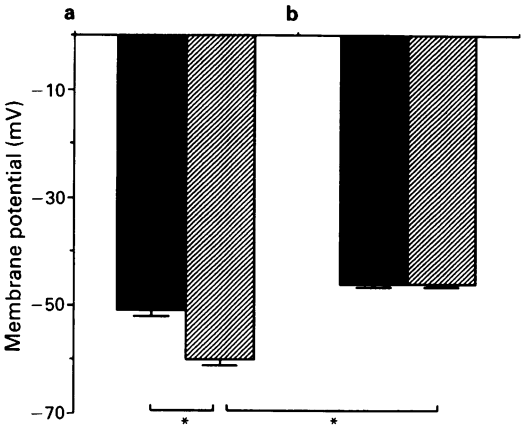

Figure 3 Amplitudes of membrane hyperpolarizations induced by bradykinin (5×10^{-8} M) in the absence (a) or presence (b) of fendiline (10^{-4} M), in the canine coronary artery. The solid and hatched columns represent membrane potential before and after the administration of bradykinin, respectively. The effects of fendiline were determined by continuous recordings of membrane potential from a single cell. Data are shown as mean ± S.E.M. With s.e.mean indicated by vertical bars ($n = 3$). *Significant difference: $P < 0.05$, analysis of variance.

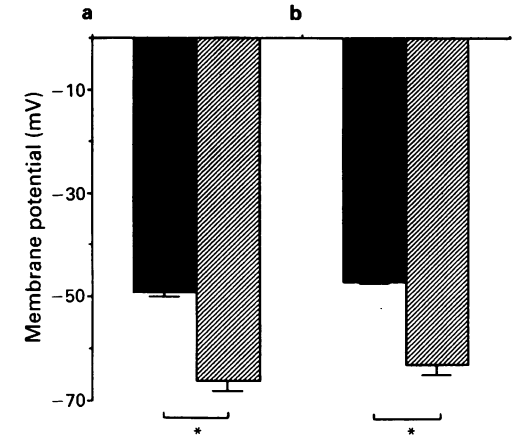

Figure 5 Amplitudes of membrane hyperpolarizations induced by lemakalim (5×10^{-8} M) in the absence (a) or presence (b) of calmidazolium (10^{-5} M), in the canine coronary artery. The membrane potential was measured by means of repeated impalements of the cells. The solid and hatched columns represent membrane potential before and after the administration of lemakalim, respectively. Data are shown as mean with s.e.mean indicated by vertical bars (6–10 impalements from 4–7 animals). *Significant difference: $P < 0.05$, analysis of variance.

Discussion

The present study demonstrates that endothelium-dependent hyperpolarization is inhibited by calmodulin antagonists and thus suggests a possible involvement of calmodulin in the generation of the electrical response. In the canine coronary artery, calmidazolium inhibits the relaxations elicited by bradykinin and A23187 that are resistant to nitro-L-arginine (a competitive inhibitor of nitric oxide-synthase) and indomethacin (an inhibitor of cyclo-oxgenase) (Illiano *et al.*, 1992). Since, in the presence of the two inhibitors, the relaxations are mediated by endothelium-dependent hyperpolarizations (Nagao & Vanhoutte, 1991; 1992), the observation reinforces the conclusion that the calmodulin antagonist inhibits endothelium-dependent hyperpolarizations in the canine coronary artery. The concentrations of calmidazolium (10^{-5} M) and fendiline (10^{-4} M) used in the present experiments are one log unit above the EC_{50} of the antagonists described *in vitro* (Johnson & Wittenauer, 1983; Gietzen, 1983). Such concentrations were used to allow a maximal inhibition and to compensate for the poor accessibility of the compounds to the inside of the cells (Ahlijanian *et al.*, 1987). Several studies on the role of calmodulin in endothelium-dependent responses have been performed with the same concentration of calmidazolium (Weinheimer & Osswald, 1986; Busse *et al.*, 1988; Förstermann *et al.*, 1991; Fleming *et al.*, 1991).

It is not likely that the inhibition of endothelium-dependent hyperpolarization by the calmodulin antagonists is due to a nonspecific action of the compounds for the following reasons: (a) Although these compounds might have effects on targets other than calmodulin (Stoclet *et al.*, 1987), calmidazolium is one of the most potent and specific calmodulin inhibitors known (Gietzen, 1983; Stoclet *et al.*, 1987). In

addition, two structurally different calmodulin antagonists had similar inhibitory effects, which may also argue against the possibility of a direct interaction between endothelium-derived hyperpolarizing factor and these compounds; (b) Calmidazolium inhibited endothelium-dependent hyperpolarizations induced by two different mechanisms; bradykinin (receptor-mediated) and A23187 (receptor-independent). This rules out the possibility of an antagonism at the receptor level; and (c) calmidazolium did not interfere with the hyperpolarization induced by lemakalim ((−)-cromakalim, an ATP-sensitive K^+channel opener: Weir & Weston, 1986; Quast, 1988). Thus, calmidazolium does not have an inhibitory effect on this class of K^+-channels. If endothelium-dependent hyperpolarizations were evoked by activation of ATP-sensitive K^+-channels in the canine coronary artery as they are in the middle cerebral artery of the rabbit (Standen *et al.*, 1989; Brayden, 1990) this observation rules out the view that calmidazolium exerts its effect at the smooth muscle (K^+-channel) level. Even though K^+-channels other than ATP-sensitive ones are responsible for the endothelium-dependent hyperpolarization in the canine coronary and in other arteries (Fujii *et al.*, 1990; Chen *et al.*, 1991; Van de Voorde *et al.*, 1992), it can be concluded, at least, that calmidazolium is not a nonspecific blocker of K^+-channels on the smooth muscle. In further support of this conclusion, calmidazolium does not inhibit the activation of Ca^{2+}-activated K^+-channels (Kihira *et al.*, 1990). Thus, the inhibition by calmodulin antagonists appears to be selective for endothelium-dependent membrane hyperpolarizations.

The production/release of nitric oxide is dependent on Ca^{2+} (Singer & Peach, 1982; Busse & Mülsch, 1990) and may require calmodulin, as suggested by the effects of calmodulin antagonists in isolated blood vessels (Weinheimer & Osswald, 1986). However, in cultured endothelial cells, these antagonists augment rather than depress the release of endothelium-derived relaxing factor (Busse *et al.*, 1988). In the carotid artery of the rabbit, endothelium-dependent hyperpolarizations depend on the availability of Ca^{2+} (Chen & Suzuki, 1990). This Ca^{2+}-dependency is supported by the finding that the Ca^{2+}-ionophore A23187 induces endothelium-dependent membrane hyperpolarizations (Chen & Suzuki, 1990; Nagao & Vanhoutte, 1992; present study). Taken in conjuction with the overall importance of Ca^{2+} in the generation of the electrical events, the present findings with calmodulin antagonists strongly suggest that the formation of a Ca^{2+}-calmodulin complex, following the elevation of Ca^{2+} in endothelial cells, is a key step in the production or release of EDHF.

In summary, the effects of A23187 and calmodulin antagonists suggest that both Ca^{2+} and calmodulin are required for the generation of endothelium-dependent membrane hyperpolarizations in the canine coronary artery.

This work was supported in part by NIH grants HL 31183 and HL 31547 and by an unrestricted Research Award of the Bristol-Myers Research Institute. Lemakalim was kindly provided by Beecham Pharmaceutical Company.

References

AHLIJANIAN, M.K. & COOPER, D.M.F (1987). Antagonism of calmodulin-stimulated adenylate cyclase by trifluoperazine, calmidazolium and W-7 in rat cerebellar membranes. *J. Pharmacol. Exp. Ther.*, **241**, 407–414.

BÉNY, J.-L. & BRUNET, P.C. (1988). Neither nitric oxide nor nitroglycerin accounts for all the characteristics of endothelially mediated vasodilatation of pig coronary arteries. *Blood Vessels*, **25**, 308–311.

BOULANGER, C., HENDRICKSON, H., LORENZ, R.R. & VANHOUTTE, P.M. (1989). Release of different relaxing factors by cultured porcine endothelial cells. *Circ. Res.*, **64**, 1070–1078.

BRAYDEN, J.E. (1990). Membrane hyperpolarization is a mechanism of endothelium-dependent cerebral vasodilatation. *Am. J. Physiol.*, **259**, H688–H673.

BREDT, D. & SNYDER, S.H. (1990). Isolation of nitric oxide synthase, a calmodulin-requiring enzyme. *Proc. Natl. Acad. Sci. U.S.A.*, **87**, 682–685.

BUSSE, R., LÜCKHOFF, A., WINTER, I., MÜLSCH, A. & POHL, U. (1988). Fendiline and calmidazolium enhance the release of endothelium-derived relaxant factor and of prostacyclin from cultured endothelial cells. *Naunyn-Schmiedebergs Arch. Pharmacol.*, **337**, 79–84.

BUSSE, R. & MÜLSCH, A. (1990). Calcium-dependent nitric oxide synthesis in endothelial cytosol is mediated by calmodulin. *FEBS*, **256**, 133–136.

CHEN, G. & SUZUKI, H. (1990). Calcium-dependency of the endothelium-dependent hyperpolarization in smooth muscle cells of the rabbit carotid artery. *J. Physiol.*, **421**, 521–534.

CHEN, G., SUZUKI, H. & WESTON, A.H. (1988). Acetylcholine releases endothelium-derived hyperpolarizing factor and EDRF from rat blood vessels. *Br. J. Pharmacol.*, **95**, 1165–1174.

CHEN, G., YAMAMOTO, Y., MIWA, K. & SUZUKI, H. (1991). Hyperpolarization of arterial smooth muscle by endothelial humoral substances. *Am. J. Physiol.*, **260**, H1888–H1892.

CHEUNG, W.Y. (1980). Calmodulin plays a pivotal role in cellular regulation. *Science*, **207**, 19–27.

FELETOU, M. & VANHOUTTE, P.M. (1988). Endothelium-dependent hyperpolarisation of canine coronary smooth muscle. *Br. J. Pharmacol.*, **93**, 515–524.

FLEMING, I., GRAY, G.A., SCHOTT, C. & STOCKLET, J.C. (1991). Inducible but not constitutive production of nitric oxide by vascular smooth muscle cells. *Eur. J. Pharmacol.*, **200**, 375–376.

FÖRSTERMANN, U., POLLOCK, J.S., SCHMIDT, H.H., HELLER, M. & MURAD, F. (1991). Calmodulin-dependent endothelium-derived relaxing factor/nitric oxide synthase activity is present in the particulate and cytosolic fractions of bovine aortic endothelial cells. *Proc. Natl. Acad. Sci. U.S.A.*, **88**, 1788–1792.

FUJII, K., KOBAYASHI, K., KOGA, T. & FUJISHIMA, M. (1990). Decreased endothelium-dependent hyperpolarization in spontaneously hypertensive rats (SHR). *Circulation*, **82** (Suppl 4), III–344.

FURCHGOTT, R.F. (1988). Studies on relaxation of rabbit aorta by sodium nitrate: the basis for the proposal that the acid-activatable inhibitory factor from bovine retractor penis is inorganic nitrate and the endothelium-derived relaxing factor is nitric oxide. In *Mechanism of Vasodilatation*, ed. Vanhoutte, P.M. Vol. 4, pp. 401–414. Raven Press: New York, U.S.A.

FURCHGOTT, R.F. & ZAWADZKI, J.V. (1980). The obligatory role of endothelial cells in the relaxation of the arterial smooth muscle by acetylcholine. *Nature*, **286**, 373–376.

GIETZEN, K. (1983). Comparison of the calmodulin antagonist compound 48/80 and calmidazolium. *Biochem. J.*, **216**, 611–616.

HOEFFNER, U., FELETOU, M., FLAVAHAN, N.A. & VANHOUTTE, P.M. (1989). Canine arteries release two different endothelium-derived relaxing factors. *Am. J. Physiol.*, **257**, H330–H333.

IGNARRO, L.J., BYRNS, R.E., BUGA, G.M. & WOODS, K.S. (1987). Endothelium-derived relaxing factor from pulmonary artery and vein possesses pharmacologic and chemical properties identical to those of nitric oxide radical. *Circ. Res.*, **61**, 866–879.

ILLIANO, S.C., NAGAO, T. & VANHOUTTE, P.M. (1992). Calmidazolium inhibits endothelium-dependent relaxations that are resistant to nitro-L-arginine in the canine coronary artery. *Br. J. Pharmacol.*, **107**, 387–392.

JOHNSON, J.D. & WITTENAUER, L.A. (1983). A fluorescent calmodulin that reports the binding of hydrophobic inhibitory ligands. *Biochem. J.*, **211**, 473–479.

KAMM, K.E. & STULL, J.T. (1985). The function of myosin and myosin light chain kinase phosphorylation in smooth muscle. *Annu. Rev. Pharmacol. Toxicol.*, **25**, 593–620.

KIHIRA, M., MATSUZAWA, K., TOKUNO, H. & TOMITA, T. (1990). Effects of calmodulin antagonists on calcium-activated potassium channels in pregnant rat myometrium. *Br. J. Pharmacol.*, **100**, 353–359.

MYERS, P.R., MINOR, R.L. Jr, GUERRA, R. Jr, BATES, J.N. & HARRISON, D.G. (1990). Vasorelaxant properties of the endothelium-derived relaxing factor more closely resemble S-nitrosocysteine than nitric oxide. *Nature*, **345**, 161–163.

NAGAO, T. & VANHOUTTE, P.M. (1991). Membrane hyperpolarization contributes to endothelium-dependent relaxations induced by acetylcholine in the femoral vein of the rat. *Am. J. Physiol.*, H1034–H1038.

NAGAO, T. & VANHOUTTE, P.M. (1992). Hyperpolarization as a mechanism for endothelium-dependent relaxations in porcine coronary arteries. *J. Physiol.*, **445**, 355–368.

PALMER, R.M.J., FERRIGE, A.G. & MONCADA, S. (1987). Nitric oxide release accounts for the biological activity of endothelium-derived relaxing factor. *Nature*, **327**, 524–526.

QUAST, U. (1988). Inhibition of the effects of K^+ channel stimulator cromakalim (BRL 34915) in vascular smooth muscle by glibenclamide and forskolin. *Naunyn-Schmiedebergs Arch. Pharmacol.*, **337** (suppl.), R72.

SINGER, H.A. & PEACH, M.J. (1982). Calcium- and endothelium-mediated smooth muscle relaxation in rabbit aorta. *Hypertension*, **4** (suppl. II), II19–II25.

STANDEN, N.B., QUAYLE, J.M., DAVIES, N.W., BRAYDEN, J.E., HUANG, Y. & NELSON, M.T. (1989). Hyperpolarizing vasodilators activate ATP-sensitive K^+-channels in arterial smooth muscle. *Science*, **245**, 177–180.

STOCLET, J.C., GERARD, D., KILHOFFER, M.-C., LUGNIER, C. & SCHAEFFER, P. (1987). Calmodulin and its role in intracellular calcium regulation. *Prog. Neurobiol.*, **29**, 321–364.

TAYLOR, S.G. & WESTON, A.H. (1988). Endothelium-derived hyperpolarizing factor: a new endogenous inhibitor from the vascular endothelium. *Trends Pharmacol. Sci.*, **9**, 72–74.

VAN DE VOORDE, J., VANHEEL, B. & LEUSEN, I. (1992). Endothelium-dependent relaxation and hyperpolarization in aorta from control and renal hypertensive rats. *Circ. Res.*, **70**, 1–8.

WEINHEIMER, G. & OSSWALD, H. (1986). Inhibition of endothelium-dependent smooth muscle relaxation by calmodulin antagonists. *Naunyn-Schmiedebergs Arch. Pharmacol.*, **33**, 391–397.

WEIR, S. & WESTON, A.H. (1986). The effects of BRL 34915 and nicorandil on electrical and mechanical activity on ^{86}Rb efflux in rat blood vessels. *Br. J. Pharmacol.*, **88**, 121–128.

(Received October 4, 1991
Revised April 27, 1992
Accepted June 1, 1992)

Br. J. Pharmacol. (1992), **107**, 387–392

Calmidazolium, a calmodulin inhibitor, inhibits endothelium-dependent relaxations resistant to nitro-L-arginine in the canine coronary artery

Stephane Illiano, Tetsu Nagao & [1]Paul M. Vanhoutte

Center for Experimental Therapeutics, Baylor College of Medicine, Houston, TX 77030, U.S.A.

1 The role of calmodulin in endothelium-dependent relaxations in the canine coronary artery, was investigated by use of the inhibitor of calmodulin, calmidazolium.

2 The endothelium-dependent relaxations to adenosine diphosphate (ADP) and nebivolol, a β-adrenoceptor antagonist, in control solution, and to bradykinin in high potassium solution (to inhibit endothelium-dependent hyperpolarization), were abolished by nitro-L-arginine (30 μM), an inhibitor of nitro oxide-synthase. Calmidazolium (10 μM) did not inhibit these relaxations.

3 Calmidazolium did not affect the endothelium-independent relaxations to SIN-1, an exogenous donor of nitric oxide (NO).

4 The relaxations to bradykinin and to the calcium ionophore A23187 in control solution were inhibited to a small extent by calmidazolium (10 μM).

5 Bradykinin and A23187 induced relaxations in the presence of nitro-L-arginine (30 μM) that were abolished by calmidazolium (10 μM) but not affected by glibenclamide (10 μM), an inhibitor of ATP-sensitive K^+ channels.

6 The endothelium-independent relaxations to lemakalim, an ATP-sensitive K^+ channel opener, were not affected by calmidazolium (10 μM) but were inhibited by glibenclamide (10 μM).

7 These results suggest that calmidazolium does not inhibit the endothelium-dependent relaxations due to endothelium-derived NO in the canine coronary artery but inhibits either the production of endothelium-derived hyperpolarizing factor (EDHF) from endothelial cells or its effects on vascular smooth muscle cells. Furthermore these results suggest that EDHF contributes to endothelium-dependent relaxations in the canine coronary artery.

Keywords: Nitric oxide; endothelium-derived hyperpolarizing factor; calmidazolium; calmodulin; coronary artery; nitro-L-arginine

Introduction

The activation of endothelial cells by an increase in shear stress or by a variety of vasoactive stimuli, such as acetylcholine (Furchgott & Zawadzki, 1980), adenosine nucleotides or bradykinin, evokes the release of non prostanoid endothelium-derived relaxing factors (EDRF; Furchgott, 1983). One of these, nitric oxide (NO) (Palmer *et al.*, 1987; Furchgott, 1988; Ignarro *et al.*, 1987), or a related compound (Myers *et al.*, 1990) is produced from L-arginine by NO synthase and evokes relaxation by activation of soluble guanylate cyclase in vascular smooth muscle cells (Rapoport & Murad, 1983; Ignarro & Kadowitz, 1985). Another endothelium-derived substance (endothelium-derived hyperpolarizing factor; EDHF), distinct from nitric oxide, induces relaxation via hyperpolarization of the smooth muscle cells (Feletou & Vanhoutte, 1988; Beny & Brunet, 1988; Chen *et al.*, 1988; Komori *et al.*, 1988; Taylor & Weston, 1988). Elevation of cytosolic Ca^{2+} is an essential step in the synthesis or release of these endothelium-derived relaxing factors (Lückhoff *et al.*, 1988; Rubanyi *et al.*, 1988; Busse *et al.*, 1988a; Chen & Suzuki, 1990). Calmodulin modulates many intracellular Ca^{2+}-regulated enzymatic processes (Means & Dedman, 1980; Cheung, 1980). Furthermore, Ca^{2+} and calmodulin are co-factors for NO-synthase activity in several tissues (Bredt & Snyder, 1990; Föstermann *et al.*, 1991). This dependency on calmodulin may explain the requirement for Ca^{2+} in the regulation of endothelium-dependent relaxations of vascular smooth muscle (Singer & Peach, 1982).

In isolated coronary arteries, bradykinin, or the Ca^{2+} ionophore A23187 evoke relaxations which are not abolished by nitro-L-arginine (Nagao & Vanhoutte, 1992), an inhibitor of NO synthase (Moore *et al.*, 1990), or methylene blue, an inhibitor of guanylate cyclase (Martin *et al.*, 1985; Ignarro & Kadowitz, 1985). A diffusible factor, distinct from NO, may play a role in the endothelium-dependent relaxation induced by these agonists (Huang *et al.*, 1988; Boulanger *et al.*, 1989; Chen *et al.*, 1991; Nagao & Vanhoutte, 1991).

The present experiments used a calmodulin inhibitor to determine the role of calmodulin in endothelium-dependent relaxations mediated either by NO, or the other non-prostanoid endothelium-derived relaxing substance (presumably EDHF). Electrophysiological experiments performed in the laboratory demonstrated that both fendiline (10^{-4} M) and calmidazolium inhibit endothelium-dependent hyperpolarization of canine coronary smooth muscle cells (Nagao *et al.*, 1992). However, preliminary studies revealed that fendiline (but not calmidazolium) inhibited in a non specific way the contractions of canine isolated coronary arteries. Therefore only calmidazolium was used in the present study.

Methods

Mongrel dogs (15–30 kg) were anaesthetized with sodium pentobarbitone (30 mg kg^{-1}, intravenously) and exsanguinated. The hearts were removed and the coronary arteries excised and placed in cold modified Krebs-Ringer bicarbonate solution [composition in mM: NaCl 118.3, KCl 4.7,

[1] Author for correspondence.

$CaCl_2$ 2.5, $MgSO_4$ 1.2, KH_2PO_4 1.2, $NaHCO_3$ 25, glucose 11.1, calcium disodium edetate 0.026, pH 7.4 (control solution)]. Tissues were cleaned of connective tissue and cut into rings (3–4 mm). In some rings, the endothelium was removed mechanically by inserting the tips of a watchmaker's forceps into the lumen and rolling the preparation back and forth over a paper towel wetted with control solution. All experiments were carried out in the presence of indomethacin (10 μM) to prevent the production of vasodilators prostanoids.

Organ chamber studies

Coronary rings were suspended between two stirrups in organ chambers (25 ml) filled with control solution (gassed with 95% O_2 plus 5% CO_2 maintained at 37°C, pH 7.4). One of the stirrups was anchored inside the organ chamber and the other connected to a force transducer (Gould CT 2) to record changes in isometric force. The rings were stretched to the optimal point of their length-active tension relationship (8.1 ± 1.2 g) as determined by the contractile response to 60 mM KCl at progressive levels of stretch. The rings were incubated either in control solution or in the presence of N^G-nitro-L-arginine (30 μM), an inhibitor of NO-synthase, glibenclamide (10 μM), an inhibitor of ATP-sensitive K^+ channels, and/or calmidazolium (10 μM), a calmodulin inhibitor, for 60 min before inducing contraction with prostaglandin $F_{2\alpha}$ (2×10^{-6} M). Relaxations were obtained with bradykinin, the calcium ionophore A23187, adenosine diphosphate (ADP), nebivolol, (a vasodilator β-adrenoceptor antagonist, that releases NO without causing endothelium-dependent hyperpolarizations of canine coronary smooth muscle; Gao *et al.*, 1991), SIN-1, an exogenous donor of NO (Feelisch *et al.*, 1989), and lemakalim ((-)-cromakalim; an ATP-sensitive K^+ channel opener: Quast, 1988).

In certain experiments, rings of dog coronary arteries were contracted into 60 mM KCl and once the contraction had stabilized, N^G-nitro-L-arginine (30 μM) or calmidazolium (10 μM) were added for 45 min. Concentration-response curves to bradykinin and SIN-1 were then obtained in succession.

Drugs and chemicals

The following drugs were used; A23187, ADP, bradykinin, glibenclamide, indomethacin, methylene blue, prostaglandin $F_{2\alpha}$, (all from Sigma, St-Louis, MO, U.S.A.), N^G-nitro-L-arginine (Aldrich, Milwaukee, WI, U.S.A.), calmidazolium (Boehringer Manheim GmbH, Germany), lemakalim (Beecham Company, United Kingdom), o(±)-nebivolol (Janssen Pharmaceutica, Belgium), and SIN-1 (N-ethoxycarbonyl-3-morpholino-sydnonimine; Hoechst Paris, France). Drugs were prepared in water except for calmidazolium, glibenclamide and calcium ionophore A23187 which were dissolved in dimethyl sulphoxide (Sigma) and lemakalim which was dissolved in ethanol. The higher concentrations (10^{-2} M) of these drugs were prepared in these solvents and the subsequent dilutions were made in distilled water. Indomethacin was dissolved in distilled water and an equimolar concentration of Na_2CO_3 (10^{-5} M).

Statistical analysis

In each experimental group, n refers to the number of animals. Results are expressed as the mean ± s.e.mean. The negative logarithm of the concentrations of the agonists causing 50% relaxation of the contraction evoked by prostaglandin $F_{2\alpha}$ is defined as IC_{50}. Statistical comparisons were performed by means of a two way analysis of variance (ANOVA) or Student's t test for paired or unpaired observations. Differences were considered to be significant when P was less than 0.05.

Results

Contractions

The two solvents dimethyl sulphoxide and ethanol, at the highest concentration used (0.1% of the final volume in the organ chamber), had no effect either on resting tension or elevated tone. Calmidazolium (10 μM) did not affect the contractions evoked by prostaglandin $F_{2\alpha}$ (2 μM) (control 6.2 ± 1.3 g; calmidazolium 5.8 ± 0.8 g) or by 60 mM KCl (8.4 ± 0.6 in control and 8.1 ± 0.7 in treated). The addition of nitro-L-arginine (30 μM) induced small contractions of the coronary rings (0.9 ± 0.3 g). The final level of contraction induced by prostaglandin $F_{2\alpha}$ (2 μM) was significantly increased in the presence of nitro-L-arginine (6.2 ± 1.3 g in control and 7.8 ± 0.7 g in treated rings).

Endothelium-dependent relaxations

Bradykinin In control solution, bradykinin induced relaxation of rings with endothelium intact, that had been contracted with prostaglandin $F_{2\alpha}$ (2 μM). The concentration-response curve was not significantly shifted to the right by calmidazolium (10 μM) (IC_{50}: 8.6 ± 0.2 in control and 8.12 ± 0.4 in treated) but the maximal response was significantly reduced (control 99.6 ± 5% and calmidazolium 76.7 ± 9.8%) (Figure 1). In rings without endothelium, bradykinin did not induce relaxations (data not shown).

In the presence of nitro-L-arginine (30 μM), the concentration-response curve to bradykinin was shifted to the right in rings with endothelium intact, that had been contracted with prostaglandin $F_{2\alpha}$ as compared to controls. The IC_{50} could not be calculated for the nitro-L-arginine-treated rings. The maximal response was significantly reduced (control 99.6 ± 5%, and nitro-L-arginine treated 28.5 ± 7%). The relaxations in the presence of nitro-L-arginine were inhibited by calmidazolium (10 μM) but not affected by glibenclamide (10 μM) (Figure 1).

In rings contracted with 60 mM potassium, bradykinin induced concentration-dependent relaxations which were not affected significantly by calmidazolium (IC_{50}: 7.94 ± 0.27 and 7.62 ± 0.3, respectively), but abolished by nitro-L-arginine (30 μM) (Figure 2).

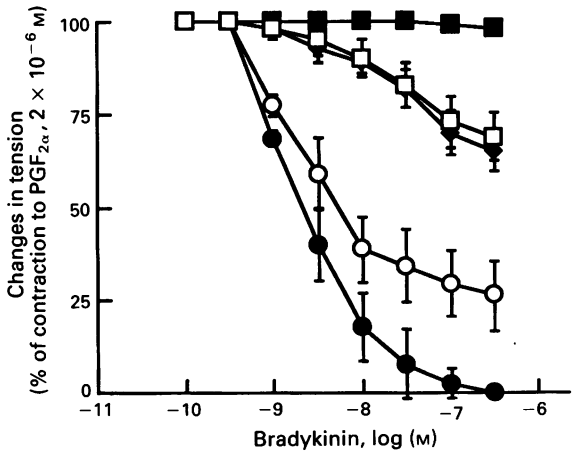

Figure 1 Effect of calmidazolium on relaxations to bradykinin in rings of canine coronary artery with endothelium intact, contracted with prostaglandin $F_{2\alpha}$ (2 μM) in control solution or in the presence of nitro-L-arginine (30 μM). The experiments were performed in the presence of indomethacin (10 μM). When nitro-L-arginine was present experiments were performed with dimethylsulphoxide (DMSO, vehicle), calmidazolium (10 μM) or glibenclamide (10 μM). Data are expressed as percentage of the contraction induced by prostaglandin $F_{2\alpha}$ and shown as mean ± s.e.mean (vertical bars) ($n = 6$). (●) Control; (○) in the presence of calmidazolium; (□) in the presence of nitro-L-arginine; (■) in the presence of nitro-L-arginine and calmidazolium; (◆) in the presence of nitro-L-arginine and glibenclamide.

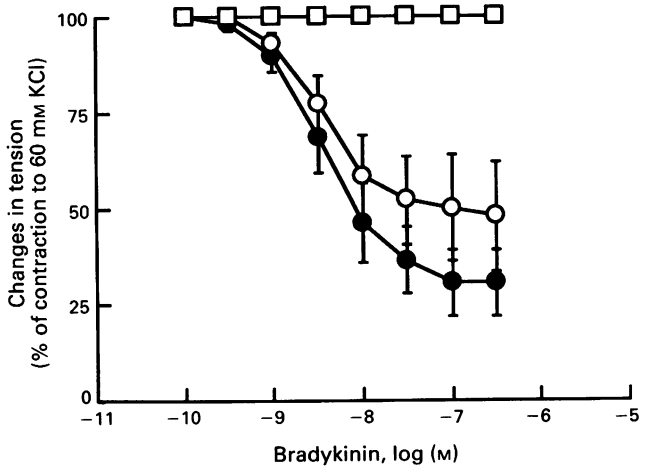

Figure 2 Effect of calmidazolium (10 μM) on relaxations to bradykinin in canine coronary arteries with endothelium intact, contracted with 60 mM KCl. The experiments were performed in the presence of indomethacin (10 μM). Data are expressed as percentage of the contraction induced by 60 mM and shown as mean ± s.e.mean (vertical bars) ($n = 6$). (●) Control; (○) in the presence of calmidazolium; (□) in the presence of nitro-L-arginine.

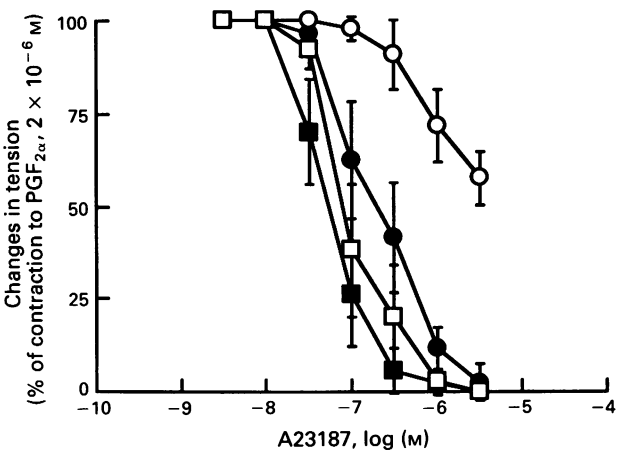

Figure 4 Effect of calmidazolium (10 μM) on relaxations elicited by A23187 in canine coronary artery with endothelium intact, contracted with prostaglandin $F_{2\alpha}$ (2 μM) in control solution or in the presence of nitro-L-arginine (30 μM). The experiments were performed in the presence of indomethacin (10 μM). Data are expressed as percentage of the contraction induced by prostaglandin $F_{2\alpha}$ and shown as mean ± s.e.mean (vertical bars) ($n = 6$). (■) Control; (□) in the presence of calmidazolium; (●) in the presence of nitro-L-arginine; (○) in the presence of nitro-L-arginine and calmidazolium.

ADP In control solution, the concentration-relaxation curve to adenosine diphosphate of rings with endothelium intact, that had been contracted with prostaglandin $F_{2\alpha}$, was not affected significantly by calmidazolium (IC_{50}: 6.61 ± 0.16 in treated and 6.84 ± 0.1 in control rings) (Figure 3).

In the presence of nitro-L-arginine (30 μM), ADP induced modest endothelium-dependent relaxations at the highest concentration tested (3 μM). These relaxations were inhibited by calmidazolium (10 μM) (Figure 3).

A23187 The calcium ionophore, A23187, induced relaxations in rings with endothelium intact, that had been contracted with prostaglandin $F_{2\alpha}$, which were not affected by calmidazolium (IC_{50}; 7.27 ± 0.15 and 6.98 ± 0.19, respectively) (Figure 4).

In the presence of nitro-L-arginine (30 μM) alone, the concentration-relaxation curves to A23187 were not significantly shifted to the right (IC_{50}: 7.27 ± 0.15 in control, and 6.93 ± 0.12 in treated rings). When the rings were incubated with nitro-L-arginine (30 μM) plus calmidazolium (10 μM), the concentration-relaxation curve to A23187 was significantly shifted to the right (the IC_{50} could not be calculated) and the maximal response was decreased (41.2 ± 5.1% compared to 92 ± 7.2% in controls) (Figure 4). In rings without endothelium A23187 did not induce relaxations (data not shown).

Nebivolol Nebivolol induced endothelium-dependent relaxations in rings of canine coronary artery contracted with prostaglandin $F_{2\alpha}$, which were not affected significantly by calmidazolium (IC_{50}: 5.08 ± 0.18 versus 5.22 ± 0.08 in control) (Figure 5).

Endothelium-independent relaxations

SIN-1 SIN-1 induced concentration-dependent relaxations in rings without endothelium, contracted with prostaglandin

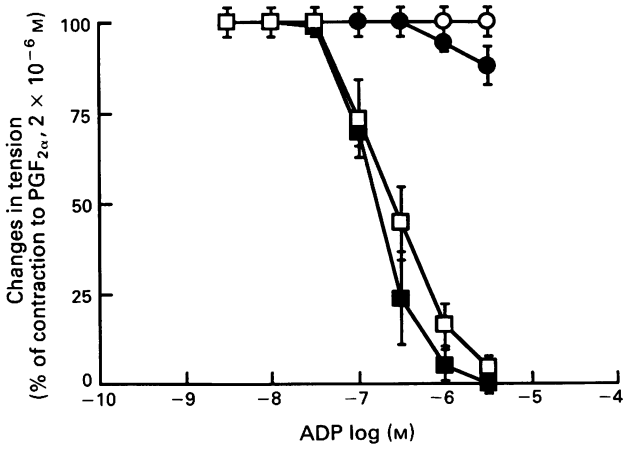

Figure 3 Effect of calmidazolium (10 μM) on relaxations to ADP in canine coronary artery with endothelium intact, contracted with prostaglandin $F_{2\alpha}$ (2 μM) in control solution or in the presence of nitro-L-arginine (30 μM). The experiments were performed in the presence of indomethacin (10 μM). Data are expressed as percentage of the contraction induced by prostaglandin $F_{2\alpha}$ and shown as mean ± s.e.mean (vertical bars) ($n = 5$). (■) Control; (□) in the presence of calmidazolium; (●) in the presence of nitro-L-arginine; (○) in the presence of nitro-L-arginine and calmidazolium.

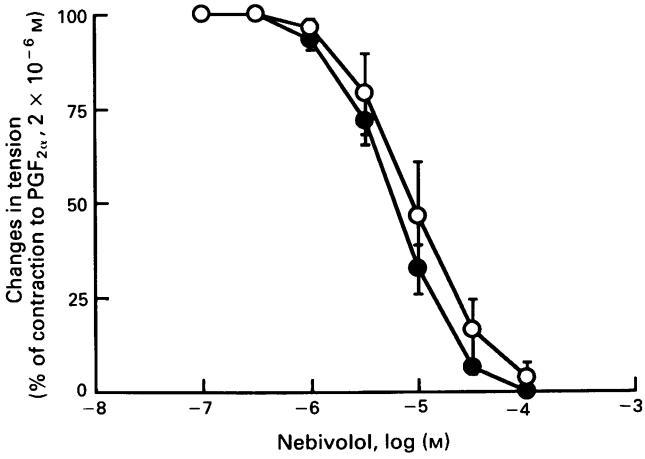

Figure 5 Effect of calmidazolium (10 μM) on relaxations elicited by nebivolol in canine coronary arteries with endothelium intact, contracted with prostaglandin $F_{2\alpha}$ (2 μM) in control solution. The experiments were performed in the presence of indomethacin (10 μM). Data are expressed as percentage of the contraction induced by prostaglandin $F_{2\alpha}$ and shown as mean ± s.e.mean (vertical bars) ($n = 5$). (●) Control; (○) in the presence of calmidazolium.

$F_{2\alpha}$, (IC_{50}: 7.3 ± 0.05). These relaxations were not affected significantly by calmidazolium (10 μM) (IC_{50}; 7.25 ± 0.11) (Figure 6a).

In rings contracted with 60 mM potassium, the relaxations to SIN-1 were not altered significantly by calmidazolium (IC_{50}; 6.47 ± 0.16 and 6.39 ± 0.15 respectively) (Figure 6b).

Lemakalim Lemakalim induced relaxations in rings without endothelium, that had been contracted with prostaglandin $F_{2\alpha}$, (IC_{50}; 6.48 ± 0.21) which were not affected significantly by calmidazolium (IC_{50}; 6.39 ± 0.16) but abolished by glibenclamide (10 μM) (Figure 7).

Discussion

This study demonstrates that calmidazolium inhibits differentially NO-dependent and NO-independent relaxations in canine coronary arteries. Calmidazolium was used at a concentration of one log unit above its EC_{50} on calmodulin *in vitro* (Gietzen, 1983; Johnson & Wittenauer, 1983). This concentration of calmidazolium, has been used by others to study endothelium-dependent responses (Weinheimer & Osswald, 1986; Busse *et al.*, 1988b; Förstermann *et al.*, 1991; Fleming *et al.*, 1991; Schini & Vanhoutte, 1992), in order to reach maximal inhibition and compensate for the poor accessibility of the compound to the inside of cells (Stoclet *et al.*, 1987).

Calmidazolium did not affect relaxations of canine coronary artery rings induced by ADP, nebivolol, or the calcium ionophore A23187, and had minimal effect on the endothelium-dependent responses to bradykinin in high potassium solution. NO is the EDRF which mediates the relaxations of canine coronary artery to ADP and nebivolol (Gao *et al.*, 1991), and the response to bradykinin in high potassium solution. This interpretation is confirmed in the present study by the abolition of these endothelium-dependent relaxations by nitro-L-arginine, an inhibitor of NO synthase (Mülsch & Busse, 1990). By contrast, calmidazolium did not influence these relaxations. Also, the compound had no effect on relaxations elicited by SIN-1, an exogenous donor of nitric oxide. The present finding may indicate that the relaxations elicited by NO in the canine coronary artery are insensitive to calmodulin inhibitors. This interpretation is at variance with the observations that NO synthase purified from the cerebellum of the rat or from bovine or porcine aortic endothelial cells is Ca^{2+} and calmodulin-sensitive (Busse & Mülsch, 1990; Bredt & Snyder, 1990; Föstermann *et al.*, 1991) and that, in the rat aorta calmodazolium, at the concentration used in the present study, inhibits the constitutive NO-synthase (Schini & Vanhoutte, 1992). Alternatively, in the canine coronary artery, calmidazolium may exert effects not related to calmodulin inhibition. In the present study experiments could not be performed with trifluoperazine, fendiline, other calmodulin inhibitors, at concentrations high enough to inhibit calmodulin activity (Weinheimer & Osswald, 1986) without deeply affecting vascular tone. As the effects of calmodulin inhibitors on endothelium-dependent relaxations are controversial (Johnson & Fugman, 1983; Weinheimer & Osswald, 1986; Busse *et al.*, 1988b; Schini & Vanhoutte, 1992) the use of these drugs might not be sufficient to assess the calmodulin-dependency of the NO synthase in the canine coronary artery. Since calmodulin activates several phosphodiesterases in vascular smooth muscle (Levin & Weiss, 1977; Hidaka *et al.*, 1979), inhibition of guanosine 3':5'-cyclic monophosphate (cyclic GMP) phosphodiesterase by calmidazolium might explain why, even under conditions of reduced NO-release, enough of the endogenous nitrate is produced to elevate the cyclic GMP content of the vascular smooth muscle cells and induce full relaxation. However, since calmidazolium did not affect the action of SIN-1, this interpretation is not tenable.

Endothelial cells can release a diffusible substance distinct from NO that causes hyperpolarization of the underlying vascular smooth muscle cells (Chen *et al.*, 1988; Feletou & Vanhoutte, 1988; Beny & Brunet, 1988; Komori & Van-

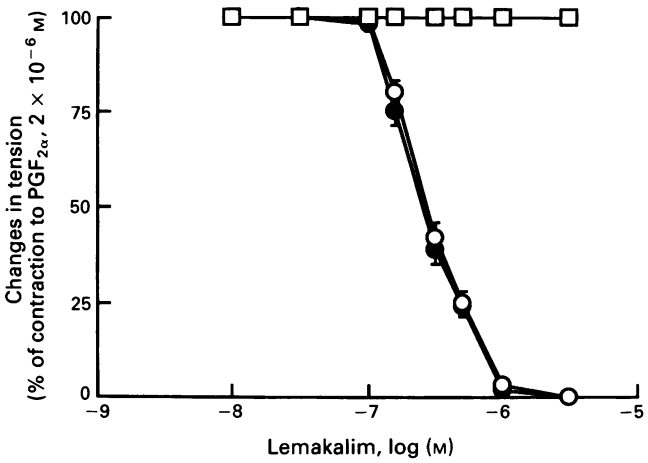

Figure 7 Effect of calmidazolium (10 μM) on relaxations to lemakalim in canine coronary artery without endothelium, contracted with prostaglandin $F_{2\alpha}$ (2 μM) in control solution or in the presence of glibenclamide (10 μM). The experiments were performed in the presence of indomethacin (10 μM). Data are expressed as percentage of the contraction induced by prostaglandin $F_{2\alpha}$ and shown as mean ± s.e.mean (vertical bars) ($n = 5$). (●) Control; (○) in the presence of calmidazolium; (□) in the presence of glibenclamide.

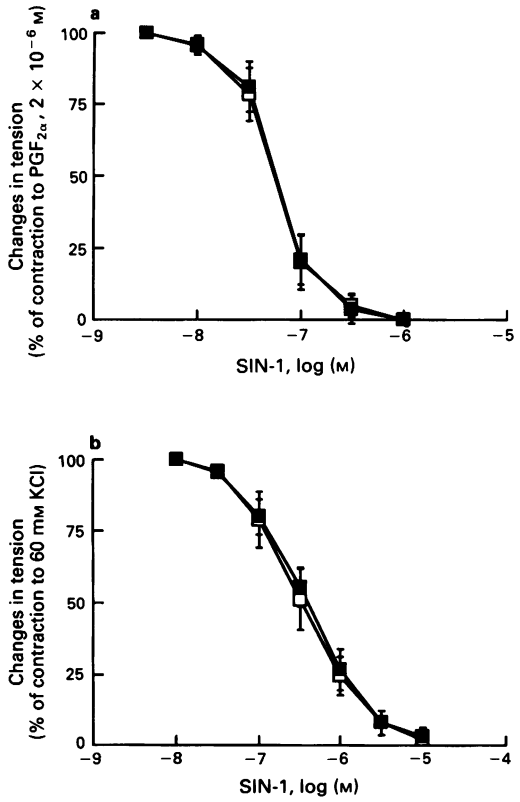

Figure 6 Effect of calmidazolium (10 μM) on relaxations to SIN-1 in canine coronary arteries without endothelium, contracted with prostaglandin $F_{2\alpha}$ (2 μM) (a) or 60 mM KCl (b). The experiments were performed in the presence of indomethacin (10 μM). Data are expressed as percentage of the contraction induced by prostaglandin $F_{2\alpha}$ (a) or 60 mM KCl (b) and shown as mean ± s.e.mean (vertical bars) ($n = 5$). (■) Control; (□) in the presence of calmidazolium.

houtte, 1990; Bray & Quast, 1991; Chen *et al.*, 1991). This endothelium-derived hyperpolarizing factor (EDHF), contributes to endothelium-dependent relaxations in arteries and veins (Nagao & Vanhoutte, 1991; 1992).

Nitro-L-arginine induced small contractions in the coronary artery due to the inhibition of the basal release of NO. This observation is in agreement with previous observations made in porcine or canine coronary with other inhibitors of the L-arginine NO pathway (Flavahan *et al.*, 1989; 1991). At the concentration used in this study, nitro-L-arginine allows maximal inhibition of NO-synthase (Illiano *et al.*, 1992). In the presence of the NO-synthase inhibitor, the relaxations of smooth muscle elicited by bradykinin or the calcium ionophore A23187 are mediated by hyperpolarization of smooth muscle cells (Nagao & Vanhoutte, 1992; Mombouli *et al.*, 1992). In the present study, the endothelium-dependent relaxations elicited by bradykinin that were resistant to nitro-L-arginine were prevented by calmidazolium. Likewise, the endothelium-dependent relaxations induced by the calcium ionophore A23187 in the presence of the NO-synthase inhibitor, were abolished by the calmodulin antagonist. Electrophysiological studies demonstrate that endothelium-dependent hyperpolarizations induced by A23187 and bradykinin are blocked by calmidazolium (Nagao *et al.*, 1992). The relaxations of coronary rings induced by bradykinin or A23187 which were resistant to nitro-L-arginine were not inhibited by glibenclamide, a specific blocker of the ATP-sensitive potassium channels (Quast, 1988), suggesting that EDHF does not mediate its action through these channels in canine coronary smooth muscle cells. By contrast, endothelium-dependent relaxations of vessels elicited by lemakalim, an ATP-sensitive potassium channel opener (Weir & Weston, 1986), were unaffected by calmidazolium, but blocked by glibenclamide. Calmodulin antagonists also do not prevent the activity of Ca^{2+} dependent potassium channels (Kihira *et al.*, 1990). Taken in conjunction, these observations suggest that in canine coronary smooth muscle the effects of calmidazolium described in the present study are due to specific inhibition, which can reasonably be attributed to endothelium-dependent hyperpolarization, and do not involve ATP-sensitive or Ca^{2+} dependent potassium channels.

An alternative explanation is that the inhibitor of calmodulin blocks the production of the hyperpolarizing mediator from the endothelial cells. The hyperpolarization induced by acetylcholine in endothelial cells is Ca^{2+} dependent (Busse *et al.*, 1988a) as are the endothelium-dependent hyperpolarizations in the carotid artery of the rabbit (Chen & Suzuki, 1990). Furthermore, the calcium ionophore A23187, induces endothelium-dependent hyperpolarization in canine coronary arteries (Nagao *et al.*, 1992). These results suggest that the increase in cytoplasmic Ca^{2+} is a key step in the production of EDHF and that Ca^{2+} calmodulin complex formation plays a role in the regulation of its synthesis or release.

In conclusion, the present findings in the canine coronary artery taken in conjunction with electrophysiological studies in the same tissue (Nagao *et al.*, 1992) indicate that calmidazolium does not inhibit significantly relaxations of canine coronary artery caused by endothelium-derived NO but inhibits the synthesis/release or the action of EDHF. Furthermore, the effects of the compound, on the relaxations elicited by bradykinin and the calcium ionophore A23187, in the presence of an inhibitor of NO-synthase indicate that EDHF contributes to the endothelium-dependent relaxations of canine coronary artery. Calmidazolium appears to be a convenient pharmacological tool to inhibit selectively this phenomenon.

The authors would like to thank Dr Keith Morrison for his critical input in this paper. This work was supported in part by NIH grant HL 31183 and HL 31547 and by an unrestricted Research Award of the Bristol-Myers Squibb Research Institute. Lemakalim was kindly provided by Beecham Pharmaceutical Company, SIN-1 by Hoechst laboratories (France), and nebivolol by Janssen Company.

References

BENY, J.-L. & BRUNET, P.C. (1988). Neither nitric oxide nor nitroglycerin accounts for all the characteristics of endothelially mediated vasodilatation of pig coronary arteries. *Blood Vessels*, **25**, 308–311.

BOULANGER, C., HENDRICKSON, H., LORENZ, R.R. & VANHOUTTE, P.M. (1989). Release of different relaxing factors by cultured porcine endothelial cells. *Circ. Res.*, **64**, 1070–1078.

BRAY, K. & QUAST, U. (1991). Differences in the K^+-channels opened by cromakalim, acetylcholine and substance P in rat aorta and porcine coronary artery. *Br. J. Pharmacol.*, **102**, 585–594.

BREDT, D. & SNYDER, S.H. (1990). Isolation of nitric oxide synthase, a calmodulin-requiring enzyme. *Proc. Natl. Acad. Sci. U.S.A.*, **87**, 682–685.

BUSSE, R., FICHTNER, H., LÜCKHOFF, A. & KOHLARDT, M. (1988a). Hyperpolarization and increased free calcium in acetylcholine-stimulated endothelial cells. *Am. J. Physiol.*, **255**, H965–H969.

BUSSE, R., LÜCKHOFF, A., WINTER, I., MÜLSCH,A. & POHL, U. (1988b). Fendiline and calmidazolium enhance the release of endothelium-derived relaxant factor and of prostacyclin from cultured endothelial cells. *Naunyn-Schmiedebergs Arch. Pharmacol.*, **337**, 79–84.

BUSSE, R. & MÜLSCH, A. (1990). Calcium-dependent nitric oxide synthesis in endothelial cytosol is mediated by calmodulin. *FEBS*, **256**, 133–136.

CHEN, G. & SUZUKI, H. (1990). Calcium dependency of the endothelium-dependent hyperpolarization in smooth muscle cells of the rabbit carotid artery. *J. Physiol.*, **421**, 521–534.

CHEN, G., SUZUKI, H. & WESTON, A.H. (1988). Acetylcholine releases endothelium-derived hyperpolarizing factor and EDRF from rat blood vessels. *Br. J. Pharmacol.*, **95**, 1165–1174.

CHEN, G., YAMAMOTO, Y., MIWA, K. & SUZUKI, H. (1991). Hyperpolarization of arterial smooth muscle induced by endothelial humoral substances. *Am. J. Physiol.*, **260**, H1888–H1892.

CHEUNG, W.Y. (1980). Calmodulin plays a pivotal role in cellular regulation. *Science*, **207**, 19–27.

FEELISCH, M., OSTROWSKI, J. & NOACK, E. (1989). On the mechanism of NO release from sydnonimines. *J. Cardiovasc. Pharmacol.*, **14** (Suppl 11), S13–S22.

FELETOU, M. & VANHOUTTE, P.M. (1988). Endothelium-dependent hyperpolarization of canine coronary smooth muscle. *Br. J Pharmacol.*, **93**, 515–524.

FLAVAHAN, N.A., SHIMOKAWA, H. & VANHOUTTE, P.M. (1989). Pertussis toxin inhibits endothelium-dependent relaxations to certain agonists in porcine coronary artery. *J. Physiol.*, **408**, 549–560.

FLAVAHAN, N.A., SHIMOKAWA, H. & VANHOUTTE, P.M. (1991). Inhibition of endothelium-dependent relaxations by phorbol-myristate in canine coronary arteries: role of a Pertussis toxin-sensitive G-protein. *J. Pharmacol. Exp. Ther.*, **256**, 50–55.

FLEMING, I., GRAY, G.A., SCHOTT, C. & STOCLET, J.C. (1991). Inducible but not constitutive production of nitric oxide by vascular smooth muscle cells. *Eur. J. Pharmacol.*, **200**, 375–376.

FÖRSTERMANN, U., POLLOCK, J.S., SCHMIDT, H.H.H., HELLER, M. & MURAD, F. (1991). Calmodulin-dependent endothelium-derived relaxing factor/nitric oxide synthase activity is present in the particulate and cytosolic fractions of bovine aortic endothelial cells. *Proc. Natl. Acad. Sci. U.S.A.*, **88**, 1788–1792.

FURCHGOTT, R.F. (1983). Role of endothelium in responses of vascular smooth muscle. *Circ. Res.*, **53**, 557–573.

FURCHGOTT, R.F. (1988). Studies on relaxation of rabbit aorta by sodium nitrite: the basis for the proposal that acid-activatable inhibitory factor from bovine retractor penis factor is inorganic nitrite and the endothelium-derived relaxing factor is nitric oxide. In *Vasodilatation*. ed. Vanhoutte, P.M. pp. 401–414. New York: Raven Press.

FURCHGOTT, R.F. & ZAWADZKI, J.V. (1980). The obligatory role of endothelial cells in the relaxation of arterial smooth muscle of acetylcholine. *Nature*, **288**, 373–376.

GAO, Y., NAGAO, T., BOND, R., JANSSENS, W.J. & VANHOUTTE, P.M. (1991). Nebivolol induces endothelium-dependent relaxations of canine coronary arteries. *J. Cardiovasc. Pharmacol.*, **17**, 964–969.

GIETZEN, K. (1983). Comparison of the calmodulin antagonist compound 48/80 and calmidazolium. *Biochem. J.*, **216**, 611–616.

HIDAKA, H., YAMAKI, T., TOTSUAKA, T. & ASANO, M. (1979). Selective inhibitors of Ca^{2+}-binding modulator of phosphodiesterase produce vascular relaxation and inhibit actin-myosin interaction. *Mol. Pharmacol.*, **15**, 49–59.

HUANG, A.H., BUSSE, R. & BASSENGE, E. (1988). Endothelium-dependent hyperpolarization of smooth muscle cells in rabbit femoral arteries is not mediated by EDRF (nitric oxide). *Naunyn Schmiedebergs Arch. Pharmacol.*, **338**, 438–442.

IGNARRO, L.J., BYRNS, R.E., BUGA, G.M. & WOODS, K.S. (1987). Endothelium-derived relaxing factor from pulmonary artery and vein possesses pharmacologic and chemical properties identical to those of nitric oxide radical. *Circ. Res.*, **61**, 866–879.

IGNARRO, L.J. & KADOWITZ, P.J. (1985). Pharmacological and physiological role of cyclic GMP in vascular smooth muscle relaxation. *Annu. Rev. Pharmacol.*, **25**, 171–191.

ILLIANO, S.C., NAGAO, T. & VANHOUTTE, P.M. (1992). Effect of calmodulin inhibitors on endothelium-dependent relaxations to bradykinin in porcine and canine coronary arteries. In *Biology of Nitric Oxide*. ed. Moncada, S., Marletta, M.A. & Hibbs, J.B. London: Portland Press (in press).

JOHNSON, J.D. & FUGMAN, D.A. (1983). Calcium and calmodulin antagonists binding to calmodulin and relaxation of coronary segments. *J. Pharmacol. Exp. Ther.*, **226**, 330–334.

JOHNSON, J.D. & WITTENAUER, L.A. (1983). A fluorescent calmodulin that reports the binding of hydrophobic inhibitory ligands. *Biochem. J.*, **211**, 473–479.

KIHIRA, M., MATSUZAWA, K., TAKUNO, H. & TOMITA, T. (1990). Effects of calmodulin antagonists on calcium-activated potassium channels in pregnant rat myometrium. *Br. J. Pharmacol.*, **100**, 353–359.

KOMORI, K., LORENZ, R.R. & VANHOUTTE, P.M. (1988). Nitric oxide, ACh, and electrical and mechanical properties of canine arterial smooth muscle. *Am. J. Physiol.*, **255**, H207–H212.

KOMORI, K. & VANHOUTTE, P.M. (1990). Endothelium derived hyperpolarizing factor. *Blood Vessels*, **27**, 238–245.

LEVIN, R.M. & WEISS, B. (1977). Binding of trifluoperazine to the calcium-dependent activator of cyclic nucleotide phosphodiesterase. *Mol. Pharmacol.*, **13**, 690–697.

LÜCKHOFF, A., POHL, U., MÜLSCH, A. & BUSSE, R. (1988). Differential role of extra- and intracellular calcium in the release of EDRF and prostacyclin from cultured endothelial cells. *Br. J. Pharmacol.*, **95**, 189–196.

MARTIN, W., VILLANI, G.M., JOTHIANADAN, D. & FURCHGOTT, R.F. (1985). Selective blockade of endothelium-dependent glyceryltrinitrate-induced relaxations by hemoglobin and by methylene blue in the rabbit aorta. *J. Pharmacol. Exp. Ther.*, **232**, 708–716.

MEANS, A.R. & DEDMAN, J.R. (1980). Calmodulin, an intracellular calcium receptor. *Nature*, **285**, 73–77.

MOMBOULI, J.V., ILLIANO, S., NAGAO, T., SCOTT-BURDEN, T. & VANHOUTTE, P.M. (1992). The potentiation of endothelium-dependent relaxations to bradykinin by angiotensin I converting enzyme inhibitors in the canine coronary artery involves both endothelium-derived relaxing and hyperpolarizing factors. *Circ. Res.*, **71**, 137–143.

MOORE, P.K., SWAYEH, O.A., CHONG, N.W.S., EVANS, R.A. & GIBSON, A. (1990). L-N^G-nitro arginine (L-NOARG), a novel, L-arginine-reversible inhibitor of endothelium-dependent vasodilatation *in vitro*. *Br. J. Pharmacol.*, **99**, 408–412.

MÜLSCH, A. & BUSSE, R. (1990). L-N^G-nitro-L-arginine (N^5-[amino (nitroamino)methyl]-L-ornithine) impairs endothelium-dependent dilations by inhibiting nitric oxide synthesis from L-arginine. *Naunyn Schmiedebergs Arch. Pharmacol.*, **341**, 143–147.

MYERS, P.R., MINOR, R.L.Jr., GUERRA, R.Jr., BATES, J.N. & HARRISON, D.G. (1990). Vasorelaxant properties of the endothelium-derived relaxing factor more closely resemble S-nitrocysteine than nitric oxide. *Nature*, **345**, 161–163.

NAGAO, T. & VANHOUTTE, P.M. (1992). Hyperpolarization as a mechanism for endothelium-dependent relaxations in the porcine coronary artery. *J. Physiol.*, **445**, 355–367.

NAGAO, T. & VANHOUTTE, P.M. (1991). Membrane hyperpolarization contributes to endothelium-dependent relaxations induced by acetylcholine in the femoral vein of rat. *Am. J. Physiol.*, **261**, H1034–H1037.

NAGAO, T., ILLIANO, S.C. & VANHOUTTE, P.M. (1992). Calmodulin antagonists inhibit endothelium-dependent hyperpolarisation in the canine coronary artery. *Br. J. Pharmacol.*, **107**, 382–386.

PALMER, R.M.J., FERRIGE, A.G. & MONCADA, S. (1987). Nitric oxide release accounts for the biological activity of endothelium-derived relaxing factor. *Nature*, **327**, 524–526.

QUAST, U. (1988). Inhibition of the effects of K^+ channel stimulator cromakalim (BRL 34915) in vascular smooth muscle by glibenclamide and forskolin. *Naunyn-Schmiedebergs Arch. Pharmacol.*, **337** (Suppl.), R72.

RAPOPORT, R.M. & MURAD, F. (1983). Agonist-induced endothelium-dependent relaxations in rat thoracic aorta may be mediated through cGMP. *Circ. Res.*, **52**, 352–357.

RUBANYI, G.M., SCHWARTZ, A. & VANHOUTTE, P.M. (1988). Calcium transport mechanisms in endothelial cells regulating the synthesis and release of endothelium-derived relaxing factor. In *Relaxing and Contracting Factor*. ed. Vanhoutte, P.M. Clifton, NJ: The Humana Press.

SCHINI & VANHOUTTE, P.M. (1992). Inhibitors of calmodulin impair the constitutive but not the inducible nitric oxide synthase activity in the rat aorta. *J. Pharmacol. Exp. Ther.*, **261** (in press).

SINGER, H.A. & PEACH, M.J. (1982). Calcium- and endothelium-mediated smooth muscle relaxation in rabbit aorta. *Hypertension*, **4** (Suppl. II), II19–II25.

STOCLET, J.C., GERARD, D., KILHOFFER, M.-C., LUGNIER, C. & SCHAEFFER, P. (1987). Calmodulin and its role in intracellular calcium regulation. *Prog. Neurobiol.*, **29**, 321–364.

TAYLOR, S.G. & WESTON, A.H. (1988). Endothelium-derived hyperpolarizing factor: a new endogenous inhibitor from the vascular endothelium. *Trends Pharmacol. Sci.*, **9**, 72–74.

WEINHEIMER, G. & OSSWALD, H. (1986). Inhibition of endothelium-dependent smooth muscle relaxation by calmodulin antagonists. *Naunyn-Schmiedebergs Arch. Pharmacol.*, **33**, 391–397.

WEIR, S. & WESTON, A.H. (1986). The effects of BRL 34915 and nicorandil on electrical and mechanical activity on ^{86}Rb efflux in rat blood vessels. *Br. J. Pharmacol.*, **88**, 121–128.

(Received October 4, 1991
Revised April 27, 1992
Accepted June 1, 1992)

Br. J. Pharmacol. (1992), **107**, 393–399

Endothelium-dependent relaxation and noradrenaline sensitivity in mesenteric resistance arteries of streptozotocin-induced diabetic rats

[1] Paul D. Taylor, *Andrew L. McCarthy, **Chris R. Thomas & Lucilla Poston

Divisions of Physiology, *Obstetrics and **Unit of Endocrinology and Diabetes, United Medical and Dental Schools, St. Thomas' Campus, London SE1 7EH

1 Noradrenaline sensitivity and acetylcholine-induced relaxation were investigated in mesenteric resistance arteries of control and streptozotocin-induced diabetic rats.

2 The diabetic rats demonstrated enhanced vascular sensitivity to noradrenaline compared with age-matched controls (pEC_{50} 5.99 ± 0.06 for diabetic rats, $n = 25$, versus 5.82 ± 0.03 for controls, $n = 45$, $P < 0.05$).

3 Significant impairment of acetylcholine-induced relaxation was observed in arteries from the diabetic animals compared with controls (pEC_{50} 6.81 ± 0.17 for diabetic rats, $n = 21$, versus 7.54 ± 0.17 for controls, $n = 45$, $P < 0.001$).

4 The difference between acetylcholine-induced relaxation in diabetic and control arteries remained in the presence of 10 μM indomethacin (pEC_{50} 6.41 ± 0.11 for diabetic rats, $n = 16$, versus 7.59 ± 0.08 for controls, $n = 20$, $P < 0.001$).

5 The nitric oxide synthase inhibitor, N^G-monomethyl-L-arginine (L-NMMA, 1 mM) produced profound inhibition of acetylcholine-induced relaxation in diabetic arteries but partial inhibition in controls. The incomplete inhibition of acetylcholine-induced relaxation by L-NMMA in the control arteries was the result of ineffective inhibition of nitric oxide synthase since an alternative inhibitor, N^G-nitro-L-arginine methyl ester (L-NAME, 0.1 mM), led to similar inhibition to that seen in the diabetic arteries with L-NMMA. The endothelium-derived relaxing factor (EDRF)-mediated component of acetylcholine-induced relaxation determined by use of the nitric oxide synthase inhibitors was, therefore, apparently reduced in diabetic rats compared with control animals.

6 In further experiments L-NAME was found to enhance the response to noradrenaline in control rats but not in diabetic animals, suggesting that the abnormal response to noradrenaline in the diabetic animals was also due to reduced EDRF release.

7 Nitroprusside-induced relaxation (endothelium-independent) was similar in arteries from control and diabetic rats (pEC_{50} 7.61 ± 0.13 for diabetic arteries, $n = 18$, versus 7.68 ± 0.15 in the controls, $n = 20$, P not significant).

8 These results suggest that endothelial function is abnormal in mesenteric resistance arteries of streptozotocin-induced diabetic rats and that this is predominantly due to reduced EDRF release.

Keywords: Mesenteric resistance arteries; vascular endothelium; vascular smooth muscle; chemically-induced diabetes in rats; streptozotocin; endothelium-derived relaxing factor; nitric oxide synthase inhibitors

Introduction

Vascular disease is a well recognized complication of diabetes mellitus (Christlieb *et al.*, 1976). Alterations in the reactivity of blood vessels to neurotransmitters and circulating hormones have been implicated in the underlying mechanism of microvascular disease and hypertension associated with diabetes (Weidmann *et al.*, 1979). The endothelial cell layer is now established as being an important modulator of vascular smooth muscle tone (Furchgott & Zawadzki, 1980) and abnormal endothelial function has been suggested as a contributary factor in diabetic microvascular dysfunction (Porta *et al.*, 1987). There is one study in human diabetes in which a defect in endothelium-dependent relaxation of the smooth muscle of the corpora cavernosa from diabetic men has been implicated in the high incidence of impotence associated with this disease. The degree of impairment was also found to be related to the duration of diabetes (De Tajada *et al.*, 1989).

In animal models of diabetes there is both histological (Arbogast *et al.*, 1984) and functional evidence that the vascular endothelium is abnormal. In chemically induced diabetes in animals, several studies have demonstrated reduced endothelium-dependent relaxation (Oyama *et al.*, 1986; Pieper & Gross, 1988; Durante *et al.*, 1988; Kamata *et al.*, 1989; Tanz *et al.*, 1989; Mayhan, 1989; Abiru *et al.*, 1990; Tesfamariam *et al.*, 1990; Mayhan *et al.*, 1991) but others have not found any impaired response (White & Carrier, 1986; Wakabayashi *et al.*, 1987; Head *et al.*, 1987; Gebremedhin *et al.*, 1988; Mulhern & Docherty, 1989). Some studies have documented an increase in sensitivity to noradrenaline in arteries from diabetic animals (MacLeod & McNeill, 1985; Harris & MacLeod, 1988; Pieper & Gross, 1988; White & Carrier, 1988; Cohen *et al.*, 1990), but not all (Gebremedhin *et al.*, 1989). It is not established whether this is attributable to abnormal sensitivity of vascular smooth muscle or to reduced relaxing factor production, due to impaired endothelial function.

Most of the *in vitro* studies to date have been investigations of large arteries obtained from diabetic animals and, therefore, have little relevance to the microcirculation or to

[1] Author for correspondence.

the local control of blood flow or the blood pressure. Two reports have investigated endothelial function in small arteries from the cerebral vasculature in an *in vivo* preparation and have found evidence of dysfunction (Mayhan, 1989; Mayhan *et al.*, 1991). In a recent study resistance artery function of rats has been investigated indirectly by measurement of regional haemodynamics with the technique of Doppler flow (Kiff *et al.*, 1991a,b) and, of the vascular beds investigated, endothelial dysfunction was found in the hindquarters circulation alone (Kiff *et al.*, 1991b). To our knowledge no *in vitro* study has investigated resistance vascular function in small arteries from diabetic animals.

We have, therefore, compared the endothelium-dependent and -independent relaxation, and noradrenaline sensitivity of resistance arteries obtained from streptozotocin-induced diabetic rats and age-matched controls. Using nitric oxide synthase inhibitors and an inhibitor of cyclo-oxygenase we have also attempted to define the role of nitric oxide and prostanoid dilators in endothelium-dependent relaxation in control and diabetic animals.

Methods

Female CSE rats (220–260 g) were injected i.p with streptozotocin (STZ, 56 mg kg^{-1}) in citrate buffer. Control rats were housed separately and both groups given free access to food and water. After 5–6 weeks the animals were killed by cervical dislocation and blood samples obtained by cardiac puncture for glucose determination (glucose oxidase method; YSI Model 23 AM Glucose Analyzer). The mesentery was removed and placed in physiological saline solution (PSS). The solution consisted of (mM): NaCl 119, KCl 4.7, $CaCl_2$ 2.5, $MgSO_4$ 1.17, $NaHCO_3$ 25, NaH_2PO_4 1.18, EDTA 0.026 and glucose 5.5, pH 7.4 and bubbled with 5% CO_2/95% O_2.

Small arteries (control internal diameter mean ± s.e.mean; 264 ± 7 μm, $n = 47$; diabetic 284 ± 9 μm, $n = 23$, P not significant) were dissected free from connective tissue using a light microscope and mounted as ring preparations on a small vessel myograph (Mulvany & Halpern, 1977) capable of measuring isometric tension. Arteries were bathed in PSS at 37°C and bubbled with 5% CO_2/95% O_2 and their passive tension and internal circumference were determined. The arteries were set to an internal circumference equivalent to 90% of that which they would have had when relaxed *in situ* under a transmural pressure of 100 mmHg (the maximum active tension for the minimum resting tension is developed at approximately this circumference; Mulvany & Halpern, 1977). In order to obtain arteries of approximately equal diameter in control and diabetic animals the third branch mesenteric arteries were routinely dissected from control rats and the fourth branch dissected from diabetic rats. To assess their contractile responses the arteries were then contracted for 2 min every 10 min on four occasions using the following protocol. The first and fourth contractions were produced with 5 μM noradrenaline in 125 mM potassium solution (KPSS, made by equimolar substitution of KCl for NaCl in PSS). The second was with 5 μM noradrenaline in PSS and the third with KPSS. Any artery failing to produce a maximum active tension equivalent to a pressure of 100 mmHg on the fourth contraction was rejected.

After the routine run-up procedure, the cumulative responses of vessels to noradrenaline were determined (0.05 μM–5.00 μM), the concentration being increased at 3 min intervals. Arteries were then washed three times with PSS and a 15 min washout period allowed before continuation of the protocol.

Arteries were then submaximally contracted with 3 μM noradrenaline for 3 min and relaxation responses to acetylcholine subsequently determined by adding increasing concentrations of acetylcholine at 2 min intervals (final bath concentration 1 nM–10 μM). After a further 5 min indomethacin (10 μM) was added to the bath for 10 min and the arteries again contracted with 3 μM noradrenaline in the continued presence of indomethacin. A second concentration-effect curve to acetylcholine was then determined in the continued presence of indomethacin. After a further 5 min, L-NMMA (N^G-monomethyl-L-arginine, 10 mM) was added to the bath for 10 min and a third acetylcholine concentration-effect curve then determined. After a 15 min recovery period arteries were again pre-contracted with 3 μM noradrenaline and subjected to increasing concentrations of sodium nitroprusside at 2 min intervals (1 nM–10 μM). In order to determine whether noradrenaline contractions were sustained and reproducible throughout the duration of the experimental period, four sequential contractions to 3 μM noradrenaline were performed in the absence of acetylcholine, but in the presence of the inhibitors as appropriate. Similarly, the reproducibility of the acetycholine relaxation was determined by eliciting three consecutive concentration-response curves to acetylcholine in the absence of the inhibitors. These separate time-control studies were carried out on arteries from both diabetic and control populations.

In a further set of experiments the acetylcholine-induced relaxation in arteries from control animals was determined as above but in the presence of the nitric oxide synthase inhibitor, N^G-nitro-L-arginine methyl ester, L-NAME (0.1 mM).

A separate investigation into the mode of action of the inhibitor L-NMMA was also carried out in control arteries. Instead of pre-incubating the arteries with L-NMMA, and then determining an acetylcholine concentration-effect curve, arteries were relaxed with acetylcholine (1–100 nM) prior to the addition of L-NMMA (1 mM).

A separate study was also carried out to investigate the role of EDRF in modulating the response to noradrenaline in control and diabetic rat arteries. Seven rats were injected with STZ as above and were killed after 2–3 weeks. Noradrenaline concentration-effect curves were determined as described above. The arteries were then incubated for 10 min with L-NAME (0.1 mM) and the noradrenaline concentration-effect curves repeated in the continued presence of the nitric oxide synthase inhibitor.

Drugs

Chemicals used in this investigation were noradrenaline (Winthrop Laboratories); acetylcholine, indomethacin, sodium nitroprusside, L-NAME, (all from Sigma); L-NMMA (Calbiochem); streptozotocin (gift from Dr Macleod, Upjohn Co., Kalamazoo, U.S.A.). Chemicals were prepared as stock solutions solubilized in PSS except indomethacin which was prepared as a 1 mM stock solution in phosphate buffer (0.02 M KH_2PO_4, 0.12 M $NaH_2PO_4.2H_2O$, pH balanced to 7.8). All concentrations are expressed as the final molar concentration in the organ bath.

Statistical analysis

All values are given as the mean ± s.e.mean. Tension was expressed as mean mN mm^{-1} artery length and the relaxant responses to acetylcholine as a percentage of the initial pre-contraction to noradrenaline. The − log concentration of the drug required to produce 50% of the maximum response (pEC_{50}) was calculated for each concentration-effect curve using the sigmoid equation from the curve fitting programme 'GraphPad' (GraphPad Software Inc., San Diego, CA, U.S.A.). Statistical comparison of the pEC_{50} values for diabetic and control rats was performed with Student's independent t test. Paired t tests were used to compare pEC_{50} values calculated from consecutive concentration-effect curves within control or diabetic artery populations. Where curve fitting was not appropriate the mean values for maximal relaxation between diabetic and control data were analysed by Student's unpaired t test. Significance was assumed if $P < 0.05$.

Results

Five weeks after i.p injection of STZ the plasma glucose concentration was found to be significantly elevated compared with that of the age-matched control animals (45.1 ± 7.5 mmol l^{-1}, in the STZ-treated animals, $n = 15$ versus 7.3 ± 1.1 mmol l^{-1}, in the controls, $n = 14$, $P < 0.001$). Blood glucose levels were not measured in the control animals used for the time-control experiments.

Arteries from diabetic and control rats contracted in a concentration-dependent manner in response to noradrenaline. The concentration-effect curve to noradrenaline was, however, shifted to the left in the diabetic animals, (control arteries pEC_{50} 5.82 ± 0.03, $n = 45$, versus diabetic arteries 5.99 ± 0.06, $n = 25$, $P < 0.05$, Figure 1).

Acetylcholine caused concentration-dependent relaxations in diabetic and control arteries submaximally contracted with noradrenaline, but relaxation was significantly attenuated between 10–100 nM acetylcholine in the diabetic arteries compared with controls (control arteries pEC_{50} 7.54 ± 0.17, $n = 36$; diabetic 6.81 ± 0.17, $n = 21$, $P < 0.001$, Figure 2). Maximum relaxation was, however, not significantly different in diabetic compared with control arteries (Figure 2). Control contractions to noradrenaline without the addition of acetylcholine demonstrated a time-dependent decrease in tension which was not significantly different between diabetic and control arteries.

The addition of indomethacin (10 μM) led to a significant reduction of the noradrenaline pre-contraction in control and diabetic arteries compared with the previous response obtained in the absence of indomethacin (control arteries with indomethacin 2.63 ± 0.20 mN mm^{-1} versus 3.32 ± 0.20 mN mm^{-1}, without indomethacin, $n = 20$, $P < 0.001$; diabetic arteries with indomethacin 3.19 ± 0.25 mN mm^{-1} versus 3.56 ± 0.24 mN mm^{-1}, without indomethacin, $n = 18$, $P < 0.001$). Indomethacin effected no significant change in the subsequent response to acetylcholine in either control or diabetic rats and acetylcholine-induced relaxation remained significantly attenuated in diabetic arteries compared with controls (control arteries in the absence of indomethacin pEC_{50} 7.54 ± 0.16, $n = 36$, versus 7.59 ± 0.08 in the presence of indomethacin, $n = 20$, P significant; diabetic arteries in the absence of indomethacin 6.81 ± 0.17, $n = 21$, versus 6.41 ± 0.11, $n = 16$, in the presence of indomethacin, P not significant, Figure 3a,b). Time-control noradrenaline-induced contractions in the absence of acetylcholine again demonstrated no significant difference in time-dependent relaxation between diabetic and control arteries.

The addition of 1 mM L-NMMA (in the continued presence of 10 μM indomethacin) resulted in an increase in

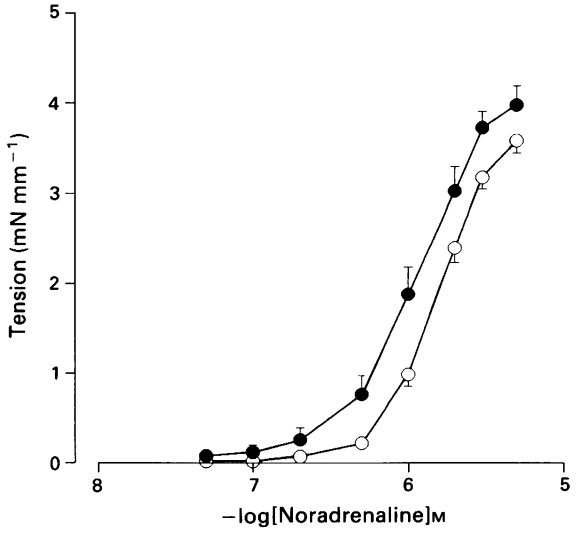

Figure 1 Noradrenaline concentration-effect curves for control (○, $n = 45$) and streptozotocin-diabetic (●, $n = 26$) rat mesenteric resistance arteries.

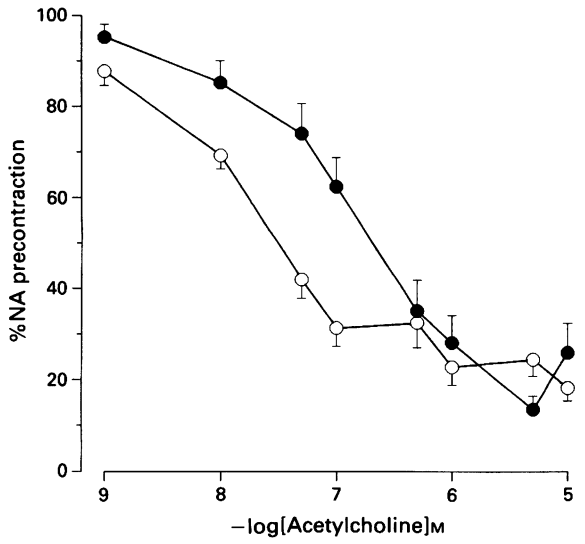

Figure 2 Acetylcholine-induced relaxation after precontraction with 3 μM noradrenaline in control (○, $n = 36$) and streptozotocin diabetic rat mesenteric resistance arteries (●, $n = 24$).

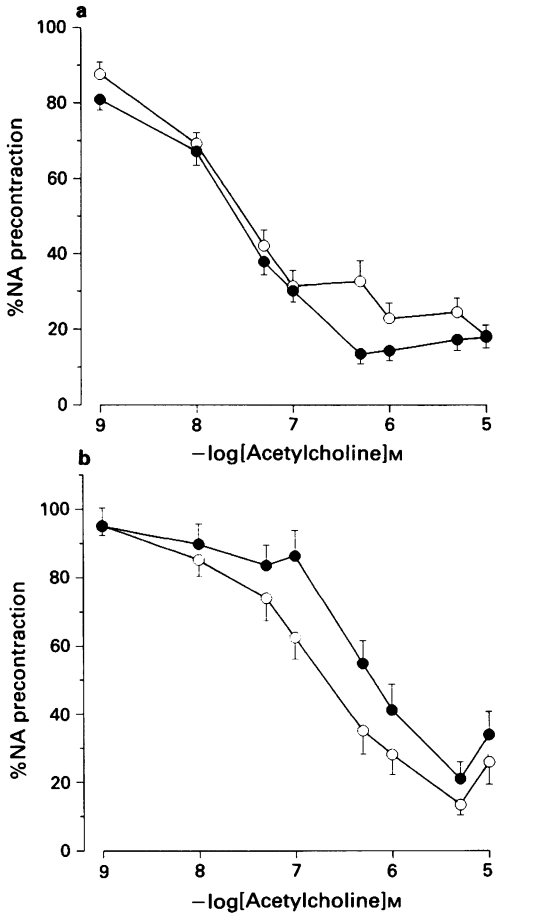

Figure 3 A comparison of the acetylcholine concentration-effect curves after precontraction with 3 μM noradrenaline in arteries taken from (a) control, $n = 20$ and (b) diabetic rats, $n = 18$. Responses were carried out before (○) and after (●) pre-incubation with 10 μM indomethacin.

the noradrenaline pre-contraction in both diabetic and control animals when compared with that obtained in the presence of indomethacin alone (diabetic arteries in indomethacin and L-NMMA, tension = 3.89 ± 0.18 mN mm^{-1} versus 3.19 ± 0.25 mN mm^{-1} indomethacin alone, $n = 18$, $P < 0.005$; control arteries in indomethacin and L-NMMA, tension = 3.42 ± 0.21 mN mm^{-1} versus 2.63 ± 0.20 mN mm^{-1}, in indomethacin alone, $n = 20$, $P < 0.001$). The maximum relaxation to acetylcholine (in the continued presence of indomethacin and L-NMMA) in both diabetic and control arteries was significantly attenuated when compared with the response to indomethacin alone. L-NMMA was, however, more effective as an inhibitor of acetylcholine-induced relaxation in the diabetic arteries which demonstrated 62.6 ± 7.3% inhibition ($n = 18$), whereas control arteries demonstrated only 30.8 ± 5.5% inhibition ($n = 20$, $P < 0.001$, Figure 4a,b). In the time-controls, in the presence of L-NMMA and indomethacin, the precontracted diabetic arteries maintained their initial tension over the duration of the experimental period (percentage change in tension + 0.9 ± 3.2%, $n = 5$) whereas control arteries did relax by a small but significant amount (− 17.5 ± 3.8%, $n = 9$, $P < 0.05$).

The reproducibility of repeated acetylcholine concentration-effect curves was assessed by carrying out three acetylcholine-induced relaxations over the same period involved in the procedures described above. There were no significant differences in the maximal relaxations or pEC_{50} values between the consecutive concentration-effect curves in the arteries from diabetic or control animals.

In order to determine whether the incomplete inhibition of acetylcholine-induced relaxation observed in control arteries in the presence of indomethacin and L-NMMA reflected ineffective inhibition of nitric oxide synthase or the presence of a relaxing factor other than nitric oxide, further experiments were undertaken. Arteries from control rats were subject to the routine 'run-up' procedure and the protocol followed as above but with substitution of the nitric oxide synthase inhibitor, L-NAME (0.1 mM) for L-NMMA (1 mM). The results are presented in Figure 4 (a) which shows a comparison of the acetylcholine response in the presence of indomethacin and either L-NMMA or L-NAME in control arteries. L-NAME effected greater overall inhibition of acetylcholine-induced relaxation than did L-NMMA (L-NAME achieving 69.7 ± 12.0% inhibition, $n = 5$, versus 30.8 ± 5.5% inhibition with L-NMMA, $n = 20$, $P < 0.05$), and the effect was similar to that observed with L-NMMA in the diabetic arteries (L-NMMA effecting 62.6 ± 7.3% inhibition in the diabetic arteries, $n = 18$, compared with 69.7 ± 12.0% inhibition by L-NAME in the controls, $n = 5$, P not significant). In a second set of experiments arteries were pre-contracted with 3 μM noradrenaline and a partial concentration-effect curve to acetylcholine (1–100 nM) determined. L-NMMA (1 mM) was then added to the bath with the subsequent concentrations of acetylcholine (0.5–10 μM) required to complete the concentration-effect curve. The results are shown in Figure 5. Late addition of L-NMMA had a profound effect on acetylcholine-induced relaxation leading to significant constriction relative to the initial tension. (i.e. 5 μM acetylcholine plus indomethacin, tension = 42.83 ± 7.09% of the initial value, $n = 20$; 5 μM acetylcholine plus indomethacin combined with late addition of L-NMMA, tension = 153.5 ± 21.1%, of initial value, $n = 3$, $P < 0.001$).

The responses of arteries pre-contracted with noradrenaline and subjected to increasing concentrations of nitroprusside were similar in control and diabetic arteries (control arteries pEC_{50} 5.68 ± 0.15, $n = 18$, versus 5.61 ± 0.13 in diabetic arteries, $n = 20$, P not significant; Figure 6).

In further experiments, in which rats were studied 2–3 weeks after injection of STZ, the blood glucose values (40.1 ± 6.9 mmol l^{-1}), were comparable to those in rats investigated after 5–6 weeks. In the presence of L-NAME

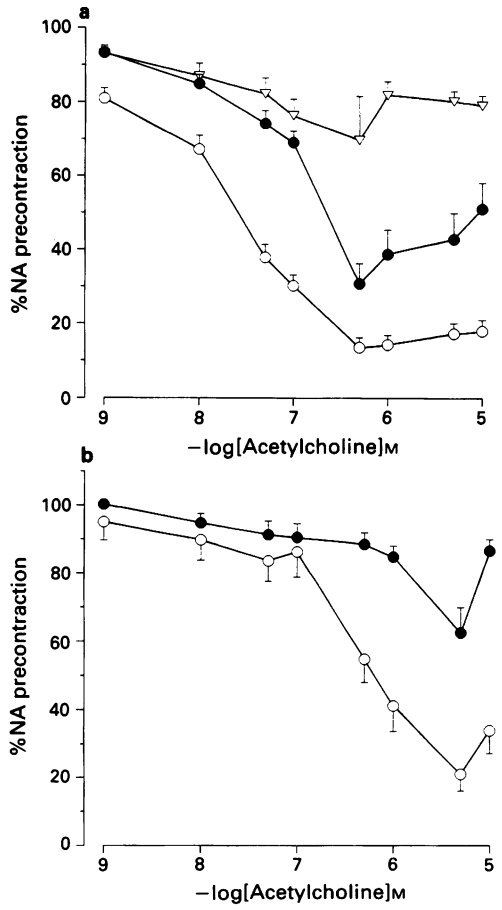

Figure 4 A comparison of the acetylcholine concentration-effect curves after pre-contraction with 3 μM noradrenaline in (a) control; $n = 20$, and (b) streptozotocin-diabetic rat mesenteric resistance arteries; $n = 18$. Responses were carried out in the presence of indomethacin alone (○) and, after pre-incubation in 10 μM indomethacin and 1 mM N^G-monomethyl-L-arginine (L-NMMA) (●). (a) Also includes the acetylcholine concentration-effect curve of a further group of control arteries ($n = 5$) incubated in 10 μM indomethacin plus 0.1 nM L-NAME (▽).

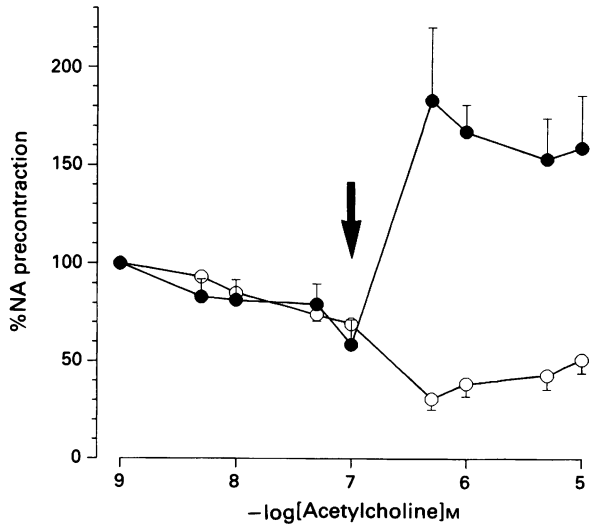

Figure 5 Acetylcholine-induced relaxation in control rat mesenteric resistance arteries demonstrating the profound effect of the bolus addition of N^G-monomethyl-L-arginine (L-NMMA, indicated by the arrow) to partially relaxed vessels (●, $n = 3$) compared with that of vessels incubated for 10 min with L-NMMA prior to exposure to acetylcholine (○, $n = 20$).

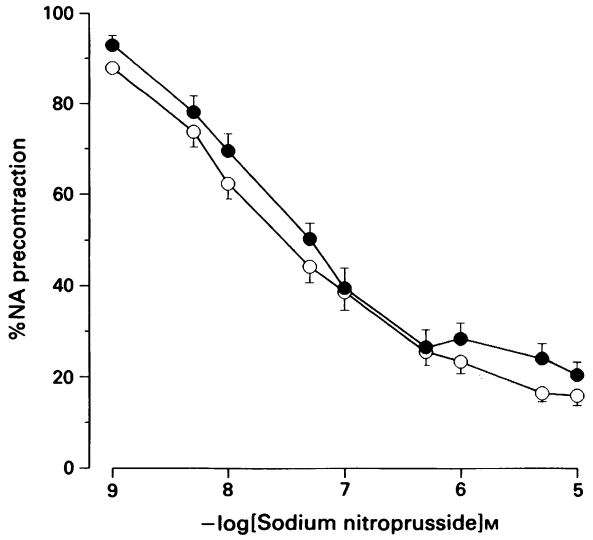

Figure 6 Sodium nitroprusside (SNP) concentration-effect curves for control (○, $n = 20$) streptozotocin-diabetic (●, $n = 18$) rat mesenteric resistance arteries, following pre-contraction with 3 μM noradrenaline.

(0.1 mM) concentration-effect curves to noradrenaline were shifted to the left in arteries from control animals (Figure 7a), but not in those from diabetic rats (Figure 7b; in the absence of L-NAME, control pEC_{50} 5.79 ± 0.08 versus 5.91 ± 0.04, in the presence of L-NAME, $n = 11$, $P < 0.05$; diabetic arteries in the absence of L-NAME pEC_{50} 5.69 ± 0.05 versus 5.70 ± 0.06, in the presence of L-NAME, $n = 14$, P not significant).

Discussion

These results demonstrate enhanced sensitivity to noradrenaline in resistance arteries of rats with STZ-induced diabetes. This enhanced pressor reactivity is in agreement with most studies of conduit arteries in experimental diabetes, the majority of which have investigated chemically-induced diabetes in the rat (MacLeod & McNeill, 1985; Pieper & Gross, 1988; White & Carrier, 1988; Harris & MacLeod, 1988). One study of small arteries found no difference in response to contractile stimuli between cerebral arteries of STZ diabetic rats compared with arteries from control animals (Mayhan *et al.*, 1991). A comparison of the studies is difficult because of the different techniques employed, but the apparent discrepancy between results could be explained by the severity of the diabetes as the rats in this study had higher levels of blood glucose than those of Mayhan *et al.* (1991).

The mechanism for this enhanced noradrenaline sensitivity could be the result of endothelial dysfunction. This was investigated in a further group of diabetic rats and in arteries from control animals. The addition of the nitric oxide synthase inhibitor, L-NAME, potentiated the response to noradrenaline in control arteries, but was without effect in the diabetic animals. This indicates that noradrenaline-induced contractions are normally attenuated by nitric oxide release and agrees with the study of Dohi *et al.* (1990) in which experimental removal of the endothelium in mesenteric resistance arteries of normal rats led to increased reactivity to noradrenaline. This was also suggested by the earlier studies in rat aorta by Martin *et al.* (1986). The lack of effect of L-NAME in the diabetic arteries would suggest a reduced release of nitric oxide. This is in agreement with some, but not all, of the previous investigations of conduit arteries in diabetes. The removal of the endothelium, whilst increasing the contractile response to noradrenaline, did not alter the

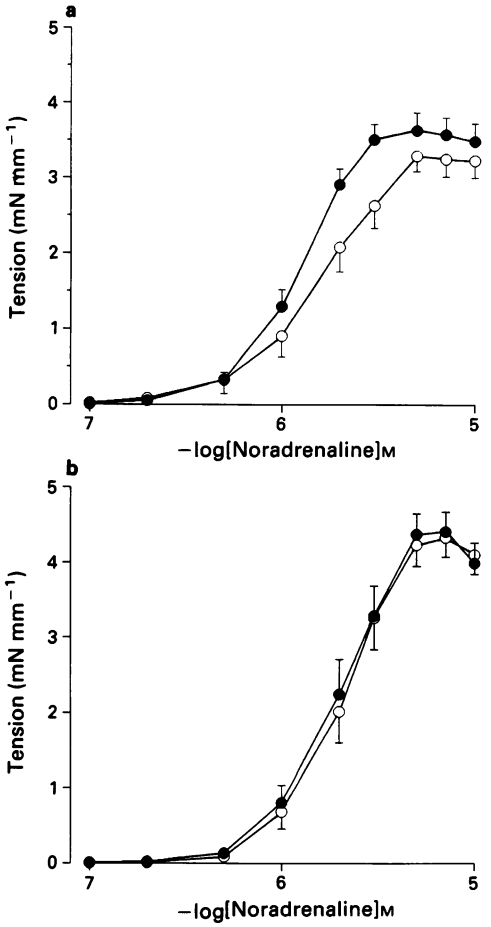

Figure 7 Noradrenaline concentration-response curves in arteries from (a) control rats ($n = 11$) and (b) diabetic rats ($n = 13$) both before (○) and after (●) the addition of N^G-nitro-L-arginine methyl ester (0.1 mM).

enhanced responsiveness to noradrenaline in the arteries of diabetic compared with control rats in studies by Harris & MacLeaod (1988) and by White & Carrier (1988). In contrast, in another study of diabetic rabbits (alloxan-induced) endothelial denudation of control rabbit aorta led to an enhanced response to noradrenaline identical to that seen in diabetic animals (Abiru *et al.*, 1990).

The resistance arteries of diabetic rats demonstrated profound impairment of relaxation to acetylcholine, indicating substantial endothelial dysfunction. This is in agreement with the majority of studies in the conduit arteries of rats with experimentally induced diabetes (Oyama *et al.*, 1986; Pieper & Gross, 1988; Durante *et al.*, 1988; Tanz *et al.*, 1989; Kamata *et al.*, 1989). Studies of cerebral arterioles in the rat (Mayhan, 1989; Mayhan *et al.*, 1991) also showed severe impairment of endothelial function as the responses to ADP and 5-hydroxytryptamine were depressed. Kappagoda *et al.* (1989) found no abnormality in conduit arteries of rats with STZ-induced diabetes, but did in vessels of the BB rat which is genetically susceptible to diabetes, as had been reported by Meraji *et al.* (1987). There is no immediately obvious explanation for the disparities between this study and those showing no impairment of endothelium-dependent relaxation (see Introduction), other than the duration and severity of diabetes which differs from study to study. It is of interest, however, that the data of Harris & MacLeod (1988) initially supported a reduction in sensitivity to acetylcholine in the diabetic rat aorta, but further experiments revealed that this was the result of the very considerable difference in the initial tension (due to the enhanced sensitivity of the diabetic

arteries to noradrenaline). Standardization of tension was found to elicit greater acetylcholine-induced relaxation in diabetic animals than controls. In that study the initial contraction was 50–60% greater in diabetic arteries compared with controls. In the present study there was a small, non-significant difference (<10%) in the initial contraction to noradrenaline but this would be unlikely to account for the very substantial difference in response to acetylcholine.

The results from the present investigation are not in agreement with a recent *in vivo* study by Kiff *et al.* (1991b) which suggested that there was an abnormality of EDRF production in the hindquarters circulation of STZ-treated rats, but not in the mesenteric circulation, which was relatively dilated compared to controls (Kiff *et al.*, 1991a). The studies are not directly comparable as the present experiments were carried out in arteries pre-contracted with noradrenaline. Again there is no obvious explanation for the disparity of results. It is not possible to compare blood glucose concentrations as all values were quoted as being above the upper detection limit of 20 mmol l^{-1} (Kiff *et al.*, 1991a).

Few studies have investigated whether the origin of impaired endothelium-dependent relaxation in diabetic animals lies in abnormalities of the production of different dilator or constrictor stimuli. In this study we hve demonstrated that inhibition of cyclo-oxygenase-dependent pathways by indomethacin had no significant effect on acetylcholine-dependent relaxations in control or diabetic animals, and it is unlikely, therefore, that a dilator prostanoid plays a significant role in acetylcholine-induced relaxation in this vascular bed. In a study of cerebral arterioles in diabetic rats, Mayhan *et al.* (1991) found that indomethacin normalized the reduced dilator response to acetylcholine and suggested that the predominant defect was due to the production of a constrictor prostanoid. Production of a constrictor prostanoid has also been implicated by Tesfarmariam *et al.* (1989) in a study of the aorta in diabetic rabbits. Pre-incubation with the nitric oxide synthase inhibitor, L-NMMA, led to a statistically greater rise in noradrenaline-induced tension in control arteries compared to those from diabetic rats, providing further evidence for reduced nitric oxide production in the diabetic rats.

The response to acetylcholine in the presence of indomethacin and L-NMMA resulted in proportionally greater inhibition of acetylcholine-induced relaxation in the vessels from diabetic rats when compared to controls. This could be interpreted as EDRF playing a greater role in acetylcholine-induced relaxation in the diabetic rats, and would, therefore, imply that the residual acetylcholine-induced relaxation in the control animals was mediated by a compound other than nitric oxide or a prostanoid. This was indeed the interpretation of the data obtained by Dohi *et al.* (1990) who found similar incomplete inhibition of acetylcholine-induced relaxation by L-NMMA and indomethacin in mesenteric resistance arteries from normal Wistar Kyoto rats. However, an alternative explanation to a third component of endothelium-dependent relaxation must be that L-NMMA is selectively ineffective as an inhibitor of nitric oxide synthase in healthy arteries from this vascular bed. In another vascular bed (human subcutaneous fat) we have previously found 1 mM L-NMMA to be an effective inhibitor of acetylcholine-induced relaxation (Woolfson & Poston, 1990), and using the same concentration, this inhibitor has been shown to be as potent as a number of other related compounds tested in rat aorta (Rees *et al.*, 1990). In the mesentery of the control rats in this study the alternative inhibitor L-NAME demonstrated much greater inhibition of nitric oxide synthase than did L-NMMA. L-NAME inhibited acetylcholine-induced relaxation by 69%, thus achieving similar inhibition to that found in the diabetic arteries treated with L-NMMA. An explanation for the different potency of these compounds may lie in their metabolism. Hecker *et al.* (1990) have found L-NMMA to be extensively metabolized in rabbit endothelial cells to L-citrulline and subsequently to L-arginine, whereas another nitric oxide synthase inhibitor, N^G-nitro-L-arginine, was not metabolized (L-NAME was not investigated). During pre-incubation the potential intracellular level of L-NMMA might be quite low if there is very rapid metabolism in the rat mesenteric vascular bed. This hypothesis is supported by the profound and immediate effect of the addition of L-NMMA to control arteries which had been relaxed with acetylcholine. In an earlier study in rabbit aorta, addition of L-NMMA to arteries partially relaxed by acetylcholine was similarly shown to cause immediate inhibition of relaxation, whereas responses of arteries pre-incubated with the inhibitor were inhibited to a lesser extent (Furchgott, 1990). This, it was suggested, could be explained if nitric oxide synthase required stimulation before L-NMMA gained access to, or interacted with it. It could also have been due to rapid metabolism of L-NMMA.

The rate of metabolism of L-NMMA may also provide an explanation for the apparently greater efficacy of L-NMMA in the arteries of diabetic rats as damage to the vascular endothelium might lead to reduced metabolism of L-NMMA. Alternatively, the data could simply reflect reduced acetylcholine-induced release of EDRF (and reduced nitric oxide synthase activity) in the diabetic rats and thus apparently greater efficiency of the inhibitor. Taken together, the data obtained with the two inhibitors L-NMMA and L-NAME suggest that the EDRF-mediated component of acetylcholine-induced relaxation in diabetic rat mesenteric resistance arteries is less than that of the control animals. This has been suggested by one previous study of the diabetic rat aorta in which basal and acetylcholine-induced guanosine levels of cyclic GMP in the vascular smooth muscle were significantly reduced (Kamata *et al.*, 1989). As EDRF leads to vasodilatation through elevation of cyclic GMP, this was indicative of abnormal nitric oxide synthesis. However, that report is in disagreement with another in which cyclic GMP levels were found to be similar in arteries of diabetic and control rats both in the presence and absence of acetylcholine (Harris & MacLeod, 1988).

In this study no attempt has been made to elucidate the mechanisms behind the observed endothelial dysfunction; however, hyperglycaemia itself may play an important role. Elevated glucose concentrations have been found to depress endothelium-dependent relaxation through activation of protein kinase C (Tesfamariam *et al.*, 1991).Together with results from an earlier study in the same laboratory (Tesfamariam *et al.*, 1990) the authors concluded that elevated glucose led to the release of constrictor prostanoids, and thus to inhibition of relaxation.

The reduced endothelium-dependent relaxation in the diabetic animals was unlikely to be the result of impairment of the response of the underlying vascular smooth muscle to EDRF since nitroprusside induced similar concentration-dependent relaxations in vessels from diabetic and control rats. Nitroprusside spontaneously forms nitric oxide in solution and, therefore, provides an estimate of the functional response of the vascular smooth muscle to EDRF (Furchgott & Vanhoutte, 1989). A normal response to nitrovasodilators has also been reported in many studies of conduit arteries from diabetic animals (Durante *et al.*, 1988; Pieper & Gross, 1988; Kamata *et al.*, 1989; Tanz *et al.*, 1989; Tesfamariam *et al.*, 1989).

In conclusion, the resistance arteries in the mesenteric circulation of rats with STZ-induced diabetes demonstrate many of the abnormalities reported in conduit arteries. Since these small arteries are involved in the local control of blood flow and the control of blood pressure, these results indicate that defective endothelial function, manifest by reduced EDRF production may play an important role in the recognized complications of the microvasculature in diabetes.

This research was funded as part of a collaborative PhD studentship between the Medical Research council and ICI Pharmaceuticals.

References

ABIRU, T., KAMATA, K., MIYATA, N. & KASUYA, Y. (1990). Differences in vascular responses to vasoactive agents of basilar artery and aorta from rabbits with alloxan-induced diabetes. *Can. J. Physiol. Pharmacol.*, **68**, 882–888.

ARBOGAST, B.W., BERRY, D.L. & NEWELL, C.L. (1984). Injury of arterial endothelial cells in diabetic sucrose fed and aged rats. *Atherosclerosis*, **51**, 31–45.

CHRISTLIEB, A.R., JANKA, H.U., KRAUS, B., GLEASON, R.E., ICASES-CABRAL, E.A., AIELLO, L.M., CABRAL, B.V. & SOLANO, A. (1976). Vascular reactivity to angiotensin II and to norepinephrine in diabetic subjects. *Diabetes*, **25**, 268–274.

COHEN, R.A., TESFAMARIAM, B., WEISBROD, R.M. & ZITNAY,K.M. (1990). Adrenergic denervation in rabbits with diabetes mellitus. *Am. J. Physiol.*, **259**, H55–H61.

DE TEJADA, I.S., GOLDSTEIN, I., AZADZOI, K., KRANE, R.J. & COHEN, R.A. (1989). Impaired neurogenic and endothelium-mediated relaxation of penile smooth muscle from diabetic men with impotence. *New Engl. J. Med.*, **320**, 1025–1030.

DOHI, Y., THIEL, M.A., BUHLER, F.R. & LUSCHER, T.F. (1990). Activation of endothelial L-arginine pathway in resistance arteries. *Hypertension*, **15**, 170–179.

DURANTE, W., SEN, A.K. & SUNAHARA, F.A. (1988). Impairment of endothelium-dependent relaxation in aortae from spontaneously diabetic rats. *Br. J. Pharmacol.*, **94**, 463–468.

FURCHGOTT, R.F. (1990). Endothelium derived relaxing factor: some old and new findings. In *Nitric Oxide from L-Arginine: a Bioregulatory System.* Chapter 2, pp. 5–17. ed. Moncada, S. & Higgs, E.A. Amsterdam: Elsevier.

FURCHGOTT, R.F. & VANHOUTTE, P.M. (1989). Endothelium-derived relaxing and contracting factors. *FASEB J.*, **3**, 2007–2018.

FURCHGOTT, R.F. & ZAWADZSKI, J.V. (1980). The obligatory role of endothelial cells in the relaxation of arterial smooth muscle by acetylcholine. *Nature*, **288**, 373–376.

GEBREMEDHIN, D., HADHAZY, P., KOLTAI, M.Z. & POGATSA, G. (1988). Contractile and relaxant properties of diabetic dog femoral arteries. *Acta Physiol. Hung.*, **71**, 213–217.

GEBREMEDHIN, D., KOLTAI, M.Z., POGATSA, G., MAGYAR, K. & HADHAZY, P. (1989). Altered responsiveness of diabetic dog renal arteries to acetylcholine and phenylephrine: role of endothelium. *Pharmacology*, **38**, 177–184.

HARRIS, K.H. & MACLEOD, M. (1988). Influence of the endothelium on contractile responses of arteries from diabetic rats. *Eur. J. Pharmacol.*, **153**, 55–64.

HEAD, R.J., LONGHURST, P.A., PANEK, R.L. & STITZEL, R.E. (1987). A contrasting effect of the diabetic state upon the contractile responses of aortic preparations from the rat and rabbit. *Br. J. Pharmacol.*, **91**, 275–287.

HECKER, M., MITCHELL, J.A., HARRIS, H.J., KATSURA, M., THIEMERMANN, C. & VANE, J.R. (1990). Endothelial cells metabolize N^G-monomethyl-L-arginine to L-citrulline and subsequently to L-arginine. *Biochem. Biophys. Res. Commun.*, **167**, 1037–1043.

KAMATA, K., MIYATA, N. & KASUYA, Y. (1989). Impairment of endothelium-dependent relaxation and changes in levels of cyclic GMP in aorta from streptozotocin-induced diabetic rats. *Br. J. Pharmacol.*, **97**, 614–618.

KAPPAGODA, T., JAYAKODY, L., RAJOTTE, R., THOMSON, A.B. & SENARATNE, M.P. (1989). Endothelium-dependent relaxation to acetylcholine in the aorta of STZ diabetic rat and BB-diabetic rat. *Clin. Invest. Med.*, **12**, 187–193.

KIFF, R.J., GARDINER, S.M., COMPTON, A.M. & BENNETT, T. (1991a). The effect of endothelin-1 and N^G-nitro-L-arginine methyl ester on regional haemodynamics in conscious rats with streptozotocin-induced diabetes mellitus. *Br. J. Pharmacol.*, **103**, 1321–1326.

KIFF, R.J., GARDINER, S.M., COMPTON, A.M. & BENNETT, T. (1991b). Selective impairment of hindquarters vasodilator responses to bradykinin in conscious Wistar rats with streptozotocin-induced diabetes mellitus. *Br. J. Pharmacol.*, **103**, 1357–1362.

MACLEOD, K.M. & MCNEILL, J.H. (1985). Influence of chronic experimental diabetes on contractile response of rat isolated blood vessels. *Can. J. Physiol. Pharmacol.*, **63**, 52–57.

MARTIN, W., FURCHGOTT, R.F., VILLANI, G.M. & JOTHIANANDAN, D. (1986). Depression of contractile responses in rat aorta by spontaneously released endothelium-derived relaxing factor. *J. Pharmacol. Exp. Ther.*, **237**, 529–538.

MAYHAN, W.G. (1989). Impairment of endothelium-dependent dilatation of cerebral arterioles during diabetes mellitus. *Am. J. Physiol.*, **256**, H621–H625.

MAYHAN, W.G., SIMMONS, L.K. & SHARPE, G.M. (1991). Mechanism of impaired responses of cerebral arterioles during diabetes mellitus. *Am. J. Physiol.*, **260**, H319–H326.

MERAJI, S., JAYAKODY, L., SENARATINE, P.J., THOMSON, A.B.R. & KAPPAGODA, T. (1987). Endothelium-dependent relaxation in aorta of BB rat. *Diabetes*, **36**, 978–981.

MULHERN, M. & DOCHERTY, J.R. (1989). Effects of experimental diabetes on the responsiveness of rat aorta. *Br. J. Pharmacol.*, **97**, 1007–1012.

MULVANY, M.J. & HALPERN, W. (1977). Contractile properties of small arterial resistance arteries in spontaneously hypertensive and normotensive rats. *Circ. Res.*, **41**, 19–26.

OYAMA, Y., KAWASAKI, H., HATTORI, Y. & KANNO, M. (1986). Attenuation of endothelium-dependent relaxation in aorta from diabetic rats. *Eur. J. Pharmacol.*, **131**, 75–78.

PIEPER, G.M. & GROSS, G.J. (1988). Oxygen free radicals abolish endothelium dependent relaxation in diabetic rat aorta. *Am. J. Physiol.*, **255**, H825–H833.

PORTA, M., LA SELVA, M., MOLINATTI, P. & MOLINATTI, G.M. (1987). Endothelial cell function in diabetic microangiopathy. *Diabetologia*, **30**, 601–609.

REES, D.D., PLAMER, R.M.J., SCHULZ, H.F., HODSON, H.F. & MONCADA, S. (1990). Characterization of three inhibitors of endothelial nitric oxide synthase *in vitro* and *in vivo*. *Br. J. Pharmacol.*, **101**, 746–752.

TANZ, R.D., CHANG, K.S.K. & WELLER, T.S. (1989). Histamine relaxation of aortic rings from diabetic rats. *Agents Actions*, **28**, 2–8.

TESFAMARIAM, B., BROWN, M.L., DEYKIN, D. & COHEN, R.A. (1990). Elevated glucose promotes generation of endothelium-derived vasoconstrictor prostanoids in rabbit aorta. *J. Clin. Invest.*, **85**, 929–932.

TESFAMARIAM, B., BROWN, M.L. & COHEN, R.A. (1991). Elevated glucose impairs endothelium-dependent relaxation by activating protein kinase C. *J. Clin. Invest.*, **87**, 1643–1648.

TESFAMARIAM, B., JAKUBOWSKI, J.A. & COHEN, R.A. (1989). Contraction of diabetic rabbit aorta caused by endothelium-derived PGH_2-TxA_2. *Am. J. Physiol.*, **257**, H1327–H1333.

WAKABAYASHI, I., HATAKA, N., KIMURA, E., KAKISHITA, E. & NAGAI, K. (1987). Modulation of vascular tonus by the endothelium in experimental diabetes. *Life Sci.*, **40**, 643–648.

WEIDMANN, P., BERETTA, P., COLLI, C., KEUSCH, G., GLUCK, Z., MUJAGIC, M., GRIMM, M., MEIER, A. & ZEIGLER, W.H. (1979). Sodium-volume factor, cardiovascular reactivity and hypotensive mechanism of diuretic therapy in mild hypertension associated with diabetes mellitus. *Am. J. Med.*, **67**, 779–784.

WHITE, R.E. & CARRIER, G.O. (1986). Supersensitivity and endothelium dependency of histamine-induced relaxation in mesenteric arteries from diabetic rats. *Pharmacology*, **33**, 34–38.

WHITE, R.E. & CARRIER, G.O. (1988). Enhanced vascular α-adrenergic neuroeffector system in diabetes: importance of calcium. *Am. J. Physiol.*, **255**, H1036–H1042.

WOOLFSON, R.G. & POSTON, L. (1990). Effect of N^G-monomethyl-L-arginine on endothelium-dependent relaxation of human subcutaneous resistance arteries. *Clin. Sci.*, **79**, 273–278.

(Received February 5, 1992
Revised June 1, 1992
Accepted June 2, 1992)

Br. J. Pharmacol. (1992), **107**, 400-406

The actions of capsaicin applied topically to the skin of the rat on C-fibre afferents, antidromic vasodilatation and substance P levels

[1]B. Lynn, [2]W. Ye & B. Cotsell

Department of Physiology, University College London, Gower Street, London WC1E 6BT

1 Single applications of solutions of capsaicin were made to the intact skin of anaesthetized rats and the effects on cutaneous blood flow and the firing of C-nociceptor afferents determined. Blood flow was measured by laser-Doppler flowmetry. C-fibre activity was recorded from filaments dissected from the saphenous nerve.

2 Following the application of a capsaicin solution (concentration $\geqslant$ 1 mM) to rat saphenous skin, low frequency firing occurred in C-polymodal nociceptors that sometimes continued for $>$ 10 min. At the some time, large increases in skin blood flow occurred exceeding 300% in some instances.

3 After the initial excitation, some C-polymodal nociceptors lost their sensitivity to pressure whilst their sensitivity to heat was lost or enhanced depending on the vehicle used.

4 Sensitivity of C-polymodal nociceptors to heat recovered in $<$ 1 day following a single application of 33 mM capsaicin. Thresholds to mechanical pressure, however, were still significantly elevated by 123% on day 1, but had recovered on day 2.

5 Vasodilatation in response to saphenous nerve stimulation ('antidromic vasodilatation') was significantly reduced by 35%, 2 days after a single application of 33 mM capsaicin, but was normal at 4 days.

6 Following a single application of 33 mM capsaicin, skin substance P levels fell to only half the normal value at day 1 and remained at this level throughout the 4 day period examined.

7 It is suggested that the ability of relatively low concentrations of capsaicin to desensitize C-fibre nociceptors may underlie the analgesic action of topical capsaicin in man.

Keywords: Capsaicin; C-fibre; neurogenic inflammation; nociceptor; substance P; laser-Doppler flowmeter; skin blood flow

Introduction

Topical application of capsaicin to human skin causes, initially, vasodilatation and a hot painful sensation. On repeated treatment, these effects diminish or disappear, and there is also loss or reduction of the vasodilator flare around localized skin injuries (Bernstein *et al.*, 1981; Carpenter & Lynn, 1981). Changes also occur in sensitivity to noxious stimuli. Initially the skin is markedly hyperalgesic to heat, but over 24–48 h this changes to a slight hypo-algesia (Carpenter & Lynn, 1981). Treatment of painful skin areas in patients, for example in post-herpetic neuralgia, with topical capsaicin creams has also been claimed to produce useful analgesia (Bernstein *et al.*, 1989).

On rat, rabbit and primate skin, local application of capsaicin selectively excites C-polymodal nociceptors (C-PMNs) (Kenins, 1982; Konietzny & Hensel, 1983; Szolcsanyi, 1987; Baumann *et al.*, 1991). This *in vivo* action presumably operates via the receptor-cation channel complex defined by *in vitro* studies on cells from the dorsal root ganglion of the rat (Baccaglini & Hogan, 1983; Wood *et al.*, 1988; Bevan & Szolcsany, 1990). Topical application of high concentrations of capsaicin in dimethylsulphoxide (DMSO) has also been shown to desensitize C-PMNs (Kenins, 1982). Overall the picture from experimental studies is of a dual action of capsaicin on nociceptor terminals, an initial excitation followed by a period of desensitization.

The present study set out to examine in more detail the effect of topically applied capsaicin on afferent and 'efferent' functions of C-PMNs in the same preparation and for this purpose the skin of the anaesthetized rat was used. The dose-dependence of the initial excitation of C-PMNs and of the simultaneous increase in local blood flow was assessed and the changes in C-PMN heat and pressure thresholds were compared with the reduction in antidromic vasodilatation over a period from immediately after treatment to 4 days later. This study also examined whether treatment of the skin with capsaicin could lead to long-term loss of C-PMNs, as has been observed after treatment of nerve trunks (Pini & Lynn, 1991). Finally, we have examined the levels in the skin of substance P, a peptide that may play a role in neurogenic inflammation (Holzer, 1988), for 1–4 days following a single topical treatment with capsaicin.

Two preliminary accounts of parts of this work have appeared (Lynn *et al.*, 1991; Lynn & Cotsell, 1992a).

Methods

Experiments were carried out on albino rats (SD or Wistar) anaesthetized with urethane (i.p. 1.5–1.8 g kg^{-1}) or sodium pentobarbitone (Sagatal, May and Baker; initial i.p. injection, 50–80 mg kg^{-1}; maintained by additional 20 mg kg^{-1} h^{-1} given i.v. or i.a.). Results were similar with both strains. Unit data were similar for either anaesthetic, but antidromic vasodilatation was greater with pentobarbitone anaesthesia. All antidromic vasodilatation data reported here have been taken from pentobarbitone-anaesthetized preparations. Cannulae were inserted in the trachea, one common carotid artery and one jugular vein. Blood pressure was measured via the carotid cannula. Rectal temperature was measured with a thermistor and was maintained at 36–38°C by automatic

[1] Author for correspondence.
[2] Present address: Department of Biology, Shanghai Teacher's University, Shanghai 200234, China.

control of a heating pad.

The saphenous nerve was exposed for recording and stimulation in the thigh and was cut proximally. A pool of mineral oil was formed around the nerve and a pair of platinum electrodes was placed under the nerve for electrical stimulation. When recordings were made, the stimulating electrodes were positioned just above the knee and the proximal cut end of the nerve was placed on a small mirrored platform. Recordings were made from fine filaments dissected from the proximal cut end of the nerve. Units were identified by maximal electrical stimulation of the nerve. Receptive fields were located by searching the skin of the anterior and medial aspects of the lower leg and foot with mechanical and thermal stimuli. C-polymodal nociceptor (C-PMN) units were identified by their slow conduction velocity (0.5–1.5 m s^{-1}) and ability to respond both to strong pressure and to heating to 40–65°C.

When antidromic vasodilatation was studied, stimulating electrodes were placed on the cut end of the nerve. In some experiments, compound action potentials were recorded from the nerve between the stimulating site and the skin. Stimuli were adjusted to be maximal for the C-fibre component of the compound action potential or to give a maximum blood flow response. Typically, maximal antidromic vasodilatation and compound action potentials occurred with stimuli of 1-3 mA (pulse width 0.5 ms)..

Capsaicin (Merck or Sigma) solutions were applied to the skin with a small paint brush or a cotton wool bud. To examine the recovery from local application, preliminary treatment was given to skin in the saphenous area under general anaesthesia (sodium pentobarbitone or halothane (2–4%) in 67% nitrous oxide: 33% oxygen), with the skin being washed with ethanol after 15 min. Three vehicles were used for experiments on the immmediate effects on C-fibre units. These were (1) ethanol, (2) 50% DMSO + 50% ethanol, and (3) a vehicle ('vehicle 3') comprising 48% ethanol, 25% propylene glycol, 25% water and 2% methyl laurate (Carter & Francis, 1991). Only vehicle 3 was used for the blood flow experiments, both those on immediate effects and on recovery over 4 days, and for the experiments on recovery of function by C-fibres.

To examine the immediate effects of topical capsaicin, controlled heat and mechanical stimulators were mounted so that identical repeated stimuli could be applied to the receptive field of a unit. Mechanical stimuli were forces of 10–100 mN applied for 15 s to a fine (0.24–0.8 mm diameter) probe. Heat stimuli were 1°C s^{-1} ramps starting from a hold temperature of 35°C and stopping at 45–62°C. Stimuli were generated with a focused projector bulb and were monitored by a fine thermocouple pressing on the skin. Alternate heat and mechanical stimuli were given at 2–3 min intervals to minimize fatigue. Once a stable baseline was achieved the test solution was applied to the receptive field with a small paintbrush. In most cases the heat and mechanical stimuli were stopped for 15 min so that any firing could be observed continuously. In two instances stimulation continued throughout the application period. No difference was observed between these two protocols. After 15 min, the skin was washed several times with alcohol and mechanical and thermal testing continued. Excitability was followed for around 1 h after a single application.

To ascertain the proportions of different classes of C-fibre after pretreatment, only filaments with a small number (1–5) of electrically driven C-units were examined. The saphenous skin was tested systematically with gentle mechanical stimulation, strong pressure, cooling with ice, and heating to 52°C. Units were classified into the major classes of mechanoreceptors, thermoreceptors and nociceptors found in earlier studies on the saphenous nerve (Lynn & Carpenter, 1982). Heat thresholds were measured with 1°C s^{-1} 'ramp' stimuli; pressure thresholds were determined with calibrated von Frey bristles. As described previously (Lynn & Carpenter, 1982), the distribution of pressure thresholds is positively skewed. However, the distribution of log thresholds is approximately normal, so the statistical analysis used log pressure thresholds in units of log mN.

Skin blood flow was determined by use of 2 laser-Doppler flow meters, one with a single channel (Moor Instruments MBF2) and another with two channels (Moor Instruments MBF3D). The single channel flowmeter used optic fibre light guides of 1 mm diameter, with the collecting and transmitting fibres separated by 1.2 mm. The two channel meter used 0.2 mm diameter fibres separated by 0.4–0.65 mm. Both meters used near infra red (approx 800 nm) laser diodes. Probes were standardized by immersing them in a 0.5% solution of 0.48 μm diameter polystyrene microspheres and the Brownian motion of the microspheres was used as a fixed velocity source. Where appropriate, flux data are expressed as '% standard' units. However, data are normally expressed as % initial baseline level since we found that, on average, effects such as antidromic vasodilatation or the peak flow following capsaicin treatment were proportional to the baseline flow. We found it necessary to avoid locations immediately over the saphenous neurovascular bundle. At these locations a large flow signal was measured that changed little when the nerve was stimulated antidromically. We concluded that the flowmeters were detecting a signal from the deep vessels that only to a small degree reflected fluctuations in local skin blood flow.

To determine their substance P content, skin samples (weight 58–102 mg) from the area innervated by the saphenous nerve were removed at the end of experiments and were dropped into approximately 10 volumes of boiling 0.5 M acetic acid for 10 min. Extracts were stored frozen and radioimmunoassay (RIA) was performed on 0.2 ml aliquots (Lynn & Shakhanbeh, 1988a). Skin from untreated or vehicle-treated rats contained 3 to 10 pmol g^{-1} wet wt. substance P. To allow for the substantial rat-to-rat variation, data have usually been expressed as % contralateral (untreated control) levels.

Variability of measurements is given as ± 1 standard error (s.e.); t tests were used to compare 2 means, except where distributions were very non-normal or variances differed markedly when the Mann-Whitney U-test (unpaired data) or the Wilcoxon signed rank test (paired data) were used. In some cases, comparisons of >2 means was by 1-way analysis of variance and either t tests for specified trends or the Newman-Keuls test for comparing all differences between group means were used.

Results

Immediate effects of capsaicin application on C-polymodal nociceptors (C-PMNs)

Afferent units of the C-PMN class were isolated from the saphenous nerve and their properties examined during, and for up to 1 h after, topical administration of capsaicin. Painting 1% capsaicin on to the receptive fields of 29 C-PMN units caused irregular low frequency firing for many minutes (Figure 1a,b). Firing was usually greatest 1–4 min after application, although occasionally firing built up only slowly or, on 2 occasions, after a delay of several minutes (e.g. see Figure 1b). The degree of firing varied between the 3 vehicles used for dissolving capsaicin (Figure 1c). Capsaicin in 50% DMSO caused most firing, with an average of 79 spikes (± 30, ± s.e., $n = 11$) recorded during the period from 0.5 to 2.5 min after application. In contrast, capsaicin in ethanol caused firing of only 24 (± 13, $n = 10$) spikes in the same period. Capsaicin in vehicle 3 (48% ethanol, 25% propylene glycol, 25% water and 2% methyl laurate) produced intermediate levels of firing, with 36 (± 13, $n = 8$) spikes recorded over the 0.5–2.5 min period after application. Capsaicin in vehicle 3 appeared to be the most effective in generating firing at times greater than 6 min after application (see

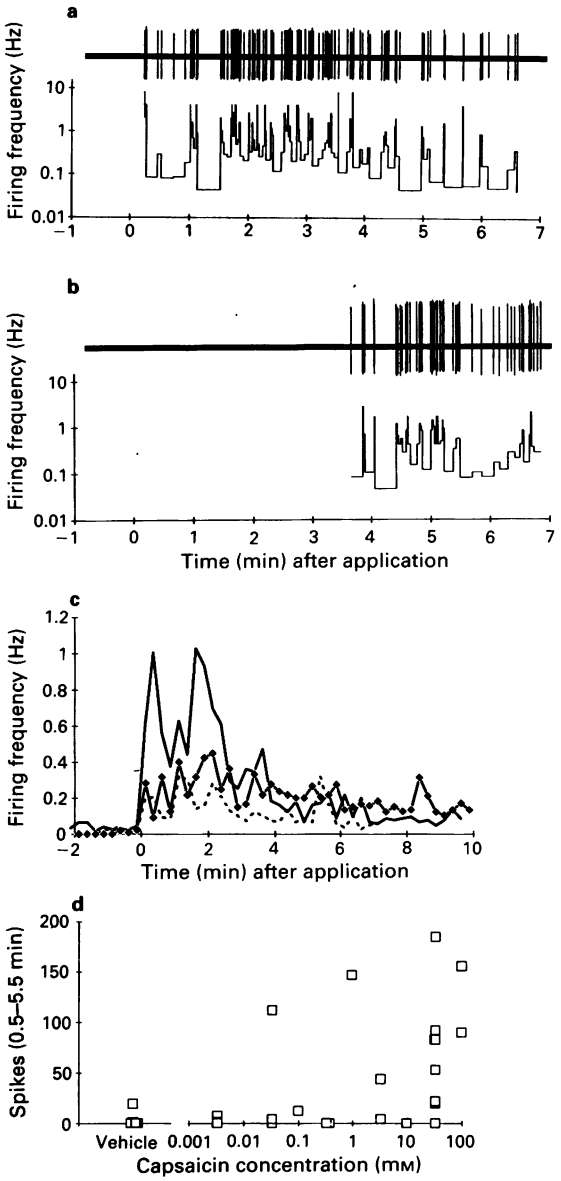

Figure 1 Responses of C-polymodal nociceptor (C-PMN) units recorded from the rat saphenous nerve after topical application of capsaicin. (a) Action potentials (upper trace) and instantaneous frequency (lower trace, on logarithmic scale) recorded in response to topical application of 33 mM capsaicin in 50% dimethyl sulphoxide (DMSO)-ethanol. (b) Action potentials from another unit in response to capsaicin dissolved in vehicle 3 (48% ethanol, 25% propylene glycol, 25% water and 2% methyl laurate), plotted as in (a). Note that the delay before firing started was unusually long in this unit. (c) Average firing of 8–11 units after topical 1% capsaicin in 3 different vehicles. Dashed line, capsaicin in ethanol; ◆, in vehicle 3; solid line, in 50% DMSO/ethanol. (d) Dose-dependence of firing for capsaicin in vehicle 3. Ordinate scale, total number of spikes fired from 0.5 to 5.5 min after application. Note great variability between units in amount of firing.

Figure 1c). Firing following application of vehicle alone was negligible for ethanol and for 6 out of 7 units tested with vehicle 3. However, 50% DMSO did produce significant firing in 4 out of 11 units tested, with an average (over all 11 units) of 15 (± 9) spikes fired from 0.5 to 2.5 min after application.

The dose-dependency of firing to topical capsaicin has been examined with vehicle 3 and the data are presented in Figure 1d. Above 1 mM most units fired and there was a general trend for firing to increase with increasing concentration. There were marked variations in the degree of response from unit to unit. Thus at 0.03 mM, 1 out of 3 units fired strongly but the others fired hardly or not at all. At 33 mM, most units fired strongly, but 1 out of the 8 examined did not fire at all.

Responses to mechanical pressure were depressed or abolished following topical capsaicin (e.g. see Figure 2, upper traces). Effects were seen on most units with $\geqslant 100\,\mu$M topical capsaicin in vehicle 3 (Figure 3c). There was again considerable variation between units in the effectiveness of capsaicin. For example, topical treatment with 3–33 mM (in vehicle 3) greatly depressed pressure-evoked firing in 7/11 units, but in 3/11 units caused no significant change (Figure 3c). The average reduction in firing to a fixed pressure stimulus was by 77% (± 9%, $n = 11$) and this reduction was maintained for at least 45 min (Figure 3a). Again, like the effects on spontaneous firing, actions of topical capsaicin varied with the vehicle used. Topical treatment with 33 mM in 50% DMSO always abolished mechanical responses whilst the same concentration in ethanol had no significant effect.

Responses to skin heating were severely depressed or abolished by topical treatment with 33 mM capsaicin in DMSO. However, topical treatment with $\geqslant 1$ mM capsaicin in vehicle 3 or with 33 mM in ethanol usually led to marked sensitization of heat responses as shown in the lower traces in Figure 2. Firing thresholds to a 1°C s^{-1} heat ramp fell (Figure 3b) and the number of spikes evoked by a constant heat stimulus increased. The average fall in heat threshold 5–25 min after application of 3–100 mM was 8.8°C (± 2.5°C, $n = 11$) and there was some recovery, by 4.5°C (± 2.0°C) over the next 20 min (Figure 3b). The dose-dependence of the fall in heat threshold is shown in Figure 3d. Note that not all units sensitized after topical capsaicin in vehicle 3, and two units actually desensitized substantially. Overall, however, most units showed simultaneous sensitization to skin heating and depression of responses to pressure following application of $\geqslant 1$ mM topical capsaicin in vehicle 3.

Immediate effects on skin blood flow

Painting capsaicin solutions onto the skin caused a slow, dose-dependent, rise in the laser-Doppler flux signal, with maximum flux usually occurring at 10–30 min (Figure 4a). After application of a 33 mM solution, blood flow recovered to baseline in 2–4 h (4 preparations). As shown in Figure 4b, no significant effect was seen with 0.3 mM capsaicin, but 1 mM caused an average increase of 60% (± 25%, $n = 6$), a rise that is just significant ($P < 0.05$, 1-tailed t test). The average increase with 33 mM capsaicin was 171% (± 23%, $n = 7$) and increases of over 300% were seen at some locations.

Immediate effects on antidromic vasodilatation

Electrical stimulation of the distal cut end of the saphenous nerve caused the blood flow to increase transiently. As reported previously (Lynn, 1988; Janig & Lisney, 1989), a stimulus intensity sufficient to activate unmyelinated (C) fibres was needed to generate reliable, large antidromic vasodilatation. A typical response for 10 stimuli at 1 Hz and maximum C-fibre strength (the standard stimulus used) is shown in Figure 5a. Antidromic vasodilatation was greatly reduced or abolished following capsaicin application (Figure 5b).

Analysis of the reduction in antidromic vasodilatation after topical capsaicin treatment was complicated by the simultaneous large rise in baseline blood flow. Expressing antidromic vasodilatation as % baseline indicates a dose-dependent fall in antidromic vasodilatation over the range 1–100 mM. A significant reduction in the absolute flux increase, in standard units (see methods), was only seen for concentrations $\geqslant 10$ mM. When there was a very high baseline flow after topical capsaicin, antidromic stimulation sometimes produced only a marked vasoconstriction. This presumably represents

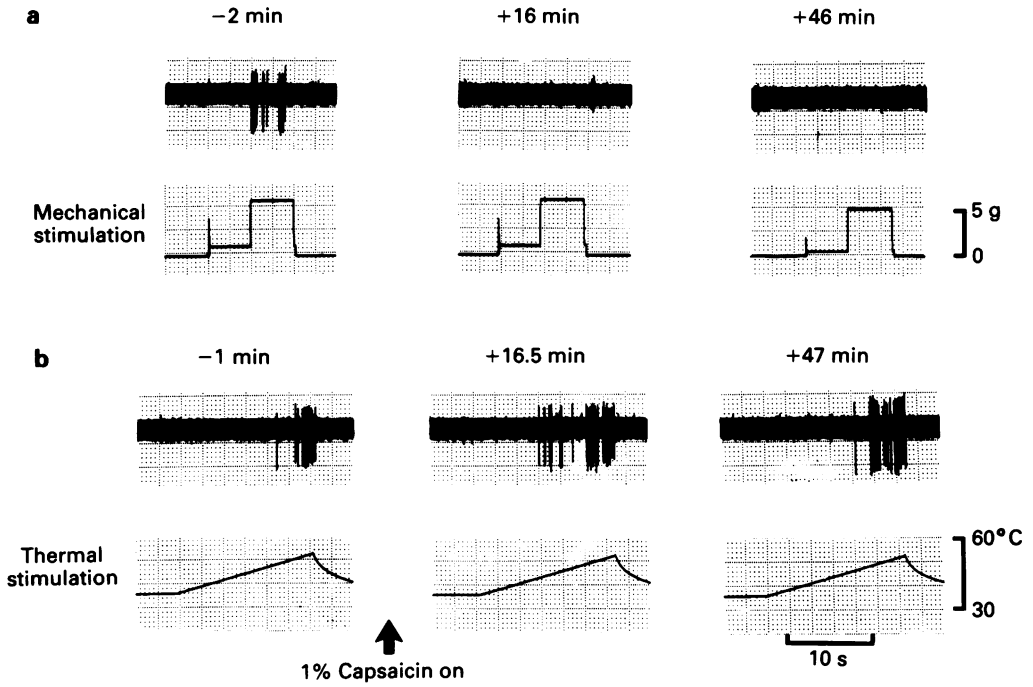

Figure 2 Responses of a typical C-polymodal nociceptor (C-PMN) unit to heat and pressure stimuli after topical capsaicin treatment. Traces of action potentials fired in response to punctuate pressure (a) and skin heating (b) before (left) and 16 and 46 – 7 min after (middle and right traces) application of 33 mM capsaicin in vehicle 3.

an action of sympathetic efferents (Lembeck & Holzer, 1979) that can become prominent when antidromic vasodilatation is blocked and there is a high baseline blood flow.

The time course of antidromic vasodilatation was not significantly altered in the first hour after topical treatment. Time for half recovery towards baseline ($t_{\frac{1}{2}}$) was 3.2 min before treatment and 2.8 min over the 15–60 min after treatment with 10–33 mM capsaicin. In 4 experiments antidromic vasodilatation was examined for 2–4 h after a single topical application of capsaicin. Peak antidromic vasodilatation showed some recovery over this period, but was still significantly reduced at 2–4 h by 41% (± 9%). Recovery of antidromic vasodilatation was therefore slower than the return of baseline blood flow to pre-application levels since at 2–4 h baseline blood flow was back to pretreatment levels in the same preparations.

Effects of C-fibre afferents 1–2 days after a single application of 33 mM capsaicin in vehicle 3

The types of afferent fibre present and the properties of C-fibre PMNs have been examined 'blind' in 13 rats treated 1–2 days previously with either capsaicin (33 mM in vehicle 3) or vehicle alone. The numbers and proportions of the major classes of afferent found after vehicle or capsaicin treatment were similar and are also similar to those reported previously for the rat saphenous nerve (Lynn & Carpenter, 1982; Pini *et al.*, 1990; Pini & Lynn, 1991). Note in particular that the proportion of C-PMN units in treated skin (63% of 40 C-units excited from the skin on day 1; 78% of 36 on days 2) was close to the value in vehicle-treated skin (69% out of 49 units). A proportion of afferents cannot be driven from the skin, and this group is usually around 25% for the C-fibre sample (Pini & Lynn, 1991; Koltzenberg *et al.*, 1991). This proportion was also unchanged following topical capsaicin treatment, the proportions of inexcitable units being 23% (± 3%, $n = 4$ preparations) for vehicle treatment, 27% (± 6%, $n = 5$) at 1 day after capsaicin treatment, 10% (± 4%, $n = 3$) at 2 days.

Heat thresholds of C-PMN units were similar for vehicle and for capsaicin treatment (Figure 6a). However, there was a significant rise in pressure thresholds 1 day after capsaicin treatment, with full recovery at 2 days (Figure 6b). Average thresholds after vehicle treatment were 0.88 ± 0.08 log mN ($n = 38$), similar to previously published values. At 2 days after capsaicin treatment thresholds were again similar at 0.95 ± 0.07 log mN ($n = 28$), but at 1 day thresholds were significantly raised ($P < 0.01$, Newman-Keuls test) at 1.23 ± 0.07 log mN ($n = 36$). This rise of 0.35 log units is equivalent to an average elevation of threshold by 123%.

Antidromic vasodilatation 4 h to 4 days after a single application of 33 mM capsaicin

Baseline blood flow and antidromic vasodilatation were measured at 12–18 sites on each leg in rats pretreated 4–9 h ($n = 2$) or 1 ($n = 5$), 2 ($n = 5$) or 4 ($n = 4$) days previously by a topical application of 33 mM capsaicin in vehicle 3 for 15 min. No differences in baseline blood flow were present between vehicle and capsaicin-treated legs at any time from 4–9 h to 4 days. This is consistent with the finding from acute experiments that the blood flow had returned to normal by around 3 h. Antidromic vasodilatation was, however, significantly depressed until 4 days (Figure 7). Peak flow was 51 ± 3% of control at 4–9 h, 86 ± 11% at 1–2 days and 99 ± 14% at 4 days. Similarly, responses were of shorter duration with $t_{\frac{1}{2}}$ (the time for half recovery) at 64 ± 3% of vehicle at 4–9 h, 78 ± 7% at 1–2 days and 105 ± 7% at 4 days. Figure 7 uses a response 'area' measure (the product of peak [% baseline] times $t_{\frac{1}{2}}$) and this shows a highly significant time trend ($P < 0.01$, 1-way analysis of variance) from 4–9 h to 4 days.

Substance P levels 1–4 days after a single application of 33 mM capsaicin

Substance P levels were determined by RIA in samples taken 1–4 days after a 15 min treatment with 33 mM capsaicin in vehicle 3. Substance P levels were significantly reduced throughout this period. Levels in vehicle-treated contralateral legs averaged 5.4 pmol g^{-1} wet wt (± 0.4 pmol g^{-1}, $n = 14$). Levels in treated skin fell to 41% (± 8%, $n = 4$) of control

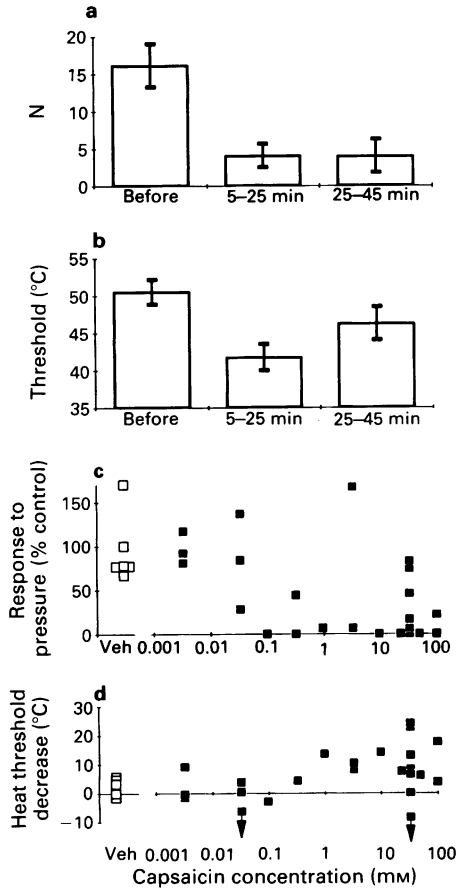

Figure 3 Average trends in (a,b) and dose-dependence of (c,d) alterations in C-polymodal nociceptors (C-PMN) afferent function after topical application of capsaicin in vehicle 3. (a,b) Average changes (± s.e., vertical bars) in number of spikes fired to a constant mechanical stimulus (a) and in heat threshold (b) over 5–25 and 25–45 min after treatment with 3–100 mM capsaicin. Data from 11 units. Mean numbers of spikes in (a) are significantly below control levels at both times after capsaicin application ($P<0.01$; Wilcoxon signed rank test), but values at the two times do not differ significantly. Heat thresholds (b) at 5–25 min are significantly less than control levels ($P=0.006$, t test) and levels at 25–45 min ($P=0.04$). Mean threshold at 25–45 min is not significantly different from control. (c,d) Effect of different concentrations on mechanically-evoked responses (c) and heat thresholds (d) 5–25 min after treatment.

values on day 1, to 50% (± 5%, $n=5$) on day 2 and to 51% (± 8%, $n=5$) on day 4.

Discussion

As has previously been reported, topical application of capsaicin to rat skin leads to excitation of afferents of the C-PMN class (Kenins, 1982) and to increases in skin blood flow (Jancso, 1968). In this study, vasodilatation was detectable with concentrations above 1 mM, and this was also the concentration above which excitation of C-PMNs was regularly seen. The C-fibre firing was low in frequency, with average rates typically in the range 0.1–0.3 Hz for 33 mM capsaicin. Vasodilatation, on the other hand, was large and 33 mM capsaicin caused increases averaging 171%. Note, however, that as has been described in other species (Celander & Folkow, 1953; Lynn & Shakhanbeh, 1988b), substantial vasodilatation has been found to occur in rat skin with low frequency stimulation of cutaneous nerves (Lynn & Cotsell, 1992b). For example, the dilatation during a 10 min, 0.2 Hz stimulation of the saphenous nerve averaged 218% above baseline in 4 rats (Lynn & Cotsell, unpublished data).

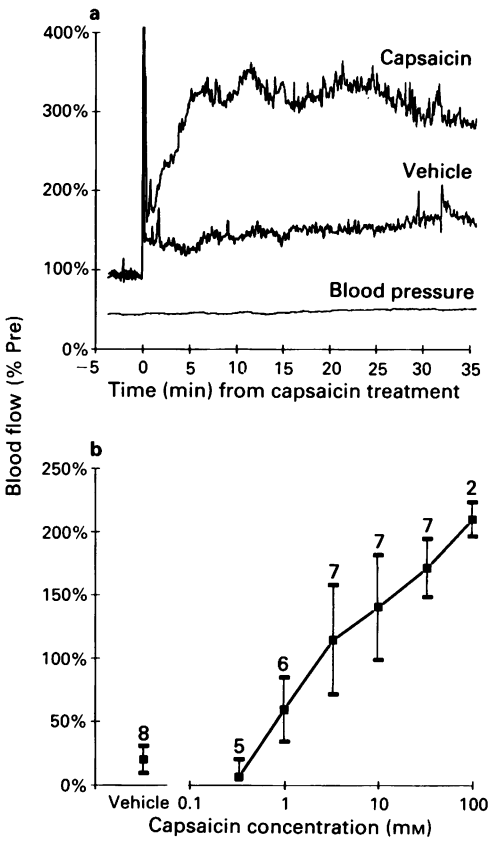

Figure 4 Skin blood flow after topical capsaicin application to the skin. (a) Laser Doppler flux expressed as % pre-application levels (upper trace); systolic blood pressure (lower trace; 100% = 200 mmHg). Application at time zero of 33 mM capsaicin in vehicle 3. Note lack of effect of vehicle 3 alone (a, middle trace), although a small shift in signal level was registered, probably an artefact due to small movement of probe. (b) Average increases in blood flow 15–60 min after topical application of different concentrations of capsaicin. Data from 5 rats tested at 3 to 6 sites on each leg. Increases expressed as % of baseline flow. Numbers of repeats are given next to each upper error bar. Blood flow with 1 mM capsaicin is just significantly above vehicle and 0.3 mM ($P=0.04$; Mann-Whitney test, 1-tailed); with >1 mM blood flow is always significantly above vehicle ($P<0.02$).

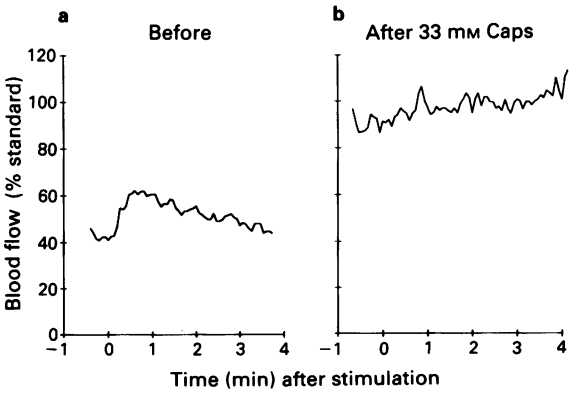

Figure 5 Antidromic vasodilatation before (a) and 15–60 min after (b) local capsaicin treatment (33 mM in vehicle 3). Antidromic vasodilation produced by stimulation of saphenous nerve at maximal C-fibre strength and with 10 shocks at 1 Hz. Average of 3 trials.

Thus our examination of C-PMN firing and vasodilatation after topical capsaicin and of antidromic vasodilatation under the same conditions, fits well with the widely accepted

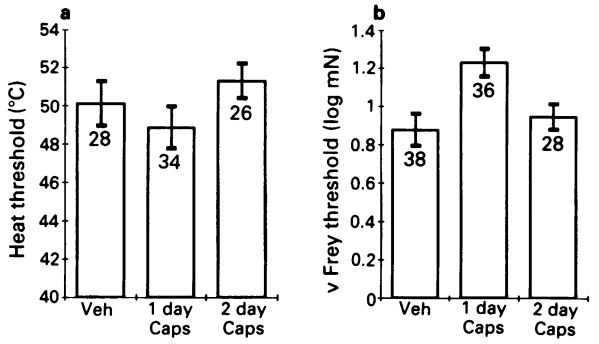

Figure 6 Firing thresholds (± s.e., vertical bars) of C-polymodal nociceptor (C-PMN) units 1–2 days after topical 33 mM capsaicin (Caps) treatment. Numbers of units given next to error bars. (a) Heat thresholds for 1°C s^{-1} ramp stimulus. No significant differences between groups. (b) Pressure thresholds for von Frey bristles. Note logarithmic force scale. Thresholds at 1 day are significantly greater than vehicle or 2 days ($P<0.01$, Newman-Keuls test); there is no significant difference between thresholds at 2 days and those with vehicle (Veh).

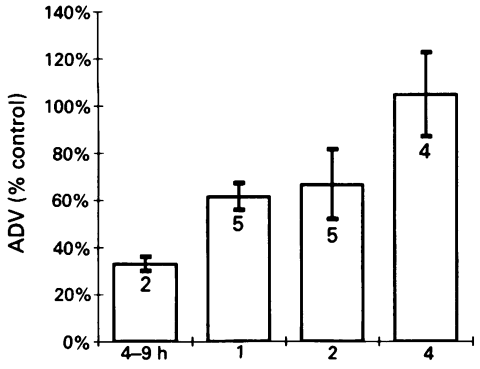

Figure 7 Antidromic vasodilatation response up to 4 days after topical treatment with 33 mM capsaicin. In each preparation 12–18 sites were measured by laser-Doppler flowmetry on each leg. One leg was vehicle-treated, the other capsaicin-treated. The ratios of the average antidromic vasodilatation (ADV) (capsaicin side/vehicle side) for each preparation were in turn averaged over the 2–5 preparations studied at each time interval. Antidromic vasodilatation measure was response 'area' defined as the product of peak flow (% baseline) and time for 50% recovery ($t_{\frac{1}{2}}$, min). Reduction compared with contralateral control was significant at 4–9 h, 1 day and 2 days (t tests, 1-tailed, $P<0.05$); there was no significant difference in the reductions at these times, but analysis of variance showed a significant 'linear' time trend from 4–9 h to 4 days ($P=0.03$).

view that capsaicin-induced vasodilatation results from the release of vasodilator peptides from C-PMN afferent terminals in response to their excitation by capsaicin (e.g. see Holzer, 1988; 1991).

Following the initial excitation of C-PMN units by capsaicin in 50% DMSO/ethanol there was a loss of sensitivity to mechanical and heat stimuli, as reported by Kenins (1982). With vehicle 3 (containing ethanol, propylene glycol and methyl laurate, but not DMSO) there was a dose-dependent reduction in mechanical sensitivity with effects reliably observed for concentrations above 0.1 mM. However, with vehicle 3, C-PMNs usually showed enhanced heat sensitivity. The more marked depressant effects of capsaicin in DMSO, along with the greater initial firing, may be because drug penetration through the skin is more rapid in this vehicle (Scheuplein & Bronaugh, 1983). In primates, capsaicin in DMSO has been found to cause heat sensitization of C-PMNs along with little change in mechanical thresholds (Baumann *et al.*, 1991). In man over the first 24 h of topical capsaicin treatment of the skin, heat pain thresholds fall and skin heating becomes more painful (Carpenter & Lynn, 1981; Simone & Ochoa, 1991). In rats treated repeatedly with capsaicin cream, withdrawal latencies for noxious heating became shorter (McMahon *et al.*, 1991). Thus it appears that capsaicin has a widespread ability to potentiate the transducer mechanism underlying heat sensitivity, while not affecting, or even depressing, the operation of the transduction mechanism for pressure.

Afferent and efferent functions of C-fibres recovered at slightly different rates following a single treatment with 33 mM capsaicin. Afferent functions recovered first, with C-PMN heat sensitivity at normal levels on day 1 and mechanical thresholds showing full recovery by 48 h. There was also no increase at any time after topical capsaicin treatment in the proportion of C-fibres that had no cutaneous receptive fields. In this respect, skin treatment differs markedly from the effects of applying similar concentrations of capsaicin to the saphenous nerve itself when a large fall in the proportion of C-PMNs that can be excited from the skin and a corresponding increase in inexcitable C-fibres occurs (Pini & Lynn, 1991). Antidromic vasodilatation recovered more slowly than afferent sensitivity, remaining depressed at 2 days but showed complete recovery at 4 days. Other experiments with topical capsaicin have shown marked reductions in neuro-inflammatory reactions. For example, after repeated application of capsaicin, flare is absent or reduced in human skin (Carpenter & Lynn, 1981; Simone & Ochoa, 1991) and neurogenic plasma extravasation is reduced in the rat (McMahon *et al.*, 1991). This difference in rate of recovery between afferent C-PMN function and antidromic vasodilatation could be because the mechanisms involved in release of vasoactive agents from C-PMN terminals are affected more severely by capsaicin than those involved in sensory transduction. On the other hand, it may reflect the possibility that classes of C-fibre other than PMNs are involved in antidromic vasodilatation and other neurogenic inflammatory responses. For example it has been suggested that the lack of significant mechanically-evoked vasodilatation in normal rat skin indicates that most C-PMNs cannot cause antidromic vasodilatation (Lynn & Cotsell, 1992b). It has also been suggested that a special population of chemo-sensitive C-fibres trigger secondary hyperalgesia (LaMotte *et al.*, 1991). Note however, that if a special population of non-PMN C-fibres is involved in generating antidromic vasodilatation, then these would have to show the same sensitivity to capsaicin as do C-PMNs.

One possible mediator, the release of which might cause vasodilatation, is substance P (Lembeck & Holzer, 1979) and this peptide is known to be present in many afferent C-fibres (McCarthy & Lawson, 1989). Levels of substance P in skin showed little sign of recovery, even 4 days after topical 33 mM capsaicin. A similar situation of normal antidromic vasodilatation when substance P levels are still depressed occurs 2 weeks after intradermal injection of capsaicin into rat skin (Lynn, 1992). A lack of substance P might well reduce efferent functions of C-fibres more than afferent ones. Certainly, whatever the exact nature of the C-fibres that are involved in antidromic vasodilatation, our results show that afferent and efferent functions of C-fibres can be normal when, as at 4 days after topical capsaicin, total levels of substance P are only just over half of normal.

The ability of topical capsaicin concentrations of 0.1–1 mM to cause significant effects on C-PMN function is of particular interest in view of the finding that treatment of patients with low concentration (0.025%, approx 0.8 mM) capsaicin creams can give significant pain relief (Bernstein *et al.*, 1989). In the clinical situation, repeated application appears to be needed to achieve useful pain relief. The long duration of densensitization following topical capsaicin, at least after single applications at 33 mM, would in principle allow the effects of daily treatments to summate.

This work was supported in part by a contract from The Proctor & Gamble Company and a grant from the Wellcome Trust. We wish to thank Dr J. Foreman for the substance P antibody.

References

BACCAGLINI, P.I. & HOGAN, P.G. (1983). Some rat sensory neurons in culture express characteristics of differentiated pain sensory cells. *Proc. Natl. Acad. Sci. U.S.A.*, **80,** 594–598.

BAUMANN, T.K., SIMONE, D.A., SHAIN, C.H. & LAMOTTE, R.H. (1991). Neurogenic hyperalgesia: the search for the primary cutaneous afferent fibers that contribute to capsaicin-induced pain and hyperalgesia. *J. Neurophysiol.*, **66,** 212–227.

BERNSTEIN, J.E., KORMAN, N.J., BICKERS, D.R., DAHL, M.V. & LAWRENCE, L.E. (1989). Topical capsaicin treatment of chronic postherpetic neuralgia. *J. Am. Acad. Dermatol.*, **21,** 265–270.

BERNSTEIN, J.E., SWIFT, R.M., SOLTANI, K. & LORINCZ, A.L. (1981). Inhibition of axon reflex vasodilatation by topically applied capsaicin. *J. Invest. Dermatol.*, **76,** 394–395.

BEVAN, S. & SZOLCSANYI, J. (1990). Sensory neuron-specific actions of capsaicin: mechanisms and applications. *Trends Pharmacol. Sci.*, **11,** 330–333.

CARPENTER, S.E. & LYNN, B. (1981). Vascular and sensory responses of human skin to mild injury after topical treatment with capsaicin. *Br. J. Pharmacol.*, **73,** 755–758.

CARTER, R.B. & FRANCIS, W.R. (1991). Capsaicin desensitization to plasma extravasation evoked by antidromic C-fibre stimulation is not associated with antinociception in the rat. *Neurosci. Lett.*, **127,** 49–52.

CELANDER, O. & FOLKOW, B. (1953). The correlation between the stimulation frequency and the dilator response evoked by 'antidromic' excitation of the thin afferent fibres in the dorsal roots. *Acta Physiol. Scand.*, **29,** 371–376.

HOLZER, P. (1988). Local effector functions of capsaicin-sensitive sensory nerve endings: involvement of tachykinins, calcitonin gene-related peptide and other neuropeptides. *Neuroscience*, **24,** 739–768.

HOLZER, P. (1991). Capsaicin: cellular targets, mechanisms of action, and selectivity for thin sensory neurones. *Pharmacol. Rev.*, **43,** 143–201.

JANSCO, N. (1968). Desensitization with capsaicin and related acylamides as a tool for studying the function of pain receptors. In *Pharmacology of Pain.* ed. Lim, R.K.S., Armstrong, D. & Pardo, E.G. pp. 35–55. Oxford: Pergamon.

JANIG, W. & LISNEY, S.J.W. (1989). Small diameter myelinated afferents produce vasodilatation but not plasma extravasation in rat skin. *J. Physiol.*, **415,** 477–486.

KENINS, P. (1982). Responses of single nerve fibres to capsaicin applied to the skin. *Neurosci. Letts.*, **29,** 83–88.

KOLTZENBERG, M., KRESS, M., REEH, P.W. & HANDWERKER, H.O. (1991). Mechanically insensitive unmyelinated afferents supplying the hairy skin of the rat in vitro. *J. Physiol.*, **438,** 164P.

KONIETZNY, F. & HENSEL, H. (1983). The effect of capsaicin on the response characteristics of human C-polymodal nociceptors. *J. Thermal. Biol.*, **8,** 213–215.

LAMOTTE, R.H., SHAIN, C.N., SIMONE, D.A. & TSAI, E.-F.P. (1991). Neurogenic hyperalgesia: psychophysical studies of underlying mechanisms. *J. Neurophysiol.*, **66,** 190–211.

LEMBECK, F. & HOLZER, P. (1979). Substance P as neurogenic mediator of antidromic vasodilatation and neurogenic plasma extravasation. *Naunyn-Schmiedebergs Arch. Pharmacol.*, **310,** 175–183.

LYNN, B. (1988). Neurogenic inflammation. *Skin Pharmacol.*, **1,** 217–224.

LYNN, B. (1992). Capsaicin: actions on C fibre afferents that may be involved in itch. *Skin Pharmacol.*, **5,** 9–13.

LYNN, B. & CARPENTER, S.E. (1982). Primary afferent units from the hairy skin of the rat hind limb. *Brain. Res.*, **238,** 29–43.

LYNN, B. & COTSELL, B. (1992a). Action of topical capsaicin on blood flow and C-fibre nociceptors in the skin of anaesthetized rats. *Br. J. Pharmacol.*, **105,** 131P.

LYNN, B. & COTSELL, B. (1992b). Blood flow increases in the skin of the anaesthetized rat that follow antidromic sensory nerve stimulation and strong mechanical stimulation. *Neurosci. Lett.*, **137,** 249–252.

LYNN, B. & SHAKHANBEH, J. (1988a). Substance P content of the skin, neurogenic inflammation and numbers of C-fibres following capsaicin application to a cutaneous nerve in the rabbit. *Neuroscience*, **24,** 769–775.

LYNN, B. & SHAKHANBEH, J. (1988b). Neurogenic inflammation in the rabbit. *Agents & Actions*, **25,** 228–230.

LYNN, B., YE, W. & COTSELL, B. (1991). The effect of topical capsaicin on the sensitivity to mechanical and heat stimulation of C-polymodal nociceptors in the skin of the anaesthetized rat. *J. Physiol.*, **438,** 164P.

MCCARTHY, P.W. & LAWSON, S.N. (1989). Cell type and conduction velocity of rat primary sensory neurons with substance P-like immunoreactivity. *Neuroscience*, **28,** 745–753.

MCMAHON, S.B., LEWIN, G. & BLOOM, S.R. (1991). The consequences of long-term topical capsaicin application in the rat. *Pain*, **44,** 301–310.

PINI, A. & LYNN, B. (1991). C-fibre function during the 6 weeks following brief application of capsaicin to a cutaneous nerve in the rat. *Eur. J. Neurosci.*, **3,** 274–284.

PINI, A., BARANOWSKI, R. & LYNN, B. (1990). Long-term reduction in the number of C-fibre nociceptors following capsaicin treatment of a cutaneous nerve in adult rats. *Eur. J. Neurosci.*, **2,** 89–97.

SCHEUPLEIN, R.J. & BRONAUGH, R.L. (1983). Percutaneous absorption. In *Biochemistry and Physiology of the Skin*, 1st edn. ed. Goldsmith, L.A. pp. 1255–1295. New York: O.U.P.

SIMONE, D.A. & OCHOA, J. (1991). Early and late effects of prolonged topical capsaicin on cutaneous sensibility and neurogenic vasodilatation in humans. *Pain*, **47,** 285–294.

SZOLCSANYI, J. (1987). Selective responsiveness of polymodal nociceptors of the rabbit ear to capsaicin, bradykinin and ultraviolet radiation. *J. Physiol.*, **388,** 9–23.

WOOD, J.N., WINTER, J., JAMES, I.F., RANG, H.P., YEATS, J. & BEVAN, S. (1988). Capsaicin-induced ion fluxes in dorsal root ganglion cells in culture. *J. Neuroscience*, **8,** 3207–3220.

(Received March 5, 1992
Revised May 6, 1992
Accepted June 2, 1992)

Br. J. Pharmacol. (1992), **107**, 407–413

Reduced relaxant potency of nitroprusside on pulmonary artery preparations taken from rats during the development of hypoxic pulmonary hypertension

[1]Janet C. Wanstall, [2]Ian E. Hughes & Stella R. O'Donnell

Pulmonary Pharmacology Group, Department of Physiology and Pharmacology, The University of Queensland, Brisbane, Queensland 4072, Australia

1 Relaxant responses to nitroprusside were examined on U46619-contracted pulmonary artery ring preparations from rats exposed to hypoxia, in chambers containing 10% oxygen, for 1, 3, or 14 days, or for 14 days followed by 12 days in room air. Control rats were housed in room air.

2 After 3 days of hypoxia (but not 1 day), rats had elevated pulmonary artery pressure, right ventricular hypertrophy and polycythemia. After 14 days of hypoxia there was, in addition, hypertrophy of the pulmonary artery. In rats returned to room air for 12 days after 14 days of hypoxia, there was still some right ventricular and vascular hypertrophy but no increase in pulmonary artery pressure or polycythemia.

3 The potency (neg log EC_{50}) of nitroprusside on pulmonary arteries taken from rats after 3 or 14 days of hypoxia was significantly less than on preparations from control rats (3 and 11 fold, respectively). This was not seen after 1 day of hypoxia or after 14 days of hypoxia followed by 12 days in room air. Removal of the endothelium from the preparations had no effect on the potency of nitroprusside in control or hypoxic rats (14 days).

4 In preparations from hypoxic, but not control, rats (14 days), the maximum response to nitroprusside was $>100\%$ (177% reversal of the U46619 contraction) in the absence, but not in the presence, of the endothelium, indicating that pulmonary arteries from hypoxic rats had inherent tone which could be counteracted by a relaxing factor from the endothelium.

5 Exposure of rats to hypoxia (14 days) did not affect the potency of nitroprusside on aorta or trachea.

6 It is concluded that exposure of rats to hypoxia results in reversible desensitization of the vascular smooth muscle of pulmonary artery to nitroprusside. The time course of this desensitization suggests that it is probably associated with the elevated pulmonary artery pressure or maintained hypoxaemia rather than with the vascular hypertrophy.

7 It is postulated that the increase in pulmonary artery pressure and/or the maintained hypoxaemia may cause chronic release of nitric oxide from the pulmonary vascular endothelium or smooth muscle resulting in desensitization of soluble guanylate cyclase to the action of nitroprusside.

Keywords: Hypoxia; pulmonary hypertension; nitroprusside; rat pulmonary artery; endothelium

Introduction

Exposure of rats to chronic hypoxia leads to the development of pulmonary hypertension (Herget *et al.*, 1978; Reid, 1979; Kay, 1980) and to changes in the reactivity of pulmonary blood vessels to various vasoactive agents (Emery *et al.*, 1981; Lowen *et al.*, 1987; Barer *et al.*, 1989; Wanstall & O'Donnell, 1992). One particular change in reactivity is a 5–10 fold reduction in the potency of the vasodilator drug, nitroprusside. This was seen on pulmonary arteries taken from rats exposed to hypoxia for 14 days (Wanstall & O'Donnell, 1992). In these rats, the characteristic pathophysiological features of hypoxic pulmonary hypertension were already well developed (Wanstall & O'Donnell, 1992). Hence it was not known whether the loss of vascular reactivity to nitroprusside coincided with the rise in pulmonary artery pressure, the onset of vascular hypertrophy and/or the maintained arterial hypoxaemia.

The aim of the present study was to compare the time course of the decline in pulmonary vascular reactivity to nitroprusside with that of the appearance of the various pathophysiological features of hypoxic pulmonary hypertension by studying rats exposed to hypoxia for different periods of time. We have also investigated whether the reactivity of pulmonary arteries to nitroprusside reverted to normal if, after exposure to hypoxic conditions, rats were allowed to recover (for 12 days) in room air.

To obtain information on the mechanism(s) underlying the reduction in the potency of nitroprusside, we have investigated whether the exposure of rats to hypoxia affected (1) the responses of pulmonary artery to the spasmogen used to contract the preparations, (2) the influence, if any, of the endothelium on responses to nitroprusside, and (3) the sensitivity of smooth muscle in other tissues to nitroprusside. The thromboxane analogue, U46619, was selected as the contractile spasmogen (in contrast to noradrenaline used in our previous study, Wanstall & O'Donnell, 1992), and data have been obtained on pulmonary artery preparations with and without endothelium, and on tissues other than pulmonary artery, *viz.* a non-pulmonary blood vessel, aorta, and non-vascular tissue from the airways, trachea.

A preliminary account of some of these data was presented to a meeting of the Australasian Society of Clinical and Experimental Pharmacologists (Wanstall *et al.*, 1990).

[1] Author for correspondence.
[2] On study leave from The Department of Pharmacology, University of Leeds, U.K.

Methods

Exposure of rats to hypoxia

Male Wistar rats were exposed to chronic hypoxia for 1, 3 and 14 days in chambers containing 10–11% oxygen (Wanstall & O'Donnell, 1992). Control rats were housed in room air (21% oxygen) for the same periods of time. An additional group of rats was exposed to hypoxia for 14 days and subsequently allowed to recover in room air for 12 days. All rats were the same age (8–9 weeks old) at the completion of the period of exposure to hypoxia.

The hypoxic chamber was continuously flushed with a mixture of nitrogen and compressed air, at a flow rate of 1.7 l min^{-1}. The ratio of nitrogen to air was adjusted so that the oxygen component of the gas in the chamber was 10–11% (measured with a Datex Normocap Gas Monitor). Trays of soda lime were included in the chamber to maintain the CO_2 content below 0.5%. The rats were removed from the chamber for a maximum of 15 min each day, when the chamber was cleaned and food and drinking water were replenished.

On the day of the experiment, the rats were anaesthetized with pentobarbitone (90 mg kg^{-1}, i.p.), were artifically ventilated via a tracheal cannula (60 breaths min^{-1}), and the pulmonary artery pressure (PAP) was recorded via a hypodermic needle inserted into the pulmonary artery through the right ventricle (Wanstall & O'Donnell, 1990). Mean PAP was calculated as diastolic PAP + 1/3 [systolic – diastolic PAP]. A blood sample was removed for measurement of the haematocrit. After removal of the pulmonary artery (and, in some experiments, the aorta and trachea) the heart and lungs were removed and weighed for the determination of the ratio of the weight of right ventricle to the weight of left ventricle plus septum (RV/LV + S), and the ratio of lung wet to dry weight, as described previously (Wanstall & O'Donnell, 1990). Increases in PAP, RV/LV + S, haematocrit and lung wet/dry weight were taken as indications of pulmonary hypertension, right ventricular hypertrophy, polycythemia and lung oedema respectively.

Blood vessel preparations

Single ring preparations (3 mm in length) of main pulmonary artery and ventral aorta were set up in physiological salt solution (PSS), at 37°C, around 2 stainless steel wires in a vertical organ bath. In one series of experiments on pulmonary artery, the endothelium was removed by gently rubbing the luminal surface of the preparations with small forceps. In the remaining preparations care was taken not to damage the endothelium. Force in the circular muscle was recorded isometrically with a Statham Universal Transducer (UC3 + UCL) attached to a micrometer (Mitutoyo, Tokyo, Japan), as described previously (Wanstall & O'Donnell, 1988). The composition of the PSS was (mM): NaCl 118, KCl 5.9, $CaCl_2$ 1.5, $MgSO_4$ 0.72, $NaHCO_3$ 25, glucose 11.7, ascorbic acid 1.14 (95% O_2/5% CO_2; pH 7.4).

Pulmonary artery preparations were set up under resting forces of 10 mN (control) or 20 mN (hypoxic), and aortic preparations (control and hypoxic) under a resting force of 65 mN. These resting forces were selected in order to reflect the circumferential wall tensions corresponding to the different pressures in these arteries *in vivo*, and were determined, in separate experiments, from passive length/tension studies and the Laplace equation, as described in detail elsewhere (Wanstall & O'Donnell, 1990).

At the completion of the experiment, the distance between the 2 horizontal wires (with the preparation under the selected resting force, see above) was measured with the micrometer holding the transducer, and the wet weight of the preparation was determined. The cross sectional area of the preparation, in the plane perpendicular to the direction of the applied force, was then calculated as described by Wanstall & O'Donnell (1988), from the formula: cross-sectional area = w $(hd)^{-1}$ where h = distance between the wires plus the diameters of the wires (mm), w = wet weight (mg) and d = density = 1.06 mg mm^{-3}. Since all the preparations were the same length (3 mm, see above), differences in cross-sectional area between vessels reflected differences in vessel wall thickness. Thus an increase in cross-sectional area indicated the development of vascular hypertrophy.

Tracheal preparations

Segments of trachea, 4 cartilage rings wide, were taken from the bronchial end of the trachea and set up, with the cartilage cut, in PSS under a resting force of 10 mN. Changes in force in the smooth muscle were measured isometrically.

Experimental protocols

Blood vessel preparations were allowed to equilibrate for 1 h. They were then contracted with 0.1 μM noradrenaline and, when the contraction was stable, acetylcholine (ACh 1 μM) was added. A relaxant response to ACh indicated the presence of a functional endothelium. After washing with PSS, a contraction to potassium-depolarizing PSS (in which 80 mM NaCl was replaced with 80 mM KCl) was obtained. The preparations were then washed, allowed to relax and a cumulative concentration-response (contraction) curve to U46619 was then determined. The preparations were again washed and allowed to relax. They were then submaximally contracted with 10 nM U46619 (approximate EC_{70} on pulmonary artery and EC_{90} on aorta), and a cumulative concentration-response (relaxation) curve to nitroprusside was determined.

Tracheal preparations were allowed to equilibrate for 1 h and were then contracted with 10 μM carbachol. This was followed, after washout with PSS, by a contraction to potassium-depolarizing PSS. The preparations were then washed, allowed to relax, and a cumulative concentration-response (contraction) curve to carbachol was obtained. After wash-out, the preparations were submaximally contracted with 1 μM carbachol (EC_{70-80}) and a cumulative concentration-response (relaxation) curve to nitroprusside was determined.

Analysis of data

Contractile responses to U46619 on pulmonary artery and aorta were determined as force (mN) and expressed as stress (mN mm^{-2}) by dividing by the cross-sectional area of the preparations. Contractile responses to carbachol on trachea were expressed as force (mN). Relaxant responses to nitroprusside were expressed as 'percentage reversal' of the contraction induced by either 10 nM U46619 (pulmonary artery and aorta) or 1 μM carbachol (trachea). The potency of U46619 and nitroprusside was expressed as the negative log EC_{50} (where EC_{50} is the concentration producing 50% of the maximum contraction or relaxation to U46619 or nitroprusside, respectively).

Preliminary experiments

The pulmonary artery preparations from control (normotensive) and hypoxic (pulmonary hypertensive) rats were set up at different resting forces, in order to try to mimic *in vivo* wall tensions (see above). Thus concentration-response curves to nitroprusside were also obtained on preparations from control rats set up at a resting force of 20 mN, i.e. the resting force used in experiments on pulmonary arteries from hypoxic rats. These curves, in which the nitroprusside negative log EC_{50} was 8.00 ± 0.07 and maximum relaxation was 96 ± 1.1% ($n = 4$), were superimposable on curves obtained on control preparations set at a resting force of 10 mN (control values in Table 3). Thus the use of a higher resting force for the preparations from hypoxic rats, compared with

control rats, was not responsible for the differences in reactivity to nitroprusside reported in the Results section for the different groups of rats.

Drugs and solutions

Acetylcholine chloride (ACh, Sigma); carbamylcholine (carbachol, Sigma); (−)-noradrenaline acid tartrate (Sigma); sodium nitroprusside (Sigma); U46619 ((1,5,5)-hydroxy-11α, 9α-(epoxymethano) prosta 5Z, 13E-dienoic acid; Upjohn).

Solutions of drugs were prepared as follows: ACh (1 mM), carbachol (10 mM) and nitroprusside (10 mM) in deionised water; noradrenaline (10 mM) in 10 mM HCl; U46619 (10 mM) in absolute ethanol. Dilutions were made in PSS and kept on ice during the course of an experiment.

Statistical analyses

Mean values are quoted together with their standard errors (s.e.mean). The significance of differences between mean values has been assessed by Student's *t* test, except for percentage values, which were assessed by Mann Whitney U-test.

Results

Effects of hypoxia on the rats

All control rats housed in room air gained weight. Rats exposed to hypoxia for 1 or 3 days lost weight. Rats exposed to hypoxia for 14 days gained weight but this gain was significantly less than that in the corresponding control rats (Table 1).

After 3 days exposure to hypoxia (but not 1 day) rats had significantly elevated pulmonary artery pressures, right ventricular hypertrophy and polycythemia (Table 1). When the time of exposure to hypoxia was increased to 14 days, these changes were more pronounced and there was, in addition, pulmonary vascular hypertrophy (Table 1). In rats exposed to hypoxia for 14 days and then allowed to recover in room air for 12 days, pulmonary artery pressure was not significantly different from controls and there was no polycythemia, but there was still significant right ventricular and pulmonary vascular hypertrophy (Table 1).

There was no lung oedema in the hypoxic rats (Table 1), and all the pulmonary artery preparations relaxed equally well in response to ACh (33–49% reversal of a noradrenaline-induced contraction), indicating the presence of a functional pulmonary vascular endothelium in all rats irrespective of treatment.

Effects of exposure of rats to hypoxia on responses of isolated tissue preparations

The potency of U44619 in contracting pulmonary arteries was the same on preparations from control and hypoxic rats (Table 2). The magnitude of the submaximal contraction to 10 nM U46619 was also the same on all preparations, with one exception, *viz.* on endothelium-denuded preparations taken from rats exposed to hypoxia for 14 days this contraction was significantly less than in the corresponding controls (Table 2).

The potency of nitroprusside, when compared with controls, was significantly less on pulmonary arteries taken from rats exposed to 3 or 14 days of hypoxia (3 and 11 fold less potent, respectively), but not on those from rats exposed to only 1 day of hypoxia (Table 3; Figure 1). The decrease in the potency of nitroprusside was apparently reversible in that it was not seen on preparations from rats allowed to recover in room air for 12 days after exposure to 14 days of hypoxia (Table 3; Figure 1). The reduction in potency associated with 14 days of hypoxia was also seen in preparations without endothelium, since removal of the endothelium did not affect the potency of nitroprusside in preparations from either the control or the hypoxic rats (Table 3). However in the endothelium-denuded preparations from the hypoxic rats, in contrast to matching preparations from control rats, there was greater than 100% reversal of the U46619-induced contractions (Figure 2). This was not seen in any of the other groups of rats studied (Table 3).

In contrast to the findings on pulmonary artery, there was no change in the potency or maximum relaxation to nitroprusside on preparations of aorta or trachea taken from the rats exposed to hypoxia for 14 days (Table 4; Figure 3). It was noted that both the potency and maximum relaxation to nitroprusside on trachea were less than on the vascular preparations (Table 4).

Discussion

In the present study, nitroprusside was less potent in relaxing isolated preparations of pulmonary artery from rats made pulmonary hypertensive by exposure to hypoxia for 14 days, than in preparations from control rats, i.e. the tissues were desensitized to nitroprusside. The preparations were contracted with the thromboxane analogue, U46619, and the data confirmed a previous finding on preparations contracted with noradrenaline (Wanstall & O'Donnell, 1992). Thus the influence of hypoxic pulmonary hypertension on pulmonary vascular reactivity to nitroprusside is not restricted to vessels contracted by noradrenaline. Furthermore the desensitization

Table 1 Effects of exposure of rats to 10% oxygen (hypoxia) or room air (control) for different periods of time

	1 day		*3 days*		*14 days*		*14 days plus 12 days recovery*	
	Control ($n=4$)	*Hypoxia* ($n=4$)	*Control* ($n=4$)	*Hypoxia* ($n=4$)	*Control* ($n=9$)	*Hypoxia* ($n=8$)	*Control* ($n=4$)	*Hypoxia* ($n=4$)
Initial weight (g)	287 ± 10	292 ± 7	229 ± 7	240 ± 10	198 ± 10	194 ± 13	183 ± 13	186 ± 14
Change in weight (g)[a]	1 ± 1	−35 ± 3***	28 ± 3	−26 ± 1***	96 ± 13	33 ± 5***	184 ± 9	135 ± 7**
Mean PAP (mmHg)	13 ± 1	14 ± 2	10 ± 2	19 ± 2*	13 ± 2	26 ± 2***	14 ± 2	18 ± 2
RV/(LV + S)[b]	0.34 ± 0.01	0.37 ± 0.01	0.33 ± 0.01	0.42 ± 0.01**	0.34 ± 0.01	0.64 ± 0.05***	0.34 ± 0.01	0.45 ± 0.02**
Haematocrit (%)	44 ± 1	47 ± 2	43 ± 1	52 ± 3*	43 ± 1	57 ± 2***	45 ± 1	44 ± 1
Lung wet/dry weight	4.56 ± 0.07	4.56 ± 0.03	4.77 ± 0.04	4.92 ± 0.05	4.69 ± 0.04	4.68 ± 0.04	4.47 ± 0.03	4.65 ± 0.03
Cross-sectional area of pulmonary artery preparations (mm^2)[c]	0.71 ± 0.04	0.60 ± 0.06	0.67 ± 0.06	0.69 ± 0.04	0.66 ± 0.03	1.13 ± 0.07***	0.65 ± 0.04	0.88 ± 0.08*

Values are means ± s.e.mean

[a]Positive values indicate weight gain and negative values indicate weight loss during period of exposure to hypoxia or room air. [b]Weight of right ventricle ÷ weight of left ventricle plus septum. [c]For definition see Methods.

*Value significantly different from corresponding control value: *$0.05 > P > 0.01$; **$0.01 > P > 0.001$; ***$P < 0.001$ (Student's *t* test).

Table 2 U46619: potency (negative log EC_{50}) and submaximal contraction (to 10 nM) on pulmonary artery preparations from rats exposed to 10% O_2 (hypoxia) or room air (control) for different times

	Neg log EC_{50}		*10 nM contraction*[a] (mN mm^{-2})	
Time of exposure	*Control*	*Hypoxia*	*Control*	*Hypoxia*
1 day	8.35 ± 0.08 (4)	8.46 ± 0.05 (4)	24.2 ± 2.9 (4)	33.9 ± 4.5 (4)
3 days	8.32 ± 0.10 (4)	8.65 ± 0.11 (4)	25.2 ± 1.6 (4)	31.2 ± 4.2 (4)
14 days	8.26 ± 0.06 (5)	8.32 ± 0.08 (4)	19.5 ± 1.5 (5)	16.4 ± 3.0 (4)
14 days (+ 12 days recovery in room air)	8.26 ± 0.04 (4)	8.36 ± 0.10 (4)	24.4 ± 3.4 (4)	23.7 ± 4.3 (4)
14 days (preparations without endothelium)	8.38 ± 0.03 (4)	8.46 ± 0.14 (4)	22.1 ± 3.1 (4)	8.2 ± 1.0** (4)

Values are mean ± s.e.mean (numbers of preparations from different rats in parentheses). [a]Submaximal contractions to U44169 (10 nM) used for nitroprusside concentration-response (relaxation) curves.
**Value significantly lower than control value $0.01 > P > 0.001$. (Student's t test).

Table 3 Nitroprusside: potency (negative log EC_{50}) and maximum relaxation on pulmonary artery preparations from rats exposed to 10% O_2 (hypoxia) or room air (control) for different times

	Neg log EC_{50}		*Max relaxation (%)*[a]	
Time of exposure	*Control*	*Hypoxia*	*Control*	*Hypoxia*
1 day	7.98 ± 0.12 (4)	7.99 ± 0.09 (4)	104 ± 1 (4)	98 ± 1 (4)
3 days	8.12 ± 0.06 (4)	7.65 ± 0.12* (4)	104 ± 3 (4)	89 ± 3 (4)
14 days	8.03 ± 0.08 (5)	7.00 ± 0.14*** (4)	99 ± 1 (5)	86 ± 10 (4)
14 days (+ 12 days recovery in room air)	8.22 ± 0.15 (4)	7.92 ± 0.09 (4)	101 ± 1 (4)	101 ± 5 (4)
14 days (preparations without endothelium)	8.22 ± 0.08 (4)	7.02 ± 0.04*** (4)	104 ± 1 (4)	177 ± 12† (4)

Values are mean ± s.e.mean (numbers of preparations from different rats in parentheses) [a]Maximum relaxation expressed as a percentage of the U44619 (10 nM)-induced contraction. *Value significantly lower than corresponding control value: $*0.05 > P > 0.01$; $***P < 0.001$ (Student's t test).
†Value significantly greater than corresponding control value: $P < 0.05$ (Mann Whitney U test).

to nitroprusside in rats exposed to hypoxia was not a non-specific effect on either blood vessels or lung tissues in general, since the potency of nitroprusside on preparations of aorta and trachea from the same animals was not affected. The desensitization was not the indirect result of an effect of the hypoxic treatment on responses to the spasmogen, since the potency of U46619 and the magnitude of the contraction to 10 nM U46619 (the concentration used in the nitroprusside experiments) were unchanged.

The reduction in the potency of nitroprusside on pulmonary arteries was not an acute response to hypoxia since it was not apparent after the first 24 h of exposure. However, it was seen in preparations from rats after 3 days of hypoxia and appeared to be progressive, in that the potency of the drug was even less after an exposure time of 14 days. The potency was not reduced in preparations taken from rats that were returned to room air for 12 days after 14 days exposure to hypoxia, indicating that the desensitization to nitroprusside was completely reversible.

The time-course for the desensitization to nitroprusside was compared with that for the various pathophysiological changes associated with hypoxic pulmonary hypertension in an attempt to determine which of these changes might account for the desensitization. Desensitization appeared to parallel the increase in pulmonary artery pressure and the development of polycythemia, in that each of these three changes occurred in rats exposed to hypoxia for 3 or 14 days, but not in the hypoxic rats that had been returned to room air for 12 days. In contrast, desensitization to nitroprusside did not coincide with vascular hypertrophy; vascular hypertrophy was seen after 14, but not after 3 days, of hypoxia, and persisted up to 12 days after hypoxic rats had been returned to room air. These observations suggest that the desensitization to nitroprusside may result either from the elevated pulmonary artery pressure (although not from the vascular hypertrophy arising from this) or from the maintained hypoxaemia (which gives rise to the polycythemia). Further experiments over a wider range of exposure and recovery times will be required to substantiate this suggestion.

The results of the present study showed that pulmonary artery pressure reverted to normal if rats exposed to hypoxia for 14 days were returned to room air for 12 days (see above). This was in contrast to findings in rats exposed to hypoxia for 3–4 weeks, where pulmonary artery pressure was still elevated even after 6 weeks in room air (Herget *et al.*, 1978; Kay, 1980). The recovery period in room air required for reversal of the increase in pulmonary artery pressure may therefore depend on the duration of the initial hypoxic exposure. The same may apply to the desensitization to nitroprusside, if, as postulated above, desensitization is associated with the increase in pulmonary artery pressure. We have not yet explored this possibility.

In seeking to provide an explanation for the reduction in the potency of nitroprusside on pulmonary arteries from hypoxic rats, the possible role of the endothelium was investigated. Although nitroprusside is not an endothelium-dependent vasodilator (Shirasaki & Su, 1985), there is evidence

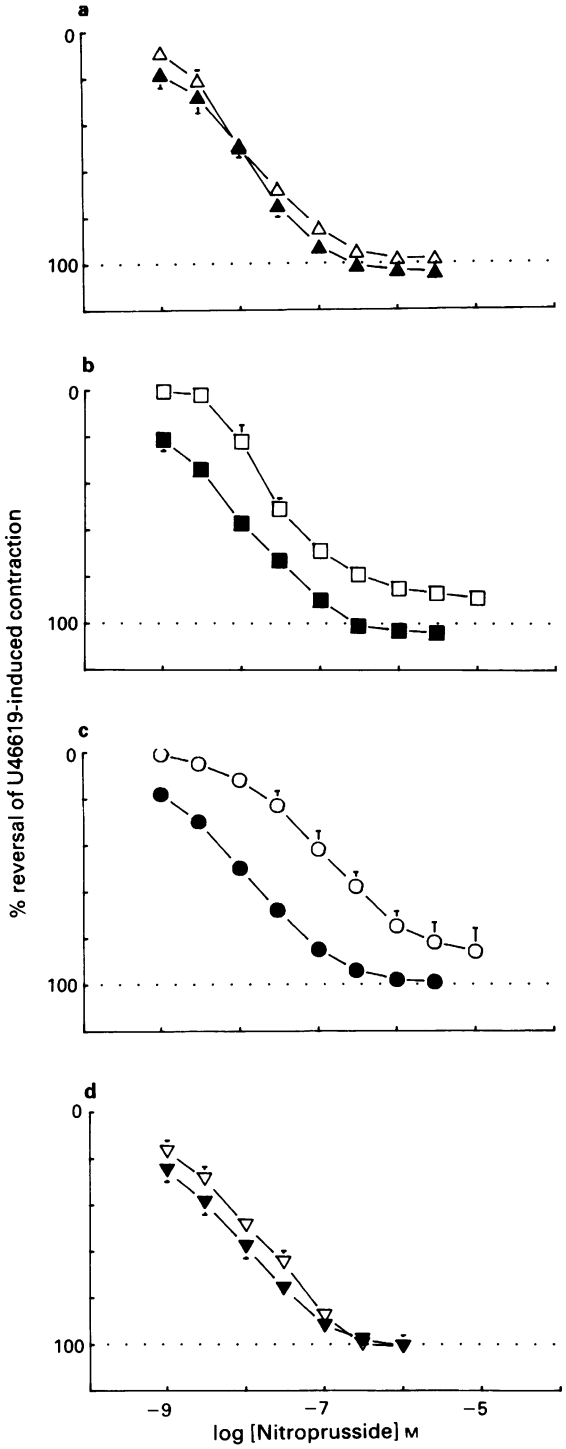

Figure 1 Mean concentration-response (relaxation) curves for nitroprusside on U46619 (10 nM)-contracted preparations of pulmonary artery taken from rats housed in room air (control; closed symbols) or 10% oxygen (hypoxia; open symbols) for (a) 1 day (b) 3 days (c) 14 days and (d) 14 days, followed by 12 days recovery in room air. Responses are expressed as percentage reversal of the U46619-induced contraction. Points are means with s.e. mean shown by vertical bars except when smaller than the size of the symbols. For numbers of observations refer to Table 3.

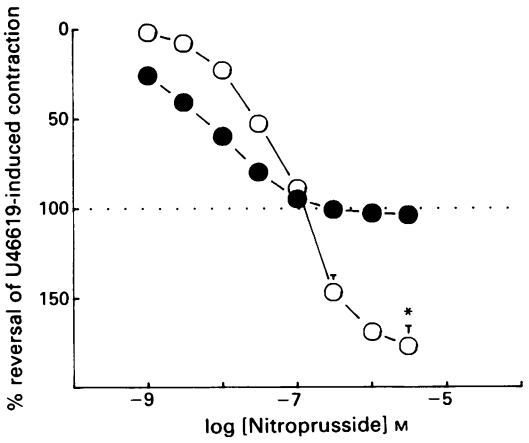

Figure 2 Preparations without endothelium. Mean concentration-response (relaxation) curves ($n = 4$) to nitroprusside on U46619 (10 nM)-contracted preparations of pulmonary artery taken from rats housed in room air (control; ●) or 10% oxygen (hypoxia; ○) for 14 days. Responses are expressed as percentage reversal of the U46619-induced contraction. Points are means with s.e. mean, when not smaller than the size of the symbols, shown by a vertical bar. The asterisk indicates that the maximum relaxation was significantly greater than the corresponding value in the control preparations ($P < 0.05$, Mann Whitney U test).

that in some, but not all, vessell types, relaxant responses to this drug are less when the endothelium is present than when it is absent (Shirasaki & Su, 1985; Shirasaki *et al.*, 1986; Pohl & Busse, 1987). Shirasaki *et al.* (1986) suggested that this could be due to the release by nitroprusside of a contractile substance from the endothelium, which would presumably act as a functional antagonist of nitroprusside. In contrast, Pohl & Busse (1987) postulated that continual basal release of nitric oxide (EDRF) from the endothelium might either compete with the nitroprusside for soluble guanylate cyclase or interfere with the relaxant response at a site distal to guanylate cyclase activation.

In the present study the potency of nitroprusside on pulmonary arteries was the same whether or not the endothelium had been removed, i.e. *in vitro*, the endothelium did not modulate responses to nitroprusside on this vessel type. Furthermore, in vessels from rats exposed to hypoxia for 14 days, the potency of nitroprusside was reduced by the same amount in preparations with and without endothelium. These findings are in contrast to the results of experiments on systemic vessels (aorta and mesenteric artery) taken from rats with systemic hypertension where the endothelium did modulate responses to nitroprusside, and where a reduction in the potency of nitroprusside was seen in the hypertensive rats, but only on preparations with an intact endothelium (Shirasaki *et al.*, 1986). Thus it appears that desensitization of systemic vessels to nitroprusside in systemic hypertension involves a change in the influence of the endothelium on responses of the smooth muscle (Shirasaki *et al.*, 1986), whereas that in pulmonary arteries in pulmonary hypertension reflects a change in the responsiveness of the smooth muscle itself.

The removal of the endothelium from vessels from 14 days hypoxic rats did result in a dramatic increase in the maximum relaxant response to nitroprusside such that reversal of the contraction to U46619 was greater than 100%. This provides evidence that the smooth muscle of pulmonary arteries from 14 day hypoxic rats had significant inherent tone, which may, in turn, explain the reduction in the size of the contraction to U46619 that was also seen on these preparations. This evidence for inherent tone was not seen in matching preparations with intact endothelium, suggesting that, when present, the endothelium may continuously release a relaxing factor that can effectively counteract (and therefore conceal) the inherent tone in the smooth muscle. It was not the purpose of this study to establish the nature of the relaxing factor involved, but one could predict that it might be either nitric oxide (Palmer *et al.*, 1987) or endothelium-derived hyperpolarizing factor (Chen *et al.*, 1988).

Table 4 Nitroprusside: potency (negative log EC_{50}) and maximum relaxation on aortic and tracheal preparations from rats exposed to 10% O_2 (hypoxia) or room air (control) for 14 days

	Neg log EC_{50}		*Maximum relaxation (%)*[c]	
	Control	*Hypoxia*	*Control*	*Hypoxia*
Aorta[a]	7.73 ± 0.20	8.01 ± 0.20	102 ± 2	105 ± 3
	(5)	(4)	(5)	(4)
Trachea[b]	6.11 ± 0.10	6.00 ± 0.12	75 ± 2	58 ± 15
	(4)	(4)	(4)	(4)

Values are mean ± s.e.mean (numbers of preparations from different rats in parentheses). [a]Aortic preparations submaximally contracted with 10 nM U46619. [b]Tracheal preparations submaximally contracted with 1 μM carbachol. [c]Maximum relaxation expressed as a percentage of the U46619- or carbachol-induced contraction.

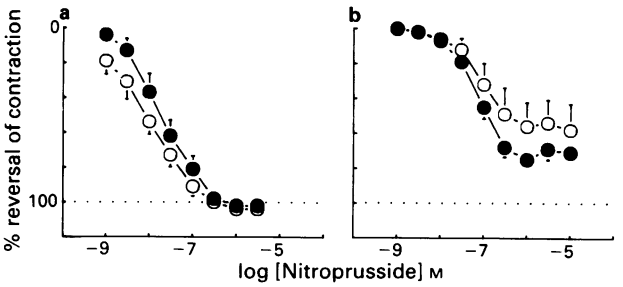

Figure 3 Aorta and trachea. Mean concentration-response (relaxation) curves for nitroprusside on preparations of (a) aorta and (b) trachea taken from rats housed in room air (control; closed symbols) or 10% oxygen (hypoxia; open symbols) for 14 days. The aortic preparations were contracted with 10 nM U46619 (contractions were (mN mm^{-2}): controls 36.0 ± 3.7 ($n = 5$); hypoxia 36.1 ± 3.7 ($n = 4$)). The tracheal preparations were contracted with 1 μM carbachol (contractions were (mN): control 7.4 ± 0.88 ($n = 4$); hypoxia 11.0 ± 3.01 ($n = 4$)). Responses are expressed as percentage reversal of the induced contractions. Points are means, with s.e. mean shown by vertical bars except when smaller than the size of the symbols.

The mechanisms underlying the two functional changes in the smooth muscle of pulmonary arteries from hypoxic rats reported in this study, *viz.* the desensitization of the smooth muscle to the relaxant effects of nitroprusside and the development of inherent tone, remain to be established. It is possible that depolarization of the smooth muscle cell membrane, which has been described by Suzuki & Twarog (1982) in main pulmonary arteries from hypoxic rats, could explain the inherent tone. Explanations for the reduced sensitivity to nitroprusside remain speculative. It is possible that during prolonged exposure of rats to hypoxia the resultant increased pulmonary artery pressure and/or the maintained hypoxaemia could stimulate or augment the release of nitric oxide *in vivo*. This might then downregulate or desensitize the soluble guanylate cyclase on which both nitric oxide and nitroprusside act, as suggested previously (Wanstall & O'Donnell, 1992). The source of the nitric oxide could be either the endothelium (Palmer *et al.*, 1987) or the smooth muscle (Mollace *et al.*, 1991). Alternatively the hypoxaemia might inhibit hydrogen peroxide-dependent activation of guanylate cyclase. The latter is a novel, oxygen-dependent mechanism for vascular smooth muscle relaxation proposed by Burke-Wolin & Wolin (1989).

In conclusion, this study has shown that in rats with hypoxic pulmonary hypertension there is a reduction in the relaxant potency of nitroprusside on isolated pulmonary artery preparations. This desensitization to nitroprusside is reversible and appears to be due to an alteration in the responsiveness of the pulmonary vascular smooth muscle and not to an alteration in the influence, *in vitro*, of the endothelium on responses of the underlying smooth muscle. It is unlikely that this functional change reflects the structural changes to the pulmonary artery that occur in hypoxic pulmonary hypertension, since the time course did not coincide with the development and reversal of vascular hypertrophy. It is more likely to be associated with the rise in pulmonary artery pressure or the maintained hypoxaemia, both of which followed the same time course as the changes in the functional response to nitroprusside. It is postulated that the increase in pressure and/or the maintained hypoxaemia could give rise, *in vivo*, to sustained release of nitric oxide, which might desensitize soluble guanylate cyclase in the smooth muscle thereby reducing responsiveness to nitroprusside.

This research was supported by the National Health and Medical Research Council of Australia. J.C.W. is an NH&MRC Research Scientist. Financial assistance to I.E.H. from the Royal Society of London is gratefully acknowledged. We thank Agatha Gambino for excellent technical assistance.

References

BARER, G.R., CAI, Y., RUSSELL, P.C. & EMERY, C. (1989). Reactivity and site of vasomotion in pulmonary vessels of chronically hypoxic rats: relation to structural changes. *Am. Rev. Resp. Dis.*, **140**, 1483–1485.

BURKE-WOLIN, T. & WOLIN, M.S. (1989). H_2O_2 and cGMP may function as an O_2 sensor in the pulmonary artery. *J. Appl. Physiol.*, **66**, 167–170.

CHEN, G., SUZUKI, H. & WESTON, A.H. (1988). Acetylcholine releases endothelium-derived hyperpolarizing factor and EDRF from rat blood vessels. *Br. J. Pharmacol.*, **95**, 1165–1174.

EMERY, C.J., BEE, D. & BARER, G.R. (1981). Mechanical properties and reactivity of vessels in isolated perfused lungs of chronically hypoxic rats. *Clin. Sci.*, **61**, 569–580.

HERGET, J., SUGGETT, A.J., LEACH, E. & BARER, G.R. (1978). Resolution of pulmonary hypertension and other features induced by chronic hypoxia in rats during complete and intermittent normoxia. *Thorax*, **33**, 468–473.

KAY, J.M. (1980). Effect of intermittent normoxia on chronic hypoxic pulmonary hypertension, right ventricular hypertrophy, and polycythemia in rats. *Am. Rev. Resp. Dis.*, **121**, 993–1001.

LOWEN, M.A., BERGMAN, M.J., CUTAIA, M.V. & PORCELLI, R.J. (1987). Age-dependent effects of chronic hypoxia on pulmonary vascular reactivity. *J. Appl. Physiol.*, **63**, 1122–1129.

MOLLACE, V., SALVEMINI, D., ANGGARD, E. & VANE, J. (1991). Nitric oxide from vascular smooth muscle cells: regulation of platelet reactivity and smooth muscle cell guanylate cyclase. *Br. J. Pharmacol.*, **104**, 633–638.

PALMER, R.M.J., FERRIDGE, A.G. & MONCADA, S. (1987). Nitric oxide release accounts for the biological activity of endothelium-derived relaxing factor. *Nature*, **327**, 524–526.

POHL, U. & BUSSE, R. (1987). Endothelium-derived relaxant factor inhibits effects of nitrocompounds in isolated arteries. *Am. J. Physiol.*, **252**, H307–H313.

REID, L.M. (1979). The pulmonary circulation; Remodelling in growth and disease. *Am. Rev. Resp. Dis.*, **119**, 531–546.

SHIRASAKI, Y. & SU, C. (1985). Endothelium removal augments vasodilation by sodium nitroprusside and sodium nitrite. *Eur. J. Pharmacol.*, **114**, 93–96.

SHIRASAKI, Y., SU, C., LEE, T.J.-F., KOLM, P., CLINE JR, W.H. & NICKOLS, G.A. (1986). Endothelial modulation of vascular relaxation to nitrovasodilators in aging and hypertension. *J. Pharmacol. Exp. Ther.*, **239**, 861–866.

SUZUKI, J. & TWAROG, B.M. (1982). Membrane properties of smooth muscle cells in pulmonary hypertensive rats. *Am. J. Physiol.*, **242**, H907–H915.

WANSTALL, J.C., HUGHES, I.E. & O'DONNELL, S.R. (1990). Nitroprusside-induced relaxation of isolated pulmonary artery from rats exposed to hypoxia for different times. *Clin. Exp. Pharmacol. Physiol.*, Suppl. **17**, 83.

WANSTALL, J.C. & O'DONNELL, S.R. (1988). Inhibition of norepinephrine contractions by diltiazem on aorta and pulmonary artery from young and aged rats: influence of receptor reserve. *J. Pharmacol. Exp. Ther.*, **245**, 1016–1020.

WANSTALL, J.C. & O'DONNELL, S.R. (1990). Endothelin and 5-hydroxytryptamine on rat pulmonary artery in pulmonary hypertension. *Eur. J. Pharmacol.*, **176**, 159–168.

WANSTALL, J.C. & O'DONNELL, S.R. (1992). Responses to vasodilator drugs on pulmonary artery preparations from pulmonary hypertensive rats. *Br. J. Pharmacol.*, **105**, 152–158.

(Received May 5, 1992
Accepted June 2, 1992)

Br. J. Pharmacol. (1992), **107**, 414–417

Evidence for a noradrenergic innervation to α_{1A}-adrenoceptors in rat kidney

[1]David R. Blue, Jr., Rachel L. Vimont & David E. Clarke

Institute of Pharmacology, Syntex Research, 3401 Hillview Avenue, Palo Alto, California 94304, U.S.A.

1 Experiments were undertaken to characterize the α_1-adrenoceptor subtype mediating vasoconstrictor responses to periarterial noradrenergic nerve stimulation (PNS) in the isolated perfused kidney of the rat.

2 Vasoconstrictor responses to nerve stimulation were inhibited by prazosin (10 nM), 5-methyl-urapidil (30 nM), and nitrendipine (1 μM) but were resistant to inhibition by chloroethylclonidine (100 μM).

3 5-Methyl-urapidil (30 nM), chloroethylclonidine (100 μM) and nitrendipine (1 μM) did not inhibit the neuronal release of tritium from nerves loaded with [^{3}H]-noradrenaline.

4 The results suggest that renovascular α_{1A}-adrenoceptors receive a noradrenergic innervation and that the innervated receptors are coupled to dihydropyridine-sensitive calcium channels.

Keywords: α_{1A}-adrenoceptors; 5-methyl-urapidil; chloroethylclonidine; dihydropyridine-sensitive calcium channels; innervation; kidney

Introduction

Recently subtypes of α_1-adrenoceptors have been proposed based upon radioligand binding studies in which two distinct binding sites have been resolved (Morrow & Creese, 1986). Binding sites with high affinity for WB 4101, phentolamine (Morrow & Creese, 1986), 5-methyl-urapidil (Gross *et al.*, 1988) and (+)-niguldipine (Boer *et al.*, 1989) have been designated α_{1A}-adrenoceptors, whereas binding sites with low affinity for these ligands have been designated α_{1B}-adrenoceptors. The α_{1B}-adrenoceptor binding site is further defined by its high sensitivity to alkylation by chloroethylclonidine (Johnson & Minneman, 1987). Functional studies provide support for such a subdivision of α_1-adrenoceptors (Han *et al.*, 1987a,b; 1990; Clarke *et al.*, 1991).

α_1-Adrenoceptor subtypes have also been shown to couple to distinct mechanisms of calcium mobilisation (Han *et al.* 1987a). It is generally thought that α_{1A}-adrenoceptors are coupled to the influx of extracellular calcium via dihydropyridine (DHP)-sensitive calcium channels, whereas α_{1B}-adrenoceptors are coupled to inositol phosphate formation and the release of intracellular calcium (for review see Minneman, 1988). Apparent exceptions to these effector mechanisms for α_{1A}- and α_{1B}-adrenoceptors, however, have been reported (Reynolds & Dubyak, 1985; Wilson & Minneman, 1990; Clarke *et al.*, 1991; Blue *et al.*, 1991).

Few studies have addressed the issue as to whether α_{1A}- or α_{1B}-adrenoceptors receive a sympathetic noradrenergic innervation (Spriggs *et al.*, 1991; Sulpizio & Hieble, 1991). Thus, the present study was conducted to identify and characterize the α_1-adrenoceptor mediating vasoconstrictor responses to periarterial nerve stimulation (PNS) in the isolated perfused kidney of the rat. The rat kidney was chosen because vasoconstrictor responses to PNS are mediated by α_1-adrenoceptors (Charlton *et al.*, 1984; Schwartz & Malik, 1989). Furthermore, recent studies in rat kidney have revealed that the α_{1A}-adrenoceptor subtype mediates vasoconstrictor responses to noradrenaline (NA) (Blue *et al.*, 1991; Clarke *et al.*, 1991; Munavvar & Johns, 1991; Eltz *et al.*, 1991; Elhawary *et al.*, 1992), although a limited involvement of α_{1B}-adrenoceptors has not been excluded (Clarke *et al.*, 1991). Finally α_{1A}-adrenoceptors in rat kidney appear to couple to either DHP-sensitive or DHP-insensitive calcium channels (Clarke *et al.*, 1991; Blue *et al.*, 1991) and it was of interest to determine which of these two receptor-effector mechanisms is triggered by the renal sympathetic, noradrenergic innervation.

[1] Author for correspondence.

Methods

Isolation and removal of kidneys

Male Sprague-Dawley (Charles River) rats (300–350 g) were anaesthetized with sodium pentobarbitone (55 mg kg^{-1}, i.p.) and the renal artery and right kidney were isolated as described previously (Charlton *et al.*, 1984; 1986). A cannula was placed in the mesenteric artery and advanced across the abdominal aorta into the renal artery. The kidney was removed and immediately perfused (6 ml min^{-1}) with Krebs bicarbonate solution (pH 7.4, 37°C) of the following composition (mM): NaCl 118.5; KCl 4.8, $CaCl_2$ 2.5, $MgSO_4$ 1.2, KH_2PO_4 1.2, $NaHCO_3$ 25 and dextrose 5. The Krebs solution was bubbled continually with a 95% O_2: 5% CO_2 mixture. Bipolar platinum electrodes were placed around the renal artery for PNS. Perfusion pressure was measured by a Spectramed physiological pressure transducer (model number: P23XL) positioned near the kidney and displayed on a Beckman physiograph (model R611).

Experimental protocol

The following procedures were carried out to obviate the potentially confounding influence of neuronally-released ATP (Schwartz & Malik, 1989). Kidneys were given a bolus dose of ATP (100 μg in 0.1 ml of 0.9% saline). After perfusion pressure returned to baseline, α-β-methylene ATP (1 μM) was added to the Krebs solution and perfused through the kidney to desensitize P_{2X}-purinoceptors (Schwartz & Malik, 1989). Desensitization of P_{2X}-purinoceptors was confirmed by injecting ATP (100 μg) 10 min after starting the infusion of α-β-methylene ATP. The effect of α-β-methylene ATP (1 μM) upon vasoconstrictor responses to infused noradrenaline (NA) and PNS was determined in a separate set of experiments. A 60 min infusion of α-β-methylene ATP (1 μM) did not alter significantly the EC_{50} or maximum response to NA (EC_{50}s to NA before α-β-methylene ATP and during infusion of α-β-methylene ATP were 0.20 μM and 0.25 μM respectively). Similarly, a 60 min infusion of α-β-methylene ATP

did not alter significantly the maximum response to PNS (maximum responses to 3 and 10 Hz before α-β-methylene ATP were 31 ± 12.7 and 184 ± 7.3 and during infusion of α-β-methylene ATP were 38 ± 6.3 and 195 ± 20.9). Furthermore, the appearance of vasoconstrictor responses to PNS were not altered by α-β-methylene ATP. However, as a precaution against the potential involvement of ATP, α-β-methylene ATP was retained in the Krebs solution in subsequent experiments.

For PNS, priming stimulations were carried out at 10 Hz (1 ms pulse duration) to determine supramaximal voltage (≈70 V). Subsequently kidneys were allowed to equilibrate for 45 min to yield a stable baseline perfusion pressure (40–60 mmHg).

Vasoconstrictor responses to 3 and 10 Hz stimulations were elicited until steady-state, control vasoconstrictor responses were obtained. Perfusion pressure was allowed to return to baseline between stimulations. The kidneys were then perfused for 60 min with Krebs solution containing vehicle or antagonist, after which responses to 3 and 10 Hz stimulations were repeated in the presence of the antagonist or vehicle (time control). The protocol differed for experiments with chloroethylclonidine. After control responses were obtained, kidneys were perfused with chloroethylclonidine (100 μM) for 20 min and then perfused for 40 min with Krebs solution free of chloroethylclonidine. Responses to 3 and 10 Hz stimulations were then repeated.

In a separate series of experiments, the effect of chloroethylclonidine (100 μM), 5-methyl-urapidil (30 μM) and nitrendipine (1 μM) was determined upon the stimulus-induced release of [^{3}H]-NA from postganglionic sympathetic nerves to the kidney. Postganglionic sympathetic nerves were loaded with (−)-[7,8-^{3}H]-NA (specific activity: 8–15 Ci mmol^{-1}) by perfusing kidneys for 30 min with Krebs solution containing [^{3}H]-NA (3.7 nM), followed by a 60 min perfusion with Krebs solution free of [^{3}H]-NA. Three sets of stimulations with 3 and 10 Hz were conducted at 10 min intervals. Following the third set of control stimulations, kidneys were perfused for 60 min with Krebs solution containing an antagonist or vehicle. Stimulations were then obtained in the presence of the antagonist or vehicle, the latter serving as a time control. With chloroethylclonidine, kidneys were perfused with Krebs solution containing chloroethylclonidine (100 μM) or vehicle for 20 min and then perfused with chloroethylclonidine-free Krebs solution for 40 min. Stimulations were then repeated.

Basal (non-stimulated) release of tritium was obtained by collecting the venous effluent for 20 s before each stimulation. The venous effluent was then collected during a 20 s stimulation and for an additional 20 s following stimulation (i.e. a total of 40 s). Stimulus-induced release was calculated by subtracting basal release from that due to stimulation. The basal efflux of tritium, and that due to stimulation, was counted in 0.5 ml samples of the venous effluent plus 4.5 ml of Ready Safe by liquid scintillation spectrometry with quench correction.

The effect of each treatment on stimulus-induced release of tritium is expressed as a percentage of the third set of control stimulations. This procedure was employed to obviate the decreases in tritium release with the first two stimulations.

Statistics

Data are expressed as the mean ± the standard error of the mean (s.e.mean) with 95% confidence limits. Each experiment was compared to its own control (100%) by a paired *t* test (two tailed). The effect of each antagonist was compared to the time control by an unpaired *t* test (two tailed). A probability of less than 0.05 was considered significant.

Drugs

Drugs were obtained from the following sources: prazosin hydrochloride (Pzifer Inc., Groton, CT, U.S.A.), 5-methyl-urapidil and chloroethylclonidine (Research Biochemicals Inc., Natick, MA, U.S.A.), ATP and α-β-methylene ATP (Sigma Chemical Co., St. Louis, MO, U.S.A.), nitrendipine (Syntex Research, Palo Alto, CA, U.S.A.) and [^{3}H]-noradrenaline (New England Nuclear, Boston, MA, U.S.A.).

Stock solutions were prepared in deionized water with the exception of nitrendipine which was dissolved in 100% ethanol and 5-methyl-urapidil which was dissolved in hydrochloric acid (1 N) and then made up to the desired concentration by adding deionized water.

Results

Periarterial nerve stimulation

PNS produced frequency-dependent vasoconstrictor responses in the rat isolated perfused kidney (Figure 1). Mean vasoconstrictor responses (± s.e.mean) to 3 and 10 Hz stimulations were 28.8 ± 5.5 mmHg and 185 ± 5.6 mmHg ($n = 23$) respectively. The mean stimulus-induced release of tritium in response to 3 and 10 Hz stimulations was 1839 ± 177 d.p.m. and 6850 ± 716 d.p.m. ($n = 16$) respectively. Basal, non-stimulated release of tritium was approximately 350 d.p.m. and was not affected by any of the drugs used.

Effects of antagonists on vasoconstrictor responses

Figure 2 shows the effect of α_1-adrenoceptor antagonists and nitrendipine on PNS-induced vasoconstrictor responses. Vasoconstrictor responses did not vary significantly with time. However, vasoconstrictor responses were reduced significantly by the non-selective α_1-adrenoceptor antagonist, prazosin (10 nM), the selective α_{1A}-adrenoceptor antagonist, 5-methyl-urapidil (30 nM), and the DHP calcium channel antagonist, nitrendipine (1 μM). In contrast, vasoconstrictor responses were not altered by chloroethylclonidine (100 μM).

Effect of antagonists on the stimulus-induced release of tritium

Figure 3 shows the effect of α_1-adrenoceptor subtype selective antagonists and nitrendipine upon stimulus-induced release of tritium. Control experiments showed that the release of tritium in response to stimulations of 3 and 10 Hz was reduced significantly compared with control responses when elicited after a 60 min perfusion with Krebs solution alone. However, 5-methyl-urapidil (30 nM), chloroethylclonidine (100 μM) and nitrendipine (1 μM) failed to inhibit stimulus-induced release of tritium. In fact, stimulus-induced release of tritium in response to 10 Hz was increased significantly over the time control by both 5-methyl-urapidil and nitrendipine.

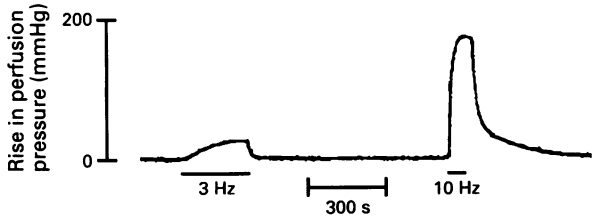

Figure 1 Representative vasoconstrictor responses to 3 and 10 Hz periarterial nerve stimulations in rat isolated perfused kidney. Kidneys were stimulated at supramaximal voltage (≈70 V) until steady-state vasoconstrictor responses were obtained (1 ms pulse duration). Baseline perfusion pressure was approximately 50 mmHg.

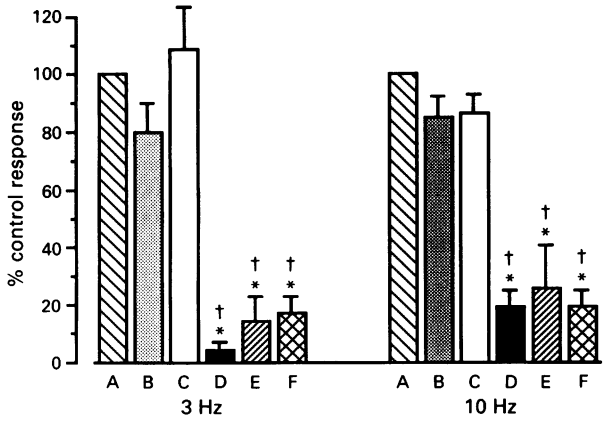

Figure 2 The effect of α_1-adrenoceptor antagonists and nitrendipine upon periarterial nerve stimulation-induced vasoconstrictor responses in the rat isolated perfused kidneys. Kidneys were perfused with antagonists for 60 min before testing. For chloroethylclonidine, kidneys were perfused with chloroethylclonidine for 20 min and then washed with Krebs solution free of chloroethylclonidine for 40 min before testing. Column (A), responses to 3 and 10 Hz before perfusion with vehicle or antagonist (set to 100%); column (B), vehicle; column (C), chloroethylclonidine (100 μM); column (D), prazosin (10 nM); column (E), 5-methyl-urapidil (30 nM) and column (F), nitrendipine (1 μM). Significantly different from column A (*) and B (†) at $P<0.05$. Columns B to F represent the mean value (± s.e.mean, vertical bars) obtained from 4 kidneys.

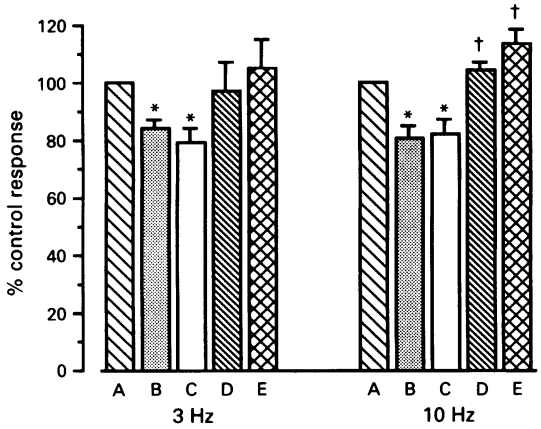

Figure 3 The effect of 5-methyl-urapidil, chloroethylclonidine and nitrendipine upon periarterial nerve stimulation-induced tritium release to 3 and 10 Hz in the rat isolated perfused kidney. Kidneys were perfused with antagonists for 60 min before testing. For chloroethylclonidine, kidneys were perfused with chloroethylclonidine for 20 min and then washed with Krebs solution free of chloroethylclonidine for 40 min before testing. Column (A), responses to 3 and 10 Hz before perfusion with vehicle or antagonist (set to 100%); column (B), vehicle; column (C), chloroethylclonidine (100 μM); column (D), 5-methyl-urapidil (30 nM) and column (E), nitrendipine (1 μM). Significantly different from column A (*) and B (†) at $P<0.05$. Columns B to E represent the mean value (± s.e.mean, vertical bar) obtained from 4 kidneys.

Discussion

The present study is the first to show innervation of α_{1A}-adrenoceptors. Furthermore, these receptors appear to be coupled to DHP-sensitive calcium channels.

Vasoconstrictor responses to PNS were inhibited by the non-selective α_1-adrenoceptor antagonist, prazosin, at a concentration, 10 nM, which is approximately 30 times its equilibrium dissociation constant for α_1-adrenoceptors in rat kidney (Clarke *et al.*, 1990; Blue *et al.*, 1991). This result confirms previous reports that α_1-adrenoceptors mediate responses to PNS in rat kidney (Charlton *et al.*, 1984; Schwartz & Malik, 1989).

α_1-Adrenoceptor-mediated vasoconstriction was further characterized by use of the selective α_{1A}-adrenoceptor antagonist, 5-methyl-urapidil (Gross *et al.*, 1988) and the preferential α_{1B}-adrenoceptor alkylating agent, chloroethylclonidine (Johnson & Minneman, 1987). 5-Methyl-urapidil, at a concentration of 30 nM (approximately 30 times its equilibrium dissociation constant for α_{1A}-adrenoceptors in rat kidney; Clarke *et al.*, 1991), inhibited responses to PNS. This result suggests that α_{1A}-adrenoceptors mediate the response to PNS as 5-methyl-urapidil is approximately 70-fold selective for the α_{1A}-adrenoceptor subtype (Gross *et al.*, 1988; Boer *et al.*, 1989; Hanft & Gross, 1989). In addition, it should be noted that the concentrations of 5-methyl-urapidil and prazosin were selected to produce equal occupancy of α_{1A}-adrenoceptors (see above). Therefore, equal antagonism toward vasoconstrictor responses to PNS by 5-methyl-urapidil and prazosin again suggests the singular involvement of the α_{1A}-adrenoceptor subtype. Furthermore, the irreversible α_{1B}-adrenoceptor antagonist, chloroethylclonidine, failed to inhibit vasoconstrictor responses to PNS. Kidneys were exposed to chloroethylclonidine for 20 min. This concentration and treatment protocol for chloroethylclonidine has been shown previously to inactivate irreversibly α_{1B}-adrenoceptors in several tissues (Johnson & Minneman, 1987; Han *et al.*, 1987b; 1990; Minneman *et al.*, 1988), including rat kidney (Sharif *et al.*, 1991). Taken together, the results with 5-methyl-urapidil and chloroethylclonidine demonstrate that vasoconstrictor responses to PNS are mediated by α_{1A}-adrenoceptors.

The inhibition of PNS-induced vasoconstriction by 5-methyl-urapidil cannot be explained by prejunctional inhibition of noradrenaline release. Indeed, 5-methyl-urapidil increased tritium release at the 10 Hz stimulation. In this regard, evidence exists for inhibitory prejunctional α_1-adrenoceptors in rat kidney (Rump & Majewski, 1987; Murphy & Majewski, 1991). The lack of an effect of chloroethylclonidine on PNS-induced release of tritium suggests that prejunctional α_1-adrenoceptors may be of the α_{1A}-subtype.

Previous attempts to characterize α_1-adrenoceptor-mediated responses to nerve stimulation have met with limited success. In field stimulated rat vas deferens, contractile responses to single stimuli have been reported to be mediated by α_{1B}-adrenoceptors (Mallard *et al.*, 1990; 1992) whereas both α_{1A}- and α_{1B}-adrenoceptors may be activated by trains of stimuli (Spriggs *et al.*, 1991; Mallard *et al.*, 1992). In these studies, however, α_{1A}- and α_{1B}-adrenoceptor-mediated responses were defined by sensitivity to inhibition by nifedipine and chloroethylclonidine respectively. Characterization of α_{1A}-adrenoceptors on the basis of nifedipine is dubious as α_{1A}-adrenoceptors have been shown to couple to calcium influx via both dihydropyridine-sensitive and dihydropyridine-*insensitive* calcium channels (Wilson & Minneman, 1990; Clarke *et al.*, 1991). Furthermore, α_{1B}-adrenoceptors may couple to DHP-sensitive channels (Reynolds & Dubyak, 1985; Clarke *et al.*, 1991).

In contrast to studies in rat vas deferens, Sulpizio & Hieble (1991) used the selective α_{1A}-adrenoceptor antagonists 5-methyl-urapidil and WB 4101 in addition to chloroethylclonidine to characterize biphasic contractile responses to field stimulation in the rat perfused caudal artery. However, these authors were unable to show selective inhibition of either phase. It was concluded that the α_1-adrenoceptor involved did not fit the current classification scheme.

Previous studies using infused NA suggest that α_{1A}-adrenoceptors in rat kidney are coupled to DHP-sensitive and DHP-insensitive calcium channels (Clarke *et al.*, 1991; Blue *et al.*, 1991). The present study demonstrates that sympathetic nerve stimulation activates only those α_{1A}-adrenoceptors which are coupled to DHP-sensitive channels. This selectivity of the innervation suggests that the α_{1A}-adreno-

ceptors linked to DHP-insensitive calcium channels may lie outside vascular neuro-effector junctions and, as such, may subserve a role for circulating adrenaline. Diverse ways of gating calcium may underlie important differences in the physiological roles of neuronal versus hormonal regulation of renal vascular resistance.

In summary, inhibition of PNS-induced vasoconstrictor responses by prazosin, 5-methyl-urapidil and nitrendipine, but not by chloroethylclonidine, demonstrates that α_{1A}-adrenoceptors coupled to DHP-sensitive calcium channels receive a sympathetic noradrenergic innervation in the isolated perfused kidney of the rat.

References

BLUE, D.R., WHITING, R.L. & CLARKE, D.E. (1991). Pharmacological profile of an alpha$_{1A}$-adrenoceptor in the renal vasculature: studies with (+)- and (−)-niguldipine. In *Adrenoceptors: Structure, Mechanisms, Function: Advances in Pharmacological Science*, ed. Abadi, S.Z. pp. 373–374. Birkhauser Verlag, Basel.

BOER, R., GRASSEGGER, A., SCHUDT, C. & GLOSSMANN, H. (1989). (+)-Niguldipine binds with very high affinity to Ca^{2+} channels and to a subtype of α_1-adrenoceptors. *Eur. J. Pharmacol.*, **172,** 131–145.

CHARLTON, K.G., BOND, R.A. & CLARKE, D.E. (1986). An inhibitory prejunctional 5-HT$_1$-like receptor in the isolated perfused rat kidney: apparent distinction from the 5-HT$_{1A}$, 5-HT$_{1B}$, and 5-HT$_{1C}$ subtypes. *Naunyn-Schmiedebergs Arch. Pharmacol.*, **332,** 8–15.

CHARLTON, K.G., JOHNSON, T.D. & CLARKE, D.E. (1984). Vasoconstrictor and norepinephrine potentiating action of 5-hydroxytrypamine in the isolated perfused rat kidney: involvement of serotonin receptors and alpha$_1$-adrenoceptors. *Naunyn-Schmiedebergs Arch. Pharmacol.*, **328,** 154–159.

CLARKE, D.E., VIMONT, R.L. & BLUE, Jr, D.R. (1990). Vascular alpha$_1$-adrenoceptors in rat kidney: agonist and antagonist [prazosin, idazoxan, WB 4101, (+)-niguldipine] characterization. *Eur. J. Pharmacol.*, **183,** 733.

CLARKE, D.E., WHITING, R.L., PFISTER, J. & BLUE, D.R. (1991). Antagonism of α_1-adrenoceptor subtypes by niguldipine and 5-methyl-urapidil in rat kidney. *Br. J. Pharmacol.*, **102,** 196P.

ELHAWARY, A.M., PETTINGER, W.A. & WOLFF, D.W. (1992). Subtype-selective alpha-1 adrenoceptor alkylation in the rat kidney and its effect on the vascular pressor response. *J. Pharmacol. Exp. Ther.*, **260,** 709–713.

ELTZE, M., BOER, R., SANDERS, K.H. & KOLASSA, N. (1991). Vasodilatation elicited by 5-HT$_{1A}$ receptor agonists in constant-pressure-perfused rat kidney is mediated by blockade of α_{1A}-adrenoceptors. *Eur. J. Pharmacol.*, **202,** 33–44.

GROSS, G., HANFT, G. & RUGEVICS, C. (1988). 5-Methyl-urapidil discriminates between subtypes of the α_1-adrenoceptor. *Eur. J. Pharmacol.*, **151,** 333–335.

HAN, C., ABEL, P.W. & MINNEMAN, K.P. (1987a). α_1-Adrenoceptor subtypes linked to different mechanisms for increasing intracellular Ca^{2+} in smooth muscle. *Nature*, **329,** 333–335.

HAN, C., ABEL, P.W. & MINNEMAN, K.P. (1987b). Heterogeneity of α_1-adrenergic receptors revealed by chlorethylclonidine. *Mol. Pharmacol.*, **32,** 505–510.

HAN, C., LI, J. & MINNEMAN, K.P. (1990). Subtypes of α_1-adrenoceptors in rat blood vessels. *Eur. J. Pharmacol.*, **190,** 97–104.

HANFT, G. & GROSS, G. (1989). Subclassification of α_1-adrenoceptor recognition sites by urapidil derivatives and other selective antagonsist. *Br. J. Pharmacol.*, **97,** 691–700.

JOHNSON, R.D. & MINNEMAN, K.P. (1987). Differentiation of α_1-adrenergic receptors linked to phosphatidylinositol turnover and cyclic AMP accumulation in rat brain. *Mol. Pharmacol.*, **31,** 239–246.

MALLARD, N.J., MARSHALL, R.W., SITHERS, A.J. & SPRIGGS, T.L.B. (1992). Separation of putative α_{1A}- and α_{1B}-adrenoceptor mediated components in the tension response of the rat vas deferens to electrical field stimulation. *Br. J. Pharmacol.*, **105,** 727–731.

MALLARD, N.J., MARSHALL, R.W. & SPRIGGS, T.L.B. (1990). Neuronally-released noradrenaline acts at different α_1-adrenoceptors to exogenous noradrenaline in rat vas deferens. *Br. J. Pharmacol.*, **100,** 359P.

MINNEMAN, K.P. (1988). α-Adrenergic receptor subtypes, inositol phosphates, and sources of cell Ca^{2+}. *Pharmacol. Rev.*, **40,** 87–119.

MINNEMAN, K.P., HAN, C. & ABEL, P.W. (1988). Comparison of α_1-adrenergic receptor subtypes distinguished by chlorethylclonidine and WB 4101. *Mol. Pharmacol.*, **33,** 509–514.

MORROW, A.L. & CREESE, I. (1986). Characterization of α_1-adrenergic receptor subtypes in rat brain: a reevaluation of [^{3}H]-WB4014 and [^{3}H] prazosin binding. *Mol. Pharmacol.*, **29,** 321–330.

MUNAVVAR, A.S. & JOHNS, E.J. (1991). Characteristics of α-adrenoceptors in the rat renal vasculature. *Br. J. Pharmacol.*, **104,** 318P.

MURPHY, T.V. & MAJEWSKI, H. (1991). Prejunctional α_1-adrenoceptors in the rat kidney. *Br. J. Pharmacol.*, **104,** 288P.

REYNOLDS, E.E. & DUBYAK, G.R. (1985). Activation of calcium mobilization and calcium influx by α_1-adrenergic receptors in a smooth muscle cell line. *Biochem. Biophys. Res. Commun.*, **130,** 627–632.

RUMP, L.C. & MAJEWSKI, H. (1987). Modulation of norepinephrine release through α_1- and α_2-adrenoceptors in rat isolated kidney. *J. Cardiovasc. Pharmacol.*, **9,** 500–507.

SCHWARTZ, D.D. & MALIK, K.U. (1989). Renal periarterial nerve stimulation-induced vasoconstriction at low frequencies is primarily due to release of a purinergic transmitter in the rat. *J. Pharmacol. Exp. Ther.*, **250,** 764–771.

SHARIF, N.A., SHIEH, I.A., BLUE, D.R. & CLARKE, D.E. (1991). Localization and function of alpha$_1$-adrenoceptor (α_1-AR) subtypes in rat kidney. *Pharmacologist*, **33,** 214.

SPRIGGS, T.L.B., MALLARD, N.J., MARSHALL, R.W. & SITHERS, A.J. (1991). Functional discrimination of α_{1A} and α_{1B} adrenoceptors in rat vas deferens. *Br. J. Pharmacol.*, **102,** 17P.

SULPIZIO, A. & HIEBLE, J.P. (1991). Lack of a pharmacological distinction between *alpha*-1 adrenoceptors mediating intracellular calcium-dependent and independent contractions to sympathetic nerve stimulation in the perfused rat caudal artery. *J. Pharmacol. Exp. Ther.*, **257,** 1045–1052.

WILSON, K.M. & MINNEMAN, K.P. (1990). Pertussis toxin inhibits norepinephrine-stimulated inositol phosphate formation in primary brain cell cultures. *Mol. Pharmacol.*, **38,** 274–281.

(Received April 6, 1992
Revised June 1, 1992
Accepted June 3, 1992)

Br. J. Pharmacol. (1992), **107**, 418–421

Effect of the thromboxane A_2-mimetic U46619 on 5-HT_1-like and 5-HT_2 receptor-mediated contraction of the rabbit isolated femoral artery

[1]Stephen J. MacLennan & Graeme R. Martin

Analytical Pharmacology Group, Biochemical Sciences, Wellcome Research Laboratories, Beckenham, Kent BR3 3BS

1 The influence of the thromboxane A_2-mimetic U46619 (11α,9α-epoxymethano PGH_2) on 5-hydroxytryptamine (5-HT)-induced contractions of the rabbit isolated femoral artery has been examined.

2 In the absence of U46619, 5-HT responses were mediated predominantly by 5-HT_2-receptors as judged by potent, surmountable antagonism by the selective 5-HT_2 receptor antagonists, spiperone and ketanserin. Both antagonists unmasked a population of 5-HT_1-like receptors which accounted for approximately 10–15% of the 5-HT maximum response.

3 In the presence of U46619 (3–10 nM), 5-HT-induced contractions were largely resistant to blockade by 5-HT_2 receptor antagonists since 5-HT_1-like receptor-mediated contraction now accounted for approximately 60% of the 5-HT maximum response.

4 These results show that activation of thromboxane A_2 receptors in a tissue possessing both 5-HT_2 and 5-HT_1-like receptors can convert 5-HT-induced contraction from one mediated predominantly by 5-HT_2 receptors to one which is mediated predominantly by 5-HT_1-like receptors.

Keywords: 5-HT_1-like receptors; 5-HT_2 receptors; thromboxane A_2; amplification; smooth muscle; rabbit femoral artery; contraction

Introduction

5-Hydroxytryptamine (5-HT) has a long-standing implied role in the pathophysiology of cardiovascular disease involving vasospasm. Such disease states include angina pectoris, cerebral vasospasm which follows subarachnoid haemorrage, and Raynaud's phenomenon. Evidence for this is provided largely by clinical observations that the concentrations of platelet release products, including 5-HT and thromboxane A_2 (TxA_2), are elevated significantly in patients with vasospastic disease (Robertson *et al.*, 1981; Rubenstein *et al.*, 1981; Van den Berg *et al.*, 1986; Reilly *et al.*, 1986).

Coronary vasospasm, occurring spontaneously or induced by ergonovine, is not prevented by the 5-HT_2 receptor antagonist ketanserin; hence the role of 5-HT in vasospastic angina has been questioned (De Caterina *et al.*, 1984; Freedman *et al.*, 1984). However, it is now apparent that in some human blood vessels, including the umbilical, coronary, basilar and pial arteries, 5-HT can elicit contraction via ketanserin-resistant 5-HT_1-like receptors in addition to ketanserin-sensitive 5-HT_2 receptors (MacLennan *et al.*, 1989; Connor *et al.*, 1989; Parsons *et al.*, 1989; Hamel & Bouchard, 1991). Furthermore, responses mediated by 5-HT_1-like receptors can be 'uncovered' or enhanced following concomitant exposure to other vasoactive agents such as TxA_2 and $PGF_{2\alpha}$ (Templeton *et al.*, 1991; Sahin-Erdemli *et al.*, 1991). The purpose of this study was to examine the interaction between 5-HT and TxA_2 receptors in the rabbit femoral artery. Initial studies showed that 5-HT-induced contraction of this tissue is mediated predominantly by 5-HT_2 receptors and to a lesser extent by 5-HT_1-like receptors (MacLennan *et al.*, 1991). Using this tissue we sought to investigate how TxA_2 receptor activation might influence the relative contributions made by these receptors to the net response elicited by 5-HT.

[1] Author for correspondence.

Methods

All experiments were conducted on femoral arteries from male New Zealand White rabbits (2.4–3.0 kg) killed by intravenous injection of pentobarbitone sodium (Sagatal: 80 mg kg^{-1}, i.v.) and exsanguination. Ring segments (2.0 mm length) were prepared after first removing adhering connective tissue. The endothelium was removed by gently rolling the tissue around a thin wire. Vascular rings were suspended between two wire hooks (diameter 250 μm) and immersed in 20 ml organ baths containing Krebs solution (pH 7.4) of the following composition (mM): NaCl 118.41, $NaHCO_3$ 25.00, KCl 4.75, KH_2PO_4 1.19, $MgSO_4$ 1.19, glucose 11.10 and $CaCl_2$ 2.50. This was maintained at 37°C and continually gassed with 95% O_2/5% CO_2. In all experiments prazosin and mepyramine (both 0.3 μM) were included in the Krebs solution to exclude actions at α_1-adrenoceptors and histamine-H_1 receptors respectively.

Experimental protocol

After a 15 min stabilization period, tissues were exposed for 30 min to pargyline (500 μM) to inactivate monoamine oxidase. During this period each ring segment was set at a passive tension equivalent to 90% of the internal circumference of that artery if it was relaxed and perfused with a transmural pressure of 100 mmHg. For most tissues this tension was 25.5 mN (2.6 g). This procedure is set out in detail elsewhere (Angus *et al.*, 1986) and is an extension of studies in microvessels (Mulvany & Halpern, 1977). Tissues were contracted with KCl (80 mM) to assess tissue viability and provide a reference contracture for subsequent data analysis. Following washout, a single cumulative concentration-effect (E/[A]) curve was constructed either in the absence or presence of antagonists which had been added 60 min previously.

The influence of TxA_2 receptor activation was examined by exposing tissues to the stable mimetic U46619 (11α,9α-epoxymethano PGH_2) to achieve a contraction equal to 30%

of its maximal effect ([A_{30}] = 3–10 nM). E/[A] curves to 5-HT were then constructed in the presence or absence of either spiperone or ketanserin (both 0.3 μM) which had been added 60 min previously. To characterize further the receptors mediating 5-HT-induced contraction (in the presence of U46619) some tissues were concomitantly exposed to spiperone (0.3 μM) and either the 5-HT$_3$-receptor antagonist MDL72222 (1.0 μM) or the non-selective 5-HT$_1$-like/5-HT$_2$ receptor antagonist methiothepin (10 nM). The tissues were then exposed to U46619 ([A_{30}]) before constructing a single E/[A] curve to 5-HT.

Data analysis

In the absence of antagonists, 5-HT E/[A] curves appeared symmetrical and monophasic and hence the following logistic function was fitted to the data:

$$E = \frac{\alpha . [A]^m}{[A_{50}]^m + [A]^m} \quad (1)$$

in order to estimate the upper asymptote (α), mid-point location ([A_{50}]) and the slope parameter (m). Location parameters were actually estimated as logarithms ($-\log_{10}[A_{50}]$). In experiments employing antagonists, 5-HT E/[A] curves were overtly biphasic with a clear-cut inflection. In these experiments only the appropriate antagonist-shifted phase of the 5-HT curve was analysed by equation (1) to provide an estimate of [A_{50}] in the presence of antagonist; from this r, the mid-point concentration-ratio between control and antagonist (B)-treated tissues was calculated. In this way the antagonist dissociation constant (or rather the apparent pK_B) was estimated from the equation:

$$pK_B = \log(r-1) - n.\log[B] \quad (2)$$

where n, the slope of the Schild regression, is unity, i.e. assuming simple competitive antagonism.

Drugs

5-Hydroxytryptamine hydrochloride, prazosin and spiperone were purchased from Sigma (U.K.). U46619 was purchased from Cayman Chemical (U.K.). Mepyramine maleate, methiothepin mesylate, MDL72222 (1αH, 3α, 5αH-tropan-3-yl 3,5-dichlorobenzoate methane sulphonate) and GR32191 ([1α(Z), 2β, 3β, 5α](+)-7-[5-[1,1'-biphenyl]-4-ylmethoxy)-3-hydroxy-2(1-piperidinyl) cyclopentyl]-4-heptonoic acid) were gifts from Rhone Poulenc (U.K.), Pharmaceutical and Biochemical Research Institute (Czechoslovakia), Marrion Merell-Dow (France) and Glaxo Group Research (U.K.) respectively. All drugs were dissolved and diluted in distilled water with the exception of prazosin and spiperone. Prazosin was dissolved (at 2 mM) in absolute ethanol and diluted in distilled water. Spiperone was dissolved (at 2 mM) in dimethyl sulphoxide (DMSO, 100%) and diluted in distilled water. The final concentrations of vehicle (0.015% v/v) did not influence tissue responsiveness.

Results

5-HT E/[A] curves

In untreated rings of rabbit isolated femoral artery, 5-HT produced apparently monophasic E/[A] curves with a mid-point location (p[A_{50}]) of 7.16 ± 0.09 (mean ± s.e.mean, n = 4) and maximum response (relative to 80 mM KCl) of 147 ± 5% (Figure 1a). However, in the presence of the 5-HT$_2$ receptor antagonists, spiperone (Figure 1a) or ketanserin (Figure 1b), 5-HT effects became clearly biphasic, revealing a component of the response to lower concentrations of 5-HT which was resistant to 5-HT$_2$-receptor antagonism. This resistant component comprised approximately 10–15% of the maximum response to 5-HT. Affinity estimates (apparent pK_B) for spiperone and ketanserin at the receptor mediating the second phase of the effects of 5-HT, calculated from equation (2), were 9.45 ± 0.18 (n = 4) and 8.76 ± 0.08 (n = 5) respectively. These estimates are similar to pK_B values of 9.28 and 8.56 determined previously at the 5-HT$_2$ receptor in rabbit aorta (Leff & Martin, 1986).

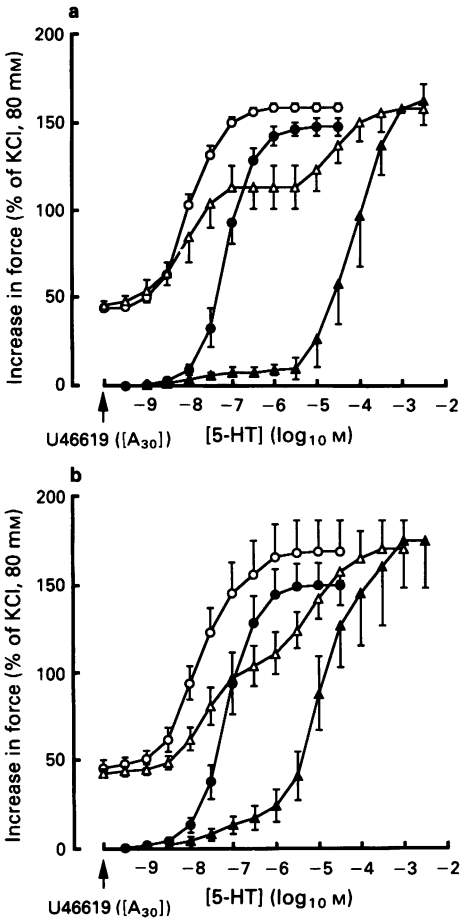

Figure 1 Effect of spiperone (a) and ketanserin (b) on concentration-effect (E/[A]) curves to 5-HT in the rabbit isolated femoral artery. Responses to 5-HT were obtained in the presence (open symbols) or absence (closed symbols) of U46619. U46619 was added cumulatively to some tissues until a response equal to 30% of its own maximum was achieved ([A_{30}]). E/[A] curves to 5-HT were then constructed in control tissues (○, ●) or in the presence (△, ▲) of spiperone (0.3 μM, n = 4) or ketanserin (0.3 μM, n = 5).

5-HT was significantly more potent in tissues exposed to U46619 (p[A_{50}] = 7.99 ± 0.05, n = 4) than in control tissues (p[A_{50}] = 7.16 ± 0.09) (Figure 1a). Furthermore, in the presence of U46619, 5-HT-induced contractions up to 0.1 μM were largely resistant to antagonism by spiperone (0.3 μM) and accounted for approximately 60% of the maximum effect. Similar results to those described for spiperone were obtained with ketanserin although there was a less clearly defined plateau between the two phases of the effects of 5-HT (Figure 1b). From visual inspection of the average 5-HT E/[A] curves constructed in the presence of U46619, affinity (apparent pK_B) estimates for spiperone and ketanserin, calculated from the E/[A] curve midpoint concentration-ratios, were 9.35 and 8.57 respectively indicating that antagonism of the second phase of the curve was consistent with 5-HT$_2$ receptor blockade.

Responses to 5-HT in the presence of spiperone (0.3 μM) were analysed further by use of the 5-HT receptor antagonists methiothepin (Figure 2a) and MDL72222 (Figure 2b). The first phase but not the second phase of 5-HT-induced contractions was antagonized by methiothepin (10 nM; pK_B = 9.24 ± 0.10, n = 6) whereas neither phase was antagonized by MDL72222 (1 μM).

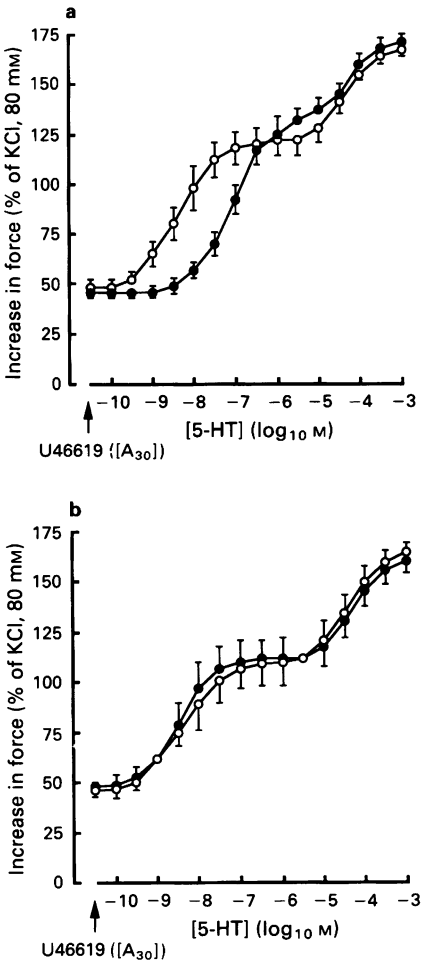

Figure 2 Effect of methiothepin (a) and MDL72222 (b) on concentration-effect (E/A) curves to 5-HT in the rabbit isolated femoral artery. All responses to 5-HT were obtained in the presence of spiperone (0.3 μM). U46619 ([A_{30}]) was added to all tissues before constructing E/[A] curves to 5-HT in the absence (○) or in the presence (●) of methiothepin (10 nM, $n = 6$) or MDL72222 (1.0 μM, $n = 5$).

U46619 E/[A] curves

E/[A] curves to U46619 were competitively antagonized by the selective TxA_2 receptor antagonist, GR32191 (0.1–3.0 μM); the pK_B was 7.09 ± 0.13 ($n = 4$) and the slope of the Schild plot was 1.12 ± 0.09 (not significantly different from unity). This estimate for GR32191 is similar to the value reported at the TxA_2 receptor in rabbit aorta ($pA_2 = 7.21$, Lumley *et al.*, 1989).

Discussion

The most important observation of this study is that activation of TxA_2 receptors, with low concentrations of the mimetic U46619, converted 5-HT-induced contractions of rabbit femoral artery from being predominantly 5-HT_2 receptor-mediated to being mediated predominantly by 5-HT_1-like receptors. In the absence of TxA_2 receptor activation, 5-HT-induced contractions were largely sensitive to the archetypal 5-HT_2 receptor antagonists spiperone and ketanserin. In the presence of these antagonists, 5-HT E/[A] curves became overtly biphasic revealing a population of receptors resistant to blockade by 5-HT_2 receptor antagonists but which accounted for 10% only of the maximum response. The effect of U46619 was to amplify the phase which was resistant to 5-HT_2 antagonism from representing approximately 10% of the maximum response to 5-HT in control tissues to approximately 60%. This spiperone- and ketanserin-resistant phase of the effects of 5-HT was potently antagonized by the 5-HT_1/5-HT_2 receptor antagonist methiothepine ($pK_B = 9.24$) but not by the selective 5-HT_3 receptor antagonist MDL72222 (1.0 μM), thus implying involvement of a 5-HT_1-like receptor (Bradley *et al.*, 1986). The high affinity of methiothepin for this receptor is similar to that quoted for the 5-HT_1-like receptor in rabbit saphenous vein ($pK_B = 9.45$, Martin *et al.*, 1991) and suggests that this antagonist has an affinity for vascular 5-HT_1-like receptors in rabbit tissue somewhat greater than reported in other species such as the dog saphenous vein ($pA_2 = 8.26$, Perren *et al.*, 1991), human basilar artery ($pA_2 = 8.80$, Parsons *et al.*, 1989) or guinea-pig iliac artery ($pK_B = 8.07$, Sahin-Erdemli *et al.*, 1991). Furthermore this affinity estimate for methiothepin is considerably higher than for any of the 5-HT_1 binding sites (Hoyer, 1989) suggesting the 5-HT_1-like receptor in rabbit femoral artery may not be identical to any of the 5-HT_1 recognition sites.

Methiothepin (10 nM) did not cause a further shift of the 5-HT_2-receptor-mediated phase of the effects of 5-HT (Figure 2a) which suggests that this antagonist has an affinity lower than 10 nM for the 5-HT_2 receptor in the rabbit femoral artery. In binding experiments methiothepin has a somewhat higher affinity at the 5-HT_2 recognition site ($pK_i = 8.8$, Hoyer, 1989). With one exception, methiothepin does not behave as a competitive antagonist at peripheral 5-HT_2 receptors (see Mylecharane, 1990) and thus rigorous estimates of its affinity are uncommon. In dog femoral artery methiothepin is a competitive antagonist with a pA_2 of 8.80 (Cohen, 1986). Thus methiothepin appears to have a lower affinity for the 5-HT_2 receptor in rabbit femoral artery than in other tissues, although a more rigorous analysis has to be carried out.

Augmentation of 5-HT_1-like receptor-mediated responses in rabbit femoral artery is not exclusive to U46619. Similar augmentation can be achieved with threshold concentrations of angiotensin II and histamine (unpublished observations). Since each of these agents augment 5-HT_1-like responses in a similar manner, it is probable that the transduction pathways associated with their receptors share common elements, which, in some way, leads ultimately to their effects on 5-HT_1-like receptor-mediated effects. The mechanism(s) underlying this augmentation are presently under investigation.

It is apparent from our results that the maximum response to 5-HT is not changed by U46619, implying that 5-HT_2 receptor-mediated effects are not augmented. We have previously examined the interaction between TxA_2 and 5-HT_2 receptors in more detail (MacLennan *et al.*, 1991). U46619 is able to potentiate the effects of (±)-α-methyl-5-HT acting at 5-HT_2 receptors but this potentiation is characterized by a small leftward shift only of (±)-α-methyl-5-HT curves (less than three fold) without an increase of the maximum response. Thus, with respect to 5-HT receptors in the rabbit femoral artery, U46619 exclusively augments 5-HT_1-like mediated effects.

The ability of U46619 to augment 5-HT_1-like responses is directly related to occupancy of TxA_2 receptors rather than to any non-specific action since in tissues exposed to U46619 (EC_{30}) and in the presence of GR32191 (3 μM) such that no contraction is observed, 5-HT_1-like receptor-mediated responses are not augmented (unpublished observations).

From our observations in the rabbit femoral artery it is intriguing to speculate whether such amplification of 5-HT_1-like responses occurs in other vascular smooth muscle tissues such as the human coronary artery in which 5-HT_1-like receptors normally contribute minimally to the total effects of 5-HT (Connor *et al.*, 1989). The concentrations of both 5-HT and TxA_2 released presumably from aggregating platelets, are elevated in the coronary sinus blood of patients with angina involving coronary artery disease and vasospasm (Robertson *et al.*, 1981; Van den Berg *et al.*, 1989). In this scenario it

would be anticipated from our results that 5-HT$_1$-like receptor-mediated contraction would be augmented and thus provide an explanation for the failure of 5-HT$_2$ receptor antagonists such as ketanserin to relieve vasospastic angina (De Caterina *et al.*, 1984; Freedman *et al.*, 1984).

We would like to thank Mary Bolofo for excellent technical assistance.

References

ANGUS, J.A., COCKS, T.M. & SATOH, K. (1986). α_2-Adrenoceptors and endothelium-dependent relaxation in canine large arteries. *Br. J. Pharmacol.*, **88**, 767–777.

BRADLEY, P.B., ENGEL, G., FENIUK, W., FOZARD, J.R., HUMPHREY, P.P.A., MIDDLEMISS, D.N., MYLECHARANE, E.J., RICHARDSON, B.P. & SAXENA, P.R. (1986). Proposals for the classification and nomenclature of functional receptors for 5-hydroxytryptamine. *Neuropharmacol.*, **25**, 563–576.

COHEN, R.A. (1986). Contractions of isolated canine coronary arteries resistant to S2-Serotonergic blockade. *J. Pharmacol. Exp. Ther.*, **237**, 548–552.

CONNOR, H.E., FENIUK, W. & HUMPHREY, P.P.A. (1989). 5-Hydroxytryptamine contracts human coronary arteries predominantly via 5-HT$_2$ receptor activation. *Eur. J. Pharmacol.*, **161**, 91–94.

DE CATERINA, R., CARPEGGIANI, C. & L'ABBATE, A. (1984). A double-blind, placebo controlled study of ketanserin in patients with Printzmetal's angina. *Circulation*, **69**, 889–894.

FREEDMAN, S.B., CHIERCHIA, S., RODRIGUEZ-PLAZA, L., BUGIARDINI, R., SMITH, G. & MASERI, A. (1984). Ergonovine-induced myocardial ischaemia: no role for serotonergic receptors? *Circultion*, **70**, 178–183.

HAMEL, E. & BOUCHARD, D. (1991). Contractile 5-HT$_1$ receptors in human isolated pial arterioles: correlation with 5-HT$_{1D}$ binding sites. *Br. J. Pharmacol.*, **102**, 227–233.

HOYER, D. (1989). 5-Hydroxytryptamine receptors and effector coupling mechanisms in peripheral tissues. In *The Peripheral Actions of 5-Hydroxytryptamine*. ed. Foxard, J.R. pp. 72–99. Oxford: Oxford University Press.

LEFF, P. & MARTIN, G.R. (1986). Peripheral 5-HT$_2$-like receptors. Can they be classified with the available antagonists? *Br. J. Pharmacol.*, **88**, 585–593.

LUMLEY, P., WHITE, B.P. & HUMPHREY, P.P.A. (1989). GR32191, a highly potent and specific thromboxane A$_2$ receptor blocking drug on platelets and vascular and airways smooth muscle *in vitro*. *Br. J. Pharmacol.*, **97**, 783–794.

MACLENNAN, S.J., WHITTLE, M.J. & MCGRATH, J.C. (1989). 5-HT$_1$-like receptors requiring functional cyclo-oxygenase and 5-HT$_2$ receptors independent of cyclo-oxygenase mediate contraction of the human umbilical artery. *Br. J. Pharmacol.*, **97**, 921–933.

MACLENNAN, S.J., TURNER, M.A., PRENTICE, D.J. & MARTIN, G.R. (1991). Amplifying interactions between 5-HT$_1$-like, 5-HT$_2$ and thromboxane A$_2$ receptors in vascular smooth muscle. *Br. J. Pharmacol.*, **102**, 203P.

MARTIN, G.R., PRENTICE, D.J. & MACLENNAN, S.J. (1991). The 5-HT receptor in rabbit saphenous vein, pharmacological identity with the 5-HT$_{1D}$ recognition site? *Fundam. Clin. Pharmacol.*, **5**, 417.

MULVANY, M.J. & HALPERN, W. (1977). Contractile properties of small arterial resistance vessels in spontaneously hypertensive and normotensive rats. *Circulation Res.*, **41**, 19–26.

MYLECHARANE, E.J. (1990). Agonists and antagonists of 5-HT$_2$ receptors. In *Cardiovascular Pharmacology of 5-Hydroxytryptamine*. ed. Saxena, P.R., Wallis, W., Wouters, W. & Bevan, P. pp. 81–100. Dordrecht: Kluwer Academic Press.

PARSONS, A.A., WHALLEY, E.T., FENIUK, W., CONNOR, H.E. & HUMPHREY, P.P.A. (1989). 5-HT$_1$-like receptors mediate 5-hydroxytryptamine-induced contraction of human isolated basilar artery. *Br. J. Pharmacol.*, **96**, 434–440.

PERREN, M.J., FENIUK, W. & HUMPHREY, P.P.A. (1991). Vascular 5-HT$_1$-like receptors that mediate contraction of the dog isolated saphenous vein and carotid arterial vasoconstriction in anaesthetised dogs are not of the 5-HT$_{1A}$ or 5-HT$_{1D}$ subtype. *Br. J. Pharmacol.*, **102**, 191–197.

REILLY, I.A.G., ROY, L. & FITZGERALD, G.A. (1986). Biosynthesis of thromboxane in patients with systemic sclerosis and Raynaud's phenomenon. *Br. Med. J.*, **292**, 1037–1039.

ROBERTSON, R.M., ROBERTSON, D., ROBERTS, L.J., MAAS, R.L., FITZGERALD, G.A., FRIESINGER, G.C. & OATES, J.A. (1981). Thromboxane A$_2$ in vasotonic angina pectoris. Evidence from direct measurements and inhibitor trials. *New Engl. J. Med.*, **304**, 998–1003.

RUBENSTEIN, M.D., WALL, R.T., BAIM, D.S. & HARRISON, D.C. (1981). Platelet activation in clinical coronary artery disease and spasm. *Am. Heart. J.*, **102**, 363–367.

SAHIN-ERDEMLI, I., HOYER, D., STOLL, A., SEILER, M.P. & SCHOEFFTER, P. (1991). 5-HT$_1$-like receptors mediate 5-hydroxytryptamine-induced contraction of guinea-pig isolated iliac artery. *Br. J. Pharmacol.*, **102**, 386–390.

TEMPLETON, A.G.B., MCGRATH, J.C. & WHITTLE, M.J. (1991). The role of endogenous thromboxane in contractions to U-46619, oxygen, 5-HT and 5-CT in the human isolated umbilical artery. *Br. J. Pharmacol.*, **103**, 1079–1084.

VAN DEN BERG, E.K., SCHMITZ, J.M., BENEDICT, C.R., MALLOY, C.R., WILLERSON, J.T. & DEHMER, G.J. (1989). Transcardiac serotonin concentration is increased in selected patients with limiting angina and complex coronary lesion morphology. *Circulation*, **79**, 116–124.

(Received April 9, 1992
Revised May 29, 1992
Accepted June 4, 1992)

Br. J. Pharmacol. (1992), **107**, 422–428

Control of cyclic AMP levels in primary cultures of human tracheal smooth muscle cells

[1] I.P. Hall, S. Widdop, P. Townsend & K. Daykin

Department of Therapeutics, University Hospital of Nottingham, Nottingham NG7 2UH

1 [^{3}H]-adenosine 3':5'-cyclic monophosphate ([^{3}H]-cyclic AMP) responses were studied in primary cultures of human tracheal smooth muscle cells derived from explants of human trachealis muscle and in short term cultures of acutely dissociated trachealis cells.

2 Isoprenaline induced concentration-dependent [^{3}H]-cyclic AMP formation wtih an EC_{50} of 0.2 μM. The response to 10 μM isoprenaline reached a maximum after 5–10 min stimulation and remained stable for periods of up to 1 h. After 10 min stimulation, 1 μM isoprenaline produced a 9.5 fold increase over basal [^{3}H]-cyclic AMP levels. The response to isoprenaline was inhibited by ICI 118551 (10 nM), (apparent K_A 1.9×10^9 M^{-1}) indicating the probable involvement of a β_2-adrenoceptor in this response in human cultured tracheal smooth muscle cells. However, with 50 nM ICI 118551 there was a reduction in the maximum response to isoprenaline. Prostaglandin E_2 also produced concentration-dependent [^{3}H]-cyclic AMP formation (EC_{50} 0.7 μM, response to 1 μM PGE_2 6.4 fold over basal).

3 Forskolin (1 nM–100 μM) induced concentration-dependent [^{3}H]-cyclic AMP formation in these cells. A 1.6 fold (over basal) response was also observed following stimulation with NaF (10 mM).

4 The nonselective phosphodiesterase inhibitor 3-isobutyl-1-methylxanthine (IBMX) (0.1 mM) and the type IV, cyclic AMP selective, phosphodiesterase inhibitor rolipram (0.1 mM) both elevated basal [^{3}H]-cyclic AMP levels by 1.8 and 1.5 fold respectively. IBMX (1–100 μM) and low concentrations of rolipram (< 10 μM), also potentiated the response to 1 μM isoprenaline. Inhibitors of the type III phosphodiesterase isoenzyme (SK&F 94120 and SK&F 94836) were without effect upon basal or isoprenaline-stimulated cyclic AMP responses in these cells.

5 Carbachol (1 nM–100 μM) produced concentration-dependent inhibition of the [^{3}H]-cyclic AMP response to 1 μM isoprenaline in human cultured tracheal smooth muscle cells (IC_{50} 0.24 μM). Carbachol (1 μM) inhibited the [^{3}H]-cyclic AMP response to 1 μM isoprenaline by 60%. This effect of carbachol was itself inhibited by atropine (50 nM) (K_A 2.3×10^9 M^{-1}) indicating the involvement of a muscarinic receptor.

6 These results show that primary cultures of human tracheal smooth muscle cells demonstrate cyclic AMP responses to direct receptor stimulation, adenylyl cyclase activation and inhibition with nonselective and type IV-selective cyclic AMP phosphodiesterase isoenzyme inhibitors, and that the cyclic AMP response to isoprenaline can be inhibited by muscarinic receptor stimulation.

Keywords: Cyclic AMP; human tracheal smooth muscle; cell culture; forskolin; phosphodiesterase inhibitors; β_2-adrenoceptors; muscarinic receptors

Introduction

Agents which elevate tissue adenosine 3':5'-cyclic monophosphate (cyclic AMP) content can relax airway smooth muscle preparations (Barnes, 1986). This response is believed to be a consequence of several different intracellular effects of cyclic AMP including activation of Ca^{2+} gated K^+ channel activity (Kume *et al.*, 1989), sequestration of intracellular calcium (Mueller & van Breeman, 1979), and alteration of the sensitivity of the contractile apparatus to changes in intracellular calcium concentrations (Silver & Stull, 1982). The mechanisms underlying control of tissue cyclic AMP levels have been investigated in a range of experimental animal airway tissues including bovine and canine trachealis (Torphy, 1988; Torphy *et al.*, 1988; Hall *et al.*, 1989; 1990a; Harris *et al.*, 1989). However, it has proved difficult to investigate the control of cyclic AMP levels in human airway smooth muscle due to the problem of obtaining sufficient tissue for studies to be performed. In order to examine the mechanisms underlying control of tissue cyclic AMP content in human tracheal smooth muscle, we have established primary cultures of tracheal smooth muscle cells from human trachealis muscle. This paper describes the basic characteristics in human cultured tracheal smooth muscle of the cyclic AMP responses to a range of agents capable of altering cyclic AMP content through receptor stimulation, phosphodiesterase inhibition and direct activation of adenylyl cyclase and G_s. A preliminary account of this work has been presented to the British Pharmacological Society (Hall *et al.*, 1992).

Methods

Primary culture of human tracheal smooth muscle cells

Human tracheal smooth muscle cells were grown from explants of trachealis muscle obtained at *post mortem* performed within 8 h of death. Tissue was used from donors with no history of respiratory disease. A strip of trachealis taken from immediately above the carina and about 2 × 1 cm was dissected clear of surrounding tissue and transported to the laboratory in Dulbecco's Modified Eagles Medium (DMEM) containing penicillin G (200 u ml^{-1}), streptomycin (200 μg l^{-1}) and amphotericin B (0.5 μg l^{-1}). The tissue was washed twice in 10 ml of DMEM containing antibiotics and anitfungal agents. Next, overlying mucosa was dissected free

[1] Author for correspondence.

from the tracheal smooth muscle under sterile conditions. Small (0.2 × 0.2 cm) explants of tracheal muscle were then excised and about 15 explants placed in a 60 mm dish. After allowing explants to adhere, DMEM containing antibiotics, amphotericin B, 10% foetal calf serum (FCS) and glutamine (2 mM) was added to just cover the explants. Smooth muscle cell growth usually occurred about 7 days after placing explants in culture. Cultures were supplemented with fresh DMEM containing FCS and glutamine about every four days. When cells were approaching confluence in some parts of the dish, explants were removed, and 24 h later cells harvested by trypsinization. Cells from an individual dish were then plated in one 75 cm flask and grown to confluence. When confluent, each flask was split 1:4. Antibiotics and amphotericin were not added to the medium used for all subsequent passages after this stage (passage 2). Cells for experiments measuring cyclic AMP accumulation were plated in 24 (× 1 cm) well plates and studied when confluent.

Preparation of acutely dissociated tracheal smooth muscle cells

Acutely dissociated tracheal smooth muscle cells were prepared by a modification of the method previously described by Kotlikoff (1990). A strip of trachealis, dissected as described above, was coarsely minced with scissors and the resulting tissue fragments transferred to a Universal containing 10 ml of DMEM (without FCS) and collagenase type II (Sigma) (1 mg ml^{-1}). These were then incubated at 37°C for 1 h with frequent agitation. The resultant suspension was filtered through gauze (mesh), mixed 50/50 with 10% FCS to inactivate collagenase and pelleted by centrifugation at 1500 r.p.m. for 5 min. Cells were resuspended in DMEM containing 10% FCS, glutamine, antibiotics and antifungal agents then plated as described above.

Immunocytochemistry

All primary cell lines from each donor were examined by use of anti smooth muscle actin antibody (1:100 dilution) (Sigma) to confirm the presence of smooth muscle type cells by standard immunocytochemical techniques. Primary cell cultures used for the experiments described in this paper showed >95% of cells staining for smooth muscle actin.

Accumulation of [^{3}H]-cyclic AMP

Accumulation of [^{3}H]-cyclic AMP was measured by a modification of a previously described method (Ruck *et al.*, 1991). In brief, confluent monolayers of cells plated in 24 well plates were labelled with [^{3}H]-adenine (2 μCi/well) for 2 h in DMEM at 37°C in an incubator constantly gassed with air /CO_2 (5%). At the end of this period cells were washed three times with 1 ml of Hanks/HEPES buffer, and then allowed to rewarm to 37°C for 10 min in the presence or absence of antagonists and/or phosphodiesterase inhibitors. At the end of this period, agonists were finally added for 10 min before reactions were terminated by the addition of 50 μl of concentrated HCl. Cells were then stored at − 20°C. [^{3}H]-cyclic AMP was determined following rethawing by column chromatography as previously described (Donaldson *et al.*, 1988; Hall *et al.*, 1989). Aliquots of [^{14}C]-cyclic AMP were added to each sample and the counts obtained from this recovery marker used to correct for variations in recovery from each column. In addition, a 100 μl aliquot was taken from each well of the plate after stopping reactions and counted for tritium in order to correct for variations in the number of cells per well.

Statistics

The affinity constant (K_A) for ICI 118551 and atropine was determined from shifts in the agonist concentration-response curve by use of the relationship:

$$K_A = (K_2/K_1\text{-}1)/A$$

where A is the concentration of antagonists, K_1 is the concentration of agonist producing half maximal response and K_2 is the concentration of agonist producing a half maximal response in the presence of antagonist. Dose-response curves were drawn with the curve fitting programme Graphpad. Statistical analysis of data was performed by paired or unpaired *t* tests as appropriate. All values in the text represent mean ± s.e.mean of *n* separate experiments. Cells from 5 individual primary tissue preparations from 3 individuals were used.

Materials

DMEM and FCS were obtained from Northumbria Biologicals Ltd. Plasticware was obtained from Falcon and Costar. 8-[^{14}C]-cyclic AMP (specific activity 42.4 μCi $mmol^{-1}$) and 2,8-[^{3}H]-adenine (specific activity 26 μCi $mmol^{-1}$) were obtained from Amersham. Gifts of ICI 118551 (erythro-dl-1-(7-methylindan-4-yloxy)-3-isopropylaminobutan-2-ol; ICI) SK&F 94120 (5-(4-acetamidophenyl)pyrazin-2-[1H]-one), SK&F 94836 (2-cyano-1-methyl-3-[4-(4-methyl-6-oxo-1,4,5,6 tetrahydropyridazine-3-yl)phenyl]quinidine; Smith Kline & Beecham, England) and rolipram (Schering AG, Germany) are gratefully acknowledged. All other chemicals were obtained from Sigma. The antibodies used for immunocytochemistry were anti smooth muscle actin (Sigma A2547) and mouse IgG whole molecule (host goat) (Sigma F0257).

Results

Effect of isoprenaline

Isoprenaline (10 μM) produced accumulation of [^{3}H]-cyclic AMP in human cultured tracheal smooth muscle cells, the response reaching maximum after between 5 and 10 min of stimulation and remaining stable for periods of up to 1 h thereafter (Figure 1). The stimulation observed with 1 μM isoprenaline was 9.5 ± 1.3 fold over basal (unstimulated) ($n = 47$). All subsequent experiments were performed with a 10 min stimulation period.

The concentration-response curve for [^{3}H]-cyclic AMP accumulation by isoprenaline is shown in Figure 2, and the inhibition of the response to a range of concentrations of isoprenaline by the β_2-selective antagonist, ICI 118551

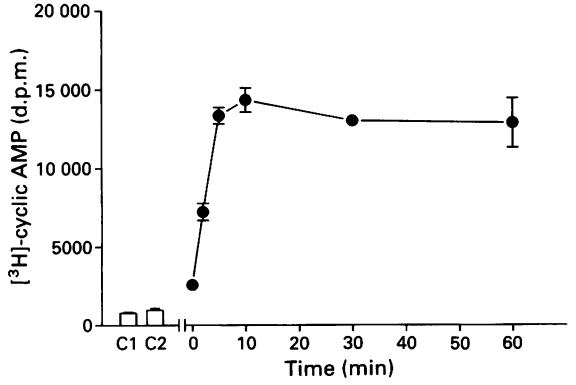

Figure 1 Time course of the [^{3}H]-cyclic AMP response to 10 μM isoprenaline in human cultured tracheal smooth muscle cells. Each point represents the mean (± s.e.mean, vertical bars) of triplicate determinations. The basal (unstimulated) accumulation of [^{3}H]-cyclic AMP at time zero (C1) and after 60 min (C2) are also shown. Data are from a representative experiment which was repeated three times with similar results on cells from a range of different passage numbers between 4 and 10. Where error bars are not shown they lie within data points.

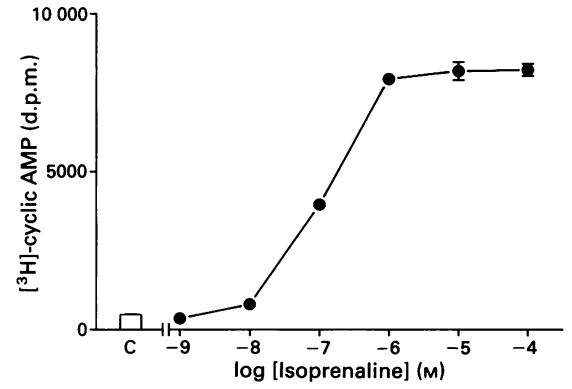

Figure 2 The effect of varying concentrations of isoprenaline on formation of [^{3}H]-cyclic AMP in human cultured tracheal smooth muscle cells. The basal (unstimulated) level of [^{3}H]-cyclic AMP is shown by the bar marked C, and the response to different concentrations of isoprenaline by the filled circles. Each point represents the mean (± s.e.mean, vertical bars) of triplicate determinations in an experiment performed in a single plate of cells. The experiment was performed 15 times with similar results.

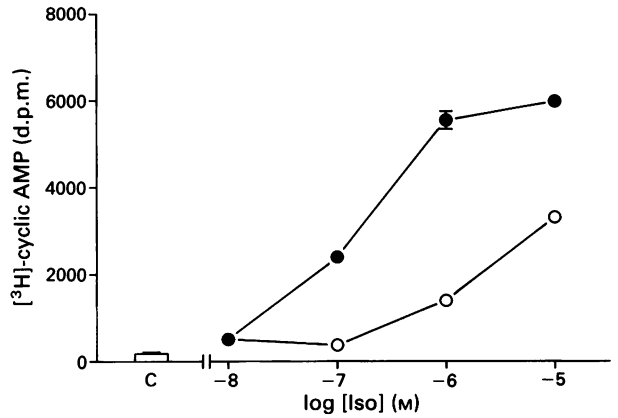

Figure 3 The effect of the β_2-adrenoceptor-selective antagonist ICI 118551 (10 nM) (○) on [^{3}H]-cyclic AMP formation in response to varying concentrations of isoprenaline (●). The basal (unstimulated) response is shown in the column marked C. Each point represents the mean (± s.e.mean, vertical bars) of triplicate determinations in a single experiment. The experiment was repeated five times with similar results.

(10 nM) (Bilski *et al.*, 1983) in Figure 3. The calculated EC_{50} for isoprenaline was $2.0 \pm 0.3 \times 10^{-7}$ M ($n = 16$), and the apparent K_A value for ICI 118551 (10 nM) was $1.9 \pm 0.3 \times 10^9$ M^{-1} ($n = 6$), indicating the probable involvement of the β_2-receptor subtype in this response in cultured human tracheal smooth muscle cells. However, in contrast to the parallel shift in the concentration-response curve produced by 10 nM ICI 118551 when 10 nM to 10 μM isoprenaline was used as agonist (Figure 3), in experiments examining the effect of ICI 118551 (50 nM) upon the response to the higher concentrations of isoprenaline used (> 10 μM), ICI 118551 produced a nonparallel shift of the concentration-response curve to isoprenaline, with a reduction in the maximum response to isoprenaline (Figure 4).

Effect of passage number on isoprenaline response

In order to define the stability of the cyclic AMP response in cells from different passage numbers, the fold stimulation and EC_{50} for isoprenaline induced [^{3}H]-cyclic AMP formation was compared between cells from passage 4 and 12. No significant change was seen with increasing passage number during this period. However, after passage 12 some decline in the maximum stimulation by isoprenaline was observed. All subsequent experiments were therefore performed on cells

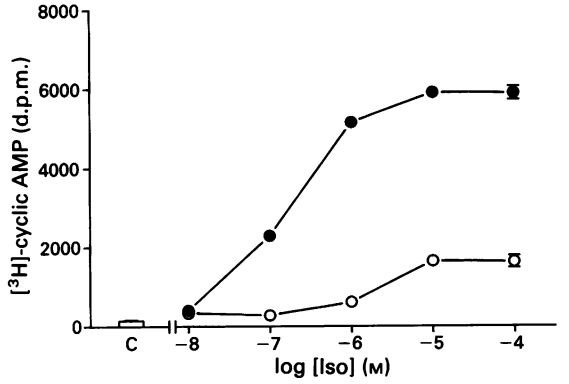

Figure 4 The effect of the β_2-adrenoceptor-selective antagonist ICI 118551 (50 nM) (○) upon [^{3}H]-cyclic AMP formation in response to isoprenaline (●). The basal (unstimulated) response is shown by the column marked C. Each point represents the mean (± s.e.mean, vertical bars) of triplicate determinations in a single experiment. The experiment was repeated three times with similar results.

from passages between 4 and 12. The effect of passage number upon the responses to prostaglandin E_2 (PGE_2), forskolin and rolipram were also examined. The potency of these agents and the stimulation observed with these agents remained stable between passages 4 and 12.

Response to isoprenaline in collagenase-treated cell preparations

In order to compare the response of cells after several passages with cells maintained in short term culture, experiments were performed using cells acutely dissociated with collagenase and plated in 24 well plates to examine the responses to isoprenaline. From a single tissue preparation, inadequate cell numbers were obtained to perform full concentration-response curves to agonists. Therefore, cells obtained by primary collagenase digestion were grown to confluence in 24 well plates and responses to isoprenaline examined (i.e. passage 2). The EC_{50} for isoprenaline-induced cyclic [^{3}H]-cyclic AMP formation was $9 \pm 1 \times 10^{-7}$ M ($n = 4$), comparing well with the responses seen in cells after repeated passage.

Effect of prostaglandin E_2

Prostaglandin E_2 (PGE_2) also stimulated concentration-dependent [^{3}H]-cyclic AMP formation in primary cultures of human tracheal smooth muscle cells (Figure 5). The EC_{50} for

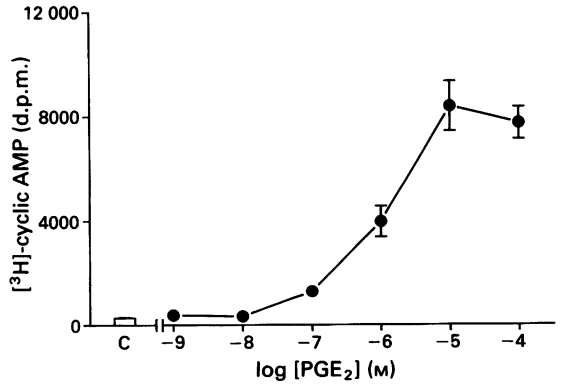

Figure 5 The effect of varying concentrations of prostaglandin E_2 (PGE_2) on [^{3}H]-cyclic AMP formation in human cultured tracheal smooth muscle cells. Data are shown from a single representative experiment which was repeated four times with similar results. Each point represents the mean (± s.e.mean, vertical bars) of triplicate determinations. The control response is shown by the column marked C.

this response to PGE_2 was $1.1 \pm 0.2 \times 10^{-6}$ M ($n = 5$). The response to 1 μM PGE_2 was 6.4 ± 0.5 fold over basal (unstimulated) ($n = 5$).

Effect of forskolin

The adenylyl cyclase activator, forskolin, produced concentration-related [^{3}H]-cyclic AMP formation in human cultured tracheal smooth muscle cells as shown in Figure 6. This response was non-maximal with the concentrations of forskolin used (10 nM to 100 μM). The response to 1 μM forskolin was increased in the presence of the nonselective phosphodiesterase (PDE) inhibitor 3-isobutyl-1-methylxanthine (IBMX) (0.1 mM) (Figure 6). The direct acting G protein stimulant, NaF (10 mM), also elevated cell [^{3}H]-cyclic AMP content to 1.6 ± 0.3 fold over basal ($P<0.05$, $n = 4$).

Effect of phosphodiesterase inhibitors

The effect of the nonselective PDE inhibitor, IBMX, on both basal and isoprenaline-stimulated cyclic AMP responses is shown in Figure 7. It can be seen that alone, IBMX produced a small but significant elevation of tissue cyclic AMP content. In addition, the response to isoprenaline (1 μM) was also increased in the presence of IBMX (10 μM–1 mM) (Figure 7, Table 1).

In order to attempt to define the PDE isoenzymes important for the physiological control of whole cell cyclic AMP content, the effects of both type III and type IV PDE inhibitors were examined. The data obtained from these experiments with the type III selective inhibitors, SK&F 94120 and SK&F 94836, and the type IV selective inhibitor, rolipram, are shown in Table 2. It can be seen that whilst inhibitors of the type III isoenzyme produced no significant effect on basal cyclic AMP responses, rolipram, an inhibitor of the high K_m, cyclic AMP hydrolysing isoenzyme present in tracheal smooth muscle (Nicholson *et al.*, 1990) produced significant elevation of cyclic AMP levels (Table 1). Low concentrations of rolipram (< 10 μM) in the presence of 1 μM isoprenaline produced a small concentration-related increase in cyclic AMP levels (response to 1 μM rolipram 1.7 ± 0.2 fold over response to 1 μM isoprenaline alone, $n = 10$, $P<0.05$; EC_{50} 0.3 ± 0.1 μM, $n = 6$). However, high concentrations of rolipram (> 10 μM) had no significant effect upon the response to 1 μM isoprenaline (Table 2).

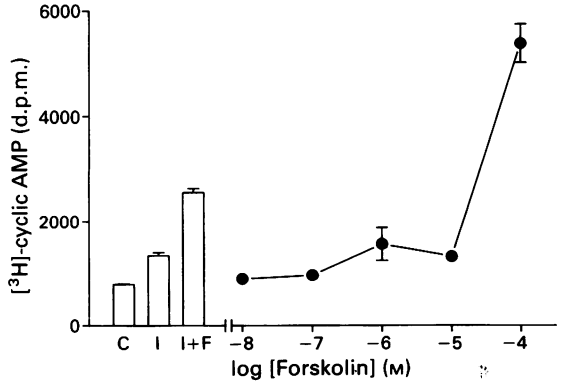

Figure 6 The effect of varying concentrations of forskolin (●) on [^{3}H]-cyclic AMP formation in human cultured tracheal smooth muscle cells. Also shown are the basal (unstimulated) response in these cells (C), the response to 3-isobutyl-1-methylxanthine (IBMX) (0.1 mM) (I) and the response to forskolin (1 μM) and IBMX (0.1 mM) together (I + F). Each point represents the mean (± s.e.mean, vertical bars) of triplicate determinations. The experiment was repeated twice with similar results.

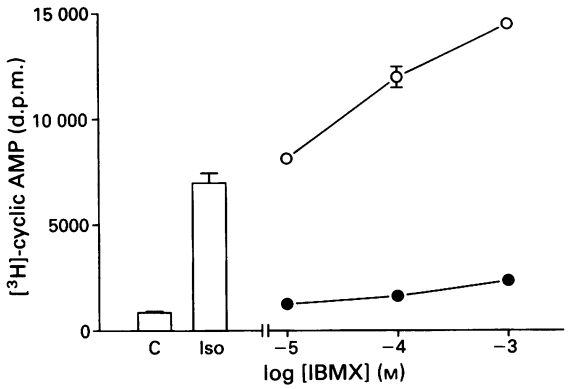

Figure 7 The effect of varying concentrations of 3-isobutyl-1-methylxanthine (IBMX) on [^{3}H]-cyclic AMP formation in human cultured tracheal smooth muscle cells in the absence (●) and presence (○) of 1 μM isoprenaline. The basal (unstimulated) level, and the response to 1 μM isoprenaline alone are shown in the columns marked C and Iso respectively. Each point represents the mean (± s.e.mean, vertical bars) of triplicate determinations in a single plate of cells. The experiment was repeated three times with similar results. The mean changes in [^{3}H]-cyclic AMP levels with these agents are summarized in Table 2.

Table 1 Effect of a range of agents on [^{3}H]-cyclic AMP formation in human tracheal smooth muscle cells

Agent	*Fold stimulation over control* − *IBMX* (n)	+ *IBMX* (0.1 mM) (n)
Isoprenaline (1 μM)	9.5 ± 1.3 (47)	28.5 ± 1.9 (9)
Forskolin (1 μM)	2.0 ± 0.3 (5)	4.4 ± 0.4 (3)
Prostaglandin E_2 (1 μM)	6.4 ± 0.5 (5)	ND
NaF (10 mM)	1.6 ± 0.3 (4)	ND

The responses to all agents were significantly ($P<0.05$) larger than unstimulated values for [^{3}H]-cyclic AMP accumulation.
ND = not determined. All responses are given as the mean fold stimulation over basal in n separate experiments 3-Isobutyl-1-methylxanthine (IBMX) (0.1 mM) alone produced a 1.8 fold increase over basal.

Effects of carbachol upon isoprenaline-stimulated cyclic AMP responses

In order to examine for the possibility of the involvement of muscarinic receptor stimulation in inhibiting adenylyl cyclase activity in human cultured tracheal smooth muscle cells, the effect of the muscarinic agonist, carbachol, on isoprenaline-stimulated cyclic AMP formation was examined (Figure 8). Carbachol produced concentration-dependent inhibition of the [^{3}H]-cyclic AMP response to 1 μM isoprenaline, with an IC_{50} value of $2.4 \pm 0.2 \times 10^{-7}$ M ($n = 6$). Carbachol (1 μM) inhibited the response to 1 μM isoprenaline by $60 \pm 1\%$ ($n = 8$, $P<0.001$). The effect of carbachol was itself inhibited by atropine (50 nM) (K_A $2.3 \pm 0.5 \times 10^9$ M^{-1}, $n = 4$), indicating the involvement of a muscarinic receptor in this response (Figure 9).

Discussion

In this paper, we describe the characteristics of the cyclic AMP responses to a range of agents in primary cultures of human tracheal smooth muscle grown from tissue explants. Elevation of cellular cyclic AMP content in primary cultures of human tracheal smooth muscle cells was observed following stimulation with isoprenaline, prostaglandin E_2, inhibition of phosphodiesterase activity by nonselective and type

Table 2 Effect of phosphodiesterase inhibitors on [^{3}H]-cyclic AMP responses in human tracheal smooth muscle cells

Agent	Fold stimulation over control	
	− Isoprenaline (n)	+ Isoprenaline (1 μM) (n)
IBMX (0.1 mM)	1.8 ± 0.3* (9)	2.1 ± 0.2* (9)
Rolipram (0.1 mM)	1.5 ± 0.2* (9)	1.0 ± 0.1 (9)
SK&F 94120 (0.1 mM)	1.0 ± 0.1 (4)	0.8 ± 0.1 (4)
SK&F 94836 (0.1 mM)	1.0 ± 0.2 (8)	0.9 ± 0.1 (5)

*$P < 0.05$ compared with control.
The response to 1 μM isoprenaline alone was 9.5 ± 1.3 fold over control. The responses shown in the presence of isoprenaline are the fold stimulation compared with the response to 1 μM isoprenaline alone. Responses shown are the mean (± s.e.mean) values relative to either unstimulated or 1 μM isoprenaline-stimulated cells obtained from *n* separate experiments. IBMX = 3-isobutyl-1-methylxanthine.

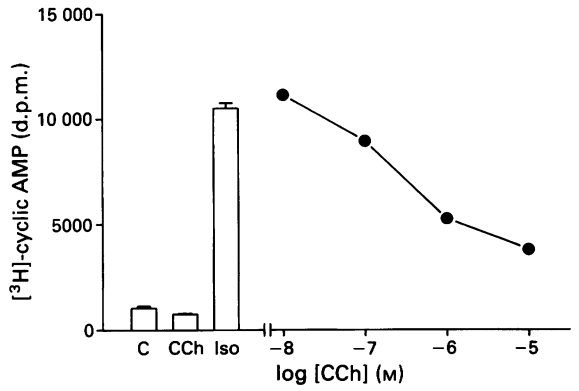

Figure 8 The inhibition of the [^{3}H]-cyclic AMP response to 1 μM isoprenaline by varying concentrations of carbachol (CCh) (●). The control response to 1 μM isoprenaline is shown by the column marked Iso and the basal (unstimulated) level by the column marked C. Each point represents the mean (± s.e.mean, vertical bars) of triplicate determinations in a single experiment which was repeated three times with similar results. The effect of 1 mM carbachol alone on [^{3}H]-cyclic AMP formation is shown in the column marked CCh.

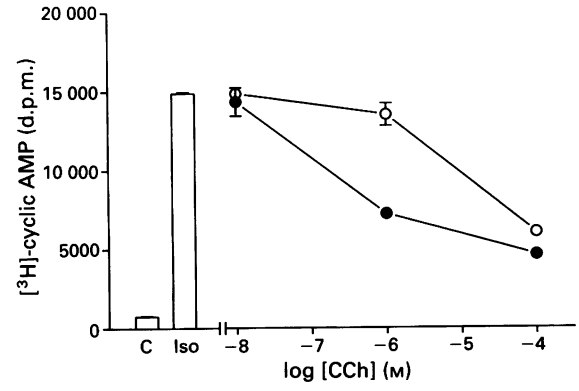

Figure 9 The effect of atropine (50 nM) (○) on the inhibition of the [^{3}H]-cyclic AMP response to 1 μM isoprenaline by varying concentrations of carbachol (CCh) (●). The control response to isoprenaline (1 μM) is shown by the column marked Iso and the basal response by the column marked C. Each point represents the mean (± s.e.mean, vertical bars) of triplicate determinations in a single experiment which was repeated three times with similar results.

IV (cyclic AMP)-selective phosphodiesterase inhibitors, and by direct stimulation of adenylyl cyclase or G_s by forskolin and NaF respectively. Both prostaglandin E_2 and isoprenaline induced concentration-related cyclic AMP formation in human cultured tracheal smooth muscle. The response to isoprenaline was inhibited by the β_2-adrenoceptor-selective antagonist, ICI 118551 (Bilski *et al.*, 1983), indicating the probable involvement of the β_2-receptor subtype in this response. The observed K_A value of 1.4×10^9 M^{-1}, is similar to the value previously reported for inhibition of β_2-responses in guinea-pig atria (Bilski *et al.*, 1983), and for the β_2-receptor-mediated inhibition of histamine-stimulated inositol phosphate formation in bovine tracheal smooth muscle slices (Hall & Hill, 1988), but approximately 100 fold higher than the value for inhibition of β_1-receptor responses in uterus (Bilski *et al.*, 1983). However, when concentrations of isoprenaline producing maximal cyclic AMP responses were used, 50 nM ICI 188551 produced a greater degree of inhibition than would have been expected from the data obtained with 10 nM ICI 118551 using lower concentrations of isoprenaline as agonist. The explanation for this observation is not clear, although one possibility is that with the higher concentration of ICI 118551, the antagonist may be behaving in a noncompetitive manner. This possibility would be worthy of further study in other cell lines expressing β_2-adrenoceptors.

The adenylyl cyclase activator forskolin, as would be expected, also induced [^{3}H]-cyclic AMP formation, the response being nonmaximal over the concentration-range examined (10 nM − 100 μM). In addition, NaF also produced elevation of cell cyclic AMP content, presumably through activation of G_s. These data are in keeping with previous observations in bovine tracheal smooth muscle, where NaF produced significant elevation of cyclic AMP levels (Hall *et al.*, 1990a). In this latter study, NaF also inhibited forskolin-induced cyclic AMP formation, presumably by a direct action on G_i.

A range of phosphodiesterase isoenzymes are present in smooth muscle homogenates from both human (Torphy & Undem, 1991) and animal (Torphy & Cieslinski, 1990; Nicholson *et al.*, 1991; Shahid *et al.*, 1991) airways. We have previously shown that in bovine trachealis muscle, the type IV enzyme is important in controlling tone (Hall *et al.*, 1990b,c) and cyclic AMP content (Hall *et al.*, 1989). Rolipram is an effective and potent inhibitor of the type IV isoenzyme in homogenates from this tissue (Nicholson *et al.*, 1990). The role for the type III isoenzyme remains less clear. Inhibitors of the type III isoenzyme have been shown to produce small degrees of relaxation of precontracted airway smooth muscle preparations from a range of species at concentrations similar to those used in the present study, although these agents do not necessarily elevate whole tissue cyclic AMP content (Gristwood *et al.*, 1986; Silver *et al.*, 1988; Torphy *et al.*, 1988; Hall *et al.*, 1989; 1990b). This may be due to a degree of compartmentalisation within the cell of phosphodiesterase isoenzymes and/or pools of cyclic AMP. The results obtained in the present study are consistent with this suggestion. We observed increases in both basal and isoprenaline-induced cyclic AMP responses in the presence of the nonselective phosphodiesterase inhibitor, IBMX. In keeping with previous observations, the absolute rise in cyclic

AMP levels seen with IBMX in the absence of another agent to stimulate adenylyl cyclase was small, suggesting that the basal level of cyclic AMP production in tracheal smooth muscle cells is low. Rolipram, an inhibitor of the high K_m, cyclic AMP hydrolysing isoenzyme present in human airway smooth muscle (Torphy & Undem, 1991) and a potent bronchodilator *in vivo* (Harris *et al.*, 1989) elevated basal cyclic AMP levels in human cultured tracheal smooth muscle cells, and at concentrations selective for the type IV isoenzyme produced a small potentiation of the response to 1 μM isoprenaline with an EC_{50} of 0.3 μM, similar to that reported in other animal studies (Shahid *et al.*, 1991; Torphy & Undem, 1991). However, high (> 10 μM) concentrations of rolipram had no significant effect upon isoprenaline-induced cyclic AMP formation. The type III (low K_m cyclic AMP hydrolysing) phosphodiesterase isoenzyme inhibitors, SK&F 94120 and SK&F 94836, (Reeves *et al.*, 1987; Torphy *et al.*, 1988) were without significant effect upon basal cyclic AMP levels. The effects of these agents upon basal levels of cyclic AMP accumulation are similar to those previously reported in bovine trachealis (Hall *et al.*, 1989). The lack of effect of high (as opposed to low) concentrations of rolipram upon isoprenaline-stimulated cyclic AMP formation does, however, remain to be explained.

In some cell types, muscarinic receptor stimulation inhibits adenylyl cyclase activity through stimulation of M_2 or M_4 receptor subtypes. In the present study, marked reduction of the cyclic AMP response to isoprenaline was observed in the presence of the muscarinic agonist, carbachol. These results are in agreement with previous observations in canine trachealis (Jones *et al.*, 1987; Torphy *et al.*, 1987; Sankary *et al.*, 1988) but in contrast to findings in whole tissue from bovine trachealis (Hall *et al.*, 1990c). The results in the study described in this paper would argue for the presence of an inhibitory effect of muscarinic receptor stimulation on cyclic AMP levels in human airway smooth muscle. A similar inhibitory effect of carbachol on isoprenaline-induced cyclic AMP formation was observed in a recent study in canine tracheal smooth muscle cells (Yang *et al.*, 1991).

In primary cultures of human tracheal smooth muscle, cyclic AMP responses to isoprenaline, forskolin and phosphodiesterase inhibitors remained stable over a period of at least 8 cell passages, demonstrating that primary cultures of human tracheal smooth muscle cells provide a potentially useful model system for the study of the regulation of airway cyclic AMP responses. The response to isoprenaline in cells from passages 4 to 12 was similar to the response seen in acutely dissociated cells grown to confluence in short term cultures. It was also hoped to compare the response in cultured cells with the response in acutely dissociated cells *ex vivo* but inadequate cell numbers precluded accurate estimation of concentration-response curves in the acutely dissociated cell preparations. Even if this were possible, however, collagenase treatment could potentially affect cell surface receptor number. Further evidence to suggest that coupling of the β-adrenoceptor to adenylyl cyclase in cultured cells is similar to coupling *in vivo* is provided from the observation that the EC_{50} value for isoprenaline induced cyclic AMP formation in the cultured cells compares well with the value obtained for this response in previous studies of canine trachealis muscle (about 0.2 μM, Fujiwara *et al.*, 1988).

The concentration-response curve for isoprenaline-induced cyclic AMP formation in primary cultures of human tracheal smooth muscle cells, and in previous studies of canine tracheal smooth muscle *ex vivo*, both lie approximately one log point to the right of the concentration-response curve for relaxation of human airway preparations (de Jongste *et al.*, 1989). This would imply that a significant spare receptor reserve exists for β_2-adrenoceptor-induced cyclic AMP formation in human airway smooth muscle.

In conclusion, this study describes the characteristics of the cyclic AMP responses to isoprenaline, prostaglandin E_2, forskolin, NaF, nonselective phosphodiesterase inhibition and a range of phosphodiesterase inhibitors in primary cultures of human tracheal smooth muscle cells. These responses are quantitatively and qualitatively similar to those previously described in *ex vivo* airway smooth muscle preparations from other species. We conclude that primary culture of human tracheal smooth muscle cells provide a useful model system for the study of the regulation of cyclic AMP responses in human airway smooth muscle.

References

BARNES, P.J. (1986). Bronchodilator mechanisms. In *Asthma: Clinical Pharmacology and Therapeutic Progress*. ed. Kay, A.B. pp. 146–160. Oxford: Blackwell.

BILSKI, A.J., HALLIDAY, S.E., FITZGERALD, J.D. & WALE, J.L. (1983). The pharmacology of a beta 2 selective adrenoceptor antagonist (ICI 118551). *J. Cardiovasc. Res.*, **5**, 430–437.

DONALDSON, J., HILL, S.J. & BROWN, A.M. (1988). Kinetic studies on the mechanism by which histamine H1 receptors potentiate cyclic AMP accumulation in guinea-pig cerebral cortical slices. *Mol. Pharmacol.*, **33**, 626–633.

FUJIWARA, T., SUMIMOTO, K., ITOH, T., SUZUKI, H. & KURIYAMA, H. (1988). Relaxing actions of procaterol, a β_2-adrenoceptor stimulant, on smooth muscle cells of the dog trachea. *Br. J. Pharmacol.*, **93**, 199–209.

GRISTWOOD, R.W., EDEN, R.J., OWEN, D.A.A. & TAYLOR, E.M. (1986). Pharmacological studies with SK&F 94120, a novel positive inotropic agent with vasodilator activity. *J. Pharm. Pharmacol.*, **38**, 452–459.

HALL, I.P., DONALDSON, J. & HILL, S.J. (1989). Inhibition of histamine stimulated inositol phospholipid hydrolysis by agents which increase cyclic AMP levels in bovine tracheal smooth muscle. *Br. J. Pharmacol.*, **97**, 603–613.

HALL, I.P., DONALDSON, J. & HILL, S.J. (1990a). Modulation of fluoroaluminate-induced inositol phosphate formation by increases in tissue cyclic AMP content in bovine tracheal smooth muscle. *Br. J. Pharmacol.*, **100**, 646–650.

HALL, I.P., DONALDSON, J. & HILL, S.J. (1990c). Modulation of carbachol-induced inositol phosphate formation in bovine tracheal smooth muscle by cyclic AMP phosphodiesterase inhibitors. *Biochem. Pharmacol.*, **39**, 1357–1363.

HALL, I.P. & HILL, S.J. (1988). β-Adrenoceptor stimulation inhibits histamine-stimulated inositol phospholipid hydrolysis in bovine tracheal smooth muscle. *Br. J. Pharmacol.*, **95**, 1204–1212.

HALL, I.P., WALKER, D., HILL, S.J. & TATTERSFIELD, A.E. (1990b). Effect of isozyme selective phosphodiesterase inhibitors on bovine tracheal smooth muscle tone. *Eur. J. Pharmacol.*, **183**, 1096–1097.

HALL, I.P., TOWNSEND, P., DAYKIN, K. & WIDDOP, S. (1992). Control of tissue cyclic AMP content in primary cultures of human airway smooth muscle cells. *Br. J. Pharmacol.*, **105**, 71P.

HARRIS, A.L., CONNELL, M.J., FERGUSON, E.W., WALLACE, A.M., GORDON, R.J., PAGANI, E.D. & SILVER, P.J. (1989). Role of low Km cyclic AMP phosphodiesterase inhibition in tracheal relaxation and bronchodilation in the guinea pig. *J. Pharmacol. Exp. Ther.*, **251**, 199–206.

JONES, C.A., MADISON, J.M., TOM-MOY, M. & BROWN, J.K. (1987). Muscarinic cholinergic inhibition of adenylate cyclase in airway smooth muscle. *Am. J. Physiol.*, C97–104.

DE JONGSTE, J.C., MONS, H., BONTA, I.L. & KERRIBIJN, K.F. (1989). Relaxation of human peripheral airway smooth muscle preparations in vitro does not correlate with severity of chronic airflow limitation in vivo. *Pulmonary Pharmacol.*, **2**, 75–79.

KOTLIKOFF, M.I. (1990). Potassium currents in canine airway smooth muscle cells. *Am. J. Physiol.*, **259**, L384–395.

KUME, H., TAKAI, A., TOKUNO, H. & TOMITO, T. (1989). Regulation of Ca^{2+}-dependent K^+-channel activity in tracheal myocytes by phosphorylation. *Nature*, **341**, 152–154.

MUELLER, E. & VAN BREEMAN, C. (1979). Role of intracellular Ca^{2+} sequestration in beta adrenergic relaxation of airway smooth muscle. *Nature*, **281**, 682–683.

NICHOLSON, C.D., CHALLISS, R.A.J. & SHAHID, M. (1991). Differential modulation of tissue function and therapeutic potential of selective inhibitors of cyclic nucleotide phosphodiesterase isoenzymes. *Trends Pharmacol. Sci.*, **12**, 19–27.

NICHOLSON, C.D., SHAHID, M., VAN AMSTERDAM, R.G.M. & ZAAGSMA, J. (1990). Cyclic nucleotide phosphodiesterase (PDE) isoenzymes in bovine tracheal smooth muscle and the ability of isoenzyme inhibitors to relax precontracted preparations. *Eur. J. Pharmacol.*, **183**, 1097–1098.

REEVES, M.L., LEIGH, B.K. & ENGLAND, P.J. (1987). The identification of a new cyclic nucleotide phosphodiesterase activity in bovine and guinea pig cardiac ventricle. *Biochem. J.*, **241**, 535–541.

RUCK, A., KENDALL, D.A. & HILLS, S.J. (1991). Alpha and beta adrenergic regulation of cyclic AMP accumulation in cultured rat astrocytes. *Biochem. Pharmacol.*, **42**, 59–69.

SANKARY, R.M., JONES, C.A., MADISON, J.M. & BROWN, J.K. (1988). Muscarinic cholinergic inhibition of cyclic AMP accumulation in airway smooth muscle: role of a pertussis toxin sensitive protein. *Am. Rev. Resp. Dis.*, **138**, 145–150.

SHAHID, M., VAN AMSTERDAM, R.G.M., DE BOER, J., TEN BERGE, R.E., NICHOLSON, C.D. & ZAAGSMA, J. (1991). The presence of five cyclic nucleotide phosphodiesterase isoenzyme activities in bovine tracheal smooth muscle and the functional effects of selective inhibitors. *Br. J. Pharmacol.*, **104**, 471–477.

SILVER, P.J., HAMEL, L.T., PERRONE, M.H., BENTLEY, R.G., BUSHOVER, C.R. & EVANS, D.B. (1988). Differential pharmacologic sensitivity of cyclic nucleotide phosphodiesterase isoenzymes isolated from cardiac muscle, arterial and airway smooth muscle. *Eur. J. Pharmacol.*, **150**, 85–94.

SILVER, P.J. & STULL, J.T. (1982). Regulation of myosin light chain kinase and phosphorylase phosphorylation in tracheal smooth muscle. *J. Biol. Chem.*, **257**, 6145–6150.

TORPHY, T.J., BURMAN, M., HUANG, L.B.F., HOROHONICH, S. & CIESLINSKI, L.B. (1987). Regulation of cAMP content and cAMP dependent protein kinase activity in airway smooth muscle. *Prog. Clin. Biol. Res.*, **245**, 263–275.

TORPHY, T.J., BURMAN, M., HUANG, L.B.F. & TUCKER, S.S. (1988). Inhibition of the low Km cyclic AMP phosphodiesterase of SK&F 94836: mechanical and biochemical responses. *J. Pharmacol. Exp. Ther.*, **246**, 843–850.

TORPHY, T.J. (1988). In *Directions for new Anti-Asthmatic Drugs*. ed. O'Donnel, S.R. & Persson, C.G.A. pp. 37–58. London: Birkhauser-Verlag.

TORPHY, T.J. & CIESLINSKI, L.B. (1990). Characterisation and selective inhibition of cyclic nucleotide phosphodiesterase isoenzymes in canine tracheal smooth muscle. *Mol. Pharmacol.*, **37**, 206–214.

TORPHY, T.J. & UNDEM, B.J. (1991). Phosphodiesterase inhibitors: new opportunities for the treatment of asthma. *Thorax*, **46**, 512–523.

YANG, C.M., CHOU, S.P. & SUNG, T.-C. (1991). Muscarinic receptor subtypes coupled to generation of different second messengers in isolated tracheal smooth muscle cells. *Br. J. Pharmacol.*, **104**, 613–618.

(Received February 17, 1992
Revised May 19, 1992
Accepted June 3, 1992)

Br. J. Pharmacol. (1992), **107**, 429–436

Tachykinin receptors in rabbit airways — characterization by functional, autoradiographic and binding studies

[1]J.L. Black, L.M. Diment, L.A. Alouan, P.R.A. Johnson, *C.L. Armour, †T. Badgery-Parker & †E. Burcher

Departments of Pharmacology and *Pharmacy, The University of Sydney, and †School of Physiology and Pharmacology, University of NSW, NSW, Australia

1 In many species, both NK_1 and NK_2 tachykinin receptors appear to be important in mediating the contraction of airway smooth muscle. We have examined the distribution and characterization of receptors for tachykinins in rabbit airways using functional length tension studies, autoradiography and radioligand binding studies.

2 Contractile responses to tachykinins were elicited in four different areas of the respiratory tree – trachea, and three progressively more distal areas of the right bronchus. The NK_2 receptor-preferring agonists, neurokinin A (NKA), neuropeptide gamma (NPγ) and the NK_2-selective [Lys^5 $MeLeu^9$, Nle^{10}]-NKA(4–10) [NKA (4–10) analogue] produced similar contraction in all four areas. Substance P (SP) and the NK_1-selective [Sar^9,$Met(O_2)^{11}$]-SP (Sar-SP) exhibited a marked location-dependence in the magnitude of contraction, producing minimal contraction in the trachea and more proximal bronchi with contractions becoming progressively larger in the more distal airways. Senktide (which is selective for the NK_3 receptor) produced negligible contraction in all areas.

3 The NK_2-selective antagonist, MDL29,913, was a weak antagonist of NKA and NKA(4–10) analogue. At a concentration of 2 μM, it produced a small but significant shift in the response curve to NKA and a greater shift (8 fold) in the curve to NKA(4–10) analogue, but it had no effect on responses to Sar-SP. The non peptide NK_1 receptor antagonist, CP-96,345, was also unexpectedly weak in this preparation. The pD_2 value for Sar-SP was decreased 27 fold by CP-96,345 at a concentration of 1 μM, without alteration in the maximum response.

4 Autoradiographic binding sites to [^{125}I]-NKA were sparse over smooth muscle in proximal airway preparations and markedly increased in density in the more distal airways. There was negligible binding over vascular smooth muscle and epithelium.

5 Radioligand binding studies revealed binding to [^{125}I]-NKA which was 82% specific. The order of potency for inhibition of [^{125}I]-NKA binding was SP > = Sar-SP > NKA = NPγ > CP-96,345 > NKA (4–10) analogue > NKB ⋙ MEN 10207 (the NK_2 subtype selective antagonist) > MDL 29,913 > senktide. This profile indicates binding predominantly to NK_1 receptors.

6 These results suggest that there are at least two types of tachykinin receptors in rabbit airways, a population of NK_1 receptors, the density of which is greatest in the periphery and, in addition, NK_2 receptors which are uniformly distributed throughout the airways. These receptors have unusual characteristics in that the NK_1 antagonist, CP-96,345 and the NK_2 antagonist, MDL 29,913 respectively exhibited only weak potency.

Keywords: Tachykinin receptor; rabbit airways; autoradiography; radioligand binding; functional studies in airway muscle.

Introduction

The properties of tachykinins, which include bronchial smooth muscle contraction (Lundberg *et al.*, 1983; Advenier *et al.*, 1987), mucus secretion, changes in vascular permeability (Barnes, 1991) and modulation of neural responses (Black *et al.*, 1990b) raise the possibility that they play a significant role in the pathogenesis of airway diseases such as asthma. If this is so then specific tachykinin antagonists may be of importance in future therapeutic strategies and this underlines the importance of identifying the receptors which mediate these effects.

Three general classes of tachykinin receptors have been proposed: NK_1, NK_2 and NK_3 for which substance P (SP), neurokinin A (NKA) and neurokinin B (NKB) are the preferred endogenous ligands respectively (Buck & Burcher, 1986; Guard & Watson, 1991). However, they are not absolutely selective for their preferred receptor type, and several new agonists, more selective than the natural tachykinins, are now available. These include [Sar^9,$Met(O_2)^{11}$]-SP (Sar-SP) for the NK_1 receptor, [Lys^5,$MeLeu^9$,Nle^{10}]-NKA(4–10) (Chassaing *et al.*, 1991) for the NK_2 receptor and senktide for the NK_3 receptor. Recently, selective peptide antagonists for NK_2 receptors have been developed (Maggi *et al.*, 1991; van Giersbergen *et al.*, 1991). In addition, highly selective non-peptide antagonists e.g. CP-96,345, may discriminate between subtypes of the NK_1 receptor in different species (Snider *et al.*, 1991; McLean *et al.*, 1991; Gitter *et al.*, 1991; Rouissi *et al.*, 1991).

We have previously reported that the contractile response to substance P in the rabbit is proportionately greater in the distal rather than the proximal airways (Black *et al.*, 1990a). In that study, the density of autoradiographically visualised binding sites for [^{125}I]-Bolton-Hunter SP (BHSP) showed a similar marked location-dependence. This non-uniform distribution of receptors has been reported for other agonists and in other species. Receptors for histamine are more numerous in the distal airways of the rabbit whereas those for carbachol are located more proximally (Armour *et al.*, 1984). In human airways, neuropeptide receptor distribution is also location-dependent. Receptors for vasoactive intestinal peptide are localized to the large airways (Palmer *et al.*, 1986) while those for SP and NKA may be concentrated in the periphery (Frossard & Barnes, 1991).

[1] Author for correspondence at Department of Pharmacology, University of Sydney, New South Wales, Australia, 2006.

In many species, both NK_1 and NK_2 tachykinin receptors appear to be important in contraction of airway smooth muscle (Ireland *et al.*, 1991; Maggi *et al.*, 1991) but whether this is the case for rabbits is not known. Interpretation of earlier studies is complicated by the lack of selectivity of the endogenous tachykinins and by regional differences in receptor distribution (Cook *et al.*, 1990; Black *et al.*, 1990a). In this study, we have used selective tachykinin receptor agonists and antagonists to investigate contractile effects throughout rabbit airways. We have carried out parallel autoradiographic studies to determine the regional distribution of binding sites for the NK_2 receptor-preferring radioligand [^{125}I]-NKA and, at the location of greatest density of these binding sites, have characterized the receptors using radioligand binding with compounds with known specificity for the three different receptor types.

Methods

Functional studies

New Zealand White rabbits were killed by cervical dislocation, the trachea and lungs removed *en bloc* and placed into Krebs-Henseleit solution (composition mM: NaCl 118.4, KCl 4.7, $CaCl_2 2H_2O$ 2.5, $MgSO_4.7H_2O$ 1.2, KH_2PO_4 1.2, $NaHCO_3$ 25.0, and (+)-glucose 11.1) which was continually aerated with 5% CO_2 in O_2. Four areas of the respiratory tree were selected for study, an area from the middle portion of the trachea (T_1) and three areas of the right main bronchus (B_1, B_2, B_3 respectively) (Figure 1), and this selection process was followed for each experiment. Ring preparations in duplicate from each area, were dissected as previously (Black *et al.*, 1988). Tracheal preparations were suspended under a 2 g load and bronchial preparations under a 1 g load (Armour *et al.*, 1988) in siliconized organ baths containing Krebs-Henseleit solution at 37°C aerated with 5% CO_2 in O_2. Over a 1–2 h equilibration period, the load was readjusted to the initial value and the preparations were washed every 20 min by exchange of the bath fluid. Changes in tension in response to addition of drugs were measured isometrically with Grass FTO3 transducers and recorded on a Grass polygraph. At the end of the equilibration period, when baseline tone was established, phosphoramidon (10 μM) was added to each tissue to inhibit endogenous endopeptidase. Cumulative concentration-responses to NKA, NKA(4–10) analogue, Sar-SP, senktide and NPγ were then constructed in each preparation. In a separate series of experiments we investigated the activity of the NK_2 receptor antagonist, MDL 29,913 and the NK_1 antagonist, CP-96,345. For these studies, 4 bronchial rings taken from areas B2 and B3 as above were selected in each experiment. After the initial equilibration period, a contractile response was elicited to 1 mM acetylcholine. After the contraction had reached a plateau, the tissues were washed and baseline tone re-established at which stage phosphoramidon (10 μM) was added. Tissues were studied in pairs and in duplicate. In one member of each pair, response curves to the agonist (NKA, Sar-SP, NKA(4–10) analogue, or NPγ) alone were elicited and in the other, responses were obtained in the presence of the antagonist (either MDL 29,913 or CP-96,345) which was added approximately 20 min before the start of the agonist-response curve.

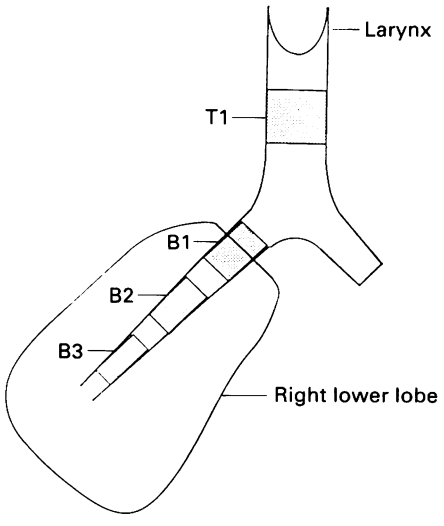

Figure 1 Diagrammatic representation of the rabbit respiratory tree depicting the areas of trachea (T1) and proximal, mid, and distal bronchus (B1, B2 and B3 respectively) used for study in both the functional and autoradiography experiments.

Functional studies – data analysis

From each response relationship a curve was constructed in which increasing log concentrations of agonist were plotted either against mg tension or, in the case of the antagonist studies, expressed as a percentage of the contraction induced by acetylcholine. From this curve an EC_{50} (the concentration of agonist which produced half the maximum response) and thence a pD_2 value was calculated. Mean pD_2 values and s.e.mean were then calculated for each type of airway preparation and in the absence and presence of antagonists. Subsequently, mean concentration-response curves were constructed from all experiments. Mean values for actual T_{max} (mg) were also calculated from all experiments. Statistical comparison were made between values obtained for the most NK_1 selective agonist, Sar-SP, and the most NK_2 selective, NKA(4–10) analogue. Differences between values for T_{max} and between mean pD_2 values were assessed by means of 2-tailed Student's *t* test for paired data. Differences were considered significant at $P<0.05$.

Autoradiographic studies

New Zealand White rabbits were killed as described above ($n = 3$). Tissuc segments corresponding to those used in the functional studies were then frozen above liquid nitrogen and stored at −70°C before sectioning: 10 μm sections were cut with a cryostat and thaw-mounted onto gelatin subbed slides.

Sections from each segment were preincubated in 50 mM Tris-HCl buffer (pH 7.4) with 0.02% bovine serum albumin (BSA) for 15 min then in the same solution at 25°C for 2 h with $MnCl_2$, the peptidase inhibitors chymostatin (4 mg ml^{-1}) and leupeptin (2 mg ml^{-1}), bacitracin (40 mg ml^{-1}) and the neutral endopeptidase inhibitor phosphoramidon 10 μM (Black *et al.*, 1990a) plus 0.07 nM [^{125}I]-NKA. After incubation, sections were washed in ice cold Tris-HCl buffer at pH 7.4 with 0.02% BSA, then briefly washed in ice cold distilled water and rapidly dried. Non specific binding was determined by treating alternate serial sections in the same manner but with the addition of 1 μM non-labelled NKA in the incubation mixture. Sections were stored at 4°C overnight in a vacuum desiccator to complete the drying process.

Coverslips which had been previously coated with Kodak NTB3 nuclear emulsion (diluted 1:1 with distilled water) were placed in apposition to the slides and stored for 7 days at 0–4°C. The slide/coverslip assemblies were developed at 18°C with film strength Kodak D19 developer for 4 min, then rinsed in water and fixed for 6 min in Kodafix or 30% sodium thiosulphate and then washed for 6 min in water. Sections were then stained with 1% methyl green pyronin and coverslips placed permanently in apposition with DPX mounting medium.

Autoradiographic studies – data analysis

Sections were viewed with an Olympus BH2 microscope with bright and dark field illumination. In order to avoid bias, slides were coded by one investigator. Density of specific

binding sites over smooth muscle was graded independently by two investigators using a scale from 0 (no binding sites visualised) to 5 (very dense binding). Sections from each of the 4 areas studied (25 sections in total) were observed in this manner from 1 rabbit and the remaining slides from the other two rabbits viewed by one investigator only. Correlation coefficients for the grading by the two investigators were obtained by linear regression analysis using the method of least squares.

Radioligand binding studies

In a separate series of experiments a further 4 rabbits were killed as described above. After the lungs were removed the areas containing trachea and hilar bronchus were discarded as was the outer parenchyma. The remaining tissue which thus contained the bronchus designated as B2 and B3 as depicted in Figure 1, was frozen and used for binding studies.

Lung tissue was finely diced, suspended in ice-cold 50 mM Tris HCl (pH 7.4, 4°C) containing NaCl (120 mM) and KCl (5 mM) and homogenized in a Kinematica GmbH Krienz-Luzern polytron (setting 6) for 30 s. The tissue suspensions were centrifuged in a Beckman J2-21 centrifuge at 17500 *g* at 4°C for 20 min. The supernatant was discarded and the pellet resuspended in 50 mM Tris HCl (pH 7.4, 4°C) containing KCl (300 mM) and EDTA (10 mM) for 60 min before repeating centrifugation. Pellets were resuspended in 50 mM Tris HCl (pH 7.4, 4°C) centrifuged as before and the procedure repeated before finally suspending the tissues in incubation buffer consisting of 50 mM Tris HCl (pH 7.4, 25°C), $MnCl_2$ (3 mM), bovine serum albumin (BSA) (0.02%) and the peptidase inhibitors chymostatin (4 $\mu g\ ml^{-1}$) and phosphoramidon (10 μM) as previously described (Geraghty *et al.*, 1992).

Aliquots (250 μl) of the tissue homogenate (final concentration 3%) were incubated at 25°C for 1 h with 0.08 nM [^{125}I]-NKA and incubation buffer (pH 7.4) in the absence and presence of competing agents to give a total volume of 500 μl. Nonspecific binding was defined by use of 1 μM NKA. Incubations were terminated by rapid filtration and washing with ice cold Tris (containing $MnCl_2$ and BSA). Bound radioligand was quantified with a Packard Minaxi gamma counter (72% efficiency).

Radioligand binding studies – data analysis

Raw d.p.m. were processed by the computer programme EBDA in conjunction with the nonlinear iterative curve fitting programme LIGAND. The *F*-test was used to determine whether the data fitted a multiple-site model rather than a single site model. A *P* value of less than 0.05 was considered to be statistically significant.

Chemicals

Neurokinin A (NKA), neuropeptide gamma (NPγ), [Sar^9,Met$(O_2)^{11}$]-SP (Sar-SP), senktide, and MDL 29,913 (cyclo [Gln-Trp-Phe-Gly-Leu-CH_2NCH_3-Leu]) were obtained from Auspep, Victoria, Australia. [Lys^5,MeLeu^9,Nle^{10}]-NKA(4–10) [NKA(4–10) analogue] was kindly donated by Dr S. Laviellle, Université Pierre et Marie Curie, Paris. [^{125}I]-NKA was purchased from Amersham and the specific activity was 2,000 Ci $mmol^{-1}$. Chymostatin, leupeptin, bacitracin and phosphoramidon (N-αrhamnopyranosyl-oxyhydroxyphosphinyl-L-leucyl L-tryptophan ammonium salt) and Tris buffer were all obtained from Sigma Chemical Co. CP-96,345 ([2S,3S)-cis-2-(diphenylmethyl)-N-(2-methoxyphenyl)methyl]-1-azabicyclo [2.2.2]octan-3-amine mandelate) was a gift from Dr S.H. Buck, Marion Merrell Dow Research Institute, Cincinnati, U.S.A., MEN 10,207 (Asp-Tyr-DTrp-Val-DTrp-DTrp-Arg-NH_2) was a kind gift from Dr C.A. Maggi, Menarini Pharmaceuticals, Italy. NKA, NPγ, Sar-SP and NKA(4–10) analogue were all dissolved in dilute acetic acid (0.01 mM) to form stock solutions which were stored at −70°C in plastic vials.

Dilutions of the peptides for use in the functional studies were made in Krebs-Henseleit solution and kept on ice for the duration of each experiment. All pipettes and containers used were plastic and organ baths were siliconized with Coatasil (Ajax Chemicals, Australia). All other reagents were of analytical grade.

Results

Functional studies

Agonist studies All tachykinins studied produced concentration-dependent contraction in the rabbit airways except for senktide, which produced only a weak response at the highest concentration used (4.2 ± 1.9% of the acetylcholine maximal response at 1 μM, $n = 4$). Responses to NKA, NPγ and NKA(4–10) analogue were very similar and the magnitude of the contraction in all four areas studied was comparable (Table 1). However Sar-SP exhibited a marked location-dependence in the magnitude of contraction. Unlike NKA, NPγ and NKA(4–10) analogue, which gave appreciable contraction in the more proximal airway preparations (T1 and B1, Table 1), Sar-SP in all 4 rabbits studied produced minimal contraction in the tracheal and more proximal bronchial preparations. Conversely, contractions to Sar-SP became progressively larger in the more distal preparations (Table 1). Thus the efficacy of NKA(4–10) analogue in tracheal and bronchial segments (T1 and B1 respectively) was significantly greater ($P < 0.01$) than that in response to Sar-SP (Table 1).

The potency of all the tachykinins was similar although, as above, Sar-SP was a weak agonist in tracheal preparations. Sar-SP was significantly more potent ($P < 0.05$) in the more distal preparations (B2 and B3) than NKA4–10 analogue (Table 2).

The values for the maximal tension generated by the four tachykinins in the different regions of the airways and the pD_2 are shown in Tables 1 and 2.

Table 1 Contractile responses to neurokinin A (NKA), [Sar^{9}Met$(O_2)^{11}$]-substance P (Sar-SP), neuropeptide gamma (NPγ) and [Lys^{5}MeLeu^{9}Nle^{10}]-NKA(4–10) [NKA(4–10) analogue] in the 4 areas of the rabbit airways depicted in Figure 1

	T1	*B1*	*B2*	*B3*
NKA	3178	3460	4341	3040
	(358)	(303)	(679)	(691)
NPγ	5347	4672	6613	5018
	(898)	(958)	(983)	(1135)
NKA(4–10) analogue	4538**	5440**	4758	3717
	(615)	(139)	(880)	(560)
Sar-SP	240	1811	3388	5055
	(174)	(575)	(941)	(1295)

Mean values from 4–7 rabbits for maximal tension (mg) are shown together with s.e. in parentheses.
**indicates significant difference ($P \leq 0.01$) from corresponding values for Sar-SP.

Table 2 Mean pD_2 values with s.e. from 4–7 rabbits for neurokinin A (NKA), [Sar^{9}Met$(O_2)^{11}$]-substance P (Sar-SP), neuropeptide γ (NPγ) and [Lys^{5}MeLeu^{9}Nle^{10}]-NKA(4–10) [NKA (4–10) analogue] in the 4 areas of the rabbit airways depicted in Figure 1

	T1	*B1*	*B2*	*B3*
NKA	8.0 ± 0.2	8.1 ± 0.2	8.0 ± 0.2	7.7 ± 0.2
NPγ	8.8 ± 0.1	8.8 ± 0.2	8.5 ± 0.1	8.4 ± 0.1
NKA(4–10) analogue	8.6 ± 0.4	7.8 ± 0.2	7.5 ± 0.3*	7.4 ± 0.1*
Sar-SP	—	8.7 ± 0.2	8.9 ± 0.2	9.1 ± 0.3

* indicates significant difference ($P<0.05$) from corresponding values for Sar-SP.
— denotes the fact that no pD_2 value could be obtained for Sar-SP in the tracheal segments.

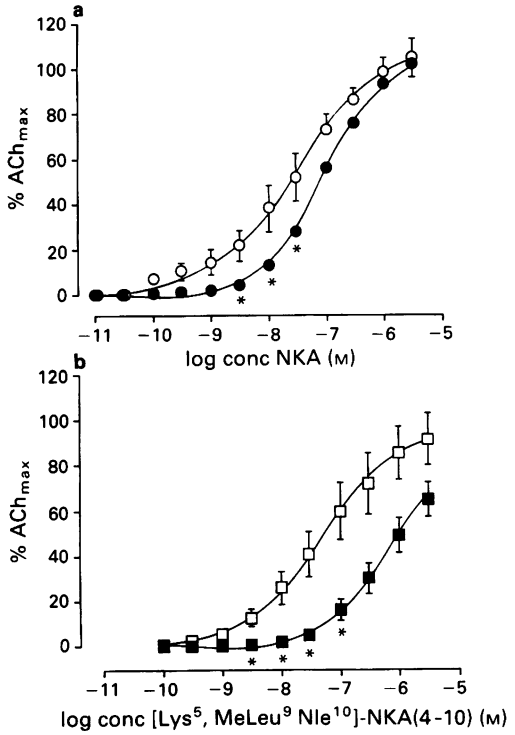

Figure 2 Concentration-response curves to neurokinin A (NKA) (a) and [Lys^5,MeLeu^{9}Nle^{10}]-NKA(4–10) (b) in the absence (open symbols) and presence (closed symbols) of MDL 29,913 at 2 μM. Points are mean values from 4 animals. Vertical bars represent s.e.mean and * designates a significant difference from corresponding control value, $P<0.05$.

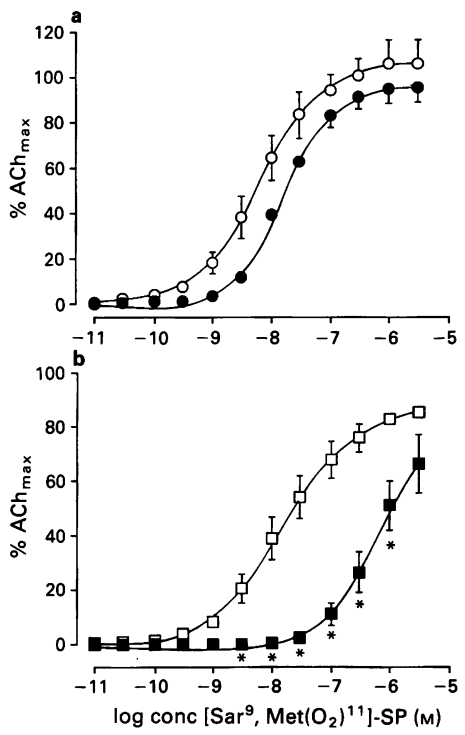

Figure 3 Concentration-response curves to [Sar^9,Met$(O_2)^{11}$]-SP in the absence (open symbols) and presence (closed symbols) of MDL 29,913, at 2 μM (a) and CP-96,345 at 1 μM (b). Points are mean values from 3 and 4 animals respectively. Vertical bars represent s.e.mean and * designates a significant difference from corresponding control value, $P<0.05$.

Table 3 Effect of MDL 29,913 and CP 96,345 on contractile responses to neurokinin A (NKA), [Lys^5,MeLeu^9,Nle^{10}]-NKA4–10 [NKA(4–10) analogue] and [Sar^9-Met-$(O_2)^{11}$]-substance P (Sar-P)

Agonist	*Antagonist*	n	pD_2 ± s.e.	T_{max} (% ACh ± s.e.)
NKA	—	4	7.9 ± 0.3	107.4 ± 7.5
NKA	MDL 29913 2 μM	4	7.3 ± 0.3*	104.7 ± 9.7
NKA(4–10) analogue	—	4	7.4 ± 0.3	90.6 ± 11.5
NKA(4–10) analogue	MDL 29913 2 μM	4	6.5 ± 0.1*	64.3 ± 7.6
Sar-SP	—	4	8.1 ± 0.1	106.0 ± 10.5
Sar-SP	MDL 29913 2 μM	4	7.8 ± 0.0	95.5 ± 6.7
Sar-SP	—	4	7.8 ± 0.2	85.3 ± 2.6
Sar-SP	CP 96345 1 μM	4	6.3 ± 0.1*	66.4 ± 10.7

Values for pD_2 are means with s.e. and maximal tension is expressed as a percentage of contraction to 1 mM acetylcholine.
* Significant difference $P<0.05$, from values obtained in the absence of antagonist.

Antagonist studies The effects of the two antagonists MDL 29,913 (NK_2 selective) and CP-96,345 (NK_1 selective) were studied in those airway preparations which had been detected in the autoradiographic studies (Figure 4) to contain the highest density of binding sites i.e. areas B2 and B3 (Figure 1). MDL 29,913 at a concentration of 2 μM produced a small but significant shift to the right in the response curve to NKA (Figure 2), with a decrease in the pD_2 value but no change in the maximal response. MDL 29,913 produced a much greater shift in the response curve to NKA(4–10) analogue (Figure 2), with nearly an 8 fold decrease in the mean pD_2 value whereas the maximum response was not depressed. In contrast, MDL 29,913 did not produce any significant shift in the response curve to Sar-SP (Figure 3). However, CP-96,345 at 1 μM produced a 27 fold rightward shift in the response curve to Sar-SP (Figure 3) without altering the maximal response. Values for maximal tension and pD_2 in the presence and absence of the antagonists are shown in Table 3.

Autoradiography

Binding of [^{125}I]-NKA on the airway smooth muscle was sparse in proximal airway preparations and increased in density in the more distal airways such that binding in B_3 was very dense (Figure 4). There was good concordance in the assessment of the density of the binding sites as judged by the scores of the two investigators (L.D. and J.B.). ($r = 0.80$, d.f. 24, $P = 0.0001$). When the binding density scores of the two observers in 25 sections from 1 rabbit were averaged, binding in T1 was 0, B1 was 1.5, B2 was 3 and B3 was 4.5. In two of the three rabbits no binding sites were visualised in the trachea or most proximal bronchus. In all three rabbits sparse binding was visible in B2 and density of binding then increased in B3.

There were negligible specific binding sites visible over structures other than airway smooth muscle i.e. vascular smooth muscle or epithelium. Nonspecific binding was uniformly low in all sections visualised (Figure 4).

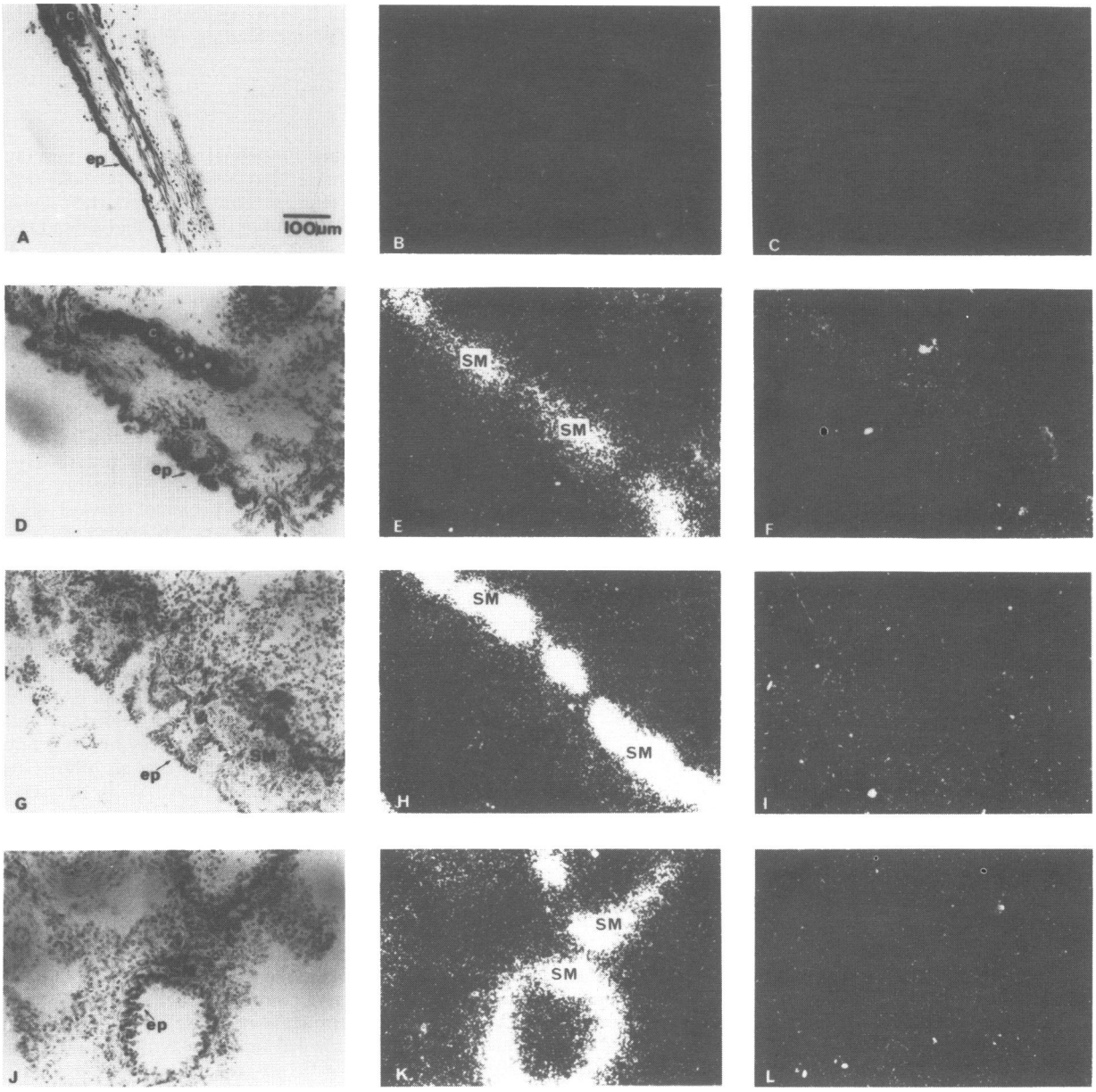

Figure 4 Visualization of autoradiographic binding sites for neurokinin A (NKA) in rabbit airways. Panels A, D, G and J, are light field photomicrographs of the areas of trachea and bronchus designated in Figure 1 as T1, B1, B2 and B3. Central and right hand panels are dark-field photomicrographs of adjacent sections incubated with [^{125}I]-NKA alone (B, E, H and K) or in combination with 1 μM non-labelled NKA (C, F, I and L). SM = smooth muscle, ep = epithelium, c = cartilage.

Table 4 Competition by tachykinins and analogues against [^{125}I]-neurokinin A ([^{125}I]-NKA) in rabbit lung membranes

Competitor	n	*Slope factor*	K_D (nM)	*RA*
Neurokinin A	4	1.01 ± 0.10	0.81 ± 0.10	100
CP-96,345	4	0.83 ± 0.26	6.4 ± 2.7	12
Substance P	5	0.44 ± 0.04	0.24 ± 0.10 (H 76%)	340
			57 ± 49 (L 24%)	1.4
[Sar^9,Met(O$_2$)^{11}]-substance P	6	0.41 ± 0.15	0.36 ± 0.18	225
Neuropeptide γ	3	1.11 ± 0.03	0.79 ± 0.14	103
Senktide	7	0.37 ± 0.11	0.8 ± 1.3 (H 36%)	100
			17000 ± 9000 (L 64%)	0.005
[Lys^5,MeLeu^9,Nle^{10}]-NKA(4–10)	5	0.69 ± 0.05	13.4 ± 2.9	6
Neurokinin B	4	0.96 ± 0.12	28.9 ± 5.9	2.8
MEN 10207	4	1.18 ± 0.25	1500 ± 400	0.05
MDL 29,913	5	1.29 ± 0.19	2000 ± 400	0.04

Values for equilibration dissociation contant (K_D) were generated by LIGAND and are the mean ± s.e. Slope factors were generated by EBDA and are the arithmetic mean ± s.e. Binding data for substance P and senktide could be resolved into two sites, of high (H) and low (L) affinity (percentages shown). RA relative affinity compared with neurokinin A.

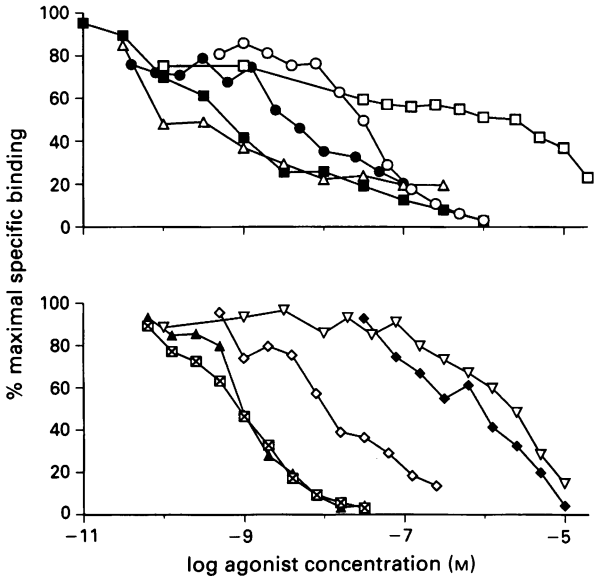

Figure 5 Competition curves for [^{125}I]-neurokinin A ([^{125}I]-NKA) binding in rabbit lung homogenates by various tachykinins and analogues. Each point represents the mean of 3–7 experiments: (■) substance P; (●) CP 96,345; (△) [Sar^9,Met(O$_2$)^{11}]-SP; (○) neurokinin B; (□) senktide; (◆) MEN 10207; (▲) neuropeptide gamma; (◇) [Lys^5,MeLeu^9,Nle^{10}]-NKA(4–10); (⊠) neurokinin A; (▽) MDL 29913.

Radioligand binding studies

Binding of [^{125}I]-NKA was approximately 82% specific. The equilibrium dissociation contant K_D, derived from 'cold' saturation curves, was 0.74 ± 0.11 nM. The order of potency for inhibition of [^{125}I]-NKA binding was SP > = Sar-SP > NKA = NPγ > CP 96,345 > NKA(4–10) analogue > neurokinin B >>> MEN 10,207 > MDL 29,913 > senktide (Table 4). This suggests binding predominantly to NK_1 receptors. The competition curve for substance P was shallow (Figure 5). LIGAND analysis showed that substance P (slope factor 0.44) was binding to two sites, of K_D 0.24 (76%) and 57 nM (24%), respectively (Table 4). Coincubation of substance P with the NK_1-selective analogue Sar-SP (10 nM) or with the NK_2-selective NKA(4–10) analogue (100 nM) gave LIGAND single-site fits for SP, of K_D 110 ± 90 and 0.46 ± 0.13 nM ($n = 6$), respectively.

The competition curve for Sar-SP was biphasic (Figure 5) and this analogue was not capable of inhibiting [^{125}I]-NKA binding more than about 80%. Senktide was found to bind to two sites, of high and of very low affinity, in a ratio of 1:2. At a concentration of 0.1 nM, senktide had already inhibited approximately 20% of the binding (Figure 5).

Discussion

We have shown, using functional, radioligand binding and autoradiographic studies that receptors for tachykinins in rabbit airways are heterogeneous and that their density is location-dependent. Our findings confirm and extend those of our previous study, which examined the distribution of substance P receptors in the rabbit respiratory tree. There, we reported that the density of substance P receptors was also location-dependent (Black *et al.*, 1990a). However, since substance P is a non selective tachykinin receptor agonist, it was possible that receptors other than the SP preferring NK_1 were being activated. In the present study, we used the selective NK_1 receptor agonist [Sar^9,Met(O$_2$)^{11}]-SP, and the pattern of response observed i.e. very little contraction in the proximal airways, with increasing efficacy progressively towards the periphery, indicates that NK_1 receptors are more numerous in the peripheral than proximal airways. That this contractile response is mediated via NK_1 receptors was confirmed by the antagonism observed with CP-96,345. Although we studied only one concentration of this antagonist, the 27 fold shift in the response curve to [Sar^9,Met(O$_2$)^{11}]-SP produced by 1 μM CP-96,345 would suggest that it is less potent in rabbit airway smooth muscle than in rabbit jugular vein (Rouissi *et al.*, 1991), rabbit aorta (Beresford *et al.*, 1991) or dog carotid artery (Snider *et al.*, 1991) in which pA_2 values of 8.9, 8.8 and 8.7 respectively have been reported. Thus, in addition to the marked species differences in the affinity of CP-96,345 for NK_1 receptors (Beresford *et al.*, 1991; Gitter *et al.*, 1991) there may also be organ or tissue differences in NK_1 receptor characteristics in the rabbit.

Our results demonstrate that, in addition to NK_1 receptors, a population of NK_2 receptors is present throughout rabbit airways. This is based on the fact that the selective NK_2 agonist, NKA(4–10) analogue, as well as the less selective NKA and its N-terminally extended form, NPγ, contracted both proximal and peripheral airways. NPγ was more potent than NKA which is consistent with our previous findings in human and guinea-pig airways (Burcher *et al.*, 1991a,b). The magnitude of the contractile response to these agonists was similar in all areas studied and the marked increase in the contractile response with progression towards the periphery noted with Sar-SP was not apparent. We expected that MDL 29,913 (an NK_2 antagonist) would antagonize responses to NKA(4–10) analogue and not those to Sar-SP and this was indeed the case. However MDL 29,913 was a rather weak antagonist as we have previously reported in human airways

(Burcher *et al.*, 1991a). This may provide further evidence for the heterogeneity of NK_2 receptors reported by others (Burcher & Mussap, 1991; Maggi *et al.*, 1991; van Giersbergen *et al.*, 1991) since another NK_2 antagonist, MEN 10376, is more potent in rabbit bronchus (Maggi *et al.*, 1992).

Our radioligand binding data suggest that, in rabbit airways, [^{125}I]-NKA binds predominantly to SP- preferring NK_1 receptors, since SP and the NK_1 selective agonist Sar-SP were the most potent competitors of [^{125}I]-NKA binding. However, Sar-SP was not capable of fully inhibiting [^{125}I]-NKA binding, suggesting that about 20% of the radioligand was binding to a site for which this analogue has no affinity. LIGAND analysis showed that the substance P competition curve could be resolved into high and low affinity sites. The high affinity sites would be NK_1 receptors; the identity of the low affinity sites is not certain but they may represent some form of NK_2 receptor. The two NK_2 subtype selective antagonists MEN 10,207 and MDL 29,913 were both extremely weak competitors of [^{125}I]-NKA binding, an observation we have previously made in guinea-pig lung homogenates (Geraghty *et al.*, 1992) and the NK_2 selective analogue NKA(4–10) analogue was not very potent. This gives rise to the possibility that [^{125}I]-NKA does not recognize NK_2 receptors in the lung as opposed to its high affinity binding to NK_2 sites elsewhere (van Giersbergen *et al.*, 1991).

The competition curve for senktide could be resolved into two sites. We have never observed this phenomenon before in lung tissue homogenates and this finding highlights the unusual nature of the tachykinin receptors in the rabbit airways.

For the radioligand binding studies, we chose the area of the lung which was likely to contain the greatest density of receptors, based on the findings in the functional and autoradiography experiments. The tissue selected contained both bronchial and a small amount of parenchymal tissue, a considerable component of which would have been vascular smooth muscle. However, it is unlikely that vascular smooth muscle binding sites could have constituted a significant proportion of those detected, since, both in this study and a previous one (Xiao *et al.*, 1992) there was negligible autoradiographic binding of [^{125}I]-NKA over vessels.

Our autoradiographic data demonstrate that binding sites for [^{125}I]-NKA increase in density from proximal to peripheral airways. This parallels the findings in our previous study (Black *et al.*, 1990a) in which binding sites for [^{125}I]-Bolton Hunter SP were similarly more dense in these smaller airways. The results of our functional experiments in the present study demonstrated increased contractile response to NK_1 agonists in the more distal airways. Taken together, our autoradiographic and functional data would suggest that [^{125}I]-NKA may have detected some NK_2 receptors in the proximal airways, but that the majority of the binding occurred non selectivity to NK_1 receptors, an observation that we have made in guinea-pig airways (Burcher *et al.*, 1989).

We have previously reported that the distribution of receptors for carbachol and histamine in rabbit airways is non-uniform (Armour *et al.*, 1984) and, indeed, this is the reason for our inability to normalize tachykinin-induced contractile responses to one of these agonists in the present study. Receptors for carbachol were more numerous in the larger airways and this is the converse of the distribution of NK_1 receptors observed in this study. It is interesting to speculate on the pathophysiological significance of regional differences in receptor populations in the airways, and whether they bear any relationship to the distribution of tachykinin-containing nerves in this species. It is possible that, if the tachykinins do play a role in regulating airway tone, then this function assumes greater significance in the more peripheral regions of the respiratory tree.

This study was supported by the National Health and Medical Research Council of Australia and the Asthma Foundation of New South Wales.

References

ADVENIER, C., NALINE, E., DRAPEAU, G. & REGOLI, D. (1987). Relative potencies of neurokinins in guinea pig and human bronchus. *Eur. J. Pharmacol.*, **139**, 133–137.

ARMOUR, C.L., BLACK, J.L. & BEREND, N. (1984). Histamine and carbachol contractile responses in proximal and distal airways of the rabbit. *Clin. Exp. Pharmacol. Physiol.*, **12**, 19–23.

ARMOUR, C.L., DIMENT, L.M. & BLACK, J.L. (1988). Relationship between smooth muscle volume and contractile response in airway tissue – isometric vs isotonic measurement. *J. Pharmacol. Exp. Ther.*, **245**, 687–691.

BARNES, P.J. (1991). Neuropeptides in the respiratory tract. *Am. Rev. Respir. Dis.*, **144**, 1187–1198.

BERESFORD, I.J.M., BIRCH, P.J., HAGAN, R.M. & IRELAND, S.J. (1991). Investigation into species variants in tachykinin NK_1 receptors by use of the non-peptide antagonist, CP-96,345. *Br. J. Pharmacol.*, **104**, 292–293.

BLACK, J.L., JOHNSON, P.R.A. & ARMOUR, C.L. (1988). Potentiation of the contractile effects of neuropeptides in human bronchus by an enkephalinase inhibitor. *Pulm. Pharmacol.*, **1**, 21–23.

BLACK, J.L., DIMENT, L.M., ARMOUR, C.L., ALOUAN, L. & JOHNSON, P.R.A. (1990a). Distribution of substance P receptors in rabbit airways – functional and autoradiographic studies. *J. Pharmacol. Exp. Ther.*, **253**, 381–386.

BLACK, J.L., JOHNSON, P.R.A., ALOUAN, L. & ARMOUR, C.L. (1990b). Neurokinin A with K^+ channel blockade potentiates contraction in human bronchus. *Eur. J. Pharmacol.*, **180**, 311–317.

BUCK, S.H. & BURCHER, E. (1986). The tachykinins: a family of peptides with a "brood" of receptors. *Trends Pharmacol. Sci.*, **7**, 65–68.

BURCHER, E., ALOUAN, L.A., JOHNSON, P.R.A. & BLACK, J.L. (1991a). Neuropeptide γ, the most potent contractile tachykinin in human isolated bronchus, acts via a "non-classical" NK2 receptor. *Neuropeptides*, **20**, 79–82.

BURCHER, E., MUSSAP, C.J., GERAGHTY, D.P., MCCLURE-SHARP, J.M. & WATKINS, D.J. (1991b). Concepts in characterization of tachykinin receptors. *Ann. N.Y. Acad. Sci.*, **632**, 123–136.

BURCHER, E. & MUSSAP, C.J. (1991). Neuropeptide γ-preferring subtypes of NK2 receptors in rat fundus and dog urinary bladder. *Soc. Neurosci. U.S.A.*, Abst. **17**, 805.

BURCHER, E., WATKINS, D.J. & O'FLYNN, N. (1989). Both neurokinin A and substance P bind to NK1 receptors in guinea-pig lung. *Pulm. Pharmacol.*, **1**, 201–203.

CHASSAING, G., LAVIELLE, S., LOEUILLET, D., ROBILLIARD, P., CARRUETTE, A., GARRET, C., BEAUJOUAN, J.C., SAFFROY, M., PETITET, F., TORRENS, Y. & GLOWINSKI, J. (1991). Selective agonists of NK-2 binding sites highly active on rat portal vein (NK-3 bioassay). *Neuropeptides*, **19**, 91–95.

COOK, J.A., BRUNNER, S.L. & TANAKA, D.T. (1990). Neurokinin receptors mediating substance P-induced contraction in adult rabbit airways. *Am. J. Physiol.*, **258**, L99–L106.

FROSSARD, N. & BARNES, P.J. (1991). Effects of tachykinins on small human airways. *Neuropeptides*, **19**, 157–162.

GERAGHTY, D.P., MUSSAP, C.J. & BURCHER, E. (1992). Radioiodinated substance P, neurokinin A and eledoisin bind predominantly to NK1 receptors in guinea-pig lung. *Mol. Pharmacol.*, **41**, 147–153.

GITTER, B.D., WATERS, D.C., BRUNS, R.F., MASON, N.R., NIXON, J.A. & HOWBERT, J.J. (1991). Species differences in affinities of non-peptide antagonists for substance P receptors. *Eur. J. Pharmacol.*, **197**, 237–238.

GUARD, S. & WATSON, S.P. (1991). Tachykinin receptor types: classification and membrane signalling mechanisms. *Neurochem. Int.*, **18**, 149–165.

IRELAND, S.J., BAILEY, F., COOK, A., HAGAN, R.M., JORDAN, C.C. & STEPHENS-SMITH, M.L. (1991). Receptors mediating tachykinin-induced contractile responses in guinea-pig trachea. *Br. J. Pharmacol.*, **103**, 1463–1469.

LUNDBERG, J.M., MARTLING, C.R. & SARIA, A. (1983). Substance P and capsaicin induced contraction of human bronchi. *Acta Physiol. Scand.*, **119,** 49–53.

MAGGI, C.A., EGLEZOS, A., QUATARA, L., PATACCHINI, R. & GIACHETTI, A. (1991). Heterogeneity of NK-2 tachykinin receptors in hamster and rabbit smooth muscles. *Reg. Peptides* (in press).

MAGGI, C.A., PATACCHINI, R., ASTOLFI, M., ROVERO, P., GIULIANI, S. & GIACHETTI, A. (1991). NK-2 receptor agonists and antagonists. *Ann. N.Y. Acad. Sci.*, **632,** 184–191.

MCLEAN, S., GANONG, A.H., SEEGER, T.F., BRYCE, D.K., PRATT, K.G., REYNOLDS, L.S., SIOK, C.J., LOWE III, J.A. & HEYM, J. (1991). Activity and distribution of binding sites in brain of a nonpeptide substance P (NK1) receptor antagonist. *Science*, **25,** 437–439.

PALMER, J.B.D., CUSS, F.M.C. & BARNES, P.J. (1986). VIP and PHM and their role in nonadrenergic inhibitory responses in isolated human airways. *J. Appl. Physiol.*, **61,** 1322–1328.

ROUISSI, N., GITTER, B.D., WATERS, D.C., HOWBERT, J.J., NIXON, J.A. & REGOLI, D. (1991). Selectivity and specificity of new, non-peptide, guinuclidine antagonists of substance P. *Biochem. Biophys. Res. Commun.*, **176,** 894–901.

SNIDER, R.M., CONSTANTINE, J.W., LOWE, J.A. III, LONGO, K.P., LEBEL, W.S., WOODY, H.A., DROZDA, S.E., DESAI, M.C., VINICK, F.C., SPENCER, R.W. & HESS, H.J. (1991). A potent nonpeptide antagonist of the substance P (NK1) receptor. *Science*, **251,** 435–437.

VAN GIERSBERGEN, P.L.M., SHATZER, S.A., HENDERSON, A.K., LAI, J., NAKANISHI, S., YAMAMURA, H.I. & BUCK, S.H. (1991). Characterization of a tachykinin peptide NK2 receptor transfected into murine fibroblasts B82 cells. *Proc. Natl. Acad. Sci. U.S.A.*, **88,** 1661–1665.

XIAO, X.-H., MUSSAP, C.J. & BURCHER, E. (1992). Characterization of the tachykinin NK2 receptor subtype in the rabbit pulmonary artery. *Peptides*, **13,** (in press).

(Received April 3, 1992
Revised May 19, 1992
Accepted June 3, 1992)

Br. J. Pharmacol. (1992), **107**, 437–442

Long-term changes in gerbil brain neurotransmitter receptors following transient cerebral ischaemia

[1]*,† Tsutomu Araki, *Hiroyuki Kato, *Kyuya Kogure &† Yasuo Kanai

*Department of Neurology, Institute of Brain Diseases, Tohoku University School of Medicine, 1-1 Seiryo-Machi, Sendai, Japan and †Pharmacological Research Laboratory, Research Laboratories, Tokyo Tanabe Co., Ltd., Tokyo, Japan

1 Receptor autoradiographic and histological techniques were used to investigate long-term changes in the gerbil brain following transient cerebral ischaemia.

2 Transient ischaemia was induced for 3 min and 10 min, and the animals were allowed to survive for 8 months.

3 Histological examination revealed that 3 min ischaemia caused neuronal damage and mild shrinkage only in the hippocampal CA1 sector. Ten minutes of ischaemia produced severe neuronal damage in the striatum and the hippocampal CA1 and CA3 sectors. Considerable shrinkage was seen in the hippocampus; the dentate gyrus, however, was not damaged.

4 Three minutes of ischaemia produced changes in the binding of [^{3}H]-quinuclidinylbenzilate ([^{3}H]-QNB), [^{3}H]-muscimol, and [^{3}H]-MK-801 in various brain regions, as determined autoradiographically. In contrast, [^{3}H]-cyclohexyladenosine ([^{3}H]-CHA) and [^{3}H]-PN200-110 ([^{3}H]-isradipine) binding in the brain was unaltered.

5 Ten minutes of ischaemia resulted in a major loss of neurotransmitter receptors, especially in the hippocampus. The substantia nigra showed a significant reduction in [^{3}H]-CHA binding, whereas the striatum, which was morphologically damaged, showed no significant changes in any of the neurotransmitter receptors examined.

6 The results demonstrated that long-term survival after transient cerebral ischaemia produced alterations in neurotransmitter receptors, especially in the hippocampal formation, where considerable shrinkage was noted. These results also suggest that the hippocampal damage was not static, but progressive.

Keywords: Cerebral ischaemia; neurotransmitter receptor; autoradiography; long-term changes; tissue shrinkage

Introduction

It is now well established that transient cerebral ischaemia can easily be produced in the Mongolian gerbil by bilaterally occluding the common carotid arteries (Crockard *et al.*, 1980; Kirino, 1982). The hippocampal CA1 sector has been shown to be the region of the brain most vulnerable to damage following brief transient ischaemia (Kirino, 1982; Araki *et al.*, 1989; 1990a), although populations of neurones in the neocortex, striatum, and thalamus are also selectively vulnerable to transient ischaemia (Wieloch, 1985). A large number of studies have explored the mechanisms underlying selective neuronal vulnerability (Jorgensen & Diemer, 1982; Pulsinelli *et al.*, 1982; Kogure *et al.*, 1988; Crain *et al.*, 1988; Siesjö & Bengtsson, 1989).

Many hypotheses have been proposed to explain the mechanisms underlying ischaemic brain damage: these include the neurotoxic action of synaptically released excitatory amino acids, such as glutamate, (Benveniste *et al.*, 1984; 1989); the pathological accumulation of intracellular calcium ions, thought to be a major factor leading to neuronal damage (Siesjö, 1981; Simon *et al.*, 1984; Benveniste *et al.*, 1988); activation of protein kinase C (Onodera *et al.*, 1988); impairment of protein synthesis (Xie *et al.*, 1989; Araki *et al.*, 1990b); lipid peroxidation (Kitagawa *et al.*, 1990); imbalance between excitatory and inhibitory inputs (Wieloch, 1985; Sternau *et al.*, 1989; Araki *et al.*, 1990c); metabolic disturbances (Munekata & Hossmann, 1987); and the alteration of intracellular signal transduction processes (Jorgensen *et al.*, 1989; Araki *et al.*, 1992a). Each of these factors has been suggested as participating in the development of ischaemic neuronal damage.

Athough many experimental investigations have addressed the short-term pathological and biochemical events that are triggered by transient ischaemia, little is known about the long-term pathological and biochemical changes following transient ischaemia. In the present study, we have utilized autoradiographs to focus on post-ischaemic alterations in the receptors for muscarinic acetylcholine, γ-aminobutyric acid$_A$ ($GABA_A$), adenosine A_1, and N-methyl-D-aspartate (NMDA), and in voltage-dependent calcium channels in the gerbil brain 8 months after transient cerebral ischaemia.

Methods

Animals and operative procedures

Male Mongolian gerbils weighing 70–95 g were maintained on a 12 h light: dark cycle and fed *ad libitum* before experimentation. Animals were anaesthetized with 2% halothane in a mixture of 70% N_2O and 30% O_2. The bilateral common carotid arteries were exposed, anaesthesia was discontinued, and the arteries were clamped with aneurysm clips for either 3 or 10 min. After occlusion, the clips were removed and ischaemic animals were allowed to survive for 8 months. Sham-operated animals were treated in the same manner, except for the clipping of the bilateral common carotid arteries. Body temperature was maintained at 37–39°C with a heating pad equipped with a thermostat until the animals began to move. For receptor autoradiography, the animals were decapitated 8 months after ischaemia. The brains were removed quickly and frozen in powdered dry-ice; saggital sections (12 μm) were cut on a cryostat at −20°C and thaw-mounted onto gelatin-coated slides. The sections were stored at −80°C until assay.

[1] Author for correspondence.

Histopathology

The gerbils were anaesthetized with pentobarbitone (50 mg kg^{-1}) intraperitoneally (i.p.) 8 months after ischaemia. They were briefly subjected to transcardiac perfusion with heparinized saline, followed by perfusion-fixation with 3.5% formaldehyde in 0.1 M phosphate buffer (pH 7.4) for 30 min. The fixed animals were then left at 4°C for 120 min, after which the brains were removed and immersed in the same fixative before being embedded in paraffin. Sections (5 μm) were stained with cresyl violet and haematoxylin-eosin. Adjacent sections prepared for receptor autoradiography were also stained with cresyl violet and haematoxylin-eosin. The sections were examined with a light microscope. Each group contained 4–7 animals.

Receptor autoradiography

[^{3}H]-quinuclidinyl benzilate ([^{3}H]-QNB) binding Autoradiographic localization of muscarinic acetylcholine receptors was performed as described previously (Araki *et al.*, 1991; Kato *et al.*, 1991). Sections were incubated with 1 nM [^{3}H]-QNB (sp. act. 41.5 Ci $mmol^{-1}$; Amersham) in phosphate buffer (pH 7.4) for 90 min at room temperature. The sections were then washed in buffer for 5 min at 4°C. Nonspecific binding was determined using 1 μM atropine (Sigma).

[^{3}H]-muscimol binding [^{3}H]-muscimol (γ-aminobutyric $acid_A$, $GABA_A$) receptor autoradiography was performed according to the method of Onodera *et al.* (1987). To remove endogenous GABA, sections were subjected to a 20 min prewash, at 4°C, in 50 mM Tris-citrate buffer (pH 7.1); they were then incubated for 40 min at 4°C in buffer containing 30 nM [^{3}H]-muscimol (sp. act. 17.1 Ci $mmol^{-1}$; New England Nuclear). The sections were then washed in buffer for 1 min at 4°C. Nonspecific binding was determined in the presence of 10 μM GABA (Sigma).

[^{3}H]-cyclohexyladenosine binding The method used for autoradiographic localization of adenosine A_1 receptors has been described previously (Araki *et al.*, 1991; Kato *et al.*, 1991). Sections were incubated with 5 nM [^{3}H]-cyclohexyladenosine (CHA, sp. act.34.4 Ci $mmol^{-1}$; New England Nuclear) and 2 units ml^{-1} adenosine deaminase (Boehringer-Mannheim) in 50 mM Tris-HCl buffer (pH 7.4) for 90 min at room temperature, after which they were washed in buffer for 1 min at 4°C. Nonspecific binding was determined with 10 μM L-phenyl-isopropyladenosine (Boehringer-Mannheim).

[^{3}H]-MK-801 binding Autoradiographic distribution of the binding of the N-methyl-D-aspartate (NMDA) antagonist, MK-801 (dizocilpine; (±)-5-methyl-10,11-dihydro-5H-dibenzo [a,d]cyclohepten-5,10-imine) was determined according to the method of Bowery *et al.* (1988), with minor modifications (Araki *et al.*, 1992b). Sections were rinsed in 50 mM Tris-HCl buffer (pH 7.4) containing 190 mM sucrose and dried in a cold air stream. They were then incubated for 20 min at room temperature in buffer containing 30 nM [^{3}H]-MK-801 (sp. act. 28.8 Cimmol^{-1}; New England Nuclear), after which they were washed in the buffer twice for 20 s at room temperature. Nonspecific binding was determined with 100 μM MK-801 (Research Biochemicals Inc., U.S.A.).

[^{3}H]-PN200-110 binding The method used for autoradiographic visualization of the binding of the voltage-dependent L-type calcium channel blocker, [^{3}H]-PN200-110 (isradipine; isopropyl methyl (±)-4-(4-benzofurazanyl)-1,4-dihydro-2,6-dimethyl-3,5-pyridinedicarboxylate), has been described previously (Araki *et al.*, 1991; Kato *et al.*, 1991). Sections were incubated with 0.1 nM [^{3}H]-PN200-110 (sp. act. 71.5 Ci-$mmol^{-1}$; New England Nuclear) in 170 mM Tris-HCl buffer (pH 7.7) for 60 min at room temperature, after which they were washed in buffer for 20 min at 4°C. Nonspecific binding was determined with 1 μM nitrendipine (Sigma).

All procedures were performed under subdued lighting conditions. The sections were dried under a cold air stream and were apposed to Hyperfilm-^{3}H (Amersham) for 2–4 weeks in X-ray cassettes with a set of tritium standards. The optical density of the brain regions was measured with a computer-assisted image analyzer. The relationship between optical density and radioactivity was obtained with reference to the ^{3}H microscale (Amersham) co-exposed with the tissue sections, using a third-order polynomial function. Anatomical structures were verified by examination of cresyl violet-stained sections, and comparison with the gerbil brain atlas of Loskota *et al.* (1974). Binding assays were performed in duplicate. Statistical comparisons were made by Duncan's multiple range test. Each group contained 4–7 animals.

Results

Histopathology

Sham-operated gerbils showed no neuronal damage in any brain region. Eight months after 3 min ischaemia, severe neuronal damage was seen only in the hippocampal CA1 sector, and mild tissue atrophy was also found in this field. Gerbils subjected to 10 min ischaemia displayed severe neuronal damage in the hippocampal CA1 and CA3 sectors (Figure 1). Further, marked tissue shrinkage was observed in the hippocampus in these animals. The dentate gyrus, however, was intact. In the striatum, most of the small- and medium-sized neurones were destroyed following ischaemia, whereas large-sized neurones, which were sparsely scattered in this region, were relatively well preserved, although they exhibited some mild degeneration (Figure 2).

Autoradiography

Quinuclidinyl benzilate binding In sham-operated gerbils, the distribution of [^{3}H]-QNB binding in the brain was strikingly heterogeneous, being greatest in the hippocampal CA1 sector and dentate gyrus, followed by the striatum, neocortex, and hippocampal CA3 sector. Other regions had a low density of [^{3}H]-QNB binding sites (Figure 3, Table 1). Eight months

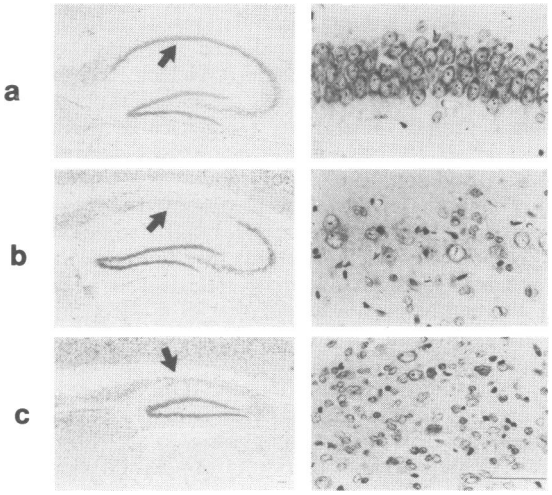

Figure 1 Representative photographs of gerbil hippocampus. Left half: whole hippocampal area; bar = 100 μm. Right half: hippocampal CA1 neurones; bar = 50 μm. (a) Sham-operated group, hippocampal CA1 sector is intact (arrow). (b) Eight months after 3 min ischaemia. Severe neuronal damage is seen in the hippocampal CA1 sector (arrow). (c) Eight months after 10 min ischaemia. Severe neuronal damage and tissue shrinkage is seen in the hippocampal CA1 sector (arrow) and hippocampal CA3 sector. Gliosis is also seen in the hippocampal CA1 sector. However, there is no neuronal damage in the dentate gyrus. Cresyl violet staining.

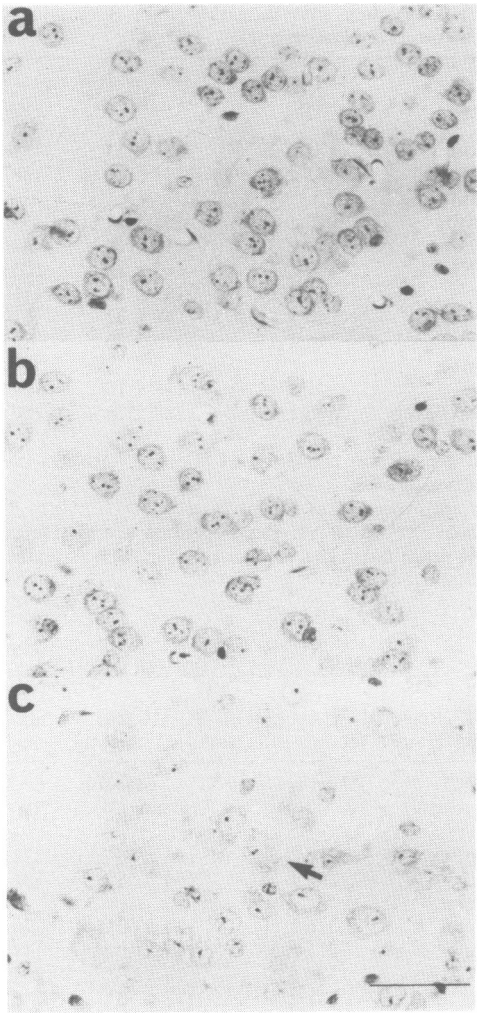

Figure 2 Representative photomicrographs of the gerbal striatum: (a) sham-operated group; (b) eight months after 3 min ischaemia; the striatal neurones are intact; (c) eight months after 10 min ischaemia; small- and medium-sized neurones are almost all destroyed, while the large-sized neurones are relatively well preserved (arrow). Cresyl violet staining. Bar = 50 μm.

Table 1 Regional distribution of [^{3}H]-quinuclidinyl benzilate ([^{3}H]-QNB) binding sites in gerbil brain 8 months after transient cerebral ischaemia

	Sham-operated (6)	*Cerebral ischaemia* 3 min (7)	10 min (4)
Frontal cortex	302 ± 42	310 ± 66	356 ± 34
Striatum	389 ± 23	371 ± 48	402 ± 112
Hippocampus			
CA1 sector	439 ± 29	248 ± 53**	115 ± 48**
CA3 sector	284 ± 17	259 ± 53	159 ± 122*
Dentate gyrus	411 ± 38	385 ± 55	451 ± 44
Thalamus	116 ± 17	92 ± 17	129 ± 59
Hypothalamus	104 ± 40	84 ± 28	145 ± 28
Substantia nigra	84 ± 21	76 ± 16	104 ± 19
Cerebellum	20 ± 4	18 ± 4	16 ± 6

Optical density was converted to fmol mg^{-1} tissue with ^{3}H microscales.
Values are expressed as means ± s.d.
*$P<0.05$; **$P<0.01$ vs. sham-operated group (Duncan's multiple-range test). The number of animals in parentheses.

after 3 min ischaemia, a significant reduction in [^{3}H]-QNB binding sites was observed only in the hippocampal CA1 sector. Gerbils subjected to 10 min ischaemia showed a significant reduction in [^{3}H]-QNB binding sites in both the hippocampal CA1 and CA3 sectors. Other regions exhibited no significant alterations in [^{3}H]-QNB binding sites.

Muscimol binding In sham-operated gerbils, [^{3}H]-muscimol binding was greatest in the thalamus, followed by the dentate gyrus, cerebellum, neocortex, hippocampal CA1 sector, substantia nigra, and striatum. The hippocampal CA3 sector exhibited a relatively low density of [^{3}H]-muscimol binding sites and in the hypothalamus these were almost undetectable (Figure 3, Table 2). Eight months after 3 min ischaemia, the hippocampal CA1 sector and CA3 sectors showed a significant reduction in binding. In contrast, the substantia nigra exhibited a significant elevation in [^{3}H]-muscimol binding. Gerbils subjected to 10 min ischaemia revealed marked reduction in [^{3}H]-muscimol binding in the hippocampal CA1 sector, hippocampal CA3 sector, and dentate gyrus. Other regions showed no significant alterations in [^{3}H]-muscimol binding.

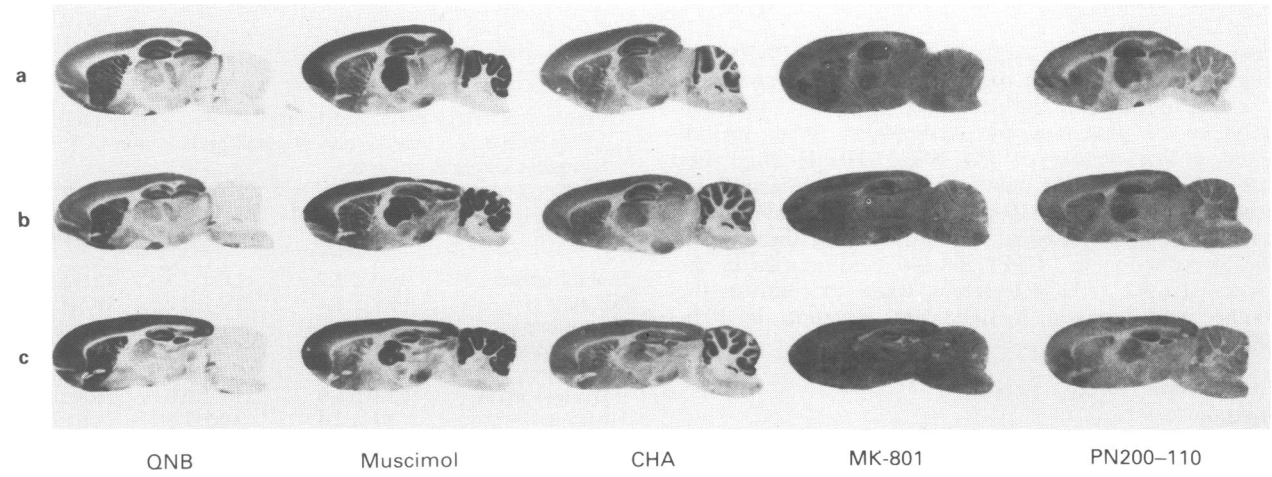

Figure 3 Representative autoradiograms of [^{3}H]-quinuclidinyl benzilate ([^{3}H]-QNB), [^{3}H]-muscimol, [^{3}H]-cyclohexyladenosine ([^{3}H]-CHA), [^{3}H]-MK-801 and [^{3}H]-isradipine ([^{3}H]-PN200-110) binding sites in gerbil brain. (a) Sham-operated group; (b) eight months after 3 min ischaemia; (c) eight months after 10 min ischaemia. A conspicuous reduction in [^{3}H]-QNB, [^{3}H]-muscimol and [^{3}H]-MK-801 binding sites is seen in the hippocampal CA1 sector, whereas [^{3}H]-CHA and [^{3}H]-PN200-110 binding show no significant reduction in this field. Further, after 10 min ischaemia, there was marked reduction in neurotransmitter receptors in the whole hippocampus; this feature, however, was not found in the striatum.

Table 2 Regional distribution of [^{3}H]-muscimol binding sites in gerbil brain 8 months after transient cerebral ischaemia

	Sham-operated (6)	*Cerebral ischaemia* 3 min (7)	10 min (4)
Frontal cortex	328 ± 32	356 ± 49	312 ± 51
Striatum	170 ± 18	186 ± 26	131 ± 40
Hippocampus			
CA1 sector	293 ± 36	224 ± 46*	42 ± 37**
CA3 sector	100 ± 30	144 ± 23	51 ± 34**
Dentate gyrus	373 ± 41	413 ± 33	313 ± 56*
Thalamus	417 ± 55	379 ± 54	337 ± 113
Hypothalamus	30 ± 17	51 ± 22	44 ± 7
Substantia nigra	186 ± 48	281 ± 76*	185 ± 34
Cerebellum	361 ± 38	370 ± 53	372 ± 37

Optical density was converted to fmol mg^{-1} tissue with ^{3}H microscales.
Values are expressed as means ± s.d.
*$P<0.05$; **$P<0.01$ vs. sham-operated group (Duncan's multiple-range test). The number of animals in parentheses.

Table 3 Regional distribution of [^{3}H]-cyclohexyladenosine ([^{3}H]-CHA) binding sites in gerbil brain 8 months after transient cerebral ischaemia

	Sham-operated (6)	*Cerebral ischaemia* 3 min (7)	10 min (4)
Frontal cortex	174 ± 39	164 ± 23	155 ± 30
Striatum	142 ± 23	131 ± 11	138 ± 16
Hippocampus			
CA1 sector	270 ± 54	267 ± 37	79 ± 44**
CA3 sector	139 ± 31	137 ± 18	62 ± 60**
Dentate gyrus	170 ± 32	163 ± 18	125 ± 48*
Thalamus	111 ± 14	107 ± 12	111 ± 5
Hypothalamus	46 ± 11	48 ± 22	61 ± 8
Substantia nigra	116 ± 27	110 ± 20	82 ± 18*
Cerebellum			
Average	141 ± 15	136 ± 16	129 ± 20
Molecular layer	306 ± 19	288 ± 28	280 ± 44

Optical density was converted to fmol mg^{-1} tissue with ^{3}H microscales.
Values are expressed as means ± s.d.
*$P<0.05$; **$P<0.01$ vs. sham-operated group (Duncan's multiple-range test). The number of animals in parentheses.

Cyclohexyladenosine binding In sham-operated gerbils, [^{3}H]-CHA binding was greatest in the hippocampal CA1 sector and the molecular layer of the cerebellum, with significant binding also being detected in the dentate gyrus, hippocampal CA3 sector, neocortex, striatum, thalamus, and substantia nigra. Other regions exhibited a low density of [^{3}H]-CHA binding sites (Figure 3, Table 3). Eight months after 3 min ischaemia, [^{3}H]-CHA binding showed no significant alteration in any brain region. Gerbils subjected to 10 min ischaemia, in contrast, showed a significant decrease in [^{3}H]-CHA binding in the hippocampus and substantia nigra. Other regions showed no significant alterations in [^{3}H]-CHA binding.

MK-801 binding In sham-operated gerbils, [^{3}H]-MK-801 binding was greatest in the hippocampal CA1 sector and dentate gyrus, followed by the thalamus, striatum, neocortex, and hippocampal CA3 sector. The hypothalamus, substantia nigra, and cerebellum also had a relatively high density of [^{3}H]-MK-801 binding sites (Figure 3, Table 4). Eight months after 3 min ischaemia, the striatum, hippocampal CA1 sector, dentate gyrus, and cerebellum showed a significant reduction in [^{3}H]-MK-801 binding sites. In gerbils subjected to 10 min ischaemia, in contrast, there was a significant reduction in [^{3}H]-MK-801 binding only in the hippocampal CA1 sector.

Isradipine binding In sham-operated gerbils, [^{3}H]-PN200-110 binding was greatest in the dentate gyrus and hippocampal CA3 sector, followed by the neocortex, striatum, hippocampal CA1 sector, thalamus, and cerebellum. Other regions exhibited a low density of [^{3}H]-PN200-110 binding sites (Figure 3, Table 5). Eight months after 3 min ischaemia, no alterations in [^{3}H]-PN200-110 binding sites were seen in any region. In gerbils subjected to 10 min ischaemia there was a significant reduction in [^{3}H]-PN200-110 binding sites in the hippocampal CA1 and CA3 sectors, while, in contrast, the substantia nigra showed a significant elevation in [^{3}H]-PN200-110 binding sites.

Table 4 Regional distribution of [^{3}H]-MK-801 binding sites in gerbil brain 8 months after transient cerebral ischaemia

	Sham-operated (6)	*Cerebral ischaemia* 3 min (7)	10 min (4)
Frontal cortex	244 ± 74	196 ± 48	222 ± 62
Striatum	249 ± 74	164 ± 28*	181 ± 30
Hippocampus			
CA1 sector	326 ± 60	134 ± 60**	76 ± 67**
CA3 sector	211 ± 63	150 ± 40	147 ± 22
Dentate gyrus	308 ± 51	198 ± 53**	267 ± 9
Thalamus	257 ± 51	187 ± 33*	216 ± 55
Hypothalamus	196 ± 52	155 ± 38	138 ± 40
Substantia nigra	186 ± 62	142 ± 41	158 ± 89
Cerebellum	177 ± 31	115 ± 22**	146 ± 48

Optical density was converted to fmol mg^{-1} tissue with ^{3}H microscales.
Values are expressed as means ± s.d.
*$P<0.05$; **$P<0.01$ vs. sham-operated group (Duncan's multiple-range test). The number of animals in parentheses.

Table 5 Regional distribution of [^{3}H]-isradipine ([^{3}H]-PN200-110) binding sites in gerbil brain 8 months after transient cerebral ischaemia

	Sham-operated (6)	*Cerebral ischaemia* 3 min (7)	10 min (4)
Frontal cortex	10.3 ± 3.7	11.0 ± 2.3	12.9 ± 1.5
Striatum	9.8 ± 3.4	9.7 ± 2.2	10.5 ± 2.5
Hippocampus			
CA1 sector	9.1 ± 3.2	6.5 ± 2.5	4.5 ± 2.0*
CA3 sector	12.8 ± 2.2	15.3 ± 2.3	5.6 ± 5.9**
Dentate gyrus	23.3 ± 6.0	25.3 ± 2.9	26.6 ± 3.9
Thalamus	9.1 ± 2.4	9.9 ± 1.3	11.6 ± 1.5
Hypothalamus	1.5 ± 1.0	3.2 ± 2.9	4.4 ± 2.3
Substantia nigra	4.0 ± 1.8	4.3 ± 2.1	7.0 ± 1.6*
Cerebellum	7.7 ± 4.3	8.9 ± 1.3	8.1 ± 2.4

Optical density was converted to fmol mg^{-1} tissue with ^{3}H microscales.
Values are expressed as means ± s.d.
*$P<0.05$; **$P<0.01$ vs. sham-operated group (Duncan's multiple-range test). The number of animals in parentheses.

Discussion

The present study clearly demonstrated that long-term survival after transient cerebral ischaemia in the gerbil produced alterations in various neurotransmitter receptors, particularly in the hippocampal formation, where considerable shrinkage was noted. Three minutes of ischaemia produced neuronal damage and mild shrinkage only in the hippocampal CA1 sector. Ten minutes of ischaemia, in contrast, caused severe

neuronal damage and marked shrinkage in the hippocampal CA1 and CA3 sectors. The dentate gyrus, however, was not damaged. Thus, the histopathological observations in this study agreed, in part, with previous reports of tissue shrinkage in the hippocampal CA1 region following 5 min ischaemia (Mudrick & Baimbridge, 1989; Kirino *et al.*, 1990).

In the present study, [^{3}H]-QNB binding sites were significantly reduced only in the hippocampal CA1 sector 8 months after 3 min ischaemia, while 10 min ischaemia caused a marked reduction in these binding sites in the hippocampal CA1 and CA3 sectors. Thus, the post-ischaemic reduction in [^{3}H]-QNB binding sites that occurred with long-term survival of recirculation was noted only in the hippocampal CA1 and CA3 sectors, i.e., those which were most vulnerable to ischaemia. By contrast, [^{3}H]-CHA and [^{3}H]-PN200-110 binding showed no significant alteration in any regions 8 months after 3 min ischaemia. However, 8 months after 10 min ischaemia, [^{3}H]-CHA binding was significantly reduced in the hippocampal CA1 and CA3 sectors, dentate gyrus, and substantia nigra; [^{3}H]-PN200-110 binding was also significantly reduced in the hippocampal CA1 and CA3 sectors, although it was significantly elevated in the substantia nigra. That is, there were post-ischaemic alterations in [^{3}H]-CHA and [^{3}H]-PN200-110 binding not only in the hippocampal CA1 and CA3 sectors, but also in the dentate gyrus and substantia nigra. Interestingly, the reduction in [^{3}H]-CHA binding in the dentate gyrus, a region which was resistant to ischaemia, was significant. This finding is essentially in agreement with our previous finding of a reduction in [^{3}H]-CHA binding in the dentate gyrus just 1 month after 10 min ischaemia (Araki *et al.*, 1991); this phenomenon thus seems to indicate long-lasting post-ischaemic neurotransmitter alterations in the dentate gyrus. We have previously reported in another study (Araki *et al.*, 1989) that transient ischaemia caused neuronal damage not only in selectively vulnerable areas, but also in such brain stem components as the substantia nigra and inferior colliculus; the decrease in [^{3}H]-CHA binding sites in the substantia nigra thus seems to reflect ischaemic damage. The significantly elevated [^{3}H]-PN200-110 binding observed in the substantia nigra in this study, however, is difficult to explain. This phenomenon seems to suggest that the elimination of nigral neurones may be involved in the induction of synaptic modifications in the neurotransmitter system, which modifications result in an increase of receptor density on surviving neurones or glial cells. The precise mechanisms responsible for such findings should be investigated in further studies.

[^{3}H]-muscimol binding in the hippocampal CA1 sector was reduced 8 months after 3 min ischaemia, while it was significantly elevated in the hippocampal CA3 sector and substantia nigra, where no morphological neuronal damage was seen. Eight months after 10 min ischaemia, however, [^{3}H]-muscimol binding showed a significant reduction only in the hippocampus. Although the reason for the increased [^{3}H]-muscimol binding activity in the hippocampal CA3 sector and substantia nigra is unclear at present, this phenomenon suggests possible alteration in [^{3}H]-muscimol binding in these areas after ischaemia.

Eight months after 3 min ischaemia, [^{3}H]-MK-801 binding also showed significant reduction not only in the hippocampal CA1 sector, but also in the striatum, dentate gyrus, thalamus, and cerebellum, where no neuronal damage was seen. It is of interest that alterations in [^{3}H]-MK-801 binding after ischaemia occurred in various brain regions that exhibited no morphological neuronal damage. MK-801 is one of the most potent non-competitive NMDA antagonists (Wong *et al.*, 1986); the NMDA receptor mediates synaptic transmission and plasticity in widespread regions of the central nervous system (Monaghan *et al.*, 1989; Monaghan, 1991). Further, this receptor contributes to neuronal damage resulting from elevated extracellular glutamate levels in pathological conditions (Choi & Rothmann, 1990). The NMDA receptor may therefore play a crucial part in modifying the efficacy of synaptic transmission and in the degeneration of neuronal cells. Thus, the alteration in [^{3}H]-MK-801 binding may reflect mild modifications of synaptic transmission or receptor sensitivity in various brain regions that exhibit no cell loss, even 8 months after 3 min ischaemia. Ten minutes of ischaemia, in contrast, caused a reduction in [^{3}H]-MK-801 binding only in the hippocampal CA1 sector. Westerberg *et al.* (1989) have previously suggested that 10 min ischaemia in rats caused a reduction in NMDA binding sites in the hippocampal CA1 sector and dentate gyrus after 1 week of recirculation. They also suggested that the reduction in NMDA binding decreased progressively in the hippocampal CA1 sector following ischaemia, whereas that in the dentate gyrus was no longer present 2 weeks after ischaemia. Furthermore, they demonstrated that the NMDA receptors were strikingly resistant to degenerative processes afer ischaemia. These observations agree, at least in part, with our present findings. Therefore, our results in the present study appear to suggest that severe ischaemia, compared with a brief ischaemic insult, does not always produce synaptic rearrangement or plasticity. However, we cannot rule out the possibility that the lack of reduction in [^{3}H]-MK-801 binding 8 months after severe ischaemia may reflect a result of tissue shrinkage. Further studies are needed to investigate the precise mechanisms underlying synaptic modification, plasticity, and receptor sensitivity following ischaemia.

Interestingly, there were no alterations in the binding sites of any of the ligands used in the striatum, which was the region most vulnerable to 10 min ischaemia. The reason for this result is unclear. However, our histological study of specimens prepared 8 months after 10 min ischaemia showed that, although the small- and medium-sized neurones in the striatum were almost all destroyed, the large-sized neurones were relatively well preserved and were sparsely scattered in this field. This result is in accord with previous studies (Pulsinelli *et al.*,1982; Smith *et al.*, 1984). In a previous investigation, it was suggested that GABA receptors were located predominantly on cholinergic neurones (large-sized neurones) in the striatum, which is resistant to ischaemia (Francis & Pulsinelli, 1983). Thus, these large-sized neurones may have a high density of [^{3}H]-CHA, [^{3}H]-MK-801, and [^{3}H]-PN200-110, as well as [^{3}H]-QNB and [^{3}H]-muscimol, binding sites. The possible contribution of presynaptic components, glial cells, and blood vessels to these residual binding sites should also be considered. Furthermore, mild tissue shrinkage may occur in the striatum 8 months after ischaemia. Thus, progression of neuronal damage and the alterations that occur in various neurotransmitter receptors in the hippocampus and striatum with long-term survival following ischaemia may have different underlying mechanisms.

In conclusion, the present study demonstrated that long-term survival after transient cerebral ischaemia could modify alterations in neurotransmitter receptors, especially in the hippocampal formation, where considerable shrinkage was noted. These results also suggest that the hippocampal damage, compared with that in other regions, is not static, but progressive.

References

ARAKI, T., KATO, H. & KOGURE, K. (1989). Selective neuronal vulnerability following transient cerebral ischemia in the gerbil: distribution and time course. *Acta Neurol. Scand.*, **80**, 548–553.

ARAKI, T., KATO, H. & KOGURE, K. (1990a). Neuronal damage and calcium accumulation following repeated brief cerebral ischemia in the gerbil. *Brain Res.*, **528**, 114–122.

ARAKI, T., KATO, H., INOUE, T. & KOGURE, K. (1990b). Regional impairment of protein synthesis following brief cerebral ischemia in the gerbil. *Acta Neuropathol.*, **79,** 501–505.

ARAKI, T., KATO, H., KOGURE, K. & INOUE, T. (1990c). Regional neuroprotective effects of pentobarbital on ischemia-induced brain damage. *Brain Res. Bull.*, **25,** 861–865.

ARAKI, T., KATO, H. & KOGURE, K. (1991). Postischemic alteration of muscarinic acetylcholine, adenosine A_1 and calcium antagonist binding sites in selectively vulnerable areas: an autoradiographic study of gerbil brain. *J. Neurol. Sci.*, **106,** 206–212.

ARAKI, T., KATO, H., HARA, H. & KOGURE, K. (1992a). Postischemic binding of [^{3}H]phorbol 12,13-dibutyrate and [^{3}H]inositol 1,4,5-trisphosphate in the gerbil brain: an autoradiographic study. *Neuroscience*, **46,** 973–980.

ARAKI, T., KATO, H., KOGURE, K., SHUTO, K. & ISHIDA, Y. (1992b). Autoradiographic mapping of neurotransmitter system receptors in mammalian brain. *Pharmacol. Biochem. Behav.*, **41,** 539–542.

BÈNVENISTE, H., DREJER, J., SCHOUSBOE, A. & DIEMER, N.H. (1984). Elevation of the extracellular concentrations of glutamate and aspartate in the rat hippocampus during transient cerebral ischemia monitored by microdialysis. *J. Neurochem.*, **43,** 1369–1376.

BENVENISTE, H., JORGENSEN, M.B., DIEMER, N.H. & HANSEN, A.J. (1988). Calcium accumulation by glutamate receptor activation is involved in hippocampal cell damage after ischemia. *Acta Neurol. Scand.*, **78,** 529–536.

BENVENISTE, H., JORGENSEN, M.B., SANDBERG, M., CHRISTENSEN, T., HAGBERG, H. & DIEMER, N.H. (1989). Ischaemic damage in hippocampal CA1 is dependent on glutamate release and intact innervation from CA3. *J. Cereb. Blood Flow Metab.*, **9,** 629–639.

BOWERY, N.G., WONG, E.H.F. & HUDSON, A.L. (1988). Quantitative autoradiography of [^{3}H]-MK-801 binding sites in mammalian brain. *Br. J. Pharmacol.*, **93,** 944–954.

CHOI, D.W. & ROTHMAN, S.M. (1990). The role of glutamate neurotoxicity in hypoxic-ischemic neuronal death. *Annu. Rev. Neurosci.*, **13,** 171–182.

CRAIN, B.J., WASTERKAM, W.D., HARRISON, A.H. & NADLER, J.V. (1988). Selective neuronal death after transient forebrain ischemia in the Mongolian gerbil: a silver impregnation study. *Neuroscience*, **27,** 387–402.

CROCKARD, A., BANNOTTI, F., HUNSTOCK, A.T., SMITH, R.D., HARRIS, R.J. & SYMON, L. (1980). Cerebral blood flow and edema following carotid occlusion in the gerbil. *Stroke*, **11,** 494–498.

FRANCIS, A. & PULSINELLI, W.A. (1983). Increased binding of [^{3}H]GABA to striatal membranes following ischemia. *J. Neurochem.*, **40,** 1497–1499.

JORGENSEN, M.B. & DIEMER, N.H. (1982). Selective neuron loss after cerebral ischemia in the rat: possible role of transmitter glutamate. *Acta Neurol. Scand.*, **66,** 536–546.

JORGENSEN, M.B., DECKERT, J. & WRIGHT, D.C. (1989). Binding of [^{3}H]inositolphosphate and [^{3}H]phorbol 12,13-dibutyrate in the rat hippocampus following transient global ischemia: a quantitative autoradiographic study. *Neurosci. Lett.*, **103,** 219–224.

KATO, H., ARAKI, T., HARA, H. & KOGURE, K. (1991). Sequential changes in muscarinic acetylcholine, adenosine A_1 and calcium antagonist binding sites in the gerbil hippocampus following repeated brief ischemia. *Brain Res.*, **553,** 33–38.

KIRINO, T. (1982). Delayed neuronal death in the gerbil hippocampus following ischemia. *Brain Res.*, **239,** 57–69.

KIRINO, T., TAMURA, A. & SANO, K. (1990). Chronic maintenance of presynaptic terminals in gliotic hippocampus following ischemia. *Brain Res.*, **510,** 17–25.

KITAGAWA, K., MATSUMOTO, M., ODA, T., NIINOBE, M., HATA, R., HANDA, N., FUKUNAGA, R., ISAKA, Y., KIMURA, K., MAEDA, H., MIKOSHIBA, K. & KAMADA, T. (1990). Free radical generation during brief periods of cerebral ischemia may trigger delayed neuronal death. *Neuroscience*, **35,** 551–558.

KOGURE, K., TANAKA, J. & ARAKI, T. (1988). The mechanism of ischemia-induced brain cell injury. *Neurochem. Pathol.*, **9,** 145–170.

LOSKOTA, W.J., LOMAX, P. & VERITY, M.A. (1974). *A Stereotoxic Atlas of the Mongolian Gerbil Brain.* Michigan: Ann Arbor Science.

MONAGHAN, D.T. (1991). Differential stimulation of [^{3}H]MK-801 binding to subpopulations of NMDA receptors. *Neurosci. Lett.*, **122,** 21–24.

MONAGHAN, D.T., BRIDGES, R.J. & COTMANN, C.W. (1989). The excitatory amino acid receptors: their classes, pharmacology and distinct properties in the function of the central nervous system. *Annu. Rev. Pharmacol. Toxicol.*, **29,** 365–402.

MUDRICK, L.A. & BAIMBRIDGE, K.G. (1989). Long-term structural changes in the rat hippocampal formation following cerebral ischemia. *Brain Res.*, **493,** 179–184.

MUNEKATA, K. & HOSSMANN, K.-A. (1987). Effects of 5-minute ischemia on regional pH and energy state of the gerbil brain: relation to selective vulnerability of the hippocampus. *Stroke*, **18,** 412–417.

ONODERA, H., SATO, G. & KOGURE, K. (1987). Quantitative autoradiographic analysis of muscarinic cholinergic and adenosine A_1 binding sites after transient forebrain ischemia in the gerbil. *Brain Res.*, **415,** 309–322.

ONODERA, H., ARAKI, T. & KOGURE, K. (1988). Protein kinase C in the rat hippocampus after forebrain ischemia: autoradiographic analysis by [^{3}H]phorbol 12,13-dibutyrate. *Brain Res.*, **481,** 1–7.

PULSINELLI, W.A., BRIERLEY, J.B. & PLUM, F. (1982). Temporal profile of neuronal damage in a model of transient forebrain ischemia. *Ann. Neurol.*, **11,** 491–498.

SIESJÖ, B.K. (1981). Cell damage in the brain: a speculative synthesis. *J. Cereb. Blood Flow Metab.*, **1,** 155–185.

SIESJÖ, B.K. & BENGTSSON, F. (1989). Calcium flues, calcium antagonists and calcium-related pathology in brain ischemia, hypoglycemia, and spreading depression: a unifying hypothesis. *J. Cereb. Blood Flow Metab.*, **9,** 127–140.

SIMON, R.P., GRIFFITHS, T., EVANS, M.C., SWAN J.H. & MELDRUM, B.S. (1984). Calcium overload in selective vulnerable neurons of the hippocampus during and after ischemia: an electron microscopy study in the rat. *J. Cereb. Blood Flow Metab.*, **4,** 350–361.

SMITH, M.L., AUER, R.N. & SIESJÖ, B.K. (1984). The density and distribution of ischemic brain injury in the rat following 2–10 min of forebrain ischemia. *Acta Neuropathol.*, **64,** 319–332.

STERNAU, L., LUST, W.D., RICCI, A.J. & RATCHESON, R. (1989). Role of γ-aminobutyric acid in selective vulnerability in gerbils. *Stroke*, **20,** 281–287.

WESTERBERG, E., MONAGHAN, D.T., KALIMO, H., COTMAN, C.W. & WIELOCK, T.W. (1989). Dynamic changes of excitatory amino acid receptors in the rat hippocampus following transient ischemia. *J. Neurosci.*, **9,** 798–805.

WIELOCH, T. (1985). Neurochemical correlates to selective neuronal vulnerability. *Prog. Brain Res.*, **63,** 69–85.

WONG, E.H.F., KEMP, J.A., PRIESTLY, T., KNIGHT, A.R., WOODRUFF, G.N. & IVERSEN, L.L. (1986). The anticonvulsant MK-801 is a potent N-methyl-D-aspartate antagonist. *Proc. Natl. Acad. Sci. U.S.A.*, **83,** 7104–7108.

XIE, Y., SEO, K. & HOSSMANN, K.-A. (1989). Effect of barbiturate treatment on post-ischemic protein biosynthesis in gerbil brain. *J. Neurol. Sci.*, **92,** 317–328.

(Received February 10, 1992
Revised May 28, 1992
Accepted June 8, 1992)

Br. J. Pharmacol. (1992), **107**, 443–447

Bradykinin B_2 receptor-mediated phosphoinositide hydrolysis in bovine cultured tracheal smooth muscle cells

[1]Katrina A. Marsh & Stephen J. Hill

Department of Physiology and Pharmacology, Medical School, Queen's Medical Centre, Clifton Boulevard, Nottingham NG7 2UH

1 Bovine tracheal smooth muscle cells were established in culture to study agonist-induced phosphoinositide (PI) hydrolysis in this tissue.

2 Bradykinin (0.1 nM–10 μM) evoked a concentration-dependent increase (log EC_{50} (M) = -9.4 ± 0.2; $n = 8$) in the accumulation of total [^{3}H]-inositol phosphates in cultured tracheal smooth muscle cells whereas the selective B_1 receptor agonist des-Arg^9-bradykinin (10 μM) was significantly less effective (16% of bradykinin maximal response; relative potency = 0.2 with respect to bradykinin = 100).

3 The bradykinin-induced increase in PI hydrolysis was unaffected by the B_1 receptor antagonist des-Arg^9[Leu^8]-bradykinin (1 nM–1 μM) but showed marked attenuation in the presence of the B_2 receptor antagonists D-Arg,[Hyp^3,D-Phe^7]-bradykinin (10 nM–10 μM) or D-Arg[Hyp^3,Thi^{5,8},D-Phe^7]-bradykinin (10 nM–10 μM). The estimated K_B values obtained for these two compounds, assuming competitive antagonism, were 40 ± 14 nM and 8.6 ± 2.8 nM for D-Arg,[Hyp^3,D-Phe^7]-bradykinin and D-Arg[Hyp^3,Thi^{5,8},D-Phe^7]-bradykinin respectively.

4 We conclude that bradykinin B_2 receptors are expressed in cultured bovine tracheal smooth muscle cells and are coupled to PI hydrolysis mechanisms.

Keywords: Bradykinin; phosphoinositide hydrolysis; trachea; cultured smooth muscle

Introduction

Bradykinin has been implicated in the pathogenesis of asthma as it has been shown that, following allergen challenge, kinin levels are elevated in allergic asthmatics (Christiansen *et al.*, 1987). Bradykinin receptors have classically been divided into two subtypes which are dependent on the relative potencies of antagonists and agonists of bradykinin and are named the B_1 and B_2 receptors (Regoli & Barabe, 1980; Steranka *et al.*, 1989). More recently however, studies by Farmer and colleagues have indicated that bradykinin-induced contraction of guinea-pig tracheal smooth muscle strip preparations are insensitive to the bradykinin B_1 receptor antagonist, des-Arg^9, [Leu^8]-bradykinin and the bradykinin B_2 receptor antagonists, D-Arg,[Hyp^3,D-Phe^7]-bradykinin and D-Arg [Hyp^3, Thi^{5,8},D-Phe^7]-bradykinin were virtually inactive as antagonists in this system (Farmer *et al.*, 1989). These findings led the group to suggest the presence of a bradykinin B_3 receptor in airway smooth muscle.

The mechanisms underlying smooth muscle contraction are not entirely understood particularly in the airways. However it has been proposed that one of the more important mechanisms for initiating smooth muscle contraction is the receptor-mediated hydrolysis of phosphatidylinositol 4,5-bisphosphate to produce inositol 1,4,5-triphosphate which itself causes a release of calcium ions from intracelluar stores (Somlyo *et al.*, 1988). It is this mechanism which is responsible for the initial transient increase in intracellular calcium concentration leading to the activation of myosin light chain kinase and tension development (Chilvers *et al.*, 1989; Murray *et al.*, 1989).

In addition to its many other actions, bradykinin has been used as a tool for producing phosphoinositide hydrolysis in cell cultures (Yano *et al.*, 1984; Jackson *et al.*, 1987; Fasolato *et al.*, 1988) and the aim of this present study was primarily to establish a cell culture system with which to study agonist-induced phosphoinositide hydrolysis in airway smooth muscle. The smooth muscle of the bovine trachea, as a slice preparation, has been shown to be sensitive to several spasmogens including histamine, carbachol, 5-hydroxytryptamine (5-HT) and the fluoroaluminate ion producing an increase in phosphoinositide hydrolysis (Hall & Hill, 1988, Hall *et al.*, 1989; 1990). We have therefore used this tissue, with a known phosphoinositide response to spasmogens, to establish long term cultures in order to study the effects of bradykinin. This paper describes the establishment of bovine tracheal smooth muscle cells in culture and the effects of bradykinin on phosphoinositide hydrolysis in these cells. Bradykinin was shown to induce an increase in phosphoinositide hydrolysis in bovine tracheal smooth muscle (BTSM) cells which was attenuated by the bradykinin B_2 receptor antagonists, D-Arg,[Hyp^3,D-Phe^7]-bradykinin and D-Arg[Hyp^3,Thi^{5,8},D-Phe^7]-bradykinin. A preliminary account of this work has been presented to the British Pharmacological Society (Marsh & Hill, 1992).

Methods

Establishment of cell cultures

Bovine tracheae were obtained fresh from the local abattoir and transported on ice to the laboratory. Tracheal smooth muscle was dissected free from the mucosa and surrounding connective tissue and chopped into approximately 1 mm^3 pieces. These explants were then transfered to 75 cm^2 tissue culture treated plastic flasks to which was added 10 ml of D-Val substituted minimum essential media containing 10% foetal calf serum (FCS), 100 u ml^{-1} penicillin G, 100 μg ml^{-1} streptomycin and 250 ng ml^{-1} amphotericin B and maintained at 37°C in a humidified 10% CO_2 atmosphere. Flasks remained undisturbed for 10 days after which time cells were fed twice weekly by a complete medium change without supplementation with antibiotics. Explants were removed when sufficient growth had occurred around each one. Cells were routinely subcultured by treatment with trypsin (0.05% in versene, Glasgow formula). Cells were screened for mycoplasma contamination using the Hoechst 33258 staining method (Chen, 1977). All cell experiments were performed between passages 3 and 9.

[1] Author for correspondence.

Immunocytochemical analysis

Indirect immunocytochemistry was used to confirm the identity of the smooth muscle cells. Briefly cells were grown on 22 mm × 22 mm glass coverslips in Dulbecco's modified Eagle's medium (DMEM) containing 10% FCS until confluency. Cells were then washed (3 × 5 min in phosphate buffered saline, (PBS)) and fixed for 10 min at − 20°C in ice cold methanol. Coverslips were then washed again (3 × 5 min in PBS) and incubated for 30 min in 10% horse serum in PBS at room temperature. The monoclonal antibody anti-smooth muscle alpha actin (1:50 in 10% horse serum in PBS) or 10% horse serum in PBS controls were then incubated with the cells overnight at 4°C. Cells were again washed (3 × 5 min in PBS) and exposed to the second layer of fluorescein isothiocyanate-conjugated rabbit anti-mouse antibody (1:20 in 10% horse serum in PBS). Cells were viewed under a Zeiss epifluorescent photomicroscope III using the 487710 filter set.

Accumulation of [^{3}H]-inositol phosphates

For measurement of the production of total [^{3}H]-inositol phosphates, cells were grown to confluency in 24-well plates in DMEM containing 10% FCS. Washed cells were then incubated for 72 h at 37°C with [^{3}H]-*myo*-inositol (1 μCi/well) in 0.7 ml inositol-free DMEM supplemented with 0.5% FCS. This medium was then removed and cells were washed twice in 1 ml/well Hanks/HEPES (9.76 g l^{-1}:20 mM, pH 7.4). Following this, cells were incubated for 30 min at 37°C in 290 μl Hanks/HEPES containing 20 mM lithium chloride. Where appropriate, antagonists were added after 28 min incubation. Agonists were added in 10 μl of Hanks/HEPES with LiCl for incubation times of 2.5 to 40 min. Stimulation was stopped by the removal of agonists and the addition of 1 ml ice cold methanol/0.12 M HCl (1:1). Cells were left overnight at − 20°C before neutralisation with 25 mM Tris:0.5 M NaOH:H_2O (11:1.2:34). Total inositol phosphates were finally separated from free [^{3}H]-*myo*-inositol by anion exchange chromatography (Hall & Hill, 1988). Tritium was determined by liquid scintillation counting.

Data analysis

Concentration-response curves from individual experiments were fitted to a Hill equation using the non-linear programme ALLFIT (DeLean *et al.*, 1978). The equation fitted was:

$$\% \text{ of maximal response} = E_{max} \times D^n/D^n + (EC_{50})^n$$

where D is the agonist concentration, n is the Hill coefficient, EC_{50} is the concentration of agonist giving half maximal response and E_{max} is the maximal stimulation. Apparent dissociation constants (K_B) of receptor antagonists were determined, assuming competitive antagonism, from shifts in the agonist concentration-response curves using the relationship:

$$K_B = D/(K_2/K_1 - 1)$$

where D is the concentration of antagonist (10 μM), K_1 is the concentration of agonist producing half maximal response and K_2 is the concentration of agonist producing the same response in the presence of antagonist. Quadruplicate determinations (i.e. separate culture wells) were made in each experiment. Statistical analysis of differences between separate treatments within an experiment were made by unpaired *t* tests. Individual experiments were repeated at least three times and, unless otherwise stated, the mean ± s.e.mean cited in the text refer to the mean data obtained in *n* separate experiments. Analysis of the extent of stimulation of inositol phospholipid hydrolysis by various agonists (e.g. Figure 2) was performed by use of paired *t*-tests of the mean basal and agonist-stimulated data obtained in each of n separate experiments.

Chemicals

Anti-alpha smooth muscle actin monoclonal antibody and FITC-conjugated rabbit-anti-mouse antibody were purchased from Dako Ltd. [^{3}H]-myo-inositol (20 Ci mmol^{-1}) was obtained from New England Nuclear Products. Histamine dihydrochloride, carbachol chloride, bradykinin acetate. D-Arg,[Hyp^3,D-Phe^7]-bradykinin,D-Arg[Hyp^3,Thi^{5,8},D-Phe^7]-bradykinin, des-Arg^9,[Leu^8]-bradykinin, des-Arg^9-bradykinin, Hoechst 33258 and 5-hydroxytryptamine creatinine sulphate were purchased from Sigma.

Results

Cells were seen to grow from the explants of bovine tracheal smooth muscle after approximately ten days in culture. All cultures tested for mycoplasma contamination were negative. Bovine tracheal smooth muscle (BTSM) cells were found to contain alpha smooth muscle actin lying in strands along the length of the cells (Figure 1). All cell lines grown from explants contained similar amounts of alpha smooth muscle actin as judged by eye.

Agonist-induced [^{3}H]-inositol phosphate accumulation

The effect of several agonists on total [^{3}H]-inositol phosphate formation in BTSM cells is shown in Figure 2. Carbachol (1 mM, $n = 5$) and histamine (1 mM, $n = 6$) produced no significant increase in the phosphoinositide (PI) hydrolysis in these cells. 5-Hydroxytryptamine (10 mM) produced a 2.4 ± 0.4 ($n = 8$) fold increase in PI hydrolysis and 0.1 μM bradykinin effected a 5.4 ± 0.6 ($n = 11$) fold increase in [^{3}H]-inositol phosphate accumulation over basal levels. [^{3}H]-inositol phosphate production induced by bradykinin was found to increase sharply up to an incubation time of 10 min after which point the curve began to plateau (Figure 3). This incubation time of 10 min was used in all other experiments.

Bradykinin (0.1 nM−10 μM) produced a concentration-dependent increase in the accumulation of [^{3}H]-inositol phosphates in BTSM cells (Figure 4a). The mean log EC_{50} (M) value obtained from these data was − 9.4 ± 0.2 ($n = 8$). The bradykinin B_1 receptor agonist, des-Arg^9-bradykinin (1 nM−1 μM, $n = 4$) was found to produce a much smaller effect on the production of [^{3}H]-inositol phosphates in these cells

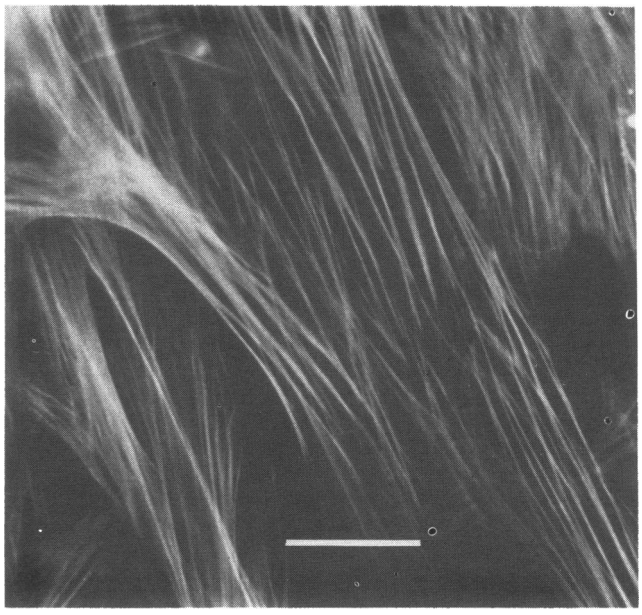

Figure 1 Monolayer of bovine tracheal smooth muscle cells fixed and stained for alpha smooth muscle actin by indirect immunocytochemical methods. Bar = 5 μM.

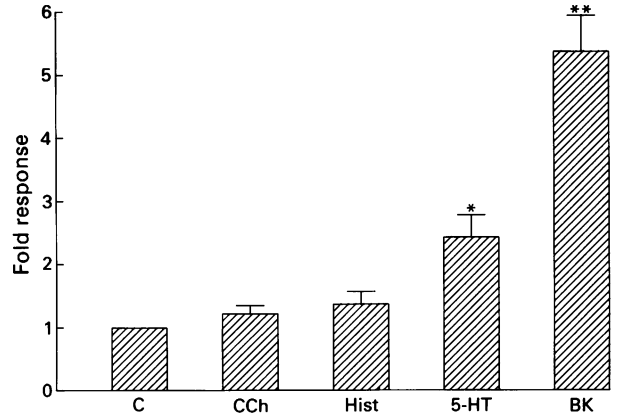

Figure 2 The effect on the accumulation of [^{3}H]-inositol phosphates in bovine cultured tracheal smooth muscle (BTSM) cells of 1 mM carbachol (CCh, $n = 5$), 1 mM histamine (Hist, $n = 6$), 100 μM 5-hydroxytryptamine (5-HT, $n = 8$) or 0.1 μM bradykinin (BK, $n = 11$). Values represent mean ($\pm$ s.e.mean, vertical bars) of the fold increase in mean [^{3}H]-inositol phosphate accumulation over basal levels (C) obtained in 5–11 separate experiments. In each experiment quadruplicate (separate culture wells) determinations were made of basal- and agonist-stimulated [^{3}H]-inositol phosphate accumulation. $*P<0.01$; $**P<0.001$ compared to corresponding basal levels (paired t test of mean basal- and agonist-stimulated responses obtained in each individual experiment). The mean basal response in these experiments was 512 ± 42 d.p.m. ($n = 32$). n represents the number of individual experiments conducted.

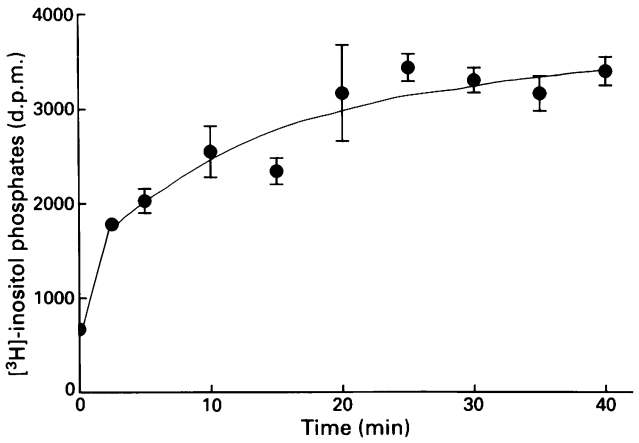

Figure 3 The effect of increasing incubation time with 0.1 μM bradykinin on total [^{3}H]-inositol phosphates accumulated. Values represent quadruplicate determinations and vertical lines indicate s.e.mean. Data are from a single experiment repeated four more times with similar results.

(Figure 4b) when compared to the response produced by bradykinin. The maximum response produced by des-Arg^9-bradykinin (10^{-5} M) was 1.7 ± 0.2 fold over basal values ($P<0.05$, paired t test; $n = 6$) and significantly less ($P<0.001$; unpaired t test) than the stimulation produced by 10^{-7} M bradykinin (5.4 ± 0.6 fold; $n = 11$). The mean log EC_{50} (M) obtained for des-Arg^9-bradykinin was -6.7 ± 0.4 ($n = 4$).

Effects of bradykinin receptor antagonists

The bradykinin B_1 receptor antagonist, des-Arg^9,[Leu^8]-bradykinin, (1 nM–1 μM, $n = 4$) was found to have no significant effect on the bradykinin-induced increase in PI hydrolysis (Figure 5a). However, both the bradykinin B_2 receptor antagonists D-Arg,[Hyp^3,D-Phe^7]-bradykinin and D-Arg[Hyp^3, Thi^{5,8},D-Phe^7]-bradykinin (Figure 5b; Figure 6) were found to decrease the elevated levels of PI hydrolysis induced by bradykinin (0.1 μM). Both B_2 receptor antagonists produced a

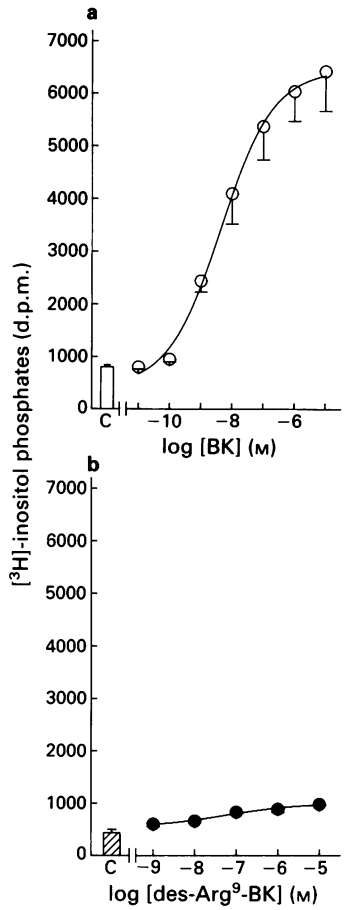

Figure 4 Concentration-response curves for bradykinin-stimulated (a) and des-Arg^9-bradykinin-stimulated (b) accumulation of [^{3}H]-inositol phosphates. The control (unstimulated) responses are shown by the columns marked C. Each data point represents the mean of quadruplicate determinations and vertical lines show s.e.mean. Data are from two individual experiments repeated at least four times more with similar results.

parallel shift of the bradykinin concentration-response curves to higher concentrations (e.g. Figure 6). K_B values calculated from the parallel shifts obtained with D-Arg,[Hyp^3,D-Phe^7]-bradykinin and D-Arg[Hyp^3, Thi^{5,8},D-Phe^7]-bradykinin (both at 10 μM) assuming competitive antagonism were 40 ± 14 nM ($n = 3$) and 8.6 ± 2.8 nM ($n = 3$) respectively.

Discussion

This study demonstrates that BTSM cells retain their 5-HT and bradykinin receptors in culture. Bradykinin was shown to induce an increase in phosphoinositide hydrolysis in these cells. The evidence obtained in this study suggests that the bradykinin-stimulated inositol phospholipid response in BTSM cells is mediated by the B_2 receptor subtype since B_2 receptor antagonists, but not B_1 receptor antagonists, are able to inhibit the bradykinin-induced increase in [^{3}H]-inositol phosphate accumulation. Furthermore the B_1 receptor agonist, des-Arg^9-bradykinin (Regoli & Barabe, 1980) produced a much weaker inositol phospholipid response than bradykinin. The maximum response produced by des-Arg^9-bradykinin (10 μM) was only 16% of that produced by bradykinin and the relative potency of this agonist (bradykinin = 100) was 0.2

It is of interest to note that bovine cultured tracheal smooth muscle cells do not retain functional muscarinic and histamine receptors which have been shown to be present in slice preparations of the same tissue (Hall & Hill, 1988). Thus, carbachol (1 mM) and histamine (1 mM) were without

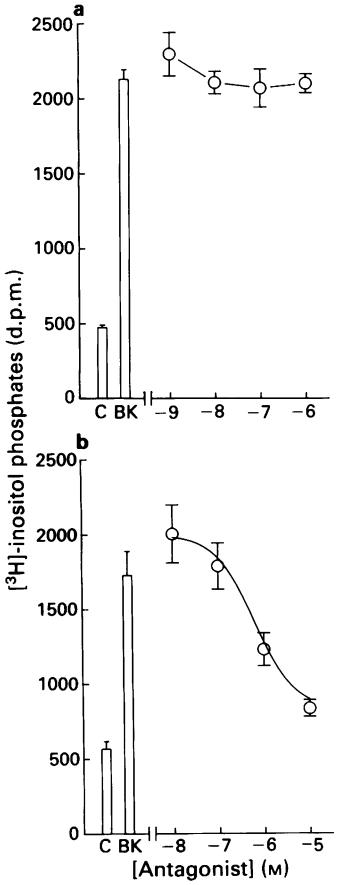

Figure 5 Effect on the inositol phosphate response to 0.1 μM bradykinin produced by des-Arg[9][Leu[8]]-bradykinin (a) or D-Arg [Hyp[3],Thi[5,8],D-Phe[7]]-bradykinin (b). The basal responses are shown by the columns marked C and the response to bradykinin by the columns marked BK. The effect of various concentrations of antagonist added 2 min prior to bradykinin are shown on the graph on the right hand side of each figure. Each data point represents the mean of quadruplicate determinations and vertical lines show s.e.mean. The experiment was repeated three times more with similar results.

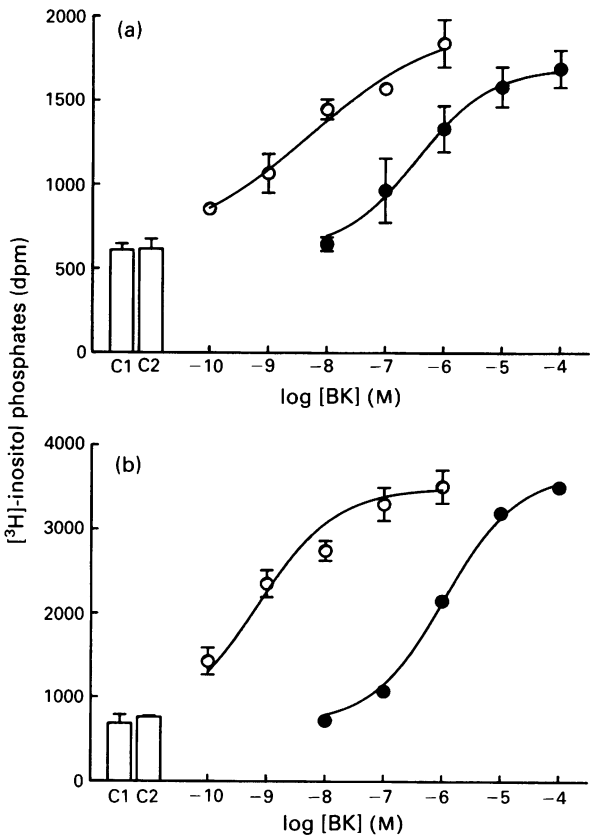

Figure 6 Concentration-response curves for bradykinin (BK)-stimulated [3H]-inositol phosphate accumulation in the absence (○) or presence (●) of either (a) D-Arg, [Hyp[3],D-Phe[7]]-bradykinin (10 μM) or (b) D-Arg[Hyp[3],Thi[5,8],D-Phe[7]]-bradykinin (10 μM). The columns represent basal responses obtained in the absence (C1) and presence (C2) of antagonist. Data points represent the mean of quadruplicate determinations obtained in a single experiment. Vertical lines show s.e.mean. Each experiment was repeated twice more with similar results.

significant effect on inositol phospholipid hydrolysis in cultured BTSM cells at concentrations which would produce maximal accumulations of [3H]-inositol phosphates in slices of bovine tracheal smooth muscle (log EC_{50} [carbachol] (M) = 5.4; log EC_{50} [histamine] (M) = 4.5; Hall & Hill, 1988) and maximal contractile activity in bovine tracheal smooth muscle strips (log EC_{50} [carbachol] (M) = 6.12 ± 0.11; log EC_{50} [histamine] (M) = 6.4 ± 0.5; Connoll & Hill, unpublished results). That changes in expression of receptors occurs when cells are taken into culture has previously been noted in airway smooth muscle. Using the guinea-pig lung *in vivo* and tracheal strips *in vitro*, Farmer *et al.* (1989) demonstrated that the B_2 receptor antagonists, D-Arg,[Hyp[3],D-Phe[7]]-bradykinin and D-Arg[Hyp[3],Thi[5,8],D-Phe[7]]-bradykinin, were weak inhibitors of bradykinin-induced bronchoconstriction *in vivo*, and virtually inactive as antagonists of bradykinin-induced tracheal smooth muscle contraction *in vitro*. In addition, D-Arg,[Hyp[3],D-Phe[7]]-bradykinin had no effect on binding of [3H]-bradykinin in fresh tissue. The same group later investigated the bradykinin receptors in cultured guinea-pig tracheal smooth muscle cells (Farmer *et al.*, 1991b). In this case they found that D-Arg,[Hyp[3],D-Phe[7]]-bradykinin was active against bradykinin-induced prostaglandin synthesis and also totally displaced [3H]-bradykinin binding. The differences noted in the expression of receptors between fresh tissue and cultured cells may be explained by the changes in the microenvironment surrounding the cells with the loss in culture of extracellular matrices and growth factors.

For bradykinin to induce smooth muscle contraction in the intact trachea it must elicit an increase in calcium ions within the smooth muscle cell either by action leading to a release of calcium ions from intracellular stores or an influx from extracellular sources. Murray & Kotlikoff (1991) have recently investigated the importance of calcium influx in the maintenance of smooth muscle contraction. Using the calcium-sensitive fluorescent probe Fura-2, they reported on a biphasic response of human airway smooth muscle cells to bradykinin. The initial transient rise in intracellular calcium was independent of extracellular calcium and was followed by a sustained influx of calcium ions. In guinea-pig tracheal smooth muscle cells, Farmer *et al.* (1989) have suggested that bradykinin-induced intracellular calcium ion mobilization is mediated by putative B_3 receptors, since the bradykinin-induced efflux of ^{45}Ca ions was unaffected by the B_2 receptor antagonist D-Arg[Hyp[3],D-Phe[7]]-bradykinin (Farmer *et al.*, 1991b), the efflux of calcium ions being the 'overflow' after intracellular calcium ion mobilisation. However, it is not known at this point whether the influx of calcium ions induced by bradykinin in guinea-pig tracheal smooth muscle is sensitive to inhibition by B_2 receptor antagonists.

The results obtained in the present study indicate that there is a marked expression of bradykinin B_2 receptors in cultured bovine tracheal smooth muscle cells and would suggest that these receptors in BTSM cells are coupled to phosphoinositide hydrolysis. In this system we found no inherent partial agonist activity was produced by either of the bradykinin B_2 receptor antagonists used which is contrary to what was found in the guinea-pig lung and tracheal strips where they produced a spasmogenic effect (Farmer *et al.*, 1989).

The K_B values obtained in BTSM cells in the present study for the B_2 antagonists D-Arg,[Hyp^3,D-Phe^7]-bradykinin and D-Arg[Hyp^3,Thi^{5,8},D-Phe^7]-bradykinin (40 nM and 8.6 nM respectively) were found to be of the same order of magnitude as those obtained from functional studies in the rabbit jugular vein which contains B_2 receptors (D-Arg,[Hyp^3,D-Phe^7]-bradykinin, 13 nM; D-Arg(Hyp^3,Thi^{5,8},D-Phe^7]-bradykinin, 10 nM; Regoli *et al.*, 1990). Preparations expressing the putative B_3 receptor demonstrated a much lower affinity for the antagonist with K_B values being in the micromolar range in the guinea-pig trachea (D-Arg,[Hyp^3,D-Phe^7]-bradykinin, 1.1 μM; D-Arg[Hyp^3,Thi^{5,8},D-Phe^7]-bradykinin, 1.3 μM; Field *et al.*, 1992) and the guinea-pig ileum (D-Arg,[Hyp^3,D-Phe^7]-bradykinin, 1.3 μM; D-Arg[Hyp^3,Thi^{5,8},D-Phe^7]-bradykinin, 1.5 μM; Field *et al.*, 1992). A comparison of these data with the values obtained in the present study confirms that cultured BTSM cells do indeed express B_2 receptors.

That bradykinin can increase phosphoinositide hydrolysis in BTSM cells via a B_2 receptor and can increase intracellular calcium ion mobilisation in guinea-pig cultured tracheal smooth muscle cells via a mechanism which is insensitive to B_2 receptor antagonists (Farmer *et al.*, 1991b) may lead one to suggest that there are species differences in the coupling of bradykinin receptors to inositol phospholipid hydrolysis and calcium ion mobilization. However, the studies performed in guinea-pig cultured tracheal smooth muscle cells are complicated by the fact that whereas intracellular calcium ion mobilisation appears to be insensitive to B_2 antagonism, the stimulation by bradykinin of prostaglandin formation (which is presumably a calcium-dependent process) can be completely attenuated by the B_2 antagonist D-Arg,[Hyp^3,D-Phe^7]-bradykinin (Farmer *et al.*, 1991b). Consequently, at this stage, it is impossible to state the role of either the B_2 or the putative B_3 receptor in the maintenance or modulation of airway smooth muscle contraction with any degree of certainty and until the advent of specific B_3 receptor antagonists this subdivision of receptors remains to be characterized. It is noteworthy that compounds from a recently developed series of analogues of B_2 receptor antagonists have been shown to produce antagonist activity in tissues normally insensitive to B_2 receptor antagonists. D-Arg[Hyp^3,Thi^5,D-Tic^7,Tic^8]-bradykinin was shown to inhibit [^{3}H]-bradykinin binding, bradykinin-induced contraction and ^{45}Ca ion efflux in guinea-pig tracheal smooth muscle (Farmer *et al.*, 1991a) and D-Arg[Hyp^3,Thi^5,D-Tic^7,Oic^8]-bradykinin (Hoe 140; Hock *et al.*, 1991) was found to antagonize potently contractile responses to bradykinin in the guinea-pig trachea (Field *et al.*, 1992).

Studies concerning the specific roles of the B_2 and B_3 receptors, if the subdivision exists, in airway smooth muscle contraction, and their relation to phosphoinositide hydrolysis and calcium ion mobilisation are in need of some clarification. To this end the culture of bovine tracheal smooth muscle cells described here will provide a most useful tool with which to study the second messenger systems involved in smooth muscle contraction. We conclude that the bradykinin-induced increase in phosphoinositide hydrolysis in BTSM cells is mediated via a B_2 receptor sensitive to the antagonists D-Arg,[Hyp^3,D-Phe^7]-bradykinin and D-Arg[Hyp^3, Thi^{5,8},D-Phe^7]-bradykinin. This culture system will also enable us to investigate the bradykinin receptors mediating calcium ion mobilisation at the single cell level which is currently in progress.

We wish to thank the A.F.R.C. for their financial support of this work.

References

CHEN, T.R. (1977). *In situ* detection of mycoplasma contamination in cell cultures by fluorescent Hoechst stain 33258. *Exp. Cell Res.*, **104**, 255–259.

CHILVERS, E.R., CHALLISS, R.A.J., BARNES, P.J. & NAHORSKI, S.R. (1989). Mass changes of inositol (1,4,5) triphosphate in trachealis muscle following agonist stimulation. *Eur. J. Pharmacol.*, **164**, 587–590.

CHRISTIANSEN, S.C., PROOD, D. & COCHRANE, C.G. (1987). Detection of tissue kallikrein in the bronchoalveolar lavage fluid of asthmatic patients. *J. Clin. Invest.*, **79**, 188–197.

DELEAN, A., MUNSON, P.J. & RODBARD, D. (1978). Simultaneous analysis of families of sigmoidal curves: application to bioassay, radioligand assay and physiological dose-response curves. *Am. J. Physiol.*, **235**, E97–E102.

FARMER, S.G., BURCH, R.M., KYLE, D.J., MARTIN, J.A., MEEKER, S.N. & TOGO, J. (1991a). D-Arg[Hyp^3-Thi^5-D-Tic^8]-bradykinin, a potent antagonist of smooth muscle BK_2 receptors and BK_3 receptors. *Br. J. Pharmacol.*, **102**, 785–787.

FARMER, S.G., BURCH, R.M., MEEKER, S.A. & WILKINS, D.E. (1989). Evidence for a pulmonary B_3 bradykinin receptor. *Mol. Pharmacol.*, **36**, 1–8.

FARMER, S.G., ENSOR, J.E. & BURCH, R.M. (1991b). Evidence that cultured airway smooth muscle cells contain bradykinin B_2 and B_3 receptors. *Am. J. Respir. Cell Mol. Biol.*, **4**, 273–277.

FASOLATO, C., PANDIELLA, A., MELDOLESI, J. & POZZAN, T. (1988). Generation of inositol phosphates, cytosolic calcium, and ionic fluxes in PC12 cells treated with bradykinin. *J. Biol. Chem.*, **263**, 17350–17359.

FIELD, J.L., HALL, J.M. & MORTON, I.K.M. (1992). Bradykinin receptors in the guinea-pig taenia caeci are similar to proposed BK_3 receptors in the guinea-pig trachea, and are blocked by HOE 140. *Br. J. Pharmacol.*, **105**, 293–296.

HALL, I.P., DONALDSON, J. & HILL, S.J. (1989). Inhibition of histamine-stimulated inositol phospholipid hydrolysis by agents which increase cyclic AMP levels in bovine tracheal smooth muscle. *Br. J. Pharmacol.*, **97**, 603–613.

HALL, I.P., DONALDSON, J. & HILL, S.J. (1990). Modulation of fluoroaluminate-induced inositol phosphate formation by increases in tissue cyclic AMP content in bovine tracheal smooth muscle. *Br. J. Pharmacol.*, **100**, 646–650.

HALL, I.P. & HILL, S.J. (1988). β2-Adrenoceptor stimulation inhibits histamine stimulated inositol phospholipid hydrolysis in bovine tracheal smooth muscle. *Br. J. Pharmacol.*, **95**, 1204–1212.

HOCK, F.J., WIRTH, K., ALBUS, U., LINZ, W., GERHARDS, H.J., WIEMER, G., HENKE, ST., BREIPOHL, G., KONIG, W., KNOLLE, J. & SCHOLKENS, B.A. (1991). Hoe 140 a new potent and long acting bradykinin-antagonist: *in vitro* studies. *Br. J. Pharmacol.*, **102**, 769–773.

JACKSON, T.R., HALLAM, T.J., DOWNES, C.P. & HANLEY, M.R. (1987). Receptor coupled events in bradykinin action: rapid production of inositol phosphates and regulation of cytosolic free calcium in a neural cell line. *EMBO J.*, **6**, 49–54.

MARSH, K.A. & HILL, S.J. (1992). Bradykinin-induced phosphoinositide hydrolysis and calcium ion mobilisation in cultured bovine tracheal smooth muscle cells. *Br. J. Pharmacol.*, (in press).

MURRAY, R.K., BENNETT, C.F., FLUHARTY, S.J. & KOTLIKOFF, M.I. (1989). Mechanism of phorbol ester inhibition of histamine-induced IP_3 formation in cultured airway smooth muscle. *Am. J. Physiol.*, **257**, L209–L216.

MURRAY, R.K. & KOTLIKOFF, M.I. (1991). Receptor-activated calcium influx in human airway smooth muscle cells. *J. Physiol.*, **435**, 123–144.

REGOLI, D. & BARABE, J. (1980). Pharmacology of bradykinin and related kinins. *Pharmacol. Rev.*, **32**, 1–46.

REGOLI, D., RHALEB, N.-E., DRAPEAU, G. & DION, S. (1990). Kinin receptor subtypes. *J. Card. Pharmacol.*, **15**, S30–S38.

SOMLYO, A.P., WALKER, J.W., GOLDMAN, Y.E., TRENTHAM, D.R., KOBAYASHI, S., KITAZAWA, T. & SOMLYO, A.V. (1988). Inositol triphosphate, calcium and muscle contraction. *Phil. Trans. R. Soc. London, B*, **320**, 399–404.

STERANKA, L.R., FARMER, S.G. & BURCH, R.M. (1989). Antagonists of B2 bradykinin receptors. *FASEB J.*, **3**, 2019–2025.

YANO, K., HIGASHIDA, H., INOUE, R. & NOZAWA, Y. (1984). Bradykinin-induced rapid breakdown of phosphatidylinositol 4,5-bisphosphate in neuroblastoma × glioma hybrid NG108-15 cells. *J. Biol. Chem.*, **259**, 10201–10207.

(Received March 23, 1992
Revised June 10, 1992
Accepted June 15, 1992)

Br. J. Pharmacol. (1992), **107**, 448–455

Short-term desensitization of the histamine H_1 receptor in human HeLa cells: involvement of protein kinase C dependent and independent pathways

[1] M.J. Smit, *S.M. Bloemers, R. Leurs, *L.G.J. Tertoolen, A. Bast, *S.W. de Laat & H. Timmerman

Department of Pharmacochemistry, Faculty of Chemistry, Vrije Universiteit, De Boelelaan 1083, 1081 HV Amsterdam, The Netherlands and *Netherland Institute for Developmental Biology, Hubrecht Laboratory, Uppsalalaan 8, 3584 CT Utrecht, The Netherlands

1 In this study we have investigated the effects of short-term exposure of cells to histamine on the subsequent H_1 receptor responsiveness in HeLa cells, using Ca^{2+} fluorescence microscopy and video digital imaging.

2 In HeLa cells, histamine (100 μM) induces an immediate H_1 receptor-mediated biphasic elevation of the intracellular Ca^{2+} concentration ($[Ca^{2+}]_i$) (basal $[Ca^{2+}]_i$: 81 ± 30 nM, histamine-induced Ca^{2+} response: first phase: 1135 ± 79 nM; second phase: 601 ± 52 nM, $n = 11$).

3 The histamine H_1 receptors on HeLa cells are readily susceptible to desensitization since repetitive exposure of the same group of cells to histamine (100 μM) markedly affected the release and influx component of the induced Ca^{2+} response (second application of histamine: first phase: 590 ± 92 nM, second phase: 279 ± 47 nM; third application of histamine: first phase: 454 ± 127 nM, second phase: 240 ± 45 nM, $n = 6$). Video digital imaging revealed an increase in the lag time between stimulation and monitoring of the Ca^{2+} response and a reduced increase in $[Ca^{2+}]_i$ after desensitization with histamine.

4 Neither the release component of the ATP response (50 μM) nor the caffeine (3 mM)-induced Ca^{2+} release were found to be affected by desensitization with 100 μM histamine. However, the second phase of the ATP response was significantly reduced after desensitization with histamine (control cells: 516 ± 33 nM; desensitized cells: 331 ± 96 nM, $n = 4$, $P < 0.05$).

5 Activation of protein kinase C (PKC) by phorbol-12-myristate-13-acetate was found to inhibit the histamine as well as ATP-induced Ca^{2+} response in a dose-dependent manner.

6 In PKC downregulated cells the second phase of the histamine-induced Ca^{2+} response was significantly elevated, indicating the involvement of PKC in the negative feedback on the Ca^{2+} influx (control cells: second phase: 601 ± 52 nM ($n = 11$); PKC downregulated cells: second phase: 890 ± 90 nM, $n = 10$, $P < 0.05$).

7 Homologous desensitization of H_1 receptor responsiveness was still observed in PKC downregulated cells, implying the rapid activation of a regulatory mechanism other than PKC.

8 Based on our experimental data we suggest that short-term desensitization of the histamine H_1 receptor evolves from two different processes: a selective reduction of the histamine-induced Ca^{2+} release, mediated by a PKC-independent pathway, and a non-selective inhibition of the receptor-mediated Ca^{2+} influx activated by a PKC-dependent pathway.

Keywords: Histamine; H_1 receptor; desensitization; Ca^{2+} signalling; video digital imaging; HeLa cells; protein kinase C; Ca^{2+} influx; Ca^{2+} release; receptor kinase

Introduction

G-protein coupled receptors frequently show a dynamic regulation, being either increased or diminished in response to various conditions. This is not only observed under *in vitro* conditions but can also occur *in vivo* (Manning *et al.*, 1987; Homcy *et al.*, 1991) and has been suggested to have consequences for drug therapy (Brodde *et al.*, 1990; Motomura *et al.*, 1990; Ghosh *et al.*, 1991; Homcy *et al.*, 1991; Stiles *et al.*, 1991).

Desensitization is regarded as one of the prominent mechanisms of receptor regulation. This process is characterized by a loss of receptor responsiveness, despite the continuous presence of a high concentration of a stimulus (Hausdorff *et al.*, 1990; Huganir & Greengard, 1990). This process can become apparent during drug therapy (Brodde *et al.*, 1990), and may have a role in several pathophysiological conditions (Homcy *et al.*, 1991; Stiles *et al.*, 1991).

In certain pathologies, e.g. an allergic reaction or asthmatic attack, histamine is released from either mast cells and basophils, resulting in a high local concentration. Thus, histamine receptors located near these sites might become desensitized. The desensitization of histamine H_1 and H_2 receptors has been reported to occur in smooth muscle preparations and various isolated cell systems (see for references Leurs *et al.*, 1990; 1991b). We have previously suggested that desensitization of the histamine H_1 receptor is homologous and caused by an alteration at the level of the histamine H_1 receptor (Leurs *et al.*, 1990; 1991b), conclusions that were based on functional studies, measurements of inositol phosphate production and radioligand binding studies. Nevertheless, the use of smooth muscle preparations has its limitations, since large quantities of material are needed for measurements of inositol phosphate production or radioligand binding studies. Moreover, since these preparations do not represent a homogeneous population of cells and histamine receptors, their use for detailed mechanistic investigation is rather limited. These considerations prompted

[1] Author for correspondence.

us to search for a well-defined cellular system.

In the present study, HeLa cells, a human uterine carcinoma cell line, was chosen as a model system to study the process of histamine H_1 receptor desensitization. Previous work from various laboratories has already revealed several characteristics with respect to the histamine H_1 receptor. Production of inositol phosphates, changes in ion permeability and Ca^{2+} signalling have been well delineated in this cell line after activation of the histamine H_1 receptor (Hazama *et al.*, 1985; Sauvé *et al.*, 1987; 1991; Volpi & Berlin, 1988; Tilly *et al.*, 1990a,b; Bristow *et al.*, 1991; Raymond *et al.*, 1991). Since these cells appear to possess a high number of [^{3}H]-mepyramine binding sites (Bristow & Young, 1991), they might be suitable for investigation of H_1 receptor regulation.

The present study was undertaken in order to examine the effects of short-term exposure of HeLa cells to histamine on the subsequent H_1 receptor responsiveness. As parameter for receptor-activation, we used the increase in intracellular Ca^{2+} levels ($[Ca^{2+}]_i$) measured by fluorescence microscopy supported by digital video recording. The advantages of this technique are its high sensitivity and the ability to monitor directly changes in $[Ca^{2+}]_i$ in groups of 6 to 8 cells stimulated repeatedly. This feature is especially important with regard to the agonist-induced desensitization.

Methods

Cell culture

Human HeLa cells were cultured at 37°C in a humidified atmosphere with 7.5% CO_2 in Dulbecco's modified Eagle's medium supplemented with 7.5% heat-inactivated foetal-calf serum (Integro, The Netherlands), 2 mM L-glutamine, 10 iu ml^{-1} penicillin and 10 $\mu g\,ml^{-1}$ streptomycin (Flow Laboratories). The cells were passaged twice a week, using trypsin (0.05%)-EDTA (0.2 $mg\,ml^{-1}$) (Flow Laboratories) and grown to sub-confluency for the fluorescence measurements.

Measurements of $[Ca^{2+}]_i$

HeLa monolayers, grown on glass coverslips, were loaded with 10 μM fura-2-AM ester in a HBS buffer (composition mM: NaCl 140, KCl 5, $CaCl_2$ 2, $MgCl_2$ 1, glucose 10 plus 0.2% bovine serum albumin (BSA) and HEPES 10 mM (pH 7.4)) for 30 min at 37°C. Ca^{2+}-dependent fura-2 fluorescence was monitored at an emission wavelength of 510 nm with an excitation wavelength of 340 nm and 380 nm, and calcium concentration calculated according to the formula derived by Grynkiewicz (1985). Fluorescence measurements were carried out at 33°C in HBS buffer by use of a fluorescence microscope (Leitz orthoplan, Ernst Leitz GHMB Wetzlar, Germany) and a SPEX dual wavelenth fluorimeter as excitation source (SPEX Industries IC, N.Y., U.S.A.). For Ca^{2+} measurements 6 to 8 cells were selected in all measurements. HeLa cells were washed every 5 min by completely exchanging the medium by rapid perfusion over a period of 10 min. Exposure of cells to a stimulus lasted for a period of 5 min. Thereafter, cells were washed rapidly three times and were exposed to another stimulus 5 min later. The background, largely due to autofluorescence, was measured before fura-2-AM loading and was corrected for when calculating the calcium concentration. Minimal fluorescence (F_{min}) was achieved by complexing calcium with 6 mM EGTA in Ca^{2+}-free HBS buffer (pH 8.0) and maximal fluorescence (F_{max}) was measured by permeabilization of cells with 3 μM ionomycin.

Video digital imaging

Changes in Ca^{2+}-dependent fura-2 fluorescence upon receptor activation in HeLa cells were simultaneously recorded at alternating 340 and 380 nm with an image intensifier coupled to a video camera. Fluorescence ratios were calculated and corrected for background fluorescence by means of a computer programme.

Chemicals

Histamine dihydrochloride, methacholine chloride, bradykinin, phorbol-12-myristate-13-acetate, ionomycin and ATP (sodium salt) were obtained from Sigma Chemical Company Ltd. (St, Louis, MO, U.S.A.), fura-2-acetoxymethylester (fura-2-AM) was from Molecular Probes (Eugene, OR, U.S.A). The enantiomers of cicletanine were kindly donated by the Institute of Henri Beaufour (France).

Statistical analysis

All data shown are expressed as mean ± s.e. of at least four independent experiments. Statistical analysis was carried out by Student's t test. P values <0.05 were considered to indicate a significant difference.

Results

The histamine-induced calcium response in HeLa cells

In HeLa cells, 100 μM histamine induced an immediate biphasic elevation of the intracellular Ca^{2+} concentration ($[Ca^{2+}]_i$) as measured by fura-2 fluorescence microscopy (Figure 1a). This response was characterized by a rapid transient rise in $[Ca^{2+}]_i$ followed by a sustained increase in $[Ca^{2+}]_i$ which lasted until the agonist was removed (Figure 1). The basal level of $[Ca^{2+}]_i$ in HeLa cells was 81 ± 30 nM ($n = 11$) which, after application of 100 μM histamine, was rapidly increased to 1135 ± 79 nM (first phase, $n = 11$). After this initial rapid rise the $[Ca^{2+}]_i$ decreased to a level of 601 ± 52 nM (second phase, $n = 11$) by 30 s after addition of histamine. The initial rise is largely dependent on the release of intracellular Ca^{2+}, whereas the second phase depends on the influx of extracellular Ca^{2+} (Tilly *et al.*, 1990b). As can be seen in Figure 1b the elevation of $[Ca^{2+}]_i$ by 100 μM histamine was abolished by 1 μM (-)-cicletanine, an H_1-receptor antagonist (Schoeffter *et al.*, 1987). The inactive enantiomer, (+)-cicletanine (1 μM) did not affect the responsiveness of HeLa cells to histamine (Figure 1c). These data clearly indicate the involvement of the histamine H_1 receptor in the response to histamine.

The histamine induced Ca^{2+}-mobilization within the HeLa cells was also monitored by video digital imaging (Figure 2).

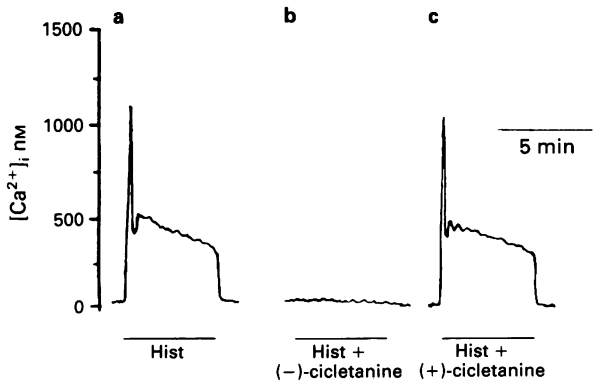

Figure 1 Intracellular free Ca^{2+} transients induced by histamine (Hist, 100 μM) (a), histamine (100 μM) in the presence of (-)-cicletanine (1 μM) (b) and histamine (100 μM) in the presence of (+)-cicletanine (1 μM) (c) in a group of 6 to 8 HeLa cells. The HeLa cells were exposed to the indicated drugs for a period of 5 min as indicated by the bars. Typical experiments out of 4 are shown.

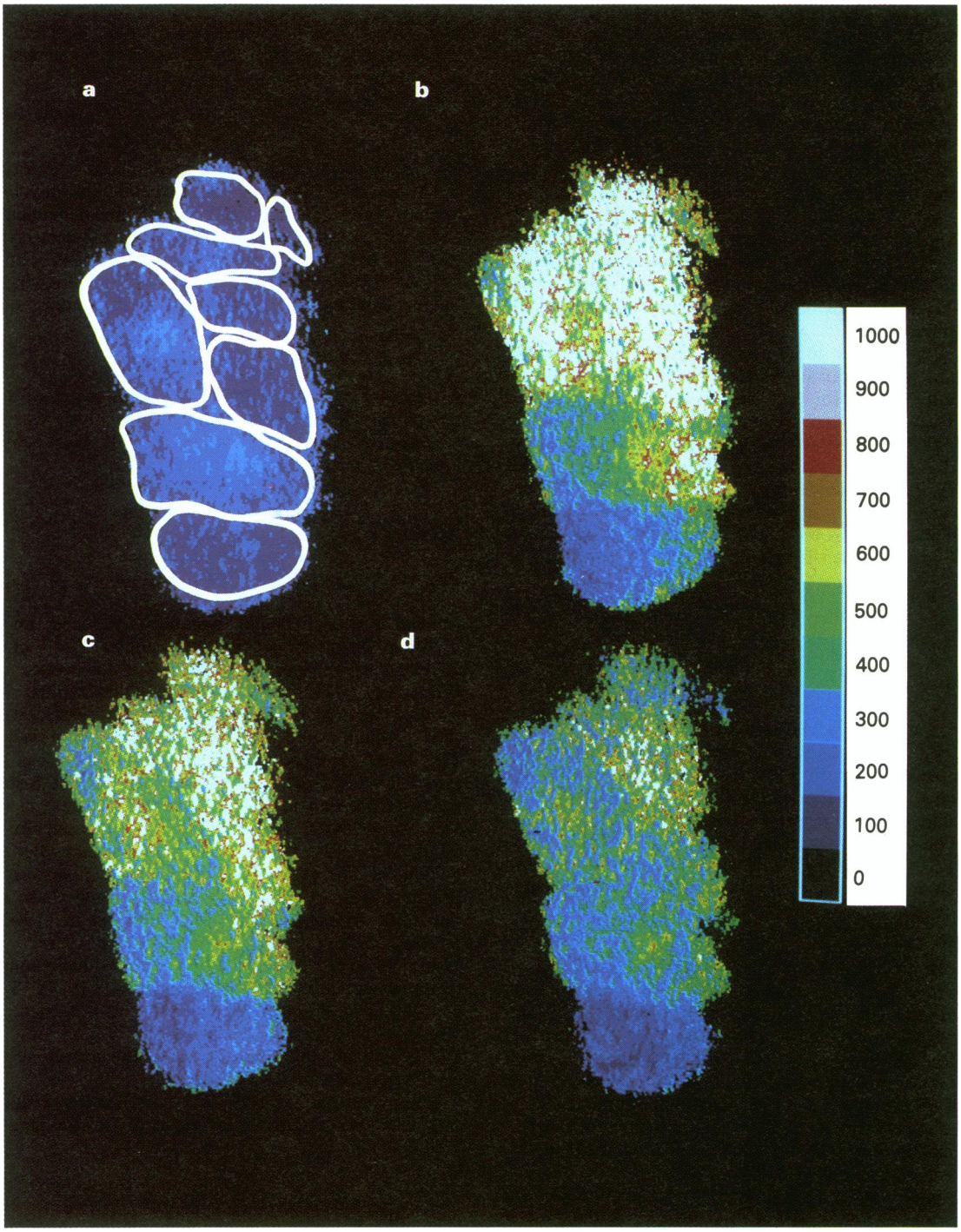

Figure 2 The histamine-induced Ca^{2+} response and desensitization of the H_1 receptor in HeLa cells illustrated by means of video digital imaging. The contour of the individual cells are marked by means of white solid lines (a). The level of $[Ca^{2+}]_i$ is depicted by a typical colour represented by the scale. (a) Represents the basal level of $[Ca^{2+}]_i$ in HeLa cells. The cells were repeatedly exposed to 100 μM histamine for a period of 5 min. After the first and second application of histamine the HeLa cells were washed three times by completely exchanging the medium by rapid perfusion. Histamine was added again after 5 min. (b), (c) and (d) show the maximal observed increase of $[Ca^{2+}]_i$ after first (b), second (c) and third (d) application of histamine (100 μM). The maximal Ca^{2+} responses of (b), (c) and (d) were recorded after 2 s, 4 s and 5 s respectively.

Upon addition of 100 μM histamine, an immediate change of colour, corresponding to a rise in $[Ca^{2+}]_i$, was observed. As can be seen in Figure 2, histamine induces a heterogeneous response, not all cells show the same extent of Ca^{2+} mobilization. A maximal response was observed 2 s after the histamine challenge (Figure 2b). Thereafter intracellular Ca^{2+} was found to expand throughout the cells with time. The latter technique clearly depicts cell-to-cell variations, which cannot be monitored by means of the former technique (Figure 1).

Desensitization of the H_1 receptor induced by 100 μM histamine

Desensitization to histamine was observed when the same group of HeLa cells was repeatedly exposed to histamine

(Figure 3b,c). As depicted in Figure 3, exposure of cells to 100 μM histamine for 5 min markedly affected the subsequent $[Ca^{2+}]_i$ transient after a washing period of 5 min. The intracellular Ca^{2+} levels of the initial peaks for the second and third application of 100 μM histamine were reduced to 590 ± 92 nM (52% reduction, $n = 6$) and 454 ± 127 nM (65% reduction, $n = 6$) respectively. The second phase measured at 30 s was reduced to 279 ± 47 nM (62% reduction, $n = 6$) and 240 ± 45 nM (70% reduction, $n = 6$) respectively (Figure 3b,c,d).

By use of video digital imaging, the process of H_1-receptor desensitization was also observed after 5 min of stimulation with 100 μM histamine followed by a washing period of 5 min (Figure 2b). Upon a second addition of histamine an average lag time of approximately 2 s between the actual application of 100 μM histamine and the rise in $[Ca^{2+}]_i$ was observed, whereas the maximal response occurred after 4 s (Figure 2c). This was in marked contrast to the immediate response recorded when the cells were exposed to histamine for the first time. Furthermore, the rise in $[Ca^{2+}]_i$ observed after receptor activation by histamine did not reach the levels of $[Ca^{2+}]_i$ attained after the first application of histamine. When HeLa cells were exposed to histamine for a third time the average lag time increased further (4 s) and the peak of intracellular Ca^{2+} level could not be achieved (Figure 2d). Thus, an incubation of 5 min with 100 μM of histamine seems sufficient to induce a rapid loss of responsiveness of the histmine H_1 receptor in HeLa cells. Moreover, histamine-induced desensitization seems to affect both the intracellular release and the influx components.

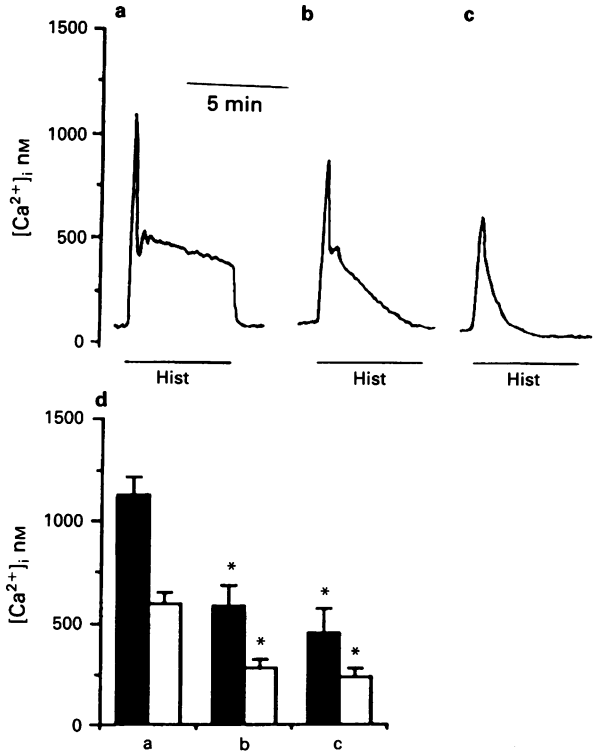

Figure 3 Desensitization of the histamine-induced Ca^{2+} transients in HeLa cells. The cells were repeatedly exposed to 100 μM histamine (Hist) for a period of 5 min. After the first application of histamine (a) the HeLa cells were washed three times by completely exchanging the medium by rapid perfusion. Histamine was added again after 5 min (b,c). A typical experiment of 6 is shown. Panel (d) shows the schematic representation of the first (solid columns) and second (open columns) phase of the histamine-induced Ca^{2+} responses, corresponding to conditions (a), (b) and (c). The second phase was recorded after 30 s of receptor activation with histamine. Data shown are the mean ± the s.e. (vertical bars) of 6 experiments. The asterisk indicates a significant difference compared to the first application of histamine.

In order to establish whether these observations of receptor desensitization were confined to the histamine H_1 receptor, we examined the effects of histamine pretreatment on the responses to other Ca^{2+}-mobilizing agents. Recent studies performed in our laboratory showed that in HeLa cells bradykinin, carbachol and ATP can also elevate the $[Ca^{2+}]_i$ levels (data not shown). The response to bradykinin (1 μM) and carbachol (300 μM) were found to be weak, yet, ATP proved to be effective in elevating $[Ca^{2+}]_i$. Pharmacological investigations revealed that on HeLa cells ATP binds to a '5'-nucleotide' type of purinoceptor, inducing a rapid rise in $[Ca^{2+}]_i$ (Smit *et al.*, unpublished observations). Video digital fluorescence microscopy showed that the same cells were activated, when exposed to either histamine or ATP (data not shown). Moreover, no additivity was monitored when cells were exposed to histamine (100 μM) and ATP (50 μM). Based on these findings, the ATP response was found to be suitable to study whether the desensitization induced by histamine was homologous or heterologous.

In HeLa cells, 50 μM ATP induced a biphasic rise of the $[Ca^{2+}]_i$ levels (Figure 4a). This response was also characterized by a rapid transient rise in $[Ca^{2+}]_i$, followed by a sustained increase in $[Ca^{2+}]_i$ (Figure 4a). After application of 50 μM ATP $[Ca^{2+}]_i$ was rapidly elevated from 71 ± 17 nM ($n = 6$) to 681 ± 140 nM (first phase, $n = 6$). After this initial rapid rise, the $[Ca^{2+}]_i$ decreased to a level of 516 ± 33 nM (second phase, $n = 6$) measured at 30 s after receptor activation.

Pretreatment of HeLa cells with 100 μM histamine for 5 min did not alter the initial transient response after application of 50 μM ATP (Figure 4c). After the desensitization with histamine the peak response after stimulation of the ATP receptor was 599 ± 110 nM, ($n = 4$). This value was not significantly different from the peak response under control

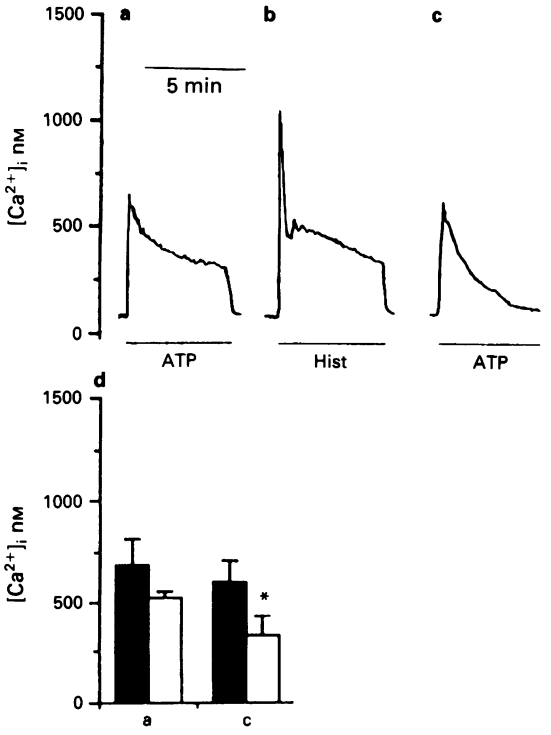

Figure 4 Intracellular free Ca^{2+} transients induced by ATP (50 μM) in control cells (a) and after (c) desensitization with histamine (100 μM) (b) (exposure 5 min). Experiments were performed as described in Figure 2. A typical experiment out of 4 is shown. Panel (d) shows the schematic representation of the first (solid columns) and second (open columns) phase of the ATP-induced Ca^{2+} responses in control cells (a) and after (c) desensitization with histamine. Data shown are the mean ± the s.e. (vertical bars) of 4 experiments.

conditions (681 ± 140 nM, $n = 6$). However, as for the second and third stimulation with histamine, the second phase of the ATP response was significantly reduced after desensitization with 100 μM histamine (control: 516 ± 33 nM, $n = 6$; desensitized: 331 ± 96, $n = 4$, $P < 0.05$) (Figure 4c).

To investigate the involvement of intracellular Ca^{2+}pools more directly, experiments with caffeine were performed. Caffeine (3 mM) induced a transient rise in $[Ca^{2+}]_i$ in HeLa cells (568 ± 149 nM, $n = 4$). After the histamine-induced desensitization, the response to caffeine did not significantly alter (560 ± 180 nM, $n = 4$). These data indicate that in contrast to the Ca^{2+} influx the effects of desensitization on the Ca^{2+} release component are confined to H_1 receptor responsiveness.

Role of protein kinase C in the process of desensitization

In many cell systems protein kinase C (PKC) has been implicated in negative feedback modulation of histamine H_1 receptor-mediated responses (Volpi & Berlin, 1988; Dillon-Carter & Chuang, 1989; Leurs *et al.*, 1990; 1991a; Tilly *et al.*, 1990a,b; Fukui *et al.*, 1991). Pretreatment of HeLa cells with increasing concentrations of the PKC activator phorbol-12-myristate-13-acetate (PMA), also resulted in a decrease in subsequent responsiveness to histamine (Figure 5c). Initial responses of histamine were hardly affected by pretreatment of cells with 20 nM PMA for 5 min. Reasonable reduction was observed following pretreatment with 0.2 μM PMA, whereas complete inhibition was achieved at 2 μM PMA. Based on these observations, a concentration of 0.2 μM of PMA was used for further investigation concerning the role of PKC. Inhibition exerted by PMA on the histamine-induced response resulted particularly in a decrease of the second phase of the Ca^{2+} transient (Figure 5b). After treatment of HeLa cells with 20 nM and 0.2 μM PMA for 5 min, the $[Ca^{2+}]_i$ levels were drastically reduced to 149 ± 16 nM ($n = 6$) and 114 ± 18 nM ($n = 6$) respectively after 30 s of stimulation with 100 μM histamine. These values were significantly lower than the elevation of $[Ca^{2+}]_i$ under control conditions (second phase: 601 ± 52 nM, $n = 11$). Thus, the percentage of inhibition by PMA of this second phase of the histamine response is considerably larger than the effects on the rapid, initial elevation of $[Ca^{2+}]_i$ (Figure 5b,c).

To assess the specificity of the inhibitory activity of PMA, we examined the effects of PMA on the ATP response. Pretreatment of HeLa cells with increasing concentrations of PMA resulted in a dose-dependent inhibition of the ATP response (50 μM) (Figure 6).

In order to examine the possible involvement of other regulatory mechanisms in the process of desensitization, PKC activity was downregulated by incubating HeLa cells for 20 h with 0.2 μM PMA, as described previously (Tilly *et al.*, 1990a,b). As a control experiment, total exclusion of PKC activity was determined by pretreating the downregulated cells with 0.2 μM PMA for 5 min (Table 1). Yet, no significant decrease of the responsiveness to histamine was observed after short PMA treatment, justifying the elimination of PKC activity (Table 1). As can be seen in Table 1, histamine still elicited an initial response, which was comparable to the initial response in untreated cells. However, the characteristics of the histamine-induced Ca^{2+} response changed (Figure 7a). The second phase of the histamine response in these cells significantly ($P < 0.05$) exceeded the Ca^{2+} level of the histamine response in untreated cells (Table 1).

When PKC downregulated cells were exposed to another dose of histamine (100 μM), marked desensitization was again observed (Figure 7b). The initial Ca^{2+} response induced by a second application of histamine was significantly decreased to 519 ± 139 nM ($n = 6$). Compared to the initial response of the first application (1177 ± 185 nM, Table 1) this corresponded to an inhibition of 58%. These data imply that homologous

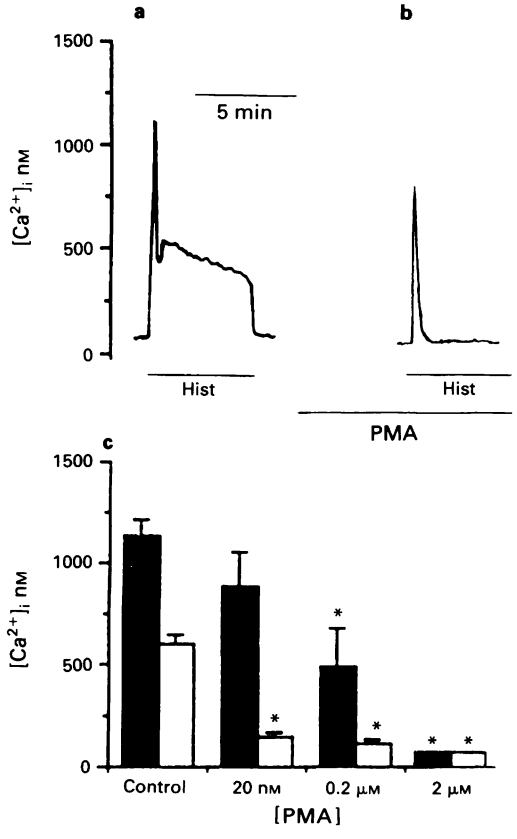

Figure 5 Intracellular free Ca^{2+} transient induced by histamine (Hist, 100 μM) (a), and by histamine (100 μM) in the presence of 0.2 μM phorbol-12-myristate-13-acetate (PMA) after 5 min pretreatment of the cells with 0.2 μM PMA (b). Effects of increasing concentrations of PMA on the first (solid columns) and second phase (open columns) of the histamine-induced Ca^{2+} response (100 μM) are shown in (c). The histamine-induced Ca^{2+} transients were recorded after pretreatment of cells with various doses of PMA for 5 min, and in the presence of the respective PMA concentration. No histamine-induced Ca^{2+} response was observed when cells were exposed to 2 μM PMA. Data shown are the mean ± s.e. (vertical bars) of 6 experiments.

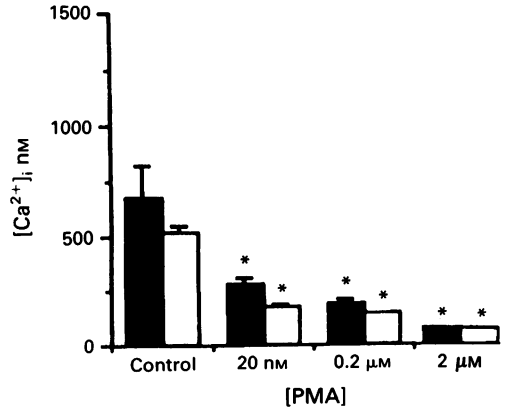

Figure 6 Effects of increasing concentrations of phorbol-12-myristate-13-acetate (PMA) on the first (solid columns) and second phase (open columns) of the ATP-induced Ca^{2+} response (100 μM). The ATP-induced Ca^{2+} transients were recorded after pretreatment of cells with various doses of PMA for 5 min, and in the presence of the respective PMA concentration. No ATP-induced Ca^{2+} response was observed when cells were exposed to 2 μM PMA. Data shown are the mean ± s.e. (vertical bars) of 6 experiments. The asterisk indicates a significant difference compared to the control histamine-induced response.

Table 1 The $[Ca^{2+}]_i$ of the first and second phase of the histamine (100 μM)-induced response in control, protein kinase C (PKC) downregulated and PKC downregulated cells pretreated with 0.2 μM phorbol-12-myristate-13-acetate (PMA) for 5 min

Cell treatment	*1st phase $[Ca^{2+}]_i$ (nM)*	n	*2nd phase $[Ca^{2+}]_i$ (nM)*	n
Control	1135 ± 79	(11)	601 ± 52	(11)
PKC downregulated	1121 ± 124	(10)	890 ± 90*	(10)
PKC downregulated + 5 min 0.2 μM PMA	1011 ± 156	(4)	720 ± 75	(4)

The second phase was recorded 30 s after receptor activation with histamine. The asterisk indicates a significant difference compared to the control response of histamine.
n: number of experiments.

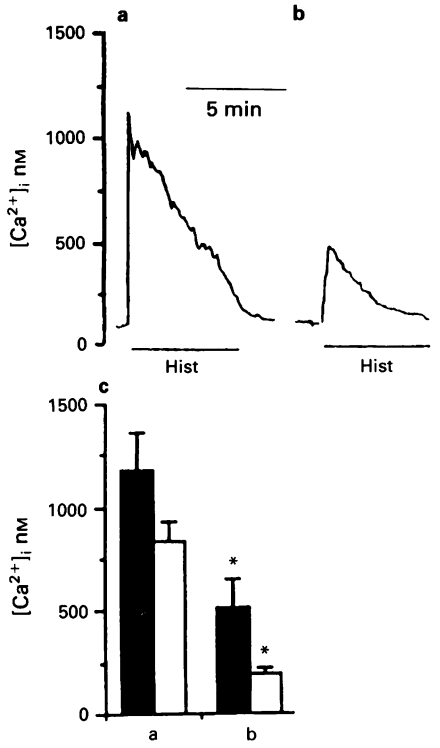

Figure 7 Histamine (Hist)-induced Ca^{2+} responses in protein kinase C downregulated cells. The HeLa cells were incubated for 20 h with 0.2 μM phorbol-12-myristate-13-acetate (PMA). After the first application of histamine (exposure of 5 min) (a) the cells were washed for 5 min and exposed to another dose of histamine (exposure of 5 min) (b). A typical experiment out of 6 is shown. Panel (c) shows the schematic representation of the first (solid columns) and second (open columns) phase of the histamine-induced Ca^{2+} responses, corresponding to conditions (a) and (b). Data shown are the mean ± the s.e. (vertical bars) of 6 experiments. The asterisk indicates a significant difference compared to the first application of histamine.

desensitization of the histamine H_1 receptor may result from a regulation mechanism other than PKC activation.

Discussion

The histamine H_1 receptor belongs to the class of receptors that is coupled to phosphatidyl inositol turnover (Haaksma *et al.*, 1990; Hill, 1990). The process of receptor desensitization of this class of receptors remains to be elucidated. In this study we used fluorometric Ca^{2+} measurements to define the mechanism underlying short-term receptor desensitization of the H_1 receptor in HeLa cells.

Histamine induces an immediate H_1 receptor-mediated biphasic rise in $[Ca^{2+}]_i$ in human HeLa cells (Figure 1). This response was heterogeneous as not all cells respond to histamine in a similar way (Figure 2). The H_1 receptors on HeLa cells were readily susceptible to desensitization since repetitive exposure of the same group of cells to histamine (100 μM) markedly affected the rise in $[Ca^{2+}]_i$ (Figure 3). Video digital imaging revealed an increase of the lag time between the stimulation and the actual monitoring of the Ca^{2+} response, and a reduced increase of $[Ca^{2+}]_i$ (Figure 2). The experimental data show that desensitization of the histamine H_1 receptor is associated with the reduction of both the Ca^{2+} release and influx component. The histamine-induced release component appears to be reduced in a selective manner, as neither the caffeine-induced Ca^{2+} release nor the release component of the ATP response were affected. Thus, desensitization of the H_1 receptor does not affect the intracellular Ca^{2+} pool, as reported previously (Hishinuma & Uchida, 1988; McDonough *et al.*, 1988; Leurs *et al.*, 1990). However, the influx component of both the histamine and ATP response was impaired. These data indicate that desensitization of the histamine H_1 receptor evolves from two different mechanisms; a selective reduction of the histamine-induced Ca^{2+} release, associated with a homologous desensitization, and a non-selective inhibition of the receptor-mediated Ca^{2+} influx, corresponding to a heterologous desensitization.

Receptor desensitization of the G-protein-coupled receptors is thought to be associated with post-translational modification of the receptor by phosphorylation reactions (Hausdorff *et al.*, 1990; Huganir & Greengard, 1990). Kinases, such as PKA, PKC and specific receptor kinases seem to play crucial roles in the mechanism underlying receptor desensitization (Huganir & Greengard, 1990; Palczewski & Benovic, 1991) and in several receptor systems PKC has been found to account for a negative feedback on the histamine H_1 receptor-mediated response (Volpi & Berlin, 1988; Dillon-Carter & Chuang, 1989; Leurs *et al.*, 1990; Tilly *et al.*, 1990a,b; Fukui *et al.*, 1991).

PKC was found to inhibit the histamine as well as ATP responses in HeLa cells, affecting both the Ca^{2+} release and in particular the Ca^{2+} influx (Figures 5 and 6). A decrease of $^{45}Ca^{2+}$ influx in HeLa cells upon short-term exposure to PMA was also reported by Marunaka *et al.* (1985). Earlier studies showed an impaired formation of inositol phosphates upon H_1 receptor stimulation after activation of PKC in HeLa cells (Tilly *et al.*, 1990a,b). The GTPγS induced formation of inositol phosphates was also found to be reduced, indicating that effects on the G-protein rather than on the H_1 receptor might explain these data (Tilly *et al.*, 1990a). These findings may explain the observed reduction of the initial rise in Ca^{2+} of the histaminergic, as well as purinergic responses after pretreatment with PMA (Berridge & Irvine, 1989). Based upon the model proposed by Irvine, coupling the Ca^{2+} release to the Ca^{2+} influx, the reduced Ca^{2+} release may partly account for the impaired influx of extracellular Ca^{2+} (Irvine, 1990). However, the sensitivity of the Ca^{2+} influx to PMA is much more pronounced, implying that PKC may

exert a negative feedback on other molecular entities, such as the receptor operated Ca^{2+} channels. Recently Peppelenbosch *et al.* (1991) developed a model in which it was suggested that the receptor-operated Ca^{2+} influx was mediated by transactivation of hyperpolarization-activated Ca^{2+} channels and Ca^{2+}-activated K^+ channels. In this model, it was proposed that activation of PKC had an inhibitory effect on the K^+ channels leading to a decrease of the Ca^{2+} influx (Peppelenbosch *et al.*, 1991). Since the H_1 receptor activation in HeLa cells is also associated with hyperpolarization of the cell membrane (Hazama *et al.*, 1985; Sauvé *et al.*, 1987; Tilly *et al.*, 1990b), it is likely that the H_1 receptor is subjected to a similar negative feedback induced by PKC. This suggestion is further corroborated by the experiments with PKC down-regulated HeLa cells (Figure 7, Table 1). In these cells the second phase of the histamine-induced response was found to be significantly elevated, implying the involvement of PKC in the negative feedback on the influx of extracellular Ca^{2+}.

In contrast to the involvement of PKC in the heterologous desensitization of the Ca^{2+} influx, it is highly unlikely that PKC activation is implicated in the selective reduction of the initial H_1 receptor response. Although PKC activation can inhibit the Ca^{2+} release component (see above), this effect is clearly not restricted to the H_1 receptor since purinoceptor responses are also inhibited. Furthermore, in the PKC down-regulated cells, desensitization of the H_1 receptor was still observed (Figure 7). Based on these data we suggest that during short-term exposure of HeLa cells to histamine besides PKC another regulatory mechanism is rapidly activated. This, as yet unknown, mechanism is reponsible for a selective desensitization of the H_1 receptor response. The number of H_1 receptors, measured as [^{3}H]-mepyramine binding sites, did not alter after an incubation of 5 min with 100 μM of histamine (unpublished observations). Similar findings were observed in smooth muscle preparations (Leurs *et al.*, 1991b). It is therefore unlikely that short-term desensitization is associated with receptor internalisation. The rapid loss of responsiveness is probably caused by alterations in efficacy of the H_1 receptor to activate the appropriate G-proteins.

During the preparation of this manuscript, the gene encoding the H_1 receptor was cloned by Yamashita *et al.* (1991). Like all other G-protein coupled receptors, the H_1 receptor was found to contain seven putative transmembrane domains. The β-adrenoceptor (βAR) is one of the best characterized receptors of the G-protein coupled receptors. As extensive structural analogy was found between this receptor and the other G-protein coupled receptors, the β-adrenoceptor provides a model for elucidating characteristics of receptor regulation mechanisms, such as desensitization (Hausdorff *et al.*, 1990; Huganir & Greengard, 1990). Rapid desensitization of the β-adrenoceptor is associated with phosphorylation of the receptor by protein kinase A (PKA) and the β-adrenoceptor kinase (βARK), resulting in the functional uncoupling of the receptor from its effector system (Benovic *et al.*, 1989). These kinases were found to phosphorylate the receptor at specific serine and threonine residues. The latter kinase is only activated when the receptor is occupied. The primary sequence of the H_1 receptor reveals the existence of several serines and threonines, which may serve as potential phosphorylation sites for such kinases (Yamashita *et al.*, 1991). Based on these findings we therefore hypothesize that the homologous desensitization of the H_1 receptor is associated with the activation of a receptor kinase and the non-specific, heterologous, desensitization with activation of PKC. PKC might play a role comparable to PKA in the process of desensitization. Moreover, the identification and cloning of β-adrenoceptor kinase-related genes, i.e. βARK2, rhodopsin kinase implies the existence of a family of receptor kinases (Benovic *et al.*, 1991; Lorenz *et al.*, 1991). The β-adrenoceptor kinase showed differences in phosphorylating the β-adrenoceptor and rhodopsin, suggesting that these kinases have distinct substrate specificities (Benovic *et al.*, 1991). Furthermore, as other G-protein coupled receptors were found to be substrates for β-adrenoceptor kinase, it is feasible that this class of receptors is regulated by a general mechanism in which specific receptor kinases are responsible for the stimulus-dependent phosphorylation (Benovic *et al.*, 1989). Differences in the number and location of potential phosphorylation sites of various cloned G-protein coupled receptors, suggest that these receptors might be regulated in distinct ways under different physiological conditions.

In conclusion, results of this study show that histamine induces a rapid H_1 receptor-mediated Ca^{2+} response in HeLa cells. PKC appears to be responsible for negative feedback on the Ca^2 influx. Moreover, H_1 receptors in HeLa cells are readily susceptible to desensitization. Based upon our experimental data we suggest that short-term desensitization of the H_1 receptor is mediated by two distinct pathways; a PKC-dependent and PKC-independent pathway. For future experiments, the recent cloning of the histamine H_1 receptor (Yamashita *et al.*, 1991) offers new possibilities, with regard to the elucidation of the mechanism underlying receptor desensitization.

References

BENOVIC, J.L., DEBLASI, A., STONE, W.C., CARON, M.G. & LEFKOWITZ, R.J (1989). Beta-adrenergic receptor kinase: primary structure delineates a multigene family. *Science*, **246**, 235–240.

BENOVIC, J.L., ONORATO, J.J., ARRIZA, J.L., STONE, W.C., LOHSE, M., JENKINS, N.A., GILBERT, D.J., COPELAND, N.G., CARON, M.J. & LEFKOWITZ, R.J. (1991). Cloning, expression, and chromosomal localization of β-adrenergic receptor kinase 2. *J. Biol. Chem.*, **266**, 14939–14946.

BERRIDGE, M.J. & IRVINE, R.F. (1989). Inositol phosphates and cell signalling. *Nature*, **341**, 197–205.

BRISTOW, D.R., ARIAS-MONTANO, J.A. & YOUNG, J.M. (1991). Histamine-induced inositol phosphate accumulation in HeLa cells: lithium sensitivity. *Br. J. Pharmacol.*, **104**, 667–684.

BRISTOW, D.R. & YOUNG, J.M. (1991). Characteristics of histamine-induced inositol phospholipid hydrolysis in HeLa cells. In *New Perspectives in Histamine Research*. ed. Van der Goot, H. & Timmerman, H. pp. 381–387. Berlin: Birkhäuser Verlag.

BRODDE, O.E., DAUL, A., MICHELREHER, M., BOOMSMA, F., VELD, A.J.M.I., SCHLIEPER, P. & MICHEL, M.C. (1990). Agonist-induced desensitization of beta-adrenoceptor function in humans - Subtype-selective reduction in beta-1-adrenoceptor or beta-2-adrenoceptor mediated physiological effects by xamoterol or procaterol. *Circulation*, **81**, 914–921.

DILLON-CARTER, O. & CHUANG, D. (1989). Homologous desensitisation of muscarinic cholinergic, histaminergic, adrenergic and serotonergic receptors coupled to phospholipase C in cerebellar granule cells. *J. Neurochem.*, **52**, 598–603.

FUKUI, H., INAGAKI, N., ITO, S., KUBO, H., YAMATODANI, A. & WADA, H. (1991). Histamine H_1 receptor on astrocytes in primary cultures: a possible target for histamine neurons. In *New Perspectives in Histamine Research*. ed. Van der Goot, H. & Timmerman, H. pp. 161–181. Berlin: Birkhäuser Verlag.

GHOSH, S.K., VOS DE, C., MCILROY, I. & PATEL, K.R. (1991). Effects of cetirizine on histamine- and leukotriene D4 induced bronchoconstriction in patients with atopic asthma. *J. All. Clin. Immunol.*, **87**, 1010–1013.

GRYNKIEWICZ, G., POENIE, M. & TSIEN, R.Y. (1985). A new generation of Ca^{2+} indicators with greatly improved fluorescence properties. *J. Biol. Chem.*, **260**, 3440–3450.

HAAKSMA, E.E.J., LEURS, R. & TIMMERMAN, H. (1990). Histamine receptors: subclasses and specific ligands. *Pharmacol. Ther.*, **47**, 73–104.

HAUSDORFF, W.P., CARON, M.C. & LEFKOWITZ, R.J. (1990). Turning of the signal: desensitization of β-adrenergic receptor function. *FASEB J.*, **4**, 2881–2889.

HAZAMA, A., YADA, T. & OKADA, Y. (1985). Hela cells have histamine H_1-receptors which mediate activation of the kalium conductance. *Biochim. Biophys. Acta*, **845**, 249–253.

HILL, S.J. (1990). Distribution, properties and functional characteristics of three classes of histamine receptors. *Pharmacol. Rev.*, **42**, 45–83.

HISHINUMA, S. & UCHIDA, M.K. (1988). Short-term desensitization of guinea-pig taenia caecum induced by carbachol occurs at intracellular Ca^{2+} stores and that by histamine at the H_1-receptor. *Br. J. Pharmacol.*, **91**, 882–889.

HOMCY, C.J., VATNER, S.F. & VATNER, D.E. (1991). Beta adrenergic receptor regulation in the heart in pathophysiological states: abnormal adrenergic responsiveness in cardiac disease. *Annu. Rev. Physiol.*, **53**, 139–157.

HUGANIR, R.L. & GREENGARD, P. (1990). Regulation of neurotransmitter receptor desensitization by protein phosphorylation. *Neuron*, **5**, 555–567.

IRVINE, R.F. (1990). 'Quantal' Ca^{2+} release and the control of the entry by inositol phosphates–a possible mechanism. *FEBS Lett.*, **263**, 5–9.

LEURS, R., SMIT, M.J., BAST, A. & TIMMERMAN, H. (1990). Different profiles of desensitization dynamics in guinea-pig jejunal smooth muscle after stimulation with histamine and metacholine. *Br. J. Pharmacol.*, **101**, 881–888.

LEURS, R., SMIT, M.J., BAST, A. & TIMMERMAN, H. (1991a). Is protein kinase C involved in histamine H_1-receptor desensitization? In *New Perspectives in Histamine Research*. ed. Van der Goot, H. & Timmerman, H. pp. 393–403. Berlin: Birkhäuser Verlag.

LEURS, R., SMIT, M.J., BAST, A. & TIMMERMAN, H. (1991b). Homologous desensitization of the histamine H_1 receptor leads to a reduction of H_1-agonist efficacy. *Eur. J. Pharmacol.*, **196**, 319–322.

LORENZ, W., INGLESE, J., PALCZEWSKI, K., ONORATO, J.J., CARON, M.J. & LEFKOWITZ, R.J. (1991). The receptor kinase family: Primary structure of rhodopsin kinase reveals similarities to the β-adrenergic receptor kinase. *Proc. Natl. Acad. Sci. U.S.A.*, **88**, 8715–8719.

MANNING, P.J., JONES, G.L. & O'BYRNE, P.M. (1987). Tachyphylaxis to inhaled histamine in asthmatic subjects. *J. Appl. Physiol.*, **63**, 1572–1577.

MARUNAKA, Y., YAMANISHA, K. & NISHINO, H. (1985). The inhibitory action of 12-O-tetradeconoylphorbol 13-acetate (TPA) on Ca^{2+} transport in HeLa cells; direct action on the plasma membrane. *IRSC Med. Sci.*, **13**, 455–456.

MCDONOUGH, P.M., EUBANKS, J.H. & HELLER BROWN, J. (1988). Desensitization and recovery of muscarinic and histaminergic Ca^{2+} mobilization in 1321N1 astrocytoma cells. *Biochem. J.*, **249**, 135–141.

MOTOMURA, S., DEIGHTON, N.M., ZERKOWSKI, H.R., DOETSCH, N., MICHEL, M.C. & BRODDE, O.E. (1990). Chronic β_1-adrenoceptor antagonist treatment sensitizes β_2-adrenoceptors, but desensitizes M_2-muscarinic receptors in the human right atrium. *Br. J. Pharmacol.*, **101**, 363–369.

PALCZEWSKI, K. & BENOVIC, J.L. (1991). G-protein coupled receptor kinases. *Trends Biol. Sci.*, **16**, 387–391.

PEPPELENBOSCH, M.P., TERTOOLEN, L.G.J. & DE LAAT, S.W. (1991). Epidermal growth factor-activated calcium and potassium channels. *J. Biol. Chem.*, **266**, 19938–19944.

RAYMOND, J.R., ALBERS, F.J., MIDDLETON, J.P., LEFKOWITZ, R.J., CARON, M.G., OBEID, L.M. & DENNIS, V.W. (1991). 5-HT1A and Histamine H_1 receptors in HeLa cells stimulate phosphoinositide hydrolysis and phosphate uptake via distinct G-protein pools. *J. Biol. Chem.*, **266**, 372–379.

SAUVE, R., PARENT, S.L. & ROY, G. (1987). Oscillary activation of calcium dependent potassium channels in Hela cells induced by histamine H_1 receptor stimulation: a single channel study. *J. Memb. Biol.*, **96**, 199–208.

SAUVE, R., DIARRA, A., CHAHINE, M., SIMONEAU, C., MORIER, N. & ROY, G. (1991). Ca^{2+} oscillations induced by histamine-H_1 receptor stimulation in HeLa cells –Fura-2 and patch clamp analysis. *Cell Calcium*, **12**, 165–176.

SCHOEFFTER, P., GHYSEL-BURTON, J., CABANIE, M. & GODFRAIND, T. (1987). Competitive and stereoselective histamine H_1 antagonistic effect of cicletanide in guinea pig ileum. *Eur. J. Pharmacol.*, **136**, 235–237.

STILES, G.L. (1991). Adrenergic receptor responsiveness and congestive heart failure. *Am. J. Cardiol.*, **67**, 13–17.

TILLY, B.C., LAMBRECHTS, A.C., TERTOOLEN, L.G.J., DE LAAT, S.W. & MOLENAAR, W.H. (1990a). Regulation of phosphoinositide hydrolysis induced by histamine and guanine nucleotides in human HeLa carcinoma cells. *FEBS Lett.*, **265**, 80–84.

TILLY, B.C., TERTOOLEN, L.G.J., LAMBRECHTS, A.C., REMOIRE, R., DE LAAT, S.W. & MOLENAAR, W.H. (1990b). Histamine H_1 receptor mediated phosphoinositide hydrolysis, calcium signalling and membrane potential oscillations in human Hela carcinoma cells. *Biochem. J.*, **226**, 235–243.

VOLPI, M. & BERLIN, R.D. (1988). Intracellular elevations of free calcium induced by activation of histamine H_1 receptors in interphase and mitotic Hela cells; hormone signal transduction is altered during mitosis. *J. Cell. Biol.*, **107**, 2533–2539.

YAMASHITA, M., FUKUI, H., SUGAMA, K., HORIO, Y., ITO, S., MIZUGUCHI, H. & WADA, H. (1991). Expression cloning of a cDNA encoding the bovine histamine H_1 receptor. *Proc. Natl. Acad. Sci. U.S.A.*, **88**, 11515–11519.

(Received June 5, 1992
Accepted June 19, 1992)

Br. J. Pharmacol. (1992), **107**, 456–462

A pertussis toxin-sensitive mechanism of endothelin action in porcine coronary artery smooth muscle

Yoshitoshi Kasuya, *Yoh Takuwa, †Masashi Yanagisawa, **Tomoh Masaki & [1]Katsutoshi Goto

Department of Pharmacology, Institute of Basic Medical Sciences, University of Tsukuba, Tsukuba, Ibaraki 305, Japan; *Department of Vascular Biology, University of Tokyo School of Medicine, Hongo 113, Japan; †Howard Hughes Medical Institute, and Department of Molecular Genetics, University of Texas, Dallas, Texas 75235-9050, U.S.A. and **Department of Pharmacology, Kyoto University Faculty of Medicine, Kyoto 606, Japan.

1 Endothelin-1 (ET-1)-induced contraction of porcine coronary artery strips may be mediated via at least two intracellular signalling mechanisims, the activation of dihydropyridine-sensitive voltage-dependent Ca^{2+} channels and the stimulation of phosphoinositide breakdown. Here we have investigated the possible involvement of pertussis toxin (PT)-sensitive guanosine-5'-triphosphate (GTP)-binding proteins (G-proteins) in ET-1-induced activation of these two signalling pathways in porcine coronary artery smooth muscle.

2 Increase in extracellular K^+ concentration (10, 15 mM) shifted the dose-response relationship for the ET-1-induced contraction to the left.

3 The dihydropyridine Ca^{2+} channel blocker, nifedipine (10^{-8} M), induced a rightward shift in the dose-response curve for ET-1. Pretreatment of the arterial strips with PT (0.1 $\mu g\ ml^{-1}$) induced a similar rightward shift of the ET-1 dose-response curve but not of the KCl response. Nifedipine (10^{-8} M) did not further attenuate the ET-1-induced contraction in the PT-pretreated strips.

4 The pretreatment with PT significantly reduced $^{45}Ca^{2+}$ uptake of the arterial strips stimulated by ET-1, but had no effect on ET-1-induced production of inositol phosphates.

5 The contractile response of the arterial strips to phorbol dibutyrate, an active phorbol ester, was not significantly affected by 10^{-8} M nifedipine.

6 We confirmed that the pretreatment of the tissue with PT induced ADP-ribosylation of a 41 kDa membrane protein.

7 These findings indicate that activation of dihydropyridine-sensitive voltage-dependent Ca^{2+} channels by ET-1 in this tissue is mediated via a PT-sensitive G-protein in a manner apparently independent of the ET-1-induced activation of protein kinase C. It is concluded that the action of ET-1 in porcine coronary artery is mediated via two distinct signal transduction pathways, which are coupled to PT-sensitive and PT-insensitive GTP-binding proteins, respectively.

Keywords: GTP-binding proteins; dihydropyridines; phosphoinositides turnover; phorbol esters

Introduction

Endothelin-1 (ET-1) provokes a strong and sustained contraction of isolated vascular smooth muscle from different species (Kasuya *et al.*, 1989a; Saitoh *et al.*, 1989). Previous studies have demonstrated that the mechanisms of ET-1-induced vasoconstriction may involve both the activation of dihydropyridine-sensitive voltage-dependent Ca^{2+} channels (Goto *et al.*, 1989; Kasuya *et al.*, 1989a) and inositol phospholipid hydrolysis (Kasuya *et al.*, 1989b). However, it is still unknown whether these two signal transduction mechanisms are independent of each other.

Heterotrimeric guanine nucleotide-binding regulatory proteins (G-proteins) act as transducers between membrane receptors for extracellular signals and intracellular effectors controlling the concentration of cytosolic signalling molecules such as adenosine 3':5'-cyclic monophosphate (cyclic AMP), Ca^{2+}, and inositol phosphates. It has been established that receptor activation of numerous hormones and neurotransmitters is coupled to phospholipase C activation via G-proteins in various cells (Smith *et al.*, 1985; Martin *et al.*, 1986). It has also been demonstrated that extracellular ligands directly (Yatani *et al.*, 1987; Toselli *et al.*, 1989) or indirectly (Osterrieder *et al.*, 1982; Shearman *et al.*, 1989) regulate plasma membrane channels for K^+ or Ca^{2+} through G-proteins. We and others have recently demonstrated that ET-1 receptor is coupled to phospholipase C via a pertussis toxin (PT)-insensitive G-protein in cultured vascular smooth muscle cells (Bobik *et al.*, 1990; Takuwa *et al.*, 1990).

In this study, in order to understand the mechanism for activation by ET-1 of dihydropyridine-sensitive voltage-dependent Ca^{2+} channels, we investigated the effect of PT on ET-1-induced contraction and Ca^{2+} influx in isolated coronary artery smooth muscle of the pig. The results suggested that ET-1-induced activation of the voltage-dependent Ca^{2+} channels is mediated by a PT-sensitive G-protein.

Methods

Measurement of contraction of arterial strips

Right coronary arteries were isolated from fresh adult porcine hearts obtained from a local slaughterhouse. Arterial segments were cut into 2 × 15 mm helical strips with endothelial cells removed by rubbing the intimal surface with a cotton swab, and suspended in 5 ml of siliconized glass organ chambers filled with a Krebs-Ringer solution of the following composition (in mM): NaCl 113, KCl 4.8, $CaCl_2$ 2.2, KH_2PO_4 1.2, $MgCl_2$ 1.2, $NaHCO_3$ 25 and glucose 5.5. The solution was maintained at 37°C and gassed with 5% CO_2/95% O_2.

[1] Author for correspondence at: Department of Pharmacology, Institute of Basic Medical Sciences, University of Tsukuba, Tsukuba, Ibaraki 305, Japan.

Arterial strips were equilibrated at a passive tension of 1.25 g until the contractile tension induced by 50 mM KCl attained a steady state. Isometric contraction was measured as previously described (Kasuya *et al.*, 1989a).

Treatment with pertussis toxin

After equilibration by repetitive application of 50 mM KCl, arterial strips were incubated for 15 h in the Krebs-Ringer solution containing 0.1 $\mu g\,ml^{-1}$ PT. During the incubation period, the solution was changed every 3 h with fresh solution of the same composition, and maintained at 37°C and gassed with 5% CO_2/95% O_2. Arterial strips showed comparable contractile responses to 50 mM KCl before and after the treatment with PT. Control muscle strips were similarly incubated in the Krebs-Ringer solution without PT for 15 h.

$^{45}Ca^{2+}$-uptake

Arterial strips were cut into small segments and equilibrated for 2 h in the Krebs-Ringer solution gassed with 5% CO_2/95% O_2 at 37°C. After the equilibration period, the segments weighing 15 mg were transferred into a N-2-hydroxyethylpiperazine-N'-2-ethanesulphonic acid (HEPES)-buffered solution of the following composition (in mM): NaCl 140, KCl 5.9, $CaCl_2$ 1.5, glucose 11.0 and 5 HEPES-tris(hydroxymethyl)aminomethane (Tris) buffer (pH 7.4). After further 30 min equilibration at 37°C, the incubation with human ET-1 (Peptide Institute, Osaka, Japan) or 50 mM KCl for 30 min was started. $^{45}CaCl_2$ (74 MBq ml^{-1}, 740 GBq $mmol^{-1}$; Amersham) was added 10 min before the end of the stimulation period. The segments were briefly washed three times with ice-cold, calcium-free HEPES-buffered solution containing 2 mM ethylene glycol-*bis*(b-aminoethyl ether)-N,N,N',N'-tetraacetic acid (EGTA). After the final washing, the segments were blotted between two sheets of filter paper (Whatman 3MM) and homogenized with a glass-glass homogenizer in scintillation solution (ACS II, Amersham). The radioactivity was then determined by a Beckman liquid scintillation counter. The Ca^{2+} uptake of the tissues was calculated as nmol Ca^{2+} per g wet tissue.

Measurement of inositol phosphate production

Arterial strips were cut into small segments and labelled by incubation in the aerated Krebs-Ringer solution containing 9.25 MBq ml^{-1} *myo*-[1,2-^{3}H]-inositol (1.66~2.96 TBq $mmol^{-1}$, New England Nuclear) at 37°C for 6 h. After washing three times with [^{3}H]-inositol-free Krebs-Ringer solution, the segments (30 mg) were preincubated at 37°C in 1 ml of the Krebs-Ringer solution containing 10 mM LiCl for 10 min and then stimulated with ET-1 for 15 min. The reaction was terminated by adding ice-cold perchloric acid to a final concentration of 10% (v/v), and the segments were homogenized with a glass-glass homogenizer. The supernatants of the homogenates were neutralized and applied to a Dowex 1X-8 anion exchange column for the separation of inositol phosphates as described previously (Kasuya *et al.*, 1989b).

In vitro *ADP-ribosylation of arterial smooth muscle cell membrane*

To estimate the effectiveness of PT-treatment under our experimental conditions, *in vitro* ADP-ribosylation was performed in the presence of ^{32}P NAD, using the membranes prepared from arterial strips, either untreated or treated with PT as described above. Arterial strips, either untreated or treated with PT, were washed twice with phosphate buffered saline (PBS), minced to small pieces, and homogenized in buffer of the following composition (in mM): Tris-HCl (pH 7.4) 10, dithiothreitol 1, and ethylene diamine N,N,N',N'-tetraacetic acid (EDTA) 5. The homogenates were sonicated for 2 min and centrifuged at 500 *g* for 5 min. The resulting supernatants were centrifuged at 10,000 *g* for 5 min. The resulting precipitates were resuspended in the homogenization buffer and used as membrane samples. The membranes (30 μg protein/sample) were incubated with 25 $\mu g\,ml^{-1}$ PT for 75 min at 25°C in a reaction buffer of the following composition (in mM): Tris-HCl (pH 7.5) 20, thymidine 10, [adenylate-^{32}P]-nicotinamide adenine dinucleotide 0.04, (NAD; 740 GBq $mmol^{-1}$, New England Nuclear), ATP 1, EDTA 0.5, dithiothreitol 20, and $MgCl_2$ 1. The reaction was terminated by adding perchloric acid (PCA) to a final concentration of 10% (v/v), and the membranes were washed once with 10 mM Tris-HCl (pH 7.5). The washed membranes were solubilized in sodium dodecyl sulphate (SDS)-sampling buffer and analyzed by SDS/9% polyacrylamide gel electrophoresis (PAGE) followed by autoradiography.

Drugs

The following drugs were used: nifedipine and phorbol 12,13-dibutyrate were from Sigma Chemical Co. Ltd. Endothelin-1 was obtained from Peptide Institutes (Osaka, Japan). Pertussis toxin (islet-activating protein: IAP) was from Funakoshi Co. Ltd. (Tokyo, Japan).

Statistical analysis of data

Values are expressed as means ± s.e. Comparisons were made by a one-way analysis of variance followed by the Bonferroni method (Figure 1, Table 1), or Student's *t* test for unpaired values (Figures 3 and 4). The level of statistically significant difference was $P<0.05$.

Results

Effect of membrane depolarization on endothelin-1-induced contraction

Our previous studies demonstrated that ET-1 activates the dihydropyridine-sensitive voltage-dependent Ca^{2+} channels in porcine coronary artery smooth muscle. In order to confirm whether the voltage-dependent process actually constitutes a part of the mechanisms by which ET-1 induces contraction, we investigated the effect of membrane depolarization on the dose-response relationships for ET-1-induced contraction. The elevation of extracellular K^+ concentration induced a small contraction in the absence of ET-1 (Figure 1a); the contractile responses to 5 mM, 10 mM and 15 mM K^+ expressed as percentages of tension generated by 50 mM KCl were 0 ± 0%, 1.7 ± 0.1% and 17.3 ± 2.0%, respectively. The cumulative addition of ET-1 superimposed a slowly-developing, dose-dependent contraction which attained a steady state after 15–20 min (Figure 1a). Increased extracellular K^+ significantly augmented the plateau tension induced by a low concentration of ET-1, whereas the maximum contraction induced by 10^{-7} M ET-1 was not significantly different (Figure 1b).

Effect of pertussis toxin-pretreatment on the endothelin-1-induced contraction

To elucidate whether a PT-sensitive G-protein is involved in the action of ET-1, we treated porcine coronary artery strips with PT as described under Methods. To verify the effectiveness of the PT-pretreatment, we incubated plasma membranes prepared from the PT-treated and control strips with PT *in vitro* in the presence of [^{32}P]-NAD. The labelled membrane proteins were separated by SDS-PAGE and visualized by autoradiography. In the control strips, a single 41 kDa species of the membrane protein was ADP-ribosylated (Figure 2). The pretreatment of intact strips with PT greatly reduced the additional ADP-ribosylation *in vitro* of the 41 kDa membrane protein, indicating that the pretreatment

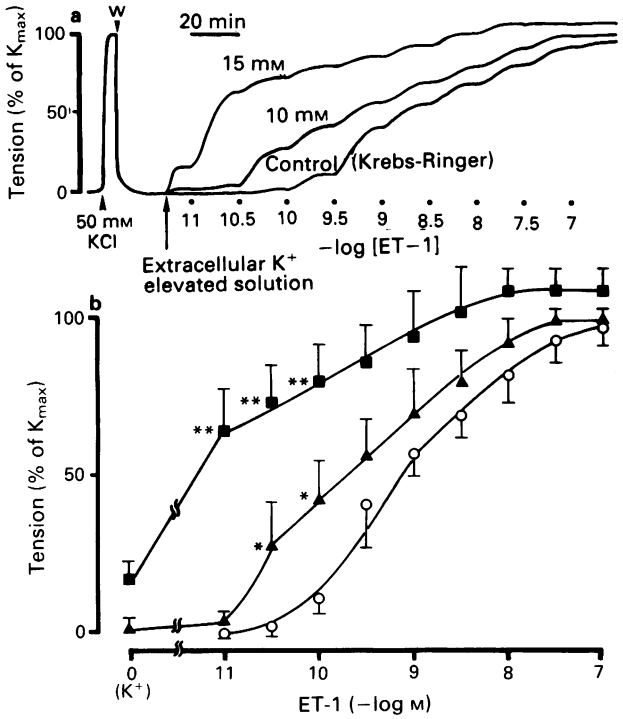

Figure 1 (a) Typical contractile response of porcine coronary artery strips to cumulatively applied endothelin-1 (ET-1) in high-K^+ Krebs Ringer solutions. (b) Dose-response relationships for vasoconstriction superimposed by cumulatively added ET-1 under conditions of elevated extracellular K^+: 15 mM (■); 10 mM (▲); control (○). Contractile responses induced by ET-1 are expressed as percentages of maximum tension induced by 50 mM KCl; since increase of extracellular KCl induced a small vasoconstriction, the steady-state contractile tension induced by KCl alone was subtracted when measuring ET-1-induced tensions. Points represent means with s.e. shown by vertical bars ($n = 4$). *Significantly different from values with normal KCl; **significantly different from values with 10 mM KCl ($P < 0.05$, ANOVA with Bonferroni method).

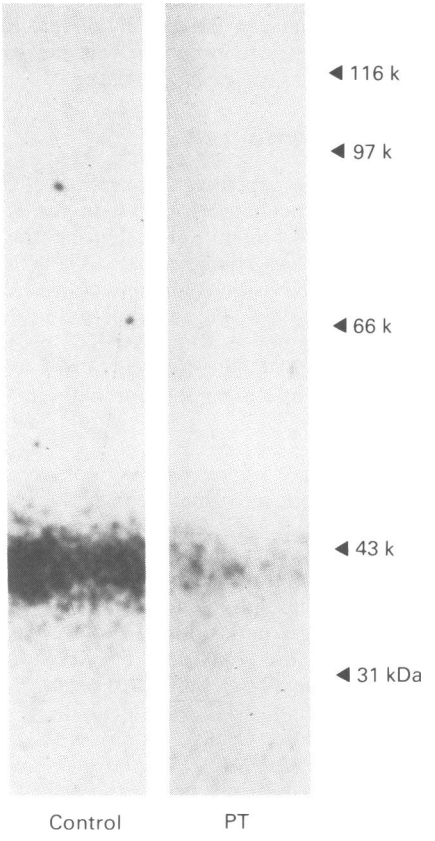

Figure 2 *In vitro* ADP-ribosylation of a 41-kDa protein in plasma membranes prepared from porcine coronary artery smooth muscle. The coronary artery strips were incubated with or without pertussis toxin (PT) 0.1 μg ml^{-1} for 15 h and crude membrane fractions were prepared. The membranes were then incubated with PT 25 μg ml^{-1} in the presence of [^{32}P]-NAD. Membrane proteins were resolved by SDS-PAGE and autoradiography.

with PT effectively ADP-ribosylated this protein in the intact tissue.

Pretreatment of arterial strips with PT did not significantly affect KCl-induced contraction (Figure 3a). In contrast, PT-pretreatment caused a significant reduction of ET-1-induced contraction. The extent of the attenuation of ET-1-induced contraction by pretreatment with PT was greater at lower doses of ET-1 (10^{-10}–3×10^{-9} M), so that the cumulative dose-response curves apparently shifted to the right and steepened. The apparent EC_{50} values were 5.3×10^{-9} M (95% confidence interval, $2.3 \times 10^{-9} \sim 1.6 \times 10^{-8}$ M) in PT-pretreated strips and 4.7×10^{-10} M ($2.3 \times 10^{-10} \sim 9.8 \times 10^{-10}$ M) in control strips. A low dose (10^{-8} M) of nifedipine induced a similar rightward shift of the cumulative dose-response curve for ET-1-induced contraction in strips not pretreated with PT. In contrast, the same concentration of nifedipine did not significantly affect the dose-response curve for ET-1 in PT-pretreated strips (Figure 3b).

Effect of pertussis toxin-pretreatment on calcium influx induced by endothelin-1

We investigated whether the inhibitory effect of PT on ET-1-induced contraction is due to the inhibition of ET-1-induced Ca^{2+} influx, which plays an important role in ET-1-induced contraction of this smooth muscle. As shown in Table 1, 10^{-9} M ET-1 augmented Ca^{2+} uptake of the control coronary artery strips by 47 ± 4.5%. We previously demonstrated that nicardipine inhibits this ET-1-stimulated Ca^{2+} uptake (Kasuya *et al.*, 1989a). Pretreatment of coronary artery strips with PT almost completely inhibited ET-1-stimulated Ca^{2+} uptake (Table 1). Elevation of extracellular K^+ concentration (50 mM; equimolar substitution for Na^+) also induced an increase in Ca^{2+} uptake by 29 ± 9.1%. However, unlike the ET-1-induced Ca^{2+} uptake, the KCl-induced Ca^{2+} uptake was not significantly suppressed by PT-pretreatment.

Effect of pertussis toxin-pretreatment on inositol phosphates production induced by endothelin-1

We examined the effect of PT-treatment on ET-1-induced phosphoinositide hydrolysis, which is also thought to be a signalling pathway evoked by ET-1. As shown in Figure 4, ET-1 stimulated the production of inositol phosphates in the control coronary artery strips. The pretreatment with PT did not significantly affect the ET-1-induced production of total inositol phosphates.

Effect of nifedipine on contractile response to phorbol ester

In order to clarify whether the ET-1-induced activation of the voltage-dependent Ca^{2+} channels is secondary to the activation of protein kinase C evoked through the ET-1-induced phosphoinositide hydrolysis, we investigated the effect of nifedipine on phorbol ester-induced contraction. Phorbol 12,13-dibutyrate (PDBu), an active phorbol ester, induced contraction of porcine coronary artery strips in a dose-dependent manner (Figure 5a), whereas the biologically inactive enantiomer, 4a-phorbol 12,13-dibutyrate, did not (data not shown). In contrast to contraction induced by ET-1, nifedipine (10^{-8} M) did not significantly affect contrac-

tion induced by PDBu (Figure 5b). This indicates that the activation of the Ca^{2+} channel is not involved in phorbol ester-induced contraction of this particular smooth muscle tissue.

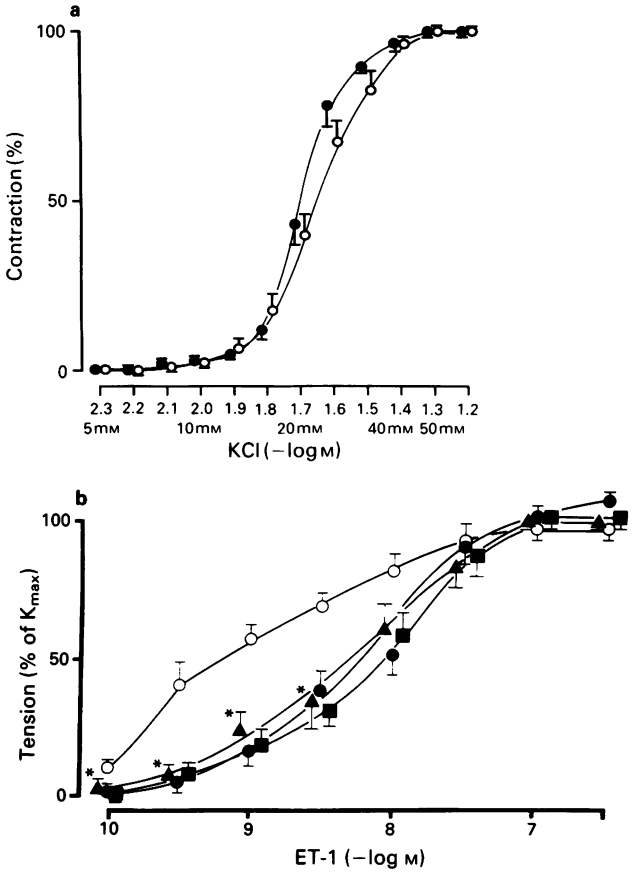

Figure 3 (a) Dose-response relationships for KCl-induced contraction of porcine coronary artery strips pretreated with pertussis toxin (PT, ●) or with vehicle (○). (b) Effects of PT pretreatment and of nifedipine on cumulative dose-response curves of endothelin-1 (ET-1)-induced contraction of porcine coronary artery strips. Dose-response relationships of intact vascular strips to cumulative ET-1 in the absence (○) and presence (●) of 10^{-8} M nifedipine are compared with those in the absence (▲) or presence (■) of 10^{-8} M nifedipine for the vascular strips pretreated with 0.1 μg ml^{-1} PT. Nifedipine was added 15 min before the first dose of ET-1. Contractile responses are expressed as percentages of maximum tension induced by 50 mM KCl. Bars represent ± s.e. ($n = 4$–6). *Significantly different from control levels with $P < 0.05$ (Student's t test for unpaired values).

Table 1 Effect of pretreatment with pertussis toxin (PT) on endothelin-1 (ET-1)-induced Ca^{2+} uptake in porcine coronary artery smooth muscle

	Ca^{2+} *uptake* (nmol g^{-1} tissue)	
	Intact	*PT-treated*
Unstimulated	992 ± 35	962 ± 22
KCl 50 mM	1281 ± 90*	1192 ± 90*
ET-1 10^{-9} M	1462 ± 45*	1005 ± 6†

Data are means ± s.e. ($n = 3$).
*Significantly different from unstimulated values for intact tissues with $P < 0.05$ (ANOVA with Bonferroni method);
†Significantly different from values for intact tissues stimulated with ET-1, $P < 0.05$ (Student's t test for unpaired values).

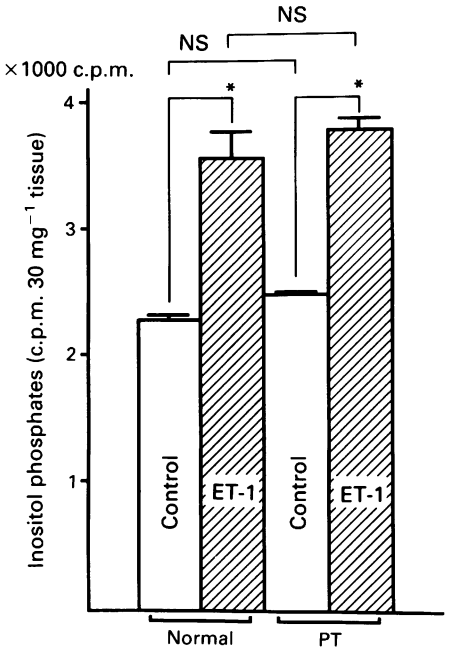

Figure 4 Stimulation by endothelin-1 (ET-1, 10^{-7} M) of production of total [^{3}H]-inositol phosphates (c.p.m. 30 mg^{-1} tissue) in porcine coronary artery strips preincubated with or without pertussis toxin (PT). Error bars represent ± s.e. ($n = 4$). *Significantly different with $P < 0.05$; NS, not significantly different (Student's t test for unpaired values).

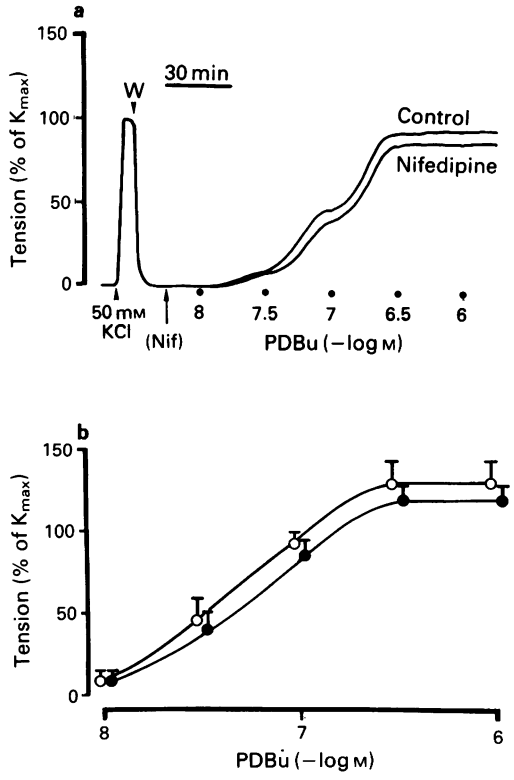

Figure 5 (a) Typical contractile response of porcine coronary artery strips to cumulatively applied phorbol 12,13-dibutyrate (PDBu) in the absence or in the presence of 10^{-8} M nifedipine. (b) Effect of nifedipine on cumulative dose-response curves of PDBu-induced vasoconstriction of porcine coronary artery strips. Dose-response relationships for PDBu in the absence (○) and presence (●) of 10^{-8} M nifedipine are shown. Contractile responses are expressed as percentages of maximum tension induced by 50 mM KCl. Bars represent ± s.e. ($n = 4$).

Discussion

The activation of voltage-dependent Ca^{2+} channels by ET-1 has been demonstrated in various types of cells (Ishikawa *et al.*, 1989; Matsumura *et al.*, 1989; Saitoh *et al.*, 1989; Yoshizawa *et al.*, 1989; Nakao *et al.*, 1990). Our previous studies demonstrated that the Ca^{2+} influx through the dihydropyridine-sensitive voltage-dependent Ca^{2+} channels plays an important role for ET-1-induced contraction of porcine coronary artery (Yanagisawa *et al.*, 1988; Goto *et al.*, 1989; Kasuya *et al.*, 1989a). We have shown in the present study that ET-1-induced contraction over low dose range ($10^{-11} \sim 10^{-10}$ M) is greatly enhanced by membrane depolarization (Figure 1b). This is consistent with the notion that the activation of voltage-dependent Ca^{2+} channels is an important process for the action of low doses of ET-1 in this tissue, since, if the Ca^{2+} influx is assumed to be independent of the membrane potential, the ET-1-induced contraction should be rather inhibited by membrane depolarization because of a decreased driving force for Ca^{2+} influx. We previously demonstrated that ET-1-induced depolarization of the smooth muscle membrane alone is not sufficient to explain the activation of the Ca^{2+} channels by ET-1 (Kasuya *et al.*, 1989a), and that ET-1 has its specific receptor that is separate from the dihydropyridine receptor complex (Miyazaki *et al.*, 1990). Moreover, it has been reported that ET receptor subtypes belong to the superfamily of G protein-coupled receptors (Arai *et al.*, 1990; Sakurai *et al.*, 1990). These observations raise the possibility that the putative receptor(s) for ET-1 may modulate the Ca^{2+} channel through a transducer molecule such as membrane G-proteins. ET-1 also activates phospholipase C with production of two second messengers, inositol trisphosphate and 1,2-diacylglycerol, leading to the mobilization of intracellular Ca^{2+} and activation of protein kinase C in porcine coronary artery. The ET-1-induced activation of phospholipase C is independent of Ca^{2+} influx (Kasuya *et al.*, 1989b). Further, it has previously been demonstrated that the activation of protein kinase C by active phorbol esters can enhance the inward Ca^{2+} current via the voltage-dependent Ca^{2+} channels in various types of cells (Dosemeci *et al.*, 1988; Vivaudou *et al.*, 1988). These findings suggest the possibility that the activation of voltage-dependent Ca^{2+} channels is secondary to the activation of phospholipase C by ET-1. We designed the present study to resolve these possibilities by dissecting the intracellular signalling mechanisms by virtue of PT.

The apparent effect of the pretreatment of coronary artery strips with PT on ET-1-induced contraction closely mimicked the action of nifedipine, in that contraction to relatively low concentrations of ET-1 (10^{-10}–3×10^{-9} M) was preferentially inhibited by the PT-pretreatment (Figure 3b). The effects of the PT-pretreatment and nifedipine were not additive; treatment with 10^{-8} M nifedipine of the PT-pretreated strips did not further attenuate the ET-1-induced contraction. This suggests that the nifedipine-sensitive component of ET-1-induced contraction may be selectively removed by the pretreatment with PT. Furthermore, the pretreatment of the coronary artery strips with PT also inhibits the Ca^{2+} uptake induced by a low concentration of ET-1 (10^{-9} M), which is previously demonstrated (Kasuya *et al.*, 1989a) to be completely inhibited by nicardipine (Table 1). These results suggest that ET-1-induced activation of the voltage-dependent Ca^{2+} channel is mediated by a PT-sensitive signalling pathway. In contrast, ET-1-induced production of inositol phosphates was not significantly affected by the pretreatment of the arterial strips with PT (Figure 4), consistent with our previous findings with rat A10 smooth muscle cells in culture (Takuwa *et al.*, 1990).

A possible pathway of the ET-1-induced activation of the Ca^{2+} channels would be via the stimulation of protein kinase C secondary to the ET-1-induced breakdown of phosphoinositides. A prerequisite of this hypothesis is that the activation of protein kinase C opens the Ca^{2+} channels. However, the dose-response relationship for phorbol ester-induced contraction of porcine coronary artery was not significantly affected by nifedipine at the dose that reduced the ET-1-induced contraction (Figure 5). Moreover, the contractile response induced by PDBu at the dose which induces the maximum tension (10^{-6} M) was not significantly inhibited by the removal of extracellular Ca^{2+} (data not shown). These results indicate that the voltage-dependent Ca^{2+} channels are not actively involved in the contraction elicited by the activation of protein kinase C in this particular tissue, and hence, that the ET-1-induced activation of the Ca^{2+} channel is unlikely to be a secondary event following the activation of protein kinase C due to the stimulation of phosphoinositide turnover by ET-1. This idea is also consistent with the previous demonstration that the active phorbol ester, tetradecanoylphorbol 13-acetate, neither positively nor negatively affects the Ca^{2+} influx via the voltage-dependent Ca^{2+} channels in this particular tissue (Itoh *et al.*, 1986).

The possibility existed that the long incubation of the tissue in PT-containing solution might bring about a membrane hyperpolarization or a reduction in the density of ET receptors; the response of the arterial tissue to agonists might be attenuated through these 'indirect' effects of PT rather than through a specific inhibition of the ET-1-induced activation of the Ca^{2+} channels. We examined these possibilities as follows: (i) if the PT-pretreatment somehow caused a membrane hyperpolarization, responses of the tissue to raised concentrations of KCl would also be affected. However, the PT-treatment did not alter the dose-response relationships for KCl-induced contraction (Figure 3a). Furthermore, the arterial strips showed a similar KCl-induced Ca^{2+} uptake before and after the PT-treatment (Table 1). (ii) If the pretreatment with PT resulted in a reduction in the density of ET receptors, the PT-treatment would cause not only a decrease of ET-1-induced Ca^{2+} entry but also a suppression of ET-1-induced phosphoinositide hydrolysis. However, the PT-pretreatment did not affect ET-1-stimulated production of inositol phosphates (Figure 4). These findings support the view that the PT-treatment under the experimental conditions used in the present study selectively blocked the signal transduction pathway from ET receptors to voltage-dependent Ca^{2+} channels in porcine coronary artery smooth muscle.

We demonstrated in the present study that the treatment of the coronary artery strips with PT efficiently ADP-ribosylated a 41 kDa membrane protein, which most likely represents the α-subunit of a G-protein (Figure 2). This further substantiates the idea that a certain G-protein, sensitive to PT, mediates the activation of the voltage-dependent Ca^{2+} channels by ET-1. In accordance with this notion, it has recently been demonstrated that *in vivo* pressor action of ET-3 in rats is apparently mediated by Ca^{2+} influx evoked via a PT-sensitive G-protein (Tabrizchi & Triggle, 1990). It has also been demonstrated that ET-1-induced Ca^{2+} influx is mediated through a PT-sensitive G-protein in striatal astrocytes (Martin *et al.*, 1991). PT prevents functional coupling of activated receptors and certain classes of G-proteins such as G_i and G_o by specifically ADP-ribosylating them. In favour of this argument, recent studies have demonstrated that the voltage-dependent Ca^{2+} channels are directly modulated by a number of G-proteins (Rosenthal *et al.*, 1988a). For example, a G_o-protein directly mediates the ligand-induced inhibition of voltage-dependent Ca^{2+} channels in various neuronal cells (Holz *et al.*, 1986; Hescheler *et al.*, 1987; Wanke *et al.*, 1987; Bergamaschi *et al.*, 1988). In addition, a G_i-protein and a G_s-protein directly mediate the stimulation of the voltage-dependent Ca^{2+} channel by hormones in endocrine cells (Hescheler *et al.*, 1988; Rosenthal *et al.*, 1988b) and cardiac cells (Yatani *et al.*, 1987), respectively. At present, however, it cannot be concluded unequivocally whether the PT-sensitive G-protein(s) that are coupled to ET receptor directly interact with the voltage-dependent Ca^{2+} channels or whether they affect the Ca^{2+} channel via an indirect mechanism.

The observations presented in this and previous studies (Goto *et al.*, 1989; Kasuya *et al.*, 1989a,b) indicate that ET-1 may evoke two independent pathways of intracellular signal transduction in porcine coronary artery smooth muscle: one pathway leads to the activation of dihydropyridine-sensitive voltage-dependent Ca^{2+} channels via a PT-sensitive G-protein, and the other involves the stimulation of phosphoinositides turnover through a PT-insensitive mechanism. Further study is required to examine whether these two signalling systems are coupled to different subtypes of the ET receptor or to a single class of ET receptor. Two distinct subtypes of endothelin receptor, name ET_A and ET_B receptors, have recently been cloned and pharmacologically characterized (Arai *et al.*, 1990; Sakurai *et al.*, 1990; Hosoda *et al.*, 1991); ET_A receptors have much higher affinity for ET-1 and ET-2 as compared with ET-3, while ET_B receptors almost equally accept all three isopeptides of endothelin. However, radioligand binding studies and affinity cross-linking studies have detected only a single class of specific binding sites for ET-1 on the membrane fraction from porcine coronary artery smooth muscle, with pharmacological profiles consistent with the ET_A receptors (unpublished observation). Although the possibility remains that there might exist more than one sub-subclass of ET_A receptors, no positive evidence suggesting ET_A receptor sub-subtypes has been presented thus far. It is therefore tempting to suggest that two distinct signalling systems of ET-1 in porcine coronary artery smooth muscle cells are coupled to a single ET-1 receptor. In this context, it is worth noting that both M_1 and M_4 subtypes of muscarinic acetylcholine receptors may each be coupled to two different classes of G-proteins that are distinguishable by sensitivity to PT (Ashkenazi *et al.*, 1989). Nichols *et al.* (1989) showed that, in a rat *in vivo* model, the pressor response mediated by an apparently single subclass of α_1-adrenoceptors may be coupled to both phospholipase C and dihydropyridine-sensitive Ca^{2+} channels via PT-insensitive and PT-sensitive G-proteins, respectively. Besides the phosphoinositides turnover response, a concomitant activation of the voltage-dependent Ca^{2+} channels via a PT-sensitive pathway may represent a newly recognized signalling mechanism for various G-protein-coupled agonists, including the endothelins, in a number of vascular smooth muscle tissues.

This work was supported in part by grants from the University of Tsukuba Project Research; the Ministry of Education, Science and Culture of Japan; Toray Foundation; and the Uehara Memorial Foundation.

References

ARAI, H., HORI, S., ARAMORI, I., OHKUBO, H. & NAKANISHI, S. (1990). Cloning and expression of a cDNA encoding an endothelin receptor. *Nature*, **348**, 730–732.

ASHKENAZI, A., PERALTA, E.G., WINSLOW, J.W., RAMACHANDRAN, J. & CAPON, D.J. (1989). Functionally distinct G proteins selectively couple different receptors to PI hydrolysis in the same cell. *Cell*, **56**, 487–493.

BERGAMASCHI, S., GOVONI, S., COMINETTI, P., PARENTI, M. & TRABUCCHI, M. (1988). Direct coupling of a G-protein to dihydropyridine binding sites. *Biochem. Biophys. Res. Commun.*, **156**, 1279–1286.

BOBIK, A., GROOMS, A., MILLAR, J.A., MITCHELL, A. & GRINPUKELS, S. (1990). Growth factor activity of endothelin on vascular smooth muscle. *Am. J. Physiol.*, **258**, C408–C415.

DOSEMECI, A., DHALLAN, R.S., COHEN, N.M., LEDERER, W.J. & ROGERS, T.B. (1988). Phorbol ester increases calcium current and stimulates the effects of angiotensin II in cultured neonatal rat heart myocytes. *Circ. Res.*, **62**, 347–357.

GOTO, K., KASUYA, Y., MATSUKI, N., TAKUWA, Y., KURIHARA, H., ISHIKAWA, T., KIMURA, S., YANAGISAWA, M. & MASAKI, T. (1989). Endothelin activates the dihydropyridine-sensitive, voltage-dependent Ca^{2+} channel in vascular smooth muscle. *Proc. Natl. Acad. Sci. U.S.A.*, **86**, 3915–3918.

HESCHELER, J., ROSENTHAL, W., TRAUTWEIN, W. & SCHULTZ, G. (1987). The GTP-binding protein, Go, regulates neuronal calcium channels. *Nature*, **325**, 445–447.

HESCHELER, J., ROSENTHAL, W., HINASCH, K.-D., WULFERUN, M., TRAUTWEIN, W. & SCHULTZ, G. (1988). Angiotensin II-induced stimulation of voltage-dependent Ca^{2+} currents in an adrenal cortical cell line. *EMBO J.*, **7**, 619–624.

HOLZ, G.G. IV., RANE, S.G. & DUNLAP, K. (1986). GTP-binding proteins mediated transmitter inhibition of voltage-dependent calcium channels. *Nature*, **319**, 670–672.

HOSODA, K., NAKAO, K., ARAI, H., SUGA, S., OGAWA, Y., MUKOYAMA, M., SHIRAKAMI, G., SAITO, Y., NAKANISHI, S. & IMURA, H. (1991). Cloning and expression of human endothelin-1 receptor cDNA. *FEBS Lett.*, **287**, 23–26.

ISHIKAWA, T., YANAGISAWA, M., KIMURA, S., GOTO, K. & MASAKI, T. (1989). Positive inotropic action of novel vasoconstrictor peptide endothelin on guinea pig atria. *Am. J. Physiol.*, **255**, H970–H973.

ITOH, T., KANMURA, Y., KURIYAMA, H. & SUMIMOTO, K. (1986). A phorbol ester has dual actions on the mechanical response in the rabbit mesenteric and porcine coronary arteries. *J. Physiol.*, **375**, 515–534.

KASUYA, Y., ISHIKAWA, T., YANAGISAWA, M., KIMURA, S., GOTO, K. & MASAKI, T. (1989a). Mechanism of contraction to endothelin in isolated porcine coronary artery. *Am. J. Physiol.*, **257**, H1828–H1835.

KASUYA, Y., TAKUWA, Y., YANAGISAWA, M., KIMURA, S., GOTO, K. & MASAKI, T. (1989b). Endothelin-1 induces vasoconstriction through two functionally distinct pathways in porcine coronary artery: contribution of phosphoinositide turnover. *Biochem. Biophys. Res. Commun.*, **161**, 1049–1055.

MARTIN, P., DEJUMEAUE, J.C., DURIEU-TRAUTMANN, O., NGUYEN, D.L., PREMONT, J., STROSBERG, A.D. & COURAUD, P.O. (1991). Are several G proteins involved in the different effects of endothelin-1 in mouse striatal astrocyte? *J. Neurochem.*, **56**, 1270–1275.

MARTIN, T.F.J., BAJJAJIEH, S.M., LUCAS, D.O. & KOWALCHYK, J.A. (1986). Thyrotropin-releasing hormone stimulation of polyphosphoinositide hydrolysis in GH3 cell membranes is GTP dependent but insensitive to cholera or pertussis toxin. *J. Biol. Chem.*, **261**, 10041–10049.

MATSUMURA, Y., NAKASE, K., IKEGAWA, R., HAYASHI, K., OHYAMA, T. & MORIMOTO, S. (1989). The endothelium-derived vasoconstrictor peptide endothelin inhibits renin release *in vitro*. *Life Sci.*, **44**, 149–157.

MIYAZAKI, H., KONDOH, M., WATANABE, H., MASUDA, Y., MURAKAMI, K., TAKAHASHI, M., YANAGISAWA, M., KIMURA, S., GOTO, K. & MASAKI, T. (1990). Affinity labeling of endothelin receptor and characterization of solubilized endothelin-endothelin receptor complex. *Eur. J. Biochem.*, **187**, 125–129.

NAKAO, K., INOUE, Y., OIKE, M., KITAMURA, K. & KURIYAMA, H. (1990). Mechanisms of endothelin-induced augmentation of the electrical and mechanical activity in rat portal vein. *Pflügers Arch.*, **415**, 526–532.

NICHOLS, A.J., MOTLEY, E.D. & RUFFOLO, R.R. Jr. (1989). Effect of pertussis toxin treatment on postjunctional alpha-1 and alpha-2 adrenoceptor function in the cardiovascular system of the pithed rat. *J. Pharmacol. Exp. Ther.*, **249**, 203–209.

OSTERRIEDER, W., BRUM, G., HESCHELER, J., TRAUTWEIN, W., FLOCKERZI, V. & HOFMANN, F. (1982). Injection of subunits of cyclic AMP-dependent protein kinase into cardiac myocytes modulates Ca^{2+} current. *Nature*, **298**, 576–578.

ROSENTHAL, W., HESCHELER, J., TRAUTWEIN, W. & SCHULTZ, G. (1988a). Control of voltage-dependent Ca^{2+} channels by G protein-coupled receptors. *FASEB J.*, **2**, 2784–2790.

ROSENTHAL, W., HESCHELER, J., HINSCH, K.-D., SPICHER, K., TRAUTWEIN, W. & SCHULTZ, G. (1988b). Cyclic AMP-independent, dual regulation of voltage-dependent Ca^{2+} currents by LHRH and somatostatin in a pituitary cell line. *EMBO J.*, **7**, 1627–1633.

SAITOH, A., SHIBA, R., KIMURA, S., YANAGISAWA, M., GOTO, K. & MASAKI, T. (1989). Vasoconstrictor response of large cerebral arteries of cats to endothelin, an endothelin-derived vasoactive peptide. *Eur. J. Pharmacol.*, **162**, 353–358.

SAKURAI, T., YANAGISAWA, M., TAKUWA, Y., MIYAZAKI, H., KIMURA, S., GOTO, K. & MASAKI, T. (1990). Cloning of a cDNA encoding a non-isopeptide-selective subtype of the endothelin receptor. *Nature*, **348**, 732–735.

SHEARMAN, M.S., SEKIGUCHI, K. & NISHIZUKA, Y. (1989). Modulation of ion channel activity: a key function of the protein kinase C enzyme family. *Pharmacol. Rev.*, **41**, 211–237.

SMITH, C.D., LANE, B.C., KUSAKA, I., VERGHESE, M.W. & SNYDERMAN, R. (1985). Chemoattractant receptor-induced hydrolysis of phosphatidylinositol 4,5-bisphosphate in human polymorphonuclear leukocyte membranes. *J. Biol. Chem.*, **260**, 5875–5878.

TABRIZCHI, R. & TRIGGLE, C.R. (1990). Comparison between the vasoactive actions of endothelin and arginine vasopressin in pithed rats after pretreatment with BAY K 8644, nifedipine or pertussis toxin. *J. Pharmacol. Exp. Ther.*, **253**, 272–276.

TAKUWA, Y., KASUYA, Y., TAKUWA, N., KUDO, M., YANAGISAWA, M., GOTO, K., MASAKI, T. & YAMASHITA, K. (1990). Endothelin receptor is coupled to phospholipase C via a pertussis toxin-insensitive guanine nucleotide-binding regulatory protein in vascular smooth muscle cells. *J. Clin. Invest.*, **85**, 653–658.

TOSELLI, M., LANG, J., COSTA, T. & LUX, H.D. (1989). Direct modulation of voltage-dependent calcium channels by muscarinic activation of a pertussis toxin-sensitive G-protein in hippocampal neurons. *Pflügers Arch.*, **415**, 255–261.

VIVAUDOU, M.B., CLAPP, L.H., WALSH, J.V. Jr. & SINGER, J.T. (1988). Regulation of one type of Ca^{2+} current in smooth muscle cells by diacylglycerol and acetylcholine. *FASEB J.*, **2**, 2497–2504.

WANKE, E., FERRONI, A., MALGAROL, A., AMBROSINI, A., POZZAN, T. & MELDOLESI, J. (1987). Activation of a muscarinic receptor selectively inhibits a rapidly inactivated Ca^{2+} current in rat sympathetic neurons. *Proc. Natl. Acad. Sci. U.S.A.*, **84**, 4313–4317.

YANAGISAWA, M., KURIHARA, H., KIMURA, S., TOMOBE, Y., KOBAYASHI, M., MITSUI, Y., YAZAKI, Y., GOTO, K. & MASAKI, T. (1988). A novel potent vasoconstrictor peptide produced by vascular endothelial cells. *Nature*, **332**, 411–415.

YATANI, A., CODINA, J., IMOTO, Y., REEVES, J.P., BIRNBAUMER, L. & BROWN, A.M. (1987). A G protein directly regulates mammalian cardiac calcium channels. *Science Wash. DC*, **238**, 1288–1292.

YOSHIZAWA, T., KIMURA, S., KANAZAWA, I., UCHIYAMA, Y., YANAGISAWA, M. & MASAKI, T. (1989). Endothelin localizes in the dorsal horn and acts on the spinal neurons: possible involvement of dihydropyridine-sensitive calcium channels and substance P release. *Neurosci. Lett.*, **102**, 179–184.

(Received March 31, 1992
Revised June 22, 1992
Accepted June 24, 1992)

Br. J. Pharmacol. (1992), **107**, 463–470

The effect of SK&F 95654, a novel phosphodiesterase inhibitor, on cardiovascular, respiratory and platelet function

[1] Kenneth J. Murray, Roger J. Eden, John S. Dolan, David C. Grimsditch, Catherine A. Stutchbury, Bella Patel, Aileen Knowles, Angela Worby, James A. Lynham & William J. Coates

SmithKline Beecham Pharmaceuticals, The Frythe, Welwyn, Herts AL6 9AR

1 SK&F 95654 inhibited the guanosine 3':5'-cyclic monophosphate (cyclic GMP)-inhibited phosphodiesterase (cGI-PDE) with an IC_{50} value of 0.7 μM. The IC_{50} values were greater than 100 μM for the other four phosphodiesterase isoenzymes tested. The **R**-enantiomer of SK&F 95654 (IC_{50} = 0.35 μM) was a more potent inhibitor of cGI-PDE than was the **S**-enantiomer (IC_{50} = 5.3 μM).

2 In the guinea-pig working heart, SK&F 95654 produced a positive inotropic response without altering heart rate.

3 Oral administration of SK&F 95654 to conscious dogs caused dose-dependent increases in left ventricular dp/dt_{max} in the range 10–50 μg kg^{-1}. These positive inotropic responses were maintained for 3 h without simultaneous changes in heart rate or blood pressure. The peak effects on left ventricular dp/dt_{max} were similar for orally and intravenously administered compound, indicating good oral bioavailability.

4 SK&F 95654 caused a potent inhibition of U46619-induced aggregation in both a human washed platelet suspension (WPS) (IC_{50} = 70 nM) and in human platelet-rich plasma (PRP) (IC_{50} = 60 nM), indicating that the compound shows negligible plasma binding.

5 The **R**-enantiomer of SK&F 95654 was twenty fold more potent as an inhibitor of platelet aggregation than was the **S**-enantiomer. The similarity of this ratio to that obtained on the cGI-PDE suggests that SK&F 95654 inhibits platelet aggregation via its effects on cGI-PDE. This was also indicated by studies which showed that SK&F 95654 increased adenosine 3':5'-cyclic monophosphate (cyclic AMP) levels and activated cyclic AMP-dependent protein kinase in human platelets.

6 Collagen-induced aggregation of rat PRP was also inhibited by SK&F 95654 (IC_{50} = 65 nM). The effects of SK&F 95654, administered intravenously, on *ex vivo* platelet aggregation were studied in the conscious rat. At 1 mg kg^{-1}, SK&F 95654 inhibited aggregation for at least 4 h post dose and was more potent than the two other cGI-PDE inhibitors studied (siguazodan and SK&F 94120).

7 In contrast to its potent effects on heart and platelets, SK&F 95654 caused only a modest relaxation of histamine- or U46619-induced bronchoconstriction in the anaesthetized, ventilated guinea-pig.

8 Taken together, these results indicate that SK&F 95654 may be a suitable agent for the treatment of congestive heart failure.

Keywords: Phosphodiesterase; inhibitor; heart; platelet; SK&F 95654; cyclic AMP

Introduction

Cyclic nucleotide phosphodiesterases (PDEs) may be classified into five isoenzyme families according to their amino-acid sequence, kinetic properties and sensitivity to physiological and pharmacological modulators (Beavo & Reifsnyder, 1990). The guanosine 3':5'-cyclic monophosphate (cyclic GMP)-inhibited PDE (cGI-PDE), also known as PDE III (Weishaar *et al.*, 1986; Reeves *et al.*, 1987), forms one of these families. Inhibitors of cGI-PDE have been shown to be inotropes (Gristwood *et al.*, 1986; Muller *et al.*, 1990), relaxants of vascular (Silver *et al.*, 1988; Lindgren & Andersson, 1991) and airway smooth muscle (Torphy *et al.*, 1988; Heaslip *et al.*, 1991) and inhibitors of platelet aggregation (Simpson *et al.*, 1988; Murray *et al.*,1990a; Seiler *et al.*, 1987; 1991). In general, however, the effects of an agent on these various physiological parameters have not been systematically compared. In this manuscript we have investigated the effects of a SK&F 95654, a cGI-PDE inhibitor with a novel structure, on PDE isoenzymes and on cardiovascular, respiratory and platelet function. We have also performed studies in human platelets to investigate the mechanism of action of SK&F 95654, and the relationship between increases in adenosine 3':5'-cyclic monophosphate (cyclic AMP) levels and effects on aggregation is discussed.

[1] Author for correspondence.

Methods

Isolation and assay of phosphodiesterases

PDE isoenzymes were isolated by a mixture of anion-exchange and affinity chromatography as previously described (Murray *et al.*,1991). The Ca^{2+}/calmodulin-stimulated PDE (PDE I, see Beavo & Reifsnyder (1990) for nomenclature) was prepared from bovine cardiac ventricle. Cyclic GMP-stimulated PDE (PDE II), cyclic GMP-inhibited PDE (PDE III) and cyclic AMP-specific PDE (PDE IV) were all isolated from guinea-pig cardiac ventricle. Cyclic GMP-selective PDE (PDE V) was obtained from porcine lung. With the exception of PDE II, which displayed positive cooperativity, all the preparations showed simple Michaelis-Menten kinetics. The PDEs also responded to pharmacological and physiological modulators in a predictable

fashion. PDE activity was assayed by the boronate column method (Reeves *et al.*, 1987) with 1 μM cyclic GMP as a substrate for PDE I (in the absence of Ca^{2+} and calmodulin), PDE II and PDE V and with 1 μM cyclic AMP as a substrate for PDE III and PDE IV.

Guinea-pig isolated working heart

Male Dunkin-Hartley guinea-pigs (450–600 g) were killed by cervical dislocation 20 min after the administration of heparin (2,000 i.u., i.p). The heart and lungs were removed rapidly and placed in Krebs solution at 4°C. The lungs and extraneous pericardial tissue were then removed and the heart mounted on the working heart apparatus (Flynn *et al.*, 1978). Krebs solution, gassed with 5% CO_2 in O_2 at 37.5°C, entered the right atrium and was pumped by the left ventricle against a 70 cm column of Krebs solution. Both the coronary and aortic flow were normally recirculated. Aortic flow was measured by a flow meter (Gould Statham), by use of probe of 6.0 mm i.d. situated just after the aortic cannula. Left ventricular (LV) pressure was measured by a Bell & Howell pressure transducer connected by a saline (0.9%) filled polythene tubing to a 23 swg needle pushed into the left ventricle. The left ventricular pressure signal was amplified (Devices preamplifier 3552), differentiated (Devices differentiator 3640) and the derived signal, LV dp/dt_{max}, used as an index of left ventricular contractility. Instantaneous heart rate was measured by a rate meter triggered by the left ventricular pulse. All four parameters were recorded by a Devices M19 six channel recorder. Coronary flow, which dripped from the ventricle, was measured by collection into a volumetric measuring cylinder over 1 min periods and recorded on the chart. Total cardiac output was obtained from the sum of the coronary and aortic flows. Coronary flow and cardiac output were expressed per g dry weight heart tissue, determined after placing the hearts in an oven at 84°C for 24 h.

Cardiovascular studies in conscious dogs

The methods for measurement of cardiovascular and left ventricular function parameters have been described in detail elsewhere (Gristwood *et al.*, 1988). Briefly, unilateral carotid loops were produced in beagle dogs by aseptic techniques under general anaesthesia maintained with halothane in 50% nitrous oxide in oxygen. The carotid loop was approximately 7 cm long and could be used 6 weeks after surgery. When the carotid loops were healed a second surgical procedure to implant a left ventricular pressure transducer was performed. Using a left thoracotomy in the fifth intercostal space, a Konigsberg P-22 solid state pressure transducer was implanted into the left ventricle through a stab wound in the apex of the heart. The animals were allowed a minimum of six weeks to recover from the surgery before the first experiment was performed.

Carotid blood pressure was measured by introducing a teflon cannula (Surflo or Angiocath 20 gauge 2 inch) into the looped carotid artery and connecting it via a three-way tap to a Micron miniature pressure transducer, Model MP 15D (Micron Instruments Inc.) used in conjunction with a Lectromed 3552 preamplifier. The left ventricular pressure transducer was energized by a Lectromed 3559 preamplifier and the resulting signal electronically differentiated to give LV dp/dt_{max}. Lead II ECG signals were detected with subcutaneous titanium electrodes, implanted under general anaesthesia, one over the right shoulder and a second over the left hip. The signals were recorded on a Lectromed M19 polygraph and led to a CED 1401 interface connected to a Micro-Vax II computer (Digital).

Platelet studies

Human platelet-rich plasma (PRP) and a washed platelet suspension (WPS) were prepared from whole blood, freshly drawn from healthy volunteers who gave informed consent, as previously described (Murray *et al.*, 1990a; Merritt *et al.*, 1991). Aggregation was measured in a 4-channel PAP4 Biodata aggregometer. Aliquots, at a final count of 1.5×10^8 platelets ml^{-1}, were equilibrated to 37°C before being placed in the sample chamber and were then incubated for 5 min with various concentrations of SK&F 95654. After the addition of the agonist, aggregation was determined by the change in absorbance monitored for 4 min. Cyclic AMP levels and the cyclic AMP-dependent protein kinase activity ratio were measured in human WPS, that had been incubated with various concentrations of SK&F 95654 for 5 min, as previously described (Murray *et al.*, 1990a,b; Merritt *et al.*, 1991).

Blood obtained from the vena cava of anaesthetized male rats (Sprague-Dawley) was immediately mixed with 0.1 volume of 102 mM sodium citrate for the preparation of rat PRP. PRP was prepared by centrifugation (450 *g* for 5 min) and diluted to 4×10^8 cells ml^{-1} by the addition of autologous platelet-free plasma. Aggregation was determined as described above. For the studies of their effects on *ex vivo* aggregation, test compounds were dissolved in 40% (v/v) polyethylene glycol-400 and administered intravenously into the tail vein. Anaesthesia was induced by Sagatal (60 mg kg^{-1}, i.p.) 8 min before the collection of blood. PRP was prepared, and aggregation monitored, as described above.

Assessment of bronchodilator activity in guinea-pigs

Male Dunkin-Hartley guinea-pigs (450–600 g), were anaesthetized (Sagatal 50 mg kg^{-1}, i.p.) and during the experiment supplements of the anaesthetic (6 mg kg^{-1}, i.v.) were given as required. The trachea was cannulated and the animals ventilated by the use of a Palmer constant volume respiration pump at a frequency of 53 strokes min^{-1}. The stroke volume (6–10 ml) was adjusted to produce a basal airways inflation pressure (AIP) of 15 mmHg. Changes in AIP at a constant airflow were measured with a Bell & Howell 0–750 mmHg physiological pressure transducer connected to a side arm of the inflow circuit. Systemic blood pressure and heart rate were recorded from a cannula inserted into one carotid artery and the pulse pressure used to trigger an instantaneous rate meter to measure heart rate. Both jugular veins were cannulated for administration of drugs and supplementary anaesthetic. Heparin (100 i.u. kg^{-1}, i.v.) was also administered to maintain the patency of cannulae. The animals were maintained at 37°C and histamine (100 nmol kg^{-1}) or U46619 (10 nmol kg^{-1}), administered by i.v. injections, was used to increase bronchial tone at the times indicated.

For *in vitro* studies, sheets of guinea-pig tracheae containing four or five cartilage bands were dissected essentially as described by Hay *et al.* (1987). The tissues were mounted, under 2.5 g tension, in organ baths filled with gassed (95% O_2:5% CO_2) Krebs-Hensleit buffer (composition, mM: NaCl 118, KCl 4.7, $NaHCO_3$ 25, $MgSO_4$ 1.18, $K_2H_2PO_4$ 1.18, (+)-glucose 5.5, Na pyruvate 2, $CaCl_2$ 2.5, pH 7.4) at 37°C. The sheets were primed three times with 1 μM carbachol and, after removal of the carbachol, the strips were left until a steady tone was produced. The effects of SK&F 95654 on this spontaneously generated tension were studied in a cumulative manner.

Drugs

SK&F 95654 (**R,S**-4,5-dihydro-6-[4-(1,4-dihydro-4-oxopyridin-1-yl)phenyl]-5-methyl-3(2H)-pyridazinone; see Figure 1), siguazodan (SK&F 94836, **R,S**-2-cyano-1-methyl-3-[4-(1, 4,5, 6-tetrahydro-4-methyl-6-oxo-3-pyridazinyl)phenyl]guanidine) and SK&F 94120 (5-(4-acetamidophenyl)pyrazin-2-(1H)-one) were prepared in the laboratories of SmithKline Beecham Pharmaceuticals, Welwyn, as previously described (Coates *et al.*, 1983; Burpitt *et al.*, 1988). The **R**- and **S**-enantiomers of

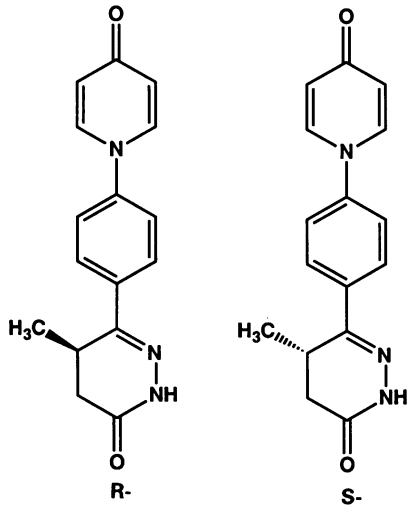

Figure 1 The structure of SK&F 95654 (4,5-dihydro-6-[4-(1,4-dihydro-4-oxopyridin-1-yl)phenyl]-5-methyl-3(2H)-pyridazinone).

SK&F 95654 were prepared from a chiral intermediate as described (Owings *et al.*, 1991). U46619 (15S-hydroxy-11α,9α-(epoxymethano)prosta-5Z,13E-dienoic acid) was obtained from Upjohn (Kalamazoo, U.S.A.) and collagen from Hormon-Chemie (Munich, Germany). Other drugs and chemicals were obtained from Sigma Chemical Company Ltd (Poole, Dorset) and radiochemicals were from Amersham International (Amersham, Bucks).

Analysis of data

All values are reported as means ± s.e.mean. Significant differences between two means were determined with Student's *t* test for unpaired observations and for paired observations (data in Figure 2). $P<0.05$ level was considered significant for all tests. Concentration-inhibition curves were fitted to the logistic equation by the programme, ALLFIT (De Lean *et al.*, 1978).

Results

Effects of SK&F 95654 on PDE isoenzymes

Table 1 shows the IC_{50} values for SK&F 95654 (racemate) and its enantiomers on cGI-PDE isolated from guinea-pig heart. SK&F 95654 potently inhibited cGI-PDE with the R-enantiomer being a more potent inhibitor than the S-enantiomer. The IC_{50} value was greater than 100 μM for the other four PDE isoenzymes tested demonstrating that SK&F 95654 is a potent, selective inhibitor of cGI-PDE. For comparison, the results obtained with previous SmithKline Beecham compounds and clinically used cGI-PDE inhibitors are shown. It can be seen that the potency and selectivity of SK&F 95654 are similar to those of siguazodan and that these compounds are more potent inhibitors of cGI-PDE than either enoximone or amrinone. Milrinone, while being a potent cGI-PDE inhibitor, shows decreased selectivity with respect to PDE IV (cyclic AMP-specific, rolipram inhibited PDE).

Effects of SK&F 95654 on guinea-pig working heart

The effects of SK&F 95654 on the guinea-pig working heart are shown in Figure 2. SK&F 95654 (0.1–10 μM) caused a positive inotropic response with maximal effect at 1 μM and with no significant effect on heart rate. Cardiac output and coronary flow remained constant over the same concentration-range but were reduced at 10 μM. SK&F 95654, therefore, shows selectivity as a positive inotropic agent *in vitro*.

Table 1 Inhibition of cyclic GMP-inhibited phosphodiesterase (cGI-PDE) and other PDE isoenzymes by SK&F 95654 and other selected cGI-PDE inhibitors

Inhibitor	*Isoenzyme* III	I	II	IV	V
	(IC_{50} μM or % inhibition at 100 μM)				
RS-SK&F 95654	**0.7**	14%	33%	31%	24%
R-SK&F 95654	**0.4**	0%	13%	14%	43%
S-SK&F 95654	**5.3**	0%	3%	10%	6%
Enoximone	**13**	11%	20%	25%	15%
Amrinone	**52**	0%	0%	10%	12%
Milrinone	**2**	25%	0%	**33**	27%
Siguazodan	**0.8**	7%	3%	4%	24%
SK&F 94120	**12**	21%	0%	13%	15%

cGI-PDE (PDE III) and other PDE isoenzymes were isolated from guinea-pig cardiac ventricle and other tissues and assayed for PDE activity with 1 μM cyclic AMP or 1 μM cyclic GMP as described under Methods. PDE I is the Ca^{2+}/calmodulin-stimulated PDE; PDE II is the cyclic GMP-stimulated PDE; PDE III is the cyclic GMP-inhibited PDE; PDE IV is the cyclic AMP-specific PDE; PDE IV is the cGMP-specific PDE; for further details see Beavo & Reifsnyder (1990). The IC_{50} (in μM) value is shown in bold, when this is greater than 100 μM the % inhibition obtained at 100 μM drug is shown.

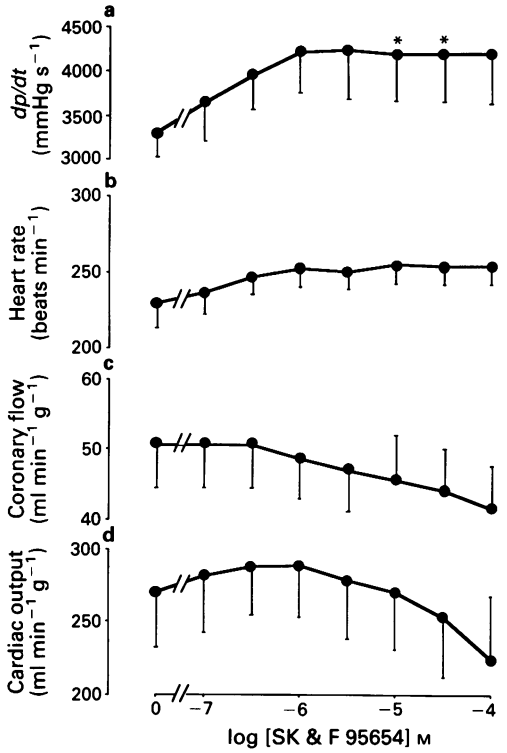

Figure 2 Effect of SK&F 95654 on guinea-pig isolated working heart. Guinea-pig hearts were set up and the various parameters measured as described under Methods. Cumulative dose-response curves to SK&F 95654 were constructed and the effects on (a) LV*dp/dt*, (b) heart rate, (c) coronary flow and (d) cardiac output were determined. Results are mean with s.e.mean shown by vertical bars ($n = 5$).

Results were analysed by Student's *t* test vs. zero SK&F 95654; $*0.05>P>0.01$.

Effects of SK&F 95654 on cardiovascular parameters in conscious dogs.

Single oral administration of SK&F 95654, 10, 25 or 50 $\mu g\,kg^{-1}$ caused a dose-related increase in myocardial contractility (measured as LV dp/dt_{max}), with no concomitant increase in heart rate or reduction of MABP (Figure 3). Parallel changes were seen when contractility was computed as dp/dt at 40 mmHg, an index independent of changes to afterload. Onset of the response was rapid, with a significant effect 20 min after administration at the highest dose. Contractility remained increased for the duration of the 3 h post dosing experimental period. Figure 4 compares the effects of SK&F 95654 administered as an intravenous bolus with those as a single oral dose. The similarity of the effects indicates excellent oral absorption of the compound, a lack of first pass metabolism and good bioavailability. Figure 5 compares the *in vivo* force/rate relationship of the compound with that of the β-adrenoceptor agonist, isoprenaline, which in contrast to SK&F 95654 caused a marked chronotropic as well as inotropic response. Thus SK&F 95654 shows force selectivity *in vivo*.

Effects of SK&F 95654 on human platelets

Table 2 shows the effects of SK&F 95654 and its enantiomers on U46619-stimulated aggregation in suspensions of washed human platelets and in human PRP. The similarity of the values in washed platelets and PRP suggest that SK&F 95654 has a low binding to plasma proteins. In both washed platelets and PRP, R-SK&F 95654 was a twenty fold more potent inhibitor of aggregation than the S-enantiomer. This ratio is very similar to that observed on the cGI-PDE and suggests that the effects of SK&F 95654 on platelet aggregation are due to cGI-PDE inhibition. SK&F 95654 increased the cyclic AMP content in a washed human platelet suspension in a dose-related manner (Figure 6). The activity of cyclic AMP-dependent protein kinase was increased by SK&F 95654 over the same concentration-range (Figure 6).

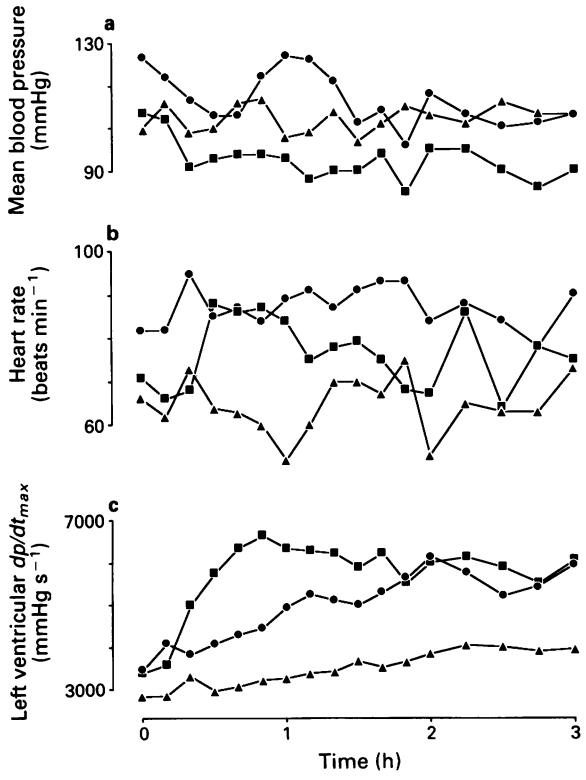

Figure 3 Haemodynamic changes following three doses of SK&F 95654 orally (in distilled water) to conscious instrumented dogs. The parameters measured were mean blood pressure (a), heart rate (b) and left ventricular dp/dt_{max} (c). The doses used were 10 $\mu g\,kg^{-1}$ (▲), 25 $\mu g\,kg^{-1}$ (●) and 50 $\mu g\,kg^{-1}$ (■). Points are means of $n = 3$; significant increases in LV dp/dt_{max} occurred at all dose levels.

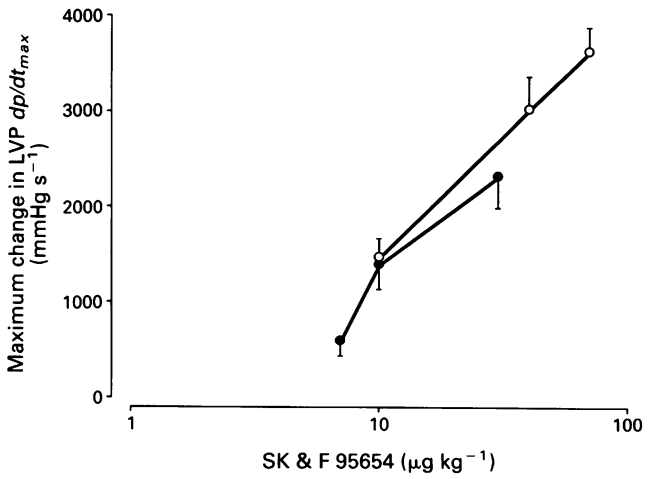

Figure 4 Comparison of the maximum inotropic response obtained from intravenously and orally administered SK&F 95654. SK&F 95654 was administered intravenously (●) or orally (○) to conscious instrumented dogs and the maximum increase in left ventricular dp/dt_{max} over the subsequent 3 h was recorded. Points are means with s.e.means shown by vertical bars ($n = 3$).

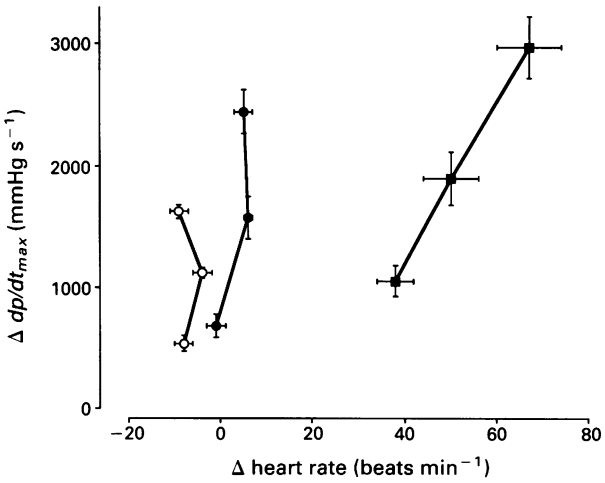

Figure 5 Comparison of the contractility/rate response relationship between SK&F 95654 and isoprenaline. SK&F 95654 was administered by oral (●) or by bolus intravenous injection (○), to conscious instrumented dogs. The points are the mean with s.e.mean (vertical and horizontal bars) ($n = 3$) of isochronous measurements taken at 5 min intervals. The doses used were 10, 25 and 50 $\mu g\,kg^{-1}$ (oral) and 5, 10 and 20 $\mu g\,kg^{-1}$ (i.v.). The values for isoprenaline (■) are taken from Gristwood *et al.* (1988).

Effects of SK&F 95654 on rat platelets

Collagen-induced aggregation of rat PRP was inhibited by SK&F 95654 (Table 2). SK&F 95654 and two other cGI-PDE inhibitors, siguazodan (Murray *et al.*, 1990a) and SK&F 94120 (Simpson *et al.*, 1988), were administered intravenously to rats and their effects on platelet aggregation in PRP obtained from blood taken 15 min after the dose studied. All three agents caused a dose-related inhibition of *ex-vivo* platelet aggregation, with SK&F 95654 being the

Table 2 Inhibition of platelet aggregation by SK&F 95654 and its enantiomers

Platelet preparation	*Stimulus*	**RS-*95654***	**R-*95654*** IC_{50} (nM)	**S-*95654***
Human WPS	U46619 (1 μM)	70 ± 24 (5)	30 ± 13 (3)	633 ± 76 (3)
Human PRP	U46619 (1 μM)	60 ± 27 (5)	31 ± 8 (3)	615 ± 209 (3)
Rat PRP	Collagen (2.5 μg ml^{-1})	65 ± 45 (2)	ND	ND
Rat PRP	Collagen (3.75 μg ml^{-1})	150 ± 40 (2)	ND	ND

Platelet-rich plasma (PRP) or a washed platelet suspension (WPS) was incubated with various concentrations of SK&F 95654 or its enantiomers for 5 min before the addition of U46619 or collagen, aggregation was monitored for the subsequent 4 min. The values shown are the calculated IC_{50} (in nM) for the inhibition of aggregation.
ND = not determined.

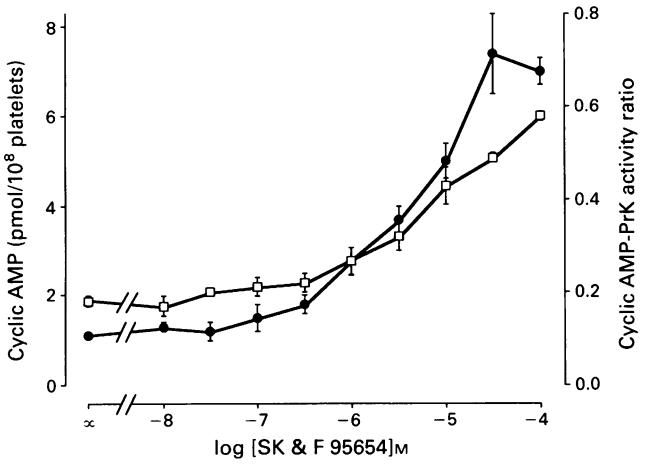

Figure 6 Effect of SK&F 95654 on cyclic AMP content and activity of cyclic AMP-dependent protein kinase (PrK) in washed human platelets. Washed platelet suspensions were incubated with SK&F 95654 and assayed for cyclic AMP (□) and cyclic AMP-dependent protein kinase (●) as described under Methods. Values are shown as means with s.e.mean (vertical bars) ($n = 4$); significant increases ($P < 0.05$) in both parameters were observed for concentrations of SK&F 95654 $> 10^{-6}$ M.

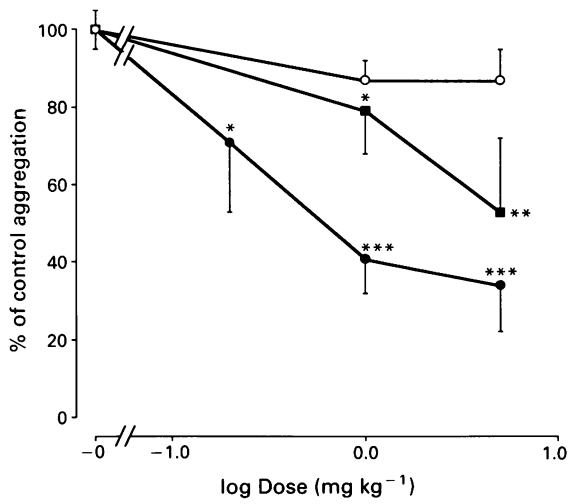

Figure 7 Comparison of the effects of SK&F 95654 (●), siguazodan (■) and SK&F 94120 (○) on platelet aggregation measured *ex vivo* in the rat. Compounds were administered as a bolus intravenous injection to rats and blood withdrawn 15 min later as described under Methods. Platelet aggregation was initiated with 3.75 μg ml^{-1} collagen. Values are means with s.e.mean (vertical bars) ($n = 6$–20) and were compared to vehicle-treated animals by use of Student's t test: *$0.05 > P > 0.01$; **$0.01 > P > 0.001$; ***$P > 0.001$.

most effective (Figure 7). The effects of SK&F 95654 (1 mg kg^{-1}; i.v.) on aggregation were still apparent 4 h after the dose when 2.5 μg ml^{-1} collagen was used as the challenge and for 2 h after the dose when 3.75 μg ml^{-1} collagen was used (Table 3).

Effects of SK&F 95654 on tracheal pressure in the anaesthetized guinea-pig and on isolated tracheal sheets

The effects of SK&F 95654 on U46619- and histamine-induced increases in airway inflation pressure in anaesthetized, ventilated guinea-pigs are shown in Table 4. The doses of U46619 (10 nmol kg^{-1}, i.v.) and histamine (100 nmol kg^{-1}, i.v.) caused an increase in airway inflation pressure of 26 ± 2 mmHg ($n = 12$) and 28 ± 3 mmHg ($n = 8$) respectively. SK&F 95654 caused a dose-dependent decrease in U46619-induced bronchoconstriction and was also effective, to a lesser extent, in reducing histamine-induced rises in airway inflation pressure. In these experiments SK&F 95654 (3 mg kg^{-1}, i.v.) caused a rapid fall in MABP from an initial value of 53 ± 4 mmHg to 29 ± 2 mmHg ($n = 6$); the decrease was evident for the 90 min duration of the experiment.

Racemic SK&F 95654 was a potent relaxant of spontaneous tone in guinea-pig isolated tracheal sheets (EC_{50} = 0.2 ± 0.02 μM) and some stereospecificity was observed (R-SK&F 95654 EC_{50} = 0.3 ± 0.09 μM; S-SK&F 95654 EC_{50} = 1.0 ± 0.07 μM) ($n = 3$, for all values). However, greater stereoselectivity was observed at lower levels of relaxation as indicated by the corresponding EC_{10} values (**RS-SK&F 95654**

Table 3 Effect of SK&F 95654 on *ex vivo* platelet aggregation in the rat

Collagen	*% of control aggregation at time after dose* 0 min	15 min	60 min	120 min	240 min
n =	(20)	(17)	(4)	(7)	(6)
2.5 μg ml^{-1}	100 ± 11	8 ± 3***	2 ± 2***	4 ± 4***	45 ± 27*
3.75 μg ml^{-1}	100 ± 5	41 ± 9***	32 ± 20***	47 ± 18*	95 ± 11

SK&F 95654 was administered as a 1 mg kg^{-1} bolus intravenous injection to rats and blood was withdrawn at the indicated times as described under Methods. Platelet aggregation was initiated by 2.5 or 3.75 μg ml^{-1} collagen. Values were compared by Student's t test to vehicle-treated controls: *$0.05 > P > 0.01$, *** > 0.001.

Table 4 Effect of SK&F 95654 on U46619- and histamine-induced increase in airway inflation pressure in anaesthetized, ventilated guinea-pigs

SK&F 95654 mg kg^{-1}	*Agonist*	*% of pre-dose increase in AIP* 5 min	15 min	30 min	60 min	90 min
0	U46619 ($n = 3$)	92 ± 6	102 ± 6	102 ± 13	119 ± 16	113 ± 4
3	U46619 ($n = 6$)	43 ± 8**	48 ± 7**	62 ± 6*	72 ± 5**	81 ± 7*
10	U46619 ($n = 3$)	18 ± 10**	15 ± 3***	21 ± 4**	40 ± 7**	ND
0	Histamine ($n = 4$)	107 ± 2	112 ± 6	110 ± 10	121 ± 7	124 ± 7
10	Histamine ($n = 4$)	46 ± 4***	73 ± 9*	97 ± 7	109 ± 14	130 ± 10

SK&F 95654 was administered as a bolus intravenous injection to anaethetized guinea-pigs and changes in airways inflation pressure (AIP) induced by U46619 or histamine measured as described under Methods. Values were compared by Student's t test to vehicle treated controls; *$0.05 > P > 0.01$, **$0.01 > P > 0.001$, ***$P > 0.001$.

$EC_{10} = 0.017\ \mu M$; **R**-SK&F 95654 $EC_{10} = 0.007\ \mu M$; **S**-SK&F 95654 $EC_{10} = 0.1\ \mu M$) perhaps indicating additional non cGI-PDE mediated effects at the higher concentrations of SK&F 95654.

Discussion

The results obtained with isolated PDE isoenzymes show that SK&F 95654 is a selective inhibitor of cGI-PDE. A range of dihydropyridazinones have been described in the literature as cGI-PDE inhibitors in which the activity is enhanced by the presence of a 5-methyl substituent in the dihydropyridazinone ring (e.g. Robertson *et al.*, 1986). Such compounds are chiral due to the asymmetric carbon at the 5-position and, for the first time, we present detailed results which show that the **R**-enantiomer is the active form for both biochemical and pharmacological action. The results are consistent with a model (Davis *et al.*, 1987) for the mimicry of cyclic AMP by dihydropyridazinone derivatives in which the **R**-5-methyl group is well accommodated in the region usually occupied by the ribose phosphate ring junction. The **S**-5-methyl would, less favourably, replace the hydroxylic function of the ribose phosphate. Similar results have previously been noted for SK&F 93505, the precursor of SK&F 95654 (Davis *et al.*, 1987).

In common with most other cGI-PDE inhibitors, SK&F 95654 had positive inotropic properties in both guinea-pig and dog with no effect on heart rate. In addition to increased cardiac contractility, it is thought that vasodilatation, resulting in reduction in both pre- and after-load, provides some of the therapeutic benefit of cGI-PDE inhibitors (Cargnelli *et al.*,1989). Although oral administration of SK&F 95654 caused an increase in LV dp/dt_{max} it had no effect on MABP in conscious dogs. However, similar results were obtained with the cGI-PDE inhibitor, siguazodan, which reduced MABP in anaesthetized, but not conscious, dogs (Gristwood *et al.*, 1988). Therefore, although not directly assessed in these studies, it is likely that SK&F 95654 also acts as a vasodilator. Indeed, in the anaesthetized guinea-pig SK&F 95654 caused a pronounced and long lasting fall in MABP, indicating it is probable that SK&F 95654 acts as an 'inodilator' (Cargnelli *et al.*, 1989). SK&F 95654 shows excellent bioavailability as demonstrated by the similarity of the doses required to obtain maximum changes in LV dp/dt_{max} when the compound is administered orally and intravenously. This, coupled with the sustained inotropic action observed after oral dosing, indicates that SK&F 95654 could be suitable for the treatment of congestive heart failure.

There is, at present, considerable debate as to benefit of cGI-PDE inhibitors in the treatment of congestive heart failure. Although clinical studies have shown that cGI-PDE inhibitors cause beneficial changes in the cardiovascular system (Murray & England, 1992), there is current concern regarding the increased mortality associated with two of these agents, milrinone (Packer *et al.*, 1991) and enoximone (Uretsky *et al.*, 1990). Failing human heart shows decreased production of cyclic AMP due to changes in both β-adrenoceptor density and subtype and also to increased levels of inhibitory G proteins (Brodde, 1991; Eschenhagen *et al.*, 1992); in contrast, PDE activity is unaffected (Movsesian *et al.*, 1991). If the reduction in cyclic AMP is regarded as a protective mechanism of the failing heart (Katz, 1990) then, as a class, cGI-PDE inhibitors by re-raising cyclic AMP levels could have undesirable effects.

However, it may be premature to judge all cGI-PDE inhibitors on the basis of current clinical results. Amrinone is usually regarded as the prototype of this class of compound although it is a very weak cGI-PDE inhibitor and almost certainly has other modes of action. Its successor, milrinone, is a potent cGI-PDE inhibitor although its selectivity with regard to inhibition of the cyclic AMP-specific PDE (PDE IV) is not great and it is now known that these two classes of PDE inhibitor interact in various cardiac preparations (Murray & England, 1992). Milrinone has also been reported to have various cyclic AMP-independent effects; for example, it has been reported to activate the calcium release channel of cardiac sarcoplasmic reticulum (Holmberg & Williams, 1991). It has also been postulated that other PDE inhibitors exert their cardiac stimulatory actions by alternate mechanisms, notably sensitization of the contractile proteins (Beier *et al.*, 1991). Therefore, clinical evaluation of novel cGI-PDE inhibitors may help in determining the benefit, or otherwise, of this class of compound.

Although the risk/benefit ratio of long term support with current cGI-PDE inhibitors and other inotropic agents is at present not acceptable, there is no doubt that such agents are suitable for the treatment of acute heart failure and as temporary support for patients waiting for heart transplants (Curfman, 1992). In this respect, the increased aqueous solubility of SK&F 95654 (430 mg l^{-1}) makes it a more suitable agent than siguazodan (51 mg l^{-1}) for acute intravenous treatment and its heightened bioavailability over siguazodan could be advantageous for oral medication. The enhanced anti-platelet action of SK&F 95654 over siguazodan (Figure 7) could also prove to be of benefit.

SK&F 95654 inhibited human and rat platelet aggregation in response to both U46619 and collagen. As previously observed with other cGI-PDE inhibitors, SK&F 95654 was apparently more potent when U46619 was the agonist (Simpson *et al.*, 1988; Murray *et al.*, 1990a). This difference in potency may reflect the ability of the cGI-PDE inhibitor to increase cyclic AMP levels in the presence of different agonists or could be due to differing functional antagonism of the signal transduction pathways used by the agonists (Murray *et al.*, 1990a). However, another explanation could simply be the concentration of agonist used as, when the concentration of collagen was lowered to 2.5 μg ml^{-1}, SK&F 95654 inhibited aggregation in rat PRP with an identical potency to that for inhibition of U46619-stimulated aggregation.

The addition of SK&F 95654 to a washed human platelet

suspension caused parallel increases in the cyclic AMP content and activity of cyclic AMP-dependent protein kinase over the concentration range 0.1–100 μM. These results, coupled with those of the enantiomers on platelet aggregation, indicate cGI-PDE inhibition as the mechanism, at least in part, by which the physiological effects of SK&F 95654 occur. There is an obvious discrepancy between the concentrations of SK&F 95654 required to increase cyclic AMP levels and cyclic AMP-PrK activity and those which inhibit platelet aggregation. A similar observation has been made with the imidazoquinolone cGI-PDE inhibitor, BMY-20844 (Seiler *et al.*, 1991) and with the adenylate cyclase stimulators, iloprost and octimabate (Merritt *et al.*, 1991). As discussed above, this discrepancy may, to some extent, be due to the conditions under which platelet aggregation is measured. By using an 'appropriate' agonist and by varying its concentration and the platelet count, it is possible that conditions will be found where the inhibition of aggregation and increase in cyclic AMP content occur over the same concentration-range. However, the small rises in cyclic AMP caused by cGI-PDE are suggestive of a pool or compartment of cyclic AMP within the platelet (Simpson *et al.*, 1988; Seiler *et al.*, 1987; 1991). When compared to receptor agonists, the compartment of cyclic AMP raised by cGI-PDE inhibition appears to be particularly effective in activating cyclic AMP-PrK. For example when 10 nM iloprost is added to human platelets, a cyclic AMP-dependent protein kinase activity ratio of 0.74 is observed and this is accompanied by a 20 fold increase in the cyclic AMP content (Merritt *et al.*,1990). However, 30 μM SK&F 95654 causes a similar increase in activity ratio with a less than three fold increase in cyclic AMP levels.

As well as inhibiting platelet aggregation *in vitro*, SK&F 95654 inhibited aggregation measured *ex vivo* when administered i.v. to the conscious rat. Aggregation was attenuated by 1 mg kg^{-1} SK&F 95654 for 2–4 h, depending on the concentration of collagen used to induce aggregation. The duration and potency of the effects of SK&F 95654 on platelet aggregation are similar to those on cardiac contraction. Therefore, it can be expected that anti-platelet action will be obtained at doses of SK&F 95654 that produce positive inotropic effects and this could well be of clinical benefit. Although SK&F 95654 and siguazodan have similar potencies with respect to inhibition of cGI-PDE and cardiovascular effects, SK&F 95654 is a more effective inhibitor of platelet aggregation in the rat (Figure 7). In this respect, it is worthy of note that the cGI-PDE inhibitor BMY-43351 has antithrombotic activity in anaesthetized dogs at doses that do not produce cardiovascular effects (Fleming *et al.*, 1991).

Intravenous administration of SK&F 95654 to anaesthetized guinea-pigs diminished bronchoconstriction caused by histamine or U46619. As with platelet aggregation, SK&F 95654 was more potent when U46619 was the agonist. The doses of histamine and U46619 used caused very similar levels of bronchoconstriction suggesting that the different efficacy of SK&F 95654 against these two agonists is not due either to relaxing from different absolute contractions. In this case, it may well be that the increased potency of SK&F 95654 against U46619-induced bronchoconstriction is due to it being a more effective functional antagonist of the particular biochemical changes invoked by this agonist although more detailed experiments are required to establish this. In this series of experiments it was noted that the effects on MABP were more pronounced and longer lasting than those on bronchodilatation and a non-uniform tissue distribution of the compound could explain these results, especially as SK&F 95654 was a potent relaxant of spontaneous tone in an isolated tracheal preparation. The apparently weaker bronchodilator effects observed *in vivo* could also be due to the fact that agonist induced tone was measured in this preparation.

Significant inotropic effects were observed in the dog at doses of SK&F 95654 of 10 μg kg^{-1} and inhibition of platelet aggregation in the rat was found at doses of 200 μg kg^{-1}, whereas 3 mg kg^{-1} SK&F 95654 was required to attenuate bronchoconstriction in the guinea-pig. It is possible that this apparent selectivity of SK&F 95654 for effects on heart and platelets over those on bronchodilatation is due to species variation. Although measurement of these effects in the same species is obviously required to address this, the magnitude of the different doses required for the cardiac and respiratory effects indicate that SK&F 95654 may show genuine tissue selectivity in its actions. In the anaesthetized dog, the cGI-PDE inhibitors CI-930 and imazodan have been reported to show no selectivity or bronchial selectivity, respectively. In these experiments preconstriction with 5-hydroxytryptamine was used to measure bronchodilatation and the dogs were treated with a β-adrenoceptor antagonist (Heaslip *et al.*, 1991). In all cases, methodology, species and the choice and concentration of the agonist could affect the apparent potencies and selectivities observed. As has already been noted above for BMY-43351, it would appear that individual cGI-PDE inhibitors have the potential to show tissue and/or specifies selectivity; therefore, it is inappropriate to extrapolate clinical benefit from the results of animal experiments.

In conclusion, the results obtained with SK&F 95654 show it to be a potent, selective inhibitor of cGI-PDE. The sustained and potent beneficial cardiovascular and platelet effects coupled with oral availability, low plasma binding and aqueous solubility indicate that SK&F 95654 could be a potential agent for the treatment of congestive heart failure. However, the recent clinical data with other cGI-PDE inhibitors coupled with observed differences between cGI-PDE inhibitors means that the therapeutic benefit of SK&F 95654 can only be determined in clinical trials specifically designed to address this point. The observations that the biological activity of SK&F 95654 is largely due to the **R**-enantiomer suggests that this, and not the racemate, may be the most appropriate compound to develop although, again, specific experimentation is required to establish this.

We are grateful to Janine Lamb for experimental work, to Dr A.M. Brown for his critical reading of the manuscript and to Sally Bradbury for help in its preparation.

References

BEAVO, J.A. & REIFSNYDER, D.H. (1990). Primary sequence of cyclic nucleotide phosphodiesterase isozymes and the design of selective inhibitors. *Trends Pharmacol. Sci.*, **11**, 150–155.

BEIER, N., HARTING, J., JONAS, R., KLOCKOW, M., LUES, I. & HAEUSLER, G. (1991). The novel cardiotonic agent EMD 53 998 is a potent calcium sensitizer. *J. Cardiovasc. Pharmacol.*, **18**, 17–27.

BRODDE, O.-E. (1991). α_1- and α_2-adrenoceptors in the human heart: Properties, function and alterations in chronic heart failure. *Pharmacol. Rev.*, **43**, 203–242.

BURPITT, B.E., CRAWFORD, L.P., DAVIES, B.J., MISTRY, J., MITCHELL, M.B., PANCHOLI, K.D. & COATES, W.J. (1988). 6-(Substituted phenyl)-5-methyl-4,5-dihydropyridazin-3(2H)-ones of medicinal interest. The synthesis of SK&F 94836 and SK&F 95654 . *J. Heterocycl. Chem.*, **25**, 1689–1695.

CARGNELLI, G., PIOVAN, D., BOVA, S., PADRINI, R. & FERRARI, M. (1989). Present and future trends in research and clinical applications of inodilators. *J. Cardiovasc. Pharmacol.*, **14** (Suppl 8), S124–S132.

COATES, W.J., EMMETT, J.C., SLATER, R.A. & WARRINGTON, B.H. (1983). Arylpyrazinones. *Eur. Pat.*, 96,517.

CURFMAN, G.D. (1991). Inotropic therapy for heart failure–an unfulfilled promise. *New Engl. J. Med.*, **325**, 1509–1510.

DAVIS, A., WARRINGTON, B.H. & VINTER, J.G. (1987). Strategic approaches to drug design. II. Modelling studies on phosphodiesterase substrates and inhibitors. *J. Comput. Aided Mol. Des.*, **1**, 97–120.

DE LEAN, A., MUNSON, P.J. & RODBARD, D. (1978). Simultaneous analysis of families of sigmoidal curves: application to bioassay, radioligand assay and physiological dose response curves. *Am. J. Physiol.*, **253**, E97–E102.

ESCHENHAGEN, T., MENDE, U., NOSE, M., SCHMITZ, W., SCHOLZ, H., HAVERICH, A., HIRT, S., DORING, V., KALMAR, P., HOPPNER, W. & SEITZ, H.-J. (1992). Increased messenger RNA level of the inhibitory G protein α subunit $Gi_{\alpha-2}$ in human end-stage heart failure. *Circ. Res.*, **70**, 688–696.

FLEMING, J.S., BUCHANAN, J.O., SIELER, S.M. & MEANWELL, N.A. (1991). Antithrombotic activity of BMY-43351,a new imidazoquinoline with enhanced aqueous solubility. *Thromb. Res.*, **63**, 145–155.

FLYNN, S.B., GRISTWOOD, R.W. & OWEN, D.A.A. (1978). Characterization of an isolated, working guinea-pig heart including effects of histamine and noradrenaline. *J. Pharmacol. Meth.*, **1**, 183–195.

GRISTWOOD, R.W., COMER, M.B., EDEN, R.J., TAYLOR, E.M., TURNER, J.A., WALLDUCK, M. & OWEN, D.A.A. (1988). *In vivo* pharmacological studies with SK&F 94836, a potent inotrope/vasodilator with a sustained duration of action. *Br. J. Pharmacol.*, **93**, 893–901.

HAY, D.W.P., FARMER, S.G., RAEBURN, D., MUCCITELLI, R.M., WILSON, K.A. & FEDAN, J.S. (1987). Differential effects of epithelium removal on the responsiveness of guinea-pig tracheal smooth muscle to bronchoconstrictors. *Br. J. Pharmacol.*, **92**, 381–388.

HEASLIP, R.J., BUCKLEY, S.K., SICKELS, B.D. & GRIMES, D. (1991). Bronchial vs. cardiovascular activities of selective phosphodiesterase inhibitors in the anesthetized beta-blocked dog. *J. Pharmacol. Exp. Ther.*, **257**, 741–747.

HOLMBERG, S.R.M. & WILLIAMS, A.J. (1991). Phosphodiesterase inhibitors and the cardiac sarcoplasmic reticulum calcium release channel: differential effects of milrinone and enoximone. *Cardiovasc. Res.*, **25**, 537–545.

LINDGEN, S. & ANDERSSON, K.-E. (1991). Effects of selective phosphodiesterase inhibitors on isolated coronary, lung and renal arteries from man and rat. *Acta Physiol. Scand.*, **142**, 77–82.

KATZ, A.M. (1990). Cardiomyopathy of overload: a major determinant of prognosis in congestive heart failure. *New Engl. J. Med.*, **322**, 100–110.

MERRITT, J.E., HALLAM, T.J., BROWN, A.M., BOYFIELD, I., COOPER, D.G., HICKEY, D.M.B., JAXA-CHAMIEC, A.A., KAUMANN, A.J., KEEN, M., KELLY, E., KOZLOWSKI, U., LYNHAM, J.A., MOORES, K., MURRAY, K.J., MACDERMOT, J. & RINK, T.J. (1991). Octimibate, a potent non-prostanoid inhibitor of platelet aggregation, acts via the prostacyclin receptor. *Br. J. Pharmacol.*, **102**, 251–259.

MOVSESIAN, M.A., SMITH, S.J., KRALL, J., BRISTOW, M.R. & MANGANIELLO, V.C. (1991). Sarcoplasmic reticulum-associated cyclic adenosine 3',5'-monophosphate phosphodiesterase activity in normal and failing human hearts. *J. Clin. Invest.*, **88**, 15–19.

MULLER, B., LUGNIER, C. & STOCKLET, J.-C. (1990). Implication of cyclic AMP in the positive inotropic effects of cyclic GMP-inhibited cyclic AMP phosphodiesterase inhibitors on guinea pig isolated left atria. *J. Cardiovasc. Pharmacol.*, **15**, 444–451.

MURRAY, K.J., EDEN, R.J., ENGLAND, P.J., DOLAN, J., GRIMSDITCH, D.C., STUTCHBURY, C.A., PATEL, B., REEVES, M.L., WORBY, A., TORPHY, T.J., WOOD, L.M., WARRINGTON, B.H. & COATES, W.J. (1991). Potential use of selective phosphodiesterase inhibitors in the treatment of asthma. *Agents Actions*, Supplement 34, *New Drugs for Asthma Therapy* ed. Anderson, G.P., Chapman, I.D. & Morley, J., pp. 27–46.

MURRAY, K.J. & ENGLAND, P.J. (1992). Inhibitors of cyclic nucleotide phosphodiesterases as therapeutic agents. *Biochem. Soc. Trans.*, **20**, 460–464.

MURRAY, K.J., ENGLAND, P.J., HALLAM, T.J., MAGUIRE, J., MOORES, K., REEVES, M.L., SIMPSON, A.W.M. & RINK, T.J. (1990a). The effects of siguazodan, a selective phosphodiesterase inhibitor, on human platelet function. *Br. J. Pharmacol.*, **99**, 612–616.

MURRAY, K.J., ENGLAND, P.J., LYNHAM, J.A., MILLS, D., SCHMITZ-PEIFFER, C. & REEVES, M.L. (1990b). Use of a synthetic dodecapeptide (malantide) to measure the cyclic AMP-dependent kinase activity ratio. *Biochem. J.*, **267**, 703–708.

OWINGS, F.L., FOX, M., KOWALSKI, C.J. & BAINE, N.H. (1991). An enantiomeric synthesis of SK&F 93505, a key intermediate for preparing cardiotonic agents. *J. Org. Chem.*, **56**, 1963–1966.

PACKER, M. FOR THE PROMISE STUDY RESEARCH GROUP (1991). Effect of oral milrinone on mortality in severe chronic heart failure. *New Engl. J. Med.*, **325**, 1468–1475.

REEVES, M.L., LEIGH, B.K. & ENGLAND, P.J. (1987). The identification of a new cyclic nucleotide phosphodiesterase activity in human and guinea-pig cardiac ventricle. *Biochem. J.*, **241**, 535–541.

ROBERTSON, D.W., KRUSHINSKI, J.H., BEEDLE, E.E., WYSS, V., POLLOCK, G.D., WILSON, H., KAUFFMAN, R.F. & HAYES, J.S. (1986). Dihydropyridazinone cardiotonics. The discovery and inotropic activity of 1,3-dihydro-3,3-dimethyl-5-[D(1,4,5,6-tetrahydro-6-oxo-3-pyridazinyl)-2H-indol-2-one. *J. Med. Chem.*, **29**, 1832–1840.

SEILER, S., ARNOLD, A.J., GROVE, R.I., FIFER, C.A., KEELY, S.L., JR., & STANTON, H.C. (1987). Effects of anagrelide on platelet cyclic AMP levels, cyclic AMP-dependent protein kinase and thrombin-induced Ca^{++} fluxes. *J. Pharmacol. Exp. Ther.*, **243**, 767–774.

SEILER, S., GILLESPIE, E., ARNOLD, A.J., BRASSARD, C.L., MEANWELL, N.A. & FLEMING, J.S. (1991). Imidazoquinoline derivatives: potent inhibitors of platelet cyclic AMP phosphodiesterase which elevate cyclic AMP levels and activate protein kinase in platelets. *Thrombosis Res.*, **62**, 31–42.

SILVER, P.J., LEPORE, R.E., O'CONNOR, B., LEMP, B.M., HAMEL, L.T., BENTLEY, R.G. & HARRIS, A.L. (1988). Inhibition of the low K_m cyclic AMP phosphodiesterase and activation of the cyclic AMP system in vascular smooth muscle by milrinone. *J. Pharmacol. Exp. Ther.*, **247**, 34–42.

SIMPSON, A.W.M., REEVES, M.L. & RINK, T.J. (1988). Effects of SK&F 94120, an inhibitor of cyclic nucleotide phosphodiesterase type III, on human platelets. *Biochem. Pharmacol.*, **37**, 2315–2320.

TORPHY, T.J., BURMAN, M., HUANG, L.B.F. & TUCKER, S.S. (1988). Inhibition of the low K_m cyclic AMP phosphodiesterase in intact canine trachaelis by SK&F 94836: mechanical and biochemical responses. *J. Pharmacol. Exp. Ther.*, **246**, 843–850.

URETSKY, B.F., JESSUP, M., KONSTAM, M.A., DEC, G.W., LEIER, C.V., BENOTTI, J., MURALI, S., HERRMANN, H.C. & SANDBERG, J.A., FOR THE ENOXIMONE MUTLICENTER TRIAL GROUP (1990). Multicenter trial of oral enoximone in patients with moderate to moderately severe congestive heart failure. Lack of benefit compared with placebo. *Circulation*, **82**, 774–780.

WEISHAAR, R.E., BURROWS, S.D., KOBYLARZ, D.C., QUADE, M.M. & EVANS, D.B. (1986). Multiple molecular forms of cyclic nucleotide phosphodiesterase in cardiac and smooth muscle and in platelets. *Biochem. Pharmacol.*, **35**, 787–800.

(Received January 22, 1992
Revised May 20, 1992
Accepted June 8, 1992)

Br. J. Pharmacol. (1992), **107**, 471–475

Effects of noradrenaline on rat paratracheal neurones and localization of an endogenous source of noradrenaline

Fiona M. Reekie & [1] Geoffrey Burnstock

Department of Anatomy and Developmental Biology and Centre for Neuroscience, University College London, Gower Street, London WC1E 6BT

1 Intracellular recording techniques were used to study the actions of exogenous noradrenaline (NA) on rat paratracheal neurones *in situ*. The receptor subtypes underlying these actions were investigated by application of selective adrenoceptor antagonists.

2 Application of NA (0.1–10 μM) by superfusion evoked a membrane depolarization in 85% (52 out of 61) of all paratracheal neurones studied. The response consisted of a slow depolarization which was sometimes accompanied by action potential discharge. In 26 out of 31 cells the response was associated with a change in input resistance of the cell membrane. In 22 out of 26 cells there was a 30% increase, whilst in a further 4 cells there was a 15% decrease in input resistance. The amplitude of the NA depolarization was concentration-dependent.

3 The depolarization evoked by NA was reversibly antagonized by prazosin (1 μM) but unaffected by yohimbine (1 μM) or propranolol (1–10 μM).

4 High performance liquid chromatography with electrochemical detection (h.p.l.c.-e.c.d.) was used to assay for NA and dopamine in samples containing mainly paratracheal ganglia and in samples of tracheal smooth muscle with mucosa. NA was present in all samples assayed at a level of 1.6 μg NA g^{-1} and 0.5 μg NA g^{-1} wet weight of the two sample types respectively. Dopamine was not detected in any samples of either ganglia or smooth muscle with mucosa.

5 It is concluded that NA-evoked depolarizations of rat paratracheal neurones result from stimulation of α_1-adrenoceptors, and that local levels of NA may be sufficiently high to activate these receptors directly.

Keywords: Trachea; ganglia; noradrenaline

Introduction

The intramural parasympathetic ganglia of the airways are thought to be the integrative sites of the neural output controlling smooth muscle tension, mucosal secretion and tracheobronchial reflexes (Richardson, 1979). The parasympathetic intracardiac (Jacobowitz, 1967) and vesical ganglia (Hamberger & Norberg, 1965a,b; Norberg & Sjöqvist, 1966; De Groat & Saum, 1971) have been shown to be adrenergically innervated.

Three membrane responses to noradrenaline (NA) have been recorded in various autonomic ganglia: hyperpolarizations, depolarizations; and biphasic responses consisting of a hyperpolarization followed by depolarization (Morita & North, 1981; Nakamura *et al.*, 1984; North & Surprenant, 1985; Akasu *et al.*, 1985). In the parasympathetic submandibular and vesical ganglia, the most frequently observed response to NA is a hyperpolarization mediated through α_2-adrenoceptors (Suzuki & Volle, 1979; Akasu *et al.*, 1985). Similarly, in sympathetic superior cervical ganglia, hyperpolarization to NA is mediated by α_2-adrenoceptors (Ashe & Libet, 1982). In contrast, the depolarizations in parasympathetic ganglia have been shown to be mediated through α_1-adrenoceptors (Akasu *et al.*, 1985) and in sympathetic ganglia they are mediated through β-adrenoceptors (De Groat & Volle, 1966; Brown & Dunn, 1983). Noradrenaline has also been shown to inhibit excitatory nicotinic neurotransmission in the paratracheal ganglia of the ferret (Baker *et al.*, 1983) and in parasympathetic ganglia of urinary bladder (Tsurasaki *et al.*, 1990).

Evidence for adrenergic innervation of paratracheal ganglia is sparse. However, adrenergic nerve fibres have been found terminating near airway ganglia of the calf (Jacobowitz *et al.*, 1973; Phipps *et al.*, 1982) and noradrenergic varicose fibres have also been localized in the mucosa, tracheal muscle and around arteries in the rat trachea (Baluk & Gabella, 1989). Whilst adrenergic fibres were found to be absent from rat paratracheal ganglia, a population of the neurones have been shown to express partially a noradrenergic phenotype (Baluk & Gabella, 1989).

In this paper we describe the effect of NA on rat paratracheal neurones and attempt to determine the receptor subtypes responsible for mediating this response. In addition, we have carried out assays for NA and dopamine in order to determine local catecholamine levels. Finally, we discuss the possible implications of these findings for airway function.

Methods

All experiments were performed on 15–18 day old Sprague-Dawley rat pups of either sex. Animals were stunned by a blow to the back of the head and then killed by cervical dislocation. The trachea was excised from the base of the carina to the bifurcation of the main bronchi and cut midline along the length of its ventral surface. The trachea was pinned out, dorsal side uppermost, onto a small block of Sylgard (Dow Corning) prebonded to a glass slide which formed the base of the recording chamber. The adventitia were then removed to expose the intramural paratracheal ganglia. The assembled chamber was then clamped to the stage of a Zeiss Ergoval microscope equipped with Hoffman

[1] Author for correspondence.

modulation contrast optics giving 40 and 640 fold magnification. The preparation was superfused at a rate of 6 ml min^{-1} with Krebs solution of composition (mM): NaCl 118.1, KCl 4.7, $MgSO_4$ 1.2, KH_2PO_4 1.2, $CaCl_2$ 2.5, $NaHCO_3$ 25, glucose 10, and gassed with 95% O_2/5% CO_2. The temperature was maintained at 34–36°C by a remote thermostatically-controlled heating coil and monitored by a thermistor positioned next to the trachea. Impalements were made with electrodes having d.c. resistances between 80 and 110 MΩ and filled with 2.3 M potassium citrate (pH 7.1). The electrodes were connected to an amplifier with an active bridge circuit that allowed simultaneous current injection and voltage recording (Axoclamp 2A). Electrode resistance and tip offset potentials were nulled before impalement to allow estimations of input resistance and membrane potential to be made during the recording. In order to aid placement of electrodes and impalement of neurones, the final 2–3 mm of the electrodes were bent through an angle of 45–70° before being filled. Input resistance measurements were made by passing 100 ms current pulses of known intensity across the cell membrane and measuring the amplitudes of the hyperpolarizations evoked. Drugs were applied by bath superfusion from small drug reservoirs connected by a multi-way tap. The time for drugs to reach the bath from the reservoirs was approximated by use of fast green dye. This was found to be around 40 s. Data were either stored on tape for future analysis (Racal store 4 DS) or displayed on a Textronix storage oscilloscope (Model D13) and a Gould pressure ink recorder (Model 2200 S).

H.p.l.c. analysis of paratracheal ganglia and smooth muscle with mucosa

Tracheae from 15–17 day old rats were dissected and pinned out as previously described. The paratracheal ganglia were then dissected from the trachealis under × 50 magnification and stored in liquid nitrogen. The underlying smooth muscle with mucosa was then dissected and also stored in liquid nitrogen. Samples were pooled from 5–6 animals and high performance liquid chromatography with electrochemical detection (h.p.l.c.-e.c.d.) was used to measure the levels of NA and dopamine present. The pooled samples of dissected ganglia and muscle were blotted dry, weighed and homogenized in 500 µl 0.1 M perchloric acid/0.4 mM sodium bisulphite containing 25 ng ml^{-1} dihydroxybenzylamine (DHBA) as an internal standard. After centrifugation the supernatants were subjected to alumina extraction as described previously (Griffith *et al.*, 1982). NA and DHBA were eluted from the alumina into 300 µl 0.1 M perchloric acid/0.4 mM sodium bisulphite and 50 µl samples were injected for h.p.l.c.-e.c.d. Separation was carried out on a 10 cm 5 µm C18 reverse phase column (Spherisorb 500DS2, Hichrom) with a mobile phase of 0.1 M phosphate buffer (pH 5.0), 0.1 mM ethylenediaminetetraacetate (EDTA) and 5 mM heptane sulphonate containing 10% (v/v) methanol (Moyer & Jiang, 1978) at a flow rate of 2 ml min^{-1}. Quantification was achieved with a Coulochem detector (Model 5100A, Severn Analytical) set at the following potentials: guard cell, + 0.25 V; electrode 1, + 0.21 V; electrode 2, − 0.23 V. Concentrations of NA and DHBA were determined by reference to the elution times and peak heights of standard solutions and the concentration of NA was corrected for recovery from the alumina extraction by use of the DHBA internal standard.

Statistical analysis

Results are expressed as means ± s.e.mean. Differences between means were analysed by Student's *t* test (paired or unpaired as appropriate). A *P* value of less than or equal to 0.05 was considered to be significant.

Drugs

Noradrenaline bitartrate, prazosin hydrochloride and yohimbine hydrochloride were obtained from Sigma, United Kingdom. Propranolol hydrochloride was obtained from ICI, United Kingdom. Noradrenaline and propranolol were dissolved in 100 µM ascorbic acid at a concentration of 100 µM. Yohimbine was dissolved in 25% methanol at a concentration of 1 mM. All drugs were diluted in Krebs solution for superfusion.

Results

Membrane responses to noradrenaline

Superfusion of NA (0.1–10 µM) onto rat paratracheal neurones evoked a slow depolarization in 85% (52 out of 61) of neurones. Of 49 neurones (RMP = 48.6 ± 1.0 mV) tested with 10 µM NA, 46 (94%) were depolarized (8.3 ± 0.7 mV) (Figure 1). In 55% of these neurones, this depolarization was accompanied by action potential discharge (Figure 1). The amplitude of the evoked depolarization was concentration-

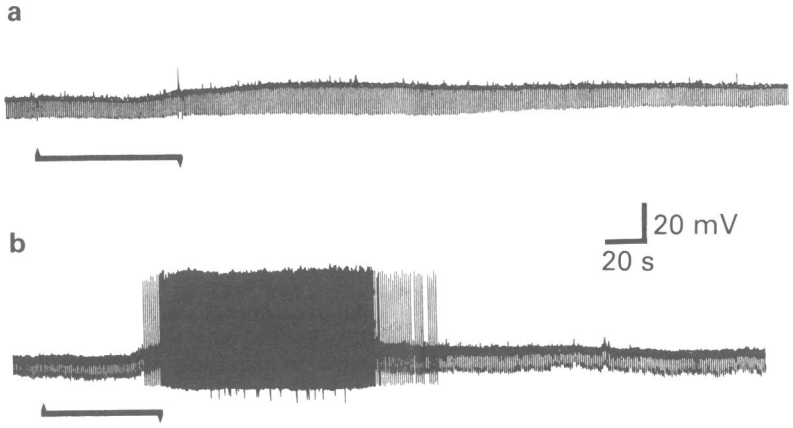

Figure 1 The effects of superfusion of 10 µM noradrenaline (NA) on rat paratracheal neurones. The open channel of the multiway tap is connected to the drug reservoir at the point indicated by ▲, and reconnected to the Krebs solution at the point indicated by ▼. An artefact is occasionally seen at these points. (a) NA elicited a slow depolarization which was accompanied by an increase in input resistance of the membrane (from 10 MΩ resting to 14 MΩ). Resting membrane potential − 62 mV. (b) In another cell, the NA-evoked depolarization was accompanied by spontaneous firing of action potentials. Resting membrane potential − 50 mV, input resistance 9 MΩ. The downward deflections are the membrane responses to constant current hyperpolarizing pulses (100 pA), as an indicator of membrane input resistance changes.

dependent with 0.1, 1 and 10 μM NA producing a depolarization of 0.8 ± 0.8 mV ($n = 6$), 4.1 ± 1.5 mV ($n = 6$) and 8.3 ± 0.7 mV ($n = 49$) respectively. A change of input resistance of the cell membrane accompanying the response to NA was not easily detected. Of 26 cells in which an apparent change in input resistance accompanying the NA-evoked depolarizations was observed, 22 cells displayed an increase in resting resistance (30 ± 5%) and 4 a small decrease (15 ± 6%). In one cell there was no change in resistance accompanying the rising phase of the depolarization although the falling phase was accompanied by a decrease in input resistance. In a further 4 neurones no change of input resistance was observed. The depolarization was unaffected by 0.5 μM tetrodotoxin (TTX) indicating no involvement of intermediary synapses.

Receptors mediating the noradrenaline response

The effects of adrenoceptor antagonists were examined to determine the receptor subtype responsible for mediating the NA response (Table 1, Figure 2). Prazosin (1 μM), a selective α_1-adrenoceptor antagonist abolished the depolarization elicited by 10 μM NA in all neurones tested ($n = 8$). Prazosin was difficult to wash out but the reversibility of the antagonism was shown in 4 cells. Prazosin (0.1 μM) exhibited less effective antagonism of the response to NA showing 40% inhibition ($n = 2$). High concentrations of NA (4 mM) were required to overcome the inhibition by 1 μM prazosin ($n = 2$). Yohimbine (1 μM), a selective α_2-adrenoceptor antagonist had no significant effect on the NA depolarization ($n = 8$). Propranolol (10 μM), a non selective β-adrenoceptor antagonist, did not inhibit the depolarization evoked by 10 μM NA ($n = 4$). In a further 4 cells the NA response also persisted in Krebs solution containing 10 μM propranolol. Phenylephrine (10 μM), an α_1-adrenoceptor agonist also elicited a depolarization similar to that produced by NA (unpublished observation).

H.p.l.c. analysis of catecholamine levels in paratracheal ganglia and of smooth muscle with mucosa

The samples containing paratracheal ganglia and those containing smooth muscle with mucosa were analysed by h.p.l.c. techniques for NA and dopamine. NA was found in both paratracheal ganglia samples (1.6 ± 0.4 μg NA g^{-1} tissue w.wt.) and smooth muscle with mucosa samples (0.5 ± 0.1 μg NA g^{-1} tissue w.wt.). These values were significantly different ($P < 0.05$, $n = 6$). Dopamine was not detected in any samples of either paratracheal ganglia or smooth muscle with mucosa.

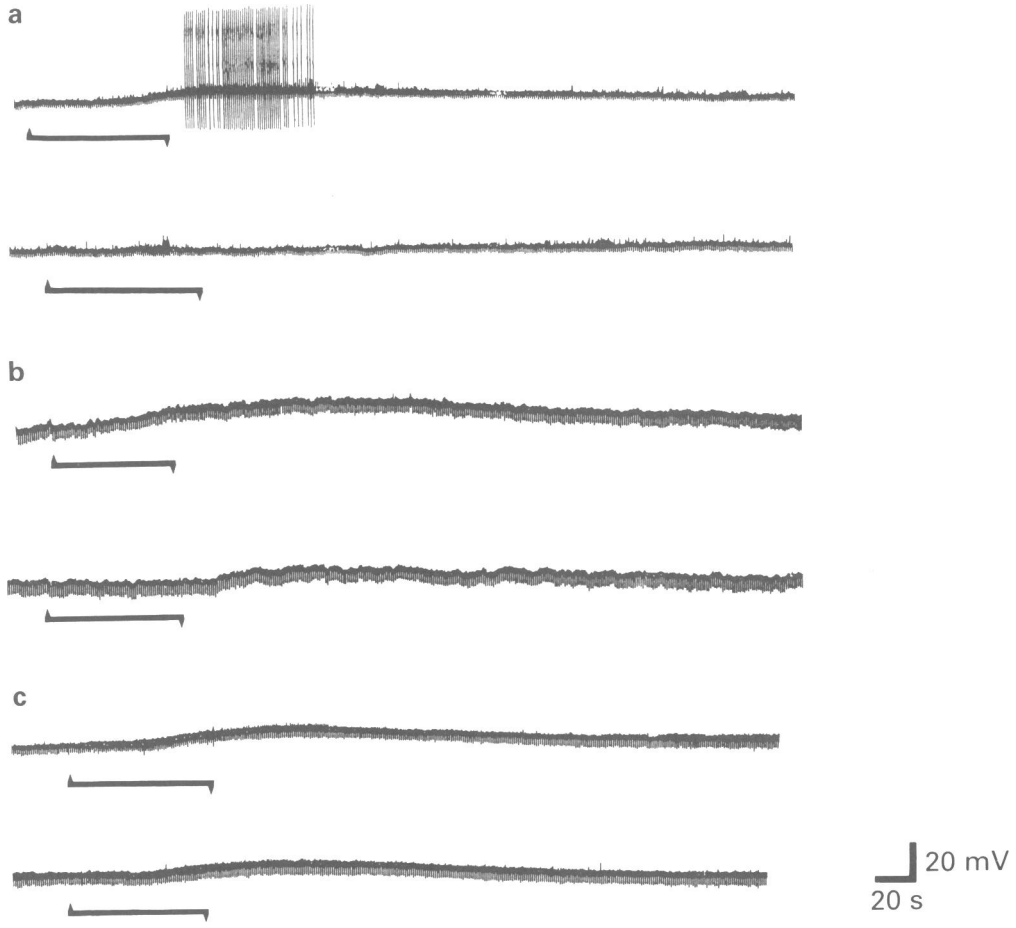

Figure 2 The effects of the α-adrenoceptor antagonists, prazosin (1 μM) and yohimbine (1 μM) and the β-adrenoceptor antagonist, propranolol (10 μM) on the response to 10 μM noradrenaline (NA). The paratracheal neurones were superfused with antagonist for 2 min before superfusion with both antagonist and NA. The open channel of the multiway tap was connected to the reservoir containing NA or NA and antagonist at the point indicated by ▲ and reconnected to Krebs solution at the point indicated by ▼. An artefact is occasionally seen at these points. (a) The effect of NA in the absence (upper panel) and presence (lower panel) of 1 μM prazosin. In the presence of prazosin both the depolarization and the spontaneous firing evoked by NA were abolished. Resting membrane potential − 45 mV, input resistance 57 MΩ. (b) The effect of NA in the absence (upper panel) and presence (lower panel) of 1 μM yohimbine. In the presence of yohimbine the onset of depolarization was delayed. This was probably the consequence of an increased time taken for the NA and yohimbine to reach the bath from the reservoir. Resting membrane potential − 60 mV, input resistance 143 MΩ. (c) The effect of NA in the absence (upper panel) and presence (lower panel) of 10 μM propranolol. Resting membrane potential − 50 mV, input resistance 88 MΩ. The downward deflections are the membrane voltage responses to constant hyperpolarizing current pulses (50 pA), as an indicator of membrane input resistance changes.

Table 1 Effects of adrenoceptor antagonists on the response to 10 μM noradrenaline (NA)

		Amplitude of depolarization (mV)			
	(μM)	*Control (NA)*	*Drug*	*Resting membrane potential (mV)*	(n)
Prazosin	(1)	7.9 ± 0.4	0***	51.5 ± 0.9	8
Yohimbine	(1)	7.5 ± 0.9	6.3 ± 0.7 NS	57.1 ± 3.9	8
Propranolol	(10)	6.8 ± 0.7	6.8 ± 0.7 NS	45.9 ± 1.5	8

***Significant difference $P<0.001$ between responses in the absence and presence of antagonist. NS = no significant difference.

Discussion

The primary aims of these experiments were to determine the response of rat paratracheal neurones to exogenous NA and to detect any NA present in the ganglia.

The findings of the present study showed that NA exerted a powerful and direct effect upon a high proportion (85%) of the parasympathetic intramural neurones of rat trachea. In over half of these neurones the depolarization produced by NA raised the excitability of the cell sufficiently to evoke firing of action potentials. The apparent increase in the input resistance of the cell membrane which accompanied the depolarization in some of the cells suggests a decrease in conductance of the membrane. A similar response has previously been observed in vesical parasympathetic neurones where the depolarization evoked by NA was also mediated via α_1-adrenoceptors (Akasu *et al.*, 1985). In other autonomic ganglia NA has been shown to evoke hyperpolarizations, depolarizations and biphasic responses. Furthermore, in vesical parasympathetic ganglia and enteric ganglia the most frequently observed response to NA is a hyperpolarization (Hirst & Silinksy, 1975; Akasu *et al.*, 1985; North & Surprenant, 1985). In contrast to other parasympathetic ganglia, the rat paratracheal neurones in the present study were consistently depolarized by NA and no paratracheal neurones studied were hyperpolarized by NA.

It has been shown that in both myenteric neurones and parasympathetic ganglia, the hyperpolarization elicited by NA is mediated by α_2-adrenoceptors and the depolarizations are mediated by α_1-adrenoceptors (Morita & North, 1981; Akasu *et al.*, 1985; Schemann, 1991). This is in contrast to sympathetic ganglia where the NA-induced hyperpolarization has been shown to be mediated by α_2-adrenoceptors and the depolarization by β-adrenoceptors (Brown & Dunn, 1983). In the present experiments it was found that the depolarization evoked by NA was reversibly inhibited by prazosin and unaffected by yohimbine and propranolol. Furthermore the depolarization elicited by NA was mimicked by the α_1-adrenoceptor agonist, phenylephrine.

In conclusion, the depolarization of rat paratracheal neurones by NA appears to be mediated by α_1-adrenoceptors. This is consistent with other parasympathetic ganglia where a depolarization to NA is also mediated by α_1-adrenoceptors. It has been determined that rat paratracheal neurones exhibit two extremes of behaviour in response to prolonged intrasomal current injection (Allen & Burnstock, 1990a). However, with respect to their response to NA, they appear to be a homogeneous population, as they were reported to be in response to γ-aminobutyric acid (GABA) (Allen & Burnstock, 1990b).

Given the powerful effect that NA exerted upon rat paratracheal neurones it is important to determine if there is any endogenous NA within the airways. Baluk & Gabella (1989) have shown that although the trachea is sympathetically innervated, the paratracheal ganglia themselves lack a sympathetic innervation. However, they have also demonstrated that the paratracheal neurones express a partial noradrenergic phenotype and are capable of taking up amine precursors and under some circumstances may synthesize NA (Baluk & Gabella, 1989). Nonetheless, the release of NA from these neurones has not yet been reported. If there are no sympathetic nerve pericellular baskets around the ganglia, it is pertinent to ask how NA reaches paratracheal neurones. Other possible sources of NA to be considered which could act upon these neurones are from small intensely fluorescent (SIF) cells and circulating NA. SIF cells have been found to contain catecholamines and peptides (Elfvin *et al.*, 1975; Pakpa *et al.*, 1987) and in the autonomic nervous system SIF cells have been shown to perform both interneuronal and paraneuronal roles (Williams & Jew, 1983). The interneuronal role has been observed in the superior cervical ganglion where concomitant changes in formaldehyde-induced fluorescence of the SIF cells and in slow inhibitory postsynaptic potentials associated with release of catecholamines were induced by stimulation of the preganglionic nerve (Libet & Owman, 1974). Furthermore, they have been located histochemically in the rat trachea within the paratracheal ganglia and associated with blood vessels (Baluk & Gabella, 1989). In the rat, NA is a presumptive SIF cell transmitter (Erankö & Erankö, 1971; Lever *et al.*, 1976; König & Heym, 1978). It is possible that under some conditions the contents of the SIF cells could be released and act locally on the paratracheal neurones or be released into the blood vessels with which they are associated and transported in the blood to act on neurones at some distance from the point of release (paracrine role). Intraganglionic blood vessels have been shown to be present in paratracheal ganglia (Baluk *et al.*, 1985). In the present study the samples containing ganglia were assayed for, and found to contain, NA. There was a significantly greater level of NA in the samples of paratracheal ganglia compared with those of smooth muscle with mucosa ($P<0.05$). If the NA detected is from SIF cells located within the ganglia, it is quite plausible that locally released NA can be of sufficient levels to depolarize the neurones and thereby modulate their excitability. This could have consequences for airway function. Previously, it has been shown that rat paratracheal neurones display a high level of subthreshold spontaneous synaptic activity (Allen & Burnstock, 1990a). High levels of subthreshold synaptic activity have also been observed in cat tracheal ganglia *in vivo*, and it has been suggested that synchronization of multiple inputs are required to elicit action potential discharge in these cells (Mitchell *et al.*, 1987). The decrease in membrane potential elicited by NA in this study would mean that the overall intensity of vagal and/or laryngeal nerve input required to elicit action potential discharge would be decreased by NA acting on α_1-adrenoceptors and raising the excitability of the ganglion cells.

The authors would like to thank D. Blundell for carrying out the assays and Drs J. Lincoln and T.G.J. Allen for advice. The authors would also like to thank Dr E. Price for editorial assistance in preparation of this manuscript. This work was supported by the Medical Research Council.

References

AKASU, T., GALLAGHER, J.P., NAKAMURA, T., SHINNICK-GALLAGHER, P. & YOSHIMURA, M. (1985). Noradrenaline hyperpolarization and depolarization in cat vesical parasympathetic neurones. *J. Physiol.*, **361**, 165–184.

ALLEN, T.G.J. & BURNSTOCK, G. (1990a). A voltage-clamp study of the electrophysiological characteristics of the intramural neurones of the rat trachea. *J. Physiol.*, **423**, 593–614.

ALLEN, T.G.J. & BURNSTOCK, G. (1990b). $GABA_A$ receptor-mediated increase in membrane chloride conductance in rat paratracheal neurones. *Br. J. Pharmacol.*, **100**, 261–268.

ASHE, J.H. & LIBET, B. (1982). Pharmacological properties and monoaminergic mediation of the slow IPSP, in mammalian sympathetic ganglion. *Brain Res.*, **424**, 345–349.

BAKER, D.G., BASBAUM, C.B., HERBERT, D.A. & MITCHELL, R.A. (1983). Transmission in airway ganglia of ferrets: inhibition by norepinephrine. *Neurosci. Lett.*, **41**, 139–143.

BALUK, P., FUJIWARA, T. & MATSUDA, S. (1985). The fine structure of the ganglia of the guinea-pig trachea. *Cell Tiss. Res.*, **239**, 51–60.

BALUK, P. & GABELLA, G. (1989). Tracheal parasympathetic neurones of rat, mouse and guinea pig: partial expression of noradrenergic phenotype and lack of innervation from noradrenergic nerve fibres. *Neurosci. Lett.*, **102**, 191–196.

BROWN, D.A. & DUNN, P.M. (1983). Depolarization of rat isolated superior cervical ganglia mediated by β_2-adrenoceptors. *Br. J. Pharmacol.*, **79**, 429–439.

DE GROAT, W.C. & SAUM, W.R. (1971). Adrenergic inhibition in mammalian parasympathetic ganglia. *Nature New Biol.*, **231**, 188–189.

DE GROAT, W.C. & VOLLE, R.L. (1966). The actions of catecholamines on transmission in the superior cervical ganglia of the cat. *J. Pharmacol. Exp. Ther.*, **154**, 1–13.

ELFVIN, L.G., HOKFELT, T. & GOLDSTEIN, M. (1975). Fluorescence microscopical, immunohistochemical and ultrastructural studies on sympathetic ganglia of the guinea-pig, with special reference to the SIF cells and their catecholamine content. *J. Ultrastruct. Res.*, **51**, 377–396.

ERÄNKO, L. & ERÄNKO, O. (1971). Effect of guanethidine on nerve cells and small intensely fluorescent cells in sympathetic ganglia of new born and adult rats. *Acta Pharmacol. Toxicol.*, **30**, 403–416.

GRIFFITH, S.G., CROWE, R., LINCOLN, J., HAVEN, A.J. & BURNSTOCK, G. (1982). Regional differences in the density of perivascular nerves and varicosities, noradrenaline content and responses to nerve stimulation in the rabbit ear artery. *Blood Vessels*, **19**, 41–52.

HAMBERGER, B. & NORBERG, K.-A. (1965a). Studies on some systems of adrenergic synaptic terminals in the abdominal ganglia of the cat. *Acta Physiol. Scand.*, **65**, 235–242.

HAMBERGER, B. & NORBERG, K.-A. (1965b). Adrenergic synaptic terminals and nerve cells in bladder ganglia of the cat. *Int. J. Neuropharmacol.*, **4**, 41–45.

HIRST, G.D.S. & SILINSKY, E.M. (1975). Some effects of 5-hydroxytryptamine, dopamine and noradrenaline on neurones in the submucous plexus of guinea-pig small intestine. *J. Physiol.*, **251**, 817–832.

JACOBOWITZ, D. (1967). Histochemical studies of the relationship of chromaffin cells and adrenergic nerve fibres to the cardiac ganglia of several species. *J. Pharmacol. Exp. Ther.*, **158**, 227–240.

JACOBOWITZ, D., KENT, K.M., FLEISCH, J.H. & COOPER, T. (1973). Histofluorescent study of catecholamine-containing elements in cholinergic ganglia from the calf and dog lung. *Proc. Soc. Exp. Biol. Med.*, **144**, 464–466.

KÖNIG, R. & HEYM, C. (1978). Immunofluorescence localization of dopamine-β-hydroxylase in small intensely fluorescent cells of the rat superior cervical ganglion. *Neurosci. Lett.*, **10**, 187–191.

LEVER, J.D., SANTER, R.M., LU, K.S. & PRESLEY, R. (1976). Electron probe X-ray microanalysis of small granulated cells in rat sympathetic ganglia after sequential aldehyde and dichromate treatment. *J. Histochem. Cytochem.*, **25**, 275–279.

LIBET, B. & OWMAN, CH. (1974). Concomitant changes in formaldehyde-induced fluorescence of dopamine interneurones and in slow inhibitory post-synaptic potentials of the rabbit superior cervical ganglion, induced by stimulation of the preganglionic nerve or by a muscarinic agent. *J. Physiol.*, **237**, 635–662.

MITCHELL, R.A., HERBERT, D.A., BAKER, D.G. & BASBAUM, C.B. (1987). In vivo activity of tracheal parasympathetic ganglion cells innervating tracheal smooth muscle. *Brain Res.*, **437**, 157–160.

MORITA, K. & NORTH, R.A. (1981). Clonidine activates membrane potassium conductance in myenteric neurones. *Br. J. Pharmacol.*, **74**, 419–428.

MOYER, T.P. & JIANG, N.-S. (1978). Optimized isocratic conditions for analysis of catecholamines by high-performance reversed-phase paired-ion chromatography with amperometric detection. *J. Chromatog.*, **153**, 365–372.

NAKAMURA, T., YOSHIMURA, M., SHINNICK-GALLAGHER, P., GALLAGHER, J.P. & AKASU, T. (1984). α_2 and α_1-adrenoceptors mediate opposing actions on parasympathetic neurones. *Brain Res.*, **323**, 349–353.

NORBERG, K.-A. & SJÖQVIST, F. (1966). New possibilities for adrenergic modulation of ganglionic transmission. *Pharmacol. Rev.*, **18**, 743–751.

NORTH, R.A. & SURPRENANT, A. (1985). Inhibitory synaptic potentials resulting from α_2-adrenoceptor activation in guinea-pig submucous plexus neurones. *J. Physiol.*, **358**, 17–33.

PAKPA, R.E., TRAURIG, H.H. & KLENN, P. (1987). Paracervical ganglia of the female rat: histochemistry and immunohistochemistry of neurones, SIF cells, and nerve terminals. *Am. J. Anat.*, **179**, 243–257.

PHIPPS, R.J., WILLIAMS, I.P., RICHARDSON, P.S., PELL, J., PACK, R.J. & WRIGHT, N. (1982). Sympathetic drugs stimulate the output of secretory glycoproteins from human bronchi in vitro. *Clin. Sci.*, **63**, 23–28.

RICHARDSON, J.B. (1979). Autonomic control of the airways. *Annu. Rev. Respir. Dis.*, **119**, 785–802.

SCHEMANN, M. (1991). Excitatory and inhibitory effects of norepinephrine on myenteric neurons of the guinea-pig gastric corpus. *Pflügers Arch.*, **418**, 575–580.

SUZUKI, T. & VOLLE, R.L. (1979). Nicotinic, muscarinic and adrenergic receptors in a parasympathetic ganglion. *J. Pharmacol. Exp. Ther.*, **211**, 252–256.

TSURUSAKI, M., YOSHIDA, M., AKASU, T. & NAGATSU, I. (1990). α_2-adrenoceptors mediate the inhibition of cholinergic transmission in parasympathetic ganglia of the rabbit urinary bladder. *Synapse*, **5**, 233–240.

WILLIAMS, T.H. & JEW, J. (1983). Monoamine connections in sympathetic ganglia. In *Autonomic Ganglia*. ed. Elfvin, L.-G. pp .235–264. Chichester, New York: John Wiley & Sons.

(Received December 18, 1991
Revised May 18, 1992
Accepted June 8, 1992)

Br. J. Pharmacol. (1992), **107**, 476–480

N^G-hydroxy-L-arginine prevents the haemodynamic effects of nitric oxide synthesis inhibition in the anaesthetized rat

[1] Claire E. Walder, Christoph Thiemermann & John R. Vane

The William Harvey Research Institute, St. Bartholomew's Hospital Medical College, Charterhouse Square, London EC1M 6BQ

1 We have investigated the effects of L-hydroxy-L-arginine (L-HOArg), an intermediate in the biosynthesis of nitric oxide (NO) from L-arginine (L-Arg), on the haemodynamic effects (systemic blood pressure and renal blood flow) of the NO synthesis inhibitor N^G-nitro-L-arginine methyl ester (L-NAME) in the anaesthetized rat.

2 L-Arg or L-HOArg (3 mg kg^{-1} min^{-1}), but not D-arginine (D-Arg) or N^G-hydroxy-D-arginine (D-HOArg), elicited a slight but significant increase in total renal blood flow (RBF) of 11 ± 2% and 11 ± 1%. Since mean arterial blood pressure (MAP) did not change this dose of L-Arg or L-HOArg resulted in a reduced renal vascular resistance (RVR) of the same magnitude.

3 Bolus injections of L-NAME, at 0.3 or 1 mg kg^{-1} i.v., produced a significant fall in RBF of 11 ± 2% and 32 ± 5% and an increase in MAP of 7 ± 3 mmHg and 22 ± 5 mmHg, respectively. Consequently, RVR was elevated by 21 ± 5% and 52 ± 10%.

4 L-Arg or L-HOArg (3 mg kg^{-1} min^{-1}) reduced the L-NAME-induced (0.3 or 1 mg kg^{-1}) falls in RBF and increases in RVR by more than 65%. Neither D-Arg nor D-HOArg (3 mg kg^{-1} min^{-1}) had any significant effect on the changes in RBF or RVR induced by L-NAME.

5 L-Arg or L-HOArg (3 mg kg^{-1} min^{-1}) attenuated the pressor effect of L-NAME (3 mg kg^{-1}) by 73% and 64%, respectively, while neither the D-isomer of arginine nor hydroxyarginine had any effect.

6 These results demonstrate that L-HOArg antagonizes the haemodynamic effects of NO-biosynthesis inhibition *in vivo*, thus supporting the hypothesis that L-HOArg is an intermediate in the formation of NO from L-Arg.

Keywords: Endothelium-derived relaxing factor; L-arginine; D-arginine; N^G-hydroxy-D-arginine; ultrasound flowmeter

Introduction

Endothelium-derived relaxing factor (EDRF) or nitric oxide (NO) (Palmer *et al.*, 1987) is released by the vascular endothelium and contributes to the regulation of the underlying vascular smooth muscle tone. NO is enzymatically synthesized from a terminal guanidino nitrogen of L-arginine (L-Arg) (Palmer *et al.*, 1988) by an NO synthase (NOS). The NOS enzymes, of which there are at least two distinct forms, are NADPH-dependent dioxygenases which possess different co-factor requirements depending on their source. The constitutive, calcium/calmodulin-dependent NOS is predominantly found in endothelial cells (Förstermann *et al.*, 1991) and neuronal cells (Bredt & Snyder, 1990), whereas the inducible, calcium-independent enzyme is largely present in activated macrophages (Marletta *et al.*, 1988), Kupffer cells (Billiar *et al.*, 1989), hepatocytes (Curran *et al.*, 1989) and smooth muscle cells (Busse & Mülsch, 1990).

Until recently, the exact biosynthetic pathways of NO synthesis from L-Arg remained uncertain, although an initial N-oxidation step to generate N^G-hydroxy-L-arginine (L-HOArg) had been postulated (Marletta *et al.*, 1988). It has since been demonstrated that L-HOArg is an intermediate in the biosynthesis of NO from L-Arg by the inducible NOS prepared from activated macrophages (Stuehr *et al.*, 1991) and the constitutive NOS from cultured endothelial cells (Zembowicz *et al.*, 1991).

N^G-monomethyl-L-arginine (L-NMMA), is a competitive inhibitor of the formation of NO by endothelial cells (Palmer *et al.*, 1988). Similarly, N^G-nitro-L-arginine methyl ester (L-NAME) inhibits endothelium-dependent vasodilatation *in vitro* (Moore *et al.*, 1990) as well as NO release from cultured endothelial cells (Hecker *et al.*, 1990; Ishii *et al.*, 1990) and is more potent than L-NMMA. Both inhibitors produce a sustained rise in systemic blood pressure, indicative of inhibition of basal release of NO (Rees *et al.*, 1989; Gardiner *et al.*, 1990; Hecker *et al.*, 1990).

Walder *et al.* (1991) showed that, in addition to causing a rise in systemic blood pressure, L-NMMA and L-NAME produce an L-Arg reversible fall in renal cortical blood flow suggesting a role for endogenous NO formation in the local regulation of renal blood flow. We have now investigated whether L-HOArg prevents the haemodynamic effects of NO-biosynthesis inhibition *in vivo* and have compared its potency to L-Arg.

Methods

Surgical procedure

Male Wistar rats were anaesthetized with Trapanal (120 mg kg^{-1}, i.p.). The trachea was cannulated to facilitate respiration and body temperature was maintained at 37°C by means of a rectal probe connected to a homeothermic blanket (Bioscience, Sheerness, Kent). The right carotid artery was cannulated and connected to a Transamerica type 40-422-0001 pressure transducer for the measurement of mean arterial blood pressure (MAP) and heart rate (HR) on a Grass 7D polygraph (Grass Instruments, Quincy, Mass., U.S.A.). The left jugular vein and right femoral vein were cannulated for the administration of drugs and the left femoral vein for the administration of saline (1.5 ml h^{-1}) to compensate for any fluid loss.

[1] Author for correspondence.

The left kidney was exposed via a mid-line laparotomy and the renal artery was carefully isolated. An ultrasonic flow probe (1RB, internal diameter = 1 mm), embedded in a silicone cuff to provide optimum alignment, was placed around the left renal artery for the measurement of total renal blood flow (RBF) using a Transonic T206 Small Animal Flowmeter (Transonic Systems Inc., New York, U.S.A.). A small amount of acoustical couplant (100 mg Nalco 1181, mixed with 10 ml distilled water; Nalco Chemical Co., IL., U.S.A.) was deposited in the probe's acoustic window adjacent to the artery, in order to replace all air. This flowmeter system uses an ultrasonic transit-time principle, which provides a continuous real-time measure of volume flow, in ml min^{-1}. Calibration was predetermined by the manufacturer and the zero flow value validated *in situ* in the rat at the end of the experiment. Renal vascular resistance (RVR) was calculated by dividing MAP by RBF.

Experimental design

After surgery, all animals were allowed to stabilize for 45 min before being treated with indomethacin (5 mg kg^{-1}, i.v.), to eliminate the involvement of prostanoids. Thirty minutes later, animals received infusions (0.03 ml min^{-1}) into the left jugular vein of either vehicle (saline; $n = 7$), L-Arg (1 or 3 mg kg^{-1} min^{-1}; $n = 6$), L-HOArg (1 or 3 mg kg^{-1} min^{-1}; $n = 6$), D-arginine (D-Arg; 3 mg kg^{-1} min^{-1}; $n = 4$) or N^G-hydroxy-D-arginine (D-HOArg; 3 mg kg^{-1} min^{-1}; $n = 2$) for 30 min by use of a syringe pump (Perfuser VI, Braun, Melsunge, Germany). At 10 and 20 min after the infusion started, bolus injections of L-NAME, 0.3 and 1 mg kg^{-1}, were administered into the right femoral vein.

Materials

All drugs were dissolved in 0.9% w/v saline with the exception of indomethacin, which was prepared as a 5 mg kg^{-1} solution in 5% w/v sodium bicarbonate. Sodium thiopentone (Trapanal) was obtained from BYK Gulden (Konstanz, Germany). L-Arg hydrochloride, D-Arg hydrochloride, L-NAME and indomethacin were purchased from Sigma Chemical Co. (Poole, Dorset). L-HOArg and D-HOArg were synthesized by Dr Paul Feldman (Medicinal Chemistry, Glaxo Inc., RTP, U.S.A.).

Statistical analysis

All values in the figures and text are expressed as mean ± s.e.mean of n observations. Statistical comparisons of differences within the same animal were made by Student's t test for paired determinations; comparisons of differences between groups of animals were made by Student's t test for unpaired determinations. A P value of less than 0.05 was considered significant.

Results

Resting values ($n = 37$) were 9.2 ± 0.4 ml min^{-1} for RBF, 12.5 ± 0.5 mmHg ml^{-1} min for RVR, 109 ± 2 mmHg for MAP and 324 ± 1 beats min^{-1} for HR. After indomethacin these values were 9.6 ± 0.4 ml min^{-1} for RBF, 11.6 ± 0.5 mmHg ml^{-1} min for RVR, 106 ± 2 mmHg for MAP and 325 ± 7 beats min^{-1} for HR.

Infusions of L-Arg (3 mg kg^{-1} min^{-1}) or L-HOArg (3 mg kg^{-1} min^{-1}) alone, but none of the other treatments, elicited a slight, but significant increase in RBF of 11 ± 2% or 11 ± 1%, respectively. In contrast, there was no significant effect on MAP or HR during the 10 min infusion ($P > 0.05$; data not shown). Consequently, RVR was reduced by 11 ± 2% or 11 ± 1%, respectively (Figure 1). D-HOArg produced a non-significant increase in MAP of 5 mmHg during this infusion period. However, due to short supply of D-HOArg, only 2 experiments were performed in this group.

Bolus injections of L-NAME (1 of 3 mg kg^{-1}) produced a slowly developing, dose-dependent, fall in RBF which, within 10 min, reached a maximum of 11 ± 2% and 32 ± 5% ($P < 0.05$) (Figure 2). The falls in RBF induced by L-NAME were associated with a dose-dependent increase in MAP of 7 ± 3 mmHg and 22 ± 5 mmHg ($P < 0.05$), developing over a similar time course (Figure 4), and a fall in HR of 11 ± 3 beats min^{-1} and 28 ± 9 beats min^{-1} ($P < 0.05$). As a result of the falls in RBF and increases in MAP, NO_2Arg 1 and 3 mg kg^{-1} substantially elevated RVR by 21 ± 5% and 52 ± 10%, respectively (Figure 3).

Pretreatment with L-Arg at 3 mg kg^{-1} min^{-1}, but not at 1 mg kg^{-1} min^{-1}, significantly ameliorated the L-NAME-induced falls in RBF (Figure 2) and rises in RVR (Figure 3). The effects of L-HOArg at the highest dose (3 mg kg^{-1} min^{-1}) were similar to those of L-Arg, producing a

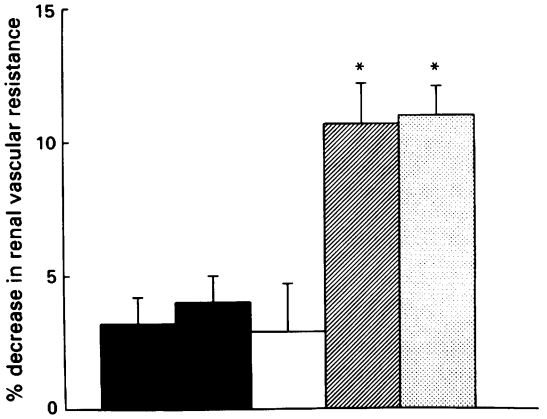

Figure 1 Infusions of L-arginine (L-Arg) or N^G-hydroxy-L-arginine (L-HOArg) produce similar decreases in renal vascular resistance (RVR) in the anaesthetized rat. When compared to saline (control; ■; $n = 7$), infusions of L-Arg (3 mg kg^{-1} min^{-1}; ▨; $n = 6$) or L-HOArg (3 mg kg^{-1} min^{-1}; ▩; $n = 6$) produced significant decreases in RVR which were of equivalent magnitude. Neither the lower dose of L-Arg (1 mg kg^{-1} min^{-1}; ■; $n = 6$) nor L-HOArg (1 mg kg^{-1} min^{-1}; □; $n = 6$) had any significant effect on RVR, suggesting their comparable potency. Data are expressed as mean with s.e.mean shown by vertical bars.
*$P < 0.05$ when compared to control.

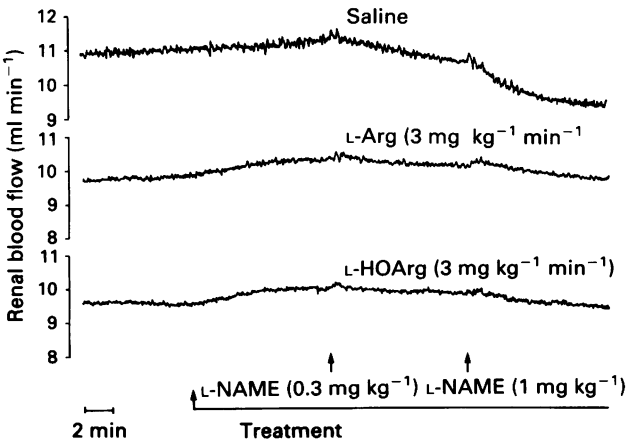

Figure 2 N^G-nitro-L-arginine methyl ester (L-NAME)-induced falls in renal blood flow (RBF) in the anaesthetized rat are attenuated by L-arginine (L-Arg) or N^G-hydroxy-L-arginine (L-HOArg). Bolus injections of L-NAME at 0.3 and 1 mg kg^{-1}, produced a fall in total renal blood flow (RBF) of 11% and 32% in the presence of saline (upper trace). Both L-Arg (middle trace) and L-HOArg (lower trace) at 3 mg kg^{-1} min^{-1} produced an increase in RBF (11%) and attenuated the L-NAME-induced falls in RBF.

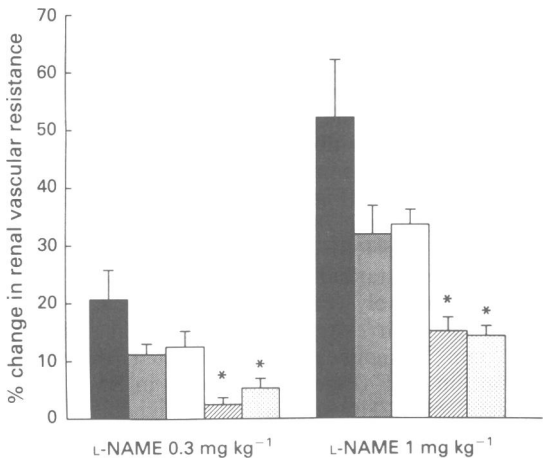

Figure 3 N^G-nitro-L-arginine methyl ester (L-NAME)-induced increases in renal vascular resistance (RVR) in the anaesthetized rat are attenuated by L-arginine (L-Arg) or N^G-hydroxy-L-arginine (L-HOArg). L-NAME (0.3 or 1 mg kg^{-1}) (control; ■; $n = 7$) produced a dose-dependent increase in RVR. Neither L-Arg (■; $n = 6$) nor L-HOArg (□; $n = 6$), at 1 mg kg^{-1} min^{-1}, had any significant effect on the L-NAME-induced elevations in RVR. However, both L-Arg (▨; $n = 6$) and L-HOArg (▩; $n = 6$), at 3 mg kg^{-1} min^{-1}, significantly attentuated the L-NAME-induced increases in RVR to a similar extent. Data are expressed as mean with s.e.mean shown by vertical bars.
*$P < 0.05$ when compared to control.

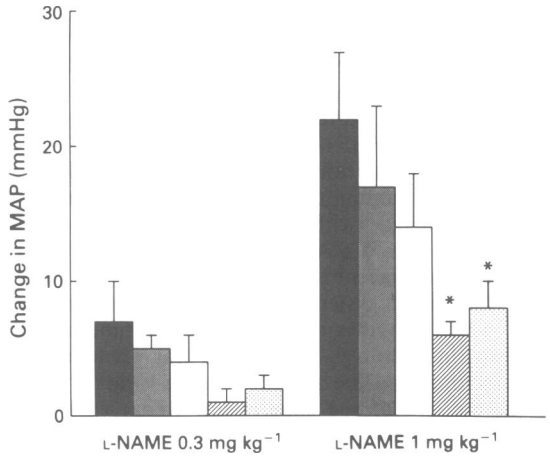

Figure 4 N^G-nitro-L-arginine methyl ester (L-NAME)-induced increases in mean arterial blood pressure (MAP) in the anaesthetized rat are attenuated by L-arginine (L-Arg) or N^G-hydroxy-L-arginine (L-HOArg). L-NAME (0.3 or 1 mg kg^{-1}) (control; ■; $n = 7$) produced a dose-dependent increase in MAP. L-Arg (3 mg kg^{-1} min^{-1}; ▨; $n = 6$) or L-HOArg (3 mg kg^{-1} min^{-1}; ▩; $n = 6$) significantly reduced the pressor response induced by the highest concentration of L-NAME (1 mg kg^{-1}), but not the lowest concentration of L-NAME (0.3 mg kg^{-1}). Neither, L-Arg (1 mg kg^{-1} min^{-1}; ■; $n = 6$) nor L-HOArg (1 mg kg^{-1} min^{-1}; □; $n = 6$), however, had any significant effect on the rise in MAP induced by either dose of L-NAME (0.3 or 1 mg kg^{-1}). Data are expressed as mean ± s.e.mean.
*$P < 0.05$ when compared to control.

significant attenuation of the L-NAME-induced falls in RBF (Figure 2) and elevations in RVR (Figure 3). The lower dose of L-HOArg (1 mg kg^{-1} min^{-1}) had no significant effect on RVR (Figure 3). In contrast, neither the D-isomer of arginine nor hydroxyarginine (3 mg kg^{-1} min^{-1}) had any significant effect on the increases in RVR induced by L-NAME at either concentration (16 ± 2% or 16 ± 2% for L-NAME 0.3 mg kg^{-1} and 35 ± 6% or 36 ± 1% for L-NAME 1 mg kg^{-1}; $P > 0.05$).

The pressor effects of L-NAME (1 mg kg^{-1}) were, likewise, significantly attenuated by pretreatment with L-Arg (3 mg kg^{-1} min^{-1}) or L-HOArg (3 mg kg^{-1} min^{-1}) (Figure 4). The corresponding doses of the D-isomer of arginine or hydroxyarginine had no significant effect on the pressor response to this dose of L-NAME (19 ± 2 mmHg or 24 ± 1 mmHg; $P > 0.05$). Although the same trends were seen with the pressor response to L-NAME at 0.3 mg kg^{-1}, the effects were not significant (Figure 4 and data not shown for D-Arg and D-HOArg 3 mg kg^{-1} min^{-1}; $P > 0.05$).

Discussion

The results from the present study demonstrate that L-HOArg attenuates the haemodynamic effects of the NO-synthesis inhibitor, L-NAME, in the anaesthetized rat. This effect resembles the actions of L-Arg, the precursor of NO, thus supporting the hypothesis that L-HOArg is an intermediate in this biosynthesis pathway.

L-Arg and L-HOArg (at 3 mg kg^{-1} min^{-1}), but not their respective D-isomers, cause an increase in renal blood flow in their own right. This finding was not entirely surprising for the following reasons. The single most important source of arginine in the body is the kidney (Featherstone *et al.*, 1973; Barbul, 1986) increasing the likelihood that L-Arg may contribute to local regulatory mechanisms in this organ. In addition, a variety of different amino acids (Epstein *et al.*, 1982; Brezis *et al.*, 1984) including L-Arg (Bhardwaj & Moore, 1989) cause an increase in renal blood flow in the isolated perfused kidney of the rat. However, the hypothesis (Bhardwaj & Moore, 1989; Walder *et al.*, 1991) that this L-Arg-induced increase in renal perfusion may be mediated by an enhanced formation of NO is difficult to test. Furthermore, L-Arg depletion caused approximately 30% reductions in renal perfusion, glomerular filtration rate and urine flow rate in the isolated perfused kidney of the rat (Radermacher *et al.*, 1991) indicating that the role of the L-Arg/NO pathway in the regulation of renal blood flow is reflected in renal function. The fact that L-Arg or L-HOArg produced a renal vasodilatation without reducing systemic blood pressure in the present study supports the above mentioned evidence that the L-Arg/NO pathway is important in the regulation of renal vascular resistance. It may be argued that the potential falls in MAP produced by either L-Arg or L-HOArg are compensated for by an increase in HR (baroreceptor reflex). Although we cannot exclude this possibility, it is evident, at least from the data presented in this study, that the protocols used for either L-Arg or L-HOArg did not result in a significant increase in HR.

The pressor effects of L-NAME and L-NMMA are associated with falls in both renal cortical blood flow in the anaesthetized rat (Walder *et al.*, 1991) and total renal blood flow in the conscious rat (Gardiner *et al.*, 1990), further pointing to a role for NO in the local regulation of renal blood flow. Our results support this evidence by showing similar dose-dependent falls in total renal blood flow induced by L-NAME, when measured by an ultrasound volume flowmeter. Moreover, intrarenal infusion of L-NMMA for 3 h is associated with an 11% decrease in renal plasma flow and a 14% increase in RVR in the conscious chronically instrumented dog. Interestingly, this infusion protocol of L-NMMA does not result in an increase in MAP, indicating that the renal vasculature is extremely sensitive to inhibition of endogenous NO formation (Granger *et al.*, 1992).

The effects of both L-NMMA and L-NAME are antagonized by L-Arg, an endogenous substrate for the biosynthesis of NO (Palmer *et al.*, 1988). However, L-NAME is much more difficult to reverse than L-NMMA requiring at least 100 fold excess of the substrate (Walder *et al.*, 1991). This is consistent with the finding that inhibition of brain

NO synthesis *in vitro* and *in vivo* by L-NAME appears to be irreversible, suggesting that L-NAME forms a strong covalent link with the enzyme (Dwyer *et al.*, 1991). For this reason we investigated whether L-Arg could prevent the effects of L-NAME rather than reverse them. We have shown that an infusion of L-Arg significantly attenuates the L-NAME induced pressor responses stereospecifically, for the same concentration of the D-isomer was without effect.

L-Arg has little or no vasorelaxant activity on freshly mounted isolated vascular strips (Gold *et al.*, 1989), nor does it potentiate the stimulated release of NO from cultured endothelial cells. In contrast, low concentrations of L-HOArg ($\geqslant 1\ \mu M$) significantly potentiate the stimulated release of NO from endothelial cells, suggesting that the constitutive NOS has a lower K_m or higher V_{max} for L-HOArg than L-Arg (Zembowicz *et al.*, 1991) which is consistent with the hypothesis that L-HOArg is an intermediate in the biosynthesis of NO from L-Arg by both the inducible and constitutive NOS (Stuehr *et al.*, 1991; Zembowicz *et al.*, 1991). Furthermore, Wallace *et al.* (1991) demonstrated that L-HOArg is able to elicit slight vasorelaxation in bovine intrapulmonary artery with greater potency than L-Arg. Thus, we expected that the effects of L-HOArg would be more potent than L-Arg *in vivo*. However, in the present experiments the haemodynamic responses to L-NAME were attenuated by L-HOArg and L-Arg to a similar extent. Furthermore, the slight increase in RBF (11%) achieved by L-HOArg alone was also of a similar magnitude to that of L-Arg. Although these results support the hypothesis that L-HOArg (even when administered intravenously) can be utilized as a substrate for the constitutive NOS present in endothelial cells, they fail to demonstrate a greater potency of L-HOArg (when compared to L-Arg) in attenuating the inhibition of NOS *in vivo*. The explanation of the equal potencies *in vivo* is at present unclear, and cannot be accounted for by a difference in uptake, since this is similar for both L-HOArg and L-Arg (Zembowicz *et al.*, 1991).

In conclusion, the present study demonstrates that L-HOArg attenuates the haemodynamic effects of NO synthesis inhibition in the anaesthetized rat, suggesting the L-HOArg is also a substrate of the constitutive NOS in endothelial cells. However, under normal physiological conditions, both L-Arg and L-HOArg produce only minor changes in organ blood flow (as demonstrated in the present study). An impairment of endothelium-dependent relaxation has been demonstrated in patients with hypercholesterolaemia (Drexler *et al.*, 1991), essential hypertension (Panza *et al.*, 1988; Linder *et al.*, 1990) and myocardial ischaemia (Drexler *et al.*, 1992). Interestingly, in patients with hypercholesterolaemia, a normal function of the coronary endothelium can be restored by short-term administration of L-Arg (Drexler *et al.*, 1991). Hence, it is intriguing to speculate that either L-Arg or L-HOArg may provide a novel therapeutic approach for the treatment of endothelial dysfunction associated with the above mentioned cardiovascular disorders.

The authors would like to thank Dr P. Feldman for the generous supply of L-HOArg and D-HOArg. This work was supported by a grant from Glaxo Group Research Ltd.

References

BARBUL, A. (1986). Arginine: biochemistry, physiology, and therapeutic implications. *J. Parenter. Enteral. Nutr.* **10,** 227–238.

BHARDWAJ, R. & MOORE, P.K. (1989). The effect of arginine and nitric oxide on resistance blood vessels of the perfused rat kidney. *Br. J. Pharmacol.*, **97,** 739–744.

BILLIAR, T.R., CURRAN, R.D., STUEHR, D.J., WEST, M.A., BENTZ, B.G. & SIMMONS, R.L. (1989). An L-arginine dependent mechanism mediates Kupffer cell inhibition of hepatocyte protein synthesis *in vitro*. *J. Exp. Med.*, **169,** 1467–1472.

BREDT, D.S. & SNYDER, S.H. (1990). Isolation of nitric oxide synthetase, a calmodulin-requiring enzyme. *Proc. Natl. Acad. Sci. U.S.A.*, **87,** 682–685.

BREZIS, M., SILVA, P. & EPSTEIN, F.H. (1984). Amino acids induce renal vasodilatation in isolated perfused kidney: coupling to oxidative metabolism. *Am. J. Physiol.*, **247,** H999–H1004.

BUSSE, R. & MULSCH, A. (1990). Induction of nitric oxide synthase by cytokines in vascular smooth muscle cells. *FEBS Lett.*, **275,** 87–90.

CURRAN, R.D., BILLIAR, T.R., STUEHR, D.J., HOFMANN, K. & SIMMONS, R.L. (1989). Hepatocytes produce nitrogen oxides from L-arginine in response to inflammatory products of Kupffer cells. *J. Exp. Med.*, **170,** 1769–1774.

DREXLER, H., LU, W., CHRISTES, A. & RIEDE, U. (1992). Impaired basal release of nitric oxide in the coronary circulation of post-infarction reactive cardiac hypertrophy. *Circulation*, (in press).

DREXLER, H., ZEIHER, A.M., MEINZER, K. & JUST, H. (1991). Correction of endothelial dysfunction in coronary microcirculation of hypercholesterolaemic patients by L-arginine. *Lancet*, **338,** 1546–1550.

DWYER, M.A., BREDT, D.S. & SNYDER, S.H. (1991). Nitric oxide synthase: irreversible inhibition by L-N^G-nitroarginine in brain *in vitro* and *in vivo*. *Biochem. Biophys. Res. Commun.*, **176,** 1136–1141.

EPSTEIN, F.H., BROSNAN, J.T., TANGE, J.D. & ROSS, B.D. (1982). Improved function with amino acids in the isolated perfused kidney. *Am. J. Physiol.*, **243,** F284–F292.

FEATHERSTON, W.R., ROGERS, Q.R. & FREEDLAND, R.A. (1973). Relative importance of kidney and liver in synthesis of arginine by the rat. *Am. J. Physiol.*, **224,** 127–129.

FORSTERMANN, U., POLLOCK, J.S., SCHMIDT, H.H.H.W., HELLER, M. & MURAD, F. (1991). Calmodulin-dependent endothelium-derived relaxing factor/nitric oxide synthase activity is present in the particulate and cytosolic fractions of bovine aortic endothelial cells. *Proc. Natl. Acad. Sci. U.S.A.*, **88,** 1788–1792.

GARDINER, S.M., COMPTON, A.M., KEMP, P.A. & BENNETT, T. (1990). Regional and cardiac haemodynamic effects of N^G-nitro-L-arginine methyl ester in conscious, Long Evens rats. *Br. J. Pharmacol.*, **101,** 625–631.

GOLD, M.E., BUSH, P.A. & IGNARRO, L.J. (1989). Depletion of L-arginine causes reversible tolerance to endothelium-dependent relaxation. *Biochem. Biophys. Res. Commun.*, **164,** 714–721.

GRANGER, J.P., SALAZAR, F.J., ALBEROLA, A. & NAKUMURA, T. (1992). Control of renal hemodynamics and sodium excretion during intrarenal blockade of endothelium-derived nitric oxide EDNO in conscious dogs. *J. Vasc. Res.*, **29,** 137.

HECKER, M., HARRIS, H., MITCHELL, J.A., KATSURA, M., THIEMERMANN, C. & VANE, J.R. (1990). Endothelial cells metabolize N^G-monomethyl-L-arginine to L-citrulline and subsequently to L-arginine. *Biochem. Biophys. Res. Commun.*, **167,** 1037–1043.

ISHII, K., CHANG, B., KERWIN, J.F.Jr., HUANG, Z.J. & MURAD, F. (1990). N_ω-nitro-L-arginine: a potent inhibitor of endothelium-derived relaxing factor formation. *Eur. J. Pharmacol.*, **176,** 219–223.

LINDER, L., KIOWSKI, W., BUHLER, F.R. & LUSCHER, T.F. (1990). Indirect evidence for release of endothelium-derived relaxing factor in human forearm circulation *in vivo*: blunted response in essential hypertension. *Circulation*, **81,** 1762–1767.

MARLETTA, M.A., YOON, P.S., IYENGAR, R., LEAF, C.D. & WISHNOK, J.S. (1988). Macrophage oxidation of L-arginine to nitrite and nitrate: nitric oxide is an intermediate. *Biochemistry*, **27,** 8706–8711.

MOORE, P.K., AL-SWAYEH, O.A., CHONG, N.S.W., EVANS, R.A. & GIBSON, A. (1990). L-N^G-nitro arginine (L-NOARG), a novel, L-arginine-reversible inhibitor of endothelium-dependent vasodilatation *in vitro*. *Br. J. Pharmacol.*, **99,** 408–412.

PALMER, R.M.J., ASHTON, D.S. & MONCADA, S. (1988). Vascular endothelial cells synthesize nitric oxide from L-arginine. *Nature*, **333,** 664–666.

PALMER, R.M.J., FERRIDGE, A.G. & MONCADA, S. (1987). Nitric oxide release accounts for the biological activity of endothelium derived-relaxing factor. *Nature*, **327,** 524–526.

PANZA, J.A., QUYYUMI, A.A. & EPSTEIN, S.E. (1988). Impaired endothelium-dependent vascular relaxation in hypertensive patients. *Circulation*, **78,** (Suppl. II), 473.

RADERMACHER, J., KLANKE, B., KASTNER, S., HAAKE, G., SCHUREK, H.-J., STOLTE, H.F. & FROLICH, J.C. (1991). Effect of arginine depletion on glomerular and tubular kidney function: studies in isolated perfused rat kidneys. *Am. J. Physiol.*, **261,** F779–F786.

REES, D.D., PALMER, R.M.J. & MONCADA, S. (1989). Role of endothelium-derived nitric oxide in the regulation of blood pressure. *Proc. Natl. Acad. Sci. U.S.A.*, **86,** 3375–3378.

STUEHR, D.J., KWON, N.S., NATHAN, C.F., GRIFFITH, O.W., FELDMAN, P.L. & WISEMAN, J. (1991). N_{ω}-hydroxy-L-arginine is an intermediate in the biosynthesis of nitric oxide from L-arginine. *J. Biol. Chem.*, **266,** 6259–6263.

WALDER, C.E., THIEMERMANN, C. & VANE, J.R. (1991). The involvement of endothelium-derived relaxing factor in the regulation of renal cortical blood flow in the rat. *Br. J. Pharmacol.*, **102,** 967–973.

WALLACE, G.C., GULATI, P. & FUKUTO, J.M. (1991). N_{ω}hydroxy-L-arginine: a novel arginine analog capable of causing vasorelaxation in bovine intrapulmonary artery. *Biochem. Biophys. Res. Commun.*, **176,** 528–534.

ZEMBOWICZ, A., HECKER, M., MACARTHUR, H., SESSA, W.C. & VANE, J.R. (1991). Nitric oxide and another potent vasodilator are formed from N^{G}-hydroxy-L-arginine by cultured endothelial cells. *Proc. Natl. Acad. Sci. U.S.A.*, **88,** 11172–11176.

(Received March 6, 1992
Revised May 2, 1992
Accepted June 9, 1992)

Br. J. Pharmacol. (1992), **107**, 481–487

Pharmacological modulation of inhaled sodium metabisulphite-induced airway microvascular leakage and bronchoconstriction in the guinea-pig

Tatsuo Sakamoto, Wayne Elwood, Peter J. Barnes & [1]K. Fan Chung

Department of Thoracic Medicine, National Heart and Lung Institute, Royal Brompton Hospital, London SW3 6LY

1 We have investigated the effects of chlorpheniramine, atropine and capsaicin pretreatment on inhaled sodium metabisulphite (MBS)-induced airway microvascular leakage and bronchoconstriction in anaesthetized guinea-pigs in order to clarify the mechanisms involved in these responses. The effects of frusemide and nedocromil sodium were also examined.

2 Lung resistance (R_L) was measured for 6 min after inhalation of MBS (20, 40, 80 and 200 mM; 30 breaths), followed by measurement of extravasation of Evans blue dye into airway tissues, used as an index of airway microvascular leakage. MBS caused an increase in R_L and leakage of dye at all airway levels in a dose-dependent manner.

3 Chlorpheniramine (10 mg kg^{-1}, i.v.), atropine (1 mg kg^{-1}, i.v.), their combination or inhaled nedocromil sodium (10 mg ml^{-1}, 7 min) had no effect against the airway microvascular leakage induced by 80 mM MBS (30 breaths). Capsaicin pretreatment (50 mg kg^{-1}, s.c.) caused a significant decrease in the leakage of dye in the main bronchi and inhaled frusemide (10 mg ml^{-1}, 7 min) also in the main bronchi and proximal intrapulmonary airway.

4 Chlorpheniramine, atropine, their combination, capsaicin pretreatment and frusemide, but not nedocromil sodium, inhibited significantly the peak R_L induced by 80 mM MBS (30 breaths) by approximately 50%.

5 We conclude that a cholinergic reflex and neuropeptides released from sensory nerve endings may participate in the mechanisms of MBS-induced airway responses. Frusemide but not nedocromil sodium may have an inhibitory effect on these neural mechanisms. The inhibitory effect of nedocromil sodium against lower doses of MBS is not excluded.

Keywords: Bronchoconstriction; capsaicin; cholinergic reflex; frusemide; histamine; microvascular permeability; nedocromil sodium; sodium metabisulphite; tachykinin

Introduction

Sodium metabisulphite (MBS) is used as a food preservative and an antioxidant, and can induce bronchoconstriction when inhaled by patients with asthma and by atopic non-asthmatic subjects (Seale *et al.*, 1988; Nichol *et al.*, 1989; Dixon & Ind, 1990). The mechanisms by which MBS induces bronchoconstriction are not clear. There is circumstantial evidence that sulphur dioxide gas released from MBS solution may be the active ingredient causing bronchoconstriction (Fine *et al.*, 1987; Hein *et al.*, 1991). Both sulphur dioxide- and MBS-induced bronchoconstriction are inhibited by nedocromil sodium (Dixon *et al.*, 1987; Dixon & Ind, 1990) and sodium cromoglycate (Snashall & Baldwin, 1982; Tan *et al.*, 1982; Myers *et al.*, 1986; Dixon & Ind, 1990), although these observations do not indicate the mechanisms involved. MBS-induced bronchoconstriction in patients with asthma is inhibited to a lesser extent by muscarinic receptor antagonists (Dixon & Ind, 1988; Seale *et al.*, 1988; Nichol *et al.*, 1989) and is not inhibited by a histamine H_1-receptor antagonist (Dixon & Ind, 1988). These studies suggest that MBS-induced airway responses may involve mechanisms other than a cholinergic reflex or histamine release.

In order to investigate further the potential mechanisms of MBS-induced bronchoconstriction, we have studied the effect of MBS aerosol in anaesthetized guinea-pigs. We have determined whether MBS can, in addition to causing bronchoconstriction (Lötvall *et al.*, 1990), induce plasma exudation in the airway. We have examined the contribution of a cholinergic reflex and of histamine release. In addition, we have tested the hypothesis that part of the effect of MBS in the airway of the guinea-pig is mediated by non-cholinergic bronchoconstrictor pathways through the release of endogenous tachykinins (Lundberg & Saria, 1987; Djokic *et al.*, 1989; Lötvall *et al.*, 1991) by studying the effect of tachykinin depletion with capsaicin pretreatment (Lundberg *et al.*, 1983; Buck & Burks, 1986). Nedocromil sodium, a drug used for the prophylaxis of asthma, and frusemide, a loop diuretic, have been shown to inhibit airway smooth muscle contraction induced by stimulation of non-cholinergic nerves in the guinea-pig *in vitro* (Elwood *et al.*, 1991; Verleden *et al.*, 1991). We studied the effect of these agents on MBS-induced airway effects in the guinea-pig *in vivo*.

Methods

Animal preparation

Female Dunkin-Hartley guinea-pigs were anaesthetized with an initial dose of urethane (1.5 g kg^{-1}) injected intraperitoneally. Additional urethane (1.0–1.5 g kg^{-1}) was given 30 min later to achieve an appropriate level of anaesthesia as evidenced by a disappearance of corneal reflex and withdrawal response to paw pinching. This level of anaesthesia was maintained throughout the experiment until the time when suxamethonium was administered. Body temperature (rectal) was maintained at about 36°C by placing the animals

[1] Author for correspondence.

under a lamp. A tracheal cannula (8 mm length and 2.7 mm internal diameter) was inserted into the lumen of the cervical trachea through a tracheostomy, and secured with a suture. A polyethylene catheter was inserted into the left carotid artery to monitor systemic mean blood pressure (BP) and heart rate with a pressure transducer (PDCR 75 S/N 1560, Druck Ltd., U.K.). The right external jugular vein was cannulated for the administration of intravenous drugs or solutions.

Measurements of airway function

Animals were placed in a supine position with an intratracheal cannula connected to a constant volume mechanical ventilator (Model 50–1718, Harvard Apparatus Ltd., Edenbridge, U.K.), and then given a single injection of suxamethonium (1–1.5 mg kg^{-1}, i.v.) to prevent interference by spontaneous respiration.

A tidal volume of 10 ml kg^{-1} and a frequency of 60 strokes min^{-1} were used. Lung resistance (R_L) and transpulmonary pressure were measured as an index of airway function and monitored throughout the experiments. Transpulmonary pressure was measured with a pressure transducer (Model FCO 40; ± 1000 mmH_2O; Furness Controls Ltd., Bexhill, U.K.) with one side attached to a catheter inserted into the right pleural cavity and the other side attached to a catheter connected to a side port of the intratracheal cannula. The ventilatory circuit had a volume of 20 ml. Airflow was measured with a pneumotachograph (Model F1L; Mercury Electronics Ltd., Glasgow, U.K.) connected to a transducer (Model FCO 40; ± 20 mmH_2O; Furness Controls Ltd.). The signals from the transducers were digitized with a 12-bit analog-digital board (NB-MIO-016; National Instruments, Austin, TX, U.S.A.) connected to a Macintosh II computer (Apple Computer Inc., Cupertino, CA, U.S.A.) and analyzed with software (LabView; National Instruments), which has programmed to calculate instantaneously R_L by the method of von Neergaard & Wirz (1927).

Measurement of microvascular leakage

Vascular permeability was quantified by the extravasation of Evans blue dye, which has been shown to correlate well with the extravasation of radiolabelled albumin in guinea-pig airways (Rogers *et al.*, 1989). Six min after inhalation of MBS or its vehicle, the thoracic cavity was opened, and a cannula was inserted into the aorta through a ventriculotomy. Perfusion was performed with 100–150 ml 0.9% w/v sodium chloride in water (0.9% saline) at a pressure of 100–120 mmHg in order to remove intravascular dye from the systemic circulation. Blood and perfused liquid were expelled through incisions in the right and left atria. Subsequently, the right ventricle was opened, and the pulmonary circulation was perfused with 30 ml of 0.9% saline. The lungs were then removed, and the connective tissues, vasculature and parenchyma were gently scraped off with a blunt scalpel until bronchial tissue was left. The tracheal portion from 6 to 13 mm distal to a tip of the tracheal cannula (TR) was collected and the main bronchi (MB) was sectioned off at a point 3 mm distal to the carina. The rest of the bronchial tract was divided into two components, arbitrarily termed 'proximal intrapulmonary airway (PIPA, the proximal 5–7 mm portion)' and 'distal intrapulmonary airway (DIPA, the remaining distal portion)'. The tissues were blotted dry, and then weighed. Evans blue dye was extracted in 2 ml of formamide at 40°C for 24 h, and measured in a spectrophotometer (Model 8480, Philips, Cambridge, U.K.) at 620 nm. The tissue content of Evans blue dye was calculated by interpolation on a standard curve of dye concentrations in the range of 0.5–10 μg ml^{-1} and expressed as ng of dye mg^{-1} of wet tissue.

Protocol

Sodium metabisulphite challenge MBS dissolved in 0.9% saline was stored at −20°C at a concentration of 1 M, and MBS solution (diluted in 0.9% saline) was prepared 24 h before experimentation. Three milliliters of the solution was then kept in a closed, air-tight container with a total capacity of 8 ml at room temperature. The container was shaken 5 times before the MBS solution was placed in an ultrasonic nebulizer (PulmoSonic Model 2511: Devilbiss Co., Somerset, PA, U.S.A.), from which MBS aerosol was generated and was administered to the airways for 30 breaths through a separate ventilatory system that bypassed the pneumotachograph. An additional five breaths was given through the nebulizer circuit to clear the system of aerosol. The volume of the circuit distal to the nebulizer was 20 ml. The output from the nebulizer at the port of the tracheal cannula, measured with airflow of 0.3 l min^{-1} (3 ml of 0.9% saline in the nebulizer), was 70 ± 5 μl min^{-1}. The mean particle size was 3.8 μm, with a geometric standard deviation of 1.3, measured with a laser droplet and particle analyzer (Model 2600C; Malvern Instruments, Malvern, U.K.).

Effect of different doses of sodium metabisulphite Animals weighing 440–500 g were divided into five groups ($n = 5$) in order to study the effects of the different concentrations of MBS (20, 40, 80 and 200 mM, 30 breaths) on R_L and dye leakage in the airway, and were compared to those of the diluent for MBS. Ten min after connection to the ventilator, Evans blue dye (20 mg kg^{-1}, i.v.) was given for a period of 1 min. One min later, each concentration of MBS or 0.9% saline was inhaled for 30 breaths. R_L was recorded every 30 s. At 5 min after the administration of MBS or 0.9% saline, the animals were hyperinflated with twice the tidal volume by manually blocking the outflow of the ventilator. One min later, recovery R_L was measured, and then the animals were perfused. Baseline R_L was determined just before challenge. In addition, the airway effects induced by 80 mM MBS and 0.9% saline were compared to those induced by 80 mM MBS prepared just before use ($n = 5$), which caused a significant increase in R_L with maximum of 2.04 ± 0.56 cmH_2O ml^{-1} s^{-1} and dye leakage only in MB (44.9 ± 4.1 ng mg^{-1} of tissue). Both these responses were significantly smaller than those by the MBS prepared 24 h before use. The pH of 80 mM MBS prepared just before use was 2.93 ± 0.006, and the other was 2.71 ± 0.007 ($P < 0.01$). Therefore, we always used MBS solutions prepared 24 h before use for our studies.

Time course of sodium metabisulphite-induced airway microvascular leakage We measured extravasated Evans blue dye into airway tissues at 2, 6 and 10 min after MBS exposure (80 mM, 30 breaths). Animals weighing 400–460 g were divided into four groups ($n = 5$). Ten min after being connected to the ventilator, Evans blue dye (20 mg kg^{-1}, i.v.) was given slowly for a 1 min period, followed 1 min later by inhalation of MBS. The perfusion was performed at the defined time. Sham-stimulated animals given 0.9% saline alone were perfused at 2 min after inhalation of 0.9% saline. R_L was measured just before and after inhalation of MBS or 0.9% saline.

Effect of chlorpheniramine and atropine Five groups of animals were used to study the effects of chlorpheniramine, atropine and their combination on airway microvascular leakage and bronchoconstriction induced by inhaled MBS (80 mM, 30 breaths). At time zero, 0.9% saline used as placebo (1 ml kg^{-1}), chlorpheniramine (10 mg kg^{-1}), atropine (1 mg kg^{-1}) or the combination (chlorpheniramine, 10 mg kg^{-1}; atropine, 1 mg kg^{-1}) was given intravenously. Ten minutes later, Evans blue dye (20 mg kg^{-1}, i.v.) was administered for a period of 1 min. After 1 min, these four groups were given the MBS aerosol. The fifth group was pretreated

with 0.9% saline (1 ml kg^{-1}, i.v.), followed by inhalation of 0.9% saline (30 breaths) as a sham control. Measurements of R_L and Evans blue dye content were performed as outlined above. Baseline R_L was determined just before pretreatment and challenge. Another two groups were treated with atropine (1 mg kg^{-1}, i.v.) and 0.9% saline (1 ml kg^{-1}, i.v.), and given 40 mM MBS aerosol (30 breaths). We chose the dose of chlorpheniramine of 10 mg kg^{-1}, i.v. because it almost completely inhibited the increase in R_L (maximum: 110.1 ± 21.5 cmH_2O ml^{-1} s^{-1}; $n = 4$) and Evans blue dye leakage (TR, 142 ± 12.4; MB, 104.9 ± 16.2; PIPA, 65 ± 11.3; DIPA, 48 ± 1.6 ng mg^{-1} of wet tissue; $n = 4$) induced by 10 mM histamine aerosol (30 breaths) in a preliminary study. Atropine at the dose of 1 mg kg^{-1}, i.v. has been shown to abolish completely bronchoconstriction induced by electrical vagal stimulation (5V, 30 Hz, pulse width 5 ms and for 30 s) in capsaicin-pretreated guinea-pigs (Ichinose & Barnes, 1990).

Effect of capsaicin We studied the effects of capsaicin pretreatment on airway microvascular leakage and bronchoconstriction induced by two different concentrations of MBS (40 and 80 mM, 30 breaths). Two groups were pretreated with capsaicin or diluent alone respectively one week before MBS challenge. We used the method of capsaicin treatment previously described by Lundberg *et al.* (1983). Briefly, the guinea-pigs were given 0.1 mg kg^{-1} terbutaline subcutaneously and 25 mg kg^{-1} aminophylline intraperitoneally 30 min before injection of capsaicin. A single dose (50 mg ml^{-1}) of capsaicin diluted in the solution containing 10% v/v ethanol, 10% v/v Tween 80 and 80% v/v 0.9% saline was injected subcutaneously 5 min after administration of ketamine (50 mg kg^{-1}, i.m.) and xylazine (0.1 mg kg^{-1}, i.m.) for anaesthesia. The control animals given the same drugs were injected with the diluent for capsaicin. These animals were injected with Evans blue dye (20 mg kg^{-1}, i.v.), followed 1 min later by inhalation of the two doses of MBS. Measurements of R_L and Evans blue dye content were performed as outlined above. Six of the animals pretreated with capsaicin were given 50 mg kg^{-1} capsaicin subcutaneously and R_L was measured for a 15 min period in order to determine whether tachykinins were depleted from airway sensory nerves.

Effect of frusemide and nedocromil sodium We used four groups in order to investigate the effects of frusemide and nedocromil sodium on airway microvascular leakage and bronchoconstriction induced by MBS (80 mM). At time zero, the aerosol of 0.9% saline (placebo control), frusemide (10 mg ml^{-1}) or nedocromil sodium (10 mg ml^{-1}) was given for 7 min from the ultrasonic nebulizer, followed 10 min later by Evans blue dye injection (20 mg kg^{-1}, i.v.). The tracheal cannula was cleared of secretions by suction just after this inhalation, and then hyperinflation with twice the tidal volume were performed at an interval of 4 min until Evans blue dye injection. After 1 min, the nebulizer circuit was opened for delivery of MBS aerosol. The other group was pretreated by inhalation of 0.9% saline (7 min), followed by inhalation of 0.9% saline (30 breaths) as a sham-stimulated group. Measurements of R_L and Evans blue dye content were performed as outlined above. The effects of nedocromil sodium (10 mg kg^{-1}, 7 min) was also examined against airway microvascular leakage and bronchoconstriction induced by 40 mM MBS inhaled for 30 breaths. This dose of nedocromil sodium was similar to that used by Church *et al.* (1989) and caused inhibition of allergen-induced bronchoconstriction in the guinea-pig.

Drugs

Nedocromil sodium was kindly donated by Fisons plc, (Loughborough, U.K.). Frusemide and aminophylline were obtained from Antigen Ltd. (Roscrea, Ireland), atropine and 0.9% saline from Phoenix Pharmaceuticals Ltd. (Gloucester, U.K.), chlorpheniramine from Allen & Hanburys Ltd. (Greenford, U.K.), ketamine from Parke, Davis & Company (Pontypool, U.K.), suxamethonium from Duncan, Flockhart & Co. Ltd. (Greenford, U.K.), terbutaline from Astra Pharmaceuticals Ltd (Kings Langley, U.K.), xylazine from Bayer U.K. Ltd. (Bury St. Edmunds, U.K.), urethane, formamide, MBS and Tween 80 from Sigma Chemical Co. Ltd. (Poole, U.K.), Evans blue dye from Aldrich Chemical Co. Ltd. (Gillingham, U.K.), ethanol from BDH Chemicals (Poole, U.K.), and capsaicin from Fluka Chemie AG (Buchs, Switzerland). Nedocromil sodium was prepared as a solution of 10 mg ml^{-1} in 0.9% saline. Urethane (25% w/v in 0.9% saline) was used. Evans blue dye dissolved in 0.9% saline (20 mg ml^{-1}) was filtered through a 5.0 μm Millipore membrane.

Statistical analysis

All values are expressed as means ± s.e.mean. Mann-Whitney U test (two-tailed) was used to test the significance of differences in mean values between the two independent groups, and Wilcoxon test (two-tailed) for testing the differences within each group. P values less than 0.05 were considered to be significant.

Results

Effect of inhaled sodium metabisulphite

There was no significant difference in baseline R_L between any of the groups used for the study of dose-related responses to MBS (data not shown). MBS at all concentrations caused a significant concentration-dependent increase in R_L throughout the time course ($P < 0.01$, Figure 1) except that 20 mM MBS did not significantly increase R_L between 1 and 5 min. The maximum increase in R_L at each concentration was found immediately after challenge and recovery was rapid.

MBS induced extravasation of Evans blue dye at all airway levels in a concentration-dependent manner (Figure 2). MBS at concentrations of and above 40 mM caused significant dye leakage at all airway levels; at 20 mM, MBS did not induce

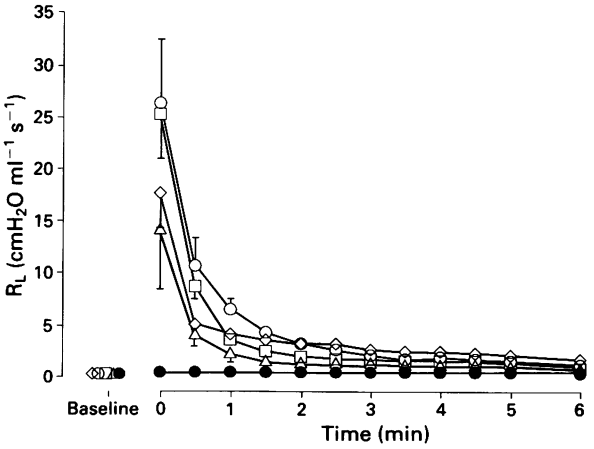

Figure 1 Time-course of increase in lung resistance (R_L) induced by the different concentrations (20 mM △, 40 mM □, 80 mM ○, 200 mM ◇; 30 breaths) of inhaled sodium metabisulphite (MBS) and its vehicle (0.9% saline, ●, 30 breaths) alone. Recovery R_L was determined 1 min after hyperinflation with twice the tidal volume at 5 min following inhalation challenge. Data are expressed as mean (s.e.mean shown by vertical bars) of 5 experiments. MBS at all concentrations caused a significant increase in R_L ($P < 0.01$ compared with 0.9% saline alone) throughout the time course, except that 20 mM MBS did not significantly increase R_L between 1 and 5 min after challenge or recovery R_L. There was no significant difference in baseline R_L between any of the groups studied.

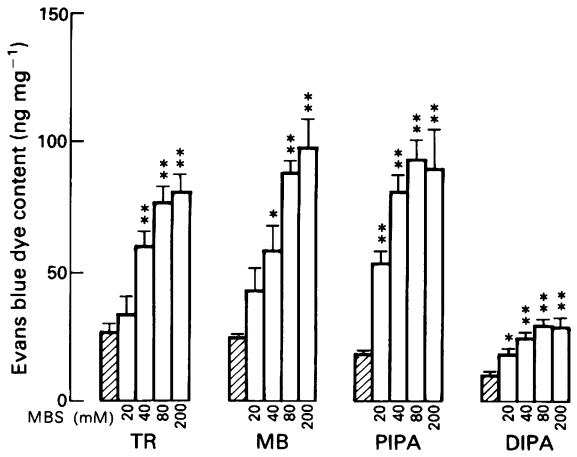

Figure 2 Evans blue dye extravasation induced by the different concentrations of sodium metabisulphite (MBS; 20, 40, 80 and 200 mM) and its vehicle (0.9% saline) alone at the airway levels of trachea (TR), main bronchi (MB), and proximal and distal intrapulmonary airways (PIPA and DIPA, respectively). Data are shown as mean (s.e.mean indicated by vertical bars) of 5 experiments. Hatched columns represent vehicle control. Statistical significance: $*P<0.05$; $**P<0.01$ compared with vehicle control.

dye extravasation in TR or MB. In the time-course study, the leakage of dye induced by 80 mM MBS was significantly increased at 6 min after inhalation with a further increase at 10 min at all airway levels (Figure 3). There was no significant difference in the peak R_L achieved by 80 mM MBS between the three groups for the time-course study (data not shown).

Effect of chlorpheniramine and atropine (Figure 4)

Intravenous administration of chlorpheniramine, atropine or the combination did not significantly alter baseline R_L. There was no significant difference in baseline R_L between the different treatment groups (Table 1). Chlorpheniramine and atropine inhibited the peak R_L by approximately 50%, but not the extravasation of Evans blue dye at any airway level. There was no additive effect of the combined injection of chlorpheniramine and atropine. A similar effect of atropine was found against the increase in R_L induced by 40 mM MBS.

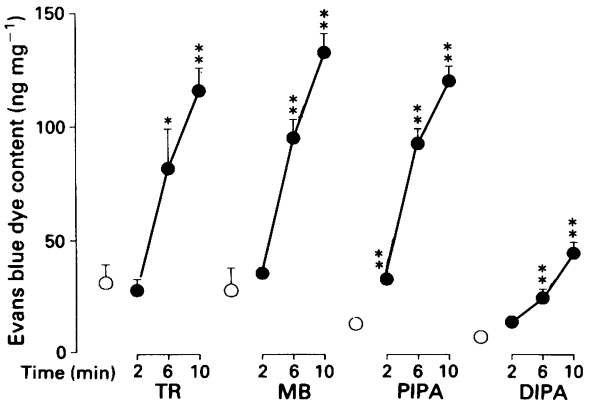

Figure 3 Time-course of extravasated Evans blue dye content at the airway levels of trachea (TR), main bronchi (MB) and proximal and distal intrapulmonary airways (PIPA and DIPA, respectively) induced by inhaled sodium metabisulphite (80 mM, 30 breaths). Evans blue dye content extravasated for 2 min after inhalation of 0.9% saline was used for comparison (O). Data are expressed as mean (s.e.mean indicated by vertical bars) of 5 experiments. Statistical significance: $*P<0.05$; $**P<0.01$ compared with saline-treated group.

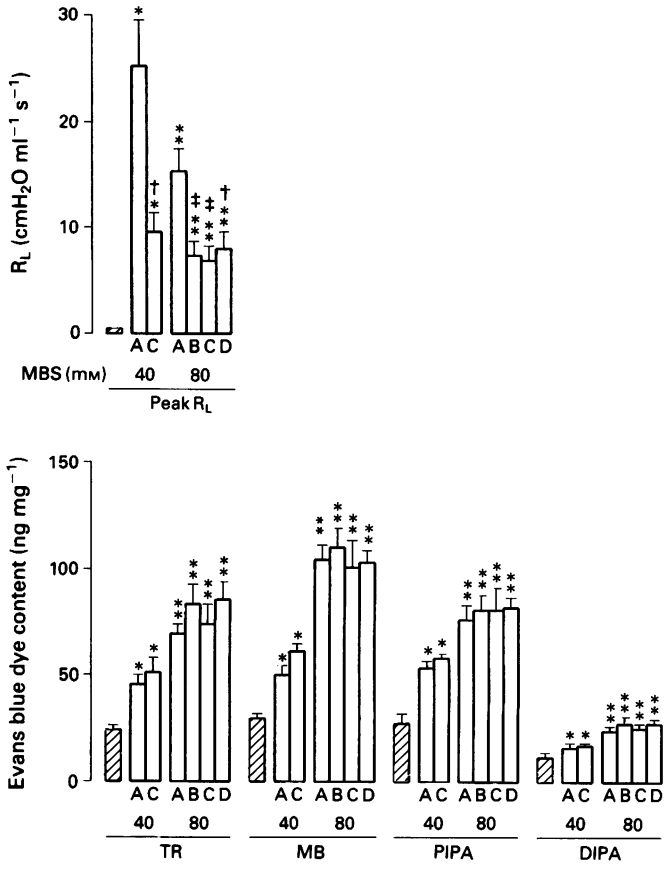

Figure 4 Effects of intravenous administration of chlorpheniramine (10 mg kg^{-1}), atropine (1 mg kg^{-1}) and their combination on sodium metabisulphite (MBS; 40 or 80 mM, 30 breaths)-induced peak lung resistance (R_L), which was always observed immediately after MBS challenge, and extravasation of Evans blue dye in trachea (TR), main bronchi (MB), and proximal and distal intrapulmonary airways (PIPA and DIPA, respectively). The effects induced by 0.9% saline (30 breaths, hatched columns) were used for comparison. (A) 0.9% saline + MBS: (B) chlorpheniramine + MBS; (C) atropine + MBS; (D) (chlorpheniramine + atropine) + MBS. Data are expressed as mean with s.e.mean indicated by vertical bars. Statistical significance: $*P<0.05$; $**P<0.01$ compared with sham-stimulated group; $\dagger P<0.05$; $\dagger\dagger P<0.01$ compared with saline control group (A).

Effect of capsaicin (Figure 5)

Subcutaneous capsaicin (50 mg kg^{-1}, s.c.) did not cause a significant increase in R_L in the six capsaicinized guinea-pigs (from 0.12 ± 0.01 to 0.15 ± 0.03 cmH$_2$O ml^{-1} s^{-1}), suggesting that the capsaicin pretreatment certainly depleted tachykinins from the airway sensory nerves. There was no significant difference in baseline R_L between the groups pretreated with capsaicin and without capsaicin (Table 1). Capsaicin pretreatment partly but significantly inhibited the peak R_L induced by both concentrations of MBS, whereas only dye leakage in MB induced by 80 mM MBS was significantly inhibited.

Effect of frusemide and nedocromil sodium (Figure 6)

Inhalation pretreatments with frusemide, nedocromil sodium and 0.9% saline caused a small but significant increase in R_L. However, no significant difference in baseline R_L between the groups was found after these pretreatments (Table 1). Frusemide caused a significant decrease in the peak R_L and Evans blue dye content in MB and PIPA. By contrast, nedocromil sodium had no significant effect on the airway responses induced by both doses of MBS.

Table 1 Body weight and baseline lung resistance (R_L) of guinea-pigs in the different treatment groups

Treatment + challenge	n	*Body weight* (g)	($cmH_2O\ ml^{-1}\ s^{-1}$) 1	*Baseline* R_L 2
Saline + MBS (80 mM)	10	536 ± 13	0.09 ± 0.01	0.10 ± 0.01
Chlorpheniramine + MBS (80 mM)	10	533 ± 20	0.10 ± 0.01	0.12 ± 0.01
Atropine + MBS (80 mM)	6	551 ± 23	0.11 ± 0.02	0.11 ± 0.02
(Chlorpheniramine + atropine) + MBS (80 mM)	6	554 ± 18	0.10 ± 0.01	0.12 ± 0.02
Saline + saline	5	628 ± 12	0.10 ± 0.03	0.11 ± 0.04
Saline + MBS (40 mM)	4	448 ± 16	0.12 ± 0.01	0.13 ± 0.01
Atropine + MBS (40 mM)	4	484 ± 27	0.08 ± 0.02	0.09 ± 0.02
Saline + saline	5	462 ± 8	0.11 ± 0.01	0.12 ± 0.01
Vehicle + MBS (80 mM)	7	570 ± 11	/	0.13 ± 0.02
Capsaicin + MBS (80 mM)	5	541 ± 10	/	0.12 ± 0.02
Vehicle + MBS (40 mM)	8	419 ± 5	/	0.12 ± 0.01
Capsaicin + MBS (40 mM)	6	429 ± 4	/	0.12 ± 0.02
Saline + MBS (80 mM)	11	447 ± 18	0.11 ± 0.02	0.22 ± 0.03
Frusemide + MBS (80 mM)	8	407 ± 13	0.14 ± 0.02	0.20 ± 0.02
Nedocromil sodium + MBS (80 mM)	6	513 ± 9	0.10 ± 0.01	0.21 ± 0.02
Saline + saline	7	441 ± 12	0.10 ± 0.01	0.19 ± 0.02
Saline + MBS (40 mM)	7	450 ± 33	0.09 ± 0.01	0.23 ± 0.02
Nedocromil sodium + MBS (40 mM)	7	424 ± 26	0.12 ± 0.01	0.25 ± 0.03

Data are expressed as mean ± s.e.mean. Baseline R_L 1 and 2 were determined just before and after treatment, respectively, with various drugs.
MBS: sodium metabisulphite.

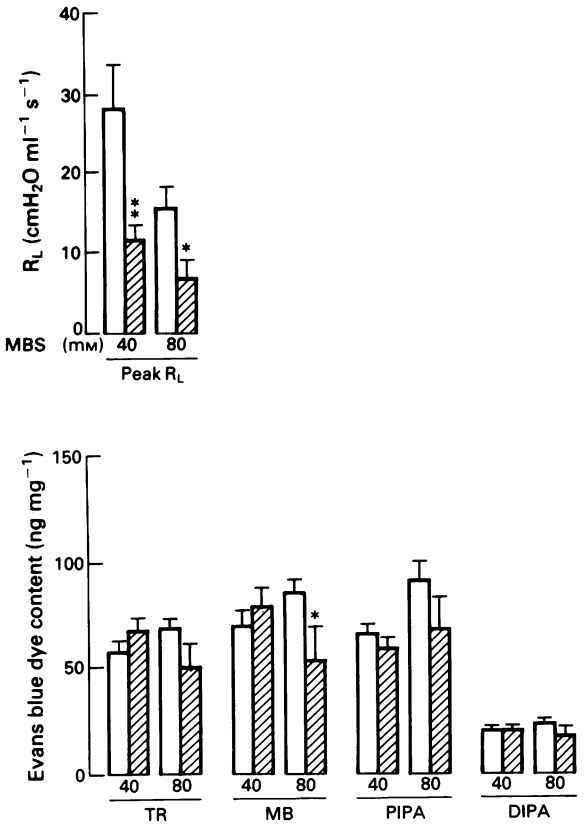

Figure 5 Effects of capsaicin pretreatment on sodium metabisulphite (MBS; 40 or 80 mM, 30 breaths)-induced peak lung resistance (R_L), which was always observed immediately after MBS challenge, and extravasation of Evans blue dye in trachea (TR), main bronchi (MB), and proximal and distal intrapulmonary airways (PIPA and DIPA, respectively). Data are expressed as mean with s.e.mean indicated by vertical bars. Hatched and open columns represent capsaicin- and its vehicle-pretreated groups, respectively. Statistical significance: $*P<0.05$; $**P<0.01$ compared with vehicle-pretreated (control) group.

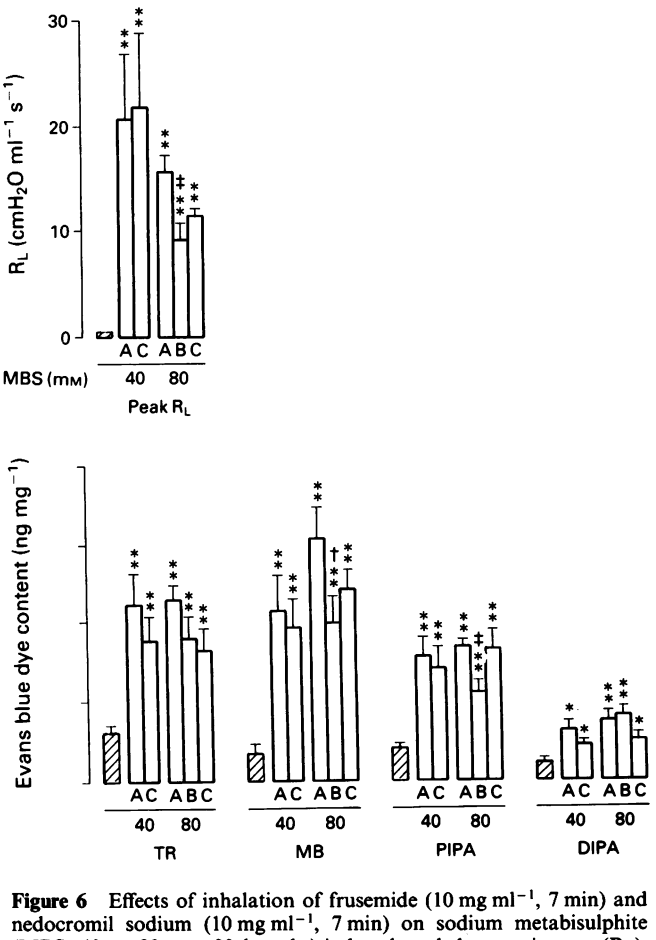

Figure 6 Effects of inhalation of frusemide (10 mg ml^{-1}, 7 min) and nedocromil sodium (10 mg ml^{-1}, 7 min) on sodium metabisulphite (MBS; 40 or 80 mM, 30 breaths)-induced peak lung resistance (R_L), which was always observed immediately after MBS challenge, and extravasation of Evans blue dye in trachea (TR), main bronchi (MB), and proximal and distal intrapulmonary airways (PIPA and DIPA, respectively). Inhalation of 0.9% saline (30 breaths) was used as a sham stimulation (hatched columns). (A) 0.9% saline + MBS; (B) frusemide + MBS; (C) nedocromil sodium + MBS. Data are given as mean with s.e.mean indicated by vertical bars. Statistical significance: $*P<0.05$; $**P<0.01$ compared with sham-stimulated group: $\dagger P<0.05$, $\dagger\dagger P<0.01$ compared with control group (A).

Discussion

We have demonstrated that inhalation of MBS caused significant concentration-dependent bronchoconstriction and airway microvascular leakage at all airway levels in the guinea-pig. The bronchoconstrictor effect was partially mediated by activation of cholinergic pathways. In addition, we have obtained evidence for a significant contribution of non-cholinergic capsaicin-sensitive pathways for both bronchoconstriction and airway microvascular leakage induced by MBS. Frusemide, which has been shown to inhibit both cholinergic and non-cholinergic airway responses in the guinea-pig *in vitro* (Elwood *et al.*, 1991), also caused a significant inhibition of MBS-induced bronchoconstriction and airway microvascular leakage.

Capsaicin pretreatment partly inhibited airway microvascular leakage in main bronchi induced by MBS at a high concentration, suggesting that neuropeptides released from airway sensory nerves contribute to the leakage in main bronchi rather than in the other parts of the respiratory tract. Lundberg *et al.* (1983) have shown that main bronchi are most densely innervated by substance P-immunoreactive nerves. In addition, the effect of electrical vagal stimulation on airway microvascular leakage in main bronchi is more prominent than in the trachea or intrapulmonary airway (Belvisi *et al.*, 1989). Our results are consistent with these observations, as is the finding that frusemide caused significant inhibition of MBS-induced microvascular leakage in the main bronchi. However, other mechanisms causing the increased airway microvascular leakage remain to be defined. Histamine is a potent bronchoconstrictor and inducer of airway microvascular permeability in the guinea-pig (Drazen & Austen, 1974; Evans *et al.*, 1989). However, i.v. chlorpheniramine did not suppress the plasma exudation at any airway level, although it partly inhibited the bronchoconstriction. Furthermore, the combined pretreatment of chlorpheniramine and atropine had no additive effect. Therefore, it appears that histamine only participates in MBS-induced bronchoconstriction and that this effect is likely to be mediated by an activation of cholinergic pathways (Douglas *et al.*, 1973; Drazen & Austen, 1975). This conclusion is supported by the demonstration that atropine caused a similar profile of inhibition to chlorpheniramine, with a significant effect on R_L but not on airway microvascular leakage. The mechanisms of MBS-induced airway microvascular leakage are different from those of antigen-induced plasma extravasation, as ovalbumin-induced airway microvascular leakage is significantly reduced by histamine H_1-receptor antagonists in ovalbumin-sensitized guinea-pigs (Saria *et al.*, 1983; Evans *et al.*, 1988). We have previously reported that inhaled MBS caused bronchoconstriction in guinea-pigs which was not dependent on a cholinergic reflex (Lötvall *et al.*, 1990), but the discrepant results between the two studies may be due to the much greater degree of bronchoconstriction induced in the present study. The cholinergic reflex may only be contributory during severe bronchoconstriction.

We used the same protocol as Lundberg *et al.* (1983) to deplete the airways of bronchoconstrictor tachykinins with capsaicin and have found that capsaicin pretreatment partly inhibited the bronchoconstriction induced by MBS, indicating the involvement of non-cholinergic neural pathways in MBS-induced bronchoconstriction. Our previous study shows that capsaicin pretreatment has no effect on PC_{350} (350% increase in R_L) to MBS (Lötvall *et al.*, 1990). Taken together, these studies suggest that the contribution of non-cholinergic neural pathways may be important when more severe bronchoconstriction is induced by MBS. Similarly, capsaicin pretreatment inhibited significantly airway microvascular leakage induced by 80 mM MBS but not 40 mM MBS in the present study. The conclusion shown by the inhibitory effect of capsaicin pretreatment is also supported by the similar profile of the inhibiting effect of frusemide. In guinea-pig bronchi, frusemide has been shown to inhibit non-cholinergic excitatory nerves *in vitro* without an effect on airway smooth muscle contraction induced by substance P (Elwood *et al.*, 1991), suggesting an inhibitory effect on the release of tachykinins from these nerves. The inhibition of MBS-induced bronchoconstriction by frusemide is in accord with similar results in asthmatic subjects (Nichol *et al.*, 1990). However, nedocromil sodium which has a similar effect to frusemide *in vitro* on guinea-pig bronchi (Verleden *et al.*, 1991) had no effect on MBS-iduced airway responses although at inhaled doses similar to those used in our studies, nedocromil sodium caused significant inhibitory effects on allergen-induced bronchoconstriction in the guinea-pig (Church *et al.*, 1989). On the other hand, nedocromil sodium is very effective in blocking MBS-induced bronchoconstriction in asthmatic patients (Dixon & Ind, 1990), suggesting that different mechanisms are operating in guinea-pigs, or that this species is less responsive to nedocromil sodium than man. We have not excluded the possibility that nedocromil sodium may be active against lower degrees of MBS-induced airway effects.

MBS is one amongst many other bronchoconstrictor agents which also induce airway microvascular leakage in the guinea-pig, including substance P, bradykinin, leukotrienes, platelet-activating factor and histamine. Whether the induction of plasma exudation causes airway oedema and subsequent narrowing of the intrapulmonary airways is not clear, but it could contribute to worsening of airway function (Moreno *et al.*, 1986; Hogg *et al.*, 1987). In the present study, it is apparent that the bronchoconstrictor mechanisms are different from those underlying airway microvascular leakage, and therefore, the increase in lung resistance appears to be independent of plasma exudation in terms of the time-course and pharmacological modulation.

We have shown that both airway microvascular leakage and bronchoconstriction induced by MBS prepared 24 h before use were significantly greater than those induced by the same concentration of MBS prepared just before use. The small variation in pH between these solutions cannot explain the difference in the airway responses (Fine *et al.*, 1987). However, even this small fall in pH may cause a considerable increase in sulphur dioxide generation when these solutions are nebulized (Fine *et al.*, 1987), and therefore the difference in sulphur dioxide generation may be important in determining the degree of bronchoconstriction induced by MBS. A close correlation between bronchoconstrictor responsiveness to MBS and sulphur dioxide in asthmatic patients has been demonstrated (Hein *et al.*, 1992).

In conclusion, inhaled MBS induces airway microvascular leakage and bronchoconstriction in the guinea-pig. These airway responses may be mediated via neural mechanisms including a cholinergic reflex and release of tachykinins from airway sensory nerves. Inhaled frusemide partly inhibits these responses, suggesting that this drug may inhibit neural mechanisms *in vivo*, as has been demonstrated *in vitro*.

We thank Fisons plc, (U.K.) for the donation of nedocromil sodium and for financial support.

References

BELVISI, M.G., ROGERS, D.F. & BARNES, P.J. (1989). Neurogenic plasma extravasation: inhibition by morphine in guinea pig airways in vivo. *J. Appl. Physiol.*, **66**, 268–272.

BUCK, S.H. & BURKS, T.F. (1986). The neuropharmacology of capsaicin: review of some recent observations. *Pharmacol. Rev.*, **38**, 179–226.

CHURCH, M.K., HUTSON, P.A. & HOLGATE, S.T. (1989). Effect of nedocromil sodium on early and late phase responses to allergen challenge in the guinea-pig. *Drugs*, **37** (Suppl. 1), 101–108.

DIXON, C.M.S., FULLER, R.W. & BARNES, P.J. (1987). Effect of nedocromil sodium on sulphur dioxide induced bronchoconstriction. *Thorax*, **42**, 462–465.

DIXON, C.M.S. & IND, P.W. (1988). Metabisulfite induced bronchoconstriction: mechanisms. *Am. Rev. Respir. Dis.*, **137** (Suppl), 238.

DIXON, C.M.S. & IND, P.W. (1990). Inhaled sodium metabisulphite induced bronchoconstriction: inhibition by nedocromil sodium and sodium chromoglycate. *Br. J. Clin. Pharmacol.*, **30**, 371–376.

DJOKIC, T.D., NADEL, J.A., DUSSER, D.J., SEKIZAWA, K., GRAF, P.D. & BORSON, D.B. (1989). Inhibitors of neutral endopeptidase potentiate electrically and capsaicin-induced noncholinergic contraction in guinea pig bronchi. *J. Pharmacol. Exp. Ther.*, **248**, 7–11.

DOUGLAS, J.S., DENNIS, M.W., RIDGWAY, P. & BOUHUYS, A. (1973). Airway constriction in guinea pigs: interaction of histamine and autonomic drugs. *J. Pharmacol. Exp. Ther.*, **184**, 169–179.

DRAZEN, J.M. & AUSTEN, K.F. (1974). Effects of intravenous administration of slow-reacting substance of anaphylaxis, histamine, bradykinin, and prostaglandin $F_{2\alpha}$ on pulmonary mechanics in the guinea pig. *J. Clin. Invest.*, **53**, 1679–1685.

DRAZEN, J.M. & AUSTEN, K.F. (1975). Atropine modification of the pulmonary effects of chemical mediators in the guinea pig. *J. Appl. Physiol.*, **38**, 834–838.

ELWOOD, W., LÖTVALL, J.O., BARNES, P.J. & CHUNG, K.F. (1991). Loop diuretics inhibit cholinergic and noncholinergic nerves in guinea pig airways. *Am. Rev. Respir. Dis.*, **143**, 1340–1344.

EVANS, T.W., ROGERS, D.F., AURSUDKIJ, B., CHUNG, K.F. & BARNES, P.J. (1988). Inflammatory mediators involved in antigen-induced airway microvascular leakage in guinea pig. *Am. Rev. Respir. Dis.*, **138**, 395–399.

EVANS, T.W., ROGERS, D.F., AURSUDKIJ, B., CHUNG, K.F. & BARNES, P.J. (1989). Regional and time-dependent effects of inflammatory mediators on airway microvascular permeability in the guinea pig. *Clin. Sci.*, **76**, 479–485.

FINE, J.M., GORDON, T. & SHEPPARD, D. (1987). The roles of pH and ionic species in sulfur dioxide- and sulfite-induced bronchoconstriction. *Am. Rev. Respir. Dis.*, **136**, 1122–1126.

HEIN, H., KIRSTEN, D. & MAGNUSSEN, H. (1991). Relation between the bronchoconstrictor response to inhaled sodium metabisulfite and inhaled sulphur dioxide in patients with bronchial asthma. *Am. Rev. Respir. Dis.*, **143** (Suppl), 437.

HOGG, J.C., PARE, P.D. & MORENO, R.H. (1987). The effect of submucosal edema on airways resistance. *Am. Rev. Respir. Dis.*, **135** (Suppl), S54–56.

ICHINOSE, M. & BARNES, P.J. (1990). A potassium channel activator modulates both excitatory noncholinergic and cholinergic neurotransmission in guinea pig airways. *J. Pharmacol. Exp. Ther.*, **252**, 1207–1212.

LÖTVALL, J.O., SKOOGH, B.-E., LEMEN, R.J., ELWOOD, W., BARNES, P.J. & CHUNG, K.F. (1990). Bronchoconstriction induced by inhaled sodium metabisulfite in the guinea pig. *Am. Rev. Respir. Dis.*, **142**, 1390–1395.

LÖTVALL, J.O., TOKUYAMA, K., LÖFDAHL, C.-G., ULLMAN, A., BARNES, P.J. & CHUNG, K.F. (1991). Peptidase modulation of noncholinergic vagal bronchoconstriction and airway microvascular leakage. *J. Appl., Physiol.*, **70**, 2730–2735.

LUNDBERG, J.M., BRODIN, E. & SARIA, A. (1983). Effects and distribution of vagal capsaicin-sensitive substance P neurons with special reference to the trachea and lungs. *Acta Physiol. Scand.*, **119**, 243–252.

LUNDBERG, J.M. & SARIA, A. (1987). Polypeptide-containing neurons in airway smooth muscle. *Annu. Rev. Physiol.*, **49**, 557–572.

MORENO, R.H., HOGG, J.C. & PARE, P.D. (1986). Mechanics of airway narrowing. *Am. Rev. Respir. Dis.*, **133**, 1171–1180.

MYERS, D.J., BIGBY, B.G. & BOUSHEY, H.A. (1986). The inhibition of sulphur dioxide-induced bronchoconstriction in asthmatic subjects by cromolyn is dose dependent. *Am. Rev. Respir. Dis.*, **133**, 1150–1153.

NICHOL, G.M., NIX, A., CHUNG, K.F. & BARNES, P.J. (1989). Characterisation of bronchoconstrictor responses to sodium metabisulphite aerosol in atopic subjects with and without asthma. *Thorax*, **44**, 1009–1014.

NICHOL, G.M., ALTON, E.W.F.W., NIX, A., GEDDES, D.M., CHUNG, K.F. & BARNES, P.J. (1990). Effect of inhaled furosemide on metabisulphite- and methacholine-induced bronchoconstriction and nasal potential difference in asthmatic subjects. *Am. Rev. Respir. Dis.*, **142**, 576–580.

ROGERS, D.F., BOSCHETTO, P. & BARNES, P.J. (1989). Plasma exudation: correlation between Evans Blue dye and radiolabeled albumin in guinea-pig airways in vivo. *J. Pharmacol. Methods*, **21**, 309–315.

SARIA, A., LUNDBERG, J.M., SKOFITSCH, G. & LEMBECK, F. (1983). Vascular protein leakage in various tissues induced by substance P, capsaicin, bradykinin, serotonin, histamine and by antigen challenge. *Naunyn-Schmiedebergs Arch. Pharmacol.*, **324**, 212–218.

SEALE, J.P., TEMPLE, D.M. & TENNANT, C.M. (1988). Bronchoconstriction by nebulized metabisulfite solutions (SO_2) and its modification by ipratropium bromide. *Ann. Allergy*, **61**, 209–213.

SNASHALL, P.D. & BALDWIN, C. (1982). Mechanisms of sulphur dioxide induced bronchoconstriction in normal and asthmatic man. *Thorax*, **37**, 118–123.

TAN, W.C., CRIPPS, E., DOUGLAS, N. & SUDLOW, M.F. (1982). Protective effect of drugs on bronchoconstriction induced by sulphur dioxide. *Thorax*, **37**, 671–676.

VERLEDEN, G.M., BELVISI, M.G., STRETTON, C.D. & BARNES, P.J. (1991). Nedocromil sodium modulates nonadrenergic, noncholinergic bronchoconstrictor nerves in guinea pig airways in vitro. *Am. Rev. Respir. Dis.*, **143**, 114–118.

VON NEERGAARD, K. & WIRZ, K. (1927). Die Messung der Strömungswiderstände in den Atemwegen des Menschen, insbesondere bei Asthma und Emphysem. *Z. Klin. Med.*, **105**, 51–82.

(Received April 8, 1992
Revised June 4, 1992
Accepted June 9, 1992)

Br. J. Pharmacol. (1992), **107**, 488–493

Cytosolic calcium increase in coronary endothelial cells after H_2O_2 exposure and the inhibitory effect of U78517F

[1]Masaaki Kimura, [2]Kaori Maeda & [1,3]Shigehiro Hayashi

Department of Pharmacology, Tsukuba Research Laboratories, Upjohn Pharmaceuticals Limited, Japan

1 Cytosolic calcium concentrations ($[Ca^{2+}]_i$ were determined with fura-2 on both resting (unstimulated) and A23187-stimulated coronary endothelial cells following injury by hydrogen peroxide (H_2O_2).

2 Treatment of cells with H_2O_2 (10^{-4} M) caused an increase in the resting $[Ca^{2+}]_i$, which reached a maximum of five fold after 3 h.

3 The increase in resting $[Ca^{2+}]_i$ was significantly attenuated by treatment with U78517F, a potent inhibitor of lipid peroxidation, at a concentration of 10^{-6} M or greater. Catalase (50 u ml^{-1}) also markedly inhibited the H_2O_2-induced rise in $[Ca^{2+}]_i$. Pretreatment with verapamil (10^{-5} M), nifedipine (10^{-6} M) or diltiazem (10^{-5} M) had no effect on the increase in $[Ca^{2+}]_i$ following addition of H_2O_2.

4 A23187 produced a transient increase in $[Ca^{2+}]_i$ followed by a sustained plateau. The initial peak and plateau phase responses to A23187 were augmented by H_2O_2. This augmentation of $[Ca^{2+}]_i$ was suppressed by U78517F or catalase but not by Ca-entry blockers.

5 Thus, it is likely that lipid peroxidation plays a critical role in the sustained increase in $[Ca^{2+}]_i$ that occurs following treatment with H_2O_2 and that this continues in the presence of agonists which stimulate the endothelium. Voltage-gated Ca^{2+} channels do not seem to be involved in the genesis of cellular damage associated with sustained large increases in $[Ca^{2+}]_i$.

Keywords: Intracellular calcium concentration; endothelial cell; cell injury; lipid peroxidation; hydrogen peroxide; U78517F

Introduction

There is a growing body of evidence which suggests that endothelial dysfunction occurs in a number of cardiovascular diseases, including hypertension (Lüscher *et al.*, 1986), diabetes (Mayhan, 1989), atherosclerosis (Förstermann *et al.*, 1988) and ischaemia/reperfusion (Mehta *et al.*, 1989) and thus results in impaired endothelium-dependent vasodilatation. Since the endothelium is often exposed to a reactive oxygen burst, it is likely to be the first site of damage in the vascular wall. Xanthine oxidase (XO)-derived oxidation is a critical pathway in microvascular and parenchymal tissue injury (Granger, 1988). Following production of superoxide anion, H_2O_2 generated extracellularly can readily diffuse into the endothelial cell, resulting in degradation of ATP (Spragg *et al.*, 1985) and increased substrate availability for XO. Highly reactive oxidants (Kvietys *et al.*, 1989) such as hydroxyl radical are formed through interaction of H_2O_2 and intracellular iron. Prime targets for free radical reactions are the unsaturated bonds in membrane lipids. Consequent lipid peroxidation results in a loss of membrane fluidity, receptor alignment, and potentially cellular lysis (Machlin & Bendich, 1987), associated with uncontrolled, sustained rises in cytosolic Ca^{2+} concentration (Nicotera *et al.*, 1988).

Release of endothelium-derived relaxing factor (EDRF) and prostaglandin I_2 (PGI_2) following agonist-stimulation in endothelial cells requires the presence of extracellular Ca^{2+} (Adams *et al.*, 1989). When the endothelium is stimulated by an agonist such as bradykinin, the cytosolic Ca^{2+} concentration ($[Ca^{2+}]_i$) increases with an initial peak due to inositol-1, 4,5-triphosphate (IP_3)-mediated Ca^{2+} release from intracellular stores, followed by a sustained plateau that is dependent on the presence of extracellular Ca^{2+}. However, it is not clear how $[Ca^{2+}]_i$ changes in response to an agonist under oxidative stress and subsequent cell injury.

The exact mechanisms involved in the regulation of intracellular calcium levels are not yet elucidated. The present study was carried out to delineate the relationship between $[Ca^{2+}]_i$ in resting and A23187-stimulated endothelial cells following treatment with the oxidant, H_2O_2. To avoid excess radical formation which is likely to cause untreatable severe cell damage accompanied with massive Ca^{2+} influx into the cell, relatively low concentrations of H_2O_2 were used. The present study clearly demonstrates that U78517F (2-[[4-(2, 6-di-1-pyrrolidinyl-4-pyrimidinyl)-1-piperazinyl]methyl]-3, 4-dihydro-2, 5, 7, 8-tetramethyl-2H-1-benzopyran-6-ol, dihydrochloride), an inhibitor of lipid peroxidation (Hall *et al.*, 1990), protects cultured coronary endothelial cells from reactive oxygen-induced increases in $[Ca^{2+}]_i$.

Methods

Endothelial cells in culture

Porcine hearts were obtained at a local slaughter house, and kept under sterile conditions for the short period (approximately 30 min) of transportation. The coronary arterial segments of left circumflex, right circumflex and left descending arteries were cleaned of surrounding adipose and connective tissue, and cut open longitudinally. The endothelial cells were harvested by scraping the luminal surface of the coronary artery with a razor blade gently under aseptic conditions. The collected cells were suspended in Dulbecco's modified Eagle's medium (DME) supplemented with 10% foetal bovine serum (FBS), 100 u ml^{-1} penicillin G and 100 $\mu g\ ml^{-1}$ streptomycin, seeded onto gelatin-coated culture dishes (60 mm of diameter), and cultured under a humidified atmosphere containing 5% CO_2 at 37°C. After the first medium change, the concentration of penicillin G and streptomycin was reduced to 10 u ml^{-1} and 10 $\mu g\ ml^{-1}$, respectively. The cells used in the study had undergone less than

[1] Present address: Pharmacology, R & D of Sandoz Pharmaceuticals Ltd., 4-17-30 Nishi-Azabu, Minato-ku, Tokyo 106, Japan.
[2] Present address: Department of Anesthesiology & Critical Care Medicine, Johns Hopkins Univ. School of Medicine, Baltimore, U.S.A.
[3] Author for correspondence.

eight passages. Cells which reached confluence were dispersed in the medium containing 0.05% trypsin and 0.53 mM EDTA for 3 to 5 min at 37°C. Thereafter, cells were centrifuged at 800 r.p.m. in HEPES-buffered solution (HBS) of the following composition (mM): NaCl 150, KCl 5.6, $CaCl_2$ 2.0, $MgCl_2$ 1.0 and HEPES 10.0 at pH of 7.4 for 6 min and resuspended with fresh HBS.

Intracellular calcium concentration

Intracellular Ca^{2+} concentration ($[Ca^{2+}]_i$) was determined with the fluorescent calcium indicator fura-2 (Grynkiewicz *et al.*, 1985). The cells were incubated in 10 ml of HBS containing 3×10^{-6} M fura-2 AM and 1 mg ml^{-1} bovine serum albumin (BSA) at 25°C. Detergent was not used for loading of fura-2 to avoid damage to the cell membrane. Sixty minutes later, the cells were centrifuged, and rinsed with HBS containing 0.5 mg ml^{-1} BSA. The concentration of the cells was adjusted to 3 to 7×10^5 ml^{-1} and cells were stored at 2°C on ice. Before the measurement of fluorescence, aliquots of 0.5 ml were placed in a cuvette, and centrifuged to eliminate the leaked fura-2 in HBS. Cells were put into fresh HBS at the same volume, and kept in suspension in the cuvette at 22°C with a magnetic stirrer before measurement of $[Ca^{2+}]_i$.

Fluorescence was measured with a fluorometer of dual wavelength excitation (CAF-100, Japan Spectroscopic, Tokyo, Japan) to detect changes in Ca^{2+}-sensitive fura-2 fluorescence. Dye-stained specimens were alternately excited at wavelengths of 340 (F_{340}) and 380 nm (F_{380}) at a frequency of 48 Hz, and the ratio (R) of F_{340} to F_{380} at an emission wavelength of 500 nm was estimated. $[Ca^{2+}]_i$ was assessed according to the following equation:

$$[Ca^{2+}]i = K_d \cdot B \cdot (R-R_{min})/(R_{max}-R) \qquad [1]$$

The dissociation constant (K_d) for Ca^{2+}-fura-2 complex at 20°C was assumed to be 135 nM (Grynkiewicz *et al.*, 1985). B is the ratio of F_{380} in Ca^{2+}-free solution with 20 mM EGTA to that in Ca^{2+} containing solution with 0.2% Triton X-100. Cells were treated with 0.2% Triton X-100 in HBS and 20 mM EGTA in 60 mM Tris solution (pH 8.3), to obtain maximum (R_{max}) and minimum (R_{min}) fluorescence ratios, respectively; slight fluorescence (2% or less of baseline fluorescence) of Triton X-100 and EGTA solution was calibrated for net fluorescence of fura-2. $MnCl_2$ at 20 mM was added to the cell suspension in Ca^{2+}-free solution to obtain the autofluorescence generated spontaneously from cells. Autofluorescence was subtracted to obtain values of $[Ca^{2+}]_i$ of the cell according to equation [1]. The slight fluorescence of 10^{-6} M A23187 did not influence measurement of $[Ca^{2+}]_i$.

After the cells in the cuvette were equilibrated for 10 to 15 min, the resting fluorescence of the cells was measured. Cells were then exposed to hydrogen peroxide (H_2O_2) at 10^{-4} M, and each cuvette incubated for 0.5, 1, 2 and 3 h at 22°C. Before the measurement of fluorescence was taken in the presence and absence of H_2O_2, cells were centrifuged, washed and resuspended. The fluorescence of the cell suspension for the calcium transient response to A23187 (10^{-6} M) was measured after an equilibration period of 5 min. Cells were treated with U78517F, Ca^{2+} antagonists and catalase 5 min before the addition of H_2O_2 to the cell suspension. Saline was used as a control.

Since fura-2 loaded in cells may leak out due to injury with consequent influence on net assessment of $[Ca^{2+}]_i$, care was taken to minimize leak from the cell just before measurement of $[Ca^{2+}]_i$ as follows: (1) centrifugation of the cell suspension and subsequent replacement with fresh HBS, and (2) maintenance at a low temperature of 22°C to reduce any leak of fura-2 (Schilling *et al.*, 1988).

Release of lactate dehydrogenase

Confluent cells plated on 24-well were incubated in DME medium containing 10^{-4} M H_2O_2 for 3 h. Lactate dehydrogenase (LDH) released into the external medium from cells was assessed by the first order rate of NADH oxidation at 340 nm using pyruvate and NADH (Kornberg, 1955).

Materials and statistical analysis

The following were used: Dulbecco's modified Eagles medium (Sigma Chemical, St. Louis, MO, U.S.A.), foetal bovine serum (FBS, Hyclone Lab., Logan, Utah, U.S.A.), penicillin G sodium salt (Sigma), streptomycin sulphate (Sigma), trypsin-EDTA (Gibco, Grand Island, NY, U.S.A.), ethylenediamine tetraacetic acid sodium salt (Na_2EDTA, Sigma), N-[2-hydroxyethyl] piperazine-N'-[2-ethanesulphonic acid] (HEPES, Sigma), fura-2 acetoxymethyl ester (Dojin, Kumamoto, Japan), bovine serum albumin (Sigma), ethyleneglycol *bis*-(beta-aminoethyl ether)-N,N,N',N'-tetraacetic acid (EGTA, Sigma), tris (hydroxymethyl) aminomethane (Tris, Sigma), $MnCl_2$ (Wako, Osaka, Japan), calcium ionophore A23187 (Sigma), catalase (Sigma), hydrogen peroxide (H_2O_2, Wako), diltiazem hydrochloride (Wako), verapamil hydrochloride (Wako), nifedipine (Sigma), catalase (Sigma), ionomycin (Carbiochemical Co., Belmont, CA, U.S.A.) and U78517F (2-[[4-(2,6-di-1-pyrrolidinyl-4-pyrimidinyl)-1-piperazinyl]methyl]-3, 4-dihydro -2, 5, 7, 8- tetramethyl-2H-1- benzopyran-6-ol, dihydrochloride) (Upjohn, Kalamazoo, MI, U.S.A.).

Statistical analyses were made according to the unpaired Student's *t* test. A *P* value less than 0.05 was regarded as significant.

Results

Treatment of coronary endothelial cells with H_2O_2 at a concentration of 10^{-4} M resulted in gradual increase in cytosolic Ca^{2+} concentration ($[Ca^{2+}]_i$). After a 3 h treatment, $[Ca^{2+}]_i$ was increased five fold over the control levels (Figure 1).

There was a release of LDH into external medium following treatment of cells with 10^{-4} M H_2O_2 for 3 h; when expressed as a percentage increase over total LDH content (0.199 ± 0.013 u/well) in cells, it was 11% (0.022 ± 0.02 u/well) for control and 19% (0.038 ± 0.013 u/well) for H_2O_2-treatment.

A23187 at 10^{-6} M produced a transient increase in $[Ca^{2+}]_i$ within 3 min, followed by the sustained plateau phase (Figures 2 and 3). Both peak and sustained responses to A23187

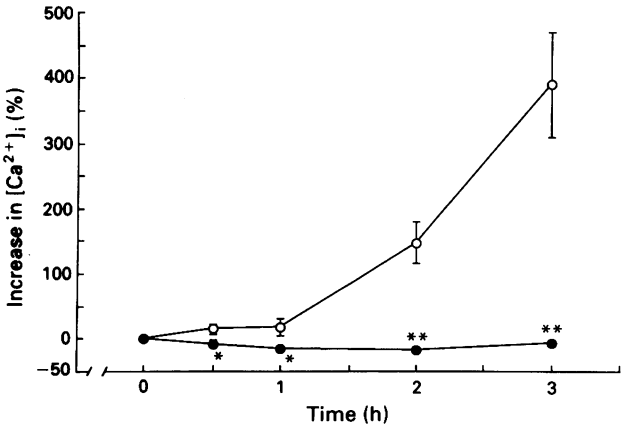

Figure 1 The time-dependent increase in resting $[Ca^{2+}]_i$ following addition of 10^{-4} M H_2O_2 to cell suspensions in the absence (○) and presence of U78517F at 10^{-6} M (●). Endothelial cells were exposed to 10^{-4} M H_2O_2 at zero time on the axis. The increase in the $[Ca^{2+}]_i$ is expressed as a percentage increase over the original $[Ca^{2+}]_i$ determined before treatment with 10^{-4} M H_2O_2, which ranged from 28.3 to 32.6 nM. Each point with vertical bars shows the mean ± s.e.mean ($n = 5$). *Significantly different from cells not exposed to U78517F; *$P < 0.05$; **$P < 0.01$.

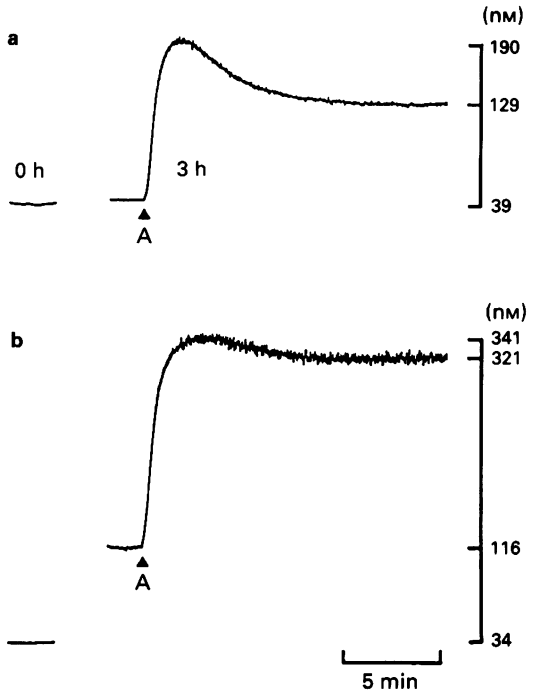

Figure 2 Typical tracing for calcium transient responses to A23187 (A, 10^{-6} M) of endothelial cells. After 3 h of treatment with (b) or without (a) 10^{-4} M H_2O_2, A23187 was added to the medium.

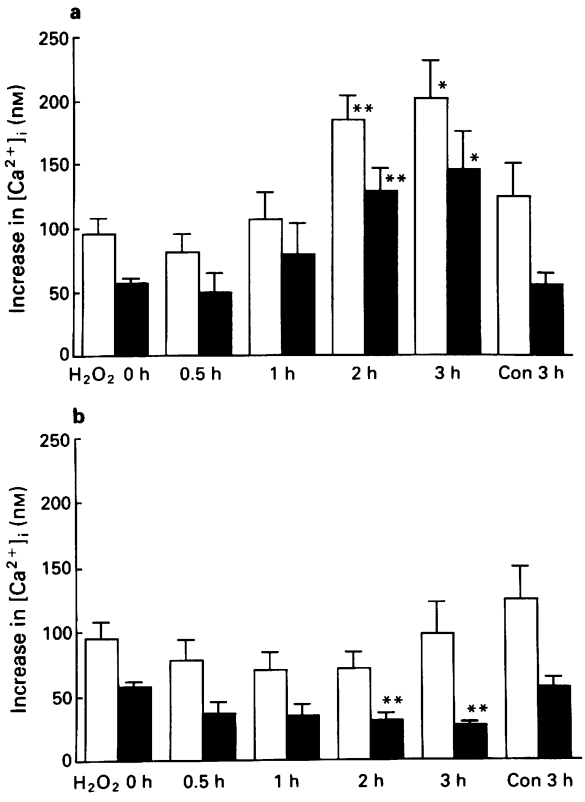

Figure 3 Calcium responses to A23187 at 10^{-6} M after exposure of the endothelial cells to 10^{-4} M H_2O_2 in the absence (a) and presence of U78517F at 10^{-6} M (b). Open and shaded columns indicate increase in $[Ca^{2+}]_i$ of peak and plateau phases in response to A23187 after the exposure to H_2O_2, respectively. A23187-stimulated increase in $[Ca^{2+}]_i$ was assessed before (0 h) and 0.5 h, 1 h, 2 h and 3 h after the exposure to H_2O_2. For the control, cells were left in HBS without exposure to H_2O_2 for 3 h (Con 3h). Each column with vertical bars shows the mean ± s.e.mean ($n = 5$). *Significantly different from H_2O_2 at 0 h; $*P<0.05$; $**P<0.01$.

for $[Ca^{2+}]_i$ were augmented in endothelial cells treated with 10^{-4} M H_2O_2; significantly augmented responses were seen at 2 h and 3 h. U78517F at 10^{-6} M inhibited the H_2O_2-induced potentiation of the rise in $[Ca^{2+}]_i$ in response to A23187 (Figure 1), while there was no significant alteration of the $[Ca^{2+}]_i$ rise in the absence of H_2O_2 (data not shown).

The H_2O_2-induced increase in resting $[Ca^{2+}]_i$ was attenuated by U78517F dose-dependently; the maximum inhibitory effect was obtained at 10^{-6} M (Figure 4). In the absence of H_2O_2, cells which were treated with U78517F at 10^{-6} M for 3 h did not show any change in the resting $[Ca^{2+}]_i$ (data not shown). The augmented responses to A23187 in H_2O_2-treated cells was inhibited by U78517F in a concentration-dependent fashion (Figure 5). U78517F at 10^{-6} M had no effect on A23187-stimulated responses in the absence of H_2O_2 (Table 1).

Treatment with 10^{-6} M nifedipine, 10^{-5} M diltiazem or 10^{-5} M verapamil, failed to attenuate the increase in $[Ca^{2+}]_i$ resulting from exposure of the cells to either H_2O_2 or H_2O_2 plus A23187 (data not shown). None of the Ca^{2+}-entry blockers altered either the resting $[Ca^{2+}]_i$ in the absence of H_2O_2 or the A23187-stimulated $[Ca^{2+}]_i$ in the absence and presence of H_2O_2 (Table 1).

Catalase at 50 u ml^{-1} attenuated both the increase in resting $[Ca^{2+}]_i$ (Figure 4) and augmented responsiveness to A23187 (Figure 5) following treatment of cells with H_2O_2 for 3 h.

Discussion

Disruption of calcium homeostasis, leading to a sustained and excess increase in cytosolic Ca^{2+} levels, is associated with cytotoxicity of hepatocytes (Nicotera *et al.*, 1988). The present study clearly demonstrated slowly increasing $[Ca^{2+}]_i$ in endothelial cells in response to H_2O_2. The concentration of H_2O_2 employed in the present study (10^{-4} M) was low relative to that associated with injury-induced release of lactate dehydrogenase; a cytotoxic effect has previously been reported at 10^{-3} M after 60 min (Sacks *et al.*, 1978; Weiss *et al.*, 1981; Harlan *et al.*, 1984). After a latent period of 1 h, H_2O_2 gradually increased resting $[Ca^{2+}]_i$ in coronary endothelial cells by as much as five times over the pretreatment level, suggesting sustained accumulation of cytosolic calcium. It is

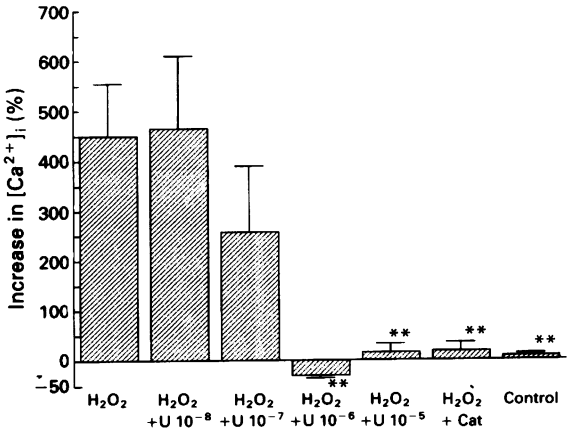

Figure 4 The inhibitory effect of U78517F or catalase against H_2O_2-induced increases in resting $[Ca^{2+}]_i$. The increases in $[Ca^{2+}]_i$ are expressed as a percentage increase over the original $[Ca^{2+}]_i$, which ranged from 32.8 to 39.0 nM. Endothelial cells were exposed to H_2O_2 for 3 h in the absence and presence of U78517F at 10^{-8} M (H_2O_2 + U 10^{-8}), 10^{-7} M (H_2O_2 + U 10^{-7}), 10^{-6} M (H_2O_2 + U 10^{-6}), 10^{-5} M (H_2O_2 + U 10^{-5}) or 50 unit ml^{-1} catalase (H_2O_2 + Cat). For the controls, cells were placed in HBS without H_2O_2 for 3 h (Control). Each column with vertical bars shows the mean ± s.e.mean ($n = 5$ to 7). **Significantly different from H_2O_2 alone; $P<0.01$.

Table 1 Effects of inhibitors on calcium responses to A23187 at 10^{-6} M in the absence of H_2O_2

Treatment	Concentration (M)	Increase in $[Ca^{2+}]_i$ (nM) Peak phase[1]	Plateau phase[2]
Control		229.2 ± 14.5	53.9 ± 11.9
U78517F	10^{-6}	219.3 ± 51.4	51.4 ± 8.6
Diltiazem	10^{-5}	204.8 ± 15.7	62.9 ± 8.7
Verapamil	10^{-6}	194.7 ± 9.4	56.5 ± 8.9
Nifedipine	10^{-6}	237.6 ± 0.6	54.5 ± 9.1

Increases in $[Ca^{2+}]_i$ in responses to A23187 are expressed as both peak[1] and plateau[2] phases. There was no significant difference between control and drug-treated values ($n = 3$, $P > 0.05$).

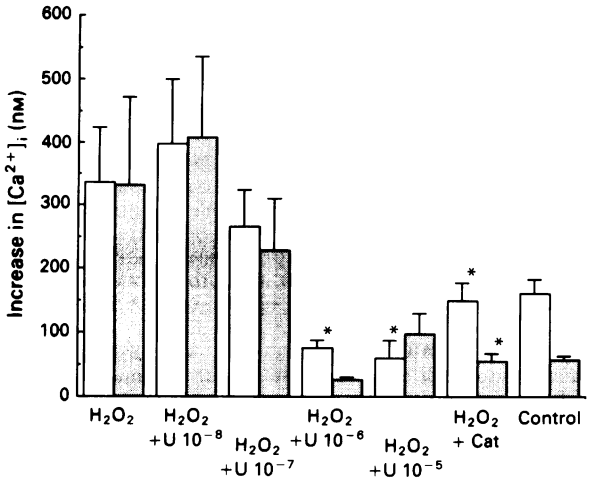

Figure 5 Inhibitory effect of U78517F or catalase on calcium responses to A23187 in the presence of H_2O_2. Open and shaded columns indicate $[Ca^{2+}]_i$ of peak and plateau phases in response to A23187 (10^{-6} M) after exposure to H_2O_2, respectively. Endothelial cells were exposed to 10^{-4} M H_2O_2 for 3 h in the absence (H_2O_2) and presence of U78517F at 10^{-8} M (H_2O_2 + U 10^{-8}), 10^{-7} M (H_2O_2 + U 10^{-7}), 10^{-6} M (H_2O_2 + U 10^{-6}), 10^{-5} M (H_2O_2 + U 10^{-5}) and 50 unit ml^{-1} catalase (H_2O_2 + Cat). For the controls, cells were placed in HBS without H_2O_2 for 3 h. Each column with vertical bars shows the mean ± s.e.mean ($n = 5$ to 7). *Significantly different from H_2O_2 alone; $P < 0.05$.

postulated that the sustained increase in $[Ca^{2+}]_i$ of cells arises from disturbed membrane Ca^{2+} permeability, depressed extrusion of Ca^{2+} from the cell secondary to an energy deficit, and/or altered release/sequestration of Ca^{2+} within the cell. The cytosolic Ca^{2+} concentration was assessed, assuming that fura-2 is located exclusively in the cell cytoplasm and that the fluorescence reflects cytosolic free Ca^{2+} (Grynkiewicz *et al.*, 1985; Morgan-Boyd *et al.*, 1987; Schilling *et al.*, 1988). However, microscopic examination of bovine aortic endothelial cells loaded with fura-2 reveals fluorescence associated with discrete intracellular structures rather than the homogeneous distribution expected for a cytosolic stain (Steinberg *et al.*, 1987). The precise location of the signal from each of the fluorescent Ca^{2+} indicator dyes after exposure of cells to H_2O_2 remains to be determined. With respect to lactate dehydrogenase activity, it was seen even in cells that had not been injured by reactive oxygen species. However, this does not suggest that cells are exposed to an injurious environment irrespective of H_2O_2-treatment, since there is baseline level of lactate dehydrogenase activity observed in cultured endothelial cells (Acosta & Li, 1979; Brigham *et al.*, 1987).

There is a great deal of evidence that release of EDRF in response to endothelium-dependent vasodilators depends on the presence of extracellular Ca^{2+} (Peach *et al.*, 1987; Luckhoff *et al.*, 1988), while release of PGI_2 is less dependent (Luckhoff *et al.*, 1988). Therefore, facilitated transport of Ca^{2+} across the membrane seems a prerequisite for triggering endothelial activation. It is conceivable that a sustained rise of $[Ca^{2+}]_i$ in the resting stage is induced by the reactive oxygen through an altered transport mechanism for Ca^{2+} across the membrane. A critical role of sustained increases in $[Ca^{2+}]_i$ in cell injury is supported by a study showing that deletion of extracellular Ca^{2+} inhibits cytotoxicity induced by lymphokine-activated killer cells (Kotasek *et al.*, 1988). Our findings in endothelial cells are consistent with those obtained in hepatocytes where oxidative stress by tert-butyl hydroperoxide at toxic concentrations increases $[Ca^{2+}]_i$ (Nicotera *et al.*, 1988). Voltage-gated Ca^{2+} channels are not involved in excitation-secretion coupling in endothelial cells (Spedding *et al.*, 1986; Jayakody *et al.*, 1987), but could possibly be involved in cell injury. We found, however, that Ca^{2+}-entry blockers of three different types, verapamil, nifedipine and diltiazem, at concentrations high enough to be effective (Hayashi & Toda, 1977; Godfraind & Miller, 1983), failed to suppress the rise of $[Ca^{2+}]_i$ following addition of H_2O_2 to endothelial cells. Our findings are consistent with those in non-injured cells where verapamil at 10^{-5} M does not alter resting $[Ca^{2+}]_i$ (Peach *et al.*, 1987; Morgan-Boyd *et al.*, 1987). Thus, the voltage-gated Ca^{2+} channel is unlikely to be activated by oxygen radicals. As suggested in hepatocytes, inhibition of the Ca^{2+}-ATPase that extrudes cytosolic Ca^{2+} may also be involved in the intracellular calcium accumulation through oxidation of the enzyme (Nicotera *et al.*, 1985).

In addition to the rise in resting $[Ca^{2+}]_i$, H_2O_2 enhanced the calcium responses of cultured cells to the calcium ionophore A23187 (Reed & Lardy, 1972). Potentiation of the calcium responses was seen for both phases, i.e. the initial peak and sustained plateau of $[Ca^{2+}]_i$, suggesting an increase in inositol-1,4,5-trisphosphate-mediated Ca^{2+} release from intracellular stores and greater membrane permeability to Ca^{2+}. A23187 stimulates not only Ca^{2+} influx but also Ca^{2+} release from the internal stores (Itoh *et al.*, 1985). Therefore, it seems reasonable to suggest that the increase in $[Ca^{2+}]_i$ continues in the presence of agonists which stimulate the endothelium during the course of cell injury.

The increases in $[Ca^{2+}]_i$ of resting and A23187-stimulated cells following treatment with H_2O_2 was attenuated by U78517F at a very low concentration compared with other inhibitors of reactive oxygen species (10^{-6} M U78517F vs. 5×10^{-3} M deferoxamine, an iron chelator: Kvietys *et al.*, 1989). H_2O_2 which is implicated as a primary effector of endothelial cell lysis by neutrophils (Sacks *et al.*, 1978; Weiss *et al.*, 1981; Harlan *et al.*, 1984) is relatively innocuous, but can readily pass through cell membranes and interact with intracellular iron to form highly reactive oxidants such as hydroxyl radical (Grisham & Granger, 1988). The radicals can attack many biological molecules, including membrane lipids, which undergo metal iron-dependent peroxidation (Braughler *et al.*, 1988; Gutteridge & Halliwell, 1990), and as a consequence may allow more Ca^{2+} to enter the cell. Although the rise in cytosolic Ca^{2+} after oxidative stress is not a universal factor in cell damage (Starke *et al.*, 1986; Herman *et al.*, 1990), there is evidence that cell death can be mediated by a sustained elevation of $[Ca^{2+}]_i$ (Chien *et al.*, 1978; Nicotera *et al.*, 1986). Thus, measuring resting $[Ca^{2+}]_i$ may be a useful means of assessing cytotoxicity. Since U78517F at 10^{-6} M had no effect in non-injured cells on resting or A23187-stimulated levels of $[Ca^{2+}]_i$, it is unlikely to inhibit Ca^{2+} mobilization. U78517F has a ring portion, i.e. a chromanol moiety of α-tocopherol, in which the hydroxyl group at the 6 position of the methylchroman ring structure serves as a reducing agent of lipid peroxyl radicals (Hall *et al.*, 1990; 1991). In a preliminary study (unpublished data, Maeda *et al.*), U78517F markedly suppressed formation of malonyldialdehyde, which is presumed to be closely related to progress of lipid peroxidation, in cultured coronary artery

endothelial cells exposed to a reaction mixture of xanthine (5×10^{-4} M) and xanthine oxidase (0.02 u ml^{-1}); $83 \pm 6\%$ ($n = 3$) inhibition by 10^{-6} M U78517 was obtained. Hall and colleagues have also demonstrated that U78517F at 10^{-6} M inhibits iron catalyzed lipid peroxidation in rat brain homogenates by approximately 90% (Hall *et al.*, 1991). Thus, U78517F is likely to exert an inhibitory action on lipid peroxidation and consequently suppress the sustained increase in $[Ca^{2+}]_i$ of endothelial cells exposed to cytotoxic reactive oxygen species.

In summary, H_2O_2 at a low concentration gradually increased $[Ca^{2+}]_i$ of coronary endothelial cells in culture. In the course of injury, the increase in $[Ca^{2+}]_i$ continues in the presence of agonists which stimulate the endothelium. Voltage-gated Ca^{2+} channels do not play a role in the genesis of cellular damage associated with increased $[Ca^{2+}]_i$. $[Ca^{2+}]_i$ increases simultaneously with cell injury presumably as a consequence of lipid peroxidation which is inhibited by U78517F.

The authors are grateful to Dr Karen Leach and Dr James L. Robotham for their critical review and valuable comments on the manuscript, and Ms Taeko Someya for her secretarial assistance with careful preparation of the manuscript. The authors gratefully acknowledge Dr Teruyuki Yanagisawa for helpful discussion on the method of fluorescent calcium measurement.

References

ACOSTA, D. & LI, C.-P. (1979). Injury to primary cultures of rat heart endothelial cells by hypoxia and glucose deprivation. *In vitro*, **15**, 929–934.

ADAMS, D.J., BARAKEH, J., LASKEY, R. & VAN BREEMAN, C. (1989). Ion channels and regulation of intracellular calcium in vascular endothelial cells. *FASEB J.*, **3**, 2389–2400.

BRAUGHLER, J.M., BURTON, P.S., CHASE, R.L., PREGRNZER, J.F., JACOBSEN, E.J., VAN DOORNIK, F.J., TUSTIN, J.M., AYER, D.E. & BUNDY, G.L. (1988). Novel membrane localized iron chelators as inhibitors of iron-dependent lipid peroxidation. *Biochem. Pharmacol.*, **37**, 3853–3860.

BRIGHAM, K.L., MEYRICK, B., BERRY, L.C. & REPINE, J. (1987). Antioxidants protect cultured bovine lung endothelial cells from injury by endotoxin. *Am. J. Physiol.*, **63**, 840–850.

CHIEN, K.R., ABRAMS, J., FERRONI, A., MARTIN, J.T. & FARBER, J.L. (1978). Accelerated phospholipid degradation and associated membrane dysfunction in irreversible ischemic liver cell injury. *J. Biol. Chem.*, **253**, 4809–4817.

FÖRSTERMANN, U., MÜGGE, A., ALHEID, U., HAVERICH, A. & FRÖLICH, J.C. (1988). Selective attenuation of endothelium-mediated vasodilatation in atherosclerotic human coronary arteries. *Circ. Res.*, **62**, 185–190.

GODFRAIND, T. & MILLER, R.C. (1983). Specificity of action of Ca^{2+} entry blockers: a comparison of their actions in rat arteries and in human coronary arteries. *Circ. Res.*, **52**(suppl. I), 81–91.

GRANGER, D.N. (1988). Role of xanthine oxidase and granulocytes in ischemia-reperfusion injury. *Am. J. Physiol.*, **255**, H1269–H1275.

GRISHAM, M.B. & GRANGER, D.N. (1988). Neutrophil-mediated mucosal injury. Role of reactive oxygen metabolites. *Dig. Dis. Sci.*, **33**, 6S–15S.

GRYNKIEWICZ, G., POENIE, M. & TSIEN, R.Y. (1985). A new generation of Ca^{2+} indicators with greatly improved fluorescence properties. *J. Biol. Chem.*, **260**, 3440–3450.

GUTTERIDGE, J.M.C. & HALLIWELL, B. (1990). The measurement and mechanism of lipid peroxidation in biological system. *Trends Biol. Sci.*, **15**, 129–135.

HALL, E.D., BRAUGHLER, J.M., YONKERS, P.A., SMITH, S.L., LINSEMAN, K.L., MEANS, E.D., SCHERCH, H.M., VON VOIGHTLANDER, P.F., LAHTI, R.A. & JACOBSEN, E.J. (1991). U-78517F: a potent inhibitor of lipid peroxidation with activity in experimental brain injury and ischemia. *J. Pharmacol. Exp. Ther.*, **258**, 688–694.

HALL, E.D., PAZARA, K.E., BRAUGHLER, J.M., LINSEMAN, K.L. & JACOBSEN, E.J. (1990). Nonsteroidal lazaloid U78517F in models of focal and global ischemia. *Stroke*, **21**(suppl. III), III-83–III-87.

HARLAN, J.M., LEVINE, J.D., CALLAHAN, K.S., SCHWARTZ, B.R. & HARKER, L.A. (1984). Glutathione redox cycle protects cultured endothelial cells against lysis by extracellularly generated hydrogen peroxide. *J. Clin. Invest.*, **73**, 706–713.

HAYASHI, S. & TODA, N. (1977). Inhibition by Cd^{2+}, verapamil and papaverine of Ca^{2+}-induced contractions in isolated cerebral and peripheral arteries of the dog. *Br. J. Pharmacol.*, **60**, 35–43.

HERMAN, B., GORES, G.J., NIEMINEN, A.-L., KAWANISHI, T., HERMAN, A. & LEMASTERS, J.J. (1990). Calcium and pH in anoxic and toxic injury. *Crit. Rev. Toxicol.*, **21**, 127–148.

ITOH, T., KANMURA, Y. & KURIYAMA, H. (1985). A23187 increases calcium permeability of stores sites more than of surface membranes in rabbit mesenteric artery. *J. Physiol.*, **359**, 467–484.

JAYAKODY, R.L., KAPPAGODA, C.T., SENARATNE, M.P.J. & SREEHARAN, N. (1987). Absence of effect of calcium antagonists on endothelium-dependent relaxation in rabbit aorta. *Br. J. Pharmacol.*, **91**, 155–164.

KORNBERG, A. (1955). Lactic dehydrogenase of muscle. *Methods Enzymol.*, **1**, 441–443.

KOTASEK, D., VERCELLOTTI, G.M., OCHOA, A.C., BACH, F.H., WHITE, H.G. & JACOB, H.S. (1988). Mechanism of cultured endothelial injury induced by lymphokine-activated killer cells. *Cancer Res.*, **48**, 5528–5532.

KVIETYS, P.R., INAUTEN, W., BACON, B.R. & GRISHAM, M.B. (1989). Xanthine oxidase-induced injury to endothelium: role of intracellular iron and hydroxyl radical. *Am. J. Physiol.*, **257**, H1640–H1646.

LUCKHOFF, A., POHL, U., MULSCH, A. & BUSSE, R. (1988). Differential role of extra- and intracellular calcium in the release of EDRF and prostacyclin from cultured endothelial cells. *Br. J. Pharmacol.*, **95**, 189–196.

LÜSCHER, T.F. & VANHOUTTE, P.M. (1986). Endothelium-dependent responses to platelets and serotonin in spontaneously hypertensive rats. *Hypertension*, **8**(suppl. II), II55–II60.

MACHLIN, L.J. & BENDICH, A. (1987). Free radical tissue damage: protective role of antioxidant nutrients. *FASEB J.*, **1**, 441–445.

MAYHAN, W.G. (1989). Impairment of endothelium-dependent dilation of cerebral arterioles during diabetes mellitus. *Am. J. Physiol.*, **256**, H621–H625.

MEHTA, J.L., NICHOLS, W.W., DONNELLY, W.H., LAWSON, D.L. & SALDEEN, T.G.P. (1989). Impaired canine coronary vasodilator response to acetylcholine and bradykinin after occlusion-reperfusion. *Circ. Res.*, **64**, 43–54.

MORGAN-BOYD, R., STEWART, J.M., VAVREK, R.J. & HASSID, A. (1987). Effects of bradykinin and angiotensin II on intracellular Ca^{2+} dynamics in endothelial cells. *Am. J. Physiol.*, **253**, C588–C598.

NICOTERA, P., HARTZELL, P., BALDI, C., SVENSSON, S.-A., BELLOMO, G. & ORRENIUS, S. (1986). Cystamine induces cytotoxicity in hepatocytes through the elevation of cytosolic Ca^{2+} and the stimulation of a non-lysosomal proteolytic system. *J. Biol Chem.*, **261**, 14628–14635.

NICOTERA, P., MCCONKEY, D.J., SVENSSON, S.A., BELLOMO, G. & ORRENIUS, S. (1988). Correlation between cytosolic Ca^{2+} concentration and cytotoxicity in hepatocytes exposed to oxidative stress. *Toxicology*, **52**, 55–63.

NICOTERA, P., MOORE, M., MIRABELLI, F., BELLOMO, G. & ORRENIUS, S. (1985). Inhibition of hepatocyte plasma membrane Ca^{2+}-ATPase activity by menadione metabolism and its restoration by thiols. *FEBS Lett.*, **181**, 149–153.

PEACH, M.J., SINGER, H.A., IZZO, N.J. & LOEB, A.L. (1987). Role of calcium in endothelium-dependent relaxation of arterial smooth muscle. *Am. J. Cardiol.*, **59**, 35A–43A.

REED, P.W. & LARDY, H.A. (1972). A23187: a divalent cation ionophore. *J. Biol. Chem.*, **247**, 6970–6977.

SACKS, T., MOLDOW, C.F., CRADDOCK, P.R., BOWERS, T.K. & JACOB, H.S. (1978). Oxygen radicals mediate endothelial cell damage by complement-stimulated granulocytes: an in vitro model of immune vascular damage. *J. Clin. Invest.*, **61**, 1161–1167.

SCHILLING, W.P., RITCHIE, A.K., NAVARRO, L.T. & ESKIN, S.G. (1988). Bradykinin-stimulated calcium influx in cultured bovine aortic endothelial cells. *Ann. J. Physiol.*, **255**, H219– 227.

SPEDDING, M., SCHINI, V., SCHOEFFTER, P. & MILLER, R.C. (1986). Calcium channel activation does not increase release of endothelium-derived relaxing factor (EDRF) in rat aorta although tonic release of EDRF may modulate calcium channel activity in smooth muscle. *J. Cardiovasc. Pharmacol.*, **8**, 1130–1137.

SPRAGG, R.G., HINSHAW, D.B., HYSLOP, P.A., SCHRAUFSTATTER, I.U. & COCHRANE, C.G. (1985). Alteration in adenosine triphosphate and energy charge in cultured endothelial and P388 D1 cells after oxidant injury. *J. Clin. Invest.*, **76**, 1471–1476.

STARKE, P.E., HOEK, J.B. & FARBER, J.L. (1986). Calcium-dependent and calcium-independent mechanisms of irreversible cell injury in cultured hepatocytes. *J. Biol. Chem.*, **261**, 3006–3012.

STEINBERG, S.F., BILEZIKIAN, J.P. & AL-AWQATI, Q. (1987). Fura-2 fluorescence is localized to mitochondria in endothelial cells. *Am. J. Physiol.*, **253**, C744–C747.

WEISS, S.J., YOUNG, J., LOBUGLIO, A.F., SLIVKA, A. & NIMEH, N.F. (1981). Role of hydrogen-peroxide in neutrophil-mediated destruction of cultured endothelial cells. *J. Clin. Invest.*, **68**, 714–721.

(Received November 18, 1991
Revised June 5, 1992
Accepted June 9, 1992)

Br. J. Pharmacol. (1992), **107**, 494–501

L-689,660, a novel cholinomimetic with functional selectivity for M_1 and M_3 muscarinic receptors

[1]R.J. Hargreaves, A.T. McKnight, K. Scholey, N.R. Newberry, L.J. Street, P.H. Hutson, J.E. Semark, E.A. Harley, S. Patel & S.B. Freedman

Merck Sharp and Dohme Research Laboratories, Neuroscience Research Centre, Terlings Park, Eastwick Road, Harlow, Essex CM20 2QR

1 L-689,660, 1-azabicyclo[2.2.2]octane, 3-(6-chloropyrazinyl)maleate, a novel cholinomimetic, demonstrated high affinity binding (pK_D (apparent) 7.42) at rat cerebral cortex muscarinic receptors. L-689,660 had a low ratio (34) of pK_D (apparent) values for the displacement of binding of the antagonist [^{3}H]-N-methylscopolamine ([^{3}H]-NMS) compared with the displacement of the agonist [^{3}H]-oxotremorine-M ([^{3}H]-Oxo-M), in rat cerebral cortex. Low NMS/Oxo-M ratios have been shown previously to be a characteristic of compounds that are low efficacy partial agonists with respect to stimulation of phosphatidyl inositol turnover in the cerebral cortex.

2 L-689,660 showed no muscarinic receptor subtype selectivity in radioligand binding assays but showed functional selectivity in pharmacological assays. At M_1 muscarinic receptors in the rat superior cervical ganglion, L-689,660 was a potent (pEC_{50} 7.3 ± 0.2) full agonist in comparison with (±)-muscarine. At M_3 receptors in the guinea-pig ileum myenteric plexus-longitudinal muscle or in trachea, L-689,660 was again a potent agonist (pEC_{50} 7.5 ± 0.2 and 7.7 ± 0.3 respectively) but had a lower maximum response than carbachol. In contrast L-689,660 was an antagonist at M_2 receptors in guinea-pig atria (pA_2 7.2 (95% confidence limits 7, 7.4)) and at muscarinic autoreceptors in rat hippocampal slices.

3 The putative M_1-selective muscarinic agonist, AF102B (*cis*-2-methylspiro-(1,3-oxathiolane 5,3′)-quinuclidine hydrochloride) was found to have a profile similar to L-689,660 but had up to 100 times less affinity in binding and functional assays. RS-86 (2-ethyl-8-methyl-2,8-diazospiro[4,5]decan 1,3-dione hydrochloride) also had lower affinity than L-689,660, and had no binding selectivity for muscarinic receptor subtypes. RS-86 had a higher NMS/Oxo-M ratio than L-689,660 and was a full agonist at M_1, M_2 and M_3 receptors in the functional pharmacological assays.

4 The functional selectivity of L-689,660 in muscarinic pharmacological assays is consistent with the effects of a low efficacy partial agonist in tissues with different effective receptor reserves.

Keywords: Cholinomimetic; muscarinic receptor; low efficacy; functional selectivity; M_1 receptor agonist; M_3 receptor agonist; M_2 receptor antagonist

Introduction

Therapeutic approaches that aim to provide symptomatic relief in Alzheimer's disease have been directed by reports of specific cholinergic deficits in brain tissue when patients diagnosed as having Alzheimer's dementia were examined post-mortem (Davis & Maloney, 1976; Perry *et al.*, 1977). These observations gave rise to the cholinergic hypothesis of dementia (Bartus *et al.*, 1982) and the suggestion that cholinergic replacement therapy would provide relief from the deficits in cognition and memory function that occur in this disorder (Bartus *et al.*, 1985; Perry, 1986). The two most widely studied approaches to improvement of cholinergic function are the use of acetylcholinesterase inhibitors and a replacement strategy using directly acting cholinomimetic drugs (Hollander *et al.*, 1986; Gray *et al.*, 1989). Clinical trials with cholinergic replacement therapy have, however, been generally disappointing, often because of the incidence of side-effects at potential therapeutic doses.

Previous studies from our laboratories have described a series of azabicyclic oxadiazole compounds that are centrally active non-selective full muscarinic agonists (Freedman *et al.*, 1990). The use *in vivo* of such non-selective compounds that have high intrinsic activity is associated with a range of peripheral and central side effects, especially through activation of muscarinic receptors within cardiovascular systems (Pazos *et al.*, 1986; Sapru, 1989) and this prevented their use in the clinic.

Three distinct muscarinic receptor subtypes M_1, M_2 and M_3 have been distinguished from binding and functional studies (Hulme *et al.*, 1990) and these have been shown to have similar binding properties to the m1, m2 and m3 muscarinic receptors expressed in CHO cells transfected with the corresponding genes (Buckley *et al.*, 1989). Using *in situ* hybridization techniques these muscarinic receptor subtypes have been shown to be localized in discrete brain regions associated with distinct CNS functions. High levels of m1 and m3 receptor mRNA transcripts have been demonstrated in rat cortex and hippocampus (Brann *et al.*, 1988) whereas m2 transcripts appeared much rarer and were shown in the basal forebrain, thalamus and hindbrain (Buckley *et al.*, 1988). Since the cognitive and memory effects of muscarinic agents are thought to be localized to the cortex and hippocampus (Ridley *et al.*, 1985; 1986; 1989) and M_1 muscarinic receptors to be relatively preserved in Alzheimer's disease (Probst *et al.*, 1988; Araujo *et al.*, 1988), it was postulated that agonist drugs selective for this subtype may be of value in cognitive disorders as side-effects mediated by other muscarinic receptor subtypes would be minimized (Gray *et al.*, 1989; Quirion *et al.*, 1989).

Agents that are truly selective agonists at particular muscarinic receptor subtypes have not yet been reported. However, as Kenakin (1986) proposed, it may be possible to achieve functional receptor subtype selectivity by use of non-selective low efficacy agonists. These compounds could

[1] Author for correspondence.

discriminate between target tissues and others, that could potentially be the sites of mediation for dose limiting side effects, on the basis of their effective receptor reserve.

The present studies describe the affinity for muscarinic binding sites and the pharmacological characterization of a novel low efficacy cholinomimetic, L-689,660 (1-azabicyclo[2.2.2]octane, 3-(6-chloropyrazinyl)maleate) (Baker *et al.*, 1991).

L-689,660 has been studied in muscarinic radioligand binding assays in the cerebral cortex and in assays that determine functional muscarinic receptor subtype selectivity. In the cortical binding assays, [^{3}H]-oxotremorine-M (Oxo-M) was used to label the high-affinity state of the muscarinic receptor in rat cerebral cortex and [^{3}H]-N-methylscopolamine (NMS) to label predominantly the low affinity state. Agonists such as carbachol recognise preferentially the high-affinity state of the receptor and so display high affinity in the agonist binding assay whereas antagonists such as atropine show similar affinity in both assays. The NMS/Oxo-M ratio has been shown previously to be correlated directly with the ability of compounds to stimulate phosphatidyl inositol turnover in the cerebral cortex and has been proposed for use as an index of efficacy at cortical muscarinic receptors (Freedman *et al.*, 1988; 1990).

The functional pharmacology of L-689,660 has been assessed at muscarinic receptors in the rat superior cervical ganglion (M_1), guinea-pig atria (M_2), guinea-pig ileum, myenteric plexus-longitudinal muscle (M_3) and guinea-pig trachea (M_3). The profile of L-689,660 has been compared with that of the putative M_1-selective muscarinic agonist AF102B (*cis*-2-methylspiro-(1,3-oxathiolane 5,3')-quinuclidine hydrochloride) (Fisher *et al.*, 1989), and of the non-selective muscarinic agonist RS-86 (2-ethyl-8-methyl-2,8-diazospiro [4,5]decan 1, 3-dione hydrochloride) (Palacios *et al.*, 1986). A preliminary account of these studies has been given to the British Pharmacological Society (Hargreaves *et al.*, 1991).

Methods

Receptor binding studies in vitro

[^{3}H]-NMS/[^{3}H]-Oxo-M binding ratio The preparation of a rat cerebral cortex membrane fraction and the assay conditions for [^{3}H]-N-methylscopolamine ([^{3}H]-NMS) and [^{3}H]-oxotremorine-M ([^{3}H]-Oxo-M) radioligand binding studies have been described previously in detail (Freedman *et al.*, 1990). Binding parameters were determined by fitting a single site model to the data by a non-linear least squares regression analysis and an iterative procedure in the RS1 software package (BBN Software Products Corporation Cambridge MA).

Binding selectivity at subtypes of muscarinic receptors

Rat cerebral cortex (M_1) A crude preparation of cortical membranes was made by homogenizing the cerebral cortex from Sprague-Dawley rats (500 r.p.m. 10 strokes) in modified Krebs solution buffer (pH 7.4) with HEPES (composition, mM:NaCl 118, KCl 4.7, $MgSO_4$ 1.2, $NaHCO_3$ 5, KH_2PO_4 1.2, $CaCl_2$ 2.5, glucose 11, HEPES, 20). The resulting homogenate was then diluted with the same buffer containing 100 μM Gpp(NH)p to a final concentration of 0.55% wet w/v. The membranes were preincubated for 10 min at 30°C to remove endogenous acetylcholine. Muscarinic binding was determined in 750 μl of homogenate (4.17 mg tissue) and 1 nM N-methyl-[^{3}H]-pirenzepine in a final assay volume of 1 ml. Non-specific binding was defined with 2 μM atropine. Incubation with radiolabel was for 60 min at 30°C and assays were terminated by filtering the membranes using a Brandel Cell Harvester onto GB/B filters pre-soaked in 0.1% polyethyleneimine. Samples were washed twice in 10 ml ice cold 0.9% w/v saline. Filters were then placed in 10 ml scintillation fluid and radioactivity estimated by liquid scintillation spectrophotometry. Data from this assay (and the M_2 and M_3 assay detailed below) were analysed in the manner described above for [^{3}H]-NMS and [^{3}H]-Oxo-M.

Rat heart (M_2) Sprague-Dawley rat hearts were perfused *in situ* with 10 ml of ice-cold modified Krebs solution buffer with HEPES (pH 7.4), cleared of connective tissue, removed and cut into pieces. The cardiac tissue was then transferred into plastic centrifuge tubes with 10 ml buffer containing 100 μM Gpp(NH)p. The tissue was disrupted by ultrasound (Polytron 2 × 20 s) and the resulting suspension homogenized (500 r.p.m., 20 strokes) and filtered coarsely by passing it through two layers of cheese cloth. This crude preparation of heart membranes was then preincubated for 10 min at 30°C and resuspended in buffer at a concentration of 0.83% wet w/v. Muscarinic binding was determined in 750 μl of homogenate (6.25 mg tissue) and [^{3}H]-NMS (0.1 nM) in the final assay volume of 1 ml. Incubation with radiolabel was for 60 min at 30°C. Non-specific binding was defined with 2 μM atropine. Assays were terminated and the samples washed and counted for radioactivity as before.

Rat lachrymal gland (M_3) Lachrymal glands were removed from male Sprague-Dawley rats, chopped with scissors, suspended in 10 ml modified Krebs solution buffer with HEPES (pH 7.4) and disrupted by ultrasound as described above. This crude preparation of lachrymal membranes was then homogenized and filtered as described for heart before centrifugation at 35 000 *g* for 20 min. The membrane pellet was resuspended in buffer containing 100 μM Gpp(NH)p at 0.05% wet w/v. Binding was determined in 750 μl homogenate (3.75 mg tissue) and [^{3}H]-NMS (0.1 nM) in a final assay volume of 1 ml. Incubation with radiolabel was for 60 min at 30°C. Non-specific binding was defined with 2 μM atropine. Assays were terminated and the samples washed and counted for radioactivity as before.

Functional pharmacological assays

In all pharmacological assays the drug effects on each tissue preparation have been normalized by relating the responses to drug to the effects of a reference compound as internal standard. In the rat superior cervical ganglion preparation (±)-muscarine was used as the standard to exclude nicotinic effects, whilst in the atria, ileum, and trachea, carbachol was used as the reference compound.

Rat superior cervical ganglion Superior cervical ganglia from male Sprague-Dawley rats were set up as described previously by Newberry & Priestley (1987) as an assay for activity at M_1 muscarinic receptors. Ganglia were excised, desheathed and submerged in a three compartment bath with the ganglion in the central compartment and the pre- and postganglionic nerve trunks projecting through greased gaps into the outer compartments. Each compartment contained 0.5 ml bathing medium (composition mM: NaCl 125, KCl 5, KH_2PO_4 1, $CaCl_2$ 2.5, $MgSO_4$ 1, $NaHCO_3$ 25, glucose 10) equilibrated with 5% CO_2/95% O_2. The central compartment was continuously perfused with gassed medium at a temperature of 25°C and a flow rate of 1–2 ml min^{-1}. Potential difference between the ganglion body and the internal carotid nerve was recorded across the greased gap with Ag/AgCl electrodes and monitored by use of a d.c. amplifier connected to a chart recorder. Before determining the concentration-response relationship to the test compounds, a reproducible response to a superfusion of 1 μM (±)-muscarine chloride was obtained on each ganglion. The test compounds were then superfused at increasing concentrations for a 1 min period at 10 min intervals. Since the response did not return to baseline during the 9 min wash period, calculations were made from the extrapolated baseline. Responses were related to the depolarizing response to the 1 μM (±)-muscarine dose that was given an arbitrary value of 100.

Guinea-pig isolated tissues Isolated tissues (atria, ileum longitudinal muscle-myenteric plexus strips, spiral cut tracheal strips) were obtained from male Dunkin-Hartley guinea-pigs and used in assays for pharmacological activity at M_2 and M_3 muscarinic receptors. Unless otherwise stated, tissues were mounted for isometric tension recording (Dynamometer UFI transducer, Pioden Controls Ltd) in 3 ml siliconized organ baths containing Krebs Henseleit solution (composition mM: NaCl 118, KCl 4.7, $CaCl_2$ 2.5, KH_2PO_4 1.2, $MgSO_4$ 1.2, $NaHCO_3$ 25, glucose 11) and gassed with 95% O_2 and 5% CO_2. The bathing solution for the atria contained 22 mM glucose. The temperature of the bathing medium was 30°C for the atrial and 37°C for the ileum and tracheal preparations. Tissues were allowed to equilibrate under a tension of 1 g for at least 1 h before exposure to test compounds and during this time were washed continuously by overflow of bathing medium.

The isolated atria used as the M_2 assay, were allowed to beat spontaneously during the equilibration period before being paced by electrical field stimulation (3–4 Hz frequency, pulse duration 2–3 ms) at supramaximal voltage using platinum electrodes. Pulses were given a biphasic component by placing a 2 μF condenser in series. On all atrial preparations, non-cumulative concentration-response curves were first constructed to carbachol, allowing exposure to any one application until the maximum negative inotropic effect was observed, before examining the activity of the test compounds.

The longitudinal muscle-myenteric plexus preparation and spiral strips of trachea were first exposed sequentially to increasing concentrations of carbachol. Dose cycles of 10–12 min were used. The contractile responses to the agonist were allowed to reach a clear peak (2–3 min), as shown by a sustained fall in tension from the maximum observed, before washout.

In all preparations to determine agonist potency, the initial concentration-response curve to carbachol was followed by a concentration-response curve to the test compound. A period of at least 45 min was allowed between the curves. With this protocol the initial carbachol concentration-response curve could be reproduced when repeated 45 min later in the tissues in which it was used as the standard agonist. Antagonist activity was examined after the initial concentration-response curve to carbachol by equilibration of the tissues with test compound for at least 30 min before repetition of the carbachol concentration-response curve in the continuing presence of antagonist.

Calculations

Agonist potency was determined by fitting the equation $Y = Y_{max}/1 + (EC_{50}/\text{agonist concentration})^{nH})$ to concentration-response curves by non-linear least squares regression analysis and an iterative procedure in RS1 software. In this equation EC_{50} is the concentration required to evoke a half maximal response (Y_{max}) and nH is the Hill coefficient. Potency was then expressed as the negative $\log_{10}$ EC_{50} (pEC_{50}) and is given for each agonist as the mean ± s.e.mean of the pEC_{50}'s in the preparations used. The activity of the compounds was also assessed by comparing the maximum response produced by the test compound to the maximum produced by the appropriate standard agonist ((±)-muscarine or carbachol) on the same preparation (relative maximum, RM × 100%). Data are given for each agonist as the mean ± s.e.mean of the RM's in the preparations used.

Antagonism was assessed from the degree of rightward shift of the log concentration-response curves to carbachol observed in the presence of antagonist with respect to the control curve (concentration-ratio CR). The CR was calculated at the response level at the EC_{50} in the control curve. Antagonist activity (pA_2) was obtained by the line of best fit (least squares – RS1 software) to the Schild regression (Arunlakshana & Schild, 1959) using four or more observations at each of four or more concentrations of antagonist.

Acetylcholine release from rat hippocampal slices

The methodology used has been described in detail by Nordstrom & Bartfai (1980). Coronal slices (400 μm) of rat hippocampus were prepared with a McIlwain chopper then loaded with 0.1 μM [^{3}H]-choline for 30 min in Krebs buffer (composition mM: NaCl 135, KCl 5, $CaCl_2$ 1.3, KH_2PO_4 1.25, $MgSO_4$ 1, $NaHCO_3$ 25, glucose 10) at 37°C. The slices were then washed 3 times with an equal volume of buffer and transferred to a superfusion apparatus. Slices were allowed to equilibrate at a superfusion rate of 1 ml min^{-1} for 50 min and then given two separate periods of field electrical stimulation (2 min, frequency 3 Hz, current 22 mA, pulse duration 2 ms) with platinum electrodes at 60 and 105 min after the start of superfusion. The superfusion buffer was Krebs containing 10 μM of both hemicholinium and physostigmine. Drugs were introduced into the superfusate 20 min before the second period of electrical stimulation. The effects of the drugs were assessed in terms of (S_2/S_1), the ratio of acetylcholine release in the presence of drug (S_2) to that in its absence (S_1).

Materials

Radioligands were purchased from New England Nuclear ([^{3}H]-N-methylscopolamine, NET 636, 70–87 Ci $mmol^{-1}$, methyl[^{3}H]-oxotremorine-M, NET 671 70–90 Ci $mmol^{-1}$; N-methyl-[^{3}H]-pirenzepine, NET 780, 70–87 Ci $mmol^{-1}$; [^{3}H]-choline chloride, 77.9 Ci $mmol^{-1}$). L-689,660 (1-azabicyclo [2.2.2]octane, 3-(6-chloropyrazinyl)maleate), AF102B (*cis*-2-methylspiro-(1,3,oxatriolane 5,3')-quinuclidine hydrochloride) and RS-86 (2-ethyl 8-methyl-2,8-diazaspiro [4,5]decan 1,3-dione hydrochloride) were synthesized in the Department of Chemistry at Merck Sharp and Dohme, Terlings Park, Harlow. All other compounds were obtained from Sigma Chemical Co.

Results

Receptor binding studies

Table 1 shows the binding profiles of L-689,660, AF102B and RS-86 in the NMS and Oxo-M binding assays in rat cerebral cortex. Data for carbachol, arecoline and atropine (Freedman *et al.*, 1990) are shown for comparison. The results indicate that L-689,660 had 100 fold higher affinity

Table 1 Binding profiles in N-methylscopolamine (NMS)/oxotremorine-M (Oxo-M) assays in rat cerebral cortex

Compound	*[^{3}H]-NMS* (pK_D(app) M)	*[^{3}H]-Oxo-M* (pK_D(app) M)	*NMS/Oxo-M ratio*
Carbachol*	4.66 (0.05)	8.32 (0.12)	4600
Arecoline*	5.21 (0.01)	7.97 (0.04)	580
Atropine*	9.00 (0.03)	9.32 (0.08)	2.1
RS-86	5.32 (0.05)	7.40 (0.07)	120
AF102B	5.51 (0.01)	7.11 (0.05)	40
L-689,660	7.42 (0.02)	8.95 (0.06)	34

Results are given as the $-\log_{10}$ of the apparent affinity constant (pK_D(app)) that has been corrected for ligand occupancy using the Cheng & Prusoff (1973) equation. The values given are arithmetic means of at least 3 separate determinations. Numbers in parentheses indicate the s.e.mean. Inhibition studies were carried out with 0.1 nM [^{3}H]-N-methylscopolamine and 3 nM [^{3}H]-oxotremorine-M. *Data from Freedman *et al.*, 1990.

than AF102B and RS-86 at cortical muscarinic receptors. The similarity of the NMS/Oxo-M ratios for L-689,660 and AF102B predicts that these compounds will have similar activity at cortical muscarinic receptors. The NMS/Oxo-M values for L-689,660 and AF102B are low compared to carbachol and arecoline. Low NMS/Oxo-M values are a characteristic of muscarinic agonists with low efficacy in the cerebral cortex (Freedman *et al.*, 1988). The NMS/Oxo-M ratio for RS-86 is intermediate in value suggesting that it will have greater activity at cortical muscarinic receptors than L-689,660 or AF102B. The NMS/Oxo-M ratio for RS-86 is similar to that reported previously for pilocarpine (Freedman *et al.*, 1988).

Muscarinic receptor subtype selectivity The binding selectivity of L-689,660, AF102B and RS-86 for cortical M_1, cardiac M_2 and glandular M_3 muscarinic receptors is shown in Table 2. The studies measured the low-affinity state of each receptor by the inclusion of 100 μM Gpp(NH)p in all assays. Reference data from concurrent experiments with the selective muscarinic antagonist pirenzepine and the muscarinic agonist McN-A-343 are shown for comparison.

L-689,660 displaced binding at all three muscarinic receptor subtypes with high affinity and showed slight selectivity (5 fold) for cortical M_1 muscarinic receptors, compared with cardiac or glandular muscarinic receptors; AF102B and RS-86 had much lower affinity (100 to 200 fold less) at muscarinic receptors than L-689,660, and less selectivity for the M_1 receptor subtype.

Pharmacological assays Cumulative concentration-depolarization curves for the effects of L-689,660, AF102B and RS-86 on M_1 muscarinic receptors in the rat superior cervical ganglion are shown in Figure 1. L-689,660 was a potent agonist with a maximum response equal to that to muscarine. The maximum responses to AF102B and RS-86 were also similar to those to muscarine but they were 200 fold and 20 fold less potent than L-689,660 respectively. The depolarizing responses to near maximum doses of L-689,660 (0.3 μM), RS-86 (3 μM) and AF102B (100 μM) were completely blocked by pretreatment with 0.1 μM pirenzepine (data not shown).

Figure 2 shows that RS-86 had full agonist activity at M_2 muscarinic receptors in guinea-pig atria and that weak agonist activity was detected with AF102B in this preparation. In contrast, L-689,660 had little agonist activity (maximum $<15\%$ of the maximum to carbachol at 10 μM). L-689,660 antagonized the responses to carbachol producing parallel shifts to the right of the concentration-response curve. The slope of the Schild regression was not significantly different from unity and this is consistent with a competitive interaction at M_2 atrial muscarinic receptors (Figure 3a). The pA_2 for L-689,660 was 7.2 indicating an affinity at M_2 muscarinic receptors that is commensurate with the binding data (Tables 1 and 2).

AF102B was shown also to antagonize the responses of the atria to carbachol. A Schild regression was used to explore

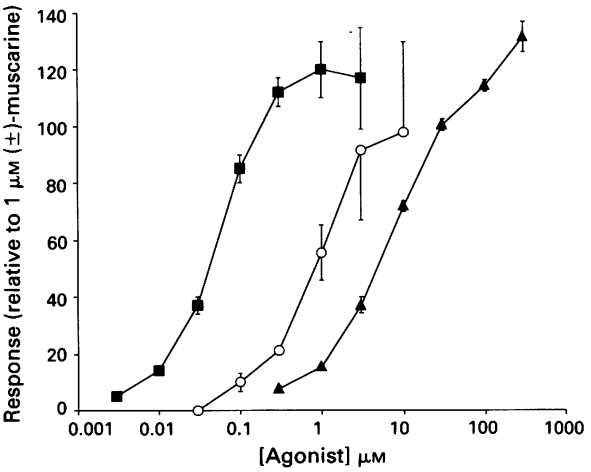

Figure 1 Depolarizing action of L-689,660, AF102B and RS-86 at M_1 muscarinic receptors in rat superior cervical ganglion. Cumulative log concentration-response curves for the effects of L-689,660 (■), AF102B (▲) and RS-86 (○) in the rat superior cervical ganglion. Responses are expressed relative to the response to 1 μM (±)-muscarine. Each point is the mean of four to six observations; s.e.mean shown by vertical bars.

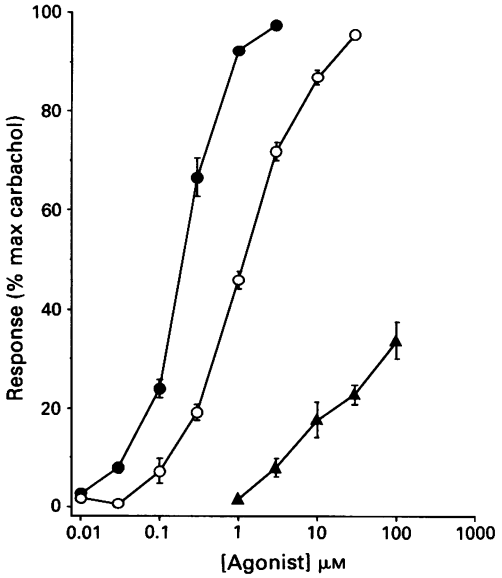

Figure 2 Agonist action of RS-86 and AF102B at M_2 muscarinic receptors in guinea-pig atria. Log concentration-response curves for the negative inotropic effects of carbachol (●), RS-86 (○) and AF102B (▲) on guinea-pig isolated atria. Responses are expressed in terms of the maximum response to carbachol in individual preparations. Each point is the mean of 4–6 separate observations; s.e.mean shown by vertical bars.

Table 2 Selectivity of L-689,660, AF102B, RS-86, McN-A-343 and pirenzepine for muscarinic receptor subtypes in rat tissues

Compound	*Cerebral cortex* M_1 (pK_D(app) M)	*Heart* M_2 (pK_D(app) M)	*Lachrymal gland* M_3 (pK_D(app) M)	*Selectivity* M_2/M_1	M_3/M_1
Pirenzepine	7.82 (0.03)	6.20 (0.05)	6.68 (0.06)	42	14
McN-A-343	5.26 (0.14)	4.39 (0.16)	4.85 (0.15)	7.4	2.6
L-689,660	7.68 (0.04)	6.96 (0.11)	7.04 (0.01)	5.2	4.4
AF102B	5.49 (0.11)	5.04 (0.02)	5.04 (0.07)	2.8	2.8
RS-86	5.41 (0.08)	4.81 (0.13)	5.51	4.0	0.8

Results are expressed as the $-\log_{10}$ of the apparent affinity constant (pK_d(app)) that has been corrected for ligand occupancy by use of the Cheng & Prusoff (1973) equation. The values are arithmetic means of at least 3 independent determinations except RS-86 in the M_3 assay. Numbers in parentheses indicate the s.e.mean.

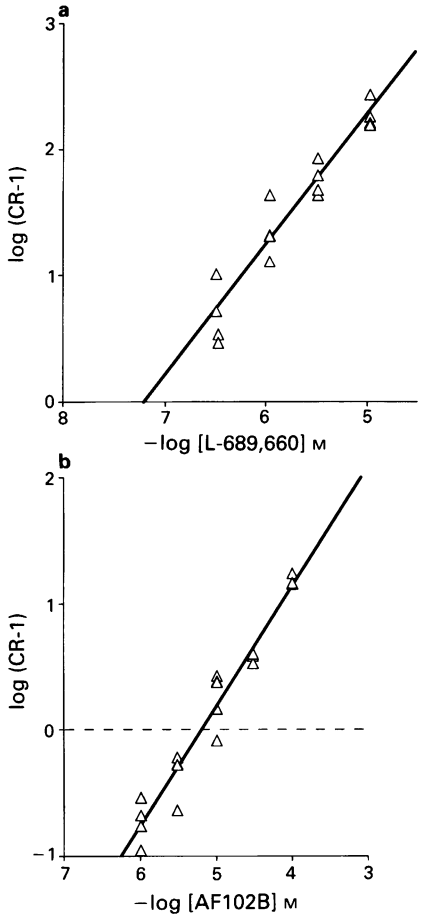

Figure 3 Antagonist action of (a) L-689,660 and (b) AF102B at M_2 muscarinic receptors in guinea-pig atria. Schild plot for the antagonism of carbachol by L-689,660 (△) or AF102B (△) in guinea-pig atria. Points are individual observations for log (CR − 1), $n = 4$ at each concentration. The concentration-ratio was calculated at the EC_{50} as a measure of the rightward shift of the log dose-response curve to carbachol by L-689,660 or AF102B. The lines are the best fit (least squares) to the data points and in neither case is the slope significantly different from unity.

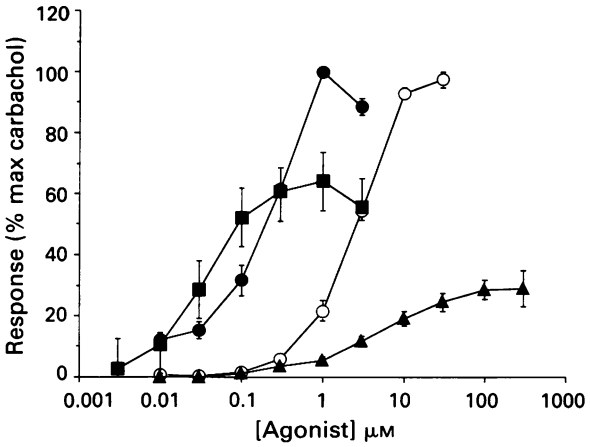

Figure 4 Agonist action of L-689,660, AF102B and RS-86 at M_3 muscarinic receptors in guinea-pig myenteric plexus-longitudinal muscle preparation. Log concentration-response curves for contractions of the ileum to carbachol (●), L-689,660 (■), AF102B (▲) and RS-86 (○). Each point is the mean for RS-86 ($n = 6$), AF102B ($n = 10$) and L-689,660 ($n = 4$); vertical bars show s.e.mean.

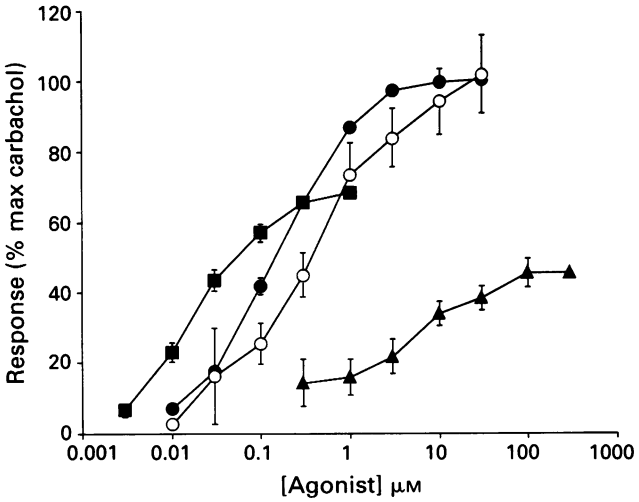

Figure 5 Agonist action of L-689,660, AF102B and RS-86 at M_3 receptors in guinea-pig trachea. Log concentration-response curves for contractions of the trachea spiral strip to carbachol (●), L-689,660 (■), AF102B (▲) and RS-86 (○). Responses are expressed in terms of the maximum response to carbachol in individual preparations. Each point is mean; L-689,660 ($n = 5$), RS-86 ($n = 4$), AF102B ($n = 7$); vertical bars show s.e.mean.

this interaction (see Discussion) and gave a line of best fit that had a slope that was not significantly different from unity. This analysis yielded an apparent pA_2 of 5.2 indicative of an affinity at M_2 muscarinic receptors some 100 times lower than L-689,660 (Figure 3b) in line with the binding data (Tables 1 and 2).

Figure 4 compares the agonist action of L-689,660, AF102B and RS-86 at M_3 muscarinic receptors in the guinea-pig ileum myenteric plexus-longitudinal muscle preparation. In this preparation L-689,660, was a potent agonist although its maximum response was less than could be obtained with carbachol. AF102B was again some 200 times less potent than L-689,660 and its maximum response was lower still than L-689,660. RS-86 was a full agonist with respect to carbachol but was less potent than L-689,660. In the ileum, as in the atria, antagonism of carbachol-induced contractions could be demonstrated with AF102B. Schild analysis (see Discussion) gave a line of best fit with slope of 0.5 and an apparent pA_2 of 5.5 suggestive of low affinity at M_3 muscarinic receptors (data not shown).

The agonist action of L-689,660, AF102B and RS-86 at M_3 receptors in the trachea is shown in Figure 5. The potency and maximum response relative to carbachol of L-689,660 on the trachea were similar to its agonist activity on the guinea-pig ileum. AF102B was again 100 times less potent than L-689,660 and had a lower maximum response. RS-86 was a full agonist at M_3 muscarinic receptors in this tissue although it was more potent than in the ileum.

The effects of L-689,660 or atropine on the release of acetylcholine from rat hippocampal slices is shown in Figure 6. L-689,660 and atropine caused a concentration-dependent increase in electrically-stimulated acetylcholine release from brain slices. Neither compound showed any effect on the basal release of acetylcholine. In the presence of an acetylcholinesterase inhibitor, acetylcholine released by electrical field stimulation is thought to interact with a terminal M_2 muscarinic autoreceptor (Richards, 1990) to reduce release and this is attenuated by muscarinic autoreceptor antagonists (James & Cubeddu, 1984). The present results therefore indicate that L-689,660 has antagonist properties at the muscarinic M_2 autoreceptor in the hippocampus in agreement with the activity detected in the guinea pig atria.

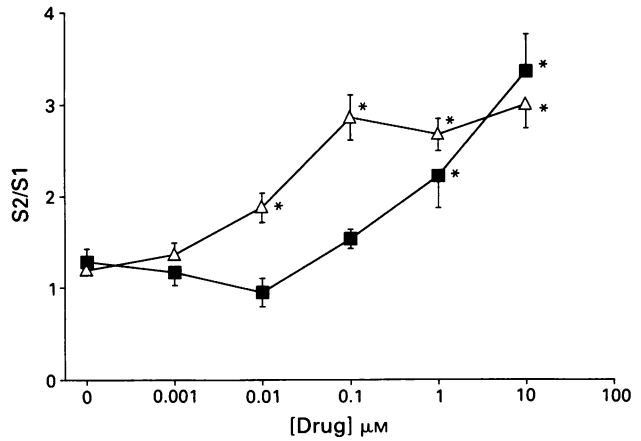

Figure 6 The effects of L-689,660 or atropine on the release of acetycholine from rat hippocampal slices. The actions of L-689,660 (■) and atropine (Δ) are shown as the ratio of electrically evoked acetylcholine release in the presence (S_2) and absence (S_1) of test compound. Results for S_2/S_1 are mean (± s.e mean vertical bars) for atropine ($n = 3-9$) or L-689,660 ($n = 5$). Points of significance are with respect to control period with no added drug ($P < 0.05$, paired t-test).

Discussion

L-689,660 had high affinity for muscarinic receptor binding sites in the rat cerebral cortex (pK_D (apparent) = 7.42). The NMS/Oxo-M ratio for L-689,660 is intermediate in value between that found for pilocarpine (ratio 100) and pirenzepine (ratio 2.2) in our earlier experiments (Freedman *et al.*, 1988). In studies on cortical phosphatidyl inositol turnover in rat cerebral cortex (Freedman *et al.*, 1988), pilocarpine was a partial agonist (pEC_{50} 5.23 with a maximum response relative to 1 mM carbachol of 11%) whilst pirenzepine was an antagonist (pIC_{50} 6.8). L-689,660 would therefore be expected to be a weak partial agonist with only small effects, if any, on phosphatidyl-inositol turnover in the cerebral cortex.

The binding assay values for pirenzepine at M_1, M_2 and M_3 receptors were in excellent agreement with the average affinity constants collated from the literature by Hulme *et al.* (1990) for binding studies using the same mammalian tissues as in the present experiments. The values also agree well, given likely differences in assay conditions, with the affinity of pirenzepine for cloned muscarinic m1, m2 and m3 receptors obtained by transfecting CHO cells with the appropriate muscarinic receptor gene (Buckley *et al.*, 1989).

Despite having no true selectivity for any particular muscarinic receptor subtype in the binding assays, L-689,660 was selective in functional pharmacological assays for tissues containing M_1 and M_3 muscarinic receptors (Table 3). This selectivity presumably reflects the low intrinsic activity of L-689,660 that confers an ability to exploit differences in effective muscarinic receptor reserve (Kenakin, 1986) between the preparations used in the functional studies. However, a further possibility that is not discounted by the present data is that the intrinsic activity of L-689,660 actually differs at the various muscarinic receptor subtypes.

The phenomenon of functional selectivity on the basis of effective receptor reserve was highlighted previously by Eglen & Whiting (1986) in their consideration of the pharmacology of the low efficacy muscarinic agonist McN-A-343. McN-A-343 was shown previously to have an NMS/Oxo-M ratio of 120 predictive of a partial agonist, and to elicit only modest (11%) increases in phosphatidyl inositol turnover in rat cerebral cortex (Freedman *et al.*, 1988). The present observations on L-689,660 together with those on McN-A-343 continue to support the hypothesis (Kenakin, 1986) that apparent receptor site specificity can be obtained with low efficacy partial agonist compounds. The findings also highlight the difficulty of using data from agonists, particularly those with low efficacy, as criteria in receptor classification since the relative potencies in different tissues are dependent critically upon the effective receptor reserve.

Previous studies have demonstrated a pharmacological profile similar to L-689,660 with an oxotremorine analogue, BM-5 (N-methyl-N-(1-methyl-4-pyrrolidino-2-butynyl)acetamide), that was a low efficacy muscarinic agonist with no true muscarinic receptor subtype selectivity (Hawkins *et al.*, 1992). In the guinea-pig ileum, BM-5 was found to antagonize presynaptic muscarinic autoreceptors, but to be an agonist, with lower efficacy than carbachol, at postsynaptic muscarinic sites (Nordstrom *et al.*, 1983). Similar observations have been reported with other oxotremorine-based muscarinic partial agonists that stimulated guinea-pig ileum and blocked muscarinic responses in guinea-pig bladder (Ringdahl, 1987a,b; Ringdahl & Markovicz, 1987). The profile of L-689,660 in the present functional pharmacological assays suggests that the effective muscarinic receptor reserve in the various assay tissues used has the order: rat superior cervical ganglion > guinea-pig ileum = trachea > guinea-pig atria and hippocampal presynaptic receptors.

The present binding results failed to confirm the M_1 muscarinic receptor selectivity claimed (Fisher *et al.*, 1989) for AF102B (Table 2). Despite the much lower potency of AF102B compared to L-689,660, the similarity of their NMS/Oxo-M ratios (Table 1) predicts that these compounds would

Table 3 Summary of the effects of L-689,660, AF102B and RS-86 in functional pharmacological assays

Assay	*L-689,660* (R-enantiomer)	*AF102B* (Racemic)	*RS-86* (Achiral)
M_1 Rat ganglion (pirenzepine-sensitive depolarization)			
pEC_{50}[a]	7.3 ± 0.1	5.1 ± 0.1	6.0 ± 0.2
RM(%)[b]	120 ± 10	130 ± 6	100 ± 24
M_2 Guinea-pig paced atria (negative inotropy)			
pA_2[c]	7.2 (7,7.4)	5.2 (5,5.3)	–
pEC_{50}	–	5.0 ± 0.6	6.0 ± 0.1
RM(%)[d]	–	34 ± 4	98 ± 3
M_3 Guinea-pig ileum (contraction)			
pA_2		5.5 (5.3, 5.6)[e]	
pEC_{50}	7.5 ± 0.2	5.3 ± 0.3	5.6 ± 0.1
RM(%)[d]	64 ± 8	29 ± 5	98 ± 3
M_3 Guinea-pig trachea (contraction)			
pEC_{50}	7.7 ± 0.3	5.4 ± 0.7	6.4 ± 0.2
RM(%)[d]	65 ± 3	44 ± 5	100 ± 10

[a]pEC_{50} = -log EC_{50} ± s.e.mean; [b]relative to the depolarizing responses to 1 μM (±)-muscarine; [c]pA_2 (95% confidence limits); [d]relative to the maximum response of carbachol; [e]apparent pA_2 (slope 0.5).

have similar activity at muscarinic receptors and therefore that their muscarinic activity profiles in isolated tissues would be the same. AF102B was found to be an agonist in M_1 and M_3 assays (confirmed recently by Boddeke & Buttini, 1991) and to antagonize the effects of carbachol on the atria (Table 3).

The weak agonist activity of AF102B detected in the atria complicated assessment of its antagonist profile at these M_2 muscarinic receptors. It is acknowledged that the underlying assumption of the Schild analysis that equal response to agonist in the presence and absence of antagonist represents equal receptor occupancy by the agonist are not strictly met when assessing a partial agonist. Nonetheless, the responses to the addition of the full agonist, carbachol, in the presence of increasing concentrations of AF102B were shifted to the right in a parallel fashion. Plots of the CR − 1 (concentration-ratio − 1) against AF102B concentration yielded graphs that were best fitted by a line with a slope not significantly different from unity, suggesting a competitive interaction (Figure 3b). The apparent pA_2 for AF102B estimated by this analysis was 5.2 indicating an apparent affinity that was commensurate with the binding data for AF102B (Tables 1 and 2). The apparent affinity of AF102B is therefore 100 times lower than L-689,660 ($pA_2 = 7.2$) at M_2 muscarinic receptors in atria when antagonism in M_2 functional assays is measured by Schild analysis. This ratio of 100 is similar to the ratio of 83 for their relative affinities in the M_2 radioligand binding studies (Table 2).

Interpretation of the pharmacological profile of AF102B is further complicated by its low potency and the consequent need to use relatively high concentrations in pharmacological assays thereby incuring a risk of provoking non-specific effects. Furthermore, AF102B is a racemic mixture and the presence within the compound of two different chemical enantiomers, that may have differing agonist profiles adds to the uncertainty in the definition of its activity.

In functional pharmacological assays, RS-86 was a full agonist with similar potency at M_1, M_2 and M_3 receptor subtypes. The potency estimates for RS-86 in rat ganglia and guinea-pig ileum (Table 3) confirm earlier observations with this compound (Palacios *et al.*, 1986). The present binding studies show that RS-86 had no selectivity for muscarinic receptor subtypes and a higher NMS/Oxo-M ratio than L-689,660 (NMS/Oxo-M ratio 120 compared with 34 respectively) that is predictive of greater activity at cortical muscarinic receptors (Tables 1 and 2). Studies *in vivo* with RS-86 (Pazos *et al.*, 1986) have shown that non-selective muscarinic agonists with this level of efficacy have the capacity to induce a range of side effects at CNS-active doses particularly on the cardiovascular system (Brezenoff & Guiliano, 1982; Pazos *et al.*, 1986; Sapru, 1989; Palacios *et al.*, 1990).

The clinical value of functional receptor selectivity achieved by controlling efficacy is difficult to predict. The approach is limited by the relative agonist potency in target versus side-effect tissues being dependent upon their effective receptor reserves and these cannot be manipulated. In the early stages of Alzheimer's disease, M_1 receptors are thought to be relatively preserved (Probst *et al.*, 1988; Araujo *et al.*, 1988; Quirion *et al.*, 1989) whereas M_2 autoreceptors are lost progressively as nerve terminals degenerate (Sims *et al.*, 1985; Mash *et al.*, 1985; Araujo *et al.*, 1988; Palacios *et al.*, 1990). The effective receptor reserve in target tissues relative to others that mediate side-effects may therefore alter when pathological changes occur (Kenakin, 1990). As a result, the pharmacological profile of a partial agonist may change with the progression of a disorder.

There are a number of questions that remain to be answered *in vivo* with L-689,660. Is its efficacy set at a level that will target the abundant m1 and m3 muscarinic receptors in cortex and hippocampus (Buckley *et al.*, 1988; Brann *et al.*, 1988) but remain relatively inactive at cardiovascular M_2 (central and peripheral) and peripheral M_3 receptors that could mediate side-effects? Is there a difference *in vivo* between the apparent effective receptor reserve of postsynaptic and prejunctional M_2 receptor-mediated responses that would favour increased acetylcholine release over M_2-mediated side-effects?

Preliminary accounts of studies *in vivo* with L-689,660 indicate that the potential therapeutic window for low efficacy muscarinic agonists differs from that of higher efficacy compounds. L-689,660 has been shown to produce hypothermia and antinociception through central cholinergic mechanisms (Dawson *et al.*, 1991; Freedman *et al.*, 1991) and to have smaller cardiovascular side-effects at CNS-active doses than the higher efficacy muscarinic agonist RS-86 (Freedman *et al.*, 1991). Studies on the effects of L-689,660 in behavioural tests of long term and working memory are in progress.

The authors would like to thank Mrs E. Brawn and Mr A. Butler for their help in the preparation of this manuscript.

References

ARAUJO, D.M., LAPCHAK, P.A., ROBITAILLE, Y., GAUTHIER, S. & QUIRION, R. (1988). Differential alteration of various cholinergic markers in cortical and subcortical regions of the human brain in Alzheimer's disease. *J. Neurochem.*, **50**, 1914–1923.

ARUNLAKSHANA, O. & SCHILD, H.O. (1959). Some quantitative uses of drug antagonists. *Br. J. Pharmacol. Chemother.*, **14**, 48–58.

BAKER, R., STREET, L.J., REEVE, A.J. & SAUNDERS, J. (1991). Synthesis of azabicyclic pyrazine derivatives as muscarinic agonists and the preparation of a chloropyrazine analogue with functional selectivity at subtypes of the muscarinic receptor. *J. Chem. Soc. Chem. Commun.*, **11**, 760–762.

BARTUS, R.T., DEAN, R.L., BEER, B. & LIPPA, A.S. (1982). The cholinergic hypothesis of geriatric memory dysfunction. *Science*, **217**, 408–417.

BARTUS, R.T., REGINALD, L.D., PONTECORVO, M.J. & FLICKER, C. (1985). The cholinergic hypothesis: a historical overview, current perspective and future directions. In *Memory Dysfunctions: An integration of Animal and Human Research from Preclinical and Clinical perspectives*. ed. Olton, D.S., Gamzu, E. & Corkin, S. pp. 332–358. New York: New York Academy of Sciences.

BODDEKE, H.W.G.M. & BUTTINI, M. (1991). Pharmacological properties of cloned muscarinic receptors expressed in A9 L cells; comparison with *in vitro* models. *Eur. J. Pharmacol.*, **202**, 151–157.

BRANN, M.R., BUCKLEY, N.J. & BONNER, T.I. (1988). The striatum and cerebral cortex express different muscarinic receptor mRNAs. *FEBS Lett.*, **230**, 90–94.

BREZENOFF, H.E. & GUILIANO, R. (1982). Cardiovascular control by cholinergic mechanisms in the central nervous system. *Annu. Rev. Pharmacol. Toxicol.*, **22**, 341–381.

BUCKLEY, N.J., BONNER, T.I. & BRANN, M.R. (1988). Localization of a family of muscarinic receptor mRNAs in rat brain. *J. Neurosci.*, **8**, 4646–4652.

BUCKLEY, N.J., BONNER, T.I., BUCKLEY, C.M. & BRANN, M.R. (1989). Antagonist binding properties of five cloned muscarinic receptors expressed in CHO-K1 cells. *Mol. Pharmacol.*, **35**, 469–476.

CHENG, Y. & PRUSOFF, W.H. (1973). Relationship between the inhibition constant (K_i) and the concentration of inhibitor which causes 50 percent inhibition. *Biochem. Pharmacol.*, **22**, 3099–3108.

DAVIS, P. & MALONEY, A.J.F. (1976). Selective loss of central cholinergic neurons in Alzheimer's disease. *Lancet*, **ii**, 1403.

DAWSON, G.R., JOHNSTONE, S., BAYLEY, P. & IVERSEN, S.D. (1991). The effects of a novel muscarinic receptor agonist, L-689,660 in the mouse tail flick test of antinociception. *Br. J. Pharmacol.*, **104**, 110P.

EGLEN, R.M. & WHITING, R.L. (1986). Muscarinic receptor subtypes: a critique of the current classification and a proposal for a working nomenclature. *J. Auton. Pharmacol.*, **5**, 323–346.

FISHER, A., BRANDEIS, R., KARTAN, I., PITTEL, Z., DACHIR, S., SAPIR, M., GRUNFELD, Y., LEVY, A. & HELDMAN, E. (1989). AF102B: A novel M_1 agonist as a rational treatment strategy in Alzheimer's disease. In *Novel Approaches to the Treatment of Alzheimer's Disease*. ed. Meyer, E.M., Simpkins, J.W. & Yamamoto, J. pp. 11–16. New York & London: Plenum Press.

FREEDMAN, S.B., HARLEY, E.A. & IVERSEN, L.L. (1988). Relative affinities of drugs acting at cholinoceptors in displacing agonists and antagonist radioligands: the NMS/Oxo-M ratio as an index of efficacy at cortical muscarinic receptors. *Br. J. Pharmacol.*, **93**, 437–445.

FREEDMAN, S.B., HARLEY, E.A., PATEL, S., NEWBERRY, N.R., GILBERT, M.J., MCKNIGHT, A.T., TANG, J.K., MAGUIRE, J.J., MUDUNKOTUWA, N.T., BAKER, R., STREET, L.J., MACLEOD, A.M., SAUNDERS, J. & IVERSEN, L.L. (1990). A novel series of non-quaternary oxadiazoles acting as full agonists at muscarinic receptors. *Br. J. Pharmacol.*, **101**, 575–580.

FREEDMAN, S.B., PATEL, S., MARWOOD, R., MCKNIGHT, A.T., NEWBERRY, N., HURLEY, C.J., HILL, R.G. & HARGREAVES, R.J. (1991). The pharmacology *in vivo* of L-689,660, a functionally selective M_1/M_3 muscarinic agonist. *Br. J. Pharmacol.*, **104**, 457P.

GRAY, J.A., ENZ, A. & SPIEGEL, R. (1989). Muscarinic agonists for senile dementia: past experience and future trends. *Trends Pharmacol. Sci.*, **10**, Suppl. 85–88.

HARGREAVES, R.J., MCKNIGHT, A.T., NEWBERRY, N., SCHOLEY, K., TANG, J., STREET, L., BAKER, R., HUTSON, P., SEMARK, J., HARLEY, E.A., PATEL, S. & FREEDMAN, S.B. (1991). L-689,660 a functionally selective agonist at M_1 and M_3 muscarinic receptors. *Br. J. Pharmacol.*, **104**, 456P.

HAWKINS, J., RILEY, G.J., BROWN, F. & CLARK, M.S.G. (1992). Neurodegeneration of the Alzheimer type: muscarinic agonists for counteracting the acetylcholine deficit. Selectivity studies on human muscarinic receptor subtypes hm1-hm4 expressed in CHO cells. In *Neurodegeneration*. ed. Hunter, A.J. & Clark, M. p. 240 London: Academic Press.

HOLLANDER, E., MOHS, R.C. & DAVIS, K.L. (1986). Cholinergic approaches to the treatment of Alzheimer's disease. *Br. Med. Bull.*, **42**, 97–100.

HULME, E.C., BIRDSALL, N.J.M. & BUCKLEY, N.J. (1990). Muscarinic receptor subtypes. *Annu. Rev. Pharmacol. Toxicol.*, **30**, 633–673.

JAMES, M.K. & CUBEDDU, L.X. (1984). Frequency-dependent muscarinic receptor modulation of acetylcholine and dopamine release from rabbit striatum. *J. Pharmacol. Exp. Ther.*, **229**, 98–104.

KENAKIN, T.P. (1986). Tissue and receptor selectivity: similarities and differences. *Adv. Drug Res.*, **15**, 71–109.

KENAKIN, T. (1990). Drugs and receptors: an overview of the current state of knowledge. *Drugs*, **40**, 666–687.

MASH, D.C., FLYNN, D.D. & POTTER, L.T. (1985). Loss of M_2 muscarinic receptors in the cerebral cortex in Alzheimer's disease and experimental cholinergic denervation. *Science*, **228**, 1115–1117.

NEWBERRY, N.R. & PRIESTLY, T. (1987). Pharmacological differences between two muscarinic receptor responses of the rat superior cervical ganglion *in vitro*. *Br. J. Pharmacol.*, **93**, 817–826.

NORDSTROM, O. & BARTFAI, T. (1980). Muscarinic autoreceptors regulate acetylcholine release in rat hippocampus. *Acta Physiol. Scand.*, **108**, 347–353.

NORDSTROM, O., ALBERTS, P., WESTLIND, A., UNDEN, A. & BARTFAI, T. (1983). Presynaptic antagonist – post synaptic agonist at muscarinic cholinergic synapses. N-methyl-N-(1-methyl-4-pyrrolidine-2-butynyl)acetamide. *Mol. Pharmacol.*, **24**, 1–5.

PALACIOS, J.M., BOLLIGER, G., CLOSSE, A., ENZ, A., GMELIN, G. & MALANOWSKI, J. (1986). The pharmacological assessment of RS-86 (2-ethyl-8-methyl-2,8-diazospiro-[4,5]-decan-1,3-dion hydrobromide). A potent, specific muscarinic acetylcholine receptor agonist. *Eur. J. Pharmacol.*, **125**, 45–62.

PALACIOS, J.M., MENGOD, G., VILARO, M.T., WIEDERHOLD, K.H., BODDEKE, H., ALVAREZ, F.J., CHINAGLIA, G. & PROBST, A. (1990). Cholinergic receptors in the rat and human brain: microscopic visualization. *Progr. Brain Res.*, **84**, 243–254.

PAZOS, A., WIEDERHOLD, K.H. & PALACIOS, J.M. (1986). Central pressor effects induced by muscarinic receptor agonists: evidence for a predominant role of the M_2 receptor subtype. *Eur. J. Pharmacol.*, **125**, 63–70.

PERRY, E.K., PERRY, R.H., BLESSED, G. & THOMLINSON, B.E. (1977). Necropsy evidence of central cholinergic deficits in senile dementia. *Lancet*, **i**, 189.

PERRY, E.K. (1986). The cholinergic hypothesis – ten years on. *Br. Med. Bull.*, **42**, 63–69.

PROBST, A., CORTES, R., ULRICH, J. & PALACIOS, J.M. (1988). Differential modification of muscarinic cholinergic receptors in the hippocampus of patients with Alzheimer's disease: an autoradiographic study. *Brain Res.*, **45**, 190–201.

QUIRION, R., AUBERT, I., LAPCHAK, P.A., SCHAUM, R.P., TEOLIS, S., GAUTHIER, S. & ARAUJO, D.M. (1989). Muscarinic receptor subtypes in human neurodegenerative disorders: focus on Alzheimer's disease. *Trends Pharmacol. Sci.*, **10**, Suppl. 80–85.

RICHARDS, M.H. (1990). Rat hippocampal muscarinic autoreceptors are similar to the M_2 (cardiac) subtype: comparison with hippocampal M_1, atrial M_2 and ileal M_3 receptors. *Br. J. Pharmacol.*, **99**, 753–761.

RIDLEY, R.M., AITKEN, D.M. & BAKER, H.F. (1989). Learning about rules but not about reward is impaired following lesions of the cholinergic projection to the hippocampus. *Brain Res.*, **502**, 306–318.

RIDLEY, R.M., BAKER, H.F., DREWETT, B. & JOHNSON, J.A. (1985). Effects of ibotenic acid lesions of the basal forebrain on serial reversal learning in marmosets. *Psychopharmacology*, **86**, 438–443.

RIDLEY, R.M., MURRAY, T.K., JOHNSON, J.A. & BAKER, H.F. (1986). Learning impairment following lesion of the basal nucleus of Meynert in the marmoset: modification by cholinergic drugs. *Brain Res.*, **376**, 108–116.

RINGDAHL, B. (1987a). Selectivity of partial agonists related to oxotremorine based on differences in muscarinic receptor reserve between the guinea pig ileum and urinary bladder. *Mol. Pharmacol.*, **31**, 351–356.

RINGDAHL, B. (1987b). Structural requirements for affinity and efficacy of N-(4-amino-2-butynyl)succinimides at muscarinic receptors in the guinea pig ileum and urinary bladder. *Eur. J. Pharmacol.*, **139**, 13–23.

RINGDAHL, B. & MARKOWICZ, M.E. (1987). Muscarinic and antimuscarinic activity of acetamides related to oxotremorine in the guinea pig urinary bladder. *J. Pharmacol. Exp. Ther.*, **240**, 789–794.

SAPRU, H.N. (1989). Cholinergic mechanisms subserving cardiovascular function in the medulla and spinal cord. *Progr. Brain Res.*, **81**, 171–179.

SIMS, N.R., BOWEN, D.M., ALLEN, S.J., SMITH, C.C.T., NEARY, D., THOMAS, D.J. & DAVISON, A.N. (1985). Presynaptic cholinergic dysfunction in patients with dementia. *J. Neurochem.*, **40**, 503–509.

(Received March 6, 1992
Revised June 8, 1992
Accepted June 9, 1992)

Br. J. Pharmacol. (1992), **107**, 502–509

Effects of long-term oral administration of amiodarone on the electromechanical performance of rabbit ventricular muscle

[1] Itsuo Kodama, Ryoko Suzuki, Kaichiro Kamiya, Hirokazu Iwata & Junji Toyama

Department of Circulation, Research Institute of Environmental Medicine, Nagoya University, Nagoya 464-01, Japan

1 The effects of long-term administration of oral amiodarone on transmembrane action potential and contraction of ventricular muscle were investigated in rabbits.

2 ECGs of rabbits that received oral amiodarone 50 mg or 100 mg kg^{-1} daily for 4 weeks, showed a significant prolongation of RR, QT and corrected QT (QTc) intervals, whereas PQ and QRS were unaffected. Serum and myocardial tissue amiodarone concentrations were 0.14–0.18 $\mu g\ ml^{-1}$ and 1.47–3.63 $\mu g\ g^{-1}$ wet wt. respectively.

3 Right ventricular papillary muscles isolated from treated rabbits were characterized by a moderate prolongation of action potential duration (APD) compared with controls. A slight decrease of the maximum upstroke velocity ($\dot{V}_{max}$) was also observed at the higher dose. The APD prolongation by chronic amiodarone, unlike acute effects of sotalol, E-4031, Cs^+ and 4-aminopyridine, did not show marked reverse use-dependence.

4 APD and $\dot{V}_{max}$ restitution following slow basic stimuli (0.03 Hz) were unaffected by chronic treatment with amiodarone.

5 Acute application of amiodarone (10 μM) caused a significant decrease in APD and developed tension, as well as a marked use-dependent $\dot{V}_{max}$ inhibition with fast recovery kinetics.

6 These findings suggest that a major and consistent electro-physiological effect of chronic amiodarone is repolarization delay (Class-III action) showing minimal frequency-dependence. However, when amiodarone above a certain concentration is present in the extracellular space, a fast kinetic Class-I action would be added as an acute effect.

Keywords: Amiodarone; ventricular muscle; action potential; $\dot{V}_{max}$; frequency-dependence

Introduction

It is now well established that long-term treatment of patients with oral amiodarone is extremely effective for prophylactic control of most supraventricular and ventricular tachyarrhythmias (Heger *et al.*, 1984; Zipes *et al.*, 1984). Amiodarone has long been referred to as a Class III antiarrhythmic agent, because it prolongs both the action potential duration (APD) and the refractory period of cardiac muscle especially when administered chronically (Vaughan Williams, 1984). Many recent studies, however, have shown that the pharmacological actions of this compound are complex. For instance, it possesses an inhibitory effect on the fast sodium channels as well as on the slow calcium channels (Mason, 1987; Singh *et al.*, 1989). Amiodarone also has non-competitive antisympathetic effects and an action to modulate thyroid function (Singh, 1990). Which action or which combinaiton of actions is fundamental and salutory for its potent antiarrhythmic activity is not known. This question is still a matter of debate, and no unequivocal answer has been presented. In order to obtain further insight into this point, we investigated the electromechanical performance of ventricular muscles isolated from rabbits following long-term oral administration of amiodarone, since this animal (and the dog) are more predictive for cardiac electrophysiology in man than any other species. Our major aims were to determine whether chronic amiodarone exerts use-dependent sodium channel inhibitory actions like local anaesthetic type (Class I) antiarrhythmic drugs, and whether the Class III action of chronic amiodarone depends on stimulation frequency. We also examined the acute effects of amiodarone in some experiments to obtain a better understanding of its total electropharmacological profile.

[1] Author for correspondence.

Methods

Experimental protocol

Japanese white rabbits of either sex weighing 1.8 to 2.2 kg were treated for 4 weeks with oral amiodarone. The dose was 20 mg kg^{-1} daily for 5 rabbits, 50 mg kg^{-1} daily for 8 and 100 mg kg^{-1} daily for 6 rabbits. On the last day of drug treatment, peripheral venous blood sampling was carried out to measure serum amiodarone concentrations. Scalar electrocardiograms (ECGs) of extremity leads (I, II) were also recorded from the conscious rabbits caged in a small dark box. The rabbits were then killed by intravenous administration of pentobarbitone sodium (30 mg kg^{-1}), and the right ventricular papillary muscles removed. Fifteen untreated rabbits of corresponding weight were used as references. The muscles (0.4 to 0.6 mm in diameter and 3 to 4 mm in length) were mounted in a tissue bath (0.5 ml) and superfused at 32°C with Krebs-Ringer solution gassed with 95% O_2 and 5% CO_2. The composition of the solution was as follows (in mM): NaCl 120.3, KCl 4.0, $CaCl_2$ 1.2, $MgSO_4$ 1.3, $NaHCO_3$ 25.2 and glucose 5.5 (pH 7.4). The base of the muscle was fixed, and the tendinous end connected to a force-displacement transducer (Nihon Kohden TB 612T) for isometric tension recording. The resting tension was adjusted to obtain maximal twitch contraction during the equilibration period. The preparation was stimulated through a pair of 1.0 mm platinum wire electrodes placed 1 mm apart on either side of the muscle. By means of this field stimulation technique, the whole muscle was excited simultaneously, and no conduction occurred within the preparation. Unless otherwise stated, pulses used for stimulation were 2 ms in duration and 1.2 times diastolic threshold. Transmembrane potential was recorded through two glass microelectrodes filled with 3 M KCl, one intracellularly and the other extracellularly,

placed close together. The electrodes were each connected by Ag-AgCl wire to a high input-impedance buffer amplifier connected to a differentiated amplifier (Nihon Kohden, MEZ-7101). The maximum upstroke velocity ($\dot{V}_{max}$) of the action potential was obtained by electronic differentiation. Action potential duration (APD) was measured by an electronic device, which produced a ramp voltage corresponding to APD at a given level of membrane potential (Kentish & Boyett, 1983). Single cell impalements of the microelectrodes were maintained throughout each experiment.

A stabilization period of 3 to 4 h under constant stimulation at 1.0 Hz was allowed before data were collected. Frequency-dependent effects were assessed during fixed-rate pacing at cycle lengths of 10 s, 5 s, 2 s, 1 s, 500 ms and 330 ms. Measurements at steady-state were obtained 3 to 5 min after pacing at each cycle length. To study restitution of the action potential configuration, regular basic stimuli at a long cycle length (30 s) were followed by a single test stimuli with various coupling intervals. The intensity of the test stimulus was adjusted to obtain a constant latency from the stimulus artifact to the initiation of the action potential upstroke.

In some experiments, amiodarone (1, 10 μM), Cs (5 mM), 4-aminopyridine (4-AP, 2 mM), E-4031 (N-[4-[[1-[2-(6-methyl-2-pyridinyl)ethyl]-4-piperidinyl]carbonyl]phenyl]methane sulphonamide dihydrochloride dihydrate; 0.1 μM) and sotalol (30 μM) were added to the superfusate for 30 to 180 min to examine their acute effects.

All the data were digitized at a sampling interval of 5 kHz for ECGs, action potentials and contraction curves, or at 20 kHz for the derivative of action potential upstroke, and recorded on a magnetic tape (SONY PC-108M) for off-line computer analysis (NEC 9801-DA). From 16 s consecutive ECG records of each rabbit, mean values of RR, PQ, QT and QRS intervals were calculated through the use of ECG processing software (Softron EP98-1). The mean QT interval was divided by the root mean of the RR interval to provide the corrected QT interval (QTc). Parameters measured in papillary muscles were resting membrane potential (RP), amplitude of action potential (AMP), $\dot{V}_{max}$, APD at − 70 mV, peak developed tension (DT) and time to peak tension (tPT).

Blood samples withdrawn into heparinized tubes were centrifuged at room temperature, and the serum removed and frozen. The ventricle remaining after excision of the papillary muscle was also frozen. Amiodarone and its major active metabolite, desethylamiodarone in the serum and in the ventricular myocardial tissues homogenates were measured by high performance liquid chromatography as modified by Brien *et al.* (1983). The limit of sensitivity for amiodarone and desethylamiodarone was 0.025 μg ml^{-1} of serum and 0.1 μg g^{-1} wet weight of ventricular tissue samples.

Drugs and data analysis

Amiodarone HCl was kindly donated by Taisho Pharmaceutical Co. Ltd. (Tokyo, Japan), and E-4031 by Eisai Pharmaceutical Co. Ltd. (Tokyo, Japan). Sotalol and 4-aminopyridine (4-AP) were purchased from Sigma Chemical Co. E-4031, sotalol and 4-AP were dissolved in deionized water and diluted with superfusate (Krebs-Ringer solution) to achieve the final concentrations required. In experiments to test the acute effects of amiodarone, the compound was dissolved in Krebs-Ringer solution containing ethanol (0.005–0.05 mg 100 ml^{-1}) and bovine serum albumin (0.1–1.0%) as described previously (Honjo *et al.*, 1991). At the concentration used in the present study (1–10 μM), there was no visible precipitation of amiodarone in the superfusate.

Values given are means or means ± s.e. One-way analysis of variance with an *F*-test was applied to evaluate the chronic effects of amiodarone in comparison with control animals. Dunnett's test was used, and differences were considered significant at $P<0.05$. The time course of $\dot{V}_{max}$ recovery was defined using a least square exponential fitting routine.

Results

Electrocardiograms and amiodarone concentration

There were no significant differences in RR, PQ, QT and QRS intervals between untreated conscious control rabbits and rabbits that received amiodarone at 20 mg kg^{-1} daily (data not shown). In rabbits that received amiodarone at 50 mg or 100 mg kg^{-1} daily, RR, QT and QTc were significantly prolonged in comparison with controls (Table 1); PQ and QRS remained unchanged.

Table 2 summarizes serum and myocardial tissue amiodarone concentrations in rabbits which received amiodarone at 50 mg and 100 mg kg^{-1} daily. Amiodarone levels in both serum and myocardium tended to be higher in the 100 mg kg^{-1} daily group than in the 50 mg kg^{-1} daily group. These differences were not however statistically significant because of relatively large variability among the animals. Desethylamiodarone concentrations in 100 mg kg^{-1} daily group were 0.04 ± 0.01 μg ml^{-1} in serum ($n = 6$), and 2.18 ± 0.48 μg g^{-1} wet weight in myocardium ($n = 6$).

Action potential characteristics and contraction in papillary muscles

Steady-state action potentials and contractions during stimulation at 1.0 Hz were compared. There were no significant differences in RP, AMP, $\dot{V}_{max}$, DT and tPT between muscles excised from control animals and those taken from animals treated with 20 mg kg^{-1} daily amiodarone. In muscles from the 50 mg kg^{-1} daily amiodarone group, APD at − 70 mV was significantly prolonged, whereas RP, AMP, $\dot{V}_{max}$, DT and tPT were similar to control (Table 3). In muscles from the 100 mg kg^{-1} daily amiodarone group, APD was further prolonged. A slight decrease in $\dot{V}_{max}$ and DT was also observed, but RP, AMP and tPT were still unchanged (Table 3, Figure 1).

When the cycle length of stimulation to the control preparations was shortened in steps from 10 s (0.1 Hz) to 330 ms (3.0 Hz), APD was initially increased and then decreased resulting in a bell-shaped frequency-response curve (Figure 2). The longest APD was obtained at a cycle length of 2.0 s (0.5 Hz). $\dot{V}_{max}$ was slightly decreased at a cycle length

Table 1 Effects of oral amiodarone administration on electrocardiograms (ECGs) of rabbits

	(n)	*RR* (ms)	*PQ* (ms)	*QRS* (ms)	*QT* (ms)	*QTc*
Control	15	257 ± 8	47 ± 2	40 ± 3	156 ± 6	308 ± 7
Amiodarone						
50 mg kg^{-1} daily	8	315 ± 20**	51 ± 1	43 ± 2	196 ± 9**	353 ± 9**
100 mg kg^{-1} daily	6	300 ± 23*	51 ± 2	45 ± 4	198 ± 11**	363 ± 7**

Values are means ± s.e. *n*: number of rabbits treated or untreated with oral amiodarone for 4 weeks.
Significant difference from control at *$P<0.05$ and at **$P<0.01$.

shorter than 1.0 s (Figure 3a). Since, the $\dot{V}_{max}$ reduction was not accompanied by a decrease in RP, it may reflect insufficient recovery of sodium channels from the slow inactivation (Saikawa & Carmeliet, 1982). DT was increased progressively at the shorter cycle length reflected in a positive staircase of contraction (Figure 3b).

In the preparations treated with amiodarone, 50 mg or 100 mg kg^{-1} daily, APD was prolonged over the entire range of cycle lengths (Figures 1 and 2). Absolute changes in APD from control were larger at the longer cycle length within a range from 330 ms to 2.0 s (Table 4). However, the frequency-dependence of APD prolongation by chronic amiodarone was relatively small, and the bell-shaped cycle length-APD relationship as observed for controls was well preserved (Figure 2). The frequency-response relationship of $\dot{V}_{max}$ and that of DT were also essentially unchanged from control (Figure 3).

Figure 4 compares the percentage changes of APD by chronic amiodarone with those induced by acute application of 4-AP (2 mM), Cs (5 mM), E-4031 (0.1 μM) and sotalol (30 μM). With the exception of 4-AP, all the drugs tested prolonged APD even at the shortest cycle length. The APD prolongation by E-4031, sotalol, Cs and 4-AP was enhanced progressively at the longer cycle length, giving rise to a marked 'reverse use-dependence' (Hondeghem & Snyder, 1990). Chronic amiodarone differed from the other drugs in that such a marked reverse use-dependence was not seen.

Table 2 Serum and myocardial concentration of amiodarone

	(n)	*Serum* ($\mu g\ ml^{-1}$)	*Myocardial tissue* ($\mu g\ g^{-1}$)
Amiodarone			
50 mg kg^{-1} daily	(8)	0.14 ± 0.05	1.47 ± 0.48
100 mg kg^{-1} daily	(6)	0.18 ± 0.06	3.63 ± 1.20

Values are means ± s.e. *n*: number of rabbits treated with oral amiodarone for 4 weeks.

Restitution of action potential configuration

Restitution of the action potential configuration was examined by applying a single test stimulus following a very slow basic cycle length (30 s) with various coupling intervals. As in controls, $\dot{V}_{max}$ recovered rapidly after full repolarization of the basic action potential in muscles taken from animals given amiodarone, 100 mg kg^{-1} daily. The recovery process was approximated by a single exponential function with a time constnat (τR) of 42 ± 11 ms ($n = 4$) for amiodarone-

Table 3 Effects of chronic oral amiodarone on transmembrane action potential and contraction in rabbit papillary muscle

	(n)	*RP* (*mV*)	*AMP* (*mV*)	$\dot{V}_{max}$ ($V\ s^{-1}$)	*APD* − 70 mV (*ms*)	*DT* (*mg*)	*tPT* (*ms*)
Control	(15)	− 88 ± 1	120 ± 2	209 ± 11	277 ± 7	288 ± 41	169 ± 6
Amiodarone							
50 mg kg^{-1} daily	(8)	− 90 ± 1	121 ± 2	196 ± 6	312 ± 8*	218 ± 32	171 ± 6
100 mg kg^{-1} daily	(6)	− 87 ± 1	119 ± 1	172 ± 8*	333 ± 6*	207 ± 29*	175 ± 8

Values are means ± s.e. *n*: number of rabbits. Oral amiodarone was administered at a dose of 50 mg kg^{-1} daily or 100 mg kg^{-1} daily for 4 weeks. RP: resting membrane potential. AMP: amplitude of action potential. $\dot{V}_{max}$: the maximum upstroke velocity of action potential. APD − 70 mV: action potential duration at − 70 mV. DT: peak developed tension. tPT: time to peak tension. Significantly different from control at $^*P < 0.05$.

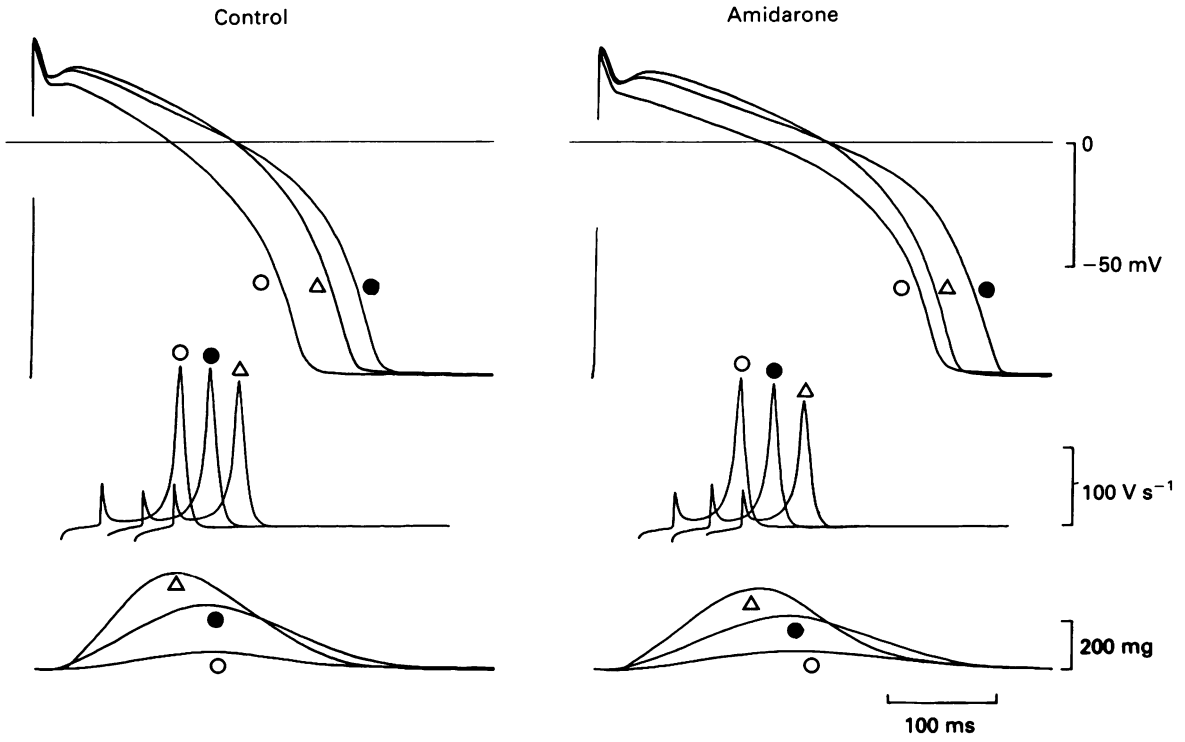

Figure 1 Effects of chronic amiodarone on transmembrane action potential and contraction of rabbit papillary muscles. The preparations from an untreated rabbit (control) and a rabbit treated with amiodarone (100 mg kg^{-1} daily) were stimulated at 0.1 Hz (○), 1.0 Hz (●) and 3.0 Hz (△). The differentiated upstroke spike ($\dot{V}_{max}$) of the action potential (middle traces) was recorded at a faster sweep velocity.

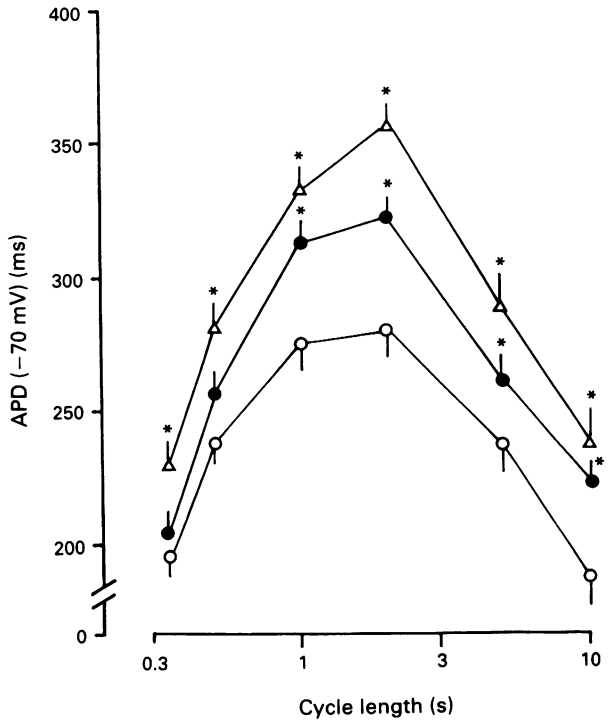

Figure 2 Relationship between action potential duration and stimulation frequency. Ordinate scale: action potential duration (APD) at − 70 mV. Abscissa scale: cycle length of stimulation. Data were obtained from 15 untreated preparations (control, ○), 8 treated with 50 mg kg^{-1} daily amiodarone (●) and 6 with 100 mg kg^{-1} daily amiodarone (△). Values are means; vertical lines show s.e.mean. *The change was statistically significantly different from control at $P<0.05$.

treated preparations and 38 ± 9 ms ($n = 4$) for untreated ones. There was no significant difference between the two values.

Figure 5 shows restitution of APD. In both control and amiodarone-treated muscles, increasing the coupling interval from 200 ms induced a progressive increase in APD reaching a peak at around 300 to 400 ms. Further prolongation of the coupling interval was associated with a gradual shortening of APD toward the level of basic action potential. Percentage decrease of APD in association with a prolongation of coupling interval from 400 ms to 10 s was 46 ± 5% in control preparations ($n = 4$). Comparable values (41 ± 6%, $n = 4$) were obtained in amiodarone-treated muscles.

Acute effects of amiodarone

In the above-mentioned experiments, papillary muscles were superfused with drug-free Krebs-Ringer solution for longer than 3 h. In other words, the data were obtained, unlike *in vivo* experiments or clinical cases, in the presence of negligible extracellular levels of amiodarone. We, therefore, tested the additional acute effects of amiodarone in four preparations which had been pretreated with oral amiodarone, 100 mg kg^{-1} daily for 4 weeks.

Application of 1 μM amiodarone to the superfusate for 120 to 180 min caused no significant changes in action potential configuration or in contractility (data not shown). Application of amiodarone at 10 μM resulted in a significant shortening in APD and a decrease in DT at all the stimulation

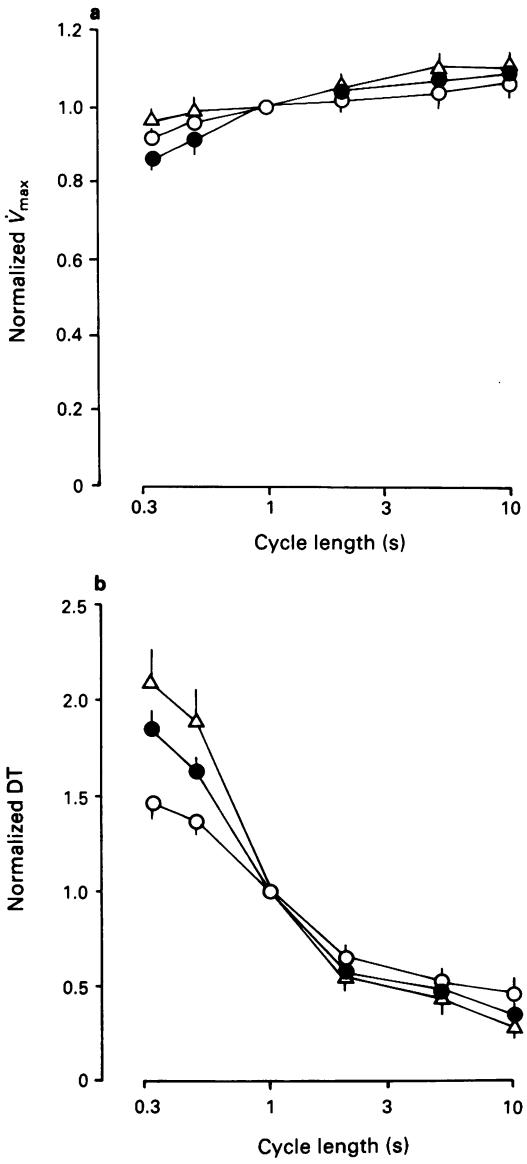

Figure 3 Frequency-response relationship of the maximum upstroke velocity ($\dot{V}_{max}$) and the peak developed tension (DT). Ordinate scale: $\dot{V}_{max}$ (a) and DT (b) normalized by the values at 1.0 Hz stimulation. Abscissa scales: cycle length of stimulation. Data were obtained from 15 untreated preparations (control, ○), 8 treated with 50 mg kg^{-1} daily amiodarone (●), and 6 with 100 mg kg^{-1} daily amiodarone (△). Values are means; vertical lines show s.e.mean.

Table 4 Prolongation of action potential duration in rabbit papillary muscles by chronic treatment with amiodarone

		Cycle length (s)					
	(n)	0.33	0.5	1.0	2.0	5.0	10.0
Amiodarone							
50 mg kg^{-1} daily	(8)	+ 11	+ 19	+ 38	+ 43	+ 24	+ 36
100 mg kg^{-1} daily	(6)	+ 34	+ 43	+ 58	+ 75	+ 52	+ 50

Values are absolute differences (ms) in means of action potential duration (APD) at − 70 mV between amiodarone-treated groups and control ($n = 15$). Data were obtained from the same experiments as in Figure 2.

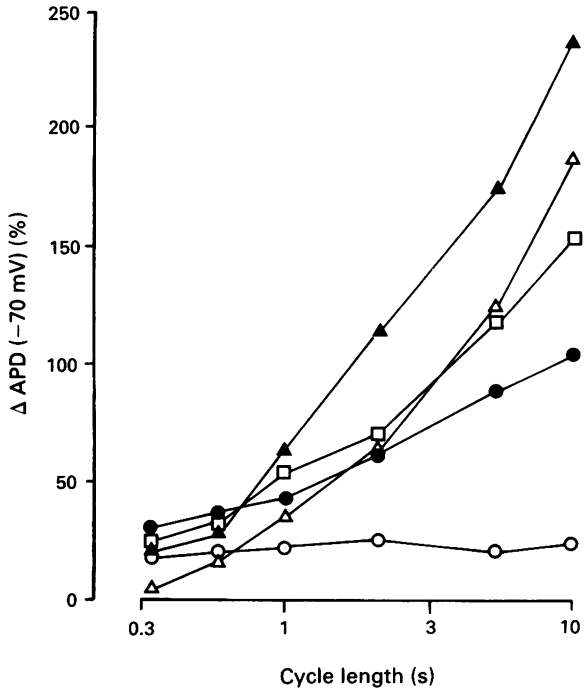

Figure 4 Frequency-dependence of APD prolongation by chronic amiodarone and by acute application of Cs, 4-aminopyridine (4-AP), E-4031 or sotalol in rabbit papillary muscles. Ordinate scale: percentage prolongation of action potential duration (APD) at −70 mV compared with control. Abscissa scale: cycle length of stimulation. Values are means of 6 preparations treated with 100 mg kg^{-1} daily amiodarone (○), and 4 treated with acute application of Cs 5 mM (▲), 4-AP 2 mM (△), E-4031 0.1 μM (●) or sotalol 30 μM (□).

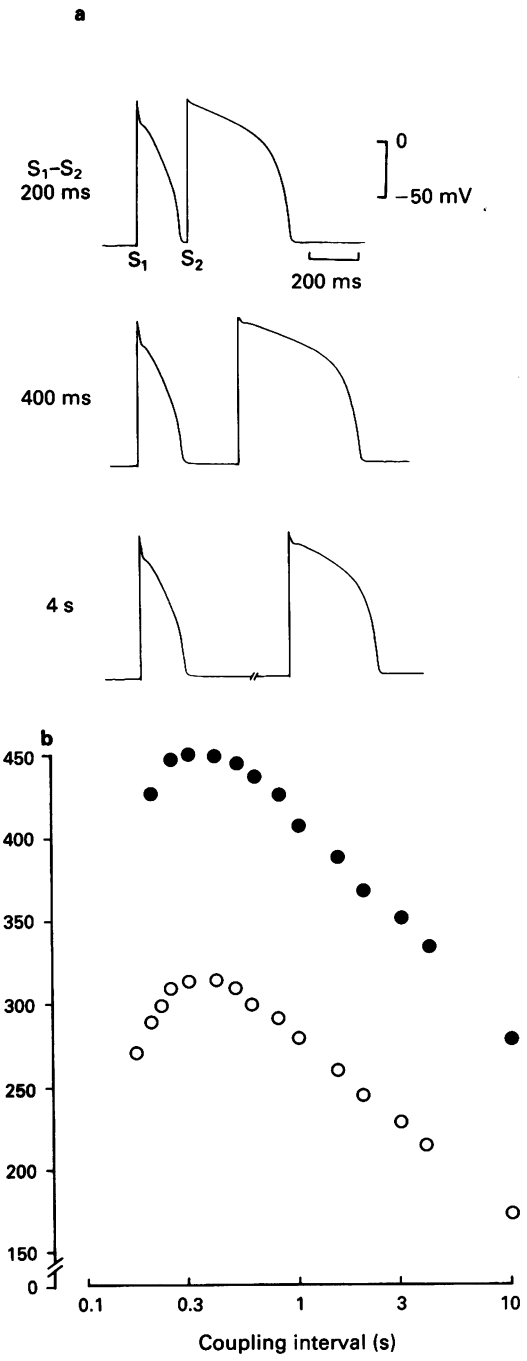

Figure 5 Restitution of action potential duration (APD) of rabbit papillary muscle. Panel (a) shows action potentials elicited by a slow basic stimulus (S1−S1 = 30 s) followed by a test stimulus (S2) with a coupling interval of 200 ms, 400 ms and 4 s. The records were obtained from a preparation treated with amiodarone (100 mg kg^{-1} daily). In (b) are shown restitution curves of APD at −70 mV in the amiodarone-treated muscle (●) and in control muscle (○).

frequencies used (0.1 to 3.0 Hz) (Figure 6). $\dot{V}_{max}$ was also decreased significantly at a frequency higher than 1.0 Hz.The higher the stimulation frequency, the greater the $\dot{V}_{max}$ reduction. Thus, the $\dot{V}_{max}$ inhibition by acute amiodarone was 'use-dependent'.

The recovery of $\dot{V}_{max}$ from use-dependent block was studied by applying a single test stimulus at various coupling intervals following a simulation train for 60 s at 1.0 Hz. Before the addition of amiodarone to the superfusate, $\dot{V}_{max}$ of the test action potential recovered almost completely within 100 ms of full repolarization. After addition of 10 μM amiodarone, a much slower recovery of $\dot{V}_{max}$ was observed (Figure 7). The recovery time course of $\dot{V}_{max}$ with a diastolic interval longer than 100 ms was approximated by a single exponential function with a mean time constant of 452 ± 23 ms ($n = 4$).

Similar APD shortening and use-dependent $\dot{V}_{max}$ inhibition were obtained when 10 μM amiodarone was added to untreated (control) papillary muscle preparations (data not shown).

Discussion

The present study showed that long-term oral administration of amiodarone (50 mg and 100 mg kg^{-1} daily for 4 weeks) caused a significant prolongation of action potential duration (APD) of rabbit papillary muscles. The muscles treated by the higher dose of amiodarone (100 mg kg^{-1} daily) also showed a slight decrease in $\dot{V}_{max}$ and peak developed tension (DT); the changes were independent of stimulation frequencies. The APD prolongation by chronic amiodarone was quite different from that induced by acute application of sotalol, E-4031, Cs and 4-AP in terms of their frequency-dependence; the former was enhanced only minimally, whereas the latter was greatly enhanced at the lower stimulation frequency within a range from 0.1 to 3.0 Hz.

There is a general agreement between previous investigators that chronic treatment of mammals with amiodarone for several weeks causes moderate prolongation of APD throughout the entire heart (Mason, 1987; Singh *et al.*, 1989). However, only limited information is available as to the frequency-dependence of this Class III action. Anderson *et al.* (1989) demonstrated in dogs *in vivo* that repolarization intervals and refractory periods of epicardial ventricular muscle assessed by surface electrograms were prolonged to a similar extent over stimulation frequencies ranging from 1 to

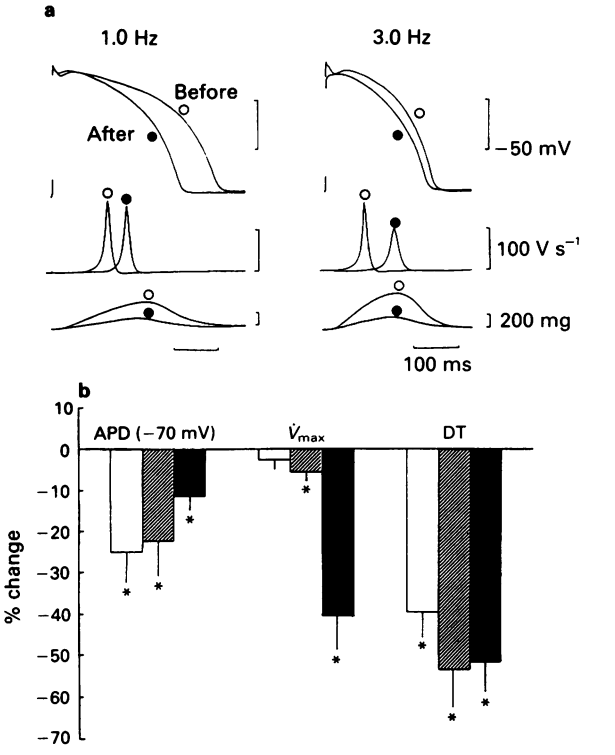

Figure 6 Effects of acute amiodarone on transmembrane action potential and force of contraction of papillary muscles. In (a) are shown superimposed records of membrane action potential (top traces), their differentiated upstroke spikes (middle traces) and isometric tension curves (bottom traces) before (○) and 120 min after (●) application of 10 μM amiodarone. The preparation was stimulated at 1.0 Hz (left) and at 3.0 Hz (right). (b) The change in action potential duration (APD) at − 70 mV, the maximum upstroke velocity ($\dot{V}_{max}$) and peak developed tension (DT) at three different stimulation frequencies; 0.1 Hz (open columns), 1.0 Hz (hatched columns) and at 3.0 Hz (solid columns). Values are presented as % change from control (means with s.e.mean (vertical bars), $n = 4$). *Significantly different from control at $P < 0.05$.

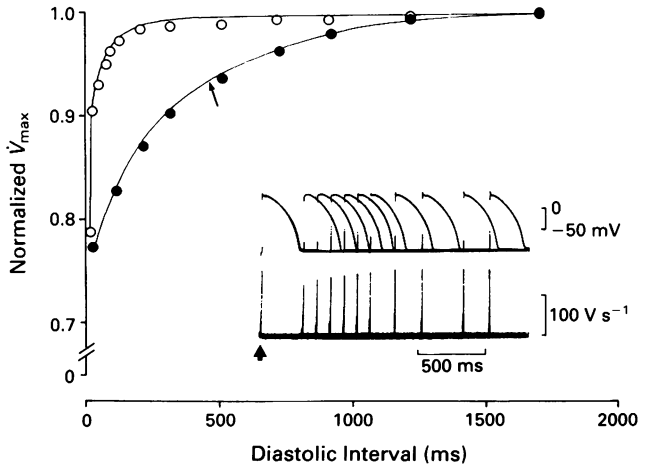

Figure 7 Recovery of $\dot{V}_{max}$ from the use-dependent block by acute amiodarone. Inset shows superimposed records of action potentials (upper trace) and their differentiated upstroke spikes (lower trace) after acute application of amiodarone (10 μM). Following 1.0 Hz stimulation for 60 s, a single test stimulus was applied with various coupling intervals. (A thick arrow indicates the last conditioning stimulus). The graph shows $\dot{V}_{max}$ recovery before (○) and after (●) acute application of amiodarone (10 μM). Ordinate scale: normalized $\dot{V}_{max}$ of test action potential with a reference to the value after full recovery. Abscissa scale: diastolic interval (an interval from the end of the last conditioning action potential to the upstroke of the test action potential). The $\dot{V}_{max}$ recovery after amiodarone was approximated by a single exponential function at a time constant of 460 ms (thin arrow) for the data with diastolic intervals of over 100 ms.

5 Hz. Hondeghem & Snyder (1990) have suggested in their recent review that such a frequency-independent Class III action of amiodarone (unlike other agents causing greater Class III action at the lower stimulation frequency) might be important for its more antiarrhythmic and less proarrhythmic activities. Our results also revealed much less 'reverse use-dependence' of APD prolongation by chronic amiodarone than that by other Class III agents.

Biphasic restitution curves of APD in control preparations (Figure 5) were similar to those reported by previous investigators using multicellular ventricular tissue preparations (Gibbs & Johnson, 1961; Kukushkin *et al.*, 1983) or single ventricular myocytes (Hiraoka & Kawano, 1987) isolated from rabbit hearts. Based on membrane current analysis during voltage-clamp experiments, Hiraoka & Kawano (1987, 1989) suggested that APD prolongation with progressively longer coupling intervals up to 0.3 s may reflect a relatively fast recovery of high threshold (L-type) inward calcium current (I_{Ca}) from inactivation, whereas APD shortening with further prolongation of coupling intervals is the result of very slow recovery of the transient outward current (I_{to}) from inactivation. Since the APD restitution curves of untreated and amiodarone-treated preparations were virtually identical, the effects of chronic amiodarone on the kinetics of I_{Ca} and I_{to} would be minimal or negligible. Nevertheless, extensive voltage-clamp studies on single ventricular cells isolated from amiodarone-treated rabbits are required to substantiate this assumption.

There is considerable controversy regarding the Class I action of chronic amiodarone. Mason *et al.* (1984) showed a marked use-dependent $\dot{V}_{max}$ inhibition in guinea-pig papillary muscles after chronic treatment with amiodarone, similar to the acute effects of the drug. In support of this finding, Anderson *et al.* (1989) demonstrated a rate-dependent decrease in conduction velocity in the epicardium of dogs after chronic treatment with amiodarone. Epstein *et al.* (1991) also showed use-dependent slowing of conduction in the His-Purkinje system in dogs after chronic amiodarone treatment. The use-dependent His-ventricular conduction delay has also been demonstrated in patients receiving long-term oral amiodarone therapy (Shenasa *et al.*, 1984; Cascio *et al.*, 1988).

In contrast, Singh and his colleagues (Singh & Vaughan Williams, 1970; Ikeda *et al.*, 1984; Venkatesh *et al.*, 1986; Kato *et al.*, 1988) showed minimal or no significant change in $\dot{V}_{max}$ in atrial and ventricular muscles from rabbits after long-term amiodarone treatment. Gallagher *et al.* (1989) also showed in their blood cross-perfusion experiments that Purkinje fibres obtained from dogs after long-term amiodarone treatment did not show use-dependent $\dot{V}_{max}$ inhibition even at higher stimulation frequencies. Our data showing no use-dependent $\dot{V}_{max}$ inhibition and rapid restitution of $\dot{V}_{max}$ (τR 42 ms) are in accordance with the latter group.

These discrepancies concerning Class I actions of chronic amiodarone could be attributed to differences in experimental and clinical conditions. For instance, serum and myocardial concentrations of amiodarone found in experiments conducted by Anderson *et al.* (1989) were several times higher than those found by others (Ikeda *et al.*, 1984; Kato *et al.*, 1988; Gallagher *et al.*, 1989) including us. Species and tissue differences in response to the chronic effects of amiodarone (and its active metabolite) might also play a part.

Acute treatment with 10 μM amiodarone had quite different effects on papillary muscles than chronic treatment. Acute administration caused a significant shortening of APD and a substantial decrease of DT. A marked use-dependent $\dot{V}_{max}$ reduction was also observed. Since the first description by Mason *et al.* (1983), many experimental studies have confirmed the local anaesthetic (Class I) actions of acute amiodarone (Varro *et al.*, 1985; Yabek *et al.*, 1985; 1986; Pallandi & Campbell, 1987; Follmer *et al.*, 1987; Kohlhardt & Fichtner, 1988; Honjo *et al.*, 1991). According to the data presented by Mason *et al.* (1983, 1984) and by Honjo *et al.*

(1991), acute amiodarone may block sodium channels by binding mainly during the inactivated state. There is some discrepancy as to the recovery time constant from use-dependent block by acute amiodarone. Mason *et al.* (1984) and Pallandi & Campbell (1987) reported values of 1.48 to 1.63 s, whilst Varro *et al.* (1985) and Honjo *et al.* (1991) obtained a much shorter time constant (from 282 to 460 ms). The recovery time constant found in the present study (452 ms) is in agreement with the latter reports.

Reports of the effects of acute amiodarone on APD have been conflicting. Some studies have shown minimal to moderate APD prolongation, whilst others have shown an appreciable APD shortening (Singh *et al.*, 1989; Gallagher *et al.*, 1989). This may be explained at least in part by different ionic currents responsible for the repolarization of action potential in different animal species and in different cardiac tissues. In voltage-clamp experiments, acute application of amiodarone has been shown to inhibit not only the fast inward sodium current (I_{Na}), the slow inward calcium current (I_{Ca}) (Nishimura *et al.*, 1989) but also outward potassium currents including the delayed rectifier current (I_K) (Colatsky *et al.*, 1990; Balser *et al.*, 1991). In rabbit ventricular muscle, the action of amiodarone on the inward currents might be greater than that on the outward currents.

The above discussion indicates that the major electrophysiological effect of chronic amiodarone on the ventricle appears to be repolarization delay (Class III action) showing minimal frequency-dependence. Relatively high concentrations of amiodarone in the extracellular space cause additional use-dependent sodium channel inhibition (Class I action). Acute amiodarone may also induce calcium channel inhibition (Class IV action) leading to a negative inotropic effect. In patients receiving long-term oral amiodarone, the serum drug level covers a wide range (0.06 to 4.5 $\mu g\,ml^{-1}$ corresponding to approximately to 0.1 to 7.6 μM) (Harris *et al.*, 1983; Raeder *et al.*, 1985). Accordingly, in individual cases of long-term amiodarone treatment, Class I, II and IV actions may contribute to the antiarrhythmic efficacy of this agent.

This study was supported in part by Grant-in-Aid for Scientific Research 02257103 from the Japanese Ministry of Education, Science and Culture.

References

ANDERSON, K.P., WALKER, R., DUSTMAN, T., LUX, R.L., ERSHLER, P.R., KATES, R.E. & URIE, P.M. (1988). Rate-related electrophysiologic effects of long-term administration of admiodarone on canine ventricular myocardium in vivo. *Circulation*, **79**, 948–958.

BALSER, J.R., BENNETT, P.B., HONDEGHEM, L.M. & RODEN, D.M. (1991). Suppression of time-dependent outward current in guinea pig ventricular myocytes. Actions of quinidine and amiodarone. *Circ. Res.*, **69**, 519–529.

BRIEN, J.F., JIMMO, S. & ARMSTRONG, P.W. (1983). Rapid high-performance liquid chromatographic analysis of amiodarone and N-desethylamiodarone in serum. *Can. J. Physiol. Pharmacol.*, **61**, 245–248.

CASCIO, W.E., WOELFEL, A., KNISLEY, S.B., BUCHANAN, J.W.Jr., FOSTER, J.R. & GETTES, L.S. (1988). Use dependence of amiodarone during the sinus tachycardia of exercise in coronary artery disease. *Am. J. Cardiol.*, **61**, 1042–1045.

COLATSKY, T.J., FOLLMER, C.H & STARMER, C.F. (1990). Channel specificity in antiarrhythmic drug action. Mechanism of potassium channel block and its role in suppressing and aggravating cardiac arrhythmias. *Circulation*, **82**, 2235–2242.

EPSTEIN, L.M., SCHEINMAN, M.M., CHIN, M.C. & KATZUNG, B.G. (1991). The use-dependent effects of acute and chronic amiodarone administration on His-Purkinje conduction and the interaction of beta-adrenergic stimulation. *J. Cardiovasc. Electrophysiol.*, **2**, 156–167.

FOLLMER, C.H., AOMINE, M., YEH, J.Z. & SINGER, D.H. (1987). Amiodarone-induced block of sodium current in isolated cardiac cells. *J. Pharmacol. Exp. Ther.*, **243**, 187–194.

GALLAGHER, J.D., BIANCHI,J. & GESSMAN, L.J. (1989). A comparison of the electrophysiologic effects of acute and chronic amiodarone administration on canine Purkinje fibers. *J. Cardiovasc. Pharmacol.*, **13**, 723–729.

GIBBS, C.L. & JOHNSON, E.A. (1961). Effect of changes in frequency of stimulation upon rabbit ventricular muscle action potential. *Circ. Res.*, **9**, 165–170.

HARRIS, L., MCKENNA, W.J., ROWLAND, E., HOLT, D.W., STOREY, G.C.A., & KRIKLER, D.M. (1983). Side effects of long-term amiodarone therapy. *Circulation*, **67**, 45–51.

HEGER, J.J., PRYSTOWSKY, E.N., MILES, W.M. & ZIPES, D.P. (1984). Clinical use and pharmacology of amiodarone. *Med. Clin. North Amer.*, **68**, 1339–1366.

HIRAOKA, M. & KAWANO, S. (1987). Mechanism of increased amplitude and duration of the plateau with sudden shortening of diastolic intervals in rabbit ventricular cells. *Circ. Res.*, **60**, 14–26.

HIRAOKA, M. & KAWANO, S. (1989). Calcium-sensitive and insensitive transient outward current in rabbit ventricular myocytes. *J. Physiol.*, **410**, 187–212.

HONDEGHEM, L.M. & SNYDER, D.J. (1990). Class III antiarrhythmic agents have a lot of potential but a long way to go. Reduced effectiveness and danger of reverse use dependence. *Circulation*, **81**, 686–690.

HONJO, H., KODAMA, I., KAMIYA, K. & TOYAMA, J. (1991). Block of cardiac sodium channels by amiodarone studied by using $\dot{V}max$ of action potential in single ventricular myocytes. *Br. J. Pharmacol.*, **102**, 651–656.

IKEDA, N., NADEMANEE, K., KANNAN, R. & SINGH, B.N. (1984). Electrophysiologic effects of amiodarone: Experimental and clinical observation relative to serum and tissue drug concentrations. *Am. Heart J.*, **108**, 890–898.

KATO, R., VENKATESH, N., KAMIYA, K., YABECK, S., KANNAN, R. & SINGH, B.N. (1988). Electrophysiologic effects of desethylamiodarone, an active metabolite of amiodarone: Comparison with amiodarone during chronic administration in rabbits. *Am. Heart J.*, **115**, 351–359.

KENTISH, J.C. & BOYETT, M.R. (1983). A simple electronic circuit for monitoring changes in the duration of the action potential. *Pflügers Arch.*, **398**, 233–235.

KOHLHARDT, M. & FICHTNER, H. (1988). Block of single cardiac Na^+ channels by antiarrhythmic drugs: The effect of amiodarone, propafenone and diprafenone. *J. Memb. Biol.*, **102**, 105–119.

KUKUSHKIN, N.I., GUINULLIN, R.Z. & SOSUNOV, E.A. (1983). Transient outward current and rate-dependence of action potential duration in rabbit ventricular muscle. *Pflügers Arch.*, **399**, 87–92.

MASON, J.W. (1987). Amiodarone. *N. Engl. J. Med.*, **316**, 455–466.

MASON, J.W., HONDEGHEM, L.M. & KATZUNG, B.G. (1983). Amiodarone blocks inactivated cardiac sodium channels. *Pflügers Arch.*, **396**, 79–81.

MASON, J.W., HONDEGHEM, L.M. & KATZUNG, B.G. (1984). Block of inactivated sodium channels and of depolarization-induced automaticity in guinea pig papillary muscle by amiodarone. *Circ. Res.*, **55**, 277–285.

NISHIMURA, M., FOLLMER, C.H. & SINGER, D.H. (1989). Amiodarone blocks calcium current in single guinea pig ventricular myocytes. *J. Pharmacol. Exp. Ther.*, **252**, 650–659.

PALLANDI, R.T. & CAMPBELL, T.J. (1987). Resting and rate-dependent depression of $\dot{V}max$ of guinea-pig ventricular action potentials by amiodarone and desethylamiodarone. *Br. J. Pharmacol.*, **92**, 97–103.

RAEDER, E.A., PORDRID, P.J & LOWN, B. (1985). Side effects and complications of amiodarone therapy. *Am. Heart J.*, **109**, 975–983.

SAIKAWA, T. & CARMELIET, E. (1982). Slow recovery of the maximum rate of rise ($\dot{V}max$) of the action potential in sheep Purkinje fibers. *Pflügers Arch.*, **394**, 90–93.

SHENASA, M., DENKER, S., MAHMUD, R., LEHMANN, M., ESTRADA, A. & AKHTAR, M. (1984). Effect of amiodarone on conduction and refractoriness of the His-Purkinje system in the human heart. *J.A.C.C.*, **4**, 105–110.

SINGH, B.N. (1990). Amiodarone: Electropharmacologic properties. In *Antiarrhythmic Drugs*. ed. Vaughan Williams, E.M. pp. 335–364. Berlin, Heidelberg, New York, London, Paris, Tokyo: Springer-Verlag.

SINGH, B.N. & VAUGHAN WILLIAMS, E.M. (1970). The effect of amiodarone, a new anti-anginal drug, on cardiac muscle. *Br. J. Pharmacol.*, **39,** 657–667.

SINGH, B.N., VENKATESH, N., NADEMANEE, K., JOSEPHSON, M.A. & KANNAN, R. (1989). The historical development, cellular electrophysiology and pharmacology of amiodarone. *Prog. Cardiovas. Dis.*, **31,** 249–280.

VARRO, A., NAKAYA, Y., ELHARRAR, V. & SURAWICZ, B. (1985). Use-dependent effects of amiodarone on $\dot{V}$max in cardiac Purkinje and ventricular muscle fibers. *Eur. J. Pharmacol.*, **112,** 419–422.

VAUGHAN WILLIAMS, E.M. (1984). A classification of antiarrhythmic action reassessed after a decade of new drugs. *J. Clin. Pharmacol.*, **24,** 129–147.

VENKATESH, N., SOMANI, P., BERSOHN, M., PHARI, R., KATO, R. & SINGH, B.N. (1986). Electropharmacology of amiodarone: Absence of relationship to serum, myocardial, and cardiac sarcolemmal drug concentration. *Am. Heart J.*, **112,** 916–922.

YABEK, S., KATO, R. & SINGH, B. (1985). Acute effects of amiodarone on the electrophysiologic properties of isolated neonatal and adult cardiac fibers. *J.A.C.C.*, **5,** 1109–1115.

YABEK, S., KATO, R. & SINGH, B. (1986). Effects of amiodarone and its metabolite, desethylamiodarone, on the electrophysiologic properties of isolated cardiac muscle. *J. Cardiovasc. Pharmacol.*, **8,** 197–207.

ZIPES, D.P., PRYSTOWSKY, E.N. & HEGER, J.J. (1984). Amiodarone: Electrophysiologic actions, pharmacokinetics and clinical effects. *J.A.C.C.*, **3,** 1059–1072.

(Received February 24, 1992
Revised June 1, 1992
Accepted June 10, 1992)

Br. J. Pharmacol. (1992), **107**, 510–514

Involvement of multiple receptors in the biological effects of calcitonin gene-related peptide and amylin in rat and guinea-pig preparations

[1]Sandro Giuliani, *Sunil J. Wimalawansa & Carlo Alberto Maggi

Pharmacology Department, A. Menarini Pharmaceuticals, Via Sette Santi 3, 50131, Florence Italy and *Biochemical Endocrinology Unit, Department of Chemical Pathology, Royal Postgraduate Medical School, Du Cane Road, London W12

1 The activity of rat α and β calcitonin gene-related peptide (CGRP) as compared to the structurally related peptide, rat amylin, has been investigated in the guinea-pig isolated left atrium (electrically driven), in mucosa-free strips from the base of the guinea-pig urinary bladder and in the rat isolated vas deferens (pars prostatica). The antagonist activity of the C-terminal fragment of human αCGRP, αCGRP(8-37), was also investigated.

2 In the guinea-pig isolated left atrium the three peptides produced a concentration-related positive inotropic effect, amylin being about 16 and 31 times less potent than α or βCGRP, respectively. Human αCGRP(8-37) produced a rightward displacement of the log concentration-response curve to the three agonists tested, without depression of maximal response attainable. Apparent pK_B values calculated on the basis of the displacement produced by 1 μM human αCGRP(8-37) indicated an agonist-independent affinity of the antagonist (6.66 ± 0.11 for αCGRP, 6.42 ± 0.17 for βCGRP and 6.95 ± 0.11 for amylin).

3 In the guinea-pig isolated urinary bladder, α or βCGRP or amylin produced a concentration-related inhibition of twitch contractions evoked by train electrical field stimulation (10 Hz frequency, 0.25 ms duration at 100 V for 0.5 s every 60 s). Amylin was about 100 times less potent than α or βCGRP. Human αCGRP(8-37) (3 μM) did not significantly affect the inhibitory action of the three agonists tested.

4 In the rat isolated vas deferens, α or βCGRP or amylin produced a concentration-related inhibition of twitch contractions evoked by electrical field stimulation (0.2 Hz frequency, 0.5 ms duration at 60 volts). Amylin was about 100 times less potent than α or βCGRP. Human αCGRP(8-37) at 3 μM did not significantly affect the inhibitory action of amylin and at 3 μM antagonized the responses to rat α and βCGRP with apparent pK_B values of 5.86 ± 0.15 and 6.11 ± 0.13, respectively.

5 These findings indicate that multiple receptors mediate the actions of peptides of the CGRP/amylin family in the preparations investigated. In the guinea-pig atrium both α and β forms of rat CGRP as well as amylin act by stimulating a single class of receptors which are sensitive to the inhibitory action of human αCGRP(8-37). In rat isolated vas deferens, at least two receptors could be present, one activated by α and βCGRP and partially sensitive to human αCGRP(8-37) and another which is sensitive to amylin but not recognised by human αCGRP(8-37). This latter type of receptor could be entirely responsible for the action of the agonists in the guinea-pig urinary bladder.

Keywords: Calcitonin gene-related peptide; CGRP receptors; rat α and β-CGRP; rat amylin; CGRP antagonist

Introduction

Calcitonin gene-related peptide (CGRP) is a 37 amino acid residue neurotransmitter peptide widely distributed in the central and peripheral nervous system in mammals (Yamamoto & Tohyama, 1989, for review). CGRP is produced through an alternate splicing of the calcitonin gene and is the predominant form expressed in the neuronal tissue. Various molecular forms of CGRP have been described in various species, which produce their biological actions through specific receptors expressed on the membrane of target cells (see Breimer *et al.*, 1988, for review). Two forms of CGRP, termed α and β are produced in both rat and man which differ in a few residues only. Both α and β forms of CGRP are endowed with biological activity in various assays including powerful vasodilator, cardiac positive inotropic and smooth muscle relaxant activities. Recently, it has been discovered that the C-terminal fragment, human αCGRP(8-37), binds with relatively high affinity to CGRP receptors but does not possess intrinsic activity to stimulate the biological response (Chiba *et al.*, 1989). According to these biochemical observations, human αCGRP(8-37) acts as a competitive antagonist at certain CGRP receptors (e.g. Dennis *et al.*, 1990; Maggi *et al.*, 1991). The use of these fragments has been instrumental in proving definitively the neurotransmitter role of CGRP in e.g. nerve-mediated responses in the guinea-pig atrium (Maggi *et al.*, 1991), guinea-pig ileum (Bartho *et al.*, 1991), guinea-pig ureter and renal pelvis (Maggi & Giuliani, 1991; Maggi *et al.*, 1992) and rat vas deferens (Maggi *et al.*, 1991).

Owing to various pharmacological criteria, including the different potency of human CGRP(8-37) in antagonizing the actions of CGRP in various biassays, the proposal has been advanced (Dennis *et al.*, 1989; 1990; Mimeault *et al.*, 1991; Quirion *et al.*, 1992) that two subtypes of CGRP receptors may exist, which have been termed $CGRP_1$ and $CGRP_2$. It has been proposed that certain preparations such as the guinea-pig atrium are rich in $CGRP_1$ receptors, while others, such as the rat vas deferens preferentially express $CGRP_2$ receptors (Dennis *et al.*, 1989; 1990). The existence of multiple receptors raises the question as to whether the various forms of endogenous CGRP may have preferential affinity for the various receptor subtypes, as has been demonstrated with peptides of other families. The first aim of this study was to compare the action of the α and β forms of rat CGRP in the guinea-pig isolated atrium and rat vas deferens. The

[1] Author for correspondence.

guinea-pig isolated bladder was also included in the study because it is a sensitive bioassay for CGRP (Maggi *et al.*, 1988) and comparison with the data obtained in the atrium may indicate whether CGRP receptors in different organs of the same species have different pharmacology.

Amylin, also known as islet amyloid peptide, is a 37 amino acid residue peptide originally isolated from amyloid plaques in the pancreas of patients with non-insulin-dependent diabetes mellitus (Westermark *et al.*, 1987; Cooper *et al.*, 1987). Amylin is produced from a distinct gene and mature amylin shares about 50% homology with CGRP peptides: the genes encoding amylin and CGRP/calcitonin are believed to belong to a superfamily derived by duplication of a common ancestral gene (Cooper *et al.*, 1989). Interestingly, amylin and CGRP/calcitonin peptides share some biological activities such as regulation of glycogen metabolism in smooth muscles (Leighton & Cooper, 1988), calcium metabolism (Datta *et al.*, 1989) and haemodynamic actions (Brain *et al.*, 1990; Gardiner *et al.*, 1991). The haemodynamic actions produced by amylin infusion in rats are blocked by human αCGRP(8-37) suggesting stimulation of a common population of receptors (Gardiner *et al.*, 1991). CGRP and amylin have been shown to interact at the same receptor sites in rat liver and skeletal muscle membranes by use of ^{125}I-labelled human αCGRP as ligand (Chantry *et al.*, 1991), while a recent report (Poyner *et al.*, 1992) failed to indicate a substantial interaction of amylin with CGRP receptors on rat L6 myocytes. We have therefore included amylin in the study and have investigated the ability of human CGRP(8-37) to prevent the action of this peptide.

Methods

Male albino guinea-pigs (250–300 g) and male albino rats of Wistar strain (300–340 g) were stunned and bled.

For experiments on the guinea-pig atrium the animals received reserpine (5 mg kg^{-1}, i.p., 48–96 h before the experiment). Reserpine pretreatment was found to enhance the response to exogenous CGRP and improve reproducibility of concentration-response curves to CGRP in this preparation (Giuliani, unpublished data). The guinea-pig left atrium was quickly removed and placed in oxygenated Tyrode solution containing atropine (1 μM) and prepared for isometric tension recording, as described previously (Giuliani *et al.*, 1989; 1991; Maggi *et al.*, 1991). The atria were electrically driven at a frequency of 3 Hz (0.5 ms duration at maximal voltage) in order to obtain a stable baseline inotropic activity. Addition of human αCGRP produced concentration-dependent positive inotropic effect suitable for assessing CGRP receptor antagonism (Maggi *et al.*, 1991).

The guinea-pig urinary bladder and rat vas deferens (pars prostatica) were excised and placed in oxygenated Krebs solution. A mucosa-free strip of smooth muscle was prepared from the base of the guinea-pig urinary bladder as described previously (Maggi *et al.*, 1988). A 10 mm segment of the rat vas deferens or the muscle strip from the guinea-pig bladder was prepared for isometric tension recording under a resting load of 5 mN, as described previously (Maggi *et al.*, 1988).

In each preparation, cumulative concentration-response curves to rat α or βCGRP and amylin were constructed, the next concentration being added when the effect of the preceding one had reached a steady state. Concentrations of amylin higher than 3 μM were not tested because of the limited amount of the peptide. In each preparation, the effect of the three putative agonists was investigated in the absence and the presence of the C-terminal fragment of human αCGRP, CGRP(8-37), which acts as a competitive antagonist at certain CGRP receptors. The effects of the antagonist were determined after having recorded two reproducible concentration-response curves to the agonists. Human αCGRP (8-37) (1–3 μM) was added to the bath 5 min before the beginning of the concentration-response curve to the agonist. All experiments were performed in the presence of 10 μM thiorphan to reduce possible degradation of CGRP by endopeptidases (Le Greves *et al.*, 1989). No agonist effect of human CGRP(8-37) was observed.

Data evaluation

EC_{50} values in the absence and presence of the CGRP receptor antagonist were calculated by linear regression and the least squares method. Apparent pK_B values were calculated from dose-ratios produced by the stated concentration of the CGRP antagonists tested from the equation: $pK_B = \log (x - 1) - \log[\text{antagonist}]$.

Parallelism of the concentration-response curves to CGRP obtained in the presence and absence of various concentrations of antagonists was assessed by use of the Parallel Lines I computer programme described by Tallarida & Murray (1981).

Drugs

Human αCGRP(8-37) (hCGRP(8-37)), rat α and βCGRP and rat amylin were from Peninsula (USA). Stock solutions of the peptides (final concentration 1 mM) were prepared in distilled water and diluted in saline just before use. Other drugs used were: thiorphan (Bachem, Switzerland), atropine and reserpine (Serva, Germany).

Results

Guinea-pig atrium

In the electrically driven guinea-pig left atrium, rat αCGRP produced a concentration-related positive inotropic effect, as described previously (Maggi *et al.*, 1991). Both amylin and rat βCGRP mimicked the action of rat αCGRP and approached the same maximum effect (expressed as % increase in resting inotropism) (Figures 1 and 2, Table 1). Amylin was about 16 and 31 times less potent than α or βCGRP, respectively.

hCGRP(8-37) (1 μM) antagonized the positive inotropic effect of both rat α and βCGRP and amylin in the guinea-pig left atrium, without depressing the maximum response to the agonist (Figure 3). From the dose-ratios obtained in the presence and absence of the antagonist, an apparent pK_B value of 6.66 ± 0.11 ($n = 5$), 6.42 ± 0.17 ($n = 4$) and 6.95 ± 0.11 ($n = 4$) was calculated with rat αCGRP, rat βCGRP or amylin as agonists, respectively.

Guinea-pig urinary bladder

In muscle strips obtained from the guinea-pig isolated urinary bladder, rat αCGRP produced a concentration-related depression of the electrically-evoked (trains of pulses at a frequency of 10 Hz, 0.25 ms duration at 100 volts for 0.5 s every 60 s), tetrodotoxin-sensitive twitch contractions produced by electrical field stimulation (Figure 1). Rat βCGRP was as potent and effective as rat αCGRP in this assay (Figure 2, Table 1). Amylin (30 nM–3 μM) was significantly less potent than the α or β forms of CGRP and, at the highest concentration tested it produced about 70% of the maximal inhibitory effect of CGRP (Figure 2). Amylin was about 100 times less potent than α or β forms of rat CGRP in this assay. Thus, the same degree of inhibition produced by rat αCGRP at 10 nM (36 ± 10% inhibition of twitches) was produced by amylin at 1 μM (37 ± 11%).

Human αCGRP(8-37) (3 μM) was without effect on the inhibitory action produced by rat αCGRP, rat βCGRP or amylin in the guinea-pig urinary bladder (Figure 3).

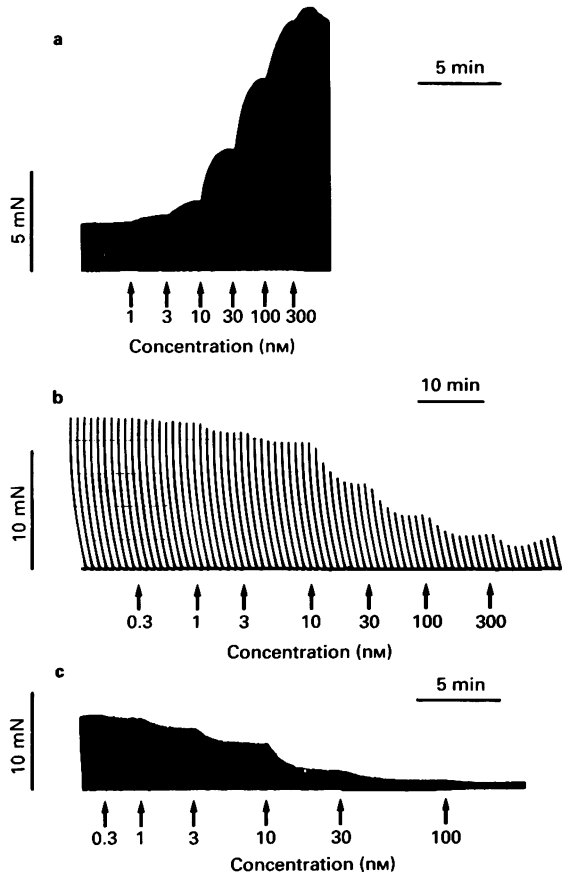

Figure 1 Typical tracings illustrating the concentration-related positive inotropic response to rat α calcitonin gene-related peptide (αCGRP) in the electrically driven guinea-pig isolated left atrium (a), and the concentration-related inhibitory effect of rat αCGRP toward electrically-evoked nerve-mediated contrations of the guinea-pig isolated urinary bladder (b) and rat vas deferens (c).

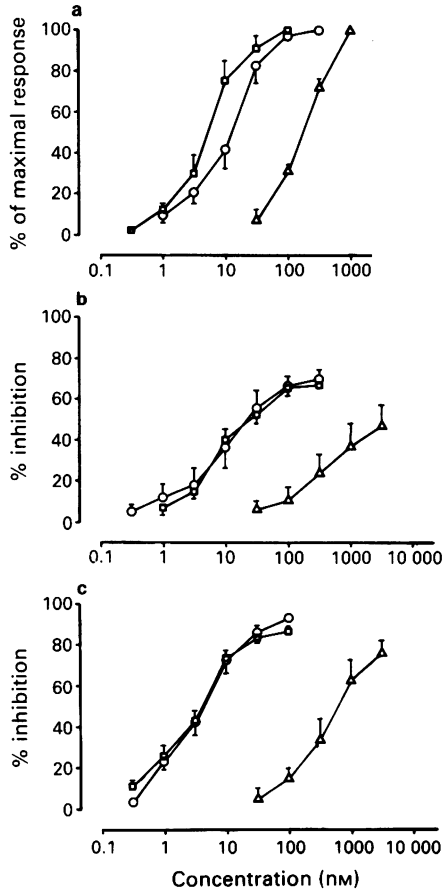

Figure 2 Concentration-related effects of rat α calcitonin gene-related peptide (αCGRP) (○), rat βCGRP (□) and amylin (△) in the guinea-pig left atrium (a) guinea-pig urinary bladder (b) and rat vas deferens (c). Each value is mean with s.e.mean (vertical bars) of 4–5 experiments.

Table 1 EC_{50} (nM) and 95% confidence limits (in parentheses) and maximal effect (E_{max}, expressed as % of the maximal response to rat α calcitonin gene-related peptide (αCGRP)) for rat α or βCGRP and amylin in the guinea-pig atrium, urinary bladder and rat vas deferens

	Rat αCGRP	*Rat βCGRP*	*Amylin*
Guinea-pig atrium			
EC_{50} (nM)	9.9 (6–24)	5.1 (3–11)	158 (65–618)
E_{max}	100	100	100
Guinea-pig urinary bladder			
EC_{50} (nM)	8.0 (5–27)	8.1 (4–66)	NE
E_{max}	100	100	67 ± 6*
Rat vas deferens			
EC_{50} (nM)	4.1 (3–6)	18 (10–38)	NE
E_{max}	100	100	82 ± 5*

Each value is mean of 4–5 experiments.
NE = not evaluable.
*Maximal effect produced at 3 μM.

Rat vas deferens

In the rat isolated vas deferens, rat αCGRP produced a concentration-related inhibition of electrically-evoked (0.2 Hz, 60 V, 0.5 ms pulse width) twitches (Figure 1). Rat βCGRP was as potent and effective as rat αCGRP in this bioassay (Figure 2, Table 1). Amylin was significantly less potent than α or β CGRP and at the highest concentration tested (3 μM) produced 81% of the maximum response to rat αCGRP (Figure 2, Table 1). As observed in the guinea-pig urinary bladder, amylin was about 100 times less potent than the α or β forms of rat CGRP, as judged by the concentration of the various agonists required to produce a similar submaximal inhibitory effect (Figure 2).

Human αCGRP(8-37) (3 μM) produced a rightward displacement of the concentration-response curve to rat α and βCGRP, without producing depression of the maximum response attainable. From the dose-ratios obtained in the presence and absence of antagonist, apparent pK_B values of 5.86 ± 0.15 and 6.11 ± 0.13 were calculated for human αCGRP (8-37) against rat α and βCGRP, respectively (Figure 3).

Human αCGRP(8-37) did not significantly affect the inhibitory action of rat amylin in the rat isolated vas deferens (Figure 3).

Discussion

The present findings provide further evidence suggesting a heterogeneity of CGRP receptors in rat and guinea-pig tissue. Furthermore, evidence is presented indicating that amylin may act as an agonist at certain CGRP receptors such as those present in the guinea-pig left atrium. The studies of Quirion and coworkers (Dennis *et al.*, 1989; 1990; Mimeault *et al.*, 1991), summarized by Quirion *et al.* (1992) have provided evidence for the existence of two subtypes of CGRP receptor, which have been termed $CGRP_1$ and $CGRP_2$. $CGRP_1$ receptors, for which the guinea-pig atrium is a prototypical assay, are recognized with relatively high affinity by C-terminal fragments of human αCGRP such as CGRP(8-37) or CGRP(12-37). $CGRP_2$ receptors, for which the rat vas

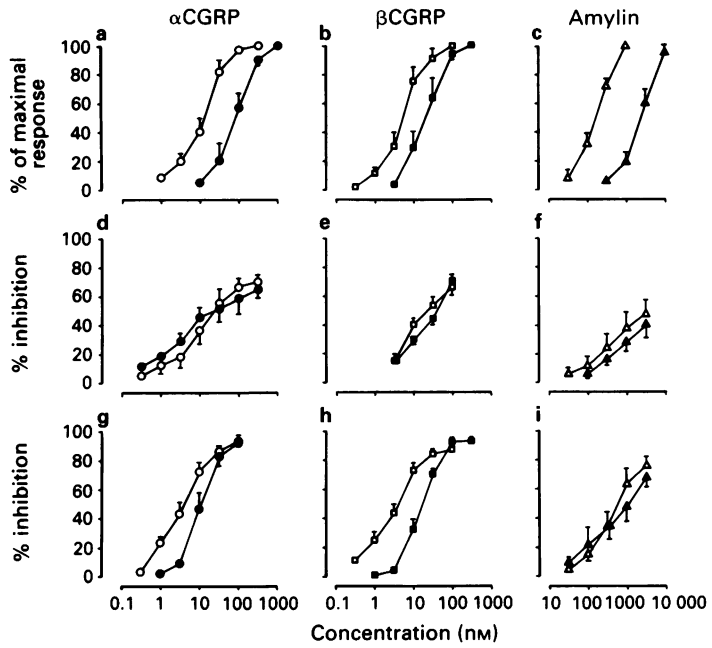

Figure 3 Effect of human α calcitonin gene-related peptide(8-37) (αCGRP(8-37)) on the response to rat αCGRP, rat βCGRP and amylin in the guinea-pig left atrium (a,b,c), guinea-pig urinary bladder (d,e,f) and rat vas deferens (g,h,i). In each panel the effects of peptide alone (control) (open symbols), and in the presence of human αCGRP(8-37) (closed symbols) is shown. Concentration of human αCGRP(8-37) is 1 μM in the atrium, and 3 μM in the other two preparations. Each value is mean with s.e.mean (vertical bars) of 4–5 preparations.

deferens is a prototypical assay, are recognized with lower affinity by CGRP(8-37) while CGRP(12-37) seems inactive as an antagonist at these sites (Mimeault *et al.*, 1991). Thus the ability of human CGRP(8-37) to block the action of the agonist seems crucial to discriminate between the proposed $CGRP_1$ and $CGRP_2$ receptor subtypes: such a discriminating ability of the antagonist has been demonstrated also in *in vivo* assays involving the hypophagic and hypothermic response to central administration of human αCGRP in rats (Quirion *et al.*, 1992) and the gastric antisecretory and antiulcer activity in the same species (Evangelista *et al.*, 1992).

Human αCGRP(8-37) competitively interacts with CGRP binding sites without stimulating them (Chiba *et al.*, 1989). Its competitive antagonist properties against exogenously administered CGRP have been repeatedly demonstrated (see Introduction for References) whilst no inhibitory action toward other agonists (bradykinin, histamine, substance P, vasoactive intestinal polypeptide, isoprenaline, adrenaline or neurotensin) has been reported in various experimental test objects (Donoso *et al.*, 1990; Maggi *et al.*, 1991; Barthó *et al.*, 1991; Chakder & Rattan, 1991). The present findings confirm a somewhat greater affinity of human αCGRP(8-37) at CGRP receptors in the guinea-pig left atrium vs. CGRP receptors in the rat vas deferens and extend the investigations to two other main questions: (a) do the α and β forms of CGRP act on the same receptor population and (b), does amylin interact with the CGRP receptor? Our results indicate that in the guinea-pig left atrium, the α and β forms of rat CGRP, as well as amylin, interact with a single class of CGRP receptors. In fact the agonist action of the three peptides was antagonized by human αCGRP(8-37) in an agonist-independent manner, indicative of a common site of action.

In the rat vas deferens, the action of amylin was not antagonized by hCGRP(8-37); in agreement with the $CGRP_1$ and $CGRP_2$ receptor hypothesis (see above), hCGRP(8-37) was weakly active against rat α or βCGRP, with lower affinity as compared to the guinea-pig atrium. The present findings may be interpreted as indicating that both $CGRP_1$ and $CGRP_2$ sites are present in the vas deferens. Amylin could be acting preferentially at the $CGRP_2$ sites while rat α and βCGRP could act on both sites, thus accounting for the lower potency of hCGRP(8-37) as an antagonist in this assay. According to this interpretation, the guinea-pig urinary bladder base may contain a pure population of the putative $CGRP_2$ receptor sites. In fact human CGRP(8-37) failed to antagonize the action of the three agonists at this level. The role of amylin as a CGRP receptor agonist could be interpreted in the same way: amylin may act as an agonist at both $CGRP_1$ and $CGRP_2$ receptors, although with different affinities. Alternatively, the possibility that amylin is acting, in the guinea-pig urinary bladder and rat vas deferens, at other receptors distinct from those activated by CGRP, cannot be excluded.

In conclusion, the present findings provide additional evidence that CGRP receptors are heterogeneous: the $CGRP_1$ /$CGRP_2$ receptor classification may need adaptation to accommodate the findings obtained with βCGRP and amylin as agonists at the putative CGRP receptor subtypes. Amylin acts as an agonist at the CGRP receptor in the guinea-pig atrium and may have preferential affinity for $CGRP_2$ vs. $CGRP_1$ receptors.

References

BARTHÓ, L., KOCZAN, G., HOLZER, P., MAGGI, C.A. & SZOLCSÁNYI, J. (1991). Antagonism of the effects of CGRP and of capsaicin on the guinea-pig isolated ileum by human αCGRP(8-37). *Neurosci. Lett.*, **29**, 156–159.

BRAIN, S.D., WIMALAWANSA, S., MCINTYRE, I. & WILLIAMS, T.J. (1990). The demonstration of vasodilator activity of pancreatic amylin in the rabbit. *Am. J. Pathol.*, **136**, 487–490.

BREIMER, L.H., MACINTYRE, I. & ZAIDI, M. (1988). Peptides from the calcitonin genes: molecular genetics, structure and function. *Biochem. J.*, **255**, 377–390.

CHAKDER, S. & RATTAN, S. (1991). Antagonism of CGRP by human CGRP(8-37): role of CGRP in internal anal sphincter relaxation. *J. Pharmacol. Exp. Ther.*, **256**, 1019–1024.

CHANTRY, A., LEIGHTON, B. & DAY, A.J. (1991). Cross-reactivity of amylin with CGRP binding sites in rat liver and skeletal muscle membranes. *Biochem. J.*, **277**, 139–143.

CHIBA, T., YAMAGUCHI, A., YAMATANI, T., NAKAMURA, A., MORISHITA, T., INUI, T., FUKASE, M., NODA, T. & FUJITA, A. (1989). CGRP receptor antagonist hCGRP(8-37). *Am. J. Physiol.*, **256**, E331–E335.

COOPER, G.J.S., DAY, A.J., WILLIS, A.C., ROBERTS, A.N., REID, K.B.M. & LEIGHTON, B. (1989). Amylin and the amylin gene: structure, function and relationship to islet amyloid and to diabetes mellitus. *Biochim. Biophys. Acta*, **1014**, 247–258.

COOPER, G.J.S., WILLIS, A.C., CLARK, A., TURNER, R.C., SIM, S.B. & REID, K.B.M. (1987). Purification and characterization of a peptide from amyloid rich pancreases of type 2 diabetic patients. *Proc. Natl. Acad. Sci. U.S.A.*, **84**, 8628–8632.

DATTA, H.K., ZAIDI, M., WIMALAWANSA, S.J., GHATEI, M.A., BEACHAM, J.L., BLOOM, S.R. & MCINTYRE, I. (1989). In vivo and in vitro effects of amylin and amylin-amide on calcium metabolism in the rat and rabbit. *Biochem. Biophys Res. Commun.*, **162**, 876–881.

DENNIS, T., FOURNIER, A., ST PIERRE, S., & QUIRION, R. (1989). Structure-activity profile of calcitonin gene-related peptide in peripheral and brain tissue. Evidence for receptor multiplicity. *J. Pharmacol. Exp. Ther.*, **251**, 718–725.

DENNIS, T., FOURNIER, A., CADIEAUX, A., POMERLAU, F., JOLICOEUR, F.B., ST PIERRE, S. & QUIRION R. (1990). hCGRP(8-37) a CGRP antagonist revealing CGRP receptor heterogeneity in brain and periphery. *J. Pharmacol. Exp. Ther.*, **254**, 123–128.

DONOSO, M.V., FOURNIER, A., ST PIERRE, S. & HUIDOBRO-TORO, P. (1990). Pharmacological characterization of CGRP1 receptor subtype in the vascular system of the rat: studies with hCGRP fragments and analogs. *Peptides*, **11**, 885–889.

EVANGELISTA, S., TRAMONTANA, M. & MAGGI, C.A. (1992). Pharmacological evidence for the involvement of multiple calcitonin gene-related peptide (CGRP) receptors in the antisecretory and antiulcer effect of CGRP in rat stomach. *Life Sci.*, **50**, P13–P18.

GARDINER, S.M., COMPTON, A.M., KEMP, P.A., BENNETT, T., BOCE, C., FOULKES, R. & HUGHES, B. (1991). Antagonistic effect of human αCGRP(8-37) on regional hemodynamic actions of rat islet amyloid polypeptide in conscious Long-Evans rats. *Diabetes*, **40**, 948–951.

GIULIANI, S., MAGGI, C.A. & MELI, A. (1989). Prejunctional modulatory action of neuropeptide Y on peripheral terminals of capsaicin-sensitive sensory nerves. *Br. J. Pharmacol.*, **98**, 407–412.

GIULIANI, S., SANTICIOLI, P., TRAMONTANA GEPPETTI, P. & MAGGI, C.A. (1991). Peptide N-formyl-methionyl-leucyl-phenylalanine (FMLP) activates capsaicin-sensitive primary afferent nerves in guinea-pig atria and urinary bladder. *Br. J. Pharmacol.*, **102**, 730–734.

LE GREVES, P., NYBERG, F., HOKFELT, T. & TERENIUS, L. (1989). CGRP is metabolized by an endopeptidase hydrolizing substance P. *Regul. Pept.*, **25**, 277–286.

LEIGHTON, B. & COOPER, G.J.S. (1988). Pancreatic amylin and CGRP cause resistance to insulin in skeletal muscle in vitro. *Nature*, **335**, 632–635.

MAGGI, C.A., CHIBA, T. & GIULIANI, S. (1991). Human α-calcitonin gene-related peptide (8-37) as an antagonist of exogenous and endogenous calcitonin gene-related peptide. *Eur. J. Pharmacol.*, **192**, 85–88.

MAGGI, C.A. & GIULIANI, S. (1991). The neurotransmitter role of CGRP in the rat and guinea-pig ureter: effect of a CGRP antagonist and species-related differences in the action of omega conotoxin on CGRP release from primary afferents. *Neuroscience*, **43**, 261–268.

MAGGI, C.A., SANTICIOLI, P., PATACCHINI, R., GEPPETTI, P., GIULIANI, S., ASTOLFI, M., BALDI, E., PARLANI, M., THEODORSSON, E., FUSCO, B. & MELI, A. (1988). Regional differences in the motor response to capsaicin in the guinea-pig urinary bladder: relative role of pre- and postjunctional factors related to neuropeptide-containing sensory nerves. *Neuroscience*, **27**, 675–688.

MAGGI, C.A., THEODORSSON, E., SANTICIOLI, P. & GIULIANI, S. (1992). Tachykinins and CGRP as co-transmitters in local motor responses produced by sensory nerve activation in the guinea-pig isolated renal pelvis. *Neuroscience*, **46**, 549–559.

MIMEAULT, M., FOURNIER, A., DUMONT, Y., ST PIERRE, S. & QUIRION, R. (1991). Comparative affinities and antagonistic potencies of various human CGRP fragments on CGRP receptors in brain and periphery. *J. Pharmacol. Exp. Ther.*, **258**, 1084–1090.

POYNER, D.R., ANDREW, D.P., BROWN, D., BOSE, C. & HANLEY, M.R. (1992). Pharmacological characterization of a receptor for calcitonin gene-related peptide on rat L6 myocytes. *Br. J. Pharmacol.*, **105**, 441–447.

QUIRION, R., VAN ROSSUM, D., DUMONT, Y., ST PIERRE, S. & FOURNIER, A. (1992). Characterization of $CGRP_1$ and $CGRP_2$ receptor subtypes. *Ann. New York Acad. Sci.*, (in press).

TALLARIDA, R.J., MURRAY, R.B. (1981). *Manual of Pharmacologic Calculations with Computer Programs*. New York: Springer Verlag.

WESTERMARK, P., WERNSTEDT, C., WILANDER, E., HAYDEN, D.W., O'BRIEN, T.D. & JOHNSON, K.D. (1987). Amyloid fibrils in human insulinoma and islets of Langerhans of the diabetic cat are derived from a neuropeptide-like protein also present in normal islet cells. *Proc. Natl. Acad. Sci. USA*, **84**, 3881–3885.

YAMAMOTO, A.I. & TOHYAMA, M. (1989). CGRP in the nervous tissue. *Prog. Neurobiol.*, **33**, 335–395.

(Received May 6, 1992
Revised June 8, 1992
Accepted June 11, 1992)

Br. J. Pharmacol. (1992), **107**, 515–520

Electrophysiological effects of CRE-1087 in guinea-pig ventricular muscles

Eva Delpón, Carmen Valenzuela, Onésima Pérez & [1]Juan Tamargo

Department of Pharmacology, School of Medicine, Universidad Complutense, 28040 Madrid, Spain

1 The electrophysiological effects of CRE-1087, a new antiarrhythmic drug, were studied in guinea-pig papillary muscles.

2 CRE-1087 (10^{-7} M–10^{-4} M) produced a concentration-dependent decrease in the action potential amplitude and V_{max} of the upstroke without altering the action potential duration or the resting membrane potential.

3 At 5×10^{-6} M, CRE-1087 produced a $5.0 \pm 1.0\%$ tonic V_{max} block and this value was not modified at the different rates of stimulation tested. In the presence of CRE-1087, trains of stimuli at rates between 0.5 and 3 Hz led to an exponential decline in V_{max} (frequency-dependent V_{max} block) which augmented at higher rates of stimulation. At 2 Hz the onset kinetics of the frequency-dependent V_{max} block was fitted by a monoexponential function being the K value 0.099 ± 0.012 AP^{-1}. The time constant for the recovery of V_{max} from the frequency-dependent block was prolonged to 18.3 ± 1.5 s.

4 CRE-1087 (5×10^{-6} M) did not shift the membrane responsiveness curve.

5 CRE-1087 had no effect on the characteristics of the slow action potentials elicited by isoprenaline in ventricular fibres depolarized by 27 mM KCl, which suggested that CRE-1087 did not exhibit class IV (Ca antagonist) antiarrhythmic actions.

6 The slow onset and the slow offset kinetics of frequency-dependent V_{max} block during repetitive activity suggested that in guinea-pig ventricular muscle fibres CRE-1087 exhibited class Ic antiarrhythmic actions.

Keywords: CRE-1087; ventricular muscle; action potential; use-dependent V_{max} block; antiarrhythmics

Introduction

CRE-1087, 1-(2-methoxyphenoxy)-2,3-bis (2-diethylaminoethoxy) propane dicitrate, is a new antiarrhythmic drug which exhibits local anaesthetic properties (Priego *et al.*, 1984; Statkow *et al.*, 1985; Delpón *et al.*, 1991a). In preliminary experiments it has been shown that CRE-1087 is effective in suppressing cardiac arrhythmias induced by aconitine, digitalis and chloroform-adrenaline in dogs, cats and rats (Statkow *et al.*, 1985). However, CRE-1087 had no effect on the positive inotropic and chronotropic responses induced by isoprenaline in guinea-pig isolated atria (Delpón *et al.*, 1991a) which suggests that it did not exhibit class II (antisympathetic) antiarrhythmic actions. Moreover, preliminary microelectrode studies in guinea-pig ventricular muscle fibres indicated that CRE-1087 decreases the maximal rate of depolarization (V_{max}) of the action potential, suggesting a class I mechanism of action, i.e., fast Na channel block (Delpón *et al.*, 1991a).

Thus the present experiments were undertaken to: (a) characterize the cellular electrophysiological effects of CRE-1087 in guinea-pig ventricular muscle fibres and (b) determine its effects on the onset and recovery kinetics of the sodium channel as reflected by its effects on V_{max}. Moreover, since the prevailing classification of antiarrhythmic drugs is based on changes in action potential duration, refractoriness and onset and offset kinetics of the frequency-dependent block of fast sodium channels (Vaughan Williams, 1984), the present experiments were also carried out in order to (c) place this drug in the appropriate class I subgroup (i.e., class Ia, Ib, Ic).

[1] Author for correspondence.

Methods

General procedure

Guinea-pigs of either sex weighing 250–350 g were killed by a blow on the head. The hearts were rapidly removed and brought into a dissection chamber where papillary muscles (2–3 mm in length, less than 1 mm in diameter) were excised from the right ventricle. The muscles were pinned to the bottom of a Lucite chamber and superfused continuously at a constant rate of 7 ml min^{-1} with Tyrode solution of the following composition (mM): NaCl 137, KCl 5.4, $CaCl_2$ 1.8, $MgCl_2$ 1.05, $NaHCO_3$ 11, NaH_2PO_4 0.42 and glucose 5.5. The solutions were bubbled with 95% O_2 and 5% CO_2 and maintained at 34 ± 0.5°C (pH = 7.4). The preparations were initially driven at 1 Hz and a period of 1 h was allowed for equilibration during which a stable impalement was obtained. Driving stimuli were rectangular pulses (2 ms duration, twice threshold strength) delivered to the preparation from a multipurpose programmable stimulator (Cibertec CS-220, Cibertec S.A., Madrid, Spain). Electrical stimulation was applied to the surface of the preparation thought Teflon-coated bipolar electrodes of silver wire.

Transmembrane action potentials were conventionally recorded through glass microelectrodes filled with 3 M KCl (tip resistance of 8–15 MΩ). The microelectrode was connected via Ag-AgCl wire to high impedance, capacity neutralizing amplifiers (WPI model 701, New Haven, CT, U.S.A.). The action potential was differentiated electronically in order to measure the maximal rate of depolarization (V_{max}) (Valenzuela *et al.*, 1988; 1989; Delpón *et al.*, 1989; 1990). The differentiator used had an upper limit of linearity of 1000 $V s^{-1}$ and variable input filters (3 Hz–260 kHz, E. Ehler, Homburg/Saar, Germany). The suitable frequency filter for minimizing noise without reducing the V_{max} was selected in

each experiment. Another distortion of V_{max} can arise from the formation of the foot of the rising phase of the electrical stimulus. This phenomenon is accompanied by a reduced interval between stimulus artifact and the upstroke of the action potential particularly when strong electrical stimuli are applied. In order to diminish this artifact, stimulus intensity and duration were adjusted throughout each experiment to maintain a constant latency (1–2 ms) between stimulus and upstroke of the action potential (Valenzuela *et al.*, 1988; 1989). Both action potential and V_{max} were displayed on a storage oscilloscope (Tektronix Inc., Beaverton, OR, U.S.A.) and the oscilloscope traces were photographed with a kymographic camera (Grass C4, Grass Instrument Co., Quincy, MA, U.S.A). All experimental results were obtained from a single continuous impalement through the whole experiment.

To study the rate-dependent effects of CRE-1087 on V_{max}, preparations were driven at a basal rate of 0.02 Hz. Following the equilibration period, the preparations were driven by trains of stimuli at various rates ranging from 0.5 to 3 Hz for 40 s (0.5, 1 and 2 Hz) and 16 s (3 Hz). Rest periods of 5 min, which were sufficient to ensure full recovery from frequency-dependent decrease in V_{max}, were interpolated between the trains of stimuli (Valenzuela *et al.*, 1988; Delpón *et al.*, 1989; 1990). This experimental protocol was repeated in the absence and presence of CRE-1087 and indicated that CRE-1087 at any given rate produced two types of V_{max} inhibition, a tonic and a frequency-dependent blockade. Tonic blockade is the decrease of V_{max} of the first action potential preceded by the rest period, whereas frequency-dependent blockade is the decrease of V_{max} during a train from the value of the first action potential to a new steady-state.

Recovery of V_{max} from the frequency-dependent block was studied by applying a single test stimulus at various coupling intervals after a stimulation train for 8 s at 3 Hz (Valenzuela *et al.*, 1988; Delpón *et al.*, 1989). The intensity and duration of the test and conditioning stimuli were adjusted to obtain a constant latency from the stimulus artifact to the initiation of the upstroke of the action potential. The effective refractory period (ERP) was measured by introducing premature test-stimuli of twice threshold strength at different intervals from the preceding basic action potential (Delpón *et al.*, 1989).

Effects of CRE-1087 on the relationship between V_{max} and the resting membrane potential, i.e., membrane responsiveness, was studied in papillary muscles driven at 0.02 Hz and the resting membrane potential was depolarized by increasing the $[K]_o$ from 2.7 to 15 mM (Delpón *et al.*, 1990). The V_{max} was measured each time after an equilibration period of 8 min. Curves were obtained in the absence and after 30 min exposure to 5×10^{-6} M CRE-1087.

To study the effects of CRE-1087 on slow action potentials, papillary muscles were equilibrated in Tyrode solution and then rendered inexcitable by depolarizing the membrane potential with high (27 mM) K Tyrode solution (Delpón *et al.*, 1989). Under these conditions papillary muscle became inexcitable despite intense stimulation. Excitability was restored, i.e. slow action potentials, in muscles driven at a basal rate of 0.1 Hz by addition of isoprenaline (10^{-6} M) to the bathing medium.

Drugs

The following drugs were used: CRE-1087 (Cermol S.A., Geneve, Switzerland) and isoprenaline hydrochloride (Sigma Chemical Co., London). CRE-1087 as a powder was dissolved in distilled deionized water. Further dilutions were carried out in Tyrode solution to obtain final concentrations between 10^{-7} M and 10^{-4} M.

Throughout the paper data are expressed as the mean ± s.e.mean and paired Student's *t* test was used to estimate the significance of differences from control values. For statistical comparison of more than two groups, a one-way analysis of variance was performed (Wallenstein *et al.*, 1980). A *P* value of less than 0.05 was considered as significant. More details on each procedure are given under 'Results'.

Results

Effects of CRE-1087 on transmembrane action potentials

The effects of a wide range of concentrations of CRE-1087 (10^{-7} M to 10^{-4} M) were studied on 9 papillary muscles. The onset of action of CRE-1087 was approximately 5 min after beginning the perfusion and reached steady-state values within 30 min. Therefore, results obtained under control conditions and 30 min after each increment in drug concentration are shown in Table 1. In ventricular muscle fibres CRE-1087, at concentrations higher than 10^{-7} M produced a significant decrease ($P<0.01$) in V_{max}, which at concentrations $\geq 5 \times 10^{-5}$ M was accompanied by a significant decrease in action potential amplitude ($P<0.01$). However, at all concentrations tested, CRE-1087 had no effect on either the resting membrane potential or the action potential duration at both 50% (APD_{50}) and 90% (APD_{90}) of repolarization.

In 6 papillary muscles the ventricular ERP averaged 199.3 ± 8.5 ms. CRE-1087, 10^{-7} M–10^{-4} M, produced a dose-dependent lengthening of the ERP. Since the lengthening of the ERP was greater than that observed in the APD_{90} values, CRE-1087 also increased the ERP/APD_{90} ratio at 5×10^{-5} M and 10^{-4} M from 1.03 ± 0.02 to 1.12 ± 0.03 ($P<0.05$) and 1.20 ± 0.02 ($P<0.01$), respectively.

Frequency-dependent effects of CRE-1087

The effectiveness of many class I antiarrhythmic drugs in inhibiting the fast inward sodium current (I_{Na}) is strongly dependent on the frequency of stimulation. Thus, the influence of stimulation frequency on the depressant effect of CRE-1087 on V_{max} was studied in papillary muscles by applying trains of pulses at different rates (0.5, 1, 2 and 3 Hz), separated from one another by a rest period of 5 min.

Table 1 Electrophysiological effects of CRE-1087 on transmembrane action potentials in guinea-pig ventricular muscles driven at 1 Hz

Drug concentration (M)	*RMP* (mV)	*APA* (mV)	V_{max} (V s^{-1})	APD_{50} (ms)	APD_{90} (ms)
0	81 ± 2	122 ± 2	218 ± 7	156 ± 6	197 ± 8
10-7	81 ± 2	123 ± 2	218 ± 7	167 ± 9	203 ± 5
10-6	81 ± 2	122 ± 1	166 ± 9[b]	160 ± 5	197 ± 2
10-5	81 ± 2	120 ± 1	137 ± 9[b]	172 ± 7	210 ± 7
5 × 10-5	81 ± 2	114 ± 2	58 ± 8[c]	175 ± 9	211 ± 12
10-4	81 ± 2	110 ± 1[b]	40 ± 4[c]	178 ± 7	220 ± 11

x ± s.e.mean, $n = 9$
[a]$P<0.05$; [b]$P<0.01$; [c]$P<0.001$.

In the presence of CRE-1087 this experimental protocol demonstrated the existence of two types of V_{max} inhibition, i.e. tonic and frequency-dependent V_{max} block. In the experiment shown in Figure 1, following perfusion with 5×10^{-6} M CRE-1087 the V_{max} of the first action potential of each train preceded by a rest period was reduced from 200 V s^{-1} to 212 V s^{-1}, i.e. it produced a 3.6% tonic V_{max} block. In 5 experiments the degree of tonic V_{max} block induced by 5×10^{-6} M CRE-1087 averaged 5.0 ± 1.0% and this value was not modified at the different rates of stimulation tested. These data indicated that CRE-1087 exhibits a low affinity for the resting state of the sodium channel.

Following a train of pulses in the presence of CRE-1087, there was a gradual decrease of V_{max} from beat to beat until a new steady-state occurred (frequency-dependent V_{max} block), which depended on the stimulation frequency. Figure 1 shows a typical experiment in the presence of 5×10^{-6} M of CRE-1087. The percentage decrease of V_{max} from the first action potential of the train to a new steady-state level in the absence and presence of 5×10^{-6} M CRE-1087 at different stimulation frequencies (0.5–3 Hz) is summarized in Table 2. At all stimulation rates tested CRE-1087 significantly increased ($P<0.001$) the frequency-dependent block. Moreover, it can be observed that the degree of frequency-dependent V_{max} block increased when the rate of stimulation increased from 0.5 to 2 Hz, while at 3 Hz the degree of frequency-dependent V_{max} block was similar to that observed at 2 Hz. This result suggests that at frequencies higher than 2 Hz the V_{max} block apparently achieved a steady-state value.

Onset kinetics of frequency-dependent V_{max} block can be defined either in terms of a time- or a rate-dependent process. In both cases, the decline of V_{max} during stimulation trains represents a first or second order process and can be well fitted by a single or biexponential function (Courtney, 1980; Grant *et al.*, 1984; Delpón *et al.*, 1991b). The time-constant (τ_{on}, s) and the onset rate per action potential [K, (AP^{-1})] at which V_{max} decreased to a new steady-state level was calculated from the regression lines in semilogarithmic plots. As can be predicted from the equation for the the two-state model (Courtney, 1983) the onset rate of the frequency-dependent V_{max} block, expressed as a fractional decrease per action potential (K), was dependent on the stimuation frequency, being always higher at lower stimulation frequencies at any drug concentration tested. This is shown in Table 3. Thus, at 0.5, 1 and 2 Hz, τ_{on} values progressively decreased in the presence of CRE-1087 from 9.4 ± 0.6 s to 5.2 ± 0.7 s, respectively. On the other hand, at frequencies of stimulation between 0.5 and 2 Hz the rate-constants (K) decreased from 0.216 ± 0.013 AP^{-1} to 0.099 ± 0.012 AP^{-1}. However, at 3 Hz the onset kinetics of the frequency-dependent V_{max} block was better fitted by a biexponential function the K values of the fast and slow components being 0.393 ± 0.08 AP^{-1} and 0.070 ± 0.02 AP^{-1}, respectively (Table 3).

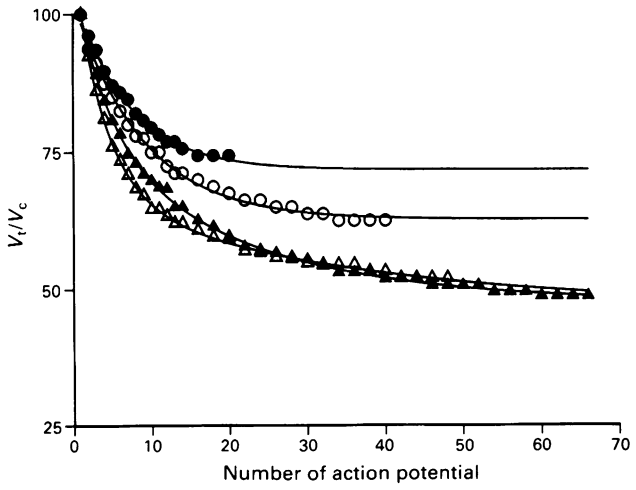

Figure 1 Onset of frequency-dependent depression of V_{max} induced by 5×10^{-6} M CRE-1087 in guinea-pig papillary muscles driven by trains of stimuli at various rates (0.5, 1, 2 and 3 Hz). Stimulation caused a frequency-dependent blockade which disappeared, whereas the tonic V_{max} block persisted. The tonic block (percentage) results from [1-V_{max} (first beat, drug)/V_{max} (rested, drug free)] × 100% and the frequency-dependent block (percentage) from [1-V_{max} (ss, drug)/V_{max} (first beat, drug)]. V_{max} (ss) is the steady-state value attained during continuous stimulation and V_{max} (first beat) is the value of the first beat of each train of stimuli. (●) 0.5 Hz, (○) 1 Hz, (▲) 2 Hz, (△) 3 Hz.

Table 2 Frequency-dependent V_{max} block induced by 5×10^{-6} M CRE-1087 in papillary muscles driven at different stimulation rates

Frequency of stimulation (Hz)	*Frequency-dependent V_{max} block (%)* *Control* (%)	*CRE-1087* (%)
0.5	0.5 ± 0.4	19.3 ± 3.3[a]
1.0	2.9 ± 0.6	28.4 ± 4.9[a]
2.0	11.3 ± 0.9	42.0 ± 4.0[a]
3.0	18.7 ± 1.0	43.1 ± 2.0[a]

X ± s.e.mean, $n = 5$.
[a] $P<0.001$.
The percentage of frequency-dependent V_{max} block was calculated as indicated in Figure 1.

Recovery kinetics of frequency-dependent V_{max} block

The effects of CRE-1087 on the recovery kinetics of frequency-dependent V_{max} block were also studied in 6 papillary muscles. In this group of experiments, muscles were driven every 3 min by a train of stimuli at a frequency of 3 Hz for 8 s and a test-stimulus was applied at variable coupling intervals from 500 ms to 36 s. Recovery from frequency-dependent V_{max} block occurred as a monoexponential process for which a single time constant (τ_{re}) can be estimated by regression analysis of the data. Under control conditions, the τ_{re} was 28.5 ± 3.2 ms whereas in the presence of 5×10^{-6} M CRE-1087 (Figure 2) the τ_{re} was prolonged to 18.3 ± 1.5 s ($P<0.001$). The y-intercept of this slow phase of recovery can be taken as the fraction of sodium channels blocked by CRE-1087, which rose to a value of 85.4 ± 2.0%. Thus, these results indicated that CRE-1087 must be considered as belonging to the kinetically slow group of class I antiarrhythmic drugs (Campbell, 1983a,b: Trump *et al.*, 1989).

Effect on membrane responsiveness

The relationship between V_{max} and the membrane resting potential from which the action potential arises, i.e. membrane responsiveness, was analyzed in 5 papillary muscles driven at a basal rate of 0.02 Hz. The resting membrane potential was depolarized stepwise to approximately − 60

Table 3 Effect of 5×10^{-6} M CRE-1087 on the onset kinetics of frequency-dependent V_{max} block

Frequency of stimulation (Hz)	τ_{on} (s)	*Onset rate per AP* (AP^{-1})
0.5	9.4 ± 0.6	0.216 ± 0.013
1.0	8.6 ± 0.5	0.117 ± 0.006
2.0	5.2 ± 0.7	0.099 ± 0.012
3.0	2.8 ± 0.5	0.393 ± 0.080
	12.2 ± 2.3	0.070 ± 0.020

X ± s.e.mean, $n = 5$.

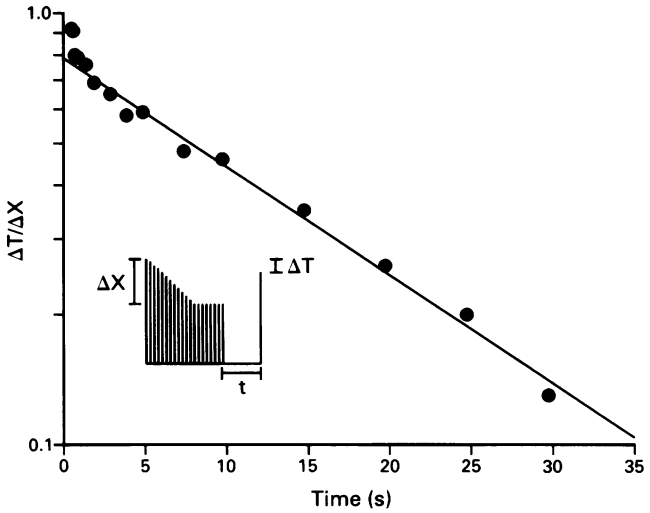

Figure 2 Effects of CRE-1087 (5×10^{-6} M) on the recovery process of V_{max} block after trains of action potentials at 3 Hz for 8 s. ΔT: V_{max} of the first action potential of the train minus V_{max} of the test response; ΔX = V_{max} of the first action potential minus steady-state value of V_{max} reached during the train. Time = interval (s) between the last action potential of the train and the test response. First-order regressions of the slow component were fitted by the method of least squares.

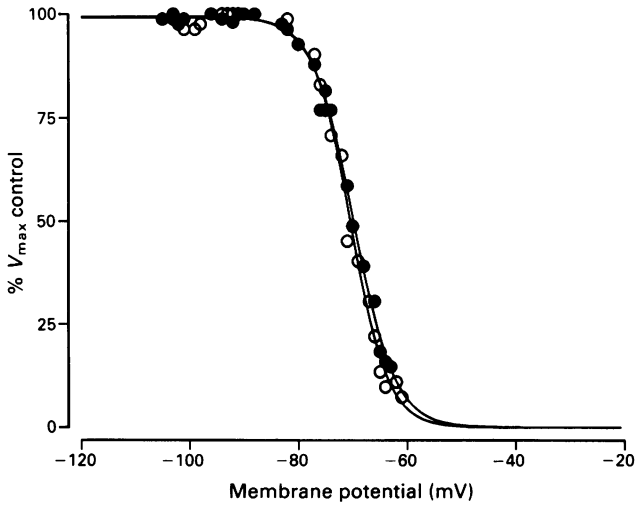

Figure 3 Effect of CRE-1087 (5×10^{-6} M) on the relationship betwen V_{max} and the resting membrane potential at which the action potential is generated (i.e. membrane responsiveness). Ordinate scale: normalized V_{max} values ($V\ s^{-1}$). Abscissa scale: membrane potential (mV). Controls (●), CRE-1087 (○).

mV by increasing the $[K]_o$ from 2.7 to 15 mM and the V_{max} value was measured when the resting membrane potential reached steady-state values at each $[K]_o$. Results of a typical experiment are shown in Figure 3. It can be observed that 5×10^{-6} M CRE-1087 did not shift the membrane-responsiveness curve.

Effect on the slow action potentials

The effects of CRE-1087 on the slow action potentials were studied in papillary muscles perfused with 27 mM K Tyrode solution and driven at a basal rate of 0.1 Hz. Under these conditions the resting membrane potential depolarized from -81.5 ± 2.4 mV to -45.7 ± 1.6 mV ($n = 6$) and ventricular fibres became inexcitable. Excitability, i.e. slow action potentials, was restored by adding isoprenaline (10^{-6} M) to the perfusate. CRE-1087, 10^{-4} M, had no effect on the amplitude (83.5 ± 2.1 mV vs 81.3 ± 2.4 mV), V_{max} ($8.9 \pm 1.2\ V\ s^{-1}$ vs $8.3 \pm 1.1\ V\ s^{-1}$) and duration of the action potential measured at 90% of repolarization (356.0 ± 32.1 vs 336.5 ± 34.5 ms) or the resting membrane potential (-45.6 ± 1.4 mV vs -45.8 ± 1.2 mV).

Discussion

In this study the effects of CRE-1087, a new antiarrhythmic drug, were analyzed on the electrophysiological properties of guinea-pig ventricular muscle fibres. Also, the onset and recovery kinetics of frequency-dependent V_{max} block were studied in order to determine the subclassification of this compound. The present results indicated that in ventricular muscle fibres, CRE-1087 produced a concentration-dependent decrease in V_{max} values which occurred even at concentrations that had no effect on other action potential characteristics or resting membrane potential. Therefore, these findings suggested that the depressive effect on V_{max} is probably due to an inhibition of the I_{Na}, and the rate-dependent effect of the drug on V_{max} suggests that CRE-1087 has an effect compatible with that of class I antiarrhythmic drugs having slow kinetics (Ic).

In the present experiments the V_{max} values were used as an indirect index of the I_{Na}. Although there is no doubt that most of the ionic current crossing the cell membrane at the V_{max} time is the I_{Na} (Hondeghem, 1978; Sheets *et al.*, 1988), there is also evidence that the relationship between the Na conductance (G_{Na}) and the V_{max} values is a monotonic but not a linear index (Walton & Fozzard, 1979). Thus, the use of V_{max} can introduce a variable error in the quantitative measurements which can overestimate the I_{Na} block induced by the drug. Whether or not possible non-linearities between V_{max} and G_{Na} affect the present results remains to be seen in reliable voltage-clamp experiments under the same conditions of temperature and external sodium concentration as used in the present experiments.

Class I antiarrhythmic drugs are characterized by their ability to depress the V_{max} of the cardiac action potentials as a consequence of interaction of these drugs with sodium channels. The characteristics of the Na-channel block can be interpreted within the framework of the 'modulated receptor hypothesis' proposed by Hondeghem & Katzung (1977, 1984) to explain the interaction between local anaesthetic-type antiarrhythmic drugs with cardiac Na channels. According to this hypothesis, reduction of I_{Na} is due to the accumulation of drug-associated nonconducting channels (blocked channels). Accumulation results from the binding of drugs to a channel receptor that changes state or conformation as the channel cycles through the resting, activated and inactivated states (Hondeghem & Katzung, 1977; 1984; Hondeghem, 1987; Tamargo *et al.*, 1989). The affinity of the drug receptor differs in the three different receptor conformations. At therapeutic concentrations most class I antiarrhythmic drugs exhibit little or no tonic V_{max} block (Campbell, 1983a,b; Hondeghem & Katzung, 1984; Valenzuela *et al.*, 1988; 1989; Delpón *et al.*, 1989; 1990) and CRE-1087 was no exception. The fact that little resting block was found with normally polarized ventricular fibres suggests that CRE-1087 exhibits little affinity for the resting state of the sodium channel.

In contrast, during stimulation trains, sodium channels spend proportionately more time in the activated state during the upstroke and in the activated state during the plateau. If CRE-1087 has a higher affinity for the receptor of an activated or inactivated channel than for a resting channel receptor, an accumulation of the blocked channels during the

stimulation train leading to a use-dependent block of V_{max} would be expected. The decrease in V_{max} increased progressively when the preparations were stimulated at progressively increasing driving rates between 0.5 and 2 Hz and the onset rate of frequency-dependent block decreased as the stimulation rate was increased. At 2 Hz the onset rate value of the frequency-dependent V_{max} block was 0.099 AP^{-1}, a value which is similar to that of drugs which had been proposed as slow kinetics class I drugs by Campbell (1983a,b). The recovery from frequency-dependent V_{max} block (reactivation) induced by CRE-1087 was also a slow process. In fact, the value of τ_{re} found in this study is quite similar to that described with other class Ic antiarrhythmic drugs, like propafenone (Kohlhardt & Seifert, 1983; Valenzuela *et al.*, 1989) or flecainide (Campbell & Vaughan Williams, 1983; Delpòn *et al.*, 1991b). Thus, CRE-1087 can be categorized as a slow kinetic class I drug, according to the classification of Vaughan Williams (1984), judging from the value of τ_{re}. The τ_{re} is one of the most reliable parameters for subdivision of the class I antiarrhythmic drugs because it is little affected by changes in drug concentration and stimulation frequencies (Courtney, 1980; Campbell, 1983a,b).

The relationship between V_{max} and the resting membrane potential was studied in muscles driven with an interstimulus interval of 50 s, which is three times longer than the τ_{re} value. Since this diastolic interval is much longer than the τ_{re}, under these conditions an inhibition of V_{max} may reflect only the tonic block induced by CRE-1087. In the present study CRE-1087 did not shift this relationship, thus suggesting that the drug exhibits little or no affinity for the inactivated state of the Na channel. On the other hand, it has been proposed that class I antiarrhythmic drugs with slow or intermediate onset of frequency-dependent V_{max} block (like CRE-1087) may have a significant affinity for the open-activated channel state only (Campbell, 1989; Snyders & Hondeghem, 1990), and that they also exhibit a long τ_{re} because the primary route for unblocking is associated with activation (Snyders & Hondeghem, 1990). In fact, in the present paper the degree of frequency-dependent V_{max} block induced by CRE-1087 at frequencies of stimulation higher than 2 Hz apparently achieved a steady-state value. This result can be explained because with this experimental approach, very high frequencies of stimulation not only increase the number of activations per time unit, but also, and more importantly, increase the percentage of Na channels in the inactivated state. Furthermore, the small voltage-shift induced by CRE-1087 suggests that at any potential, there will be more activation unblock than desired for optimal sequestration of depolarized tissue into the drug-bound inactivated state. Unfortunately our experiments do not allow us to estimate the relative contribution of block of activated vs. inactivated sodium channels.

Class Ic antiarrhythmic drugs characterized by a slow onset of and recovery from V_{max} block are often very effective in suppressing both early and late premature beats since they will find a significant fraction of non-conducting sodium channels (Hondeghem & Katzung, 1977; 1984). Moreover, in the presence of tachyarrhythmias, sodium channels are in activated and/or inactivated states for a longer period and there is less time to recover from block between beats. Because in the presence of CRE-1087 the recovery kinetics from V_{max} block is a very slow process (τ_{re} about 18 s), the diastolic interval during the trains is not long enough to bring about a complete reactivation of V_{max}. As a consequence, during a train of pulses this drug would produce an accumulation of blocked sodium channels during each successive action potential until a new steady-state is reached.

The present results indicate that CRE-1087 had no effect on ventricular action potential duration. This can be due to the fact that it had no effect and/or exhibited opposite effects on the ionic currents responsible for repolarization of ventricular muscle fibres, i.e. the slow inward Ca current, the outward repolarizing potassium current (I_K) and the late sodium current flowing during the plateau (Carmeliet & Vereecke, 1979; Kiyosue & Arita, 1989).

To ascertain whether CRE-1087 may inhibit the slow inward Ca current, its effects were analyzed on the slow action potentials elicited by isoprenaline in K-depolarized fibres. CRE-1087 had no effect on the electrophysiological characteristics of these slow action potentials, which suggests that it did not exhibit class IV activity in guinea-pig papillary muscles. Thus, even though in the present experiments a direct analysis of the outward K current (I_K) was not performed, it seems unlikely that CRE-1087 exerts a significant effect on this current.

The results of the Cardiac Arrhythmia Suppression Trial (CAST, 1989) demonstrated that antiarrhythmic drugs with class Ic actions (flecainide and encainide) produced an approximately threefold increase in arrhythmic deaths in patients with prior myocardial infarction and asymptomatic ventricular arrhythmias compared to their respective placebo group. Even though caution should be exercised in extrapolating the CAST data to other class I antiarrhythmics or for other patient groups, it seems that class Ic drugs, like CRE-1087, should be restricted to the treatment of cardiac arrhythmias in patients with no structural heart disease (Pratt *et al.*, 1990). In patients with structural heart disease the risk-benefit ratio is critical in clinical decision, particularly when the benefit of class Ic therapy may be low and the risk extremely high (Morganroth, 1992).

On the basis of the present results obtained in guinea-pig ventricular muscle fibres, it can be concluded that CRE-1087 is a class I antiarrhythmic agent which can be classified as a kinetically slow class Ic agent.

The authors would like to thank Dr P. Statkow for the generous supply of CRE-1087. Financial support was provided by a CAICYT Grant and by Laboratories Cermol-Alter S.A.

References

CAMPBELL, T.J. (1983a). Importance of physico-chemical properties in determining the kinetics of the effects of Class I antiarrhythmic drugs on maximum rate of depolarization in guinea-pig ventricle. *Br. J. Pharmacol.*, **80**, 33–40.

CAMPBELL, T.J. (1983b). Kinetics of onset of rate-dependent effects of class I antiarrhythmic drugs are important in determining their effects on refractoriness in guinea-pig ventricle, and provide a theoretical basis for their subclassification. *Cardiovasc. Res.*, **17**, 344–352.

CAMPBELL, T.J. (1989). Subclassification of class I antiarrhythmic drugs. In *Handbook of Experimental Pharmacology*, Vol. 89., ed. Vaughan Williams, E.M. & Campbell, T.J. pp. 135–155. Berlin: Springer Verlag.

CAMPBELL, T.J. & VAUGHAN WILLIAMS, E.M. (1983). Voltage- and time-dependent depression of maximum rate of depolarization of guinea-pig ventricular action potentials by two new antiarrhythmic drugs, flecainide and lorcainide. *Cardiovasc. Res.*, **17**, 251–258.

THE CARDIAC ARRHYTHMIA SUPPRESSION TRIAL (CAST) INVESTIGATORS (1989). Effect of encainide and flecainide on mortality in a randomized trial of arrhythmia suppression after myocardial infarction. *N. Engl. J. Med.*, **321**, 406–412.

CARMELIET, E. & VEREECKE, J. (1979). Electrogenesis of the action potential and automaticity. In *Handbook of Physiology. The Cardiovascular System.* Vol. 1, ed. Berne, E., Speralakis, N. & Geiger, S. pp. 269–334. Bethesda, Maryland: American Physiological Society.

COURTNEY, K. (1980). Interval-dependent effects of small antiarrhythmic drugs on excitability of guinea-pig myocardium. *J. Mol. Cell. Cardiol.*, **12**, 1273–1286.

COURTNEY, K. (1983). Quantifying antiarrhythmic drug blocking during action potentials in guinea-pig papillary muscle. *J. Mol. Cell. Cardiol.*, **15**, 749–757.

DELPON, E., VALENZUELA, C. & TAMARGO, J. (1989). Electrophysiological effects of E-3753, a new antiarrhythmic drug, in guinea-pig ventricular muscles. *Br. J. Pharmacol.*, **96**, 970–976.

DELPON, E., VALENZUELA, C. & TAMARGO, J. (1990). Tonic and use-dependent Vmax block induced by imipramine in guinea-pig ventricular muscle fibres. *J. Cardiovasc. Pharmacol.*, **15**, 414–420.

DELPON, E., VALENZUELA, C. & TAMARGO, J. (1991a). Electrophysiological effects of CRE-1087, a new antiarrhythmic drug, in guinea-pig ventricular papillary muscles. *Br. J. Pharmacol.*, **104**, 179P.

DELPON, E., VALENZUELA, C. & TAMARGO, J. (1991b). Electrophysiological effects of the combination of mexiletine and flecainide in guinea-pig ventricular fibres. *Br. J. Pharmacol.*, **103**, 1411–1416.

GRANT, A., STARMER, C. & STRAUSS, H. (1984). Antiarrhythmic drug action. Blockade of the sodium current. *Circ. Res.*, **55**, 427–439.

HONDEGHEM, L.M. (1978). Validity of Vmax as a measure of the sodium current in cardiac and nervous tissue. *Biophys. J.*, **23**, 147–152.

HONDEGHEM, L.M. (1987). Antiarrhythmic agents: modulated receptor applications. *Circulation*, **75**, 514–520.

HONDEGHEM, L.M. & KATZUNG, B. (1977). Time- and voltage-dependent interactions of antiarrhythmic drugs with cardiac sodium channels. *Biochim. Biophys. Acta*, **472**, 377–398.

HONDEGHEM, L.M. & KATZUNG, B. (1984). Antiarrhythmic agents: The modulated receptor mechanism of sodium and calcium channel-blocking agents. *Annu. Rev. Pharmacol Toxicol.*, **24**, 387–423.

KIYOSUE, T. & ARITA, M. (1989). Late sodium current and its contribution to action potential configuration in guinea-pig ventricular myocytes. *Circ. Res.*, **64**, 389–397.

KOHLHARDT, M. & SEIFERT, C. (1983). Tonic and phasic I_{Na} blockade by antiarrhythmics. Different properties of drug binding to fast sodium channels as judged from Vmax studies with propafenone and derivatives in mammalian ventricular myocardium. *Naunyn-Schmiedebergs Arch. Pharmacol.*, **296**, 199–209.

MORGANROTH, J. (1992). Early and late proarrhythmia from antiarrhythmic drug therapy. *Cardiovasc. Drugs Ther.*, **6**, 11–14.

PRATT, C.M., BRATER, D.C., HARRELL, F.E., KOWEY, P.R., LEIER, C.V., LOWENTHAL, D.T., MESSERLI, F., PACKER, M., PRITCHETT, E.L.C. & RUSKIN, J.N. (1990). Clinical and regulatory implications of the Cardiac Arrhythmia Suppression Trial. *Am. J. Cardiol.*, **65**, 103–105.

PRIEGO, J., STATKOW, P., FAU, M. & SUNKEL, C. (1984). Pharmacokinetic studies with the new antiarrhythmic CRE-1087 in rats. *Proceedings of the IUPHAR 9th International Congress of Pharmacology*, London, 1815P.

SHEETS, M., HANCK, D. & FOZZARD, H. (1988). Nonlinear relation between Vmax and I_{Na} in cardiac Purkinje fibres. *Circ. Res.*, **63**, 386–398.

SNYDERS, D.J. & HONDEGHEM, L.M. (1990). Effects of quinidine on the sodium current of guinea-pig ventricular myocytes. *Circ. Res.*, **66**, 565–579.

STATKOW, P., STRAUMANN, D., SUNKEL, C., FAU, M. & PRIEGO, J. (1985). A new product with potent antiarrhythmic activity in animal models and patients with atrial and ventricular arrhythmias. *Proceedings of the International Symposium on Cardiovascular Therapy*, Geneva. Abstract 58.

TAMARGO, J., VALENZUELA, C. & DELPON, E. (1989). Modulated receptor hypothesis: selectivity and interactions of antiarrhythmic drugs. *News Physiol. Sci.*, **4**, 88–90.

VALENZUELA, C., DELPON, E. & TAMARGO, J. (1988). Tonic and frequency-dependent Vmax block induced by 5-hydroxypropafenone in guinea-pig ventricular muscles. *J. Cardiovasc. Pharmacol.*, **12**, 423–431.

VALENZUELA, C., DELPON, E. & TAMARGO, J. (1989). Electrophysiological interactions between mexiletine and propafenone in guinea-pig papillary muscles. *J. Cardiovasc. Pharmacol.*, **14**, 351–357.

VAUGHAN WILLIAMS, E. (1984). A classification of antiarrhythmic actions reassessed after a decade of new drugs. *J. Clin. Pharmacol.*, **24**, 129–147.

WALLENSTEIN, S., ZUCKER, S. & FLEISS, J. (1980). Some statistical methods useful in circulation research. *Circ. Res.*, **47**, 1–9.

WALTON, M. & FOZZARD, H. (1979). The relation of Vmax to I_{Na}, G_{Na} and h, in a model of the cardiac Purkinje fiber. *Biophys. J.*, **25**, 407–420.

(Received December 9, 1991
Revised May 20, 1992
Accepted June 11, 1992)

Br. J. Pharmacol. (1992), **107**, 521–527

Changes in intrinsic inhibition in isolated hippocampal slices during ethanol withdrawal; lack of correlation with withdrawal hyperexcitability

M.A. Whittington, [1] H.J. Little & *[2] J.D.C. Lambert

Department of Pharmacology, The Medical School, University of Bristol, University Walk, Bristol BS8 1TD and *PharmaBiotec, Institute of Physiology, University of Aarhus, DK-8000 Aarhus C, Denmark

1 Intracellular recordings were made from pyramidal cells in area CA1 in mouse isolated hippocampal slices, after chronic ethanol treatment *in vivo*.

2 Fast i.p.s.ps were isolated by injection of the impaled neurones with QX314 (to block fast sodium currents and the slow i.p.s.p.) and stimulating the interneurones in the presence of the glutamatergic blockers, CNQX and APV.

3 The isolated fast-inhibitory postsynaptic potential (f.-i.p.s.p.) was measured at intervals during the 7 h withdrawal period. The reversal potential and sensitivity to bicuculline suggested that the isolated f.-i.p.s.p. was mediated by activation of the $GABA_A$ receptor-chloride ionophore complex.

4 Measurement of stimulus-response relationships for the f.-i.p.s.ps revealed an initial increase in the maximum size of the i.p.s.p., evoked from a membrane potential of -50 mV, seen at 2 h into ethanol withdrawal. This was attributed to a negative shift in the reversal potential, $E_{i.p.s.p.}$, with no observed change in conductance, $G_{i.p.s.p.}$.

5 No differences in f.-i.p.s.ps evoked during ethanol withdrawal or in control slices were seen at 4 h or 6 h. At these times, epileptiform activity was seen in previous field potential recordings.

6 Paired pulse depression of the f.-i.p.s.p. was significantly increased at 2 h into withdrawal, when a 150 ms pulse interval was used. No differences were seen at later times in the ethanol withdrawal period.

7 The results suggest that ethanol withdrawal hyperexcitability in isolated hippocampal slices is not caused by primary decreases in inhibition mediated by the $GABA_A$ receptor-chloride ionophore complex. The increase in the f.-i.p.s.p. during the initial stages of the withdrawal might prevent the overt expression of epileptiform activity at this time.

Keywords: Ethanol withdrawal; hippocampus; inhibition; $GABA_A$ receptor

Introduction

Withdrawal from long-term ethanol intake results in neuronal hyperexcitability. In man, this withdrawal syndrome is seen as tremor, hallucinations and seizures; the latter can be fatal. It has long been thought that the hyperexcitability may be due to deceased γ-aminobutyric acid (GABA)-mediated inhibition. This has been suggested to occur as an adaptation to the potentiation of GABA transmission that can develop after acute application of ethanol (Nestoros, 1980; Agueyo, 1990).

Much evidence has been cited in support of this hypothesis. GABA agonists, such as muscimol and 4,5,6,7-tetrahydroisazoxolo[4,5-C]pyridin-3-ol (THIP), and agents that increase GABA concentrations, such as amino-oxyacetic acid (AOAA) and sodium valproate, or which potentiate GABA, such as the benzodiazepines, have been found to decrease the ethanol withdrawal syndrome (Goldstein, 1973; 1979; Cooper *et al.*, 1979; Frye *et al.*, 1983; Gonzales & Hettinger, 1984). Clinically, benzodiazepines are widely used to treat the abstinence syndrome. Chronic ethanol treatment has been reported to decrease the number and affinity of GABA receptor sites. Ticku (1980) showed that there was a temporal correlation between the binding changes and the appearance of withdrawal behaviour. Decreases in GABA binding have also been reported by others (Ticku & Burch, 1980; Linnoila *et al.*, 1981; Ticku *et al.*, 1983; Volicer & Biagioni, 1982), although Hunt & Dalton (1981) did not find changes. Studies on GABA-agonist stimulated chloride flux into membrane vesicles have shown tolerance to the potentiating effect of ethanol on the actions of GABA after chronic ethanol treatment, but no changes in GABA-stimulated chloride flux in the absence of ethanol (Allan & Harris, 1987; Morrow *et al.*, 1988).

There have been only a few electrophysiological studies made after chronic ethanol administration. Durand & Carlen (1984) found decreased after-hyperpolarizations and decreased spike frequency adaptation to depolarizing current in CA1 neurones in rat isolated hippocampal slices three weeks after cessation of chronic ethanol treatment. These authors also reported decreased i.p.s.ps in dentate granule and CA1 neurones. However, when the same measurements were made 24 h after ethanol withdrawal, a different pattern was seen, with no change in i.p.s.ps and increases in after-hyperpolarizations (Reynolds *et al.*, 1990). These authors saw no overt withdrawal syndrome after their ethanol treatment, and the studies were made at later times than those at which withdrawal hyperexcitability might have expected. The persistence of these electrophysiological changes suggests that they are unlikely to be involved in the behavioural withdrawal signs, unless some compensatory adaptations took place at other sites to terminate the withdrawal hyperexcitability. Takada *et al.* (1989) studied the effects of GABA by extracellular recordings on hippocampal slices prepared from rats four days after cessation of chronic ethanol treatment. Inhibition by exogenous GABA of the population spikes occurred to the same extent after this chronic treatment as in control slices. The potentiation of this effect by ethanol at concentrations above 70 mM, seen in control preparations, was however, lost after the chronic treatment.

[1] Author for correspondence.
[2] Author to whom reprint requests should be addressed

We have described patterns of hyperexcitability in extracellular recordings from area CA1 in isolated hippocampal slices, prepared immediately on withdrawal from chronic ethanol treatment (Whittington & Little, 1990; 1991). The treatment schedule used caused behavioural hyperexcitability on cessation of treatment (Littleton *et al.*, 1990; Green *et al.*, 1990). The changes seen in the electrophysiological studies followed different time courses and suggested that several different mechanisms may underlie the withdrawal hyperexcitability. The first change, seen within 2 h of the slice preparation (i.e. from ethanol withdrawal) was an increase in paired pulse potentiation of the population spike. This reached maximum at 2 h 15 min, then decreased to normal values by 4 h into withdrawal. Decreases in the thresholds for eliciting single and multiple population spikes and epileptiform activity were then seen, that reached maximum at 5 h–7 h into the withdrawal period. In the present study we have examined changes in inhibition mediated specifically by the $GABA_A$ receptor-chloride ionophore complex, using intracellular recordings from CA1 pyramidal cells, during the withdrawal period, immediately after chronic ethanol administration *in vivo*.

Methods

Chronic ethanol treatment

Male C57 mice, 28–39 g, were given either ethanol 24% v/v in tap water as sole fluid, or tap water alone for between 15 and 18 weeks. Ethanol intake was measured every 3 to 4 days, giving a mean (± s.e.mean) intake of 19.2 ± 0.6 g kg^{-1} daily. Mice were housed singly and both treatment groups were kept under identical conditions. A 12 h light/dark cycle was used (08 h 00 min to 20 h 00 min).

Preparation of hippocampal slices

On each day of the study, each mouse was killed by cervical dislocation between 08 h 45 min and 09 h 15 min. The ethanol drinking fluid was not removed from the cages before this. The times in which data were gathered are all expressed with reference to this, expressed as time 0 h (i.e. time from dissection or time from cessation of chronic ethanol treatment). Transverse hippocampal slices, 400 μm thick, were prepared from the middle third of the hippocampus; slices from the septal and temporal ends were not used in this study. Slices were immediately transferred to the recording chamber and perfused with artificial CSF for the duration of each experiment.

Intracellular recordings

Intracellular recordings were made from the somata of CA1 pyramidal neurones with electrodes (50–80 MΩ) filled with 4 M KAc and 50 mM of the quaternary derivative of lignocaine (QX314). The latter blocks both the sodium action potential and the slow inhibitory postsynaptic potential (Nathan *et al.*, 1990). Diffusion of QX314 into the cell was facilitated by depolarizing current pulses. On two occasions, recordings were taken with electrodes filled with potassium acetate alone to examine sodium spikes and slow inhibition. The criteria for accepting neurones on impalement were a stable resting membrane potential more negative than − 50 mV and input resistances greater than 30 MΩ. Membrane potentials were corrected for both potentials measured after withdrawing from the cell.

Bipolar stimulating electrodes were placed both proximal to the recording site, in the stratum radiatum at the subicular end of area CA1, and distal to the recording site in the stratum radiatum of area CA3 (Figure 1). The fast inhibitory component (f.-i.p.s.p.) of the compound synaptic potential, evoked by proximal stimulation, was isolated by use of QX314, 50 mM in the recording electrode, as described above, and blockade of glutamatergic excitation by addition of both the N-methyl-D-aspartate (NMDA) receptor antagonist, (DL)-2-amino-5-phosphovaleric acid (APV), 50 μM, and the non-NMDA receptor antagonist 6-cyano-7-nitro quinoxaline-2,3-dione (CNQX), 10 μM, to the perfusion solution. This combination of pharmacological agents blocked all measurable synaptic activity induced by distal stimulation in this study, but left the single f.-i.p.s.p. intact upon proximal stimulation (Nathan *et al.*, 1991), as illustrated in Figure 1.

The aim of this study was to measure the f.-i.p.s.ps at three time points in the ethanol withdrawal period, during each experiment, 2 h, 4 h and 6 h from the time of dissection (i.e. from cessation of chronic ethanol treatment). The measurement protocol described below took 30 min to complete and was therefore carried out from 15 min before to 15 min after each of the 2 h, 4 h and 6 h time points.

During each time period the stimulus-response relationship for the f.-i.p.s.p. was examined by use of stimuli from 25–500 μA (duration 50 μs, frequency 0.1 Hz). The membrane potential was held at − 50 mV by depolarizing current injection to increase the size of the f.-i.p.s.p. and to normalize the influence of membrane potential on this f.-i.p.s.p. Measurements of f.-i.p.s.p. size, duration and time-to-peak were made with a Nicolet digital oscilloscope (4049C).

Paired pulse depression of the f.-i.p.s.p. was examined with two interpulse intervals; 70 ms, to correspond with the interval producing maximum potentiation of the population spike in the mouse hippocampus (Whittington & Little, 1990) and 150 ms to correspond with the interval producing maximal depression of the second evoked f.-i.p.s.p. in the rat hippocampus (Nathan *et al.*, 1991). Paired pulse depression was expressed as the amplitude of the second evoked f.-i.p.s.p. as a percentage of the first.

The voltage-dependency of the f.-i.p.s.p. was examined by evoking maximal f.-i.p.s.ps (stimulus intensities 250–500 μA) with the membrane potential held sequentially at − 50, − 60, − 70 and − 80 mV for 2–3 min at each level. Steps were always performed in the hyperpolarizing direction. The reversal potential for the f.-i.p.s.p. ($E_{i.p.s.p.}$) was measured as the membrane potential at which no hyperpolarizing or depolarizing potential change was seen in response to maximal stimulation. Conductance changes associated with the f.i.p.s.p. ($G_{i.p.s.p.}$) were measured by comparison of the absolute membrane potential for a given magnitude of current injected at the cell soma both with and without the evoked f.-i.p.s.p. Values of the f.-i.p.s.p. conductance were derived from the slope of the *I*/V relationship at the peak of the f.-i.p.s.p. and subtracting the value for the resting membrane conductance.

Statistical analysis

All comparisons between data from slices from control mice and mice treated with ethanol were made within the three discrete time-windows, as described above. Each measurement protocol at each time was performed on separate hippocampal slices not previously exposed to APV or CNQX. Recordings were made from only one cell per slice and only one slice per mouse was used. Comparisons were made by Student's nonpaired *t* test, with significance at the 0.05 level.

Composition of solutions

The composition of the perfusion fluid was (mM): NaCl 124, KCl 3.25, NaH_2PO_4 1.25, $NaHCO_3$ 20.0, $MgSO_4$ 2.0, $CaCl_2$ 2.0, and (+)-glucose 10.0. The pH was 7.2 at 30°C. CNQX (Novo-Nordisk) was dissolved at 10 mM in NaOH at pH 8 and diluted in the artificial CSF. QX314 bromide (Astra) was dissolved in 4 M potassium acetate. Bicuculline methobromide and DL-APV were obtained from Tocris (Bristol).

Results

Isolation of the monosynaptic f.-i.p.s.p.

Pyramidal cells in area CA1, impaled with potassium acetate-filled electrodes, showed a characteristic triphasic synaptic potential with either proximal or distal stimulation (Figure 1a). Impalement with electrodes filled with QX314 (50 mM) after repeated depolarizing current injection, removed both the fast sodium spike and the slow phase of the i.p.s.p. (Figure 1b). Perfusion with medium containing both APV 50 μM, and CNQX, 10 μM, resulted in an absence of post-synaptic potentials with distal stimulation, even at maximal stimulation amplitude (500 μA). However, a single, hyper-polarizing potential was evoked by proximal stimulation (Figure 1c). This postsynaptic potential, termed the f.-i.p.s.p., was completely blocked by addition of 30 μM bicuculline to the perfusion medium.

Magnitude of the f.-i.p.s.p. during ethanol withdrawal

Stimulus-response relationships for the peak potential change during the f.-i.p.s.p. (Em = − 50 mV) and the stimulus intensity showed an increase in the maximum size of the evoked f.-i.p.s.p. at 2 h into ethanol withdrawal (Figure 2a). At stimulus intensities greater than 100 μA, the i.p.s.ps from slices from mice treated with ethanol were significantly larger than controls ($P<0.05$). No significant differences were seen in this measurement at lower stimulus intensities, or at later times (4 h and 6 h) in the withdrawal period (Figure 2c, $P>0.05$).

Neither the f.-i.p.s.p. duration nor time to peak were significantly different when comparison was made, throughout the withdrawal period, between results from control slices and slices from mice treated with ethanol (Figure 3, $P>0.05$).

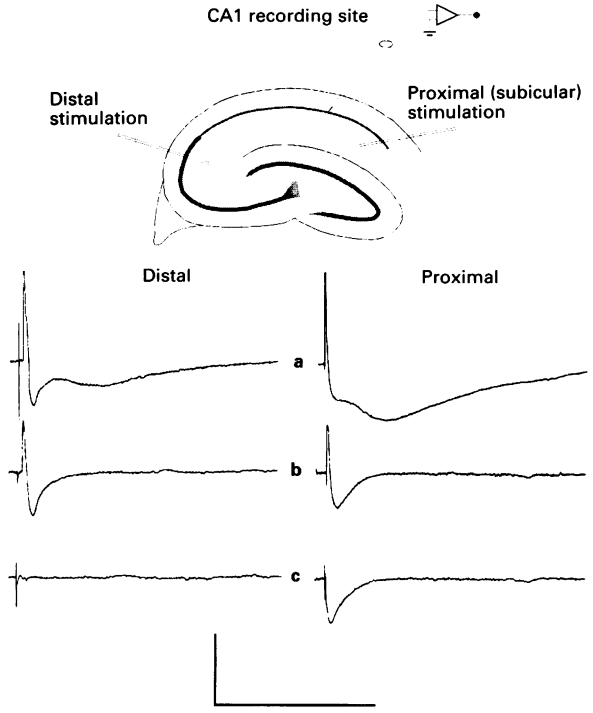

Figure 1 Example of the compound synaptic potentials evoked in CA1 pyramidal cells. (a) Slices bathed in normal artifical CSF, recording electrode containing 4 M KAc only. (b) Normal artificial CSF, electrode contained 4 M KAc and 50 nM QX314. Responses were recorded after a 5 min period of repeated injections of depolarizing current pulses. (c) Responses in CSF containing APV, 50 μM, and CNQX, 10 μM, the recording electrode contained QX314. All responses evoked by single 500 μA stimulus pulse. Scale bar; 10 mV, 400 ms. For abbreviations, see text.

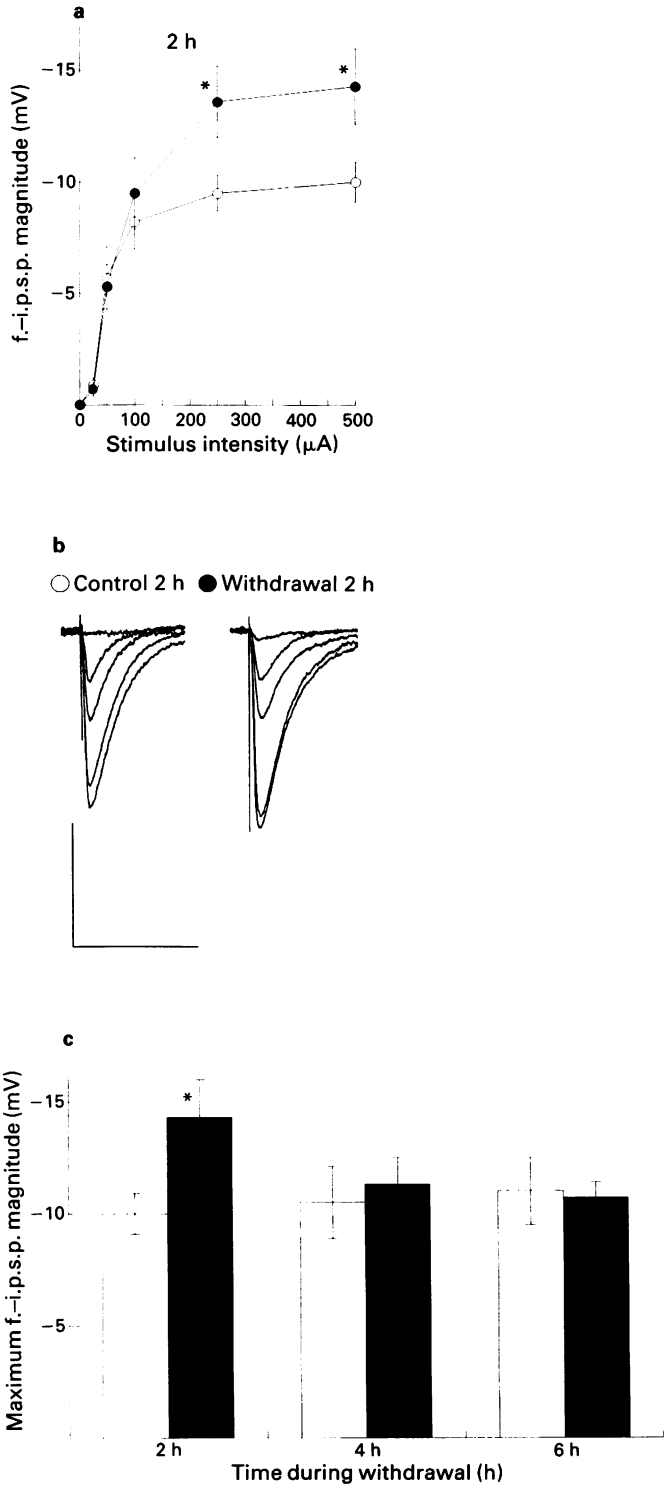

Figure 2 Fast-i.p.s.p. magnitude during ethanol withdrawal. (a) Stimulus-response relationship for proximal stimulation of CA1 pyramidal cells 2 h after dissection in slices from control mice (○, $n = 7$) and mice treated with ethanol (●, $n = 8$). Data expressed as mean with s.e.mean shown by vertical bars. $*P<0.05$ for comparison between control and ethanol withdrawal. (b) Sample traces showing the stimulus response relationship of the f.-i.p.s.p. 2 h after dissection in a control neurone and a neurone after ethanol withdrawal. Stimulus intensities were at the five values between 25–500 μA shown in (a). Scale bar; 10 mV, 150 ms. Each trace is a digital average of at least 8 consecutive responses. (c) Time course of changes in f.-i.p.s.p. magnitude in cells from control slices (open columns, $n = 7$) and cells from slices from mice treated with ethanol (solid columns, $n = 8$). All values are maximal f.-i.p.s.p. amplitude, mean with s.e.mean shown by vertical bars. $*P<0.05$.

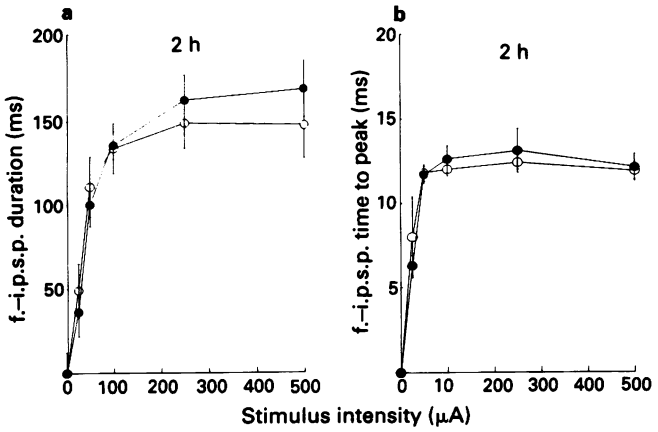

Figure 3 Lack of effect of ethanol withdrawal on f.-i.p.s.p. duration and time to peak. (a) Stimulus-response relationship of f.-i.p.s.p. duration measurements in slices from control mice (○, $n = 7$) and mice treated with ethanol (●, $n = 8$). (b) Corresponding measurements of time to peak.

Changes in paired pulse depression of the f.-i.p.s.p. during ethanol withdrawal.

When paired stimuli were given, with interpulse intervals of 70 ms or 150 ms, a decrease in the size of the second evoked f.-i.p.s.p., compared with the first, was seen at maximum stimulation levels in all slices, as illustrated in Figure 4 (Em = − 50mV). This paired-pulse depression of the second f.-i.p.s.p. appeared greater when interpulse intervals of 150 ms, as opposed to 70 ms, were used.

No significant differences in paired-pulse depression of the f.-i.p.s.p. were seen with interpulse intervals of 70 ms, at any time during the withdrawal period, although the mean values at the 2 h and 4 h times were lower after the ethanol treatment than in the controls (Figure 4c). At the 2 h interval, the percentage control value was 80 ± 3, and the ethanol withdrawal value, 73 ± 2 (mean ± s.e.mean, $P > 0.05$).

At 2 h into ethanol withdrawal, a significant increase was seen in the paired-pulse depression of the f.-i.p.s.p., when the 150 ms interval was used. At this time, the mean percentage control value was 74 ± 4, and the ethanol withdrawal value 63 ± 2 ($P < 0.05$). The differences were not significant at any other time interval (Figure 4a). Although at the 4 h interval the mean differences were actually larger than at 2 h, the variance of the data was greater and the difference was not significant ($P > 0.05$).

The second f.-i.p.s.p. during ethanol withdrawal was unaltered with respect to control values ($P > 0.05$ for comparison between the second evoked f.-i.p.s.p. in control slices and during ethanol withdrawal throughout the stimulus range, Figure 5a). The increase in paired pulse depression of the second f.-i.p.s.p. therefore appeared to be due entirely to the increase in the size of the first f.-i.p.s.p.

Potential dependence of the f.-i.p.s.p.

The maximum size of the f.-i.p.s.p. was measured at membrane potentials from − 50 mV down to − 80 mV, in 10 mV steps. Measurements revealed a shift in the f.-i.p.s.p. reversal potential to more hyperpolarizing membrane potentials during the initial stages of the withdrawal period; control values for the first f.-i.p.s.p. were − 69 ± 1 mV, ethanol withdrawal values were − 75 ± 2 mV, at 2 h into withdrawal (Figures 6a and b). This shift was significant 2 h into ethanol withdrawal ($P < 0.05$) and was completely absent at the end of the 7 h recording period (Figure 6c).

The magnitude of paired f.-i.p.s.ps at the above membrane potentials showed that the degree of paired pulse depression appeared to increase with increasing levels of depolarization

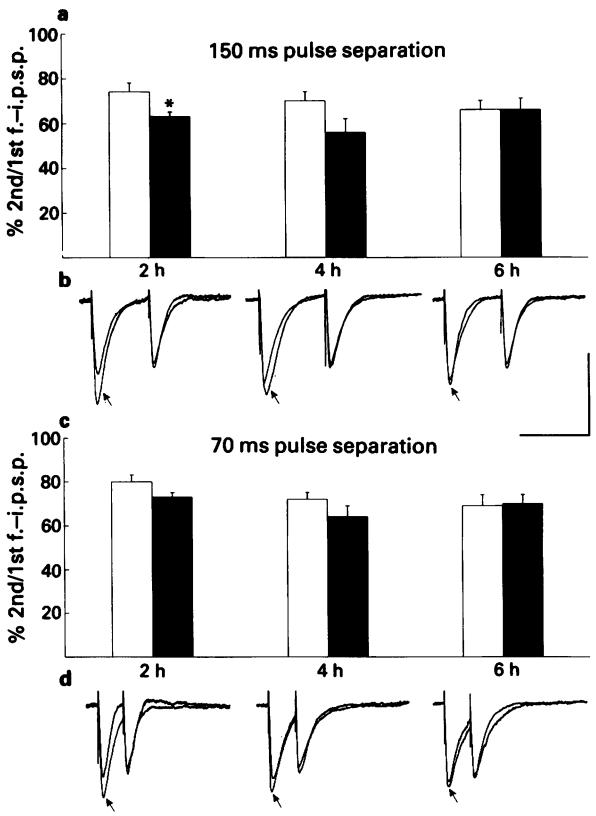

Figure 4 Paired pulse depression of the f.-i.p.s.p. (a) Percentage size of the second compared with the first evoked f.-i.p.s.p. at maximal stimulus intensity with a pulse interval of 150 ms. Data expressed as mean with s.e.mean (vertical bars) from slices from control mice (open columns, $n = 7$) and mice treated with ethanol (solid columns, $n = 8$). $^*P < 0.05$ for comparison between ethanol withdrawal and control. (c) Percentage size of the second compared with the first evoked f.-i.p.s.p. as in (a) but with a pulse interval of 70 ms. Data expressed as mean with s.e.mean, $n = 7-8$. (b & d) Superimposed sample recordings of paired f.-i.p.s.ps evoked in control slices and slices prepared after chronic ethanol treatment. Each trace is a digital average of at least 6 consecutive paired responses, with interpulse intervals of 150 ms (b) and 70 ms (d). Arrows indicate response evoked during ethanol withdrawal at the times shown. Scale bar; 10 mV, 200 ms.

from the reversal potential, in both controls and during ethanol withdrawal, indicating that, at a given membrane potential the degree of paired pulse depression was related to the reversal potential (Figure 5b). Measurements of the gradient of the plot of transmembrane current versus maximum potential change during the f.-i.p.s.p. gave estimates of the total membrane conductance change during the f.-i.p.s.p. response (Figure 6b). No significant difference in this measurement was seen at 2 h into withdrawal, when the maximum increase in the size of the first i.p.s.p. was seen (control $G_{i.p.s.p.} = 58 \pm 9$ nS, ethanol withdrawal $G_{i.p.s.p.} = 49 \pm 5$ nS, $P > 0.05$).

Discussion

The reversal potential and the bicuculline sensitivity of the i.p.s.ps recorded in this study demonstrated that they were monosynaptic i.p.s.ps, mediated by GABA release from interneurones acting on postsynaptic $GABA_A$ receptors. These responses are known to be due to increased chloride conductance. The amplitudes of the control f.-i.p.s.ps were virtually identical at the beginning and the end of the recording period, demonstrating the stability of the preparations.

The results showed clearly that these fast, GABA-

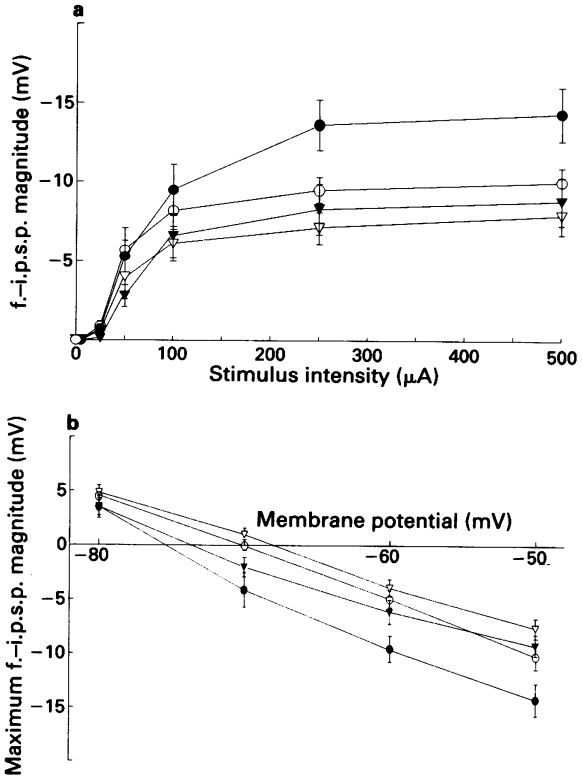

Figure 5 Relationship between first and second evoked f.-i.p.s.ps using paired pulses (150 ms interpulse interval). All data taken 2 h after dissection. (a) Stimulus-response relationships for the first (○) and second (△) evoked f.-i.p.s.ps in control slices ($n = 7$) and the first (●) and second (▲) evoked f.-i.p.s.ps in slices from mice treated with ethanol ($n = 8$). Data expressed as mean with s.e.mean shown by vertical bars. $n = 7-8$. (b) Membrane potential dependency of the relationship between first (○) and second (△) evoked f.-i.p.s.ps in control slices and the first (●) and second (▲) evoked f.-i.p.s.ps in slices from mice treated with ethanol. All data expressed as in (a).

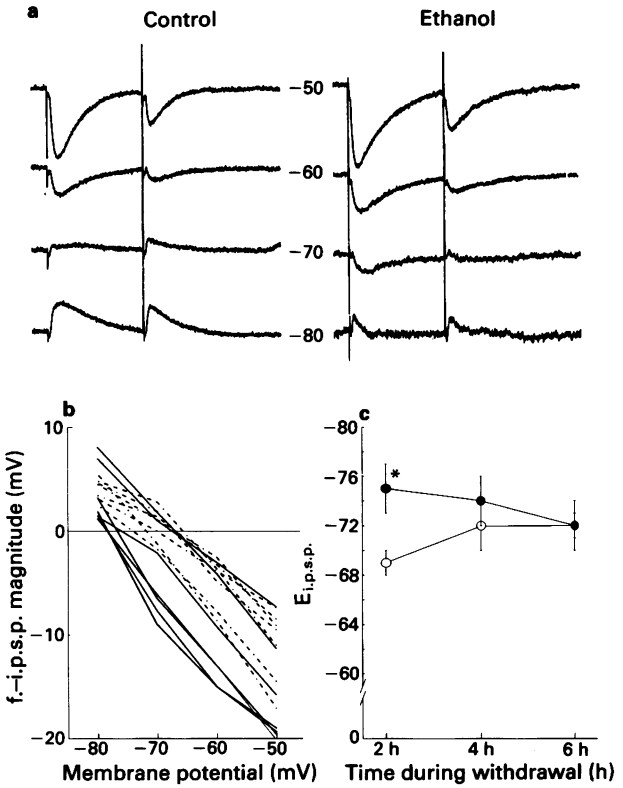

Figure 6 Potential dependence of the f.-i.p.s.p. (a) Example recordings taken 2 h after dissection. Each trace is an average of at least 6 responses at each membrane potential. Paired pulse interval was 150 ms, with maximal stimulation. (b) Potential dependence of f.-i.p.s.ps for cells from seven control slices (- - -) and seven slices from ethanol-treated mice (——). $E_{i.p.s.p.}$ was derived from the interpolation of these relationships with the line drawn for an f.-i.p.s.p. magnitude of 0 mV. (c) Time course of changes in $E_{i.p.s.p.}$. Data expressed as mean with s.e.mean (vertical bars) from control slices (○) and slices from ethanol-treated mice (●). $^*P < 0.05$.

mediated, i.p.s.ps were not decreased at any time during the ethanol withdrawal period, when epileptiform activity was seen in our earlier field potential recordings. As described in the introduction, biochemical and behavioural evidence has previously been cited in support of the suggestion that the hyperexcitability seen during ethanol withdrawal is due to decreases in GABAergic inhibition. The present study, however, is the first, to our knowledge, to investigate by electrophysiological means whether or not such a decrease actually does occur.

The isolated hippocampal slice appears to be a valid model for withdrawal hyperexcitability and pharmacological prevention of behavioural syndrome could be achieved with the same compounds that blocked the epileptiform activity in the hippocampal slices, for example, dihydropyridine calcium channel antagonists (Littleton *et al.*, 1990; Whittington & Little, 1991) and NMDA antagonists (Ripley *et al.*, 1991). At the concentrations effective against the withdrawal hyperexcitability, the former compounds did not alter the hyperexcitability produced by the GABA antagonist, bicuculline, in hippocampal slices from naive animals. The maximum changes in behaviour of the mice occurred between 5 h and 8 h after cessation of this chronic ethanol treatment (Littleton *et al.*, 1990; Green *et al.*, 1990), but the time course of withdrawal hyperexcitability *in vitro* would be expected to be more rapid, as the *in vivo* metabolism of ethanol would be slower than the wash-out of ethanol from the hippocampal slices.

The increase in the maximum amplitude of the f.-i.p.s.ps, seen at 2 h into ethanol withdrawal, suggested that excitability of the hippocampal slice may be lowered during the intial stages of ethanol withdrawal. Some indication of such a decrease in excitability was seen in our extracellular studies, as the thresholds for eliciting single population spikes were increased slightly during the first part of the recording period (Whittington & Little, 1990).

The mice were allowed access to the ethanol drinking fluid up to the time of dissection. Although there would have been some individual variation in the amount drunk by each mouse immediately before the slice preparation, these animals consume most fluid at night, as would be expected from their nocturnal habits. Ethanol would therefore have been present in the tissues before dissection and would have been expected to wash rapidly out of the slices during perfusion. As described in the introduction, although ethanol can acutely potentiate the effects of GABA (Nestoros, 1980; Celentano *et al.*, 1988), this effect has not been found in all studies (for review see Little, 1991).It is now known that this potentiation occurs only in certain neurones (Agueyo, 1990). It is possible that residual ethanol may have contributed to the increase in maximal i.p.s.p. amplitude during the early part of the recording period in the present study, but it is unlikely that sufficient would have remained 2 h into withdrawal to have had a significant effect on the f.-i.p.s.p. The only study that examined the acute and chronic effects of ethanol on GABA inhibition found that tolerance developed to the acute potentiating action after the chronic ethanol (Takada *et al.*, 1989). It is therefore unlikely that $GABA_A$ inhibition was increased at the end of the chronic ethanol administration, immediately prior to the preparation of the slices.

The increase in the f.-i.p.s.ps, seen 2 h into withdrawal,

could have arisen either because a larger number of ionophores participate in the generation of the f.-i.p.s.p., or because the electrochemical gradient for chloride was increased. The absence of significant changes in the kinetics (time-to-peak and duration) suggested that neither an increase in the number of $GABA_A$ receptor-ionophore complexes or an increase in the amount of GABA released accounted for the increase in the f.-i.p.s.p. Furthermore, the conductance change underlying a single (i.e. the first) i.p.s.p. was the same in control and ethanol-treated slices, suggesting that GABA release was unaltered. On the other hand, the i.p.s.p. reversal potential was increased at 2 h into the withdrawal period. Assuming the i.p.s.p. reversal potential is equal to the chloride reversal potential, it can be calculated, using the Nernst equation, that the internal chloride concentration would be 9.33 mM for control slices and 7.41 mM for slices prepared after ethanol withdrawal, at 2 h after the start of withdrawal. Active outward chloride transport maintains the internal chloride concentration below that dictated by passive diffusion (Misgeld *et al.*, 1986; Thompson *et al.*, 1988). Chloride ions are co-transported with potassium ions using the energy stored in the potassium gradient. An increase in the chloride reversal potential could result from one or more of the following: (1) a decrease in resting chloride permeability; (2) alterations of the transmembrane potassium gradient, which would alter the internal chloride concentration according to the quasi-Donnan conditions prevailing across neuronal membranes; (3) an increase in the activity of the chloride extrusion mechanism.

There were no significant differences between either the resting membrane potential or resting membrane conductance between ethanol withdrawal and control slices. This suggests that the potassium distribution was not changed during withdrawal and that the membrane permeability to chloride was not altered to such an extent that this could be seen as a change in the overall input membrane conductance. However, Thompson & Gähwiler (1989a) have pointed out that chloride permeability is relatively low in hippocampal pyramidal cells and that the majority of chloride entry at 'rest' results from spontaneous inhibitory activity. It is not yet known whether this differs between control hippocampal slices and those prepared after chronic ethanol treatment. The other remaining possibility exists that the activity and/or affinity of the chloride extrusion mechanism is increased during the early phase of withdrawal.

Paired-pulse depression of the f.-i.p.s.p. was present in both control and withdrawal slices. A decrease in the equilibrium potential for the i.p.s.p. on presentation of multiple stimuli has been widely reported for rat slices (McCarren & Alger, 1985; Deisz & Prince, 1989; Thompson & Gähwiler, 1989b; Nathan & Lambert, 1991), and has now been shown here for the mouse. The inward chloride flux underlying the first f.-i.p.s.p. would increase the internal chloride concentration, which would cause a transient positive shift in the chloride equilibrium potential. Since the shift between the first and second responses was about + 2 mV, in both control and withdrawal slices, this cannot explain the increase in paired-pulse depression of the f.-i.p.s.p. in slices after ethanol withdrawal, which was due entirely to an increase in the first f.-i.p.s.p. The mechanism underlying the depression of the f.-i.p.s.p. is thought to involve activation of presynaptic $GABA_B$ receptors autoreceptors (Deisz & Prince, 1989; Thompson & Gähwiler, 1989c; Davies *et al.*, 1990; Nathan & Lambert, 1991). It is possible that activity mediated by these receptors is transiently increased during the early withdrawal period, thereby causing a relatively larger reduction of the second f.-i.p.s.p.

It is notable that the time of appearance of the decrease in the paired pulse depression of the f.-i.p.s.p., the shift in the reversal potential and that of the increase in maximum i.p.s.p. amplitude, at 2 h into withdrawal, were similar to that seen for the increase in paired pulse potentiation of the population spike in our extracellular recordings during ethanol withdrawal (Whittington & Little, 1990; 1991). However, in the previous studies the pulse interval used was 70 ms (giving maximal potentiation of population spikes in the mouse hippocampus), but the changes in the paired pulse depression of the f.-i.p.s.p. in the present study were not significant when the 70 ms interval was used. It has previously been shown, in rat hippocampal slices, that paired pulse depression of f.-i.p.s.ps underlies paired pulse potentiation of the late phase of the field e.p.s.p. (maximum potentiation at 125 ms), and was not involved in potentiation of the population spike (maximum potentiation at 50 ms interval) (Nathan *et al.*, 1990; 1991). Others have suggested that paired pulse potentiation of the population spike is due to increased intracellular calcium accumulation (Creager *et al.*, 1980; Konnerth & Heinemann, 1983).

The present work therefore provides evidence against primary decreases in $GABA_A$-mediated inhibition being the cause of withdrawal hyperexcitability in the hippocampus. On the contrary, the initial increase in GABAergic inhibition may prevent the expression of overt hyperexcitability in the early part of the withdrawal period. It is possible, however, that $GABA_A$ inhibition could be decreased by primary changes at other sites, where the responses were blocked in the present recordings. We have recently reported an increase in NMDA-mediated excitatory transmission in isolated hippocampal slices during the later phase of ethanol withdrawal and it is likely that this is an important factor in the epileptiform activity (Whittington *et al.*, 1992).

We are grateful to the PharmaBiotec Biotechnology programme, the Danish Medical Research Council, the British Medical Research Council, the European Science Foundation, and the Wellcome Trust for financial support for this work. H.J.L. is a Wellcome Trust Senior Lecturer. We thank T. Honore (Novo-Nordisk) for the gift of CNQX, Astra for QX314 bromide and Tocris (Bristol) for bicuculline and APV.

References

AGUEYO, L. (1990). Ethanol potentiates the $GABA_A$-activated Cl^- current in mouse hippocampal and cortical neurones. *Eur. J. Pharmacol.*, **187**, 127–130.

ALLAN, A.M. & HARRIS, R.A. (1987). Acute and chronic ethanol treatments alter GABA receptor-operated chloride channels. *Pharmacol. Biochem. Behav.*, **27**, 665–670.

CELENTANO, J.J., GIBBS, T.T. & FARB, D.H. (1988). Ethanol potentiates GABA- and glycine-induced chloride currents in chick spinal cord neurones. *Brain Res.*, **455**, 377–380.

COOPER, B.R., VIIK, K., FERRIS, R.M. & WHITE, H.L. (1979). Antagonism of the enhanced susceptibility to audiogenic seizures during alcohol withdrawal in the rat by gamma-aminobutyric acid (GABA) and 'GABA-mimetic' agents. *J. Pharmacol. Exp. Ther.*, **209**, 396–403.

CREAGER, R., DUNWIDDIE, T. & LYNCH, G. (1980). Paired pulse and frequency facilitation in the CA1 region of the in vitro rat hippocampus. *J. Physiol.*, **299**, 409–424.

DAVIES, C.H., DAVIES, S.N. & COLLINGRIDGE, G.L. (1990). Paired pulse depression of monosynaptic GABA mediated inhibitory postsynaptic responses in rat hippocampus. *J. Physiol.*, **424**, 513–531.

DEISZ, R.A. & PRINCE, D.A. (1989). Frequency-dependent depression of inhibition in guinea pig neocortex *in vitro* by $GABA_B$ receptor feed-back on GABA release. *J. Physiol.*, **412**, 513–542.

DURAND, D. & CARLEN, P.L. (1984). Decreased neuronal inhibition in vitro after long-term administration of ethanol. *Science*, **224**, 1359–1361.

FRYE, G.D., MCGOWAN, J. & BREESE, G.R. (1983). Differential sensitivity of ethanol withdrawal signs in the rat to gamma-aminobutyric acid (GABA)-mimetics: blockade of audiogenic seizures but not forelimb tremors. *J. Pharmacol. Exp. Ther.*, **226**, 720–726.

GOLDSTEIN, D.B. (1973). Alcohol withdrawal reactions in mice: effects of drugs that modify neurotransmission. *J. Pharmacol. Exp. Ther.*, **186,** 1–9.

GOLDSTEIN, D.B. (1979). Sodium bromide and sodium valproate: effective suppressants of ethanol withdrawal reactions in mice. *J. Pharmacol. Exp. Ther.*, **208,** 223–227.

GONZALES, L.P. & HETTINGER, M.K. (1984). Intranigral muscimol suppresses ethanol withdrawal seizures. *Brain Res.*, **298,** 163–166.

GREEN, A.R., DAVIES, M., WHITTINGTON, M.A., LITTLE, H.J. & CROSS, A.J. (1990). Action of chlormethiazole in a model of ethanol withdrawal. *Psychopharmacology*, **102,** 239–242.

HUNT, W.A. & DALTON, T.K. (1981). Neurotransmitter receptor binding in various brain regions in ethanol dependent rats. *Pharmacol. Biochem. Behav.*, **14,** 733–739.

KONNERTH, A. & HEINEMANN, U. (1983). Presynaptic involvement in frequency facilitation in the hippocampal slice. *Neurosci. Lett.*, **42,** 255–260.

LINNOILA, M., STOWELL, L., MARANGOS, P.J. & THURMAN, R.G. (1981). Effect of ethanol and ethanol withdrawal on [^{3}H]-muscimol binding and behaviour in the rat: a pilot study. *Acta Pharmacol. Toxicol.*, **49,** 407–411.

LITTLE, H.J. (1991). Mechanisms that may underlie the behavioural effects of ethanol. *Progr. Neurobiol.*, **36,** 171–194.

LITTLETON, J.M., LITTLE, H.J. & WHITTINGTON, M.A. (1990). Effects of dihydropyridine calcium channel antagonists in ethanol withdrawal; doses required, stereospecificity and actions of BAY K 8644. *Psychopharmacology*, **100,** 387–392.

MCCARREN,M. & ALGER, B.E. (1985). Use-dependent depression of IPSPs in rat hippocampal pyramidal cells in vitro. *J. Neurophysiol.*, **53,** 557–571.

MISGELD, U., DEISZ, R.A., DODT, H.U. & LUX, H.D. (1986). The role of chloride transport in postsynaptic inhibition of hippocampal neurones. *Science*, **232,** 1413–1415.

MORROW, A.L., SUZDAK, P.D., KARANIAN, J.W. & PAUL, S.M. (1988). Chronic ethanol administration alters GABA, pentobarbitol and ethanol mediated 36Cl- uptake in cerebral cortical synaptoneurosomes. *J. Pharmacol. Exp. Ther.*, **246,** 158–164.

NATHAN, T., JENSEN, M.S. & LAMBERT, J.D.C. (1990). The slow inhibitory postsynaptic potential in rat hippocampal CA1 neurones is blocked by intracellular injection of QX-314. *Neurosci. Lett.*, **110,** 309–313.

NATHAN, T. & LAMBERT, J.D.C. (1991). Depression of the fast IPSP underlies paired-pulse facilitation in area CA1 of the rat hippocampus. *J. Neurophysiol.*, **66,** 1704–1715.

NESTOROS, J.N. (1980). Ethanol specifically potentiates GABA mediated neurotransmission in feline cerebral cortex. *Science*, **209,** 708–710.

REYNOLDS, J.N., WU, P.H., KHANNA, J.M. & CARLEN, P.L. (1990). Ethanol tolerance in hippocampal neurones: adaptive changes in cellular responses to ethanol measured in vitro. *J. Pharmacol. Exp. Ther.*, **252,** 265–271.

RIPLEY, T.L., RABBANI, M. & LITTLE, H.J. (1991). A competitive antagonist at NMDA receptors, at low doses, protects against the ethanol withdrawal syndrome. *Eur. J. Pharmacol.*, Suppl. 4, 322.

TAKADA, R., SAITO, K., MATSURA, H. & INOKI, R. (1989). Effect of ethanol on hippocampal receptors in the rat brain. *Alcohol*, **6,** 115–119.

THOMPSON, S.M., DEISZ, R.A. & PRINCE, D.A. (1988). Relative contribution of passive equilibrium and active transport to the distribution of chloride in mammalian cortical neurons. *J. Neurophysiol.*, **60,** 105–124.

THOMPSON, S.M. & GÄHWILER, B.H. (1989a). Activity-dependent disinhibition. II. Effects of extracellular potassium, furosemide, and membrane potential on E_{Cl-} in hippocampal CA3 neurons. *J. Neurophysiol.*, **61,** 512–522.

THOMPSON, S.M. & GÄHWILER, B.H. (1989b). Activity-dependent disinhibition. I. Repetitive stimulation reduces IPSP driving force and conductance in the hippocampus in vitro. *J. Neurophysiol.*, **61,** 501–511.

THOMPSON, S.M. & GÄHWILER, B.H. (1989c). Activity-dependent disinhibition. III. Desensitization and $GABA_B$ receptor-mediated presynaptic inhibition in the hippocampus in vitro. *J. Neurophysiol.*, **61,** 524–533.

TICKU, M.K. (1980). The effect of acute and chronic ethanol administration and its withdrawal on gamma-aminobutyric acid receptor binding in rat brain. *Br. J. Pharmacol.*, **70,** 403–410.

TICKU, M.K. & BURCH, T. (1980). Alterations in gamma-aminobutyric acid receptor sensitivity following acute and chronic ethanol treatments. *J. Neurochem.*, **34,** 417–423.

TICKU, M.K., BURCH, T.P. & DAVIS, W.C. (1983). The interactions of ethanol with the benzodiazepine-GABA-receptor ionophore complex. *Pharmacol. Biochem. Behav.*, **18,** 15–18.

VOLICER, L. & BIAGIONE, T.M. (1982). Effect of ethanol administration and withdrawal on GABA receptor binding in rat cerebral cortex. *Subst. Alc. Actions/Misuse*, **3,** 31–39.

WHITTINGTON, M.A. & LITTLE, H.J. (1990). Patterns of changes in field potentials in the isolated hippocampal slice on withdrawal from chronic ethanol treatment of mice in vivo. *Brain Res.*, **523,** 237–244.

WHITTINGTON, M.A. & LITTLE, H.J. (1991). A calcium channel antagonist stereoselectivity decreases ethanol withdrawal hyperexcitability but not that due to bicuculline, in hippocampal slices. *Br. J. Pharmacol.*, **103,** 1313–1320.

WHITTINGTON, M.A., LAMBERT, J.D.C. & LITTLE, H.J. (1992). Withdrawal from in vivo chronic ethanol treatment increases APV-sensitive transmission in isolated mouse hippocampal slices. *J. Physiol.*, (in press).

(Received March 31, 1992
Revised June 6, 1992
Accepted June 12, 1992)

Br. J. Pharmacol. (1992), **107**, 528–531

Effect of histamine and histamine analogues on human isolated myometrial strips

María Inocencia Martínez-Mir, Luis Estañ, Francisco J. Morales-Olivas & [1]Elena Rubio

Departament de Farmacologia, Universitat de València, València, Spain

1 The effect of histamine and histamine H_1- and H_2-receptor agonists on isolated myometrium strips of premenopausal women has been examined. The effect of acetylcholine was also determined.

2 Histamine, 2-pyridylethylamine, 4-methylhistamine and acetylcholine, but not dimaprit, produced a concentration-related contractile response in human isolated myometrial strips. Histamine also produced a further contraction in human isolated myometrial strips precontracted with KCl (55 mM).

3 The contractile response to histamine was antagonized by the histamine H_1-receptor angatonist, clemizole (0.1 μM) but was potentiated by the histamine H_2-receptor antagonist, ranitidine (10 μM). Clemizole (0.1 nM to 10 nM) competitively antagonized the contractile effect of 2-pyridylethylamine ($-\log K_B = 10.5 \pm 0.5$). The concentration-response curve for acetylcholine was displaced to the right by atropine 0.1 μM.

4 Atropine (0.1 μM), propranolol (0.1 μM), prazosin (0.1 μM) and indomethacin (1 μM) failed to modify the contractile response to histamine.

5 In human isolated myometrial strips precontracted with KCl (55 mM), clemizole at 1 μM completely abolished the contractile response to histamine and revealed a concentration-dependent relaxation. Dimaprit alone and 4-methylhistamine (in the presence of clemizole), produced concentration-related relaxation with a magnitude similar to that in response to histamine. The relaxant response to dimaprit was antagonized by ranitidine.

6 It is concluded that human isolated uterine strips possess histamine H_1- and H_2-receptors: the former mediating contraction and the latter relaxation. The predominant response to histamine in this tissue is contraction.

Keywords: Histamine; histamine receptors; histamine H_1-receptor agonists; histamine H_2-receptor agonists; human isolated myometrium

Introduction

Responses of uterine smooth muscle to histamine vary widely between species. Thus, histamine produces contractions of guinea-pig uterine horns, but causes relaxation of the rat uterus. The receptors involved in these two effects are classified as histamine H_1- and H_2-receptors respectively (Black *et al.*, 1972; Tozzi, 1973; Goyal & Verma, 1981; Rubio *et al.*, 1982; Cortijo *et al.*, 1984). However, there is little information on the effect of histamine on the human uterus, and previous studies reported in the literature have come to differing conclusions. Farmer & Lehrer (1966) reported that histamine had a contractile effect on uteri *in vitro*, but in contrast Dai *et al.* (1982) failed to observe any effect of histamine on spontaneous activity in isolated myometrium. We have recently reported a contractile response to histamine in human myometrial strips (Martínez-Mir *et al.*, 1990) and the object of the present investigation was to establish the role of histamine H_1- and H_2-receptors in this response.

Methods

Tissues

Myometrial tissues were obtained from 60 non-pregnant women who underwent hysterectomy for various pathological gynaecological conditions. All patients were pre-menopausal and were 27–57 years of age. These women were operated on for gynaecological conditions that did not affect the uterus ($n = 16$), for uterine myoma ($n = 33$) and for uterine adenomyosis ($n = 11$). The pathological diagnosis and the phase of menstrual cycle were checked by histological examination and the final diagnoses were as described previously (Martínez-Mir *et al.*, 1990).

Isolated strips of uterus

Immediately after abdominal hysterectomy, muscle strips from an intermediate layer were cut longitudinally from the anterior part of the corpus of the uteri. Care was taken to use only specimens from muscle tissue which appeared to be non-pathological. The tissue was rapidly immersed in Jalon solution of the following composition (in mM): NaCl 155.17, KCl 5.68, $CaCl_2$ 0.41, $NaHCO_3$ 5.95 and glucose 2.78. Samples were then transported to the laboratory. The tissue samples were stored at 4°C until the next day. Longitudinal muscle strips measuring approximately 2 × 3 × 35 mm were dissected out and then suspended under a load of 1 g in a 20 ml organ bath containing Jalon solution aerated with 5% CO_2 in O_2. The temperature was maintained at 31 ± 1°C in order to prevent spontaneous contractions. Isometric tension was recorded by a Ugo Basile C 40 7010 transducer connected to a Ugo Basile mod Gemini 7070 recorder. The preparations were allowed to equilibrate in Jalon solution for 1 h before any drugs were added. At the end of the equilibration period, two different experiments were performed: (i) concentration-response curves to histamine or other agonists were obtained by adding the drugs cumulatively; (ii) a submaximal well-maintained plateau-contraction was obtained by adding KCl (55 mM) and then a cumulative concentration-response curve to agonists was performed as in (i). Only one complete dose-response curve to histamine was constructed for each myometrial strip, in view of the tachyphylaxis to histamine that has been reported for the rat uterus (Tozzi,

[1] Author for correspondence at: Departament de Farmacologia, Facultat de Medicina i Odontologia, Avda. Blasco Ibañez, 15, 46010-València, Spain.

1973; Cortijo *et al.*, 1984). Therefore, separate strips from the same uteri were used in parallel experiments, one strip acting as the control for the other. Strips were incubated with antagonists for 15 min, before the addition of agonists. Immediately after completion of the experiment, the tissue was removed from the bath, heated at 65 ± 1°C for 24 h and then weighed on a precision balance.

Analysis of data

Contractile responses to agonists were determined as changes in isometric tension and transformed into tension (i.e. force (g).g^{-1} tissue dry weight (g_F/g_W)). Relaxant responses to agonists were expressed as the percentage inhibition of the KCl-induced contraction.

Maximum response (E_{max}) and the half-maximal effective concentrations (EC_{50}) of agonists were calculated from concentration-response curves by fitting the experimental data to a logistic equation by non-linear regression analysis (Graph Pad Software; San Diego, California, U.S.A.). The pA_2 value was calculated according to the method of Arunlakshana & Schild (1959) as previously described (Aguilar *et al.*, 1986).

All data are given as mean ± s.e.mean. Significance of differences was assessed with either a paired or unpaired Student's *t* test at a 5% significance level.

Drugs

The following drugs were used: acetylcholine chloride, atropine sulphate, histamine dihydrochloride, propranolol hydrochloride and ranitidine hydrochloride (Sigma Chemical Co St. Louis. MO U.S.A.), dimaprit, 4-methylhistamine dihydrochloride and 2-pyridylethylamine dihydrochloride (Smith-Kline Beecham R & D), clemizole hydrochloride (Schering España SA), prazosin hydrochloride (Pfizer), indomethacin (Liade). All drugs were prepared in Jalon solution before being added to the bath. The histamine stock solution was adjusted to pH = 7.4 with sodium hydroxide. Stock solutions of indomethacin were prepared in absolute ethanol; the final concentration of ethanol in the organ bath has been shown previously not to alter either the baseline tension or the drug-induced responses (Fuchs & Fuchs, 1973).

Results

Contractile effects of agonists on human isolated myometrium in the resting state

Concentration-response curves for histamine, 2-pyridylethylamine, dimaprit, 4-methylhistamine and acetylcholine are shown in Figure 1. With the exception of dimaprit, all agonists produced concentration-related contractions of human uterine strips.

Histamine increased the force of contraction with a maximum of 48.9 ± 3.6 g_F/g_W. The EC_{50} value was 40.2 ± 10.6 μM ($n = 60$). The histamine receptor agonists, 2-pyridylethylamine and 4-methylhistamine also produced a contractile effect of isolated myometrial strips. 2-Pyridylethylamine appeared to be a partial agonist (E_{max} = 30.1 ± 7.2; EC_{50} = 14.5 ± 6.6 μM), while 4-methylhistamine produced an appreciable response only at concentrations ⩾ 0.1 mM and even at 1 mM the response was much less than that to histamine. The selective histamine H_2-receptor agonist, dimaprit, up to 0.1 mM, had no apparent effect.

The myometrial force of contraction was also increased in a dose-related manner by acetylcholine. It reached a maximum effect of 31.3 ± 6.7 g_F/g_W. The EC_{50} value was 4.1 ± 1.5 μM. The response to 55 mM KCl was 53% of the maximum induced by histamine (Figure 1).

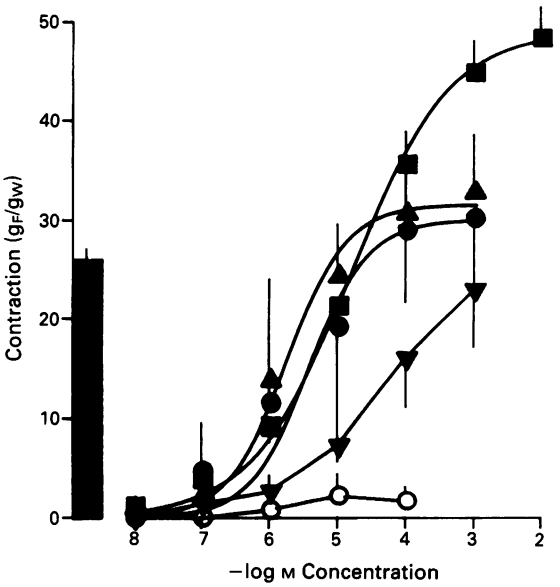

Figure 1 Concentration-response curves to histamine ($n = 60$) (■), 2-pyridylethylamine ($n = 6$) (●), 4-methylhistamine ($n = 6$) (▼), dimaprit ($n = 6$) (○) and acetylcholine ($n = 8$) (▲), and contractile response to K^+ 55 mM ($n = 15$) (histogram) in human isolated myometrial strips. g_F/g_W = force(g).g^{-1} tissue dry weight. *n* is the number of experiments. The curves for histamine, 2-pyridylethylamine and acetylcholine are the best-fit lines calculated as described under Methods.

Effect of antagonists

The histamine H_1-receptor blocker, clemizole (0.1 μM), shifted the concentration-response curve for histamine-induced contraction to the right without any significant change in the maximum response. Ranitidine (1 μM), a selective histamine H_2-receptor antagonist, did not modify the contractile effect of histamine, but 10 μM ranitidine displaced the histamine concentration-response curve to the left (Figure 2).

The contractile response to histamine was not significantly altered by propranolol (0.1 μM), prazosin (0.1 μM), atropine (0.1 μM) or indomethacin (1 μM). The EC_{50} values were: 49 ± 39 μM; 20 ± 7 μM; 42 ± 4 μM and 22 ± 12 μM, respectively; the EC_{50} value for the control group was 25 ± 10 μM.

The histamine H_1-receptor antagonist, clemizole (0.1 nM to 10 nM), produced a parallel shift of concentration-response curves for 2-pyridylethylamine to the right, without affecting the maximal response. A Schild plot is shown in Figure 3. The slope of regression line was not significantly different from unity (0.96 ± 0.10) and the $-\log K_B$ value obtained for clemizole was 10.5 ± 0.5.

The muscarinic receptor blocker, atropine (0.1 μM), shifted the concentration-response curve for acetylcholine to the right increasing the EC_{50} 333 fold ($n = 6$), without any modification in the maximal effect. The dissociation constant calculated for atropine was 0.6 nM.

Relaxant effects of agonists on human isolated myometrium precontracted with KCl

Relaxant effects of histamine were investigated by cumulative addition to isolated myometrial strips precontracted with KCl. As shown in Figure 4a, histamine at low concentrations (0.01, 0.1 and 1 μM) did not modify the K^+-induced contractions, but higher concentrations of histamine (10 μM to 10 mM) produced a further contraction.

Clemizole, 1 μM, acting alone, had a relaxant effect (21.6 ± 7.2%) on the contraction produced by 55 mM KCl. After blockade of the histamine H_1-receptor with clemizole, the contractile effect of histamine was abolished and a relaxa-

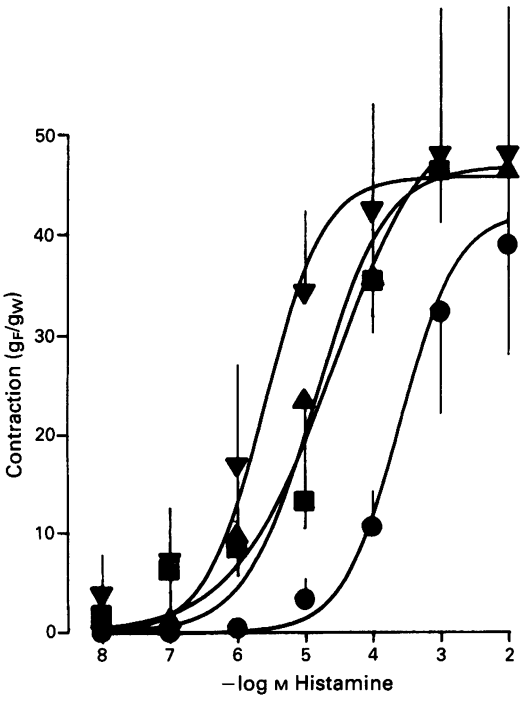

Figure 2 Concentration-response curves to histamine in human isolated myometrial strips. Control ($n = 24$) (■); in the presence of 1 μM ($n = 8$) (▲) and 10 μM ($n = 8$) (▼) ranitidine; in the presence of 0.1 μM clemizole ($n = 8$) (●). g_F/g_W = force(g).g^{-1} tissue dry weight. n is the number of experiments. The curves for histamine, 2-pyridylethylamine and acetylcholine are the best-fit lines calculated as described under Methods.

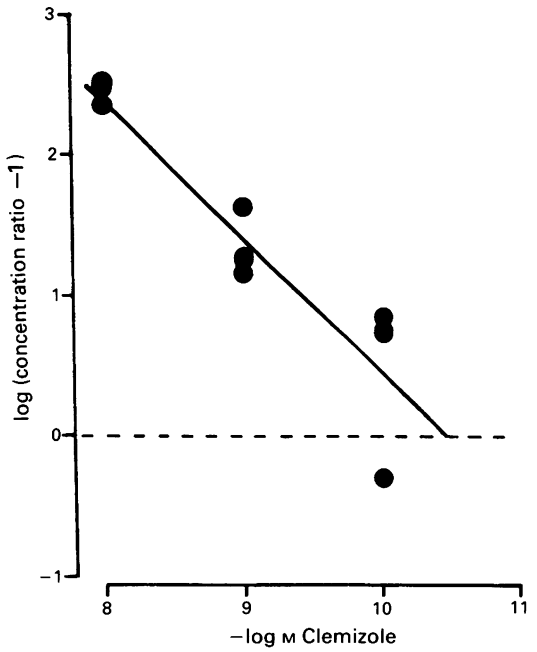

Figure 3 Schild plot of the antagonism by clemizole of the response to 2-pyridylethylamine. The line drawn was calculated by linear-regression analysis.

tion response observed (Figure 4a). 4-Methylhistamine in the presence of 1 μM clemizole also relaxed K^+-precontracted strips ($E_{max} = 24.5 \pm 6.1\%$; $EC_{50} = 9.9 \pm 8.6$ μM).

Dimaprit produced a concentration-related relaxation of isolated uterine strips depolarized with K^+. The EC_{50} value was 18.2 ± 10.3 μM and the maximal effect was $31.7 \pm 8.1\%$. Ranitidine 1 μM produced a significant decrease in the relaxant response to dimaprit and 10 μM rantidine abolished it (Figure 4b).

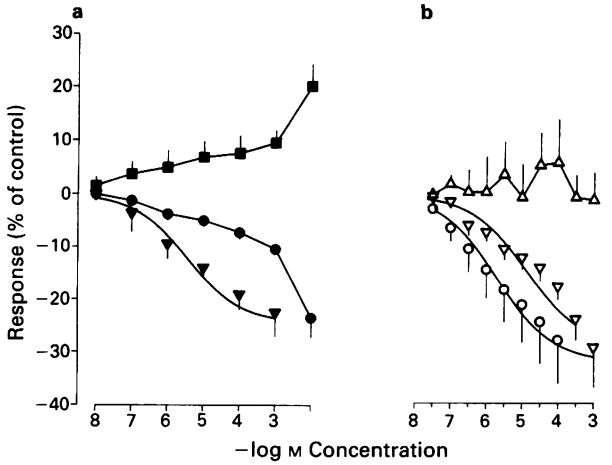

Figure 4 (a) Concentration-response curves to histamine alone ($n = 6$) (■), histamine in the presence of 1 μM clemizole ($n = 6$) (●) and 4-methylhistamine in the presence of 1 μM clemizole ($n = 6$) (▼) in human isolated myometrial strip precontracted with KCl (55 mM). The response is expressed as a percentage of the response to KCl alone or KCl plus clemizole. (b) Concentration-response curves to dimaprit alone ($n = 6$) (○), dimaprit in the presence of 1 μM ($n = 6$) (▽) and 10 μM ($n = 6$) (△) ranitidine in human isolated myometrial strip precontracted with KCl (55 mM). n is the number of experiments. The curves for 4-methylhistamine in the presence of 1 μM clemizole, dimaprit alone and dimaprit in the presence of 1 μM ranitidine are the best-fit lines calculated as described under Methods.

Discussion

We have demonstrated that histamine causes a dose-dependent contractile effect in human isolated myometrial strips both in the resting and submaximally precontracted states of the tissue. However, after blockade of histamine H_1-receptors, histamine produced a slight inhibitory effect in strips precontracted by KCl. The contractile effect of histamine observed in this study resembles that described by Goyal & Verma (1981) in guinea-pig isolated uterus, where histamine produced a dose-related contraction with a similar potency. Our results also confirmed those described by Farmer & Lehrer (1966) in human isolated myometrium, although a comparative analysis of the findings is difficult because the authors did not give the details of their experimental procedure and used only single doses of histamine. In contrast, our results do not accord with the observations of Dai *et al.* (1982), who showed that histamine did not influence the spontaneous activity of human isolated myometrial strips. Isolation of the strips from uteri in different phases of the oestrus cycle does not explain the discrepancy, since we have previously found no significant changes in the contractile uterine effect of histamine during the menstrual cycle (Martínez-Mir *et al.*, 1990). On the other hand, the contractile responses to acetylcholine and potassium that we observed agree well with previous findings in human uterus (Sandberg *et al.*, 1957; Nakanishi & Wood, 1971; Sanger & Bennet, 1981). Moreover, the antagonism of the response to acetylcholine by atropine is in accord with binding studies in this tissue (Vauquelin *et al.*, 1984). The lack of modification by muscarinic, α- and β-adrenoceptor blockade and prostaglandin synthesis inhibition of the contractile response to histamine, argues against the participation of endogenous acetylcholine, catecholamines and prostaglandins and indicates that this effect is probably due to a direct stimulation of histamine receptors. The fact that the dose-response curve to histamine was shifted to the right by clemizole (0.1 μM) but not modified by ranitidine (1 μM) suggests that the receptor involved in the contractile effect of histamine in human isolated uterine strips is the histamine H_1-receptor subtype. However, the concentration-ratio observed with clemizole is lower than expected; moreover, ranitidine (10 μM) shifted to

the left the dose-response curve to histamine. All this suggests some participation of histamine H_2-receptors. To characterize further the receptor subtype mediating contractile responses to histamine, we examined the effect of 2-pyridylethylamine, 4-methylhistamine and dimaprit. The selective histamine H_1-receptor agonist, 2-pyridylethylamine, produced a concentration-dependent contractile effect with a similar EC_{50} to histamine. Although 2-pyridylethylamine appears to be a partial agonist (Figure 1), paired experiments showed that the maximal effects of both compounds were similar. This finding agrees with previous results in various tissues, including the guinea-pig isolated uterus, although in this latter study 2-pyridylethylamine was shown to be less potent than histamine (Duncan *et al.*, 1980; Goyal & Verma, 1981; Schmidt *et al.*, 1987). The contractile effect of 4-methylhistamine agrees with a similar result in guinea-pig uterus and confirms previous findings were 4-methylhistamine was a histamine H_1-agonist (Goyal & Verma, 1981; Black *et al.*, 1972). This underlines the importance of the numbers of histamine H_1-: histamine H_2-receptors in a tissue for the observed effect of agonists which are not very selective (Barker & Hough, 1983).

The $-\log K_B$ value (pA_2) for clemizole, 10.5 ± 0.5, agrees closely with those obtained by Aguilar *et al.* (1986) (10.45 ± 0.44) and Martínez-Mir *et al.* (1988) (10.54 ± 0.44) in other tissues and supports the existence of histamine H_1-receptor in human isolated myometrium.

In human isolated uterus submaximally contracted with KCl, histamine still caused a contractile effect. A weak histamine-mediated relaxation occurred only in the presence of the histamine H_1-receptor antagonist clemizole (1 μM). Moreover, dimaprit and 4-methylhistamine (in the presence of H_1-blockade) also produced a similar relaxant effect. Although 4-methylhistamine and dimaprit have been reported to be less potent than histamine (Hill, 1990), we found that both were more potent. However, in guinea-pig airways, for example, both agonists were equipotent and the EC_{50} calculated with dimaprit and 4-methylhistamine (in the presence of H_1-blockade), were similar to those obtained in the present study. No comparison with histamine was made by the authors (Tomioka & Yamada, 1982). A complicating factor in the analysis of the response to histamine is the relaxation produced by clemizole. Given that studies in our laboratory have shown that clemizole is a selective histamine H_1-receptor antagonist (Aguilar *et al.*, 1986; Martínez-Mir *et al.*, 1988), a possibility that needs investigation is that KCl might release endogenous histamine. The inhibition by ranitidine of the relaxant response to dimaprit, taken together with the potentiation of the histamine-induced contraction by 10 μM ranitidine, is evidence for histamine H_2-receptor-mediated relaxation. Similar results have been described by Ginsburg *et al.* (1980) in human arteries. A predominance of the histamine H_1-receptor-mediated contraction over the histamine H_2-receptor-mediated relaxation can be explained by the balance of apparent affinities for histamine H_1- and H_2-receptors. Consistent with this is the fact that the selective histamine H_2-receptor agonist, dimaprit, relaxed the precontracted uterine strip in the absence of H_1-blockade.

We are grateful to Dr M.E. Parsons for his valuable advice, the staff of the Obstetrics and Gynaecologic Service of the Hospital Clínico Universitario for their cooperation in providing specimens of uterus, Mr P.S. Derrick for correcting the English text and Liade, Pfizer, Schering España SA and SmithKline Beecham R & D for generous gifts of drugs.

References

AGUILAR, M.J., MORALES-OLIVAS, F.J. & RUBIO, E. (1986). Pharmacological investigation into the effects of histamine and histamine analogues on guinea-pig and rat colon in vitro. *Br. J. Pharmacol.*, **88,** 501–506.

ARUNLAKSHANA, O. & SCHILD, H.O. (1959). Some quantitative uses of drug antagonists. *Br. J. Pharmacol. Chemother.*, **14,** 48–58.

BARKER, L.A. & HOUGH, L.B. (1983). Selectivity of 4-methylhistamine at H_1- and H_2-receptors in the guinea-pig isolated ileum. *Br. J. Pharmacol.*, **80,** 65–71.

BLACK, J.W., DUNCAN, W.A.M., DURANT, G.J., GANELLIN, C.R. & PARSONS, M.E. (1972). Definition and antagonism of histamine H_2-receptors. *Nature*, **236,** 385–390.

CORTIJO, J., ESPLUGUES, J., MORALES-OLIVAS, F.J. & RUBIO, E. (1984). The inhibitory effect of histamine on the motility of rat uterus in vivo. *Eur. J. Pharmacol.*, **97,** 7–12.

DAI, S., OGLE, C.W. & LEUNG, P.M.K. (1982). The lack of effect of histamine on spontaneous activity in the isolated human myometrium. *Agents Actions*, **12,** 608–611.

DUNCAN, P.G., BRINK, C., ADOLPHSON, R.L. & DOUGLAS, J.S. (1980). Cyclic nucleotides and contraction/relaxation in airway muscle: H_1 and H_2 agonists and antagonists. *J. Pharmacol. Exp. Ther.*, **215,** 434–442.

FARMER, J.B. & LEHRER, D.N. (1966). The effect of isoprenaline on the contraction of smooth muscle produced by histamine, acetylcholine or other agents. *J. Pharm. Pharmacol.*, **18,** 649–656.

FUCHS, A.R. & FUCHS, F. (1973). Possible mechanisms of inhibition of labour by ethanol. In *Uterine Contraction – Side Effects of Steroidal Contraceptives*. ed. Josimovich, J.B. pp. 287–300. New York: John Wiley & Sons, Inc.

GINSBURG, R., BRISTOW, M.R., STINSON, E.B. & HARRISON, D.C. (1980). Histamine receptors in the human heart. *Life Sci.*, **26,** 2245–2249.

GOYAL, R.K. & VERMA, S.C. (1981). Pharmacological investigations into the effects of histamine and histamine analogs on guinea-pig and rat uterus. *Agents Actions*, **11,** 312–317.

HILL, S.J. (1990). Distribution, properties, and functional characteristics of three classes of histamine receptor. *Pharmacological Rev.*, **42,** 45–83.

MARTINEZ-MIR, I., ESTAÑ, L., MORALES-OLIVAS, F.J. & RUBIO, E. (1990). Studies of the spontaneous motility and the effect of histamine on isolated myometrial strips of the nonpregnant human uterus: The influence of various uterine abnormalities. *Am. J. Obstet. Gynecol.*, **163,** 189–195.

MARTINEZ-MIR, I., ESTAÑ, L., RUBIO, E. & MORALES-OLIVAS, F.J. (1988). Antihistaminic and anticholinergic activities of mequitazine in comparison with clemizole. *J. Pharm. Pharmacol.*, **40,** 655–656.

NAKANISHI, H. & WOOD, C. (1971). Cholinergic mechanisms in the human uterus. *J. Obstet. Gynaec. Br. Commonwealth.*, **78,** 716–723.

RUBIO, E., ESPLUGUES, J., MARTI-BONMATI, E., MORCILLO, E. & MORALES-OLIVAS, F.J. (1982). Action inhibitrice de l'histamine sur l'uterus isolée de rat. *J. Pharmacol. (Paris)*, **13,** 543–552.

SANDBERG, F., INGELMAN-SUNDBERG, A., LINDGREN, L. & RYDEN, G. (1957). In vitro studies of the motility of the human uterus. Part III. The effects of adrenaline, noradrenaline and acetylcholine on the spontaneous motility in different parts of the pregnant and non-pregnant uterus. *J. Obstet. Gynaec. Br. Empire*, **64,** 965–972.

SANGER, G.J. & BENNETT, A. (1981). Secoverine hydrochloride is a muscarinic antagonist in human isolated gastrointestinal muscle and myometrium. *J. Pharm. Pharmacol.*, **33,** 711–714.

SCHMIDT, G., KANNISTO, P., OWMAN, C. & SJÖBERG, N.-O. (1987). Alteration by histamine of the sympathetic nerve-mediated contractions in the bovine ovarian follicle wall in vitro. *Eur. J. Pharmacol.*, **135,** 11–22.

TOMIOKA, K. & YAMADA, T. (1982). Effects of histamine H2-receptor agonists and antagonists on isolated guinea-pig airways muscles. *Arch. Int. Pharmacodyn.*, **255,** 16–26.

TOZZI, S. (1973). The mechanism of action of histamine on the isolated rat uterus. *J. Pharmacol. Exp. Ther.*, **187,** 511–517.

VAUQUELIN, G., WEMERS, C., VOKAER, A., KAIVEZ, E., LESCRAINIER, J.P. & BOTTARI, S.P. (1984). Identification of muscarinic acetylcholine receptors in human myometrium by [^{3}H]-3-quinuclidinyl benzylate binding. In *Uterine Contractility*. ed. Bottari, S., Thomas, J.P., Vokaer, A. & Vokaer, R. pp. 185–194. New York: Masson Publishing USA, Inc.

(Received September 30, 1991
Revised May 26, 1992
Accepted June 12, 1992)

Br. J. Pharmacol. (1992), **107**, 532–538

Millimolar amiloride concentrations block K conductance in proximal tubular cells

Françoise Discala, Philippe Hulin, Fouzia Belachgar, Gabrielle Planelles, Aleksander Edelman &[1]Takis Anagnostopoulos

INSERM U.323, Faculté de Médecine Necker Enfants-Malades 156, Rue de Vaugirard 75730 Paris Cedex, France

1 Amiloride, applied at millimolar concentrations, results in the blockade of K^+ conductance in amphibian proximal convoluted cells (PCT), fused into giant cells.

2 Amiloride results directly in a blockade of K^+ conductance that is not related to inhibition of the Na^+-H^+ antiport, which would lower intracellular pH, adversely affecting K^+ conductance. On the contrary, high amiloride concentrations promote entry of this lipophilic base in the cell, leading to higher cell pH.

3 Under voltage clamp conditions, control vs. amiloride, current-voltage curves from PCT fused giant cells intersect at -86.2 ± 3.4 mV, a value close to the equilibrium potential for potassium.

4 Hexamethylene amiloride, 10^{-5} M, irreversibly depolarizes the membrane potential.

5 Barium decreased by 50% the initial slope of realkalinization, following removal of a solution containing NH_4Cl, as did amiloride. In addition, these blockers reduced membrane conductance by 40%, suggesting that a fraction of the amiloride-suppressible NH_4^+ efflux may be conductive.

6 Amiloride does not directly inhibit the Na^+-K^+, ATPase in our preparation, contrary to the prevalent belief.

7 *In vivo* studies show that amiloride interferes with an apical K^+ conductance but it does not alter basolateral K^+ conductance.

Keywords: Amiloride; K^+ conductance; Na^+-H^+ antiport; Na^+-K^+ , ATPase; proximal tubule

Introduction

Amiloride is a substituted pyrazine ring, bearing an acyl-guanidine group. It exerts several different inhibitory biological effects. For example, amiloride has been shown to inhibit Na^+ transport across the frog skin epithelium (Eigler *et al.*, 1967). Initial studies suggested that amiloride blocks Na^+ entry only into electrically tight epithelia; however, this notion was subsequently extended to leaky epithelia (Cuthbert *et al.*, 1979), and more recently, it has been shown that even the leakiest epithelium, the proximal convoluted tubule (PCT), (actually an established cell line with characteristics of proximal tubular cells), is sensitive to this drug (Cantiello *et al.*, 1987). The blocking effect of amiloride on epithelial Na^+ channels has also been confirmed at the single channel level, by patch-clamp techniques (Palmer, 1987). In contrast, whereas micromolar amiloride concentrations interfere with passive Na^+ diffusion, millimolar concentrations of this drug inhibit the PCT Na^+-H^+ antiport (Kinsella & Aronson, 1981a), as well as apical and basolateral Na^+-H^+ antiporters in a proximal cell line (Haggerty *et al.*, 1988), and also other Na^+-H^+ epithelial and non-epithelial antiports (Frelin *et al.*, 1987). Inhibition of the Na^+-H^+ antiport generally results in a fall of intracellular pH (pH_i), which may adversely affect potassium conductance(s), since lowering pH_i has been shown to inhibit the PCT basolateral K^+ conductance (Anagnostopoulos, 1972; Kubota *et al.*, 1983). It has also been reported that amiloride enters cell and, by virtue of its being a weak base ($pK \approx 9.0$), it may buffer intracellular protons (Benos *et al.*, 1983). Amiloride at millimolar concentrations has also been reported to inhibit the Na^+,K^+ pump of rabbit PCT (Soltoff & Mandel, 1983). We report in this study a novel action of amiloride, in a preparation of amphibian PCT cells. Amiloride, at a concentration currently used to suppress the Na^+-H^+ antiporter, directly blocks a barium-sensitive K^+ conductance.

[1] Author for correspondence.

Methods

Two experimental preparations were used: (i) frog PCT cells fused into 'giant' cells *in vitro*, and (ii) *in vivo* studies of membrane potential on the PCT of *Necturus*.

Fusion of PCT cells into giant cells

About 15–40 cells, making up a PCT fragment, were fused into giant cells, according to technique originally described by Oberleithner *et al.* (1986, 1987), and modified in our laboratory (Bouachour *et al.*, 1988; Discala *et al.*, 1992). The renal vasculature of frog kidney (*Rana ridibunda*) was washed with an amphibian physiological salt solution via the aorta (in a retrograde fashion) and both portal renal veins, to remove blood cells completely, following which collagenase (IA, Sigma), 450 u ml^{-1}, was added to the portal perfusate to digest connective tissue. The composition of the physiological salt solution, in mM, was NaCl 82, KCl 3, $CaCl_2$ 1.8, $MgCl_2$ 1, Na_2HPO_4 1, Na-pyruvate 1, buffered with N-tris (hydroxy-methyl) methyl-2 amino-ethane sulphonic acid (TES) and appropriate amounts of NaOH, to pH 7.5. Small fragments of the kidney were cut, then placed in the physiological salt solution supplemented with collagenase, 3000 u ml^{-1}, for 1 h at 26°C. One hundred to 150 PCTs were microdissected, collected and stored in the physiological salt solution at 4°C, in siliconized test tubes. Mechanical treatment yielded fragments of an average size of 100–150 μm. Fusion of a few individual cells or small fragments into a single (giant) cell was achieved by exposure to a 'fusion medium'. This solution is made up of 7.4 g polyethylene glycol (Mr 4000), dissolved in 25 ml Leibovitz-15 medium and 14 ml H_2O, buffered with TES at pH 8.6. This medium was removed after centrifugation, the pellet was resuspended in a modified Leibowitz medium (L15) as described earlier (Bouachour *et al.*, 1988), total osmolality 200 mOsm l^{-1}, pH 7.6. Clusters of cells were deposited onto glass plates,

coated with a thin collagen layer, for 24 h at 4°C. Most clusters achieved complete fusion into giant cells and adhered firmly to the plate.

Electrical recording

Fused cells, placed on the stage of a microscope (Nikon, Diaphot) were initially superfused with a control solution and then with the aid of an electronically controlled switch, the control superfusate was alternated with any of up to six other 'experimental' solutions depending on different protocols (half-time of complete bath replacement was approximately 5 s); thus, each cell served as its own control. In most experiments, a single giant cell was impaled with two borosilicate microelectrodes, (having tip resistance between 40–70 MΩ) by use of hydraulic micromanipulators (Narishige MO-103). Both microelectrodes were filled with 1 M KCl, and were connected to the input of an electrometer (Axoclamp 2A, Axon Instr.) via AgCl/Ag bridges. An identical (macro)-electrode placed down-stream in the effluent served as the reference. The cell was impaled with two microelectrodes, one to record membrane potential and the other to inject 750 ms duration current pulses (≈ ± 1 nA), to yield voltage transients, depolarizing ($\Delta\Psi^+$)/hyperpolarizing ($\Delta\Psi^-$). Current injection was triggered by an Axoclamp programme (version 5.3), as described in a recent study (Discala *et al.*, 1992). Changes in membrane conductance were expressed as a ratio, provided by the following expression: $G_{m(exp)}/G_{m(ctr)} = \Delta\Psi_{(ctr)}/\Delta\Psi_{(exp)}$, where $\Delta\Psi$ is the sum of $\Delta\Psi^+$ and $\Delta\Psi^-$ and G_m is membrane conductance; ctr and exp refer to control and experimental states. Each $\Delta\Psi_{(exp)}$ is referred to the preceding $\Delta\Psi_{(ctr)}$.

To measure simultaneously membrane potential and a given intracellular ionic activity (αX_i), double barrelled borosilicate microelectrodes were constructed, as described previously (Teulon & Anagnostopoulos, 1982; Planelles *et al.*, 1984; Anagnostopoulos & Planelles, 1987). After exposure of the ion-selective barrel to vapours of dimethyl-trimethyl-silylamine (Fluka 41716) and baking (120°C for 2 h), a droplet of a neutral ion-exchanger (Fluka sodium cocktail 71176, Fluka potassium cocktail 60308 or Fluka proton cocktail 95291) was introduced near the tip of the silanized barrel, and allowed to slip overnight down to the extreme tip. On the next day, the non-selective-barrel was filled with 1 M KCl, and the ion-selective barrel with an appropriate solution: Na^+ electrodes, 100 mM NaCl; K^+ electrodes, 100 mM KCl; H^+ electrodes, NaCl 67 mM plus 40 mM KH_2PO_4, pH 7.00. The electrode slope, expressed per decade of ionic activity (within the relevant activity αX_i range prevailing *in vivo*) was: 40–50 mV for Na^+ microelectrodes, 45–55 mV for K^+ microelectrodes and 50–58 mV for pH microelectrodes. These electrodes were used to measure αNa_i, αK_i, and pH_i, respectively. In contrast to the Fluka K^+ cocktail, which is specific to K^+ ions, the K^+ Corning 477317 ligand displays selectivity to amiloride. These latter electrodes in the presence of amiloride (1 mM) exhibit a maximal signal equivalent to 230 mM αK_i within the cell, and 2500 mM *in vitro*. These electrodes were useful to establish the entry of amiloride into the cells. Ion activities were measured with an ultra-high impedance electrometer (FD 223, WPI, New Haven, CT, U.S.A.); its output was displayed on a Linseis (LS 4) chart recorder.

It has been reported that (low-resistance) selective borosilicate microelectrodes may develop a leak resistance across the glass wall, thereby altering both membrane potential and ion activity (Lewis & Wills, 1980). Consequently, these authors recommended the use of high resistivity glass wall, e.g. aluminosilicate glass. Thus, we used an experimental protocol close to that of Lewis & Wills (1980), to determine whether borosilicate microelectrodes exhibit leak resistance comparable to the tip resistance: a microelectrode connected to a current generator was inserted into a PCT lumen of *Necturus in vivo*. A second, conventional (borosilicate) microelectrode was inserted into the same PCT, ≈300 μm apart, first in the superficial cell layer then into the lumen, to record voltage transepithelial/basolateral resistance ratio. Then, this procedure was repeated with a borosilicate Na^+-selective microelectrode, at about the same distance from the source as above, to again determine the voltage divider ratio. Lack of shunting across the glass wall should produce identical results with either conventional or selective microelectrodes. The average voltage divider ratio was 2.6 ± 0.3 with a non-selective electrode and 2.3 ± 0.05 with a selective electrode ($n = 3$); this difference is statistically insignificant, suggesting the absence of significant artifacts. Discrepancies between the data of Lewis & Wills (1980) and our own observations may be explained by different methods of silanization. However, we also carried out a few αNa_i measurements with double-barrelled aluminosilicate microelectrodes: similar results were obtained using borosilicate selective microelectrodes (see Results section).
similar results were obtained using borosilicate selective microelectrodes (see Results section).

Three additional experimental protocols were carried out. First, fused cells were exposed to 15 mM NH_4Cl solution for approximately 5 min, in order to estimate the initial slope of realkalinization following ammonia withdrawal (Boron & De Weer, 1976), in the absence and in the presence of Ba^{2+} or amiloride. Second, we generated current-voltage curves by applying three ± 20 mV voltage steps (500 ms duration each) on either side of the control membrane potential. Third, hexamethylene-amiloride was used in some experiments, in place of amiloride.

In vivo *studies*

This protocol was designed to identify the location of the amiloride-sensitive K^+ conductance within the PCT, i.e. either apical, or basolateral. *Necturuses* were anaesthetized by immersion into a 7% Tricain solution for 15 min, following which this solution was diluted fivefold for the remainder of the experiment. Dissection of the peritoneal cavity, exposure of the kidneys, and their superfusion with a physiological salt solution have been described previously (Edelman *et al.*, 1981). Double barrelled micropipettes (tip diameter, ≈10 μm) were filled with a physiological salt solution for amphibia, one barrel of which was supplemented with amiloride, at a concentration of 1 mM. The micropipette was inserted into a peritubular capillary, to perfuse alternately, control and amiloride solutions while also recording the membrane potential in a PCT cell adjacent to the tip of the micropipette. In a separate experiment, these solutions were delivered alternately into a PCT lumen, while monitoring membrane potential in a PCT cell. In order to avoid luminal distension, a second micropipette (inserted upstream) collected both the artificial solutions, (which were delivered retrogradely) and the tubular fluid originating in the glomerulus.

Solutions and drugs

The composition of experimental solutions was similar to the control salt solution, supplemented by an appropriate drug. The single exception was addition of NH_4Cl, 15 mM, at the expense of NaCl.

Amiloride and ouabain were purchased from Sigma, and hexamethylene-amiloride from RBI; hexamethylene-amiloride was dissolved in HCl, then buffered at pH 7.4 before use.

Statistics

Data are presented as means ± s.e.mean. Statistical significance was assessed by the use of a paired or unpaired *t* test, as appropriate.

Results

Amiloride inhibits the K^+ conductance of PCT fused cells

Figure 1 depicts the effects of increasing amiloride concentrations on membrane potential and membrane conductance. Low concentrations of amiloride (10^{-6} M and 10^{-5} M) failed to alter membrane potential, although higher concentrations produced concentration-dependent and reversible depolarization, which reached a plateau value of $+22.8 \pm 1.7$ mV at the highest amiloride concentration used, 3×10^{-3} M (Table 1). Membrane conductance decreased monotonically, to achieve a minimum value of $54 \pm 2\%$ with respect to control (Table 1). Because the membrane potential moved away from the equilibrium potential for potassium (depolarization) and the membrane conductance was almost halved by addition of amiloride, it is likely that amiloride predominantly blocked potassium conductance. In fused cells, potassium conductance is the main conductance (Discala *et al.*, 1992).

To ascertain whether not only amiloride, but also some its analogues display similar properties, we tested the effects of hexamethylene-amiloride. This compound (10^{-6} M) elicited a 7.5 ± 2.7 mV depolarization ($n = 4$, $P < 0.05$), which was partly reversible (net loss of 2.0 ± 0.8 mV), whereas hexamethylene-amiloride, 10^{-5} M, resulted in 22.5 ± 4.4 mV depolarization ($P < 0.005$, $n = 4$, different series), irreversible in three experiments and partly reversible in one (data not shown). Since no vehicle was added to hexamethylene-amiloride, the irreversible effects on membrane potential may indicate that hexamethylene-amiloride covalently binds a receptor site or, alternatively, hexamethylene-amiloride may induce irreversible membrane damage. In single cells, membrane conductance increased with time, irreversibly.

Amiloride does not reduce potassium conductance by lowering pH_i

Millimolar amiloride concentrations inhibit the apical Na^+-H^+ PCT antiport (Kinsella & Aronson, 1981a), thereby lowering pH_i, which, in turn, reduces PCT K^+ conductance (Anagnostopoulos, 1972; Kubota *et al.*, 1983). To ascertain whether amiloride indeed lowers pH_i in fused cells, membrane potential and pH_i were measured with double-barrelled H^+-selective microelectrodes. Increasing amiloride concentrations (10^{-6}–3×10^{-3} M) resulted in a dose-dependent reduction of membrane potential, to reach a peak depolarization of 29.7 ± 2.5 mV at the highest amiloride concentration (3×10^{-3} M) tested (Table 2). Concomitantly, pH_i changes, though not statistically significant, had a downward tendency at low amiloride concentrations (10^{-6}–10^{-4} M), which contrasts with a significant rise in pH_i, of $+0.15 \pm 0.05$ pH u over control ($P < 0.01$), at the highest amiloride concentration (3×10^{-3} M) tested. The observation that amiloride (3 mM) is associated with intracellular alkalinization rules out acidification-induced blockade of K^+ conductance. With respect to the size of the effects of amiloride on pH_i, there were in fact two groups: for control pH_i between 7.01 and 7.25, ΔpH_i in response to high concentrations of amiloride was significantly greater ($\Delta pH_i = +0.22 \pm 0.07$ pH, $n = 5$), than the ΔpH_i for those cells which control pH_i was in the range 7.26 to 7.51 ($\Delta pH_i = +0.06 \pm 0.03$, $n = 4$). This can be seen in Figure 2.

Direct demonstration that amiloride blocks K^+ conductance

To establish beyond reasonable doubt that amiloride directly blocks K^+ conductance, we measured the currents associated with voltage steps from a holding potential set at control membrane potential, both in the absence and in the presence of amiloride, 1 mM. Figure 3 shows the data from such an experiment and it can be seen that the current-voltage curve intersects at -88 mV. The average current-voltage intersection in five such experiments was -86.2 ± 3.4 mV, a value close to the equilibrium potential for potassium (E_K) of -79 mV, calculated from our average αK_i figure (53.5 ± 1.0 mM, Table 4) and an extracellular K^+ activity of 2.3 mM, determined using an activity coefficient of 0.77 (Robinson & Stokes, 1970).

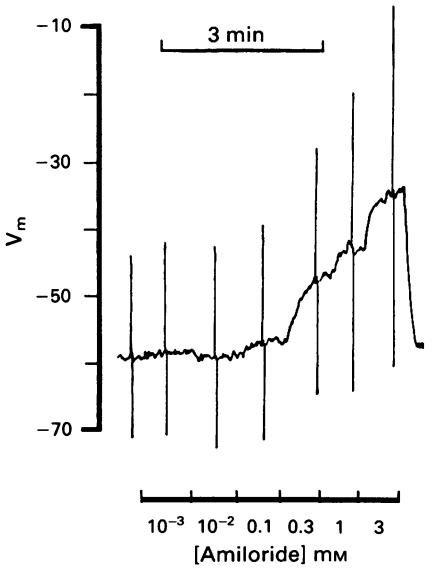

Figure 1 Original tracing, illustrating the effects of amiloride on giant PCT fused cells. Amiloride concentration was raised stepwise from 10^{-6} M to 3×10^{-3} M, as shown between vertical marks, on abscissa scale. Rectangular constant current pulses, ± 1 nA, were applied via a single microelectrode across the membrane, in the control state and during exposure to each amiloride concentration. Resulting vertical voltage transients (using a second microelectrode), in presence of amiloride, were compared to the first (control) vertical pulse, to determine the fractional change in membrane conductance, at each concentration (see Methods section).

Table 1 Effect of increasing amiloride concentrations (M), on membrane potential (top row) and membrane conductance (bottom) ($n = 5$)

	Control	10^{-6}	10^{-5}	10^{-4}	3×10^{-4}	10^{-3}	3×10^{-3}
Membrane potential (mV)	-55.4 ± 2.3	NS -55.2 ± 2.4	NS -56.2 ± 2.8	* -53.7 ± 2.5	* -50.4 ± 2.7	*** -41.4 ± 1.6	*** -32.6 ± 1.1
Membrane conductance (% of control)	1	** 0.96 ± 0.02	** 0.92 ± 0.02	** 0.87 ± 0.02	*** 0.78 ± 0.03	*** 0.65 ± 0.03	*** 0.54 ± 0.02

Values are means $\pm$ s.e.mean of 5 experiments.
NS, not significant.
*$P < 0.05$, **$P < 0.01$, ***$P < 0.001$ (statistical significance with respect to control values).

Table 2 Effect of increasing concentrations of amiloride (M), on membrane potential (mV) (top row) and intracellular pH (bottom) ($n = 9$)

	Control	10^{-6}	10^{-5}	10^{-4}	3×10^{-4}	10^{-3}	3×10^{-3}
Membrane potential		*	**	***	***	***	***
	-53.9 ± 3.3	-52.9 ± 3.4	-51.8 ± 3.4	-51.1 ± 3.3	-47.4 ± 3.1	-36.9 ± 2.5	-24.2 ± 2.1
		*	NS	*	NS	NS	**
pH_i	7.23 ± 0.05	7.21 ± 0.04	7.20 ± 0.04	7.20 ± 0.04	7.20 ± 0.04	7.27 ± 0.03	7.38 ± 0.03

Double-barrelled pH-selective microelectrodes recorded membrane potential and intracellular pH, during exposure to increasing amiloride concentrations, as indicated.
NS, not significant.
*$P<0.05$, **$P<0.01$, ***$P<0.001$ (statistical significance with respect to the appropriate control).

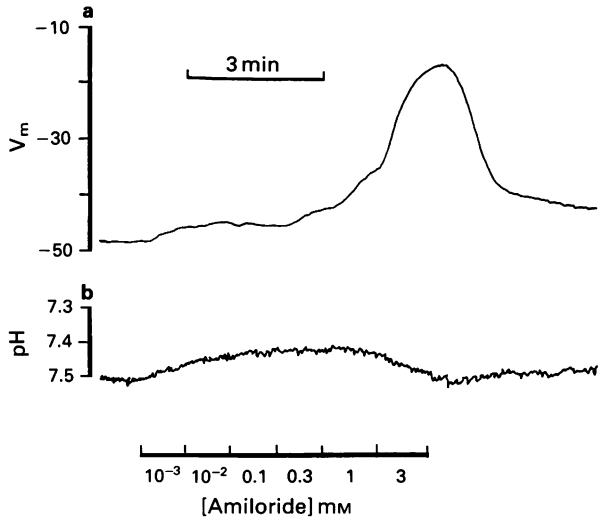

Figure 2 Original tracing, obtained with a double-barrelled microelectrode, and recording simultaneously membrane potential (a) and intracellular pH (b). Amiloride was continuously applied at various concentrations, for the periods indicated by the bars under the traces.

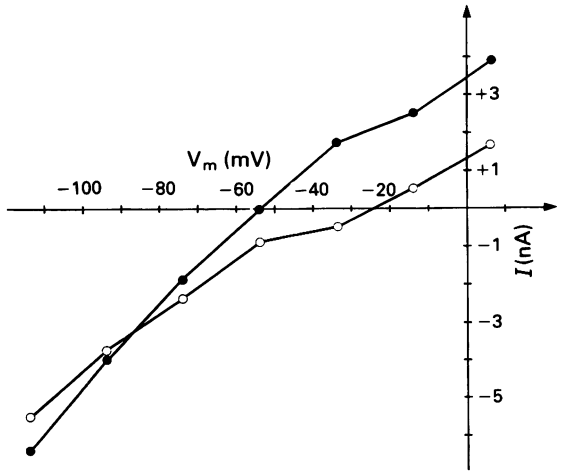

Figure 3 Voltage-clamp experiment illustrating the effects of amiloride, 1 mM. Control state (●); 1 mM amiloride (○). Control membrane potential was − 54 mV. Three voltage steps of ± 20, 40 and 60 mV were carried out, each of them in the absence, then in the presence of amiloride.

Exclusion of direct inhibition of the Na^+-K^+, ATPase by amiloride

Amiloride has been reported to inhibit directly the PCT Na^+-K^+, ATPase. It has been shown that incubation of PCTs in presence of millimolar amiloride concentrations decreases the ouabain-sensitive fraction of oxygen consumption (Soltoff & Mandel, 1983). To examine if the above mechanism (inhibition of the Na^+-K^+, ATPase) could account for the present data, we compared the effects of amiloride (1 mM) to ouabain, (10^{-4} and 10^{-3} M), and to Ba^{2+} (2.5×10^{-4} M), an effective blocker of PCT K^+ conductance (Planelles *et al.*, 1981), on membrane potential and intracellular Na^+ or K^+ activities.

Table 3 summarizes the data carried out with Na^+-selective microelectrodes. Application of Ba^{2+} results in a 18.7 ± 1.5 mV ($n = 7$) depolarization in reversible fashion as does amiloride, yet the size of the depolarization is smaller (12.9 ± 1.0 mV). Ouabain, 10^{-4} M, reduces the membrane potential by 8.1 ± 0.5 mV, followed by partial recovery after withdrawal of the cardiac glucoside (Table 3). Subsequent exposure to ouabain, 10^{-3} M, elicits a 7.9 ± 0.8 mV depolarization; however, following the final ouabain wash, there is only a partial recovery of membrane potential, compared to the preceding 'control'. The net reduction in membrane potential between control state before application of ouabain, 10^{-4} M, and the last wash (3–6 min) following ouabain, 10^{-3} M, amounts to 7.1 ± 2.1 mV. Control αNa_i in this series was 9.9 ± 0.5 mM (Table 3). This value was unaltered by the presence of either Ba^{2+} or amiloride (Table 3). In contrast, ouabain, 10^{-4} M , did increase αNa_i by 0.9 ± 0.3 mM after 1 min, and removal of the cardiac glucoside led to a further increase in αNa_i (by 1.2 ± 0.4 mM). The higher ouabain concentration (10^{-3} M) increased αNa_i by a further 0.8 ± 0.3 mM; then, subsequent washout again led to a further increase of αNa_i by 2.2 ± 0.3 mM within the following 3–6 min. The cumulative rise of αNai by this procedure was 5.8 ± 0.6 mM. Taken together, these observations indicate that the effects of amiloride (Ba^{2+}) differ radically from those of ouabain, both quantitatively and qualitatively (Figure 4).

In a comparable series of experiments, the effects of amiloride (Ba^{2+}) and ouabain on membrane potential and on αK_i were compared. Exposure to Ba^{2+}, followed by amiloride resulted in 21.6 ± 1.2 and 14.1 ± 1.1 mV depolarizations, respectively (as in the above series), and an associated peak rise of αK_i of 2.9 ± 0.6, and 3.6 ± 0.8 mM, respectively. Withdrawal of the Ba^{2+} and the amiloride leads to repolarization within $\leqslant 1.5$ min which contrasts however with the sustained rise of αK_i (Figure 5), which, on washout of drug, relaxes slowly ($\approx$3–6 min) towards the control αK_i value. As in the above series, ouabain, 10^{-4} M, its subsequent wash followed by the higher ouabain concentration and its eventual removal resulted in progressive depolarization, to attain a cumulative reduction of membrane potential of 7.6 ± 0.7 mV (Table 4). αK_i underwent a net loss in the presence of ouabain, 10^{-4} M, ouabain, 10^{-3} M, and also after each withdrawal of the cardiac glucoside, so that the total fall of αK_i summed up to 8.1 ± 1.0 mM (Table 4 and Figure 5). Once again, the pattern associated with Ba^{2+} or amiloride compared to that of ouabain are clearly distinct. The former alter membrane potential and αK_i in reversible fashion, even though the rise in αK_i relaxes over several minutes. Ouabain, unlike amiloride or Ba^{2+}, lowers αK_i, irreversibly (Figure 5 and Table 4).

Table 3 Comparison of the effects of amiloride (Am), relative to those of Ba^{2+} and ouabain (Oua) on membrane potential (mV) and αNa_i (mM) ($n = 7$)

	Control 1	*Ba*	*Ctrl 2*	*Am*	*Ctrl 3*	*Oua 10^{-4}*	*Ctrl 4*	*Oua 10^{-3}*	*Ctrl 5*
Membrane potential		***		***		***	●	***	●
	−49.0 ± 3.1	−30.3 ± 2.4	−48.7 ± 2.7	−35.9 ± 2.9	−48.7 ± 2.7	−40.7 ± 2.6	−43.7 ± 2.2	−35.9 ± 2.1	−41.6 ± 2.5
		NS		NS		*	●●	**	●●●
αNa_i	9.9 ± 0.5	9.3 ± 0.5	10.2 ± 0.6	9.8 ± 0.6	10.6 ± 0.7	11.4 ± 0.5	12.6 ± 0.5	13.5 ± 0.6	15.7 ± 0.7

Differences between an experimental solution and its preceding control (Ctrl) are indicated by asterisks. Dots denote differences between indicated column and Ctrl 3 column, i.e. the first column before exposure to ouabain.
NS, not significant, with regard to previous control.
*$P<0.05$, **$P<0.01$, ***$P<0.001$ (statistical significance with regard to previous control).

Table 4 Comparison of the effects of amiloride, relative to those of Ba^{2+} and ouabain on membrane potential (mV) and αK_i (mM) ($n = 7$)

	Control 1	*Ba*	*Ctrl 2*	*Am*	*Ctrl 3*	*Oua 10^{-4}*	*Ctrl 4*	*Oua 10^{-3}*	*Ctrl 5*
Membrane potential		***		***		***	●●●	***	●●●
	51.1 ± 2.8	−29.6 ± 2.7	−51.3 ± 3.0	−37.1 ± 3.7	−51.7 ± 3.2	−44.4 ± 3.0	−47.2 ± 3.2	−41.6 ± 3.0	−44.1 ± 3.2
		**		**		NS	NS	*	●●●
αK_i	53.5 ± 1.0	56.4 ± 0.7	55.0 ± 1.2	58.6 ± 0.7	56.5 ± 0.9	56.1 ± 0.8	55.4 ± 1.3	53.3 ± 0.8	48.7 ± 0.9

Differences between an experimental solution and its preceding control (Ctrl) are indicated by asterisks. Dots denote differences between indicated column and Ctrl 3 column, i.e. the first column before exposure to ouabain.
NS, not significant, with regard to previous control.
*$P<0.05$, **$P<0.01$, ***$P<0.001$ (statistical significance with regard to previous control).

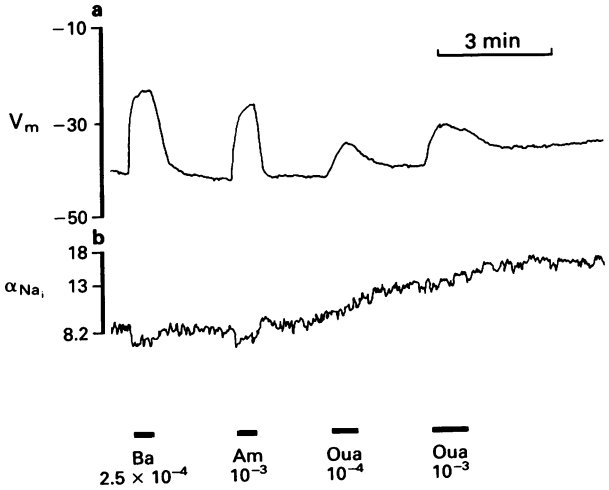

Figure 4 Effects of Ba^{2+}, amiloride (Am) and ouabain (Oua), as indicated, on membrane potential (a) and αNa_i (b). Drugs were applied during the time indicated by the bars under the trace. Ba^{2+} and amiloride elicit depolarization and small decrease in αNa_i, essentially reversible. Ouabain alters membrane potential and αNa_i, irreversibly.

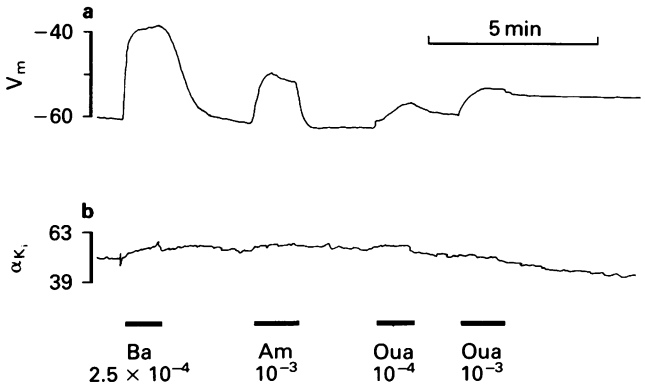

Figure 5 Effects of Ba^{2+}, amiloride (Am) and ouabain (Oua) on membrane potential (a) and αK_i (b). The effects of these agents on membrane potential are comparable to those of Figure 4. Drugs were applied during the time indicated by the bars under the trace. Ba^{2+} raises αK_i; however, removal of this blocker does not lead to recovery of αK_i within the 2–3 min following withdrawal of Ba^{2+}. Qualitatively similar effects were obtained with amiloride. Exposure to ouabain moderately lowers αK_i, but an even greater fall of αK_i is observed after withdrawal of ouabain.

To ascertain whether different glass microelectrodes yield similar results, we assessed αNa_i with aluminosilicate glass in control state and during a brief exposure to Ba^{2+} and amiloride: control αNa_i was 10.8 ± 0.5; αNa_i under amiloride was 10.1 ± 0.4, whereas in presence of Ba^{2+} this value was 11.3 ± 0.8 ($n = 4$, NS with regard to its paired control). Apparently, both, control αNa_i and $\Delta\alpha Na_i$ values with K^+ channel blockers are comparable, regardless of the glass used in these experiments.

Barium- and amiloride-sensitive NH_4^+ transport

Exposure of fused cells for approximately 5 min to a solution containing NH_3/NH_4^+, 15 mM, at the expense of NaCl, followed by its withdrawal results in cellular alkalinization. Taking the tangent to the initial rise of pH_i provides an estimate of NH_4^+ efflux (Boron & DeWeer, 1976). This approach has been widely used to assess the rate of Na^+-NH_4^+ antiport, whereby the Na^+ influx promotes NH_4^+ efflux. However, the present data support Ba^{2+}- and amiloride-sensitive K^+ conductive transport in fused PCT cells. In a separate experiment, we compared, in paired fashion, the effects of Ba^{2+} (2.5×10^{-4} M), and amiloride (10^{-3} M), on membrane conductance: membrane conductance decreased to 57 ± 4% and 60 ± 4%, respectively, with regard to control ($n = 11$). These means are not different from one another. The fused cells ($n = 9$) were then exposed to the NH_3/NH_4^+ pulse: in the control state the initial rate of alkalinization was 0.20 ± 0.02 pH u min^{-1}, which was reduced to 0.09 ± 0.02 in the presence of Ba^{2+} and to 0.11 ± 0.02 pH u min^{-1} in the presence amiloride (Figure 6). The latter two figures are statistically indistinguishable, but significantly lower than control ($P<0.005$). In summary, Ba^{2+} and amiloride, at the stated concentrations, lower the membrane conductance to about 60% of control, and they reduce the initial slope of realkalinization, by ≈10% less than the reduction of membrane conductance. Although these observations may not have an unequivocal meaning, it is tempting to ascribe an appreciable fraction of the amiloride-blockade of the NH_4^+ fluxes to a conductive process.

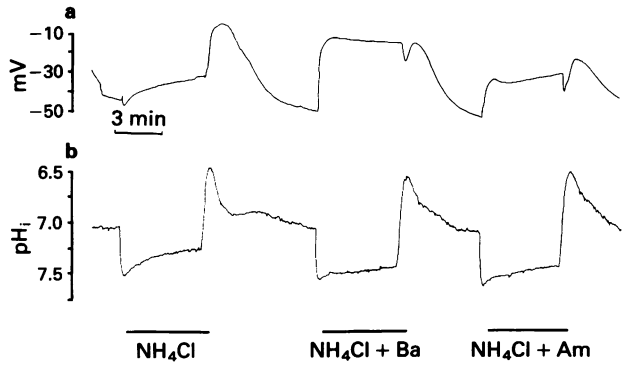

Figure 6 Effects of ≈5 min exposure of fused cells to 15 mM NH_4Cl solution alone (at the expense of NaCl) or in presence of Ba^{2+}, 2.5×10^{-4} M or amiloride (Am) 10^{-3} M: (a) membrane potential; (b) pH_i. The initial rate of cellular acidification, during NH_4Cl exposure is an index of the NH^+_4 influx into the cell. Ba^{2+} and amiloride reduce the initial rate of acidification with regard to control.

Identification of the epithelial membrane carrying an amiloride-sensitive K^+ conductance, in vivo

Since the above experiments have been performed on an *in vitro* preparation, in which the cytoskeleton was reshuffled during the fusion process (Oberleithner *et al.*, 1986), it was important to check whether the present data pertain to the native state. We used double-barrelled micropipettes, to alternate perfusion between a physiological salt solution, and the same solution plus amiloride, 1 mM. Peritubular capillary perfusion with amiloride failed to alter membrane potential ($\Delta V_m = 0.6 \pm 0.5$ mV, $n = 7$, NS). By contrast, delivery of an amiloride-containing solution into the tubular lumen resulted in a significant (7.6 ± 0.6 mV) depolarization which was reversible ($n = 8$). Since the PCT apical-to-basolateral (specific) resistance ratio *in vivo* is two to one, and recalling that the presence of a paracellular pathway generates intraepithelial circular current, during step-concentration changes in luminal fluid, the actual ΔV_m value in presence of amiloride is underestimated (Anagnostopoulos *et al.*, 1980).

Discussion

This study establishes that millimolar amiloride concentrations directly block K^+ conductance in amphibian PCT cells. Whereas high concentrations of amiloride were used in this study, similar concentrations have been currently applied in the past to silence the Na^+-H^+ antiport. Amiloride-induced inhibition of the Na^+-H^+ antiport elicits a fall of pH_i (Roos & Boron, 1981) and low pH_i in turn leads to K^+ conductance blockade (Anagnostopoulos, 1972; Kubota *et al.*, 1983). That amiloride concentrations $\geqslant 3 \times 10^{-4}$ M block K^+ conductance in amphibian PCT cells is established by several observations; this concentration-range results in depolarization of membrane potential and a reduction in membrane conductance, both of which return to control values upon removal of the drug. Blockade of Na^+ conductance by amiloride (Gögelein & Greger, 1986) should hyperpolarize membrane potential, as we observed on occasion at low amiloride concentrations. Similarly, amiloride-induced blockade of a non-selective cation channel (Light *et al.*, 1988) should also lead to hyperpolarization. Although a macroscopic Cl^- conductance has not been demonstrated in the PCT (Anagnostopoulos & Planelles, 1979; Guggino *et al.*, 1982), inhibition of a hypothetical Cl^- conductance by amiloride should also yield hyperpolarization, if fused cells *in vitro* retained the properties observed *in vivo*, where the Cl^- equilibrium potential has been estimated at − 36 mV (Edelman *et al.*, 1981). In short, electrophysiological analysis of the effects of amiloride in fused PCT cells does indicate an amiloride-induced blockade of K^+ conductance. Furthermore, our voltage-clamp studies, strongly suggest that amiloride inhibits potassium conductance.

With regard to the effects of amiloride on pH_i, it is interesting to note that high amiloride concentrations elevate pH_i in PCT fused cells, although high amiloride concentrations (2 mM) are required to establish the amphibian PCT Na^+-H^+ antiport (Boron & Boulpaep, 1983). In that study, the evidence for a Na^+-H^+ antiport relied upon the capacity of PCT cells to remove H^+ ions, following exposure to an acid imposed load. Whereas the Na^+-H^+ antiport exchange rate is sensitive to the absolute pH_i, it may not be active under resting (physiological) pH_i (Aronson *et al.*, 1982). In the present study, high amiloride concentrations elicit moderate alkalinization. At least two mechanisms may account for this observation: (i) the lipophilic properties of amiloride favour its diffusion into fused cells and due to its high pK it may increase pH_i. The data using Corning K^+-selective microelectrodes confirmed this hypothesis. (ii) Amiloride-induced membrane depolarization should alter the driving force of the PCT $Na^+/(HCO_3^-)_{n>1}$ symport, leading to decreased HCO_3^- efflux, or even reversing this flux, to promote net HCO_3^- influx (Planelles & Anagnostopoulos, 1991).

We also used the 'ammonium pulse' technique to assess the intrinsic capacity of fused cells to remove an acid load. In general, this procedure is used to quantify the ability of the Na^+-H^+ antiport to remove acid, because this antiport is the main extruder of protons. In the presence of NH_4Cl, the antiport carries NH_4^+ rather than H^+ ion (Kinsella & Aronson, 1981b), because the NH_4^+ concentration is orders of magnitude higher than that of H^+ ions. However, NH_4^+ ions share K^+ permeable pathways, including K^+ conductances (channels), secondary active transport (mainly Na^+-K^+-$2Cl^-$ cotransport) and even the Na^+-K^+, ATPase (Knepper *et al.*, 1989). That Ba^{2+} and amiloride curtail membrane conductance by 40% of control and that NH_4^+ efflux rates in presence of these blockers decrease by 50% with regard to control, suggests that a substantial fraction of amiloride-blockable NH_4^+ efflux may be conductive.

Our data are in conflict with direct inhibition of the Na^+-K^+, ATPase by amiloride in this preparation. Although Soltoff & Mandel (1989) observed a 35% reduction of Na^+-K^+ pump activity after 15–20 min exposure of PCT cells to amiloride, their results do not rule out the possibility that this reduction may be secondary to other changes induced by amiloride. According to the pump-leak hypothesis (Schultz, 1981), direct inhibition of the pump gives rise to homeostatic decrease of K^+ conductance and, reciprocally, primary K^+ conductance blockade leads to down-regulation of the Na^+-K^+, ATPase. In the present work, amiloride, like Ba^{2+}, reversibly depolarizes membrane potential and had no effect on αNa_i, whereas they elicited an initial increase of αK_i, which then relaxes back to previous levels over several minutes (Figure 5). Slow recovery could indicate the absence of, or poor, αK_i regulation. Alternatively, accumulation of K^+ ions into the cell under K^+ conductance blockade may be associated with cell volume expansion, the regulation of which may have priority over that of αK_i (Völkl & Lang, 1990). In sharp contrast to the effects of amiloride (Ba^{2+}), application of ouabain elicits irreversible changes of intracellular ion activities (rise of αNa_i, and fall of αK_i) and of membrane potential. Irreversible alteration of αNa_i, αK_i and membrane potential within $\leqslant 1$ min have been also observed in presence of ouabain in the amphibian cortical collecting tubule (Horisberg & Giebisch, 1989). Taken together these observations suggest that amiloride-induced K^+ conductance blockade is the primary cause which may ultimately result in down-regulation of the Na^+-K^+, ATPase during prolonged exposure to amiloride.

The amphibian PCT displays basolateral (Hunter, 1991) and apical (Kawahara *et al.*, 1987) K^+ channels and so does the mammalian PCT (Lang & Rehwald, 1992). Our observa-

tions indicate that amiloride blocks the apical PCT K^+ conductance, which is presumably assigned to K^+ secretion. This pathway may also serve for NH_4^+ secretion into the lumen. It may also be pertinent to recall that a PCT 250 pS maxi-K^+ channel has been identified in rabbit renal brush-border membrane vesicles (Zweifach *et al.*, 1991), that is inhibited by methylisobutyl amiloride. Whether an apical maxi-K channel is also present in the amphibian PCT to contribute to K^+ and NH_4^+ secretion, cannot be established from the present data.

In conclusion, we have demonstrated a novel action of amiloride: at concentrations currently used to study the Na^+-H^+ antiport, amiloride directly blocks an apical PCT K^+ conductance. Further studies are needed to determine whether amiloride-associated blockade of K^+ conductance is also present in other segments of the nephron.

The authors appreciate the secretarial work of M. Poitou.

References

ANAGNOSTOPOULOS, T. (1972). Effects of pH on electrical properties of peritubular membrane and shunt pathway of *Necturus* kidney. Abstr. 5th Internat. Congr. Nephrology (Mexico City) p. 104.

ANAGNOSTOPOULOS, T. & PLANELLES, G. (1979). Organic anion permeation at the proximal tubule of *Necturus*. An electrophysiological study of the peritubular membrane. *Pflügers Arch.*, **381**, 231–239.

ANAGNOSTOPOULOS, T. & PLANELLES, G. (1987). Cell and luminal activities of chloride, potassium, sodium and protons in the late distal tubule of *Necturus* kidney. *J. Physiol.*, **393**, 73–80.

ANAGNOSTOPOULOS, T., TEULON, J. & EDELMAN, A. (1980). Conductive properties of the proximal tubule in *Necturus* kidney. *J. Gen. Physiol.*, **75**, 553–589.

ARONSON, P.S., NEE, J. & SHUM, M.A. (1982). Modifier role of internal H^+ in activating the Na^+-H^+ exchanger in renal microvillus membrane vesicule. *Nature*, **299**, 161–163.

BENOS, D.J., REYES, J. & SHOEMAKER, D.G. (1983). Amiloride fluxes across erythrocyte membranes. *Biochem. Biophys. Acta*, **734**, 99–104.

BORON, W.F. & BOULPAEP, E.L. (1983). Intracellular pH regulation in the renal proximal tubule of the salamander. Na-H exchange. *J. Gen. Physiol.*, **81**, 29–52.

BORON, W.F. & DE WEER, P. (1976). Active proton transport stimulated by CO_2/HCO_3^-, blocked by cyanide. *Nature*, **259**, 240–241.

BOUACHOUR, G., PLANELLES, G. & ANAGNOSTOPOULOS, T. (1988). Fusion of amphibian proximal convoluted cells into giant cells. *Pflügers Arch.*, **441**, 220–222.

CANTIELLO, H.F., SCOTT, J.A. & RABITO, C.A. (1987). Conductive Na^+ transport in an epithelial cell line (LLC-PK_1) with characteristics of proximal tubular cells. *Am. J. Physiol.*, **252**, F590–F597.

CUTHBERT, A.W., FANELLI, G.M. & SCRIABINE, A. ed. (1979). *Amiloride and Epithelial Sodium Transport*. Baltimore Md: Urban & Schwarzenberg.

DISCALA, F., BELACHGAR, F., PLANELLES, G., HULIN, P. & ANAGNOSTOPOULOS, T. (1992). Barium- or quinine-induced depolarization activates K, Na and cationic conductances in frog proximal tubular cells. *J. Physiol.*, **448**, 525–537.

EDELMAN, A., BOUTHIER, M. & ANAGNOSTOPOULOS, T. (1981). Chloride distribution in the proximal convoluted tubule of *Necturus* kidney. *J. Membr. Biol.*, **62**, 7–18.

EIGLER, J., KELTER, J. & RENNER, E. (1967). Wirkungscharacterisk eines neuen acylguanidins Amiloride (MK 870) an der isolierten Haut von Amphibien. *Klin. Wochenschr.*, **45**, 737–738.

FRELIN, C., VIGNE, P., BARBRY, P. & LAZDUNSKI, M. (1987). Molecular properties of amiloride action and of its Na^+ transporting targets. *Kidney Intern.*, **32**, 785–793.

GÖGELEIN, H. & GREGER, R. (1986). Na^+ selective channels in the apical membrane of rabbit late proximal tubules (pars recta). *Pflügers Archiv.*, **406**, 198–203.

GUGGINO, W.B., BOULPAEP, E.L. & GIEBISCH, G. (1982). Electrical properties of chloride transport across the *Necturus* proximal tubule. *J. Membr. Biol.*, **65**, 185–196.

HAGGERTY, J.G., AGARWAL, N., REILLY, R.F., ADELBERG, E.A. & SLAYMAN, C.W. (1988). Pharmacological different Na/H antiporters on the apical and basolateral surfaces of cultured porcine kidney cells (LLC-PK_1). *Proc. Natl. Acad. Sci. U.S.A.*, **85**, 6797–6801.

HORISBERGER, J.-D. & GIEBISCH, G. (1989). Na-K pump current in the *Amphiuma* collecting tubule. *J. Gen. Physiol.*, **94**, 493–510.

HUNTER, M. (1991). Potassium-selective channels in the basolateral membrane of single proximal tubular cells of frog kidney. *Pflügers Arch.*, **418**, 26–34.

KAWAHARA, K., HUNTER, M. & GIEBISCH, G. (1987). Potassium channels in *Necturus* proximal tubule. *Am. J. Physiol.*, **253**, F488–F494.

KINSELLA, J.L. & ARONSON, P.S. (1981a). Amiloride inhibition of the Na^+/H^+ exchanger in renal microvillus membrane vesicles. *Am. J. Physiol.*, **241**, F374–F379.

KINSELLA, J.L. & ARONSON, P.S. (1981b). Interaction of NH_4^+ and Li^+ with the renal microvillus membrane N^+-H^+ exchanger. *Am. J. Physiol.*, **241**, C220–C226.

KNEPPER, M.A., PACKER, R. & GOOD, D.W. (1989). Ammonium transport in the kidney. *Physiol. Rev.*, **69**, 179–249.

KUBOTA, T., BIAGI, B.A. & GIEBISCH, G. (1983). Effects of acid base disturbances on basolateral membrane potential and intracellular potassium activity in the proximal tubule of *Necturus*. *J. Membr. Biol.*, **73**, 61–68.

LANG, F. & REHWALD, W. (1992). Potassium channels in renal epithelial transport regulation. *Physiol Rev.*, **72**, 1–72.

LEWIS, S.A. & WILLS, N.K. (1980). Resistive artifacts in liquid-ion exchanger microelectrode estimates of Na^+ activity in epithelial cells. *Biophys. J.*, **13**, 127–138.

LIGHT, D.B., MCCANN, F.V., KELLER, T.M. & STANTON, B.A. (1988). Amiloride-sensitive cation channel in apical membrane of inner medullary collecting duct. *Am. J. Physiol.*, **255**, F278–F286.

OBERLEITHNER, H., SCHMIDT, B. & DIETL, P. (1986). Fusion of epithelial cells: a model for studying cellular mechanisms of ion transport. *Proc. Natl. Acad. Sci. U.S.A.*, **83**, 3547–3551.

OBERLEITHNER, H., WEIGT, M., WESTPHALE, H.-J. & WANG, W. (1987). Aldosterone activates Na^+/H^+ exchange and raises cytoplasmic pH in target cells of the amphibian kidney. *Proc. Natl. Acad. Sci. U.S.A.*, **84**, 1464–1468.

PALMER, L.G. (1987). Ion selectivity of epithelial Na channels. *J. Membr. Biol.*, **96**, 97–106.

PLANELLES, G. & ANAGNOSTOPOULOS, T. (1991). Basolateral electrogenic Na/HCO_3 symport in the amphibian distal tubule. *Pflügers Archiv.*, **417**, 582–590.

PLANELLES, G., KURKDJIAN, A. & ANAGNOSTOPOULOS, T. (1984). Cell and luminal pH in the proximal tubule of *Necturus* kidney. *Am. J. Physiol.*, **247**, F932–F938.

PLANELLES, G., TEULON, J. & ANAGNOSTOPOULOS, T. (1981). The effects of barium on the electrical properties of the basolateral membrane in proximal tubule. *Naunyn-Schmied. Arch. Pharmacol.*, **318**, 135–141.

ROBINSON, R.A. & STOKES, R.H. (1970). *Electrolyte Solutions*. London: Butterworths.

ROOS, A. & BORON, W.F. (1981). Intracellular pH. *Physiol. Rev.*, **61**, 296–434.

SCHULTZ, S.G. (1981). Homocellular regulatory mechanisms in sodium-transporting epithelia: avoidance of extinction by 'flush-through'. *Am. J. Physiol*, **241**, F579–F590.

SOLTOFF, S.P. & MANDEL, L. (1983). Amiloride directly inhibits the Na,K-ATPase activity of rabbit kidney proximal tubules. *Science*, **220**, 957–959.

TEULON, J. & ANAGNOSTOPOULOS, T. (1982). Proximal K^+ activity: technical problems and dependence on plasma K^+ concentration. *Am. J. Physiol.*, **243**, F12–F18.

VÖLKL, H. & LANG, F. (1990). Effect of potassium on cell regulation in renal straight proximal tubules. *J. Membr. Biol.*, **117**, 113–122.

ZWEIFACH, A., DESIR, G.V., ARONSON, P.S. & GIEBISCH, G. (1991). Ca-activated K channel from rabbit renal brush-border membrane vesicles in planar lipid bilayers. *Am. J. Physiol.*, **261**, F187–F196.

(Received January 2, 1992
Revised May 7, 1992
Accepted June 12, 1992)

Br. J. Pharmacol. (1992), **107**, 539–543

Agonist analysis of 2-(carboxycyclopropyl)glycine isomers for cloned metabotropic glutamate receptor subtypes expressed in Chinese hamster ovary cells

*†Yasunori Hayashi, *Yasuto Tanabe, *Ichiro Aramori, *Masayuki Masu, **Keiko Shimamoto, **Yasufumi Ohfune & [1],*Shigetada Nakanishi

*Institute for Immunology and †Department of Pharmacology, Kyoto University Faculty of Medicine, Kyoto 606 and **Suntory Institute for Bioorganic Research, Shimamoto-cho, Mishima-gun, Osaka 618, Japan

1 2-(Carboxycyclopropyl)glycines (CCGs) are conformationally restricted glutamate analogues and consist of eight isomers including L- and D-forms. The agonist potencies and selectivities of these compounds for metabotropic glutamate receptors (mGluRs) were studied by examining their effects on the signal transduction of representative mGluR1, mGluR2 and mGluR4 subtypes in Chinese hamster ovary cells expressing the individual cloned receptors.

2 Two extended isomers of L-CCG, L-CCG-I and L-CCG-II, effectively stimulated phosphatidylinositol hydrolysis in mGluR1-expressing cells. The rank order of potencies of these compounds was L-glutamate > L-CCG-I > L-CCG-II.

3 L-CCG-I and L-CCG-II were effective in inhibiting the forskolin-stimulated adenosine 3':5'-cyclic monophosphate (cyclic AMP) accumulation in mGluR2-expressing cells. Particularly, L-CCG-I was a potent agonist for mGluR2 with an EC_{50} value of 3×10^{-7} M, which was more than an order of potency greater than that of L-glutamate.

4 L-CCG-I evoked an inhibition of the forskolin-stimulated cyclic AMP production characteristic of mGluR4 with a potency comparable to L-glutamate.

5 In contrast to the above compounds, the other CCG isomers showed no appreciable effects on the signal transduction involved in the three mGluR subtypes.

6 This investigation demonstrates not only the importance of a particular isomeric structure of CCGs in the interaction with the mGluRs but also a clear receptor subtype specificity for the CCG-receptor interaction, and indicates that the CCG isomers would serve as useful agonists for investigation of functions of the mGluR family.

Keywords: Excitatory amino acids; glutamate analogue; agonist potency; agonist selectivity; metabotropic glutamate receptor; receptor-expressing cell; signal transduction

Introduction

L-Glutamate, a major excitatory neurotransmitter in the central nervous system (CNS), plays an important role in neuronal plasticity and neurotoxicity (Monaghan *et al.*, 1989; Collingridge & Singer, 1990; Meldrum & Garthwaite, 1990). Glutamate receptors are classified into two distinct groups termed ionotropic receptors and metabotropic receptors (mGluRs) (Monaghan *et al.*, 1989). The ionotropic receptors comprise integral cation-specific channel complexes and are further subdivided into the receptors for N-methyl-D-aspartate (NMDA) and the non-NMDA receptors for kainate/α-amino-3-hydroxy-5-methyl-4-isoxazolepropionate (AMPA) (Monaghan *et al.*, 1989). The mGluRs are coupled to intracellular signalling transduction via guanine nucleotide-binding proteins (G proteins) (Schoepp *et al.*, 1990; Récasens *et al.*, 1991). Recently, we isolated complementary DNAs (cDNAs) for five different subtypes of the rat mGluR family (mGluR1-mGluR5) (Masu *et al.*, 1991; Tanabe *et al.*, 1992; Abe *et al.*, 1992). The mGluR family shares no sequence similarity with the other members of G protein-coupled receptors and possesses a large extracellular domain preceding the seven putative transmembrane segments (Masu *et al.*, 1991; Houamed *et al.*, 1991; Tanabe *et al.*, 1992). The mGluR subtypes differ in the signal transduction and agonist selectivity and are expressed in specialized neuronal and glial cells of the CNS (Masu *et al.*, 1991; Tanabe *et al.*, 1992; Abe *et al.*, 1992).

Specific agonists and antagonists for glutamate receptors are indispensible for receptor research and have been extensively developed for the ionotropic receptors (Watkins *et al.*, 1990). However, there have been no selective or potent agonists and no antagonists for the mGluR subtypes (Schoepp *et al.*, 1990). Furthermore, the precise characterization of the agonist and antagonist selectivity has been limited in tissue and cell preparations, because of the ambiguity resulting from the presence of multiple subtypes of the glutamate receptors in these preparations. The functional assay of a single cloned receptor expressed in animal cells provides a useful system to determine accurately the selectivity and potencies of agonists and antagonists.

2-(Carboxycyclopropyl)glycine (CCG) is a conformationally restricted glutamate analogue in which the cyclopropyl group fixes the glutamate chain in either an extended or a folded form (Kurokawa & Ohfune, 1985; Yamanoi *et al.*, 1988; Shimamoto *et al.*, 1991). CCG has 8 stereoisomers including L- and D-forms (Figure 1) and serves as a valuable compound for investigating the interaction of glutamate molecules with glutamate receptor subtypes (Shinozaki *et al.*, 1989). Shinozaki and his colleagues reported that the two extended isomers of CCG with L-configuration (2**S**, 1'**S**,2'**S**) isomer (L-CCG-I) and (2**S**,1'**R**,2'**R**) isomer (L-CCG-II), are capable of selectively activating mGluR and thus cause the induction of an electrophysiological response in *Xenopus* oocytes injected with rat brain poly(A)$^+$ RNA (Ishida *et al.*, 1990) and the stimulation of phosphatidylinositol (PI) hydrolysis in rat hippocampal synaptoneurosome (Nakagawa *et al.*,

[1] Author for correspondence.

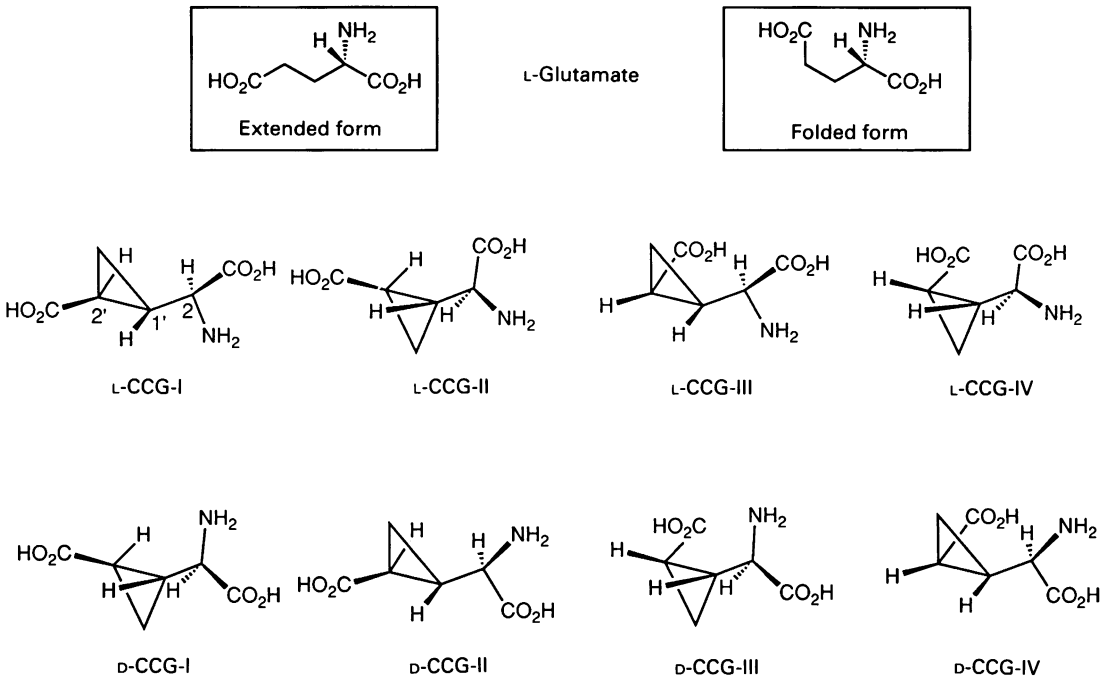

Figure 1 Eight diastereomers of 2-(carboxycyclopropyl)glycine (CCG).

1990). In this investigation, we tested the agonist effects and selectivities of the 8 CCG isomers on the activities of different mGluR members by measuring intracellular second messengers in Chinese hamster ovary (CHO) cells expressing individual receptor subtypes. We confirmed that L-CCG-I and L-CCG-II specifically activate PI hydrolysis of mGluR1 among the 8 CCG isomers. Furthermore, we found that L-CCG-I acts as a more potent and selective agonist for mGluR2 than for the other members of mGluRs.

Methods

Measurements of phosphatidylinositol hydrolysis

CHO cell lines stably expressing mGluR1 and mGluR2 were described in our previous papers (Aramori & Nakanishi, 1992; Tanabe *et al.*, 1992). Those expressing mGluR4 were established according to the procedures used for the development of mGluR1-expressing cell lines (Aramori & Nakanishi, 1992). The agonist activity for mGluR1 was assessed by measuring agonist-induced stimulation of total inositol phosphate formation in mGluR1-expressing cells as described previously (Aramori & Nakanishi, 1992). Briefly, mGluR1-expressing cells were seeded in 6-well plates at a density of 3×10^5 cells per well and cultured for 24 h. The cells were labelled with fresh medium containing [^{3}H]-inositol (1 μCi ml^{-1}) for 24 h. They were washed with phosphate buffered-saline solution (PBS) and incubated with the same solution for 20 min and then with PBS containing 10 mM LiCl (PBS-Li) for 20 min at 37°C. Agonist stimulation was started by replacing the medium with fresh PBS-Li containing various concentrations of test agents. After incubation for 20 min, the medium was removed, and the reaction was terminated with 5% (w/v) trichloroacetic acid (TCA). The TCA fraction was applied on a Bio-Rad AG1-X8 anion exchanger column, and a mixture of ^{3}H-labelled inositol mono-, bis- and tris-phosphates was eluted from the column with 0.1 M formic acid/1.0 M ammonium formate. The radioactivity of eluate was determined by a liquid scintillation spectrometer.

Measurements of adenosine 3':5'-cyclic monophosphate (cyclic AMP) formation

Agonist activities for mGluR2 and mGluR4 were evaluated by measuring an agonist-dependent inhibition of forskolin-induced cyclic AMP formation in mGluR2- and mGluR4-expressing cells as described (Tanabe *et al.*, 1992). Briefly, CHO cells expressing either mGluR2 or mGluR4 were seeded in 12-well plates at a density of 1.5×10^5 cells per well and grown for 2 to 3 days. The cells were washed with PBS containing 1 mM 3-isobutyl-1-methylxanthine (IBMX) (PBS-IBMX) and incubated for 20 min in the same solution. The reaction was started by replacing the medium with fresh PBS-IBMX containing 10 μM forskolin and various concentrations of test agents. After incubation for 10 min, the medium was removed, and the reaction was terminated with 5% (w/v) TCA. Cyclic AMP levels were determined by the cyclic AMP radioimmunoassay kit.

Materials

Eight stereoisomers of CCG [the (2S,1'S,2'S) isomer (L-CCG-I), (2S,1'R,2'R) isomer (L-CCG-II), (2S,1'S,2'R) isomer (L-CCG-III), (2S,1'R,2'S) isomer (L-CCG-IV), (2R, 1'R,2'R) isomer (D-CCG-I), (2R,1'S,2'S) isomer (D-CCG-II), (2R,1'R, 2'S) isomer (D-CCG-III) and (2R,1'S,2'R) isomer (D-CCG-IV)] (Figure 1) were synthesized according to previously described procedures (Yamanoi *et al.*, 1988; Shimamoto *et al.*, 1991); the carbons 1' and 2' were previously numbered as 3 and 4, respectively, and are renumbered according to the IUPAC nomenclature. Enantiomeric purity of these compounds (>99%) was ascertained by high performance liquid chromatography analysis using an optically active column (Daicel Chemical Industries Ltd., Crownpack CR(+), aqueous $HClO_4$ (pH 2.0) as an eluent). Other chemicals used were of reagent grade and were obtained as described previously (Tanabe *et al.*, 1992).

Statistical analysis

All experiments for measurements of PI hydrolysis and cyclic

AMP formation were carried out in triplicate at least twice. Statistical significance was examined by analysis of variance with Williams multiple-range test.

Results

Effects of CCG isomers on mGluR1

The five mGluR subtypes can be subclassified into three groups on the basis of the sequence similarity of their primary structures and their signalling cascades: mGluR1/5, mGluR2/3, and mGluR4. They show about 60–70% amino acid homology within the same group of the receptors and about 40% sequence similarity between different groups of the receptors (Tanabe *et al.*, 1992; Abe *et al.*, 1992). mGluR1 and mGluR5 are coupled to PI hydrolysis with a similar profile of the agonist selectivity (Abe *et al.*, 1992). In contrast, mGluR2 and mGluR4 are linked to the inhibitory cyclic AMP cascade in response to the interaction with L-glutamate (Tanabe *et al.*, 1992; see also below). However, the agonist selectivity profiles of these two receptors are clearly different from each other. The rank order of potencies of agonists for mGluR2 was L-glutamate≈(1S*,3R*)-1-aminocyclopentane-1,3-dicarboxylate (tACPD)>ibotenate>quisqualate (Tanabe *et al.*, 1992), whereas the agonist activity of tACPD, quisqualate and ibotenate was very weak or almost negligible for mGluR4 (Tanabe & Nakanishi, unpublished data). This difference probably reflects a low homology between the primary structures of mGluR2 and mGluR4. We chose mGluR1, mGluR2 and mGluR4 as representatives of each group of the receptors and investigated the effects of the 8 CCG isomers on the signal transduction characteristic of the respective receptors. In addition, we included L-glutamate as a control compound for the subsequent analysis of the 8 isomers in receptor-expressing cells. We also confirmed that none of the 8 CCG isomers produced any effects on the signal transduction described below in untransfected cells or cells transfected with the vector DNA alone (data not shown).

The potencies of the 8 CCG isomers for mGluR1 were first examined by determining dose-response curves of these compounds for the stimulation of PI hydrolysis in mGluR1-expressing cells (Figure 2). PI hydrolysis was measured by incubating cells with an individual CCG isomer for 20 min to allow maximal stimulation of inositol phosphate formation, while blocking further dephosphorylation by LiCl. L-Glutamate added to mGluR1-expressing cells evoked stimulation of PI hydrolysis with an EC_{50} value of 1×10^{-5} M. The two extended CCG isomers with L-configuration, L-CCG-I and L-CCG-II, similarly showed the stimulation of PI hydrolysis in mGluR1-expressing cells (Figure 2a). The EC_{50} value of L-CCG-I was about 5×10^{-5} M, while the potency of L-CCG-II was much lower than that of L-CCG-I. In contrast, no response in the stimulation of PI hydrolysis was evoked by the two folded isomers of L-CCG (L-CCG-III and IV) or by the four D-CCG isomers (D-CCG-I to IV), regardless of whether the structure of D-CCG was extended or folded (Figure 2a and 2b). The result obtained thus demonstrates that the extended isomers of L-CCG specifically interact with mGluR1 but are less potent than L-glutamate in inducing mGluR1-mediated PI hydrolysis.

Effects of CCG isomers on mGluR2

As shown previously (Tanabe *et al.*, 1992), mGluR2 mediates the inhibitory cyclic AMP cascade. In the experiments shown in Figure 3, incubation of mGluR2-expressing cells with 10 μM forskolin evoked cyclic AMP accumulation of approximately 30 times above the basal levels. This accumulation was reduced in a dose-dependent manner by increasing concentrations of L-glutamate and was lowered to about 10% of the maximally accumulated cyclic AMP levels at 1×10^{-4} M L-glutamate; the EC_{50} value of L-glutamate was about 2×10^{-5} M. Similarly, L-CCG-I and L-CCG-II effectively inhibited the forskolin-stimulated cyclic AMP accumulation and maximally reduced the cyclic AMP formation (Figure 3a). Furthermore, L-CCG-I was highly effective for this receptor and was more potent than L-glutamate in inhibiting the cyclic AMP accumulation. The EC_{50} values of L-CCG-I and L-CCG-II were 3×10^{-7} M and 3×10^{-4} M, respectively. Folded isomers of L-CCG, on the other hand, showed only a weak agonist activity at the concentration of 1×10^{-3} M (Figure 3a). Among the 4 isomers with D-configuration, D-CCG-I exhibited a significant inhibitory activity at high concentrations (Figure 3b). The purity of all isomers of the CCG tested was estimated to be more than 99%. However, because D-CCG-I and its enantiomer, L-CCG-I, showed about 3 orders of magnitude difference in the effective concentrations, it could not be ascertained whether the effect of D-CCG-I reflects its intrinsic activity or arises from the possible presence of a trace amount of L-CCG-I in our D-CCG-I preparation.

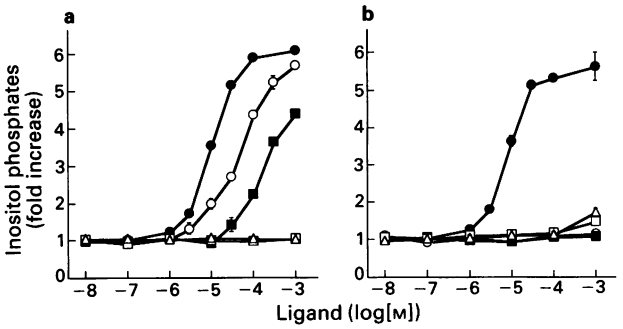

Figure 2 Dose-response curves of 8 2-(carboxycyclopropyl)glycine (CCG) isomers for stimulation of phosphatidylinositol (PI) hydrolysis in mGluR1-expressing cells. Receptor-expressing cells were incubated with indicated concentrations of L-CCG isomers (a) and D-CCG isomers (b) for 20 min and inositol phosphate formation determined. In (a), L-glutamate (●), L-CCG-I (○), L-CCG-II (■), L-CCG-III (□) and L-CCG-IV (△) were added. In (b), L-glutamate (●), D-CCG-I (○), D-CCG-II (■), D-CCG-III (□) and D-CCG-IV (△) were examined. The inositol phosphate formation is expressed as multiples of inositol phosphate levels in agonist-untreated cells. Basal levels of total inositol phosphates were 1254 ± 142 c.p.m. The data indicated were taken from a representative experiment and the values are means with s.e. (vertical bars) of triplicate determinations.

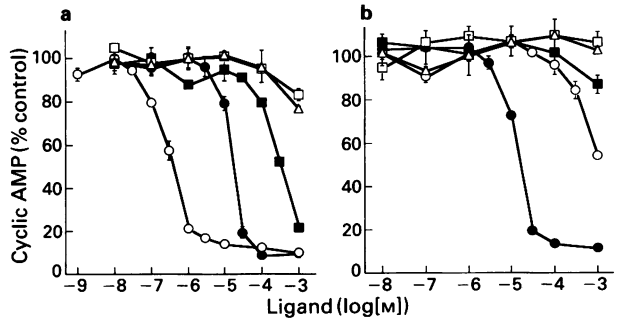

Figure 3 Dose-response curves of 8 2-(carboxycyclopropyl)glycine (CCG) isomers for inhibition of the forskolin-stimulated cyclie AMP formation in mGluR2-expressing cells. Receptor-expressing cells were incubated with indicated concentrations of L-CCG isomers (a) and D-CCG isomers (b) in the presence of 10 μM forskolin and intracellular cyclic AMP levels determined. Cyclic AMP levels in cells treated and untreated with 10 μM forskolin were 169.1 ± 2.9 and 5.5 ± 0.1 nmol per well, respectively. The former levels were taken as 100%. For further explanation, see Figure 2.

Effects of CCG isomers on mGluR4

As shown in Figure 4, L-glutamate inhibited the forskolin-stimulated cyclic AMP accumulation in mGluR4-expressing cells, but this inhibition did not extend beyond about 40% of the maximally stimulated levels even by the addition of higher concentrations of L-glutamate. Because the partial inhibition of the cyclic AMP formation was consistently observed in several independent mGluR4-expressing cell lines, this inhibition pattern probably represents a feature characteristic of the signal transduction mediated by mGluR4. In mGluR4-expressing cells, L-CCG-I elicited a partial inhibition of the forskolin-stimulated cyclic AMP accumulation (Figure 4a). The potency of this compound was comparable to L-glutamate; the EC_{50} value of L-CCG-I was about 5×10^{-5} M, when the maximal inhibition was assumed to occur at 1×10^{-3} M L-CCG-I. In contrast to L-CCG-I, none of the other compounds including D-CCG isomers produced any remarkable effects on the mGluR4 activity, though some of these compounds showed a slight inhibition at the concentration of 1×10^{-3} M.

Discussion

The mGluR family consists of multiple receptor subtypes and the expressions of the individual receptors overlap in many neuronal cells (Tanabe *et al.*, 1992; Abe *et al.*, 1992). The determination of the subtype specificity of possible agonists thus requires an assay system in which a single receptor subtype can be characterized without any cross-reactivity of the agonists to other receptor subtypes. In this investigation, we adopted clonal cell lines expressing an individual cloned mGluR subtype to examine the agonist properties of the 8 CCG isomers for mGluRs and to clarify their subtype specificity. Our results unequivocally demonstrate that L-CCG-I and L-CCG-II specifically interact with mGluR1 and thus stimulate PI hydrolysis in mGluR1-expressing cells. This observation is in good agreement with previous studies on rat hippocampal synaptoneurosome and *Xenopus* oocytes injected with brain poly(A)$^+$ RNA (Nakagawa *et al.*, 1990; Ishida *et al.*, 1990). Furthermore, the extended isomers of L-CCG act not only on mGluR1 but also on other mGluR subtypes. Notably, L-CCG-I has a strong potency to interact with mGluR2 and thus effectively inhibits the forskolin-stimulated cyclic AMP formation in mGluR2-expressing cells. The EC_{50} value of L-CCG-I for mGluR2 is 3×10^{-7} M, and this potency is more than one order higher than those of L-glutamate and tACPD (Tanabe *et al.*, 1992). The latter compound is the only one that is currently available as an mGluR-specific agonist, but L-CCG-I is more potent than tACPD as an agonist for both mGluR1 and mGluR2; the EC_{50} values of tACPD for mGluR1 and mGluR2 are about 1×10^{-3} M and 5×10^{-6} M, respectively (Aramori & Nakanishi, 1992; Tanabe *et al.*, 1992). With respect to the subtype specificity of L-CCG-I, the possible reactivity of this compound with mGluR3 must be taken into consideration. We have not yet succeeded in characterizing the agonist selectivity of mGluR3, because of the difficulty in developing cell lines expressing mGluR3 (the reasons for this are unknown). However, mGluR3 shows a high degree of sequence similarity (about 70%) with mGluR2 (Tanabe *et al.*, 1992). It is thus likely that mGluR3 shares similar properties with mGluR2 in signal transduction and the agonist selectivity. Remarkably, L-CCG-I is capable of producing an almost full activity of mGluR2 at low concentrations (e.g. 1×10^{-6} M), where virtually no effects on mGluR1 and mGluR4 are produced. Furthermore, electrophysiological and binding studies have indicated that L-CCG-I is only weakly active for the NMDA receptor at high concentrations (1×10^{-4} M) and is totally inactive for the kainate/AMPA receptors (Ishida *et al.*, 1990; Kawai *et al.*, 1992). L-CCG-I may thus be useful for distinguishing functions not only between the ionotropic and metabotropic receptors but also within different subtypes of the mGluR family.

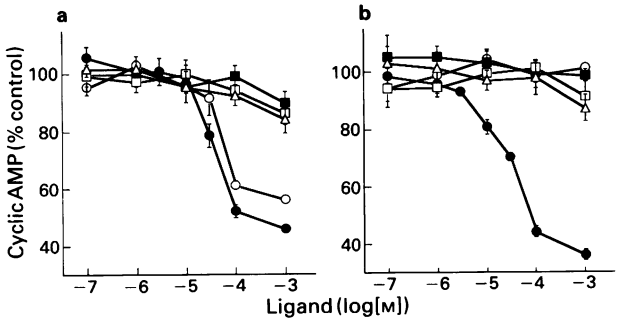

Figure 4 Dose-response curves of L-2-(carboxycyclopropyl)glycine (L-CCG) isomers (a) and D-CCG isomers (b) for inhibition of the forskolin-stimulated cyclic AMP formation in mGluR4-expressing cells. Intracellular cyclic AMP levels in cells treated and untreated with 10 μM forskolin were 182.2 ± 14.1 and 5.3 ± 0.5 nmol per well, respectively. For further explanation, see Figure 3.

Recently accumulated evidence has indicated that mGluRs play an important role in mediating synaptic transmission in the CNS. Activation of mGluR has been reported to regulate neuronal excitability in the hippocampus through suppression of a Ca^{2+}-dependent K^+ current and a voltage-gated K^+ current (Charpak *et al.*, 1990; Baskys *et al.*, 1990; Desai & Conn, 1991). The involvement of mGluR has also been reported in the depression of synaptic transmission in the hippocampal CA1 synapses (Baskys & Malenka, 1991). mGluRs may also be involved in the neuronal functions of glutamate in other parts of the brain. For example, the functional cooperation of both the AMPA receptor and mGluR seems to be required for long-term depression in cerebellar Purkinje cells (Linden *et al.*, 1991). Glutamate-induced depression of spike discharge observed in cerebellar slice preparations could also result from activation of mGluR in Golgi cells (Yamamoto *et al.*, 1976), where mGluR2 mRNA is prominently expressed (Tanabe *et al.*, 1992). It has been thought that the major effects associated with mGluR activation result solely from the stimulation of PI hydrolysis/Ca^{2+} signal transduction. However, it has now been established that there are several subtypes of mGluRs which are coupled to distinct signal transduction (Tanabe *et al.*, 1992). It has also recently been reported that the selective mGluR activation results in the inhibition of cyclic AMP formation in hippocampal slices (Schoepp *et al.*, 1992). L-CCG isomers selective to mGluR subtypes would thus provide a new tool to investigate which subtype of the mGluRs is responsible for the induction and depression of neuronal transmission as described above.

L-CCG isomers are not only valuable as specific mGluR agonists but also may serve as leading compounds for the synthesis of more specific ligands for mGluRs. Our study has revealed that the agonist activity of CCG isomers for mGluRs is confined to the extended form with the L-configuration at the α-carbon moiety. Conformationally restricted glutamate analogues have provided useful tools for the development of agonists and antagonists for glutamate receptors (Watkins *et al.*, 1990). Fixation of the main chain of glutamate or its longer chain analogues by incorporation of a cyclic structure or a double bond directs the ω-anionic group into a particular steric arrangement with respect to the α-carbon moiety. This strategy has been used successfully for the synthesis of NMDA receptor antagonists (Davies *et al.*, 1986; Murphy *et al.*, 1988; Sills *et al.*, 1991). Therefore, structural modification of L-CCG isomers may be designed to produce specific agonists and antagonists for a certain mGluR subtype. Noteworthy also here is that the only avail-

able radiolabelled compound for the mGluR family is [^{3}H]-glutamate. However, no significant binding of [^{3}H]-glutamate to membrane fractions prepared from mGluR-expressing cells was discernible by filter binding and centrifugation assays, due to high levels of endogenous [^{3}H]-glutamate binding (Aramori & Nakanishi, 1992; Abe *et al.*, 1992). In addition, rapid dissociation of [^{3}H]-glutamate binding is expected from the EC_{50} value of this compound. Thus, incorporation of a tritium into L-CCG-I or its derivative may provide a high-affinity radioligand applicable for a simple binding assay of an mGluR subtype.

In conclusion, this investigation has explored the selectivity and potencies of the 8 CCG isomers for 3 representative subtypes of the mGluR family by examining the effects of these compounds on the signal transduction characteristic of the individual receptors. Our results demonstrate that the two extended isomers of L-CCG specifically interact with the mGluR family. It is particularly interesting that L-CCG-I acts as a potent agonist for mGluR2. These compounds may thus facilitate investigations of the function and role of mGluRs as well as development of specific agonists and antagonists for these receptors.

This work was supported in part by research grants from the Ministry of Eduction, Science and Culture of Japan and the Ministry of Health and Welfare of Japan.

References

ABE, T., SUGIHARA, H., NAWA, H., SHIGEMOTO, R., MIZUNO, N. & NAKANISHI, S. (1992). Molecular characterization of a novel metabotropic glutamate receptor mGluR5 coupled to inositol phosphate/Ca^{2+} signal transduction. *J. Biol. Chem.*, (in press).

ARAMORI, I. & NAKANISHI, S. (1992). Signal transduction and pharmacological characteristics of a metabotropic glutamate receptor mGluR1 in transfected Chinese hamster ovary cells. *Neuron*, **8**, 757–765.

BASKYS, A., BAROLET, A.W. & CARLEN, P.L. (1990). Quisqualate induces suppression of the calcium-dependent potassium current via a mechanism involving G proteins. *Can. J. Physiol. Pharmacol.*, **68**, Aii.

BASKYS, A. & MALENKA, R.C. (1991). Trans-ACPD depresses synaptic transmission in the hippocampus. *Eur. J. Pharmacol.*, **193**, 131–132.

CHARPAK, S., GÄHWILER, B.H., DO, K.Q. & KNÖPFEL, T. (1990). Potassium conductances in hippocampal neurons blocked by excitatory amino-acid transmitters. *Nature*, **347**, 765–767.

COLLINGRIDGE, G.L. & SINGER, W. (1990). Excitatory amino acid receptors and synaptic plasticity. *Trends Pharmacol. Sci.*, **11**, 290–296.

DAVIES, J., EVANS, R.H., HERRLING, P.L., JONES, A.W., OLVERMAN, H.J., POOK, P. & WATKINS, J.C. (1986). CPP, a new potent and selective NMDA antagonist. Depression of central neuron responses, affinity for [^{3}H]D-AP5 binding sites on brain membranes and anticonvulsant activity. *Brain Res.*, **382**, 169–173.

DESAI, M.A. & CONN, P.J. (1991). Excitatory effects of ACPD receptor activation in the hippocampus are mediated by direct effects on pyramidal cells and blockade of synaptic inhibition. *J. Neurophysiol.*, **66**, 40–52.

HOUAMED, K.M., KUIJPER, J.L., GILBERT, T.L., HALDEMAN, B.A., O'HARA, P.J., MULVIHILL, E.R., ALMERS, W. & HAGEN, F.S. (1991). Cloning, expression, and gene structure of a G protein-coupled glutamate receptor from rat brain. *Science*, **252**, 1318–1321.

ISHIDA, M., AKAGI, H., SHIMAMOTO, K., OHFUNE, Y. & SHINOZAKI, H. (1990). A potent metabotropic glutamate receptor agonist: electrophysiological actions of a conformationally restricted glutamate analogue in the rat spinal cord and *Xenopus* oocytes. *Brain Res.*, **537**, 311–314.

KAWAI, M., HORIKAWA, Y., ISHIHARA, T., SHIMAMOTO, K. & OHFUNE, Y. (1992). 2-(Carboxycyclopropyl)glycines: binding, neurotoxicity and induction of intracellular free Ca^{2+} increase. *Eur. J. Pharmacol.*, **211**, 195–202.

KUROKAWA, N. & OHFUNE, Y. (1985). The palladium(II)-assisted syntheses of (±)-α-(methylenecyclopropyl)glycine and (±)-trans-α-(carboxycyclopropyl)glycine, two bioactive amino acids. *Tetrahedron Lett.*, **26**, 83–84.

LINDEN, D.J., DICKINSON, M.H., SMEYNE, M. & CONNOR, J.A. (1991). A long-term depression of AMPA currents in cultured cerebellar Purkinje neurons. *Neuron*, **7**, 81–89.

MASU, M., TANABE, Y., TSUCHIDA, K., SHIGEMOTO, R. & NAKANISHI, S. (1991). Sequence and expression of a metabotropic glutamate receptor. *Nature*, **349**, 760–765.

MELDRUM, B. & GARTHWAITE, J. (1990). Excitatory amino acid neurotoxicity and neurodegenerative disease. *Trends Pharmacol. Sci.*, **11**, 379–387.

MONAGHAN, D.T., BRIDGES, R.J. & COTMAN, C.W. (1989). The excitatory amino acid receptors: their classes, pharmacology, and distinct properties in the function of the central nervous system. *Annu. Rev. Pharmacol. Toxicol.*, **29**, 365–402.

MURPHY, D.E., HUTCHISON, A.J., HURT, S.D., WILLIAMS, M. & SILLS, M.A. (1988). Characterization of the binding of [^{3}H]-CGS 19755: a novel N-methyl-D-aspartate antagonist with nanomolar affinity in rat brain. *Br. J. Pharmacol.*, **95**, 932–938.

NAKAGAWA, Y., SAITOH, K., ISHIHARA, T., ISHIDA, M. & SHINOZAKI, H. (1990). (2S,3S,4S)α-(Carboxycyclopropyl)glycine is a novel agonist of metabotropic glutamate receptors. *Eur. J. Pharmacol.*, **184**, 205–206.

RÉCASENS, M., MAYAT, E. & GUIRAMAND, J. (1991). Excitatory amino acid receptors and phosphoinositide breakdown: facts and perspectives. In *Current Aspects of the Neurosciences*, Vol.3. ed. Osborne, N.N., pp. 103–175. New York: Macmillan Press.

SCHOEPP, D.D., BOCKAERT, J. & SLADECZEK, F.A.J. (1990). Pharmacological and functional characteristics of metabotropic excitatory amino acid receptors. *Trends Pharmacol. Sci.*, **11**, 508–515.

SCHOEPP, D.D., JOHNSON, B.G. & MONN, J.A. (1992). Inhibition of cyclic AMP formation by a selective metabotropic glutamate receptor agonist. *J. Neurochem.*, **58**, 1184–1186.

SHIMAMOTO, K., ISHIDA, M., SHINOZAKI, H. & OHFUNE, Y. (1991). Synthesis of four diastereomeric L-2-(carboxycyclopropyl)glycines. Conformationally constrained L-glutamate analogues. *J. Org. Chem.*, **56**, 4167–4176.

SHINOZAKI, H., ISHIDA, M., SHIMAMOTO, K. & OHFUNE, Y. (1989). Potent NMDA-like actions and potentiation of glutamate responses by conformational variants of a glutamate analogue in the rat spinal cord. *Br. J. Pharmacol.*, **98**, 1213–1224.

SILLS, M.A., FAGG, G., POZZA, M., ANGST, C., BRUNDISH, D.E., HURT, S.D., WILUSZ, E.J. & WILLIAMS, M. (1991). [^{3}H]CGP 39653: a new N-methyl-D-aspartate antagonist radioligand with low nanomolar affinity in rat brain. *Eur. J. Pharmacol.*, **192**, 19–24.

TANABE, Y., MASU, M., ISHII, T., SHIGEMOTO, R. & NAKANISHI, S. (1992). A family of metabotropic glutamate receptors. *Neuron*, **8**, 169–179.

WATKINS, J.C., KROGSGAARD-LARSEN, P. & HONORÉ, T. (1990). Structure-activity relationships in the development of excitatory amino acid receptor agonists and competitive antagonists. *Trends Pharmacol. Sci.*, **11**, 25–33.

YAMAMOTO, C., YAMASHITA, H. & CHUJO, T. (1976). Inhibitory action of glutamic acid on cerebellar interneurones. *Nature*, **262**, 786–787.

YAMANOI, K., OHFUNE, Y., WATANABE, K., LI, P.N. & TAKEUCHI, H. (1988). Syntheses of trans- and cis-α-(carboxycyclopropyl)glycines. Novel neuroinhibitory amino acids as L-glutamate analogue. *Tetrahedron Lett.*, **29**, 1181–1184.

(Received February 12, 1992
Revised April 23, 1992
Accepted June 15, 1992)

Br. J. Pharmacol. (1992), **107**, 544–552

Capsazepine: a competitive antagonist of the sensory neurone excitant capsaicin

[1]S. Bevan, S. Hothi, G. Hughes, I.F. James, H.P. Rang, K. Shah, C.S.J. Walpole & J.C. Yeats

Sandoz Institute for Medical Research, 5 Gower Place, London WC1E 6BN

1 Capsazepine is a synthetic analogue of the sensory neurone excitotoxin, capsaicin. The present study shows the capsazepine acts as a competitive antagonist of capsaicin.

2 Capsazepine (10 μM) reversibly reduced or abolished the current response to capsaicin (500 nM) of voltage-clamped dorsal root ganglion (DRG) neurones from rats. In contrast, the responses to 50 μM γ-aminobutyric acid (GABA) and 5 μM adenosine 5'-triphosphate (ATP) were unaffected.

3 The effects of capsazepine were examined quantitatively with radioactive ion flux experiments. Capsazepine inhibited the capsaicin (500 nM)-induced $^{45}Ca^{2+}$ uptake in cultures of rat DRG neurones with an IC_{50} of 420 ± 46 nM (mean ± s.e.mean, $n = 6$). The $^{45}Ca^{2+}$ uptake evoked by resiniferatoxin (RTX), a potent capsaicin-like agonist was also inhibited. (Log concentration)-effect curves for RTX (0.3 nM–1 μM) were shifted in a competitive manner by capsazepine. The Schild plot of the data had a slope of 1.08 ± 0.15 (s.e.) and gave an apparent K_d estimate for capsazepine of 220 nM (95% confidence limits, 57–400 nM).

4 Capsazepine also inhibited the capsaicin- and RTX-evoked efflux of $^{86}Rb^+$ from cultured DRG neurones. The inhibition appeared to be competitive and Schild plots yielded apparent K_d estimates of 148 nM (95% confidence limits, 30–332 nM) with capsaicin as the agonist and 107 nM (95% confidence limits, 49–162 nM) with RTX as agonist.

5 A similar competitive inhibition by capsazepine was seen for capsaicin-induced [^{14}C]-guanidinium efflux from segments of adult rat vagus nerves (apparent $K_d = 690$ nM; 95% confidence limits, 63 nM–1.45 μM). No significant difference was noted in the apparent K_d estimates for capsazepine in assays on cultured DRG neurones and vagus nerve as shown by the overlap in the 95% confidence limits.

6 Capsazepine, at concentrations up to 10 μM, had no significant effects on the efflux of $^{86}Rb^+$ from cultured DRG neurones evoked either by depolarization with high (50 mM) K^+ solutions or by acidification of the external medium to pH 5.0–5.6. Similarly capsazepine had no significant effect on the depolarization (50 mM KCl)-induced efflux of [^{14}C]-guanidinium from vagus nerve preparations.

7 Ruthenium Red was also tested for antagonism against capsaicin evoked [^{14}C]-guanidinium release from vague nerves and capsaicin induced $^{45}Ca^{2+}$ uptake in cultures of DRG neurones. In contrast to capsazepine the inhibition by Ruthenium Red (10–500 nM in DRG and 0.5–10 μM in vagus nerve experiments) was not consistent with a competitive antagonism, but rather suggested a more complex, non-competitive inhibition.

Keywords: Capsaicin; resiniferatoxin; Ruthenium Red; capsazepine; sensory neurones

Introduction

Capsaicin, the pungent ingredient in hot chilli peppers, has a unique excitatory action on a sub-population of afferent sensory neurones. When capsaicin interacts with these neurones a cation selective ion channel is opened (Wood *et al.*, 1988; see review by Bevan & Szolcsanyi, 1990). This allows sodium and calcium ions to enter and potassium ions to leave the cell. The net effect is an inward current that depolarizes and thus excites the neurones. Not all sensory neurones are depolarized by capsaicin; the chemosensitivity is restricted to some somatic and visceral afferents with conduction velocities in the C- and Aδ-range. The capsaicin-sensitive somatic neurones include the polymodal nociceptors, which are sensitive to a variety of noxious chemical, thermal and mechanical stimuli, while the visceral neurones mediate important autonomic reflexes (see Szolcsanyi, 1990; Holzer, 1991). There is also increasing evidence that, in addition to their afferent functions, these neurones have efferent functions in the target tissues possibly as a result of neuropeptides released from the peripheral terminals (see Szolcsanyi, 1984; Holzer, 1988; Maggi & Meli, 1988 for reviews).

In addition to its specific agonist action on sensory neurones, capsaicin has also been reported to inhibit or to modify voltage-gated sodium, potassium and calcium currents in a variety of neurones (Dubois, 1982; Erdelyi & Such, 1984; Yamanaka *et al.*, 1984; Petersen *et al.*, 1987; 1989; Docherty *et al.*, 1991) and also to inhibit contraction of cardiac, visceral and vascular smooth muscle (Szolcsanyi & Bartho, 1978; Donnerer & Lembeck, 1982; Zernig *et al.*, 1984). Other effects on cellular functions such as prostanoid formation (Juan *et al.*, 1980; Flynn *et al.*, 1986) and platelet aggregation (Wang *et al.*, 1984; 1985) have also been reported. The concentration of capsaicin necessary to show these effects is usually higher than that required to show the sensory neurone-specific membrane action, which is postulated to involve specific membrane receptors. Nevertheless such findings raise the possibility that some of the actions of capsaicin could be unrelated to its action on the sensory neurone membrane. The availability of a specific capsaicin antagonist would greatly assist studies on the physiological functions of capsaicin sensitive nerves as well as the mechanisms of action of capsaicin and a related compound, resiniferatoxin (RTX).

Recent studies have demonstrated that RTX, which is a compound isolated from some plants of the genus *Euphorbia*,

[1] Author for correspondence.

has similar effects to capsaicin (de Vries & Blumberg, 1989; Szallasi & Blumberg, 1989; Dray *et al.*, 1990a; Szallasi & Blumberg, 1990a). RTX shows some structural similarities to capsaicin (see Figure 1). Both compounds appear to act on the same neurones, to have a similar, if not identical, mechanism of action (Szallasi & Blumberg, 1989; Winter *et al.*, 1990) and to share a common, membrane associated binding site (Szallasi & Blumberg, 1990b). The difference is that RTX is usually active at 100 to 1000 times lower concentrations than capsaicin (see. e.g. Maggi *et al.*, 1989). It is unclear, however, if all the effects of RTX are due to an action at capsaicin binding sites rather than to activation of protein kinases (cf. Ryves *et al.*, 1989).

The inorganic dye, Ruthenium Red, inhibits the effects of capsaicin on sensory neurones and has been used as a capsaicin antagonist (Maggi *et al.*, 1988a,b; 1989; Amann & Lembeck, 1989; Chahl, 1989; Franco-Cereceda *et al.*, 1989; Dray *et al.*, 1990b). Unfortunately, Ruthenium Red can inhibit the responses to other agents (see Maggi, 1991) and this non-specificity limits its usefulness as a capsaicin antagonist. In this paper we describe the discovery and characterization of a competitive antagonist of both capsaicin and RTX. This antagonist, capsazepine (see Figure 1) has already been shown to antagonize the actions of capsaicin in the spinal cord (Dickenson & Dray, 1991) and will be a valuable tool in future studies on the cellular actions of these agents and the physiological functions of capsaicin-sensitive nerves.

Preliminary reports on the pharmacology of capsazepine have been published (Bevan *et al.*, 1991; Dray *et al.*, 1991).

Methods

Dorsal root ganglion neurone experiments

Cell dissociation Dissociated DRG neurones were prepared from neonatal rats by enzymatic and mechanical dissociation as described in detail elsewhere (Wood *et al.*, 1988). In brief, neonatal animals were killed by decapitation after cervical dislocation. Spinal ganglia were removed aseptically from all levels of the spinal cord. Ganglia were incubated for 30 min at 37°C with F-14 medium (Gibco) containing 0.125% collagenase (Boehringer Mannheim) and 10% horse serum (Gibco) and then for 15–30 min with 0.25% trypsin (Worthington) in F-14 medium. Cells were dissociated by trituration through a flame polished Pasteur pipette, centrifuged and the cell pellet resuspended in F-14 medium containing 10% horse serum and 200 ng ml^{-1} nerve growth factor. Cells were either used immediately for electrophysiology or placed in culture.

For experiments on cultured neurones, dissociated DRG cells were plated either on sterile 13 mm glass coverslips or Terasaki plates. Both substrates were previously coated with 10 $\mu g\ ml^{-1}$ poly-D-ornithine (Sigma) and 5 $\mu g\ ml^{-1}$ laminin (Gibco). Cells were maintained at 37°C in an humidified incubator gassed with 3% CO_2 in air.

Electrophysiology Experiments were done on dissociated cells shortly (4–12 h) after plating on laminin-coated glass coverslips. DRG neurones were voltage-clamped by the whole cell, tight seal method with an Axopatch 1B amplifier. Wide bore 'patch' pipettes were pulled from 1.5 mm external diameter glass fibre-filled capillaries (Clark Electromedical GC150F) in a 3 stage pull on a P-80 Brown-Flaming micropipette puller (Sutter Instrument Co.). These were fire polished and had a final resistance of 2–5 MΩ when filled. Intracellular, pipette-filling solutions were composed of (mM) KCl 130, $MgCl_2$ 1, $CaCl_2$ 1, EGTA 11, HEPES (N-[2-hydroxyethyl]piperazine-N'-[2-ethanesulphonic acid]) 10, pH 7.4. For most experiments pipettes were coated with Repelcote (Sigma) to reduce electrode capacitance.

Recordings were made on the stage of an inverted phase contrast microscope (Nikon Diaphot) in a flow chamber of a design similar to that described by McBurney & Neering (1985). The basic external solution of (mM) NaCl 130, KCl 3.5, $CaCl_2$ 2, $MgCl_2$ 1, glucose 5 and sucrose 40, was buffered to pH 7.4 with 10 mM HEPES. Drugs were applied to the cells from a U-tube, which allowed rapid application (< 300 ms) of solutions (Fenwick *et al.*, 1982). All experiments were done at room temperature 20–23°C.

Radioactive ion flux experiments

Efflux experiments were performed on cultures of neonatal rat DRG neurones plated at high density (5000–10 000 per 13 mm diameter coverslip). Either Rb^+ or guanidinium ions were studied as both ions are readily permeant through capsaicin activated (Wood *et al.*, 1988), proton activated and depolarization activated (Bevan & Yeats, 1991) channels. The choice of cation was largely a matter of availability. Three to six day old cultures were loaded to equilibrium with either radioactive Rb^+ or guanidinium ions by incubation for 2 h at 37°C in medium containing either 2 $\mu Ci\ ml^{-1}$ $^{86}RbCl$ (300 Ci mol^{-1}; Amersham) or 10 $\mu Ci\ ml^{-1}$ [^{14}C]-guanidine HCl (54 Ci mol^{-1}; Amersham). Coverslips were then dipped in non-radioactive medium and mounted in an enclosed chamber (0.5 ml volume), similar in design to that used for electrophysiology. The chamber was perfused at a rate of 1 ml min^{-1} with non-radioactive medium. Cells were perfused for 10 min to remove extracellular radioactivity. The efflux of radioactive ions was then followed by subsequent collection of solution at 1 min intervals. The standard solutions for efflux studies was composed of (mM): NaCl 150, KCl 5, $CaCl_2$ 2, $MgCl_2$ 1 and HEPES 5, titrated to pH 7.4 with NaOH. In experiments designed to investigate the effects of capsazepine on proton-induced permeability changes, the external medium was acidified by replacement of the HEPES buffered solution with a 10 mM MES (2-[N-morphilino]-ethanesulphonic acid) buffered solution (pH 5.0–5.6). Experiments were performed at room temperature (20–23°C). At the end of the experiment, the amount of radioactivity

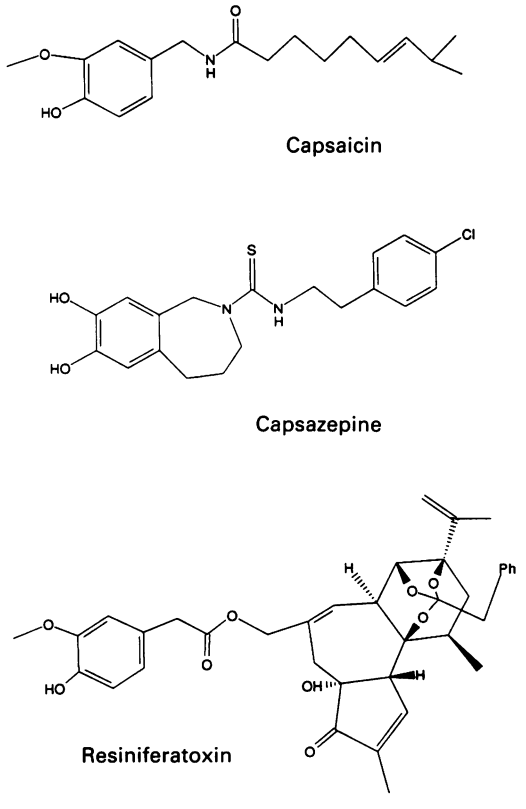

Figure 1 Structures of capsaicin, resiniferatoxin and capsazepine.

remaining in the cells was determined after solubilization of the cells in 0.2% sodium dodecylsulphate (SDS). The rate of efflux was expressed as a rate constant by calculating the amount of radioactivity released in each 1 min period as a fraction of the amount present at the beginning of the period. The mean efflux for each experimental condition was estimated from at least 4 replicate cultures (usually 5–9). Agonists were applied for 2–3 min and the agonist-induced efflux calculated as the peak increase in efflux rate coefficient.

$^{45}Ca^{2+}$ uptake experiments were carried out on 3–5 day old cultures of DRG neurones plated on 60 well Terasaki plates. The method has been described in detail by Wood *et al.* (1988). In brief, calcium uptake was measured at room temperature over a 10 min incubation period in a nominally calcium-free medium with 10 μCi ml^{-1} $^{45}Ca^{2+}$ added. The incubation medium contained varying concentrations of either capsaicin or RTX. The background uptake in the absence of agonist was also determined for each plate. Six replicate wells were used to assess the uptake for each condition tested. At the end of the incubation period the plates were washed with at least 6 changes (10 ml each) of calcium-free medium, the cells were solubilised in 1% SDS and the amount of radioactivity in each sample measured by liquid scintillation counting.

Vagus nerve experiments

Rats (Sprague-Dawley, about 220 g) were killed with chloroform and both cervical vagus nerves removed. The nerves were desheathed and placed overnight at room temperature in 1–2 ml of Locke solution (mM: NaCl 154, KCl 5.6, $CaCl_2$ 2, $NaHCO_3$ 1.8, D-glucose 1.8, Tris-HCl buffer 10, pH 7.4) containing [^{14}C]-guanidine HCl (approximately 10 μCi ml^{-1}). The nerves were then mounted in stainless steel tubes (1 mm internal diameter) through which Locke solution was perfused at a constant rate (1 ml min^{-1}) by a peristaltic pump. The emerging solution was collected at 1 min intervals, and the radioactivity was determined by liquid scintillation counting. At the end of the experiments, the nerve was removed, dissolved in 2 N NaOH, and the residual radioactivity was counted. The rate of efflux was expressed as a rate constant. After mounting the nerve and perfusing with Locke solution for 20–30 min, the solution was changed for 5 min to one containing capsaicin or, in some control experiments, 50 mM KCl. In some experiments the preparation was perfused for 5 min with antagonist (capsazepine or Ruthenium Red) alone before changing the solution to one containing capsaicin (or 50 mM KCl) and antagonist. The effect of capsaicin was expressed as the increase in efflux rate constant during the 2 min test perfusion period. Each nerve was tested only once with capsaicin, to avoid problems of desensitization. Each drug combination was tested on 2–4 preparations.

Drugs

Capsazepine (2-[2-(4-chlorphenyl)ethylamino-thiocarbonyl]-7, 8-dihydroxy-2,3,4,5 tetrahydro-1H-2-benzazepine) was synthesized at the Sandoz Institute for Medical Research. Capsaicin, GABA, ATP and Ruthenium Red were obtained from Sigma Chemical Co. Resiniferatoxin was purchased from Fluka.

Statistics

Except where noted, Student's *t* test, modified where appropriate for small sample sizes, was used for statistical analysis of drug effects. Schild plots were constructed from the (log concentration)-response curves by estimating the concentration of agonist to produce a 50% maximum effect. A line was fitted to the Schild plot data by a least squares algorithm (BBN Software Products Corporation, Cambridge, Massachusetts, USA). The asymmetrical confidence limits for the apparent K_d estimates were calculated with Fieller's theorem (see Colquhoun, 1971). Results are given as mean ± s.e.mean.

Results

Electrophysiological studies

The effects of capsazepine on the chemosensitivity of isolated dorsal root ganglion (DRG) neurones was examined electrophysiologically in voltage-clamped cells. Figure 2a shows the response of an adult rat DRG neurone at a holding potential of −80 mV. Capsaicin (500 nM) evoked an inward current that was reversibly abolished by exposure to a high concentration (10 μM) of capsazepine. Similar results were observed in 10 other cells examined in this way. The mean amplitude of the current in the presence of capsazepine (0.06 ± 0.03 nA, s.e.mean) was only 4% of that before capsazepine (1.38 ± 0.28 nA). After washing out the capsazepine, the response to capsaicin always increased in size although it usually did not return to the initial level (mean amplitude = 0.71 ± 0.15 nA). This reduction in amplitude after washout of capsazepine probably reflects some degree of desensitization induced by the first application of capsaicin (Yeats *et al.*, 1991). Desensitization made it difficult to make a detailed quantitative study of the effects of capsazepine with electrophysiological methods.

In contrast to the effect on capsaicin-induced currents, 10 μM capsazepine had no obvious effect on the response to either GABA (Figure 2b) or ATP (Figure 2c). These two agonists were chosen as they evoke reliable and easily studied electrophysiological responses in DRG neurones. The responses to GABA were studied relatively easily as there was little or no desensitization when the drug was applied at 2 min intervals. The mean amplitude of the response to 50 μM GABA in the presence of 10 μM capsazepine was 2.12 ± 0.34 nA; this was 1.03 ± 0.08 ($n = 7$) times that of the response to GABA alone.

The effects of capsazepine on ATP responses were less easily studied as ATP responses normally showed a significant degree of desensitization. The responses shown in Figure 2 were atypical as little desensitization was noted in this cell. Nevertheless, they clearly show that 10 μM capsazepine had no effect on the ATP response. In other experiments different protocols were required. In one set of experiments the ATP sensitivity of the population was sampled either in normal external solution ($n = 14$) or in the presence of 10 μM capsazepine ($n = 13$). The amplitude of the response in the presence of capsazepine (0.43 ± 0.11 nA) was not significantly different ($P > 0.05$) from that in control solutions (0.37 ± 0.09 nA). The possible effect of capsazepine on the responses to ATP was also studied in single cells by alternating between normal and capsazepine-containing solutions.

In 9 experiments ATP was first applied in normal medium and then in the presence of capsazepine, while in a further 5 experiments ATP was initially applied in capsazepine containing solution and then again 3–4 min after washing out the casazepine. The mean ratio (response amplitude with capsazepine/'control' amplitude) calculated from these experiments was 1.34 ± 0.34, which indicates that capsazepine had no significant effect on the paired responses of individual cells ($P > 0.1$). In view of the large variance of the ratio, these data were also analyzed with a non-parametric test (Wilcoxon sign rank test). This analysis also indicated that capsazepine had no significant ($P > 0.3$) effect on the response of DRG neurones to ATP.

Ion flux studies on cultured DRG neurones

The agonist actions of capsaicin and RTX can be studied quantitatively by following the transmembrane flux of radioactive ions (Wood *et al.*, 1988; Winter *et al.*, 1990). Figure 3

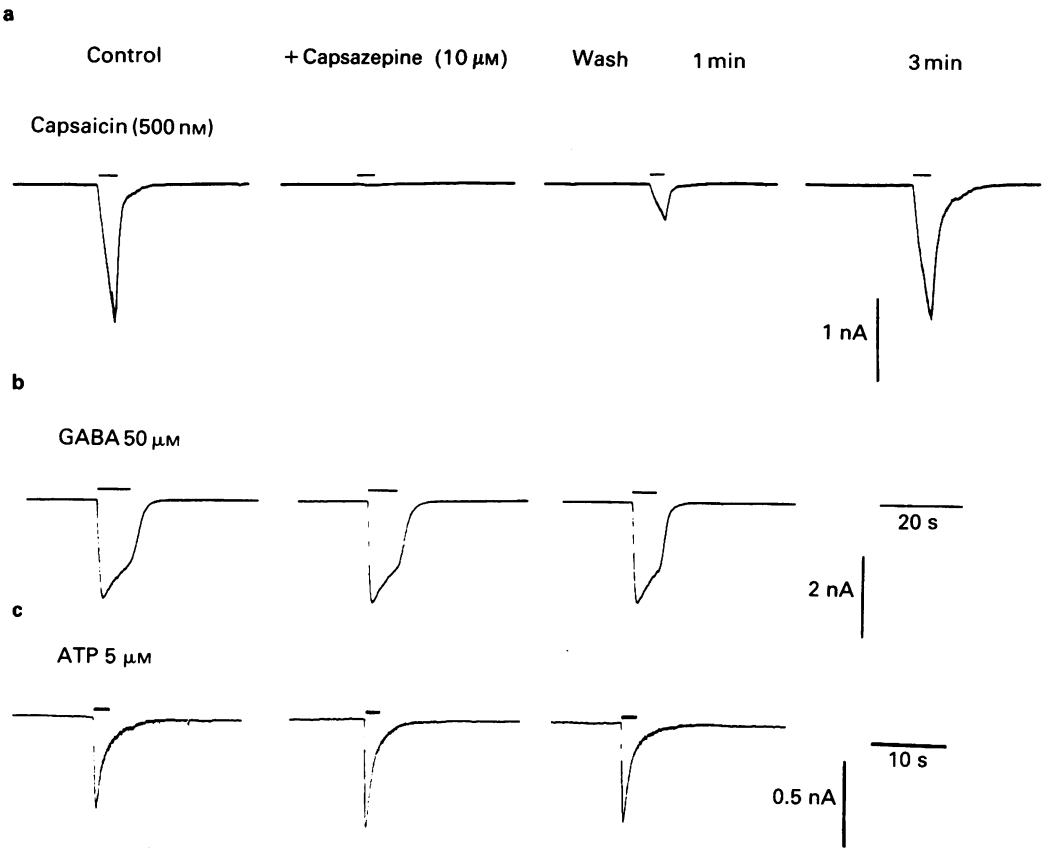

Figure 2 Effect of 10 μM capsazepine on current responses of neonatal rat DRG neurones evoked by 500 nM capsaicin (a), 50 μM γ-aminobutyric acid (GABA, b) and 5 μM adenosine 5'-triphosphate (ATP, c). Responses measured before, during and after exposure to capsazepine. Each agonist tested on a different cell. Cells were pre-incubated with capsazepine for 3 min before application of each agonist together with capsazepine. For the recovery from capsazepine treatment, responses after two wash times (1 and 3 min) are shown for capsaicin, whereas the responses after 3 min wash periods in capsazepine-free medium are shown for the GABA and ATP experiments. Current calibrations shown for each cell. Time calibration is 20 s for capsaicin and GABA experiments, 10 s for ATP experiment.

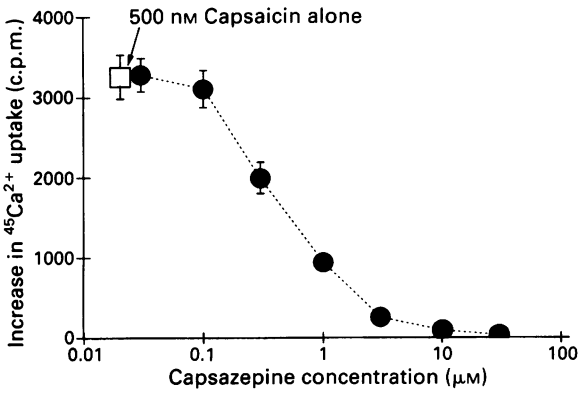

Figure 3 Inhibition by capsazepine of the uptake of $^{45}Ca^{2+}$ evoked by administration of 500 nM capsaicin to neonatal rat cultured DRG neurones. Data shown as mean with s.e.mean indicated by vertical bars, $n = 6$.

shows the results of a study of the uptake of $^{45}Ca^{2+}$ into cultures of neonatal rat DRG neurones. When tested against 500 nM capsaicin, capsazepine inhibited the uptake with an IC_{50} of 420 ± 46 nM ($n = 6$). Attempts to study this inhibition with capsaicin as the agonist were hampered by the finding that high (⩾ 10 μM) concentrations of capsaicin alone inhibited the $^{45}Ca^{2+}$ accumulation to give a 'bell-shaped' (log-concentration)-effect curve (data not shown). For this reason it was not possible to overcome the capsazepine inhibition by raising the capsaicin concentration. Such experiments were, however, possible with RTX as the agonist because no depression of the maximum $^{45}Ca^{2+}$ uptake was noted even with the highest RTX concentrations used (Figure 4a). RTX induced a concentration-dependent uptake of $^{45}Ca^{2+}$ with an EC_{50} of 3 nM, which is similar to previously published values (Winter *et al.*, 1990). Capsazepine shifted the (log-concentration)-effect curves to the right, but the inhibition was surmountable when the RTX concentration was raised (Figure 4a). No inhibition of the maximum RTX induced $^{45}Ca^{2+}$ was noted in the presence of either 5 μM (3 experiments) or 10 μM (2 experiments) capsazepine ($P > 0.1$ in each experiment). Figure 4e shows the Schild plot constructed from the data in Figure 4a; this had a slope of 1.08 ± 0.15 and yielded a K_d estimate of 220 nM (95% confidence limits, 57–400 nM).

The accumulation of $^{45}Ca^{2+}$ requires several steps including sequestration by intracellular organelles (Wood *et al.*, 1988). Experiments were therefore done to examine the effects of capsazepine on capsaicin- and RTX-induced efflux of $^{86}Rb^{+}$ from cultured DRG neurones, which is a more direct measure of the plasma membrane permeability changes. Capsaicin alone evoked a concentration-dependent increase in $^{86}Rb^{+}$ efflux rate with an EC_{50} of 60 nM (Figure 4c). Increasing concentrations of capsazepine shifted the (log-concentration)-response curves to the right. The Schild plot for these data was linear with a slope of 1.21 ± 0.07 and gave a K_d for capsazepine of 148 nM (95% confidence limits, 30–332 nM, see Figure 4f). RTX also evoked a $^{86}Rb^{+}$ efflux ($EC_{50} = 0.9$ nM) and this was similarly inhibited by capsa-

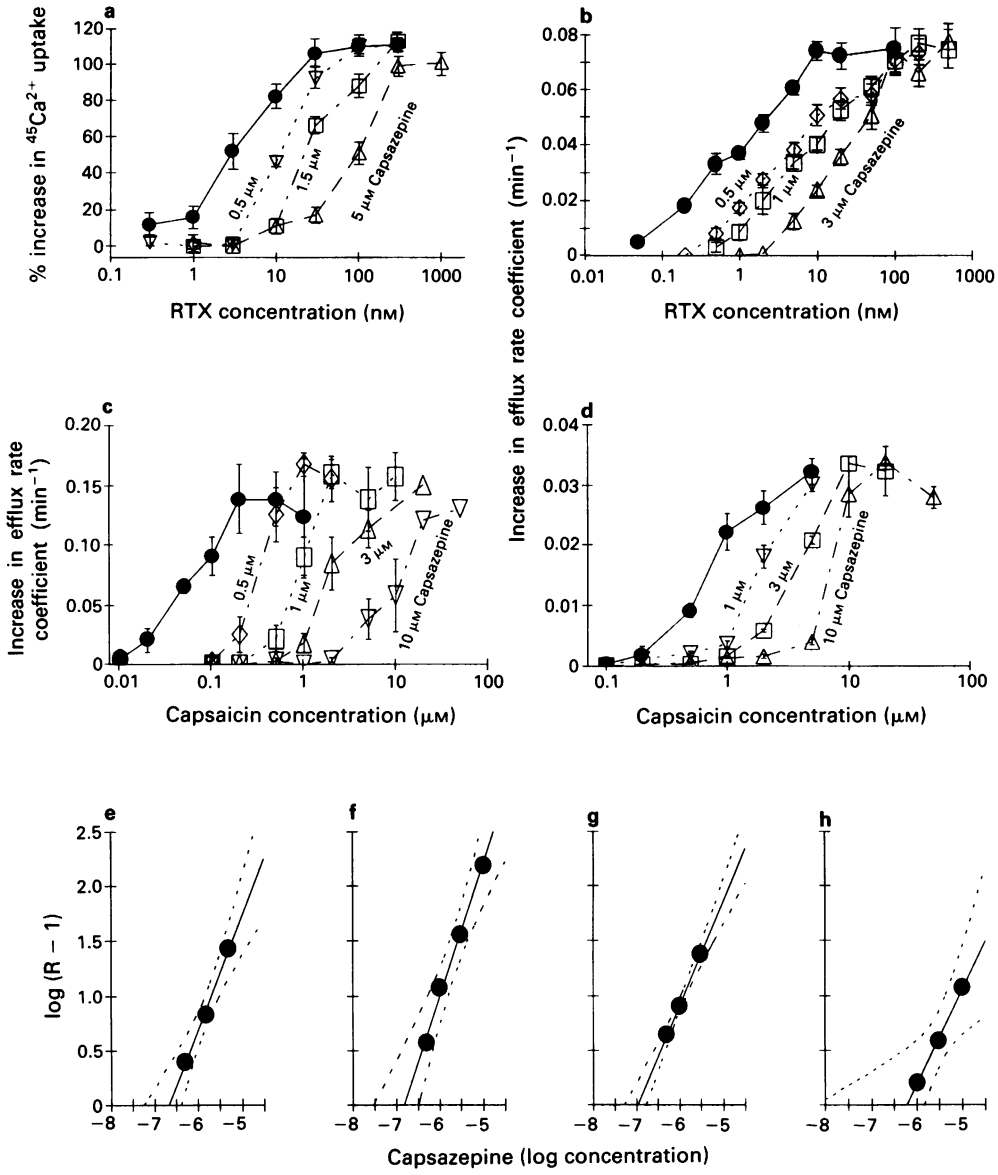

Figure 4 (a–d) (Log-concentration)-effects curves for capsazepine on (a) resiniferatoxin (RTX)-induced $^{45}Ca^{2+}$ uptake by neonatal rat DRG cultures: (b) RTX-induced $^{86}Rb^{+}$ efflux, cultured DRG neurones: (c) capsaicin-evoked efflux of $^{86}Rb^{+}$, cultured DRG neurones: (d) capsaicin-evoked efflux of [^{14}C]-guanidinium from pre-loaded rat vagus nerves. (Log-concentration) – effect curves are shown for agonists alone and in the presence of the indicated concentrations of capsazepine: data shown as mean with s.e.mean shown by vertical bars. (e–h). Schild plots for the data shown in (a–d) respectively. (e) slope = 1.08 ± 0.15, K_d = 220 nM (95% confidence limits, 57–400 nM): (f) slope = 1.21 ± 0.07, K_d = 148 nM (95% confidence limits, 49–162): (g) slope = 0.95 ± 0.03, K_d = 107 nM (95% confidence limits, 30–332 nM): (h) slope = 0.87 ± 0.03, K_d = 690 nM (95% confidence limits, 63 nM–1.45 μM).

zepine with a K_d of 107 nM (95% confidence limits, 49–162 nM) as shown in Figure 4b and g.

An increase in the efflux rate of $^{86}Rb^{+}$ was evoked when cultured DRG neurones were depolarized by a challenge with 150 mM KCl (replacement for NaCl). The potassium evoked $^{86}Rb^{+}$ efflux was not inhibited by 10 μM capsazepine, which was included in the pre-challenge solutions as well as in the high K^{+} solution. The increase in efflux rate coefficient in the presence of capsazepine (0.0418 ± 0.0066 min^{-1}, $n = 5$) was not significantly different ($P > 0.1$) from the increase evoked by KCl alone (0.0508 ± 0.0074 min^{-1}, $n = 5$).

Acidification of the external medium to pH < 6.4 evokes a sustained inward, depolarizing current in a subset of DRG neurones. The channels responsible for this current are permeable to Rb^{+} and guanidinium ions and so the efflux of either $^{86}Rb^{+}$ or [^{14}C]-guanidinium ions from pre-loaded DRG cultures can be used as a measure of the proton evoked response (Bevan & Yeats, 1991). Figure 5 shows the results of such an experiment with $^{86}Rb^{+}$. Acidification of the external medium elicited an increase in the efflux rate, which was not significantly different when 10 μM capsazepine was included in the perfusion medium. Experiments were done with solutions of various pH (5.0–5.6). The ratio (increase in efflux rate in the presence of capsazepine)/(increase in rate for control) was calculated for pH 5.0, 5.2, 5.4 and 5.6 solutions with 4–6 estimates of rate coefficient for each condition. The mean ratio over this pH range was 1.06 ± 0.24 for [^{14}C]-guanidinium ($P > 0.1$: total number of preparations: control, $n = 21$; capsazepine, $n = 22$) and 0.98 ± 0.33 for $^{86}Rb^{+}$ ($P > 0.1$, control, $n = 17$; capsazepine, $n = 18$).

Ion flux studies on rat vagus nerves

Radioactive efflux studies were also carried out on vagus nerves from adult rats to examine whether the action of the antagonist was restricted to cells maintained in culture. In

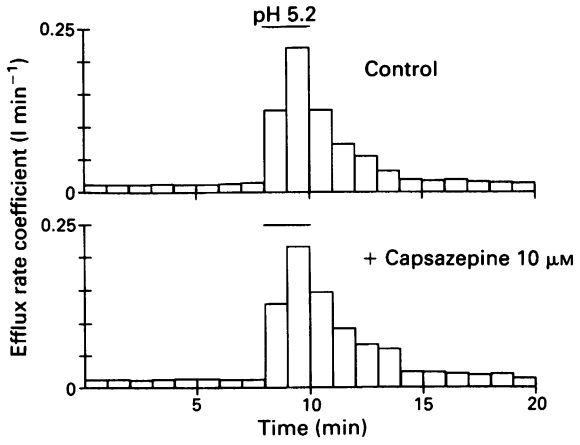

Figure 5 Lack of effect of 10 μM capsazepine on proton-evoked efflux of $^{86}Rb^+$ from neonatal rat DRG cultures. Each column represents the amount of radioactivity released during a 1 min collection period. Time of application of the acidic solutions shown by bars.

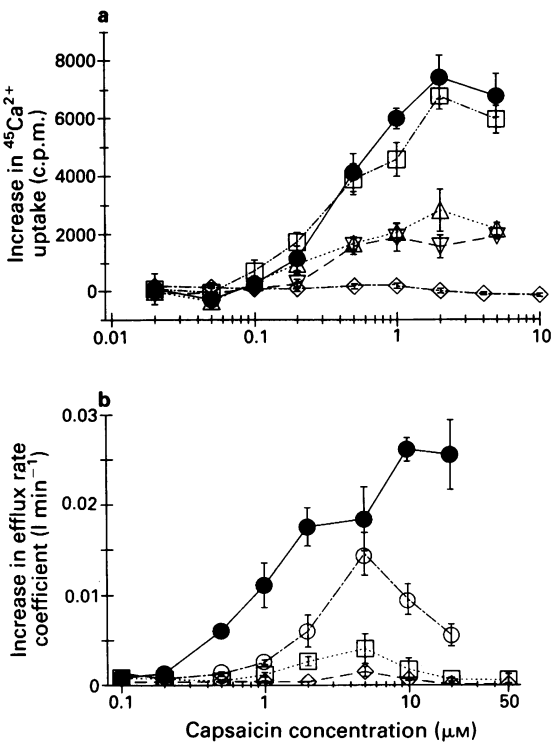

Figure 6 Effect of Ruthenium Red on capsaicin induced ion fluxes. (Log-concentration)-effect curves. (a) $^{45}Ca^{2+}$ uptake in neonatal rat DRG cultures; Ruthenium Red tested at 5 (□), 25 (Δ), 50 (▽) and 250 (◇) nM. (b) [^{14}C]-guanidinium efflux from adult rat vagus nerves in the absence and presence of 0.1 (○), 0.2 (□) and 5 μM (◇) capsazepine. Preparations pre-incubated with Ruthenium Red for at least 5 min before co-application of agonist. Data shown as mean with s.e.mean indicated by vertical bars.

these experiments [^{14}C]-guanidinium ion was used as a convenient permeant cation to study as this, like Rb^+, flows through the capsaicin-operated channel (Wood *et al.*, 1988; C.A. Forbes & S. Bevan, unpublished observations). The results were qualitatively similar to those obtained with $^{86}Rb^+$ on cultured DRG neurones. Capsazepine alone, in concentrations up to 10 μM, had no significant effect ($P>0.05$) on the resting efflux rate of guanidinium (control 0.00411 ± 0.00007 min^{-1}, $n = 31$, 10 μM capsazepine 0.00435 ± 0.00010, $n = 19$). However, capsazepine produced a dose-dependent inhibition of the capsaicin-evoked guanidinium efflux that could be surmounted by an increase in the capsaicin concentration (Figure 4d). The Schild plot constructed from the (log-concentration)-effect curves showed a slope of 0.87 ± 0.03 (s.e.) and an apparent K_d of 690 nM (Figure 4h; 95% confidence limits, 63 nM–1.45 μM).

Capsazepine was tested for any possible effects on guanidinium efflux elicited by depolarization of the nerve with 50 mM K^+. Little or no inhibition was noted over the concentration range 1–10 μM. A challenge with 50 mM KCl alone raised the efflux rate by 0.0087 ± 0.00052 min^{-1} ($n = 6$), while similar increases of 0.0082 ± 0.0054 min^{-1} ($n = 6$) and 0.0070 ± 0.0031 min^{-1} ($n = 10$) were noted in the presence of 1 and 10 μM capsazepine ($P>0.1$).

Inhibition of response to capsaicin by Ruthenium Red

Two sets of experiments were done to investigate the ways in which Ruthenium Red, a reported antagonist, inhibited the actions of capsaicin. The effects of various concentrations of Ruthenium Red on the $^{45}Ca^{2+}$ accumulation by cultured DRG neurones and the capsaicin-induced [^{14}C]-guanidinium efflux from vagus nerve are shown in Figure 6a and b. Ruthenium Red inhibited the response to capsaicin in both preparations. However, in contrast to capsazepine, Ruthenium Red flattened the (log dose)-response curves and reduced the maximal responses. No obvious rightward shift in the curves was noted; for example, in the $^{45}Ca^{2+}$ uptake experiments (Figure 6a) the estimated EC_{50} value in control conditions (0.43 ± 0.03 μM) was not significantly different ($P>0.1$) from the estimates in the presence of either 50 nM (0.29 ± 0.08 μM) or 100 nM (0.32 ± 0.07 μM) Ruthenium Red. These data suggest that the inhibition is non-competitive.

Discussion

The quantitative results of ion flux experiments have shown that capsazepine acts as a competitive antagonist not only for capsaicin but also for the more potent agonist RTX. The slopes of the Schild plots for the experiments on cultured DRG neurones were not significantly different from 1 ($P>0.05$). A similar affinity for capsazepine was estimated from $^{45}Ca^{2+}$ accumulation ($K_d = 220$ nM) and $^{86}Rb^+$ efflux ($K_d = 107$ nM) experiments on cultured DRG neurones when RTX was the agonist. The $^{45}Ca^{2+}$ accumulation assay is a measure of both the influx and the sequestration of $^{45}Ca^{2+}$ and so inhibition could occur at an intracellular site and not at the plasma membrane. In contrast, the efflux experiments are a direct measure of plasma membrane effects. The similarity in the results of both influx and efflux experiments therefore suggests that the inhibition observed in the $^{45}Ca^{2+}$ experiments represents an inhibition at the plasma membrane.

Capsazepine also showed competitive antagonism in the rat vagus nerve preparation with a slope for the Schild plot that was not significantly different from 1 ($P>0.1$). The apparent K_d values for capsazepine in assays on cultured DRG neurones and vagus nerve were not significantly different as shown by the extensive overlap in the 95% confidence limits. Thus these data indicate that capsazepine acts at a very similar, if not identical, binding site in both cultured neonatal rat cells and in acutely isolated tissue from adult animals.

The effects of RTX are very similar to those of capsaicin. Both agents act on the same population of DRG neurones with a similar mode of action (Winter *et al.*, 1990). In addition, the structural similarity between parts of the RTX and capsaicin molecules led to the suggestion that both

molecules act at the same cellular site (de Vries & Blumberg, 1989). However, RTX also shows considerable structural similarity to phorbol esters and has been reported to activate a protein kinase (Ryves *et al.*, 1989). It has therefore been possible to argue that RTX acts, at least in part, at a different site from capsaicin. The findings that capsazepine was a competitive antagonist of RTX and that essentially identical K_d estimates for capsazepine were obtained with either RTX or capsaicin as the agonist (capsaicin 148 nM; RTX 107 nM, $^{86}Rb^+$ efflux assay, overlapping 95% confidence limits), argue that for Rb^+ efflux both agonists operate by binding to the same site. As capsaicin is known to activate ion channels in isolated patches of plasma membrane (Forbes & Bevan, 1988), the binding site for these agents must be in, or intimately associated with, the membrane.

The inhibition by capsazepine was specific to the capsaicin response. The responses to GABA, ATP and protons were not inhibited by high concentrations of capsazepine (10 μM). Similarly, capsazepine did not reduce the ion flux evoked by K^+ induced depolarization of either vagus nerve (guanidinium ions) or cultured DRG neurones ($^{86}Rb^+$). In these latter experiments only ion flux through slowly inactivating or non-inactivating voltage-sensitive channels would have been measured with the protocols used. Guanidinium ions are permeant through Ca^{2+} channels (McCleskey & Almers, 1985) but not through delayed rectifier K^+ channels, whereas Rb^+ is highly permeant through K^+ channels (see Hille, 1984). The failure to inhibit [^{14}C]-guanidinium and $^{86}Rb^+$ fluxes suggests that capsazepine has little or no effect on these channel types. Of course, the use of these ions is not a definitive test for the activity of voltage-gated Ca^{2+} or delayed rectifier K^+ channels, nevertheless, the lack of inhibition of the depolarization-induced ion flux shows that capsazepine does not act on a significant population of voltage-gated ion channels.

Ruthenium Red has been used previously as a capsaicin antagonist although it is unclear how it acts (see Amman & Maggi, 1991; Maggi, 1991 for reviews). It does not block the binding of RTX to DRG membranes (Szallasi & Blumberg, 1990) although it does inhibit the activity of capsaicin operated ion channels (Dray *et al.*, 1990b). Observations on single capsaicin-activated channels suggest that, unlike lanthanum, Ruthenium Red does not act as a simple open channel blocker (Dray *et al.*, 1990b). Our experiments indicate that Ruthenium Red is not a competitive antagonist of capsaicin. It depressed the maximum $^{45}Ca^{2+}$ accumulation evoked by capsaicin in cultures of DRG neurones, without any marked parallel shift in the (log-concentration)-response curves. This calcium accumulation involves not only calcium entry but also sequestration by intracellular compartments (see Wood *et al.*, 1988) and so the failure to observe any obvious competitive inhibition by Ruthenium Red could reflect actions at steps subsequent to ion entry. However, similar results were noted in efflux experiments made on vagus nerve preparations, which give a more direct measure of plasma membrane permeability. Together these experiments suggest that Ruthenium Red acts as a non-competitive capsaicin antagonist.

Other experiments have shown that the use of Ruthenium Red as a capsaicin antagonist has to be restricted to a narrow range of concentrations (0.1–10 μM, see Maggi, 1991). Even at these concentrations, it is not specific for capsaicin and can prevent primary afferent nerve activation induced by noxious heat (Amman *et al.*, 1990), toluene diisocyanate (Mapp *et al.*, 1991a), protons (Geppetti *et al.*, 1991) and prostacyclin (PGI_2) (Mapp *et al.*, 1991b). Similar concentrations of Ruthenium Red also affect some types of ion channels and receptors in a wide range of cell types (Weiss, 1977; Adams *et al.*, 1985; Tapia *et al.*, 1985; Ong *et al.*, 1987; Robertson & Wann, 1987; Davidson *et al.*, 1988; Grasso & Reichert, 1989; Williams *et al.*, 1990). Furthermore Ruthenium Red is known to inhibit intracellular Ca^{2+} transport processes and thereby raise the level of intracellular free Ca^{2+} in intact preparations (Rossi *et al.*, 1973; Raess & Vincenzi, 1980; Bernath & Vizi, 1987). Therefore, although it may be a useful tool, the lack of specificity of Ruthenium Red limits its use in the study of the action of capsaicin.

Our data indicate that capsazepine is a specific antagonist of the sensory neurone actions of capsaicin and RTX. In this respect it differs from Ruthenium Red, which has a non-competitive mode of action and can also interfere with the activity of other receptors and ion channels. At present it is unclear whether capsaicin and RTX simply mimic the actions of endogenous, structurally similar molecules or whether they activate an ion channel that is not normally operated in such a way. Capsazepine will be of use in addressing such a problem. In addition capsazepine provides us with a tool to dissect the specific, sensory neurone actions of capsaicin from the non-specific actions (see introduction) and so will allow us to investigate, more precisely, the physiological roles of capsaicin sensitive neurones. Already capsazepine has been shown to antagonize the actions of capsaicin *in vivo* (Dray *et al.*, 1991) and has been used to provide evidence that capsaicin exerts an anti-nociceptive effect by acting on specific receptors localized to sensory nerve fibres within the spinal cord (Dickenson & Dray, 1991).

References

ADAMS, D.J., TAKEDA, K. & UMBACH, J.A. (1985). Inhibitors of calcium buffering depress evoked transmitter release at the squid giant synapse. *J. Physiol.*, **369**, 145–159.

AMMAN, R. & LEMBECK, F. (1989). Ruthenium Red selectivity prevents capsaicin induced nociceptor stimulation. *Eur. J. Pharmacol.*, **161**, 227–229.

AMMAN, R. & MAGGI, C.A. (1991). Ruthenium red as a capsaicin antagonist. *Life Sci.*, **49**, 849–856.

AMMAN, R., DONNERER, J. & LEMBECK, F. (1990). Activation of primary afferent neurons by thermal stimulation. Influence of ruthenium red. *Naunyn Schmiedebergs Arch. Pharmacol.*, **341**, 108–113.

BERNATH, S. & VIZI, E.S. (1987). Inhibitory effect of ionized free intracellular calcium enhanced by ruthenium red and m-chlorocarbonylcyanide phenylhydrazone on the evoked release of acetylcholine. *Biochem. Pharmacol.*, **36**, 3683–3687.

BEVAN, S., HOTHI, S., HUGHES, G., JAMES, I.F., RANG, H.P., SHAH, K., WALPOLE, C.S.J. & YEATS, J.C. (1991). The development of a competitive antagonist for the sensory neurone excitant, capsaicin. *Br. J. Pharmacol.*, **102**, 77P.

BEVAN, S. & SZOLCSANYI, J. (1990). Sensory neuron-specific actions of capsaicin: mechanisms and applications. *Trends Pharmacol Sci.*, **11**, 330–333.

BEVAN, S. & YEATS, J. (1991). Protons activate a cation conductance in a sub-population of rat dorsal root ganglion neurones. *J. Physiol.*, **433**, 145–161.

CHAHL, L. (1989). The effects of ruthenium red on the response of guinea-pig ileum to capsaicin. *Eur. J. Pharmacol.*, **169**, 241–247.

COLQUHOUN, D. (1971). *Lectures on Biostatistics*. Oxford: Clarendon Press.

DAVIDSON, J.S., WAKEFIELD, I.K., KING, J.A., MULLIGAN, G.P. & MILLAR, R.P. (1988). Dual pathways of calcium entry in spike and plateau phases of luteinizing hormone release from chicken pituitary cells: sequential activation of receptor-operated and voltage-sensitive calcium channels by gonadotropin-releasing hormone. *Mol. Endocrinol.*, **2**, 382–390.

DE VRIES, D.J. & BLUMBERG, P.M. (1989). Thermoregulatory effects of resiniferatoxin in the mouse: comparison with capsaicin. *Life Sci.*, **44**, 711–715.

DICKENSON, A.H. & DRAY, A. (1991). Selective antagonism of capsaicin by capsazepine: evidence for a spinal receptor site in capsaicin-induced antinociception. *Br. J. Pharmacol.*, **104**, 1045–1049.

DOCHERTY, R.J., ROBERTSON, B. & BEVAN, S. (1991). Capsaicin causes prolonged inhibition of voltage-activated calcium currents in adult rat dorsal root ganglion neurones in culture. *Neuroscience*, **40**, 513–521.

DONNERER, J. & LEMBECK, F. (1982). Analysis of the effect of intravenously injected capsaicin in the rat. *Naunyn Schmiedebergs Arch. Pharmacol.*, **320**, 54–57.

DRAY, A., BETTANY, J. & FORSTER, P. (1990a). Resiniferatoxin: a potent capsaicin-like stimulator of peripheral nociceptors in the neonatal rat tail *in vitro*. *Br. J. Pharmacol.*, **99**, 323–326.

DRAY, A., CAMPBELL, E.A., HUGHES, G.A., PATEL, I.A., PERKINS, M.N., RANG, H.P., RUEFF, A., SENO, N., URBAN, L. & WALPOLE, C.S.J. (1991). Antagonism of capsaicin-induced activation of C-fibres by a selective capsaicin antagonist, capsazepine. *Br. J. Pharmacol.*, **99**, 78P.

DRAY, A., FORBES, C.A. & BURGESS, G.M. (1990b). Ruthenium Red blocks the capsaicin-induced increase in intracellular calcium and activation of membrane currents in sensory neurons as well as the activation of peripheral nociceptors *in vitro*. *Neurosci. Lett.*, **110**, 52–59.

DUBOIS, J.M. (1982). Capsaicin blocks one class of K-channels in the frog node of Ranvier. *Brain Res.*, **245**, 372–375.

ERDELYI, L. & SUCH, G. (1984). The effects of capsaicin on the early outward current in identified snail neurones. *Neurosci. Lett.*, **48**, 349–353.

FENWICK, E.M., MARTY, A. & NEHER, E. (1982). Sodium and calcium channels in bovine chromaffin cells. *J. Physiol.*, **331**, 599–635.

FLYNN, D.L., RAFFERTY, M.F. & BOCTOR, A.M. (1986). Inhibition of human neurotrophil 5-lipoxygenase activity by gingerdione, shogaol, capsaicin and related pungent compounds. *Prostaglandins Leuk. Med.*, **24**, 195–198.

FRANCO-CERECEDA, A., LOU, Y.-P. & LUNDBERG, J.M. (1989). Ruthenium red differentiates between capsaicin and nicotine effects on cardiac sensory nerves. *Acta Physiol. Scand.*, **137**, 457–458.

FORBES, C.A. & BEVAN, S. (1988). Single channels activated by capsaicin in patches of membranes from adult rat sensory neurones in culture. *Neurosci. Lett. Suppl.*, **32**, S3.

GEPPETTI, P., DEL BIANCO, E., PATACCHINI, R., SANTICIOLI, P., MAGGI C.A. & TRAMONTANA, M. (1990). Low pH-induced release of calcitonin gene-related peptide from capsaicin-sensitive sensory nerves: mechanisms of action and biological response. *Neuroscience*, **41**, 295–301.

GRASSO, P. & REICHERT, L.E. (1989). FSH receptor-mediated uptake of calcium-45 by proteoliposomes and cultured rat sertoli cells: evidence for involvement of voltage activated and voltage-independent calcium channels. *Endocrinology*, **125**, 3029–3036.

HILLE, B. (1984). *Ionic Channels in Excitable Membranes*. Sunderland, Mass. USA: Sinauer Associates.

HOLZER, P. (1988). Local effector functions of capsaicin-sensitive sensory nerve endings: involvement of tachykinins, calcitonin gene-related peptide and other neuropeptides. *Neuroscience*, **24**, 739–768.

HOLZER, P. (1991). Capsaicin: cellular targets, mechanisms of action, and selectivity for thin sensory neurons. *Pharmacol. Rev.*, **43**, 143–201.

JUAN, H., LEMBECK, F., SEEWAN, S. & HACK, U. (1980). Nociceptor stimulation and PGE_2 release by capsaicin. *Naunyn Schmiedebergs Arch. Pharmacol.*, **312**, 139–143.

MAGGI, C.A. (1991). Capsaicin and primary afferent neurons: from basic science to human therapy. *J. Autonom. Nerv. Syst.*, **33**, 1–14.

MAGGI, C.A. & MELI, A. (1988). The sensory-efferent function of capsaicin-sensitive neurons. *Gen. Pharmacol.*, **19**, 1–43.

MAGGI, C.A., PATACCHINI, R., SANTICIOLI, P., GUILIANI, S., GEPPETTI, P. & MELI, A. (1988a). Protective action of ruthenium red toward capsaicin desensitization of sensory fibres. *Neurosci. Lett*, **88**, 201–205.

MAGGI, C.A., SANTICIOLI, P., GEPPETTI, P., PARLANI, M., ASTOLFI, M., PRADELLES, P., PATACCHINI, R. & MELI, A. (1988b). The antagonism induced by ruthenium red of the actions of capsaicin on the peripheral terminals of sensory neurone: further studies. *Eur. J. Pharmacol.*, **154**, 1–10.

MAGGI, C.A., GUILIANI, S. & MELI, A. (1989). Effect of ruthenium red on responses mediated by activation of capsaicin-sensitive nerves of the rat urinary bladder. *Naunyn Schmiedebergs Arch. Pharmacol.*, **340**, 541–546.

MAPP, C.E., BONIOTTI, A., GRAF, P.D., CHITANO, P., FABRRI, L.M. & NADEL, J.A. (1991a). Bronchial smooth muscle responses evoked by toluene diisocyanate are inhibited by ruthenium red and by indomethacin. *Eur. J. Pharmacol.*, **200**, 73–76.

MAPP, C.E., FABBRI, L.M., BONIOTTI, A. & MAGGI, C.A. (1991b). Prostacyclin activates tachykinin release from capsaicin sensitive afferents in guinea-pig bronchi through a ruthenium red-sensitive pathway. *Br. J. Pharmacol.*, **104**, 49–52.

MCBURNEY, R.N. & NEERING, I.R. (1985). The measurement of changes in intracellular free calcium during action potentials in mammalian neurones. *J. Neurosci. Methods*, **13**, 65–76.

MCCLESKEY, E.W. & ALMERS, W. (1985). The calcium channel in skeletal muscle is a large pore. *Proc. Natl. Acad. Sci. U.S.A.*, **82**, 7149–7153.

ONG, J., KERR, D.I. & JOHNSTON, G.A. (1987). Calcium dependence of baclofen- and GABA-induced depression of responses to transmural stimulation in the guinea-pig isolated ileum. *Eur. J. Pharmacol.*, **24**, 369–372.

PETERSEN, M., PIERAU, F.-K. & WEYRICH, M. (1987). The influence of capsaicin on membrane currents in dorsal root ganglion neurones of guinea-pig and chicken. *Pflüger Arch.*, **409**, 403–410.

PETERSEN, M., WAGNER, G. & PIERAU, F.-K. (1989). Modulation of calcium-currents by capsaicin in a subpopulation of sensory neurones of guinea pig. *Naunyn Schmiedebergs Arch. Pharmacol.*, **339**, 184–191.

RAESS, B.U. & VINCENZI, F.F. (1980). Calmodulin activation of red blood cells Ca^{2+} and Mg^{2+}-ATPase and its antagonism by phenothiazines. *Mol. Pharmacol.*, **18**, 253–258.

ROBERTSON, B. & WANN, K.T. (1987). On the action of ruthenium red and neuraminidase at the frog neuromuscular junction. *J. Physiol.*, **382**, 411–423.

ROSSI, C.S., VASINGTON, F.D. & CARAFOLI, E. (1973). The effect of ruthenium red on the uptake and release of Ca^{2+} by mitochondria. *Biochem. Biophys. Res. Commun.*, **50**, 846–852.

RYVES, W.J., GARLAND, L.G., EVANS, A.T. & EVANS, F.J. (1989). A phorbol ester and a daphnane ester stimulate a calcium-independent kinase activity from human mononuclear cells. *FEBS Lett.*, **245**, 159–163.

SZALLASI, A. & BLUMBERG, P.M. (1989). Resiniferatoxin: a phorbol-related diterpene, acts as an ultrapotent analog of capsaicin, the irritant constituent in red peppers. *Neurosci.*, **30**, 515–520.

SZALLASI, A. & BLUMBERG, P.M. (1990a). Resiniferatoxin and its analogue provide novel insights into the pharmacology of the vanilloid (capsaicin) receptors. *Life Sci.*, **47**, 1399–1408.

SZALLASI, A. & BLUMBERG, P.M. (1990b). Specific binding of resiniferatoxin, an ultrapotent capsaicin analog, by dorsal root ganglion membranes. *Brain Res.*, **524**, 106–111.

SZOLCSANYI, J. (1984). Capsaicin-sensitive chemosensitive neural system with dual sensory-efferent function. In *Antidromic Vasodilatation and Neurogenic Inflammation*. ed. Chahl, L.A., Szolcsanyi, J. & Lembeck, F. pp. 27–52. Budapest: Akademai Kiado.

SZOLCSANYI, J. (1990). Capsaicin, irritation, and desensitization: neurophysiological basis and future perspectives. In *Chemical Senses*, Vol. 2. Ed. Green, B.G., Mason, J.R. & Kare, M.R. pp. 141–168. New York: Marcel Dekker Inc.

SZOLCSANYI, J. & BARTHO, L. (1978). New type of nerve-mediated cholinergic contractions of the guinea-pig small intestine and its selective blockade by capsaicin. *Naunyn Schmiedebergs Arch. Pharmacol.*, **305**, 83–90.

TAPAI, R., ARIAS, C. & MORALES, E. (1985). Binding of lanthanum ions and ruthenium red to synaptosomes and its effects on neurotransmitter release. *J. Neurochem.*, **45**, 1464–1470.

WANG, J.-P., HSU, M.-F., HSU, T.-P. & TENG, C.-M. (1985). Antihemostatic and antithrombotic effects of capsaicin in comparison with aspirin and indomethacin. *Thromb. Res.*, **37**, 669–679.

WANG, J.-P., HSU, M.-F. & TENG, C.-M. (1984). Antiplatelet effect of capsaicin. *Thromb. Res.*, **36**, 497–507.

WEISS, G.B. (1977). Calcium and contractility in vascular smooth muscle. In *Advances in General and Cellular Pharmacology*, ed. Narahashi, T. & Bianci, C.P. pp. 71–154. New York: Plenum.

WILLIAMS, P.F., CATERSON, I.D., COONEY, G.J., ZILKENS, R.R. & TURTLE, J.R. (1990). High affinity insulin binding and insulin receptor-effector coupling: modulation by Ca^{2+}. *Cell Calcium*, **11**, 547–556.

WINTER, J., DRAY, A., WOOD, J.N., YEATS, J.C. & BEVAN, S. (1990). Cellular mechanism of action of resiniferatoxin: a potent sensory neuron excitant. *Brain Res.*, **520**, 131–140.

WOOD, J.N., WINTER, J., JAMES, I.F., RANG, H.P., YEATS, J. & BEVAN, S. (1988). Capsaicin-induced ion fluxes in dorsal root ganglion cells in culture. *J. Neurosci.*, **8**, 3208–3220.

YAMANAKA, K., KIGOSHI, S. & MURAMATSU, I. (1984). Conduction-block induced by capsaicin in crayfish giant axon. *Brain Res.*, **300**, 113–119.

YEATS, J.C., DOCHERTY, R.J. & BEVAN, S. (1991). Calcium dependent and independent desensitization of capsaicin-evoked responses in voltage clamped adult rat dorsal root ganglion (DRG) neurones in culture. *J. Physiol.*, **446,** 390P.

ZERNIG, G., HOLZER, P. & LEMBECK, F. (1984). A study of the mode and site of action of capsaicin in guinea-pig heart and uterus. *Naunyn Schmiedebergs Arch. Pharmacol.*, **326,** 58–63.

(Received February 14, 1992
Revised June 1, 1992
Accepted June 16, 1992)

Br. J. Pharmacol. (1992), **107**, 553–558

Possible mechanisms of inhibition with atropine against noradrenaline-induced contraction in the rabbit aorta

Nobuhiro Satake, Sumio Kiyoto, [1] Shoji Shibata, *Vijayalakshmi Gandhi, *David J. Jones & Masako Morikawa

Department of Pharmacology, University of Hawaii, School of Medicine, Honolulu, Hawaii 96822 and *The University of Texas Health Science Center, Departments of Anesthesiology and Pharmacology, San Antonio, Texas 78284, U.S.A.

1 In the rabbit isolated aorta, atropine (3×10^{-6}M–10^{-4}M) inhibited contractile response to noradrenaline without affecting contraction to KCl.

2 In the presence of contraction to noradrenaline, atropine (3×10^{-7}M–10^{-4}M) caused concentration-dependent relaxation. Pretreatment with theophylline (10^{-3}M) potentiated the relaxant action of atropine. Relaxation to atropine was not affected by the specific guanosine 3':5'-cyclic monophosphate phosphodiesterase inhibitor, M & B 22,948 (10^{-4}M), tetraethylammonium (10 mM), indomethacin (10^{-5}M), propranolol (10^{-7}M), nifedipine (10^{-6}M) or removal of the endothelium.

3 Relaxation to either atropine or prazosin was not affected by preincubation with prazosin and atropine, respectively.

4 In Ca^{2+}-free medium containing EGTA and nifedipine, atropine (10^{-7}M–10^{-4}M) inhibited the residual noradrenaline response more than the subsequent Ca^{2+}-induced contraction. Pretreatment with either theophylline (10^{-3}M), forskolin (3×10^{-7}M) or a low concentration of prazosin (3×10^{-9}M) also inhibited the residual contraction to noradrenaline and Ca^{2+}. The effect of combined treatment of atropine and any of these agents was much greater than with each individual agent.

5 Atropine (10^{-6}M–10^{-4}M) also inhibited increases in the level of inositol monophosphates (IP) in response to noradrenaline. Theophylline (10^{-3}M) and a low concentration of prazosin (3×10^{-9}M) also inhibited IP formation. Combined with atropine, the effect was much greater than with each of these agents individually.

6 Atropine did not affect adenosine 3':5'-cyclic monophosphate (cyclic AMP) levels in the aorta and also failed to displace specific [^{3}H]-prazosin binding.

7 These results suggest the possibility that smooth muscle relaxation to atropine may be due to the inhibition of phosphoinositide metabolism. The relaxation is not apparently due to an action of atropine on α_1-adrenoceptors, or a change in the level of cyclic AMP.

Keywords: Atropine; anti-cholinoceptor agents; adrenoceptors; vascular smooth muscle; noradrenaline; endothelium; inositol phosphate (IP)

Introduction

It is well known that atropine ((±)-hysocyamine) is a competitive antagonist at acetylcholine-muscarinic receptor sites in smooth muscles and other tissues (see Katzung, 1987). A high concentration of atropine was reported to antagonize contraction of smooth muscle strips by noradrenaline in cattle (Denac *et al.*, 1991). It was also reported to inhibit the increased motility caused by cholecystokinin octapeptide in the jejunum and colon of dogs (Fargeas *et al.*, 1989) and abolish adenosine-induced increases in histamine contraction in canine bronchial smooth muscles (Sakai *et al.*, 1989). Recently we also found that atropine, but not scopolamine ((−)-hyoscine) and other muscarinic receptor antagonists, caused relaxation of noradrenaline-induced contractions in vascular smooth muscles of rabbit. Based on these observations, the present study was conducted to define the mechanism of the inhibitory effect of atropine on the response to noradrenaline in vascular tissue.

Methods

Rabbit aorta: isolation, preparation, and protocol

Male New Zealand white rabbits weighing 2.5–3.0 kg were killed by an air injection through an ear vein during ether anaesthesia. The thoracic aorta was isolated, excess fat and connective tissue removed, and then cut into cylindrical segments which were subsequently cut open. Preparations (approximately 3–4 mm in width and 10–13 mm in length) were mounted vertically in organ baths containing 20 ml of Krebs solution of the following composition (mM): NaCl 120.3, KCl 4.8, $CaCl_2$ 1.2, $MgSO_4$ $7H_2O$ 1.3, KH_2PO_4 1.2, $NaHCO_3$ 24.2 and glucose 5.8 at pH 7.4. The tissue bath solution was maintained at 37°C and bubbled with a 95% O_2 and 5% CO_2 gas mixture. Ca^{2+}-free solution was prepared by omitting $CaCl_2$ from the previously described solution and by including EGTA (0.01 mM) and nifedipine (10^{-6} M). Ligatures were placed around both ends of the muscle strips, one attaching the muscle to a glass holder and the other to a transducer. The preparation was adjusted to give an initial resting tension of 2 g. Changes in isometric tension were recorded through a force displacement transducer (FT-03) connected to a six-channel Grass polygraph. The contractile responses were measured as increases above rest tension. Concentration-response curves were performed in a cumulative manner. When antagonists were used, tissues were pretreated with an antagonist 10 min before the addition of an agonist. The endothelium was removed from some preparations by rubbing the intimal surface of the aorta with wet filter paper. In these preparations, acetylcholine (3×10^{-7} M) failed to relax the contraction induced by noradrenaline (3×10^{-7} M). The response in the absence of inhibitor was taken as 100%.

[1] Author for correspondence (University of Hawaii)

Measurement of inositol monophosphate

The accumulation of [^{3}H]-inositol monophosphate (IP) was determined by a slight modification of the procedure of Brown & Brown (1983) and Rapoport (1986). Briefly, rings of rabbit aorta were incubated at 37°C for 3 h in Krebs solution containing [^{3}H]-inositol (4 μCi 0.5 ml^{-1} per ring). The tissues were transferred to Krebs solution containing 10 mM LiCl and placed on ice for 30 min. Noradrenaline (10^{-5} M) and other drugs were added to the solution and the mixture was incubated at 37°C for an additional 60 min. Each tissue was then homogenized in 1.0 ml of 10% trichloroacetic acid. The homogenates were centrifuged at 300 g for 15 min and the supernatants were extracted 3 times with 2.0 ml of ether; 4 ml of 5 mM $NaHCO_3$ was added to 1 ml of the aqueous phase and the mixture was transferred to a column containing anion exchange resin (Bio-Rad AGI-X8, 100–200 mesh, formate form). The column was washed with 10 ml water to remove [^{3}H]-inositol. [^{3}H]-inositol monophosphate was eluted with 6 ml 200 mM ammonium formate in 100 mM formic acid.

Scintillation cocktail (Aquasol-2, New England Nuclear) was added to the eluate and the samples were counted in a liquid scintillation counter.

[^{3}H]-prazosin binding

Aortae were thawed in ice-cold 0.32 M sucrose. Each aorta was placed on a glass plate on an ice bath, kept moist with 0.32 M sucrose and the surrounding fat carefully trimmed, avoiding any mechanical damage to the tissue. The tissue was then crosschopped with a McIlwain tissue chopper (Surrey, England) at 300 μm and homogenized in a Brinkman Polytron (Kinematica, Switzerland) at setting 7, single burst for 30 s. The homogenate was subjected to two successive centrifugations at 1,000 g and 45,000 g for 15 and 30 min, respectively. The pellet was resuspended in 0.05 M Tris buffer pH 8.0 containing 1 mM $MgCl_2$, using the polytron at setting 7 for 30 s, and centrifuged at 45,000 g for 20 min. The final pellet was resuspended in Tris buffer at a protein concentration of 1.0–1.2 mg ml^{-1}. [^{3}H]-prazosin binding was assayed in the aortic membrane preparation as established earlier in our laboratory (Simmons & Jones, 1988). Membrane protein concentration of 0.20 to 0.25 mg per assay tube was found to produce optimum results with 60 min incubation. Specific binding was determined over a ligand concentration range of 0.1 to 10 nM and was defined as the difference between [^{3}H]-prazosin bound in the absence and presence of 10^{-5} M phentolamine. Protein was assayed by the method of Lowry et al. (1951) with bovine serum albumin used as standard.

Cyclic AMP measurement

Each rabbit aortic ring was preincubated in 1 ml of Krebs-Ringer solution for 1 h at 37°C before the incubation with atropine (10^{-6} M–10^{-4} M) for 20 min; 1 ml of 12% cold trichloroacetic acid was then added and the tissue was homogenized at 4°C. The homogenate was centrifuged at 1700 g for 10 min and the supernatant was extracted 3 times with 3 ml of water-saturated ether. Adenosine 3':5'-cyclic monophosphate (cyclic AMP) in the supernatant (100 μl) was measured by radioimmunoassay (Amersham cAMP[^{125}I] assay system, RPA.509).

Statistical analysis

Data are presented as the means ± s.e.mean and statistical analysis was performed with a Student's t test or Analysis of Variance followed by Dunnett's test. Significant differences between control and test groups were evaluated with $P<0.05$ as the level of significance.

Drugs

The following chemicals were used: noradrenaline bitartrate, phentolamine, atropine sulphate salt, prazosin HCl, scopolamine, gallamine, forskolin, tetraethylammonium chloride, pirenzepine (all Sigma); propranolol HCl (Ayerst Lab); theophylline (Matheson, Coleman & Bell); indomethacin (Merk, Sharp & Dohme); nifedipine (Pfizer); M & B 22,948 (2-O-propoxyphenyl-8-azapurine-6-one; May & Baker); *myo*-[2-^{3}H (N)]-inositol (specific activity 15.6 Ci mmol^{-1}) and [^{3}H]-prazosin ([^{3}H]-PRZ; specific activity 18.1 Ci mmol^{-1}) (New England Nuclear); cyclic AMP [^{125}I] assay system (Amersham).

Results

In rabbit isolated aorta, atropine (10^{-5} M and 10^{-4} M) inhibited contractile responses to noradrenaline (10^{-9} M–3×10^{-6} M) (Figure 1a). Specifically, atropine at 10^{-5} M and 10^{-4} M shifted the concentration-response curve for noradrenaline to the right without significantly altering the maximal contraction (Figure 1a). However, atropine at 10^{-4} M did not cause any reduction or shift in the response to KCl (10 mM–70 mM) (Figure 1b).

Following contraction of the aorta with noradrenaline (3×10^{-7} M), atropine (10^{-6} M–10^{-4} M) caused relaxation in a concentration-dependent manner (Figure 2). Scopolamine (10^{-4} M), pirenzepine (10^{-4} M) and gallamine (10^{-4} M) had only a negligible effect on the noradrenaline (3×10^{-7} M)-contracted aorta (scopolamine: 11.3 ± 3.4% reduction, $n = 4$; pirenzepine: 3.1 ± 1.7% reduction, $n = 5$; gallamine: 4.2 ± 2.3% reduction, $n = 5$). Pretreatment of the aorta with theophylline (10^{-3} M) markedly potentiated the relaxant action of atropine, although M & B 22,948 (10^{-4} M) did not have any significant effect on the relaxation (Figure 2). Similarly, pretreatment of the aorta with tetraethylammonium (TEA; 10 mM), indomethacin (10^{-5} M), propranolol (10^{-7} M) or nifedipine (10^{-6} M) did not affect the atropine-induced relaxation (Table 1). In addition, removal of endothelium also did not have any significant effect on the responses to atropine (Table 1). Prazosin (10^{-9} M) partially inhibited the contraction to noradrenaline (3×10^{-7} M) (51.2 ± 7.8% of the control) but had no effect on relaxation to atropine (10^{-7} M–10^{-4} M) (control: IC_{50} $1.26 \pm 0.21 \times 10^{-5}$ M, maximal relaxation 85.2 ± 3.0%; in the presence of prazosin: IC_{50} $1.0 \pm 0.20 \times 10^{-5}$ M, maximal relaxation 86.0 ± 3.2%, $n = 4$). Prazosin (10^{-10} M–3×10^{-6} M) also caused

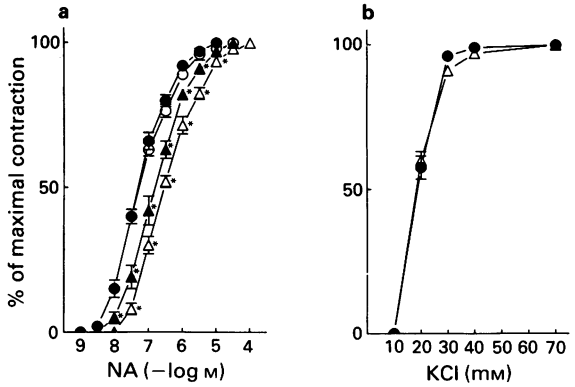

Figure 1 Inhibitory effects of atropine on contractile responses to noradrenaline (a) and KCl (b) of rabbit aorta. The maximal contractions induced by noradrenaline and KCl were 3.6 ± 0.23 g ($n = 5$) and 2.3 ± 0.10 g ($n = 3$), respectively, and were expressed as 100%. Each value is the mean (s.e.mean shown by vertical bars) of 3 to 5 experiments. Control (●); atropine at 3×10^{-6} M (○); 10^{-5} M (▲); 10^{-4} M (△).
*Significantly different from respective controls ($P<0.05$).

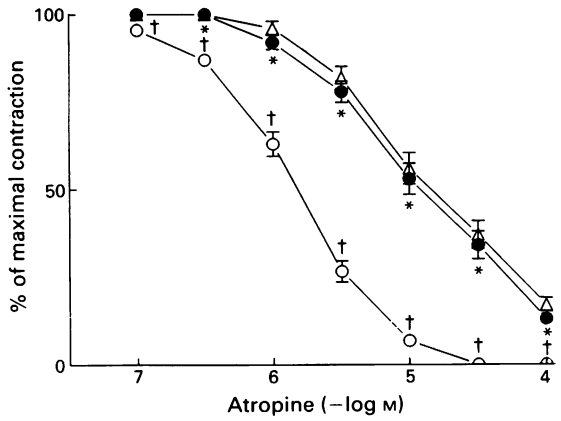

Figure 2 Vasorelaxation to atropine in rabbit aorta precontracted with noradrenaline. Tissues were precontracted with noradrenaline (3×10^{-7} M) before cumulative additions of atropine (●; 10^{-7} M–10^{-4} M). In some tissues, theophylline (○; 10^{-3} M) or M & B 22,948 (△; 10^{-4} M) was added before the noradrenaline treatment. The contraction induced by noradrenaline (3×10^{-7} M) in the absence of phosphodiesterase inhibitors prior to the addition of atropine was 2.5 ± 0.56 g ($n = 5$), 1.20 ± 0.10 g ($n = 5$) in the presence of theophylline and 1.10 ± 0.27 g ($n = 5$) in the presence of M & B 22,948. These were expressed as 100% in the figure. Each value is the mean (s.e.mean shown by vertical bars) of 5 experiments.
*Significantly different from the values before the addition of atropine ($P < 0.05$).
†Significantly different from control based on analysis of variance and Dunnett's test ($P < 0.05$).

Table 1 Effects of various treatments on vasorelaxant action of atropine (10^{-7} M–10^{-4} M) in rabbit aorta precontracted by noradrenaline (3×10^{-7} M)

	Atropine IC_{50} ($\times 10^{-5}$ M)	*Maximal relaxation* (%)
Control	1.18 ± 0.38	92.2 ± 2.3
Tetraethyl ammonium (10 mM)	1.78 ± 0.41	91.3 ± 1.8
Indomethacin (10^{-5} M)	0.98 ± 0.21	92.2 ± 1.8
Nifedipine (10^{-6} M)	0.81 ± 0.28	95.0 ± 1.4
Propranolol (10^{-7} M)	1.41 ± 0.31	96.6 ± 1.8
Endothelium-denuded	1.06 ± 0.20	87.6 ± 3.1

IC_{50} values (concentrations of atropine that inhibited 50% of the noradrenaline response) were calculated graphically. In endothelium-denuded tissues, endothelium of the aorta was removed by rubbing the tissues with wet filter paper. Each value is the mean ± s.e.mean of 5 experiments.

relaxation of the aorta precontracted by noradrenaline (3×10^{-7} M) (IC_{50} $5.96 \pm 0.32 \times 10^{-10}$ M, maximal relaxation 100%, $n = 4$). Pretreatment with atropine (10^{-5} M) partially inhibited the noradrenaline (3×10^{-7} M)-induced contraction (64.2 ± 10.9% of the control) but had no effect on relaxation to prazosin (IC_{50} $6.03 \pm 0.29 \times 10^{-10}$ M, maximal relaxation 100%, $n = 4$).

In a Ca^{2+}-free medium containing EGTA (0.01 mM) and nifedipine (10^{-6} M), noradrenaline (3×10^{-7} M) induced a phasic contraction. The subsequent addition of Ca^{2+} (1.2 mM) induced a contractile response, presumably related to the activation of non-voltage operated Ca-channels. Pretreatment with atropine (3×10^{-7} M–10^{-4} M) inhibited the residual contraction to noradrenaline in a Ca^{2+}-free medium (Figure 3a) and the subsequent contraction to Ca^{2+} (Figure 3b), both in a concentration-dependent manner. Pretreatment of the aorta with theophylline (10^{-3} M) or forskolin (3×10^{-7} M) also inhibited the residual noradrenaline response (Figure 4a) and the subsequent response to Ca^{2+} (Figure 4b). However, the inhibitory effect of a combined treatment with atropine (10^{-5} M) plus theophylline (10^{-3} M) or atropine (10^{-5} M) plus forskolin (3×10^{-7} M) was much greater than a single treatment with either atropine (10^{-5} M), theophylline (10^{-3} M) or forskolin (3×10^{-7} M) (Figure 4a,b). Similarly, pretreatment of the aorta with prazosin (3×10^{-9} M) inhibited the residual noradrenaline response (Figure 5a) and the subsequent Ca^{2+}-response (Figure 5b). The inhibitory action of a combined treatment with atropine (10^{-5} M) plus prazosin (3×10^{-9} M) was also significantly greater than that of a single treatment with either agent (Figure 5a,b).

Effect of atropine on cyclic AMP, inositol phosphates and [^{3}H]-prazosin binding

Atropine had no significant effect on cyclic AMP levels (control 128.5 ± 6.1 pmol g^{-1} net weight; atropine at 10^{-6} M, 133.2 ± 4.4; 10^{-5} M, 124.6 ± 13.0; 10^{-4} M, 125.7 ± 11.0; $n = 4$).

Noradrenaline (10^{-5} M) in the presence of LiCl (10 mM) caused an increase in the level of [^{3}H]-inositol monophosphate (IP) (Figure 6). Atropine (10^{-6} M–10^{-4} M) inhibited the increase in the [^{3}H]-IP level, in a concentration-dependent manner (Figure 6). Treatment with prazosin (3×10^{-9} M) or theophylline (10^{-3} M) also inhibited the increase in the [^{3}H]-IP level (Figure 6). In addition, the effect of a combined treatment with atropine (10^{-5} M) plus prazosin (3×10^{-9} M) was significantly greater than that of a single treatment with either agent (Figure 6). Similarly, the inhibitory effect of combined treatment with atropine (10^{-5} M) plus theophylline (10^{-3} M) was much greater than that of a single treatment with either agent (Figure 6).

A possible inhibitory effect of atropine via α-adrenoceptors was investigated with [^{3}H]-prazosin binding in rabbit aorta.

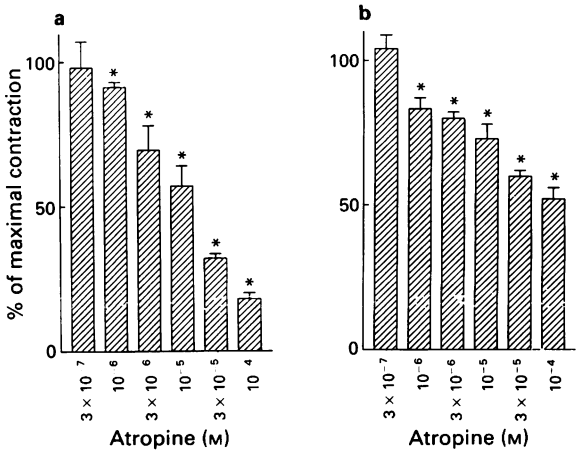

Figure 3 The effect of atropine in Ca^{2+}-free solution on the residual contraction to noradrenaline, and to Ca^{2+} in the presence of noradrenaline in rabbit aorta. Tissues were incubated in Ca^{2+}-free solution containing EGTA (0.01 mM) and nifedipine (10^{-6} M) for 15 min before (a) the addition of noradrenaline (3×10^{-7} M). (b) Ca^{2+} (1.2 mM) was added to the bath 15 min later. Atropine was added to the bath 10 min before the addition of noradrenaline. The contractions induced by (a) noradrenaline and (b) Ca^{2+} were 1.5 ± 0.21 g ($n = 6$) and 2.2 ± 0.27 g ($n = 6$), respectively, in the absence of atropine. Each value is the mean (s.e.mean shown by vertical bars) of 4 to 7 experiments.
*Significantly different from respective controls ($P < 0.05$).

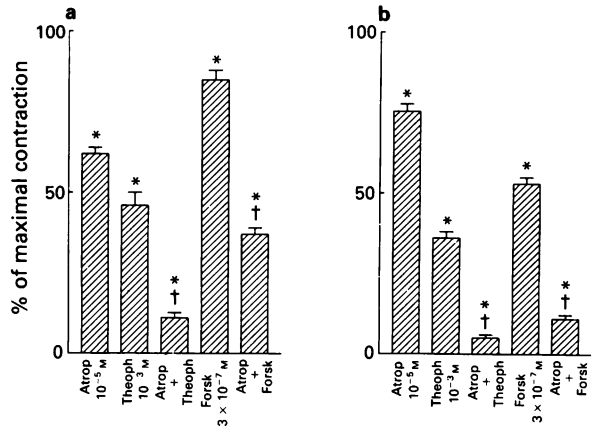

Figure 4 Effects of atropine, theophylline and forskolin on the residual contraction in response to noradrenaline and Ca^{2+} in the presence of noradrenaline in Ca^{2+}-free solution. Tissues were incubated in Ca^{2+}-free medium containing EGTA (0.01 mM) and nifedipine (10^{-6} M) for 15 min before (a) the addition of noradrenaline (3×10^{-7} M). (b) Ca^{2+} (1.2 mM) was then added to the bath 15 min later. Atropine (Atrop; 10^{-5} M), theophylline (Theoph; 10^{-3} M), forskolin (Forsk; 3×10^{-7} M), atropine (10^{-5} M) plus theophylline (10^{-3} M) (Atrop + Theoph), or atropine (10^{-5} M) plus forskolin (3×10^{-7} M) (Atrop + Forsk) was added to the bath 10 min before the addition of noradrenaline. The contractions induced by (a) noradrenaline and (b) Ca^{2+} were 1.5 ± 0.10 g ($n = 5$) and 2.3 ± 0.23 g ($n = 5$), respectively. Each value is the mean ± s.e.mean of 4 to 5 experiments.
*Significantly different from respective controls in the absence of inhibitors ($P < 0.05$).
†Significantly different from respective single treatments based on analysis of variance and Dunnett's test ($P < 0.05$).

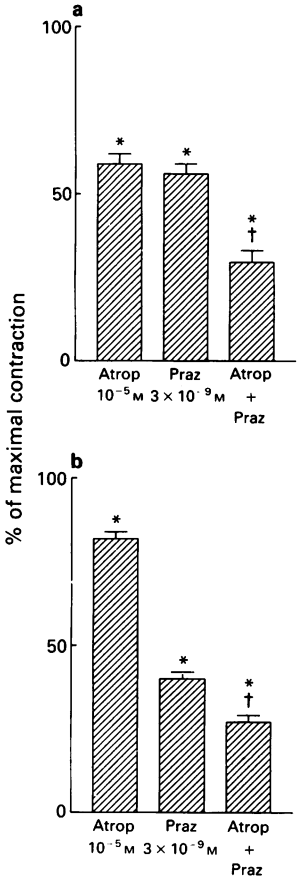

Figure 5 Effects of atropine and prazosin on the residual response to noradrenaline and on the Ca^{2+} response in the presence of noradrenaline in rabbit aorta. Tissues were incubated in Ca^{2+}-free medium containing EGTA (0.01 mM) and nifedipine (10^{-6} M) for 15 min before (a) the addition of noradrenaline (3×10^{-7} M). (b) Ca^{2+} (1.2 mM) was then added to the bath 15 min later. Atropine (Atrop; 10^{-5} M), prazosin (Praz; 3×10^{-9} M), or atropine (10^{-5} M) plus prazosin (3×10^{-9} M) (Atrop + Praz) was added to the bath 10 min before the addition of noradrenaline. The contractions induced by (a) noradrenaline and (b) Ca^{2+} were 1.8 ± 0.21 g ($n = 6$) and 2.10 ± 0.17 g ($n = 6$), respectively. Each value is the mean (s.e.mean shown by vertical bars) of 4 to 6 experiments.
*Significantly different from respective controls in the absence of any inhibitor ($P < 0.05$).
†Significantly different from respective single treatments based on analysis of variance and Dunnett's test ($P < 0.05$).

In order to evaluate this interaction the characteristics of binding of [^{3}H]-prazosin to α-receptor sites in rabbit aorta was established over a concentration-range of 0.1–10 nM [^{3}H]-prazosin. Rosenthal analysis (Rosenthal, 1967) of the saturation isotherm of binding revealed a monophasic plot with a B_{max} of 28 fmol mg^{-1} protein and a K_D of 0.44 nM (data not shown). Atropine (10^{-8} M–10^{-4} M) did not displace specific [^{3}H]-prazosin binding from the α-receptor site. Expressed as % of control [^{3}H]-prazosin binding (0.5 nM), binding varied from 99–109% in the presence of atropine.

Discussion

In the rabbit aorta, atropine inhibited contractile responses to noradrenaline, in a non-competitive manner, but had no effect on the response to KCl. Muscarinic receptors do not appear to be involved because the concentrations of atropine required were substantially higher than those effective at muscarinic receptors, and because other muscarinic antagonists did not produce similar inhibition. In addition, the results indicate that the relaxant action of atropine is not related to K^+ channels sensitive to TEA, voltage-operated Ca^{2+} channels, prostaglandins or the activation of β-adrenoceptors, since the effect of atropine was not affected by TEA, indomethacin (cyclo-oxygenase inhibitor), nifedipine (inhibitor for voltage-operated Ca^{2+} channels) or propranolol (β-adrenoceptor antagonist). The results also indicate that removal of the endothelium does not affect the relaxation to atropine, suggesting that the production of endothelium-derived relaxing factors is not involved in these responses. The present study also indicates that the relaxation to atropine is not related to interaction with α_1-adrenoceptors, because the relaxant action of either atropine or prazosin (low concentrations), an α_1-adrenoceptor antagonist, was not affected by pretreatment with prazosin or atropine, respectively. In addition, potentiation by theophylline, an inhibitor of cyclic AMP-phosphodiesterase, but not with M & B 22,948, an inhibitor of cyclic GMP-phosphodiesterase (Kukovetz *et al.*, 1979) suggests an involvement of cyclic AMP rather than cyclic GMP in the relaxation to atropine.

Agents which interfered with the intracellular mobilization of Ca^{2+} inhibited the residual noradrenaline-induced contraction in a Ca^{2+}-free solution in a number of investigations (Weishaar *et al.*, 1983; Hester, 1985; Shibata *et al.*, 1987;1988). The results in the present study indicated that atropine inhibited the residual noradrenaline response in Ca^{2+}-free solution containing EGTA and nifedipine. Atropine also inhibited the Ca^{2+} response in the presence of noradrenaline in Ca^{2+}-free solution. The inhibitory effect of atropine on the residual noradrenaline response was much greater than that on the response to Ca^{2+} in the presence of noradrenaline. This may be due to the differing background levels of tension. This agonist-induced contraction is nifedipine-insensitive, so is probably due to the activation of voltage-dependent Ca^{2+}-channels (Karaki *et al.*,1984; Hester, 1985; Shibata *et al.*, 1987; 1989). The present results suggest the possibility that atropine may interfere with intracellular

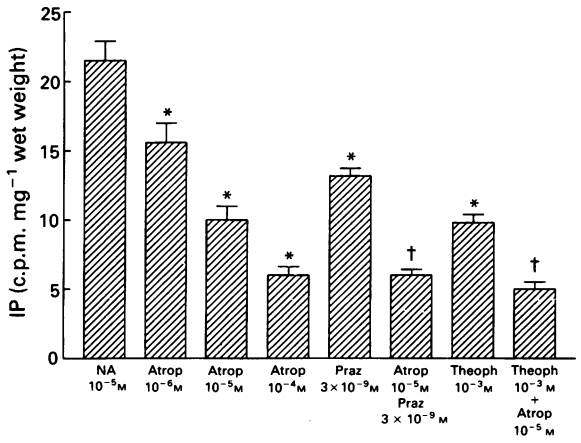

Figure 6 Effects of atropine, prazosin and theophylline on the level of inositol monophosphate (IP) in rabbit aorta. The tissue level of IP in the presence of noradrenaline (10^{-5} M) was measured in the presence of LiCl (10 mM) as described in the Methods section. In some experiments, tissues were incubated with atropine (Atrop; 10^{-6} M, 10^{-5} M and 10^{-4} M), prazosin (Praz; 3×10^{-9} M), theophylline (Theoph; 10^{-3} M), atropine (10^{-5} M) plus prazosin (3×10^{-9} M) (Atrop + Praz), or atropine (10^{-5} M) plus theophylline (10^{-3} M) (Atrop + Theoph) in addition to noradrenaline (10^{-5} M). The value for control (LiCl) in the absence of the drug was 2.92 ± 0.89 c.p.m. mg^{-1} net weight ($n = 15$). Each value is the mean (s.e.mean shown by vertical bars) of 4 to 7 experiments.
*Significantly different from the noradrenaline-control in the absence of inhibitors ($P < 0.05$).
†Significantly different from respective single treatments based on analysis of variance and Dunnett's test ($P < 0.05$).

Ca^{2+} mobilization and also Ca^{2+}-influx through receptor-operated Ca^{2+} channels.

The results also indicated that pretreatment with either theophylline or forskolin, an activator of adenylyl cyclase (Seamon *et al.*, 1981), inhibited both the residual noradrenaline response and the subsequent Ca^{2+} response. The inhibitory effects of combined treatments with atropine plus theophylline and atropine plus forskolin, however, were significantly greater than that of a single treatment with any one of these agents. If atropine was increasing cyclic AMP by inhibiting the activity of cyclic AMP-phosphodiesterase, atropine would not be expected to cause further inhibition of the responses in the presence of theophylline, since the high concentration of theophylline should have completely inhibited the enzyme activity. If atropine increases cyclic AMP by activating adenylyl cyclase at the site which forskolin activates, the effect of atropine in the presence of forskolin should not be different from the effect of single treatment. However, the results suggest that atropine may either activate the enzyme at a different site from forskolin or that the effect of atropine may not be related to activation of adenylyl cyclase. In fact, in the present study, atropine failed to affect the level of cyclic AMP. These results indicate that the mode of inhibitory action of atropine is not directly related to the absolute level of cyclic AMP. It has been proposed that phosphorylation of phospholipase C-γ by cyclic AMP-dependent protein kinase may alter its interaction with GTP-binding protein and leads to its inhibition (Kim *et al.*, 1989). Alternatively, the GTP-binding protein may be the target of cyclic AMP-dependent protein kinase (Abdel-Latif, 1991). Since atropine is lipophilic, it is conceivable that atropine may also enter the vascular smooth muscle cells and inhibit the activity of phospholipase C or G-protein itself. However, the exact mechanism for the interaction between the effect of atropine and the cyclic AMP level cannot be ascertained at this time. The results further indicated that the inhibitory effect of a combined treatment with atropine and a low concentration of prazosin was significantly greater than that of a single treatment with either agent. These results also suggest that the mechanism of action of atropine is different from that of prazosin.

The hydrolysis of inositol lipids is known to be linked to calcium signalling (Berridge & Irvine, 1984). Activation of α-adrenoceptors increases the metabolism of phosphoinositol 4,5-bisphosphate into two second messengers, inositol trisphosphate (IP_3) and diacylglycerol (Abdel-Latif, 1983; Berridge & Irvine, 1984). IP_3 and dicylglycerol release intracellular calcium and activate protein kinase C, respectively (Berridge & Irvine, 1984; Williamson *et al.*, 1985; Abdel-Latif, 1986). In the present investigation, atropine and prazosin both inhibited increases in inositol monophosphate (IP), a metabolite of IP_3,in the presence of noradrenaline and lithium. However, the effect of a combined incubation with atropine plus prazosin on the IP level was much greater than that with either agent alone. These results, therefore, indicate that the effect of atropine may be due to inhibition of the metabolism of membrane phosphoinositide and further illustrate the possibility that the mechanism of action of atropine is different from prazosin. This is further supported by the finding that atropine does not affect the binding of [^{3}H]-prazosin.

The results also indicated that theophylline could partially inhibit the accumulation of IP. However, the inhibitory effect of a combined treatment with atropine plus theophylline was much greater than that of a single treatment with either agent. Therefore, the effect of atropine on the phosphoinositide metabolism may also be different from that of theophylline.

In summary, atropine inhibited contraction to noradrenaline in the rabbit aorta, without significantly affecting the response to KCl. Atropine also inhibited the noradrenaline response due to intracellular Ca^{2+} release, and the response due to Ca^{2+} influx through receptor-operated channels. The inhibitory effect of atropine was not apparently due to an interaction with α_1-adrenoceptors but may reflect inhibition of phosphoinositide metabolism.

References

ABDEL-LATIF, A.A. (1983). Metabolism of phsophoinositides. *Handb. Neurochem.*, **3**, 91–131.

ABDEL-LATIF, A.A. (1986). Calcium-mobilizing receptors, polyphosphoinositides, and the generation of second messengers. *Pharmacol. Rev.*, **38**, 227–272.

ABDEL-LATIF, A.A. (1991). Biochemical and functional interactions between the inositol, 1,4,5-trisphosphate-Ca^{2+} and cyclic AMP signalling systems in smooth muscle. *Cell. Signal.*, **3**, 371–385.

BERRIDGE, M.J. & IRVINE, R.F. (1984). Inositol triphosphate, a novel second messenger in cellular signal transduction. *Nature*, **312**, 315–321.

BROWN, S.L. & BROWN, J.H. (1983). Muscarinic stimulation of phosphatidylinositol metabolism in atria. *Mol. Pharmacol.*, **24**, 351–356.

DENAC, M., KUMIN, G. & SCHARRER, E. (1991). Effect of noradrenaline on smooth muscle strips from the reticular groove of adult cattle. *J. Vet. Med.*, **38**, 383–388.

FARGEAS, M.J., BASSOTTI, G., FIORAMONTI, J. & BUENO, L. (1989). Involvement of different mechanisms in the stimulatory effects of cholecystokinin octapeptide on gastrointestinal and colonic motility in dogs. *Can. J. Physiol. Pharmacol.*, **67**, 1205–1212.

HESTER, R.K. (1985). The effects of 2-nicotinamidoethyl nitrate on agonist-sensitive Ca^{2+} release and Ca^{2+} entry in rabbit aorta. *J. Pharmacol. Exp. Ther.*, **233**, 100–111.

KARAKI, H., NAKAGAWA, H. & URAKAWA, N. (1984). Effects of calcium antagonists on release of [^{3}H]-norepinephrine in rabbit aorta. *Eur. J. Pharmacol.*, **101**, 177–183.

KATZUNG, B.F. (1987). Acetylcholine receptor antagonists. In *Basic and Clinical Pharmacology*. ed. Katzung, B.G. pp. 75–83. Norwalk: Appleton & Lange.

KIM, U.-H., KIM, J.W. & RHEE, S.G. (1989). Phosphorylation of phospholipase C- by cAMP-dependent protein kinase. *J. Biol. Chem.*, **264**, 20167–20170.

KUKOVETZ, W.R., HOLZMANN, S., WURM, A. & POCH, G. (1979). Evidence for cyclic GMP-mediated relaxant effects of nitrocompounds in coronary smooth muscles. *Naunyn Schmiedebergs Arch. Pharmacol.*, **310**, 129–138.

LOWRY, O.H., ROSEBROUGH, N.J., FARR, A.L. & RANDALL, R.J. (1951). Protein measurement with a Folin phenol reagent. *J. Biol. Chem.*, **193**, 265–275.

RAPOPORT, R.M. (1986). Cyclic guanosine monophosphate inhibition of contraction may be mediated through inhibition of phosphatidylinositol hydrolysis in rat aorta. *Circ. Res.*, **59**, 407–410.

ROSENTHAL, H.E. (1967). A graphic method for the determination and presentation of binding parameters in a complex system. *Anal. Biochem.*, **20**, 525–532.

SAKAI, N., TAMAOKI, J., KOBAYASHI, K., KATAYAMA, M. & TAKIZAWA, T. (1989). Adenosine potentiates neurally–and histamine-induced contraction of canine airway smooth muscle. *Int. Arch. Allergy Appl. Immunol.*, **90**, 280–284.

SEAMON, K.B., PADGETT, W. & DALY, J.W. (1981). Forskolin: Unique diterpene activator of adenylate cyclase in membranes and intact cells. *Proc. Natl. Acad. Sci. U.S.A.*, **78**, 3363–3367.

SHIBATA, S., SATAKE, N. & HESTER, R.K. (1989). Differential inhibitory effects of nitroglycerin on contractile responses to the α-adrenoceptor agonists, methoxamine and clonidine, in rabbit aorta. *J. Cardiovasc. Pharmacol.*, **13**, 245–252.

SHIBATA, S., SATAKE, N., KURAHASHI, K. & OHTSUKA, M. (1988). The vasoinhibitory action of FR 46171, a new pyridine alcohol antianginal agent, on isolated rabbit vascular smooth muscles. *J. Cardiovasc. Pharmacol.*, **11**, 601–607.

SHIBATA, S., WAKABAYASHI, S., SATAKE, N., HESTER, R.K., UEDA, S. & TOMIYAMA, A. (1987). Mode of vasorelaxing action of 5-[3-[[2-3,4-dimethoxyphenyl)-thyl] amino]-1-oxopropyl]-2,3,4,5-tetrahydro-1,5-benzothiazepine fumarate (KT-362), a new intracellular calcium antagonist. *J. Pharmacol. Exp. Ther.*, **240**, 16–22.

SIMMONS, R.M.A. & JONES, D.J. (1988). Binding of [^{3}H]prazosin and [^{3}H]p-aminoclonidine to alpha-adrenoceptors in rat spinal cord. *Brain Res.*, **445**, 338–349.

WEISHAAR, R.E., QUADE, M., SCHEDUDEN, J.A. & KAPLAN, H.R. (1983). The methylenedioxyindenes, a novel class of 'intracellular calcium antagonist': Effects on contractility and on processes involved in regulating intracellular calcium homeostasis. *J. Pharmacol. Exp. Ther.*, **227**, 767–778.

WILLIAMSON, J.R., COOPER, R.H., JOSEPH, S.K. & THOMAS, A.P. (1985). Inositol triphosphate and diacylglycerol as intracellular second messengers in liver. *Am. J Physiol.*, **248**, (Cell Physiol. 17), 203–216.

(Received February 28, 1992
Revised May 11, 1992
Accepted June 16, 1992)

Br. J. Pharmacol. (1992), **107**, 559–565

Effects of propofol and enflurane on action potentials, membrane currents and contraction of guinea-pig isolated ventricular myocytes

[1]*R.M. Puttick & D.A. Terrar

University Department of Pharmacology, Mansfield Road, Oxford, OX1 3QT and *Nuffield Department of Anaesthetics, Radcliffe Infirmary, Woodstock Road, Oxford, OX2 6HE

1 The effects of two general anaesthetics, propofol and enflurane, on electrical activity and contractions were investigated in single myocytes isolated from guinea-pig ventricles.

2 Propofol and enflurane depressed the plateau and shortened the duration of action potentials.

3 Under voltage-clamp conditions, propofol and enflurane reduced the amplitude of inward calcium current and of additional inward current activated by cytosolic calcium.

4 Contractions (measured with an optical technique) accompanying either action potentials or second inward currents (in response to depolarizations to 0 mV) were reduced by both anaesthetics. The mechanisms for calcium entry during contractions accompanying pulses to positive potentials such as + 60 mV are thought to differ from those accompanying second inward currents which are evoked by pulses from − 40 to 0 mV. Enflurane enhanced the amplitudes of contractions accompanying pulses to positive potentials; in contrast these contractions were depressed by propofol.

5 In experiments where recovery processes were investigated by use of pairs of voltage-clamp pulses with a variable interval between them, enflurane but not propofol slowed the recovery of contractions and calcium-activated 'tail' currents. These observations are consistent with the hypothesis that enflurane may impair calcium handling by the sarcoplasmic reticulum whereas propofol has little, if any, effect at this site.

6 In conclusion, the actions of propofol and enflurane on second inward currents contribute to their effects on action potentials and contraction. The negative inotropic effect of both anaesthetics may result partly from reduced calcium influx to trigger contraction, and for enflurane, partly from an impairment of calcium handling by the sarcoplasmic reticulum.

Keywords: Propofol; enflurane; calcium currents; calcium-activated currents; isolated ventricular myocytes

Introduction

Certain general anaesthetics depress myocardial contractility, an effect which may, in certain circumstances, prove harmful. Anaesthetics may depress contractility either (i) by reducing the amount of calcium available to the contractile apparatus and/or (ii) by a direct effect on the contractile proteins.

Enflurane is a halogenated inhalational anaesthetic which has negative inotropic actions in man (Calverley *et al.*, 1978), experimental animals (Cutfield, 1983) and isolated atria and ventricles of various mammalian species (Shimosato *et al.*, 1969; Brown & Crout, 1971; DeTraglia *et al.*, 1988). Several studies of the possible cellular mechanisms underlying these cardiodepressant actions have indicated that anaesthetics such as enflurane inhibit calcium influx into cardiac cells and so reduce the transient increase in cytosolic calcium concentration that triggers and controls contraction (Lynch *et al.*, 1982; Nakao *et al.*, 1988; Bosnjak *et al.*, 1991). Triggered release of calcium from the sarcoplasmic reticulum (SR) contributes to this calcium transient and thus to activation of contractile filaments. Evidence suggests that halogenated anaesthetics may inhibit calcium uptake by the SR (Su & Kerrick, 1980) and/or cause calcium to leak from the SR (Su & Kerrick, 1980; Wheeler *et al.*, 1988; 1990; Katsuoka *et al.*, 1989) via the SR calcium release channel (Herland *et al.*, 1990). These actions would also impair cardiac contractility. In addition, it has been suggested that anaesthetics reduce the calcium sensitivity of contractile proteins (Merin *et al.*, 1974; Pask *et al.*, 1981; Murat *et al.*, 1988; 1990), however, these studies indicate that if these agents do depress contractile proteins, they do so at high anaesthetic concentrations and the effects are small compared to their overall negative inotropic effects. Despite the extensive research in this field it is still not clear what cellular actions of enflurane underlie the negative inotropic effects of this agent.

There has been several reports on the effects of the intravenously-administered anaesthetic propofol (2,4-diisopropylphenol) on the circulation, the most consistently reported effects both in man and in experimental animals being depressed systolic and diastolic arterial pressures and reduced cardiac output (Al-Khudhairi *et al.*, 1982; Claeys *et al.*, 1983; Stephan *et al.*, 1986; Coetzee *et al.*, 1989; Goodchild & Serrao, 1989). It appears that the haemodynamic depression induced by propofol arises, at least in part, from a direct depression of myocardial contractility (Puttick *et al.*, 1992). To date, there are no published studies on the effects of propofol on the cellular mechanisms underlying this contractile depression.

The experiments described in this paper have examined and compared the effects of the halogenated inhalation anaesthetic enflurane and the intravenous anaesthetic propofol on membrane currents thought to underlie cardiac contraction, and the possible effects of these agents on the SR. To achieve this, action potentials, membrane currents and contraction were recorded from guinea-pig isolated ventricular myocytes. Preliminary results have been reported to the British Pharmacological Society (Puttick & Terrar, 1989).

[1] Author for correspondence at present address: Parke-Davis Neuroscience Research Centre, Addenbrookes Hospital Site, Hills Road, Cambridge CB2 2QB.

Methods

Cells were isolated from guinea-pig ventricles by collagenase digestion (Powell *et al.*, 1980; Mitchell *et al.*, 1983). Aliquots of cell suspension were mounted on the surface of an agar-coated coverslip in a perspex organ bath. The superfusing solution contained (mM): NaCl 118.5, KCl 4.2, $NaHCO_3$ 14.5, KH_2PO_4 1.18, $MgSO_4$ 1.18, glucose 11.1 and $CaCl_2$ 2.5. All solutions were bubbled with 95% O_2:5% CO_2 (pH 7.4) and maintained at 37°C. A tap at the inflow to the bath permitted rapid changeover to the anaesthetic-containing solution. Propofol was prepared at a concentration of 50 mM, in a vehicle containing 50:50 polyethyleneglycol:dimethylsulphoxide. This stock solution was applied to the reservoir to give a final concentration of 25, 50 or 100 μM. The vehicle when applied alone to the isolated cells had no apparent effect on the action potentials, membrane currents and contractions. In other experiments the superfusing solution was pre-equilibrated for at least 45 min with enflurane (Abbott) from an Enfluratec vapouriser. The enflurane concentration in the bath was assayed by infra-red spectrophotometry (Speden, 1963). The concentrations determined were: 2%, 0.90 ± 0.02 mM: 3%, 1.46 ± 0.09 mM: 4%, 2.76 ± 0.14 mM.

Heart cells were impaled with glass microelectrodes containing either 0.5 M K_2SO_4 and 10 mM KCl or 3 M KCl (resistance 18–30 MΩ). Electrodes containing 3 M $CsCl_2$ were used in a few experiments, to suppress outward potassium current.

Membrane potentials were recorded and voltage signals were fed to a preamplifier incorporating a bridge circuit (Axoclamp 2). Action potentials could be elicited by brief (2 ms) depolarizing pulses. Cells could also be voltage-clamped with a single electrode system in which the function of the electrode was switched rapidly between current passing and voltage recording (Wilson & Goldner, 1975). The Axoclamp 2 system was used at a switching rate of 2–8 kHz. Cells were clamped at a holding potential of − 40 mV to inactivate sodium current and voltage signals were displayed on a digital storage oscilloscope (Gould 4020) and recorded on magnetic tape for later analysis. The second inward current was evoked by a step depolarization from − 40 mV to 0 mV. The magnitude of this current was measured as the difference between the peak current and the steady current at the end of the pulse (Mitchell *et al.*, 1983; 1987a). In most experiments, voltage-clamp and action potential records were obtained at a steady-state stimulation rate of 0.3 Hz; however, for the purpose of the double-pulse experiments, stimulation frequency was 0.2 Hz.

Contraction was monitored by a photodiode which was mounted in the eyepiece of the microscope (Mitchell *et al.*, 1983; 1987a). Light in the field of view was restricted to the edge of the cell under study. Changes in the output of the photodiode correspond to the extent of contraction which was measured in arbitrary units.

These experiments were performed over 2 years and observations made in over 250 cells from 87 guinea-pigs. Results are displayed and either quoted as mean ± s.e.mean for both control and anaesthetic or as the mean percentage reduction ± s.e.mean evoked by the anaesthetic. Values before and after anaesthetic administration were compared (Student's paired *t* test).

Results

Both propofol and enflurane, applied at clinically relevant concentrations, in the solution bathing cardiac cells depressed the magnitude of contraction. In addition there was a depression in the plateau and a shortening of the duration of the accompanying action potential. The dose-dependence of the effects of propofol and enflurane on contraction and the time taken for 20 and 90% repolarization of the action potential (APD_{20} and APD_{90} respectively) is shown in Table 1.

Table 1 Percentage reduction of the action potential duration and accompanying contraction induced by propofol and enflurane

	Concentration (μM)		
Propofol	25	50	100
n	10	10	14
APD_{-20} (% reduction)	7 ± 1	16 ± 5*	35 ± 3**
APD_{-90} (% reduction)	7 ± 1*	15 ± 3**	21 ± 3**
Contraction (% reduction)	19 ± 6*	34 ± 9**	52 ± 6**
	Concentration (% vol)		
Enflurane	2	3	4
n	6	7	11
APD_{-20} (% reduction)	21 ± 5*	39 ± 7*	47 ± 5**
APD_{-90} (% reduction)	15 ± 3*	18 ± 3**	26 ± 3**
Contraction (% reduction)	21 ± 2*	—	42 ± 7**

APD_{-20} and APD_{-90} are the times taken for 20 and 90% repolarization of the action potential respectively. Each value represents the mean ± s.e.mean, *n* is the number of guinea-pig isolated ventricular cells.
*$P<0.05$ and **$P<0.005$ compared with control, Student's paired *t* test. Mean basal absolute APD_{-20} and APD_{-90} was 128 ± 11 ms and 253 ± 13 ms ($n = 34$), respectively, for cells exposed to propofol and 116 ± 10 ms and 240 ± 12 ms ($n = 24$), respectively, for cells exposed to enflurane.

Second inward currents were evoked by applying 200 ms step depolarizations from the holding potential of − 40 mV to 0 mV. Both propofol and enflurane, applied in the solution bathing cardiac cells depressed the second inward current and reduced the amplitude of the concomitant contraction. Table 2 shows the dose-dependence of the effects of propofol and enflurane on second inward currents and accompanying contractions. The effects of these anaesthetics on second inward currents was a consistent observation in all cells studied and would be expected to contribute to the

Table 2 Percentage depression of membrane currents and contraction induced by propofol and enflurane

	Concentration (μM)		
Propofol	25	50	100
Second inward current	5 ± 3* (23)	25 ± 3** (22)	47 ± 3* (19)
Calcium-activated 'tail' current	22 ± 3* (12)	29 ± 4** (12)	50 ± 9* (12)
Contraction	27 ± 3* (23)	31 ± 5** (22)	60 ± 3** (19)
	Concentration (% vol)		
Enflurane	2	3	4
Second inward current	22 ± 3* (9)	31 ± 3* (21)	41 ± 4** (13)
Calcium-activated 'tail' current	30 ± 4* (6)	43 ± 5** (13)	53 ± 5** (10)
Contraction	31 ± 4* (6)	42 ± 4** (14)	53 ± 5** (13)

Each value shows mean percentage reduction ± s.e.mean, the number of guinea-pig isolated ventricular myocytes is in parentheses.
*$P<0.05$/**$P<0.005$ compared with control values: Student's paired *t* test. Mean basal absolute amplitude of second inward current and calcium activated 'tail' current was − 2.2 ± 0.1 nA ($n = 64$) and − 0.6 ± 0.05 nA ($n = 36$), respectively, for cells exposed to propofol and − 2.1 ± 0.1 nA ($n = 43$) and − 0.5 ± 0.07 nA ($n = 29$), respectively, for cells exposed to enflurane.

negative inotropic effects and to the modification of the action potential configuration described above.

Voltage clamp pulses to different membrane potentials were applied and current-voltage curves constructed (Figure 1). The currents at the end of the step depolarizations were plotted as triangles and peak inward or outward currents plotted as squares. The difference between these two curves provides a measure of the amplitude of the second inward current. However, this estimate of second inward current is complicated, particularly at positive potentials, by contaminating outward currents. This problem was minimized in the cells used for this experiment by the intracellular application of the potassium channel blocker, caesium (Matsuda & Noma, 1984). Under these conditions, enflurane and propofol reduced the amplitude of the second inward current without substantial effect on the shape of the current-voltage relation (Figures 1a and 1b respectively).

On repolarization to the holding potential of − 40 mV after a 200 ms step depolarization to + 60 mV a slow 'tail' of decaying outward current can be seen. This 'tail' is thought to reflect deactivation of the delayed rectifier potassium current. Propofol (50 μM) and enflurane (3%) reduced this current by 29 ± 7% ($P<0.05$; $n=8$) and 32 ± 5% ($P<0.05$; $n=7$) respectively. A reduction of outward current might be expected to lengthen the action potential but as described above, both anaesthetics shorten action potentials. This indicates that anaesthetic effects on the counterbalancing inward currents predominate.

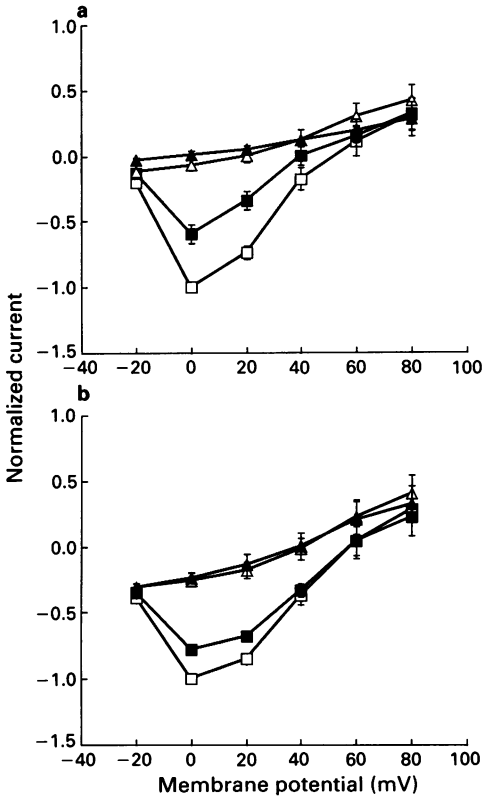

Figure 1 Normalized current as a function of membrane potential during voltage-clamp pulses measured from isolated cells loaded with Cs. Cells were voltage-clamped at − 40 mV. For each depolarization the current was measured at the end of the 200 ms depolarization (triangles) and at the peak inward or outward current (squares). All currents were normalized with respect to the peak inward current at 0 mV. Mean basal absolute current amplitude at 0 mV was − 2.3 ± 0.2 nA for cells subsequently exposed to enflurane and − 2.0 ± 0.2 nA for cells subsequently exposed to propofol. Data in the absence of anaesthetic are shown by open squares. Data in the presence of anaesthetic when a steady state was reached are shown by solid symbols. (a) Effects of 3% enflurane ($n=5$ cells) and (b) effects of 50 μM propofol ($n=8$ cells) on the current-voltage relation.

Current carried by calcium is thought to contribute the major fraction of peak second inward current. However, additional inward current appears to be activated by the increase in cytosolic calcium that accompanies the second inward current (Mitchell *et al.*, 1987b; Fedida *et al.*, 1987). This calcium-activated current may be recorded on repolarization to − 40 mV after brief (20 ms) step depolarizations to 0 mV as a slow 'tail' of decaying inward current. The percentage depression induced by various concentrations of propofol and enflurane on the calcium-activated 'tail' currents is shown in Table 2. A representative record from a single cell illustrating the effect of enflurane on this 'tail' current is shown in Figure 2.

The possibility that enflurane and propofol have actions additional to the depression in second inward current that may contribute to the contractile depression was investigated in experiments in which a paired pulse protocol was used. At various intervals (0.2–1 s) after the start of a conditioning depolarization (200 ms, from a holding potential of − 40 mV to 0 mV) to evoke the second inward current and accompanying contraction, a 'test' depolarization (to 0 mV for 20 or 200 ms) was applied to assess the recovery of second inward currents, calcium-activated 'tail' currents and contraction. The conditioning depolarizations led to substantial inactivation of calcium channels and perhaps to a depletion of calcium available for release from intracellular stores. The recovery rate of calcium-activated 'tail' current and contraction is dependent to an extent on the rate of recovery of calcium uptake/release from intracellular stores. The rationale for these experiments was to assess the extent of repriming of the mechanisms responsible for contraction and calcium-activated 'tail' currents after the conditioning depolarization. The effects of propofol and enflurane on this repriming could thus be investigated. At brief intervals between these pulses the amplitudes of second inward current, calcium-activated tail current and contractions were all depressed. The recovery of these amplitudes as the pulse interval increased is illustrated in Figures 3 and 4. In these graphs the amplitudes of the second inward current, calcium-activated 'tail' current

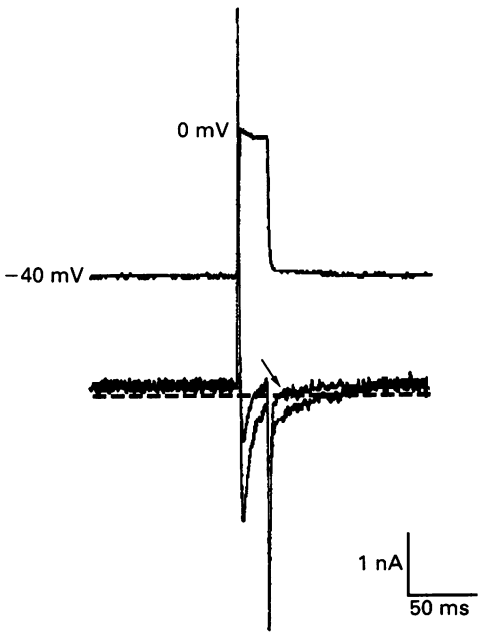

Figure 2 Membrane potential (upper trace) and current (lower trace) during 20 ms step depolarizations to 0 mV from the holding potential of − 40 mV. This protocol was used to obtain calcium-activated 'tail' currents which are seen on repolarization to − 40 mV. The arrow indicates the record obtained in the presence of 3% enflurane when a steady-state had been reached. The zero current level is shown by a dashed line.

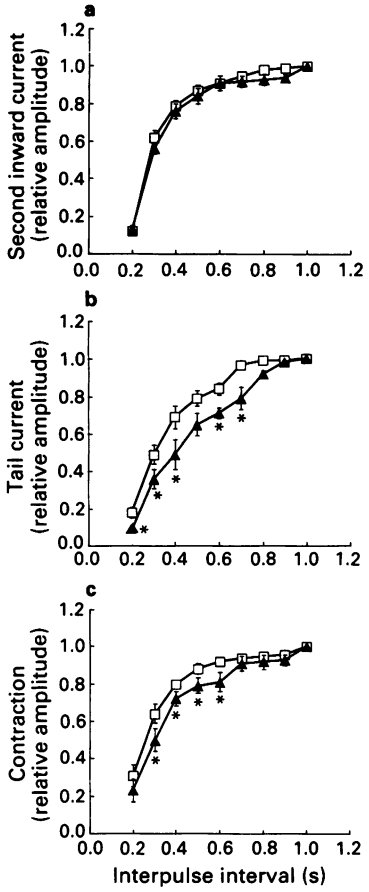

Figure 3 The effect of 3% enflurane (▲) on the recovery of second inward current (a), calcium activated 'tail' current (b) and contraction (c), in paired pulse protocols. The test pulses for (a) and (c) were 200 ms while for (b) the duration was reduced to 20 ms. The time scales show delay between the test pulse and the start of the conditioning pulse of 200 ms duration. Data are expressed as a fraction of their values at an interpulse interval of 1 s. Data obtained in the absence of anaesthetic are shown by (□). Points represent the means from 7 guinea-pig isolated ventricular myocytes; s.e.mean shown by vertical lines.

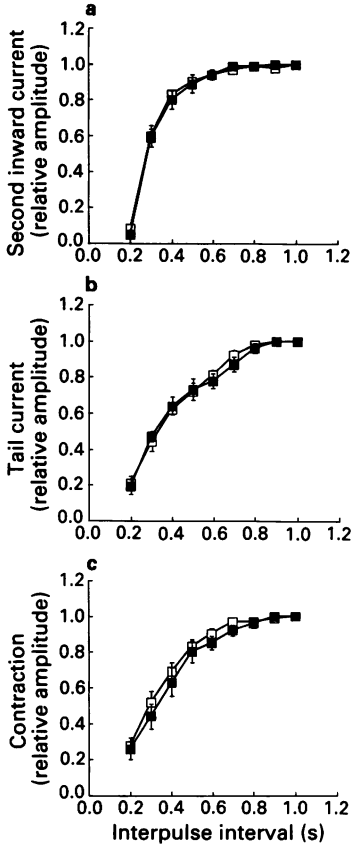

Figure 4 The effect of 50 μM propofol (■) on the recovery of second inward current (a), calcium activated 'tail' current (b) and contraction (c), in paired pulse protocols. The test pulses for (a) and (c) were 200 ms while for (b) the duration was reduced to 20 ms. The time scales show delay between the test pulse and the start of the conditioning pulse of 200 ms duration. Data are expressed as a fraction of their values at an interpulse interval of 1 s. Data obtained in the absence of anaesthetic are shown by (□). Points represent the means from 8 guinea-pig isolated ventricular myocytes; s.e.mean shown by vertical lines.

and contraction were plotted as a fraction of their value at an interpulse interval of 1 s when recovery may still have been incomplete. Propofol had no apparent effect on the recovery rate of second inward currents, calcium-activated tail currents and contraction (Figure 4). Although there was no detectable effect of enflurane (3%) on the recovery rate of the second inward current, the rate of recovery of calcium-activated tail currents and contraction was delayed (Figure 3).

Calcium channel inactivation is thought to be controlled by both calcium- and voltage-dependent mechanisms (Lee *et al.*, 1985). A possible effect of propofol and enflurane on the steady-state inactivation of calcium channels was investigated (data not shown). Propofol (50 μM) had no apparent effect on calcium channel inactivation. Enflurane (3%; 1.45 mM), however, appeared to enhance calcium channel inactivation, an effect which was significant ($P < 0.05$; $n = 8$) at negative membrane potentials where, in the absence of anaesthetic, inactivation was incomplete.

Contractions accompanying pulses to positive potentials, under certain conditions, are thought to be triggered by a different source of calcium from those accompanying pulses to 0 mV, possibly calcium entry through sodium-calcium exchange (Terrar & White, 1989). Calcium entering via this route may also trigger calcium release from the SR. To assess the effects of propofol and enflurane on contractions accompanying pulses to positive potentials, contractions were monitored accompanying 200 ms step depolarizations to + 60 mV from a holding potential of − 40 mV. The pulses to + 60 mV were immediately preceded by pulses to 0 mV to inactivate calcium channels and thus ensure no calcium entry via this route during the subsequent pulse to + 60 mV. Figure 5a and b shows the effects of 3% enflurane and 50 μM propofol, respectively, on currents and contractions accompanying pulses to 0 mV and + 60 mV. In the presence of propofol (Figure 5b) the amplitudes of the second inward current which accompanies the pulse to + 0 mV and the slowly developing outward current which accompanies the depolarization to + 60 mV were both reduced, as were the concomitant contractions. Enflurane (Figure 5a) also reduced the amplitudes of the membrane currents accompanying the pulses to 0 mV and + 60 mV and depressed the amplitude of the contraction accompanying the second inward current; however, the contraction accompanying the pulse to + 60 mV was enhanced by enflurane. These observations are illustrated graphically in Figure 6, where the anaesthetic induced percentage change in the amplitude of contraction accompanying pulses to positive potentials is plotted for the individual cells studied. Although there is some overlap in the effects of both of these anaesthetics it is apparent that the predominant effect of propofol on the contractions accompanying pulses to + 60 mV is to cause little change or a reduction in amplitude, whereas the tendency with enflurane is to cause no change or an increase in amplitude. To clarify

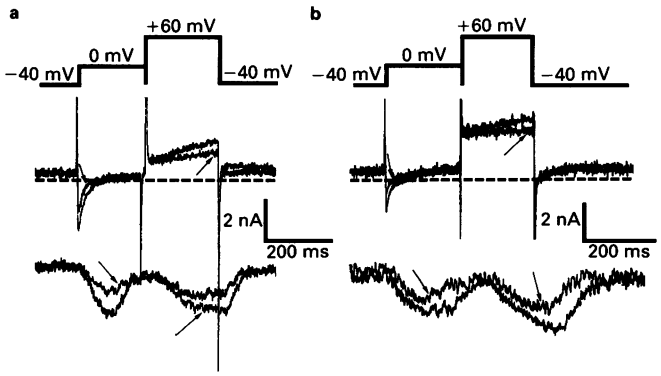

Figure 5 Membrane current (middle trace) and contraction (lower trace) evoked in response to the voltage protocol shown in the upper trace. The cells were depolarized from the holding potential of − 40 mV to + 60 mV after a 200 ms prepulse to 0 mV. Records obtained in the presence of (a) 3% enflurane and (b) 50 μM propofol when a steady state had been reached are indicated by arrows. Dashed line indicates the zero current level.

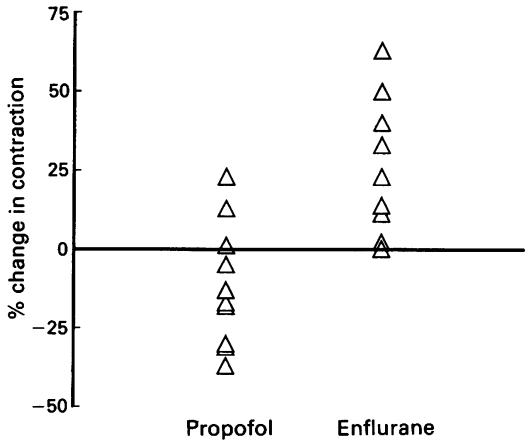

Figure 6 The effects of 50 μM propofol and 3% enflurane on contractions accompanying a 100 mV step depolarization (200 ms) from the holding potential of − 40 mV. Cells were depolarized to + 60 mV from a holding potential of − 40 mV 10 ms after a 200 ms prepulse to 0 mV. Data are expressed as percentage change compared to corresponding values obtained in the absence of anaesthetic. Each point represents data obtained from a single cell.

the events underlying this observation with propofol, experiments were performed in which the cells were perfused throughout the whole procedure i.e. during both control periods and periods of anaesthetic exposure, with either ryanodine (1 μM) or caffeine (10 mM) and the effects of propofol on contractions accompanying pulses to + 60 mV observed. The range and distribution of values from individual cells for the percentage change induced by propofol in the amplitude of contractions accompanying pulses to + 60 mV (see Figure 6), was the same in the absence or presence of ryanodine or caffeine in the solution bathing the cells ($n = 10$; $P > 0.05$ and $n = 8$; $P > 0.05$ respectively: Student's unpaired t test).

Discussion

Calcium entry during the plateau of the action potential is thought to activate and control contraction (Reuter, 1973; Fozzard, 1980). Both propofol and enflurane decreased the duration and depressed the plateau of action potentials and reduced the amplitude of the accompanying contraction. These effects would indicate that the anaesthetics reduce calcium influx into the cells. Calcium which enters the cell via 'L'-type calcium channels (Nilius *et al.*, 1985) carries the major part of the second inward current (Lee & Tsien, 1982; Mitchell *et al.*, 1983; Matsuda & Noma, 1984). Both propofol and enflurane reduced the second inward current. A reduction of the second inward current would decrease the magnitude of the cytosolic calcium transient and this may account, at least in part, for the observed depression in the amplitude of the accompanying contraction.

Calcium-activated 'tail'currents which are activated by the cytosolic calcium transient were reduced by propofol and enflurane. This implies that these anaesthetics either: (i) directly inhibited the membrane processes thought to be responsible for these tail currents, namely electrogenic sodium:calcium exchange (Mullins, 1979; Kimura *et al.*, 1986; Mechmann & Pott, 1986) and current through non-selective cation channels (Colquhoun *et al.*, 1981) or (ii) they attenuated the calcium transient. The reduction in calcium influx found with propofol and enflurane would be expected to reduce the increase in cytosolic calcium levels both directly and indirectly by reducing calcium-induced calcium release from the SR. These effects may be sufficient to account for the reduction in tail current and the depression of contractility. However, propofol and enflurane may also have additional effects on SR calcium release which could contribute to the negative inotropic actions.

Under very similar experimental conditions to those used in the experiments described in this paper, the effects of low doses of the calcium channel blockers, verapamil and nifedipine, on the percentage depression of second inward current and contraction have been studied. These studies indicate that a relatively large reduction in second inward current was required for a relatively small depression of contraction (Terrar & Victory, 1988a). In contrast, propofol and enflurane produced a greater depression of contraction than verapamil for a given reduction in second inward current. This indicates that both the anaesthetics may have actions additional to that of second inward current inhibition to account for their negative inotropic effects.

The possibility that propofol and enflurane have a direct effect on SR calcium release was investigated by use of double-pulse voltage clamp protocols. The magnitudes of the calcium-activated tail current and contraction at a given interpulse interval were taken as an index of the calcium transient, which, in turn depends on the extent of refilling of the SR. Thus, any delay in the recovery of the tail current and contraction induced by propofol when compared to the recovery of the second inward current may be explained in terms of a delay in the uptake/release of calcium from the SR. Propofol had no apparent effect on the recovery rate of second inward current, calcium-activated 'tail' current and contraction. In contrast, enflurane delayed the recovery rate of the calcium-activated 'tail' current and contraction while having little effect on the recovery rate of second inward current. In similar experiments, halothane (Terrar & Victory, 1988a) and isoflurane (Terrar & Victory, 1988b) also have been shown to delay the recovery rate of tail currents and contraction. The results with enflurane may be explained in terms of enflurane inhibiting the refilling of the SR calcium store. This may result from enflurane either inhibiting calcium uptake and/or causing calcium 'leak' from the SR. These results are consistent with those of Su & Kerrick (1980) who showed that enflurane reduced calcium uptake capacity of the SR in functionally skinned myocardial fibres from the rabbit. In addition, results of Katsuoka & Ohnishi (1989) have shown that enflurane reduces SR calcium content and that this reduction has a high degree of correlation to the negative inotropic effect of enflurane. In contrast propofol does not appear to affect calcium uptake into or release from SR calcium stores.

In guinea-pig ventricular muscle, calcium entry through

nifedipine-sensitive 'L' type channels and calcium release from intracellular stores are essential for triggering and controlling contraction (Reuter, 1979; Fozzard, 1980; Fabiato, 1983). Calcium current with these characteristics can be activated in guinea-pig ventricular myocytes at membrane potentials in the range − 40 to 0 mV (Mitchell *et al.*, 1983). As membrane potential is made more positive (to + 60 mV), contraction amplitude in these cells is not consistently blocked by nifedipine and increases even though it would be expected that calcium entry through 'L' channels would decrease (Mitchell *et al.*, 1987b). Contraction at positive potentials is thought to be via a route other than calcium channels, possibly sodium:calcium exchange (Brill *et al.*, 1987; Barcenas-Ruiz & Weir, 1987; Terrar & White, 1989).

Contractions accompanying depolarizing pulses to 0 mV were consistently depressed by both enflurane and propofol. However, there was a distinct difference between the effects of propofol and enflurane on contractions accompanying pulses to positive potentials. Enflurane enhanced (8 cells) or had no affect (1 cell) on contractions accompanying pulses to positive potentials. In contrast, most of the cells exposed to propofol exhibited a reduction (6 cells) of these contractions, with just three cells exhibiting a small increase in contraction amplitude. The effects of enflurane may be explained in terms of an inhibition of calcium uptake into the SR or a 'leak' of calcium from the SR. As sodium:calcium exchange is thought to mediate influx of calcium at positive potentials and would not be able to extrude calcium, the effects of enflurane on the SR may leave more cytosolic calcium available for contraction. Halothane has been reported to have similar effects to enflurane with regards to contraction accompanying pulses to positive potentials (Terrar & Victory, 1989).

If the effects of propofol on contractions accompanying pulses to + 60 mV were mediated via an effect on the SR one would have expected that the range and distribution of values representing percentage change in the amplitude of contractions accompanying pulses to + 60 mV would have been affected by the presence both before and during propofol administration of the inhibitors of SR function, ryanodine and caffeine. As this was not the case it may be concluded that propofol does not induce its effects on contractions accompanying pulses to positive potentials via an effect on the SR. Possible alternative explanations for the effects of propofol on contractions accompanying pulses to positive potentials include (i) a direct inhibition by propofol of calcium influx via sodium:calcium exchange, resulting in reduced calcium influx during the pulse to positive potentials or (ii) a direct reduction by propofol of the sensitivity of the contractile proteins.

In conclusion, both enflurane and propofol depress the amplitude of second inward currents and calcium-activated inward currents. There seems, however, to be a clear cut difference between propofol and halogenated anaesthetics such as enflurane (this study), halothane (Terrar & Victory, 1988a) and isoflurane (Terrar & Victory, 1988b) concerning actions which have been interpreted as resulting from a major effect of halogenated anaesthetics on the SR (double-pulse experiments and experiments using depolarizations to + 60 mV). Inhibition of calcium release from the SR by enflurane may occur via either an inhibition of calcium uptake and/or an increased leak of calcium from the SR. These actions would impair the ability of the SR to sequester calcium and would result in a reduction of the amount of calcium available for release. Both the reduction in calcium influx via second inward current and an inhibition of calcium release from intracellular stores could account for the negative inotropic effects of enflurane. In contrast, propofol does not have a major effect on SR function. Thus propofol seems to depress contractility by a reduction of second inward current and a possible depression of myofilament sensitivity.

R.M.P. was supported by a MRC Studentship.

References

AL-KHUDHAIRI, D., GORDON, G., MORGAN, M. & WHITWAM, J.G. (1982). Acute cardiovascular changes following disoprofol. *Anaesthesia*, **37**, 1007–1010.

BARCENAS-RUIZ, L. & WIER, W.G. (1987). Voltage-dependence of intracellular $[Ca]_i$ transients in guinea-pig ventricular myocytes. *Circ. Res.*, **61**, 148–154.

BOSNJAK, Z.J., SUPAN, F.D. & RUSCH, N.J. (1991). The effects of halothane, enflurane and isoflurane on calcium current in isolated canine ventricular cells. *Anesthesiology*, **74**, 340–345.

BRILL, D.M., FOZZARD, H.A., MAKIELSKI, J.C. & WASSERSTROM, J.A. (1987). Effects of prolonged depolarizations on twitch tension and intracellular sodium activity in sheep cardiac Purkinje fibres. *J. Physiol.*, **384**, 355–376.

BROWN, B.R. & CROUT, J.R. (1971). A comparative study of the effects of five general anesthetics on myocardial contractility. *Anesthesiology*, **34**, 236–245.

CALVERLEY, R.K., SMITH, N.T., PRYS-ROBERTS, C., EGER, E.I. & JONES, C.W. (1978). Cardiovascular effects of enflurane anesthesia during controlled ventilation in man. *Anesth. Analg.*, **57**, 619–628.

CLAEYS, M.A., GEPTS, E. & CAMU, F. (1988). Haemodynamic changes during anaesthesia induced and maintained with propofol. *Br. J. Anaesth.*, **60**, 3–9.

COETZEE, A., FOURIE, P., COETZEE, J., BADENHORST, E., REBEL, A., BOLLINGER, C., UEBEL, R., WIUM, C. & LOMBARD, C. (1989). Effect of various plasma propofol concentrations on regional myocardial contractility and left ventricular afterload. *Anesth. Analg.*, **69**, 473–483.

COLQUHOUN, D., NEHER, E., REUTER, H. & STEVENS, C.F. (1981). Inward current channels activated by intracellular Ca in cultured cardiac cells. *Nature*, **294**, 752–754.

CUTFIELD, G.R. (1983). The effect of anaesthesia and its interaction with critically reduced coronary perfusion upon myocardial function. *D. Phil. Thesis (Oxford)*.

DETRAGLIA, M.C., KOMAI, H. & RUSY, B.F. (1988). Differential effects of inhalation anesthetics on myocardial potentiated-state contractions in vitro. *Anesthesiology*, **68**, 534–540.

FABIATO, A. (1983). Calcium-induced release of calcium from the cardiac sarcoplasmic reticulum. *Am. J. Physiol.*, **245**, C1–C14.

FEDIDA, D., NOBLE, D., SHIMONI, Y. & SPINDLER, A.J. (1987). Inward current related to contraction in guinea-pig ventricular myocytes. *J. Physiol.*, **385**, 565–589.

FOZZARD, H.A. (1980). In *The Slow Inward Current and Cardiac Arrhythmias*. ed. Zipes, D.P., Bailey, J.C. & Elharrar, V. pp. 173–203. The Hague, Boston, London: Martinus Nijhoff.

GOODCHILD, C.S. & SERRAO, J.M. (1989). Cardiovascular effects of propofol in the anaesthetized dog. *Br. J. Anaesth.*, **63**, 87–92.

HERLAND, J.S., JULIAN, F.J. & STEPHENSON, D.G. (1990). Halothane increases Ca^{2+} efflux via Ca^{2+} channels of sarcoplasmic reticulum in chemically skinned rat myocardium. *J. Physiol.*, **426**, 1–18.

KATSUOKA, M., KOBAYASHI, K. & OHNISHI, S.T. (1989). Volatile anesthetics decrease calcium content of isolated myocytes. *Anesthesiology*, **70**, 954–960.

KATSUOKA, M. & OHNISHI, S.T. (1989). Inhalation anaesthetics decrease calcium content of cardiac sarcoplasmic reticulum. *Br. J. Anaesth.*, **62**, 669–673.

KIMURA, J., NOMA, A. & IRISAWA, H. (1986). Na-Ca exchange current in mammalian heart cells. *Nature*, **319**, 596–597.

LEE, K.S., MARBAN, E. & TSIEN, R.W. (1985). Inactivation of calcium channels in mammalian heart cells: joint dependence on membrane potential and intracellular calcium. *J. Physiol.*, **364**, 395–411.

LEE, K.S. & TSIEN, R.W. (1982). Reversal of current through calcium channels in dialysed single heart cells. *Nature*, **297**, 498–501.

LYNCH, C., VOGEL, S., PRATILA, M.G. & SPERELAKIS, N. (1982). Enflurane depression of slow action potentials. *J. Pharmacol. Exp. Ther.*, **222**, 405–409.

MATSUDA, H. & NOMA, A. (1984). Isolation of calcium current and its sensitivity to monovalent cations in dialysed ventricular cells of guinea-pig. *J. Physiol.*, **357**, 553–573.

MECHMANN, S. & POTT, L. (1986). Identification of the Na/Ca exchange current in single cardiac myocytes. *Nature*, **319**, 597–599.

MERIN, R.G., KUMAZAWA, T. & HONIG, C.R. (1974). Reversible interaction between halothane and Ca on cardiac actomyosin adenosine triphosphatase: Mechanism and significance. *J. Pharmacol. Exp. Ther.*, **190**, 1–14.

MITCHELL, M.R., POWELL, T., TERRAR, D.A. & TWIST, V.W. (1983). Characteristics of the second inward current in cells isolated from rat ventricular muscle. *Proc. Soc. B.*, **219**, 447–469.

MITCHELL, M.R., POWELL, T., TERRAR, D.A. & TWIST, V.W. (1987a). Electrical activity and contraction in cells isolated from rat and guinea-pig ventricular muscle: a comparative study. *J. Physiol.*, **391**, 527–544.

MITCHELL, M.R., POWELL, T., TERRAR, D.A. & TWIST, V.W. (1987b). Calcium-activated inward current and contraction in rat and guinea-pig ventricular myocytes. *J. Physiol.*, **391**, 545–560.

MULLINS, L.J. (1979). The generation of electric currents in cardiac fibres by Na/Ca exchange. *Am. J. Physiol.*, **236**, C103–C110.

MURAT, I., VENTURA-CLAPIER, R. & VASSORT, G. (1988). Halothane, enflurane, and isoflurane decrease calcium sensitivity and maximal force in detergent-treated rat cardiac fibers. *Anesthesiology*, **69**, 892–899.

MURAT, I., LECHENE, P. & VENTURA-CLAPIER, R. (1990). Effects of volatile anesthetics on mechanical properties of rat cardiac skinned fibres. *Anesthesiology*, **73**, 73–81.

NAKAO, S., HIRATA, H. & KAGAWA, Y. (1989). Effects of volatile anaesthetics on cardiac calcium channels. *Acta Anaesthesiol. Scand.*, **33**, 326–330.

NILIUS, B., HESS, P., LANSMAN, J.B. & TSIEN, R.W. (1985). A novel type of cardiac calcium channel in ventricular cells. *Nature*, **316**, 443–446.

PASK, H.T., ENGLAND, P.J. & PRYS-ROBERTS, C. (1981). Effects of volatile anaesthetic agents on isolated bovine cardiac myofibrillar ATPase. *J. Mol. Cell. Cardiol.*, **13**, 293–301.

POWELL, T., TERRAR, D.A. & TWIST, V.W. (1980). Electrical properties of individual cells isolated from adult rat ventricular myocardium. *J. Physiol.*, **302**, 131–153.

PUTTICK, R.M. & TERRAR, D.A. (1989). Effects of propofol on membrane currents and contraction in single myocytes isolated from guinea-pig ventricles. *Br. J. Pharmacol.*, **98**, 742P.

PUTTICK, R.M., DIEDERICKS, J., SEAR, J., GLEN, J.B., FOEX, P. & RYDER, W.A. (1992). Effects of increasing propofol infusion rates on global and regional left ventricular function of anaesthetised dogs. *Br. J. Anaesth.* (in press).

REUTER, H. (1973). Divalent cations as charge carriers in excitable membranes. *Progr. Biophys. Mol. Biol.*, **26**, 3–43.

REUTER, H. (1979). Properties of two inward membrane currents in the heart. *Annu. Rev. Physiol.*, **41**, 413–424.

SHIMOSATO, S., SUGAI., N., IWATZUKI, N. & ETSTEN, B.E. (1969). Effects of ethrane on cardiac muscle mechanics. *Anesthesiology*, **30**, 513–518.

SPEDEN, R. (1963). Kinetics and mechanism of action of some volatile anaesthetics. *D. Phil Thesis (Oxford)*.

STEPHAN, H., SONNTAG, H., SCHENK, H.D., KETTLER, D. & KHAMBATTA, H.J. (1986). Effects of propofol on cardiovascular dynamics, myocardial blood flow and myocardial metabolism in patients with coronary artery disease. *Br. J. Anaesth.*, **58**, 969–975.

SU, J.Y. & KERRICK, W.G.L. (1980). Effects of enflurane on functionally skinned myocardial fibers from rabbits. *Anesthesiology*, **52**, 385–389.

TERRAR, D.A. & VICTORY, J.G.G. (1988a). Effects of halothane on membrane currents associated with contraction in single myocytes isolated from guinea-pig ventricle. *Br. J. Pharmacol.*, **94**, 500–508.

TERRAR, D.A. & VICTORY, J.G.G. (1988b). Isoflurane depresses membrane currents associated with contraction in myocytes isolated from guinea-pig ventricle. *Anesthesiology*, **69**, 742–749.

TERRAR, D.A. & VICTORY, J.G.G. (1989). Influence of halothane on contraction at positive membrane potentials in single cells isolated from guinea-pig ventricular muscle. *Q. J. Exp. Physiol.*, **74**, 141–151.

TERRAR, D.A. & WHITE, E. (1989). Mechanisms and significance of calcium entry at positive membrane potentials in guinea-pig ventricular muscle cells. *Q. J. Exp. Physiol.*, **74**, 121–139.

WHEELER, D.M., RICE, R.T., HANSFORD, R.G. & LAKATTA, E.G. (1988). The effect of halothane on the free intracellular calcium concentration of isolated rat heart cells. *Anesthesiology*, **69**, 578–583.

WHEELER, D.M., RICE, R.T. & LAKATTA, E.G. (1990). The action on halothane on spontaneous contractile waves and stimulated contractions in isolated rat and dog heart cells. *Anesthesiology*, **72**, 911–920.

WILSON, W.A. & GOLDNER, M.M. (1975). Voltage-clamping with a single microelectrode. *J. Neurobiol.*, **6**, 411–422.

(Received May 8, 1992
Revised June 10, 1992
Accepted June 16, 1992)

Br. J. Pharmacol. (1992), **107**, 566–572

Thimerosal blocks stimulated but not basal release of endothelium-derived relaxing factor (EDRF) in dog isolated coronary artery

Peter Crack & [1] Thomas Cocks

Baker Medical Research Institute, Commercial Road, Prahran, 3181, Victoria, Australia

1 The effect of an acetly-coA lysolecithin acyltransferase inhibitor, thimerosal, on the release of endothelium-derived relaxing factor (EDRF) was examined in the greyhound isolated coronary artery.

2 Thimerosal (1–10 μM) relaxed fully, ring segments of coronary artery which were contracted with the thromboxane A_2-mimetic, U46619 (30 nM). The response was endothelium-dependent, slow in both onset and time to reach maximum. The maximum relaxation to the highest concentration of thimerosal (10 μM) was maintained for 10–20 min before the tissue slowly regained active force (1–2 h) to the same or higher level as that prior to the addition of thimerosal. At this time the endothelium-dependent relaxation responses to acetylcholine (ACh), substance P (SP), bradykinin (BK) and the calcium ionophores, ionomycin and A23187 were abolished. The endothelium-dependent contractions to the nitric oxide synthase inhibitors, N^G-nitro-L-arginine (L-NNA; 10–100 μM) and N^G-monomethyl-L-arginine (L-NMMA: 10–100 μM), however, were unaffected.

3 Thimerosal (10 μM) did not affect the relaxation curve to sodium nitroprusside (SNP) nor the contraction curve to the thromboxane A_2-mimetic, U46619.

4 Both the relaxation response to thimerosal and the selective block of the relaxation responses to stimulated EDRF release were unaffected by either indomethacin (10 μM) or superoxide dismutase (150 u ml^{-1}).

5 L-NNA (100 μM) significantly blocked the relaxation curves to thimerosal and A23187 but not that to SNP.

6 Abolition of stimulated EDRF-mediated responses with thimerosal was unlikely to result from maximal and maintained stimulation of EDRF release even when active U46619-induced force had returned to pre-thimerosal levels, since the relaxation curves to glyceryl trinitrate (GTN) and SNP were markedly attenuated in the presence of SNP and GTN respectively when active force was restored with endothelin-1 (ET-1).

7 Melittin (1 μM), ionomycin (1 μM) and A23187 (1 μM) each had selective effects on stimulated but not basal EDRF responses, similar to those of thimerosal.

8 We propose that stimulated but not 'basal' release of EDRF is dependent on the release of arachidonic acid or one of its non-cyclo-oxygenase metabolites, possibly by Ca^{2+}-dependent activation of phospholipase A_2.

Keywords: EDRF; phospholipase A_2; arachidonic acid; nitric oxide; L-arginine; coronary artery; thimerosal

Introduction

Endothelium-derived relaxing factor (EDRF) is now thought to be nitric oxide (NO; Palmer *et al.*, 1987; Moncada *et al.*, 1991) synthesized in endothelial cells from L-arginine by an enzyme termed nitric oxide synthase (NOS; Moncada *et al.*, 1991). Release of EDRF occurs basally and in response to a variety of chemical stimuli including receptor-specific agonists like acetylcholine (ACh) as well as the calcium ionophores, A23187 and ionomycin. Although there is strong evidence to suggest that EDRF is NO, the endothelial cell signalling mechanisms underlying its release are yet to be defined. The main NOS enzyme found in endothelial cells is the constitutive type, dependent on NADPH (Moncada *et al.*, 1991) and Ca^{2+} (Lopez-Jaramillo *et al.*, 1990). The current theory behind the signal transduction of EDRF suggests that receptor-mediated EDRF agonists such as ACh and substance P (SP), upon coupling with their respective receptors, activate phospholipase C (PLC), thereby causing an increase in *myo*-inositol 1,4,5-triphosphate (IP3) and diacylglycerol (DAG; see Berridge & Irvine, 1989). Intracellular free Ca^{2+} is then increased primarily by influx of extracellular Ca^{2+} through a receptor-regulated channel as well as mobilization from intracellular pools (see Angus & Cocks, 1989; Lopez-Jaramillo *et al.*, 1990). This increase in intracellular Ca^{2+} then stimulates NOS from its basal level of activity, which is also dependent on Ca^{2+} (Lopez-Jaramillo *et al.*, 1990), resulting in an increased rate of NO formation. Calcium inophores like A23187 and ionomycin on the other hand increase intracellular Ca^{2+} directly without interacting with PLC.

Analogues of L-arginine modified in either one of the guanidino nitrogens like N^G-monomethyl-L-arginine (L-NMMA) and N^G-nitro-L-arginine (L-NNA) have been shown to inhibit NOS, most probably as competitive substrate inhibitors (Rees *et al.*, 1990). The effects of these inhibitors is to raise vascular tone if basal EDRF is present and inhibit vasodilator responses to EDRF releasing agents like ACh, SP and A23187.

Several pieces of evidence suggest that phospholipid metabolism may be involved in EDRF production (for review, see Angus & Cocks, 1989). Putative inhibitors of phospholipase A_2 (PLA_2) such as mepacrine were found to

[1] Author for correspondence.

inhibit EDRF-mediated relaxation in a range of bioassays for EDRF (Furchgott, 1981; Cocks *et al.*, 1984; Förstermann & Neufang, 1985; for review see Angus & Cocks, 1989). Also, the bee-venom peptide, melittin, a potent stimulator of PLA_2 (Schier, 1979; Zeitler *et al.*, 1991) induces endothelium-dependent relaxation resistant to cyclo-oxygenase inhibition (Förstermann & Neufang, 1985). Similarly, thimerosal, a comparatively specific inhibitor of acyl-CoA: lysolecithin acyltransferase (LAT) in macrophages (Goppelt-Strübe *et al.*, 1986) has been reported to cause a long-lasting release of EDRF from both endothelial cells *in situ* and in culture (Förstermann *et al.*, 1986a,b). Thus, inhibition of LAT, which has been found in endothelial cells (Förstermann *et al.*, 1986b), would be expected to induce effects similar to stimulation of PLA_2 since these two enzymes catalyze arachidonic acid release from and re-incorporation into membrane glycerolipids respectively, in particular lecithin. This cycle of arachidonic acid metabolism is known as the Lands cycle (Lands, 1960; Lands & Merkl, 1963) and its activity within endothelial cells suggests that the resultant continuous release of arachidonic acid from the phospholipid membrane may be important for the production of EDRF. Interestingly, the original hypothesis on the nature of EDRF prior to the discovery of NO and NOS centred on the role of arachidonic acid or an arachidonate metabolite in EDRF-mediated vasorelaxation (for reviews see Furchgott, 1981; 1984; Angus & Cocks, 1989).

The present study, confirms that thimerosal induces endothelium-dependent relaxations *in situ* in the dog isolated coronary artery. The relaxations to thimerosal were not sustained and tone in the artery segments slowly returned to control values within 1–2 h. The surprising finding, however, was that following recovery from the thimerosal relaxation all response to EDRF-releasing agents like ACh, SP, bradykinin (BK), A23187 and ionomycin were abolished, yet the contractions to the NOS substrate inhibitors, L-NNA and L-NMMA remained normal. Melittin, as well as ionomycin and A23187 also relaxed the coronary artery and again, following return of tone, relaxations to all EDRF-releasing agents were blocked but contractions to L-NNA and L-NMMA were unaffected. From these results we propose that the Lands cycle or more specifically arachidonate metabolism may play an integral role in the regulation of EDRF release.

Methods

Isolated tissues

Greyhounds of either sex (20–30 kg) were deeply anaesthetized with sodium pentobarbitone (Euthatal: 60 mg kg^{-1}, i.v.) and their hearts removed. The circumflex coronary artery was then dissected free from the surrounding myocardium and connective tissue and placed in a modified Krebs solution (Cocks *et al.*, 1985) which was continually gassed with 95% O_2, 5% CO_2 and kept at room temperature (21–23°C). The artery was then cut into 3 mm long rings with a twin-bladed scalpel holder. Some rings had their endothelium removed by gently abrading the luminal surface with a Krebs-moistened filter paper taper (Cocks *et al.*, 1985). Each ring was then mounted on two parallel stainless steel hooks in a water-jacketed, 25 ml organ bath containing Krebs solution maintained at 37°C. The lower hook was attached to a plastic (PVC) support leg and the upper hook to a Grass force-displacement transducer. Changes in isometric, circumferential force were amplified and displayed on a flat-bed chart recorder. After an equilibration period of 60 min the rings were stretched to 4 g tension and allowed 30 min recovery after which time they were again stretched to 4 g. When a steady plateau of resting force was attained (30–40 min) the rings were contracted to a steady level of active force with the thromboxane A_2-mimetic, U46619 with a concentration (30 nM) which caused approximately 80% of the maximal response to U46619 (Cocks & Angus, 1984). Single concentration-responses or concentration-response curves to the compounds being tested were then obtained. At the conclusion of the experiment, the maximal relaxation to sodium nitroprusside (SNP) was obtained and all relaxation responses were then expressed as percentages of this maximal SNP response.

Statistics

All relaxation curves were normalized as percentages of the maximal relaxation to SNP. Each normalized relaxation curve was then computer-fitted with a logistic equation which gave the estimates of the concentration (EC_{50}) of the relaxing agent necessary to give 50% of the maximal response (see Nakashima *et al.*, 1982; Angus *et al.*, 1986). Differences between pairs of mean EC_{50}'s and mean maximal responses were tested for significance by an unpaired Students *t* test. A value of $P<0.05$ was considered to be statistically significant.

Drugs and their source (parentheses)

The following were used: U46619, (1,5,5-hydroxy-11,9-(epoxymethano)prosta-5Z,13E-dienoic acid, Upjohn: Kalamazoo, U.S.A.); A23187, (Calbiochem, U.S.A.); endothelin-1 (Peninsula Labs, U.S.A.); acetylcholine bromide, substance P triacetate, ionomycin, thimerosal, melittin, isoprenaline, N^G-nitro-L-arginine (L-NNA), indomethacin, superoxide dismutase (bovine erythrocytes) (all from Sigma, U.S.A.); N^G-monomethyl-L-arginine (L-NMMA: Institute of Drug Technology, Australia); bradykinin triacetate (Fluka, Switzerland); sodium nitroprusside (Roche, Australia); glyceryl trinitrate (David Bull Laboratories, Australia).

Results

Effect of thimerosal

In rings of artery contracted to a steady level of active force with U46619, thimerosal caused endothelium-dependent relaxations that were concentration-dependent for both magnitude and time to reach maximum. Low concentrations of thimerosal (0.03–1 μM) caused delayed, slowly developing relaxations over 20–40 min with maintained maxima. Higher concentrations of thimerosal (3–10 μM) caused more rapid and maximal relaxations. These relaxations, however, were not maintained. At 10 μM thimerosal, the tissue recovered its U46619-induced contraction fully over 1–2 h after maximal relaxation was maintained for 10–20 min (see Figure 1). After the tissue had relaxed maximally and recovered its U46619 active force in the presence of thimerosal (10 μM), the endothelium-dependent relaxing agents, ACh, SP, BK and the divalent cation ionophore, A23187 were all unable to cause any further relaxation (Figure 1 and Table 1). The endothelium-dependent relaxation response to the calcium ionophore, ionomycin was blocked by 80 ± 7% by this concentration of thimerosal (Table 1). The contractions to the EDRF blocking agent L-NNA (10–100 μM), however, were unaffected by thimerosal (Figure 1 and Table 2). Endothelium-dependent contractions to L-NMMA (10–100 μM) were also unaffected by thimerosal (data not shown). Similar effects as those found with thimerosal were obtained in further experiments with A23187 ($n = 6$), ionomycin ($n = 6$) and melittin ($n = 3$; see Figure 2 and Table 2). For ionomycin and A23187, the relaxation responses were endothelium-dependent but not maintained. Following return of the U46619-induced contraction, addition of other endothelium-dependent relaxing agents failed to cause further relaxations, yet the tissues were able to contract normally to L-NNA (see Figure 2 and Table 2). The same pattern of response was also seen with melittin, except the degree of

recovery over the experimental time was less than that for the other three agents (Figure 2). Melittin had no significant effect on the contraction elicited by L-NNA (Table 2).

Thimerosal (10 μM) did not cause a contraction in either

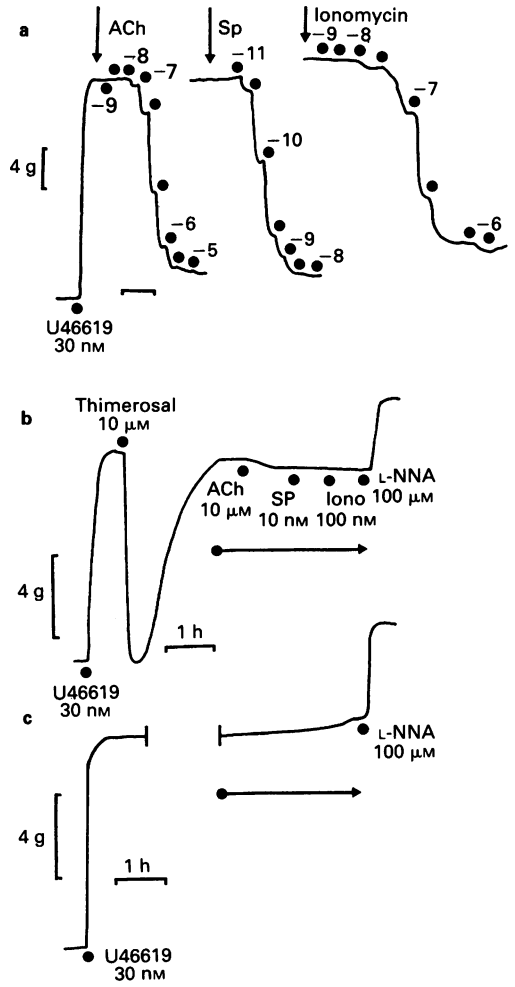

Figure 1 Representative tracings of original chart recordings from endothelium-intact rings of dog, isolated coronary artery contracted to a steady level of force with U46619. (a) Relaxations to cumulative (− log M) additions of acetylcholine (ACh), substance P (SP) and ionomycin. The time calibration bar represents 40 and 4 min before and after the vertical arrow respectively. (b) Maximal but not sustained relaxation to thimerosal followed by total block of responses to ACh, SP and ionomycin (Iono). The tissue was still able to contract normally to N^G-nitro-L-arginine (L-NNA) as compared to the time control shown in (c). The time calibration for the duration of the arrow is 6 min. Note that the break in the trace in (c) corresponds to approximately 100 min.

Table 1 The effect of thimerosal (10 μM) on the relaxation responses to maximal concentrations of acetylcholine, substance P, bradykinin, A23187 and ionomycin in the dog coronary artery

Agonist	*[Agonist]* μM	n	*Thimerosal* (% inhibition)
Acetylcholine	10.0	7	97 ± 1.8
Bradykinin	0.003	4	100 ± 0.0
Substance P	0.01	4	100 ± 0.0
A23187	1.0	4	100 ± 0.0
Ionomycin	0.3	7	80 ± 6.9

n = number of rings from separate animals.
Values are given as mean ± s.e.mean.

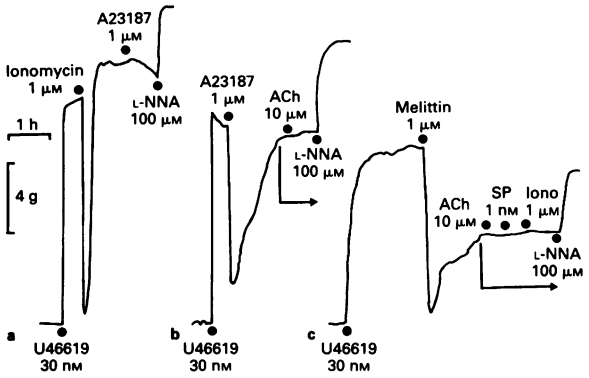

Figure 2 The selective effect of ionomycin (left panel), A23187 (middle panel) and melittin (right panel) on relaxations to EDRF agents (A23187, acetylcholine (ACh), substance P (SP) and ionomycin (Iono)) in rings of endothelium-intact, dog coronary artery contracted to a steady level of force with U46619. In each case, the contraction to N^G-nitro-L-arginine (L-NNA) was unaffected after recovery of the U46619 tone. The time calibration for the duration of the arrows represents 6 min.

Table 2 The effect of thimerosal, ionomycin, A23187 and melittin on the contractile response to N^G-nitro-L-arginine (L-NNA) in the dog coronary artery.

Drug	*[Drug]* μM	n	*[L-NNA]* (μM)	Δ *L-NNA* (% U46619)
U46619	0.003	4	30	28.9 ± 5.9
(control)		9	100	31.8 ± 4.7
Thimerosal	10.0	4	30	26.2 ± 4.3
		9	100	30.5 ± 4.4
Ionomycin	1.0	4	30	24.7 ± 6.6
		5	100	32.8 ± 7.2
A23187	1.0	4	30	32.7 ± 5.2
		5	100	34.3 ± 7.2
Melittin	1.0	4	30	14.6 ± 6.7
		5	100	20.7 ± 3.2

The contractions are expressed as percentage increases in the contraction to U46619 (30 nM).
n = number of rings from separate animals.
Values are given as mean ± s.e.mean.

endothelium-intact or denuded rings of artery without U46619-induced active force, whereas L-NNA (100 μM) contracted the endothelium-intact artery but had no effect on the denuded preparation (see Figure 3). Both the relaxation and the subsequent inhibition of further EDRF(NO) release by thimerosal were uneffected by pretreatment of the tissue with either indomethacin (10 μM) or superoxide dismutase (150 u ml^{-1}) (data not shown).

Concentration-relaxation response curves to thimerosal, A23187 and SNP were obtained in the presence and absence of L-NNA (100 μM) in endothelium-intact rings of coronary artery (Figure 4). L-NNA caused an approximate 10 fold significant rightward shift in the curve to thimerosal (mean EC_{50}'s ± s.e.mean (− log M) for control and L-NNA treatment were 7.0 ± 0.1 and 6.1 ± 0.2 (n = 3) respectively; P = 0.008, unpaired t test). The maximal relaxation to thimerosal was unaffected by L-NNA. L-NNA (100 μM) also caused an approximate 10 fold significant rightwards shift in the relaxation curve to A23187 (mean EC_{50}'s (− log M) for control and L-NNA treatment were 7.8 ± 0.1 and 6.9 ± 0.1 (n = 6 and 7) respectively; P = 0.0002, unpaired t test) although here again the maximal relaxation was not

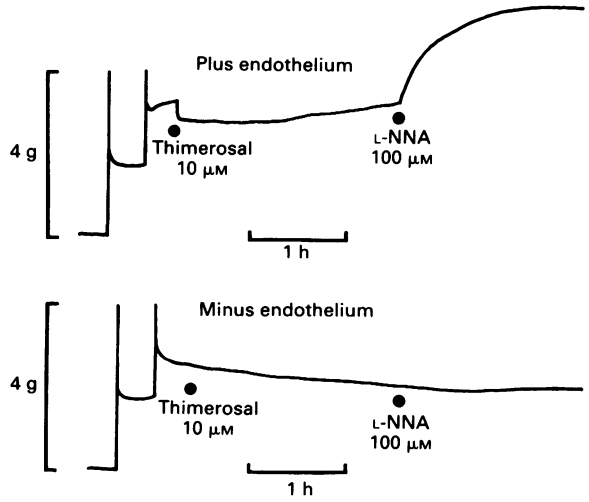

Figure 3 Tracings of original chart recordings from two rings of dog coronary artery showing the effect of removal of the endothelium on the responses to thimerosal and N^G-nitro-L-arginine (L-NNA). Each ring of artery was stretched twice to 4 g before the experiment was started.

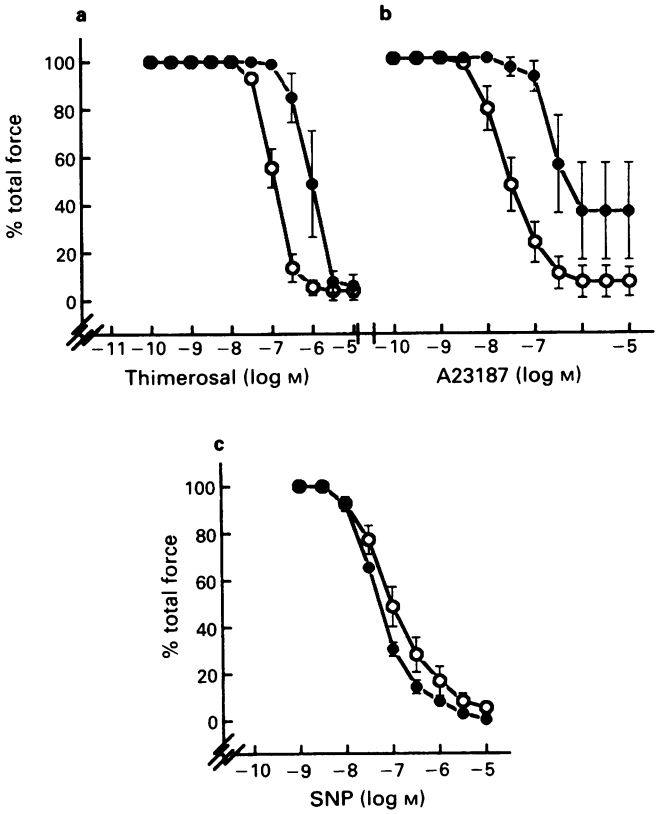

Figure 4 The effect of N^G-nitro-L-arginine (L-NNA, ●, 100 μM) on the concentration-relaxation curve to thimerosal (a), A23187 (b) and sodium nitroprusside (SNP, c) in the dog coronary artery. Open circles (○) depict the control curve for each agent. Data points are means ± s.e.mean (vertical bars).

significantly reduced. The relaxation curve to the endothelium-independent relaxing agent, SNP was unaffected by the same concentration of L-NNA (mean EC_{50}'s (− log M) for control and L-NNA treatment ($n = 6$ and 7) were 7.5 ± 0.1 and 7.4 ± 0.07 respectively; the maximal responses were not significantly different).

A further series of experiments ($n = 3$) was carried out to assess the toxicity of thimerosal on the tissue. Cumulative concentration-contraction curves to U46619 (0.1–100 nM) were obtained 5, 30 and 60 min after the addition of thimerosal (Figure 5). The curve at 5 min was markedly depressed and then showed a time-dependent recovery which approached control responses at 60 min (Figure 5).

Nitrovasodilators

Endothelium-intact rings of artery precontracted with U46619 were exposed continuously to either SNP or glyceryl trinitrate (GTN) at concentrations that caused maximal relaxations (see Figure 6). In each of three separate experiments the relaxation response recovered only poorly during maintained exposure to each of the vasodilators. A three fold higher concentration of U46619 also failed to return the active force to control levels and another constrictor, ET-1 (10 nM) was used to increase active force towards control levels. When these contractions had reached a new steady level of active force, cumulative concentration-relaxation response to the alternative nitrovasodilators were obtained and compared to those in tissues not treated with the nitrovasodilators (Figure 6). Under these conditions of maintained stimulation with either SNP or GTN, further relaxations to the alternate nitrovasodilators were virtually abolished. The tissues, however, were able to relax sensitively to a non-nitrovasodilator, isoprenaline (Figure 6). Thimerosal (100 μM) has no inhibitory effect upon cumulative concentration-relaxation curve to SNP (Figure 7).

Discussion

The major finding from this study was that thimerosal, a compound known to inhibit lysolecithin acetylCoA-transferase (LAT), within endothelial cells (Förstermann *et al.*, 1986a,b), first released EDRF then abolished any further response to a variety of EDRF-releasing agents like ACh and the calcium ionophores, ionomycin and A23187. The endothelium-dependent contractions to the EDRF synthesis inhibitors L-NNA and L-NMMA, however, were unaffected. The relaxation to thimerosal was probably due to release of arginine-derived NO or a related compound, since the res-

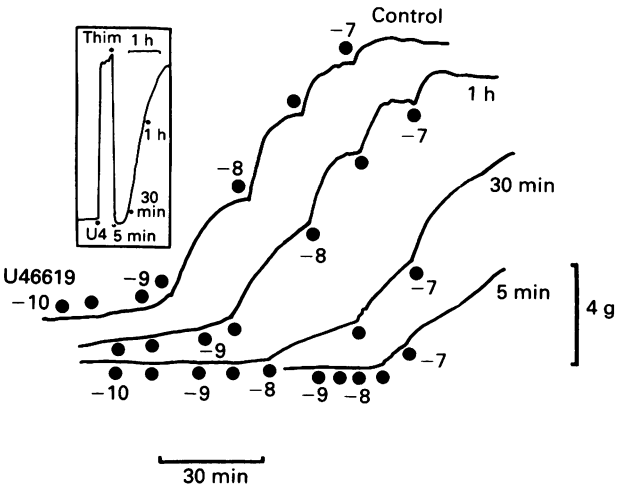

Figure 5 The effect of thimerosal (10 μM) on the cumulative contractions to U46619 in endothelium-intact rings of coronary artery from the dog. Contraction curves were carried out in rings not contracted previously (see Figure 3). The inset shows the time course of a typical response to thimerosal (Thim) in a ring of artery contracted with U46619 (U4) and the corresponding times at which the contraction curves to U46619 were carried out after addition of thimerosal.

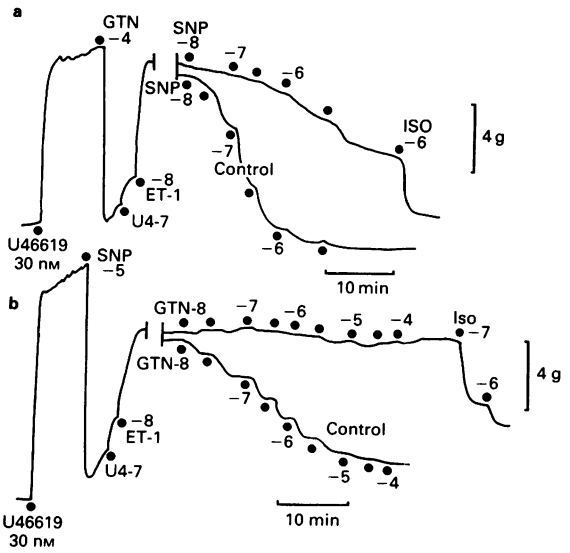

Figure 6 Tracings of original chart recordings depicting the effect of maintained, maximal relaxing concentrations of glyceryl trinitrate (GTN: a) and sodium nitroprusside (SNP: b) on the subsequent cumulative relaxation curves to SNP and GTN respectively. Note active constrictor force was restored in the presence of both nitrovasodilators with higher concentrations of U46619 (U4) and endothelin-1 (ET-1). The initial U46619 contraction for the controls have been omitted for clarity. The breaks in the traces represent 20–30 min. Isoprenaline (Iso) was added to demonstrate normal sensitivity of the nitrovasodilator-treated tissues to non-nitrovasodilators under the conditions of excess U46619 and endothelin.

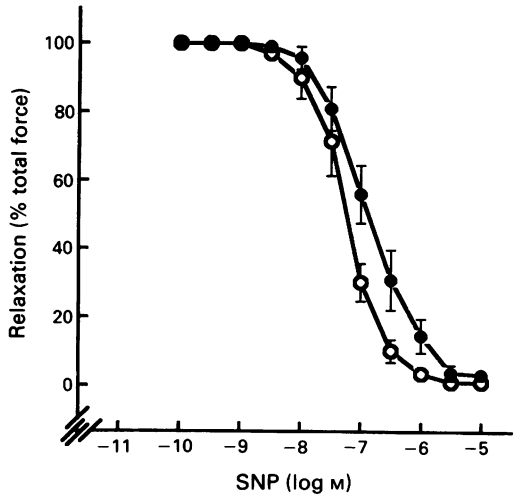

Figure 7 The effect of thimerosal (●, 100 μM) on the relaxation curves to sodium nitroprusside (SNP) in rings of dog coronary artery. Open circles (○) depict the control curve for SNP. Data points are means ± s.e.mean (vertical lines).

ponse was blocked by both L-NNA and L-NMMA. Although the block with L-NNA for thimerosal was relatively small (approximately 10 fold rightwards displacement of the EC_{50} at 100 μM L-NNA with no change in range), it was nevertheless similar to that for A23187. We have previously found that EDRF-mediated relaxations in the greyhound coronary artery *in vitro* are relatively resistant to block by the L-arginine analogues (Cocks & Angus, 1991), which probably reflects either tighter coupling or more reserve of the NOS-NO/cyclic GMP transduction system in this tissue than in other tissues like the rabbit aorta (see Martin *et al.*, 1992). Thimerosal was unlikely to have interacted with NO directly since the relaxation curve to SNP was unaffected by thimerosal.

LAT, which mediates the re-incorporation of arachidonic acid (as arachidonyl CoA) into membrane lecithin via lysolecthin constitutes one of the enzymatic arms of the Lands cycle (Lands, 1960; Lands & Merkl, 1963), the other being phospholipase A_2 which catalyzes the breakdown of membrane-bound lecithin to lysolecithin and arachidonic acid. Arachidonic acid and/or its metabolites are known to interact with other transducing systems to modulate or amplify their signals. Therefore, taken together with the early evidence that EDRF was an arachidonic acid metabolite (see below), we suggest that arachidonic acid or one of its metabolites plays an important role in the regulation of stimulated EDRF release. Such an action would be not only novel, but it would also bring together much of the pre- and post-NOS/NO literature into a unified mechanism for the regulation of EDRF synthesis.

Many studies on the nature of EDRF prior to the discovery of the NOS/NO signalling system (see Moncada *et al.*, 1991) clearly suggested a role for arachidonic acid in its synthesis and/or release (see Angus & Cocks, 1989). For example, quinacrine, a supposedly specific phospholipase A_2 inhibitor (Flower & Blackwell, 1976) was one of the most commonly used blockers of EDRF-mediated relaxation responses in isolated blood vessels (Furchgott, 1981; 1984; Cocks & Angus, 1984; Angus & Cocks, 1989). Also, the potent phospholipase A_2 inhibitor, *p*-bromophenacyl bromide (*p*-BPB) completely and irreversibly inhibited relaxation responses of isolated vessels to acetylcholine and A23187 without affecting those to endothelium-independent relaxants like sodium nitroprusside and isoprenaline (Furchgott, 1983; Chand *et al.*,1987). Endothelial cell viability may be a problem with *p*-BPB (see Furchgott, 1983) but Chand *et al.* (1987) also showed that indomethacin-sensitive and endothelium-independent relaxations of rabbit pulmonary artery were selectively blocked by *p*-BPB. Therefore, although it was possible that *p*-BPB may be toxic to endothelial cells, it selectively and potently blocked the release of prostacyclin from smooth muscle cells. Förstermann & Neufang (1985) showed that melittin, a bee venom polypeptide (Haberman, 1972) that activates release of arachidonic acid from membrane phospholipids (Schier, 1978) by stimulating phospholipase A_2, and acetylcholine both caused endothelium-dependent relaxations and release of prostacyclin in rabbit isolated aortic strips. In each case, both the relaxation response and the release of prostacyclin were blocked by quinacrine and a variety of lipoxygenase inhibitors but only the generation of prostacyclin was inhibited by indomethacin (Förstermann & Neufang, 1985). These results suggest that melittin does not act at some site distal to the release of arachidonic acid such as interaction with calmodulin (Mülsch & Busse, 1991 and see below). Förstermann and colleagues also demonstrated that thimerosal acted like melittin except that the relaxation response to thimerosal was not blocked by quinacrine whereas that to acetylcholine was (Förstermann *et al.*, 1986a,b). They suggested that thimerosal may interact with a thiol group, perhaps of LAT, since the relaxation response to thimerosal was completely blocked by thiol compounds like glutathione and 2-mercaptoethanol whilst that to acetylcholine was unaffected (Förstermann *et al.*, 1986b).

Thimerosal may also interact with thiol groups other than those on LAT. Thus Hecker *et al.* (1989) proposed that thimerosal-induced platelet aggregation occurs via oxidation of thiol groups of an internal Ca^{2+} pool which leads to release of Ca^{2+}, activation of phospholipase A_2 and subsequently release of arachidonic acid. The concentration of thimerosal used in that study, however, was 4–5 times greater than that used in ours. Also, since release of EDRF is thought to depend more on influx of extracellular calcium through a receptor-operated ion channel rather than release

from an intracellular store (Long & Stone, 1985; Griffith *et al.*, 1986; Peach *et al.*, 1987; Johns *et al.*, 1987; Lodge *et al.*, 1988; see Angus & Cocks, 1989), it is unlikely that the total block by thimerosal of relaxations to all the EDRF-releasing agonists, including the calcium ionophores, was due to block of release of calcium from an intracellular store.

Another possible explanation for the effect of thimerosal on vascular endothelial cells is a direct chemical interaction between EDRF and thimerosal if, as has been suggested, EDRF is a nitrosothiol compound and not simply NO (Myers *et al.*, 1990). The endothelium-dependent relaxation to thimerosal, combined with its total block of relaxations to EDRF-releasing agonists may indicate that if EDRF is such a nitrosothiol compound then it may be stored within endothelial cells as first suggested by Cocks & Angus (1991). Thimerosal could deplete this store by oxidizing the thiol group of EDRF, thereby releasing NO. Since thimerosal had no effect on the contractions to L-NNA and L-NMMA, basal EDRF may represent a different chemical form of EDRF, possibly NO. Others have also suggested that stimulated and basal NO release may be derived from different sources (Randall & Griffith, 1991).

Block of the relaxation responses to EDRF agonists by thimerosal, melittin and the calcium ionophores was unlikely to be due to maximal, sustained release of EDRF, even when the tissues had recovered their active force. The marked inhibition of the relaxation curves to SNP and GTN in the continual presence of a maximally-relaxing concentration of GTN or SNP respectively, but with active force restored with ET-1 indicates that sustained activation of guanylate cyclase not only maintains the vessel in a maximally relaxed state which is difficult to overcome with excess amounts of vasoconstrictors, but also when active force can be partially restored, even in the presence of maximal guanylate cyclase activation, relaxation to other nitrovasodilators is blocked. Thus if thimerosal continually released EDRF maximally, it would first be difficult to reverse this relaxation and second the relaxation curve to SNP would be expected to be blocked, both of which were found not to occur. Also thimerosal did not appear to have a toxic effect on the tissue since both the endothelium-dependent contractions to the N^G-arginine analogues (L-NNA and L-NMMA) as well as those to the thromboxane-mimetic, U46619 were unaffected by prolonged treatment with thimerosal.

Other compounds such as A23187, ionomycin and melittin had an effect comparable to that of thimerosal. Melittin is a potent activator of phospholipase A_2 and as such would be expected to cause a build-up of intracellular arachidonic acid. Part of the inhibitory effect of melittin on the release of EDRF may also be explained in terms of its ability to bind to calmodulin (see Mülsch & Busse, 1991). A calmodulin binding site has been discovered on the NOS enzyme (Bredt *et al.*, 1991), which is further evidence that Ca^{2+} plays a crucial role in the production of EDRF. The divalent cationic ionophore A23187 is also known to inhibit LAT (see Mülsch *et al.*, 1989) and thus, like thimerosal and melittin could cause an increase in intracellular arachidonic acid. It is unknown if the more selective calcium ionophore, ionomycin also inhibits LAT. Like thimerosal, however, all of these compounds released large amounts of EDRF-like material from the coronary artery which after 10–20 min was not sustained and the tissue recovered its initial level of active force. From this pattern of activity of the three different classes of compounds (thimerosal, melittin and the calcium ionophores), we suggest that both the relaxation and the recovery phases of each compound's response are caused by first accumulation and then depletion of arachidonic acid from a phospholipid pool sensitive to phospholipase A_2.

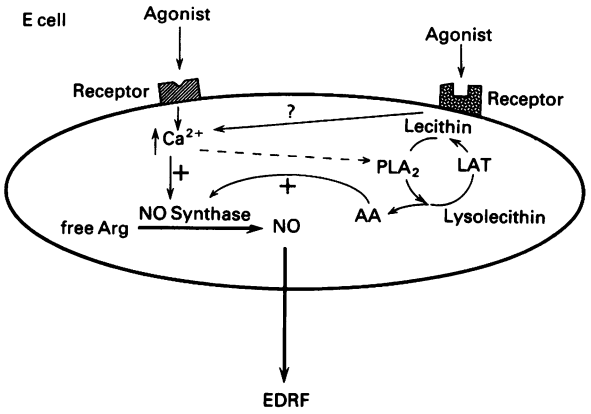

Figure 8 Schema for the proposed mechanism of action of thimerosal and role of arachidonic acid in regulation of endothelium-derived relaxing factor (EDRF) synthesis in endothelial cells (E cell). Abbreviations: free Arg, free levels of intracellular L-arginine; NO synthase, nitric oxide synthase; AA, arachidonic acid; PLA_2, phospholipase A_2; LAT, lysolecithin acylCoA-transferase.

Since L-NNA and L-NMMA were still able to contract the tissues apparently depleted of arachidonic acid, basal EDRF release does not appear to require release of arachidonic acid. There are at least two different forms of nitric oxide synthase (NOS). One, the so-called constitutive type is dependent on calcium for its activity and is the main type found in endothelial cells as well as platelets and the brain (Förstermann *et al.*, 1991). The other, the inducible form is calcium-independent and is found in a wide variety of cells (see Moncada *et al.*, 1991). Therefore basal EDRF may be synthesized from L-arginine by a different form of NOS from that which mediates agonist and ionophore-stimulated EDRF release (see also Randall & Griffith, 1992). Support for this comes from Mülsch *et al.* (1989) who demonstrated that native porcine endothelial cells synthesize EDRF from L-arginine via both a Ca^{2+}-sensitive and Ca^{2+}-insensitive pathway.

In conclusion, this study provides indirect evidence, that either arachidonate or one of its non-cyclo-oxygenase products may play an integral role in the regulation of EDRF release. Thimerosal, a known inhibitor of LAT in endothelial cells, blocked the relaxation responses to various EDRF-releasing agents whilst it had no affect on the contractions to the L-arginine analogue inhibitors of NOS, L-NNA and L-NMMA and therefore by inference had no effect on basal EDRF release. We hypothesize that arachidonic acid, possibly generated via activity of the Lands Cycle, either amplifies the activating effect of Ca^{2+} on NOS or releases more Ca^{2+} from intracellular stores which in turn stimulates NOS above its basal level of activity to generate NO (see Figure 8). Interestingly, arachidonic acid has been shown to cause endothelium-dependent relaxations in the rabbit aorta (Pinto *et al.*,1986; for review see Angus & Cocks, 1989). This finding is consistent with our hypothesis on the involvement of arachidonic acid in EDRF release. The results from the present study, however, are also compatible with the idea that stimulated EDRF is derived from a preformed 'pool', possibly as a nitrosthiol (Myers *et al.*, 1991; Ignarro, 1991; Cocks & Angus, 1991) whilst basal EDRF is simply NO.

This work was funded in part from an Institute Grant from the National Health and Medical Research Council of Australia and Glaxo Australia. We thank Dr James Angus and Dr Ian Smith for their helpful comments.

References

ANGUS, J.A., COCKS, T.M. & SATOH, K. (1986). α_2-Adrenoceptors and endothelium-dependent relaxation in canine large arteries. *Br. J. Pharmacol.*, **88**, 767–777.

ANGUS, J.A. & COCKS, T.M. (1989). Endothelium-derived relaxing factor. *Pharmacol. Ther.*, **41**, 303–351.

BERRIDGE, M.J. & IRVINE, R.F. (1989). Inositol triphosphate, a novel second messenger in cellular signal transduction. *Nature*, **312**, 315–321.

BREDT, S.D., HWANG, P.M., GLATT, C.E., LOWENSTEIN, C., REED, R.R. & SNYDER, S.S. (1991). Cloned and expressed nitric oxide synthase structurally resembles cytochrome P-450 reductase. *Nature*, **351**, 714–718.

CHAND, N., MAHONEY, T.P. Jr, DIAMANTIS, W. & SOFIA, R.D. (1987). Pharmacological modulation of bradykinin, acetylcholine and calcium ionophore A23187-induced relaxation of rabbit pulmonary arterial segments. *Eur. J. Pharmacol.*, **137**, 173–177.

COCKS, T.M. & ANGUS, J.A. (1984). Endothelium-dependent modulation of blood vessel reactivity. In *The Peripheral Circulation*. ed. Hunyor, S., Ludbrook, J., Shaw, J. & McGrath, M. pp. 9–22. Amsterdam: Elsevier.

COCKS, T.M., ANGUS, J.A., CAMPBELL, J.H & CAMPBELL, G.R. (1985). Release and properties of endothelium-derived relaxing factor (EDRF) from endothelial cells in culture. *J. Cell Physiol.*, **123**, 315–320.

COCKS, T.M. & ANGUS, J.A. (1991). Evidence that contractions of isolated arteries by L-NMMA and NOLA are not due to inhibition of basal EDRF release. *J. Cardiovasc. Pharmacol.*, **17** (Suppl. 3), S159–S164.

FLOWER, R.J. & BLACKWELL, G.J. (1976). The importance of phospholipase-A_2 in prostaglandin biosynthesis. *Biochem. Pharmacol.*, **25**, 281–291.

FÖRSTERMANN, U. & NEUFANG, B. (1985). Endothelium-dependent vasodilation by melittin: are lipoxygenase products involved? *Am. J. Physiol.*, **249**, H14–H19.

FÖRSTERMANN, U., BURGWITZ, K. & FRÖLICH, J.C. (1986a). Thimerosal induces endothelium-dependent vascular smooth muscle relaxation by interacting with thiol groups. *Naunyn-Schmiedebergs Arch. Pharmacol.*, **334**, 501–507.

FÖRSTERMANN, U., GOPPELT-STRÜBE, M., FRÖLICH, J.C. & BUSSE, R., (1986b). Inhibitors of acyl-coenzyme A:lysolecthin acyltransferase activate the production of endothelium-derived vascular relaxing factor. *J. Pharmacol. Exp. Ther.*, **238**, 352–359.

FÖRSTERMANN, U., SCHMIDT, H.H.W., POLLOCK, J.S., SHENG, H., MITCHELL, J.A., WARNER, T.D., NAKANE, N. & MURAD, F. (1991). Isoforms of nitric oxide synthase; characterization and purification from different cell types. *Biochem. Pharmacol.*, **42**, 1849–1857.

FURCHGOTT, R.F. (1981). The requirement for endothelial cells in the relaxation of arteries by acetylcholine and some other vasodilators. *Trends. Pharmacol. Sci.*, **2**, 173–176.

FURCHGOTT, R.F. (1984). The role of endothelium in the responses of vascular smooth muscle and drugs. *Annu. Rev. Pharmacol. Toxicol.*, **24**, 175–197.

GOPPELT-STRÜBE, M., KORNER, C.F., HAUSMANN, G., GEMSA, D. & RESCH, K. (1986). Control of prostanoid synthesis: role of reincorporation of released precursor fatty acids. *Prostaglandins*, **32**, 373–386.

GRIFFITH, T.M., EDWARDS, D.H., NEWBY, A.C., LEWIS, M.J. & HENDERSON, A.H. (1986). Production of endothelium derived relaxing factor is dependent on oxidative phosphorylation and extracellular calcium. *Cardiovasc. Res.*, **20**, 7–12.

HABERMAN, E. (1972). Bee and wasp venoms. *Science*, **177**, 314–322.

HECKER, M., BRÜNE, B., DECKER, K. & ULLRICH, V. (1989). The sulfhydryl reagent thimerosal elicits human platelet aggregation by mobilization of intracellular calcium and secondary prostaglandin endoperoxide formation. *Biochem. Biophys. Res. Commun.*, **159**, 961–968.

IGNARRO, L.J. (1991). Heme-dependent activation of guanylate cyclase and cyclic GMP formation by endogenous nitric oxide: A unique transduction mechanism for transcellular signaling. *Blood Vessels*, **28**, 67–73.

JOHNS, A., LATEGAN, T.W., LODGE, N.J., RYAN, U.S., VAN BREEMAN, C. & ADAMS, D.J. (1987). Calcium entry through receptor-operated channels in bovine pulmonary artery endothelial cells. *Tissue Cell*, **19**, 733–745.

LANDS, W.E.M. (1960). Metabolism of glycerolipids: the enzymatic acylation of lysolecthins. *J. Biol. Chem.*, **235**, 2233–2237.

LANDS, W.E.M. & MERKL, I. (1963). Metabolism of glycerolipids: reactivity of various acyl esters of co-enzymeA with α-acylglycero-phosphorylcholine, and positional specificities in lecithin synthesis. *J. Biol. Chem.*, **238**, 898–904.

LODGE, N.J., ADAMS, D.J., JOHNS, A., RYAN, U.S. & VAN BREEMAN, C. (1988). Calcium activation of endothelial cells. In *Proceedings of the Second International Symposium on Resistance Arteries*. ed. Halpen, W., Ithaca, New York: Perinatology Press.

LONG, C.J. & STONE, T.W. (1985). EDRF: a Ca^{2+}-dependent chemical moiety(ies). *Trends Pharmacol. Sci.*, **6**, 285.

LOPEZ-JARAMILLO, P., GONZALEZ, M.C., PALMER, R.M.J. & MONCADA, S. (1990). The crucial role of physiological Ca^{2+} concentrations in the production of endothelial nitric oxide and the control of vascular tone. *Br. J. Pharmacol.*, **101**, 489–493.

MARTIN, G.R., BOLOFO, M.L. & GILES, H. (1992). Inhibition of endothelium-dependent vasorelaxation by arginine analogues: a pharmacological analysis of agonist and tissue dependence. *Br. J. Pharmacol.*, **105**, 643–652.

MONCADA, S., PALMER, R.M.J. & HIGGS, E.A. (1991). Biosynthesis and endogenous roles of nitric oxide. *Pharmacol. Rev.*, **43**, 109–142.

MÜLSCH, A., BASSENGE, E. & BUSSE, R. (1989). Nitric oxide synthesis in endothelial cytosol: evidence for a calcium-dependent and a calcium-independent mechanism. *Naunyn-Schmiedeburgs Arch. Pharmacol.*, **340**, 767–770.

MÜLSCH, A. & BUSSE, R. (1991). Nitric oxide synthase in native and cultured endothelial cells: Calcium/calmodulin and tetrahydrobiopterin are cofactors. *J. Cardiovasc. Pharmacol.*, **17** (Suppl. 3), S52–S56.

MYERS, P.R., MINOR, R.L.Jr., GUERRA, R.Jr., BATES, J.N. & HARRISON, D.G. (1990). Vasorelaxant properties of the endothelium-derived relaxing factor more closely resemble s-nitrocysteine than nitric oxide. *Nature*, **345**, 161–163.

NAKASHIMA, A., ANGUS, J.A. & JOHNSTON, C.L. (1982). Comparison of angiotensin converting enzyme inhibitors captopril and MK4211-Diacid in guinea pig atria. *Eur. J. Pharmacol.*, **81**, 487–492.

PALMER, R.M.J., FERRIGE, A.G. & MONCADA, S. (1987). Nitric oxide release accounts for the biological activity of endothelium-derived relaxing factor. *Nature*, **327**, 524–526.

PEACH, M.J., SINGER, H.A., IZZO, N.J. & LOEB, A.L. (1987). Role of calcium in endothelium-dependent relaxation of arterial smooth muscle. *Am. J. Cardiol.*, **59**, 35A–43A.

PINTO, A., ABRAHAM, N.G. & MULLANE, K.E. (1986). Cytochrome P-450-dependent monoxygenase activity and endothelial-dependent relaxations induced by arachidonic acid. *J. Pharmacol. Exp. Ther.*, **236**, 445–451.

RANDALL, M.D. & GRIFFITH, T.M. (1991). Differential effects of L-arginine on the inhibition by N^G-nitro-L-arginine methyl ester of basal and agonist-stimulated EDRF activity. *Br. J. Pharmacol.*, **104**, 743–749.

REES, D.D., PALMER, R.M.J., SCHLUZ, R., HODSON, H.F. & MONCADA, S. (1990). Characterization of three inhibitors of endothelial nitric oxide synthase *in vitro* and *in vivo*. *Br. J. Pharmacol.*, **101**, 746–752.

SCHIER, W.T. (1978). Activation of high levels of endogenous phospholipase A_2 in cultured cells. *Proc. Natl. Acad. Sci. U.S.A.*, **76**, 195–199.

ZEITLER, P., WU, Y.Q. & HANDWERGER, S. (1991). Melittin stimulates phosphoinositide hydrolysis and placental lactogen release: Arachidonic acid as a link between phospholipase-A_2 and phospholipase C signal transduction pathways. *Life Sci.*, **48**, 2089–2095.

(Received March 23, 1992
Revised June 12, 1992
Accepted June 17, 1992)

Br. J. Pharmacol. (1992), **107**, 573–576

Effects of the δ-opioid receptor antagonist naltrindole on antinociceptive responses to selective δ-agonists in post-weanling rats

T.J. Crook, [1] I. Kitchen & *R.G. Hill

Receptors and Cellular Regulation Research Group, School of Biological Sciences, University of Surrey, Guildford, Surrey GU2 5XH and *Merck Sharp and Dohme Research Laboratories, Neuroscience Research Centre, Harlow, Essex CM20 2QR

1 Antagonism, by the selective δ-opioid receptor antagonist naltrindole, of the antinociceptive effects of [D-Pen^2, D-Pen^5] enkephalin (DPDPE), [D-Ser^2, Leu^5, Thr^6] enkephalin (DSLET) and D-Ala^2 deltorphin I (DELT I) has been studied in 25 day old rats.

2 Antinociception was measured by the 50°C tail immersion test following i.p. administration of agonists and/or antagonists.

3 Dose-related antinociception was observed with DPDPE, DSLET and DELT I and ED_{75} doses were computed (0.66 mg kg^{-1}, 0.65 mg kg^{-1}, 0.032 mg kg^{-1} respectively) and used for antagonism studies.

4 Naltrindole (0.01 mg kg^{-1}) significantly attenuated the antinociceptive effects of DPDPE and DSLET with 0.1 mg kg^{-1} producing complete reversal of the effects of the ED_{75} dose. In contrast, naltrindole at 0.01 and 0.1 mg kg^{-1} did not alter antinociceptive responses to DELT I. Naltrindole at 1 mg kg^{-1} significantly attenuated DELT I antinociception.

5 Naloxone (1 mg kg^{-1}) produced equivalent degrees of antagonism of the antinociceptive effects of DPDPE, DSLET and DELT I. ICI 174,864 (1 mg kg^{-1}) also antagonized antinociception with a differential degree of attenuation (DSLET > DPDPE > DELT I).

6 Naltrindole (1 mg kg^{-1}) had no effect on the antinociception induced by the selective μ-agonist alfentanil (60 μg kg^{-1}). Naltrindole, naloxone or ICI 174,864 had no effect on nociceptive latencies.

7 The differential antagonism by naltrindole of the effects of three selective δ-agonists suggests δ-receptor heterogeneity. Further, the lower sensitivity of response to DELT I suggests that this agent may exert its antinociceptive effects at a different δ receptor subtype from DPDPE or DSLET.

Keywords: Antinociception; δ-opioid receptors; ontogeny; naltrindole; δ-agonists

Introduction

Results from *in vitro* and *in vivo* experimental studies strongly suggest the existence of three primary opioid receptor types (μ, δ and κ) (see Paterson *et al.*, 1983). Elucidation of the role of the δ-opioid receptor has in the past been hampered because of a lack of selective, stable, non-peptide agonists and antagonists. Several high affinity, δ-selective peptide agonists have now been produced (Grace *et al.*, 1980; Mosberg *et al.*, 1983; Erspamer *et al.*, 1989) and recently a selective non-peptide antagonist, naltrindole has become available (Portoghese *et al.*, 1988). These pharmacological tools have allowed a re-examination of the possible roles of the δ-opioid receptor and, in particular, studies in mice with naltrindole and its benzofuran analogue have suggested the existence of δ-receptor subtypes (Sofuoglu *et al.*, 1991). We further addressed this possibility by studying the ability of naltrindole to antagonize the antinociceptive responses to three highly selective δ-agonists, [D-Pen^2, D-Pen^5] enkephalin (DPDPE), [D-Ser^2, Leu^5, Thr^6] enkephalin (DSLET) and D-Ala^2 deltorphin I (DELT I) in postweanling rats.

Methods

Animals and experimental conditions

Male Wistar albino rats (University of Surrey strain) 25 days old and weighing 60–90 g, were used in all studies. All rats were housed in groups of 8–10 and maintained at 22 ± 1°C in a constant 12 h light-dark cycle (lights on at 07 h 00 min). Experimental procedures were carried out in a quiet, windowless, air-conditioned laboratory between 14 h 00 min and 18 h 00 min to minimize diurnal variation. Animals were allowed to acclimatize for 2 h before experimentation.

Nociceptive testing

Animals were divided into treatment groups so that nociceptive tests took place for saline- and drug-treated animals on at least three separate days. Drugs (in 0.9% w/v saline) were administered i.p. in a dose volume no greater than 0.1 ml. Nociceptive responses were measured by the 50°C warm water tail immersion test (Janssen *et al.*, 1963) adapted for young rats (Kitchen *et al.*, 1984). Nociceptive responses were defined as withdrawal of the tail from the surface of the water and a maximum 10 s cut-off was used. Response latencies were measured 15 min before administration of the δ-agonists DPDPE, DSLET, DELT I or the μ-agonist alfentanil and nociceptive responses measured 2, 5, 10 and 15 min after treatment.

When studied, antagonists (naloxone, naltrindole or ICI 174,864) were injected 10 min before agonist administration. The ED_{75} of each of the δ-agonists was chosen for antagonism studies and calculated as the 75% of maximum effect from full dose-response curves at peak antinociception (5 min) with saline control values defined as 0%.

Drugs and statistical procedures

Drugs used were [D-Pen^2, D-Pen^5], enkephalin (DPDPE), [D-Ser^2, Leu^5, Thr^6] enkephalin (DSLET), ICI 174,864 (Allyl$_2$-

[1] Author for correspondence.

Tyr-Aib-Aib-Phe-Leu-OH; Cambridge Research Biochemicals), D-Ala^2 deltorphin I (DELT I) (Bachem), alfentanil HCl (Janssen Pharmaceuticals), naloxone (Dupont) and naltrindole HCl (NTI) (Research Biochemicals Incorporated).

Antagonism of the antinociceptive responses to the δ-agonists was analysed by analysis of variance followed by *post-hoc* analysis with Dunnett's test.

Results

Administration of increasing doses of DPDPE, DSLET and DELT I induced a dose-related antinociception with ED_{75}s of 0.66 mg kg^{-1}, 0.65 mg kg^{-1}, 0.032 mg kg^{-1} respectively. Responses to all three agonists were qualitatively similar with peak antinociception being observed 5 min after administration (Figure 1a,b,c).

Figure 2a,b,c shows the effects of NTI (0.01–1 mg kg^{-1}) on the antinociceptive responses to the ED_{75} dose of DSLET, DPDPE and DELT I respectively. NTI (0.01 mg kg^{-1}) significantly attenuated the peak response to DPDPE and DSLET, while higher doses (0.1 and 1 mg kg^{-1}) completely antagonized the antinociceptive response to DSLET. NTI (0.1 mg kg^{-1}) markedly reduced the response to DPDPE and the response following 1 mg kg^{-1} NTI was not significantly different from saline control values. In contrast, NTI (0.01 and 0.1 mg kg^{-1}) did not alter antinociception induced by DELT I, and only the highest dose of NTI (1 mg kg^{-1}) significantly antagonized antinociception induced by this agonist.

Naloxone (1 mg kg^{-1}) significantly antagonized response to DPDPE, DSLET and DELT I producing a similar degree of attenuation of the antinociceptive effects of all three agonists (Figure 3). ICI 174,864 (1 mg kg^{-1}) also significantly antagonized the antinociceptive effects of these agonists with a differential degree of attenuation (DSLET> DPDPE> DELT I). Further, ICI 174,864 (2 mg kg^{-1}) completely blocked antinociceptive responses to all the δ-agonists (data not shown) but at this dose in some animals this antagonist caused behavioural toxicity, including hindlimb stretching, flaccidity and barrel rolling. NTI and naloxone showed no overt behavioural toxicity at the highest doses used.

NTI (1 mg kg^{-1}) and ICI 174,864 (2 mg kg^{-1}) had no effect on the antinociceptive response induced by a submaximal dose (60 μg kg^{-1}) of the μ-agonist alfentanil (Figure 4).

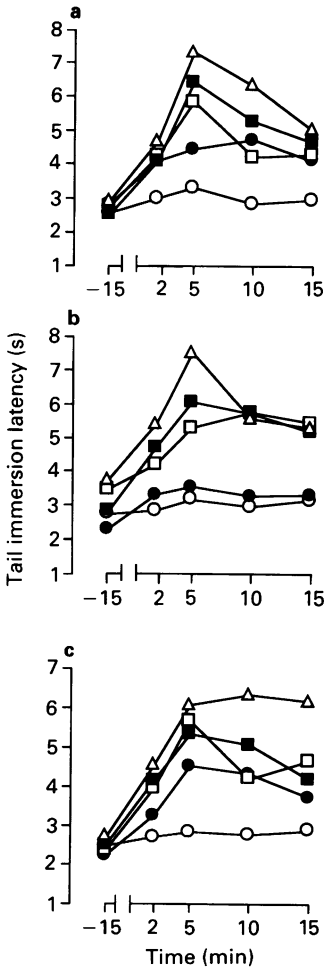

Figure 1 Time course of the antinociceptive effects of (a) [D-Ser^2, Leu^5, Thr^6] enkephalin (DSLET), (b) [D-Pen^2, D-Pen^5] enkephalin (DPDPE) and D-Ala^2 deltorphin (DELT I) in 25 day old rats using the tail immersion test. Values are means of at least six observations. Error bars are omitted for clarity of presentation; s.e.mean varied from 3–14% of the mean value. (○) Represents saline treated controls; (●) 0.25 (DSLET), 0.25 (DPDPE), 0.02 (DELT I) mg kg^{-1}; (□) 0.5 (DSLET), 0.5 (DPDPE), 0.05 (DELT I) mg kg^{-1}; (■) 0.75 (DSLET), 2 (DPDPE), 0.1 (DELT I) mg kg^{-1}; (△) 1 (DSLET), 4 (DPDPE), 0.15 (DELT I) mg kg^{-1}.

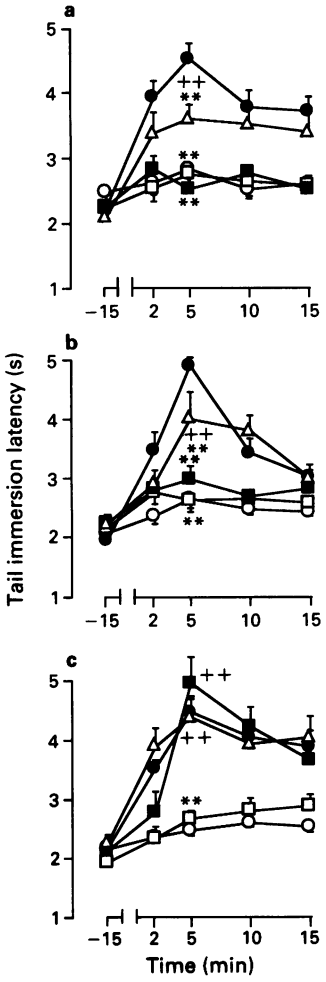

Figure 2 Effect of increasing doses of naltrindole (NTI) on the antinociceptive response to ED_{75} of (a) DSLET (b) DPDPE and (c) DELT I in 25 day old rats using the tail immersion test. Values are means ± s.e.mean of at least six observations. (○) Saline; (●) 0.65 mg kg^{-1} DSLET, 0.66 mg kg^{-1}, DPDPE, 0.032 mg kg^{-1}, DELT I; (□) agonists + 1 mg kg^{-1} NTI; (■) agonists + 0.1 mg kg^{-1} NTI; (△) agonists + 0.01 mg kg^{-1} NTI.
Significant differences vs saline control at 5 min $P<0.01$ DSLET alone, DSLET + 0.01 mg kg^{-1} NTI. Significant differences at 5 min $^{**}P<0.01$ vs agonist alone, $^{++}P<0.01$ vs saline control. Responses to antagonist alone were not significantly different from saline controls (data not shown). For abbreviations see legend to Figure 1.

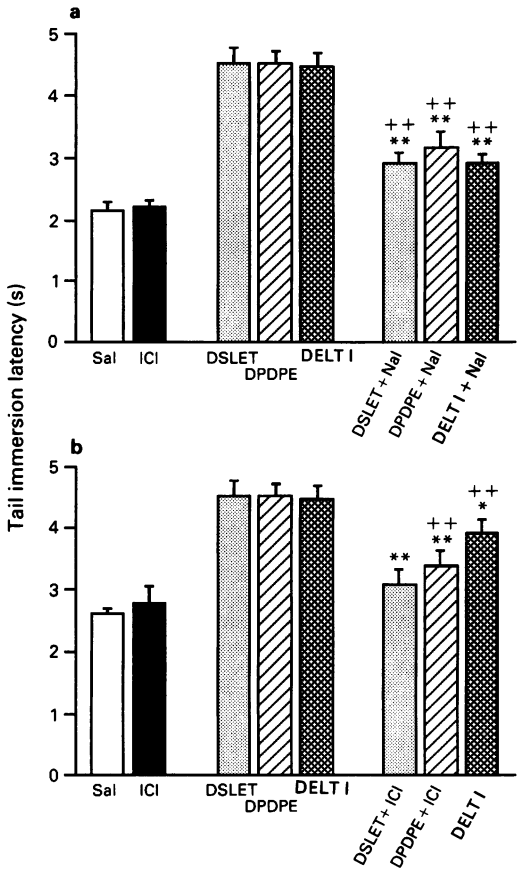

Figure 3 Effect of (a) naloxone and (b) ICI 174,864 on the peak antinociceptive response (5 min) to an ED_{75} of DSLET, DPDPE and DELT I in 25 day old rats in the tail immersion test. Values are the mean (± s.e.mean, vertical bars) of at least six observations. Sal = saline; Nal = naloxone 1 mg kg^{-1}; ICI = ICI 174,864, 1 mg kg^{-1}; DSLET 0.65 mg kg^{-1}; DPDPE 0.66 mg kg^{-1}; DELT I 0.032 mg kg^{-1}. For other abbreviations see legend to Figure 1. $^{**}P<0.01$; $^{*}P<0.05$ vs agonist alone; $^{++}P<0.01$ vs saline control.

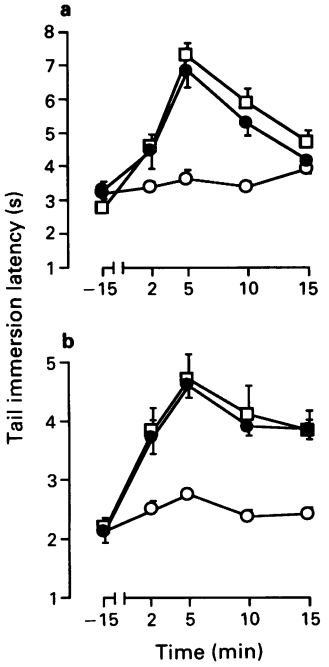

Figure 4 Effect of (a) naltrindole (NTI) and (b) ICI 174,864 on the antinociceptive response to alfentanil in 25 day old rats in the tail immersion test. Values are means (± s.e.mean, vertical bars) of at least six observations: (○) 1 mg kg^{-1} NTI (a), 2 mg kg^{-1} ICI 174,864 (b); (●) 60 μg kg^{-1} alfentanil; (□) 60 μg kg^{-1} alfentanil + 1 mg kg^{-1} NTI (a), 2 mg kg^{-1} ICI 174,864 (b). Alfentanil vs alfentanil + antagonist: not significant.

None of the antagonists (NTI, ICI 174,864 and naloxone) used had any effects on nociceptive latencies in the tail immersion test when administered alone.

Discussion

Determination of the importance of the δ-opioid receptor in mediating antinociception has been difficult because of the lack of suitable brain-penetrating selective agonists and antagonists. Studies with the selective ligand DPDPE implicate δ-sites in both spinal (Rodriguez *et al.*, 1986) and supraspinal (Heyman *et al.*, 1987) antinociception. Most studies have employed intrathecal or intracerebroventricular routes for administration of these agonists (Galligan *et al.*, 1984; Porreca *et al.*, 1987; Suh & Tseng, 1990) and administration by parental routes in the rat has been generally unsuccessful in inducing antinociception (Tavani *et al.*, 1989).

Our success in obtaining dose-related antinociceptive responses to DPDPE, DSLET and DELT I after i.p. injection most probably reflects the age of the animals used since in the rat, the blood brain barrier is not fully mature until postnatal day 30 (Keep *et al.*, 1986). We have also previously demonstrated δ-receptor operated stress-induced antinociception in 25 day old rats (Kitchen & Pinker, 1990).

NTI shows 100 fold selectivity for δ-receptors over other opioid receptors in isolated tissue preparations (Portoghese *et al.*, 1988) and in radioligand binding studies (Rogers *et al.*, 1991). The confirmation of the δ-receptor selectivity of NTI at doses used in this study was provided by lack of antagonism of the highly selective μ-agonist, alfentanil, and agrees with our previous assessment of *in vivo* selectivity of this antagonist (Kitchen & Pinker, 1990) and that of others (Calcagnetti & Holtzmann, 1991).

The observation that responses to DPDPE, DSLET and DELT I were antagonized to an equivalent degree by naloxone confirms opioid receptor mediation. The differential sensitivity to antagonism by NTI points to the possibility that these δ-agonists do not all mediate their effects via a common site. Others have found differential antagonism of DPDPE and DSLET by NTI and by its benzofuran analogue after intrathecal injection in mice (Sofuoglu *et al.*, 1991) and have suggested that these differences might be explained by the existence of δ-receptor subtypes. The differences between our work and that of Sofuoglu *et al.* (1991) could reflect the species used although route of administration may be important because Sofuoglu *et al.* (1991) did not see differential antagonism of DPDPE and DSLET after intracerebroventricular injection.

Our results also show there is not equal antagonism of the δ-agonists by ICI 174,864 and although the differences are not as marked as for NTI, it supports the possibility of δ-receptor heterogeneity. Further, the results in rats now show that DELT I provides the best discrimination of the effects of NTI with a 10 fold dose difference in sensitivity to either DPDPE or DSLET. The most marked difference is seen between DSLET and DELT I since NTI antagonism of DPDPE responses was not quite as marked as the antagonism of DSLET at 0.1 mg kg^{-1} (Figure 2b). This might suggest that DPDPE has affinity for both postulated sites. Further support for this conclusion is provided by differential functional antagonism of DPDPE and D-Ala^2 deltorphin II responses by tetraethylammonia and glibenclamide, respectively (Wild *et al.*, 1991). Other studies also suggest δ-receptor heterogeneity. For example, the two irreversible δ-antagonists, naltrindole 5′ isothiocyanate (Portoghese *et al.*, 1990) and D-Ala^2 Leu^5 Cys^6 enkephalin (Jiang

et al., 1990) differentially antagonize antinociceptive effects of D-Ala^2 deltorphin II, DSLET and DPDPE (Jiang et al., 1991).

Thus the results from our studies and that of others clearly demonstrate differential antagonism of the antinociceptive responses to selective δ-agonists by highly sensitive antagonists suggesting the presence of δ-opioid receptor subtypes in both rats and mice. The possibility that the differential antagonist effects of NTI might, in part, reflect pharmacokinetic differences in the distribution or metabolism of the three δ-agonists cannot be excluded. The differences in sensitivity to NTI are unlikely to be explained by μ-activity of DELT I since this peptide shows over 3000 fold selectivity for δ-sites in isolated tissue studies (Erspamer et al., 1989). Metabolism of DELT I to a non-selective μ/δ compound is also unlikely since its antinociceptive activity is fully reversed by ICI 174,864 and NTI at doses that have no effect on antinociception mediated by a highly selective μ-agonist (Figure 4).

In conclusion, the differential antagonism of the antinociceptive effects of three selective δ-agonists by NTI is in agreement with the proposal of the existence of δ-opioid receptor subtypes and suggests that DELT I exerts its antinociceptive effect at a different receptor subtype from DPDPE or DSLET in the rat.

T.J.C. is supported by a SERC CASE studentship with Merck Sharp and Dohme Research Laboratories.

References

CALCAGNETTI, D.J. & HOLTZMAN, S.G. (1991). Delta-opioid antagonist, naltrindole, selectively blocks analgesia induced by DPDPE but not DAGO or morphine. *Pharmacol. Biochem. Behav.*, **38**, 185–190.

ERSPAMER, Y., MELCHIORRI, P., FALCONIERI-ERSPAMER, G., NEGRI, L., CORSI, R., SERENNI, C., BARRA, D., SIMMACO, M. & KREIL, G. (1989). Deltorphins: A family of naturally occurring peptides with high affinity and selectivity for δ-opioid binding sites. *Proc. Natl. Acad. Sci. U.S.A.*, **86**, 5188–5192.

GALLIGAN, J.J., MOSBERG, H.I., HURST, R., HRUBY, V.J. & BURKS, T.F. (1984). Cerebral delta-opioid receptors mediate analgesia but not the intestinal motility effects of intracerebroventricularly administered opioids. *J. Pharmacol. Exp. Ther.*, **229**, 641–648.

GACEL, G., FOURNIE-ZALUSKI, M. & ROQUES, B.P. (1980). D-Tyr-Ser-Gly-Phe-Leu-Thr, A highly preferential ligand for δ-opiate receptors. *FEBS Lett.*, **118**, 245–247.

HEYMAN, J.S., MULVANEY, S.A., MOSBERG, H.I. & PORRECA, F. (1987). Opioid δ-receptor involvement in supraspinal and spinal antinociception in mice. *Brain. Res.*, **420**, 100–108.

JANSSEN, P.A.J., NIEMEGGERS, C.J.E. & DONY, J.G.H. (1963). The inhibitory effect of fentanyl and other morphine-like analgesics on the warm-water induced tail withdrawal reflex. *Arzneim. Forsch.*, **13**, 502–504.

JIANG, Q., BOWEN, W.D., MOSBERG, H.I., ROTHMAN, R.B. & PORRECA, F. (1990). Opioid agonist and antagonist antinociceptive properties of [D-Ala^2, Leu^5, Cys^6] enkephalin: Selective actions at the $\text{Delta}_{\text{non-complexed}}$ site. *J. Pharmacol. Exp. Ther.*, **255**, 636–641.

JIANG, Q., TAKEMORI, A.E., SULTANA, M., PORTOGHESE, P.S., BOWEN, W.D., MOSBERG, H.I. & PORRECA, F. (1991). Differential antagonism of opioid delta antinociception by [D-Ala^2, Leu^5, Cys^6] enkephalin and Naltrindole 5′-isothiocyanate: Evidence for delta receptor subtypes. *J. Pharmacol. Exp. Ther.*, **257**, 1069–1075.

KEEP, R.F., CAWKWELL, R.D. & JONES, H.C. (1986). The development of the blood-cerebrospinal fluid barrier: the relationship between structure and function in the rat choroid plexus. In *The Blood-Brain Barrier in Health and Disease*. ed. Suckling, A.J., Rumsby, M.G. & Bradbury, M.W.B. pp. 41–51. Chichester: Ellis Horwood.

KITCHEN, I., MCDOWELL, J., WINDER, C. & WILSON, J.M. (1984). Low-level lead exposure alters morphine antinociception in neonatal rats. *Toxicol. Lett.*, **22**, 119–123.

KITCHEN, I. & PINKER, S.R. (1990). Antagonism of swim-stress-induced antinociception by the δ-opioid receptor antagonist naltrindole in adult and young rats. *Br. J. Pharmacol.*, **100**, 685–688.

MOSBERG, H.I., HURST, R., HRUBY, V.J., GEE, K., YAMAMURA, M.I., GALLIGAN, J.J. & BURKS, T.F. (1983). Bis-penicillamine enkephalins possess highly improved specificity toward δ-opioid receptors. *Proc. Natl. Acad. Sci. U.S.A.*, **80**, 5871–5874.

PATERSON, S.J., ROBSON, L.E. & KOSTERLITZ, H.W. (1983). Classification of opioid receptors. *Br. Med. Bull.*, **39**, 31–36.

PORRECA, F., HEYMAN, J.S., MOSBERG, H.I., OMNAAS, J.R. & YAUGHT, J.L. (1987). Role of mu and delta receptors in the supraspinal and spinal analgesic effects of [D-Pen^2, D-Pen^5] enkephalin in the mouse. *J. Pharmacol. Exp. Ther.*, **241**, 393–400.

PORTOGHESE, P.S., SULTANA, M. & TAKEMORI, A.E. (1988). Naltrindole, a highly selective and potent non-peptide δ-opioid receptor antagonist. *Eur. J. Pharmacol.*, **146**, 185–186.

RODRIGUEZ, R.E., LEIGHTON, G., HILL, R.G. & HUGHES, J. (1986). In vivo evidence for spinal delta-opiate receptor-operated antinociception. *Neuropeptides*, **8**, 221–241.

ROGERS, H., HAYES, A.G., BIRCH, P.J., TRAYNOR, J.R. & LAWRENCE, A.J. (1990). The selectivity of the opioid antagonist, naltrindole,for δ-opioid receptors. *J. Pharm. Pharmacol.*, **42**, 358–359.

SOFUOGLU, M., PORTOGHESE, P.S. & TAKEMORI, A.E. (1991). Differential antagonism of delta opioid agonists by naltrindole and its benzofuran analog (NTB) in mice: Evidence for delta opioid receptor subtypes. *J. Pharmacol. Exp. Ther.*, **257**, 676–680.

SUH, H.H. & TSENG, L.F. (1990). Different types of opioid receptors mediating analgesia induced in mice. *Naunyn-Schmiedebergs Arch. Pharmacol.*, **342**, 67–71.

TAVANI, A., PETRILLO, P., LAKEGINA, A. & SBACCHI, M. (1990). Role of peripheral mu, delta and kappa opioid receptors in opioid-induced inhibition of gastrointestinal transit in rats. *J. Pharmacol. Exp. Ther.*, **254**, 91–97.

WILD, K.D., YANDERAH, T., MOSBERG, H.I. & PORRECA, F. (1991). Opioid δ-receptor subtypes are associated with different potassium channels. *Eur. J. Pharmacol.*, **193**, 135–136.

(Received March 17, 1992
Revised June 2, 1992
Accepted June 19, 1992)

Br. J. Pharmacol. (1992), **107**, 577–583

Lack of effect of the antimigraine drugs, sumatriptan, ergotamine and dihydroergotamine on arteriovenous anastomotic shunting in the dura mater of the pig

Marinus O. den Boer, Judith A.E. Somers & [1]Pramod R. Saxena

Department of Pharmacology, Faculty of Medicine and Health Sciences, Erasmus University Rotterdam, P.O. Box 1738, 3000 DR Rotterdam, The Netherlands

1 In anaesthetized animals, the antimigraine drugs, sumatriptan, ergotamine and dihydroergotamine, reduce carotid arteriovenous anastomotic shunting. Within the carotid vascular bed arteriovenous anastomoses are located, amongst other places in the dura mater, which is a putative site of the pain during a migraine attack.

2 In this investigation, we have localized and measured the arteriovenous shunting within the carotid vascular bed of the pig by using simultaneous intracarotid injections of radiolabelled microspheres of three different sizes (10, 15 and 50 μm), which provides an index of blood flow via arteriovenous anastomoses larger than approximately 14, 27 and 90 μm diameter, respectively. The effects of sumatriptan (0.3 mg kg^{-1}), ergotamine (0.02 mg kg^{-1}), dihydroergotamine (0.1 mg kg^{-1}) and saline were studied by repeating the injections of 15 and 50 μm spheres after the treatments.

3 There was no difference in shunting or entrapment between the 10 and 15 μm microsphere, indicating the absence of arteriovenous anastomoses with a diameter between 14 and 27 μm.

4 Arteriovenous anastomoses with a diameter between 27 and 90 μm, as indicated by the difference in blood flow measured by 15 and 50 μm spheres, were located in the dura mater, ears, skin, fat and, to a lesser extent, in the skeletal muscles and eyes.

5 Sumatriptan, ergotamine and dihydroergotamine reduced the overall flow in the smaller arteriovenous anastomoses (diameter between 27 and 90 μm), and even more in larger shunts (wider than 90 μm).

6 Locally, blood flow in the smaller arteriovenous shunts was reduced in the skin and fat, but not in the dura mater, ears, eyes and muscles. It is not possible to determine in which tissues blood flow in the larger arteriovenous anastomoses was reduced.

7 Tissue blood flow measured with 15 μm microspheres remained unchanged after the three antimigraine drugs, implying a lack of effect on capillary flow.

8 It is concluded that in the anaesthetized pigs the only evident effect of these antimigraine drugs on carotid haemodynamics is a decrease in blood flow in both smaller and larger arteriovenous anastomoses; the smaller arteriovenous anastomoses were affected in the skin and fat, but not in other tissues.

Keywords: Arteriovenous anastomoses; carotid blood flow; dihydroergotamine; dura mater; ergotamine; ergot alkaloids; 5-hydroxytryptamine receptors; migraine; sumatriptan

Introduction

The antimigraine drugs, sumatriptan, ergotamine and dihydroergotamine are vasoconstrictors. *In vitro*, different medium sized and small arteries as well as certain veins are constricted (Müller-Schweinitzer & Weidmann, 1978; Müller-Schweinitzer & Rosenthaler, 1987; Humphrey *et al.*, 1988). Amongst the arteries, those of the cranial circulation are more sensitive to these drugs than those in other body regions (Müller-Schweinitzer & Weidmann, 1978; Humphrey *et al.*, 1988). *In vivo*, these drugs cause an increase in resistance in the carotid vascular bed of different species; this increase seems to be localized only in arteriovenous anastomoses in this vascular bed, because capillary blood flow remains either unchanged or is even increased (see Saxena, 1978; Bom *et al.*, 1989; Perren *et al.*, 1989; Den Boer *et al.*, 1991a,b).

Arteriovenous anastomoses have been located in various cranial tissues, but it is at present unclear which of them is constricted by the antimigraine drugs. Furthermore, it is uncertain whether a constrictor action in anastomoses is involved at all in the clinical action of the antimigraine drugs. A possible contribution of dilatation of arteriovenous anastomoses to the migraine headache has been postulated by Heyck (1969), who found the jugular venous oxygen saturation to be elevated during a migraine attack. Interestingly, arteriovenous anastomoses have been anatomically located in the human dura mater, which is endowed with rich vascularization (Rowbotham & Little, 1965; Kerber & Newton, 1973). The dura mater is currently held as a possible origin of the migraine pain, involving vasodilatation and extravasation of plasma protein, induced by peptide release from the peripheral endings of the trigeminal nerve (Markowitz *et al.*, 1988; Goadsby *et al.*, 1990). Such vascular changes in the dura mater, when experimentally induced in rats and guinea-pigs, can be inhibited by the same antimigraine drugs (Markowitz *et al.*, 1988; Buzzi & Moskowitz, 1990). The mechanism involved in this inhibition of protein extravasation has not yet been fully elucidated; both a presynaptic inhibition of neuropeptide release (Buzzi *et al.*, 1991) and cranial vasoconstriction (Humphrey *et al.*, 1990; Saxena & Den Boer, 1991) remain as possibilities. Indeed,

[1] Author for correspondence.

sumatriptan increases vascular resistance in the human isolated, perfused dura mater (Humphrey *et al.*, 1991b). However, at present, no direct information on the effects of these antimigraine agents on dural haemodynamics *in vivo* is available.

Therefore, we studied the effects of sumatriptan, ergotamine and dihydroergotamine on the carotid circulation in anaesthetized pigs, with special emphasis on the dura mater. In order to obtain direct information about the blood flow in arteriovenous anastomoses of different tissues, we injected radioactive microspheres of different sizes into the carotid artery.

Methods

General

After an overnight fast 24 domestic pigs (Yorkshire × Landrace; 16–22 kg) were anaesthetized with azaperone (120 mg, i.m.) and metomidate (150 mg, i.v.), intubated and connected to a respirator (Bear 2E, BeMeds AG, Baar, Switzerland) for intermittent positive pressure ventilation with a mixture of room air and oxygen. Respiratory rate, tidal volume and oxygen supply were adjusted to keep arterial blood gas values within physiological limits (pH 7.35–7.48; P_{CO_2}: 35–48 mmHg; P_{O_2}: 100–120 mmHg). Anaesthesia was maintained with a continuous i.v. infusion of pentobarbitone sodium (Sanofi, Paris, France) at 20 mg kg^{-1} h^{-1} for the first hour and thereafter at 12 mg kg^{-1} h^{-1}.

Catheters were placed in the inferior vena cava via a femoral vein for the administration of drugs and in the aortic arch via a femoral artery, connected to a Statham pressure transducer (P23 Dc, Hato Rey, Puerto Rico) for the measurement of arterial blood pressure and the withdrawal of arterial blood for determining blood gases (ABL-2, Radiometer, Copenhagen, Denmark). Mean arterial blood pressure (MAP) was calculated from the systolic (SAP) and diastolic (DAP) arterial pressures: MAP = (SAP + 2 × DAP)/3. The common carotid arteries were dissected free and the cervical vagosympathetic trunks were cut. Blood flow was measured in one of the common carotid arteries with a flow probe (internal diameter: 2.5 or 3 mm) connected to a sine-wave electromagnetic flow meter (Transflow 600-system, Skalar, Delft, The Netherlands). Heart rate was measured with a tachograph triggered from the blood pressure or the flow signal, depending on their shape. A 0.6 mm (external diameter) needle, connected to a polyethylene tubing was inserted into the common carotid artery against the direction of the blood flow for the administration of radioactive microspheres. At the same side the jugular vein was cannulated in order to obtain venous blood samples for determining blood gases.

During the experiment body temperature was kept above 37°C and the animals were continuously infused with 100 ml h^{-1} saline to compensate for fluid loss.

Radioactive microsphere method

The distribution of common carotid blood flow was determined with a mixture of 10, 15 and 50 μm microspheres at baseline and of 15 and 50 μM microspheres after drug treatment. These were labelled with either ^{141}Ce (10 μm), ^{113}Sn (50 μm), ^{103}Ru (50 μm), ^{95}Nb (15 μm) or ^{46}Sc (15 μm; NEN Company, Dreieich, Germany). The order of 15 and 50 μm spheres injected before and after the drugs was randomized. The approximate number of microspheres given per isotope was: 10 μm, 700,000; 15 μm, 300,000; 50 μm, 30,000. The microspheres were vortexed for about half a minute and then injected into the carotid artery against the direction of the blood flow to ensure uniform mixing. At the end of the experiment the animals were killed and the heart, kidneys, lungs and the different cranial tissues were dissected out, weighed and put in vials. The radioactivity in these vials was counted for 5–10 min in a gamma-scintillation counter (Packard, Minaxi Autogamma 5000) using suitable windows for discriminating the different isotopes.

The ratio between the radioactivity in a particular tissue and the total radioactivity was calculated with a set of specially developed computer programmes (Saxena *et al.*, 1980). By multiplying this ratio with the total carotid blood flow value at the time of the injection, blood flow values to the lungs and tissues were determined.

By video recording the motion of microspheres in the blood vessels in the hamster cheek pouch, Dickhoner *et al.* (1978) have demonstrated that microspheres with a diameter of 9, 15 and 24 μm are trapped in blood vessels with a diameter of 11.5, 27.7 and 42.7 μm, respectively. Therefore, in the present investigation blood flow values measured with the 10, 15 and 50 μm microspheres in the lungs have been assumed to represent cranial shunt flow in arteriovenous anastomoses wider than approximately 14, 28 and 90 μm, respectively. Similarly, in the cranial tissues, the difference between blood flow values measured with 10 and 15 μm and with 15 and 50 μm microspheres was assumed to represent the flow in local arteriovenous anastomoses with a diameter, respectively, between 14 and 28 μm and between 28 and 90 μm. The rationale for these assumptions is amplified at the beginning of the discussion section.

Experimental protocol

After a stabilization period of about 1 h, arterial blood pressure, heart rate, blood flow in one of the common carotid arteries, and arterial and jugular venous blood gas values were determined. Then a mixture of 10, 15 and 50 μm microspheres was injected into the carotid artery. After another stabilization period of about 15 min, the animals received an intravenous injection of either sumatriptan (0.3 mg kg^{-1}), ergotamine (0.02 mg kg^{-1}), dihydroergotamine (0.1 mg kg^{-1}) or saline. These doses of the drugs have been shown to cause a 70 to 80% decrease in arteriovenous anastomotic shunt flow in our previous experiments (Den Boer *et al.*, 1991a,b). Fifteen minutes after this injection, systemic haemodynamic values were collated and blood gases and regional carotid haemodynamics (by use of a mixture of 15 and 50 μm microspheres) were again determined.

Data presentation and statistical analysis

All data have been expressed as means ± s.e.mean. The overall significance of the differences between the baseline flow values has been evaluated in the four groups together with a multivariate analysis of variance (repeated-measurements design). In the case of a significant F, individual differences were analyzed with a Student's t test for paired data (two-tailed). The effect of the treatment was compared in every group separately with a repeated measurements analysis of variance with the factors size and treatment. Individual differences were analyzed with a Student's t test for paired data. Statistical significance was accepted at $P < 0.05$ (two-tailed).

Drugs

Apart from the anaesthetics, azaperone and metomidate (both from Janssen Pharmaceutica, Beerse, Belgium), the drugs used in this study were: sumatriptan (Glaxo group research, Ware, U.K.), ergotamine tartrate (Wander-Pharma, Uden, The Netherlands), dihydroergotamine mesylate (Wander-Pharma, Uden, The Netherlands) and heparin sodium (Thromboliquine, Organon Teknika B.V., Boxtel, The Netherlands) to prevent clotting in the catheters. Sumatriptan was dissolved in physiological saline. All doses refer to the respective salts.

Results

Localization and size of arteriovenous anastomoses

In the carotid circulation, 63 ± 3% of 10 μm microspheres, 61 ± 3% of 15 μm spheres and 41 ± 3% of 50 μm spheres were shunted to the venous side via arteriovenous anastomoses. Arteriovenous anastomotic blood flows, measured with the 10, 15 and 50 μm microspheres, were 108 ± 11, 105 ± 11 and 71 ± 7 ml min^{-1}, respectively, so that 3 ± 1 ml min^{-1} passed through shunts with a diameter between 14 and 28 μm, 34 ± 4 ml min^{-1} through shunts of 28–90 μm diameter and 71 ± 7 ml min^{-1} through larger shunts. In the dura mater, ears, skin, fat and, to a lesser extent, skeletal muscles and eyes, the respective blood flow values measured with 15 μm microspheres were less than those measured with 50 μm microspheres, thus implying the presence of arteriovenous anastomoses with a diameter between approximately 28 and 90 μm in these tissues (Table 1; Figure 1). In the skin and the eyes there was a small, but significant, difference between entrapment of 10 and 15 μm microspheres, so that a few arteriovenous anastomoses with a diameter between approximately 15 and 30 μm appear to be present in these tissues. Since there was no difference in the blood flow measured with the microspheres of three sizes in the brain, tongue, bones and salivary glands (Table 1; Figure 1), it appears that these tissues contain no anastomoses with a diameter between 15 and 90 μm. From the present experiments, it is, however, not possible to localize the shunts larger than 90 μm.

Effects of the antimigraine drugs

Systemic haemodynamics The effects of i.v. injections of sumatriptan (0.3 mg kg^{-1}), ergotamine (0.02 mg kg^{-1}), dihydroergotamine (0.1 mg kg^{-1}) or saline on heart rate and mean arterial blood pressure are shown in Table 2. After saline and dihydroergotamine small, but statistically significant, decreases in heart rate occurred. It is, therefore, not certain, whether the small change induced by dihydroergotamine reflects a direct action of the drug (Table 2). After ergotamine and dihydroergotamine mean arterial blood pressure increased by 38 ± 8 and 34 ± 5%, respectively. Though not statistically significant, an increase in mean arterial pressure of 14 ± 8% was seen after sumatriptan.

Carotid blood flow and total arteriovenous anastomotic shunting All three antimigraine drugs, sumatriptan, ergotamine and dihydroergotamine, reduced carotid blood flow (Table 3) by −30 ± 7, −44 ± 6 and −30 ± 5%, respectively. Although a much smaller, but statistically significant, reduction of carotid blood flow was seen after saline, most of the changes after the three antimigraine drugs appear to be specific for the drugs. These decreases were not caused by a decrease in capillary flow: drug-induced changes in total capillary blood flow values, determined with 15 μm microspheres, were only −1.6 ± 1.3, 4.4 ± 5.8, −3.7 ± 8.0 and 6.6 ± 5.7 ml min^{-1}, respectively, for saline, sumatriptan, ergotamine and dihydroergotamine. On the other hand, arteriovenous shunt flow, measured with microspheres of both 15 and 50 μm was decreased by the three antimigraine drugs (Figure 2). An increase in the difference between arterial and jugular venous oxygen saturation after ergotamine or dihydroergotamine is in keeping with an effect on arteriovenous anastomoses (Table 3).

Blood flow through smaller (28–90 μm) arteriovenous anastomoses was decreased by sumatriptan and tended to decrease, although not significantly, after ergotamine and dihydroergotamine (Table 4, Figure 2). A much larger decrease in shunting was observed in the shunts wider than 90 μm after all three agents (Table 4).

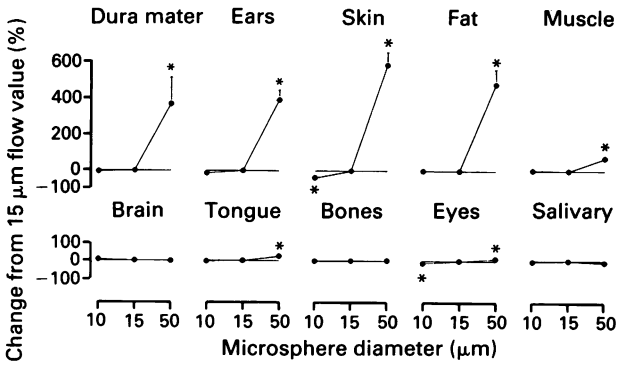

Figure 1 The localization of arteriovenous anastomoses in different cranial tissues, by differential entrapment of radioactive microspheres of 10, 15 and 50 μm diameter. All values (means ± s.e.mean) have been given as the percentage difference from the flow value, measured with 15 μm spheres. *$P<0.05$ from 15 μm flow value.

Table 2 Effect of sumatriptan (0.3 mg kg^{-1}), ergotamine (0.02 mg kg^{-1}), dihydroergotamine (0.1 mg kg^{-1}) or saline on heart rate (HR) and mean arterial blood pressure (MAP) in the pig

	HR (Beats min^{-1})		*MAP* (mmHg)	
	Before	After	Before	After
Saline	89 ± 6	87 ± 5*	92 ± 7	92 ± 7
Sumatriptan	89 ± 4	88 ± 3	94 ± 8	107 ± 11
Ergotamine	87 ± 6	85 ± 6	88 ± 4	120 ± 7*
Dihydroergotamine	91 ± 3	86 ± 4*	101 ± 6	134 ± 4*

Values are given as mean ± s.e.mean.
*$P<0.05$ versus control.

Table 3 Effect of sumatriptan (0.3 mg kg^{-1}), ergotamine (0.02 mg kg^{-1}), dihydroergotamine (0.1 mg kg^{-1}) or saline on carotid blood flow (CBF) and difference in arterial and jugular venous oxygen saturation (AVOSD) in the pig

	CBF (ml min^{-1})		*AVOSD* (%)	
	Before	After	Before	After
Saline	152 ± 17	144 ± 14*	5.4 ± 1.8	5.8 ± 1.9
Sumatriptan	157 ± 20	106 ± 9*	7.1 ± 4.3	8.9 ± 2.8
Ergotamine	181 ± 36	98 ± 18*	4.6 ± 0.9	15.3 ± 3.7*
Dihydroergotamine	170 ± 24	117 ± 18*	4.9 ± 1.4	14.9 ± 3.6*

Values are given as mean ± s.e.mean.
*$P<0.05$ versus control.

Table 1 Tissue flow values in the pig, measured with 10, 15 and 50 μm diameter radioactive microspheres

	10 μm	15 μm	50 μm
Dura mater	0.12 ± 0.02	0.13 ± 0.02	0.28 ± 0.02*
Ears	2.3 ± 0.3	2.7 ± 0.5	9.4 ± 1.0*
Skin	2.1 ± 0.1*	2.9 ± 0.3	16.9 ± 1.3*
Fat	2.6 ± 0.3	2.7 ± 0.4	11.6 ± 1.5*
Muscle	8.9 ± 0.7	8.9 ± 0.9	14.3 ± 1.2*
Brain	9.4 ± 0.9	10.3 ± 1.0	10.2 ± 1.0
Tongue	3.1 ± 0.3	3.3 ± 0.4	3.8 ± 0.3*
Bones	11.1 ± 1.0	11.3 ± 1.0	11.3 ± 1.0
Eyes	1.9 ± 0.3*	2.1 ± 0.2	2.4 ± 0.2
Salivary	7.1 ± 0.6	7.6 ± 0.8	6.5 ± 0.5

All values (ml min^{-1}) are given as means ± s.e.mean.
*$P<0.05$ vs. flow measured with 15 μm microsphere.

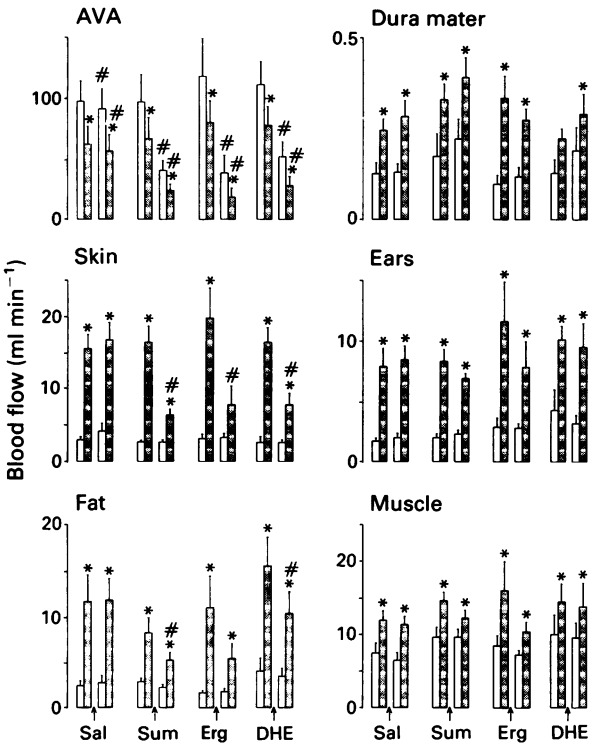

Figure 2 Effect of saline (Sal), sumatriptan (Sum, 0.3 mg kg^{-1}), ergotamine (Erg, 0.02 mg kg^{-1}) and dihydroergotamine (DHE, 0.1 mg kg^{-1}) on flow measured with 15 μm (open columns) and 50 μm (cross-hatched columns) microspheres. Values as means ± s.e.mean (vertical bars). *$P<0.05$ vs simultaneously injected 15 μm sphere; #$P<0.05$ vs same sphere before treatment.

Table 4 Effect of sumatriptan (0.3 mg kg^{-1}), ergotamine (0.02 mg kg^{-1}), dihydroergotamine (0.1 mg kg^{-1}) or saline on blood flow (ml min^{-1}) of the pig through arteriovenous anastomoses with a diameter between 28 and 90 μm or anastomoses wider than 90 μm

	28–90 μm		>90 μm	
	Before	After	Before	After
Saline	35 ± 5	35 ± 5	61 ± 14	56 ± 13*
Sumatriptan	30 ± 6	16 ± 3*	66 ± 17	24 ± 5*
Ergotamine	38 ± 14	20 ± 7	79 ± 18	18 ± 8*
Dihydroergotamine	33 ± 7	24 ± 5	77 ± 15	28 ± 7*

Values are given as mean ± s.e.mean.
*$P<0.05$ versus control.

Blood flow in tissues with arteriovenous anastomoses with a diameter between 16 and 28 μm In skin and fat, sumatriptan, ergotamine and dihydroergotamine decreased entrapment of 50 μm microspheres, while the entrapment of 15 μm microspheres remained unchanged (Figure 2). All three agents also attenuated the difference in blood flow measured with spheres of the two sizes in the skin, indicating a decrease in the blood flow through shunts with a diameter between 28 and 90 μm (Figure 2). In the fat, only dihydroergotamine significantly decreased the blood flow through these shunts, although a similar, non-significant, tendency was observed with sumatriptan and ergotamine (Figure 2). In spite of the abundance of shunts with a diameter between 28 and 90 μm in the dura mater and ears, they were not affected by any of the drugs (Figure 2). The slight amount of shunting in muscle, tongue and eyes was also not influenced by the drugs.

Blood flow in tissues without arteriovenous anastomoses with a diameter between 16 and 28 μm In the bones, salivary glands and brain, where flow through shunts with a diameter between 28 and 90 μm was completely absent, administration of neither sumatriptan, ergotamine nor dihydroergotamine produced any effect, except for an increase in salivary gland blood flow, measured with 50 μm spheres after dihydroergotamine (Figure 3).

Discussion

Use of microspheres of three sizes to measure arteriovenous anastomotic blood flow

The use of microspheres of different sizes to measure the distribution of carotid blood flow has already been extensively described by Saxena & Verdouw (1985). A clear effect of 5-hydroxytryptamine (5-HT) on arteriovenous anastomoses was observed in their experiments. From the early years of the use of radioactive microspheres to measure blood flow, non-entrapment of spheres in certain tissues has been observed (Kaihara *et al.*, 1968; Hales, 1974). The amount of non-entrapment, ascribed to arteriovenous anastomotic blood flow (Hales, 1974), is dependent on microsphere size, the tissue studied and the use of anaesthesia (Forsyth & Hoffbrand, 1970). Dickhoner *et al.* (1978) examined with a video camera the behaviour of 9, 15 and 24 μm microspheres in the hamster cheek pouch, after intracardiac injection. They demonstrated that 9, 15 and 24 μm microspheres were trapped when arriving in blood vessels with a diameter of 11.5, 27.7 and 42.7 μm, respectively, for the three microspheres. Extrapolation of these results to our experiments indicates that the 10, 15 and 50 μm diameter microspheres are expected to pass to the venous side through blood vessels with a minimum diameter larger than 14, 28

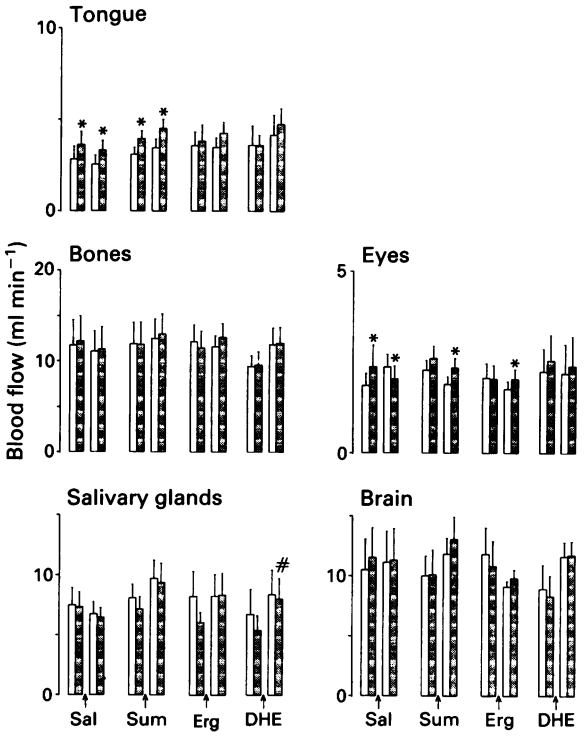

Figure 3 Effect of saline (Sal), sumatriptan (Sum, 0.3 mg kg^{-1}), ergotamine (Erg, 0.02 mg kg^{-1}) and dihydroergotamine (DHE, 0.1 mg kg^{-1}) on flow measured with 15 μm (open columns) and 50 μm (cross-hatched columns) microspheres. Values as means ± s.e.mean (vertical bars). *$P<0.05$ vs simultaneously injected 15 μm sphere; #$P<0.05$ vs same sphere before treatment.

and 90 μm, respectively. Such vessels are arteriovenous anastomoses, because capillaries have a diameter under 10 μm (for references see Saxena & Verdouw, 1985). Since, in our experiments, no radioactivity could be detected in the heart or the kidneys, the microspheres reaching the venous side by arteriovenous anastomoses were completely trapped in the lungs. Therefore, the lung blood flow value obtained with a particular microsphere reflects the total amount of arteriovenous anastomotic shunting of that microsphere (Saxena & Verdouw, 1982). The tissue blood flow value, calculated with a certain microsphere, is a measure of the flow through blood vessels in which this particular microsphere is trapped. When a tissue is devoid of arteriovenous anastomoses, microspheres of all sizes yield similar blood flow values, which are equal to the tissue capillary flow (as demonstrated e.g. in the brain in the present experiments). An increase in tissue blood flow values with increasing microsphere size indicates that arteriovenous anastomoses are present in that tissue. Using the data from Dickhoner *et al.* (1978) the difference between the blood flow values measured with 10 and 15 μm microspheres can be used as an index of blood flow in arteriovenous anastomoses with a diameter between 14 and 28 μm. Similarly, the blood flow difference between 15 and 50 μm microspheres indicates blood flow in shunt vessels between 28 and 90 μm. Blood flow in still larger arteriovenous anastomoses, which may have a diameter up to 150 μm (Sherman, 1963), cannot be calculated for individual tissues, since the use of still larger microspheres is not practical due to adverse influence on the circulation. However, the total blood flow in these largest shunts can be assessed by the lung entrapment of 50 μm spheres.

Effects of the antimigraine drugs

It has been known for some time that the antimigraine drugs ergotamine and dihydroergotamine, when administered in anaesthetized animals, decrease arteriovenous anastomotic blood flow in the carotid vascular bed (Saxena, 1978; Saxena *et al.*, 1983; Den Boer *et al.*, 1991a). Since the new antimigraine agent, sumatriptan, also has this property (Perren *et al.*, 1989; Den Boer *et al.*, 1991b), interest in this field has been renewed. Arteriovenous anastomoses have been demonstrated in different cranial tissues, but the distribution is species-dependent. Some arteriovenous anastomoses have a thermoregulatory function and they can be demonstrated e.g. in the human skin, the dog tongue and the rabbit ears (Hales & Molyneux, 1988). Others, for example those in the splanchnic region, are believed to play a role in blood pressure regulation (Hales & Molyneux, 1988). In the domestic pig, such shunts have been functionally demonstrated in the skin and ears, with radioactive microspheres of four sizes (10, 15, 25 and 35 μm diameter; Saxena & Verdouw, 1985).

A further location of arteriovenous anastomoses is the human dura mater (Rowbotham & Little, 1965; Kerber & Newton, 1973). This tissue is currently believed to play a role in the generation of the pain during a migraine attack. The three antimigraine agents used in this study can all inhibit the effects of stimulation of the trigeminal ganglion on the dura mater of rats. These effects include plasma protein extravasation and oedema caused by the release of vasoactive peptides (e.g. substance P, calcitonin gene-related peptide, neurokinin A) from trigeminal afferents (Markowitz *et al.*, 1988; Buzzi & Moskowitz, 1990). An involvement of the trigeminal system, whether confined to the dura mater or not, is probably reflected by the increased level of calcitonin gene-related peptide in the jugular venous blood, which can be observed during a migraine attack and which can equally be normalized by sumatriptan (Goadsby *et al.*, 1990; Goadsby & Edvinsson, 1991). The mechanism by which the antimigraine drugs inhibit this protein extravasation is not yet clear. A direct effect on the trigeminal afferents is possible, but a role for the vasoconstrictor effects of the antimigraine drugs cannot be excluded. In favour of this latter mechanism is the fact that these drugs have been shown to increase vascular resistance in the *in vitro*, perfused human dura mater (Humphrey *et al.*, 1991b). It is, however, not known what the effects of these drugs are on the dural haemodynamics *in vivo*, and it is with this point that the present study is concerned. Since, in our model, the major effect of the antimigraine drugs is on the arteriovenous anastomoses, we have used intracarotid injection of radioactive microspheres of different sizes to measure directly arteriovenous anastomotic blood flow in different tissues, including the dura mater. In concordance with the human dura mater (Rowbotham & Little, 1965; Kerber & Newton, 1973), arteriovenous anastomoses with a diameter between 28 and 90 μm could be functionally demonstrated in the porcine dura mater. This is different from the dog dura mater, where there was no difference in entrapment between 15 and 50 μm microspheres (Faraci *et al.*, 1989), although, as in our experiments, the animals were anaesthetized with pentobarbitone, which is known to increase shunting (Forsyth & Hoffbrand, 1970). In addition to the dura mater, arteriovenous anastomoses were demonstrated in the ears, skin and fat; in muscle and eyes there was only a very small amount of shunted blood.

As in earlier studies, sumatriptan, ergotamine and dihydroergotamine all decreased arteriovenous shunt flow in the carotid circulation. Both smaller (28–90 μm) and larger (>90 μm) shunts were affected in this way. This decrease in arteriovenous anastomotic blood flow was confined to the skin and fat, while the shunting in the dura mater, ears, muscle and eyes was not affected by the drugs. Neither was there a change in capillary blood flow to any tissue that we studied. In view of the present results, it would seem unlikely that a haemodynamic effect of the antimigraine drugs on dural arteriovenous anastomoses is responsible for the inhibition of dural protein extravasation or the clinical effect of the antimigraine drugs, although one should keep in mind that drug effects may differ among species and preparations used. Sumatriptan has been shown to increase vascular resistance in human isolated, perfused dura mater (Humphrey *et al.*, 1991b). This difference cannot be explained yet, but *post-mortem* damage to the dural vasculature or the different experimental set-up could be responsible.

The presence of a functional blood brain barrier may explain some differences in drug effects. For example, sumatriptan, which constricts pial vessels upon perivascular application in anaesthetized cats, fails to do so after intravenous administration (Humphrey *et al.*, 1991a): this may be caused by its inability to cross the blood brain barrier (Sleight *et al.*, 1990). However, the dura mater is devoid of an anatomical and functional blood-brain barrier, having fenestrated endothelium (Wislocki & Leduc, 1952; Knudsen *et al.*, 1988).

A further point to consider is the size of the arteriovenous anastomoses. In the present study, 41% of 50 μm microspheres was shunted to the lungs via arteriovenous anastomoses wider than 90 μm. The total flow in these large arteriovenous anastomoses was decreased by the antimigraine drugs, but these large shunts have not been localized. This would only be possible by use of microspheres with a diameter larger than 50 μm. However, such microspheres will undoubtedly adversely influence haemodynamics. It is possible for these large shunts to have a different pharmacological reactivity from the smaller ones. It should, however, be noted that the arteriovenous anastomoses in the human dura mater usually have a diameter between 50 and 90 μm, and that larger ones seem to be absent (Kerber & Newton, 1973).

A constrictor action of sumatriptan, ergotamine and dihydroergotamine has been demonstrated on large arteries in the cranial vasculature, both *in vitro* (Müller-Schweinitzer & Weidmann, 1978; Parsons *et al.*, 1989) and *in vivo* during migraine attacks (Friberg *et al.*, 1991; Caekebeke *et al.*, 1991). Such a constrictor action of these drugs on arteries rather than on arteriovenous anastomoses, may be the basis

of their antimigraine effect. Vasodilatation of extracranial arteries during the migraine attack and its reversal by ergotamine has been observed by Graham & Wolff (1938). Especially in the last decade the occurrence of vasodilatation has been severely questioned and both positive and negative studies have been published (for an overview, see Olesen *et al.*, 1990). However, most of these studies were concerned only with changes in cerebral blood flow, and possible changes in the diameter of the larger arteries and arteriovenous anastomoses, which may not affect tissue blood flow, have remained largely unaddressed. Only very recently, transcranial Doppler measurements of blood flow velocities in cranial arteries have provided an indirect estimate of arterial diameter (Caekebeke *et al.*, 1991; Friberg *et al.*, 1991). Whereas Friberg *et al.* (1991) found the middle cerebral artery to be dilated during the migraine headache, no such change was observed in the experiments of Caekebeke *et al.* (1991).

Therefore, it remains to be established, whether vasodilatation occurs during a migraine attack, and which vascular beds and which segments of the vascular bed are involved. A role could be assigned to arteries or arteriovenous anastomoses, both of which are affected by the antimigraine drugs. The larger arteriovenous anastomoses ($>90\,\mu m$ diameter), which are constricted by the antimigraine drugs, have still to be localized. Furthermore, the role of the trigeminal system during a migraine attack has to be elucidated and the mechanism by which the antimigraine drugs inhibit the effects of stimulation of this system. It is interesting that this effect of the antimigraine drugs seems to be specific for the dura mater, since the protein extravasation in the conjunctiva, eyelids and lips are not affected by sumatriptan (Buzzi & Moskowitz, 1990).

Part of this work was financially supported by Glaxo Group Research, Ware, U.K. The authors wish to thank Dr W. Feniuk (Glaxo Institute of Applied Pharmacology, University of Cambridge, U.K.) for his critical remarks and help in preparing the manuscript.

References

BOM, A.H., HEILIGERS, J.P.C., SAXENA, P.R. & VERDOUW, P.D. (1989). Reduction of cephalic arteriovenous shunting by ergotamine is not mediated by 5-HT_1-like or 5-HT_2 receptors. *Br. J. Pharmacol.*, **97**, 383–390.

BUZZI, M.G. & MOSKOWITZ, M.A. (1990). The antimigraine drug, sumatriptan (GR43175), selectively blocks neurogenic plasma extravasation from blood vessels in dura mater. *Br. J. Pharmacol.*, **99**, 202–206.

BUZZI, M.G., CARTER, W.B., SHIMIZU, T., HEATH, H. & MOSKOWITZ, M.A. (1991). Dihydroergotamine and sumatriptan attenuate levels of CGRP in plasma in rat superior sagittal sinus during electrical stimulation of the trigeminal ganglion. *Neuropharmacol.*, **30**, 1193–1200.

CAEKEBEKE, J.F.V., ZWETSLOOT, C.P., JANSEN, J.C., SAXENA, P.R. & FERRARI, M.D. (1991). Sumatriptan increases the cranial blood flow velocity during migraine attacks: a transcranial Doppler study. In *Migraine and other Headaches: The Vascular Mechanisms*. ed. Olesen, J. pp. 331–334. New York: Raven Press.

DEN BOER, M.O., HEILIGERS, J.P.C. & SAXENA, P.R. (1991a). Carotid vascular effects of ergotamine and dihydroergotamine in the pig: no exclusive mediation via 5-HT_1-like receptors. *Br. J. Pharmacol.*, **104**, 183–189.

DEN BOER, M.O., VILLALÓN, C.M., HEILIGERS, J.P.C., HUMPHREY, P.P.A. & SAXENA, P.R. (1991b). Role of 5-HT_1-like receptors in the reduction of porcine cranial arteriovenous anastomotic shunting by sumatriptan. *Br. J. Pharmacol.*, **102**, 323–330.

DICKHONER, W.H., BRADLEY, B.R. & HARREL, G.S. (1978). Diameter of arterial microvessels trapping 8–10 μm, 15 μm and 25 μm microspheres as determined by vital microscopy of hamster cheek pouch. *Invest. Radiol.*, **13**, 313–317.

FARACI, F.M., KADEL, K.A. & HEISTAD, D.D. (1989). Vascular responses of dura mater. *Am. J. Physiol.*, **257**, H157–H161.

FORSYTH, R.P. & HOFFBRAND, B.I. (1970). Redistribution of cardiac output after sodium pentobarbital anesthesia in the monkey. *Am. J. Physiol.*, **218**, 214–217.

FRIBERG, L., OLESEN, J., IVERSEN, H.K. & SPERLING, B. (1991). Migraine pain associated with middle cerebral artery dilatation: reversal by sumatriptan. *Lancet*, **338**, 13–17.

GOADSBY, P.J. & EDVINSSON, L. (1991). Sumatriptan reverses the changes in calcitonin gene-related peptide seen in the headache phase of migraine. *Cephalalgia*, **11** (suppl. 11), 3–4.

GOADSBY, P.J., EDVINSSON, L. & EKMAN, R. (1990). Vasoactive peptide release in the extracerebral circulation of humans during migraine headache. *Ann. Neurol.*, **28**, 183–187.

GRAHAM, J.R. & WOLFF, H.G. (1938). Mechanism of migraine headache and action of ergotamine tartrate. *Arch. Neurol. Psychiat.*, **39**, 737–763.

HALES, J.R.S. (1974). Radioactive microsphere techniques for studies of the circulation. *Clin. Exp. Pharmacol. Physiol.*, Suppl. 1, 31–46.

HALES, J.R.S. & MOLYNEUX, G.S. (1988). Control of cutaneous arteriovenous anastomoses. In *Vasodilatation: Vascular Smooth Muscle, Peptides, Autonomic Nerves and Endothelium*. ed. Vanhoutte, P.M. pp. 321–332. New York: Raven Press.

HEYCK, H. (1969). Pathogenesis of migraine. *Res. Clin. Stud. Headache*, **2**, 1–28.

HUMPHREY, P.P.A., CONNOR, H.E., STUBBS, C.M. & FENIUK, W. (1991a). Effect of sumatriptan on pial vessel diameter *in vivo*. In *Migraine and other Headaches: The Vascular Mechanisms*. ed. Olesen, J. pp. 335–338. New York: Raven Press.

HUMPHREY, P.P.A., FENIUK, W., MOTEVALIAN, M., PARSONS, A.A. & WHALLEY, E.T. (1991b). The vasoconstrictor action of sumatriptan on human isolated dura mater. In *Serotonin: Molecular Biology, Receptors and Functional Effects*. ed. Fozard, J.R. & Saxena, P.R. pp. 421–429. Basel: Birkhäuser Verlag.

HUMPHREY, P.P.A., FENIUK, W., PERREN, M.J., BERESFORD, I.J.M. & SKINGLE, M. (1990). Serotonin and migraine. *Ann. New York Acad. Sci.*, **600**, 587–598.

HUMPHREY, P.P.A., FENIUK, W., PERREN, M.J., CONNOR, H.E., OXFORD, A.W., COATES, I.H. & BUTINA, D. (1988). GR43175, a selective agonist for the 5-HT_1-like receptor in dog isolated saphenous vein. *Br. J. Pharmacol.*, **94**, 1123–1132.

KAIHARA, S., VAN HEERDEN, P.D., MIGITA, T. & WAGNER, H.N. (1968). Measurement of distribution of cardiac output. *J. Appl. Physiol.*, **25**, 696–700.

KERBER, C.W. & NEWTON, T.H. (1973). The macro and microvasculature of the dura mater. *Neuroradiology*, **6**, 175–179.

KNUDSEN, G.M., JUHLER, M. & PAULSON, O.B. (1988). Morphology, physiology and pathophysiology of the blood-brain barrier. In *Basic Mechanisms of Headache*. ed. Olesen J. & Edvinsson, L. pp. 49–60. Amsterdam, New York, Oxford: Elsevier.

MARKOWITZ, S., SAITO, K. & MOSKOWITZ, M.A. (1988). Neurogenically mediated plasma extravasation in dura mater: effect of ergot alkaloids. A possible mechanism of action in vascular headache. *Cephalalgia*, **8**, 83–91.

MÜLLER-SCHWEINITZER, E. & ROSENTHALER, J. (1987). Dihydroergotamine: Pharmacokinetics, pharmocodynamics and mechanism of venoconstrictor action in Beagle dogs. *J. Cardiovasc. Pharmacol.*, **9**, 686–693.

MÜLLER-SCHWEINITZER, E. & WEIDMANN, H. (1978). Basic pharmacological properties. In *Ergot Alkaloids and Related Compounds, Handbook of Experimental Pharmacology*, Vol. 49. ed. Berde, B. & Schild, H.O. pp. 87–232. Berlin, Heidelberg, New York: Springer-Verlag.

OLESEN, J., FRIBERG, L., SKYHØJ OLSEN, T., IVERSEN, H.K., LASSEN, N.A., ANDERSEN, A.R. & KARLE, A. (1990). Timing and topography of cerebral blood flow, aura and headache during migraine attacks. *Ann. Neurol.*, **28**, 791–798.

PARSONS, A.A., WHALLEY, E.T., FENIUK, W., CONNOR, H.E. & HUMPHREY, P.P.A. (1989). 5-HT_1-like receptors mediate 5-hydroxytryptamine-induced contraction of human isolated basilar artery. *Br. J. Pharmacol.*, **96**, 434–449.

PERREN, M., FENIUK, W. & HUMPHREY, P.P.A. (1989). The selective closure of feline carotid arteriovenous anastomoses (AVAs) by GR43175. *Cephalalgia*, **9** (suppl. 9), 41–46.

ROWBOTHAM, G.F. & LITTLE, E. (1965). New concepts on the aetiology and vascularization of meningiomata: the mechanisms of migraine: the chemical process of the cerebrospinal fluid; and the formations of the collections of blood or fluid in the subdural space. *Br. J. Surg.*, **52**, 21–24.

SAXENA, P.R. (1978). Arteriovenous shunting and migraine. *Res. Clin. Stud. Headache*, **6**, 89–102.

SAXENA, P.R. & DEN BOER, M.O. (1991). Pharmacology of antimigraine drugs. *J. Neurol.*, **238** (Suppl. 1), S28–S35.

SAXENA, P.R., KOEDAM, N.A., HEILIGERS, J. & HOF, R.P. (1983). Ergotamine-induced constriction of cranial arteriovenous anastomoses in dogs pretreated with phenotolamine and pizotifen. *Cephalalgia*, **3**, 71–81.

SAXENA, P.R., SCHAMHARDT, H.C., FORSYTH, R.P. & LOEVE, J. (1980). Computer programs for the radioactive microsphere technique. Determination of regional blood flows and other haemodynamic variables in different experimental circumstances. *Comp. Program. Biomed.*, **12**, 63–84.

SAXENA, P.R. & VERDOUW, P.D. (1982). Resdistribution by 5-hydroxytryptamine of carotid arterial blood at the expense of arteriovenous anastomotic blood flow. *J. Physiol.*, **332**, 501–520.

SAXENA, P.R. & VERDOUW, P.D. (1985). Tissue blood flow and localization of arteriovenous anastomoses in pigs with microspheres of four different sizes. *Pflügers Arch.*, **403**, 128–135.

SHERMAN, J.L. (1963). Normal arteriovenous anastomoses. *Medicine, Baltimore*, **42**, 247–267.

SLEIGHT, A.J., CERVENKA, A. & PEROUTKA, S.J. (1990). In vivo effects of sumatriptan (GR43175) on extracellular levels of 5-HT in the guinea-pig. *Neuropharmacol.*, **29**, 511–513.

WISLOCKI, G.B. & LEDUC, E.H. (1952). Vital staining of the hematoencephalic barrier by silver nitrate and trypan blue, and cytological comparisons of the neurohypophysis, pineal body, area postrema, intercolumnar tubercle and supra-optic crest. *J. Comp. Neurol.*, **96**, 371–413.

(Received April 2, 1992
Revised June 9, 1992
Accepted June 19, 1992)

Br. J. Pharmacol. (1992), **107**, 584–590

Inhibition by phosphoramidon of the regional haemodynamic effects of proendothelin-2 and -3 in conscious rats

[1] S.M. Gardiner, P.A. Kemp & T. Bennett

Department of Physiology and Pharmacology, University of Nottingham Medical School, Queen's Medical Centre, Nottingham NG7 2UH

1 Regional haemodynamic studies were carried out in conscious, Long Evans rats, chronically-instrumented with pulsed Doppler flow probes and intravascular catheters.

2 In the first experiment, proendothelin-2 and -3 (0.1 and 1.0 nmol kg^{-1}, i.v. boluses) were found to cause dose-dependent pressor, bradycardic, and renal and, particularly, mesenteric vasoconstrictor effects. The hindquarters showed an initial vasodilatation (which was not dose-dependent) followed by a vasoconstriction (which was dose-related). The pressor and renal and mesenteric vasoconstrictor effects of proendothelin-3 were greater than those of proendothelin-2.

3 In the second experiment, it was demonstrated that phosphoramidon (10 μmol kg^{-1}, i.v. bolus) abolished the pressor, bradycardic, and hindquarters vasoconstrictor effects of proendothelin-2 (1.0 nmol kg^{-1}), and inhibited significantly the renal and mesenteric vasoconstrictor actions of this peptide. Phosphoramidon had similar effects on the responses to proendothelin-3 (1.0 nmol kg^{-1}), although a slight pressor effect of this peptide remained in the presence of phosphoramidon.

4 In the third experiment, it was found that phosphoramidon had no significant effect on the pressor or vasoconstrictor responses to endothelin-2 or -3 (0.1 nmol kg^{-1}).

5 Collectively, the results indicate that the haemodynamic effects of proendothelin-2 and -3 *in vivo* in conscious rats are probably due to their conversion to endothelin-2 and -3, respectively, by an enzyme(s) that is inhibited by phosphoramidon. There appears to be no obvious difference between proendothelin-2, proendothelin-3 and proendothelin-1 in this respect.

Keywords: Proendothelin-2; proendothelin-3; phosphoramidon; haemodynamics

Introduction

No doubt as a result of the rate at which the field has developed, there are many unresolved issues relating to the biology of endothelin. This is particularly true in regard to the enzymatic processes whereby endothelin-1 is produced from its precursor, proendothelin-1 (Yanagisawa *et al.*, 1988). Although several different 'endothelin-1-converting enzyme' (ECE-1) systems have been identified, it seems most likely that a membrane-bound, phosphoramidon-sensitive metalloprotease is the major ECE-1 of endothelial cells (Matsumura *et al.*, 1990b; Okada *et al.*, 1990). However, the conversion of exogenous proendothelin-1 to endothelin-1 by the membrane fraction of porcine aortic vascular smooth muscle cells is not phosphoramidon-sensitive under normal conditions (Matsumura *et al.*, 1991b), in contrast to the membrane-bound ECE-1 of the vascular smooth muscle of bovine carotid artery (Hioki *et al.*, 1991). Matsumura *et al.* (1991b) suggested their observations were due to a 'masking' of the action of phsophoramidon-sensitive ECE-1 by the presence of a phosphoramidon-insensitive ECE-1, and by degradation of proendothelin-1 and/or endothelin-1. However, it does appear that there is a difference between the endothelial and vascular smooth muscle ECE-1 systems, because Ikegawa *et al.* (1991) observed inhibition by phosphoramidon of spontaneous production of endothelin-1 from intact, porcine, aortic endothelial cells, but not from intact vascular smooth muscle cells. Despite this difference, the production of endothelin-1 from exogenous proendothelin-1 by both cell types was sensitive to phosphoramidon.

The picture is even more complex when the activity of ECE-1 against other substrates is considered. Thus, some biochemical studies indicate that the membrane-bound ECE-1 of bovine endothelial cells converts proendothelin-3 to endothelin-3, but at a rate only 1/9 that of the conversion of proendothelin-1 to endothelin-1 (Okada *et al.*, 1990). In contrast, the soluble ECE-1 of the same cells does not appear to convert proendothelin-3 to endothelin-3 (Takada *et al.*, 1991), although the same group (Okada *et al.*, 1991) subsequently reported that both membrane-bound and soluble forms of ECE-1 from bovine endothelial cells were inactive against proendothelin-2 and proendothelin-3. ECE-1 from renal epithelial cell lines has also been found to be inactive against proendothelin-2 and -3 (Takada *et al.*, 1992), although it was acknowledged that enzyme systems other than those studied might be important *in vivo*.

In vivo, the pressor effects of exogenous proendothelin-1 can be markedly inhibited by phosphoramidon (Matsumura *et al.*, 1990a; Fukuroda *et al.*, 1990; McMahon *et al.*, 1991; Gardiner *et al.*, 1991; Le Monnier de Gouville & Cavero, 1991; Pollock & Opgenorth, 1991), and this effect is associated with a reduction in the regional vasoconstrictor effects of proendothelin-1 (Gardiner *et al.*, 1991; Pollock & Opgenorth, 1991). As pointed out elsewhere (Gardiner *et al.*, 1991), *in vivo* administration of phosphoramidon might have differential influences on the production and degradation of endothelin-1 (Vijayaraghavan *et al.*, 1990; Sokolovsky *et al.*, 1990), and hence the overall changes could be multifactorial in origin. However, with bolus administration of exogenous proendothelin-1, inhibition of the degradation of the resulting endothelin-1 is not likely to contribute greatly to the effects of phosphoramidon, since the neutral endopeptidase inhibitor, SQ 28,603, which is more potent than phosphoramidon at inhibiting degradation of endothelin-1 (Dickinson *et al.*, 1991), has no significant effects on the haemodynamic actions of exogenous endothelin-1 (Gardiner *et al.*, 1992a). Interestingly, SQ 28,603 does inhibit the pressor effects of proendothelin-1 (Gardiner *et al.*, 1992a)

[1] Author for correspondence.

indicating this compound may suppress ECE-1 activity, unlike kelatorphan, captopril or enalaprilat (McMahon *et al.*, 1991; Pollock & Opgenorth, 1991). The results with SQ 28,603 are consistent with ECE-1 being a form of neutral endopeptidase, and this is in line with the observations of McMahon *et al.* (1991) showing that thiorphan causes dose-dependent inhibition of the pressor effects of proendothelin-1. However, these findings go against those of Pollock & Opgenorth (1991) who reported that thiorphan was without effect on responses to proendothelin-1. But examination of the results of Pollock & Opgenorth (1991) shows that baseline values in the presence of thiorphan were elevated (see their Table 1), and this may have masked an inhibitory effect of thiorphan on responses to proendothelin-1. Nevertheless, the *in vivo* studies are generally consistent with the proposition that most, if not all, the cardiovascular effects of exogenous proendothelin-1 are dependent upon endothelin-1 produced by the activity of a phosphoramidon-sensitive ECE-1, that may be differentially expressed in different vascular beds (Gardiner *et al.*, 1991; Hisaki *et al.*, 1991).

In line with the apparent selectivity of ECE-1 for proendothelin-1 as a substrate, Télémaque & D'Orléans-Juste (1991) and D'Orléans-Juste *et al.* (1991) have reported that, in the vas deferens of the rat and in the intact guinea-pig, proendothelin-3 is biologically inactive. However, these findings are not easy to reconcile with our observations showing that, in conscious rats, proendothelin-3 exerts clear pressor and vasoconstrictor effects (Gardiner *et al.*, 1992c), similar in pattern to those seen with proendothelin-1 (Gardiner *et al.*, 1991; 1992c).

Since we had previously demonstrated inhibition of the haemodynamic effects of proendothelin-1 by phosphoramidon in conscious rats (Gardiner *et al.*, 1991), and considering the unresolved questions outlined above, the present work was carried out to determine whether or not the *in vivo* effects of proendothelin-3 were susceptible to inhibition by phosphoramidon. We also assessed the regional haemodynamic effects of proendothelin-2 and the effects of phosphoramidon on these. Finally, we investigated the effects of phosphoramidon on haemodynamic responses to endothelin-2 and endothelin-3, to ensure that any putative effects of phosphoramidon on responses to proendothelin-2 or -3 were not due to inhibition of the action of the peptides produced from them.

Methods

Male, Long Evans rats (400–450 g) were used in all experiments. Under sodium methohexitone anaesthesia (60 mg kg^{-1}, i.p., supplemented as required), pulsed Doppler flow probes (Haywood *et al.*, 1981) were sutured around the left renal and superior mesenteric arteries, and the distal abdominal aorta (to monitor flow to the hindquarters). The probe wires were led subcutaneously to emerge at the back of the neck where they were anchored by a suture. Following closure of incisions, animals were given ampicillin (Penbritin, Beecham, 7 mg kg^{-1}, i.m.) and returned to individual home cages with free access to food and water.

At least 7 days later, animals were anaesthetized (sodium methohexitone, 40 mg kg^{-1}, i.p., supplemented as necessary), and the signals from the pulsed Doppler probes were checked. Any animal without good quality signals (signal: noise $>$ 20:1) from all 3 probes was excluded from the study; those with 3 acceptable flow signals had an intra-arterial (distal abdominal aorta via the ventral caudal artery) and intravenous (right jugular) catheters implanted. The catheters ran subcutaneously to emerge at the same site as the probe wires. The latter were soldered into a micro-connector (Microtech Inc., Boothwyn, USA) that was held in a clamp fitted to a harness worn by the rat. The catheters ran through a flexible spring connected to the harness; the spring was supported by a counterbalanced lever system to allow the rat free movement. Animals were returned to their home cages with free access to water and food, and experiments did not commence until at least 24 h later. The following protocols were run:

Experiment 1 Cardiovascular responses to proendothelin-2 and proendothelin-3

Animals ($n = 8$) were given bolus i.v. injections of proendothelin-2 and proendothelin-3 (0.1 and 1.0 nmol kg^{-1}). The experiment ran over 2 days with animals receiving 2 injections a day. They received the peptides in random order, but the higher doses were given after the lower doses, because of the prolonged effects of the former.

Experiment 2 Effects of phosphoramidon on cardiovascular responses to proendothelin-2 and proendothelin-3

Animals ($n = 7$) were challenged with i.v. bolus injections of proendothelin-2 or proendothelin-3 (1.0 nmol kg^{-1}) in the absence, or 5 min after, i.v. bolus injection of phosphoramidon (10 μmol kg^{-1}; Gardiner *et al.*, 1991). Animals were given proendothelin-2 and proendothelin-3 in random order on separate days. Responses to either peptide in the absence and presence of phosphoramidon were measured on the same day (at least 5 h apart). In pilot experiments we determined that repeated doses of proendothelin-2 or -3, separated by 5 h, evoked similar responses.

Experiment 3 Effects of phosphoramidon on responses to endothelin-2 and endothelin-3

Animals ($n = 6$) were challenged with i.v. bolus injections of endothelin-2 or endothelin-3 (0.1 nmol kg^{-1}) before, or 5 min after, phosphoramidon. Animals were randomized to receive endothelin-2 or -3 on separate days, with the exposures to each peptide in the absence and presence of phosphoramidon being separated by at least 5 h.

Continuous recordings were made (on a Gould ES 1000 system) of phasic and mean systemic arterial blood pressure, instantaneous heart rate, and phasic and mean Doppler shift signals (Crystal Biotech VF1 system). The phasic Doppler shift signals were recorded only to ensure there were no technical problems (we have encountered circumstances when the mean Doppler signal looked acceptable although the phasic Doppler signal showed loss of pulsatility). Measurements of mean arterial blood pressure, heart rate and mean renal, mesenteric and hindquarters Doppler shift signals were made at selected time points. This was done by averaging (by eye) over 20 s epochs. Percentage changes in mean Doppler shift signals were taken as indices of changes in flow (Haywood *et al.*, 1981; Gardiner *et al.*, 1989a; 1990a,b,c; 1991; 1992a,b,c). Vascular conductances were calculated by dividing mean Doppler shift by mean blood pressure and expressing changes as percentages (Gardiner *et al.*, 1991).

Data analysis

Within-group analysis was carried out by use of Friedman's test (Theodorsson-Norheim, 1987). Comparison of responses in the same groups of animals in different experimental protocols was made on areas under or over curves (AUC and AOC, respectively, $t = 0–60$ min) by Wilcoxon's rank sums test. A P value < 0.05 was taken as significant.

Peptides

Endothelin-2, endothelin-3, proendothelin-2 (human, 1–37) and proendothelin-3 (human, 1–41 amide) were obtained from the Peptide Institute (Osaka, Japan) through their UK agents (Scientific Research Associates). The peptides were dissolved initially in aqueous acetic acid (0.1%) and stored in

100 µl aliquots at − 80°C. Before use the stock solution was diluted in saline containing 1% bovine serum albumin (Sigma, U.K.). Phosphoramidon (sodium salt, Sigma, U.K.) was dissolved in isotonic saline. All bolus injections were given in 100 µl and flushed in with 150 µl isotonic saline. Injection of vehicle solutions in these volumes had no consistent haemodynamic effects.

Results

Cardiovascular responses to proendothelin-2 and proendothelin-3

The low dose (0.1 nmol kg^{-1}) of proendothelin-2 had no significant effects on mean arterial blood pressure (MAP), but there was a transient tachycardia (Figure 1, Table 1). Renal blood flow did not change significantly, although there was a slight decrease in mesenteric blood flow and hindquarters flow showed an initial increase (Figure 1, Table 1). There was no significant decrease in renal vascular conductance, although there was a slight, but significant, mesenteric vasoconstriction, and a hindquarters vasodilatation followed by a delayed vasoconstriction (Figure 1, Table 1).

Proendothelin-3 (0.1 nmol kg^{-1}) caused a slight, but significant, rise in MAP, but this was not significantly different from the effect of proendothelin-2, and there was also a similar initial tachycardia (Figure 1, Table 1). Proendothelin-3 had no significant effect on renal blood flow, and the initial rise in hindquarters flow it caused was not different from that seen with proendothelin-2 (Figure 1, Table 1). However, the reduction in mesenteric blood flow caused by proendothelin-3 was significantly greater than that seen with proendothelin-2, as was the mesenteric vasoconstriction (Figure 1,Table 1), whereas the renal vasoconstriction and hindquarters vasodilatation were not different from the effects of proendothelin-2 (Figure 1, Table 1).

The high dose (1 nmol kg^{-1}) of proendothelin-2 caused a clear, and prolonged, rise in MAP accompanied by a sustained bradycardia (Figure 1, Table 1). There was a slight reduction in renal blood flow, a more marked reduction in mesenteric blood flow, and an initial rise followed by a non-significant reduction in hindquarters flow (Figure 1, Table 1). Renal and mesenteric vascular conductances were

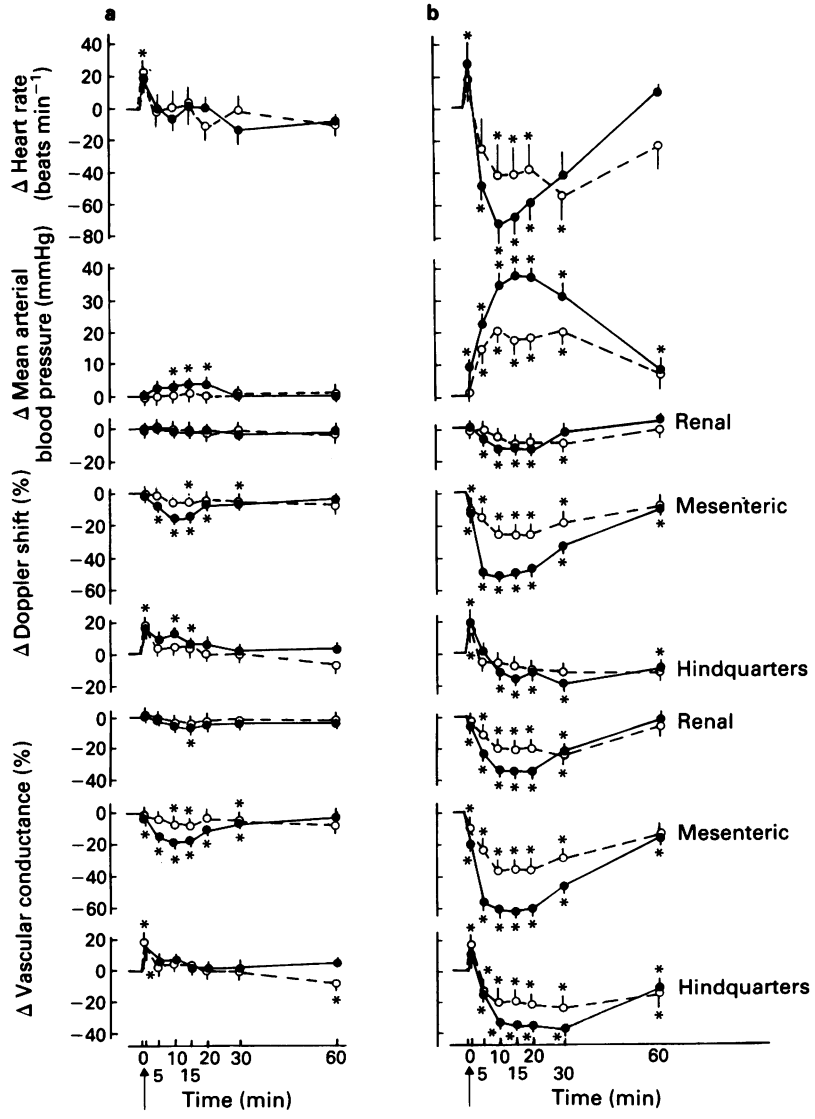

Figure 1 Cardiovascular changes in the same conscious, Long Evans rats in response to bolus i.v injections of proendothelin-2 (○) and proendothelin-3 (●) at doses of 0.1 nmol kg^{-1} (a) or 1.0 nmol kg^{-1} (b). Values are mean and vertical bars show s.e.mean ($n = 8$).
*$P < 0.05$ versus original baseline. Statistics for differences between responses to proendothelin-2 and proendothelin-3 are given in the text.

Table 1 Integrated (area under or over curve (AUC, AOC) for 0–60 min) cardiovascular response to bolus i.v. injections of proendothelin (ProEt)-2 or -3 in the same conscious, Long Evans rats ($n = 8$)

		ProEt-2 (0.1 nmol kg^{-1})	*ProEt-3* (0.1 nmol kg^{-1})	*ProEt-2* (1 nmol kg^{-1})	*ProEt-3* (1 nmol kg^{-1})
MAP (mmHg min)	AUC	NS	159 ± 62	970 ± 156	1552 ± 166†
HR (beats)	AUC	530 ± 264	336 ± 113	NS	208 ± 91
	AOC	NS	NS	2569 ± 391	2789 ± 506
Doppler shift (%min)					
Renal	AOC	NS	NS	465 ± 122	448 ± 107
Mesenteric	AOC	432 ± 65	528 ± 79†	1113 ± 106	1964 ± 167†
Hindquarters	AUC	263 ± 167	441 ± 100	114 ± 47	69 ± 19
	AOC	NS	NS	NS	853 ± 74
Vascular conductance (%min)					
Renal	AOC	NS	259 ± 79	1067 ± 95	1291 ± 148†
Mesenteric	AOC	448 ± 83	613 ± 69†	1657 ± 118	2631 ± 176†
Hindquarters	AUC	369 ± 198	489 ± 132	61 ± 29	28 ± 15
	AOC	419 ± 140	NS	1192 ± 225	1736 ± 100

Values are mean ± s.e.mean.
At the low dose, the predominant heart rate response was a tachycardia whereas at the high dose there was a marked, subsequent bradycardia. In the hindquarters vascular bed an initial vasodilatation was followed by a vasoconstriction; hence values for AUC and AOC are included.
†$P < 0.05$: significant difference from the effects of the corresponding dose of ProEt-2 (Wilcoxon's ranks sums test).
NS indicates no significant change in that variable.

decreased, and there was an initial dilatation followed by a constriction in the hindquarters vascular bed (Figure 1, Table 1).

The pattern of cardiovascular response to proendothelin-3 (1 nmol kg^{-1}) was similar to that above, although the rise in MAP and reduction in mesenteric blood flow were greater with proendothelin-3 than with proendothelin-2, as were the renal and mesenteric vasoconstrictions (Figure 1, Table 1). With proendothelin-3, the reductions in heart rate and renal flow, and the initial rise and subsequent fall in hindquarters flow and vascular conductance were not different from those seen with proendothelin-2 (Figure 1, Table 1).

Effects of phosphoramidon on cardiovascular response to proendothelin-2 and proendothelin-3

The responses to proendothelin-2 and to proendothelin-3 (1 nmol kg^{-1}) in the animals in this experiment were generally similar to those seen in the first experiment (Figure 2, Table 2). As before, the pressor effect of proendothelin-3 was greater than that of proendothelin-2. However, in this experiment the bradycardic affect of proendothelin-3 was significantly greater than that of proendothelin-2 (Figure 2, Table 2). There was no significant difference between the effects of proendothelin-2 and proendothelin-3 in respect of the reductions in renal blood flow or hindquarters blood flow (Figure 2, Table 2). However, the reduction in mesenteric blood flow evoked by proendothelin-3 was greater than that elicited by proendothelin-2. Proendothelin-3 caused more marked renal vasoconstriction and mesenteric vasoconstriction than did proendothelin-2, but the hindquarters vasoconstrictor responses to the peptides were not significantly different (Figure 2, Table 2).

Phosphoramidon had no significant haemodynamic effects itself, but it abolished the pressor, bradycardic and hindquarters vasoconstrictor effects of proendothelin-2, and reduced significantly its renal and mesenteric vasoconstrictor actions (Figure 2, Table 2).

In the presence of phosphoramidon, the pressor influence of proendothelin-3 was markedly reduced, and this effect was accompanied by an abolition of the bradycardic and hindquarters vasoconstrictor response and significant reductions of the renal and mesenteric vasoconstrictor responses (Figure 2, Table 2).

Effects of phosphoramidon on cardiovascular responses to endothelin-2 and endothelin-3

The pressor and vasoconstrictor response to endothelin-2 and -3 were as described elsewhere (Gardiner *et al.*, 1990a,b,c); phosphoramidon had no significant effects on these responses (data not shown).

Discussion

The present study has shown that proendothelin-2 and -3 have dose-dependent haemodynamic effects in conscious rats. These effects are inhibited by phosphoramidon at a dose that has no effects on the pressor or vasoconstrictor response to exogenous endothelin-2 or -3. Hence, these results are consistent with the *in vivo* haemodynamic actions of exogenous proendothelin-2 and -3 being due to their conversion into endothelin-2 and -3, respectively, by phosphoramidon-sensitive enzyme(s). In this regard, proendothelin-2 and -3 show no marked differences from proendothelin-1 (Matsumura *et al.*, 1990a,b; Fukuroda *et al.*, 1990; McMahon *et al.*, 1991; Gardiner *et al.*, 1991; Le Monnier de Gouville & Cavero, 1991; Pollock & Opgenorth, 1991).

These results are particularly striking against the background (see Introduction) of biochemical and cardiovascular studies showing that phosphoramidon-sensitive, ECE-1 does not act on proendothelin-2 or -3. Of course, it is feasible that the failure to demonstrate phosphoramidon-sensitive conversion of proendothelin-2 and -3 to endothelin-2 and -3, respectively, in the *in vitro* systems examined (Okada *et al.*, 1990; 1991; Takada *et al.*, 1992) is a reflection of the inability of such systems to represent the *in vivo* condition. However, this argument cannot pertain to the observations of D'Orléans-Juste *et al.* (1991) who found proendothelin-3, in doses as high as 20 nmol kg^{-1}, had no cardiovascular effects *in vivo*. It is possible the fundamental difference between the results of D'Orléans-Juste *et al.* (1991) and ours is due to a species difference (since they studied anaesthetized guinea-pigs), but this seems unlikely because Télémaque & D'Orléans-Juste (1991) also found proendothelin-3 was inactive in rat tissues, albeit *in vitro*. The inactivity of the proendothelin-3 used by Télémaque & D'Orléans-Juste *et al.* (1991) cannot be due to their material not being the authentic peptide, because they

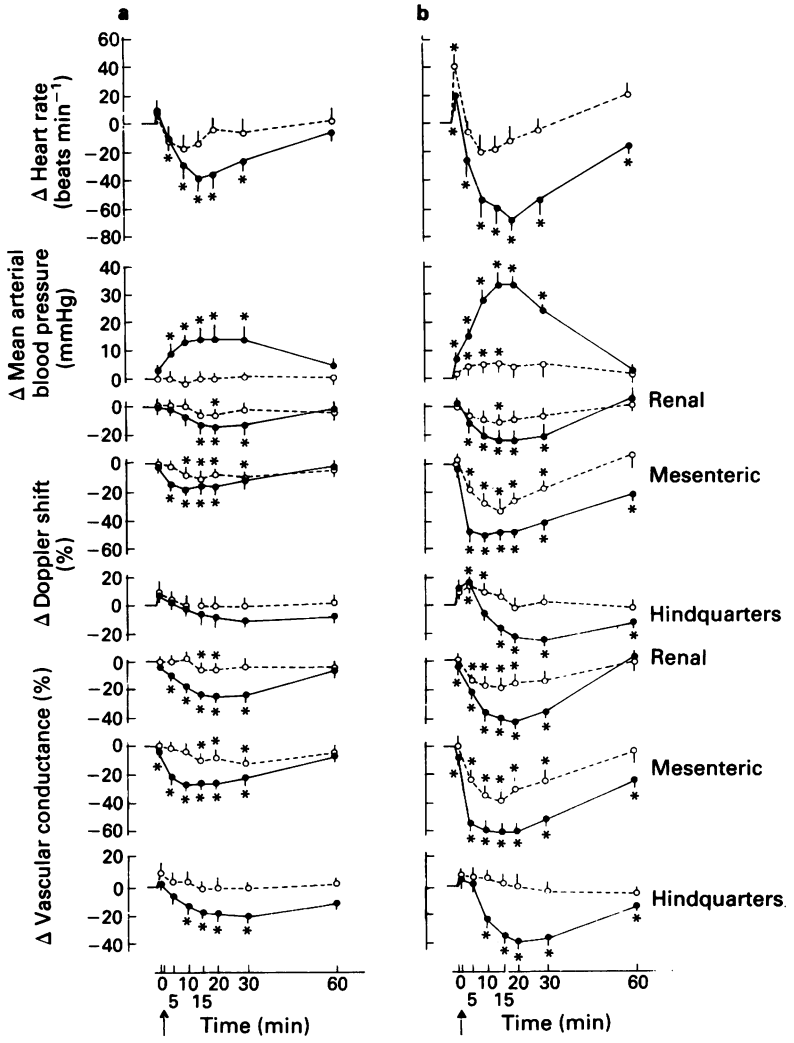

Figure 2 Cardiovascular changes in the same conscious, Long Evans rats in response to bolus injections of proendothelin-2 (1.0 nmol kg^{-1}, a) or proendothelin-3 (1.0 nmol kg^{-1}, b) before (●) and 5 min after i.v. bolus injection of phosphoramidon (10 μmol kg^{-1}, ○). Values are mean and vertical bars show s.e.mean ($n = 7$).
*$P < 0.05$ versus original baseline. Statistics for differences between responses before and after administration of phosphoramidon are given in the text.

Table 2 Integrated (area under or over curve (AUC, AOC) for 0–60 min) cardiovascular responses to bolus i.v. injections of proendothelin-2 or -3 (1 nmol kg^{-1}) before and 5 min after phosphoramidon (10 μmol kg^{-1}) in the same conscious, Long Evans rats ($n = 7$)

		Proendothelin-2	*Proendothelin-2 after phosphoramidon*	*Proendothelin-3*	*Proendothelin-3 after phosphoramidon*
MAP (mmHg min)	AUC	665 ± 132	NS*	1201 ± 66†	517 ± 129*
HR (beats)	AUC	NS	NS	108 ± 48	727 ± 181*
	AOC	1539 ± 418	NS*	2612 ± 371†	NS*
Doppler shift (%min)					
Renal	AOC	661 ± 197	316 ± 67*	1087 ± 267	523 ± 174*
Mesenteric	AOC	791 ± 179	520 ± 84*	2258 ± 200†	1046 ± 212*
Hindquarters	AUC	NS	NS	117 ± 27	399 ± 121
	AOC	NS	NS	991 ± 181	NS*
Vascular conductance (%min)					
Renal	AOC	1093 ± 210	300 ± 74*	1804 ± 170†	831 ± 260*
Mesenteric	AOC	1141 ± 219	537 ± 106*	2758 ± 174†	1325 ± 259*
Hindquarters	AUC	NS	NS	NS	NS
	AOC	981 ± 249	NS*	1666 ± 158	NS*

Values are mean ± s.e.mean.
†$P < 0.05$: significant difference from the effects of proendothelin-2.
*$P < 0.05$: significant difference from the effects seen in the absence of phosphoramidon (Wilcoxon's ranks sums test).
NS indicates no significant change in that variable.

obtained it from the same source as we did (Peptide Institute). While we have no explanation for this important disparity, we shall discuss our results on the assumption they are correct, not the least because we have found that two separate batches of proendothelin-3 had clear haemodynamic effects in several different groups of experimental animals (Gardiner *et al.*, 1992c and present study).

In the conscious rat, the cardiovascular effects of proendothelin-2 were, in several respects (pressor and renal and mesenteric vasoconstrictor actions) less than those of proendothelin-3. While this could have been due to more effective conversion of the latter to the active peptide, it is possible this was on account of the forms of peptide used (proendothelin-3 was amidated, but proendothelin-2 was not). However, it is notable that the pattern of response to proendothelin-2 and -3, with a particularly marked mesenteric vasoconstriction in both cases, was similar to that seen with proendothelin-1 (Gardiner *et al.*, 1991; 1992a), and is consistent with substantial ECE activity in this vascular bed (Hisaki *et al.*, 1991). In general, the pattern of response to proendothelin-2 and -3 was similar to that seen with endothelin-2 and -3 (Gardiner *et al.*, 1990a,b,c), consistent with these peptides being responsible for the effects of proendothelin-2 and -3, respectively. However, as noted elsewhere for proendothelin-1 (Gardiner *et al.*, 1991), proendothelin-2 and -3 exerted more marked hindquarters vasoconstrictor effects than endothelin-2 and -3. This is consistent with the endothelins causing more marked stimulation of those factors mediating the vasodilatation that opposes their vasoconstrictor influences. While it appears that endothelium-derived nitric oxide (NO) is not a major contributor to the hindquarters vasodilator effects of endothelin-1 (Gardiner *et al.*, 1989b), putative interactions between NO and endothelins should always be borne in mind. This is particularly true in the light of the recent finding that manipulating the availability of sulphydryl groups has marked effects on phosphoramidon-sensitive ECE-1 activity (Matsumura *et al.*, 1991a), since there is good evidence that NO interacts with sulphydryl groups (Moncada *et al.*, 1991); thus, NO might indirectly influence ECE activity.

The regionally differentiated effects of proendothelin-2 and -3 are consistent with the local conversion of these precursors into the active peptides, as suggested for proendothelin-1 (Gardiner *et al.*, 1991), although it does not follow that the same enzyme system(s) is responsible for the conversion of all three proendothelins. Recently, Modin *et al.* (1991) reported that phosphoramidon inhibited the pressor effects of proendothelin-1, but not the elevation in plasma endothelin-1. These results are entirely consistent with local, rather than systemic, conversion of proendothelins being responsible for their biological effects (Gardiner *et al.*, 1991; Le Monnier de Gouville & Cavero, 1991; Watanabe *et al.*, 1991). Indeed, the lack of change in plasma endothelin-1 levels under conditions in which its cardiovascular influences clearly are diminished illustrates the inability of the plasma level of endothelin-1 (and, presumably, -2 and -3) to provide information of functional significance.

The fact that phosphoramidon abolished the pressor effects of proendothelin-2, but not those of proendothelin-3, could have been due to the difference in the magnitudes of the response to these peptides in the absence of phosphoramidon. However, the latter had substantial inhibitory effects on the haemodynamic actions of both proendothelin-2 and -3, and there was no evidence that phosphoramidon was a less effective inhibitor of the effects of these peptides than of the actions of proendothelin-1 (Gardiner *et al.*, 1991). As in that instance, there was particularly marked inhibition of the hindquarters vasoconstrictor actions of proendothelin-2 and -3 by phosphoramidon. Thus, it seems likely that this effect was a major determinant of the ability of phosphoramidon to inhibit the pressor actions of the proendothelins. While a greater contribution of the hindquarters, rather than renal and/or mesenteric, vascular bed to haemodynamic status may seem surprising, it is consistent with the finding that the hindquarters vascular bed makes a particular contribution to the maintenance of hypertension following chronic inhibition of NO synthesis (Gardiner *et al.*, 1992b), for example.

In conclusion, proendothelin-2 and -3 have marked haemodynamic effects *in vivo* in conscious rats, and these effects appear to be largely-dependent on a phosphoramidon-sensitive ECE.

References

DICKINSON, K.E.J., TYMIAK, A.A., COHEN, R.B., LIU, E.C.-K., WEBB, M.L. & HEDBERG, A. (1991). Vascular A10 cell membranes contain an endothelin metabolizing neutral endopeptidase. *Biochem. Biophys. Res. Commun.*, **176**, 423–429.

D'ORLÉANS-JUSTE, P., TÉLÉMAQUE, S. & CLAING, A. (1991). Different pharmacological profiles of big-endothelin-3 and big-endothelin-1 *in vivo* and *in vitro*. *Br. J. Pharmacol.*, **104**, 440–444.

FUKURODA, T., NOGUCHI, K., TSUCHIDA, S., NISHIKIBE, M., IKEMOTO, F., OKADA, K. & YANO, M. (1990). Inhibition of biological actions of big endothelin-1 by phosphoramidon. *Biochem. Biophys. Res. Commun.*, **172**, 390–395.

GARDINER, S.M., COMPTON, A.M. & BENNETT, T. (1989a). Regional hemodynamic effects of endothelin-1 in conscious, unrestrained, Wistar rats. *J. Cardiovasc. Pharmacol.*, **13** (Suppl. 5), S202–S204.

GARDINER, S.M., COMPTON, A.M. & BENNETT, T. (1990a). Regional haemodynamic effects of endothelin-1 and endothelin-3 in conscious, Long Evans and Brattleboro rats. *Br. J. Pharmacol.*, **99**, 107–112.

GARDINER, S.M., COMPTON, A.M. & BENNET, T. (1990b). Regional hemodynamic effects of endothelin-2 and sarafotoxin-S6b in conscious rats. *Am. J. Physiol.*, **258**, R912–R917.

GARDINER, S.M., COMPTON, A.M. & BENNETT, T. (1990c). Effects of indomethacin on the regional haemodynamic responses to low doses of endothelins and sarafotoxin. *Br. J. Pharmacol.*, **100**, 158–162.

GARDINER, S.M., COMPTON, A.M., BENNETT, T., PALMER, R.M.J. & MONCADA, S. (1989b). N^G-monomethyl-L-arginine does not inhibit the hindquarters vasodilator action of endothelin-1 in conscious rats. *Eur. J. Pharmacol.*, **171**, 237–240.

GARDINER, S.M., COMPTON, A.M., KEMP, P.A. & BENNETT, T. (1991). The effects of phosphoramidon on the regional haemodynamic responses to human proendothelin [1-38] in conscious rats. *Br. J. Pharmacol.*, **103**, 2009–2015.

GARDINER, S.M., KEMP, P.A. & BENNETT, T. (1992a). Effects of the neutral endopeptidase inhibitor, SQ 28,603, on regional haemodynamic responses to atrial natriuretic peptide or proendothelin-1 [1-38] in conscious rats. *Br. J. Pharmacol.*, **106**, 180–186.

GARDINER, S.M., KEMP, P.A., BENNETT, T., PALMER, R.M.J. & MONCADA, S. (1992b). Nitric oxide synthase inhibitors cause sustained, but reversible, hypertension and hindquarters vasoconstriction in Brattleboro rats. *Eur. J. Pharmacol.*, **213**, 449–451.

GARDINER, S.M., KEMP, P.A., COMPTON, A.M. & BENNETT, T. (1992c). Coeliac haemodynamic effects of endothelin-1, endothelin-3, proendothelin-1 [1-38] and proendothelin-3 [1-41] in conscious rats. *Br. J. Pharmacol.*, **106**, 483–488.

HAYWOOD, J.R., SHAFFER, R., FASTENOW, C., FINK, G.D. & BRODY, M.J. (1981). Regional blood flow measurement with pulsed Doppler flowmeter in conscious rat. *Am. J. Physiol.*, **241**, H273–H278.

HIOKI, Y., OKADA, K., ITO, H., MATSUYAMA, K. & YANO, M. (1991). Endothelin converting enzyme of bovine carotid artery smooth muscles. *Biochem. Biophys. Res. Commun.*, **174**, 446–451.

HISAKI, K., MATSUMURA, Y., IKEGAWA, R., NISHIGUCHI, S., HAYASHI, K., TAKAOKA, M. & MORIMOTO, S. (1991). Evidence for phosphoramidon-sensitive conversion of big endothelin-1 to endothelin-1 in isolated rat mesenteric artery. *Biochem. Biophys. Res. Commun.*, **177**, 1127–1131.

IKEGAWA, R., MATSUMURA, Y., TSUKAHARA, Y., TAKAOKA, M. & MORIMOTO, S. (1991). Phosphoramidon inhibits the generation of endothelin-1 from exogenously applied big endothelin-1 in cultured vascular endothelial cells and smooth muscle cells. *FEBS Lett.*, **293**, 45–48.

LE MONNIER DE GOUVILLE, A.-C. & CAVERO, I. (1991). Cross tachyphylaxis to endothelin isopeptide-induced hypotension: a phenomenon not seen with proendothelin. *Br. J. Pharmacol.*, **104**, 77–84.

MATSUMURA, Y., HISAKI, K., TAKAOKA, M. & MORIMOTO, S. (1990a). Phosphoramidon, a metalloproteinase inhibitor, suppresses the hypertensive effect of big endothelin-1. *Eur. J. Pharmacol.*, **185**, 103–106.

MATSUMURA, Y., IKEGAWA, R., TSUKAHARA, Y., TAKAOKA, M. & MORIMOTO, S. (1990b). Conversion of big endothelin-1 to endothelin-1 by two types of metalloproteinases derived from porcine aortic endothelial cells. *FEBS Lett.*, **272**, 166–170.

MATSUMURA, Y., IKEGAWA, R., TSUKAHARA, Y., TAKAOKA, M. & MORIMOTO, S. (1991a). N-ethylmaleimide differentiates endothelin converting activity by two types of metalloproteinases derived from vascular endothelial cells. *Biochem. Biophys. Res. Commun.*, **178**, 531–538.

MATSUMURA, Y., IKEGAWA, R., TSUKAHARA, Y., TAKAOKA, M. & MORIMOTO, S. (1991b). Conversion of big endothelin-1 to endothelin-1 by two-types of metalloproteinases of cultured porcine vascular smooth muscle cells. *Biochem. Biophys. Res. Commun.*, **178**, 899–905.

MCMAHON, E.G., PALOMO, M.A., MOORE, W.M., MCDONALD, J.F. & STERN, M.K. (1991). Phosphoramidon blocks the pressor activity of porcine big endothelin-1-(1-39) *in vivo* and conversion of big endothelin-1-(1-39) to endothelin-1-(1-21) *in vitro*. *Proc. Natl. Acad. Sci. U.S.A.*, **88**, 703–707.

MODIN, A., PERNOW, J. & LUNDBERG, J.M. (1991). Phosphoramidon inhibits the vasoconstrictor effects evoked by big endothelin-1 but not the elevation of plasma endothelin-1 *in vivo*. *Life Sci.*, **49**, 1619–1625.

MONCADA, S., PALMER, R.M.J. & HIGGS, E.A. (1991). Nitric oxide: physiology, pathophysiology and pharmacology. *Pharmacol. Res.*, **43**, 109–142.

OKADA, K., MIYAZAKI, Y., TAKADA, J., MATSUYAMA, K., YAMAKI, T. & YANO, M. (1990). Conversion of big endothelin-1 by membrane-bound metalloendopeptidase in cultured bovine endothelial cells. *Biochem. Biophys. Res. Commun.*, **171**, 1192–1197.

OKADA, K., TAKADA, J., ARAI, Y., MATSUYAMA, K. & YANO, M. (1991). Importance of the C-terminal region of big endothelin-1 for specific conversion by phosphoramidon-sensitive endothelin converting enzyme. *Biochem. Biophys. Res. Commun.*, **180**, 1019–1023.

POLLOCK, D.M. & OPGENORTH, T.J. (1991). Evidence for metalloprotease involvement in the *in vivo* effects of big endothelin-1. *Am. J. Physiol.*, **261**, R257–R263.

SOKOLOVSKY, M., GALRON, R., KLOOG, Y., BDOLAH, A., INDIG, F.E., BLUMBERG, S. & FLEMINGER, G. (1990). Endothelins are more sensitive than sarafotoxins to neutral endopeptidase: Possible physiological significance. *Proc. Natl. Acad. Sci. U.S.A.*, **87**, 4702–4706.

TAKADA, J., HATA, M., OKADA, K., MATSUYAMA, K. & YANO, M. (1992). Biochemical properties of endothelin converting enzyme in renal epithelial cell lines. *Biochem. Biophys. Res. Commun.*, **182**, 1383–1388.

TAKADA, J., OKADA, K., IKENAGA, T., MATSUYAMA, K. & YANO, M. (1991). Phosphoramidon-sensitive endothelin-converting enzyme in the cytosol of cultured bovine endothelial cells. *Biochem. Biophys. Res. Commun.*, **176**, 860–865.

TÉLÉMAQUE, S. & D'ORLÉANS-JUSTE, P. (1991). Presence of a phosphoramidon-sensitive endothelin-converting enzyme which converts big-endothelin-1, but not big-endothelin-3, in the rat vas deferens. *Naunyn-Schmiedebergs Arch. Pharmacol.*, **344**, 505–507.

THEODORSSON-NORHEIM, E. (1987). Freidman and Quade tests: BASIC computer program to perform non-parametric two-way analysis of variance and multiple comparisons on ranks of several related samples. *Comput. Biol. Med.*, **17**, 85–99.

VIJAYARAGHAVAN, J., SCICLI, A.G., CARRETERO, O.A., SLAUGHTER, C., MOOMAW, C. & HERSH, L.B. (1990). The hydrolysis of endothelins by neutral endopeptidase 24.11 (enkephalinase). *J. Biol. Chem.*, **265**, 14150–14155.

WATANABE, Y., NARUSE, M., MONZEN, C., NARUSE, K., OHSUMI, K., HORIUCHI, J., YOSHIHARA, I., KATO, Y., NAKAMURA, N., KATO, M., SUGINO, N. & DEMURA, H. (1991). Is big endothelin converted to endothelin-1 in circulating blood? *J. Cardiovasc. Pharmacol.*, **17** (Suppl. 7), S503–S505.

YANAGISAWA, M., KURIHARA, H., KIMURA, S., TOMOBE, Y., KOBAYASHI, M., MITSUI, Y., YAZAKI, Y., GOTO, K. & MASAKI, T. (1988). A novel potent vasoconstrictor peptide produced by vascular endothelial cells. *Nature*, **332**, 411–415.

(Received April 8, 1992
Revised June 16, 1992
Accepted June 22, 1992)

Br. J. Pharmacol. (1992), **107**, 591–596

5-Hydroxytryptamine (5-HT) mediates potent relaxation in the sheep isolated pulmonary vein via activation of 5-HT_4 receptors

[1] T.M. Cocks & P.J. Arnold

Baker Medical Research Institute, Commercial Rd, Prahran, Victoria, 3181, Australia

1 We investigated the potent 5-hydroxytryptamine (5-HT)-mediated vasorelaxation of the sheep pulmonary vein. Here we present evidence that this response is due to activation of 5-HT_4 receptors.

2 5-HT (1–1000 nM) caused concentration-dependent, maintained relaxations ($pEC_{50} = 8.4 \pm 0.1$) of isolated rings of sheep pulmonary vein pre-contracted with endothelin-1 (3 nM).

3 The relaxation response to 5-HT was unaffected by either removal of the endothelium or by inhibition of NO-synthase by N^G-nitro-L-arginine (100 μM).

4 Ketanserin, methiothepin, methysergide and MDL 72222 at concentrations that selectively block 5-HT_2, 5-HT_1-like and 5-HT_3 receptors respectively, had no effect on the concentration-relaxation curve to 5-HT.

5 ICS 205-930 (1–10 μM) competitively antagonized the concentration-relaxation curve to 5-HT with a pA_2 of approximately 6.7.

6 Increasing the concentration of ICS 205-930 from 10 to 30 μM did not cause a further rightward shift of the 5-HT concentration-relaxation curve. The pEC_{50} of 6.50 for 5-HT in the presence of ICS 205-930 (30 μM) was taken as an estimate of the affinity of 5-HT for 5-HT_1-like receptors since methiothepin (10 nM) unmasked further competitive inhibition of 5-HT in the presence of this concentration of ICS 205-930.

7 Other 5-HT agonists including 5-carboxamidotryptamine (5-CT), α-methyl-5-HT and BIMU 8 (but not 2-methyl-5-HT) also relaxed the pulmonary vein. The response to 5-CT was inhibited by methiothepin (10 nM) and methysergide (100 nM) but unaffected by ICS 205-930 (30 μM), whilst that to α-methyl-5-HT and BIMU 8 was unaffected by methiothepin (10 nM) but blocked by ICS 205-930 (estimated pK_B values of 6.4 and 6.9 respectively). Relaxation curves to both 5-HT and BIMU 8 were unaffected by cocaine (6 μM).

8 In conclusion, these results indicate that the sheep pulmonary vein possesses 5-HT_4 receptors that mediate potent endothelium-independent relaxation. 5-HT_1-like relaxant receptors are also present in this tissue but 5-HT has a lower affinity at these receptors. This preparation may thus provide a robust and sensitive bioassay for future development of selective 5-HT_4 receptor agonists and antagonists.

Keywords: 5-Hydroxytryptamine (5-HT); vasorelaxation; sheep pulmonary vein; 5-HT_4 receptors

Introduction

Receptors for 5-hydroxytryptamine (5-HT) have been divided into three major classes; 5-HT_1-like, 5-HT_2 and 5-HT_3 (Bradley *et al.*, 1986). In addition to its action at 5-HT receptors (5-HT_2 or 5-HT_1-like) mediating vascular smooth muscle contraction, 5-HT also causes both endothelium-dependent and independent relaxation of a number of isolated blood vessels including porcine coronary artery, (Cocks & Angus, 1983) rabbit jugular vein, (Leff *et al.*, 1987) cat saphenous vein, (Feniuk *et al.*, 1983) porcine vena cava, (Sumner *et al.*, 1989; Sumner, 1991) and sheep and goat pulmonary veins (Eyre, 1975; Chand, 1981). 5-HT_1-like receptors have been found to mediate vasorelaxation in most of these cases (but see Sumner *et al.*, 1991; Leff *et al.*, 1987), and have been characterized by the following criteria: (1) susceptibility to blockade by methiothepin and methysergide; (2) resistance to blockade by 5-HT_2 and 5-HT_3 receptor selective antagonists; (3) a high agonist potency of 5-HT which is mimicked by 5-carboxamidotryptamine (5-CT) with an equal or greater potency (Bradley *et al.*, 1986). A novel 5-HT receptor site, positively coupled to adenylate cyclase, designated as 5-HT_4 has been identified in mammalian brain, (Dumuis *et al.*, 1988a,b; 1989; Bockaert *et al.*, 1990) guinea-pig ileum, (Craig & Clarke, 1989) rat oesophagus (Baxter *et al.*, 1991) porcine heart, (Villalon *et al.*, 1990; 1991) and human atria (Kaumann *et al.*, 1990; 1991). ICS 205-930 has been reported to be an antagonist at this receptor (Dumuis *et al.*, 1988b). This compound also acts as an antagonist at 5-HT_3 receptors with a pK_B of 10.2–10.6 (Richardson *et al.*, 1985). At higher concentrations, however, ICS 205-930 antagonizes the actions of 5-HT at 5-HT_4 receptors, (pK_B 6.0–6.7). Also a number of 5-HT_4 receptor agonists including 5-methoxytryptamine, α-methyl-5-HT, substituted benzamide derivatives and benzimidazolone derivatives (BIMU 8) have been described (Kaumann *et al.*, 1991; Villalon *et al.*, 1991; Schiantarelli *et al.*, 1990).

The receptor which mediates the potent vasorelaxation to 5-HT in the sheep pulmonary vein (Eyre, 1975) has not been characterized. Here we present evidence that this receptor is of the 5-HT_4 subclass which is the first account of the presence of this receptor in vascular tissue. The sheep pulmonary vein may thus provide a simple, reliable bioassay which can be used for future development of additional compounds as either 5-HT_4 receptor agonists or antagonists.

Methods

Lungs from healthy sheep, of mixed breed, age and sex were obtained from a local abattoir and placed into cold, oxygenated Krebs solution (see below) and transported quickly to the laboratory (15 min). The main pulmonary vein

[1] Author for correspondence.

and its first branches from all lungs were carefully dissected and 3 mm ring segments were cut with a fixed double-bladed scapel arrangement. Some rings had their endothelium removed by abrading the luminal surface with a tapered wooden stick (Cocks & Angus, 1983). All rings of vein were then mounted on parallel stainless steel wires (350 μm diameter) passed through the lumen and suspended in 25 or 30 ml organ baths containing Krebs solution (see below) kept at 37°C and continually gassed with carbogen (95% O_2:5% CO_2). One wire was fixed to a support leg which in turn was attached to a micrometer so that the leg could be easily moved in a vertical plane. The other wire was attached to a Grass FT.03 force-displacement transducer to record circumferential, isometric force, which was then amplified and displayed on a flat-bed chart recorder (see Angus *et al.*, 1986). The Krebs solution had the following composition (mM): Na^+ 144, K^+ 5.9, Ca^{2+} 2.5, Mg^{2+} 1.2, Cl^- 128.7, HCO_3^- 25, SO_4^{2-} 1.2 and glucose 11.

Protocol

The rings of vein were allowed to remain unstretched in the organ baths for 60 min after which time they were stretched to a passive force of 2 g. This passive force was previously determined as that required to stretch the veins such that their circumference was approximately 0.9 times that when the veins were subjected to a transmural distending pressure of 20 mmHg (see Angus *et al.*, 1986). After a further 30 min the force was reset to 2 g and the ring segments were then left to equilibrate for a further 60 min. They were then pre-contracted with endothelin-1 (ET-1) at a concentration (3 nM) which caused approximately 50% of the maximum contractile response to ET-1 (30 nM). When the contraction to ET-1 had reached its peak and either maintained a steady plateau or lost active force at a linear rate of 0.07 ± 0.01 g min^{-1}, cumulative concentration (0.5 log unit)-relaxation curves were constructed to the agonists under study. When antagonists were used they were allowed to equilibrate with the tissue for 30 min before relaxation curves were constructed. Only one agonist curve was constructed for each ring segment.

In tissues where 100% relaxation had not been obtained by the agonist, sodium nitroprusside (SNP) (10 μM) was added at the end of the experiment to show that the tissues were able to relax fully.

Statistical analysis

All relaxation responses were expressed as percentages of the contraction to ET-1. The concentration-relaxation curves were fitted to a logistic equation to determine maximum response, (E_{max}) and the negative logarithm of the molar concentration of drug that elicited 50% of the maximum relaxation, (pEC_{50}) (Nakashima *et al.*, 1982). All pEC_{50} values quoted are mean values ± s.e.mean with the number of experiments (n) given in parentheses. The effects of the antagonists and agonists on both pEC_{50} and E_{max} in different treatment groups were compared by use of the unpaired Student's t test and a P value of 0.05 or less was considered statistically significant.

Competitive antagonism of the vasodilator effects of 5-HT by ICS 205-930 was analysed by the equation of Arunlakshana & Schild (1959). pK_B estimates for antagonist experiments in which only one concentration of antagonist was used were determined from concentration-ratios by the equation for competitive inhibition at equilibrium, $pK_B = \log_{10}(x-1) - \log_{10}[A]$, where x is the concentration-ratio and [A] the applied antagonist concentration.

Drugs

Drugs and their sources (in parentheses) were: 5-hydroxytryptamine creatinine sulphate, acetylcholine bromide and N^G-nitro-L-arginine (Sigma, U.S.A.); ionomycin (Calbiochem, Australia); ketanserin (gift from Janssen-Cilag, Australia); endothelin-1 (Peninsula Laboratories, U.S.A.); 5-carboxamidotryptamine maleate, α-methyl-5-hydroxytryptamine, 2-methyl-5-hydroxytryptamine and sumatriptan (gifts from Dr P. Humphrey, Glaxo Group Research, Ware, U.K.); methiothepin (gift from Hoffman-La Roche, U.S.A.); MDL72222 (1αH,3αω5αH-tropan-3yl-3,5-dichlorobenzoate) (gift from Dr J. Fozard, formerly at Merrell Dow, Strasbourg, France); methysergide hydrochloride and ICS 205-930 ((3α-tropanyl)-1H-indole-3-carboxylic acid ester) (gifts from Dr J. Fozard, Sandoz, Basle, Switzerland); sodium nitroprusside dihydrate (Roche, Australia); BIMU 8 (endo-N-(8-methyl-8-azabicyclo [3.2.1.] oct-3-yl) -2,3-dihydro-(1-methyl) ethyl-2-oxo-1H-benzimidazole-1-carbo-oxamide hydrochloride) gift from Dr C. Rizzi, Boehringer Ingelheim, Italy); cocaine hydrochloride (gift from Alfred Hospital, Melbourne, Australia).

Results

Characterization of 5-hydroxytryptamine-mediated relaxation

5-HT (1–1000 nM) caused concentration-dependent, stable relaxations in the sheep pulmonary vein contracted with ET-1 (see Figure 1), with a pEC_{50} value of 8.4 ± 0.1 ($n = 26$) and an E_{max} of $88.7 \pm 4.7\%$ ($n = 13$). At higher concentrations (1–10 μM), 5-HT caused concentration-dependent contractions, whcih were antagonised by ketanserin (1 μM). Neither mechanical removal of the endothelium nor treatment of endothelium-intact rings with N^G-nitro-L-arginine (L-NNA; 100 μM) affected the pEC_{50} or E_{max} of the relaxation curve to 5-HT. Respective pEC_{50} and E_{max} values were 8.3 ± 0.1, $98.0 \pm 2.0\%$ ($n = 5$) and 8.2 ± 0.1, $99.5 \pm 1.7\%$ ($n = 7$) which were not significantly different from the 5-HT control ($P > 0.05$). Functional removal of the endothelium, however, proved to be difficult in this tissue since not all tissues with intact endothelium relaxed in response to acetylcholine. If relaxation was observed it was abolished by either luminal abrasion to remove the endothelial cells or L-NNA (100 μM).

The effect of 5-HT_1-like, 5-HT_2 and 5-HT_3 antagonists on the relaxation curve to 5-HT is shown in Table 1. Methiothepin (100 nM) and methysergide (100 nM) did not significantly affect the 5-HT concentration-response curve, the estimated pEC_{50} values being 8.8 ± 0.2 ($n = 8$) and 7.9 ± 0.4 ($n = 3$) respectively. Similarly, the pEC_{50} values for 5-HT in the presence of the 5-HT_2 receptor antagonist ketanserin (1 μM)

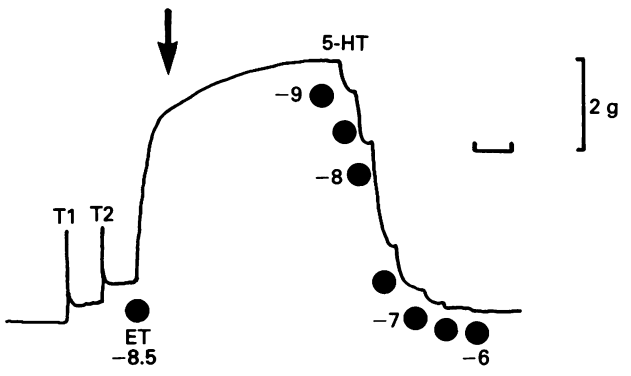

Figure 1 Tracing of a representative chart recording showing relaxation responses of the sheep isolated pulmonary vein to cumulative (log M) additions of 5-hydroxytryptamine (5-HT) contracted with endothelin-1 (ET) (3 nM). T_1 and T_2 correspond to the initial stretches of the vein to 2 g passive force. The horizontal bar represents 20 min before the arrow and 6 min after the arrow.

Table 1 Effect of 5-HT$_1$-like, 5-HT$_2$ and 5-HT$_3$ receptor antagonists on the relaxation response curve to 5-hydroxytryptamine (5-HT) in sheep isolated pulmonary vein preparations contracted with endothelin-1 (3 nM)

Antagonist	EC_{50}	n	*Maximal relaxation (%)*	n
5-HT alone	8.4 ± 0.1	26	88.7 ± 4.7	13
Methiothepin 100 nM	8.8 ± 0.2	8	94.2 ± 3.8	6
Methysergide 100 nM	7.9 ± 0.4	3	86.7 ± 6.9	3
Ketanserin 1 μM	8.3 ± 0.1	18	95.3 ± 2.8	16
MDL 72222 100 nM	7.9 ± 0.1	4	87.0 ± 6.6	4

Results are mean ± s.e.mean from *n* experiments.

and the 5-HT$_3$ receptor antagonist MDL72222 (100 nM) were 8.3 ± 0.1 ($n = 18$) and 7.9 ± 0.1 ($n = 4$) respectively, which were not significantly different from the pEC_{50} of 5-HT in the absence of antagonists ($P > 0.05$ in all cases) (see Table 1).

5-HT$_4$ receptor antagonism

ICS 205-930 (1–10 μM) caused a concentration-dependent, parallel rightward shift of the relaxation curve to 5-HT with no significant depression of the maximum response in the presence of ketanserin (1 μM) to block the contractile effects of 5-HT at higher concentrations (see Figure 2a). However, at a concentration of 30 μM ICS 205-930, no further rightward shift was observed. To test the hypothesis that the response to 5-HT in the presence of ICS 205-930 (30 μM) was due to 5-HT$_1$-like receptor activation at the higher concentrations of 5-HT, the effect of this concentration of ICS 205-930 (30 μM) was determined in the presence of methiothepin (10 nM). Under these conditions ICS 205-930 now produced a further significant approximate three fold rightward shift of the relaxation curve to 5-HT (see Figure 2a).

Figure 2b shows the Schild plot for ICS 205-930 against 5-HT, mean pEC_{50} values being used to calculate the concentration-ratios for concentrations of ICS 205-930 up to 10 μM. The pA_2 estimate obtained by Schild analysis was 6.7 (95% confidence limits 6.5, 7.0) with a slope of the regression line of 1.0 (95% confidence limits 0.8, 1.2).

Effects of other agonists

Concentration-response curves obtained to two other agonists which mediated relaxation in the sheep pulmonary vein are shown in Figure 3. 5-Carboxamidotryptamine (5-CT) (1–1000 nM) caused only relaxation but was significantly less potent than 5-HT with a similar E_{max} (Table 2), whereas α-methyl-5-HT produced relaxation at lower (1–1000 nM), and contraction at higher (1–10 μM) concentrations due to stimulation of 5-HT$_2$ receptors. Thus for the relaxation responses to α-methyl-5-HT a pEC_{50} value of 6.6 ± 0.3 ($n = 5$) and E_{max} of 62.0 ± 5.0% ($n = 3$) were obtained. In the presence of ketanserin (1 μM) the pEC_{50} estimate for α-methyl-5-HT was 6.5 ± 0.1 ($n = 4$) which was not significantly different from that observed without ketanserin but the E_{max} was significantly increased to 93.0 ± 5.0% ($n = 4$). Relaxation-response curves to α-methyl-5-HT were therefore obtained in the presence of the 5-HT$_2$ receptor antagonist, ketanserin (1 μM), to block the latter contractile response. BIMU 8 (1–1000 nM) caused concentration-dependent relaxation in the sheep pulmonary vein with a pEC_{50} value of 8.3 ± 0.1 and an E_{max} of 84.5 ± 4.1% ($n = 4$). Two other 5-HT agonists were also studied: sumatriptan (a 5-HT$_1$-like receptor agonist, see Humphrey *et al.*, 1988) and 2-methyl-5-HT (a partially selective 5-HT$_3$ receptor agonist, see Richardson *et al.*, 1985). Both agents failed to produce an effect (either relaxation or contraction) in this tissue at concentrations up to 10 μM (Table 2).

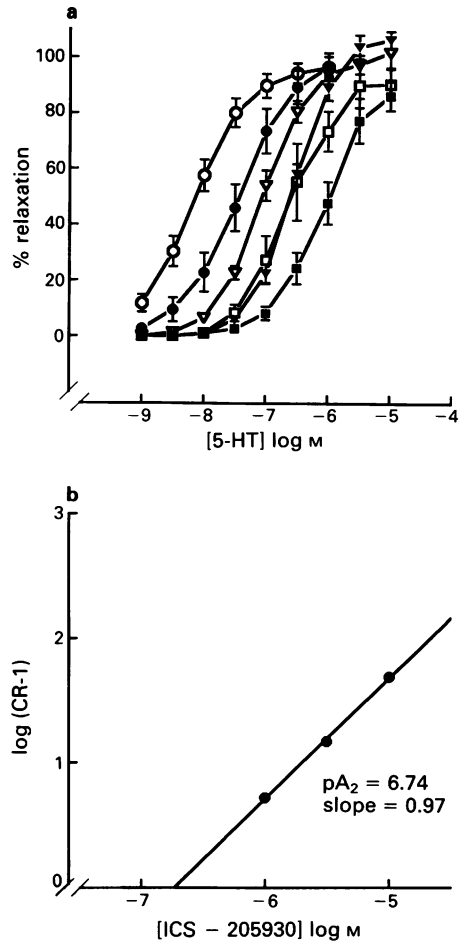

Figure 2 (a) Relaxation responses to 5-hydroxytryptamine (5-HT) alone (○; $n = 12$) or in the presence of ICS 205-930 1 μM (●; $n = 9$), 3 μM (▽; $n = 7$), 10 μM (▼; $n = 9$), 30 μM (□; $n = 7$) or 30 μM in the presence of methiothepin 10 nM (■; $n = 5$). All concentration-response curves were carried out in the presence of ketanserin (1 μM). Data points are means ± s.e.mean (vertical bars). (b) Schild plot depicting competitive antagonism by ICS 205-930 of the relaxation response curve to 5-HT. Concentration-ratios (CR) were calculated from the mean pEC_{50} values. The line through the data points was obtained by linear regression.

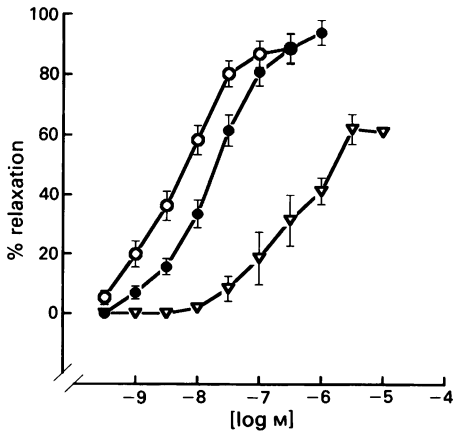

Figure 3 Relaxation response curves to 5-hydroxytryptamine (5-HT), 5-carboxamidotryptamine (5-CT) and α-methyl-5-hydroxytryptamine (α-methyl-5-HT) in sheep pulmonary vein. 5-HT (○; $n = 26$), 5-CT (●; $n = 13$), and α-methyl-5-HT (▽; $n = 5$). Data points are means ± s.e.mean (vertical bars).

Table 2 Relaxant activity of 5-hydroxytryptamine (5-HT) receptor agonists in sheep isolated pulmonary vein preparations contracted with endothelin-1 (3 nM)

Agonist	EC_{50}	n	*Maximal relaxation (%)*	n
5-HT	8.4 ± 0.1	26	88.7 ± 4.7	13
5-CT	7.7 ± 0.1	13	94.0 ± 4.2	9
α-Methyl-5-HT	6.6 ± 0.3	5	62.0 ± 5.0	3
BIMU 8	8.3 ± 0.1	4	84.5 ± 4.1	4
2-Methyl-5-HT	< 5.0	2	0	2
Sumatriptan	< 5.0	3	0	3

Results are mean ± s.e.mean from *n* experiments. For abbreviations, see text.

Characterization of 5-carboxamidotryptamine-mediated relaxation

Both methiothepin (10 nM) and methysergide (100 nM) produced significant rightward shifts of the relaxation curve to 5-CT without affecting E_{max} (see Figure 4). pEC_{50} estimates were 7.7 ± 0.1 ($n = 13$) for the 5-CT control, 5.9 ± 0.2 ($n = 6$) in the presence of methiothepin ($P < 0.001$) and 6.9 ± 0.2 ($n = 3$) in the presence of methysergide ($P = 0.005$). A pEC_{50} estimate was also obtained for 5-CT in the presence of ICS 205-930 (30 μM), giving a value of 7.9 ± 0.1 ($n = 2$) which was not significantly different from the control (data not illustrated). Also, in endothelium-denuded rings of vein, the mean pEC_{50} was 7.5 ± 0.1 ($n = 4$) which was not significantly different from the control.

Characterization of α-methyl-5-HT mediated relaxation

Methiothepin (10 nM) did not significantly affect the concentration-response curve to α-methyl-5-HT (obtained in the presence of ketanserin (1 μM)), where the pEC_{50} was 6.4 ± 0.1 ($n = 3$) and E_{max} was unchanged. ICS 205-930 (3 μM), however, caused a significant rightward shift of the relaxation curve to α-methyl-5-HT with a pEC_{50} value of 5.6 ± 0.1 ($n = 6$; $P < 0.05$), the estimated pK_B value being 6.4. E_{max} was not significantly different from the control (see Figure 5).

Characterization of BIMU 8-mediated relaxation

Neither methiothepin (10 nM) nor ketanserin (1 μM) had a significant effect on the concentration-response curve to BIMU 8. Respective pEC_{50} values were 8.8 ± 0.4 ($n = 3$) and 8.4 ± 0.3 ($n = 3$), (control $pEC_{50} = 8.3 \pm 0.1$). ICS 205-930 (10 μM), however, caused a significant rightward shift of the relaxation curve to BIMU 8 with a pEC_{50} value of 6.4 ± 0.1 ($n = 4$; $P < 0.01$). The estimated pK_B value was 6.9. E_{max} was not significantly different from the control (see Figure 6).

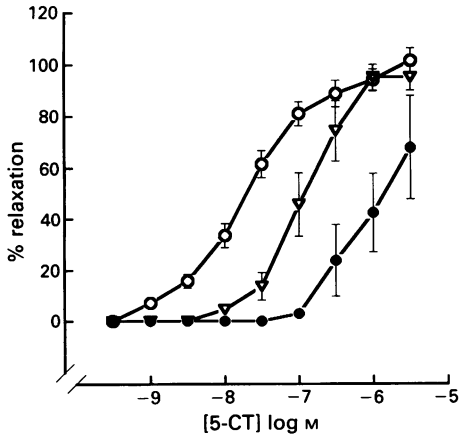

Figure 4 Effect of 5-HT_1-like receptor antagonists on the relaxation-response curve to 5-carboxamidotryptamine (5-CT). 5-CT alone (○; $n = 13$) and in the presence of methiothepin 10 nM (●; $n = 6$) or methysergide 100 nM (▽; $n = 3$). Data points are means ± s.e.mean (vertical bars).

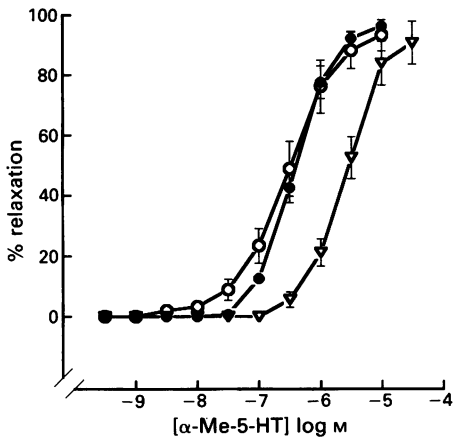

Figure 5 Effect of 5-hydroxytryptamine (5-HT) receptor antagonists on the relaxation response curve to α-methyl-5-HT: α-methyl-5-HT alone (○; $n = 4$), and in the presence of methiothepin 10 nM (●; $n = 3$) or ICS 205-930 3 μM (▽; $n = 6$). All curves were carried out in the presence of ketanserin 1 μM. Data points are means ± s.e.mean (vertical bars).

Effect of cocaine

Preincubation with cocaine (6 μM) had no effect on either 5-HT- or BIMU8-mediated relaxation. Respective pEC_{50} values for 5-HT and BIMU 8 were 8.5 ± 0.1 and 8.7 ± 0.1 in the presence of cocaine, which were not significantly different from control values of 8.4 ± 0.1 and 8.5 ± 0.1 respectively ($n = 4$ in each group).

Discussion

The results presented here strongly suggest that the potent relaxation to 5-HT in the sheep isolated pulmonary vein is due to activation of 5-HT_4 receptors. Thus the response was not blocked by 5-HT_1-like, 5-HT_2 or 5-HT_3 receptor antagonists whereas it was competitively antagonized by the 5-HT_4 receptor antagonist, ICS 205-930. The pA_2 estimate of 6.7 obtained here for ICS 205-930 was similar to that reported in the rodent brain ($pK_B = 6.2$; Dumuis *et al.*,

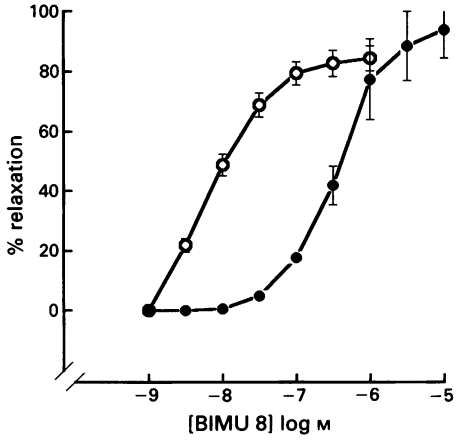

Figure 6 Effect of ICS 205-930 on the relaxation curve to BIMU 8. BIMU 8 alone (○; $n = 4$), and in the presence of ICS 205-930 (10 μM) (●; $n = 4$). Data points are means ± s.e.mean (vertical bars).

1988b) and guinea-pig ileum ($pK_B = 6.4$; Craig & Clarke, 1989), and identical to that reported in human atria ($pK_B = 6.7$; Kaumann *et al.*, 1990). We have also shown that the selective 5-HT$_4$ receptor agonist, BIMU 8, is an agonist in this tissue with a similar order of potency to 5-HT itself. The potencies of both 5-HT and BIMU 8 were unaffected by the neuronal uptake blocker, cocaine. Also, α-methyl-5-HT acts as an agonist at this receptor although less potent by approximately 2 orders of magnitude than 5-HT, which supports the findings of Villalon *et al.* (1991). Taken together our data indicate that the 5-HT receptors in the sheep pulmonary vein resemble 5-HT$_4$ receptors found in rat and guinea-pig brain, guinea-pig ileum, porcine heart and human atria.

We have also shown that relaxant 5-HT$_1$-like receptors are present in this tissue. Thus the 5-CT-mediated relaxation with a pEC_{50} value of 7.7 was blocked by the 5-HT$_1$-like antagonists, methysergide and methiothepin at concentrations that had no effect on the 5-HT-mediated response. The 5-CT-mediated relaxation was unaffected, however, by high concentrations (30 μM) of ICS 205-930. Also, failure to antagonize further the relaxation to 5-HT when the concentration of ICS 205-930 was increased from 10 to 30 μM was completely overcome by first treating the tissue with methiothepin (see Figure 2a). Under these conditions 30 μM ICS 205-930 gave a further 3 fold shift of the relaxation curve, and the value of the log (CR − 1) lay exactly on the Schild regression line (not shown). This implies that the pEC_{50} of 6.5 for 5-HT in the presence of 30 μM ICS 205-930 (without methiothepin) can be taken as a good estimate for the pEC_{50} of 5-HT at 5-HT$_1$-like receptors, and shows in accordance with convention, that 5-CT has a higher affinity for 5-HT$_1$-like receptors than 5-HT. Therefore, both 5-HT$_1$-like and 5-HT$_4$ receptors are present in sheep pulmonary vein, 5-HT being more potent at 5-HT$_4$ receptors.

Although it was relatively difficult to remove the endothelium completely in this tissue without causing damage to the underlying smooth muscle, both the 5-HT$_1$-like and 5-HT$_4$-mediated responses to 5-HT appeared to be endothelium-independent. The pulmonary vein relaxed only poorly to the endothelium-dependent agent, acetylcholine (ACh). As such there was often little or no relaxation, but a small further contraction in vessels optimally contracted with endothelin. In preparations that did relax to ACh, both mechanical damage to the intima (removal of endothelium) and treatment with the NO-synthase inhibitor L-NNA (see Moncada *et al.*, 1991) completely abolished this relaxation to reveal the direct contractile response. Both luminal damage and L-NNA, however, had no effect on the relaxation curve to 5-HT. Therefore, there appeared to be no role for the endothelium in mediating the relaxation response to 5-HT in this tissue as reported for other vessels (Cocks & Angus, 1983; Leff *et al.*, 1987; Sumner, 1991; for review see Angus & Cocks, 1989). Further evidence against 5-HT endothelial receptors in the sheep pulmonary vein was the resistance of the relaxation to methiothepin which blocked 5-HT-mediated relaxations in the rabbit jugular vein (Leff *et al.*, 1987), and the slow time-course of the relaxation compared to the responses to 5-HT in pig vena cava (Sumner, 1991).

The presence of 5-HT$_4$ receptors in the pulmonary vein appears to be species-specific, since in similar experiments on dog, pig and human pulmonary vein we have found no evidence for 5-HT$_4$-mediated relaxations (unpublished data). Preliminary experiments on bovine pulmonary vein, however, suggest that the relaxation to 5-HT (observed in the presence of ketanserin (1 μM) and methiothepin (10 nM)), could be mediated via 5-HT$_4$ receptors. The 5-HT-induced relaxation reported in the goat isolated pulmonary vein (Chand, 1981) might also be mediated via 5-HT$_4$ receptors since responses were similar in time course and occurred over a similar concentration-range to the response in the sheep. Therefore it appears that ruminants possess pulmonary vein 5-HT$_4$ receptors, but for what physiological reason remains unknown.

In conclusion, the receptors responsible for 5-HT-mediated relaxation of the sheep pulmonary vein appear identical to the 5-HT$_4$ receptors recently described in other tissues. Therefore, this is the first demonstration of vascular 5-HT$_4$ receptors. Whilst their physiological role(s) is unknown, given the availability of abattoir material, this robust and sensitive bioassay may thus prove particularly useful in the development of new selective 5-HT$_4$ agonists and antagonists provided that care is taken to eliminate possible complications of the effects of activation of 5-HT$_1$-like and 5-HT$_2$ receptors present in this tissue.

This work was supported by an Institute grant from the NH & MRC of Australia and by Glaxo Australia. We thank Drs Angus, McPherson and Fozard for their helpful comments.

References

ANGUS, J.A., COCKS, T.M. & SATOH, K. (1986). α_2-Adrenoceptors and endothelium-dependent relaxation in canine large arteries. *Br. J. Pharmacol.*, **88**, 767–777.

ANGUS, J.A. & COCKS, T.M. (1989). Endothelium-derived relaxing factor. *Pharmacol. Ther.*, **41**, 303–351.

ARUNLAKSHANA, O. & SCHILD, H.O. (1959). Some quantitative uses of drug antagonists. *Br. J. Pharmacol. Chemother.*, **14**, 48–58.

BAXTER, G.S., CRAIG, D.A. & CLARKE, D.E. (1991). 5-Hydroxytryptamine$_4$ receptors mediate relaxation of rat oesophageal tunica muscularis mucosae. *Naunyn-Schmiedebergs Arch. Pharmacol.*, **343**, 439–446.

BOCKAERT, J., SEBBEN, M. & DUMUIS, A. (1990). Pharmacological characterisation of 5-hydroxytryptamine$_4$ (5-HT$_4$) receptors positively coupled to adenylate cyclase in adult guinea pig hippocampal membranes: effect of substituted benzamide derivatives. *Mol. Pharmacol.*, **37**, 408–411.

BRADLEY, P.B., ENGEL, G., FENIUK, W., FOZARD, J.R., HUMPHREY, P.P.A., MIDDLEMISS, D.N., MYLECHARANE, E.J., RICHARDSON, B.P. & SAXENA, P.R. (1986). Proposals for the classification and nomenclature of functional receptors for 5-hydroxytryptamine. *Neuropharmacology*, **25**, 563–576.

CHAND, N. (1981). 5-Hydroxytryptamine induces relaxation of goat pulmonary veins: evidence for the noninvolvement of M and D-tryptamine receptors. *Br. J. Pharmacol.*, **72**, 233–237.

COCKS, T.M. & ANGUS, J.A. (1983). Endothelium-dependent relaxation of coronary arteries by noradrenaline and serotonin. *Nature*, **305**, 627–630.

CRAIG, D.A. & CLARKE, D. (1989). 5-Hydroxytryptamine and cholinergic mechanisms in guinea-pig ileum. *Br. J. Pharmacol.*, **96**, 247P.

DUMUIS, A., BOUHELAL, R., SEBBEN, M. & BOCKAERT, J. (1988a). A 5-HT receptor in the central nervous system positively coupled with adenylate cyclase is antagonized by ICS 205-930. *Eur. J. Pharmacol.*, **146**, 187–188.

DUMUIS, A., BOUHELAL, R., SEBBEN, M., CORY, R. & BOCKAERT, J. (1988b). A non-classical 5-hydroxytryptamine receptor positively coupled with adenylate cyclase in the central nervous system. *Mol. Pharmacol.*, **34**, 880–887.

DUMUIS, A., SEBBEN, M. & BOCKAERT, J. (1989). The gastrointestinal prokinetic benzamide derivatives are agonists at the non-classical 5-HT receptor (5-HT$_4$) positively coupled to adenylate cyclase in neurons. *Naunyn-Schmiedebergs Arch. Pharmacol.*, **340**, 403–410.

EYRE, P., (1975). Atypical tryptamine receptors in sheep pulmonary vein. *Br. J. Pharmacol.*, **55**, 329–333.

FENIUK, W., HUMPHREY, P.P.A. & WATTS, A.D. (1983). 5-hydroxytryptamine-induced relaxation of isolated mammalian smooth muscle. *Eur. J. Pharmacol.*, **96**, 71–78.

HUMPHREY, P.P.A., FENIUK, W., PERREN, M.J., CONNOR, H.E., OXFORD, A.W., COATES, I.H. & BUTINA, D. (1988). GR43175, a selective agonist for the 5-HT_1-like receptor in dog isolated saphenous vein. *Br. J. Pharmacol.*, **94,** 1123–1132.

KAUMANN, A.J., SANDERS, L., BROWN, A.M., MURRAY, K.J. & BROWN, M.J. (1990). A 5-hydroxytryptamine receptor in human atrium. *Br. J. Pharmacol.*, **100,** 879–885.

KAUMANN, A.J., SANDERS, L., BROWN, A.M., MURRAY, K.J. & BROWN, M.J. (1991). A 5-HT_4-like receptor in human right atrium. *Naunyn-Schmiedebergs Arch. Pharmacol.*, **344,** 150–159.

LEFF, P., MARTIN, G.R. & MORSE, J.M. (1987). Differential classification of vascular smooth muscle and endothelial cell 5-HT receptors by use of tryptamine analogues. *Br. J. Pharmacol.*, **91,** 321–331.

MONCADA, S., PALMER, R.M.J. & HIGGS, E.A. (1991). Nitric oxide: physiology, and pharmacology. *Pharmacol. Rev.*, **43,** 109–142.

NAKASHIMA, A., ANGUS, J.A. & JOHNSTON, C.I. (1982). Comparison of angiotensin converting enzyme inhibitors captopril and MK421-diacid in guinea-pig atria. *Eur. J. Pharmacol.*, **81,** 487–492.

RICHARDSON, B.P., ENGEL, G., DONATSCH, P. & STADLER, P.A. (1985). Identification of serotonin M-receptor subtypes and their specific blockade by a new class of drugs. *Nature*, **316,** 126–131.

SCHIANTARELLI, P., BOCKAERT, J., CESANA, R., DONETTI, A., DUMUIS, A., GIRALDO, E., LADINSKY, H., MONFERINI, E., RIZZI, C., SAGRADA, A. & SCHIAVONE, A. (1990). The prokinetic properties of new benzimidazolone derivatives are related to 5-HT_4 agonism. *Pharmacol. Res.*, **22,** (Suppl 2) 453.

SUMNER, M.J. (1991). Characterization of the 5-HT receptor mediating endothelium-dependent relaxation in porcine vena cava. *Br. J. Pharmacol.*, **102,** 938–942.

SUMNER, M.J., FENIUK, W. & HUMPHREY, P.P.A. (1989). Further characterization of the 5-HT receptor mediating vascular relaxation and elevation of cyclic AMP in porcine isolated vena cava. *Br. J. Pharmacol.*, **97,** 292–300.

VILLALON, C.M., DEN BOER, M.O., HEILIGERS, J.P.C. & SAXENA, P.R. (1990). Mediation of 5-hydroxytryptamine-induced tachycardia in the pig by the putative 5-HT_4 receptor. *Br. J. Pharmacol.*, **100,** 665–667.

VILLALON, C.M., DEN BOER, M.O., HEILIGERS, J.P.C. & SAXENA, P.R. (1991). Further characterization, by use of tryptamine and benzamide derivatives, of the putative 5-HT_4 receptor mediating tachycardia in the pig. *Br. J. Pharmacol.*, **102,** 107–112.

(Received March 27, 1992
Revised June 9, 1992
Accepted June 22, 1992)

Br. J. Pharmacol. (1992), **107**, 597–603

The role of endothelial cells in the relaxations induced by 13-hydroxy- and 13-hydroperoxylinoleic acid in canine arteries

[1]Guido R.Y. De Meyer, Hidde Bult, [2]Tony J. Verbeuren & Arnold G. Herman

Division of Pharmacology, University of Antwerp (UIA), Universiteitsplein 1, B-2610 Wilrijk, Belgium

1 One of the major fatty acids in the arterial wall is linoleic acid. It has been shown that its 13-hydroxy metabolite (13-HODE) is generated in significant amounts by cultured endothelial cells. The aim of the present study was to investigate the relaxations to 13-HODE and its hydroperoxyprecursor (13-HPODE) and to examine the role of the endothelial cells.

2 Ring segments of canine circumflex and splenic artery were mounted in organ chambers for isometric tension recording. During contractions induced by prostaglandin $F_{2\alpha}$ or noradrenaline, 13-HODE and 13-HPODE evoked dose-dependent relaxations. Removal of the endothelial cells reduced the relaxations to 13-HODE, but had no effect on those elicited by 13-HPODE.

3 Indomethacin and meclofenamate (0.3 μM to 30 μM) blocked the relaxations evoked by 13-HODE and 13-HPODE in endothelium-denuded rings. In segments with endothelium, both cyclo-oxygenase inhibitors again abolished the relaxations to 13-HODE, but only diminished those to 13-HPODE.

4 Prostacyclin biosynthesis, as measured by radioimmunoassay, increased upon incubation with 13-HODE and 13-HPODE (10 μM). Bioassay of the release of nitric oxide (NO) indicated that NO was not involved in the relaxations elicited by either metabolite. Moreover, L-N^G-nitroarginine (100 μM), a specific inhibitor of NO synthesis, did not influence the relaxations to 13-HODE and 13-HPODE. The responses to 13-HPODE were also not altered by superoxide dismutase.

5 In the splenic artery 13-HPODE and 13-HODE induced contractions above 3 μM which were blocked by the thromboxane receptor antagonist, daltroban. In the circumflex artery contractile responses to high concentrations of 13-HODE could be observed only after inhibition of cyclo-oxygenase.

6 We conclude that the vasodilatation induced by 13-HODE and 13-HPODE was due to stimulation of prostacyclin biosynthesis both in the endothelium and smooth muscle cells or other subendothelial structures. An additional, unidentified intermediate, which was neither NO nor a cyclo-oxygenase product nor superoxide anion, contributed to the relaxations to 13-HPODE in arteries with endothelium.

Keywords: 13-Hydroxylinoleic acid (13-HODE); 13-hydroperoxylinoleic acid (13-HPODE); vascular; endothelium; prostacyclin

Introduction

Arachidonic acid can be converted by vascular smooth muscle cells and endothelial cells to 15-hydroperoxyeicosatetraenoic acid (15-HPETE) which, in turn, is reduced by a peroxidase to 15-hydroxyeicosatetraenoic acid (15-HETE). These metabolites are known to evoke vasoconstriction, spontaneous rhythmic activity and relaxations in isolated blood vessels (Asano & Hidaka, 1979; Trachte *et al.*, 1979; Aharony *et al.*, 1981; Koide *et al.*, 1982; Takahashi *et al.*, 1985; Thomas & Ramwell, 1986; Van Diest *et al.*, 1986; 1991; d'Alarcao *et al.*, 1987; Uotila *et al.*, 1987; Lovelady *et al.*, 1988). Besides arachidonic acid, another major fatty acid in the arterial wall is linoleic acid (Simon *et al.*, 1989), which can be (non-)enzymatically converted to 13-hydroperoxyoctadecadienoic acid (13-HPODE). This labile intermediate is further reduced to its 13-hydroxy derivative (13-HODE) (Buchanan *et al.*, 1985; Setty *et al.*, 1987). The presence of 13-HODE has been demonstrated in rabbit, rat and bovine aorta (Funk & Powell, 1985; De Meyer *et al.*, 1991). It has been proposed that 13-HODE maintains the endothelial lining in a non-adhesive state (Buchanan *et al.*, 1985), but does not seem to play a major role in platelet-subendothelium interaction (De Graaf *et al.*, 1989). Cholesterol-induced fatty streak formation is accompanied by a decreasae in the endogenous amounts of esterified 13-HODE and 15-HETE. The reduction of the esterified 13-HODE content correlates with the severity of the lesions (De Meyer *et al.*, 1991).

Since the vascular effects of 13-HODE and its hydroperoxy precursor are poorly documented, we examined their direct and endothelium-dependent effects in canine isolated arteries, which are very sensitive to the actions of the lipoxygenase metabolites of arachidonic acid (Van Diest *et al.*, 1991), and tried to elucidate their mechanism of action.

Methods

Vascular reactivity

Mongrel dogs (15–35 kg) of either sex were anaesthetized with sodium pentobarbitone (30 mg kg^{-1}, i.v.). The heart was isolated and subsequently the splenic artery and the circumflex branch of the left coronary artery were removed. The tissues were immediately immersed in an oxygenated (95% O_2–5% CO_2) physiological salt solution. The isolated arteries were cleaned of loose connective tissue and ring segments (3 mm long) were mounted in organ chambers filled with 25 ml physiological salt solution, maintained at 37°C and continuously gassed with 95% O_2–5% CO_2 (Vanhoutte & Verbeuren, 1976). Tension was measured isometrically with a Statham UC_2 force transducer. Before mounting the tissues in the organ chambers some segments were denuded of the endothelium by rubbing the tip of a pair of forceps against the intimal surface. After an equilibration period of 15 min the preparations were gradually stretched and were

[1] Author for correspondence.
[2] Present address: Institut de recherches Servier, 11, Rue des Moulineaux, 92150, Suresnes, France.

placed at the optimal point of their length-tension relationship with either 50 mM KCl (Vanhoutte & Verbeuren, 1976) or 2 μM prostaglandin $F_{2\alpha}$ ($PGF_{2\alpha}$). The resting tension amounted to 9.2 g ± 0.8 g for splenic artery segments with endothelium, 9.0 g ± 0.5 g for splenic artery segments without endothelium, 10.5 ± 1.0 g for circumflex segments with endothelium and 11.5 g ± 1.6 g for circumflex segments without endothelium. Subsequently the segments were allowed to equilibrate for 45 min at their optimal length prior to experimentation.

After raising the tone of the vessels with $PGF_{2\alpha}$, noradrenaline (NA) or KCl, cumulative dose-response curves were constructed for prostacyclin (PGI_2), 13-HODE and 13-HPODE. Intact segments and segments without endothelium were tested in parallel to investigate the role of the endothelial cells. The rings with and without endothelium were precontracted to the same tone. The efficacy of the removal of the endothelium was examined in each ring with acetylcholine (Furchgott & Zawadzki, 1980). The thromboxane receptor antagonist daltroban (BM13505; Lefer, 1988), indomethacin, meclofenamate, L-N^G-nitroarginine (L-NNA) and superoxide dismutase (SOD) were administered 40 min before the addition of prostacyclin, 13-HODE or 13-HPODE.

Bioassay of the release of nitric oxide (NO)

A segment of the canine splenic artery (3 cm long) was used as donor vessel and mounted horizontally in a perfusion chamber filled with physiological salt solution gassed with a mixture of 20% O_2: 5% CO_2: 75% N_2 and maintained at 37°C (Bult *et al.*, 1988). It was continuously perfused with the same solution at a rate of 3 ml min^{-1}. The perfusate was dripped onto a segment of the rabbit abdominal aorta of which the endothelium had been mechanically removed. This detector segment was mounted vertically over two hooks for isometric tension recording and its initial tension was gradually set at 8 g. Thereafter, it was contracted by an infusion of NA (0.1 μM). Atropine (0.1 μM) and daltroban (1 μM) were infused above the detector tissue to block contractile effects of acetylcholine and the derivatives of linoleic acid respectively. After an equilibration period of 30 min boluses (0.3, 3 and 30 nmol) of acetylcholine, 13-HPODE and 13-HODE were injected in random order and at 20 min intervals into the physiological salt solution which perfused the donor artery.

Biosynthesis of prostacyclin

Mongrel dogs (18–32 kg) of either sex were anaesthetized with sodium pentobarbitone (30 mg kg^{-1}, i.v.). Subsequently the dogs received heparin (100 units kg^{-1}, i.v.) and 5 min later they were killed. The splenic artery was removed and immediately placed in cold physiological salt solution gassed with 95% O_2: 5% CO_2. Adjacent tissues were carefully dissected from the adventitial side and thereafter four ring segments of equal length (1 cm) were cut.

These rings were randomly divided into plastic tubes filled with physiological salt solution (1 ml) continuously gassed with 95% O_2: 5% CO_2 and maintained at 37°C. After an equilibration period of 30 min, the segments were transferred to fresh physiological salt solution. Fifteen min later this incubation fluid was collected into 30 μM indomethacin. Subsequently, fresh physiological salt solution, containing respectively 0, 1 or 10 μM 13-HPODE, or 10 μM 13-HODE was added and the rings were incubated for another 15 min ($n = 7-14$ dogs) before collecting a second sample. The amount of prostacyclin in each sample was measured by radioimmunoassay (RIA) of 6-keto-prostaglandin $F_{1\alpha}$ (Bult *et al.*, 1982). A correction for the cross-reactivity of the agonists with the assay (0.012%) was made. At the end of the experiment the rings were placed on Whatman No. 1 filter paper in order to remove adhering water and their wet weight was determined.

Preparation and h.p.l.c. analysis of 13-HPODE and 13-HODE

13-HPODE was prepared by incubation of linoleic acid (10 mg in 100 ml Tris buffer 0.2 M; pH = 9 at 4°C) with 126,000 u soybean lipoxidase type I (linoleate: oxygen oxidoreductase; EC 1.13.11.12) at 4°C. After an incubation period of 30 min a second amount of lipoxidase (126,000 u) was added for another 30 min at 4°C. In order to prepare 13-HODE, 100 mg glutathione was added after the first 30 min and the mixture was incubated during the following 30 min at room temperature. Both linoleic acid derivatives were extracted and purified by thin layer chromatography (TLC) as described (Coene *et al.*, 1986; Van Diest *et al.*, 1991). The purity of the metabolites was investigated by means of high performance liquid chromatography (h.p.l.c.) analysis with a Varian 5000 liquid chromatograph. A Nucleosil C_{18} reversed-phase column (4.6 × 250 mm, 5 μm particles, Alltech Europe, Eke, Belgium) was used and elution (1 ml min^{-1}) was carried out with a mixture of tetrahydrofuran-acetonitrile-water-acetic acid (22:40:38:0.05 by volume) (Engels *et al.*, 1986). 13-HPODE and 13-HODE were monitored at 235 nm in a Varian UV50 variable wavelength detector. They were kept in ethanol at −20°C and stored under nitrogen.

Materials

The physiological salt solution had the following composition (mM): NaCl 118, KCl 4.7, $CaCl_2$ 2.5, KH_2PO_4 1.2, $MgSO_4$ 1.2, $NaHCO_3$ 25, Ca EDTA 0.025 and glucose 11.1. Acetylcholine, atropine sulphate, glutathione, linoleic acid, L-N^G-nitro arginine, (−)-noradrenaline bitartrate and soybean lipoxidase were obtained from Sigma Chemical Corp., St. Louis, MO, U.S.A. Heparin Leo was from Therabel Pharma, Brussels, Belgium, indomethacin sodium tetrahydrate from Merck, Sharp & Dohme, München, Germany, meclofenamate sodium from Parke Davis, Bornem, Belgium, prostaglandin $F_{2\alpha}$ from Upjohn, Puurs, Belgium and sodium pentobarbitone from Psyphac, Brussels, Belgium. Acetic acid and acetonitrile for h.p.l.c. were purchased from Merck, Darmstadt, Germany, tetrahydrofuran for h.p.l.c. from Lab-Scan, Dublin, Ireland and [^{3}H]-6-keto-prostaglandin $F_{1\alpha}$ from New England Nuclear, Boston, MA, USA. Daltroban, prostacyclin (sodium salt) and bovine recombinant superoxide dismutase were gifts from Boehringer Mannheim, Mannheim, Germany, the Wellcome Foundation, Beckenham, Kent, UK and Grünenthal, Aachen, Germany, respectively.

The drugs were dissolved and diluted in distilled water; noradrenaline was dissolved in an aqueous solution of ascorbic acid (0.01%). Daltroban was dissolved in distilled water with equimolar amounts of NaOH and diluted in distilled water. The stock solutions of 13-HPODE and 13-HODE were diluted in distilled water and kept on ice. The final concentration of ethanol in the organ chambers never exceeded 0.2%. The stock solution of prostacyclin was prepared in 0.1 N NaOH and dilutions were made in Tris buffer (pH = 8.5).

Data analysis

In the organ chamber experiments the tension (g) was measured and expressed as a percentage of the initial contraction induced by $PGF_{2\alpha}$, NA or KCl. The negative logarithm of the concentration of agonist (pD_2 or $-\log EC_{50}$) that produced half of the maximal effect obtained with that agonist was calculated for each ring, by linear regression analysis (Tallarida & Murray, 1981). All data are expressed as means ± s.e.mean. The number of vessels reported (n) equals the number of dogs used. For statistical analysis, Student's t test for paired observations and analysis of variance (ANOVA) (Sokal & Rohlf, 1981) were used; P values less than 0.05 were considered to be significant.

Results

Vascular reactivity

Prostacyclin PGI_2 (1 nM to 1 μM) induced relaxation of splenic artery rings contracted with $PGF_{2\alpha}$ 1 μM or NA, 0.25 μM. Removal of endothelial cells induced a small leftward shift of the dose-relaxation curve (Table 1). The thromboxane receptor antagonist, daltroban, did not have statistically significant effects (Table 1).

13-HODE and 13-HPODE 13-HODE and 13-HPODE (10 nM to 10 μM) induced dose-dependent relaxations of coronary artery segments with endothelium contracted with 1 μM $PGF_{2\alpha}$ (Figure 1a,b). Removal of the endothelium reduced the dilator response to 13-HODE, but had no significant effect on those induced by 13-HPODE (Figure 1a,b).

In splenic artery segments with and without endothelium contracted with NA (0.25 μM), 13-HPODE induced concentration-dependent relaxations, followed by contractions at higher concentrations. Daltroban (7 μM) abolished this additional contraction and unmasked further relaxation (Figure 2).

To investigate the effect of indomethacin and meclofenamate (0.3 μM to 30 μM) on the relaxations induced by 13-HPODE and 13-HODE in the splenic artery, the concentration of NA was reduced to 60 nM in order to obtain an initial level of contraction similar to the controls. Van Diest *et al.* (1991) demonstrated that indomethacin and meclofenamate enhance contractions to NA in canine arteries. In order to block contractile responses of the linoleic acid metabolites, daltroban was added to the organ chambers. Both indomethacin and meclofenamate diminished the endothelium-dependent relaxations induced by 13-HPODE in a dose-dependent way and abolished those induced by 13-HODE (Table 2). Similar results were obtained with segments of the circumflex contracted with $PGF_{2\alpha}$ (Figure 1a,b). In segments without endothelium, indomethacin (30 μM) completely inhibited the relaxations induced by 13-HPODE and 13-HODE (Figure 1a,b). In the circumflex artery with and without endothelium, contractile responses to high concentrations of 13-HODE could be observed, but only after inhibition of cyclo-oxygenase (Figure 1a).

In both the circumflex and splenic artery L-NNA (100 μM) (Moore *et al.*, 1990) did not significantly influence the relaxations to 13-HODE and 13-HPODE. In contrast, L-NNA induced about 70% inhibition of the maximum relaxation to acetylcholine (Table 3). Incubation of the circumflex and splenic artery rings with superoxide dismutase (SOD, 20 or 40 u ml^{-1}) did not affect the relaxations to 13-HPODE (Table 4).

Bioassay of the release of NO

Stimulation of the canine splenic artery with increasing doses of acetylcholine (0.3–30 nmol) induced a dose-dependent release of NO. In contrast, neither 13-HPODE nor 13-HODE (0.3–30 nmol) evoked a release of NO from this donor vessel (Table 5). Similar results were obtained when the rabbit thoracic aorta was used as donor vessel (results not shown).

Biosynthesis of prostacyclin

Canine splenic artery segments incubated with an aerated physiological salt solution released PGI_2 under basal conditions as indicated by radioimmunoassay of 6-keto-prostaglandin $F_{1\alpha}$. There were no differences among the rings regarding the baseline 6-keto-$PGF_{1\alpha}$ biosynthesis in the preincubation period. The biosynthesis of PGI_2 increased upon treatment for 15 min with 10 μM 13-HODE and 10 μM 13-HPODE; as little as 1 μM 13-HPODE tended to augment PGI_2 biosynthesis (Figure 3).

Discussion

We investigated the relaxations to 13-HODE and 13-HPODE in canine isolated arteries and compared them to the relaxations induced by prostacyclin. The tone of the vessels was raised with either $PGF_{2\alpha}$ or NA. In addition, the effects of endothelial removal, cyclo-oxygenase inhibitors, inhibition of NO biosynthesis, and SOD on these relaxations were studied.

During NA-induced contractions, 13-HODE and 13-HPODE evoked relaxations of the splenic artery but high concentrations of these linoleic acid derivatives evoked further contraction. The thromboxane receptor antagonist, daltroban (Lefer, 1988) prevented these additional contractions and unmasked further relaxation. Hence, the highest concentrations of 13-HODE and 13-HPODE seem to have a dual effect: in addition to stimulating prostacyclin biosynthesis they induce

Table 1 Effects of contractile agonist, daltroban (7 μM) and removal of the endothelial cells on prostacyclin-induced relaxation of canine splenic artery segments

	Endothelium present	*Endothelium absent*
EC_{50} ($-\log$ M)		
(1) Contraction with $PGF_{2\alpha}$ (1 μM)		
Control	7.47 ± 0.14	7.70 ± 0.12*
(2) Contraction with NA (0.25 μM)		
Control	7.48 ± 0.14	7.98 ± 0.15**
Daltroban	7.51 ± 0.12	7.74 ± 0.10**
Maximum relaxation (%)		
(1) Contraction with $PGF_{2\alpha}$ (1 μM)		
Control	88 ± 10 (i.c. = 6.8 ± 1.7 g)	95 ± 5 (i.c. = 6.2 ± 1.7 g)
(2) Contraction with NA (0.25 μM)		
Control	78 ± 14 (i.c. = 3.3 ± 0.3 g)	95 ± 3 (i.c. = 2.5 ± 0.3 g)
Daltroban	93 ± 6 (i.c. = 2.7 ± 0.3 g)	100 ± 0 (i.c. = 2.5 ± 0.3 g)

Values are shown as means ± s.e.mean for 6 dogs. EC_{50}: concentration producing half of the maximum relaxation of segments contracted with prostaglandin $F_{2\alpha}$ ($PGF_{2\alpha}$) or noradrenaline (NA) respectively. i.c.: initial contraction.
*$P<0.05$; **$P<0.01$; significantly different from segments with endothelium (ANOVA).

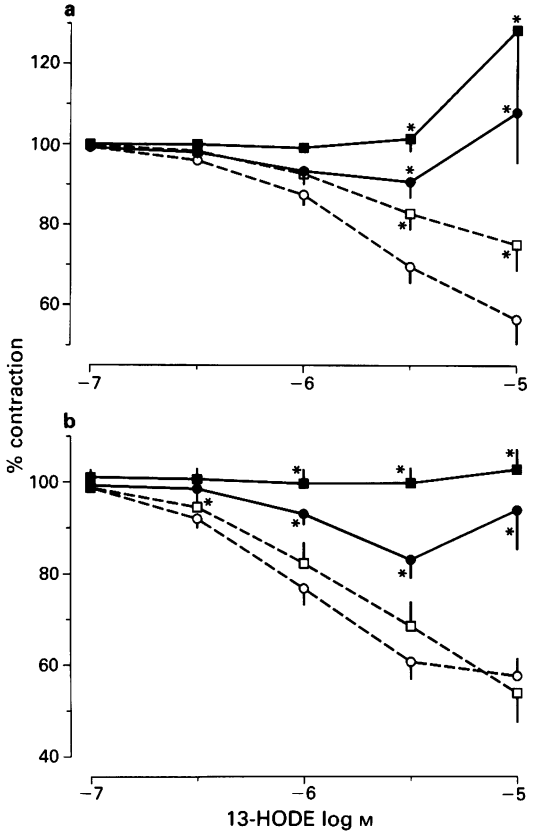

Figure 1 (a) Effect of 30 μM indomethacin on the relaxations to 13-hydroxylinoleic acid (13-HODE) in segments of canine circumflex coronary artery contracted with prostaglandin $F_{2\alpha}$ ($PGF_{2\alpha}$, 2 μM). Responses are shown as means with s.e.mean (vertical lines), and expressed as a percentage of the initial contraction. 100% = 3.0 g ± 0.5 g for control segments with endothelium (○), 3.5 g ± 0.5 g for control segments without endothelium (□), 3.3 g ± 0.9 g for indomethacin treated segments with endothelium (●) and 3.2 g ± 1.1 g for indomethacin-treated segments without endothelium (■). $*P<0.05$, (control versus indomethacin-treated), $*P<0.05$ (with endothelium versus without endothelium), Student's t test (paired, two-tailed), $n = 6$. (b) Effect of 30 μM indomethacin on the relaxations to 13-hydroperoxylinoleic acid (13-HPODE) in segments of canine circumflex coronary artery contracted with $PGF_{2\alpha}$ (2 μM). Responses are shown as means with s.e.mean (vertical lines) and expressed as a percentage of the initial contraction. 100% = 3.0 g ± 0.4 g for control segments with endothelium (○), 3.2 g ± 0.5 g for control segments without endothelium (□), 3.1 g ± 0.5 g for indomethacin-treated segments with endothelium (●), 3.2 g ± 0.4 g for indomethacin-treated segments without endothelium (■). $*P<0.05$, (control versus indomethacin-treated), Student's t test (paired, two-tailed), $n = 7$.

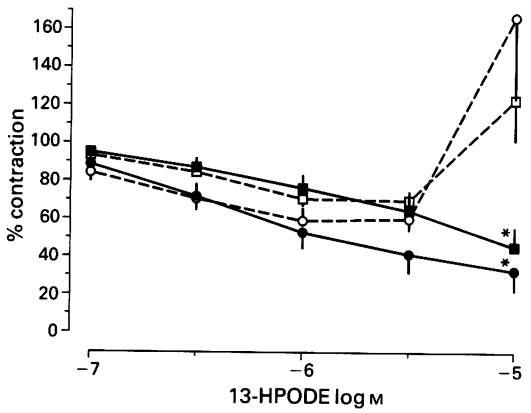

Figure 2 Effect of the thromboxane receptor antagonist, daltroban (7 μM) on the relaxations to 13-hydroperoxylinoleic acid (13-HPODE) in segments of canine splenic arteries contracted with noradrenaline (0.3 μM). Responses are shown as means with s.e.mean (vertical lines) and expressed as percentage of the initial contraction. 100% = 3.6 g ± 0.3 g for control segments with endothelium (○), 4.0 g ± 0.7 g for control segments without endothelium (□), 3.3 g ± 0.5 g for daltroban-treated segments with endothelium (●) and 4.5 g ± 1.0 g for daltroban-treated segments without endothelium (■). $*P<0.05$, Student's t test (paired, two-tailed), $n = 6$.

Table 2 Effect of indomethacin (Indo) and meclofenamate (Meclo) on 13-hydroxylinoleic acid (13-HODE) and 13-hydroperoxylinoleic acid (13-HPODE)-induced relaxation of canine splenic artery segments with endothelium

Relaxation (%)	*13-HODE* (10 μM) ($n = 5$)	*13-HPODE* (10 μM) ($n = 6$)
Control	43 ± 5 (i.c. = 5.3 ± 0.6 g)	63 ± 5 (i.c. = 6.8 ± 0.4 g)
Indo 0.3 μM	20 ± 4* (i.c. = 6.5 ± 1.2 g)	ND
Indo 3 μM	9 ± 4* (i.c. = 6.8 ± 1.2 g)	36 ± 4* (i.c. = 7.3 ± 0.7 g)
Indo 30 μM	ND	16 ± 6* (i.c. = 5.5 ± 1.0 g)
Meclo 0.3 μM	12 ± 6* (i.c. = 6.2 ± 1.0 g)	ND
Meclo 3 μM	9 ± 9* (i.c. = 5.5 ± 1.3 g)	31 ± 10* (i.c. = 8.7 ± 1.5 g)
Meclo 30 μM	ND	12 ± 5* (i.c. = 6.7 ± 0.9 g)

Values are shown as means ± s.e.mean. The segments were contracted with noradrenaline in the presence of daltroban (7 μM). In the rings treated with a cyclooxygenase inhibitor the concentration of noradrenaline was diminished in order to obtain a level of initial contraction similar to the controls. i.c.: initial contraction; ND: not done. $*P<0.05$ (ANOVA, Student-Newman-Keuls test).

contraction by activating thromboxane receptors, similar to 15-HETE and 15-HPETE (Van Diest *et al.*, 1991). In the circumflex artery the relaxant responses prevailed and contractile responses to 13-HODE were observed only after treatment with indomethacin. Presumably, this is due to inhibition of endogenous prostacyclin biosynthesis, thereby tipping the balance in favour of the contractile effect of thromboxane receptor activation by 13-HODE. Daltroban could not be used to verify this assumption, since the circumflex arteries were contracted with $PGF_{2\alpha}$ and thromboxane receptor antagonists suppress the contractile responses to $PGF_{2\alpha}$ in a competitive manner (Van Diest *et al.*, 1991).

In further experiments, we studied the role of the endothelial cells on relaxations. In both circumflex and splenic artery, removal of the endothelial cells reduced the relaxations in response to 13-HODE. This suggests an involvement of endothelium-derived vasodilators such as PGI_2 (Moncada & Vane, 1979) and/or NO (Furchgott & Zawadzki, 1980; Palmer *et al.*, 1987). It has been reported that in the canine coronary artery, the relaxations induced by 15-HETE and 15-HPETE are impaired by cyclo-oxygenase inhibitors (Takahashi *et al.*, 1985; Van Diest *et al.*, 1991). Likewise, in rings with endothelium, the relaxations were abolished (13-HODE) or diminished (13-HPODE) by indomethacin and meclofenamate. Both cyclo-oxygenase inhibitors also completely inhibited the relaxations to 13-HODE and 13-HPODE in endothelium-free segments. These results suggest that the relaxations to 13-HODE and the major part of the relaxations induced by 13-HPODE were due to stimulation of endothelial and subendothelial biosynthesis of a cyclo-oxy-

Table 3 Effect of L-N^G-nitro arginine (L-NNA) on the amplitude of 13-hydroxylinoleic acid (13-HODE), 13-hydroperoxylinoleic acid (13-HPODE) and acetylcholine (ACh)-induced relaxations of canine splenic artery and circumflex segments with endothelium

Relaxation (%)	*13-HODE* (10 μM)	*13-HPODE* (10 μM)	ACh (1 μM) + Indo 3 μM
Splenic artery ($n = 3$)			
Control (i.c. = 5.4 ± 0.8 g)	63 ± 10	66 ± 5	99 ± 1
L-NNA 100 μM (i.c. = 6.9 ± 0.9 g)	71 ± 5	78 ± 10	28 ± 2*
Circumflex ($n = 3$)			
Control (i.c. = 6.4 ± 1.7 g)	63 ± 21	59 ± 10	95 ± 3
L-NNA 100 μM (i.c. = 7.2 ± 1.2 g)	59 ± 20	50 ± 11	34 ± 4*

Values are shown as means ± s.e.mean. The segments were contracted with noradrenaline 0.3 μM in the presence of daltroban 7 μM (splenic artery) or prostaglandin $F_{2\alpha}$ ($PGF_{2\alpha}$) 2 μM (circumflex). In the inhibitor-treated rings, the concentration of noradrenaline and $PGF_{2\alpha}$ was diminished in order to obtain a level of initial contraction similar to the controls. i.c.: initial contraction.
*$P < 0.05$ (paired t test).

Table 4 Effect of superoxide dismutase (SOD) on 13-hydroperoxylinoleic acid (13-HPODE)-induced relaxation of canine splenic artery and circumflex segments

	Splenic artery ($n = 7$)	*Circumflex* ($n = 6$)
EC_{50} ($-\log$ M)		
Control	5.86 ± 0.08	5.91 ± 0.05
SOD 20 u ml^{-1}	5.99 ± 0.06	6.00 ± 0.08
SOD 40 u ml^{-1}	5.95 ± 0.08	6.00 ± 0.02
Maximum relaxation (%)		
Control	84 ± 3 (i.c. = 5.7 ± 0.9 g)	58 ± 5 (i.c. = 5.6 ± 0.8 g)
SOD 20 u ml^{-1}	75 ± 8 (i.c. = 5.0 ± 1.1 g)	61 ± 9 (i.c. = 5.3 ± 0.9 g)
SOD 40 u ml^{-1}	76 ± 11 (i.c. = 6.2 ± 1.2 g)	87 ± 7 (i.c. = 4.8 ± 0.3 g)

Values are shown as means ± s.e.mean. EC_{50}: concentration producing half of the maximum relaxation of segments contracted with noradrenaline 0.3 μM in the presence of daltroban 7 μM (splenic artery) or $PGF_{2\alpha}$ 2 μM (circumflex); i.c. = initial contraction. The effect of SOD was not significant (ANOVA, Student-Newman-Keuls test).

Table 5 Bioassay of NO induced by acetylcholine, 13-hydroxylinoleic acid (13-HODE) and 13-hydroperoxylinoleic acid (13-HPODE)

Agonist	*Bolus* (nmol)	*Relaxation* (%) ($n = 5$)
Acetylcholine	0.3	39 ± 8
	3	45 ± 9
	30	56 ± 5
13-HODE	0.3	6 ± 5
	3	1 ± 1
	30	2 ± 2
13-HPODE	0.3	0 ± 1
	3	1 ± 1
	30	3 ± 3

The canine splenic artery was used as donor vessel and the rabbit abdominal aorta denuded of endothelial cells served as detector tissue. Data are given as percentage relaxation ± s.e.mean of the detector tissue.

genase-derived vasodilator. Incubation experiments indicated that 13-HODE (10 μM) and 13-HPODE (10 μM) did indeed stimulate the biosynthesis of PGI_2. This is in agreement with the finding that 13-HODE stimulates the production of PGI_2 in cultured endothelial cells (Setty *et al.*, 1987). It has also been reported that in human umbilical vein endothelial cell monolayers, 13-HPODE, up to 20 μM, stimulated the formation of PGI_2, PGI_3 and dihomo-PGI_2 from endogenous arachidonate or exogenous eicosapentaenoic acid and docosatetraenoic acid, respectively (Bordet *et al.*, 1988). In our experiments the concentration of 13-HPODE was kept below 20 μM. Above that level 13-HPODE inhibits PGI_2 biosynthesis, presumably by destroying PGH_2 synthase activity (Hennig *et al.*, 1986; Bordet *et al.*, 1988), the rate limiting step in the formation of PGI_2 from arachidonate (De Witt *et al.*, 1983) and may act as a detergent in cell membranes (Hennig *et al.*, 1986).

It is possible that some of the effects of 13-HPODE may be due to its conversion to 13-HODE in the organ bath. However, 13-HPODE elicited an additional indomethacin- and meclofenamate-resistant, but endothelium-dependent relaxation. The possiblity that this part of the relaxation to 13-HPODE was due to stimulation of the release of NO, was ruled out by both the bioassay and the experiments with L-NNA. L-NNA is a potent, L-arginine-reversible inhibitor of endothelial NO biosynthesis (Moore *et al.*, 1990). As expected, 13-HODE did not evoke release of NO either.

Since in arteries with endothelium the 13-HPODE-induced relaxations appeared to be partly due to an intermediate different from a cyclo-oxygenase product or NO, we investigated the possibility that these relaxations were mediated by superoxide anions or superoxide-dependent relaxing factor(s)

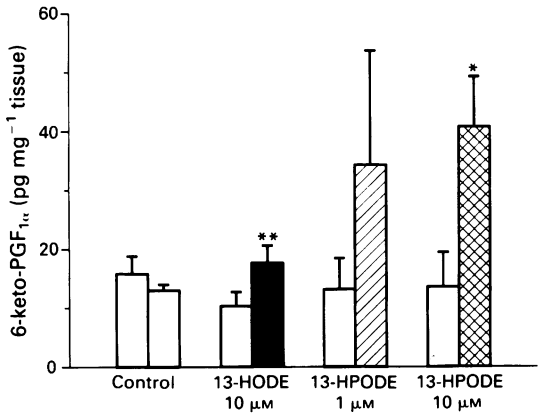

Figure 3 Influence of 13-hydroxylinoleic acid (13-HODE) and 13-hydroperoxylinoleic acid (13-HPODE) on the biosynthesis of prostacyclin by rings of the canine splenic artery. Prostacyclin production was determined after 15 min incubation before (left hand open columns) and after addition (right hand columns) of 0 or 10 μM 13-HODE ($n = 14$) or 0, 1 or 10 μM 13-HPODE ($n = 7$). Results are expressed in pg 6-keto-$PGF_{2\alpha}$ mg^{-1} tissue as means ± s.e.mean (vertical bars). $^*P<0.05$; $^{**}P<0.01$, Student's t test (paired, two-tailed).

from endothelial cells (Hong *et al.*, 1989). However, SOD, which destroys superoxide anions (McCord & Fridovich, 1969) failed to diminish the relaxations to 13-HPODE. This argues against a role of superoxide anion in the 13-HPODE induced relaxations, although it cannot be ruled out that SOD failed to diffuse into the intercellular spaces of the tissue.

In conclusion, 13-HODE and 13-HPODE induce relaxations in canine splenic and coronary arteries that are due to stimulation of PGI_2 biosynthesis, both in the endothelium and smooth muscle cells or other subendothelial structures. For 13-HPODE, an additional intermediate contributes to the relaxations of arteries with endothelium. The nature of this mediator, which is neither NO, nor a cyclo-oxygenase product, and is unlikely to be superoxide anion, is at present unknown.

We wish to thank Boehringer Mannheim, the Wellcome Foundation and Grünenthal for their gift of daltroban, prostacyclin and bovine recombinant SOD respectively. The secretarial help of Mrs Liliane Van den Eynde and Mrs Lydie Van Laerhoven is also gratefully acknowledged. G.R.Y.D.M. is a Senior Research Assistant of the National Fund for Scientific Research, Belgium.

References

AHARONY, D., SMITH, J.B., SMITH, E.F. & LEFER, A.M. (1981). Effects of arachidonic acid hydroperoxides on vascular and non-vascular smooth muscle. *Prostaglandins Med.*, **7**, 527–535.

ASANO, M. & HIDAKA, H. (1979). Contractile response of isolated rabbit aorta strips to unsaturated fatty acid peroxides. *J. Pharmacol. Exp. Ther.*, **208**, 347–353.

BORDET, J.-C., GUICHARDANT, M. & LAGARDE, M. (1988). Hydroperoxides produced by n-6 lipoxygenation of arachidonic and linoleic acids potentiate synthesis of prostacyclin related compounds. *Biochim. Biophys. Acta*, **958**, 460–468.

BUCHANAN, M.R., BUTT, R.W., MAGAS, Z., VAN RYN, J., HIRCH, J. & NAZIR, D.J. (1985). Endothelial cells produce a lipoxygenase-derived chemorepellant which influences platelet/endothelial cell interactions: effect of aspirin and salicylate. *Thromb. Haemostas.*, **53**, 306–311.

BULT, H., FRET, H.R., VAN DEN BOSSCHE, R.M. & HERMAN, A.G. (1988). Platelet inhibition by endothelium-derived relaxing factor from the rabbit perfused aorta. *Br. J. Pharmacol.*, **95**, 1308–1314.

BULT, H., HERMAN, A.G. & VAN DE VELDE, V.J.S. (1982). Effect of dipyridamole on the formation of 6-oxo-prostaglandin $F_{1\alpha}$ by the rat isolated aorta and ram seminal vesicle microsomes. *Br. J. Pharmacol.*, **76**, 453–458.

COENE, M.-C., BULT, H., CLAEYS, M., LAEKEMAN, G.M. & HERMAN, A.G. (1986). Inhibition of rabbit platelet activation by lipoxygenase products of arachidonic and linoleic acid. *Thromb. Res.*, **42**, 205–214.

D'ALARCAO, M., COREY, E.J., CUNARD, C., RAMWELL, P., WUOTILA, P., VARGAS, R. & WROBLEWSKA, B. (1987). The vasodilatation induced by hydroperoxy metabolites of arachidonic acid in the rat mesenteric and pulmonary circulation. *Br. J. Pharmacol.*, **91**, 627–632.

DE GRAAF, J.C., BULT, H., DE MEYER, G.R.Y., SIXMA, J.J. & DE GROOT, P.G. (1989). Platelet adhesion to subendothelial structures under flow conditions: no effect of the lipoxygenase product 13-HODE. *Thromb. Haemostas.*, **62**, 802–806.

DE MEYER, G.R.Y., BULT, H. & HERMAN, A.G. (1991). Early atherosclerosis is accompanied by a decreased rather than an increased accumulation of fatty acid hydroxyderivatives. *Biochem. Pharmacol.*, **42**, 279–283.

DE WITT, D.L., DAY, J.S., SONNENBURG, W.K. & SMITH, W.L. (1983). Concentrations of prostaglandin endoperoxide synthase and prostaglandin I_2 synthase in the endothelium and smooth muscle of bovine aorta. *J. Clin. Invest.*, **72**, 1882–1888.

ENGELS, F., WILLEMS, H. & NIJKAMP, F.P. (1986). Cyclooxygenase catalysed formation of 9-hydroxylinoleic acid by guinea pig alveolar macrophages under non-stimulated conditions. *FEBS Lett.*, **209**, 249–253.

FUNK, C.D. & POWELL, W.S. (1985). Release of prostaglandins and monohydroxy and trihydroxy metabolites of linoleic and arachidonic acids by adult and fetal aortae and ductus arteriosus. *J. Biol. Chem.*, **260**, 7481–7488.

FURCHGOTT, R.F. & ZAWADZKI, J.V. (1980). The obligatory role of endothelial cells in the relaxation of arterial smooth muscle by acetylcholine. *Nature*, **288**, 373–376.

HENNIG, B., ENOCH, C. & CHOW, C.K. (1986). Linoleic acid hydroperoxide increases the transfer of albumin across cultured endothelial monolayers. *Arch. Biochem. Biophys.*, **248**, 353–357.

HONG, K.W., RHIM, B.Y., LEE, W.S., JEONG, B.R., KIM, D.C. & SHIN, Y.W. (1989). Release of superoxide-dependent relaxing factor(s) from endothelial cells. *Am. J. Physiol.*, **257**, H1340–H1346.

KOIDE, T., NEICHI, T., TAKATO, M., MATSUSHITA, H., SUGOIKA, K., NAKANO, M. & HATA, S. (1982). Possible mechanisms of 15-hydroperoxy arachidonic acid-induced contraction of the canine basilar artery in vitro. *J. Pharmacol. Exp. Ther.*, **221**, 481–488.

LEFER, A.M. (1988). Daltroban (BM 13.505) – A highly specific, potent thromboxane receptor antagonist. *Drugs Fut.*, **13**, 999–1005.

LOVELADY, G.K., MIRRO, R., ARMSTEAD, W.M., BUSIJA, D.W. & LEFFLER, C.W. (1988). Effects of 15-HETE on cerebral arterioles of newborn pigs. *Prostaglandins*, **36**, 507–513.

MCCORD, J.M. & FRIDOVICH, I. (1969). Superoxide dismutase. An enzymic function for erythrocuprein (hemocuprein). *J. Biol Chem.*, **244**, 6049–6055.

MONCADA, S. & VANE, J.R. (1979). Arachidonic acid metabolites and the interactions between platelets and blood-vessel walls. *N. Engl. J. Med.*, **300**, 1142–1147.

MOORE, P.K., AL-SWAYEH, O.A., CHONG, N.W.S., EVANS, R.A. & GIBSON, A. (1990). L-N^G-nitro arginine (L-NOARG), a novel, L:-arginine-reversible inhibitor of endothelium-dependent vasodilatation *in vitro*. *Br. J. Pharmacol.*, **99**, 408–412.

PALMER, R.M.J., FERRIGE, A.G. & MONCADA, S. (1987). Nitric oxide release accounts for the biological activity of endothelium-derived relaxing factor. *Nature*, **327**, 524–526.

SETTY, B.N.Y., BERGER, M. & STUART, M.J. (1987). 13-Hydroxy-octadecadienoic acid (13-HODE) stimulates prostacyclin production by endothelial cells. *Biochem. Biophys. Res. Commun.*, **146**, 502–509.

SIMON, T.C., MAKHEJA, A.N. & BAILEY, J.M. (1989). The induced lipoxygenase in atherosclerotic aorta converts linoleic acid to the platelet chemorepellant factor 13-HODE. *Thromb. Res.*, **55**, 171–178.

SOKAL, R.R. & ROHLF, F.J. (1981). *Biometry: the Principles and Practice of Statistics in Biological Research*. 2nd edition. pp. 179–453. New York: Freeman, W.H. & Company.

TAKAHASHI, M., OZAKI, N., KAWAKITA, S., NOZAKI, M. & SAEKI, Y. (1985). Vascular effects of 15-HPETE and 15-HETE on canine arteries. *Jpn. J. Pharmacol.*, **37**, 325–334.

TALLARIDA, R.J. & MURRAY, R.B. (1981). *Manual of Pharmacological Calculations*. pp. 1–150. Berlin – Heidelberg – New York: Springer Verlag.

THOMAS, G. & RAMWELL, P. (1986). Induction of vascular relaxation by hydroperoxides. *Biochem. Biophys. Res. Commun.*, **139**, 102–108.

TRACHTE, G.J., LEFER, A.M., AHARONY, D. & SMITH, J.B. (1979). Potent constriction of cat coronary arteries by hydroperoxides of arachidonic acid and its blockade by anti-inflammatory agents. *Prostaglandins*, **18**, 909–914.

UOTILA, P., VARGAS, R., WROBLEWSKA, B., D'ALARCAO, M., MATSUDA, S.P., COREY, E.J., CUNARD, C.M. & RAMWELL, P.W. (1987). Relaxing effects of 15-lipoxygenase products of arachidonic acid on rat aorta. *J. Pharmacol. Exp. Ther.*, **242**, 945–949.

VAN DIEST, M.J., VERBEUREN, T.J. & HERMAN, A.G. (1986). Cyclooxygenase blockers influence the effects of 15-lipoxygenase metabolites of arachidonic acid in isolated canine blood vessels. *Prostaglandins*, **32**, 97–100.

VAN DIEST, M.J., VERBEUREN, T.J. & HERMAN, A.G. (1991). 15-Lipoxygenase metabolites of arachidonic acid evoke contractions and relaxations in isolated canine arteries: role of thromboxane-receptors, endothelial cells and cyclooxygenase. *J. Pharmacol. Exp. Ther.*, **256**, 194–203.

VANHOUTTE, P.M. & VERBEUREN, T.J. (1976). Inhibition by acetylcholine of the norepinephrine release evoked by potassium in canine saphenous vein. *Circ. Res.*, **39**, 263–269.

(Received January 27, 1992
Revised June 18, 1992
Accepted June 22, 1992)

Br. J. Pharmacol. (1992), **107**, 604-609

Effects of nitric oxide synthase inhibitors, L-N^G-nitroarginine and L-N^G-nitroarginine methyl ester, on responses to vasodilators of the guinea-pig coronary vasculature

Amanda Vials & [1]Geoffrey Burnstock

Department of Anatomy and Developmental Biology and Centre for Neuroscience, University College London, Gower Street, London WC1E 6BT

1 The effects of L-N^G-nitroarginine (L-NOARG) and L-N^G-nitroarginine methyl ester (L-NAME) on vasodilatation induced by ATP, substance P, 5-hydroxytryptamine (5-HT), bradykinin and sodium nitroprusside (SNP) were examined in the guinea-pig coronary bed, by use of a Langendorff technique. The effects of these inhibitors of nitric oxide synthesis were assessed on their ability to inhibit both the amplitude and the area of the vasodilator response.

2 The vasodilator responses evoked by low doses of 5-HT (5×10^{-10}–5×10^{-8} mol) were almost abolished by L-NAME and L-NOARG (both at 10^{-5}, 3×10^{-5} and 10^{-4} M), although L-NOARG (3×10^{-5} M) was significantly less potent than L-NAME (3×10^{-5} M) as an inhibitor of vasodilator responses to 5-HT (5×10^{-8} mol).

3 The vasodilator responses evoked by substance P (5×10^{-12}–5×10^{-9} mol) were reduced in the presence of L-NAME and L-NOARG (both at 10^{-5} and 3×10^{-5} M). The response to substance P was almost abolished by L-NAME and L-NOARG (both at 10^{-4} M).

4 The amplitude of the vasodilator responses to ATP (5×10^{-11} and 5×10^{-9}–5×10^{-7} mol) was little affected by either L-NAME or L-NOARG (both at 10^{-5}, 3×10^{-5} and 10^{-4} M). However, the area of the response to ATP (5×10^{-10}–5×10^{-7} mol) was inhibited by L-NAME (10^{-5}, 3×10^{-5} and 10^{-4} M) and to a lesser extent by L-NOARG (10^{-5} and 10^{-4} M).

5 The amplitude and area of the vasodilator responses to bradykinin (5×10^{-12}–5×10^{-11} mol) were reduced, but not abolished, by L-NOARG and L-NAME.

6 Neither the amplitude nor area of the responses to sodium nitroprusside (5×10^{-10}–5×10^{-7} mol) were inhibited by either L-NAME or L-NOARG (both at 10^{-5} and 3×10^{-5} M).

7 It is concluded that in the guinea-pig coronary vasculature, the vasodilatation evoked by substance P and low doses of 5-HT is mediated almost exclusively via nitric oxide, whereas the vasodilatations evoked by ATP and bradykinin appear to involve other mechanisms in addition to the release of nitric oxide. L-NAME was a more effective agent than L-NOARG in inhibiting the vasodilator actions of 5-HT and ATP in this preparation.

Keywords: Nitric oxide synthase; relaxation of smooth muscle; blood vessels; coronary vasculature; L-N^G-nitroarginine; L-N^G-nitroarginine methyl ester

Introduction

Endothelial cells play a key role in the control of vascular tone by virtue of their ability to synthesize and release endothelium-derived relaxing factors. Various agents, including substance P, adenosine 5'-triphosphate (ATP), 5-hydroxytryptamine (5-HT), acetylcholine (ACh) and bradykinin, elicit vasodilatation in the coronary bed via an action at receptors located on endothelial cells, leading to the release of these factors (Cohen *et al.*, 1983; Saeed *et al.*, 1986; Hopwood & Burnstock, 1987; Hopwood *et al.*, 1989; Hoover, 1990; Lamontagne *et al.*, 1991). These factors include prostacyclin (Moncada & Vane, 1979) and endothelium-derived relaxing factor (EDRF, Furchgott & Zawadzki, 1980). Prostacyclin is a potent vasodilator (Moncada *et al.*, 1976) which can be released from endothelial cells by a variety of stimuli including bradykinin, arachidonic acid, thrombin, the ionophore A23187, ATP and histamine (Weksler *et al.*, 1978; Pearson *et al.*, 1983). In some blood vessels the release of EDRF also mediates the vascular relaxation evoked by certain vasodilators including ACh, ATP, substance P and bradykinin (Furchgott & Zawadzki, 1980; Cherry *et al.*, 1982; Furchgott, 1983; 1984).

It has been proposed that EDRF is the free radical of nitric oxide (NO, Ignarro *et al.*, 1986; Furchgott *et al.*, 1987) and indeed, EDRF has chemical and pharmacological properties identical to those of NO (Palmer *et al.*, 1987; Ignarro *et al.*, 1987). NO is released tonically from guinea-pig isolated, perfused hearts, and ACh, bradykinin, 5-HT and ATP stimulate further release (Kelm & Schrader, 1988; 1990).

In endothelial cells, NO is produced from the conversion of the semi-essential amino acid L-arginine into L-citrulline by NO synthase (Palmer *et al.*, 1988; Schmidt *et al.*, 1988; Mayer *et al.*, 1989; Palmer & Moncada, 1989). Analogues of L-arginine are, therefore, potentially specific inhibitors of EDRF-mediated effects on vascular tone. In fact, it has been shown that L-N^G-monomethylarginine (L-NMMA) inhibits dilator responses due to ACh, A23187, substance P and L-arginine in the rabbit aorta (Rees *et al.*, 1989). L-N^G-nitroarginine (L-NOARG) is also an inhibitor of the generation of NO and has been shown to be more potent than L-NMMA (Moore *et al.*, 1990). L-NOARG has been shown to inhibit vasodilator responses to ACh and 5-HT in the rabbit isolated perfused heart (Lamontagne *et al.*, 1991), and to attenuate the duration of the vasodilator response to bradykinin in the rat isolated heart (Baydoun & Woodward, 1991). Similarly, L-N^G-nitroarginine methyl ester (L-NAME) is an inhibitor of enzymatic synthesis of NO from L-arginine (Rees *et al.*, 1990).

[1] Author for correspondence.

The purpose of this study was to compare the effects of the NO synthase inhibitors L-NOARG and L-NAME, and to ascertain the role of NO in the vasodilator responses to various agonists in the guinea-pig coronary bed.

Methods

Guinea-pigs (250–500 g) of either sex were injected with heparin (2,500 units i.p.) 15 min before being killed by cervical dislocation. The heart was quickly removed and placed in cold Krebs (4°C) to arrest the beating. Extraneous fat and large vessels were removed, the heart was cannulated via the aorta, and the coronary circulation perfused by the method of Langendorff with a modified Krebs-Henseleit solution containing (mM): NaCl 115.3, KCl 4.6, $MgSO_4.7H_2O$ 1.1, $NaHCO_3$ 22.1, KH_2PO_4 1.1, $CaCl_2$ 2.5 and glucose 11.1. Albumin (0.5 g l^{-1}) was also added to the solution to increase the oncotic pressure and prevent oedema. A water-filled silicone rubber balloon, connected to a pressure transducer (Viggo-Spectramed Bilthoven, model P23XL), was placed in the left ventricle for the measurement of left ventricular pressure. The left ventricular diastolic pressure did not exceed 10 mmHg. Perfusion pressure was monitored with a pressure transducer connected via a side arm to the aortic cannula. A pair of platinum wire electrodes were placed in the right ventricle and the heart was paced at 4 Hz with electrical pulses of 5 ms duration at supramaximal voltage (usually around 20 V). The flow rate was gradually increased to obtain a starting perfusion pressure of 50–60 mmHg using a Masterflex constant flow roller pump (Cole-Palmer Instruments Co., Chicago). The flow rate was determined by collecting the effluent over a timed period; the mean rate was 22.6 ± 0.75 ml min^{-1} ($n = 76$).

In order to look at the effect of the inhibitors L-NOARG and L-NAME, control dose-response relationships to agonists were first determined. An inhibitor was then added to the perfusing solution and the preparation allowed to equilibrate for 20 min. Dose-response relationships were re-evaluated in the presence of the inhibitor. Agonists were given as 50 µl boluses, injected over 3 s into the superfusing solution close to the heart. At least 5 min were left between administration of each agonist. For a given response, both its maximum amplitude and area were measured. The area of the vasodilator response was calculated by use of a measurement and analysis programme on an Apple II computer. The results were calculated as the means ± s.e. mean and Student's t test was used to assess significance. A value of $P < 0.05$ was taken to be significant. At the end of each experiment the heart was removed from the cannula, blotted and weighed. The mean weight was 2.3 ± 0.1 g ($n = 76$).

ATP, bradykinin, L-NOARG, L-NAME, 5-HT and sodium nitroprusside were all obtained from Sigma Chemical Co., Poole. Substance P was obtained from Cambridge Research Biochemicals and heparin was obtained form CP Pharmaceuticals Ltd, Wrexham.

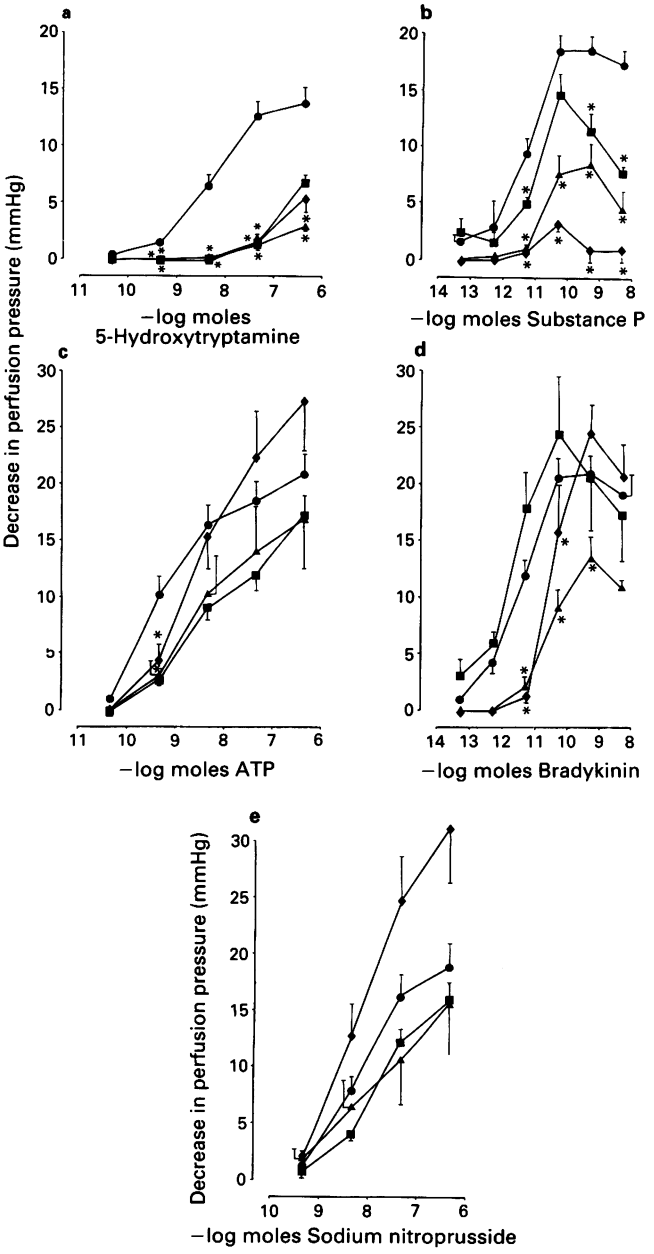

Figure 1 The amplitude of the vasodilator responses evoked by (a) 5-hydroxytryptamine, (b) substance P, (c) ATP, (d) bradykinin and (e) sodium nitroprusside, in the guinea-pig isolated perfused heart, in the absence (●; mean of all controls) and presence of N^G-nitro-L-arginine methyl ester (L-NAME) 10^{-5} M (■), 3×10^{-5} M (▲) or 10^{-4} M (◆). The graph shows the mean ($n \geq 6$) with s.e. mean indicated by vertical bars. The significant differences are $^*P < 0.05$.

Results

Effect of L-N^G-nitroarginine methyl ester on vasodilator responses of the guinea-pig coronary bed

The effect of L-NAME on the maximum amplitude of the vasodilator response (Figure 1a–e), on perfusion pressure trace response (Figure 2a–c) and on the area of the vasodilator response (Figure 4a,c,e) to various agents is demonstrated. L-NAME (10^{-5}, 3×10^{-5} and 10^{-4} M) was a potent inhibitor of vasodilator responses due to 5-HT, virtually abolishing the effects of lower doses of this agent (Figures 1a and 2c). The maximum amplitude and area of the vasodilator responses due to substance P were significantly inhibited by L-NAME (10^{-5}, 3×10^{-5} and 10^{-4} M; Figures 1b and 2b), and at 10^{-4} M it almost abolished the responses to substance P.

L-NAME (10^{-5} M) did not affect the amplitude of the dilatation evoked by ATP across its dose-range, and at 3×10^{-5} and 10^{-4} M it inhibited only a low dose of ATP (5×10^{-10} mol; Figure 1c). In contrast, the area of the vasodilator response to ATP was significantly inhibited by L-NAME (10^{-5}, 3×10^{-5} and 10^{-4} M; Figure 4a), reflecting an attenuation of the duration of the response (Figure 2a). The area of the vasodilator response to the highest dose of ATP was not inhibited by L-NAME (10^{-4} M).

The responses evoked by bradykinin were significantly inhibited by L-NAME (3×10^{-5} and 10^{-4} M; Figures 1d and 4c). Neither the amplitude (Figure 1e) nor the area (Figure 4e) of the vasodilator responses to SNP were affected by L-NAME.

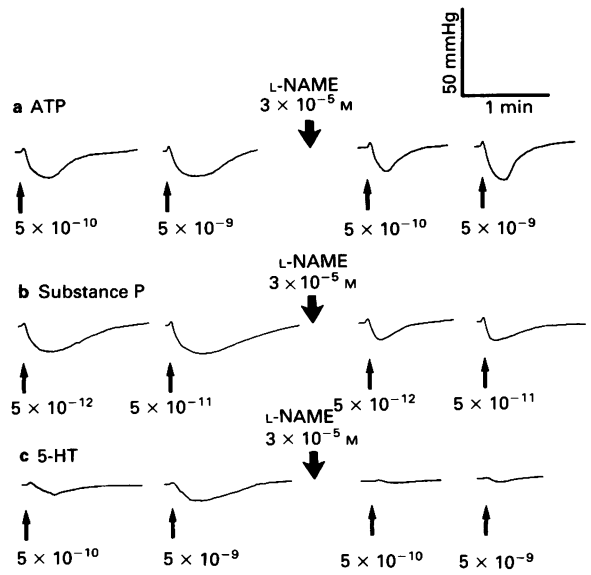

Figure 2 Typical perfusion pressure traces, obtained from guinea-pig isolated perfused hearts, showing the effects of (a) ATP, (b) substance P and (c) 5-hydroxytryptamine (5-HT) in the absence and presence (after ↑) of L-N^G-nitroarginine methyl ester (L-NAME). The dose stated is the number of moles of vasodilator agonist that is injected into the perfusion system close to the heart.

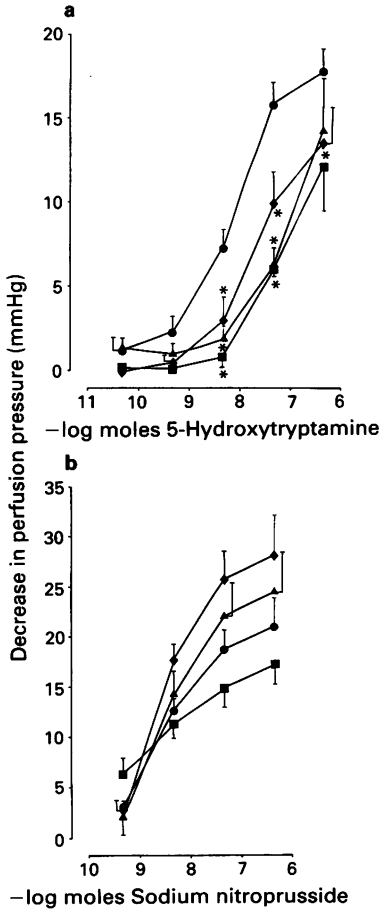

Figure 3 The amplitude of the vasodilator responses evoked by (a) 5-hydroxytryptamine, and (b) sodium nitroprusside, in the guinea-pig isolated perfused heart, in the absence (●; mean of all controls) and presence of N^G-nitro-L-arginine 10^{-5} (■), 3×10^{-5} (▲) or 10^{-4} M (◆). The graph shows the mean ($n \geq 6$) with s.e. mean indicated by vertical bars. The significant differences are $^*P < 0.05$.

Effect of L-N^G-nitroarginine on vasodilator responses of the guinea-pig coronary bed

The effect of L-NOARG on the maximum amplitude of the vasodilator response (Figure 3a–b) and on the area of the vasodilator response (Figure 4b,d,f) to various agents is shown. The amplitude of the responses evoked by 5-HT (5×10^{-10}–5×10^{-9} mol) was significantly reduced by L-NOARG (10^{-5}, 3×10^{-5} and 10^{-4} M; Figure 3a). The area of the responses to 5-HT (5×10^{-10}–5×10^{-9} mol) was also reduced by L-NOARG (10^{-5}, 3×10^{-5} and 10^{-4} M, data not shown). L-NOARG (3×10^{-5} M) was significantly less effective than L-NAME (3×10^{-5} M) at reducing the maximum amplitude of the vasodilatation due to 5-HT (5×10^{-8} mol); 84.1 ± 4.2 and 48.7 ± 13.34% inhibition of the response to 5-HT by L-NAME and L-NOARG (both at 3×10^{-5} M), respectively.

The inhibition of the responses to substance P by L-NOARG (10^{-5}, 3×10^{-5} and 10^{-4} M; data not shown) was similar to that of L-NAME (10^{-5}, 3×10^{-5} and 10^{-4} M).

L-NOARG did not inhibit the amplitude of the responses to ATP (data not shown). L-NOARG (10^{-5} and 10^{-4} M) significantly attenuated only the area of the response evoked by intermediate doses of ATP (5×10^{-10}–5×10^{-8} mol; Figure 4b). The mid-concentration of L-NOARG (3×10^{-5} M) did not have any inhibitory effect on the responses to ATP.

The amplitude of the responses evoked by bradykinin was significantly inhibited by L-NOARG (3×10^{-5} and 10^{-4} M; data not shown), although the lower concentration of L-NOARG (10^{-5} M) had no effect on the amplitude of the responses to this agent. L-NOARG (10^{-5}, 3×10^{-5} and 10^{-4} M) significantly inhibited the area of the response to bradykinin (Figure 4d). Responses (amplitude and area) due to SNP (Figure 3b and 4f) were not affected by L-NOARG.

Discussion

The results of this study show that in the guinea-pig coronary vasculature, dilator responses evoked by substance P and low concentrations of 5-HT were dependent largely upon the synthesis of NO. In contrast, vasodilator responses elicited by bradykinin and ATP appeared to be only partially dependent upon the synthesis of NO, while SNP elicited vasodilatation by a mechanism that was independent of the generation of NO.

Few studies have compared the effects of both L-NAME and L-NOARG as inhibitors of NO synthase. L-NAME has been shown to be equipotent with L-NOARG as a prejunctional inhibitor of non-adrenergic, non-cholinergic transmission in the rat anococcygeus (Hobbs & Gibson, 1990). L-NAME and L-NOARG at the same concentration, have been shown to produce similar inhibition of vasodilatation evoked by ACh in the rabbit aorta (Moore *et al.*, 1990). However, the present study demonstrates that, although L-NAME and L-NOARG exhibit similar inhibitory properties to vasodilator responses to bradykinin and substance P in the guinea-pig coronary bed, there are differences in the extent of inhibition of vasodilator responses due to 5-HT and ATP.

Responses (both the amplitude and area) due to low concentrations of 5-HT were virtually abolished by L-NAME. Consistent with this, it has been shown in the canine coronary artery that 5-HT does not act via endothelial production of prostacyclin, or following breakdown to active products by endothelial monoamine oxidase (Cohen *et al.*, 1983). Together these results suggest that the response to low doses of 5-HT was dependent almost exclusively on the production of NO. 5-HT is localized in endothelial cells in the rat heart, from where it may be released during hypoxic conditions (Burnstock *et al.*, 1988). Following release from endothelial cells, 5-HT can then act on receptors on the endothelium to elicit vasodilatation via production of NO. The higher dose

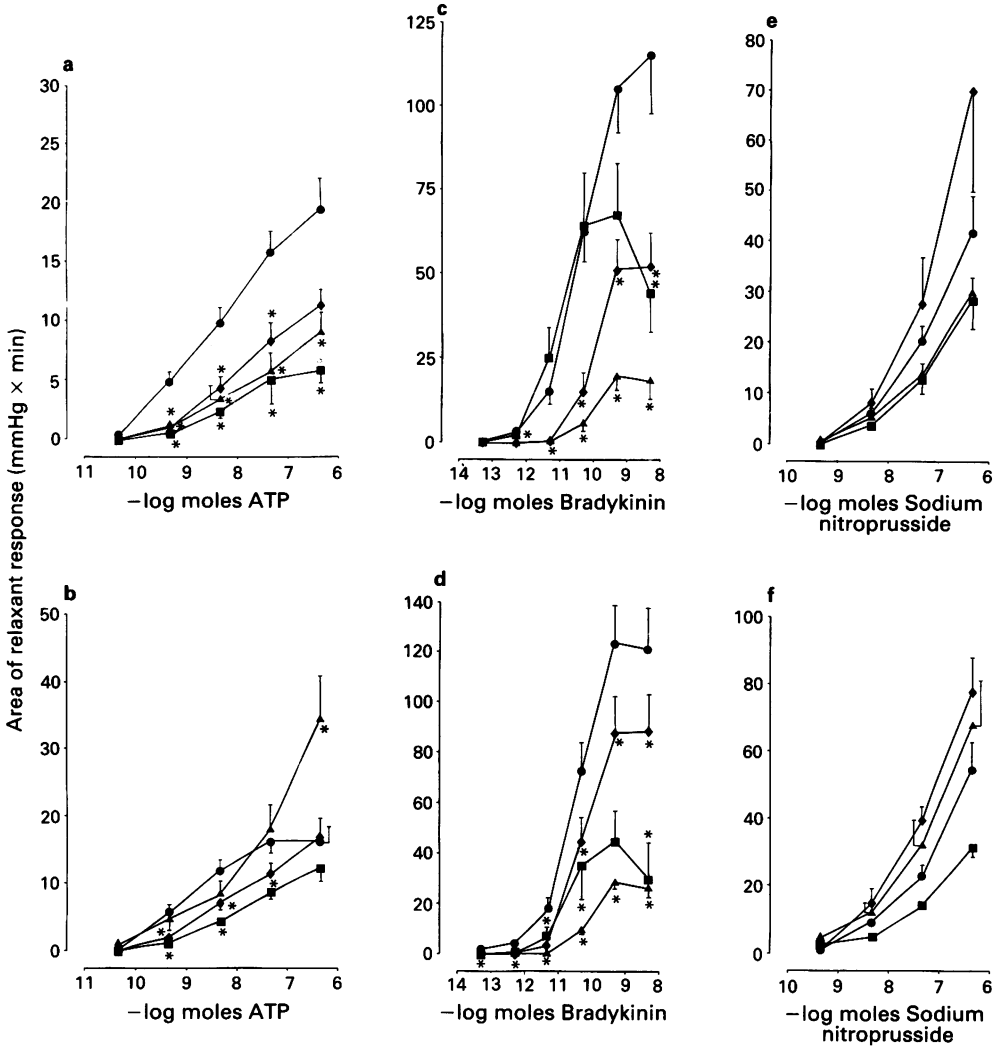

Figure 4 Area of the vasodilator response to (a) ATP, (c) bradykinin and (e) sodium nitroprusside in the guinea-pig isolated perfused heart in the absence (●; mean of all controls) and presence of L-N^G-nitroarginine methyl ester 10^{-5} (■), 3×10^{-5} (▲) or 10^{-4} M (◆), and also the area of the vasodilator response to (b) ATP, (d) bradykinin and (f) sodium nitroprusside in the absence (●; mean of all controls) and presence of L-N^G-nitroarginine 10^{-5} (■), 3×10^{-5} (▲) or 10^{-4} M (◆). The graph shows the mean ($n \geq 6$) with s.e. mean indicated by vertical bars. The significant differences are $^*P < 0.05$.

of 5-HT was not abolished by L-NAME even at its highest concentration, suggesting another mode of action of 5-HT.

L-NAME did not alter the peak vasodilatation induced by ATP, suggesting that at least this part of the response is not due to the generation of NO. However, the duration of the response was reduced by L-NAME, and therefore, part of the action of ATP occurs via the release of NO. This is supported by work on the release of NO in the guinea-pig coronary bed (Kelm & Schrader, 1990), which has shown that ATP does induce release of NO. The lack of effect of L-NOARG (at 5×10^{-4} M) on vasodilator responses of the guinea-pig coronary bed to ATP has also been found by Brown *et al.* (1991), using a constant pressure system. Thus although part of the vasodilator response to ATP is via NO, other mechanisms are also involved. Although it is not possible to extrapolate directly from studies on different species and vascular beds, the information obtained may provide clues to the other possible mechanisms of action of ATP. For example, prostacyclin production could be involved as ATP has been shown to stimulate prostacyclin production from various perfused beds and from endothelial cells in culture (Needleman *et al.*, 1974; Boeynaems & Galand, 1983; Hellewell & Pearson, 1984). Alternatively or additionally, ATP could be acting directly on the smooth muscle. It has been shown, for example, in the coronary artery of the rabbit, that ATP produces vasodilatation by a direct action on P_{2Y}-receptors on the smooth muscle (Corr & Burnstock, 1991). ATP could also be metabolized to adenosine by highly active ectonucleotidases (Fleetwood *et al.*, 1989) and as such cause relaxation via action at P_1-purinoceptors (Burnstock & Kennedy, 1986).

Bradykinin is a potent vasoactive agent which relaxes several vascular smooth muscle preparations via an endothelium-dependent mechanism (Cherry *et al.*, 1982); it also causes release of NO from guinea-pig isolated hearts (Kelm & Schrader, 1988). L-NAME and L-NOARG significantly inhibited the vasodilatation in response to bradykinin, suggesting that at least part of its action was via the release of NO from endothelial cells. The maximum inhibition of the peak response to bradykinin by L-NAME (3×10^{-5} M) was reached without abolishing the response, suggesting that bradykinin exerts its effect by a combination of mechanisms. In addition to acting via NO, it could also act via activation of endothelium-derived hyperpolarizing factor (Boulanger *et al.*, 1989) or via release of prostacyclin, although it has been shown in the porcine coronary artery that vasodilator responses to bradykinin are maintained in the presence of indomethacin (Richard *et al.*, 1990). In the rat isolated perfused heart, bradykinin mediates vasodilator effects via activation of the kinin B_2-receptor (Baydoun & Woodward, 1991), which introduces another possible vasodilator contribution in the guinea-pig coronary bed.

L-NAME and L-NOARG (both at 10^{-4} M) almost abolish the response to substance P, suggesting that it induces relaxation almost exclusively via NO release. It has been shown in various isolated coronary arteries that substance P is endothelium-dependent (Berkenboom *et al.*, 1987; Gulati *et al.*, 1987). If it is assumed that NO is released from endothelial cells, then it appears that substance P also acts by an endothelial-dependent mechanism in the guinea-pig coronary vasculature.

The action of SNP was not affected by either L-NAME or L-NOARG. Formation of NO from SNP is probably the mode for direct or indirect activation of soluble guanylate cyclase, resulting in relaxation of vascular smooth muscle (Feelisch & Noack, 1987). Thus, SNP should not be, and was not, affected by these NO synthase inhibitors as it bypasses NO formation in endothelial cells.

This study has revealed that in the guinea-pig coronary bed L-NAME and L-NOARG exhibited similar inhibitory effects on vasodilator responses, although L-NAME tended to be more potent in inhibiting relaxant responses evoked by 5-HT and ATP. The use of L-NAME and L-NOARG has established a better understanding of the role that NO plays in the relaxant response to various vasodilators of the guinea-pig coronary vasculature.

This work was supported with a grant from the Science and Engineering Research Council. Dr C.H.V. Hoyle is thanked for helpful discussion during the course of this work.

References

BAYDOUN, A.R. & WOODWARD, B. (1991). Effects of bradykinin in the rat isolated perfused heart: role of kinin receptors and endothelium-derived relaxing factor. *Br. J. Pharmacol.*, **103**, 1829–1833.

BERKENBOOM, G., DEPIERREUX, M. & FONTAINE, J. (1987). The influences of atherosclerosis on the mechanical responses of isolated coronary arteries to substance P, isoprenaline and noradrenaline. *Br. J. Pharmacol.*, **92**, 113–120.

BOEYNAEMS, J.M. & GALAND, N. (1983). Stimulation of vascular prostacyclin synthesis by extracellular ADP and ATP. *Biochem. Biophys. Res. Commun.*, **112**, 290–296.

BOULANGER, C., HENDRICKSON, H., LORENZ, R.R. & VANHOUTTE, P.M. (1989). Release of different relaxing factors by cultured porcine endothelial cells. *Circulation Res.*, **64**, 1070–1078.

BROWN, I., THOMPSON, C.I. & BELLONI, F.L. (1991). Coronary vasodilation by ATP in guinea-pig is not mediated by nitric oxide. *FASEB J.*, **5**, A694.

BURNSTOCK, G. & KENNEDY, C. (1986). Purinergic receptors in the cardiovascular system. *Prog. Pharmacol.*, **6**, 111–132.

BURNSTOCK, G., LINCOLN, J., FEHÉR, E., HOPWOOD, A.M., KIRKPATRICK, K., MILNER, P. & RALEVIC, V. (1988). Serotonin is localised in endothelial cells of coronary arteries and released during hypoxia: a possible new mechanism for hypoxia-induced vasodilatation of the rat heart. *Experientia*, **44**, 705–707.

CHERRY, P.D., FURCHGOTT, R.F., ZAWADZKI, J.V. & JOTHIANANDAN, D. (1982). Role of endothelial cells in relaxation of isolated arteries by bradykinin. *Proc. Natl. Acad. Sci. U.S.A.*, **72**, 2106–2110.

COHEN, R.A., SHEPHERD, J.T. & VANHOUTTE, P.M. (1983). 5-Hydroxytryptamine can mediate endothelium-dependent relaxation of coronary arteries. *Am. J. Physiol.*, **245**, H1077–H1080.

CORR, L. & BURNSTOCK, G. (1991). Vasodilator response of coronary smooth muscle to the sympathetic co-transmitters noradrenaline and adenosine 5'-triphosphate. *Br. J. Pharmacol.*, **104**, 337–342.

FEELISCH, M. & NOACK, E.A. (1987). Correlation between nitric oxide formation during degradation of organic nitrates and activation of guanylate cyclase. *Eur. J. Pharmacol.*, **139**, 19–30.

FLEETWOOD, G., COADE, S.B., GORDON, J.L. & PEARSON, J.D. (1989). Kinetics of adenine nucleotide catabolism in coronary circulation of rats. *Am. J. Physiol.*, **256**, H1565–H1572.

FURCHGOTT, R.F. (1983). Role of the endothelium in responses of vascular smooth muscle. *Circulation Res.*, **53**, 557–573.

FURCHGOTT, R.F. (1984). The role of the endothelium in the response of vascular smooth muscle to drugs. *Ann. Rev. Pharmacol. Toxicol.*, **24**, 175–197.

FURCHGOTT, R.F. & ZAWADZKI, J.V. (1980). The obligatory role of endothelial cells in the relaxation of arterial smooth muscle by acetylcholine. *Nature*, **288**, 373–376.

FURCHGOTT, R.F., KHAN, M.T. & JOTHIANANDAN, D. (1987). Evidence supporting the proposal that endothelium-derived relaxing factor is nitric oxide. *Thrombosis Res.*, Suppl **VII**, 5.

GULATI, N., MATHISON, R., HUGGEL, H., REGOLI, D. & BENY, J.-L. (1987). Effects of neurokinins on the isolated pig coronary artery. *Eur. J. Pharmacol.*, **137**, 149–154.

HELLEWELL, P.G. & PEARSON, J.D. (1984). Purinoceptor mediated stimulation of prostacyclin release in the porcine pulmonary vasculature. *Br. J. Pharmacol.*, **83**, 457–462.

HOBBS, A.J. & GIBSON, A. (1990). L-N^G-nitro-arginine and its methyl ester are potent inhibitors of non-adrenergic, non-cholinergic transmission in the rat anococcygeus. *Br. J. Pharmacol.*, **100**, 749–752.

HOOVER, D.B. (1990). Effects of substance P on rate and perfusion pressure in the isolated guinea-pig heart. *J. Pharmacol. Exp. Ther.*, **252**, 179–184.

HOPWOOD, A.M. & BURNSTOCK, G. (1987). ATP mediates coronary vasoconstriction via P_{2X}-purinoceptors and coronary vasodilatation via P_{2Y}-purinoceptors in the isolated perfused rat heart. *Eur. J. Pharmacol.*, **136**, 49–54.

HOPWOOD, A.M., LINCOLN, J., KIRKPATRICK, K.A. & BURNSTOCK, G. (1989). Adenosine 5'-triphosphate, adenosine and endothelium-derived relaxing factor in hypoxic vasodilatation of the heart. *Eur. J. Pharmacol.*, **165**, 323–326.

IGNARRO, L.J., WOOD, K.S. & BYRNS, R.E. (1986). Pharmacological and biochemical properties of EDRF: evidence that EDRF is closely related to nitric oxide (NO) radical. *Circulation*, **74**, 287.

IGNARRO, L.J., BYRNS, R.E., BUGA, G.M. & WOOD, K.S. (1987). Endothelium-derived relaxing factor from pulmonary artery and vein possesses pharmacologic and chemical properties identical to those of nitric oxide radical. *Cir. Res.*, **61**, 866–879.

KELM, M. & SCHRADER, J. (1988). Nitric oxide release from the isolated guinea-pig heart. *Eur. J. Pharmacol.*, **155**, 317–321.

KELM, M. & SCHRADER, J. (1990). Control of coronary vascular tone by nitric oxide. *Circ. Res.*, **66**, 1561–1575.

LAMONTAGNE, D., POHL, U. & BUSSE, R. (1991). N^G-Nitro-L-arginine antagonizes endothelium-dependent dilator responses by inhibiting endothelium-derived relaxing factor release in the isolated rabbit heart. *Pflügers Arch.*, **418**, 266–270.

MAYER, B., SCHMIDT, K., HUMBERT, P. & BÖHME, E. (1989). Biosynthesis of endothelium-derived relaxing factor: a cytosolic enzyme in porcine aortic endothelial cells Ca^{2+}-dependently converts L-arginine into an activator of soluble guanylate cyclase. *Biochem. Biophys. Res. Commun.*, **164**, 678–685.

MONCADA, S. & VANE, J.R. (1979). Pharmacology and endogenous roles of prostaglandin endoperoxides, thromboxane A_2 and prostacyclin. *Pharmacol. Rev.*, **30**, 293–331.

MONCADA, S., GRYGLEWSKI, R., BUNTING, S. & VANE, J.R. (1976). An enzyme isolated from arteries transforms prostaglandin endoperoxides to an unstable substance that inhibits platelet aggregation. *Nature*, **263**, 663–665.

MOORE, P.K., AL-SWAYEH, O.A., CHONG, N.W.S., EVANS R.A. & GIBSON, A. (1990). L-N^G-nitroarginine (L-NOARG), a novel L-arginine-reversible inhibitor of endothelium-dependent vasodilatation *in vitro*. *Br. J. Pharmacol.*, **99**, 408–412.

NEEDLEMAN, P., MINKES, M.S. & DOUGLAS, J.R. (1974). Stimulation of prostaglandin biosynthesis by adenine nucleotides. *Circulation Res.*, **34**, 455–460.

PALMER, R.M.J., FERRIDGE, A.G. & MONCADA, S. (1987). Nitric oxide release accounts for the biological activity of endothelium-derived relaxing factor. *Nature*, **327**, 524–526.

PALMER, R.M.J. & MONCADA, S. (1989). A novel citrulline-forming enzyme implicated in the formation of nitric oxide by vascular endothelial cells. *Biochem. Biophys. Res. Commun.*, **158**, 348–352.

PALMER, R.M.J., REES, D.D., ASHTON, D.S. & MONCADA, S. (1988). L-Arginine is the physiological precursor for the formation of nitric oxide in endothelium-dependent relaxation. *Biochem. Biophys. Res. Commun.*, **153**, 1251–1256.

PEARSON, J.D., SLAKEY, L.L. & GORDON, J.L. (1983). Stimulation of prostaglandin production through purinoceptors on cultured porcine endothelial cells. *Biochem. J.*, **214**, 273–276.

REES, D.D., PALMER, R.M.J., HODSON, H.F. & MONCADA, S. (1989). A specific inhibitor of nitric oxide formation from L-arginine attenuates endothelium-dependent relaxation. *Br. J. Pharmacol.*, **96**, 418–424.

REES, D.D., PALMER, R.M.J., SCHULZ, R., HODSON, H.F. & MONCADA, S. (1990). Characterization of three inhibitors of endothelial nitric oxide synthase *in vitro* and *in vivo*. *Br. J. Pharmacol.*, **101**, 746–752.

RICHARD, V., TANNER, F.C., TSCHUDI, M. & LÜSCHER, T.F. (1990). Different activation of L-arginine pathway by bradykinin, serotonin, and clonidine in coronary arteries. *Am. J. Physiol.*, **259**, H1433–H1439.

SAEED, M., SCHMIDLI, J., METZ, M. & BING, R.J. (1986). Perfused rabbit heart: endothelium-derived relaxing factor in coronary arteries. *J. Cardiovasc. Pharmacol.*, **8**, 257–261.

SCHMIDT, H.H.H.W., NAU, H., WITTFOHT, W., GERLACH, J., PRESCHER, K.E., KLEIN, M.M., NIROOMAND, F. & BÖHME, E. (1988). Arginine is a physiological precursor of endothelium-derived nitric oxide. *Eur. J. Pharmacol.*, **154**, 213–216.

WEKSLER, B.B., LEY, C.W. & JAFF, E.A. (1978). Stimulation of endothelial cell prostacyclin production by thrombin, trypsin and the ionophore A23187. *J. Clin. Invest.*, **62**, 923–930.

(Received January 23, 1992
Revised June 18, 1992
Accepted June, 24, 1992)

Br. J. Pharmacol. (1992), **107**, 610–615

In vitro denervation of the rat vas deferens through hypothermic storage

N.H. Jurkiewicz, *A.G. Garcia & [1]A. Jurkiewicz

Department of Pharmacology, Escola Paulista de Medicina, Caixa Postal 20372, São Paulo 04034, Brazil and *Department of Pharmacology, Facultad de Medicina, Universidad Autónoma de Madrid, Arzobispo Morcillo s/n, Madrid, Spain

1 The rat vas deferens was excised, stored at 4–6°C and tested after 24, 48, 72 or 96 h for its contractile activity and for the presence of innervation.

2 The maximal contractile capacity of the vas, tested through cumulative concentrations of barium chloride (3×10^{-2} M) was progressively reduced from about 110 mm to about 63 mm after 72 h, without further decay after 96 h. Spontaneous rhythmic contractions were practically absent.

3 A loss of endogenous pools of catecholamines was indicated by four parameters: (a) a decline of about 80% after 24 h and of more than 95% after 48 h of the contractile effect of the indirect sympathomimetic agonist tyramine; (b) a fall of about 20%, 50% and 85% on the concentration of noradrenaline, respectively after 24, 48 and 72 h; (c) a fall of about 25% and 90% after respectively 24 and 48 h, of the activity of dopamine-β-hydroxylase (DBH); (d) a decline of noradrenaline-induced histofluorescence on cross sections of the vas.

4 A loss of neuronal uptake capacity was indicated by: (a) a progressive variation of the apparent affinity for adrenaline, expressed as pD_2 values, that increased by about 1.5 log units (corresponding to a 30 fold potentiation) after 72 h, and (b) a reduction of the ability of cocaine to potentiate the contractile effects of adrenaline.

5 The pD_2 values for barium chloride, 5-hydroxytryptamine (5-HT) and histamine were not significantly changed, while the corresponding value for acetylcholine was slightly but significantly reduced by about 0.8 log units.

6 The maximal heights of concentration-response curves for noradrenaline, acetylcholine, histamine and 5-HT were reduced by 42–66% in relation to controls. However, when this reduction was measured in relation to the corresponding barium effect, by means of the relative responsiveness ratio (ρ), a small though significant increase was observed for noradrenaline, and a fall for the other drugs.

7 It is concluded that: (1) the values for the various biochemical and pharmacological parameters decline at different rates, though revealing altogether that denervation is completed by at least 85% after 72 h of hypothermic storage; (2) two of the results, i.e., the lack of spontaneous rhythmic contractions and the lack of increased contractile effects for acetylcholine, 5-HT and histamine, indicate that in these conditions the vas is devoid of the so-called nonspecific signs of denervation.

Keywords: Denervation; vas deferens; dopamine-β-hydroxylase; noradrenaline; acetylcholine; barium; 5-hydroxytryptamine; hypothermic storage

Introduction

It is known that adrenergic innervation can influence contractile effects induced by drug-receptor interactions in rat vas deferens (Jurkiewicz *et al.*, 1977; 1991). Thanks mainly to surgical denervation (Kasuya *et al.*, 1969; Birmingham, 1970), a number of biochemical, pharmacological and histochemical alterations could be ascribed to the degeneration of nerve terminals in this organ: a decrease of the catecholamine-storing vesicles can be detected by a decrease of the activity of dopamine-β-hydroxylase (DBH), an enzyme that is known to be present only in these vesicles (Klein, 1982); a decrease in the pools of neurotransmitter, by a fall of noradrenaline (NA) concentration, and by a decrease in the amplitude of contractions induced by the indirect agonist tyramine; a decrease of neuronal uptake, by an increase of the apparent affinities for noradrenaline and adrenaline, and by a decrease of the ability of cocaine to potentiate the contractile effects of these agonists; in addition, two other effects, the causes of which are not totally known, have been observed in denervated preparations: a non-specific increase of the maximal effect of some agonists, that can be accompanied by a leftward shift of concentration-response curves (Kasuya *et al.*, 1969; Westfall *et al.*, 1975; Kasuya & Suzuki, 1978), and the presence of spontaneous rhythmic contractions (Lee *et al.*, 1975; Goto *et al.*, 1976). Several of these changes have also been observed after other denervation procedures in vas, as for instance after treatment with 6-hydroxydopamine (Westfall & Fedan, 1975), bretylium (Murdock *et al.*, 1977), colchicine (Wakade, 1978; Goto *et al.*, 1979) and vinca alkaloids (Wakade, 1979).

In a pioneering publication, Martins & Valle (1939) reported that the vas deferens maintains its responsiveness to drugs for as much as 13 days, if stored in a regular refrigerator up to the moment of the experiment. In addition, they reported that responses to adrenaline were almost always the last to disappear, in relation to other agonists. Since this could indicate a potentiation of adrenaline effects due to nerve degeneration, experiments were carried out on the rat vas deferens submitted to hypothermic storage, to examine its innervation characteristics. This examination was performed by checking the presence, or not, of the forementioned changes described for the denervated vas.

[1] Author for correspondence.

Methods

Vas deferens excision and hypothermic storage

Wistar male rats of our own colony, BAW2 (Festing, 1980) were used. After laparotomy under ether anaesthesia, one vas deferens was cleared of surrounding tissues, and removed as previously described (Jurkiewicz *et al.*, 1977). The organ was placed in a Petri dish between two cotton layers embedded in nutrient solution of the following composition (mM): NaCl 138, KCl 5.7, $CaCl_2$ 1.8, NaH_2PO_4 0.36, $NaHCO_3$ 15.0 and glucose 5.5, prepared in distilled water. The covered Petri dish was placed in a regular refrigerator for hypothermic storage (about 4–6°C). After 24, 48, 72 or 96 h, vasa deferentia were placed in gassed nutrient solution to be processed for biochemical, pharmacological and histological analysis. Usually the contralateral vas deferens was excised under ether anaesthesia shortly before the experiment, and used as a control. In some experiments normal vasa were also used as controls.

Tissue content of noradrenaline

NA content was estimated following the fluorometric method of Anton & Sayre (1962).

Assay of tissue dopamine-β-hydroxylase activity

Tissue DBH activity was assayed according to the procedure described by Molinoff *et al.* (1971). Treated or control vasa deferentia were individually homogenized in 25 volumes (w/v) 0.005 M cold Tris-HCl buffer, pH 7.4, containing 0.2% Triton-X-100. The homogenates were centrifuged at 27,000 *g* at 2°C and the enzyme activity assayed in 200 µl aliquots of the supernatants. Several concentrations of $CuSO_4$ were tested to obtain adequate inactivation of the endogenous inhibitors of the enzyme. Maximal DBH activities were repeatedly found at 1.6×10^{-4} M (final concentration of $CuSO_4$ in the reaction mixture). The optimal pH for maximal DBH activity was 5.0. Results are expressed as nmol of octopamine formed from tyramine per hour, per g of wet tissue weight (nmol h^{-1} g^{-1}).

Localization of noradrenaline by histofluorescence

Cooled and control vasa deferentia were frozen, freeze-dried, treated with paraformaldehyde, infiltrated *in vacuo* with paraffin, and cut for examination on a fluorescence microscope, according to the technique of Falck (1962). The distribution and intensity of fluorescence were measured by eye, through an arbitrary score, by comparison with the green fluorescence of normal preparations. The background fluorescence had a homogeneous distribution, pallid yellow colour, low intensity, and could be easily differentiated from that due to NA.

Concentration-response curve studies

Cooled and control organs were washed with nutrient solution, weighed and mounted in 10 ml organ chambers containing continuously aerated nutrient solution at 30°C. Isotonic contractions were recorded on smoked drums with frontal levers, with 6 fold amplification and a load of 0.5 to 1 g.

After an initial equilibration period of 60 min, cumulative dose-response curves were obtained at 30 min intervals for the agonists under study. In some preparations, after achieving stable responses to adrenoceptor agonists, dose-response curves were repeated in the presence of cocaine. Shifts to the left of dose-response curves were always measured as dose-ratios, or log dose-ratios among EC_{50} values. At the beginning of most experiments a dose of tyramine (10^{-5} M) was given to check the release of endogenous catecholamines.

Values of pD_2 were measured as the negative logarithms of EC_{50} to express apparent affinities.

The relative responsiveness ratio (ρ) was measured as previously described (Jurkiewicz *et al.*, 1976), as the relation between the maximal effect of a full agonist (E_m) and the overall maximal effect induced through the effector system of the vas deferens (E_M):

$$\rho = E_m/E_M$$

The value of E_M was arbitrarily taken as the maximal contraction induced by barium chloride (10^{-2}–3×10^{-2} M), in the same experiment in which a full agonist was used. The maximal cumulative contractions for noradrenaline, acetylcholine, 5-hydroxytryptamine (5-HT) or histamine were taken as the respective values of E_m. In general the resting length of the control vas deferens (42.1 ± 1.4 mm, $n = 8$) was reduced by about 40% when the organ was stimulated by a maximal concentration (10^{-2} M) of $BaCl_2$ (length = 24.5 ± 2.1 mm).

Drugs

The following drugs were used: acetylcholine chloride (E. Merck), adrenaline ((−)-epinephrine-D-bitartrate, Sigma); noradrenaline ((−)-arterenol chloride, Sigma); 5-hydroxytryptamine (serotonin, Sigma), histamine (Sigma), tyramine (Schuchardt); barium chloride (J.T. Baker); cocaine hydrochloride (Sigma), and phenoxybenzamine (SKF). Stock solutions of drugs were kept in the freezer and discarded after about 15 days. Working solutions were prepared shortly before each experiment from the stock solution. EDTA (10 µg ml^{-1}) was added to catecholamine solutions to prevent catalytic oxidation by traces of heavy metals. All the chemicals used were ACS certified reagent grade.

Statistics

Significance of differences of contractile and NA release values were analyzed according to an unpaired *t* test (Snedecor & Cochran, 1967).

Results

General characteristics of the vas after hypothermic storage

Drug-induced contractions could be obtained in vas deferens after hypothermic storage, though with a lower amplitude. For instance, cumulative concentration-response curves for barium chloride, obtained after 24, 48, 72 and 96 h showed a progressive decline of the maximal heights, leading to a reduction of about 40% after 72–96 h (Figure 1). However, contrary to the expectations for denervated vasa, spontaneous rhythmic contractions were absent, except for occasional twitches in some preparations. In contrast to barium, the effects for the indirect agonist, tyramine, were reduced to less than 20% after 24 h, and were practically absent after 48 h (Figure 1), indicating a reduction of endogenous noradrenaline. In fact, noradrenaline content was lower than 20% after 72 h, and the activity of DBH had practically disappeared after 48 h (Figure 1). It is noteworthy that after 24 h, when the effects of tyramine had been strikingly reduced, the contents of noradrenaline and DBH were still relatively high, at about 80%, when compared to controls.

The reduction of endogenous NA was corroborated by fluorescence microscopy studies. It was difficult to see a smooth decline of fluorescence at 24 h intervals, due to limitations of our method of measurement and to some individual variation between preparations, but noradrenaline-induced fluorescence was clearly absent after 96 h (not shown).

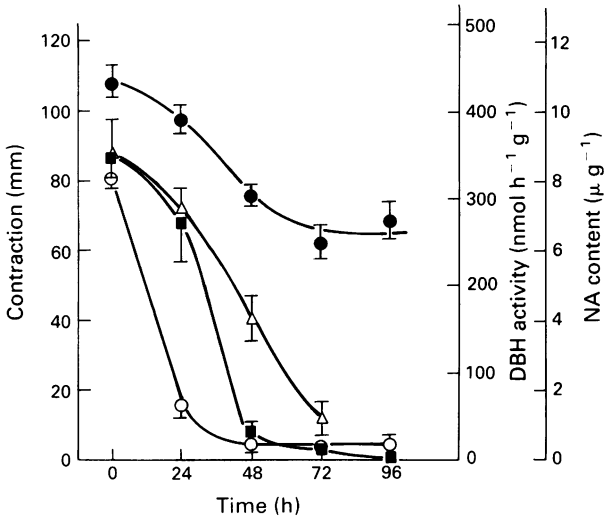

Figure 1 Variation of four pharmacological and biochemical parameters in rat vas deferens, after hypothermic storage: maximal cumulative contraction (under 1 g load and with a 6 fold amplification) for barium chloride (3×10^{-2} M, ●), contraction induced by tyramine (10^{-5} M, ○), concentration of endogenous noradrenaline (NA, △) and dopamine-β-hydroxylase activity (DBH, ■). Parameters were measured at 24 h intervals, as indicated on the abscissae. Each value represents the mean from at least 4 experiments; s.e.mean shown by vertical bars. All values were significantly lower ($P<0.05$) than the respective control (0 h).

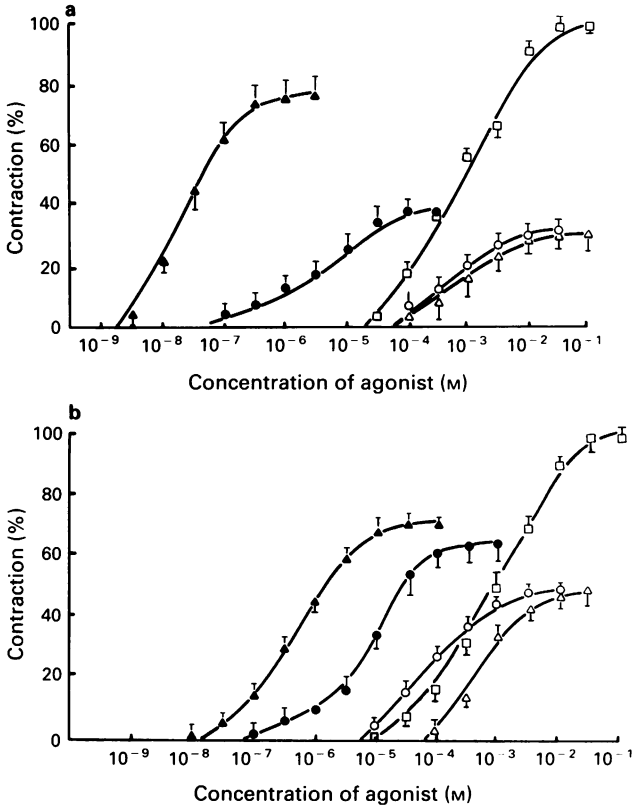

Figure 2 Mean cumulative dose-response curves for noradrenaline (▲), 5-hydroxytryptamine (●), acetylcholine (○), histamine (△) and barium chloride (□) in 72 h cold-stored (a) and contralateral control (b) vas deferens. The effects were plotted as percentages of the respective maximum effect of barium chloride. The 100% contraction was decreased from about 110 mm in controls, to about 63 mm after hypothermic storage. Note that the maximal effect of noradrenaline in relation to barium chloride, was increased after hypothermic storage. Values of pD_2, E_{max} and relative responsiveness (ρ) were measured from these experiments and are shown in Tables 1 and 2. Points are means (± s.e., vertical bars) of at least 5 experiments.

Concentration-response curves

Figure 2 shows that after 72 h, the concentration-response curves for various full agonists, except NA, were reduced after hypothermic storage, when the effects were expressed as percentage values of barium maximal contraction. In addition, a shift to the left was observed for the curve for NA. As a consequence, the value of pD_2 for NA was increased by 1.3 log units, corresponding to a 20 times potentiation. The values of pD_2 for barium chloride, 5-HT and histamine were not significantly changed, while the pD_2 for acetylcholine was slightly reduced (Table 1).

The reduction of maximal effects (Table 2) was not similar for all the agonists studied, ranging between 42 and 66%, when considering absolute contractions (mm). A proportionally larger reduction was observed for acetylcholine, 5-HT and histamine. Because of the partial loss of contractile capacity of the vas deferens after hypothermic storage (Figure 1), these differences in absolute contractions have a limited significance. Therefore, contractions were mostly analysed in relation to the maximal effects of the respective preparations, by using the relative reponsiveness ratio (ρ), as shown below. By means of this ratio, a very small though significant increase, of 10%, was obtained for noradrenaline (Table 2). Concerning the maximal effects of the other three agonists, a reduction was observed for the respective ρ ratios (Table 2), as it occurred for the absolute values.

Neuronal uptake

A reduction of neuronal uptake activity was shown indirectly by measuring two parameters: the reduction of the potentiation induced by cocaine on adrenaline (Ad) concentration-response curves, and the increase of the apparent affinity for the latter agonist. Figure 3 shows a progressive shift to the left of concentration-response curves for Ad, that was proportional to the duration of hypothermic storage. As a consequence, after 72 h the potency of Ad was increased by about 1.5 log units. The same figure shows a decline, from 28 fold to 3 fold, of the ability of cocaine to shift the curves for Ad to the left, after 72 h. As shown in Figure 3a, this decline was simultaneous with the increase of pD_2 values for the latter agonist.

Discussion

Neurochemical, histological and pharmacological parameters were used to show that the rat vas deferens is practically denervated within 72 h of hypothermic storage. In addition, it has been demonstrated that the changes in these parameters follow different time courses, indicating that some properties of the nerve terminals can be more stable than others, during the progression of nerve degeneration. Finally, it was shown that the secondary indicators of denervation, as spontaneous contractions and nonspecific sensitization (Kasuya *et al.*, 1969) could not be detected, contrary to the expectations for the denervated vas deferens.

The decrease of endogenous NA and DBH, the disappearance of fluorescent nerve terminals, and the sharp decline of the contractile activity of tyramine, are strong indications of a degeneration of nerve terminals (Jurkiewicz *et al.*, 1977; 1991). Another characteristic of sympathetic nerves, the ability to take up exogenous catecholamines, has been indirectly shown to be strikingly decreased, through the progressive growth of pD_2 values for adrenaline (Figure 3). The latter values are expected to increase after denervation, since

Table 1 Variation of pD_2 values, expressed as dose-ratios (DR), after hypothermic storage of the vas deferens at 4–6°C for 72 h

Agonist	*pD_2 for control* (A)	*pD_2 after hypothermic storage* (B)	*Log DR* (B-A)	*DR* (antilog (B-A))
Barium chloride	3.0 ± 0.1	3.1 ± 0.1	0.1	1.2
Noradrenaline	6.3 ± 0.1	7.6 ± 0.1*	1.3	20.0
Acetylcholine	4.0 ± 0.1	3.2 ± 0.1*	−0.8	−6.2
Histamine	3.3 ± 0.1	3.3 ± 0.2	0.0	1.0
5-Hydroxytryptamine	5.1 ± 0.1	5.2 ± 0.2	0.1	1.2

All the values are means ± s.e. of at least seven experiments.
*Significantly different from corresponding control value, $P<0.05$.

Table 2 Maximum cumulative effects (E_m) and relative responsiveness ratios (ρ) after hypothermic storage of the vas deferens at 4–6°C for 72 h

Parameter	*Agonist*	*Control* (A)	*After hypothermic storage* (B)	*% Decrease* (A-B)/A × 100
E_m	Barium chloride	108.7 ± 4.7	62.7 ± 4.7*	42
	Noradrenaline	77.6 ± 2.6	41.3 ± 3.7*	47
	Acetylcholine	54.9 ± 4.3	18.9 ± 2.8*	66
	Histamine	50.3 ± 3.1	18.0 ± 2.2*	64
	5-Hydroxytryptamine	67.3 ± 6.0	28.8 ± 4.5*	57
ρ ratio	Noradrenaline	0.69 ± 0.02	0.76 ± 0.03*	10†
	Acetylcholine	0.50 ± 0.02	0.31 ± 0.03*	38
	Histamine	0.48 ± 0.03	0.30 ± 0.03*	37
	5-Hydroxytryptamine	0.63 ± 0.06	0.40 ± 0.06*	36

†A percentage increase was observed in this case.
All the values are means ± s.e. of at least seven experiments.
*Significantly different from corresponding control value, $P<0.05$.

the loss of neuronal uptake permits higher concentrations of exogenous Ad to be available in the vicinity of receptors. This result was corroborated by a parallel decline in the potentiation induced by the neuronal uptake blocker, cocaine (Jurkiewicz & Jurkiewicz, 1976). The increase of pD_2 values or related parameters for NA and Ad, and the loss of cocaine-induced potentiation after inactivation of neuronal uptake, have been exhaustively described in vas, with changes ranging typically between 1.0 and 1.5 log units (Kasuya *et al.*, 1969; Birmingham, 1970; Birmingham *et al.*, 1970; Westfall & Fedan, 1975; Westfall, 1977; Jurkiewicz *et al.*, 1977; 1991). A variation on the time needed for the completion of these changes has also been reported by different authors, ranging from 24 h (Birmingham, 1970) to 4 days, or more (Westfall, 1977; Degaris & Pennefather, 1987).

Although unequal time courses could be seen for different parameters (Figures 1 and 3), most of the values were roughly stabilized within 72 h. The fastest decay was observed for tyramine contractions (Figure 1). It is noteworthy that after nerve regeneration following 5-month transplantation of the vas, the effect of tyramine is the parameter that shows the lowest (practically absent) recovery (Jurkiewicz *et al.*, 1991). Therefore, it can be concluded that the tyramine-induced contraction is the most sensitive indicator of neuronal integrity, in the vas deferens. However, it fails to indicate whether some of the nerve functions, as for instance uptake of catecholamines, are still present.

It is suprising that about 50% of NA was still present after 48 h, since several authors described a loss of at least 90% of NA within the initial 24–48 h after different types of denervation (Kasuya *et al.*, 1969; Lee *et al.*, 1975; Westfall & Fedan, 1975; Westfall *et al.*, 1975). This is probably due to the fact that enzymatic and other types of degradation of NA are diminished during hypothermic storage, thus increasing the stability of NA even if this mediator is freed into the extraneuronal space. As a matter of fact, a similar prolonged presence of NA was observed in guinea-pig taenia caecum after cold storage (Hattori *et al.*, 1972).

An additional unexpected result was the absence of the secondary indicators of denervation, such as spontaneous contractions, and nonspecific potentiation. The latter is expressed as a shift to the left and an increase of the maximal height of concentration-response curves of various unrelated agonists (Kasuya *et al.*, 1969). The shift to the left induced in NA curves cannot be included here because it is a specific phenomenon related to the blockade of neuronal uptake, as discussed. Another specific alteration would be a small shift to the left of acetylcholine curves, due to the loss of cholinesterase (Westfall *et al.*, 1974). However, it has been shown that this enzyme is still active even after 7-day cold storage of the guinea-pig taenia caecum (Hattori *et al.*, 1972), a possibility that can be extended to the vas deferens.

Regarding rhythmic contractions, it is known that the amplitudes attain a maximum after 7 days, but that 30% and 60% of these values are already observed respectively 24 h and 48 h after denervation (Lee *et al.*, 1975). The presence of spontaneous contractions is a nonspecific phenomenon, since it can also be observed in the vas deferens of castrated rats (Martins & Valle, 1939). It can also be seen in the vas deferens from 30 to 90 min after injecting 6-hydroxydopamine, probably because of the release of NA (Furness *et al.*, 1970).

In relation to nonspecific sensitization, the only alteration observed here was a trivial increase of 10% on ρ value for NA receptors. This contrasts with the high rises described for the height of concentration-response curves for NA (from about 30% to 400%) and, to a lesser degree, for acetylcholine (Kasuya *et al.*, 1969; Kasuya & Suzuki, 1978; Westfall *et al.*, 1972; 1974; Goto *et al.*, 1976; 1979; Lee *et al.*, 1975; Murdock *et al.*, 1977). Increases were also observed for 5-HT (Goto *et al.*, 1976) and for histamine in guinea-pig vas (Westfall *et al.*, 1972), but not for potassium (Lee *et al.*, 1975). An increased maximal effect can either indicate an increase in the density of receptors or a change in the chain

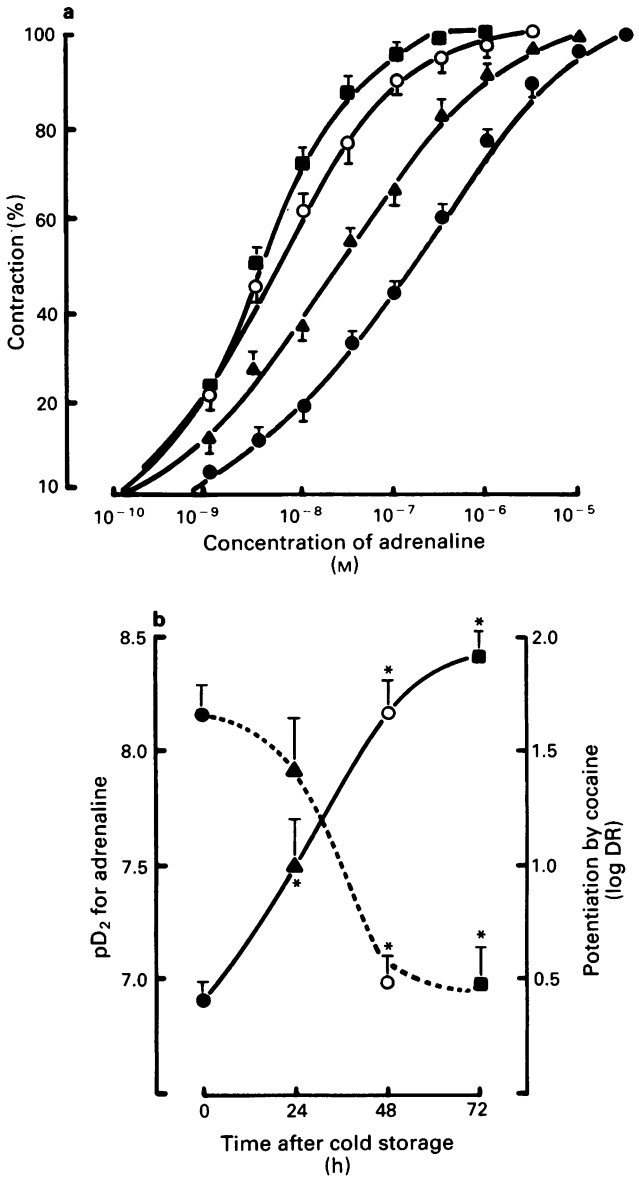

Figure 3 Concentration-response curves (a) for adrenaline in controls (●) or after hypothermic storage for 24 h (▲), 48 h (○) or 72 h (■). In (b) are shown the increase of pD_2 values for adrenaline, measured from the respective curves (complete line), as well as the decay of the potentiation induced in the respective curves by 10^{-5} M cocaine (dotted line). This potentiation was expressed as the logarithm of a dose ratio (log DR) for adrenaline, representing the leftward shift induced by cocaine on adrenaline curves. Points are means (± s.e., vertical bars) of at least 5 experiments. $^*P<0.05$ compared with controls.

of events leading from drug-receptor interaction to the effect. A theoretical analysis of the meaning and limitations of the changes of maximal effects, measured through the ρ ratio, has been presented previously (Jurkiewicz *et al.*, 1976). A few situations have been described in which a nonspecific potentiation was not observed: DeGaris & Pennefather (1987) could not detect increases in maximal effects for adrenergic and cholinergic agents by denervating only the epididymal part of the vas deferens. Kasuya & Suzuki (1978) have shown that the effect of ACh is practically abolished in the prostatic part of the vas, after denervation. In addition, Sannomiya & DeMoraes (1979), using the denervated guinea-pig vas, could not show an increased maximal effect for NA when recording contractions *in situ*, contrary to experiments *in vitro*. The results of Kasuya & Suzuki (1978) are compatible with our finding that the effects of acetylcholine are reduced (Tables 1 and 2). The reasons for this specific reduction remain to be explained.

The presence of nonspecific changes, such as spontaneous movements and sensitization, is probably due to complex mechanisms. It was previously shown that the primary changes represented by nerve degeneration are followed by secondary changes on smooth muscle tissue, that can be represented: (a) morphologically, by an increase of the number of cell-to-cell close junctions, or nexuses, that are twice as many as in controls (Westfall *et al.*, 1975); (b) electrophysiologically, by a growth of electrical coupling between cells and improved synchronization during drug-induced contractions (Lee *et al.*, 1975; Goto *et al.*, 1976); (c) histochemically, by an increase of non-neuronal ATP from the 2nd day on (Westfall *et al.*, 1975) and of endogenous peptides, such as vasoactive intestinal peptide and calcitonin gene-related peptide (Aberdeen *et al.*, 1992). The discussion of these points, as well as of the reinnervation that commences after about 4 days and takes several months to be completed (Burnstock, 1981; Jurkiewicz *et al.*, 1991), is out of the scope of the present publication.

A fall of the maximal contractile ability of the preparation (Figure 2 and Table 1) shows that smooth muscle cells were also injured during hypothermic storage denervation. When the vas undergoes hypothermic storage, the secondary mechanisms stated above are probably blocked, because of the lack of irrigation and nutrition, added to hypoxia and absence of the trophic influence of testosterone. However, one could argue that this damage is not simply due to the cooling process, since storage at room temperature would lead to a faster degeneration and loss of function. In this way cooling can be seen as a tool to slow down the degeneration process. On the other hand, since cold storage causes some changes in ionic balance in smooth muscle (Fukuda & Shibata, 1972), it is still unknown whether these electrolyte variations do influence drug-induced responses in vas.

It is concluded that hypothermic storage of the vas deferens differs from other proposed methods for denervation in at least two properties: (a) the primary pharmacological signs of nerve degeneration are not followed by the secondary indicators of denervation, such as spontaneous contractions and nonspecific sensitization; (b) from a methodological standpoint, this procedure seems to be easier to perform than *in vivo* denervations, since it avoids the postoperative maintenance of the rats, and a second surgical procedure for the removal of the vas.

References

ABERDEEN, J., MILNER, P., LINCOLN, J. & BURNSTOCK, G. (1992). Guanethidine sympathectomy of mature rats leads to increases in calcitonin gene-related peptide and vasoactive intestinal polypeptide-containing nerves. *Neuroscience*, **47**, 453–461.

ANTON, A.H. & SAYRE, D.F. (1962). A study of the factors affecting the aluminum oxide-trihydroxindole procedure for the analysis of catecholamines. *J. Pharmacol. Exp. Ther.*, **138**, 360–375.

BIRMINGHAM, A.T. (1970). Sympathetic denervation of the smooth muscle of the vas deferens. *J. Physiol.*, **206**, 645–661.

BIRMINGHAM, A.T., PATTERSON, G. & WOJCICKI, J. (1970). A comparison of the sensitivities of innervated and denervated rat vasa deferentia to agonist drugs. *Br. J. Pharmacol.*, **39**, 748–754.

BURNSTOCK, G. (1981). Development of smooth muscle and its innervation. In *Smooth Muscle: an Assessment of Current Knowledge*. ed. Bülbring, E., Brading, A.F., Jones, A.W. & Tomita, T. pp. 431–457. London: Edward Arnold.

DEGARIS, R.M. & PENNEFATHER, J.N. (1987). Prolonged supersensitivity to noradrenaline of smooth muscle of the epididymal half of the rat vas deferens denervated by vasectomy. *J. Auton. Pharmacol.*, **7**, 267–279.

FALCK, B. (1962). Observations on the possibilities of the cellular localization of monoamines by a fluorescence method. *Acta Physiol. Scand.*, **56**, 2–25.

FESTING, M.F.W. (1980). *International Index of Laboratory Animals.* UK: Medical Research Council.

FUKUDA, H. & SHIBATA, S. (1972). The effect of cold storage on the inhibitory action of isoprenaline, phenylephrine and nicotine on the mechanical and membranal activities of guinea-pig taenia caecum. *Br. J. Pharmacol.*, **46**, 438–448.

FURNESS, J.B., CAMPBELL, G.R., GILLARD, S.M., MALMFORS, T., COBB, J.L.S. & BURNSTOCK, G. (1970). Cellular studies of sympathetic denervation produced by 6-hydroxydopamine in the vas deferens. *J. Pharmacol. Exp. Ther.*, **174**, 111–122.

GOTO, K., MASAKI, T., SAITO, A. & KASUYA, Y. (1979). Denervation-like supersensitivity of the rat vas deferens induced by local application of colchicine to the hypogastric plexus. *J. Pharmacol. Exp. Ther.*, **209**, 376–381.

GOTO, K., MASUDA, Y. & KASUYA, Y. (1976). The effect of denervation on the synchronization of contraction of the rat vas deferens. *Eur. J. Pharmacol.*, **36**, 395–404.

HATTORI, K., KURAHASAHI, K., MORI, J. & SHIBATA, S. (1972). The effect of cold storage on the adrenergic mechanisms of intestinal smooth muscle. *Br. J. Pharmacol.*, **46**, 423–437.

JURKIEWICZ, A., ABDO, A.O., JURKIEWICZ, N.H., GUEDES, A.O. & SOUCCAR, C. (1976). Relative responsiveness (ρ): a critical analysis of a new method in receptor differentiation. *Gen. Pharmacol.*, **7**, 93–101.

JURKIEWICZ, N.H. & JURKIEWICZ, A. (1976). Dual effect of α-adrenoceptor antagonists in rat isolated vas deferens. *Br. J. Pharmacol.*, **56**, 169–178.

JURKIEWICZ, N.H., JURKIEWICZ, A. & GARCIA, A.G. (1991). Reinnervation of the transplanted vas deferens: differential recovery of various biochemical and pharmacological parameters. *J. Neural. Transm.*, **85**, 83–94.

JURKIEWICZ, N.H., JURKIEWICZ, A., GOMES, C.B. & AUCELIO, J.G. (1977). Pharmacodynamic analysis of the rat isolated vas deferens after transplantation to intestinal wall. *J. Pharmacol. Exp. Ther.*, **203**, 112–119.

KASUYA, Y., GOTO, K., HASIMOTO, H., WATANABE, H., MUNUKATA, H. & WATANABE, M. (1969). Nonspecific denervation supersensitivity in the rat vas deferens 'in vitro'. *Eur. J. Pharmacol.*, **8**, 177–184.

KASUYA, Y. & SUZUKI, N. (1978). Regional differences in the effects of denervation, cocaine and chronic reserpine administration on the respones of the rat vas deferens to norepinephrine and acetylcholine. *Arch. Int. Pharmacodyn.*, **236**, 202–213.

KLEIN, R.L. (1982). Chemical composition of the large noradrenergic vesicles. In *Neurotransmitter Vesicles.* ed. Klein, R.L., Lagercrants, H. & Zimmermann, H. pp. 133–174. New York: Academic Press.

LEE, T.J.-F., WESTFALL, D.P. & FLEMING, W.W. (1975). The correlation between spontaneous contractions and postjunctional supersensitivity of the smooth muscle of the rat vas deferens. *J. Pharmacol. Exp. Ther.*, **192**, 136–148.

MARTINS, T. & VALLE, J.R. (1939). Endocrine control of the motility of the male accessory genital organs. *Endocrinology*, **25**, 80–90.

MOLINOFF, P.B., WEINSHILBOUM, R. & AXELROD, J. (1971). A sensitive enzymatic assay for dopamine β-hydroxylase. *J. Pharmacol. Exp. Ther.*, **178**, 425–431.

MURDOCK, S.D., EVANS, B.K., HEATH, J.W., HILL, C.E. & BURNSTOCK, G. (1977). Effects of chronic bretylium treatment on the sympathetic neuron and the smooth muscle of the rat. *Eur. J. Pharmacol.*, **43**, 225–235.

SANNOMIYA, P. & DE MORAES, S. (1979). Denervation supersensitivity to noradrenaline in the guinea-pig vas deferens in vivo: absence of the postjunctional component. *Eur. J. Pharmacol.*, **54**, 167–171.

SNEDECOR, G.W. & COCHRAN, G.C. (1967). In *Statistical Methods.* (6th ed). Ames, Iowa, USA: Iowa State University Press.

WAKADE, A.R. (1978). Time course of degeneration of short and long postganglionic sympathetic nerve fibres and effect of pentobarbitone and colchicine on degeneration. *Br. J. Pharmacol.*, **62**, 553–561.

WAKADE, A.R. (1979). Recent developments in degeneration of the sympathetic neuron. *Gen. Pharmacol.*, **10**, 351– 357.

WESTFALL, D.P. (1977). The effects of denervation, cocaine, 6-hydroxydopamine and reserpine on the characteristics of drug-induced contractions of the depolarized smooth muscle of the rat and guinea-pig vas deferens. *J. Pharmacol. Exp. Ther.*, **201**, 267–275.

WESTFALL, D.P. & FEDAN, J.S. (1975). The effect of pretreatment with 6-hydroxydopamine on the norepinephrine concentration and sensitivity of the rat vas deferens. *Eur. J. Pharmacol.*, **33**, 413–417.

WESTFALL, D.P., LEE, T.J.-F. & STITZEL, E. (1975). Morphological and biochemical changes in supersensitive smooth muscle. *Fed. Proc.*, **34**, 1985–1989.

WESTFALL, D.P., MCPHILLIPS, J.J. & FOLEY, D.J. (1974). Inhibition of cholinesterase activity after postganglionic denervation of the rat vas deferens: evidence for prejunctional supersensitivity to acetylcholine. *J. Pharmacol. Exp. Ther.*, **189**, 493–498.

WESTFALL, D.P., MCCLURE, D.C. & FLEMING, W.W. (1972). The effects of denervation, decentralization and cocaine on the response of the smooth muscle of the guinea-pig vas deferens to various drugs. *J. Pharmacol. Exp. Ther.*, **181**, 328–338.

(Received May 27, 1992
Revised June 23, 1992
Accepted June 25, 1992)

Br. J. Pharmacol. (1992), **107**, 616–621

Endothelium-dependent modulation of resistance vessel contraction: studies with N^G-nitro-L-arginine methyl ester and N^G-nitro-L-arginine

Michael A. Bennett, Pamela A.C. Watt & [1] Herbert Thurston

Department of Medicine, Clinical Sciences Building, Leicester Royal Infirmary, PO Box 65, Leicester LE2 7LX

1 The effect of N^G-nitro-L-arginine methyl ester (L-NAME) and N^G-nitro-L-arginine (L-NOARG) on noradrenaline (NA)-induced contractility and acetylcholine (ACh)-induced endothelium-dependent relaxation was studied in rat mesenteric resistance arteries.

2 Third order branches of mesenteric arteries were dissected and mounted on two forty micron wires in a Mulvany myograph.

3 Incubation with L-NAME and L-NOARG (10 μM) caused a time-dependent shift in the 50% response to NA (ED_{50}) (0.01 μM–10 μM) but was not associated with an increase in the maximum contractile response.

4 L-NAME and L-NOARG (10 μM) caused a time-dependent inhibition of ACh (1 μM)-induced relaxation with a maximum effect after 120 min.

5 Following endothelium removal, incubation with either L-NAME or L-NOARG caused no significant shift in the ED_{50}, although the residual relaxation response to ACh (1 μM) was further attenuated.

6 Incubation with the cylco-oxygenase inhibitor, indomethacin, enhanced the relaxation to ACh and reduced the inhibitory effects of L-NAME and L-NOARG.

7 In conclusion, L-NAME and L-NOARG are potent inhibitors of acetylcholine-induced endothelium-dependent relaxation in mesenteric resistance arteries. The shift in ED_{50} associated wtih these inhibitors suggests a probable role for the endothelium in modulating the contractility of the resistance vasculature.

Keywords: Mesenteric resistance vessel; endothelium-derived relaxing factor; Wistar Kyoto rats; N^G-nitro-L-arginine methyl ester (L-NAME); N^G-nitro-L-arginine (L-NOARG); cyclo-oxygenase; indomethacin

Introduction

It is known now that many vasodilators act by causing the endothelium to release a vasorelaxant, endothelium-derived relaxing factor (EDRF) that relaxes vascular smooth muscle (Furchgott & Zawadski, 1980). The relaxing properties of EDRF have been well documented in large and medium sized arteries (Yang *et al.*, 1991) but few studies have been performed on resistance arteries. These have revealed that in normotensive rats, maximally contracted resistance vessels relax almost completely when exposed to acetylcholine (De Mey & Gray, 1985). Similar responses have been demonstrated in vessels from normotensive rabbits (Owen & Bevan, 1985) and man (Aalkjaer *et al.*, 1987). In addition, endothelium-dependent relaxation has been shown to increase as the internal diameter of the vessel decreases (Owen & Bevan, 1985). A variety of vasoconstrictor agents also induce EDRF release (Griffith *et al.*, 1985) but any vasorelaxant effect is submerged in the overriding contraction. However, there is evidence that the endothelium can reduce the contractile response to vasoconstrictors and may play an important role in the modulation of smooth muscle contraction of the small arteries concerned with the regulation of peripheral vascular resistance.

Studies of the modulating function of the endothelium in larger arteries have involved the use of physical methods (rubbing, perfusion with collagenase or detergent) to remove the endothelium (Harder, 1987; Osol *et al.*, 1989; Wiest *et al.*, 1989). Unfortunately, these techniques produce inconsistent results because of incomplete removal of the endothelium and varying degrees of damage to the underlying vascular smooth muscle. Recently it has been suggested that EDRF is nitric oxide (Palmer *et al.*, 1987) or a substance containing nitric oxide (Myers *et al.*, 1989) formed by the conversion of L-arginine to L-citrulline by the enzyme nitric oxide synthase (Mulsch & Busse, 1990). Furthermore, this led to the use of analogues of L-arginine which inhibit EDRF synthesis (Palmer *et al.*, 1988), attenuating endothelial dependent relaxation in the rabbit aorta (Rees *et al.*, 1989). Such analogues have also been used *in vivo* where the infusion of N^G-monomethyl-L-arginine (L-NMMA) into the human forearm caused inhibition of acetylcholine induced vasodilatation (Vallance *et al.*, 1989a) and arterial dilatation (Vallance *et al.*, 1989b) showing that EDRF has a major influence on basal blood flow. *In vitro* studies of rat aorta have shown that two other L-arginine analogues N^G-nitro-L-arginine (L-NOARG) and N^G-nitro-L-arginine methyl ester (L-NAME) are potent inhibitors of acetylcholine-induced endothelium-dependent relaxation (Moore *et al.*, 1990; Rees *et al.*, 1990) and similar results have been obtained in human subcutaneous resistance arteries with L-NOARG (Woolfson & Poston, 1990). The actions of the L-arginine analogues are reversible following the exposure to high concentrations of L-arginine (Levic *et al.*, 1990). The L-arginine analogues provide the opportunity to study endothelium modulation of resistance vessel contractility. Accordingly, we have studied the effects of two inhibitors of EDRF synthesis, L-NOARG and L-NAME alone or in the presence of the cyclo-oxygenase inhibitor indomethacin on the noradrenaline contraction and

[1] Author for correspondence.

acetylcholine-induced endothelium-dependent relaxation of mesenteric resistance arteries from 12 week old Wistar Kyoto rats.

Methods

Preparation of vessels

The experiments were performed on 12 week old female normotensive Wistar Kyoto rats (WKY) bred in our own colony at Leicester University. Rats were killed by stunning followed by cervical dislocation. Arterial resistance vessels were taken from the superior mesenteric bed which supplies the jejunum at a point 8–10 cm from the pylorus. Two segments 2 mm in length of the third generation branch resistance vessels, with a mean internal diameter of less than 300 μm, were dissected and mounted on two 40 μm wires in a myograph. One of the wires was attached to a force transducer and the other to a micrometer. This arrangement enables wall tension to be measured at a pre-determined internal diameter. Both dissection and mounting of the vessels were carried out in cold (4°C) physiological salt solution (PSS).

Experimental protocol and solutions

The resistance vessels were allowed to equilibrate for 1 h in PSS at 37°C. The PSS was made up of (mM): NaCl 118, $NaHCO_3$ 25, KCl 4.5, KH_2PO_4 1.0, $CaCl_2$ 2.5, $MgSO_4$ 1.0 and glucose 6. A high potassium PSS was made by replacing NaCl with KCl. All solutions were gassed with 95% O_2:5% CO_2 to achieve a pH of 7.4 at 37°C. After this equilibration period the length tension characteristic for each vessel was determined and then the internal circumference was set to $0.9 \times L_{100}$, where L_{100} is the internal circumference the artery would have had *in vivo* when relaxed and under a transmural pressure of 100 mmHg (Mulvany & Halpern, 1976). Following this normalization procedure, the vessels were incubated in PSS for a further 60 min before starting the contraction studies. Two stimulations with a high-potassium PSS were followed by one contraction with 10 μM noradrenaline. Each stimulation was maintained for 2 min before being rinsed in PSS and allowed to return to baseline. The vessels were then rinsed three times with PSS and left to recover for a further 15 min.

Cumulative dose-contraction curves to noradrenaline over the range 0.01 to 30 μM were obtained in the presence of 1 μM cocaine which was added 20 min before the start of the contraction curve. Maximally contracted vessels were then relaxed with a single dose of acetylcholine (1 μM). Following this initial contraction/relaxation curve, the vessels were selected arbitrarily for studies with either L-NAME or L-NOARG before and after incubation with indomethacin.

(1) Nine vessels with a mean internal diameter of 280 ± 17 μm served as time controls. Noradrenaline dose contraction curves in the presence of 1 μM cocaine were performed 30, 60 and 120 min after the preliminary study.

(2) Sixteen vessels with a mean internal diameter of 252 ± 11 μm were incubated with L-NOARG (10 μM) and dose-contraction curves to noradrenaline performed in the presence of 1 μM cocaine after 12, 60 and 120 min.

(3) Fifteen vessels with a mean internal diameter of 280 ± 17 μm were incubated with L-NAME (10 μM) and dose-contraction curves performed as for protocol (2). The remaining two groups of vessels were subjected to endothelial removal after the preliminary noradrenaline dose-contraction curve had been obtained. Following endothelial removal a second dose-contraction was obtained and the vessels arbitrarily selected for either protocol (4) or (5).

(4) Ten vessels with a mean internal diameter of 260 ± 9 μm were incubated with L-NAME (10 μM) and dose-contraction curves obtained in the presence of 1 μM cocaine after 12 and 60 min.

(5) Fourteen vessels with a mean internal diameter of 282 ± 10 μm were incubated with L-NOARG (10 μM) and dose-contraction curves obtained as for protocol (4).

Protocols (1), (2) and (3) were repeated in the presence of 10 μM indomethacin which was added 30 min before the start of the contraction/relaxation curve.

Endothelium removal

The endothelium was removed by the technique described by Osol *et al.* (1989). A human hair was washed in ethanol and rinsed in PSS before being inserted into the lumen of the vessel mounted under tension in the myograph. The endothelium was mechanically removed by repeatedly drawing the hair through the lumen of the vessel. Following removal of the endothelium the vessel was left for 45 min. Endothelial function was assessed by observing the relaxation produced by exposing a maximally contracted vessel to 10 μM ACh.

Drugs

All solutions were freshly prepared on the day of study. Cocaine hydrochloride, noradrenaline, acetylcholine, L-NAME, L-NOARG and indomethacin were obtained from Sigma Chemical Company, St Louis, Missouri, U.S.A. All drugs were dissolved in distilled water except for indomethacin which was dissolved in absolute ethanol. Ethanol was found to have no effect on responses induced by acetylcholine. Drugs were diluted to the final bath concentration with PSS.

Data and statistical analysis

Results are expressed as the mean ± standard error of the mean (s.e.mean) and the statistical significance determined by Student's paired *t* test with Dunnett's correction for multiple comparisons. The noradrenaline contractile responses are expressed as active tension (milli Newtons/mm) which is calculated from the measured force (milli Newtons) divided by twice the vessel length (millimetres). Noradrenaline sensitivity is expressed in terms of the ED_{50}, that is the concentration required to produce a half-maximal contraction. ACh-induced relaxations are expressed as a percentage decline of the maximum contraction.

Results

Contraction studies

The controls showed that there was no difference in either the noradrenaline sensitivity and maximum contraction between the dose-response curves performed at the baseline and after incubation in PSS for 30, 60 and 120 min (Figure 1). Incubation with L-NAME for the same time period produced a non-significant rise in the maximum contraction with an enhanced noradrenaline sensitivity (Figure 2, Table 1); the ED_{50} fell from 3.61 ± 0.72 μM at the baseline to 1.21 ± 0.27 μM after 60 min ($P<0.05$). A similar response was observed after a 2 h incubation with L-NOARG but the sensitivity was significantly increased at 12, 60 and 120 min (Figure 3, Table 1). Mechanical removal of the endothelium reduced the maximum contractile response to noradrenaline from 3.63 ± 0.21 mN mm^{-1} to 2.91 ± 0.32 mN mm^{-1} ($P<0.05$) in the group subsequently treated with L-NAME. There was no associated change in the sensitivity, the ED_{50} changed from 5.20 ± 1.03 μM to 3.26 ± 0.72 μM. This pattern was also observed in the endothelium-denuded arteries treated with L-NOARG where the maximum contraction fell from 3.06 ± 0.30 mN mm^{-1} to 2.56 ± 0.36 mN mm^{-1} ($P<0.05$) without a significant change in the ED_{50} of 3.80 ±

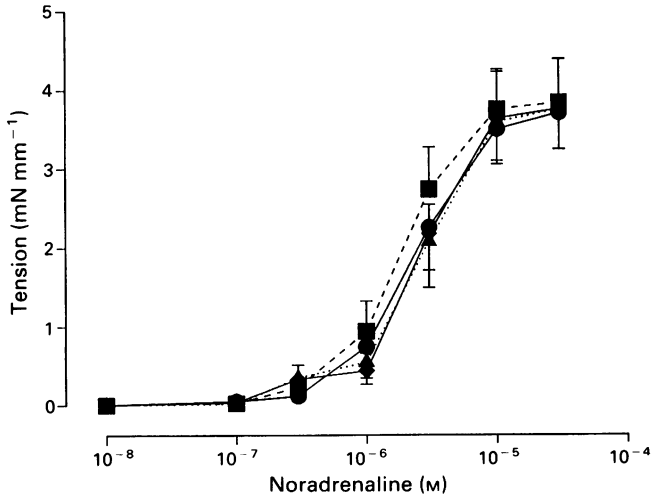

Figure 1 Noradrenaline-induced contractile responses in the control rat mesenteric resistance arteries at 0 (●), 30 (■), 60 (▲) and 120 min (◆).

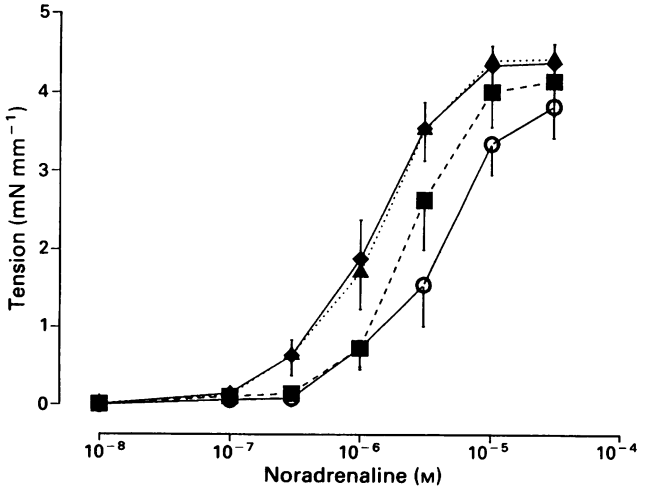

Figure 3 The contractile response to noradrenaline in intact rat mesenteric resistance vessels before (○) and after incubation with N^G-nitro-L-arginine (L-NOARG) for 12 (■), 60 (▲) and 120 min (◆).

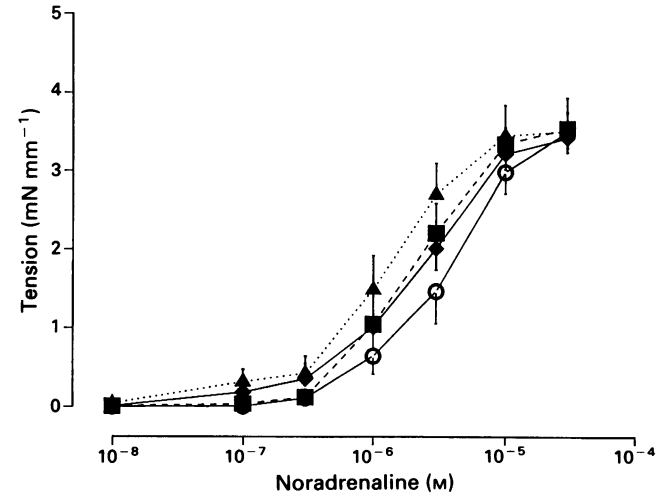

Figure 2 The contractile response to noradrenaline in intact rat mesenteric resistance vessels before (○) and after incubation with N^G-nitro-L-arginine methyl ester (L-NAME) for 12 (■), 60 (▲) and 120 min (◆).

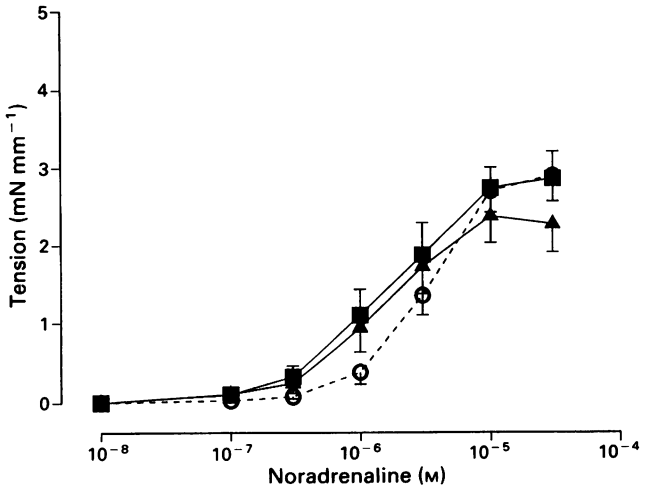

Figure 4 The contractile response to noradrenaline in endothelium-denuded rat mesenteric resistance vessels before (○) and after incubation with N^G-nitro-L-arginine methyl ester (L-NAME) for 12 (■) and 60 (▲) min.

0.65 μM in the intact arteries and 3.17 ± 0.78 μM after removing the endothelium. The effects of L-NAME (Figure 4 and Table 1) and L-NOARG (Figure 5 and Table 1) on the noradrenaline contractile response were abolished in the endothelium-denuded arteries.

Relaxation

The controls showed that there was no difference in the relaxation to ACh between curves performed at the baseline (83 ± 4%) and after incubation in PSS for 30 min (78 ± 3%), 60 min (83 ± 5%) and 120 min (74 ± 7%) (Table 3). The relaxation of maximally contracted resistance arteries decreased after incubation with L-NAME and L-NOARG in a time-dependent manner (Table 2). A bolus dose of ACh (to give a final concentration of 1 μM) produced 68 ± 4% relaxation in the untreated arteries in the group subsequently treated with L-NAME and 79 ± 4% in the L-NOARG group. Incubation with L-NAME reduced the relaxation response to 64 ± 6% at 12 min, 46 ± 8% ($P<0.05$) at 60 min and 32 ± 10% ($P<0.05$) at 120 min. Incubation with L-NOARG produced similar changes with 63 ± 4% relaxation at 12 min, 59 ± 3% ($P<0.05$) at 60 min and 44 ± 9% ($P<0.05$) after 120 min (Table 2). Endothelium removal produced a marked fall in ACh-induced relaxation. In the L-NAME group, ACh-induced relaxation was 66 ± 5% before and 10 ± 3% ($P<0.05$) after denuding the endothelium. Incubation with L-NAME further reduced the acetylcholine relaxation to 5 ± 3% at 12 min and 1 ± 1% at 60 min. In the L-NOARG group of arteries, ACh relaxation was 73 ± 4% before and 21 ± 8% ($P<0.05$) after removing the endothelium. Incubation with L-NOARG caused a reduction to 5 ± 3% at 12 min ($P<0.05$) and 2 ± 2% at 60 min (Table 2).

Indomethacin enhanced ACh-induced endothelium-dependent relaxation in mesenteric resistance arteries from the WKY. In addition the effect of L-NAME and L-NOARG was significantly reduced ($P<0.05$) in arteries which had been pre-incubated with 10 μM indomethacin (Table 3).

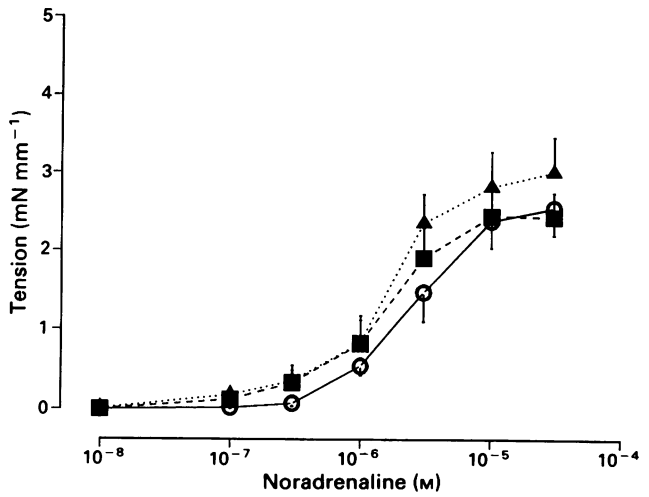

Figure 5 The contractile response to noradrenaline in endothelium-denuded rat mesenteric resistance vessels before (○) and after incubation with N^G-nitro-L-arginine (L-NOARG) for 12 (■) and 60 (▲) min.

Discussion

The present experiments show that the L-arginine analogues L-NAME and L-NOARG, are potent inhibitors of endothelium-dependent relaxation in the rat isolated mesenteric resistance artery. In addition, the enhanced vasoconstrictor response to noradrenaline after inhibition of EDRF synthesis supports an important role for the endothelium in the regulation of the contractile response of these arteries. There was a time-dependent decrease in the ED_{50} for a period up to 60 min of incubation but this was not associated with a significant increase in the maximum contraction. Moreover, the effects of both inhibitors were attenuated after mechanical removal of the endothelium by passing a human hair back and forward through the vessel lumen. Similar augmentation of vascular tone has been documented using L-NAME in the phenylephrine-contracted rat aorta (Rees *et al.*, 1990) and with L-NOARG in both the rat aorta and the rat isolated perfused mesentery (Moore *et al.*, 1990). However, by contrast incubation with another L-arginine analogue L-N^G-monomethyl-arginine (L-NMMA), did not affect the noradrenaline contractility of human subcutaneous arteries (Woolfson & Poston, 1990). This discrepancy may depend on differences between the vascular beds and also the potency of the EDRF inhibitor used. In the perfused rat mesenteric bed L-NOARG is approximately four times more active in inhibiting acetylcholine-induced endothelial-dependent relaxation than is L-NMMA. Recent evidence suggests that the difference in potency of EDRF inhibitors could be due to differences in the mechanisms by which they enter the endothelial cell (McCall *et al.*, 1991). It appears that in porcine cultured endothelial cells, L-NMMA acts by inhibiting the transport system Y^+ which is responsible for the entry of L-arginine into the endothelial cell. In contrast L-NAME and L-NOARG do not affect this system and therefore enter the cell by a different mechanism (Bogle *et al.*, 1992).

The change in noradrenaline sensitivity probably results from a decrease in basal EDRF release since there was no significant increase in the maximum contraction. However, a reduction in stimulated EDRF release cannot be excluded and it is known that noradrenaline, along with other vasoconstrictors, can stimulate the release of EDRF (Peach *et al.*, 1985). Acetylcholine evoked potent endothelium-

Table 1 The maximum contraction and the ED_{50} values for noradrenaline before and after incubation with N^G-nitro-L-arginine methyl ester (L-NAME) and N^G-nitro-L-arginine (L-NOARG) in vessels with and without an intact endothelium

		Endothelium intact			
		Control	*12 min*	*60 min*	*120 min*
L-NAME	NA_{max} (mN mm^{-1})	3.51 ± 0.21	3.64 ± 0.29	3.57 ± 0.42	3.50 ± 0.32
	ED_{50} (μM)	3.61 ± 0.72	2.37 ± 0.77	1.21 ± 0.27*	2.17 ± 0.59
L-NOARG	NA_{max} (mN mm^{-1})	4.01 ± 0.38	4.20 ± 0.40	4.53 ± 0.32	4.44 ± 0.25
	ED_{50} (μM)	3.88 ± 0.65	2.16 ± 0.42*	1.75 ± 0.32*	1.84 ± 0.42*
		Endothelium denuded			
		Before	*After* (0 min)	*12 min*	*60 min*
L-NAME	NA_{max} (mN mm^{-1})	3.63 ± 0.21	2.91 ± 0.32†	2.89 ± 0.34	2.38 ± 0.35
	ED_{50} (μM)	5.20 ± 1.03	3.26 ± 0.72	2.40 ± 0.99	1.62 ± 0.40
L-NOARG	NA_{max} (mN mm^{-1})	3.06 ± 0.30	2.56 ± 0.36†	2.49 ± 0.30	3.06 ± 0.46
	ED_{50} (μM)	3.80 ± 0.65	3.17 ± 0.78	1.76 ± 0.54	1.43 ± 0.31

*$P<0.05$ as compared to control (incubation in PSS).
†$P<0.05$ as compared to before endothelial removal.

Table 2 The maximum relaxation to acetylcholine before and after incubation with N^G-nitro-L-arginine methyl ester (L-NAME) and N^G-nitro-L-arginine (L-NOARG) in vessels with and without an intact endothelium

		Endothelium intact		
Inhibitor	*Control*	*12 min*	*60 min*	*120 min*
L-NAME	68 ± 4	64 ± 6	46 ± 8*	32 ± 10*
L-NOARG	79 ± 4	63 ± 4	59 ± 3*	44 ± 9*
		Endothelium denuded		
Inhibitor	*Before*	*After*	*12 min*	*60 min*
L-NAME	66 ± 5	10 ± 3†	5 ± 3	1 ± 1
L-NOARG	73 ± 7	21 ± 8†	5 ± 3	2 ± 2

*$P<0.05$ as compared to control (incubation in PSS).
†$P<0.05$ as compared to before endothelial removal.

Table 3 The maximum relaxation to acetylcholine in vessels incubated with N^G-nitro-L-arginine methyl ester (L-NAME) and N^G-nitro-L-arginine (L-NOARG) alone and after incubation with indomethacin (Indom)

	Control	*30 min*	*60 min*	*120 min*
PSS	83 ± 4	78 ± 3	83 ± 5	74 ± 7
Indom	74 ± 11	90 ± 4	92 ± 5	92 ± 4
	Control	*12 min*	*60 min*	*120 min*
L-NAME	68 ± 4	64 ± 6	46 ± 8*	32 ± 10*
L-NAME + Indom	88 ± 4 †	79 ± 6	73 ± 8†	71 ± 7†
L-NOARG	79 ± 4	63 ± 4	59 ± 3*	44 ± 9*
L-NOARG + Indom	93 ± 1 †	90 ± 3†	88 ± 5†	80 ± 11†

*$P<0.05$ (compared to control)
†$P<0.05$ (inhibitor vs inhibitor plus indomethacin)

dependent relaxation in the mesenteric resistance arteries which were comparable to previous studies (Watt & Thurston, 1989). Incubation with either L-NAME or L-NOARG caused a time-dependent decrease in acetylcholine-induced relaxation with maximum inhibition after 120 min. However, even after incubation with the inhibitors for 2 h, the initial burst of relaxation caused by acetylcholine was unchanged but the sustained relaxation seen in the control curve was markedly reduced. This is in keeping with the findings of Furchgott *et al.* (1990) and suggests that there are two stores of EDRF. The first is a limited and readily available store which is released almost immediately upon exposure to an endothelium-dependent agonist such as acetylcholine but becomes exhausted. The exposure to this agonist then initiates the synthesis of EDRF from L-arginine and it is this store which is responsible for the sustained relaxation seen in the control curves. It is possible that incubation with the EDRF inhibitor blocks the synthesis of this second store of EDRF and hence the relaxation seen in the treated vessels is only of a transient nature.

Neither L-NAME nor L-NOARG completely inhibited acetylcholine-induced endothelium-dependent relaxation. Thus, even after incubation with the inhibitors for 120 min there was approximately 40% relaxation (L-NAME, 32 ± 10% and L-NOARG, 44 ± 9%). It is possible that the concentration of inhibitor used in this study may not have been sufficient to inhibit completely the endothelium-dependent relaxation produced by the L-arginine pathway. However, other studies using higher concentrations of L-NAME and L-NOARG (30 μM) have achieved comparable levels of inhibition of relaxation in larger arteries (Moore *et al.*, 1990). On the other hand the residual relaxation may depend on the release of other vasodilator substances such as prostaglandin E_2 and prostacyclin. It is apparent that acetylcholine can release another EDRF which is generated from a source other than L-arginine (Ray *et al.*, 1988). This substance has been named endothelium-derived hyperpolarizing factor (EDHF) and relaxes vascular smooth muscle cells through hyperpolarization as a result of opening of potassium channels (Van de Voorde *et al.*, 1992).

We have investigated the likelihood of a cyclo-oxygenase-derived vasodilator being responsible for the residual relaxation seen after incubation with the EDRF inhibitors. The results however indicate that this is not the case since incubation with indomethacin enhanced the relaxation to a bolus dose of ACh. Furthermore, incubation with indomethacin reduced the effectiveness of both L-NAME and L-NOARG such that there was no significant inhibition of ACh-induced endothelium-dependent relaxation. These results suggest that the residual relaxation in the presence of L-NAME and L-NOARG is not due to ACh stimulated release of a cyclo-oxygenase-derived relaxing factor such as prostacyclin but may represent partial inhibition of EDRF synthesis. Moreover, the attenuation of the inhibitory effects of the EDRF inhibitors in the presence of indomethacin suggests that a contracting factor is released from the mesenteric resistance arteries taken from normotensive WKY rats. Interestingly, pre-incubation with the thromboxane A_2 antagonist, SQ 29548, did not affect the action of the EDRF inhibitors on ACh-induced endothelium-dependent relaxation. Thus it would appear that this weak contracting factor is not thromboxane A_2 but may be another vasoconstrictor prostaglandin such as prostaglandin H_2. There is evidence that the reduced endothelium-dependent relaxation seen in the spontaneously hypertensive rat (SHR) is due to a cyclo-oxygenase contracting factor (Luscher *et al.*, 1990) but as yet there is no evidence for the release of such a factor in the WKY. It appears that in the SHR the reduced relaxation arises because of a shift in the balance of relaxing and contracting factors. The discovery of a contracting factor in the WKY supports such a claim, suggesting that in the WKY the balance is in favour of relaxing factors. Furthermore since the contracting factor is only apparent after inhibition of EDRF it suggests that it is fairly weak in nature and is easily overridden by EDRF.

In conclusion we have demonstrated that both L-NAME and L-NOARG are potent inhibitors of acetylcholine-induced endothelium-dependent relaxation. Both of these inhibitors blocked endothelium-dependent regulation of vascular contraction probably by inhibiting the basal rather than the stimulated release of EDRF. These results show that the endothelium plays an important role in the modulation of the contraction of the resistance vasculature and therefore in the maintenance of vascular resistance.

This work was funded by a research grant awarded by the British Heart Foundation.

References

AALKJAER, C., HEAGERTY, A.M., SWALES, J.D. & THURSTON, H. (1987). Endothelial dependent relaxation in human subcutaneous resistance vessels. *Blood Vessels*, **24**, 85–88.

BOGLE, R.G., MONCADA, S., PEARSON, J.D. & MANN, G.E. (1992). Identification of inhibitors of nitric oxide synthase that do not interact with the endothelial cell L-arginine transporter. *Br. J. Pharmacol.*, **105**, 768–770.

DE MEY, M.P. & GRAY, S.D. (1985). Endothelium-dependent reactivity in resistance vessels. *Prog. Appl. Microcirc.*, **8**, 181–182.

FURCHGOTT, R.F. & ZAWADSKI, J.V. (1980). The obligatory role of endothelial cells in the relaxation of arterial smooth muscle by acetylcholine. *Nature*, **288**, 373–376.

FURCHGOTT, R.F., DESINGARAO, J. & FREAY, A.D. (1990). Endothelium-derived relaxing factor: some old and new findings. In *Nitric Oxide from L-Arginine: a Bioregulatory System.* ed. Moncada, S. & Higgs, E.A. pp. 5–17. Amsterdam: Elsevier Science.

GRIFFITH, T.M., EDWARDS, D.H., COLLINS, P., LEWIS, M.J. & HENDERSON, A.H. (1985). Endothelium dependent relaxation factor. *J. R.. Coll. Physicians Lon.*, **19**, 74–79.

HARDER, D.F. (1987). Pressure-induced myogenic activation of cat cerebral arteries is dependent on an intact endothelium. *Circ. Res.*, **60**, 102–107.

LEVIC, R., GROSS, S.S., LAMPARTER, B., FASEHUN, O.A., AISAKA, K., JAFFE, E.A., GRIFFITH, O.W. & STUEHR, D.J. (1990). Evidence that L-arginine is the biosynthetic precursor of vascular and cardiac NO. In *Nitric Oxide from L-Arginine: a Bioregulatory System.* ed. Moncada, S. & Higgs, E.A. p. 37. Amsterdam: Elsevier Science.

LUSCHER, T.F., AARHUS, L.L. & VANHOUTTE, P.M. (1990). Indomethacin improves the impaired endothelium dependent relaxations in small mesenteric arteries of the spontaneously hypertensive rats. *Am. J. Physiol.*, **3**, 55–58.

MCCALL, T.B., FEELISCH, M., PALMER, R.M.J. & MONCADA, S. (1991). Identification of N-iminoethyl-L-ornithine as an irreversible inhibitor of nitric oxide synthase in phagocytic cells. *Br. J. Pharmacol.*, **102**, 234–238.

MOORE, P.K., AL-SWAYEH, O.A., CHONG, N.W.S., EVANS, R.A. & GIBSON, A. (1990). L-N^G-nitro arginine (L-NOARG), a novel, L-arginine reversible inhibitor of endothelium dependent vasodilation *in vitro*. *Br. J. Pharmacol.*, **99**, 408–412.

MULSCH, A. & BUSSE, R. (1990). N^G-nitro-L-arg (N5-[imino(nitroamino)methyl]-L-ornithine) impairs endothelium dependent dilation by inhibiting cytosolic nitric oxide synthesis from L-arginine. *Naunyn-Schmiedebergs Arch. Pharmacol.*, **341**, 143–147.

MULVANY, M.J. & HALPERN, W. (1976). Mechanical properties of vascular smooth muscle cells in situ. *Nature*, **260**, 617–619.

MYERS, P.R., GUERRA, R. Jr., BATES, J.N. & HARRIS, D.G. (1989). Studies on the properties of endothelium derived-relaxing factor (EDRF), nitric oxide, and nitrosothiols: similarities between EDRF and S-nitroso-L-cysteine (cys NO). *J. Vasc. Med. Biol.*, **1**, 106.

OSOL, G., CIPOLLA, M. & KNUTSON, S. (1989). A new method for mechanically denuding the endothelium of small arteries (50–150 μm) with a human hair. *Blood Vessels*, **26**, 320–324.

OWEN, M.P. & BEVAN, J.A. (1985). Acetylcholine induced endothelial dependent vasodilation increases as artery diameter decreases in the rabbit ear. *Experientia*, **41**, 1057–1058.

PALMER, R.M.J., FERRIGE, A.G. & MONCADA, S. (1987). Nitric Oxide release accounts for the biological activity of endothelium-derived relaxing factor. *Nature*, **327**, 524–526.

PALMER, R.M.J., REES, D.D., ASHTON, D.S. & MONCADA, S. (1988). L-arginine is the physiological precursor for the formation of nitric oxide in endothelium-dependent relaxation. *Biochem. Biophys. Res. Commun.*, **153**, 1251–1256.

PEACH, M.J., LOEB, A.L., SINGER, H.A. & SAYE, J. (1985). Endothelium-derived relaxing factor. *Hypertension*, Suppl. I, **7**, I-94–I-100.

RAIJ, L., LUSCHER, T.F. & VANHOUTTE, P.M. (1988). High potassium diet augments endothelium dependent relaxations in the Dahl rat. *Hypertension*, **12**, 562–567.

REES, D.D., PALMER, R.M.J., HODSON, H.F. & MONCADA, S. (1989). A specific inhibitor of nitric oxide formation from L-arginine attenuates endothelium-dependent relaxation. *Br. J. Pharmacol.*, **96**, 418–424.

REES, D.D., PALMER, R.M.J., SCHULZ, R., HODSON, H.F. & MONCADA, S. (1990). Characterization of three inhibitors of endothelium NO synthase *in vitro* and *in vivo*. *Br. J. Pharmacol.*, **101**, 746–752.

VALLANCE, P., COLLIER, J. & MONCADA, S. (1989a). Nitric oxide synthesised from L-arginine mediates endothelium dependent relaxation in human veins in vivo. *Cardiovasc. Res.*, **23**, 1053–1057.

VALLANCE, P., COLLIER, J. & MONCADA, S. (1989b). Effects of endothelium-derived NO on peripheral arteriolar tone in man. *Lancet*, **ii**, 997–1000.

VAN DE VOORDE, J., VANHEEL, B. & LEUSEN, I. (1992). Endothelium-dependent relaxation and hyperpolarization in aorta from control and renal hypertensive rats. *Circ. Res.*, **70**, 1–8.

WATT, P.A.C. & THURSTON, H. (1989). Endothelium-dependent relaxation in resistance vessels from spontaneously hypertensive rats. *J. Hypertension*, **7**, 661–666.

WIEST, E., TRACH, V. & DAMMGEN, J. (1989). Removal of endothelial function in coronary resistance vessels by Saponin. *Basic Res. Cardiol.*, **84**, 469–478.

WOOLFSON, R.G. & POSTON, L. (1990). Effect of N^G-monomethyl-L-arginine on endothelium-dependent relaxation of human subcutaneous reistance arteries. *Clin. Sci.*, **79**, 273–278.

YANG, Z., VON SEGESSER, L., BAUER, E., STULZ, P., TURINA, M. & LUSCHER, T.F. (1991). Different activation of the endothelial L-arginine and cyclooxygenase pathway in the human internal mammary artery and saphenous vein. *Circ. Res.*, **68**, 52–60.

(Received April 30, 1992
Revised June 15, 1992
Accepted June 26, 1992)

Br. J. Pharmacol. (1992), **107**, 622–627

Differential potentiation of $GABA_A$ receptor function by two stereoisomers of diimidazoquinazoline analogues

Haesook K. Im, [1]Wha Bin Im, Jeff F. Pregenzer, James D. Petke, Beverly J. Hamilton, Donald B. Carter, Philip F. VonVoigtlander, *Holger C. Hansen & *Marit Kristiansen

CNS Diseases Research, The Upjohn Company, Kalamazoo, MI 49001, U.S.A. and *CNS Division, Novo Nordisk A/S, Novo Nordisk Park, 2760 Maaloev, Denmark

1 U-84935, diimidazo[1,5-a;1',2'-C]quinazoline,5-(5-cyclopropyl-1,2,4-oxidiazol-3yl)-2,3-dihydro, is a ligand of high affinity for the benzodiazepine site of the $GABA_A$ receptor composed of $\alpha_1\beta_2\gamma_2$ subunits.

2 The efficacy of its analogues was measured with their ability to potentiate GABA-mediated Cl^- currents in the whole cell configuration of the patch clamp techniques in human kidney cells (A293 cells) expressing the subtype of the $GABA_A$ receptor.

3 The analogues displayed various levels of efficacy including agonists, partial agonists and antagonists without marked changes in their affinity for the receptors.

4 The major determinant of their efficacy was the spacial configuration of a methyl substituent of the C2 atom of the rigid and planar diimidazoquinazoline ring: U-90167, containing the methyl substituent projected below the plane of the ring, markedly enhanced the GABA current with a maximal potentiation of $220 \pm 25\%$, while its stereoisomer, U-90168, marginally increased the GABA response with a maximal potentiation of $45 \pm 10\%$, to which its methyl group appeared to contribute very little.

5 U-90167 potentiated the GABA response with an EC_{50} of 8.1 nM and a Hill coefficient of 1.1 and did not alter the reversal potential for the Cl^- current.

6 From computational modelling, the sensitive methyl group of U-90167 could be assigned to the general region for the 5-phenyl group of diazepam. The diimidazoquinazoline, because of its rigid and plantar ring structure, may be useful to define further the out-of-plane region responsible for agonistic activity and to pinpoint other areas pivotal to the functionality of benzodiazepine ligands.

Keywords: $GABA_A$ receptor; $\alpha_1\beta_2\gamma_2$, GABA; Cl^- currents; diimidazoquinazoline; computational modelling

Introduction

$GABA_A$ receptors are the receptor-chloride channel complex of multimeric polypeptides and exert inhibitory effects on neuronal firing by hyperpolarizing neuronal membrane potential. Recent cloning studies indicate the presence of α, β, γ and δ subunits, each of which has several isotypes in mammalian brain (Barnard *et al.*, 1987; Schofield, 1989; Sigel *et al.*, 1990; Verdoorn *et al.*, 1990). Various combinations of the subunits expressed in mammalian cells displayed γ-aminobutyric acid (GABA)-mediated Cl^- currents, which were differentially modulated by allosteric ligands. In particular, benzodiazepines interact with only the cloned receptors containing γ in addition to α and β subunits: for instance, the $\alpha_1\beta_2\gamma_2$ subtype represents Type 1 receptors which interact with all the known ligands for benzodiazepine receptors while Type 2 receptors include the $\alpha_{2-5}\beta_2\gamma_2$ subtypes and are differentiated from Type 1 merely by their lower affinity for some selected ligands, such as imidazopyridines and β-carbolines (Pritchett *et al.*, 1989a, b; Puia *et al.*, 1991). All allosteric ligands of agonistic activity to the $\alpha_1\beta_2\gamma_2$ subtype are therapeutically useful as hypnotics, anxiolytics and anticonvulsants, to name a few. These drugs have diverse chemical structures such as benzodiazepines, pyrazoloquinolines, cyclopyrrolones, β-carbolines, imidazopyridines, imidazoquinoxalines, benzocinnolones and phenylquinolones (Costa, 1979; Costa & Guidotti, 1979; Yokohama *et al.*, 1982; Goldberg *et al.*, 1983; Bennett & Petrack, 1984; Petersen *et al.*, 1984; Gardener, 1988; Haefely *et al.*, 1985; Tang *et al.*, 1990; Tully *et al.*, 1991). At present the structural feature(s) central to the agonistic activity is not clear, although many models have been proposed to explain the *in vivo* efficacy of various ligands on the basis of computational modelling studies (Tebib *et al.*, 1987; Villar *et al.*, 1989; 1991). Knowledge of the key functional determinants for benzodiazepine receptor ligands in cloned $GABA_A$ receptors would be useful for understanding the ligand-receptor interactions at the molecular level and for developing new ligands with unique pharmacological and therapeutic profiles.

Recently, the derivatives of diimidazoquinazolines (Figure 1) were discovered as a new series of ligands for the benzodiazepine receptors. In this study, we characterize the binding property and efficacy of several analogues of the diimidazoquinazolines utilizing the cloned $GABA_A$ receptor consisting of $\alpha_1\beta_2\gamma_2$, the most abundant and ubiquitous subtype in mammalian brains. We will show with a pair of stereoisomers with respect to a methyl substituent at C2 of the rigid and planar diimidazoquinazoline ring that a pharmacophore for agonistic activity consists of a simple substituent like a methyl in the out of plane region with respect to the rest of the molecular structure.

Methods

Cell culture and transfection

The stable cell-lines expressing α_1 (Khrestchatisky *et al.*, 1989), β_2 (Ymer *et al.*, 1989) and γ_2 (Shivers *et al.*, 1989) subunits of $GABA_A$ receptors were derived by transfection of plasmids containing cDNA and a plasmid encoding G418 resistance into the human kidney cells (A293 cells) (Graham *et al.*, 1977). After two weeks of selection in G418 (1 mg ml^{-1}), resistant cells were assayed for the ability to synthesize

[1] Author for correspondence.

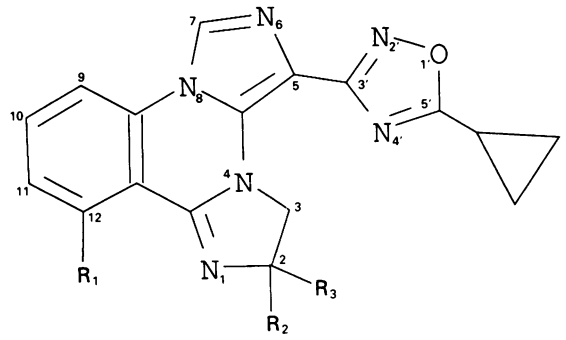

Figure 1 Molecular structure and atom numbering of U-84935 and its analogues.

all three $GABA_A$ receptor mRNAs by Northern blotting. Positive cells were used for electrophysiology to measure GABA-induced Cl^- currents. For binding studies, because of a relatively low level of expression of the $GABA_A$ receptor subtype in A293 cells (see Figure 3), we used the baculovirus system for the receptor expression in SF-9 cells, an insect ovary cell line, where a high level of expression of ion channels have already been shown (Klaiber *et al.*, 1990). We have shown earlier that the infected insect cells expressed GABA-mediated Cl^- currents as well as benzodiazepine binding sites having the same pharmacological specificity as animal cells expressing the same receptor subunits (Carter *et al.*, 1992). For instance, the GABA-induced Cl^- currents in SF-9 cells showed the GABA-sensitivity, desensitization and responsiveness to benzodiazepine receptor ligands similar to those in A293 cells. The cloned receptors in the insect cells also showed the α subunit-dependent selectivity of benzodiazepine receptor ligands and their binding parameters indistinquishable from those in A293 cells.

Electrophysiology

The whole cell configuration of the patch clamp technique (Hamill *et al.*, 1981) was used to record the GABA-mediated

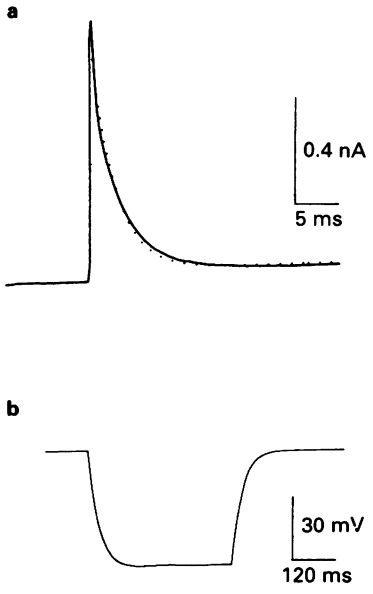

Figure 2 Current transient after a 20 mV voltage-jump (a) and voltage-change under current clamp conditions (b) recorded from a cluster of six cells. The current decay (a) was fitted to an exponential equation $(I_t - I_\infty)/I_{max} = \exp(-t/\tau)$. The values were 2.7 ms for τ and 42 pA for I_∞.

Cl^- currents. Patch pipettes made of borosilicate glass were fire-polished to a tip resistance of 0.5–2 MΩ when filled with a solution containing (mM): CsCl 140, EGTA 11, $MgCl_2$ 2, ATP 0.5 and HEPES 10, pH 7.3. The cells on the cover slip were placed in a small chamber on the stage of the inverted microscope and superfused with the external solution containing (mM): NaCl 130, KCl 5, $MgCl_2$ 1, $CaCl_2$ 1.8 and HEPES 5, pH 7.2 (Normal Saline) at a rate of 2 ml min^{-1}. GABA and drugs were dissolved at the indicated concentrations in the external solution and were applied through a Y-tube (Murase *et al.*, 1989) placed within 100 μm of the cells. Briefly, the drug solutions were held 450 mm above the level of the Y-tube tip and flowed out by gravity to a drain bottle. The position of the drain bottle was adjusted to draw also superfusing solution in the cell-chamber through the Y-tube tip. Application of the drug solution was initiated by blocking the drain with an electric valve (normally open) placed in the outflow arm of the Y-tube.

The current through the pipette was recorded with an Axopatch 1D amplifier and a CV-4 headstage (Axon Instrument Co.) A Bh-1 bath headstage was used to compensate for changes in bath potentials. The currents were recorded with a Gould Recorder 220. Experiments were carried out at the holding potential of −60 mV at room temperature (21–24°C). In this permanently expressed cell line, we often encounter cell clusters of 4 to 6 cells. Figure 2a shows a current transient after a 20 mV voltage jump in a cluster of six cells. The current decay was well fitted by a single exponential function with a time constant (τ) of 2.7 ms. In cell clusters we used, one exponential function well described the current decay and the value of τ varied from 0.5 to 2.7 ms roughly depending on the number of cells in a cluster. This is consistent with a tight electrical coupling between the cells. Otherwise, more than one exponential function is needed to describe the current decline (Jauch *et al.*, 1986). The voltage change under current clamp conditions in a cluster of six cells (Figure 2b) was uniform and further supports the existence of one electrical compartment in the cluster. In this study we used cell clusters of up to 6 cells for patch-clamp experiments. Figure 3 shows the recording from a single cell as well as from such cell clusters. The amplitude of the peak current induced with 5 μM GABA was 57, 342 and 409 pA for a single, 4-cell and 6-cell clusters, respectively, and then increased upon inclusion of 5 μM diazepam to 121, 631 and 857 pA, respectively. The percentage stimulation by diazepam was fairly constant (ranging from 185 to 209%) from the one-cell to the six-cell groups.

Equilibrium binding

For the binding study, Sf-9 cells infected with baculovirus carrying cDNA for α_1, β_2 and γ_2 subunits were harvested in 2 l batches, 60 h post infection. The membranes were prepared in normal saline after homogenization with Polytron PT 3000 (Brinkman) for 4 min. Unbroken cells and large nuclei aggregates were removed by centrifugation at 1000 *g* for 10 min. Then the membranes were recovered with a second centrifugation of the supernatant at 40,000 *g* for 50 min. The membranes were resuspended to a final concentration of 5 mg ml^{-1} in a solution containing 300 mM sucrose, 5 mM Tris/HCl, pH 7.5, and glycerol to a final concentration of 20%, and were stored at −80°C. Equilibrium binding of [^{3}H]-flunitrazepam to the $GABA_A$ receptors was measured in a 500 μl volume of normal saline containing 6 nM [^{3}H]-flunitrazepam, varying concentrations of test ligands and 50 μg of membrane protein. The mixture was incubated for 60 min at 4°C, filtered over Whatman glass fibre filter, and washed four times with cold normal saline. The filter was then counted for the radioactivity in the presence of a scintillation cocktail (Insta gel). With the insect cell membranes expressing $\alpha_1\beta_2\gamma_2$ $GABA_A$ receptor subunits, we observed a K_d of 15.8 ± 0.6 nM and B_{max} of 3.8 ± 0.7 pmol mg^{-1} protein for [^{3}H]-muscimol, and a K_d of 4.1 ± 0.1 nM and B_{max} of 2.1 ± 0.6 pmol mg^{-1}

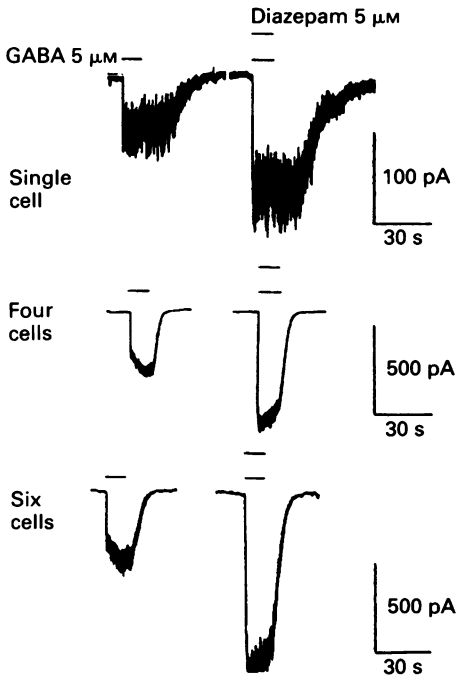

Figure 3 Comparison of the electrophysiological responses to γ-aminobutyric acid (GABA) with or without diazepam in A293 cells expressing $\alpha_1\beta_2\gamma_2$ subunits. The whole cell configuration of the patch clamp techniques was established in the cluster of single, four or six A293 cells expressing $\alpha_1\beta_2\gamma_2$. GABA (5 μM) without or with diazepam (5 μM) was applied for 10 s (as indicated with a bar above each trace) through a Y-tube located within 100 μm of the cells. The Cl^- current was measured at the holding potential of −60 mV with a symmetrical Cl^- concentration across the membrane. The amplitude of the peak current induced by 5 μM GABA was 57, 342 and 409 pA for a single, 4 cell and 6-cell clusters, respectively, and increased to 121, 631 and 857 pA in the presence of diazepam (5 μM).

protein for [^{3}H]-flunitrazepam. No considerable specific binding for the two ligands was observed in the membranes from non-transfected SF-9 cells.

Computer modelling

The conformational properties of the diimidazoquinazolines were studied with molecular mechanics methods by use of the MACROMODEL implementation of the MM2 force field (Allinger, 1977), and semi-empirical quantum mechanical techniques; Stewart, 1990).

Results

Equilibrium binding

The diimidazoquinazoline derivatives bound to the benzodiazepine site of the $\alpha_1\beta_2\gamma_2$ subtype of $GABA_A$ receptors with high affinity. Table 1 shows their K_i values computed from their ability to block [^{3}H]-flunitrazepam binding to the receptor. The parent compound, U-84935, showed a K_i value of 1.5 nM. Substituents like a halide at R1 and/or a methyl substituent at R2 or R3 produced some changes in their K_i values. For instance, U-87161 and U-85575, having a fluoro and a chloro group at R1, respectively, had a K_i of about 0.2 nM; one eighth of that for the parent compound. The methyl substituent at R2 (U-90167) or R3 (U-90168) with the chloro group at R1, however, raised their K_i values back to the range of the parent compound (K_i of 3.9 and 1.0 nM for U-90167 and U-90168, respectively). These flexible changes in their binding affinity are not marked and indicate that the analogues share the same binding pockets in the benzodiazepine binding region.

Table 1 Affinity and efficacy measurements for U-84935 and its diimidazoquinazoline analogues in the $GABA_A$ receptor made of $\alpha_1\beta_2\gamma_2$

	R1	*R2*	*R3*	*Binding* K_i (nM)	*Cl^- currents* (% of potentiation)
U-84935	H	H	H	1.5 ± 0.2	20 ± 15
U-87161	F	H	H	0.15 ± 0.05	19 ± 10
U-85575	Cl	H	H	0.24 ± 0.10	45 ± 10
U-90167	Cl	CH_3	H	3.9 ± 0.4	220 ± 25
U-90168	Cl	H	CH_3	1.0 ± 0.2	46 ± 7
Diazepam				11.2 ± 0.9	95 ± 20

The affinity of the drugs for the benzodiazepine binding site was estimated from the ability of the drugs to inhibit [^{3}H]-flunitrazepam binding in the membranes of SF-9 cells expressing $\alpha_1\beta_2\gamma_2$ subunits. The IC_{50} value was obtained from dose-response curves consisting of six different concentrations, and was converted to K_i's using the equation, $K_i = IC_{50}/(1 + [\text{Test ligand}]/K_d$ of flunitrazepam). The efficacy of the drugs (5 μM) was measured by their ability to potentiate the Cl^- current induced by 5 μM GABA using the whole cell configuration of the patch clamp techniques in A293 cells expressing $\alpha_1\beta_2\gamma_2$ subunits. The percentage potentiation was calculated from the formula, ((the amplitude of the peak Cl^- current with test drug plus GABA) − (that with GABA alone)/(that with GABA alone)) × 100. The data represent the mean of 3 to 8 separate experiments with a standard error.

Functional characteristics

Chloride currents induced by GABA at 5 μM alone or in combination with diimidazoquinazoline analogues were measured in A293 cells expressing the $\alpha_1\beta_2\gamma_2$ subtype of $GABA_A$ receptors, using the whole cell configuration of the patch clamp technique. Figure 4a shows several representative traces for the whole cell current measurements: GABA at 5 μM induced an inward current of 250 pA representing the outward movement of Cl^- at the holding potential of −60 mV and in the presence of a nearly symmetrical Cl^- gradient across the membrane (148 mM in the pipette and 141 mM in the bathing solution). The actions of drugs was examined in the presence of 5 μM GABA. Diazepam nearly doubled the GABA response. U-90167 enhanced the GABA-induced currents by more than twice (220 ± 25%), whereas its stereoisomer with respect to the methyl group, U-90168, enhanced the current by only 46 ± 7% (Table 1). The values represent the maximal responses, because the concentration of the drugs (5 μM) is at least 1000 times greater than their K_i value and well over the saturating dose in the dose-response profile for GABA currents (see below, Figure 5). U-85575, containing hydrogens instead of the methyl at C2, displayed the same degree of potentiation as U-90168. This suggests that the methyl group of U-90168 did not contribute to its potentiation of GABA response. Table 1 further shows that U-84935, the parent compound, and U-87161, containing a fluoro substituent at R1, only marginally enhanced the GABA response; 20 ± 15% for U-84935 and 19 ± 10% for U-87161.

Ro 15-1788, a classical antagonist to the benzodiazepine receptor, showed no noticeable enhancement of the GABA response, but blocked the potentiation by U-90167 (Figure 4b). The dose-response profile for the potentiation of GABA action by U-90167 is shown in Figure 5. The data were fitted to Langmuir adsorption isotherm for a single site (Im & Blakeman, 1991). U-90167 potentiated the GABA response with a half maximal dose of 8.1 ± 1.1 nM, a Hill coefficient of 1.1 ± 0.2, and the maximal potential of 220 ± 25%. Figure 6 compares the current-voltage (*I*-V) relationships in the

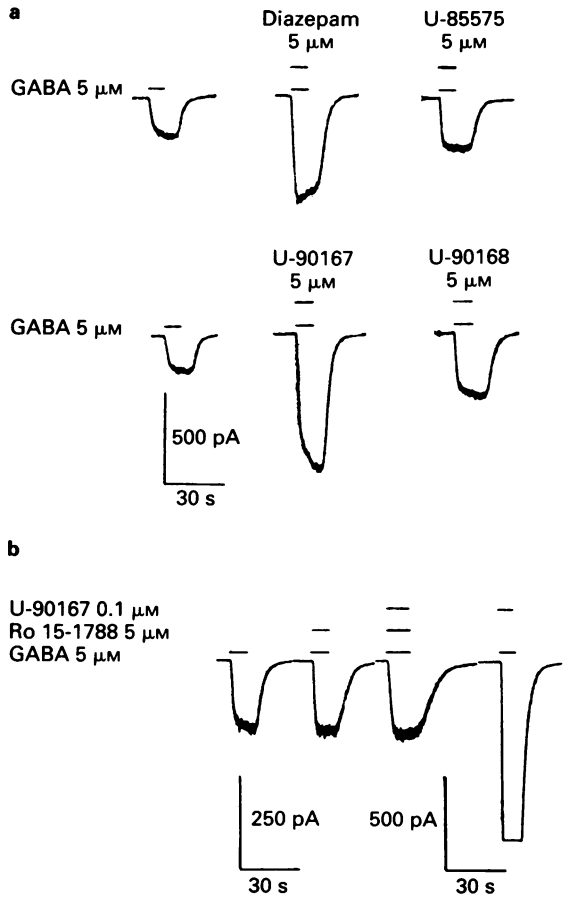

Figure 4 Representative traces showing differential potentiation of γ-aminobutyric acid (GABA)-induced Cl^- by the diimidazoquinazoline analogues in A293 cells expressing $\alpha_1\beta_2\gamma_2$. Each drug was applied for 10 s (as indicated with a bar(s) above each trace). (a) The extent of potentiation of the GABA- (5 μM) response by U-85575, U-90167 or U-90168 at a concentration (5 μM) was compared with that by diazepam. Table 1 lists the percentage potentiation obtained after normalizing the net increase of the current induced by test drugs to that by GABA alone. (b) Ro 15-1788, a classical antagonist, showed no noticeable potentiation of the GABA response by itself, but abolished the stimulatory action by U-90167.

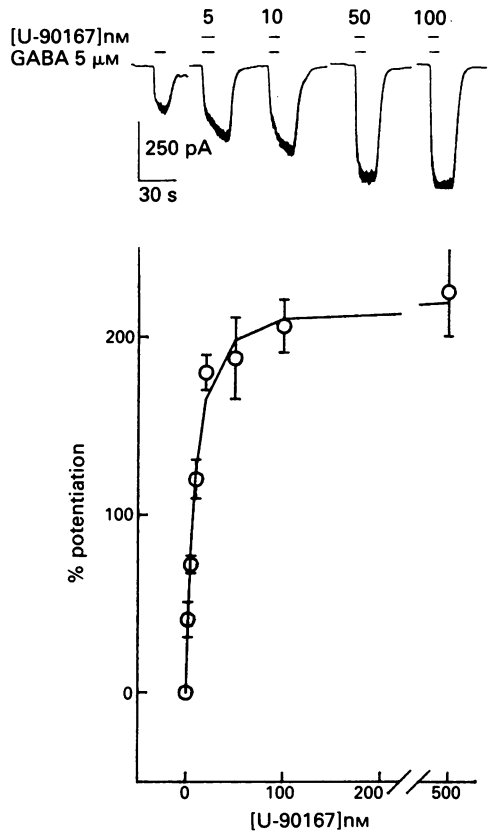

Figure 5 Graph showing dose-dependent potentiation of γ-aminobutyric acid (GABA) response by U-90167 in A293 cells expressing $\alpha_1\beta_2\gamma_2$. Representative recordings for GABA-induced currents in the presence of U-90167 at 0, 5, 10, 50 and 100 nM are shown above. The net increase of the currents induced by the drug at the various concentrations was normalized to the response to GABA alone. The potentiations, expressed as percentages of control, were plotted with the mean and standard errors from three separate experiments, and fitted to the equation, % potentiation = (([U-90167]^n × maximal potentiation)/([U90167]^n + EC_{50}^n)), where n is the Hill coefficient and the other symbols have the usual meanings. U-90167 potentiated the GABA response with an EC_{50} (a half maximal concentration) of 8.1 ± 1.1 nM, a Hill coefficient of 1.1 ± 0.2 and the maximal potentiation of 221 ± 25%.

presence of GABA with or without U-90167. The reversal potential with GABA was near 0 mV, as expected from the almost symmetrical gradient of Cl^- ion, and was not affected by the potentiation action of U-90167.

Structural characteristics

Figure 1 shows the chemical structure of the diimidazoquinazolines. Studies with molecular mechanics showed that the diimidazoquinazoline ring is largely plantar and the methyl substituent at R2 and R3 projected below and above the planar ring, respectively (Figure 7). The cyclopropyl oxidiazole group appears to be perpendicular to the plane of the diimidazoquinazoline in the low energy conformers, but may rotate freely without noticeable changes in the energy level. Substitution with a methyl or halide group at R1 (C12), R2 and R3 (C2) produced no considerable change in the configurations of their diimidazoquinazoline and oxidiazole rings.

Discussion

In this study, we have shown that the derivatives of diimidazoquinazoline interact with the $\alpha_1\beta_2\gamma_2$ subtype of $GABA_A$ receptors as shown by the displacement of [^{3}H]-flunitrazepam, a classical benzodiazepine. Functionally, the diimidazoquinazolines, although only a limited number of analogues were examined in this study, displayed various levels of efficacy as measured with their ability to potentiate GABA-mediated Cl^- currents in the $\alpha_1\beta_2\gamma_2$ subtype. For instance, they include the compounds of low efficacy (U-84935 and U-87161) like antagonists, the compounds of medium efficacy (U-85575 and U-90168) like partial agonists, and the compound of high efficacy (U-90167). The variations of the drug efficacy can be related to changes in the two substituents. The chloro group at R1 (but not the fluoro) enhanced, albeit to a minor extent, the efficacy as compared to the parent compound containing a hydrogen group at R1. A more dramatic and clearly explicable effect came from the methyl substituent at R2 (U-90167) and R3 (U-90168); U-90167 is an agonist of high efficacy while its stereoisomer, U-90168, is only a partial agonist. This indicates that a spacial configuration of the methyl moiety at C2 of the diimidazoquinazolines is largely responsible for inducing the marked agonistic activity in the $\alpha_1\beta_2\gamma_2$ subtype of $GABA_A$ receptors. As shown in Figure 6, the planar and rigid diimidazoquinazoline ring fixes the spacial configuration of the methyl moiety at the C2 to be projected below the plane of the ring, and is instrumental in pinpointing the pivotal role of the methyl group in the

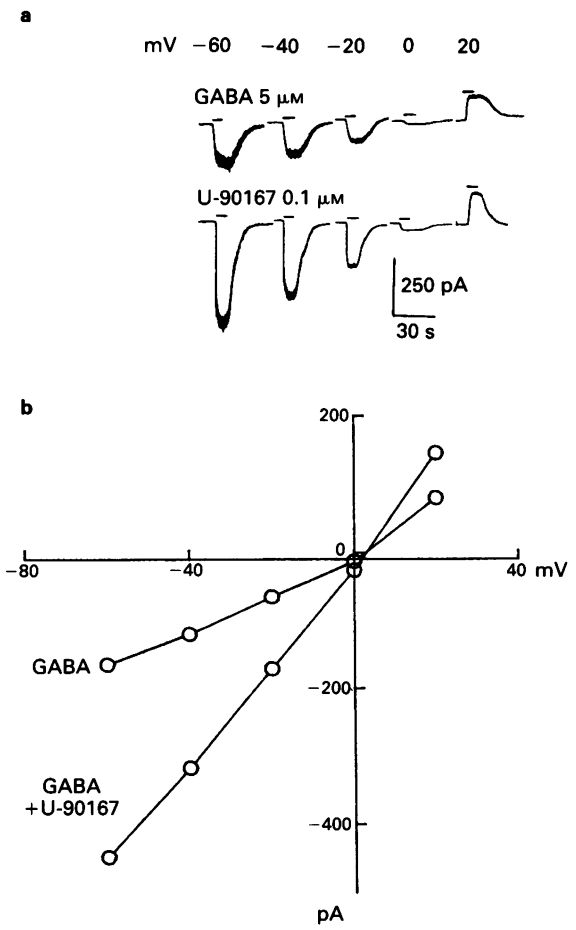

Figure 6 Current-voltage relationships for γ-aminobutyric acid (GABA)-induced Cl^- currents with or without U-90167. Panel (a) shows representative traces for GABA-induced currents with or without U-90167 at the holding potentials of −60, −40, −20, 0 and 20 mV. The chloride gradient across the membrane was nearly symmetrical. The reverse potential was near 0 mV and was not noticeably affected by the drug.

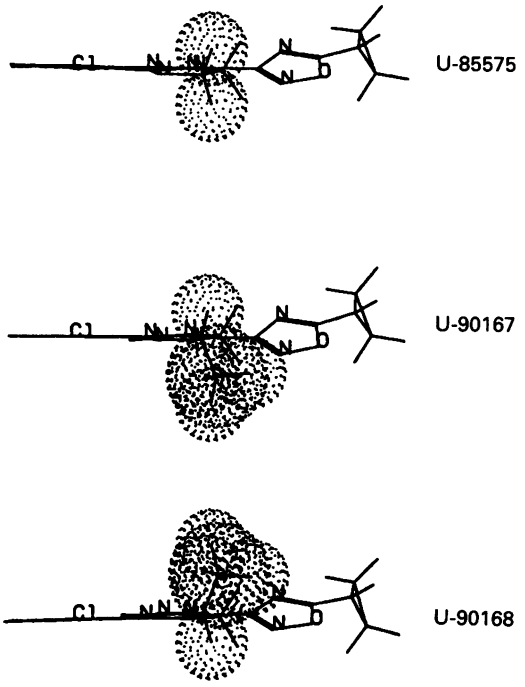

Figure 7 Side-view of minimum energy structures of U-85575, U-90167 and U-90168.

allosteric modulation of the $GABA_A$ receptor. One can also readily envision that in interacting with the receptor, the diimidazoquinazoline ring slides in the narrow binding region on the receptor like a sheet, and the methyl group, which is out of the plane with respect to the ring, is interacting in a stereospecific manner with a region of the receptors responsible for inducing the conformational changes necessary to facilitate the GABA-mediated opening of the chloride channels. We know that several series of benzodiazepine receptor ligands show noticeable variations in their efficacy upon changing substituents of the major ring system, but their functional changes could not be related to one key structural feature. This is because of involvement of more than one substituent, and because of multiple plausible conformations of the key substituents from isomerization or a large degree of their rotational freedom. For instance, in β-carbolines, replacements of more than one substituent, 4-CH_3 and 5-$OCH(-CH_3)_2$ (ZK93426) with 4-CH_2OCH_3 and 5-benzyloxy group (ZK91926) or with 6-benzyloxy (ZK93423) is required to change neutral antagonists into anticonvulsants (agonists) (Cooper, 1986; Villar *et al.*, 1989). With pryazoloquinolones, changes in the substituents of the *para*-position of the phenyl ring (CGS 9896, CGS 9895 and CGS 8216 having Cl^-, H and OCH_3, respectively) has been reported to produce anticonvulsant, pro-convulsant, and neutral antagonists (Yokohama *et al.*, 1982), but determination of the precise configuration of the group is difficult because of the existence of the tautomeric forms of pyrazoquinolone (Cooper, 1986) and a large degree of rotational freedom of the key phenyl group. Besides, these studies used anticonvulsant activity of these drugs in experimental animals as the measure of their efficacy, which could not represent their inherent modes of interactions with various $GABA_A$ receptors known to exist in the brain. Because of these weaknesses, these analogues have not been very helpful in distinguishing various models advanced to explain the functional characteristics of benzodiazepine receptor ligands (Villar *et al.*, 1991).

In this study, on the other hand, the differential agonistic activity of the two diimidazoquinazoline stereoisomers clearly points out the key functional pharmacophore for benzodiazepine receptor ligands and appears to favour one particular proposal that the agonistic activity can be attributed to the presence of a bulky group in an out-of-plane region where the 5-phenyl group of benzodiazepines has also been assigned (Tebib *et al.*, 1987). This proposal was formulated from computational modelling of diverse chemical structures including benzodiazepines, pyrazoquinolones, cyclopyrrolones, β-carbolines and imidazopyridines. Although the methyl of C2 of the diimidazoquinazoline is not bulky as compared to the groups cited in the model such as acetaamidomorpholine, pyrrolidine, and piperazine, it is certainly out of plane with respect to the rest of the molecular structure and responsible for the agonistic activity. Also when the aromatic ring of the diimidazoquinazoline is superimposed over that of diazepam, the methyl at C2 of the diimidazoquinazoline is located in the general region for the 5-phenyl group of diazepam. This suggests that our observation with the diimidazoquinazolines could be generalized to other series of benzodiazepine ligands.

In summary, we have characterized the binding and functional characteristics of the diimidazoquinazolines, a new series of benzodiazepine receptor ligands. In the $\alpha_1\beta_2\gamma_2$ subtype, the methyl substituent at C2 of the rigid and planar diimidazoquinazoline ring markedly influenced the agonistic activity in a stereo-specific manner. This identifies the out-of-plane methyl group as a key functional pharmacophore for benzodiazepine receptor ligands and supports the earlier proposal of Tebib *et al.* (1987) derived from computational modellings of the various ligands of $GABA_A$ receptors.

References

ALLINGER, N.L. (1977). Conformational analysis – 130. MM2. A hydrocarbon force field utilizing V_1 and V_2 torsional terms. *J. Am. Chem. Soc.*, **99**, 8127–8134.

BARNARD, E.A., DARLISON, M.G. & SEEBURG, P. (1987). Molecular biology of the $GABA_A$ receptor: the receptor/channel superfamily. *Trends Neuro. Sci.*, **10**, 502–509.

BENNETT, D.A. & PETRACK, B.A. (1984). CGS 9896: a non-benzodiazepine, non-sedating potential anxiolytic. *Drug Dev. Res.*, **4**, 75–82.

CARTER, D.B., THOMSEN, D.R., IM, W.B., LENNON, D.J., NGO, D.M., GALE, W., IM, H.K., SEEBURG, P.H. & SMITH, M.W. (1992). Functional expression of $GABA_A$ Cl^- channels and benzodiazepine binding sites in Baculovirus infected insect cells. *Bio/Technol.*, **10**, 678–681.

COOPER, S.J. (1986). Bidirectional effects of behavior of β-carbolines acting at central benzodiazepine receptors. *Trends Pharmacol. Sci.*, **7**, 210–212.

COSTA, E. (1979). The role of gamma-aminobutyric acid in the action of 1,4-benzodiazepines. *Trends Pharmacol. Sci.*, **1**, 41–44.

COSTA, E. & GUIDOTTI, A. (1979). Molecular mechanisms in the receptor action of benzodiazepines. *Annu. Rev. Pharmacol.*, **19**, 531–545.

GARDNER, C.R. (1988). Pharmacological profiles in vivo of benzodiazepine receptor ligands. *Drug Dev. Res.*, **12**, 1–28.

GOLDBERG, M.E., SALAMA, A.L., PATEL, L.B. & MALICK, J.B. (1983). Novel benzodiazepine anxiolytics. *Neuropharmacol.*, **22**, 1499–1504.

GRAHAM, F.L., SMILEY, J., RUSSEL, C. & NAIRN, R. (1977). Characteristics of a human cell line transformed by DNA from human adenovirus type 5. *J. Gen. Virol.*, **36**, 59–74.

HAEFELY, W., KYBURZ, E., GERECKE, M. & MOHLER, H. (1985). Recent advances in the molecular pharmacology of benzodiazepine receptors and in the structure-activity relationship of their agonists and antagonists. *Adv. Drug. Res.*, **14**, 165–322.

HAMILL, O.P., MARTY, A., NEHER, E., SAKMANN, B. & SIGWORTH, F.J. (1981). Improved patch-clamp techniques for high-resolution current recording from cells and cell-free membrane patches. *Pflügers. Arch.*, **391**, 85–100.

IM, W.B. & BLAKEMAN, D.P. (1991). Correlation between γ-aminobutyric $acid_A$ receptor ligand-induced changes in t-butylbicyclophosphoro[^{35}S]thionate binding and $^{36}Cl^-$ uptake in rat cerebrocortical membranes. *Mol. Pharmacol.*, **39**, 394–398.

JAUCH, P., PETERSEN, O.H. & LAUGER, P. (1986). Electrogenic properties of the sodium-alanine cotransporter in pancreatic acinar cells: I. Tight-seal whole-cell recordings. *J. Memb. Biol.*, **94**, 99–105.

KHRESTCHATISKY, M., MACLENNON, A.J., CHIANG, M.-Y., XU, W., JACKSON, M.B., BRECHA, N., STERNINI, C., OLSEN, R.W. & TOBIN, A.J. (1989). A novel α subunit in rat brain $GABA_A$ receptors. *Neuron*, **3**, 745–753.

KLAIBER, K., WILLIAMS, N., ROBERTS, T.M., PAPAZIAN, D.M., JAN, L.Y. & MILLER, C. (1990). Functional expression of Shaker K^+ channels in a Baculovirus-infected insect cell line. *Neuron*, **5**, 221–226.

MURASE, K., RYU, P.D. & RANDIC, M. (1989). Excitatory and inhibitory amino acids and peptide induced responses in acutely isolated rat spinal dorsal horn neurons. *Neurosci. Lett.*, **103**, 56–63.

PETERSEN, E.N., JENSEN, L.H., HONORE, J., BRAESTRUP, C., KEHER, W., STEPHENSEN, D.N., WATCHEL, H., SEIDELMAN, D. & SCHMIECHEN, R. (1984). ZK 91296, a partial agonist at benzodiazepine receptors. *Psychopharmacol.*, **83**, 240–248.

PRITCHETT, D.B., SONTHEOMER, H., SHIVERS, B.D., YMER, S., KETTENMANN, H., SCHOFIELD, P.R. & SEEBURG, P.H. (1989a). Importance of a novel $GABA_A$ receptor subunit for benzodiazepine pharmacology. *Nature*, **338**, 582–585.

PRITCHETT, D.B., LUDDENS, H. & SEEBURG, P.H. (1989b). Type I and Type II $GABA_A$-benzodiazepine receptors produced in transfected cells. *Science*, **245**, 1389–1392.

PUIA, G., VICINI, S., SEEBURG, P.H. & COSTA, E. (1991). Influence of recombinant $GABA_A$ receptor subunit composition on the action of allosteric modulators of GABA-gated Cl^- currents. *Mol. Pharmacol.*, **39**, 691–696.

SCHOFIELD, P.R. (1989). The $GABA_A$ receptor: molecular biology reveals a complex picture. *Trends Pharmacol. Sci.*, **10**, 476–478.

SHIVERS, B.D., KILLISCH, I., SPRENGEL, R., SONHEIMER, H., KOHLER, M., SCHOFIELD, P.R. & SEEBERG, P.H. (1989). Two novel $GABA_A$ receptor subunits exist in distinct neuronal subpopulations. *Neuron*, **3**, 327–337.

SIGEL, E., BAUR, R., TRUBE, G., MOHLER, H. & MALHERBE, P. (1990). The effect of subunit composition of rat brain $GABA_A$ receptors on channel function. *Neuron*, **5**, 703–711.

STEWART, J.J.P. (1990). MOPAC, a semiempirical molecular orbital program. *J. Comput.-Aided Mol. Design.*, **4**, 1–105.

TANG, A.H., FRANKLIN, S.R., HO, P.M., BLAKEMAN, D.P. & IM, W.B. (1990). U-78875, a benzodiazepine anxiolytic with potent antagonistic activity. *Psychopharmacol.*, **101**, Suppl. 1: S56.

TEBIB, S., BOURGUIGNON, J.-J. & WERMUTH, G.-G. (1987). The active analog approach applied to the pharmacophore identification of benzodiazepine receptor ligands. *J. Computer-Aided Mol. Des.*, **1**, 153–170.

TULLY, W.R., GARDENER, C.R. & WESTWOOD, R. (1991). General approach to the development of imidazoquinoline and imidazopyrimidine benzodiazepine receptor ligands. *Drug Dev. Res.*, **22**, 229–308.

VERDOORN, T.A., DRAGUHN, A., YMER, S., SEEBURG, P.H. & SAKMANN, B. (1990). Functional properties of recombinant rat $GABA_A$ receptors depend upon subunit composition. *Neuron*, **4**, 919–928.

VILLAR, H.O., UYENO, E.T., TOLL, L., POLGAR, W., DAVIS, M.F. & LOEW, G.H. (1989). Molecular determinants of benzodiazepine receptor affinities and anticonvulsant activities. *Mol. Pharmacol.*, **36**, 589–600.

VILLAR, H.O., DAVIES, M.F., LOEW, G.H. & MAGUIRE, P.A. (1991). Molecular models for recognition and activation at the benzodiazepine receptor. *Life Sci.*, **48**, 593–602.

YMER, S., SCHOFIELD, P.R., DRAGUHN, A., WERNER, P., KOHLER, M. & SEEBURG, P.H. (1989). $GABA_A$ receptor β subunit heterogeneity: functional expression of cloned cDNAs. *EMBO J.*, **6**, 1665–1670.

YOKOHAMA, J.W., RITTER, B. & NEUBERT, A.D. (1982). 2-Arylpyrazolo-[4,3-c]quinoline-3-ones: novel agonist, partial agonist, and antagonists of benzodiazepines. *J. Med. Chem.*, **25**, 337–339.

(Received April 10, 1992
Revised June 17, 1992
Accepted June 29, 1992)

Br. J. Pharmacol. (1992), **107**, 628–633

The effect of centrally acting myorelaxants on NMDA receptor-mediated synaptic transmission in the immature rat spinal cord *in vitro*

R.J. Siarey, S.K. Long & [1,*]R.H. Evans

Department of CNS-Pharmacology, SOLVAY DUPHAR BV, P O Box 900, 1380 DA Weesp, The Netherlands and *The Department of Pharmacology, University of Bristol, School of Medical Sciences, University Walk, Bristol BS8 1TD

1 The effect of the myorelaxant drugs baclofen, diazepam and tizanidine have been compared on *in vitro* preparations of baby rat spinal cord and adult rat superior cervical ganglion.

2 Dorsal root-elicited long duration (time to half decay 9.71 ± 0.29 s.e.mean, $n = 31$) ipsilateral ventral root reflexes (DR-VRP), measured as integrated area, of immature rat spinal cord preparations were abolished by **RS**-2-amino-5-phosphonopentanoate (AP5) (EC_{50} 8.13 ± 0.92 μM, $n = 3$). The initial short latency component of DR-VRP was resistant to AP5.

3 Baclofen abolished both components of the DR-VRP. Respective EC_{50} values for the AP5-insensitive and AP5-sensitive components were 237 ± 68 nM ($n \pm 7$) and 57 ± 10 nM ($n = 7$). These effects of baclofen were reversed by the $GABA_B$ antagonist, CGP35348. The apparent K_d values (16.7 ± 6.4 μM, $n = 3$ and 14.3 ± 3.9 μM, $n = 6$ respectively) for this reversal were not significantly different.

4 Tizanidine, clonidine and diazepam had no effect on the AP5-insensitive component of the DR-VRP.

5 The AP5-sensitive long duration component of the DR-VRP was depressed to respective maximal levels of 23.2 ± 1.4% ($n = 7$), 18.8 ± 3.8% ($n = 4$) and 47.6 ± 1.6% ($n = 5$) of control (100%) levels by tizanidine (EC_{50} 135 ± 33 nM), clonidine (EC_{50} 26.0 ± 2.2 nM) and diazepam (EC_{25} 114 ± 12 nM, $n = 4$). The depressant effects of tizanidine and clonidine were reversed by idazoxan (1 μM). Flumazenil (1 μM) failed to reverse the depressant effect of tizanidine. The depressant effect of diazepam was reversed by flumazenil (1 μM) but not by idazoxan (1 μM). Naloxone 1 μM did not reverse the effects of either tizanidine or diazepam.

6 In the presence of tetrodotoxin (0.1 μM) which abolished synaptic activity, clonidine, tizanidine or diazepam (10, 100 and 10 μM respectively) produced no significant antagonism of NMDA-induced depolarizations recorded from ventral roots.

7 Control (100%) synaptic responses of rat superior cervical ganglion preparations were depressed respectively to near maximal levels of 60.0 ± 5.2% ($n = 4$) and 60.7 ± 5.6% ($n = 5$) by clonidine (0.5 μM, EC_{25} 15.3 ± 3.0 nM) and tizanidine (1 μM, EC_{25} 227 ± 83 nM). These depressant effects were reversed by idazoxan (1 μM). Baclofen (EC_{25} 28.7 ± 10.0, $n = 3$) depressed the postganglionic response to a maximum level of 71.8 ± 2.4% ($n = 4$) control at a concentration of 100 μM. The latter depressant action was reversed by the $GABA_B$ receptor antagonist, CGP35348 (1 mM). Diazepam (1 μM) had no significant effect on ganglionic transmission.

8 It is concluded that the activation of benzodiazepine or α_2-noradrenaline receptors can modulate NMDA receptor-mediated excitatory synaptic pathways whereas synaptic excitation from primary afferent terminals, mediated by non-NMDA receptors, appears to lack the propensity for this type of modulation. The results show also that the isolated spinal preparation can be used to identify central myorelaxant actions that are mediated through functional benzodiazepine or α_2-noradrenaline receptors.

Keywords: Myorelaxant; spinal cord; NMDA receptors

Introduction

Baclofen, diazepam and tizanidine are centrally acting myorelaxant drugs in current use. These three drugs have differing sites of action which may contribute to their therapeutic properties. These sites are respectively $GABA_B$ receptors, benzodiazepine receptors and α_2-adrenoceptors. The purpose of the present investigation was to compare the action of these agents on the synaptic input to motoneurones of the *in vitro* spinal cord preparation.

The immature rat spinal cord preparation is of special interest for such comparison because a long duration (> 20 s) ventral root reflex (DR-VRP) of (1 to 5 day old) rat spinal cord preparations has been associated with nociceptive pathways (Akagi *et al.*, 1985). The $GABA_B$ receptor agonist, baclofen (Akagi & Yanagisawa, 1987), diazepam (Akagi & Yanagisawa, 1987) and α_2-adrenoceptor agonists (Kendig *et al.*, 1991) have all been shown to depress this long duration reflex. Tizanidine has been shown to have α_2-adrenoceptor agonist properties at dorsal horn neurones *in vivo* (Davies & Quinlan, 1985). Thus in the present investigation the action of the myorelaxant, tizanidine, has been compared with the prototypic α_2-adrenoceptor agonist, clonidine. Baclofen differs from diazepam and tizanidine in being a potent depressant of monosynaptic transmission from 1a primary afferent fibres (Edwards *et al.*, 1989).

Flumazenil, idazoxan and the $GABA_B$ antagonist, CGP-35348 (P-[3-aminopropyl]-P-diethoxymethylphosphinic acid; Bittiger *et al.*, 1990) have been used to produce rightward shifts in the concentration effect plots to respective agonists and thus obtain apparent K_d values at the receptors involved in the depressant effects of these myorelaxants.

An important feature of the long duration reflex of the *in vitro* spinal preparation is that it is mediated via neurotransmitter(s) which act at NMDA receptors (Brugger *et al.*,

[1] Author for correspondence.

1990). Thus in the present investigation the effects of an NMDA receptor antagonist have been compared with those of the other drugs.

Because α_2-adrenoceptors, benzodiazepine receptors and $GABA_B$ receptors are not confined to the central nervous system, the *in vitro* superior cervical ganglion preparation has been used in the present study in order to compare the synaptic depressant potency and selectivity of the drugs at this peripheral site with the data from the spinal cord.

Some of these results have been reported in preliminary form (Siarey *et al.*, 1991a,b).

Methods

The methods of superfusion, stimulation and recording were as described by Evans *et al.* (1982). Hemisected spinal cord preparations from rats of 2 to 5 days *post partum* age were superfused with medium containing (mM) $MgSO_4$ 1.25, $CaCl_2$ 1.5, NaCl 118, KCl 3, $NaHCO_3$ 24 and dextrose 12. Supramaximal electrical stimulation (10 to 20 times threshold) of a dorsal root (L4 or 5), cycle time 90s, was used to evoke synaptic potentials in the corresponding ventral root (DR-VRP). Superior cervical ganglion and rat vagus nerve preparations were superfused with the same medium as for spinal cord preparations excepting for the $MgSO_4$ concentration which was 0.75 mM. The presynaptic nerves of ganglia and the vagus nerves were also stimulated supramaximally but at a rate of 0.033 Hz. All preparations were maintained at 25°C.

Depressant effects of drugs on the electrically evoked responses were measured as the reduction in peak amplitude or area after integration over the complete time-course.

Depressant potencies were estimated as the concentration required to depress synaptic responses to 50% of control values (EC_{50}). This procedure was simple for those agents that could completely abolish synaptic responses. However, when the maximal depressant effect was close to 50% of control, potency was recorded as the concentration required to produce a 25% depression (EC_{25}). The latter procedure was chosen because non-specific depressant effects produced at high concentrations, as described for tizanidine below, made it difficult or impossible to determine the maximal depressant action and thus normalize the depressant responses as fractions of the maximum. Unless stated otherwise, mean values are presented ± s.e.mean.

Results

Involvement of NMDA receptors

Figure 1a illustrates the depressant effect of **RS**-2-amino-5-phosphonopentanoate (AP5) on the long duration component of the DR-VRP. Under control conditions the mean integrated area measured from 2 to 32 s was 19.5 ± 1.2 mV.s and the mean time of decay to half area of these potentials was 9.67 ± 0.49 s ($n = 31$). As expected from previous work (Evans *et al.*, 1982; Long *et al.*, 1990) the early component of the reflex was resistant to this antagonist whereas the long duration component (assessed from the area between 2 and 32 s) was depressed completely by concentrations of 100 μM or higher (EC_{50} 8.13 ± 0.92 μM, $n = 3$).

Action of α_2-adrenoceptor agonists.

Investigation of the properties of tizanidine, in relation to its myorelaxant action, was a major interest of this study. Because tizanidine has been characterized as an α_2-adrenoceptor agonist, it was of interest to compare the properties of clonidine as a prototypic α_2-adrenoceptor agonist with those of tizanidine. Figure 1b illustrates the depressant action of clonidine. The early component of the synaptic response was resistant to clonidine. The long duration DR-VRP was partially resistant to clonidine as shown by the maximal depression to 18.8 ± 3.8% of control ($n = 4$) produced by concentrations of 100 nM or higher (EC_{50} 26.0 ± 2.2 nM, $n = 4$). It can be seeen from Figure 1b that recovery of the synaptic response on removal of clonidine was very slow compared to recovery from the depressant action of AP5 (Figure 1a). Thus after 60 min washout of clonidine, the long duration DR-VRP had recovered to only 24.5 ± 3.4% ($n = 4$) of the control area. However, the depressant action of clonidine was reversed rapidly on introduction of idazoxan (1 μM) such that full recovery to the control area of synaptic response occurred within 17 ± 6 min ($n = 4$) (Figure 1b). The selectivity of idazoxan, in reversing clonidine-induced depression, was demonstrated following the depressant action of

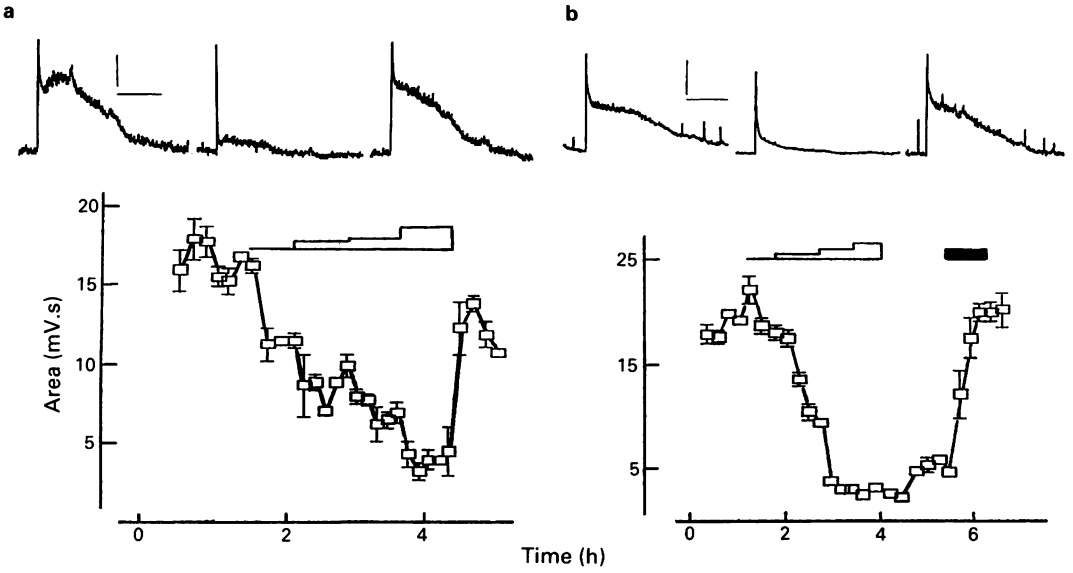

Figure 1 (a) Shows **RS**-2-amino-5-phosphonopentanoate (AP5)-sensitivity of long duration ipsilateral DR-VRP. Note return to control size of potential on washout of AP5. AP5 1, 5, 10 and 100 μM was introduced cumulatively as indicated by the bar above the plot. (b) Separate preparation showing depressant effect of clonidine and reversal by idazoxan. Clonidine was applied cumulatively at 10, 20, 100 and 300 nM. The filled bar above the plot indicates introduction of idazoxan 1 μM. Single records before, during and after the depressant effects are shown above. Each point plotted below is the mean ± s.e.mean (vertical bars) of three consecutive recordings. Vertical scale bars 0.5 mV in (a) and 1 mV in (b). Horizontal scale bars 10 s.

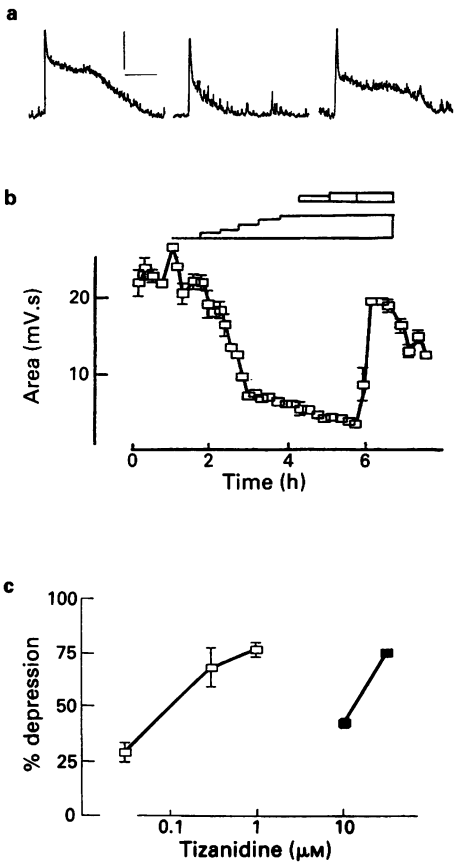

Figure 2 Depressant effect of tizanidine on the long duration DR-VRP. (a) The three recordings are shown consecutively before introduction of tizanidine, in the presence of tizanidine (1 μM) and in the presence of idazoxan (1 μM) (vertical scale bar 0.5 mV). (b) The time-course is plotted. Cumulative introduction of 0.01, 0.03, 0.1, 0.3, 1 and 3 μM tizanidine is indicated immediately above the plot. The upper bars to the right indicate consecutive introduction of prazosin (0.5 μM), naloxone (1 μM) or idazoxon (1 μM). The effect of tizanidine was reversed only when idazoxan was applied. (c) Concentration-effect plot of the depressant action of tizanidine showing the rightward displacement which occurred in the presence of idazoxan. Other details as for Figure 1.

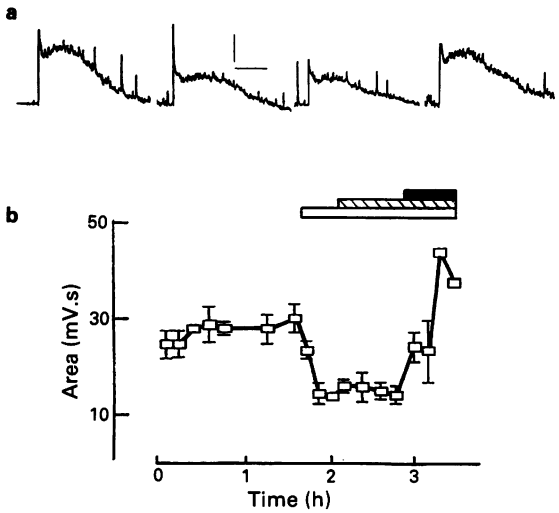

Figure 3 Depressant effect of diazepam on the long duration DR-VRP and reversal of the depression by flumazenil. (a) Consecutive records are shown before introduction of diazepam, in the presence of diazepam (1 μM), in the presence of idazoxan and in the presence of flumazenil (vertical scale bar 1 mV). (b) The bars above the time-course indicate in ascending order the introduction of diazepam (1 μM), idazoxan (1 μM) and flumazenil (1 μM). Other details as for Figure 1.

diazepam and baclofen (see below).

Figure 2 illustrates that the effect of clonidine was mimicked, in every respect examined, by tizanidine which depressed the long duration DR-VRP to 23.2 ± 1.4% of control levels (EC_{50} for depression of the long duration DR-VRP 135 nM ± 33, $n = 7$). As illustrated in Figure 2 dose-ratios for antagonism of the depressant effect by tizanidine by idazoxan were obtained in five preparations (apparent K_d 9.57 nM ± 2.14). The α_2-adrenoceptor antagonist, prazosin (0.5 μM), illustrated in Figure 2, and the opiate antagonist, naloxone (1 μM), did not reverse the depressant effect of tizanidine.

Action of diazepam

The maximal depressant effect of diazepam (decrease in control DR-VRP area to 47.6 ± 1.6% produced by 1 μM, EC_{25}, 114 nM ± 12, $n = 4$) was less than that of the α_2-adrenoceptor agonists. On all five preparations tested this depressant effect was not reversed by idazoxan (1 μM) (Figure 3). However, as illustrated in Figure 3, the depressant effect of diazepam was quickly reversed following introduction of flumazenil (1 μM).

NMDA and AMPA-induced depolarization

As illustrated by Figure 1, the component of the DRP-VRP which was most sensitive to clonidine, tizanidine and diazepam is characteristically mediated by NMDA receptors (Brugger *et al.*, 1990). Therefore the myorelaxant drugs were tested for NMDA receptor antagonist properties, particularly because of previously reported postjunctional depressant actions of tizanidine (Curtis *et al.*, 1983; Villanueva *et al.*, 1988) and diazepam (Evans *et al.*, 1977). In tetrodotoxin-blocked preparations, clonidine (10 μM), tizanidine (100 μM) and diazepam (10 μM) produced mean dose-ratios of 0.97 ± 0.03 ($n = 8$), 1.00 ± 0.003 ($n = 3$) and 1.01 ± 0.03 ($n = 3$) respectively for antagonism of depolarizations produced by 10 to 30 μM NMDA. In this series of experiments AP5 (10 μM) or kynurenate (100 μM) produced mean dose-ratios of 2.29 ± 0.08 ($n = 6$) and 2.10 ± 0.08 ($n = 6$) respectively. Consistent with the resistance of the initial component of the DR-VRP, clonidine (10 μM), tizanidine (100 μM) and diazepam (10 μM) did not alter **RS**-α-amino-3-hydroxy-5-methylisoxazole-4-propionic acid (AMPA)-induced depolarization of motoneurones in the presence of tetrodotoxin. The respective dose-ratios were 0.97 ± 0.03 ($n = 7$), 0.83 ± 0.10 ($n = 3$) and 1.02 ± 0.07 ($n = 3$). In this series of experiments kynurenate (100 μM) produced a mean dose-ratio of 1.93 ± 0.02 ($n = 6$) against the depolarizations induced by AMPA.

Action of baclofen

The potent depressant effect of baclofen on spinal transmission from primary afferent nerves has been reported on several occasions and the role of GABA receptors in mediating this depressant action has been controversial (see review by Evans, 1989). Availability of the $GABA_B$ receptor antagonist, CGP35348 for the present experiments has allowed some resolution of this controversy. In the present experiments baclofen completely abolished all the components of the DR-VRP at concentrations higher than 2 μM. The early and long duration phases of the reflex had differing sensitivities to baclofen as shown by respective EC_{50} values of 237 ± 68 nM ($n = 7$) and 57 ± 10 nM ($n = 7$). However, the sensitivity of these components to antagonism by CGP35348 was not significantly different. Thus the effects of baclofen on short and long duration components of the reflex were reversed in the presence of CGP35348, yielding respective apparent K_d values of 16.7 ± 6.4 μM ($n = 3$) and 14.3 ± 3.9 μM ($n = 6$). The latter values are not significantly different. Idazoxan (1 μM) failed to reverse the depressant effects of baclofen. These effects are illustrated in Figure 4.

Effects on the monosynaptic population e.p.s.p. from primary afferents

The initial component of the DR-VRP consists mainly of the population spike of motoneurones. Therefore it is possible that the resistance of this component to the α_2-adrenoceptor agonists and diazepam was apparent rather than real because the underlying excitatory postsynaptic potential (e.p.s.p.) could have been depressed to a level insufficient to prevent firing of motoneurones. To test this possibility the short latency population spike of the DR-VRP was blocked with kynurenic acid. In the presence of 1 mM kynurenate the initial component of the reflex then consisted of a smooth population e.p.s.p. (Figure 5) of mean latency 5.99 ± 0.62 ms, time to peak 21.7 ± 1.1 ms, peak amplitude 0.84 ± 0.12 mV and slope of 0.084 ± 0.018 V s^{-1} ($n = 10$). Clonidine (300 nM, $n = 3$), tizanidine (1 μM, $n = 3$) (Figure 5) and diazepam (1 μM, $n = 4$) (Figure 5) had no significant effect on the rising slope of these potentials. However, as illustrated by the lower traces in Figure 4, baclofen decreased the rising slope of the e.p.s.p. when applied at concentrations insufficient to block it completely. This depressant effect of baclofen was reversed also by CGP35348 (200 μM).

Effects on ganglionic transmission

Clonidine has been reported previously to depress transmission in the superior cervical ganglion by an action at α_2-adrenoceptors (Brown & Caulfield, 1979; Medgett, 1983). Thus it was of interest to compare depressant potencies of the α_2-adrenoceptor agonists at this peripheral site with their potencies for depression of the spinal preparation.

The postganglionic response of ganglion preparations had a mean latency of 12.9 ± 0.5 ms ($n = 19$). Clonidine and

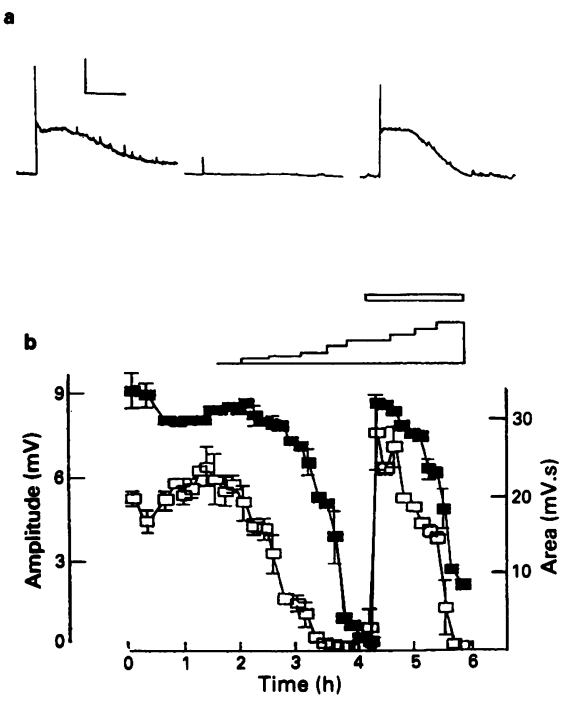

Figure 4 (b) Depressant action of baclofen on the initial monosynaptic (■, left hand ordinate scale) and the long duration (□, right hand ordinate scale) components of the DR-VRP. The recordings of the long duration DR-VRP in (a) are consecutively before introduction of baclofen, in the presence of baclofen (1 μM) and in the presence of CGP35348 (1 mM) (vertical scale bar 1 mV). Cumulative introduction of 0.01, 0.03, 0.05, 0.1, 0.3, 1, 3, 10 and 30 μM baclofen is indicated above the time-course plot in (b) and the upper bar on the right indicates introduction of CGP35348 (1 mM). Other details as for Figure 1.

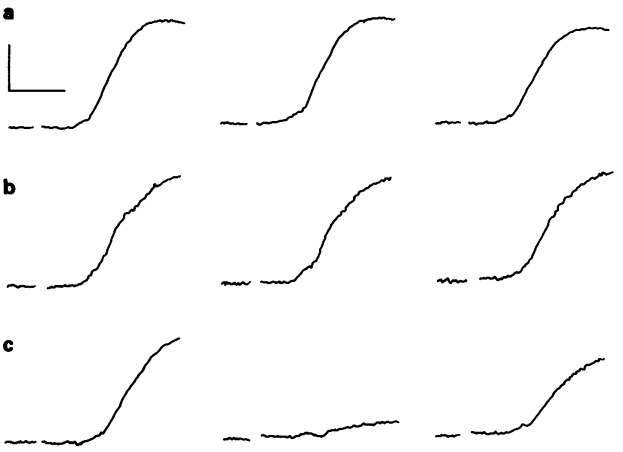

Figure 5 Effect of tizanidine (a), diazepam (b) and baclofen (c) on the population e.p.s.p. of motoneurones. The recordings were made in the presence of kynurenate (1 mM) in order to block the compound action potential of the motoneurones. Each trace is the average of four consecutive recordings. (a), (b) and (c) are from different preparations. The first column of traces was obtained before introduction of drug. The second column was obtained 40 min after introduction of tizanidine (1 μM) or diazepam (1 μM) or 15 min after introduction of baclofen (0.3 μM). The third column of traces was obtained 10 min following the respective application of (in descending order) idazoxan (1 μM), flumazenil (1 μM) or CGP35348 (0.2 mM). Only baclofen depressed the e.p.s.p. and the depression was reversed by CGP35348. Vertical scale bar 0.4 mV in (a) and (c), 0.22 mV in (b). Horizontal scale bar 10 ms.

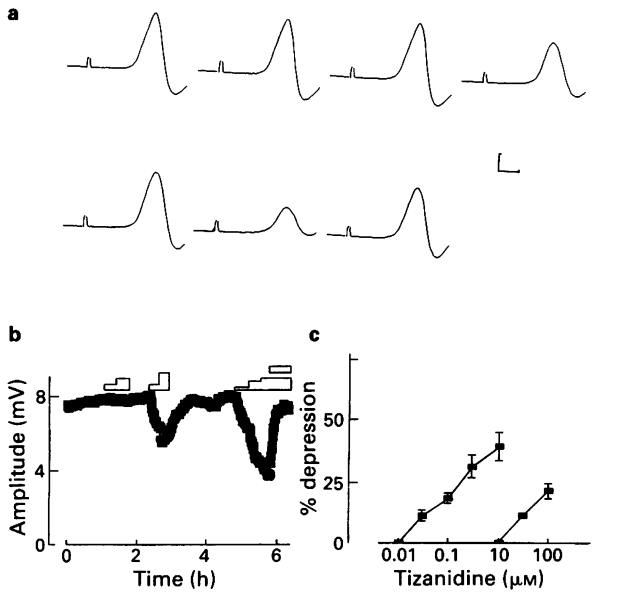

Figure 6 Effect of diazepam, baclofen and tizanidine on synaptic response of superior cervical ganglion. (a) Recordings obtained consecutively before introduction of diazepam, in the presence of diazepam (10 μM), following washout of diazepam, in the presence of baclofen (100 μM), following washout of baclofen, in the presence of tizanidine (1 μM) and in the presence of idazoxan (1 μM) as indicated above the time-course in (b) (vertical scale bar 2.5 mV, horizontal scale bar 5 ms). (b) The bars above the time-course indicate from the left introduction of diazepam (1 and 10 μM), baclofen (1 and 100 μM) and tizanidine (0.03, 0.3 and 1 μM). Introduction of idazoxan (1 μM) is indicated by the upper bar on the right above tizanidine. It can be seen that, unlike the other two drugs, diazepam had no significant depressant action. (c) Concentration-effect plot of the depressant action of tizanidine on four preparations showing the rightward shift produced in the presence of idazoxan (1 μM). Other details as for Figure 1.

tizanidine (Figure 6) depressed the population spike of this response to plateau levels of $60.0 \pm 5.2\%$ ($n = 4$) and $60.7 \pm 5.6\%$ ($n = 5$) respectively. As with the spinal cord, these depressant actions recovered very slowly on washout of drug but were quickly reversed on introduction of idazoxan (1 μM). These effects are illustrated in Figure 6. The preparation of Figure 6b was the one of the series on which tizanidine had the greatest depressant effect.

The EC_{25} values (nM) for clonidine and tizanidine were 15.3 ± 3.0 ($n = 4$) and 227 ± 83 ($n = 5$) respectively. In contrast to clonidine and tizanidine, diazepam (10 μM, $n = 6$) (Figure 6) and AP5 (100 μM, $n = 4$), at concentrations which clearly depressed the long duration DRP-VRP, failed to depress ganglionic transmission. The apparent K_d values obtained for idazoxan in reversing the spinal (9.57 ± 2.14 nM, $n = 5$) and ganglionic (12.8 ± 2.0 nM, $n = 5$) depressant effects of tizanidine were not significantly different ($P = 0.23$ Wilcoxon-Mann-Whitney).

In contrast to a previous report (Evans, 1979) the amplitude of postganglionic potentials was depressed by baclofen (EC_{25} 28.7 ± 10.0 μM, $n = 3$) to a mean maximal level of $71.8 \pm 2.4\%$ of control (100%) at 100 μM ($n = 4$). This depressant effect of 10 μM baclofen was reversed in the presence of CGP35348 (1 mM).

In three out of four ganglion preparations it was observed that application of baclofen (10 μM) produced a mean postganglionic hyperpolarization of 0.020 ± 0.007 mV. The hyperpolarizations developed over a period of 3 to 8 min and were swiftly reversed on application of CGP35348 (1 mM).

Tizanidine, at higher concentrations than those above, had a non-specific depressant action. This non-specific action was shown following application of 1 mM tizanidine to four preparations of rat vagus nerve. The amplitudes of A and C elevations in the compound action potential of the nerves were depressed to $63.3 \pm 5.0\%$ and $53.8 \pm 4.0\%$ of control (100%) levels respectively. This depression was not reversed by 1 μM idazoxan. Clonidine and diazepam were not tested on the vagus nerve.

Discussion

The long duration DR-VRP is mediated by NMDA receptors as indicated by the complete blockade which occurs in the presence of an appropriate concentration of AP5. The depressant effect of the α_2-adrenoceptor agonists on this reflex reflects intrinsic inhibitory mechanisms which operate through α_2-adrenoceptors (Taylor *et al.*, 1991). Similarly the depressant effect of diazepam is likely to reflect the operation of $GABA_A$ receptors in inhibitory pathways.

These drugs failed to depress the rising slope of the dorsal root evoked population e.p.s.p. of motoneurones which is mediated through non-NMDA receptors (Long *et al.*, 1990). These three drugs failed to antagonize NMDA- or AMPA-induced depolarizations at concentrations higher than those required for the depressant action on the long duration DR-VRP. Therefore the depressant action was unlikely to have been due to postjunctional antagonism at excitatory amino acid receptors. Diazepam has some excitatory amino acid antagonist activity but only at concentrations much higher than those used in the present study (Evans *et al.*, 1977). Thus the drugs appear to modulate selectively NMDA receptor-mediated excitatory transmission. It is implied from this that transmitters released on to NMDA receptors can be modulated separately from those released on to non-NMDA receptors. Such selectivity may be a consequence of the temporal difference between non-NMDA- and NMDA-receptor-mediated events.

The α_2-agonists produced a larger maximal depressant action than did diazepam suggesting that these two classes of drug may influence different populations of excitatory synapses.

The speedy and selective reversal of depressant effects produced by the antagonists idoxazan and flumazenil were important in demonstrating the effects of the respective agonists. The synaptic depression produced by these agonists is slow to reverse in the absence of antagonist, indicating persistence of the agonists in the tissue during the application of agonist-free wash solution.

The effects of the α_2-adrenoceptor agonists and diazepam contrast with the action of baclofen which depressed all components of the DR-VRP as expected from its action at the primary afferent synapse (Edwards *et al.*, 1989). The apparent K_d of 10.6 μM reported here for the $GABA_B$ antagonist, CGP35348, in reversing the action of baclofen is not significantly different from the value of 11.2 μM for depression of e.p.s.ps of striatal neurones (Seabrook *et al.*, 1990).

In the present experiments the different components of the DR-VRP had different sensitivities from baclofen as shown by the four fold higher EC_{50} for depression of the initial monosynaptic as compared to the long duration component. However, the dose-ratios for reversal of these depressant actions of baclofen, produced by the antagonist CGP35348 were not significantly different. Thus the antagonist is able to define only one population of $GABA_B$ receptors in this preparation.

Although in the present investigation baclofen was 500 times less potent at depressing ganglionic than it was at depressing spinal transmission, this effect of baclofen on the superior cervical ganglion preparations was unexpected since a previous study showed no action of baclofen at concentrations up to 1 mM (Evans, 1979). The failure of baclofen to depress the postjunctional response of ganglia to less than approximately 70% of control levels suggests that postjunctional hyperpolarization of ganglionic neurones may be involved rather than the depression of transmitter release.

The adrenoceptor agonists were distinguished from diazepam by their depressant action on the superior cervical ganglion preparation. The apparent K_d value of 11 nM for idazoxan-induced reversal of the effect of tizanidine applied to the ganglionic preparations was not significantly different from the value obtained with the spinal preparations or from the value of 9 nM obtained by Williams *et al.* (1985) at locus coeruleus neurones. Thus the affinities for idazoxan of spinal, cephalic and peripheral α_2-adrenoceptors are very similar if not the same.

In the present investigation, tizanidine and clonidine had a greater maximal depressant effect than diazepam on the spinal cord and baclofen and tizanidine depressed ganglionic transmission whereas diazepam did not. Thus benzodiazepine ligands can be differentiated from adrenoceptor ligands due to their lack of effect on ganglionic transmission as well as their sensitivity to flumazenil.

Muscle spasm is painful. Thus it is helpful if myorelaxant drugs are also analgesic. Baclofen (Sawynok & Reid, 1988), benzodiazepines (Goodchild & Serrao, 1987) and α_2-adrenoceptor agonists (Bonnet *et al.*, 1989) are all reported to have analgesic actions at the spinal level. It is claimed that the long duration DR-VRP is a manifestation of activity in nociceptive pathways in the spinal cord (Akagi *et al.*, 1985). This is certainly consistent with the analgesic action of intrathecally administered AP5 (Cahusac *et al.*, 1984). Thus depression of the long duration reflex by these myorelaxant drugs is consistent with the proposed link between this reflex and nociception. Therefore depression of the long duration component of the DR-VRP may be a predictor for *in vivo* centrally acting myorelaxant activity. The myorelaxant action of AP5 and other NMDA receptor antagonists (Turski *et al.*, 1984) is consistent with this expectation.

R.H.E. was supported by the Medical Research Council, The Taberner Trust and The Wellcome Trust and R.J.S. was supported by a DUPHAR research scholarship.

References

AKAGI, H., KONISHI, S., OTSUKA, M. & YANAGISAWA, M. (1985). The role of substance P as a neurotransmitter in the reflexes of slow time courses in the neonatal rat spinal cord. *Br. J. Pharmacol.*, **84**, 663–673.

AKAGI, H. & YANAGISAWA, M. (1987). GABAergic modulation of a substance P-mediated reflex of slow time course in the isolated rat spinal cord. *Br. J. Pharmacol.*, **91**, 189–197.

BITTIGER, H., FROESTL, W., HALL, R., KARLSSON, G., KLEBS, K., OLPE, H.-R., POZZA, M.F., STEINMANN, M.W. & VAN REIZEN, H. (1990). Biochemistry, electrophysiology and pharmacology of a new $GABA_B$ antagonist: CGP35348. In *$GABA_B$ receptors in Mammalian Function*. ed. Bowery, N.G., Bittiger, H. & Olpe, H.-R. pp. 47–60. Chichester, England: John Wiley.

BONNET, F., BOIES, O., ROSTAING, S., SAADA, M., LORIFERNE, J.-F., TOUBOUL, C., ABHAY, K. & GHIGNONE, M. (1989). Postoperative analgesia with extradural clonidine. *Br. J. Anaesth.*, **63**, 465–469.

BROWN, D.A. & CAULFIELD, M.P. (1979). Hyperpolarizing 'α_2'-adrenoceptors in rat sympathetic ganglia. *Br. J. Pharmacol.*, **65**, 435–445.

BRUGGER, F., EVANS, R.H. & HAWKINS, N.S. (1990). Effects of N-methyl-D-aspartate antagonists and spantide on spinal reflexes and responses to substance P and capsaicin in isolated spinal cord preparations from mouse and rat. *Neuroscience*, **36**, 611–622.

CAHUSAC, P.M.B., EVANS, R.H., HILL, R.G., RODRIGUEZ, R.E. & SMITH, D.A.S. (1984). The behavioural effects of an N-methyl-D-aspartate receptor antagonist following application to the lumbar spinal cord of conscious rats. *Neuropharmacology*, **23**, 719–724.

CURTIS, D.R., LEAH, J.D. & PEET, M.J. (1983). Spinal interneurone depression by DS103-282. *Br. J. Pharmacol.*, **79**, 9–11.

DAVIES, J. & QUINLAN, J.E. (1985). Selective inhibition of response of feline dorsal horn neurones to noxious cutaneous stimuli by tizanidine (DS103-282) and noradrenaline: involvement of α_2-adrenoceptors. *Neuroscience*, **16**, 673–682.

EDWARDS, F.R., HARRISON, P.J., JACK, J.J.B. & KULLMAN, D.M. (1989). Reduction by baclofen of monosynaptic EPSPs in lumbosacral motoneurones of the anaesthetised cat. *J. Physiol.*, **416**, 539–556.

EVANS, R.H. (1979). Baclofen: lack of effect on neurotransmission in the mouse vas deferens. *J. Pharm. Pharmacol.*, **31**, 642–643.

EVANS, R.H. (1989). The pharmacology of segmental transmission in the spinal cord. *Progr. Neurobiol.*, **33**, 255–279.

EVANS, R.H., FRANCIS, A.A., JONES, A.W., SMITH, D.A.S. & WATKINS, J.C. (1982). The effects of a series of ω-phosphonic α-carboxylic amino acids on electrically evoked and excitant amino acid-induced responses in isolated spinal cord preparations. *Br. J. Pharmacol.*, **75**, 65–75.

EVANS, R.H., FRANCIS, A.A. & WATKINS, J.C. (1977). Differential antagonism by chlorpromazine and diazepam of frog motoneurone depolarization induced by glutamate-related amino acids. *Eur. J. Pharmacol.*, **44**, 325–330.

GOODCHILD, C.S. & SERRAO, J.M. (1987). Intrathecal midazolam in the rat: evidence for spinally-mediated analgesia. *Br. J. Anaesth.*, **59**, 1563–1570.

KENDIG, J.J., SAVOLA, M.K.T., WOODLEY, S.J. & MAZE, M. (1991). α_2-Adrenoceptors inhibit a nociceptive response in neonatal rat spinal cord. *Eur. J. Pharmacol.*, **192**, 293–300.

LONG, S.K., SMITH, D.A.S., SIAREY, R.J. & EVANS, R.H. (1990). Effect of 6-cyano-2,3-dihydroxy-7-nitroquinoxaline (CNQX) on dorsal root-, NMDA, kainate- and quisqualate-mediated depolarization of rat motoneurones *in vitro*. *Br. J. Pharmacol.*, **100**, 850–854.

MEDGETT, I.C. (1983). Modulation of transmission in rat sympathetic ganglion by activation of presynaptic α- and β-adrenoceptors. *Br. J. Pharmacol.*, **78**, 17–27.

SAWYNOK, J. & REID, A. (1988). Role of ascending and descending serotonergic pathways in the antinociceptive effect of baclofen. *Naunyn Schmiedebergs Arch. Pharmacol.*, **337**, 359–365.

SEABROOK, G.R., HOWSON, W. & LACEY, M.G. (1990). Electrophysiological characterization of potent agonists and antagonists at pre- and postsynaptic $GABA_B$ receptors on neurones in rat brain slices. *Br. J. Pharmacol.*, **101**, 949–957.

SIAREY, R.J., LONG, S.K. & EVANS, R.H. (1991a). Effect of clonidine on synaptic activity of rat in vitro spinal cord preparations. *J. Physiol.*, **435**, 70P.

SIAREY, R.J., LONG, S.K. & EVANS, R.H. (1991b). Potentiation of synaptic reflexes by D-serine in the rat spinal cord in vitro. *Eur. J. Pharmacol.*, **195**, 241–244.

TAYLOR, J.S., NEAL, R.I., HARRIS, J., FORD, T.W. & CLARKE, R.W. (1991). Prolonged inhibition of a spinal reflex after intense stimulation of distant peripheral nerves in the decerebrated rabbit. *J. Physiol.*, **437**, 71–84.

TURSKI, L., SCHWARCZ, M., TURSKI, W.A., KLOCKGETHER, T., SONTAG, K.-H. & COLLINS, J.F. (1984). Muscle relaxant action of excitatory amino acid antagonists. *Neurosci. Lett.*, **53**, 321–326.

VILLANUEVA, L., CHITOUR, D. & LE BARS, D. (1988). Effects of tizanidine (DS103-282) on dorsal horn convergent neurones in the rat. *Pain*, **35**, 187–197.

WILLIAMS, J.T., HENDERSON, G. & NORTH, R.A. (1985). Characterization of α_2-adrenoceptors which increase potassium conductance in rat locus coeruleus neurones. *Neuroscience*, **14**, 95–101.

(Received June 10, 1992
Revised June 29, 1992
Accepted July 1, 1992)

British Journal of Pharmacology

VOLUME 107 (2) OCTOBER 1992

SPECIAL REPORTS

The purpose of *Special Reports* is to provide rapid publication for **new** and **important** results which the Editorial Board considers are likely to be of special pharmacological significance. *Special Reports* will have publication priority over all other material and so authors are asked to consider carefully the status of their work before submission.

In order to speed publication there is normally no revision allowed beyond very minor typographical or grammatical corrections. If significant revision is required, the Board may either invite rapid re-submission or, more probably, propose that it be re-written as a Full Paper and be re-submitted for consideration. In order to reduce delays, proofs of *Special Reports* will be sent to authors but **essential corrections must reach the Production Office within 48 hours of receipt.** Authors should ensure that their submitted material conforms exactly to the following requirements.

Special Reports should normally occupy no more than two printed pages of the Journal; two illustrations (Figures or Tables, with legends) are permitted. As a guideline, with type face of 12 pitch and double-line spacing, a page of A4 paper could contain about 400 words. The absolute maximum length of the *Special Report* is 1700 words. For each Figure or Table, please deduct 200 words. The manuscript should comprise a Title page with key words (maximum of 10), a Summary consisting of a single short paragraph, followed by Introduction, Methods, Results, Discussion and References (maximum of 10). In all other respects, the requirements are the same as for Full Papers (see current 'Instructions to Authors').

Papers will be considered for publication on all aspects of pharmacology, including chemotherapy.

Manuscripts (two copies) should be sent to Editorial Office, British Journal of Pharmacology, St. George's Hospital Medical School, Cranmer Terrace, London SW17 0RE. Authors should consult the Instructions to Authors in Vol. 105, 245–251 (1992) and the Nomenclature Guidelines for Authors in Vol. 105, 252–254 (1992). These Instructions and Guidelines also appear with the journal Index for volumes 102–104, 1991.

The *British Journal of Pharmacology* is published monthly by the Scientific & Medical Division, Macmillan Press Ltd.

The journal is covered by *Current Contents*, *Excerpta Medica* and *Index Medicus*.

All business correspondence and reprint requests should be addressed to the Scientific & Medical Division, Macmillan Press Ltd., Houndmills, Basingstoke, Hampshire RG21 2XS, UK. Telephone: (0256) 29242; Fax: (0256) 810526.

Annual subscription prices for 1992 EEC £412, elsewhere £445/US$825 (sterling rate is definitive). Orders must be accompanied by remittance. Cheques should be made payable to Macmillan Press, and sent to: Macmillan Press Ltd., Subscription Department, Brunel Road, Houndmills, Basingstoke, Hampshire RG21 2XS, UK.

Overseas subscribers may make payments into UK Post Office Giro Account No. 5192455. Full details must accompany the payment.

Second Class postage paid at Rahway NJ. US Mailing Agent: Mercury Airfreight International Ltd, Inc., 2323 Randolph Avenue, Avenel, New Jersey, NJ 07001, USA.

Enquiries concerning advertising space or rates should be addressed to: Michael Rowley, Advertisement Manager, Macmillan Press Ltd., 4 Little Essex Street, London WC2R 3LF. Telephone: 071 836 6633; Fax: 071 379 0820.

ISSN 0007–1188

0007–1188/92 $3.50 + $0.00

SPECIAL REPORTS

The purpose of *Special Reports* is to provide rapid publication for **new** and **important** results which the Editorial Board considers are likely to be of special pharmacological significance. *Special Reports* will have publication priority over all other material and so authors are asked to consider carefully the status of their work before submission.

In order to speed publication there is normally no revision allowed beyond very minor typographical or grammatical corrections. If significant revision is required, the Board may either invite rapid re-submission or, more probably, propose that it be re-written as a Full Paper and be re-submitted for consideration. In order to reduce delays, proofs of *Special Reports* will be sent to authors but **essential corrections must reach the Production Office within 48 hours of receipt.** Authors should ensure that their submitted material conforms exactly to the following requirements.

Special Reports should normally occupy no more than two printed pages of the Journal; two illustrations (Figures or Tables, with legends) are permitted. As a guideline, with type face of 12 pitch and double-line spacing, a page of A4 paper could contain about 400 words. The absolute maximum length of the *Special Report* is 1700 words. For each Figure or Table, please deduct 200 words. The manuscript should comprise a Title page with key words (maximum of 10), a Summary consisting of a single short paragraph, followed by Introduction, Methods, Results, Discussion and References (maximum of 10). In all other respects, the requirements are the same as for Full Papers (see current 'Instructions to Authors').

PREPARATION OF MANUSCRIPTS

Authors are strongly recommended to read the full *Instructions to Authors* and *Nomenclature Guidelines for Authors* (*Br. J. Pharmacol.* 1992, **105,** 245–254) before submitting a manuscript for publication in the *British Journal of Pharmacology*. The manuscript and cover letter should be checked against the following list before mailing.

The original and one copy of the manuscript must be supplied. Manuscripts must be typed in double-line spacing on one side of A4 paper, in type not smaller than 12 characters per inch or 10 point. Both copies to include Tables and a set of labelled Figures. One set of Figures without numbers or letters is also to be included. The text to be arranged in the following subsections:

1. **Title**—To have no more than 150 characters on a separate page, which should also include a Short Title (50 characters maximum) and the name and address of the author for correspondence.

2. **Summary**—To be arranged in numbered paragraphs (Full Papers) or a single paragraph (Special Reports).
   —to include aims, principal results and conclusions.
   —to include Key words (10 maximum) at end of summary.

3. **Introduction**—To contain concise statements of the problem and the aims of the investigation.

4. **Methods**—To have brief but adequate account of the procedures; *full names of drugs* (*including those referred to by manufacturer's code*), sources of drugs and statistical tests to be stated.

5. **Results**—To have no repetition of data in Figures, Tables and text.

6. **Discussion**—Findings and conclusions to be placed in context of other relevant work.
   NB Simple repetition of results and unwarranted speculation are not acceptable.

7. **Acknowledgments**—Sources of support. Sources of drugs not widely available commercially.

8. **References**—All references in the text to be included in the Reference List and *vice versa*. References in alphabetical order with complete citations; Journals publishing 'in press' papers identified.
   References to manuscripts submitted to other journals but not yet accepted are not allowed.

9. **Tables**—Each on a separate page and prepared in accordance with current requirements of the Journal.

10. **Figures**—Both labelled and non-labelled Figures to be prepared in accordance with current requirements of the Journal (see *Instructions to Authors*, 1992, **105,** 245–251) and provided with Figure Number and Authors' names on back (*in pencil*).
    —each legend to be typed on a separate page and carrying keys to symbols.
    —keys to symbols and histograms must not appear on the figures themselves, but in the respective legends.
    —'box style' figures are not in keeping with the Journal style; line drawings etc must have only left-hand and bottom axes.

11. **Manuscripts**—To be accompanied by a declaration signed by each author that
    (a) results are original
    (b) approval of all persons concerned has been given to submit manuscripts for consideration (see also 12b)
    (c) the same material is neither 'in press' (i.e. is in proof or has definitely been accepted for publication) nor under consideration elsewhere. Furthermore it will not be submitted or published elsewhere before a decision has been reached by the Editorial Board of the *British Journal of Pharmacology* and will not be submitted elsewhere if accepted by the *British Journal of Pharmacology*.
    (d) Copyright assignment is included.

12. **Cover letter**—To state clearly
    (a) Corresponding author's full postal address, telephone, telex or Fax number
    (b) where appropriate, that *either* ethical approval has been given for investigation *or* Company or Institutional permission to publish work has been received.

13. **Reminder**—Packaging to be sufficiently robust to protect Figures and to withstand mailing.

Failure to comply with *Instructions to Authors* may lead to substantial delays in processing, review and publication and may even jeopardize acceptance of the manuscript.

NOMENCLATURE

Authors are reminded that accepted receptor and associated terminology is laid out in *Nomenclature Guidelines for Authors*, as published in the *British Journal of Pharmacology, Br. J. Pharmacol., 1992,* **105,** 245–254.

BRITISH JOURNAL OF PHARMACOLOGY VOLUME 107 (2) 1992

Contents continue inside back cover

Typeset by Elite Typesetting Techniques, Southampton, Hampshire
and printed in Great Britain by Unwin Brothers Ltd., The Gresham Press, Old Woking, Surrey

See last page of issue for 'PREPARATION OF MANUSCRIPTS'